



Lecture Notes in Mechanical Engineering

Adam Hamrol  
Olaf Cizak  
Stanisław Legutko  
Mieczysław Jurczyk *Editors*

# Advances in Manufacturing

 Springer

# **Lecture Notes in Mechanical Engineering**

Lecture Notes in Mechanical Engineering (LNME) publishes the latest developments in Mechanical Engineering—quickly, informally and with high quality. Original research reported in proceedings and post-proceedings represents the core of LNME. Also considered for publication are monographs, contributed volumes and lecture notes of exceptionally high quality and interest. Volumes published in LNME embrace all aspects, subfields and new challenges of mechanical engineering. Topics in the series include:

- Engineering Design
- Machinery and Machine Elements
- Mechanical Structures and Stress Analysis
- Automotive Engineering
- Engine Technology
- Aerospace Technology and Astronautics
- Nanotechnology and Microengineering
- Control, Robotics, Mechatronics
- MEMS
- Theoretical and Applied Mechanics
- Dynamical Systems, Control
- Fluid Mechanics
- Engineering Thermodynamics, Heat and Mass Transfer
- Manufacturing
- Precision Engineering, Instrumentation, Measurement
- Materials Engineering
- Tribology and Surface Technology

More information about this series at <http://www.springer.com/series/11236>

Adam Hamrol · Olaf Ciszak  
Stanisław Legutko · Mieczysław Jurczyk  
Editors

# Advances in Manufacturing

 Springer

*Editors*

Adam Hamrol  
Poznan University of Technology  
Poznań  
Poland

Stanisław Legutko  
Poznan University of Technology  
Poznań  
Poland

Olaf Ciszak  
Poznan University of Technology  
Poznań  
Poland

Mieczysław Jurczyk  
Poznan University of Technology  
Poznań  
Poland

ISSN 2195-4356

ISSN 2195-4364 (electronic)

Lecture Notes in Mechanical Engineering

ISBN 978-3-319-68618-9

ISBN 978-3-319-68619-6 (eBook)

<https://doi.org/10.1007/978-3-319-68619-6>

Library of Congress Control Number: 2017955280

© Springer International Publishing AG 2018

This work is subject to copyright. All rights are reserved by the Publisher, whether the whole or part of the material is concerned, specifically the rights of translation, reprinting, reuse of illustrations, recitation, broadcasting, reproduction on microfilms or in any other physical way, and transmission or information storage and retrieval, electronic adaptation, computer software, or by similar or dissimilar methodology now known or hereafter developed.

The use of general descriptive names, registered names, trademarks, service marks, etc. in this publication does not imply, even in the absence of a specific statement, that such names are exempt from the relevant protective laws and regulations and therefore free for general use.

The publisher, the authors and the editors are safe to assume that the advice and information in this book are believed to be true and accurate at the date of publication. Neither the publisher nor the authors or the editors give a warranty, express or implied, with respect to the material contained herein or for any errors or omissions that may have been made. The publisher remains neutral with regard to jurisdictional claims in published maps and institutional affiliations.

Printed on acid-free paper

This Springer imprint is published by Springer Nature

The registered company is Springer International Publishing AG

The registered company address is: Gewerbestrasse 11, 6330 Cham, Switzerland

# Preface

This volume of Lecture Notes in Mechanical Engineering contains accepted papers presented at the 5th International Scientific-Technical Conference (MANUFACTURING 2017), held in Poznan, Poland, on October 24–26, 2017. The conference was organized by the Faculty of Mechanical Engineering and Management, Poznan University of Technology, under the scientific auspices of the Committee on Machine Building of the Polish Academy of Sciences, and the Committee on Production Engineering of the Polish Academy of Sciences.

The aim of the conference was to present the latest achievements in mechanical engineering and to provide an occasion for discussion and exchange of views and opinions. The scope of the conference comprised of issues relating to:

- design, building, and research of machines and devices
- technological and assembly processes planning
- cutting machining, founding, plastic forming, devices, and tool-systems
- metrology and measurement systems
- materials engineering
- quality engineering
- production engineering and management

The book is organized into five chapters, according to the main conference topics: (1) production engineering (2) design, building, and research of machines and devices (3) cutting machining and technological and assembly processes (4) measurement systems and quality engineering (5) materials engineering.

Members of the Conference Scientific Committee were experts from various areas of manufacturing systems. They were engaged in evaluating papers submitted to the conference.

The organizers received 142 manuscripts from 18 countries. After a thorough peer review process, the committee accepted 92 papers prepared by 240 authors from 18 different countries (acceptance rate of about 65%). All of these papers have been published in conference proceedings. Chosen for their excellent quality, extended versions of selected papers will be published in the scientific journals

*Management and Production Engineering Review* (published by De Gruyter and indexed by ISI/SCI) and *Archives of Mechanical Technology and Materials* (published by De Gruyter).

We would like to especially thank the members of the International Program Committee for their hard work during the review process.

We acknowledge all that contributed to the staging of MANUFACTURING 2017: authors, committees, and sponsors. Their involvement and hard work were crucial to the success of the MANUFACTURING 2017 conference.

Poznań, Poland  
October 2017

Adam Hamrol  
Olaf Ciszak  
Stanisław Legutko  
Mieczysław Jurczyk

# Organization

## Steering Committee

General Chair

Adam Hamrol, Poznan University of Technology, Poland

Chairs

Olaf Ciszak, Poznan University of Technology, Poland

Stanisław Legutko, Poznan University of Technology, Poland

Mieczysław Jurczyk, Poznan University of Technology, Poland

Jan Żurek, Poznan University of Technology, Poland

Part I Co-Editor (Production Engineering)

Justyna Trojanowska

Part II Co-Editor (Design, Building, and Research of Machines and Devices)

Grzegorz Królczyk

Part III Co-Editor (Cutting Machining and Technological and Assembly Processes)

Marcin Suszyński

Part IV Co-Editor (Measurement Systems and Quality Engineering)

Magdalena Diering

Part V Co-Editor (Materials Engineering)

Jose Machado

## Scientific Committee

Zenobia Weiss (Honorary SC Member), Poland

Stanisław Adamczak, Poland

Zbigniew Banaszak, Poland



Stefan Berczyński, Poland  
Johan Berglund, Sweden  
Christopher A. Brown, USA  
Somnath Chattopadhyaya, India  
Shin-Guang Chen, Taiwan  
Danut Chira, Romania  
Edward Chlebus, Poland  
Damir Ciglar, Croatia  
Nadežda Cuboňová, Slovakia  
Jens J. Dahlgaard, Sweden  
Łucjan Dąbrowski, Poland  
Sergey Dobrotvorskiy, Romania  
Lyudmyla Dobrovolskaya, Ukraine  
Jan Duda, Poland  
Davor Dujak, Croatia  
Sabahudin Ekinovic, Bosnia and Hercegovina  
Józef Gawlik, Poland  
Boštjan Gomišček, ZEA  
Wit Grzesik, Poland  
Michal Hatala, Slovakia  
Ivan Hudec, Slovakia  
Andrzej Jardzioch, Poland  
Wojciech Kacalak, Poland  
Lyudmila Kalafatova, Ukraine  
Mourad Keddami, Algeria  
Sławomir Kłos, Poland  
Ryszard Knosala, Poland  
Jan Kosmol, Poland  
Janusz Kowal, Poland  
Drazen Kozak, Croatia  
Bogdan Kruszyński, Poland  
Janos Kundrak, Hungary  
Maciej Kupczyk, Poland  
Ivan Kuric, Slovakia  
Piotr Łebkowski, Poland  
José Mendes Machado, Portugal  
Aleksandar Makedonski, Bulgaria  
Ilija Mamuzic, Croatia  
Krzysztof Marchelek, Poland  
Tadeusz Marciniak, Poland  
Tadeusz Markowski, Poland  
Thomas Mathia, France  
Józef Matuszek, Poland  
Adam Mazurkiewicz, Poland  
Andrzej Milecki, Poland

Piotr Moncarz, USA  
Miroslaw Pajor, Poland  
Alejandro Pereira Dominguez, Spain  
Jan Pilarczyk, Poland  
Włodzimierz Przybylski, Poland  
Luis Paulo Reis, Portugal  
Álvaro Rocha, Portugal  
Rajkumar Roy, UK  
Iwan Samardzic, Croatia  
Krzysztof Santarek, Poland  
Jarosław Sęp, Poland  
Jan Sieniawski, Poland  
Bożena Skołod, Poland  
Jerzy Sładek, Poland  
Roman Staniek, Poland  
Tomasz Sterzyński, Poland  
Maria Leonilde R. Varela, Portugal  
Sachin D. Waigaonkar, India  
Edmund Weiss, Poland  
Michał Wieczorowski, Poland  
Ralph Woll, Germany.

## **Program Committee**

Zbigniew Banaszak, Warsaw University of Technology, Poland  
Stefan Berczyński, Maritime University of Szczecin, Poland  
Johan Berglund, Swerea, Sweden  
Christopher A. Brown, Worcester Polytechnic Institute, USA  
Vladimír Bulej, University of Zilina, Slovakia  
Somnath Chattopadhyaya, Indian School of Mines, India  
Shin-Guang Chen, Tungnan University, Taiwan  
Danut Chira, University of Oradea, Romania  
Edward Chlebus, Wrocław University of Technology, Poland  
Damir Ciglar, University of Zagreb, Croatia  
Olaf Ciszak, Poznan University of Technology, Poland  
Nadežda Cuboňová, University of Zilina, Slovakia  
Jens J. Dahlgaard, Linköping University, Sweden  
Lucjan Dąbrowski, Warsaw University of Technology, Poland  
Magdalena Diering, Poznan University of Technology, Poland  
Sergey Dobrotvorskiy, National Technical University in Kharkiv, Ukraine  
Lyudmyla Dobrovolskaya, National Technical University in Kharkiv, Ukraine  
Jan Duda, Cracow University of Technology, Poland

Davor Dujak, Josip Juraj Strossmayer University of Osijek, Croatia  
Sabahudin Ekinovic, University of Zenica, Bosnia and Hercegovina  
Józef Gawlik, Cracow University of Technology, Poland  
Boštjan Gomišček, University of Wollongong in Dubai, United Arab Emirates  
Marek Góral, Rzeszow University of Technology, Poland  
Marta Grabowska, Poznan University of Technology, Poland  
Wit Grzesik, Opole University of Technology, Poland  
Adam Hamrol, Poznan University of Technology, Poland  
Michal Hatala, Technical University of Kosice, Slovakia  
Marek Hawryluk, Wroclaw University of Technology, Poland  
György Hegedűs, University of Miskolc, Hungary  
Ivan Hudec, Slovak University of Technology, Slovakia  
Andrzej Jardzioch, West Pomeranian University of Technology Szczecin, Poland  
Sabahudin Jasarevic, University of Zenica, Bosnia and Hercegovina  
Małgorzata Jasiulewicz-Kaczmarek, Poznan University of Technology, Poland  
Mieczysław Jurczyk, Poznan University of Technology, Poland  
Wojciech Kacalak, Koszalin University of Technology, Poland  
Lyudmila Kalafatova, Donetsk National Technical University, Ukraine  
Marcin Kaszuba, Wroclaw University of Technology, Poland  
Mourad Keddou, Mouloud Mammeri University of Tizi-Ouzou, Algeria  
Sławomir Kłos, University of Zielona Góra, Poland  
Ryszard Knosala, Opole University of Technology, Poland  
Jan Kosmol, Silesian University of Technology, Poland  
Janusz Kowal, AGH University of Science and Technology, Poland  
Drazen Kozak, Josip Juraj Strossmayer University of Osijek, Croatia  
Grzegorz Królczyk, Opole University of Technology, Poland  
Bogdan Kruszyński, Lodz University of Technology, Poland  
Agnieszka Kujawińska, Poznan University of Technology, Poland  
Darina Kumičáková, University of Zilina, Slovakia  
Janos Kundrak, University of Miskolc, Hungary  
Maciej Kupczyk, Poznan University of Technology, Poland  
Ivan Kuric, University of Zilina, Slovakia  
Milovan Lazarevic, University of Novi Sad, Serbia  
Stanisław Legutko, Poznan University of Technology, Poland  
Piotr Łebkowski, AGH University of Science and Technology, Poland  
José Mendes Machado, University of Minho, Portugal  
Maciej Majewski, Koszalin University of Technology, Poland  
Aleksandar Makedonski, Technical University of Sofia, Bulgaria  
Vijaya Kumar Manupati, VIT University, India  
Krzysztof Marchelek, West Pomeranian University of Technology Szczecin, Poland  
Tadeusz Marciniak, Lodz University of Technology, Poland  
Tadeusz Markowski, Rzeszow University of Technology, Poland  
Zsolt Maros, University of Miskolc, Hungary  
Thomas Gregoire Mathia, Ecole Centrale de Lyon, France

Józef Matuszek, University of Bielsko-Biala, Poland  
Adam Mazurkiewicz, Institute for Sustainable Technologies, Poland  
Andrzej Milecki, Poznan University of Technology, Poland  
Krzysztof Nadolny, Koszalin University of Technology, Poland  
Peter Nielsen, Aalborg University, Denmark  
Mirosław Pajor, West Pomeranian University of Technology Szczecin, Poland  
Justyna Patalas-Maliszewska, University of Zielona Góra, Poland  
Alejandro Pereira Dominguez, University of Vigo, Spain  
Jan Pilarczyk, Institute of Welding, Poland  
Dariusz Plinta, AGH University of Science and Technology, Poland  
Włodzimierz Przybylski, Gdańsk University of Technology, Poland  
Lorenz Ratke, German Aerospace Center, Germany  
Luis Paulo Reis, University of Minho, Portugal  
Álvaro Rocha, University of Coimbra, Portugal  
Rajkumar Roy, Cranfield University, UK  
Alessandro Ruggiero, University of Salerno, Italy  
Iwan Samardzic, Josip Juraj Strossmayer University of Osijek, Croatia  
Krzysztof Santarek, Warsaw University of Technology, Poland  
Jarosław Sęp, Rzeszow University of Technology, Poland  
Jan Sieniawski, Rzeszow University of Technology, Poland  
Bożena Skołod, Silesian University of Technology, Poland  
Jerzy Śladek, Cracow University of Technology, Poland  
Roman Staniek, Poznan University of Technology, Poland  
Beata Starzyńska, Poznan University of Technology, Poland  
Tomasz Sterzyński, Poznan University of Technology, Poland  
Krzysztof Stępień, Kielce University of Technology, Poland  
Marcin Suszyński, Poznan University of Technology, Poland  
Tibor Szalay, Budapest University of Technology and Economics, Hungary  
Tamás Török, University of Miskolc, Hungary  
Justyna Trojanowska, Poznan University of Technology, Poland  
Paweł Twardowski, Poznan University of Technology, Poland  
Wiesław Urban, Białystok University of Technology, Poland  
Maria Leonilde R. Varela, University of Minho, Portugal  
Sachin D. Waigaonkar, BITS Pilani K.K. Birla Goa Campus, India  
Michał Wieczorowski, Poznan University of Technology, Poland  
Ralph Woll, Brandenburgische Technische Universität Cottbus–Senftenberg, Germany  
Wojciech Zębała, Cracow University of Technology, Poland  
Jan Żurek, Poznan University of Technology, Poland

# Contents

## Part I Production Engineering

<b>Analysis of the Conditions for Effective Use of Numerically Controlled Machine Tools</b> .....	3
Adam Hamrol, Slawomir Zerbst, Mariusz Bozek, Marta Grabowska and Markus Weber	
<b>A Simulative Study Approach for Improving the Efficiency of Production Process of Floorboard Middle Layer</b> .....	13
Tomasz Bartkowiak, Olaf Ciszak, Piotr Jablonski, Adam Myszkowski and Marcin Wisniewski	
<b>A Methodology of Improvement of Manufacturing Productivity Through Increasing Operational Efficiency of the Production Process</b> .....	23
Justyna Trojanowska, Adam Kolinski, Dariusz Galusik, Maria L.R. Varela and Jose Machado	
<b>The Impact of Buffer Allocation in Assembly-Line Manufacturing Systems on the Effectiveness of Production Processes</b> .....	33
Slawomir Klos and Justyna Patalas-Maliszewska	
<b>Overall Equipment Effectiveness: Analysis of Different Ways of Calculations and Improvements</b> .....	45
Dorota Stadnicka and Katarzyna Antosz	
<b>Verification of the Method for Assessing Productivity, Taking into Account Logistical Processes in Manufacturing Companies</b> .....	57
Michaela Rostek and Ryszard Knosala	
<b>The Impact of Task Balancing and Sequencing on Production Efficiency</b> .....	67
Krzysztof Zywicki, Paulina Rewers, Lukasz Sobkow and Dawid Antas	

<b>Formal Description of Integrated Process and Assembly System Planning</b> . . . . .	79
Jan Duda	
<b>The Operational Validation of a Planning Process Integration Model in a Manufacturing Company</b> . . . . .	91
Michal Adamczak, Piotr Cyplik and Marek Fertsch	
<b>Job Scheduling Problem in a Flow Shop System with Simulated Hardening Algorithm</b> . . . . .	101
Andrzej Jardzioch and Bartosz Skobiej	
<b>A Study of Priority Rules for a Levelled Production Plan</b> . . . . .	111
Paulina Rewers, Justyna Trojanowska, Jacek Diakun, Alvaro Rocha and Luis P. Reis	
<b>Production Process Analysis in Conditions of Short-Term Raw Materials Expiration Dates and Long Setup Times Using Simulation Method</b> . . . . .	121
Adrian Jakobczyk, Kamil Nogaj, Jacek Diakun and Reggie Davidrajuh	
<b>Development of an Intelligent and Automated System for Lean Industrial Production, Adding Maximum Productivity and Efficiency in the Production Process</b> . . . . .	131
Adriana F. Araújo, Maria L.R. Varela, Marivan S. Gomes, Raissa C. C. Barreto and Justyna Trojanowska	
<b>The Use of Virtual Design to Accommodate a Workplace for a Hearing-Impaired Worker</b> . . . . .	141
Karolina Szajkowska and Anna Karwasz	
<b>Intelligent Platform for Supervision and Production Activity Control in Real Time</b> . . . . .	151
Gaspar G. Vieira, Maria L.R. Varela, Goran D. Putnik and Jose Machado	
<b>Definition of Smart Retrofitting: First Steps for a Company to Deploy Aspects of Industry 4.0</b> . . . . .	161
Bruno V. Guerreiro, Romulo G. Lins, Jianing Sun and Robert Schmitt	
<b>Additive Manufacturing Technologies Cost Calculation as a Crucial Factor in Industry 4.0</b> . . . . .	171
Maria Rosienkiewicz, Joanna Gabka, Joanna Helman, Arkadiusz Kowalski and Slawomir Susz	
<b>Fulfilling Individual Requirements of Customers in Smart Factory Model</b> . . . . .	185
Krzysztof Zywicki and Przemyslaw Zawadzki	

**Model of Competency Management in the Network of Production Enterprises in Industry 4.0—Assumptions** . . . . . 195  
 Magdalena Graczyk-Kucharska, Maciej Szafranski, Marek Golinski, Malgorzata Spychala and Kamila Borsekova

**The Benefits of Using Computer Simulation Models to Support Decision-Making** . . . . . 205  
 Elzbieta Malec

**Cyclic Steady-State Approach to Modelling of Multimodal Processes Flow Levelling** . . . . . 215  
 Grzegorz Bocewicz, Pawel Pawlewski and Zbigniew Banaszak

**Symbolic Representation of Production Knowledge in the Development of Knowledge Management Systems** . . . . . 227  
 Alfred Paszek

**Methodology of KBE System Development for Automated Design of Multivariant Products** . . . . . 239  
 Przemyslaw Zawadzki

**Interacting Manufacturing Features in CAPP Systems** . . . . . 249  
 Janusz Pobożniak

**Case Studies of the Process-Oriented Approach to Technology Management** . . . . . 259  
 Wieslaw Urban and Elzbieta Krawczyk-Dembicka

**Technical Product-Service Systems—A Business Opportunity for Machine Industry** . . . . . 269  
 Mariusz Salwin, Bartłomiej Gładysz and Krzysztof Santarek

**Development of a Speech System Using BCI Based on ERD/ERS for Patients Suffering from Amyotrophic Lateral Sclerosis** . . . . . 279  
 Arkadiusz Kubacki and Dominik Rybarczyk

**GPenSIM for Performance Evaluation of Event Graphs** . . . . . 289  
 Reggie Davidrajuh, Bożena Skolud and Damian Krenczyk

**Analysis of the Environmental Costs in Manufacturing Companies in the SME Sector in Poland** . . . . . 301  
 Lukasz Grudzien, Filip Osinski and Sabahudin Jasarevic

**Product Variants Recycling Cost Estimation with the Use of Multi-agent Support System** . . . . . 311  
 Ewa Dostatni, Jacek Diakun, Radoslaw Wichniarek, Anna Karwasz and Damian Grajewski

<b>The Use of Machine Learning Method in Concurrent Ecodesign of Products and Technological Processes</b> . . . . .	321
Ewa Dostatni, Izabela Rojek and Adam Hamrol	
<b>Part II Design, Building and Research of Machines and Devices</b>	
<b>Intelligent Materials Application in Mechatronic Devices</b> . . . . .	333
Andrzej Milecki	
<b>Development of Force Feedback Controller For the Loader Crane</b> . . . .	345
Dominik Rybarczyk, Piotr Owczarek and Adam Myszkowski	
<b>Analysing and Optimizing 2.5D Circular Pocket Machining Strategies</b> . . . . .	355
Adam Jacso and Tibor Szalay	
<b>Study on Mechanical Characteristics in Electromechanical Disengaging Damper</b> . . . . .	365
Grzegorz Pittner, Bartosz Minorowicz and Roman Regulski	
<b>Modeling and 3D Simulation of an Electro-hydraulic Manipulator Controlled by Vision System with Kalman Filter</b> . . . . .	375
Piotr Owczarek, Jaroslaw Goslinski, Dominik Rybarczyk, Arkadiusz Kubacki, Arkadiusz Jakubowski and Lukasz Sawicki	
<b>Trends in the Development of Rotary Tables with Different Types of Gears</b> . . . . .	385
Kamil Wojtko and Piotr Frackowiak	
<b>Survey on Design and Development of Hexapod Walking Robot, Automated Guided Vehicle and Drone</b> . . . . .	395
Bartosz Minorowicz, Mariusz Palubicki, Natan Stec, Jakub Bartoszek, Lukasz Antczak and Jakub Matyszczyk	
<b>Development of Conical Face Gear Technology Cooperation with Conical Worm in Spiroid Gear Drive</b> . . . . .	405
Piotr Frackowiak and Kamil Wojtko	
<b>Unilateral Hydraulic Telemanipulation System for Operation in Machining Work Area</b> . . . . .	415
Mateusz Sakow, Arkadiusz Parus, Miroslaw Pajor and Karol Miadlicki	
<b>Effect of Different Electrolytes on Material Removal Rate, Diameter of Hole, and Spark in Electrochemical Discharge Machining</b> . . . . .	427
Mukund L. Harugade and Sachin D. Waigaonkar	
<b>ExoArm 7-DOF (Interactive 7-DOF Motion Controller of the Operator Arm) Master Device for Control of Loading Crane</b> . . . . .	439
Pawel Herbin and Miroslaw Pajor	



**Influence of Selected Factors on Static Friction for Combination of Expanded Graphite-Steel** . . . . . 451  
 Aleksandra Rewolinska and Karolina Perz

**Development of Experimental Design for Hydraulic Active Heave Compensation Systems** . . . . . 457  
 Arkadiusz Jakubowski, Arkadiusz Kubacki and Piotr Owczarek

**Loader Crane Working Area Monitoring System Based on LIDAR Scanner** . . . . . 465  
 Karol Miadlicki, Mirosław Pajor and Mateusz Sakow

**Optimization of the Movement Trajectory of Mobile Crane Working Elements** . . . . . 475  
 Wojciech Kacalak, Zbigniew Budniak and Maciej Majewski

**Design, Manufacture, and Application of Chamber for the Magnetohydrodynamic Deposition Made of PP** . . . . . 485  
 Jeremiasz K. Koper

**Testing of Tight Crimped Joint Made on a Prototype Stand** . . . . . 497  
 Nikodem Wrobel, Michał Rejek, Grzegorz Krolczyk and Sergej Hloch

**Part III Cutting Machining & Technological and Assembly Processes**

**Computer Simulation of the Process of Regenerating the Adsorbent Using Microwave Radiation in Compressed Air Dryers** . . . . . 511  
 Sergey S. Dobrotvorskiy, Ludmila G. Dobrovol'ska and Borys A. Aleksenko

**Spatial Adjusting of the Industrial Robot Program with Matrix Codes** . . . . . 521  
 Jakub Wojciechowski and Olaf Ciszak

**Topology Optimisation Aimed at Additive—SLM Manufacturing of Metal Parts of ExoArm 7-DOF** . . . . . 533  
 Paweł Herbin, Dariusz Grzesiak and Marcin A. Krolkowski

**Applications of Optomechatronic Technologies in Innovative Industry** . . . . . 543  
 Tomasz Giesko and Adam Mazurkiewicz

**Case Study of Thermal Stress Distribution Within Coating Applied on Aluminum Plain Clutch Plate by Thermal Spray Coating Technique** . . . . . 555  
 Piotr Jablonski, Piotr Czajka, Adam Patalas, Rafał Talar and Michał Regus

<b>Augmented Reality in Training of Fused Deposition Modelling Process</b> . . . . .	565
Filip Gorski, Radoslaw Wichniarek, Wieslaw Kuczko, Pawel Bun and John A. Erkoyuncu	
<b>Complex Control Method of Degreasing Process</b> . . . . .	575
Michal Zoubek, Jan Kudlacek, Petr Chabera and Andrey Abramov	
<b>Hybrid Processing by Turning and Burnishing of Machine Components</b> . . . . .	587
Wlodzimierz Przybylski and Stefan Dzionk	
<b>Virtual Reality and CAD Systems Integration for Quick Product Variant Design</b> . . . . .	599
Przemyslaw Zawadzki, Filip Gorski, Pawel Bun, Radoslaw Wichniarek and Karina Szalanska	
<b>An Approach to Modeling and Simulation of a Complex Conveyor System Using Delmia Quest—A Case Study</b> . . . . .	609
Waldemar Malopolski and Adam Wiercioch	
<b>Prediction of HPDC Casting Properties Made of AlSi9Cu3 Alloy</b> . . . . .	621
Jakub Hajkowski, Pawel Popielarski and Robert Sika	
<b>Internal Stresses Analysis in the Shrink-Fitted Joints of the Assembled Crankshafts</b> . . . . .	633
Zbigniew Siemiatkowski, Miroslaw Rucki and Jan Kudlacek	
<b>The Influence of Composition Chemical of Nanofluids on Hardness and Wear Resistance of Laser-Treated C20 Steel</b> . . . . .	641
Wojciech Gestwa	
<b>Application of Correlation Function for Analysis of Surface Structure Shaping by Hybrid Manufacturing Technology</b> . . . . .	651
Sara Dudzinska, Michal Szydlowski, Daniel Grochala and Emilia Bachtiak-Radka	
<b>Investigation of Heat Distribution in Coated Indexable Tool Inserts</b> . . . . .	661
Marta Bogdan-Chudy, Piotr Nieslony and Grzegorz Krolczyk	
<b>Assessment of the Accuracy of High-Speed Machining of Thin-Walled EN AW-2024 Aluminium Alloy Elements Using Carbide Milling Cutter and with PCD Blades</b> . . . . .	671
Jozef Kuczmaszewski, Waldemar Login, Pawel Piesko and Magdalena Zawada-Michalowska	
<b>Effect of Heat Treatment on Mechanical Properties of Inconel 625/Steel P355NH Bimetal Clad Plate Manufactured by Explosive Welding</b> . . . . .	681
Robert Kosturek, Michal Najwer, Piotr Nieslony and Marcin Wachowski	

**Alternative Methods of Chemical Pre-Treatment on Hot-Dip Galvanization Surface for Adhesion Organic Coatings** . . . . . 687  
 Jakub Svoboda, Jan Kudlacek, Viktor Kreibich and Stanislaw Legutko

**Influence of Machining Conditions on the Energy Consumption and Productivity in Finish Hard Turning** . . . . . 697  
 Roman Chudy, Wit Grzesik and Krzysztof Zak

**Application of Principal Component Analysis and Decision Trees in Diagnostics of Cylindrical Plunge Grinding Process** . . . . . 707  
 Pawel Lajmert, Malgorzata Sikora, Bogdan Kruszynski and Dariusz Ostrowski

**Assessment of Deformation Characteristics on CW004A Copper Influenced by Acoustically Enhanced Water Jet** . . . . . 717  
 Dominika Lehocka, Vladimir Simkulet and Stanislaw Legutko

**Part IV Measurement Systems and Quality Engineering**

**Measuring the Punching Profile of a Punch And Bind Machine** . . . . . 727  
 Joao Sousa, Luis Figueiredo, Jose Machado and Joao P. Mendonca

**Influence of the Inlet Nozzle Diameter on the Air Gauge Dynamics** . . . . . 733  
 Michal Jakubowicz, Miroslaw Rucki, Gyula Varga and Radomir Majchrowski

**Accuracy of Hysteresis Modeling in Smart Actuator with MSMA** . . . . . 743  
 Bartosz Minorowicz, Grzegorz Pittner and Frederik Stefanski

**Application of Scanning Techniques in the Analysis of the Wear Forging Tools** . . . . . 753  
 Marek Hawryluk, Jacek Ziemba and Marcin Rychlik

**Comparison of Geometrical Accuracy of a Component Manufactured Using Additive and Conventional Methods** . . . . . 765  
 Witold Habrat, Maciej Zak, Jolanta Krolczyk and Pawel Turek

**Studies of Geometric Accuracy of Polygons Machined by Polygonal Turning Technique** . . . . . 777  
 Michal Regus, Bartosz Gapinski, Piotr Czajka and Piotr Jablonski

**Ensuring the Reliability of the Car Body Controls by Controlling the Current Inspection of Measuring Machines** . . . . . 787  
 Robert Koterak, Michal Wieczorowski, Piotr Znanecki and Lidia Marciniak-Podsadna

**Application of Industrial Robot as a Measuring System** . . . . . 797  
 Ksenia Ostrowska, Robert Kupiec, Malgorzata Kowalczyk, Pawel Wojakowski, Halszka Skorska and Jerzy Sladek

<b>Surface Roughness of Graphite and Aluminium Alloy After Hydro-abrasive Machining</b> . . . . .	805
Jan Carach, Dominika Lehocka, Stanislaw Legutko, Sergej Hloch, Somnath Chattopadhyaya and Amit R. Dixit	
<b>Measurement of Surface Topography Using Computed Tomography</b> . . . . .	815
Bartosz Gapinski, Michal Wieczorowski, Lidia Marciniak-Podsadna, Alejandro Pereira Domínguez, Lenka Cepova and Anton Martinez Rey	
<b>Cylindricity Measurement on a Coordinate Measuring Machine</b> . . . . .	825
Nermina Zaimovic-Uzunovic and Samir Lemes	
<b>Improvement of Acceptance Sampling Inspection for the Operation of Sealing Packages</b> . . . . .	837
Agnieszka Kujawinska, Michal Rogalewicz, Magdalena Diering, Marcin Luczak, Mariusz Bozek and Sachin D. Waigaonkar	
<b>I Spy, with My Little Eye: Quality Standards of Different Target Groups</b> . . . . .	847
Beatrice M. Rich, Jane Worlitz, Stefan Peplowsky and Ralf Woll	
<b>Reduction of Errors of the Conformity Assessment During the Visual Inspection of Electrical Devices</b> . . . . .	857
Krzysztof Knop, Manuela Ingaldi and Marta Smilek-Starczynowska	
<b>Possibilities and Limitations of Passive Experiments Conducted in Industrial Conditions</b> . . . . .	869
Michal Rogalewicz, Pawel Smuskiewicz, Adam Hamrol, Agnieszka Kujawinska and Luis P. Reis	
<b>A Study of Raters Agreement in Quality Inspection with the Participation of Hearing Disabled Employees</b> . . . . .	881
Beata Starzynska, Karolina Szajkowska, Magdalena Diering, Alvaro Rocha and Luis P. Reis	
<b>Assessment of Quality Management System Maturity</b> . . . . .	889
Marta Grabowska and Josu Takala	
<b>Organization of Visual Inspection and Its Impact on the Effectiveness of Inspection</b> . . . . .	899
Agnieszka Kujawinska, Katarzyna Vogt, Magdalena Diering, Michal Rogalewicz and Sachin D. Waigaonkar	

**Part V Materials Engineering**

**On the Formation Features and Some Material Properties of the Coating Formed by Laser Cladding of a NiCrBSi Self-fluxing Alloy** . . . . . 913  
 Oleg Devojno, Eugene Feldshtein, Marharyta Kardapolava and Nikolaj Lutsko

**Fracture Toughness of Plasma Paste-Borided Layers Produced on Nickel-Based Alloys** . . . . . 923  
 Magdalena Frackowiak, Natalia Makuch, Piotr Dziarski, Michal Kulka and Sukru Taktak

**Effect of Residual Stresses in Surface Layer of Nickel-Based Alloy—Inconel 718 on the Safety Factor of Construction** . . . . . 933  
 Joanna Krajewska-Spiewak and Jozef Gawlik

**Influence of Preparation Conditions on Final Dielectric Properties of Pure and Ca-Doped BaTiO<sub>3</sub> Ceramics** . . . . . 941  
 Izabela Szafraniak-Wiza, Anna Włodarkiewicz, Ewa Markiewicz, Bozena Hilczer, Kamil Feliksik and Lucjan Kozielski

**Wear of Solid Carbide Ball Nose End Mill** . . . . . 951  
 Iwona Lapunka, Piotr Wittbrodt and Katarzyna Marek-Kolodziej

**Author Index** . . . . . 963

**Part I**  
**Production Engineering**

# Analysis of the Conditions for Effective Use of Numerically Controlled Machine Tools

Adam Hamrol, Slawomir Zerbst, Mariusz Bozek, Marta Grabowska and Markus Weber

**Abstract** The paper demonstrates that the effective replacement of conventional machine tools with numerically controlled machinery (CNC) requires the simultaneous conducting of actions related to organization and control of production, management of human resources, and tool economy. The direct costs of machining for a selected group of surgical tools, performed with the use of conventional, as well as CNC machinery, were analyzed. The assumptions adopted for the analysis of profitability of machinery park restructuring were compared with the actual costs generated after a year from implementing the project.

**Keywords** Efficiency · Production costs · Tool economy

## 1 Introduction

A process-oriented approach to managing a manufacturing company means perceiving all actions, equipment, and machinery, such as machine tools, for instance, as links in the chain of delivery of parts or assemblies. The internal and external clients within this chain pose mutual requirements concerning the quality, costs, and timeliness of deliveries. The level of their fulfillment is the result of technological, organizational, human, material and other factors [1–3].

The technological factors (technologies and machine tools, including their accessories) play special importance here, especially in regard to the quality of the parts, subassemblies, and products manufactured, since they have a large impact on the dimensional and geometric accuracy, and the mechanical properties of the

---

A. Hamrol · M. Grabowska (✉)  
Poznan University of Technology, Poznan, Poland  
e-mail: marta.grabowska@put.poznan.pl

S. Zerbst · M. Bozek  
AesculapChifa sp. z o.o., Nowy Tomysl, Poland

M. Weber  
Aesculap AG, Tuttlingen, Germany

machined tools. The better the technology, and the better the machine tools, the better the qualitative requirements can be fulfilled.

The significance of technological factors in terms of costs and timeliness is more complex, however. On one hand, e.g., in case of numerically controlled machine tools being the subject of this paper, a number of potential benefits of using them, compared to conventional machine tools, may be pointed out [4, 5], e.g.,:

- increased flexibility, owing to the possibility of performing various operations on a single machine, and limiting the number and duration of retooling procedures,
- reduced demand for different accessories,
- limitation of the possibility of the operator's intervention in the technological process (higher repeatability of the machining conditions, limitation of human errors),
- possibility of several machines being operated by the single operator.

CNC machinery features a number of advantages compared to the conventional machines also in personnel terms [6, 7], such as:

- lower requirements for general qualifications (high qualifications are required, but in a relatively narrow scope),
- improved work conditions,
- increased workplace safety.

On the other hand, the implementation of CNC machines is related to higher costs of purchase and maintenance (service, part replacements), but also provides higher efficiency compared to conventional machines. The higher efficiency of individual work stands requires proper organization and control of production flow. If these two aspects: the stand's efficiency and production flow organization are not coordinated, then the efficiency of the entire production system is reduced (e.g., the machined or processed tools must wait in queue for subsequent operations, or large batches of parts produced too early are stored) [8, 9].

The factor that negatively impacts the effectiveness of the use of CNC machines may be the high cost of tools. Therefore, the implementation of CNC technologies must be assessed from the point of view of different criteria, including economic ones.

## **2 Assessment of Effectiveness of Implementation of New Manufacturing Methods**

Investments consisting of the replacement of machine tools and the use of modern production technologies should be profitable in economic terms, since the basic goals of any enterprise are: generating profits, gaining positive operating cash flow, and increasing value. For technological investments to achieve these goals, they should be preceded by proper financial analyses.



The process of introduction of a new technology in the enterprise is understood, from the economic point of view, as an investment action, i.e., the engagement of funds in different objects aiming at the maintaining and development of the enterprise's potential [10]. The economic assessment of the implemented investments may be measured by a number of indicators, e.g., accounting rate of return, net present value, internal rate return [10–12]. They may be measured before the commencement of investment (ex ante), or after its completion (ex post). The choice of the proper measurement should be made based on the information needs of the decision maker or investor. For the calculated indicators to reliably verify the obtained benefits (or losses), the quality of input data is very important. They should take into account the business assumptions and the further plans of the enterprise. The range and scope of parameters to be taken into account in the analysis should be agreed mutually between the department performing the investment, the financial department, and the management body. The analysis may be of direct nature—verifying the effects only in the area of implementation of the new technology, as well as direct and indirect, i.e., also taking into account the impact of the new technology on other areas. Additionally, factors must be eliminated that may impact the results of analysis, even if they are not related to the given investment (e.g., change in the method of cost allocation, budgeting, etc.).

Direct analysis, referring to effects in the area of implementation of the new technology, will be used in this article. The analysis will use data on the costs generated in the selected production division, responsible for the introduction of specific group of products.

### **3 Analysis of Profitability of Selected Investment at AesculapChifa sp. z o.o.**

AesculapChifa sp. z o.o. company (ACP) is a manufacturer of surgical tools. The assortment of the produced tools is very wide, which results from the requirements of the clients who use them to carry out different surgical procedures. At present, ACP manufactures about 3 thousand of models of surgical tools, with the annual demand for different models ranging from 10 pcs up to as much as 5 thousand pieces.

The case study concerns an investment consisting of the replacement of conventional machines with CNC machinery in machining processes of a selected group of surgical tools. The performance of investment included the following phases:

- decision-making and replacement of conventional machines with CNC ones,
- operating and economic analysis after 1 year from introducing CNC machines,
- preparation to the improvement of organizational and technological CNC processes.

### 3.1 Premises for Replacing Conventional Machines with CNC Machinery at ACP

ACP company continuously strives for improving the quality of the offered products and fulfilling the clients' requirements, e.g., concerning shorter order processing times. The high significance is also attached to improving the organization of internal processes, and optimizing production flow, e.g., through reducing inventories, both in current production as well as ready products. One of the pre-conditions for fulfilling the above goals is modernization of production resources, including the machinery park. One of the examples of actions in this field is the replacement of conventional machinery used for machining tools such as scissors or pliers with numerically controlled machines. The tools from the mentioned group may be generally characterized as: comprising of two arms joined with a single rivet joint (Fig. 1).

The process of production of tools from the scissors and pliers group includes six basic technological operations: plastic processing, machining, initial assembly, thermal treatment, grinding, and final assembly.

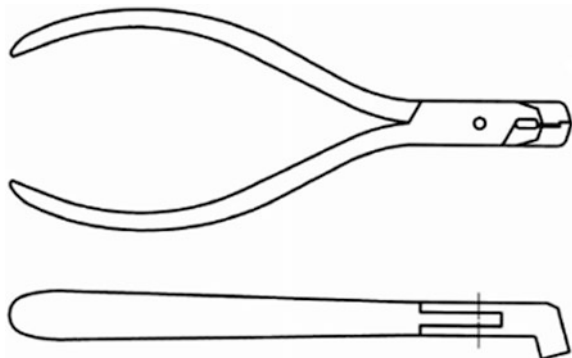
On conventional machines, each machining operation was performed on a different machine, and the quality of making was dependent on the operator's experience. Due to the necessity of transferring semi-products from one machine to another, inter-operational interruptions occurred.

With a CNC machine, all operations are performed on a single machine, in a single clamping, and the operator's work is reduced to clamping the semi-product, and then removing the ready tool arm from the machine.

The decision on modernizing the tool machines stock was preceded by carrying out an economic analysis that was based on the following goals and principles:

- the company aims at improving the production capacity of the entire mechanical processing division, but the analysis is performed for the production volume corresponding to the maximum efficiency of machinery park comprising of conventional machines

**Fig. 1** Structural drawing of an example tool from the: scissors and pliers group



- the cost of machining will be reduced, since the increase in the costs of tools used with CNC machines is compensated by the decrease in personnel costs and production area of the plant,
- the increase in quality (repeatability) of the obtained semi-products from machining will translate into shortening the preliminary assembly time and grinding work, which in turn will result in lowered costs of producing the end product.

According to the performed technological and operational analyses, it was assumed that the use of individual resources to producing the same production volume should lead to savings in terms of man-hours, number of machines, and the occupied space, as well as increased demand for tools (Fig. 2) [13–15].

Based on tool specifications and the performed research, it was calculated that the life of a single set of tools for a conventional machine, in consideration of the possibility of regeneration, is equivalent to 12 sets of tooling for a CNC lathe. Taking into account the fact that the cost of tools for conventional machinery is two times higher than for CNC machinery, it was assumed that the cost of consumption of the latter is six times higher (Table 1).

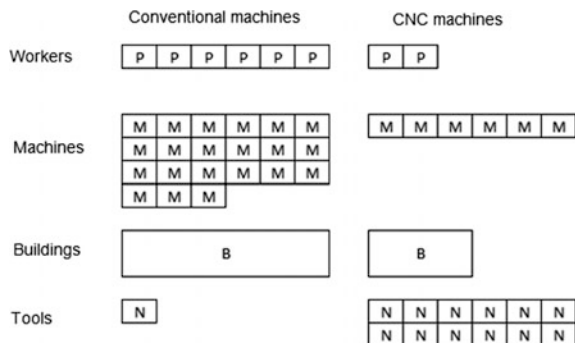
In order to compare the costs of machining in the conventional and CNC technologies, data concerning the direct costs were gathered, including:

- labor costs: personnel remunerations;
- machinery: amortization, service and repairs, supply and occupied space;
- tools: purchase, production, regeneration, and storage.

It was assumed that the direct costs borne with the use of conventional machines is 100%; they were compared to the projected costs of producing the same production batch with the use of CNC machines (Table 2).

Based on the actual and predicted costs analysis, and based on the assumptions made, it was concluded that the cost of machining on CNC machines will be 11% lower.

**Fig. 2** Comparison of projected engagement of resources for achieving the same production volume of semi-products within 1 h time



**Table 1** Comparison of selected parameters of CNC tools and conventional tools necessary for processing the same batch of products

Comparative criterion	Conventional machine tools	CNC machine tools
Life [time/pieces]	1	12
Purchase cost [PLN/set]	2	1
Consumption cost [PLN/pieces]	1	6

**Table 2** Comparison of projected cost of production of the same production volume on conventional machines and CNC machines

Cost group	Conventional machine tools (%)	CNC machine tools (%)	Shift (%)
Workers	78	22	-56
Machines	12	9	-4
Tools	10	58	+49
Total	100	89	-11

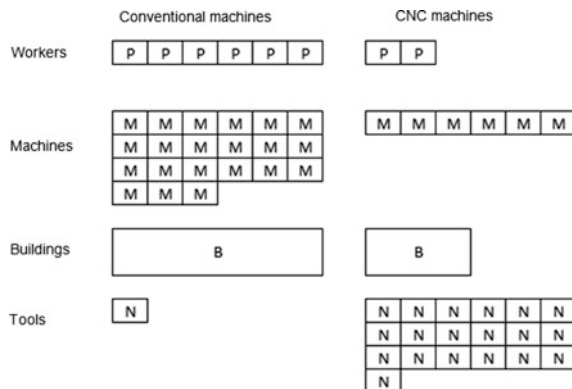
Explanation: 100% is the total direct costs when using a conventional machine

### 3.2 Operating and Economic Analysis After 1 Year from Introducing CNC Machines

After a year of use of CNC machines, operating analysis was performed aiming at verifying the assumptions preceding the decision on modernizing the machinery park (Fig. 3).

The achieved results confirmed the positive effect in terms of the time and demand for surface area. The workers and machinery engagement was reduced three times, and the space necessary for producing the assumed volume was reduced by half. As an effect, the enterprise also increased its production capacity. However, a problem was observed with achieving the planned level of tools

**Fig. 3** Comparison of actual engagement of resources for achieving the same production volume of tool arms at the same time



**Table 3** Structure of direct costs for the same production volume for conventional and CNC machines

Cost group	Conventional machine tools (%)	CNC machine tools (%)	Shift (%)
Workers	78	18	-60
Machines	12	7	-5
Tools	10	75	+65
Total	100	100	0

Explanation: 100% is the total direct costs when using the given technology

**Table 4** Comparison of manufacturing cost of the same production volume on conventional machines and CNC machines

Cost group	Conventional machine tools (%)	CNC machine tools (%)	Shift (%)
Workers	78	22	-56
Machines	12	9	-4
Tools	10	92	82
Total	100	123	+23

Explanation: 100% is the total direct costs when using a conventional machine

consumption, which was twice higher than it was assumed based on the analysis of specifications and technological trials.

The values of costs were determined based on historical data and additional operating analyses (Table 3).

The change in the cost structure after using CNC machines is confirmed by the character of the given technology: the CNC one is automated, e.g., with high capital demand, and the conventional one has high labor demand. The largest share of CNC costs belongs to the tools consumption (75%), and then workers and machinery. With conventional machinery, the key cost is worker remunerations (78%). Then, the values of actual costs of using conventional and CNC machinery for the same production volume were compared (Table 4).

The individual percentage shares of costs for CNC machines are compared to the value of the given item for direct costs when using conventional machinery. It may be noticed that:

- personnel costs after introducing CNC machines was reduced from 78 to 22%;
- machinery costs after introducing CNC machines was reduced from 12 to 9%;
- tools cost in case of CNC increased from 10 to 92%;
- as an effect, the total cost of producing the same volume on CNC is 23% higher than on conventional machines.

According to the results of operating and economic analysis, the cost of machining increased by 23%, due to the 60% higher tool wear than assumed in the business plan.

### 3.3 Preparation to Organizational and Technological Improvement of Production Processes

In order to explain the reasons for increased costs of tools, a team was appointed that comprised of: machine operators and personnel managing the machinery park, process engineers, and programmers, tool regeneration department, as well as controlling department. The first stage of the works of that team was to point out to the potential reasons for increased wear of tools compared to the assumed one. These were then grouped and presented on the Ishikawa diagram (Fig. 4).

The team agreed that the reasons from the “human” and “management” group must be eliminated in the first place, and then trials and analyses concerning the technology and tools must be carried out (Fig. 4).

It was additionally noted that, when carrying out the trials being the subject of this article, the tools consumption cost was conformant with the assumptions preceding the purchase of CNC machinery (Table 1). The explanation of that is the conclusion that both the “human” as well as “management” were directly shifted from the conventional technology that was characterized by significantly lower focus on the issue of tool costs. During the performed observations and experiments concerning tool consumption, the operators operated them with greater care, and the processes of their collection and replacement were specially supervised. It was, therefore, concluded that the most urgent improvement actions should include trainings for increasing the workers’ awareness on the losses resulting from improper fixture of tooling. Also, new principles of the tool supervision system were proposed.

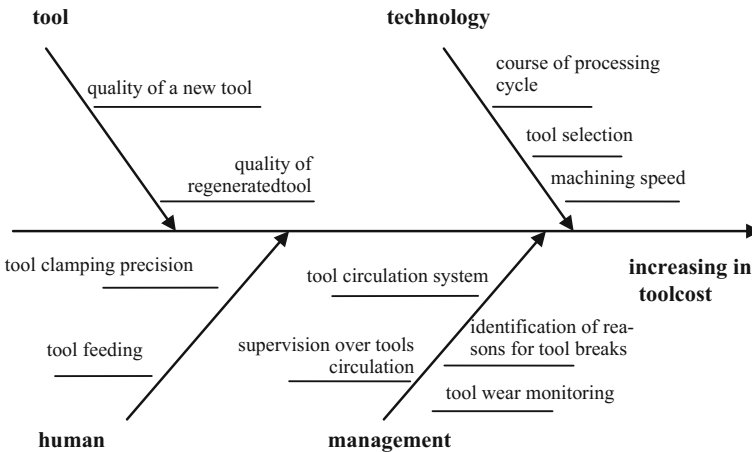


Fig. 4 Ishikawa diagram for the problem of high costs of tools for CNC machines

## 4 Summary

This article presents the results of an analysis of investment consisting of the replacement of conventional machine tools with CNC machine tools in a company producing surgical tools. An assumption was made that the comparison will be based on the direct costs of specific production volume equivalent to the maximum capacity of the machinery park owned by ACP, and comprising of conventional machine tools. The purchase value of CNC machine tools was omitted, and the significant increase in the capacity of the machinery park after the restructuring was not taken into account (for the conventional machine tools to achieve comparable efficiency, the machinery park would have to be expanded threefold, additional production halls would have to be built, and the required additional personnel employed). This detailed (focusing on a selected operation), direct approach to the analyzed effects allowed to identify the problem of high consumption costs of tooling for CNC machines, and planning improvement actions in this field. Broader analysis, from the point of view of added value in the entire chain of deliveries, clearly points out to the positive effects resulting from the use of modern numerically controlled machine tools at ACP; these include, among others: increased efficiency, increased quality of semi-products, increased process repeatability, possibilities of alternative use of the saved space and the related additional income, increased work safety.

**Acknowledgements** The presented results derive from a scientific statutory research conducted by Chair of Management and Production Engineering, Faculty of Mechanical Engineering and Management, Poznan University of Technology, Poland, supported by the Polish Ministry of Science and Higher Education from the financial means in 2017 (02/23/DSPB/7695).

## References

1. Hamrol, A.: Strategies and practices of efficient operation. Lean Six Sigma and Other (in Polish), PWN, Warsaw (2015)
2. Bicheno, J.: The Lean Toolbox. Towards Fast, Flexible Flow. PICSIE Books, Buckingham, England (2004)
3. Jasarevic, S., Diering, M., Brdarevic, S.: Opinions of the consultants and certification houses regarding the quality factors and achieved effects of the introduced quality system. *Tehnicky Vjesn. Tech. Gaz.* **19**(2), 211–220 (2012)
4. Liker, J.K.: The Toyota production system and art: making highly customized and creative products the Toyota way. *Int. J. Prod. Res.* **45**, 3681–3698 (2007)
5. Trojanowska, J., Żywicki, K., Machado, J.M., Varela, L.R.: Shortening changeover time—an industrial study. In: Proceedings of 10th Iberian Conference on Information Systems and Technologies (CISTI 2015), Agueda, Portugal, vol. II, pp. 92–97 (2015)
6. Smid, P.: CNC Programming Handbook, 3rd edn. Industrial Press, New York (2008)
7. Groover, M.P., Zimmers, E.W.: CAD/CAM: Computer Aided Design and Manufacturing. Prentice-Hall of India Private Limited, New Delhi (1998)
8. Angel, L.C., Chandra, M.J.: Performance implications of investments in continuous quality improvement. *Int. J. Oper. Prod. Manage.* **21**(1/2), 108–125 (2001)

9. Starzyńska, B., Hamrol, A.: Excellence toolbox: decision support system for quality tools and techniques selection and application. *Total Qual. Manage. Bus. Excellence* **24**(5), 577–595 (2013)
10. Wang, J., Chen, Z., Parlikad, A.: Designing performance measures for asset management systems in asset-intensive manufacturing companies: a case study. In: *Proceedings of the 10th World Congress on Engineering Asset Management (WCEAM 2015)*, Lecture Notes in Mechanical Engineering, Springer, Berlin (2016)
11. Brigham, E.F., Houston, J.F.: *Fundamentals of Financial Management* (in Polish), PWE, Warsaw (2005)
12. Drury, C., *Cost Accounting* (in Polish), PWN, Warsaw (1995)
13. Bożek, M., Kujawińska, A., Rogalewicz, M., Diering, M., Gościński, P., Hamrol, A.: Improvement of catheter quality inspection process. In: *MATEC Web of Conferences* 121, 05002, 8th International Conference on Manufacturing Science and Education—MSE Trends in New Industrial Revolution (2017)
14. Sarkar, A., Panja, S.C., Das, D., Sarkar, B.: Developing an efficient decision support system for non-traditional machine selection: an application of MOORA and MOOSRA. *Prod. Manuf. Res.* **3**(1), 324–342 (2015)
15. Roy, M.K., Ray, A., Pradhan, B.B.: Non-traditional machining process selection using integrated fuzzy AHP and QFD techniques: a customer perspective. *Prod. Manuf. Res.* **2**(1), 530–549 (2014)



# A Simulative Study Approach for Improving the Efficiency of Production Process of Floorboard Middle Layer

Tomasz Bartkowiak, Olaf Ciszak, Piotr Jablonski, Adam Myszkowski  
and Marcin Wisniewski

**Abstract** The subject of this paper is the simulation study into the improvement of the production process of floorboard middle layer. The object of our interest in the manufacturing process of wooden floorboard which consists of three layers: lower—made of softwood pieces glued together; middle—in a form a module, made of softwood slats and plywood, and hardwood upper layer. The process improvement involved a better use of raw materials in the form of plats (of variable dimension groups) by reducing losses caused by defects such as wane and knots. A simulation model of the manufacturing process was created by using DES software. Thanks to that model, buffers size and a performance of the designed systems including their anticipated breakdowns were estimated. As a result of the study, a concept of the entire production system meeting the requested production capacity and material efficiency was devised.

**Keywords** Manufacturing systems · Discrete event systems · Simulation

## 1 Introduction

In modern highly competitive industry, a company must rapidly adjust to constantly changing customers' requirements and improve the quality of its products in order to preserve on the market. Thus, an immediate response to design or technology changes and demand fluctuations becomes an important issue [1]. In addition, those adaptations have a significant impact on raw materials, semi and finished goods stock and its optimization would require either more accurate sales forecast or increasing the production frequency for maintaining high service level. The latter directly affects the performance of the production lines due to a higher number of various production batches of lower volume. A production flexibility influences the number of machine change-overs, what may also result in decreasing the capacity

---

T. Bartkowiak (✉) · O. Ciszak · P. Jablonski · A. Myszkowski · M. Wisniewski  
Institute of Mechanical Technology, Poznan University of Technology, Poznan, Poland  
e-mail: tomasz.bartkowiak@put.poznan.pl

of the line. There are also environmental aspects to be considered as there is a growing tendency to reduce CO<sub>2</sub> footprint. All the aforementioned phenomena explain why optimization of production system performance has recently received such a great attention.

A production line is a system of machines, connected by transportation elements and separated by storage zones that are used together for manufacturing process [1]. The performance of the production system depends on the performance of the individual workstations, inter-station transportation, company intralogistic system and organizational structure. System's configuration along with the specification of transportation time does influence the overall manufacturing system performance [2]. There are also storage elements called buffers that prevent the machine from stopping due to fluctuation in the production of the precedent machine [3, 4].

The improvement of the existing manufacturing system might be concentrated on the maintenance in order to reduce or eliminate machine stoppages due to breakdowns or the installation or expansion of existing buffers [5–7]. Looking from the business point of view, there might be a common denominator that combines all the quantifiable aspects of the manufacturing process in order to evaluate each of the efficiency improvement scenarios via profit and loss analysis. Each scenario might be tested through simulation of a credible verified and validated a model that include all the important components of the production system. Most of the simulations concentrate on the particular aspect of the process such as buffer allocation or maintenance strategies. There have been some recent endeavors to include financials into the complex simulation model [8]. The modern approach is to dynamically adapt to constantly changing manufacturing conditions. The so-called support vector machine simulation approach methodology has been developed and it offers better performance than the single-rule-based production control system [9].

In general, as far as manufacturing systems are concerned, two approaches are considered: analytical and simulative. Analytical solutions tend to fail because of the complexity of the large-scale environment [10]. Thus, simulation is introduced as an alternative method, which can be utilized for complex stochastic problems. The major drawback of simulation for practical applications is its high time consumption comparing to the analytical approach. Usually, in the literature, there is a lack of experimental data for complex production system [3, 11]. Simulation approach has recently received great attention and can be applied to many aspects of manufacturing systems, for example, in job-shop scheduling the simulation of dispatching rules and the assessment of the effect of different rules on the shop's ability to meet delivery dates and utilize the machines [1]. Li et al. [10] proposed a simulation model with a prioritized stochastic batch arrival mechanism for a remanufacturing system to optimize production planning and control policies. Simulation can be combined with optimization to study the sequencing and identify the optimal lot size for production and inventory systems [12]. Recently, a multi-modal-based approach has become a trend in the analysis of manufacturing processes [13].

The credibility of the simulation model of the completely novel manufacturing system can be disputable as there are usually no data for model validation. This paper is a study of the floorboard middle layer manufacturing process which is a combination of the new and existing subprocesses. The aim of this work to verify if the assumed (at the design stage) efficiency of the system is achievable for the proposed system. In addition, the inter-operational buffer size was estimated in order to check if available space for the installation of racks is sufficient.

## 2 Object of the Study

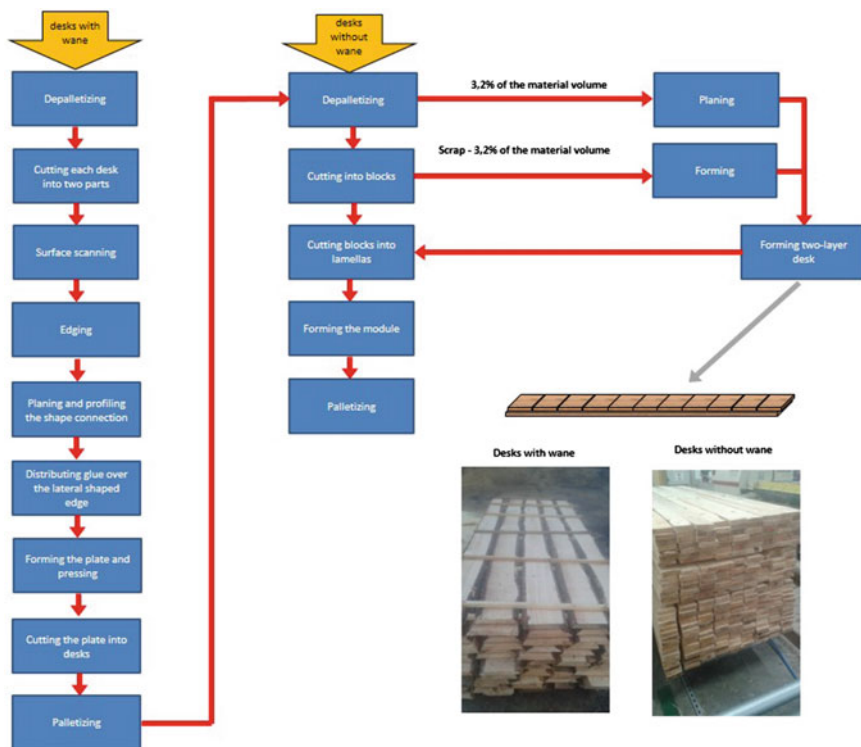
### 2.1 Production Process

This research is concentrated on the manufacturing process of a middle layer of the laminated floorboard. A laminated board consists of three individual layers that are glued together at the final stage of the process. The top layer is made of European or exotic timber of appropriate thickness, visual aesthetic properties, and hardness (usually hardwood such as oak or beech). The middle layer is made of softwood, which is positioned transversely to other two layers to reduce tension and natural deformations over time (swelling, creaking, or gapping). It also contains plywood inserts which are located on the both sides of a board, where joint grooves are milled. The bottom layer is made of soft coniferous wood [14].

This paper concentrates on the manufacturing process of the middle layer. The general diagram of the process is illustrated in Fig. 1. There are two input wood material streams in the process: desks with wane which cross-section fall short of a squared shape and desk without wane of rectangular cross-section. The occurrence of wane is directly related to the log-into-desks cutting strategy and log shape. For desks with wane, there are following operations:

- dispatching from a pallet via 3-axis Cartesian manipulator,
- cutting desk into two small parts in order to reduce the curvature,
- scanning using an optical system that identifies the location of waness and calculates the optimal cutting lines,
- edging to reduce excessive wane,
- planning and profiling the shape connection,
- distributing the glue along the lateral shaped edge and pressing in order to create plate,
- cutting the plane into modules of exact width,
- palletizing using 3-axis Cartesian manipulator.

The proposed process was designed to reduce the material scrap significantly. In the traditional process desks with wane are directly cut into blocks and lamellas, what results in either inadequately thick lamellas that can break easily during the transportation or lack of significant part of the volume. The palletized material is



**Fig. 1** The analyzed manufacturing process—material flow and operations

then transferred to buffer warehouse where it needs to rest for at least 8 h to be assured that glue has bonded sufficiently. After the “seasoning” material is transported to another shopfloor location where the other part of the manufacturing line is located. It meets there a stream of desks which are free of wanes.

In the second stage of the process, all desks are depalletized and the material is fed to the horizontal saw which cuts each desk into blocks of exact length. Blocks are then cut into lamellas which are manually sorted in order to remove the pieces that do not meet the demanded quality level (e.g., that are missing material because knag fell out during cutting). Lamellas are then formed in a module and palletized. This part of the process already exists and the maintenance data regarding the breakdowns, change-overs and micro-stoppages is available.

The simulative model of the aforementioned manufacturing process was created in simulation program FlexSim ([www.flexsim.com](http://www.flexsim.com)). That simulation environment was selected because of the following benefits it provides:

- simple to be used in real 3D dimensions utilizing drag and drop technology,
- loading production layout directly from \*.dwg file to a simulated model,
- simple to model technical systems,

- vast library of statistical models,
- built-in ExpertFit tool for fitting statistical distributions to empirical data.

## 2.2 *Statistical Input Data*

In the modeling, we assumed that there was one line dedicated for desks with wane that produced the modules and four parallel lines that processed the modules and desks with wanes to form the panel middle layer module (TAF). The performance of manufacturing process depends on many input variables, some of which might be considered as random and be described by either empirical or known statistical distributions. In the model, we consider the following phenomena to be stochastic:

- breakdowns,
- machine adjustments after change-overs,
- tool change-overs,
- machine stoppages due to insufficient quality of input material,
- other registered machine stoppages not categorized according to the above criteria.

All machines incidents are collected by the maintenance department and presented in the form a form containing the information about the duration and category as well as the actual time of the occurrence. Those data were used to build statistical distributions of TTR (Time-To-Repair) and TBF (Time-Between-Failures) in ExpertFit software (<http://www.averill-law.com/distribution-fitting/>). This software suggests the best-fit model based on the empirical data using well-known statistical tests (Anderson–Darling, Kolmogorov, Chi-Square) for 29 various continuous or discrete distributions. In case goodness of fitness is not good, application of empirical distribution is suggested. What is important from a simulation perspective, the software provides the exact representation of the statistical distribution (fitted or empirical) that can be easily implemented in FlexSim.

In addition, other production stoppages were included in the modeling:

- rest breaks for employees in accordance with the Labor Code,
- activities during the shift changes,
- machine change-overs.

In case of rest breaks and shift changes, the breakdowns are modeled using constant MTBF and MTTR values. Whereas, machine change-overs depend on the assumed production problem. There exist four types of relevant change-overs:

- type 1—related to machines where change of material thickness is crucial—lasting 20 min,
- type 2—related to machines where change of material width is crucial—lasting 40 min,

**Table 1** Number and duration of machine change-overs for the analyzed 5-day production

Line	Type 1 (20 min)	Type 2 (40 min)	Type 3 (10 min)	Type 4 (5 min)
1	0	0	3	0
2	2	0	0	0
3	0	0	0	2
4	2	0	2	1

- type 3—related to machines where change of material length is crucial—lasting 10 min,
- type 4—related to machines where change of material length is crucial—lasting 5 min.

In the model, the lines were categorized in terms of the manufactured products and input material what represent the averaged production plan variety. The resulting number of change-overs for each line is presented in Table 1. If any line completes the production plan before 5 days pass it changes over to process the not yet consumed material and manufacture TAF module in accordance with the already set processing width.

### 3 Model and Experimentation

Overview of the devised model representation in FlexSim is presented in Fig. 2. A green arrow indicates two material input streams (desk with and without wane). A black-colored arrow shows the 8-h seasoning warehouse for glued modules. Four TAF lines are evident with machines and their parameters as in the actual processes. Due to limited computational power and time, we assumed that only one production week will be simulated. The production was diversified in order to reflect the mean production variety. This caused that the volume of input material had been adjusted according to the plan but the distribution of desk dimension had been derived from annual consumption distribution. The length of the desk with and without waness was fixed and equal to 2.95 m. The other parameters varied. Processing time and geometrical parameters of the machines were taken from technical documentation and were verified with the maintenance department. The processing time was also dependent on the size of input material. Machines were connected with each other with conveyors of constant velocity. All the aforementioned information were implemented in FlexSim model using dedicated objects. In some cases, object logics were adjusted using flexscript code what allows flexible modification of object behavior in the model.

The model was verified in terms of assumed parameters. It was checked that the module production line is not a bottleneck in the process. In addition, it was verified that the simulated OEE values (circa 85%) are consistent with the actual historical results for the current process.

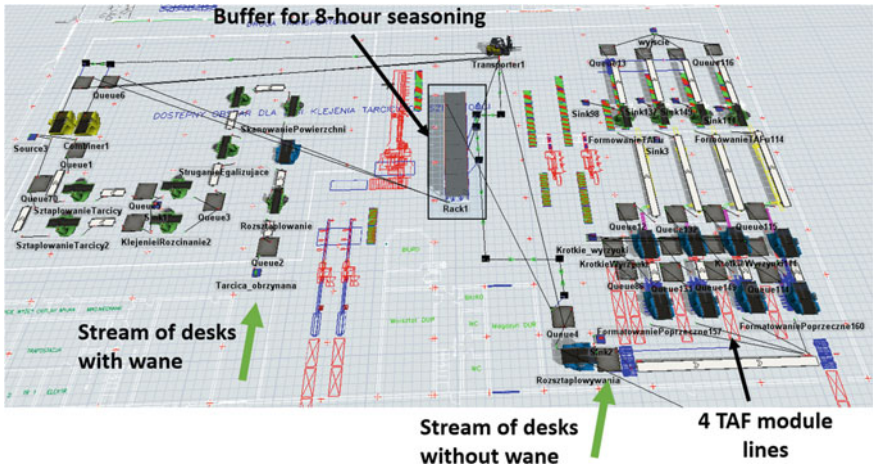


Fig. 2 The overview of graphical representation of simulation model of the manufacturing process in FlexSim environment

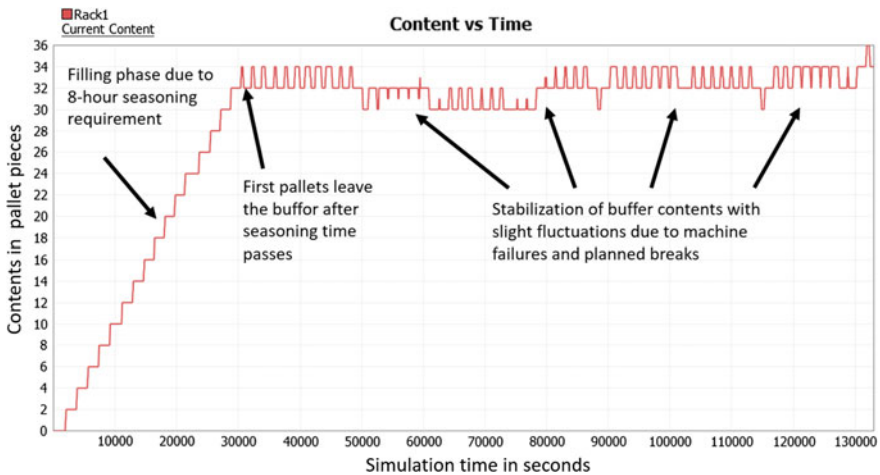


Fig. 3 The contents of the seasoning buffer with time

Two further experiments were performed. First, it was important to determine what should be the buffer capacity needed for material 8-h seasoning. In the experimentation, buffer content was observed during 1 week operations (Fig. 3). Some distinctive moments are evident:

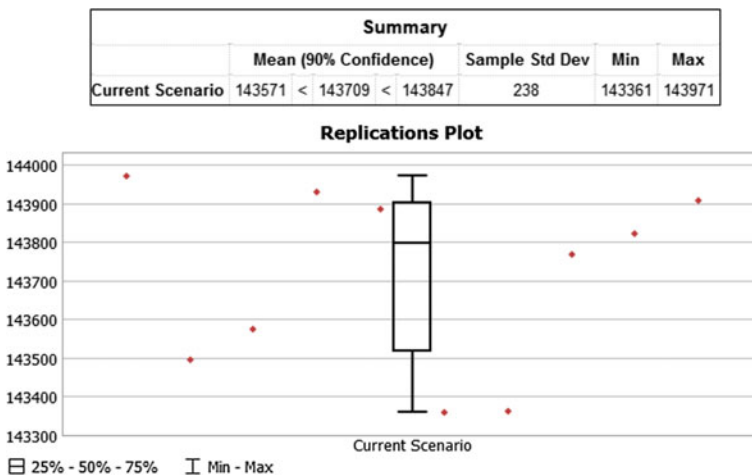
- buffer filling—the contents of the buffer increase for the first 8 h after the first pallet is delivered,
- leaving of the first after 8-h seasoning,

- stabilization of buffer contents with slight fluctuations resulting from line failures or planned breaks.

Ten different replications (of various random streams) were performed for the same scenario and the maximum buffer occupancy was no more than 36 pallets. Manufacturer’s warehouse space allows 60 pallet spaces to be accommodated. This means that the available space is sufficient for the designed process.

From the process design point of view, it was important to check whether, taking into account the failure of the machines and production interruptions, the desired number of pieces of TAF modules could be produced at assumed time—i.e., 5 days. For this purpose, a script was introduced to a model which was responsible for counting the number of modules produced with time. If, after 5 days passes, the number of pieces of the TAF module with respect to the plan, has been reached (or exceeded), then the line was designed correctly as far the performance is considered.

Due to the randomness in the model, it is not enough to make one simulation to state any conclusions. Therefore, ten replications were performed and the analysis was done based on the resulting sample. The results are shown in Fig. 4. For each replication, the entire volume of input material was consumed within 5 weeks. The aim was to make 143,530 semi-finished goods—TAF modules. The results indicate that, on average, the assumed efficiency is met. The lower confidence interval for mean at probability  $p = 0.9$  is 143,571, what is greater than the assumed value. The standard deviation from the sample is low, what suggests the small dispersion of results.



**Fig. 4** The results of experimentation—number of produced TAF modules for each iteration. Please note that statistical parameters and confidence interval for  $p = 0.9$  are presented in the framed table above the plot



## 4 Summary

The devised model in DES environment helped to confirm that the assumed performance of the proposed manufacturing system is possible to be achieved. The simulation model will be developed in order to analyze the investment or improvement scenario, when selecting or typing particular machines and devices. A complete validation of the model will be conducted once the line is installed, commissioned, and tested at the manufacturer.

We believe that the validated model can be an extremely useful tool in maintenance decision-making process. Potentially most profitable solution can be selected thanks to simulation testing of various perspective scenarios. Together with the growing computational power and popularity, the problem of time-consuming simulation and its cost will be solved. The development of new heuristic and meta-heuristic methods, in order to optimize system performance, would be a very promising direction for the further research in this area.

**Acknowledgements** The authors would like to thank Piotr Hoffman and Łukasz Hetman from Barlinek for their help with providing the accurate data and for thoughtful comments on our work. The results presented in the paper come from the R&D project: Improvement of raw wood efficiency in the industrial production processes, BIOSTRATEG2/298950/1/NCBR/2016, run by the Faculty of Mechanical Engineering and Management, Poznan University of Technology, Poland (in cooperation with Barlinek, a floorboard manufacturer in Poland), supported by the National Centre for Research and Development (NCBR) from the financial means within the BIOSTRATEG programme.

## References

1. Trojanowska, J., Varela, M.L.R., Machado, J.: The tool supporting decision making process in area of job-shop scheduling. In: Rocha, Á., Correia, A., Adeli, H., Reis, L., Costanzo, S. (eds.) *Recent Advances in Information Systems and Technologies. Advances in Intelligent Systems and Computing*, vol. 571, pp. 490–498. Springer, Berlin (2017)
2. Varela, M.R.L., Trojanowska, J., Carmo-Silva, S., Costa, N.M.L., Machado, J.: Comparative simulation study of production scheduling in the hybrid and the parallel flow. *Manage. Prod. Eng. Rev.* **8**(2), 69–80 (2017)
3. Gershwin, S.B.: *Manufacturing Systems Engineering*. Prentice-Hall, Englewood Cliffs, NJ. Currently available at <http://home.comcast.net/~hierarchy/MSE/mse.html> (1994)
4. Battini, D., Persona, A., Regattieri, A.: Buffer size design linked to reliability performance: a simulative study. *Comput. Ind. Eng.* **56**, 1633–1641 (2009)
5. Jasiulewicz-Kaczmarek, M., SWOT analysis for planned maintenance strategy—a case study. In: Dolgui, A., Grubbström, R., Ivanov, D., Yalaoui, F. (eds.) *IFAC Conference on Manufacturing Modelling, Management and Control, MIM 2016, IFAC PapersOnLine*, vol. 49, no. 12, pp. 674–679 (2016)
6. Jasiulewicz-Kaczmarek, M.: Practical aspects of the application of RCM to select optimal maintenance policy of the production line. In: Nowakowski, T., Mlynczak, M., Jodejko-Pietruczuk, A., et al. (eds.) *Safety and Reliability: Methodology and Applications—Proceedings of the European Safety and Reliability Conference, ESREL 2014*, pp. 1187–1195. Taylor & Francis Group, London (2015)

7. Vieira, G., Reis, L., Varela, M.L.R., Machado, J., Trojanowska, J.: Integrated platform for real-time control and production and productivity monitoring and analysis. *Rom. Rev. Precis. Mech. Opt. Mechatron.* **50**, 119–127 (2016)
8. Jasiulewicz-Kaczmarek, M., Bartkowiak, T.: Improving the performance of a filling line based on simulation. In: *IOP Conference Series: Materials Science and Engineering*, vol. 145, no. 4, p. 042024 (2016)
9. Manupati, V.K., Anand, R., Thakkar, J.J., Benyoucef, L., Garsia, F.P., Tiwari, M.K.: Adaptive production control system for a flexible manufacturing cell using support vector machine-based approach. *Int. J. Adv. Manuf. Technol.* **1**(4), 969–981 (2013)
10. Li, J., Gonzalez, M., Zhu, Y.: A hybrid simulation optimization method for production planning of dedicated remanufacturing. *Int. J. Prod. Econ.* **117**(2), 286–301 (2009)
11. Shi, L., Gershwin, S.B.: An efficient buffer design algorithm for production line profit maximizations. *Int. J. Prod. Econ.* **122**, 725–740 (2009)
12. Kampf, M., Kochel, P.: Simulation-based sequencing and lot size optimization for a production-and-inventory system with multiple items. *Int. J. Prod. Econ.* **104**(1), 191–200 (2006)
13. Pawlewski, P.: Multimodal approach to modeling of manufacturing processes. *Procedia CIRP* **17**, 716–720 (2014)
14. Kujawińska, A., Rogalewicz, M., Diering, M., Hamrol, A.: Statistical approach to making decisions in manufacturing process of floorboard. In: *Proceedings of 5th World Conference on Information Systems and Technologies, Recent Advances in Information Systems and Technologies*, vol. 3, pp. 499–508. Springer, Berlin, (2017)

# A Methodology of Improvement of Manufacturing Productivity Through Increasing Operational Efficiency of the Production Process

Justyna Trojanowska, Adam Kolinski, Dariusz Galusik,  
Maria L.R. Varela and Jose Machado

**Abstract** One of the most important aspects of manufacturing efficiency assessment is the determination of productivity. A study of the relevant literature and a review of business practices have led the authors to conclude that there is a niche for a comprehensive decision support methodology which would assist organizations in improving their manufacturing productivity. This paper presents a methodology of improvement of manufacturing productivity through increasing operational efficiency of the manufacturing process. The methodology was verified by a manufacturing company which is a supplier of goods for i.e. the automotive and medical industries. The effect of using methodology is reducing of cycle of lot, reducing number of changeovers and eliminating errors.

**Keywords** Productivity · Production efficiency · Production constraint

## 1 Introduction

Based on the process of matching the existing resource productivity with the forecast demand which utilizes the analysed manufacturing resources, productivity is an important issue in view of production efficiency. Analyses of manufacturing process efficiency seek to improve productivity through effective use of the available machine park within a specified timeframe (e.g. depending on the number of

---

J. Trojanowska (✉) · D. Galusik  
Poznan University of Technology, Poznań, Poland  
e-mail: justyna.trojanowska@put.poznan.pl

A. Kolinski  
Logistics Expertise Department, Institute of Logistics and Warehousing, Poznań, Poland

M.L.R. Varela  
Department of Production and Systems, School of Engineering, University of Minho,  
Guimarães, Portugal

J. Machado  
MEtRICs Research Center, School of Engineering, University of Minho, Braga, Portugal

scheduled manufacturing changes). However, we should keep in mind that productivity can be improved only provided that additionally employed workstations are used optimally in terms of operational and economic efficiency. Therefore, benefits of reduced capital expenditures and high resource utilization ratio are counterbalanced by limited manufacturing flexibility [1].

Productivity is analysed at the level of workstation and operation as well as at the level of the entire manufacturing process. Manufacturing productivity of resources is defined as the maximum number of items which can be produced within a certain timeframe [2]. The literature of the subject analyses manufacturing productivity with reference to human labour potential only [3–6], whereas, in fact, it refers to all types of resources utilized in the manufacturing process [7].

In order to improve productivity, companies seek to utilize 100% of manufacturing capacity of a resource which constrains the manufacturing system. It must be noted here that 100% utilization of a workstation poses a serious threat to the efficiency of the manufacturing processes. The highest possible level of utilization of one or more workstations being constraining resources increases the likelihood of breakdowns and may cause delays in the manufacturing process in the event of resource downtime. Manufacturing bottlenecks disrupt processes, cause inventory accumulation and downtime [8]. Therefore, when seeking to improve manufacturing productivity, it is important to make sure that processes carried out in bottlenecks are well organized.

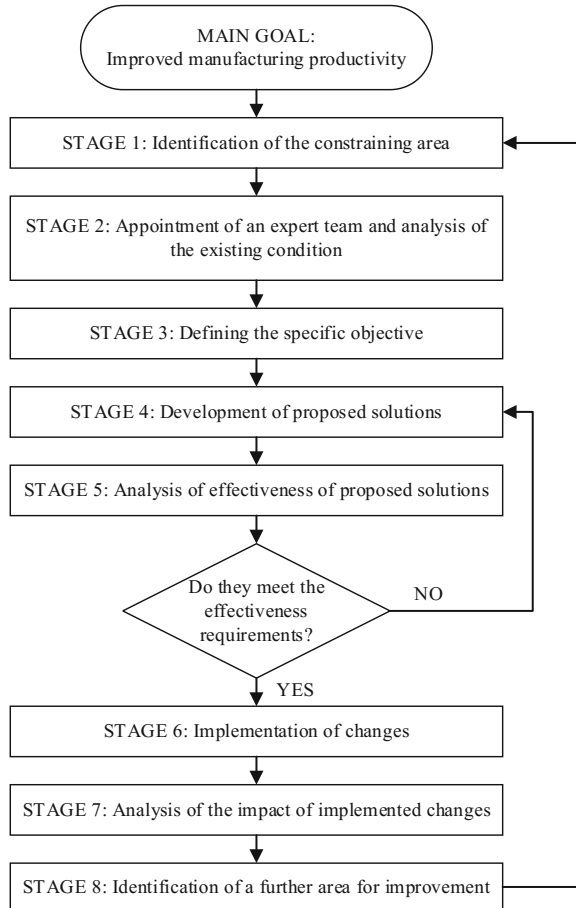
Decision-making in the area of improvement of manufacturing performance indicators is challenging due to the complexity of the issue. Increasingly often, companies use decision-making support methods for this purpose [9–12]. The literature describes many applications of the dominance-based rough set approach (DRSA) to gaining insight into the manufacturing process [13–15], minimizing losses [16–19], verifying validity of measurement and inspection tools [20–22], and applying systems which support visualization and control of manufacturing processes [23]. Analyses of productivity should also look at the economic conditions and personal features of the employee [24, 25].

What is more, productivity of a workstation being a bottleneck in the manufacturing process translates to productivity of not only the analysed manufacturing process, but also the entire manufacturing facility, and further—the entire logistic supply chain [26–29]. It should be taken into consideration in the process of designing the flow of goods between various organizations [30].

## **2 Methodology of Improvement of Manufacturing Productivity**

The research on improving manufacturing productivity was based on the application of the methodology shown in Fig. 1.

**Fig. 1** Manufacturing productivity improvement methodology



The key objective of the methodology is to improve manufacturing productivity. Its stages are described below.

Stage 1: Identification of the constraining area. The input data for the methodology is a predefined set of workstation jobs and routings, i.e. a list of technological operations required to complete certain jobs and timeframes for completion of operations on particular pieces of equipment. They serve as a basis for the calculation of the man-hours required for particular manufacturing resources. A workstation with the highest demand for man-hours is a resource constraining the manufacturing system. Therefore, to identify constraining resources, the total of man-hours required at particular workstations is calculated and the most heavily loaded workstation is identified. Organization of work and sequencing of tasks at this workstation has an impact on productivity of the entire manufacturing system within a certain timeframe.

Stage 2: Analysis of the existing condition. At this stage, the constraining factors, i.e. those which reduce productivity of the constraining workstation are identified. Various support tools may be used, such as brainstorming, process diagrams, timing, Gantt chart, the theory of constraints thinking processes, or value stream mapping (VSM).

Stage 3: Defining the specific objective. The input data for this stage are the results of the analysis of the existing condition, obtained at Stage 2. This stage aims at specifying an optimization objective at the operational level of manufacturing management. A close link between the strategic, tactical and operational levels of management justifies an analysis of deviations from the schedule at the tactical and operational levels. Compliance of current actions or optimization efforts is assessed on the basis of defined strategic goals which must be transferred into the operational level. The study carried out under the research project confirmed that successful transfer of the strategy into the tactical and operational levels has a tremendous impact on the assessment of manufacturing process efficiency.

Stage 4: Development of proposed solutions. With the specific objective defined at stage 3 and the results of the analysis of the existing condition, carried out at stage 2, areas in which improvement actions should be initiated can be determined. It is important to develop several solutions, of which the optimal one will be selected after a thorough analysis. For this purpose, a single or multiple-case study is conducted as a one-off and limited research process aimed to provide a thorough analysis, with the use of various study techniques over a long time period [31].

Stage 5: Analysis of effectiveness of proposed solutions. The methodology focuses on the analysis of operational efficiency, which is related to the technical and organizational aspects of scheduling and control of the manufacturing process. Thus, operational efficiency indirectly affects the economic performance and costs of manufacturing. Therefore, as part of the analysis of effectiveness, the methodology prescribes an analysis of selected operational indicators within the scope of:

- optimizing the manufacturing process performance,
- shortening manufacturing cycles,
- reducing manufacturing deficiencies,
- optimizing utilization of manufacturing capacity,
- balancing the manufacturing resources,
- assessing the impact of the developed solutions on the costs of manufacturing and logistic processes in the organization under analysis.

Stage 6: Implementation of proposed solutions. The proposed solutions are implemented, provided that the results of the analysis of effectiveness are satisfactory and acceptable by decision makers.

Stage 7: Analysis of the impact of implemented changes. This stage is aimed at verifying whether the objective specified at stage 3 has been obtained, and how other areas of operation of the organization have been affected. Changes implemented to increase manufacturing productivity may contribute to alteration of work

organization in the warehouse of raw materials or scheduling process. At stage 7, a further area for improvement at stage 8 is identified.

### 3 Case Study

The methodology was verified by a manufacturing company which has operated on the Polish market since 1986. As a supplier of goods for the automotive, rail, medical, furniture and machine engineering industries, the company does profile bending, welding of steel and aluminium, tool machining, steel surface finishing, and powder coating.

At stage 1, the powder coating line was identified as a resource constraining manufacturing productivity. At stage 2, the existing condition was analysed. The analysis results showed that the mean productivity of the process of coating connectors was 500 items per shift. A team of experts, including the manufacturing scheduling specialist, the coating facility manager, and the warehouse manager, carried out a thorough analysis of the existing condition and presented factors which affected the unsatisfactory productivity of the coating process.

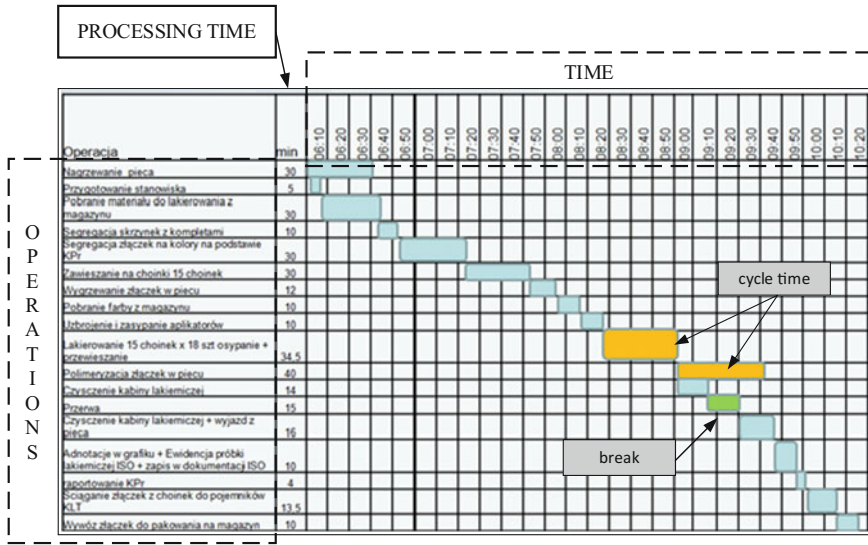
The analysis covered the following areas:

- the workload at shifts at the powder coating line,
- timeframes of task completion at the powder coating line,
- the manner of identification of connectors by powder coating line workers,
- the system of suspending the connectors,
- the procedures of loading the furnace,
- the frequency of colour changes at the powder coating line,
- the system of providing job sheets,
- queuing of jobs in the manufacturing schedule,
- the system of distribution of connectors from the raw material warehouse,
- the scope of duties of warehouse workers concerning the provision of raw materials for the powder coating line.

The process of powder coating and all the jobs performed by the powder coating line workers are presented in the Gantt chart (Fig. 2). The chart presents the pause, jobs performed within certain time units (powder coating and polymerization), and the preparation and finishing tasks.

An analysis of the Gantt chart showed that the preparation and finishing jobs had a large share in the total timeframe of process performance, and the level of utilization of the furnace was low.

The analysis of the existing condition permitted to determine the specific objective and prepare an action plan. At stage 3, the objective was specified as follows: reduction of the powder coating cycle of one lot by 50% through increased utilization of the chamber furnace for surface polymerization. At stage 4, detailed suggestions for organizational and technical changes were developed, aimed at



**Fig. 2** Gantt chart—jobs carried out at the powder coating facility before the implementation of changes

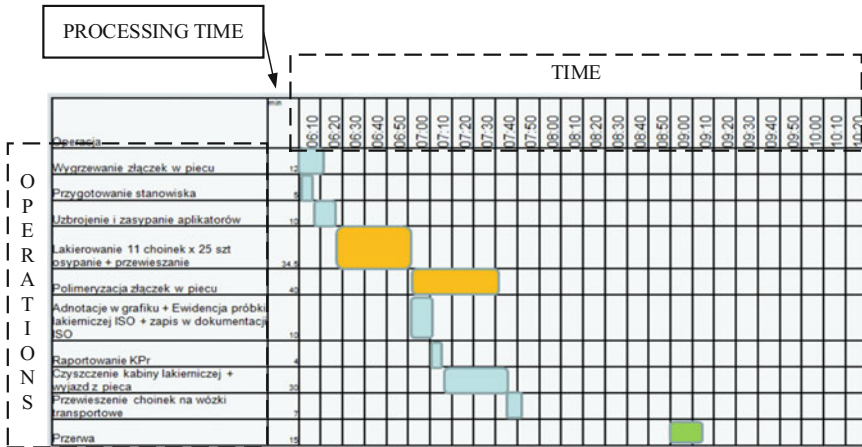
obtaining the objective. An analysis of the effectiveness of the proposed solutions, carried out at stage 5, showed that they had a positive impact on the indicators of production cycle performance, variability of jobs at workstations, and frequency of manufacturing deficiencies. Taking into consideration the results of the analysis of effectiveness, actions (aimed at achieving the objective) were taken to shorten the timeframes of preparation and finishing tasks. At stage 6, the following changes to work organization were implemented:

- the duty of switching the furnace on for pre-heating was transferred to the furnace operator at the previous shift,
- the warehouse worker was made responsible for delivering raw materials to the workstation at the powder coating facility,
- the operation of separation of stacked connectors was combined with order assembly, and the task was transferred to the warehouse worker.

One technical alteration was implemented: the way of suspending the items on the frame which is loaded into the furnace was changed. Additionally, the manner of scheduling the manufacturing was changed. After the implementation of the change, jobs to be performed at the powder coating facility were generated for each colour separately. It significantly reduced the preparation and finishing timeframes and permitted early reporting of completion of coating with particular colours.

Analysis of the effects of implemented changes was conducted at stage 7. A Gantt chart was drawn up again, showing particular jobs performed at the powder coating facility (Fig. 3).





**Fig. 3** Gantt chart—jobs carried out at the powder coating facility after the implementation of changes

An analysis of the effects proved that:

- the powder coating cycle of one lot was reduced from 240 to 112 min (down by 53.3%),
- the need for retooling was reduced from 9 to 5 times in 2 working days, through increasing the economic manufacturing lot and changes to manufacturing scheduling,
- some errors were eliminated, such as wrong identification of components or coating with a wrong colour, through the transfer of identification of components from the powder coating line to the warehouse.

To obtain the final effects, the company had to make the following investments:

- employ of a part-time worker in the warehouse to handle the rotation of raw connectors,
- arrange space in the warehouse for hanging the connectors (the warehouse of connectors was moved closer to the powder coating facility),
- cover the cost of materials and manpower for the construction of transport trolleys,
- cover the cost of arranging space for storing transport trolleys on the premises of the powder coating facility,
- cover the cost of modifying the software for generating manufacturing jobs.

The costs incurred were justified in economic terms, as they contributed to the reduction of the timeframes of preparation and finishing jobs from 165 to 37.5 min per cycle. The profits generated by the company in the first month after implementation of the changes exceeded the project investment.

One of the results of the changes implemented into the manufacturing scheduling was a several-fold increase in the number of job sheets generated for each job. Although it was a negative consequence, the key objective was to improve productivity at the bottleneck. The issue of large number of job sheets was made the topic of the next improvement project (stage 8). It is worth noting here that in spite of an improvement in productivity by more than 50%, the powder coating facility still remains a bottleneck.

## 4 Conclusion

Effectiveness of operational efficiency assessment depends on skillful transposing of strategic goals onto the tactical and operational levels of management. To effectively perform a strategic plan, it must be translated into actions, results, and indicators of an ongoing operation. For this reason, operational efficiency is related to optimization and rationalization of the manufacturing process in terms of its organization and technologies used.

An analysis of efficiency of a manufacturing process requires a multi-criteria assessment which takes into consideration the cause and effect relations not only in the manufacturing process, but also in the entire organization and its supply chain. Improvement in one area often results in deterioration in another. Analyses of effectiveness should look at the negative impact that a certain optimization may have on other business areas. A solution is beneficial for an organization only if benefits resulting from optimization of a certain area, in global terms, largely exceed additional costs or deterioration in the standards of performance in other areas of operation.

**Acknowledgements** This work had the financial support of Ministry of Science and Higher Education, Republic of Poland, under the project 02/23/DSMK/7699.

## References

1. Waters, C.D.J., Waters, D.: *Operations Management: Producing Goods and Services*. Pearson Education, UK (2002)
2. Hadas, L., Adamczak, M., Cyplik, P.: The integration of theory of constraints tools—case study. In: 21st International Conference on Production Research: Innovation in Product and Production, ICPR, Stuttgart, Germany (2011)
3. Drucker, P.F.: Knowledge-worker productivity: the biggest challenge. *Calif. Manage. Rev.* **41** (2), 79–94 (1999)
4. Heizer, J., Render, B.: *Operations Management*. Pearson Prentice Hall, New Jersey (2008)
5. de Menezes, L.M., Wood, S., Gelade, G.: The integration of human resource and operation management practices and its link with performance: a longitudinal latent class study. *J. Oper. Manage.* **28**(6), 455–471 (2010)

6. Domanski, R., Fertsch, M.: Integration of production and supply in the lean manufacturing conditions according to the lot for lot method logic-results of research. *LogForum* **11**(4), 351–358 (2015)
7. Koliński, A.: The efficiency of the production—the analyse of problems based on the literature research. *LogForum* **8**(2), 137–150 (2012)
8. APICS Dictionary, 11th Edition, American Production and Inventory Control Society, Inc., Falls Church, VA (2004)
9. Dostatni, E., Diakun, J., Grajewski, D., et al.: Multi-agent system to support decision-making process in design for recycling. *Soft. Comput.* **20**(11), 4347–4361 (2016)
10. Rogalewicz, M., Sika, R.: Methodologies of knowledge discovery from data and data mining methods in mechanical engineering. *Manage. Prod. Eng. Rev.* **7**(4), 97–108 (2016)
11. Klos, S., Patalas-Maliszewska, J.: Throughput analysis of automatic production lines based on simulation methods. In: Jackowski, K., Burduk, R., Walkowiak, K., Wozniak, M., Yin, H. (eds.) *Intelligent Data Engineering and Automated Learning—IDEAL*, Lecture Notes in Computer Science, vol. 9375, pp. 181–190 (2015)
12. Kujawińska, A., Rogalewicz, M., Diering, M.: Application of expectation maximization method for purchase decision-making support in welding branch. *Manage. Prod. Eng. Rev.* **7**(2), 29–33 (2016)
13. Bartkowiak, T., Pawlewski, P.: Reducing negative impact of machine failures on performance of filling and packaging production line—a simulative study. In: *The 2016 Winter Simulation Conference*, pp. 2912–2923 (2017)
14. Kujawińska, A., Rogalewicz, M., Piłacińska, M., Kocharński, A., Hamrol, A., Diering, M.: Application of dominance-based rough set approach (DRSA) for quality prediction in a casting process. *Metalurgija* **55**(4), 821–824 (2016)
15. Kujawińska, A., Rogalewicz, M., Diering, M., Piłacińska, M., Hamrol, A., Kocharński, A.: Assessment of ductile iron casting process with the use of the DRSA method. *J. Min. Metall. Sect. B Metall.* **52**(1), 25–34 (2016)
16. Kujawińska, A., Rogalewicz, M., Diering, M., Hamrol, A.: Statistical approach to making decisions in manufacturing process of floorboard. In: *5th World Conference on Information Systems and Technologies, Recent Advances in Information Systems and Technologies*, vol. 3, pp. 499–508, Springer, Berlin (2017)
17. Suszyński, M., Żurek, J., Legutko, S.: Modelling of assembly sequences using hypergraph and directed graph, *Tehnički Vjesnik. Technical Gazette* **21**(6), 1229–1233 (2014)
18. Krenczyk, D., Skołod, B.: Transient states of cyclic production planning and control. *Appl. Mech. Mater.* **657**, 961–965 (2014)
19. Starzyńska, B., Hamrol, A.: Excellence toolbox: decision support system for quality tools and techniques selection and application. *Total Qual. Manage. Bus. Excellence* **24**(5–6), 577–595 (2013)
20. Diering, M., Dyczkowski, K.: Assessing the raters agreement in the diagnostic catheter tube connector production process using novel fuzzy similarity coefficient. In: *IEEE International Conference on Industrial Engineering and Engineering Management*, pp. 228–232 (2016)
21. Diering, M., Dyczkowski, K., Hamrol, A.: New method for assessment of raters agreement based on fuzzy similarity. In: *10th International Conference on Soft Computing Models in Industrial and Environmental Applications, Advances in Intelligent Systems and Computing*, vol. 368, pp. 415–425, Springer, Berlin (2015)
22. Ignaszak, Z., Sika, R., Perzyk, M., Kocharński, A., Kozłowski, J.: Effectiveness of SCADA systems in control of green sands properties. *Arch. Foundry Eng.* **16**(1), 5–12 (2016)
23. Golinska, P., Kuebler, F.: The method for assessment of the sustainability maturity in remanufacturing companies. *Procedia CIRP* **15**, 201–206 (2014)
24. Hamrol, A., Kowalik, D., Kujawinska, A.: Impact of selected work condition factors on quality of manual assembly process. *Hum. Factors Ergon. Manuf. Serv. Ind.* **21**(2), 156–163 (2010)

25. Kujawińska, A., Vogt, K., Wachowiak, F.: Ergonomics as significant factor of sustainable production. In: Golińska, P., Kawa, A. (eds.) *Technology Management for Sustainable Production and Logistics*, Book Series: EcoProduction, pp. 193–203 (2015)
26. Golinska, P., Kawa, A.: Remanufacturing in automotive industry: challenges and limitations. *J. Ind. Eng. Manage.* **4**(3), 453–466 (2011)
27. Kawa, A.: SMART logistics chain. In: *Asian Conference on Intelligent Information and Database Systems*, pp. 432–438, Springer, Berlin (2012)
28. Hadas, L., Cyplik, P., Adamczak, M., Domanski, R.: Dimensions for developing supply chain integration scenarios. In: *15th International Scientific Conference*, pp. 225–239, *Business Logistics in Modern Management*, Croatia (2015)
29. Adamczak, M., Domanski, R., Hadas, L., Cyplik, P.: The integration between production-logistics system and its task environment-chosen aspects. *IFAC-PapersOnLine* **49**(12), 656–661 (2016)
30. Kawa, A.: Simulation of dynamic supply chain configuration based on software agents and graph theory. In: *International Work-Conference on Artificial Neural Networks*, pp. 346–349, Springer, Berlin (2009)
31. Maylor, H., Blackmon, K.: *Researching Business and Management*. Polgrave Macmillan, New York (2005)

# The Impact of Buffer Allocation in Assembly-Line Manufacturing Systems on the Effectiveness of Production Processes

Slawomir Klos and Justyna Patalas-Maliszewska

**Abstract** The allocation of buffers in an assembly-line manufacturing system plays an important role in the effectiveness and the work-in-progress of production processes. In this paper, the impact of buffer allocation on the throughput and average product lifespan is analysed. The behaviour of the system is investigated using the computer-simulation method and the Tecnomatix Plant Simulation software tool. The different variants of an assembly-line manufacturing system are considered (varied allocation of buffers and operation times). For the assembly-line manufacturing system, simulation experiments are prepared (varied allocation of buffer capacities and processing times). The input values of the simulation experiments, along with the different allocations of buffer capacities, are taken into account. The output values are the manufacturing system's throughput, along with the average lifespan of the products, which indicate the work-in-progress.

**Keywords** Assembly-line manufacturing system · Computer simulation  
Buffer-allocation problem · Throughput · Product lifespan

## 1 Introduction

The buffer-allocation problem is a NP-hard combinatorial optimisation issue well known in the research area of industrial engineering. On the one hand, the correct allocation of buffer capacities on production lines can result in an increase in the overall efficiency of the production system. Computer simulation is the research method of choice for the analysis of behaviour within discrete-manufacturing

---

S. Klos (✉) · J. Patalas-Maliszewska  
Faculty of Mechanical Engineering, University of Zielona Góra, Licealna 9, 65-417 Zielona Góra, Poland  
e-mail: s.klos@iizp.uz.zgora.pl

systems [1]. Using computer simulation, the impact of various parameters on the effectiveness, and on the work-in-progress, of discrete-manufacturing systems, can be evaluated. In this paper, the change of buffer allocation within an assembly-line manufacturing system is examined. The structure of the assembly-line manufacturing system is consistent with the manufacturing resources (CNC machines and assembly-line stations) and the buffers allocated between resources. It is assumed that the discrete-manufacturing system is fully automated and fully flexible, and that the availability of resources is determined as 90%.

Simulation is a very important research method for the modelling, analysis and development of manufacturing systems. Many scientific papers include the application of computer simulation, and the buffer-allocation problem in the general design of discrete-manufacturing systems and in the analysis of the operation, production planning and scheduling of the systems [2, 3]. The problem of maximising the throughput of production lines by changing buffer sizes, or locations, using simulation methods, was studied by Vidalis et al. [4]. A critical literature overview of buffer allocation and production line performance was carried out by Battini et al. [5], while Demir et al. [6] proposed a classification scheme to review the literature studies, and presented a comprehensive survey on the buffer-allocation problem in production systems. Stanley and Kim [7] presented the results of simulation experiments carried out for buffer allocations in closed-series production lines. Yamashita and Altioek [8] proposed an algorithm for minimising the total buffer allocation for the desired throughput in production lines with phase-type processing times. They implemented a dynamic programming algorithm which used the decomposition method to approximate the system's throughput at every stage. Gurkan [9] used a simulation-based optimisation method to find the optimal buffer allocations in tandem production lines where machines were subject to random breakdowns and repairs, and the product was of the fluid type. He explored some of the functional properties of the throughput of such systems and derived recursive expressions to compute one-sided directional derivatives of throughput from a single simulation run. Kujawińska et al. [10] analysed the problem of the capability assessment of a production process for manufacturing products which fulfilled certain requirements. They presented theoretical assumptions of the DRSA method for the classification of a process state based on so-called process-state measures (e.g. process parameters, diagnostic signals, events).

In this paper, the impact of different variants of discrete assembly-line manufacturing systems on the throughput and average product lifespan are analysed. The research problem can be formulated as 'Given that an assembly-line manufacturing system includes CNC machines, assembly-line stations and buffers, how does the allocation of the buffer capacity and operation times of the system influence the throughput and product lifespan?'

In the next chapter, the buffer-allocation problem is described and assembly-line manufacturing system variants are presented.

## 2 A Model for Discrete Assembly-Line Manufacturing Systems

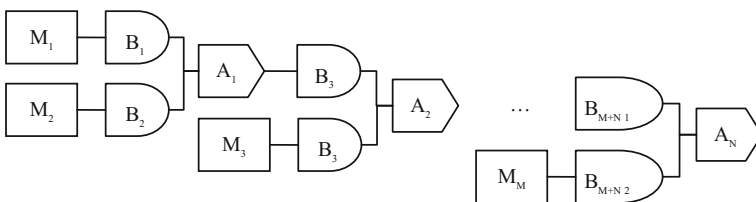
For the simulation research, a general model for three discrete-manufacturing systems is considered. The systems include, respectively, one, two and three production lines. Each line includes two manufacturing resources and two intermediate buffers. For the systems, different interconnections between the buffers and the manufacturing resources are proposed. Simulation experiments are prepared for different buffer capacities as input values.

### 2.1 The Buffer Allocation Problem (BAP)

The buffer-allocation problem (BAP) is one of the most important questions facing a serial-production designer. It is a combined, NP-hard, combinatorial, optimization problem when designing production lines, and the issue is studied by many scientists and theorists around the world [5–7]. The buffer-allocation problem is concerned with the allocation of a certain number of buffers  $P$ , among the  $N - 1$  intermediate buffer locations of a production line, in order to achieve a specific objective. A production line consists of machines working in sequence and assembly-line stations separated by buffers (Fig. 1) where the machines are denoted as  $M_1, M_2, M_M$ , assembly-line stations  $A_1, A_2, A_N$ , and the buffers as  $B_1, B_2, B_{M+N-1}$ .

In the literature, several types of the production line are considered. The classification of production lines can be based on the blocking type, i.e. those which block either before or after operation; job-transfer timing, such as asynchronous, synchronous, continuous; production-control mechanisms, such as push and pull; types of workstation and whether they are reliable or unreliable; and career requirements, whether open or closed. BAP can be formulated in three cases, depending on the function of the objective. In the first case, the main objective is the maximisation of the throughput rate for a given, fixed, number of buffers. The first BAP case is formulated as (1)–(3). Find:

$$B = (B_1, B_2, \dots, B_{M+N-1}) \tag{1}$$



**Fig. 1** A production line with  $M$  machines,  $N$  assembly-line stations and  $M + N - 1$  buffers

so as to:

$$\max f(B) \quad (2)$$

subject to:

$$\sum_{i=1}^{M+N-1} B_i = P \quad (3)$$

where  $B$  represents a buffer-sized vector and  $f(B)$  represents the throughput rate of the production line as a function of the vector size of the buffers, and  $P$  is a fixed, non-negative integer denoting the total buffer space available within the manufacturing system. The second BAP case is formulated as (4)–(6). Find:

$$B = (B_1, B_2, \dots, B_{M+N-1}) \quad (4)$$

so as to:

$$\min \sum_{i=1}^{M+N-1} B_i \quad (5)$$

subject to:

$$f(B) = f^* \quad (6)$$

where  $f^*$  is the desired throughput rate. The third **BAP** case is formulated as follows (7)–(10). Find:

$$B = (B_1, B_2, \dots, B_{M+N-1}) \quad (7)$$

so as to:

$$\min Q(B) \quad (8)$$

subject to:

$$f(B) = f^* \quad (9)$$

$$\min \sum_{i=1}^{M+N-1} B_i \leq P \quad (10)$$

where  $Q(B)$  denotes the inventory of the average work-in-progress as a function of the vector size of the buffers and  $f^*$  is the desired throughput rate. This formulation of the problems expresses the maximisation of the throughput rate for a fixed, given, number of buffers which achieves the desired throughput rate, with the



minimum total buffer size—or with the minimisation of the inventory of the average work-in-progress—which is subject to the constraints of the aggregate buffer size and the desired throughput rate.

### 2.2 A Model for Assembly-Line Manufacturing Systems

The assembly-line manufacturing system is presented in Fig. 2, and consists of intermediate buffers  $B_1, B_2, B_3, B_4, B_5, B_6$ , and manufacturing resources CNC<sub>1</sub>, CNC<sub>2</sub>, CNC<sub>3</sub>, CNC<sub>4</sub>, A<sub>1</sub>, A<sub>2</sub>, A<sub>3</sub> ( $M = 4, N = 3$ ). The model is prepared using Tecnomatix Plant Simulation software.

The operation times of the manufacturing resources are determined as uniform distribution. Uniform distribution can be used for the modelling of random numbers which are located between the ‘start-and-stop’ interval limits. This is useful when little is known about the distribution of the random numbers. The function of the probability density of the distribution for values between  $start < x < stop$  has the following form:

$$f(x) = \frac{1}{stop - start} \tag{11}$$

where the average value of the distribution is:

$$\mu = \frac{start + stop}{2} \tag{12}$$

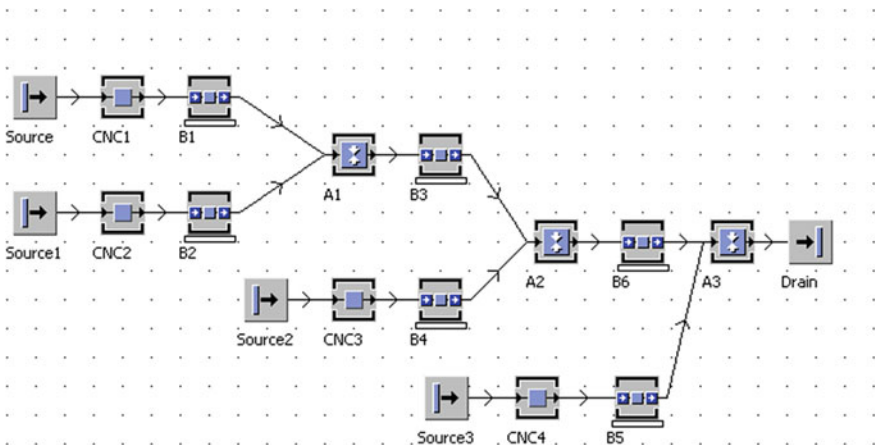


Fig. 2 A model of an assembly-line manufacturing system

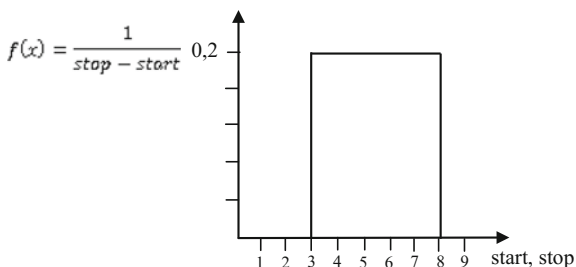
and the variant takes on the value of:

$$\sigma^2 = \frac{(\text{stop} - \text{start})^2}{2} \tag{13}$$

An example of density function of the uniform distribution is presented in Fig. 3.

The processing times for all the production resources of the investigated model are defined as start = 3:00 and stop = 5:00. It is assumed that the availability of manufacturing resources is 90%. For the model of the assembly-line manufacturing system, 26 experiments for different allocations of buffer capacities were conducted. The variants of buffer capacities (simulation experiments) are presented in Table 1. The simulation experiments were conducted for different variants of operation times of the resources (CNC machines and assembly-line stations). The variants of operation times are presented in Table 2.

**Fig. 3** The density function of the uniform distribution where start = 3 and stop = 8



**Table 1** The simulation experiments for different values of buffer capacities

	$B_1$	$B_2$	$B_3$	$B_4$	$B_5$	$B_6$		$B_1$	$B_2$	$B_3$	$B_4$	$B_5$	$B_6$
Exp 01	1	1	1	1	1	10	Exp 14	2	2	2	2	2	1
Exp 02	1	1	1	1	10	1	Exp 15	1	2	3	4	5	6
Exp 03	1	1	1	10	1	1	Exp 16	6	5	4	3	2	1
Exp 04	1	1	10	1	1	1	Exp 17	1	1	2	2	3	3
Exp 05	1	10	1	1	1	1	Exp 18	2	2	1	1	3	3
Exp 06	10	1	1	1	1	1	Exp 19	1	1	5	1	1	5
Exp 07	1	1	1	2	2	2	Exp 20	1	1	1	1	1	1
Exp 08	2	1	1	1	2	2	Exp 21	2	2	2	2	2	2
Exp 09	2	1	2	1	2	2	Exp 22	3	3	3	3	3	3
Exp 10	2	2	1	1	2	2	Exp 23	5	5	5	5	5	5
Exp 11	2	1	2	2	2	2	Exp 24	10	10	10	10	10	10
Exp 12	2	2	2	1	2	2	Exp 25	20	20	20	20	20	20
Exp 13	2	2	2	2	1	2	Exp 26	30	30	30	30	30	30

**Table 2** Different variants of operation times for the simulation model of an assembly-line manufacturing system (start-and-stop time for a uniform distribution)

	CNC <sub>1</sub>	CNC <sub>2</sub>	CNC <sub>3</sub>	CNC <sub>4</sub>	A <sub>1</sub>	A <sub>2</sub>	A <sub>3</sub>
V <sub>1</sub> —start	3:00	3:00	3:00	3:00	3:00	3:00	3:00
V <sub>1</sub> —stop	5:00	5:00	5:00	5:00	5:00	5:00	5:00
V <sub>2</sub> —start	1:00	1:00	2:00	3:00	2:00	3:00	4:00
V <sub>2</sub> —stop	2:00	2:00	3:00	4:00	3:00	4:00	5:00
V <sub>3</sub> —start	4:00	4:00	3:00	2:00	3:00	2:00	1:00
V <sub>3</sub> —stop	5:00	5:00	4:00	3:00	4:00	3:00	2:00

The operation times presented in Table 2 are ordered in the following way.

- variant V<sub>1</sub>—the same values of operating times,
- variant V<sub>2</sub>—increasing operation times,
- variant V<sub>3</sub>—decreasing operation times.

The operation times presented in Table 2 should be interpreted for example: for variant V<sub>1</sub> and CNC<sub>1</sub> start = 3:00 and stop = 5:00 for uniform distribution.

Each operation-time variant includes at least one bottleneck, where the stop parameter of the uniform distribution is 5:00. The results of the simulation experiments are presented in the next chapter.

### 3 Results of the Simulation Experiments

The output values of the simulation experiments are the throughput per hour, and the average lifespan of the products of the systems studied. In Fig. 4, the throughput values for variant V<sub>1</sub> are presented. The smallest throughput value is obtained in experiment Exp 20 ( $f_{20}(6) = 9.56$ ), where all buffer capacities are equal to 1.

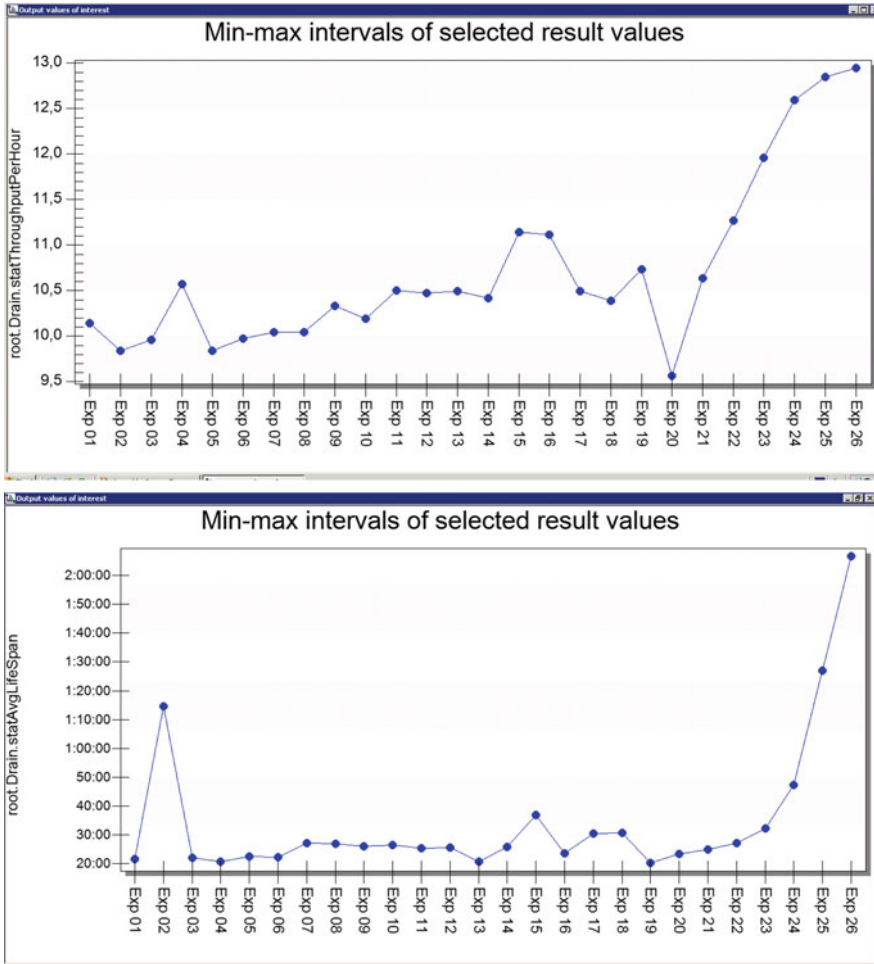
The throughput of the system increases in tandem with the increasing capacity of all buffers, reaching the greatest value ( $f_{26}(180) = 12.95$ ) in experiment Exp 26, with all buffer capacities being equal to 30. Together with increasing the buffer capacities, the average product lifespan is increased.

To evaluate the objective impact of the selected parameters on the efficiency of the system, a production-flow index  $\gamma$  is proposed

$$\gamma = f/\alpha \tag{14}$$

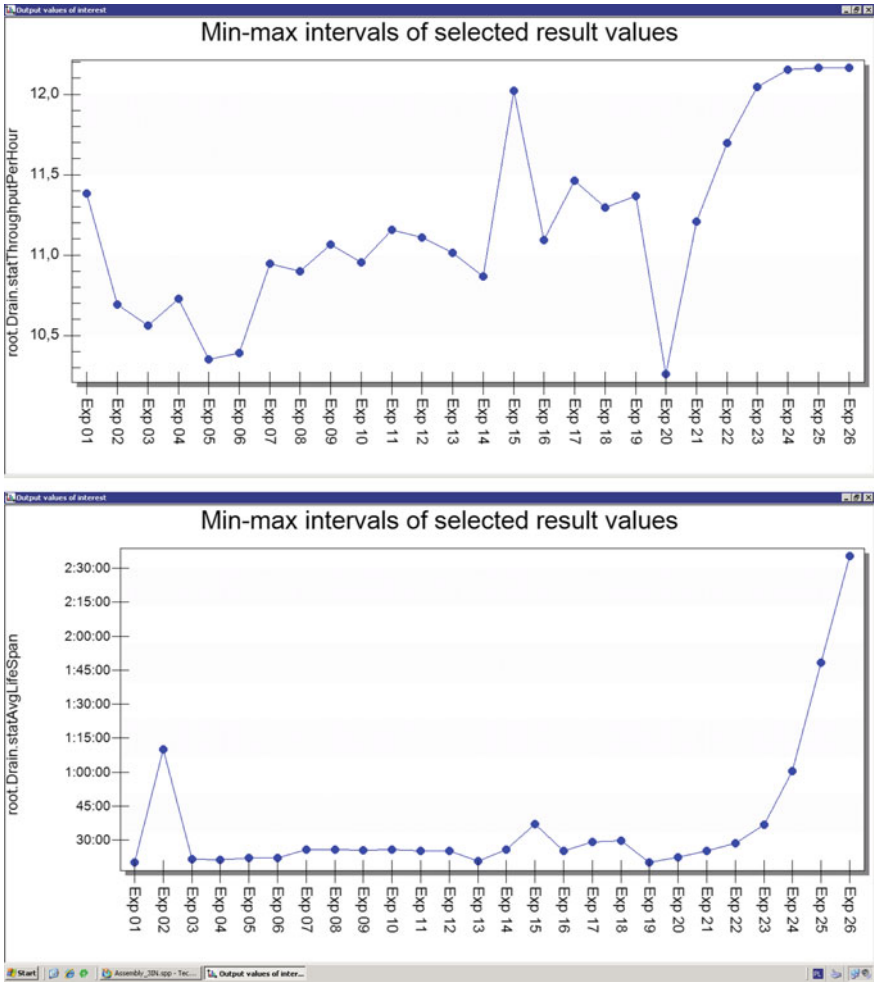
where  $f$ —the throughput of the system,  $\alpha$ —the average product lifespan.

For the variant V<sub>1</sub> the best value of production-flow index is achieved in experiment Exp 19— $\gamma = 769.76$ .



**Fig. 4** The results of the simulation experiments (throughput and average product lifespan) for variant  $V_1$

The maximum throughput of variant  $V_2$  is in experiments Exp 25 and Exp 26  $f_{25}(120) = f_{26}(180) = 12.17$  products per hour. A good result is also achieved for Exp 15, where  $f_{15}(21) = 12.02$ . The smallest throughput value is obtained in experiment Exp 20 ( $f_{20}(6) = 10.26$ ), where all buffer capacities are equal to 1. The best value of production-flow index is achieved in experiment Exp 01— $\gamma = 815.26$ .



**Fig. 5** The results of the simulation experiments (throughput and average product lifespan) for variant  $V_1$

The maximum throughput of variant  $V_2$  is in experiments Exp 25 and Exp 26  $f_{25}(120) = f_{26}(180) = 12.17$  products per hour. A good result is also achieved for Exp 15, where  $f_{15}(21) = 12.02$ . The smallest throughput value is obtained in experiment Exp 20 ( $f_{20}(6) = 10.26$ ), where all buffer capacities are equal to 1. The best value of production-flow index is achieved in experiment Exp 01— $\gamma = 815.26$  (Figs. 5 and 6).

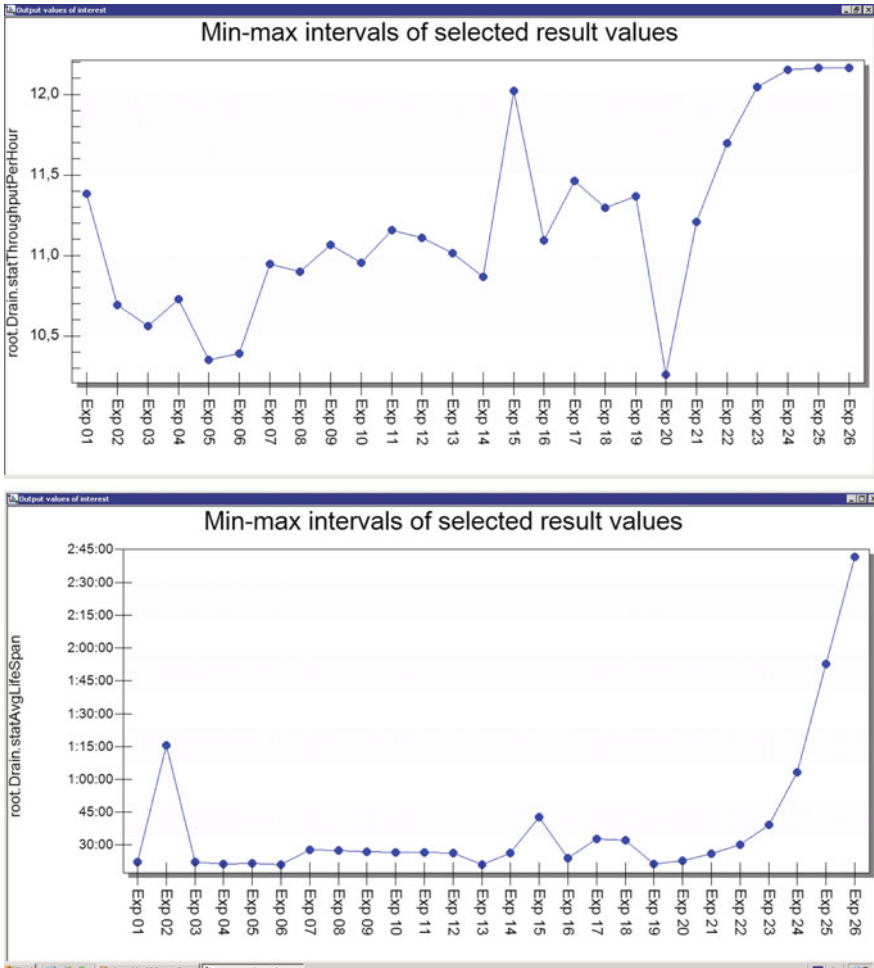


Fig. 6 The results of simulation experiments (throughput and average product lifespan) for variant  $V_3$

## 4 Conclusions

In the paper, the impacts of buffer and operation times allocation and of a assembly manufacturing system on throughput and lifespan using computer simulation method, is studied. The structure of assembly manufacturing system is proposed. Three variants of production systems are analysed. To find a good relation between throughput and average lifespan the production-flow index is proposed. On the basis of the simulation experiments conducted, the following conclusions can be formulated:

- the allocation of buffer capacity has crucial impact on the throughput and average lifespan of products. Proper buffer allocation enable to increase throughput more than 30%,
- increasing total the buffer capacity in the system results with increasing average lifespan of products,
- the greatest value of production-flow index is reached for variant  $V_2$  and Exp 01,
- the greatest value of throughput is reached for variant  $V_1$  and experiment Exp 26,
- for increasing and decreasing operation times, smaller values of system throughput is reached than for regular operation times allocation.

In further research, the more complex structures of assembly manufacturing systems will be studied using computer simulation method.

## References

1. Negahban, A., Smith, J.S.: Simulation for manufacturing system design and operation: literature review and analysis. *J. Manuf. Syst.* **33**, 241–261 (2014)
2. Kujawińska, A., Rogalewicz, M., Diering, M.: Application of expectation maximization method for purchase decision-making support in welding branch. *Manage. Prod. Eng. Rev.* **7** (2), 29–33 (2016)
3. Trojanowska, J., Żywicki, K., Machado, J.M., Varela, M.L.: Shortening changeover time—an industrial study. In: 10th Iberian Conference on Information Systems and Technologies, vol. II, pp. 92–97 (2015)
4. Vidalis, M.I., Papadopoulos, C.T., Heavey, C.: On the workload and ‘phase load’ allocation problems of short reliable production lines with finite buffers. *Comput. Ind. Eng.* **48**, 825–837 (2005)
5. Battini, D., Persona, A., Regattieri, A.: Buffer size design linked to reliability performance: a simulative study. *Comput. Ind. Eng.* **56**, 1633–1641 (2009)
6. Demir, L., Tunali, S., Eliiyi, D.T.: The state of the art on the buffer allocation problem: a comprehensive survey. *J. Intell. Manuf.* **25**, 371–392 (2014)
7. Staley, D.R., Kim, D.S.: Experimental results for the allocation of buffers in closed serial production lines. *Int. J. Prod. Econ.* **137**, 284–291 (2012)
8. Yamashita, H., Altioik, T.: Buffer capacity allocation for a desired throughput in production lines. *IIE Trans.* **30**, 83–91 (1998)
9. Gurkan, G.: Simulation optimization of buffer allocations in production lines with unreliable machines. *Ann. Oper. Res.* **93**, 177–216 (2000)
10. Kujawinska, A., Rogalewicz, M., Piłacińska, M., Kochański, A., Hamrol, A., Diering, M.: Application of dominance-based rough set approach (DRSA) for quality prediction in a casting process. *Metalurgija* **55**(4), 821–824 (2016)

# Overall Equipment Effectiveness: Analysis of Different Ways of Calculations and Improvements

Dorota Stadnicka and Katarzyna Antosz

**Abstract** An Overall Equipment Effectiveness (OEE) indicator is one of the most often used indicators, especially in large companies, to assess the level of the successful utilization of equipment. Many companies still do not calculate OEE, although the procedure of the OEE calculation is well known. On the basis of the literature review and from companies practice, it occurs that different methods of the OEE assessment are used. It is because companies identify different disturbances which influence the OEE value. The authors summarized these disturbances. In the paper, two case studies concerning the OEE calculations from manufacturing companies are presented. On the basis of the first company, it is shown how the Total Productive Maintenance (TPM) implementation may improve the value of OEE. On the base of the other company, the way the OEE calculation procedure can be improved and the results of the calculation procedure modification are presented. Finally, the authors propose to introduce weights to differentiate the influence of different OEE components. The results of the new procedure implementation are presented in the paper.

**Keywords** Overall equipment effectiveness · OEE · Production disturbances  
TPM

## 1 Introduction

Success of companies depends on how they meet customers' requirements and how much profit they can gain. Equipment effectiveness is one of the factors which have a great influence on the companies capabilities. Unfortunately, many companies still do not measure equipment effectiveness despite the fact that the procedure for calculating an Overall Equipment Effectiveness (OEE) indicator has been well known for many years [1]. There are many difficulties connected to the OEE

---

D. Stadnicka (✉) · K. Antosz  
Rzeszow University of Technology, Rzeszow, Poland  
e-mail: dorota.stadnicka@prz.edu.pl



calculations. Most of them are related to the necessity of collection the data used in the calculations of OEE and its components.

The main goal of this paper is to identify the procedures of the OEE calculations both in the literature and in practice, as well as the kind of disturbances that can influence the OEE value. Additionally, the authors wanted to present how the Total Productive Maintenance (TPM) implementation can affect the OEE value. Furthermore, the authors present the influence of different ways of the OEE calculation on the OEE value. Finally, the authors proposed the introduction of weights to differentiate the influence of different OEE components.

In this work in Sect. 2, on the basis of a literature review, the authors present an OEE origin and demonstrate the chosen methods of the OEE calculation. In Sect. 3, the review of production disturbances which can influence the OEE value are presented. Section 4 analyzes two case studies from two manufacturing companies operating in the automotive industry. The first case study presents in detail the procedure of the OEE calculation and demonstrates how the TPM implementation can improve the value of OEE. The other case study shows how by taking into consideration a planning process, disturbances concerning this process and their influence on the OEE value can be identified. In Sect. 5, discussion and the proposal of weights introduction to the OEE calculation are presented. The last section of this paper concludes the work and presents its limitations as well as the future research.

## 2 OEE Origin and Calculations

Overall Equipment Effectiveness (OEE) is a well-known indicator used for measuring manufacturing productivity for many years [1–4]. Originally, it was introduced by Seiichi Nakajima in the work [1]. OEE depends on Availability (A), Performance (P) and Quality (Q). It can be said that OEE depends on time losses, which are caused by different reasons and which result in:

- shorter planned production time than it is theoretically possible—because of errors in a planning process (schedule loss),
- shorter run time than it is theoretically possible (availability loss),
- shorter net run time than it is theoretically possible (performance loss),
- shorter fully productive time than it is theoretically possible (quality loss).

Different ways of OEE and its components calculations can be found in the literature. Some of them are presented in Table 1. The ways of the OEE calculations used in the case study companies are also included in the table.

The OEE components depend on time losses, which in turn depend on different disturbances that may appear in an organization. In order to calculate OEE, it is necessary to identify and register the losses and measure their time.

**Table 1** Ways of OEE and OEE components calculations [1, 2, 5-7]

OEE component	Planning (L)	Availability (A)	Performance (P)	Quality (Q)	OEE
Nikajima [1]	–	$\frac{LT-DT}{LT}$	$\frac{ICT \times O}{OT}$	$\frac{I-VQD}{I}$	$A \cdot P \cdot Q$
	<i>LT</i> Loading time, <i>DT</i> Downtime, <i>ICT</i> Ideal cycle time, <i>O</i> Output, <i>OT</i> Operating time, <i>I</i> Input, <i>VQD</i> Volume of quality defects				
De Groote [5]	–	$\frac{PPT-UD}{PPT}$	$\frac{AAP}{PAP}$	$\frac{AAP-NAA}{AA}$	$A \cdot P \cdot Q$
	<i>PPT</i> Planned production time, <i>UD</i> Unplanned downtime, <i>AAP</i> Actual amount of production, <i>PAP</i> Planned amount of production, <i>NAA</i> Not-accepted amount, <i>AA</i> Actual amount				
Muchiri and Pintelon [2]	–	$\frac{OT}{LT} \cdot 100$	$\frac{TCT \times AO}{OT}$	$\frac{TP-DA}{TP} \cdot 100$	$A \cdot P \cdot Q$
		$OT = LT - DT$			
	<i>OT</i> Operating time, <i>LT</i> Loading time, <i>DT</i> Downtime, <i>TCT</i> Theoretical cycle time, <i>AO</i> Actual output, <i>TP</i> Total production, <i>DA</i> Defect amount				
Sasor [6]	–	$\frac{AT}{TT} \cdot 100\%$	$\frac{PT}{AT} \cdot 100\%$	$\frac{ET}{PT} \cdot 100\%$	$A \cdot P \cdot Q$
	<i>AT</i> Available time, <i>TT</i> Total time, <i>PT</i> Productive time, <i>ET</i> Effective time				
Ptak [7] Method I	–	$\frac{AT-DT}{AT}$	$\frac{TNP}{MC}$	$\frac{TNP \times NP}{TNP}$	$A \cdot P \cdot Q$
		$DT = ST + UT + BT$			
	<i>AT</i> Available time, <i>DT</i> Downtime, <i>ST</i> Set-up time, <i>UT</i> Unplanned time, <i>BT</i> Breaks time (planned), <i>TNP</i> Total number of manufactured products, <i>MC</i> Machines capacity, <i>NP</i> Number of nonconforming products				
Ptak [7] Method II	$\frac{TAT-PDT}{NAT}$	$\frac{NAT-UDT}{NAT}$	$\frac{TNP}{MC}$	$\frac{TNP \times NP}{TNP}$	$L \cdot A \cdot P \cdot Q$
	<i>TAT</i> Total available time, <i>PDT</i> Planned downtime, <i>NAT</i> Net available time, <i>UDT</i> Unplanned downtime, <i>TNP</i> Total number of manufactured products, <i>MC</i> Machines capacity, <i>NP</i> Number of nonconforming products				

Analyzing the examples of OEE calculations presented in the Table 1, it can be said that many kinds of data have to be gathered and updated to calculate OEE [8]. The companies can utilize an automatic data acquisition systems to collect the necessary data [9, 10]. However, if they do not have any computer system such as e.g. ERP to support the maintenance process they can decide not to calculate OEE at all [8]. Although it can be recommended to calculate OEE at least for the most important machines identified with the use of the specified criteria [11]. Additionally, also production disturbances have to be identified and their time has to be measured. The disturbances are discussed in the next section of this work.

### 3 Production Disturbances and Other Wastes Influencing OEE

OEE is influenced by many production disturbances that create losses. In the literature, different kinds of disturbances and wastes that can influence equipment efficiency are presented. For example, Jonsson and Lesshamar [12] identify six big losses: **downtime losses** [(1) Breakdown losses (productivity reduction) and quantity losses (defective products). (2) Set-up (downtime) and adjustment losses (after occurring of defective products)], **speed losses** [(3) Idling and minor stoppage (interruption of production by a temporary malfunction). (4) Reduced speed losses in relation to designed speed], **quality losses** [(5) Quality defects and rework. (6) Start up losses (machine start up to stabilization at early stages of production)]. According to Jonsson and Lesshammar [12], the disturbances can be chronic and sporadic. Sporadic disturbances cause large problems, therefore they can be easy to identify. Chronic disturbances, which occur repeatedly [13], are small and hidden, and difficult in identification. They result in low utilization of equipment.

In Table 2, based on the results of the literature review [2, 12, 14], the authors present the connection of different production disturbances with the specified OEE components.

The presented disturbances cause time losses and result in the OEE minimization. Different tools, such as SMED, can be applied to minimize loss of time [15, 16].

**Table 2** Connections of production disturbances and other wastes with OEE components

Influence on OEE	Disturbances/wastes	Description
Decrease of a planned production time (an operating time)	Planning error	Machines utilization is planned incorrectly and machines are underloaded
	Shortage of staff	Because of staff shortage it was impossible to plan full machines load
	Work meetings	Time for planned meetings cannot be utilized for working
	Planned breaks	Time for planned breaks cannot be utilized for working
	Preventive maintenance	During preventive maintenance a machine cannot work
	Set-up	To prepare a machine to perform a new manufacturing task on other product
	Tool change	To perform a new manufacturing task or in case when a tool is used
	Adjustment	To adjust a machine parameters to perform a task
	Cleaning	A work stand and a machine are cleaned

(continued)

**Table 2** (continued)

Influence on OEE	Disturbances/wastes	Description
Decrease of availability	Equipment failure	Machine is not working because a failure needs to be eliminated
	Failure of software in production equipment	Machine is not working because an operating system does not work
	Failure of peripheral equipment	Material flow is disturbed because peripheral equipment does not work
Decrease of availability	Media error	Machine is not working because media are not delivered
	Subsequent stop in output flow from machine	Material flow is disturbed and the product is waiting on the work stand preventing manufacturing on the next products
	Pauses and unplanned breaks and microbreaks	Machine is not working because of small disturbances
	Incidents	Machine is not working because of operator's life-threatening incidents
Decrease of performance	Waiting time for incoming product or material	Machine is not working because of lack of materials
	Speed loss	Machine works slower because of different disturbances
	Start up	Star tup after nonconforming products identification
Decrease of quality	Start up	During start up nonconforming products can be manufactured
	Scrap or nonconforming product	Time spend for manufacturing of nonconforming products
	Human error	Errors generate manufacturing of nonconforming products
	Reprogramming	Necessary because of quality problems

## 4 The OEE Method Application in Companies—Case Studies

### 4.1 The Research Methodology

In the work, two case study companies were investigated. The main goal of this research was to identify the advantages and disadvantages of different ways of OEE calculations. The main criteria to choose the companies were that: they should be the same size companies, they should operate in the same industry, they should

have implemented TPM system and they should have different ways of OEE calculations. Both of investigated companies are large size companies and operate in the automotive industry. Both have implemented TPM system and calculate OEE indicator.

### 4.2 First Company: OEE Calculations and OEE Improvement After TPM Implementation

In the first company the manufacturing processes such as cutting, ultrasonic welding, assembly, etc., are realized. In order to calculate OEE, they collect the data concerning disturbances and connected time losses (Table 3) [6]. All registered time wastes are next assigned to an adequate category concerning availability, performance, and quality. Then, the time lost is calculated. Next, OEE is calculated. In Table 4, OEE for one machine working on one shift is calculated. It can be seen that Availability equals 86%, Performance is 93% and Quality equals 95%. Finally, OEE is 76%.

The company, in order to improve the OEE value, implemented TPM and undertaken the following activities:

- Initial cleaning—5S, identification and elimination of pollutants sources,
- Development of standards concerning maintenance of machine’s,

**Table 3** Wastes

Waste Time [min]	Quality (Q)			Performance (P)					Availability (A)				
	T	C	N	I	M	S	U	L	A	E	F	M	B
Setup										25			
Measurements	5												
Start up (idle work)				10									
Loading of material					16								
Cleaning												3	
Tool change and adjustment											12		
Tool adjustment									4				
Unplanned break													12
5S activities												5	
Scraps			9										
Repaired products		4											
Total	5	4	9	10	16	0	0	0	4	25	12	8	12
[min]	18 (Q)			26 (P)					61 (A)				

*T* Technological trials, *C* Corrections, *N* Nonconforming products, *I* Idle work, *M* Lack of material, *S* Stopping, *U* Start up, *L* Speed loss, *A* Adjustments, *E* Set-ups, *F* Failures, *M* Maintenance, *B* Breaks

**Table 4** OEE calculation; 1 shift—450 min

Indicator	Quality	Performance	Availability
OEE	$363 - 18 = 345$	$389 - 26 = 363$	$450 - 61 = 389$
0.76	$345/363 = 0.95$	$363/389 = 0.93$	$389/450 = 0.86$
76%	95%	93%	86%

**Table 5** OEE before and after TPM implementation

Machine	Q (%)	P (%)	A (%)	OEE Oct 2015 (before) (%)	OEE Apr 2016 (after) (%)
M72	100	51.8	75.7	39.2	42.10
M74	100	52	72.7	37.8	38.30
M84	100	57.9	73.9	42.8	46.70
M91	100	81.7	72.4	59.1	63.30

- Development of lists of autonomous maintenance, operators' training,
- Reorganization of work stands,
- Autonomous maintenance implementation.

The undertaken activities brought OEE improvement which is presented in Table 5 for the four chosen machines.

The company applied a standard method to calculate OEE (see Table 1—Sasor [6]) which it consequently uses.

### **4.3 The Other Company: OEE Calculations According to the Standard and Improved Method**

In the second analyzed company, the main types of the machines include hydraulic and mechanical presses. The data from own research and data from work [7] were taken for the analysis. The analyzed company calculates indicators of machine efficiency related to Performance, Quality and Availability, which are the components of the OEE indicator. In order to determine the values of these indicators the needed data, i.e., machines used in a manufacturing process, the number of manufactured products, the number of nonconforming products, planned and unplanned downtime were gathered. Initially, to calculate the components of OEE and the total value of this indicator, the standard formulas were used (see Table 1—Method D). The values calculations of OEE components were made for a chosen machine. The company was satisfied with the presented OEE calculation method. However, a detailed analysis pointed out that in calculating the indicator of Availability both planned and unplanned downtimes were taken into account.

Therefore, the company proposed to change the method of the OEE calculation, where the influence of planned and unplanned downtimes on the value of the OEE can be shown. The new way of the OEE calculation (see Table 1—Method II) uses four indicators: Planning, Availability, Performance and Quality. Planning is the total net available time per a month. It means that there is 1440 min (24 h) available per day minus all the planned downtimes such as national or local holidays, the shutdown of production, Preventive Maintenance and other planned downtimes like trainings and workshops. Unplanned downtimes include mainly failures (break-downs), the loss of speed or working on idling, and others like set-ups, waiting or material loss. Additionally, availability (net operating time) is used to calculate performance. Performance gives information about on how well the machine is used when working. Other indicators of Performance and Quality are calculated as previously. Table 6 shows the wastes which are taken into account in order to calculate OEE and which have influence on the values of all the components.

After changing the calculation method of OEE for the chosen machines the needed data were collected and the OEE values were calculated. Table 7 shows the value of OEE1 which were calculated with the new method on the selected work stand for the chosen period of time (monthly). Additionally, the difference (D) between the previous and the current values of OEE and OEE1 was shown.

Based on the OEE results, it can be observed that changing the method of OEE calculation has affected its value. In all cases, the OEE value decreased by a few percent. The highest deference of values was observed in the last period of time (3 months), and the lowest in 2 months.

**Table 6** Wastes in OEE components calculation

Planning L	Availability A	Performance P	Quality Q
National or local holidays Shutdown of production Preventive Maintenance Internal or external trainings. workshops	Failures (breakdowns) Waiting or lost for material Break caused by physiological need (i.e. breakfast. lunch). Set-up	Speed loss Start up (idle work)	Nonconforming products

**Table 7** OEE for the chosen machine after changes (monthly)

Ind.[%]	1	2	3	4	5	6	7	8	9	10
OEE Meth. I	61.13	64.10	60.87	62.16	61.68	59.29	59.73	61.24	59.66	67.08
OEE1 Meth. II	59.06	63.32	53.15	61.10	60.09	57.61	57.15	57.19	55.09	62.72
D	2.07	0.78	7.72	1.06	1.59	1.68	2.58	4.05	4.56	4.36

**Table 8** OEE values for the first company after reevaluation

Indictors [%]	1	2	3	4	5	6	7	8	9	10
Availability	79.36	79.97	77.57	79.80	77.21	74.94	75.94	76.08	74.13	78.17
Performance	77.24	80.36	78.69	78.10	80.06	79.33	78.89	80.74	80.70	85.94
Quality	99.73	99.75	99.72	99.74	99.78	99.73	99.70	99.70	99.72	99.85
OEE before	61.13	64.10	60.87	62.16	61.68	59.29	59.73	61.24	59.66	67.08
OEE after	85.05	85.98	84.44	85.44	84.55	83.26	83.66	84.10	83.12	86.23



## 5 Discussion and a Proposal for OEE Calculation Improvement

The weakness of the presented methods is that all components of the OEE calculation are treated at the same level. The Quality, Availability and Performance indicators have the same effect on the final value. However, from the company point of view, the components might have a different importance. The authors propose to introduce weights ( $w$ ) for individual components using an empirical formula (1).

$$OEE = w_1A * w_2P * w_3Q \quad (1)$$

where:  $w_1 + w_2 + w_3 = 1$ .

The weights shall be decided by the management of a particular manufacturing organization based on their needs. In the case studies analysis it was discovered that the Availability is the most important component for the companies, then Quality and Performance. Based on authors experience and discussion, weights of the formula (1) were decided as:  $w_1 = 0.5$ ,  $w_2 = 0.2$ ,  $w_3 = 0.3$ . Then, the same data gathered from the first company was reevaluated using the proposed empirical model. Table 8 shows the evaluation results.

Table 8 shows that after reevaluation the value of OEE increased. Almost all the values are close to 85%. The proposition of changing the way of OEE calculation will be discussed in the further studies.

## 6 Conclusions

The paper presents thoughts concerning the OEE indicator for the equipment efficiency assessment. On the basis of the analysis, the authors conclude that in the literature different ways of OEE calculation are presented as well as the companies utilize different ways in practice. Therefore, it may be difficult to implement benchmarking and compare one company with others when they use different calculation procedures. However, when a company decides on a calculation method. It can compare its own improvements within time.

The weakness of used models of OEE calculation is that level of excellence was set to value more than 85% of OEE [17, 18]. In many companies is very hard to achieve this level. Although, it can be said that, for example, TPM can really improve the OEE value. Additionally, the companies can experiment with the OEE calculation procedure and develop an OEE equation including the losses concerning a planning process. Generally, it will result in the minimization of the OEE value which again cannot be compared with the results of other companies. The authors also presented a way of OEE calculation, which introduces weights of OEE components what again make the calculations more complex.

The presented studies have limitations. Only two companies were analyzed in detail. Therefore, in the future studies, the proposed OEE calculation including wastes in a planning process should be tested in other companies, as well as the proposed new method for OEE calculation.

## References

1. Nakajima, S.: Introduction to Total Productive Maintenance. Productivity Press, Cambridge, MA (1988)
2. Muchiri, P., Pintelon, L.: Performance measurement using overall equipment effectiveness (OEE): literature review and practical application discussion. *Int. J. Prod. Res.* **46**(13), 3517–3535 (2008)
3. Jasiulewicz-Kaczmarek, M., Piechowski, M.: Practical aspects of OEE in automotive company—case study. In: 3rd International Conference on MSMI, 2013–2018 (2016)
4. Azizi, A.: Evaluation improvement of production productivity performance using statistical process control, overall equipment efficiency and autonomous maintenance. *Procedia Manuf.* **2**, 186–190 (2015)
5. De Groote, P.: Maintenance performance analysis: a practical approach. *J. Qual. Maintenance Eng.* **1**(2), 4–24 (1995)
6. Sasor, S.: Improvement of machines reliability by TPM implementation Left blank to preserve the authors anonymous (2016)
7. Ptak, D.: Analyze and improvement of the technological machines in the chosen company Left blank to preserve the authors anonymous (2015)
8. Kłos, S., Patalas-Maliszewska, J.: The impact of ERP on maintenance management. *Manage. Prod. Eng. Rev.* **4**(3), 15–25 (2013)
9. Hedman, R., Subramaniyan, M., Almström, P.: Analysis of critical factors for automatic measurement of OEE. *Procedia CIRP* **57**, 128–133 (2016)
10. Singh, R., Shah, D.B., Gohil, A.M., Shah, M.H.: Overall Equipment Effectiveness (OEE) calculation—automation through hardware & software development. *Procedia Eng.* **51**, 579–584 (2013)
11. Stadnicka, D., Antosz, K., Ratnayake, R.M.C.: Development of an empirical formula for machine classification: prioritization of maintenance tasks. *Saf. Sci.* **63**, 34–41 (2014)
12. Jonsson, P., Lesshamar, M.: Evaluation and improvement of manufacturing performance measurement systems—the role of OEE. *Int. J. Oper. Prod. Manage.* **19**(1), 55–78 (1999)
13. Nord, C., Pettersson, B., Johansson, B.: TPM: Total Productive Maintenance med Erfarenhet från Volvo (in Swedish), Idrottens Grafiska i Göteborg AB, Mölnlycke (1997)
14. Bokrantz, J., Skoogh, A., Ylipaa, T., Stahre, J.: Handling of production disturbances in the manufacturing industry. *J. Manuf. Tech. Manage.* **27**(8), 1054–1075 (2016)
15. Lintilä, J., Takala, J.: Reducing time losses in operational actions of a food production lines. *Manage. Prod. Eng. Rev.* **4**(1), 39–49 (2013)
16. Trojanowska, J., Żywicki, K., Machado, J.M., Varela, L.R.: Shortening changeover time—an industrial study. In: 10th Iberian Conference on Information Systems and Technologies (CISTI), vol. II, pp. 92–97 (2015)
17. Wauters, F., Mathot, J.: Overall equipment effectiveness, pp. 27–28. ABB Inc., Ohio (2002)
18. Japan Institute of Plant Maintenance: OEE for Operators: Overall Equipment Effectiveness. Productivity Press, Cambridge, MA (2010)

# Verification of the Method for Assessing Productivity, Taking into Account Logistical Processes in Manufacturing Companies

Michaela Rostek and Ryszard Knosala

**Abstract** The aim of the article is to present the results of research related to the assessment of the productivity of a manufacturing enterprise taking into account logistic processes. Verification of the method for assessing productivity in a food business was carried out. In this method, the partial indicators of productivity regard the efficiency of the use of individual logistic processes as inputs in manufacturing companies. The results have been presented in the article along with the conclusions. It was observed that logistical processes have a relation to productivity. Changes in the company's logistics processes caused changes in the productivity index.

**Keywords** Evaluation · Logistics processes · Production · Productivity measurement

## 1 Introduction

Changes in the global and domestic economy cause logistics and production management to be of more and more importance at the moment. Among the reasons for such changes are increased competition, improvement of manufacturing processes and production technology, increased emphasis on quality of processes, products, customer service, as well as increased expectations of buyers [1]. The tasks of logistics include, among all: order acceptance and coordination, production planning, synchronized supply security, relationships with suppliers, purchasing, supply chain management, transport, warehouse management. These tasks allow to perceive the functioning of the enterprise as a coupled sequence of processes [2–4].

Both productivity and logistics processes in a manufacturing enterprise are elements which should be analyzed and improved. When examining productivity, the impact of logistical processes on the performance of the indicators should be

---

M. Rostek (✉) · R. Knosala  
Opole University of Technology, Opole, Poland  
e-mail: m.rostek@po.opole.pl

taken into account. On the other hand, when analyzing individual logistical processes in a manufacturing enterprise, it is worth to focus on their ability to impact the performance indicators of the enterprise. This is why an attempt was made to examine the productivity of an enterprise in terms of logistics processes.

## 2 Productivity in Manufacturing Enterprises

Productivity is a relationship between the goods and services produced in a certain period, and the resources consumed to produce them in that period. This relationship is expressed in the equation [5–7]:

$$P = \frac{\text{Output at based period}}{\text{Total of all inputs at base period}}.$$

In literature, productivity is divided due to labor and capital, as well as materials and energy. These are the most common divisions. Productivity can be calculated as partial ratios. There are different ratios for each inputs, for example [5, 8]:

$$P_{\text{Labor}} = \frac{\text{Output at base period}}{\text{Labor input at base period}},$$

$$P_{\text{Materials}} = \frac{\text{Output at base period}}{\text{Materials input at base period}},$$

$$P_{\text{Energy}} = \frac{\text{Output at base period}}{\text{Energy input at base period}},$$

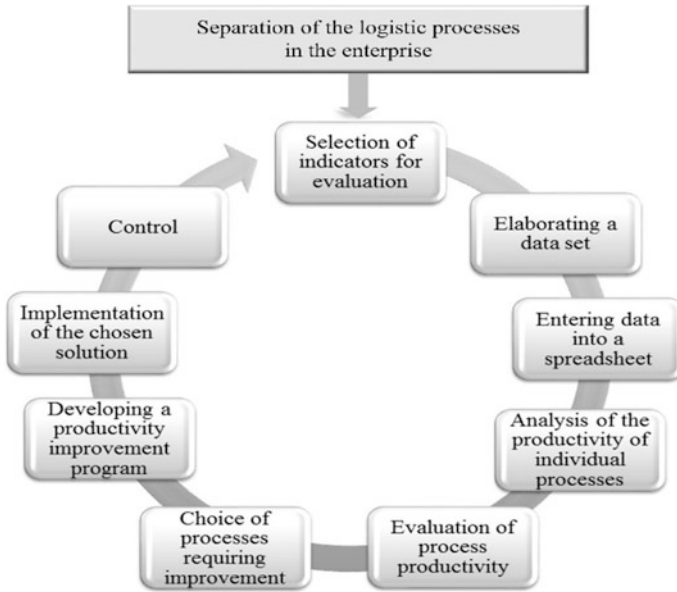
$$P_{\text{Capital}} = \frac{\text{Output at base period}}{\text{Capital input at base period}}.$$

In enterprises, productivity ratios can be shared according to departments, processes, positions, etc. [5].

There is no significant focus on logistics in an enterprise and attempts to indicate its impact on the productivity of an enterprise. The objective of productivity is to maximize output and minimize input [8–11].

## 3 Short Description of the Methodology

The proposed general model for evaluating productivity (Fig. 1) was developed with a significant focus on logistic areas in an enterprise. In the presented model, 5 stages can be distinguished, which are the next stages of the entire method:



**Fig. 1** A general model for assessing the productivity of manufacturing companies

1. extracting processes,
2. preparing data for analysis,
3. analysis and assessment of productivity,
4. developing a productivity improvement program,
5. control.

Not each of these stages has to be realized in an enterprise. In part of them, the classification of processes has already been made, then it is possible to omit this stage. The second stage should rather be implemented each time unless we perform another analysis for the same set of data. Each stage consists of different elements. Some of them may also be omitted.

Starting a productivity analysis in an enterprise, taking into account logistic processes according to the methods shown in Fig. 1, it is worth to first elaborate a map of the process. It should contain information consistent with the reality of the business. The headings should include divisions/departments/cells that will be involved in the implementation of each stage. This map will make it easier to identify the people responsible, and will also clearly indicate the next steps to be taken, with which it is worth to familiarize before undertaking a logistic process productivity test.

In the presented model, the first step is to separate the logistics processes in the enterprise. For this purpose, the person or persons responsible for the classification of logistical processes should be chosen. If there is already a clear division of

processes in the enterprise, this step can be omitted and it is possible to move on to the next phase of productivity assessment, based on the current classification in the enterprise.

The second stage consists of preparing the data for analysis, which consists of the following steps:

- selection of indicators for evaluation,
- elaborating a data set,
- entering data into a spreadsheet.

The choice of indicators for evaluation is based on familiarizing with the indicators used for this purpose and selecting for each process one representative of the process. Depending on the number of distinguished logistical processes, such an amount of productivity indicators should be analyzed. The development of data needed to carry out the assessment and further analysis is linked to the earlier step, because the choice of a specific indicator should be made in the light of the possibility of its designation.

The third stage consists of the following steps:

- analysis of the productivity of individual processes,
- evaluation of process productivity,
- choice of processes requiring improvement.

In the first place, the values of selected sub-indices for logistics processes in an enterprise should be determined. In the frame of this step, a dynamic analysis of the results, a comparative analysis, etc., is performed. The comparative analysis is performed at the time selected for analysis by comparing the results with some reference values. The model may be the value of the indicator in other units or in general for a given branch. The next step is to assess the productivity of the logistics processes. It is supposed to rely on assessing the value of the productivity ratios of each logistic process and deciding whether its level is good or whether it needs improvement. This leads to another step in which analysts should decide which processes require improvement.

The penultimate stage includes steps such as:

- developing a productivity improvement program,
- implementation of the chosen solution.

The penultimate stage requires knowledge of the processes and problems that may occur. Based on the collected data and knowledge, many alternative solutions need to be considered. A team of several people can come up with a number of solutions and think which of them has the potential to produce the expected results with the least cost and minimal changes in the system. In the beginning, a detailed improvement solution is being developed. In works related to productivity, there is mention of productivity improvement programs. This step is supposed to lead to the creation of such a program for an enterprise. Of course, you can develop several solutions at this stage, each for a different process that will create a coherent

program. In situations where there is an urgent need to improve more a few one process, it is helpful to develop a productivity improvement plan with several solutions. The next step is to implement the chosen solution. It is important to carefully and precisely carry out what was foreseen for in the productivity improvement program.

The last step in the entire method of productivity improvement is control, i.e., system monitoring after the changes have been made. Verification of the effectiveness of the implemented solution by examining the current total enterprise productivity index and the sub-indices which were previously selected for the examination. A correctly carried out method has a result of an improvement in the overall productivity index by improving the partial productivity index. Unfortunately, there might be situations where the result of a revised process will be better, and the indicator for another process will be worse. In logistical processes, it is a relation that needs to be addressed. In this case, one should focus on assessing the company's productivity.

## 4 Verification of Methodology in Enterprise

Verification was carried out in a medium company from the food industry. Based on the model presented in Fig. 1, a map of the process of implementing the productivity test with a focus on logistical processes was elaborated (Fig. 2). Next, steps were taken to verify the correctness of the proposed model and the possibility of implementation in the manufacturing company.

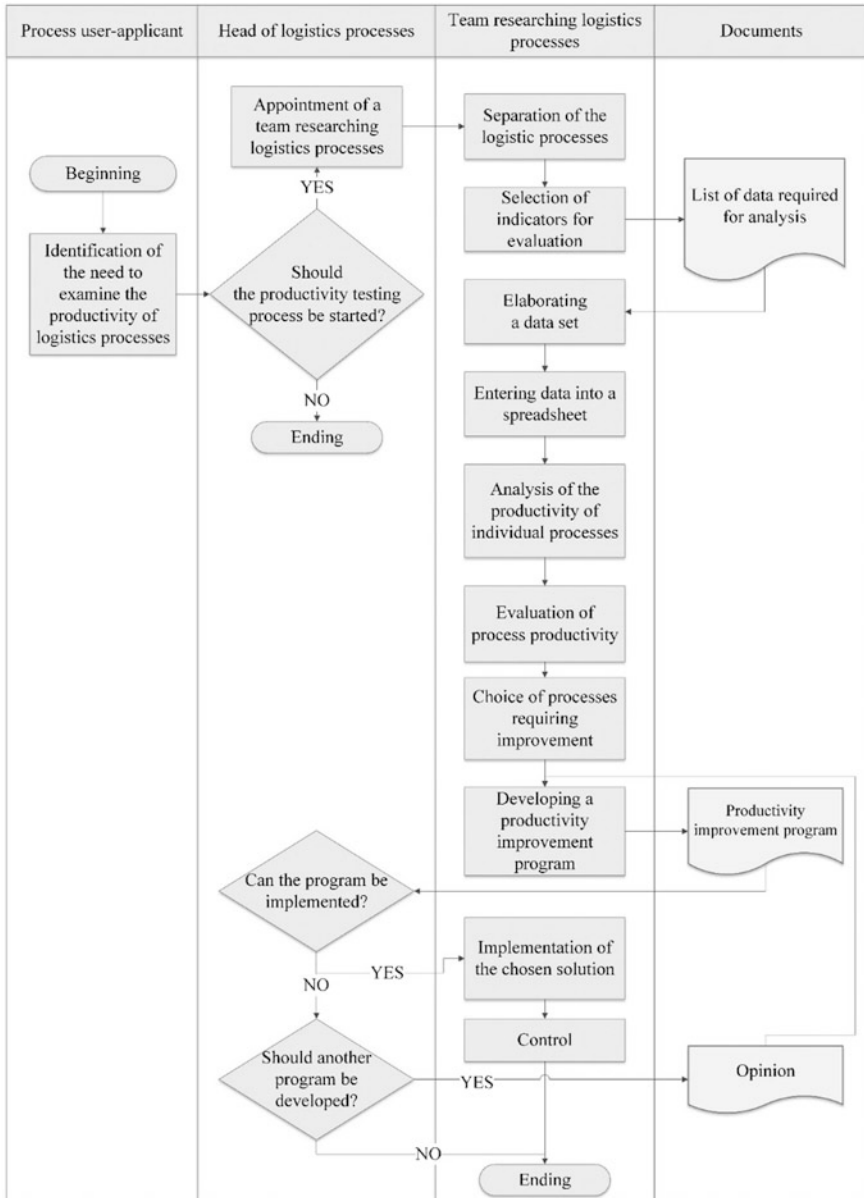
In the first stage, the division of logistic processes in the company was made. Processes were disguised: distribution, production, supplies, warehousing.

Figure 3 presents a division of productivity ratios that take into account logistical processes. This is related to the next step—the choice of indicators for analysis. By dividing the indicators in this way, it is important to remember that in addition to the logistic processes, other processes are carried out in the enterprise and have been emphasized in the figure as the productivity of the remaining processes.

In the next step, it is possible to set more specific indicators, due to the resources involved. Then, for the selected processes, additional productivity indicators are determined, due to the resources used: capital, materials, labor, energy.

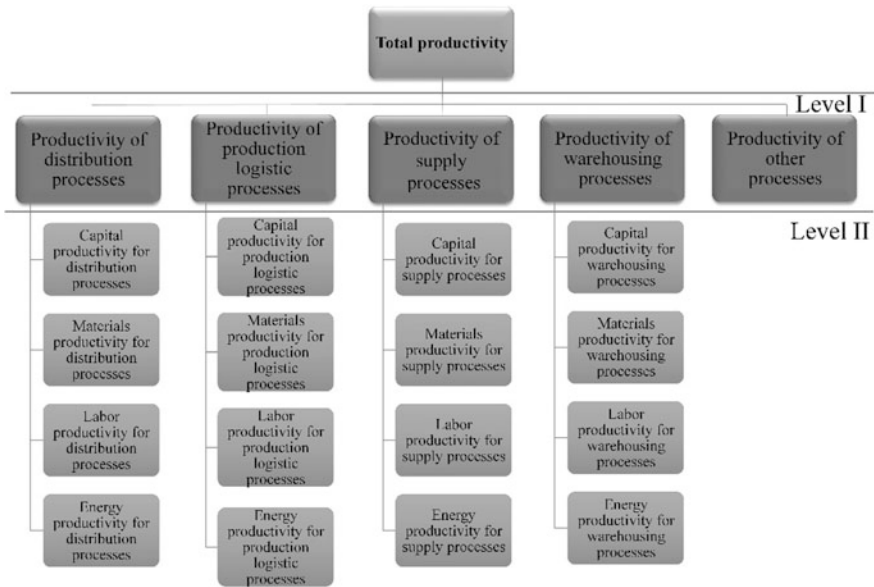
After the selection of indicators for analysis, data was collected by the person assigned to this task. The data was aggregated and segregated in a spreadsheet. Then, appropriate formulas were introduced to determine the productivity ratios.

The next step was to analyze the productivity of the logistic processes and the assessment of the situation. By dividing the productivity coefficients by logistic processes, 4 productivity ratios were determined:



**Fig. 2** Process map of the company’s productivity evaluation taking into account logistic processes for the examined company (own elaboration based on [12])





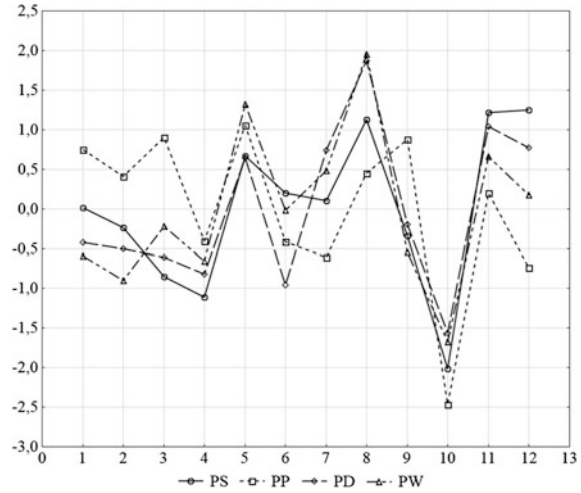
**Fig. 3** Diagram of the division of productivity indicators taking into account logistical processes [13]

- distribution (PD)—it is the relationship between sales revenue and all inputs which was needed to distribution processes,
- production (PP)—it is the relationship between sales revenue and all inputs which was needed to logistic production processes,
- warehousing (PW)—it is the relationship between sales revenue and all inputs which was needed to warehousing processes,
- supplies (PS)—it is the relationship between sales revenue and all inputs which was needed to supplies processes.

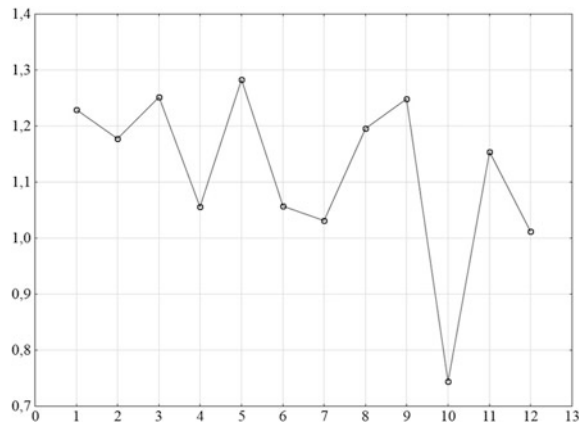
Productivity has in numerator outputs. In this case, sales revenue are used as numerator. In denominator should be inputs. In partial productivity ratios taking into account logistic processes everything what is used in each logistics process are treated as inputs. And in that way, the ratios were measured by logistic processes.

The standardized results, which were performed in the STATISTICA program for presentation in one drawing, are presented in Fig. 4. Standardization also allows comparison of these samples with respect to each other. The tenth month of analysis in which all indicators drastically decreased is characteristic. What is more, the total productivity index (Fig. 5) for this month was very low. Then, the costs exceeded sales revenue. It was one of the final months of the year in which companies make investments to reduce annual profits. It also affected productivity ratios. The development of infrastructure causes the value of resources used in processes to increase and the productivity index to decrease. According to this distribution of indicators, the productivity of distribution shows the greatest variability of all

**Fig. 4** Partial productivity for the examined enterprise, taking into account a division due to logistical processes



**Fig. 5** Total productivity for the examined enterprise



**Table 1** Coefficients of variation of sub-productivity in the examined enterprise

Productivity	PS	PP	PD	PW
Average	154.27	1.16	125.29	79.64
Standard deviation	19.32	0.16	18.89	11.61
Coefficient of variation (%)	12.52	13.72	15.08	14.57

analyzed processes (Table 1). Productivity of the warehouses has a similar variability. This is due to the dependence between these processes—if the goods are not delivered, they are therefore stored in the warehouses. Conversely, low inventory levels are due to the systematic delivery of goods coordinated with production. Based on the analysis, we have selected processes that need improvement and jointly decided to develop a solution to streamline the distribution process.

During the development of the improvement solution, one had to reflect on the possibilities of changes in distribution that would allow to improve the process. Out of several ideas, it was decided to consider in detail the employment of an additional employee. It was a real solution from the point of view of company management. This solution would enable to streamline the work of the current team and focus on gaining new orders. An additional person in the team could help improve customer service. On the negative side, there was an increase in costs associated with employing a new employee. This solution has been accepted.

Implementation of the solution took place in the 16th month. Already after the next three months, positive trends were seen, namely a gradual increase in the productivity of distribution processes. Apart from the increase in process costs, this effect was also expected to increase the sales revenue. For the overall productivity index after a slight decline, an increase in value was noted. Apart from the distribution processes, total productivity is affected by the remaining processes, so growth was not significant. Therefore, after the control period, the entire process can be started from the first stage (Fig. 1).

## 5 Conclusions

Productivity is a complex issue in manufacturing companies. It is worth analyzing it taking into account logistical processes. The paper presents the verification of the proposed methods of productivity research, with particular emphasis on logistics processes in manufacturing companies.

Verification was made in a medium-sized enterprise, where logistics, supply, distribution, and warehousing processes are implemented. Next steps were taken according to the proposed model. Each of these stages was carried out according to a map of the process of productivity research. This map identifies the steps and people responsible for their implementation. It took most of the time to collect data for analysis and carry out the analysis itself.

In the examined enterprise, not all data has been aggregated so far in such a way to immediately set performance indicators. The enterprise wanted to make changes in this area. After compiling the data, another labor-intensive phase was their analysis. The next step was the improvement of the solution, after selecting processes requiring improvements. Implementing the chosen solution (employing an additional employee) has allowed to see an increase in the productivity of the distribution process and sales revenue.

After verification, it is considered reasonable to divide the productivity ratios due to logistical processes. The proposed model of implementing productivity research in a manufacturing enterprise with a special focus on logistics is possible in medium-sized enterprises. The productivity problem is seen by management. The potential for improving the efficiency of the resources used is appreciated by the companies concerned. In the researched enterprise, the assumption of

reproducibility of the productivity analysis process was confirmed. One of the processes has been improved and it has been noted that further ones can also be streamlined.

The change in logistical processes has also resulted in a change in total productivity. The analysis of productivity in the whole examined period confirms this relationship. It is, therefore, reasonable to argue that changes in logistical processes are causing changes in the productivity of an enterprise.

## References

1. Bendkowski, J., Matuszek, M.: Production logistics practical aspects. Part I Planning and production control (in Polish), Gliwice (Silesian University of Technology) (2013)
2. Grant, D.B., et al.: Fundamentals of logistics management, Maidenhead. McGraw-Hill Education, USA (2006)
3. Krawczyk, S.: Management of logistics processes (in Polish), Warsaw (PWE) (2001)
4. Murphy, P.R. Jr., Wood, D.F.: Contemporary logistics, New Jersey. Pearson Education International, USA (2011)
5. Kosieradzka, A.: Enterprise productivity management (in Polish), Warsaw. C.H. Beck, German (2012)
6. Nagashima, S.: 100 management charts, Tokio. Asian Productivity Organization, China (1992)
7. Saari, S.: Productivity. Theory and measurement in business, European productivity conference, Finland (2006)
8. Christopher, W.F.: Productivity measurement handbook, Cambridge. Productivity Press, USA (1985)
9. A Guide to Productivity Measurement, Singapore (SPRING Singapore) (2011)
10. Sink, S.: Productivity management—planning, measurement and evaluation control and improvement, New York. Wiley, USA (1985)
11. Lovell, C.A.K.: Recent developments in productivity analysis. *Pacific Econ. Rev.* **21**, 417–444 (2016). doi:[10.1111/1468-0106.12191](https://doi.org/10.1111/1468-0106.12191)
12. Rostek, M., Knosala, R.: Research productivity of logistics as a process in manufacturing companies (in Polish), *Entrepreneurship Manag.* **XVII**(12), 2, 435–445 (2016)
13. Rostek, M., Knosala, R.: Comparison of two methods of division productivity of logistic processes in manufacturing companies (in Polish). *Bus. Manag.* **3**, 31–38 (2016)

# The Impact of Task Balancing and Sequencing on Production Efficiency

Krzysztof Zywicki, Paulina Rewers, Lukasz Sobkow and Dawid Antas

**Abstract** The paper contains an evaluation of the impact of assembly-line balancing and scheduling on production efficiency. It describes issues connected with assembly-line balancing and the rules of scheduling production tasks. Some problems are indicated connected with the functioning of assembly line before the improving actions began, which have been eliminated by means of the assembly-line balancing and a new method of scheduling. Results connected with improved productivity and production efficiency are shown.

**Keywords** Improving production · Balancing assembly processes  
Scheduling · Production efficiency

## 1 Introduction

Flow-shop manufacturing systems are currently used in many industries to manufacture various products. One of the methods of the organization is the assembly-line system in which a certain number of workstations is concentrated around a conveyor belt or another conveying system [1]. The first moving assembly line was introduced to mass production of model T Ford by Henry Ford in 1913 in his factory in Highland Park (Michigan) [2]. It became a benchmark for mass production methods worldwide. It is currently more and more frequently the case that several variants or models of products are assembled on a single line [3]. This is caused inter alia by shorter life cycle of products, very fast introduction of new models on the market and a wide range of variants of the same model. It necessitates efficient designing of products that fulfill individual requirements of

---

K. Zywicki (✉) · P. Rewers · L. Sobkow · D. Antas  
Chair of Management and Production Engineering, Poznan University of Technology,  
Piotrowo 3 Street, 60-965 Poznan, Poland  
e-mail: krzysztof.zywicki@put.poznan.pl

© Springer International Publishing AG 2018  
A. Hamrol et al. (eds.), *Advances in Manufacturing*, Lecture Notes in Mechanical Engineering, [https://doi.org/10.1007/978-3-319-68619-6\\_7](https://doi.org/10.1007/978-3-319-68619-6_7)

customers. This is possible mostly by implementing a strategy of mass customization [4]. To catch up with quickly evolving and competitive market, manufacturers must keep on improving the quality of their products, while at the same time decreasing their prices and shortening the manufacturing time. In such a case, methods connected with statistical analysis of manufacturing processes, which enable quality inspection of products and undertaking reasonable decisions, gain particularly significance [5–9]. The need of increasing the diversity of products by companies makes it necessary to ensure close integration of product design processes with production flow control [9–13].

Only then will it be possible to utilize fully the manufacturing potential of an enterprise which owns modern technical resources compliant with the concept of Industry 4.0 [14–16].

Such a situation makes proper planning of assembly process (balancing) difficult for many companies [17].

Assembly-line balancing is about striving to achieve a uniform, considering the assembly time, arrangement of a complete set of tasks on workstations connected in a series, to achieve a minimum amount of idle time. An assembly line is considered ideally balanced if the number of workstations is limited to minimum, the same number of tasks is performed on each of them, and total amount of idle time (i.e. a sum of idle times at all workstations along the line) is as short as possible with the given level of production [18].

During an assembly-line balancing, work components should be grouped by imposing the following three limitations: [19].

- cycle time  $c$ , which is interpreted as the interval between subsequent products leaving the line, longer or equal to the time of the most loaded workstation,
- sequential relations between tasks which result from construction technology of the manufactured product and which specify the possibility of their ordering. This enforces earlier completion of specific tasks in relation to others,
- number of workstations  $K$  must not be higher than the number of tasks  $N$ , however, the minimum number of workstations  $K$  is 1.

Organizational changes performed while balancing assembly-lines are most often limited by one of the following two problems:

- a defined assembly tact, the number of production workers at the line is unknown,
- a defined number of workers at a given assembly line, the assembly tact is unknown.

By analysing the diversity of products manufactured on a single assembly line, the following three forms of balancing can be specified [20]:

- reducing the number of workstations with imposed fixed tact,
- change in the line tact with a fixed number of workstations,
- increasing the assembly line efficiency by a change in the tact and the number of workstations for a given product.

An important aspect of assembly-line operation ensuring the most effective assembly is adequate planning of task performance sequence. Production schedule for multi-version lines determines the number and type of products manufactured in a given planning period. The primary goal of scheduling is to determine when a given manufacturing task should be performed, so that the cost of storage are minimized and any delay in order performance is eliminated [21]. The major problem in preparing a schedule for multi-version lines is the sequence in which subsequent production batches should be manufactured to minimize the waste time resulting from change-overs [22, 23]. Although production scheduling for products of the same tact time seems uncomplicated, planning a sequence of assembly for products of different tact times in such a way as to obtain the most efficient production is problematic.

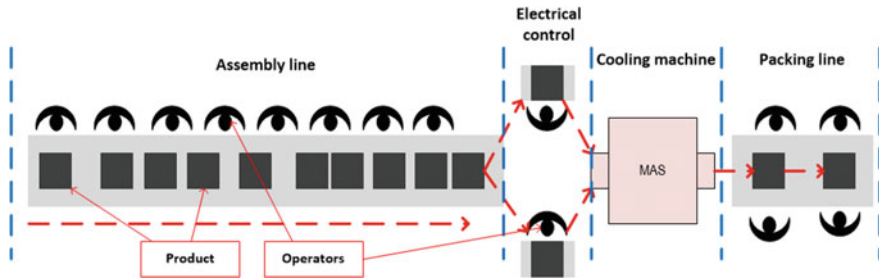
The paper describes the process of improving the assembly-line operation aiming at improving efficiency as a result of balancing and assuming the rules of production task scheduling.

## 2 Description of the Analysed Assembly Line

The example of actions undertaken in order to improve production efficiency, described in this paper, concerns the assembly line of electric cooktops used in households.

The analysed assembly line is a serial line on which 105 types of products are assembled. The high number of variants is connected with differences in labour required to perform the assembly processes. Depending on the manufactured type of product, 12–15 workers are involved in the assembly process. 6–9 operators perform work which is directly connected with assembly, two employees perform quality control (the so-called electrical inspection), and then, once the cooktops pass through the cooling tunnel (MAS) and cool down, four operators pack the finished products. The products are assembled by subsequent operators, who perform specified tasks. In theory operators are assigned to certain workstations where the necessary assembly components are stored. A semi-finished product is transferred between operators automatically on the conveyor until the finished product is packed into a cardboard box and put on the pallet. The pattern is repeated for each piece of the production batch (Fig. 1).

In the primary state of organization of assembly processes tasks were assigned in a simplified way. Due to that, a sort of freedom in performing tasks on the workstations by the employees could be noticed. During observation of the assembly process, it was often noticed that the workers who performed tasks which were less labour intensive, once they collected a certain stock of components, they helped operators who worked on more loaded workstations. Such a situation occurred when a worker who was performing less labour-intensive tasks had to wait until the preceding operator completed his/her task.



**Fig. 1** Diagram of the analysed assembly line

Thus, major disadvantages of the current system can be summarized as follows:

- lack of operator working standards;
- lack of effective production flow control system;
- lack of possibility to define precisely the cycle time (tact);
- operators moving between individual workstations on the line;
- mutual help which disturbs the organized assignment of tasks.

### 3 Improving Operation of the Assembly Line

The improvement actions aimed at enhancing the productivity and production efficiency covered the following scope of work:

1. Separating product families—to divide products by their structural similarity.
2. Analysis of the assembly labour intensity—to recognize tasks performed on individual workstations and to determine time required for the performance.
3. Assembly-line balancing—to level the load of assembly workstations.
4. Drawing up the rules of scheduling—to adopt rules of sequencing manufacturing tasks to reduce waste time resulting from changing the type of manufactured products.
5. Evaluation of the suggested solutions with regard to efficiency and production efficiency.

#### 3.1 Separating Product Families

Separating product families were connected with determining their structural similarity. It aimed at separating products for which further actions related to the analysis of labour intensity can be performed on selected representatives. Three criteria of division were assumed: type of heating—four types, number of the



heating hob—three types, the control method—two types. As a result, all the products were grouped into 11 families.

### 3.2 Analysis of Product Assembly Labour Intensity

At this stage, an analysis was performed to separate tasks performed on individual workstations for representatives of individual product families, and duration of task performance by operators was measured. The analysis was performed for three shift teams of operators in different periods of work system (production shifts). As a result, a list of tasks necessary for proper performance of assembly operations was prepared and adequate duration times for performance of the tasks were assumed.

Figure 2 shows the diagram of assembly labour intensity. The assembly process is made up of 30–50 tasks depending on the product family, which are performed by 12–15 operators assigned to 10–13 workstations.

The analysed conditions of the assembly organization did not allow to determine the actual tact *s* that would indicate the times when products leave the line, as the work was irregular because operators were moving along the assembly line. Consequently, since the tact time had not been determined, the time of the conveyor movement was set freely, not in line with the pace of work performed on individual workstations. The freely selected time of movement of the assembly line caused that the operators were in the middle of performing work on a current product when the line was moving. That was why they collected the products or followed the

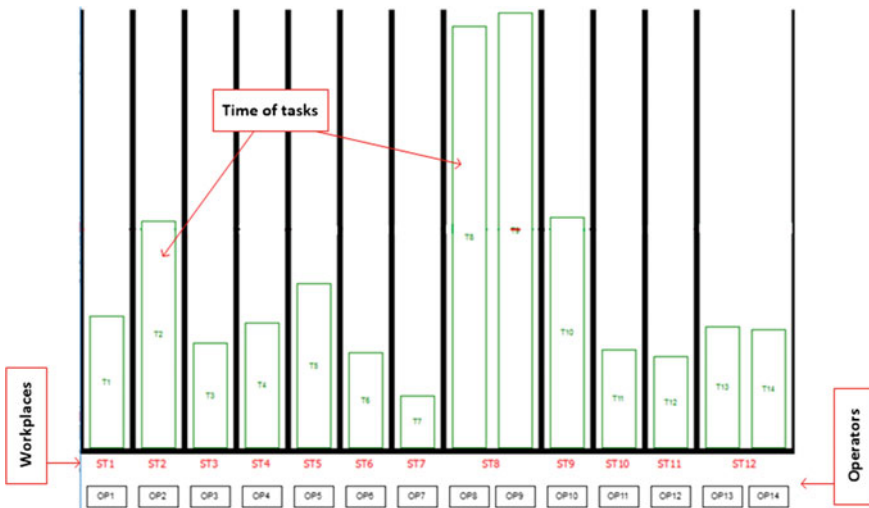


Fig. 2 Example of assembly labour intensity diagram

conveyor while it was moving to finish their tasks. Such lack of coordination results in what can be called a “hand-to-hand” work system.

### 3.3 Assembly-Line Balancing

Changes in the organization of work on the assembly line were connected with balancing the process for each product family representative. The primary rule was to balance the load of workstations connected with the performance of individual assembly tasks.

During the balancing process, structural limitations connected with a potential change in the sequence of assembly tasks were taken into account. Assembly tact (supply of product by the assembly line) was determined as a result of balancing. Tact time is determined by the most loaded workstation (Fig. 3). Simultaneously, tact time is the time during which a product stays on a given workstation, after which it is transferred to subsequent assembly workstation. As a result, seven workstations were separated on the assembly line. On stations 1–6 operators perform their assembly tasks, they do not move along the line and they do not help other operators in performing their tasks. The seventh workstation is a buffer, which enables to synchronize the assembly line with the electrical inspection workstation and no assembly work is performed there.

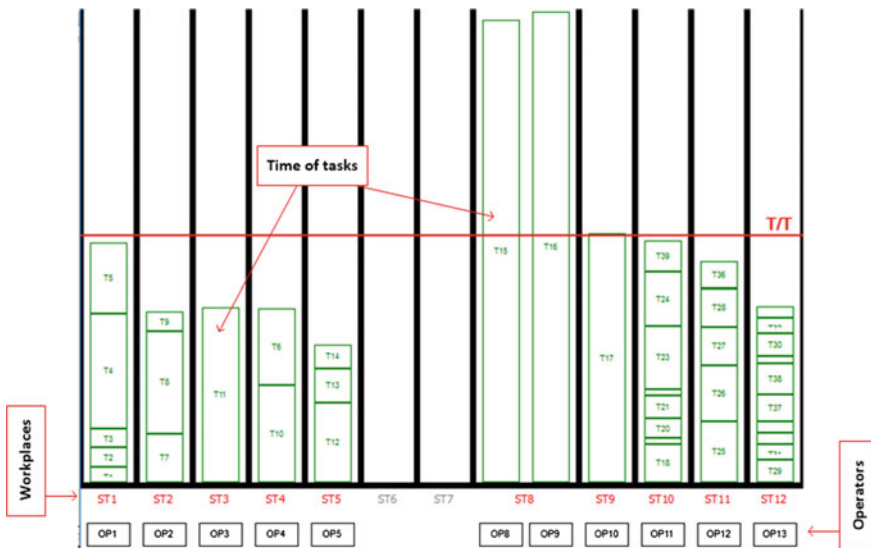


Fig. 3 Example of an assembly-line balancing graph

For some product families, the so-called sub-assembly workstations were designed, on which subcomponents of finished products later supplied to the assembly line are assembled.

As a result, we successfully limited the number of operators for most product families, mostly through the assembly-line zone. The electrical inspection station and the packing station remained unchanged, only in the case of one type of products was an inspection employee shifted to the assembly workstation.

### 3.4 Rules of Scheduling Production Task Performance

Because of the production planning system adopted in the entire company, determining new rules of scheduling production task performance was limited to one production shift as the basic time bucket. The product assembly tact was assumed as the basic parameter of scheduling. The sequence according to which a set of production tasks is performed for a given production shift is determined from the longest to the shortest tact for a given product. The number of operators involved during a single production shift (Fig. 4) was assumed as another parameter of task scheduling.

The adopted assumptions of production task scheduling affect the assembly process performed on the assembly line. When the assembly of a product of different tact time is commenced, the conveyor movement will change after the last workpiece of the preceding batch of products leaves the assembly line. This means that the first 5 workpieces from the new production task will be assembled in the tact of the previous product.

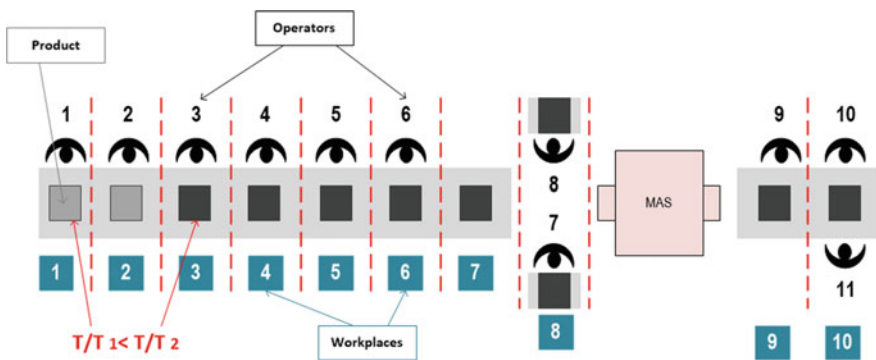


Fig. 4 Schema of scheduling rules for production orders

## 4 Evaluation of the Implemented Solutions

The above-described modifications in the operation of the assembly line were evaluated with regard to efficiency and production efficiency. Below we show the evaluation for two business days. The production results obtained in the same period before the organizational changes were assumed as the benchmark for evaluation.

The assembly-line balancing was assessed with use of efficiency ratio, which was defined as a ratio of the number of manufactured products to the number of operators involved in the production.

The analysis showed that after balancing the efficiency increased for all types of manufactured products. In the case of three types of cooktops, the efficiency decreased insignificantly, whereas in the case of two types it remained at the same level.

Changes in the production efficiency were evaluated by determining the time required to perform the assumed set of production tasks. The reference values of the manufactured number of workpieces (before changes) were achieved within 7.5 h of available assembly line work time during a shift.

As a result of calculations based on the new production task scheduling rules, in most cases products will be manufactured in time shorter than before the changes. Only in two cases was the assembly time after balancing longer than before the organizational changes. However, it should be taken into account that after the changes had been introduced the results were in most cases obtained with fewer operators involved in the assembly process.

Therefore, one can assume that faster performance of production tasks will contribute to improving the assembly efficiency (Table 1).

## 5 Summary

The paper contains an evaluation of the impact of assembly-line balancing and scheduling on production efficiency and staffing. The analysis of the assembly line, which is described in the beginning of this paper, enabled to indicate some key drawbacks in operation of the current system, including:

- lack of operator working standards;
- lack of effective production flow control system;
- lack of possibility to define precisely the cycle time (tact);
- operators moving between individual workstations on the line;
- mutual help which disturbs the assignment of tasks organized by managers.

The assembly-line balancing significantly contributed to the reduction of the number of employees required to perform the assembly. However, the suggested rules of assembly line scheduling allowed for an efficient change in the assembly of

**Table 1** Results of evaluation production efficiency

Day	Production shift	Product	Before organizational changes			After organizational changes			
			Production time [h]	Number of operators	Efficiency [Pcs./operator]	Tact [s]	Number of operators	Production time [h]	Efficiency [Pcs./operator]
1	I	I4P—400 Pcs.	7.5	13	30.8	60	11	7.4	36.4
	II	I4P—240 Pcs.	7.5	13	18.5	60	11	7.6	21.8
		I4S—60 Pcs.		15	4.0	70	12		5
		I4P—100 Pcs.		13	7.7	60	11		9.1
III	C4S—448 Pcs.	7.5	13	34.5	50	12	7	37.3	
	I4P—340 Pcs.	7.5	13	26.1	60	11	7.4	30.9	
2	I	C4S—47 Pcs.		13	3.6	50	12		3.9
		I4P—20 Pcs.		13	1.5	60	11		1.8
		I4P—400 Pcs.	7.5	13	30.8	60	11	7.65	36.4
II	I4S—10 Pcs.		15	0.7	70	12		0.8	
	I4S—70 Pcs.	7.5	15	4.7	70	12	7.11	5.8	
III	E4P—280 Pcs.		13	21.5	65	12		23.3	

different product families and engaging a constant number of workers for a single production shift. As a result of the suggested modifications, the efficiency of the assembly-line operation was improved.

**Acknowledgements** The paper is prepared and financed by scientific statutory research conducted by Chair of Management and Production Engineering, Faculty of Mechanical Engineering and Management, Poznan University of Technology, Poland, Poland, supported by the Polish Ministry of Science and Higher Education from the financial means in 2017 (02/23/DSPB/7695).

## References

1. Becker, C., Scholl, A.: A survey on problems and methods in generalized assembly line balancing. *Eur. J. Oper. Res.* **168**, 694–715 (2006)
2. Amen, M.: Cost-oriented assembly line balancing: model formulations, solution difficulty, upper and lower bounds. *Eur. J. Oper. Res.* **168**, 747–770 (2006)
3. Boysen, N., Fliedner, M., Scholl, A.: A classification of assembly line balancing problems. *Eur. J. Oper. Res.* **183**, 674–693 (2007)
4. Górski, F., Zawadzki, P., Hamrol, A.: Knowledge based engineering as a condition of effective mass production of configurable products by design automation. *J. Mach. Eng.* **16** (2016)
5. Kujawińska, A., Rogalewicz, M., Diering, M., Hamrol, A.: Statistical approach to making decisions in manufacturing process of floorboard. *Inf. Syst. Technol.* **3**, 499–508 (2017). Springer
6. Diering, M., Hamrol, A., Kujawińska, A.: Measurement system analysis combined with Shewhart's approach. *Key Eng. Mater.* **637**, 7–11 (2015)
7. Starzyńska, B., Grabowska, M., Hamrol, A.: Effective management of practitioners' knowledge—development of a system for quality tool selection, In: 3rd International Conference on Social Science (ICSS), Shanghai, China, pp. 859–865 (2016)
8. Hamrol, A., Kowalik, D., Kujawińska, A.: Impact of selected work condition factors on quality of manual assembly process. *Human Factors Ergon. Manuf. Serv. Indus.* **21**(2), 156–163 (2011)
9. Trojanowska, J., Żywicki, K., Pająk, E.: Influence of selected methods of production flow control on environment. *Inf. Technol. Environ. Eng.* **3**, 695–705 (2011)
10. Żywicki, K., Rewers, P., Bożek, M.: Data analysis in production levelling methodology. In: *Advances in Information Systems and Technologies*, 519–527 (2017)
11. Rewers, P., Hamrol, A., Żywicki, K., Kulus, W., Bożek, M.: Production leveling as an effective method for production flow control—experience of polish enterprises. *Procedia Eng.* **182**, 619–626 (2017)
12. Trojanowska, J., Varela, M.L.R., Machado, J.: The tool supporting decision making process in area of job-shop scheduling. In: Rocha Á., Correia A., Adeli H., Reis L., Costanzo S. (eds), *Recent advances in information systems and technologies*. WorldCIST, advances in intelligent systems and computing, 571, 490–498, Springer, Cham (2017)
13. Gangala, C., Modi, M., Manupati, V.K., Varela, M.L.R., Machado, J., Trojanowska, J.: Cycle time reduction in deck roller assembly production unit with value stream mapping analysis. In: Rocha Á., Correia A., Adeli H., Reis L., Costanzo S. (eds) *Recent advances in information systems and technologies*, WorldCIST, advances in intelligent systems and computing, 571, 509–518, Springer, Berlin (2017)
14. Zawadzki, P., Żywicki, K.: Smart product design and production control for effective mass customization in the Industry 4.0 concept. *Manag. Prod. Eng. Rev.* **7**(3), 105–112 (2016)

15. Żywicki, K., Zawadzki, P., Hamrol, A.: Preparation and production control in smart factory model. In: *Advances in Information Systems and Technologies*, 519–527 (2017)
16. Górski, F., Wichniarek, R., Zawadzki, P., Hamrol, A.: Computation of mechanical properties of parts manufactured by fused deposition modeling using finite element method. In: Herrero Á., Sedano J., Baruque B., Quintián H., Corchado E. (eds.) *10th International Conference on Soft Computing Models in Industrial and Environmental Applications, Advances in Intelligent Systems and Computing*, Springer, Berlin, 368, 403–413 (2015)
17. Bukchin, J., Dar-El, E.M., Rubinovitz, J.: Mixed model assembly line design in a make-to-order environment. *Comput. Ind. Eng.* **41**, 405–421 (2002)
18. Baybars, I.: A survey on exact algorithms for the simple assembly line balancing problem. *Manage. Sci.* **32**, 909–932 (1986)
19. Erel, E., Gokcen, H.: Shortest-route formulation of mixed-model assembly line balancing problem. *Eur. J. Oper. Res.* **116**, 194–204 (1999)
20. Żurek, J., Pastwa, M., Wiśniewski, M.: Simple assembly line balancing. *Arch. Mech. Technol. Autom.* **4**, 61–67 (2013)
21. Boysen, N., Fliedner, M., Scholl, A.: Production planning of mixed-model assembly lines: overview and extensions. *Prod. Plan. Control Manag. Oper.* **20**(5), 455–471 (2009)
22. Copaceanu, C.: Mixed-model assembly line balancing problem: variants and solving techniques. *Proc. ICMI* **45**, 337–360 (2006)
23. Karwasz, A., Chabowski, P.: Productivity increase through reduced changeover time. *J. Mach. Eng.* **16**(2), 61–70 (2016)

# Formal Description of Integrated Process and Assembly System Planning

Jan Duda

**Abstract** The paper presents the trends in the development of methods and systems for assembly process planning on the background of Concurrent Engineering (CE) strategies. The solutions for the functional integration of design/manufacturing and production preparation are proposed. The formal description of integrated process and assembly system planning in CE manner is presented.

**Keywords** Concurrent engineering · Process/assembly system integration · PLM

## 1 Introduction

According to the new development strategies, the product development focuses on as much as possible parallel execution of all development-related product life cycle phases, thus creating Concurrent Engineering (CE) environment [1–5]. CE strategy assumes the development of resources and production facilities at the early product design phases to shorten the production start-up time, CE is the computer-integrated environment for design and manufacturing—the common platform for computer-aided systems used in the product development [6, 7]. The key condition for the effective CE is the computer-integrated environment of design and manufacturing—the common platform for computer aided systems for the product development. This requires a formal description of the product, process, and design procedures. Discussion about integrated design of a product and assembly system is presented in [8, 9].

---

J. Duda (✉)

Institute of Production Engineering, Cracow University of Technology, Cracow, Poland  
e-mail: [duda@mech.pk.edu.pl](mailto:duda@mech.pk.edu.pl)

© Springer International Publishing AG 2018

A. Hamrol et al. (eds.), *Advances in Manufacturing*, Lecture Notes in Mechanical Engineering, [https://doi.org/10.1007/978-3-319-68619-6\\_8](https://doi.org/10.1007/978-3-319-68619-6_8)



## 2 Defining of the Product in the Live Cycle Context

The assembly process planning is a phase of the Product Life Cycle realized within the production preparation. The Product is created in design planning phase. The result of the designer work is SK—the design structure of the product:

$$SK = \{JK_1\{JK_2\{JK_3 \dots \{JK_K\}\}\}\} \quad (1)$$

where

$K$  level of product decomposition on design units,  
 $JK$  design unit.

Between of design units topological, dimensional, and accuracy constraints are defined. So the design form of the product WRK can be described as

$$WRK = \langle SK, WK, \alpha \rangle \quad (2)$$

where:

$SK$  design structure of the product,  
 $WK$  set of design constraints,  
 $\alpha$  mapping on the set of design units.

$$\alpha: JK \times JK \rightarrow WK \quad (3)$$

The product design represented in the digital form in CAD system is the base for making engineering calculations, dynamic, static, and kinematic analysis.

Design form of the product is the base for the determination of the assembly product structure.

$$SM = \{JM_M\{JM_{M-1}\{JM_{M-2} \dots JM_1\}\}\} \quad (4)$$

where:

$M$  level of product decomposition on assembly units,  
 $JM$  assembly unit.

In the set of assembly units on  $M$  level, the following elements can be separated:

- assembly aggregates which can be further decomposed into the lower aggregates,
- elementary part which cannot be further decomposed.

Thus, the product in the term of its assembly can be described as

$$WRM = \langle SM, WM, \beta \rangle \quad (5)$$

where

- SM assembly product structure,  
 WM set of assembly constraints,  
 $\beta$  mapping on the set of assembly units

$$\beta: JM \times JM \rightarrow WM \quad (6)$$

In the set of assembly units on R level, the following elements can be separated:

- assembly aggregates which can be further decomposed into the lower aggregates,
- elementary part which cannot be further decomposed.

The assembly form of the product represented in digital form in CAD system is the base for making assembly simulation of the product.

### 3 Formal Description of the Assembly Process

Assembly process plan PTM for the given product WRK is described by

$$PTM = \{E_{TRM}, E_{OPM}, E_{IDM}\}, SPM \quad (7)$$

where

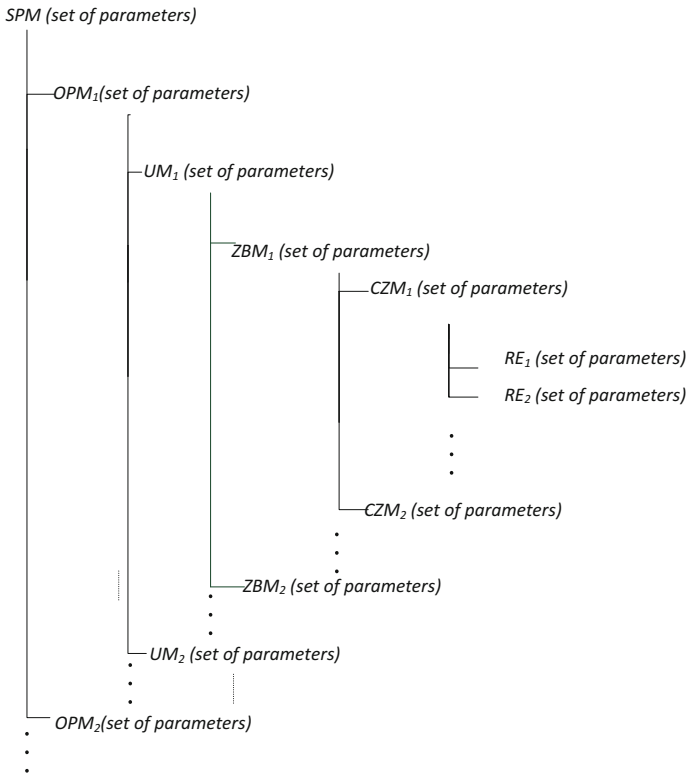
- $E_{TRM}$  assembly process actions causing permanent connection of parts,  
 $E_{OP}$  assembly process actions changing the location of the object in the system of assembly tools, assembly units, assembly equipment,  
 $E_{ID}$  control actions checking the quality of the executed assembly tasks in relation to the requirements in the process documentation,  
 SPM structure of assembly process plan.

The actions  $E_{TRM}$ ,  $E_{OPM}$ ,  $E_{IDM}$  can be described by three blocks of information: action model, execution methods, and parameters.

Assembly action  $E_{TRM}$  can be described using three blocks of information:

- action model  $AE_M$  describing in general terms the assembly task for linking assembly units and the planned method of connection,
- execution method  $BE_M$  of assembly task,
- execution parameters  $CE_M$  of assembly task.

The structure of assembly process plan SPM (Fig. 1) has the characteristic structure elements and their order depending on:



**Fig. 1** Structure of assembly process plan. **SPM** = [**OPM**—Assembly operation [**UM**—set-up [**ZBM**—Assembly treatment [**CZM**—Assembly action [**RE**—Elementary motion]]]]]

- features of product, its dimensions, and dimension constraints of location of assembly units,
- requirement no to use in the assembly operation the parts already mounted,
- size of manufacturing batch.

Assembly process plan is the result of the planning procedure, which determines the manufacturing actions and the structure of assembly process SPM, allowing to receive the design form of the product WRK proposed by the designer.

#### 4 Integrated Process and Assembly Systems Development

Features of modern development strategies indicate the need for product development phase integration. Integration and parallel execution of activities were received through the separation of the conceptual design stages, allowing for the

creation of the variant solutions. Variants are then evaluated in the view of the requirements of the next development phase [2, 3].

The integrations of process and assembly system development suggest the separation of the following phases (Fig. 2):

- conceptual process planning phase,
- detailed process planning phase.

The integrations of manufacturing and organization product development suggest the separation of the following phases:

- conceptual production organization planning phase,
- detailed production organization planning phase.

#### 4.1 Conceptual Process Planning Stage

The assembly process is created on the basis of the digital product model prepared with CAD system. The process planning activities includes the following:

- development of the product assembly structure—separation of the assembly units (assemblies, subassemblies, and parts),
- development of the assembly process plan including the basic parts for separated assembly units, methods, and hierarchical order of assembly of these units to receive the design features of the product,
- mounting of subassemblies, assemblies, and parts based on the developed assembly plan,
- assembleability analysis of the product and for iterative improvement of the design form in view of the assembly requirements.

The product assembly structures (Eq. 4) is the base for the determination of the assembly sequences [8]. They describe the order of connecting the assembly units and list of assembly actions leading to the final product. Most of the methods of assembly sequence presentation are *explicit* methods, directly precisising the assembly tasks in the representations.

On the conceptual planning stage, *implicit* methods are used, specifying only the conditions which must be satisfied by the assembly task sequences.

The determined sequence of connection of assembly units, presented as a graphical assembly plan is the base for the definition of the assembly tasks and their characteristics. On the set of assembly tasks, the graph GOK can be describing:

$$\text{GOK} = \langle \text{ZM}, \text{RK}, \mu \rangle \quad (8)$$

where

ZM set of assembly tasks,

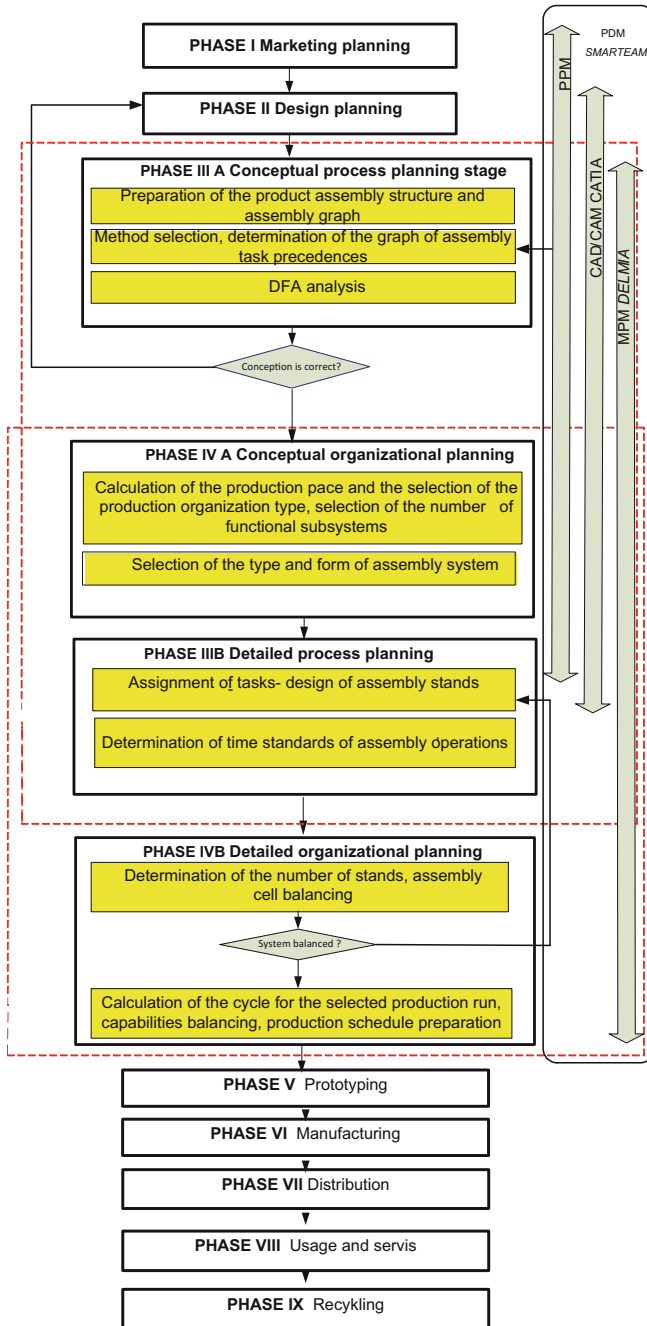


Fig. 2 Execution of product development phases

RK set of precedence relations,  
 $\mu$  mapping on the set of assembly tasks

$$\mu: ZM \times ZM \rightarrow RK \quad (9)$$

Precedence relation can be described by the matrix  $RK[rk_{ij}]_{n \times n}$   $i, j = 1 \dots n$

$$rk = \begin{cases} 1 & \text{when task } i \text{ precedes task } j \\ 0 & \text{in the other case} \end{cases}$$

The multivariant nature of the assembly processes is due to the possibility to use several assembly sequences with the application of methods and manufacturing means and different automation levels. On the base of the defined variants of manufacturing/assembly processes, the manufacturability analysis DFM and assembleability analysis DFA are carried out [10, 11]. The results of the subsequent iterations are used to simplify the product design (by minimization of the number of parts and the integration of parts), thus decreasing the time and costs of the assembly and to estimate the times and costs for different manufacturing methods of constituent product elements. DFA classifies the degree of difficulty of assembly actions and uses it for the determination of the assembly time of all assembly task  $T_i$ . The time determined by DFA methodology results from the classification of design features influencing the execution of assembly actions. On this planning phase, it is possible to evaluate the total product assembly time  $T_a$ .

The product design resulting from the subsequent iterations and its assembly plan form the base for defining the graph of the assembly activities, representing the admissible variants of the execution of product assembly.

## 4.2 Conceptual Production Organization Planning Stage

The conceptual organization stage is used to select the appropriate form of the production organization, production pace, and for the initial calculation of the number and type of functional subsystems. On this stage, also the type and organizational form of assembly system is selected.

The main goal of the conceptual organization planning is the development of the manufacturing system concept for the variants of assembly and process planning plans.

The decision taken on this stage can be changed later and should be detailed on the subsequent phases. Nevertheless, they influence further solutions. The base for taking these decisions is limited information gathered during the previous development activities, describing:

- assortment specified by the set of items  $\{WR_1, WR_2, \dots\}^M$
- production program for each assortment item,

- developed in the conceptual phase of technological design, the concepts of technological processes of assembling assortment positions.

In the first design step, the production structure of the assembly system is determined (Fig. 3).

The established number and type of functional subsystems is the basis for conducting organizational arrangements within the isolated subsystems.

Further action is dependent on the adopted variation of the production organization in the dedicated production assembly subsystem. The course of proceedings leading to the development of the concept of the assembly line was presented in [3, 10].

The outcome of these actions is the conceptual assembly system forming the base for the subsequent detailed process planning.

### 4.3 Detailed Process Planning Stage

The selected type, organizational form of the assembly, and the graphical product assembly plan are the basis for the detailed assembly process planning.

The design actions on the detailed process planning phase cover the series of activities leading to the development of assembly operations.

Within the scope of assembly process planning, these actions include:

- selection and design of assembly devices, workpiece and tool equipment,
- determination of the structure of assembly operations, activities and movements,
- development of control programs for manipulators and robots,
- preparation of documentation for assembly operations.

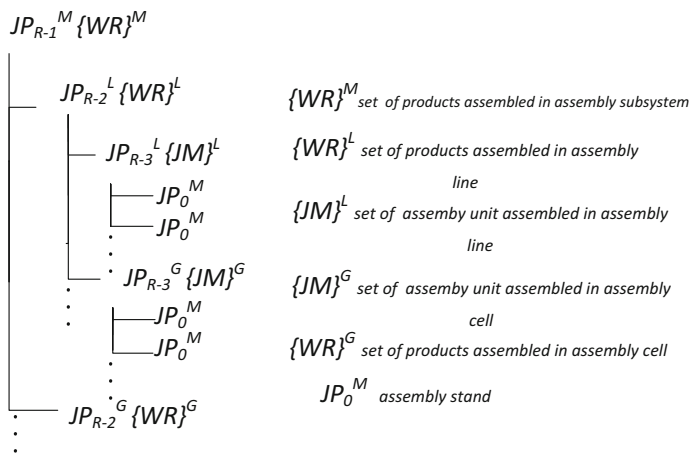


Fig. 3 Hierarchical structure of the assembly system

Within the scope of the transport between stands, these actions include:

- selection and design of transport devices,
- development of control programs for transport devices.

Within the scope of control operation design, these actions include:

- selection and design of control devices,
- development of programs for control devices,
- preparation of documentation for control operations.

The result of these actions is the set of actions  $\{E_{TRM}, E_{OPM}, E_{IDM}\}$  executed in the system and the assembly process plan structure SPM including assembly, transport, and control operations. Assembly operation consists of several interconnected elements: treatments, actions, and movements

The determined assembly process plan PTM is the base for the selection of the organization variant of the manufacturing stands and for the detailed organization planning phase including the creation of the digital model of assembly system and the time normalization of the assembly operation.

#### ***4.4 Detailed Production Organization Planning Stage***

The selected structure of the assembly process and the determined duration times of assembly activities covered by the operations are the base for the synchronization within the isolated assembly subsystem. For analyzed production organization forms, for example, production lines, these steps include the recalculation of the number of stands and line balancing [10].

The change in the assignment of tasks to the assembly stands necessitates the redesign of assembly stands and the recalculation of the assembly times. The subsequent iterations improve the assembly system. The activities for the selected organization forms (assembly stations) include ergonomic analysis too.

The outcome of the detailed production organization stage is the digital model of the manufacturing system linking all the components of the assembly system with assembly process plan stored in library and process schedule [10].

## **5 Verification and Conclusions**

The verification was done with PLM solutions offered by Dassault Systemes. These solutions include the following systems:

- CAD/CAM CATIA for product, manufacturing process and resource design,
- MPM DELMIA for process and manufacturing system design.



The proposed methodology of concurrent development and formal description of products, processes and manufacturing systems using such PLM tools like CATIA and DELMIA increases the integration of the technical production preparation phases and covers various planning actions, including the ones executed with the computer systems like Design For Manufacturing (DFM) analysis, Design for Assembly (DFA) analysis, Computer-Aided Assembly Process Planning (CAAP), MTM time analysis, ergonomic analysis and line balancing.

Nevertheless, it should be noted the PLM solutions are only the tools speeding up the organizational and process planning stages of production preparation. The key conditions to receive the good results are high qualifications of the designer, process planners, and manufacturing organization engineers developing the system components.

Additional research works are required especially for the conceptual and detailed production organization planning phases. Suggestions for the order of design actions depending on the characteristics of the process and manufacturing system shall be elaborated. Especially promising is the use of the Artificial Engineering (AI) techniques for the initial estimation of the manufacturing concepts. Nevertheless, despite the huge number of advanced computer systems for various production preparation phases, the most important decisions are still taken by experts.

## References

1. Chlebus, E.: *CAX computer technology in production engineering*, Warsaw (2000)
2. Duda, J.: Modelling of concurrent development of the products, processes and manufacturing systems in product lifecycle context. In: *New Trends in Technologies, SCIYO* (2010)
3. Duda, J.: *Management of product development in systematic approach*. Cracow University of Technology Press, Cracow (2016)
4. Duda, J., Pobożniak, J.: Concurrent development of products, processes and manufacturing systems in PLM environments. In: Pokojski, W.J., Shuishi, F., Salwiński, J. (eds.) *New Word Situation: New Direction in Concurrent Engineering*, pp. 37–44. Springer, Berlin (2010)
5. Eigner, M.: Product Lifecycle management—the backbone for engineering. In: *1st International Conference Virtual Design and Automation VIDA* (2004)
6. Eversheim, W., Rozenfeld, H., Bochtler, W., Graessler, R.: *A Methodology for Integrated Design and Process Planning on a Concurrent Engineering Reference Model*, Annals of the CIRP (1995)
7. Kahlert, T.: From PDM to PLM—from a workgroup tool to on enterprise—wide strategy. In: *First International Conference Virtual Design and Automation VIDA* (2004)
8. Łebkowski, P.: *Computer-Aided Mechanical Assembly Methods in Flexible Production Systems*. AGH University of Science and Technology Press, Poland (2000)
9. De Lit, P., Delchambre, A.: *Integrated Design of a Product Family and its Assembly System*. Springer Science + Business Media, New York (2003)
10. Duda, J.: Computer integrated development of processes and assembly systems. In: Lisowski, E., Filo, G., Filipowska, R., Fabiś-Domagala, J. (eds.) *Computer Aided Mechanical*

Engineering, vol. 1, no. 4, pp. 99–106. Cracow University of Technology Press, Technical Transaction, Mechanics (2011)

11. Duda, J., Karpiuk, M., Gawąd, P., Chromiak, M.: Design for assembly analysis in solidworks system. Eng. Des. Constr. **3** (2010)

# The Operational Validation of a Planning Process Integration Model in a Manufacturing Company

Michał Adamczak, Piotr Cyplik and Marek Fertsch

**Abstract** The article aims at verifying the possibility of implementing the authors' own operational validation method to assess a planning process integration model in a manufacturing company. The applied operational validation method is applicable to other research methods known in management sciences: process modelling and simulation. A new aspect of this work is the operational validation of a model, which was qualitatively described by means of quantitative methods. The process modelling method was a method used to translate the qualitatively described model to conditions in which the operational validation was possible to be performed by means of quantitative methods. The model of integrating planning processes in manufacturing companies was selected to be a research subject. Apart from presenting the mere method of the model operational validation, the accuracy of describing particular planning process integration levels at the same time is controlled.

**Keywords** Planning process integration · Hypothesis testing · Validation Simulation

## 1 Introduction

### 1.1 Planning Process Integration

Based on the concept valid in contemporary literature references, it is possible to state that the process integration makes it feasible to enhance its efficiency [1–5]. It is required by the internal integration to primarily integrate the process planning and control their performance [6].

One of the possible planning process integration tools is sales and operations planning (SOP). It is a set of business and technological processes that make it

---

M. Adamczak (✉) · P. Cyplik · M. Fertsch  
Chair of Logistics System, Poznań School of Logistics, Poznań, Poland  
e-mail: [michal.adamczak@wsl.com.pl](mailto:michal.adamczak@wsl.com.pl)

possible for a company to correlate the market demand with the manufacturing and procurement potential of the company in the possibly most efficient way [7]. Numerous authors present their own SOP plan definitions [8]. In the works [9], there are SOP plan structures, i.e., types of plans integrated within SOP. This structural approach was specified for the sake of SOP as a common planning and decision-making process between the functional cells [10]. SOP is properly suitable to conduct research by means of a simulation method because SOP represents the process approach [11–13]. The SOP-related research with the use of modelling and simulation methods was presented in the works by [14–17].

### 1.2 Validation of Models

The validation of models might be defined in two different ways:

- statement that the model action is justified and in line with the modelling objectives in the assumed application domain [18],
- process that specifies the degree of how faithfully the model maps the reality with respect to its intended applications [19].

The validation proceeds in 3 phases as presented in Fig. 1.

The conceptual model validation makes it possible to assess the model assumption fulfillment in the context of the identified research problem. The model verification is confined to its implementation accuracy control in a selected IT tool. The operational validation is a control of the model when its use is in progress.

In the scientific research, there are a number of validation techniques and tools [21]. A dynamic validation is the most significant validation tool from the viewpoint of this article. It is required by the dynamic validation to activate the model, to analyse its dynamic behaviour and results. As regards to the validation techniques it is worth paying attention to the following techniques:

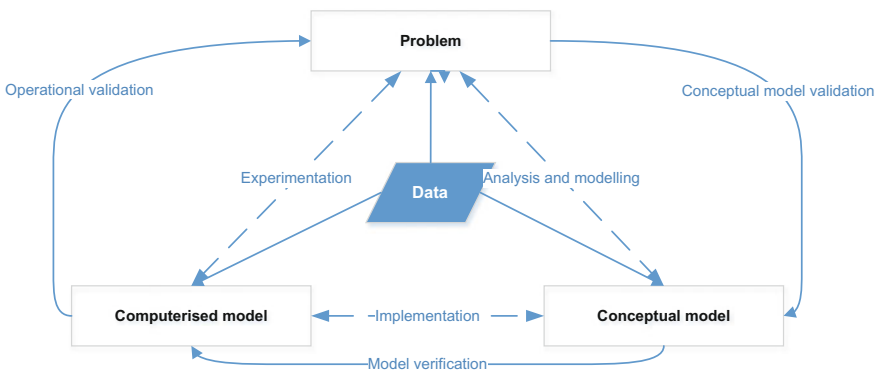


Fig. 1 Simulation model formation and assessment phases [20]

- confrontation with other models—a comparison of this model results with the results of other models which were positively validated,
- event validation—a comparison of events generated in the simulation model with events in the real system.

In the authors’ opinion, the operational validation is the most significant validation phase. As its part, one might give an answer to the question about whether a model achieves its objective and faithfully maps the reality. This is also the last validation phase and thus it gives a complex reply related to both the conceptual modelling phase and the modelling implementation in the IT environment. A positive validation in the operational phase makes it feasible to state that the two remaining phases were also correctly performed.

## 2 Planning Process Integration Model

The authors used the SOP approach while developing the planning process integration model. In the first stage of developing a conceptual model one specified an integrated planning structure, i.e. types of plans included in the model. The developed structure is presented in Fig. 2.

At the second modelling stage, the dependencies between particular plan types which formed a system with particular elements and relations is defined. Due to the large number of possible variants, it is decided to divide the dependencies into a finite number of groups. At each of the 4 distinguished levels, one described the dependencies that should exist between particular plans in order to name them as integrated plans at a given level. A detailed description of each level is presented in Table 1.

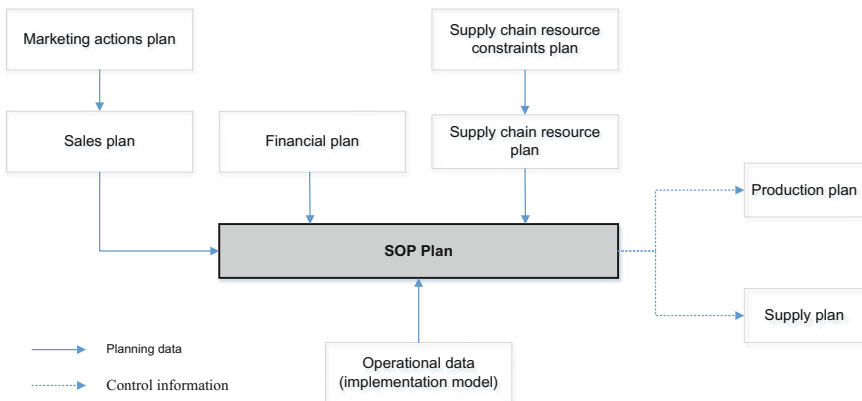


Fig. 2 Integrated planning model structure

**Table 1** Modelling of integration of planning process

Planning process integration level	Characteristics of level
D	No planning process integration, production plan developed adaptively to the sales plan, available resources at a constant level in the process duration based on standards specified in the past, no financial plan and marketing actions included in the plan
C	Corrective procedures implemented in the area of the sales and production planning and in the area of production and procurement. The objective of the procedures is to select the most appropriate solution to executing the proposed sales plan in terms of the planned profit and return on sales by the financial plan simulation, available resources specified at a constant level in the process duration based on standards specified in the past, no marketing actions included in the plan
B	Corrective actions as at level C with the financial plan, available resources specified based on real data about repairs and/or developing the resources as a result of the conducted investment actions, no marketing actions included in the plan
A	All the actions conducted as at level B without the marketing plan. At integration level A the marketing plan is formed based on real data (plan promotional campaigns, extending and enlarging market areas, product portfolios, etc.). The plan is included in the planning process structures and therefore influences the material flow plan which is under construction

Such a qualitatively described model was transformed into maps of processes that function according to the rules as described above. Apart from the process integration level, the model includes 7 other parameters of a simulation scenario. The parameters reflect the task environment influence on a manufacturing company [1, 22]:

- marketing influence on sales volume,
- random demand variability,
- demand seasonality,
- demand trend,
- random demand fluctuations,
- potential of a supplier,
- maintenance-repair plan.

Each of the above parameters might occur at one of the three defined states (small, average and large variability).

As ten iterations were assumed to be performed in the case of each simulation scenario states, 87,480 simulations of planning and material flow processes were required to be conducted. The simulation results were used to perform the model operational validation.

### 3 Operational Validation of the Model

#### 3.1 Operational Validation Methodology

The model validation is based on including the model development objective within its structure.

The developed model needed to meet 3 conditions:

- to map the planning process integration specifics,
- to present a description of the environment influence on a manufacturing company in a simplified way,
- to map the specifics of material flow through the manufacturing company and the flow influence on the customer service level and return on sales.

In the developed operational validation method, the techniques of degeneration tests and event validation is used. The created simulation model should reflect the functioning of real processes. Thereby, the positive model validation will be made feasible by obtaining results in line with the adopted assumptions or the present knowledge state. Taking the above for granted, the authors formed the operational validation methodology and simultaneously focused on defining the steps that make it possible to state unambiguously whether the obtained results confirmed the previously adopted assumptions. To achieve this goal, the authors used such statistical methods as a correlation analysis (in the correlation analysis the Spearman's rho correlation coefficient was used due to discrete values adopted by a variable named as a planning process integration level), Anderson–Darling test for normality, testing two-sided and one-sided hypotheses (by means of U-statistics in the case of results with a normal distribution and the ANOVA method in the case of other results), Tukey Pairwise Comparisons (Tukey method). An algorithmic approach to the developed methodology is presented in Fig. 3 and includes the statistical methods as presented above with their fulfillment sequence and the result influences on the model validation.

In the next part, the validation of the planning process integration model that was performed by means of the developed methodology is presented.

#### 3.2 Operational Validation of the Planning Process Integration Model

In the operational validation, the results of simulations and material flow are used. The simulations were performed in the developed planning process model (at each of 4 defined integration levels of the processes). The Minitab 17 software was used to conduct statistical analyses.

At the first operational validation stage, an analysis of the correlations between the planning process integration level in manufacturing companies and return on

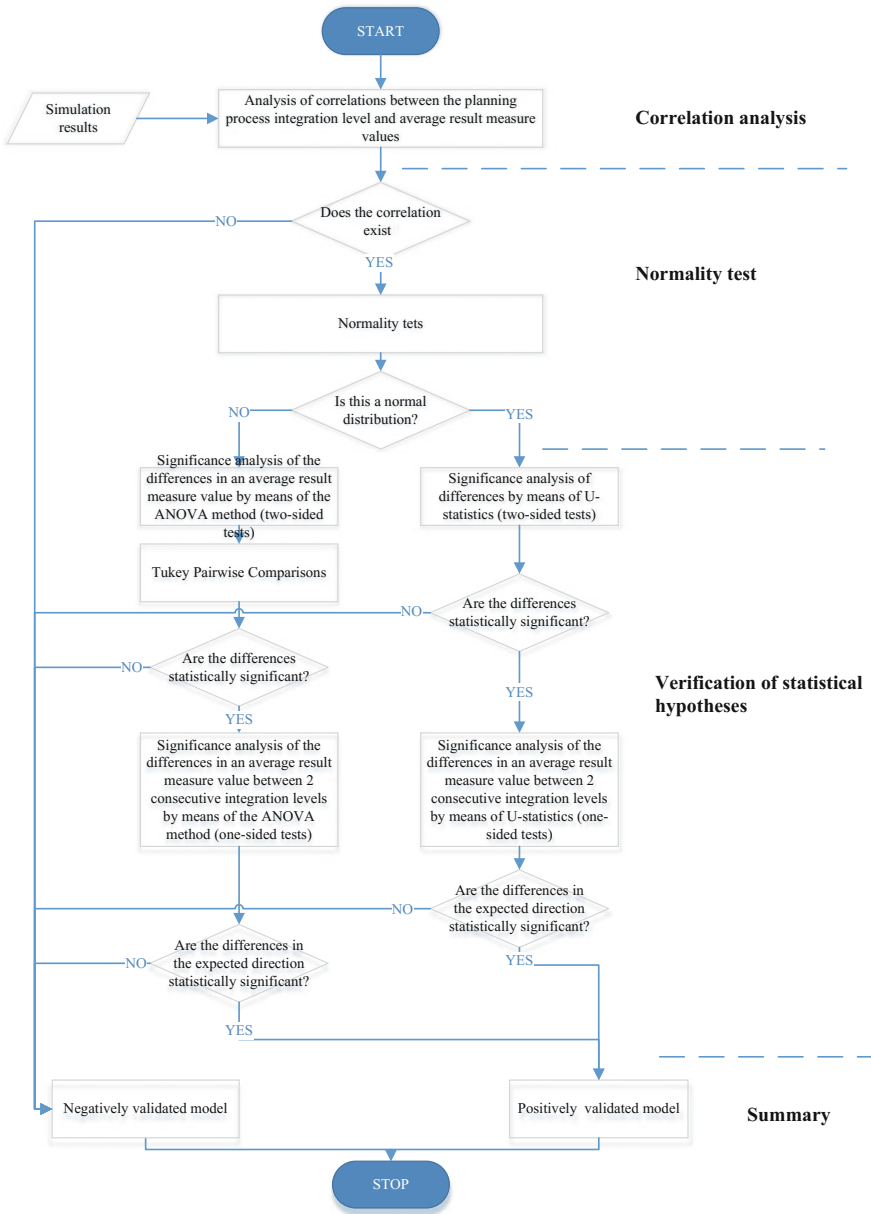


Fig. 3 Algorithm of the simulation model operational validation

sales is performed. In order to make it certain, whether the calculated the correlation coefficient value might be interpreted, the significance test in the case of this value is additionally conducted. This analysis resulted in obtaining the Spearman's rho



correlation coefficient value 0.26 and it was indicated at the same time that this value was statistically significant ( $p$ -value  $< 0.001$  with the adopted significance level 0.05). This means there is a correlation between the planning process integration level and the return on sales indicator value. This correlation is positive and it is presumed that the higher integration level the higher expected return on sales.

In order to check this correlation in detail and its existence in the case of each of the process integration levels defined according to the operational validation methodology, the verification of the statistical hypotheses related to the return on sales value in the case of each planning process integration level is used. In order to make the above feasible, it is necessary to check the empirical distribution of the return on sales value in order to select the method of verifying the hypotheses.

At the second operational validation stage, a normality test by means of the Anderson–Darling test for normality is performed. A few statistical hypotheses about the distribution normality of the return on sales indicator is formulated. This was performed in the case of each of 4 planning levels.  $P$ -value indicator values for the normal distribution test of the return on sales measure value or each planning process integration level were below 0.005. It is concluded based on  $p$ -value indicator that the results at any planning process integration level are not characterised by a normal distribution. Thereby, the ANOVA method was selected to verify the statistical hypotheses.

The third stage of the operational model validation was performed in 3 steps in accordance with the developed methodology. In the first step, using the ANOVA methodology whether the average return on sales values at each of the planning process integration levels were different from each other in terms of the statistical difference is checked. To achieve this goal a few hypotheses are formulated:

*H0: average return on sales values in the case of each planning process integration level are equal to one another;*

*H1: average return on sales values in the case of each planning process integration level are different from one another.*

The tests were conducted with the adopted significance level  $\alpha = 0.05$ . The ANOVA results are presented in Fig. 4.

As presented in Fig. 4, the  $p$ -value indicator value makes it feasible to withdraw the null hypothesis about the equality of the average return on sales values. This statement explains the performance of the Tukey Pairwise Comparisons. Its results are presented in Fig. 5. It is stated based on the results of the Tukey Pairwise

Analysis of Variance					
Source	DF	Adj SS	Adj MS	F-Value	p-Value
Planning integration level	3	98.28	32.7600	2672.51	0,000
Error	87476	1072.29	0.0123		
Total	87479	1170.57			

**Fig. 4** Report on the ANOVA variant analysis with the average value of the return on sales indicator at particular planning process integration levels

Comparisons (see Fig. 5) that the average return on sales value in the case of each planning process integration level is different from one another (results were assigned to 4 separate groups).

The last step of the third operational validation stage was to check whether the average return on sales values increase with the transition to a higher planning process integration level. To achieve this goal, one formed 3 pairs of statistical hypotheses in the case of the conterminous planning process integration levels (a pair of hypotheses for level A and B is presented below the remaining pairs are identically constructed).

$H_0 : \mu_{RENTA} = \mu_{RENTB}$  (the average return on sales values at planning process integration levels A and B are equal to each other)

$H_1 : \mu_{RENTA} > \mu_{RENTB}$  (the average return on sales values at planning process integration level A are higher than at level B)

The results of the statistical tests (with the adopted significance level  $\alpha = 0.05$ ) in the case of each of the above hypothesis pairs are presented in Table 2.

As presented in Table 2, the  $p$ -value indicator values make the null hypothesis withdrawn in the case of each of 3 pairs of the above-formulated hypotheses. Therefore, it is concluded by stating that the average return on sales value increases with the transition to higher planning process integration levels.

### 4 Summary

The authors' presented their own method of the simulation model operational validation. The authors managed to verify the quantitatively (descriptively) developed model by means of statistical measures and due to the application of modelling and process simulation method. The developed operational validation methodology is universal and is suitable to be applied to other simulation models. This is obviously conditioned by using a quantitative result measurement and the modelled process level or variants.

The operational validation of the authors' own model of the planning process integration model in manufacturing companies was presented in the article at the same time. Taking for granted the statement adopted in management sciences that the process integration enables the cost reduction of the activities undertaken by

Tukey Pairwise Comparisons Grouping Information Using the Tukey Method and 95% Confidence				
Planning integration level	N	Mean	Grouping	
A	21870	0.067623	A	
B	21870	0.042555	B	
C	21870	0.001801	C	
D	21870	-0.017889	D	

Fig. 5 Report on the pair comparison of the average value of the return on sales indicator at particular planning process integration levels by means of the Tukey Pair wise Comparisons

**Table 2** *P*-value indicator values in the case of one-sided tests of return on sales measure values

Integration levels with investigated differences	<i>p</i> -value
A–B	0.001
B–C	0.001
C–D	0.001

companies (including manufacturing companies) with a simultaneous increase in return on sales, the positive result of each of 3 operational validation stages makes it possible to state that the planning process integration levels were correctly defined. The course of processes at each integration level was also correctly specified. The processes were correctly mapped in the model frame and then transferred to the IT environment. Thereby, the developed model was positively validated at each of three validation stages as adopted in the theory of the conceptual model, model verification and operational validation.

**Acknowledgements** This paper is the result of research conducted using a Ministry of Science and Higher Education Republic of Poland grant entitled “Development of production and logistics systems” (project No. KSL 1/16) pursued at the Poznan School of Logistics in Poznan.

## References

1. Danese, P., Romano, P., Formentini, M.: The impact of supply chain integration on responsiveness: the moderating effect of using an international supplier network. *Transp. Res. Part E: Logistics Transp. Rev.* **49**(1), 125–140 (2013)
2. Hadas, L., Cyplik, P., Adamczak, M.: Dimensions for developing supply chain integration scenarios. *Bus. Logistics Modern Manag.* 225–239 (2015)
3. Kolinski, A., Śliwczyński, B.: IT support of production efficiency analysis in ecological aspect. In: Golinska, P., Kawa, A. (eds.) *Technology Management for Sustainable Production and Logistics*, pp. 205–219. Springer Verlag, Berlin (2015)
4. Pagell, M.: Understanding the factors that enable and inhibit the integration of operations, purchasing and logistics. *J. Oper. Manage.* **22**(5), 459–487 (2004)
5. Seo, Y.-J., Dinwoodie, J., Kwak, D.-W.: The impact of innovativeness on supply chain performance: is supply chain integration a missing link? *Supply Chain Manage.: Int. J.* **19**(5/6), 733–746 (2014)
6. Gimenez, C., Ventura, E.: Logistics-production, logistics-marketing and external integration: their impact on performance. *Int. J. Oper. Prod. Manag.* **25**(1), 20–38 (2005)
7. Muzumdar, M., Fontanella, J.: The secrets to S&OP success. *Supply Chain Manage. Rev.* 34–41 (2007)
8. Blackstone Jr., J.H.: *APICS Dictionary*, Twelfth edn. APICS, Georgia (2008)
9. Feng, Y., Martel, A., D’Amours, S., Beauregard, R.: Coordinated contract decision in make-to-order manufacturing supply chain: a stochastic programming approach. *Prod. Oper. Manage.* **22**(3), 642–660 (2013)
10. Grimson, J.A., Pyke, D.F.: Sales and operations planning: an exploratory study and framework. *Int. J. Logistics Manage.* **18**(3), 322–346 (2007)
11. Ivert, L.K., Jonsson, P.: The potential benefits of advanced planning and scheduling systems in sales and operations planning. *Indus. Manage. Data Syst.* **110**(5), 659–681 (2010)
12. Lapide, L.: Sales and operations planning (S&OP) mindsets. *J. Bus. Forecast.* **26**(1), 21–31 (2007)

13. Stahl, R.A.: Executive S&OP: managing to achieve consensus. *Foresight* 34–38 (2010)
14. Adamczak, M., Domański, R., Hadaś, Ł., Cyplik, P.: The integration between production-logistics system and its task environment chosen aspects. *IFAC Papersonline* **49**(12), 656–661 (2016)
15. Domański, R., Adamczak, M., Hentschel, B.: Modelling and simulation of the integration of the supply chain of forward and backward type. *Logforum* **11**(1), 63–77 (2015)
16. Hahn, G.J., Kuhn, H.: Value-based performance and risk management in supply chains: a robust optimization approach. *Int. J. Prod. Econ.* **139**(1), 135–144 (2012)
17. Olhager, J., Johansson, P.: Linking long-term capacity management for manufacturing and service operations. *J. Eng. Tech. Manage.* **29**(1), 22–33 (2012)
18. Balci, O.: Verification, validation, and certification of modeling and simulation applications. In: *Proceedings of the Winter Simulation Conference*, pp. 150–158 (2003)
19. Tucker, W.: A Glossary of Modeling and Simulation Terms for Distributed Interactive Simulation. [www.tmpo.nima.mil/guides/Glossary/](http://www.tmpo.nima.mil/guides/Glossary/) (1995). Access 14 May 2015
20. Sargent, R.G.: Verification and validation of simulation models. In: Medeiros, D.J., Watson, E.F., Carson J.S., Manivannan, M.S. (eds.) *Proceedings of the Winter Simulation Conference*, IEEE (1998)
21. Karkula, M.: Verification and validation of dynamic simulation models of logistics processes (in Polish), *Logistyka* [CD recorded material], vol. 2 (2012)
22. Hentschel, B., Domański, R., Adamczak, M., Cyplik, P., Hadaś, Ł., Kupczyk, M., Pruska, Z.: Ranking of integration factors within supply chains of forward and backward types—recommendations from researches. *Logforum* **11**(2), 161–169 (2015)

# Job Scheduling Problem in a Flow Shop System with Simulated Hardening Algorithm

Andrzej Jardzioch and Bartosz Skobieł

**Abstract** A solution to the problem of job scheduling in a flow shop system is proposed in this paper. A three-machine flow shop system is presented with 10 sets of 10 random jobs to be processed. A new approach, called Simulated Hardening (SH), is used to schedule the jobs by taking into consideration two criteria: minimal makespan and maximal profit. The results obtained are compared with First In First Out (FIFO), Earliest Due Date (EDD), Shortest Processing Time (SPT), Longest Processing Time (LPT), Time Reserve (TR), and Descending Delay Penalty (DDP) sorting methods and confronted with the results of exhaustive search. The usefulness of the new SH algorithm is estimated in terms of the quality of the results obtained.

**Keywords** Simulated hardening · Scheduling · Flow shop · Makespan · Profit

## 1 Introduction

A job scheduling problem in a flow shop production system is widely discussed in literature [1–5]. The above works show that the most common objectives of job scheduling problems are the following: minimizing waiting time [3], makespan [4] or total tardiness [5]. In everyday production, these objectives can be regarded primary. The direct impact of makespan and tardiness factor on various Key Performance Indicators (KPIs) cannot be denied. However, there is one more issue within the scope of researchers' interest—economic factors. The correlation between time factors and profit resulting from a given scheduling still poses a challenge. The number of available works on profit optimization issues is somehow limited and not so widely discussed as the time-related problems. A few profit-related optimization problems related to job scheduling can be found in [6–9]. In this study, a specific time–profit correlation is adopted from [10] and thoroughly

---

A. Jardzioch (✉) · B. Skobieł  
West Pomeranian University of Technology, Szczecin, Poland  
e-mail: andrzej.jardzioch@zut.edu.pl

described in Chap. 2. The abovementioned correlation was also successfully implemented by the authors in [11, 12]. It is worth mentioning that a time–profit correlation is not the only one profit-related correlation that a researcher may find interesting to investigate. Among many profit-related optimizations, one can point out a material waste minimizing method [13, 14] or an energy-saving method [15, 16]. One should also keep in mind that modern production systems are highly integrated with Quality Management Systems (QMSs). As a result, the quality approach can also provide optimization tools and techniques [17, 18].

## 2 Problem Description

The main objective of the research, in the case discussed, is to create a job schedule that will provide a satisfactory result in the context of fulfilling the criteria. The flow shop production line consists of three machines: M1, M2, and M3. Each sorting consists of 10 random jobs processed on M1, M2, and M3 respectively. Each job is described by seven attributes:

- job number, from 1 to 10,
- potential profit, between 1 and 100,
- penalty factor, between 1 and 10,
- due date of the job, between 300 and 900,
- processing time on machine 1 (M1), between 1 and 100,
- processing time on machine 2 (M2), between 1 and 100,
- processing time on machine 3 (M3), between 1 and 100.

Two criteria are considered: makespan and profit. In order to define the criteria values for each sorting, a full job schedule is created. On the basis of the schedule obtained, the makespan is defined as the completion time of the last job in the schedule. The profit value is described as the result of the Eq. (1), adopted from [10],

$$P_s = \sum_{i=1}^N p_{\text{job}(i)} - w_{\text{job}(i)} \max\{0, t_{\text{job}(i)} - d_{\text{job}(i)}\} \quad (1)$$

where

- $P_s$  profit gained from job sorting,
- $N$  number of jobs,
- $p_{\text{job}(i)}$  profit gained from the  $i$ th job,
- $w_{\text{job}(i)}$  the penalty factor for the  $i$ th job,
- $t_{\text{job}(i)}$  completion time of the  $i$ th job,
- $d_{\text{job}(i)}$  due date of the  $i$ th job.

A practical implementation of the Eq. (1) is introduced in Fig. 1, where two exemplary schedules for three jobs are presented. The makespan in both cases is similar, but the calculated profit differs significantly. In the case of sorting 1, 2, 3 the job no. 2 is delayed by 30 time units and the penalty factor for job no. 2 is very high and equals 9. The Eq. (1) serves to evaluate the delay impact on the profit:  $30 * 9 = 270$ . For sorting 2, 1, 3, the job no. 1 is delayed by 70 time units, but the penalty factor for this job is low, and equals 1. The delay impact in this case is  $70 * 1 = 70$ . As can be seen in Fig. 1, sorting 2, 1, 3 is more profitable in spite of generating more delays.

In this study, 5 basic methods of job sorting were selected and implemented, apart from the SH algorithm:

- FIFO First In First Out, jobs are sorted by the time of arrival,
- EDD Earliest Due Date, jobs are sorted by the due date of each job,
- DDP Descending Delay Penalty, jobs are sorted by the penalty factor,
- SPT Shortest Processing Time, jobs are sorted by the sum of their processing times,
- TR Time Reserve, jobs are sorted by the values of (due date—the sum of processing times) evaluated for each job.

### 3 Simulated Hardening Algorithm

The SH algorithm is a heuristic method of searching a quasi-optimal solution in a given limited amount of time. The aim of the first operation of the algorithm is to import or to create an initial sorting of the jobs. The second step is to run the mechanism that creates a new sorting. That mechanism is based on random swap places idea, also known as a swap mutation in Genetic Algorithms (GA) domain. The idea of a swap mutation is shown in Fig. 2.

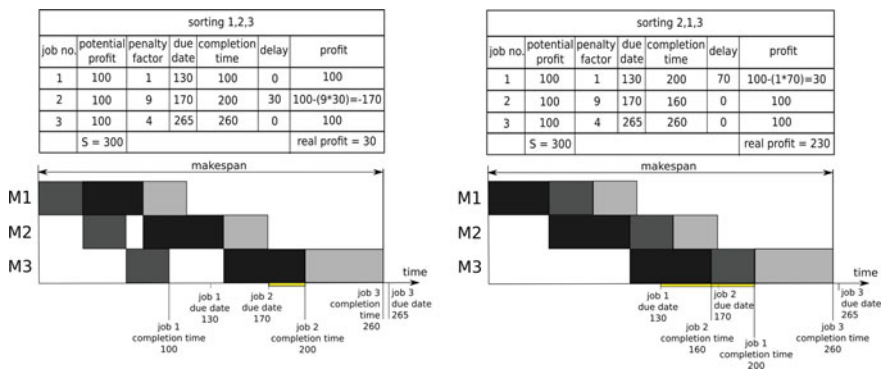


Fig. 1 Two exemplary schedules of three jobs with profit evaluation

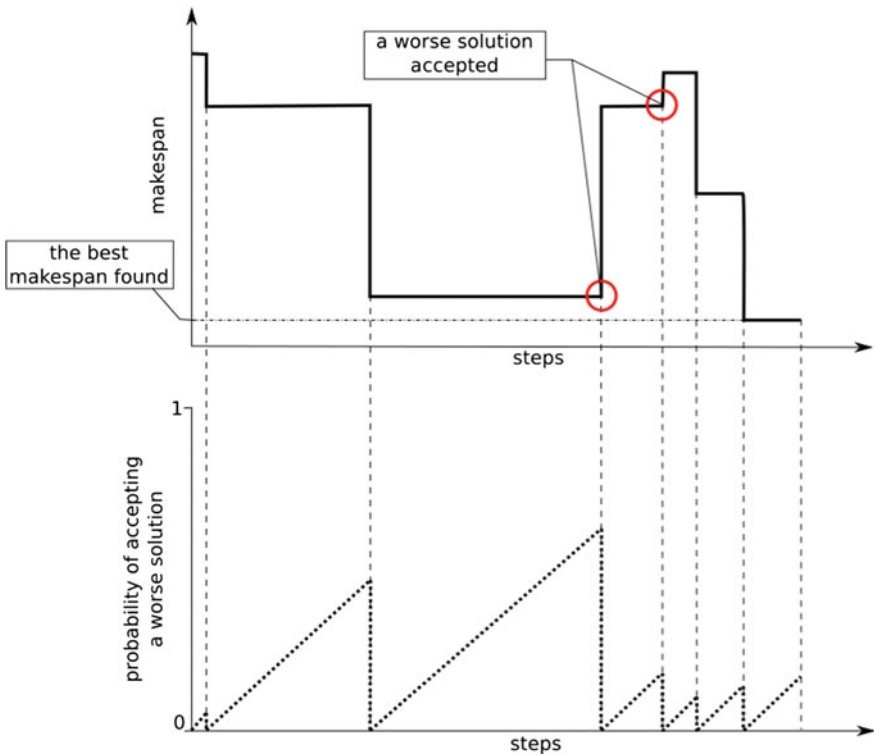
**Fig. 2** The idea of a swap mutation

1	2	3	4	5	6	7	8	before
1	2	7	4	5	6	3	8	after

After a new sorting is created, the solution is evaluated. If the evaluation of the new sorting results in a better fitness value (in the context of the criterion) than the previous one—it is considered as the “new best” solution. If however, the fitness value is worse than in the previous sorting, one can accept the worse solution with a given probability.

The concept of the SH algorithm, as well as that of the Simulated Annealing (SA) algorithm, is derived from metallurgy. In the case discussed, the temperature as it is known in thermodynamics, is represented as a probability function of accepting a worse solution, while the SH algorithm does not improve the results. The probability function can, therefore, be regarded as a defense mechanism against premature convergence of the SH algorithm (Fig. 3).

In every step of the SH algorithm, a new sorting is created and the evaluation of the new sorting is performed. The fitness value of the new sorting is then compared



**Fig. 3** The idea of probability function in SH algorithm and its influence on the results



with the fitness value of the previous sorting. In each stage of the SH algorithm operation, three decisions can be made: accepting the better solution, accepting the worse solution, maintaining the current solution. In case the new solution is worse than the previous one, a random number between 0 and 1 is generated and compared to the current probability value, also ranged between 0 and 1. If the random number is lower than the probability value, then the worse solution is accepted as the current one. The process described above can be followed by looking at the pseudocode below.

A pseudocode of the SH algorithm for profit criterion:

```

/* values defined by the user: q - increase in probability
per step, end_step - limit of steps */
probability = 0;
step = 0;
create sorting;
DO
{
    create new_sorting from sorting;
    fitness(sorting) = evaluate sorting;
    fitness(new_sorting) = evaluate new_sorting;
    IF (fitness(new_sorting) > fitness(sorting))
    {
        best_fitness(step) = fitness(new_sorting);
        sorting = new_sorting;
        probability = 0; }

    ELSE
    {
        roulette = rand (0,1);
        IF (roulette < probability)
        {
            best_fitness(step) = fitness(new_sorting);
            sorting = new_sorting;
            probability = 0; }

        ELSE
        {
            probability + q; }
    }
    step ++;
}
WHILE (step < end_step);
best_result = max(best_fitness);
best_sorting = sorting(best_result);

```

In the presented case, the operational time of SH algorithm is limited by the number of steps that is defined by the user. For the sake of research, the limit of steps is set to 1000 and the increase in probability per step is set to 0.001. The probability of accepting the worse solution will then rise 0.1% per step if no progress is detected. In the end, the overall best result of fitness function is determined and the corresponding sorting is returned as the best sorting found.

## 4 Results

The results obtained are presented in Tables 1 and 2. Table 1 shows the values of time for the minimization of the makespan criterion for every sorting method used. The optimal values obtained with the exhaustive search method are highlighted.

Table 2 shows the values of profit for every sorting method used. The optimal values obtained from the exhaustive search method are highlighted.

Figure 4 presents the median and min-max distance from the optimal values of makespan. The optimal value equals 100%.

In case of minimal makespan search, only 2 out of the total number of 6 methods produced optimal results at least once—the SH and TR. The distance between the median value and the optimum for TR method is 21.8% and is regarded as the worst median result of all. Therefore, in spite of achieving the best makespan result once, the TR method is not recommended in this case. The SH method, on the other hand, proved its usability and, with the median in the optimum, is preferable.

Figure 5 presents the median and min-max distance to the optimal values of profit. The optimal value equals 100%.

In case of profit search, a significant spread of results is observed. Only 3 out of all tested methods placed median values of results at the optimum: the EDD, TR,

**Table 1** Makespan values for every sorting method and jobs set

	Set 1	Set 2	Set 3	Set 4	Set 5	Set 6	Set 7	Set 8	Set 9	Set 10
optimal	<b>672</b>	<b>483</b>	<b>528</b>	<b>609</b>	<b>573</b>	<b>574</b>	<b>760</b>	<b>607</b>	<b>689</b>	<b>539</b>
FIFO	749	607	584	695	753	654	885	731	839	619
EDD	700	608	573	708	773	673	922	695	774	645
DDP	794	670	691	680	728	669	868	680	745	748
SPT	764	577	633	702	666	649	881	658	806	692
TR	767	608	<b>528</b>	753	733	711	959	728	821	645
SH	690	<b>483</b>	<b>528</b>	<b>609</b>	<b>573</b>	585	<b>760</b>	<b>607</b>	730	575

**Table 2** Profit values for every sorting method and jobs set

	Set 1	Set 2	Set 3	Set 4	Set 5	Set 6	Set 7	Set 8	Set 9	Set 10
optimal	<b>541</b>	<b>509</b>	<b>576</b>	<b>648</b>	<b>620</b>	<b>402</b>	<b>429</b>	<b>411</b>	<b>449</b>	<b>440</b>
FIFO	-1949	-727	408	113	-829	-198	-1876	-2245	-3047	-2591
EDD	463	<b>509</b>	<b>576</b>	<b>648</b>	<b>620</b>	<b>402</b>	-2652	<b>411</b>	<b>449</b>	<b>440</b>
DDP	-726	-409	420	85	227	-395	-2652	-567	-192	-522
SPT	-758	-446	<b>576</b>	<b>648</b>	122	-2904	-2994	-324	-2277	322
TR	-981	<b>509</b>	<b>576</b>	<b>648</b>	<b>620</b>	<b>402</b>	-3314	<b>411</b>	<b>449</b>	<b>440</b>
SH	517	<b>509</b>	<b>576</b>	<b>648</b>	<b>620</b>	<b>402</b>	<b>429</b>	<b>411</b>	<b>449</b>	<b>440</b>

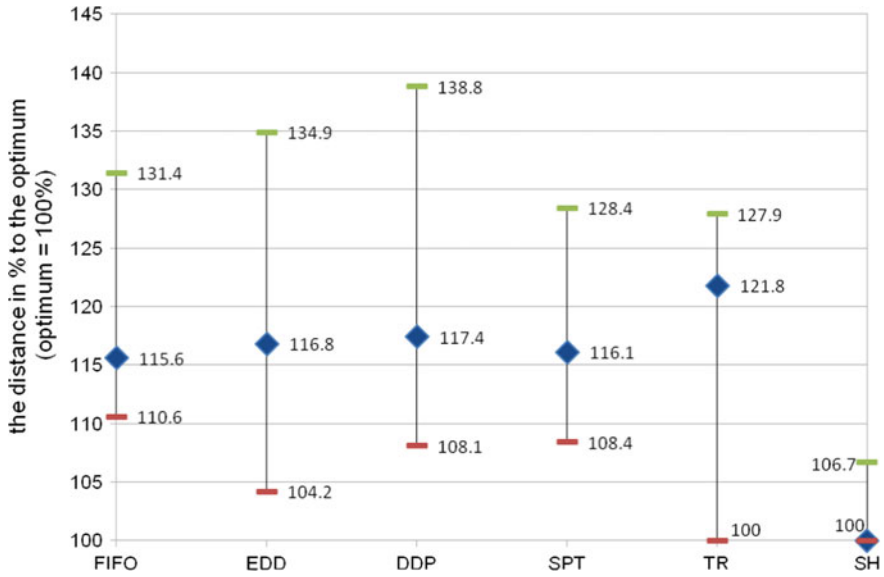


Fig. 4 Median, min-max distance to the optimum of makespan results

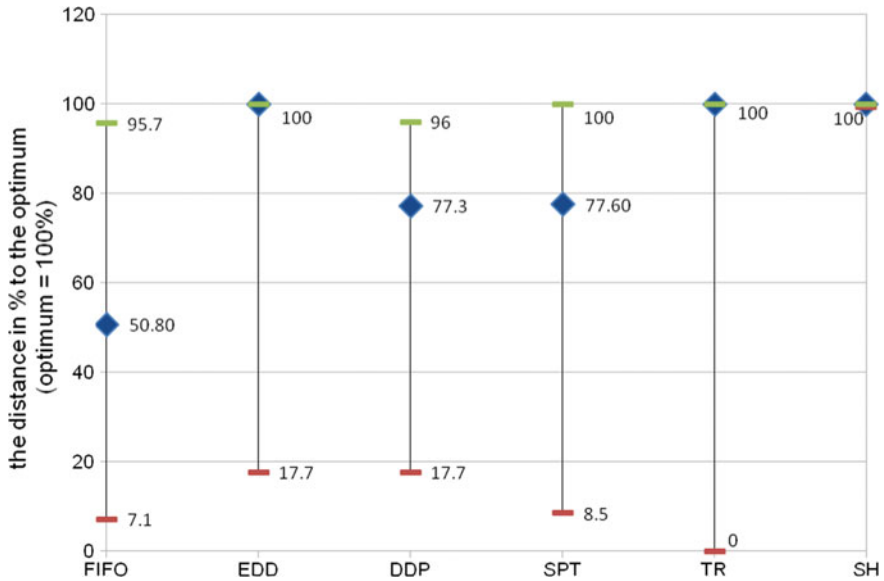


Fig. 5 Median, min-max distance to the optimum of profit results

and SH. It is worth mentioning that the EDD and TR methods occasionally produced very poor results, both for Set 1 and Set 7. It may suggest that those two

specific sets are not meant to be sorted with EDD or TR method. Instead, the SH method is preferable for sorting Set 1 and Set 7, as well as for other sets.

## 5 Conclusion

The objective of the conducted study was to investigate the new SH algorithm in the context of job sorting with regard to two criteria: minimal makespan and maximal profit. For 10 sets of 10 jobs with known optimal solution, the SH algorithm produces 6 optimal solutions out of 10 for the makespan criterion and 9 optimal solutions out of 10 for the profit criterion. The solutions were obtained for the discrete space of  $10!$  results in 0 s time (below 1 s). The study proved that the SH algorithm is able to discover the optimal sorting where other selected methods fail. The main reason why the SH algorithm is regarded as the best approach in this study is its ability to search for a solution while testing many job sorting. On the other hand, the basic methods also called static methods, e.g., EDD, FIFO, SPT, result in finding just a one solution. Therefore, the authors find it practical to compare the SH algorithm results against other heuristic, fast-computational methods in future articles.

## References

1. Emmons, H., Vairaktarakis, G.: *Flow Shop Scheduling*. Springer, New York, US (2013)
2. Knosala, R, Wal, T.: A production scheduling problem using genetic algorithm. *J. Mat. Process. Technol.* **109**(1–2), 90–95 (2001) (Elsevier Science SA)
3. Pugazhenthii, R., Xavior, M.A.: A Heuristic Toward Minimizing Waiting Time of Critical Jobs in a Flow Shop. In: *Lecture Notes on Mechanical Engineering. Emerging Trends in Science, Engineering and Technology*, pp. 343–350. Springer, India (2012)
4. Laha, D, Chakraborty, U.K.: An efficient hybrid heuristic for make span minimization in permutation flow shop scheduling. *Int. J. Adv. Manuf. Technol.* **44**, 555–569 (2009) (Springer-Verlag)
5. Xiaoping, L., Long, C., Haiyan, X., Gupta, J.N.D.: Trajectory scheduling methods for minimizing total tardiness in a flowshop. *Oper. Res. Perspect.* **2**, 13–23 (2015) (Elsevier B.V)
6. Chapadosa, N., Joliveaub, M., L'Ecuyera, P., Rousseau, L.-M. Retail store scheduling for profit. *Eur. J. Oper. Res.* **239**(3), 609–624 (2014) (Elsevier B.V)
7. Qi, X.: Production scheduling with subcontracting: the subcontractor's pricing game. *J. Sched.* **15**(6), 773–781 (2012) (Springer, USA)
8. Sereshti, N., Bijari, M.: Profit maximization in simultaneous lot-sizing and scheduling problem. *Appl. Math. Model.* **37**(23), 9516–9523 (2013) (Elsevier B.V)
9. Dylewski, R., Jardzioch, A., Krebs, I.: the optimal sequence of production orders, taking into account the cost of delays. *Manage. Prod. Eng. Rev.* **7**(2), 21–28 (2016) (Production Engineering Committee of the Polish Academy of Sciences)
10. Wang, X., Xie, X., Cheng, T.C.E.: A modified artificial bee colony algorithm for order acceptance in two-machine flow shops. *Int. J. Prod. Econ.* **141**(1), 14–23 (2013) (Elsevier B. V)

11. Jardzioch, A., Skobiej, B.: Analysis of variable changeover times impact on the revenue in manufacturing process. *Acad. J. Manuf. Eng.* **11**(4), 114–117 (2013) (Editura Politehnica)
12. Jardzioch, A., Skobiej, B.: Simulated hardening algorithm application in advanced planning and scheduling. *Entrepreneurship Manage.* **XVII**(12), part II, 105–117 (2016) (Wydawnictwo Spolecznej Akademii Nauk)
13. Dylewski, R., Jardzioch, A.: Scheduling production orders, taking into account delays and waste. *Manage. Prod. Eng. Rev.* **5**(3), 3–8 (2014) (Production Engineering Committee of the Polish Academy of Sciences)
14. Mallak, S.K., Ishak, M.B., Kasim, M.R.M., Abu Samah, M.A.: Assessing the effectiveness of waste minimization methods in solid waste reduction at the source by manufacturing firms in Malaysia. *Polish J. Environ. Stud.* **24**(5), 2063–2071 (2015) (Hard Publishing)
15. Cantore, N.: Factors affecting the adoption of energy efficiency in the manufacturing sector of developing countries. *Energy Effi.* **10**(3), 743–752 (2017) (Springer)
16. Terelak-Tymczyna, A., Miadlicki, K., Nowak, M.: The energy efficiency of the machining process on the example of rolling, (in Polish). *Mechanik*, No. 10/2016, pp 1307–1308, Redakcja Mechanik (2016)
17. Starzynska, B., Hamrol, A.: Excellence toolbox: decision support system for quality tools and techniques selection and application. *Total Qual. Manage. Bus. Excellence* **24**(5–6), 577–595 (2013) (Taylor & Francis Ltd)
18. Meng, K., Lou, P.H., Pengm, X.H., Prybutok, V.: Multi-objective optimization decision-making of quality dependent product recovery for sustainability. *Int. J. Prod. Econ.* **188**, 72–85 (2017) (Elsevier Science BV)

# A Study of Priority Rules for a Levelled Production Plan

Paulina Rewers, Justyna Trojanowska, Jacek Diakun, Alvaro Rocha  
and Luis P. Reis

**Abstract** This paper looks at initial results of research into the validity of application of selected priority rules in the development of a levelled production plan. The development of a levelled production plan is the key stage of the authors' own methodology of levelling production to mitigate the adverse impact of variable demand. A levelled production plan permits to maximize effects, defined as being able to deliver diverse products in a timely manner and at the same time reduce stocks and optimize efficient use of manufacturing resources. Application of an appropriate priority rule in the development of a levelled production plan is the key factor determining the effectiveness of the developed methodology. Initial research has been conducted for twenty automatically generated task sets. One hundred manufacturing schedules have been developed in total—five schedules for each set, according to the selected priority rules (shortest task time, longest task time, shortest processing time, longest processing time, first in first out). The schedules have been assessed in terms of meeting the selected key criteria for the objectives of levelled production.

**Keywords** Levelling production · Levelled production plan · Production scheduling · Priority rules

---

P. Rewers · J. Trojanowska (✉) · J. Diakun  
Chair of Management and Production Engineering,  
Poznan University of Technology, Poznan, Poland  
e-mail: justyna.trojanowska@put.poznan.pl

A. Rocha  
Department of Informatics Engineering,  
University of Coimbra, Coimbra, Portugal

L.P. Reis  
Department of Information Systems, University of Minho, Braga, Portugal

# 1 Introduction

Rapid developments in the economic environment pose a challenge to manufacturing companies of continual improvement in order to respond to increasing customer requirements. Variable demand causes frequent changes to production schedules, which generate increasing stocks of finished goods on one hand, and difficulties in timely delivery of finished goods on the other. Various production management methods and tools are implemented to solve ongoing issues at manufacturing companies. An analysis of the literature of the subject shows that companies implement solutions which support quality management [1–4], decision-making processes [5–8], and lean manufacturing [9].

The concept of lean manufacturing (LM) seeks to eliminate all forms of waste in manufacturing processes and thus permits to reduce lead time. It originates from the Toyota Production System (TPS), created by Japanese engineers Sakichi Toyoda, Ki'ichirō Toyoda and Taiichi Ohno [10].

One of the methods of improvement of production flow is *Heijunka*, i.e., production levelling, aimed at mitigating the effect of variable demand [11]. The concept underlying production levelling is based on sequencing and controlling the volume of inflow of goods from manufacturing processes, which ensure that stocks of finished goods match ongoing demand and no rapid changes in the production schedule are required. The production schedule should remain fixed over a certain period of time. The overall objective is to manufacture goods in a certain sequence and in smallest possible lots [12]. In other words, production levelling ensures availability of goods through a repeatable and smooth inflow of goods.

The key objectives of levelled production, as described in the literature of the subject, include:

- ensuring smooth flow throughout the supply chain [13],
- smoothing out production peaks and troughs [11],
- reducing inventories [14],
- avoiding excessive work load [15],
- increasing manufacturing capacity [16],
- maximizing effectiveness of manufacturing resources [17],
- increasing competitiveness [18].

The greatest challenge faced during implementation of levelled production is the development of an appropriate production plan. The literature of the subject offers many production scheduling algorithms. In practice, however, heuristic methods are the most popular. They do not guarantee an optimal solution, but generate a permissible solution within an acceptable time span. Heuristic methods are based on priority rules.

In the literature of the subject, no guidelines related to priority rules dedicated to levelling production were found. The research aims at evaluation of validity of the use of priority rules in the development of a levelled production plan. The paper presents results of the study for selected priority rules. The developed production

schedules have been evaluated and compared on the basis of three criteria with assigned weights.

## 2 Levelled Production Implementation Methodology

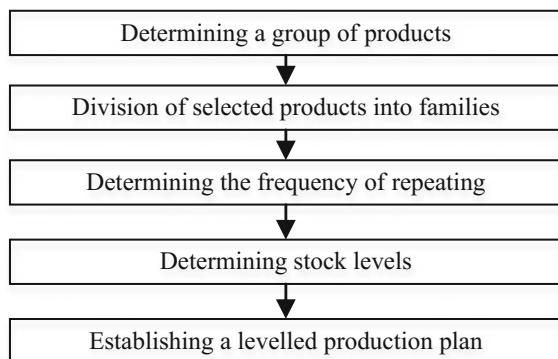
The levelled production implementation methodology proposed by the authors was first presented in [12]. It comprises the following stages (Fig. 1):

- Selection of the group of goods for which levelled production will be implemented—the objective of this stage is to select goods which are sold in the largest quantities or rotate most frequently;
- Grouping of the goods into families on the basis of their technological similarities;
- Determination of the quantity of inventories—the objective of this stage is to calculate the quantity of inventories in the supermarket;
- Determination of the intervals in which certain families of goods will be manufactured—the objective of this stage is to determine how frequently a certain quantity of goods should be manufactured;
- Development of a levelled production schedule, i.e., sequencing of manufacturing and determination of the quantity of goods to be manufactured.

At the first stage of the methodology, the group of goods for which levelled production will be implemented is determined. The range of products can be classified on the basis of the Glenday Sieve or ABC/XYZ analysis. Both methods permit to determine the group of products manufactured in the largest quantities, for which levelled production is implemented in the first place.

Next, the goods need to be divided into families based on the criterion of technological similarity. A family is understood as a group of goods manufactured

**Fig. 1** Levelled production implementation methodology





in similar technological processes. Families are identified by the use of the technology similarity matrix.

At the third stage, manufacturing intervals are determined with the use of the Every Part Every Interval (EPEI) index. The index provides data on time intervals in which lots of a given product are manufactured.

At the next stage, inventories of finished goods in the supermarket are determined. The supermarket is understood as a warehouse where certain goods have their assigned location, the First In First Out (FIFO) rule is in place, and the maximum and minimum stock levels are explicitly specified.

There are three types of inventories in the supermarket [19]:

- Rotating inventories—goods required to meet regular demand;
- Buffer inventories—good required to meet variable demand;
- Safety inventories—goods required to cover internal losses.

At the last stage of the methodology, a levelled production plan is developed. This is the most important, and at the same time the most challenging stage. The authors undertook to study the validity of application of particular priority rules in the levelled production plan. The priority rules were evaluated based on three criteria: the makespan ( $C_{\max}$ ), the machine utilization level, and the standard deviation of the differences between the end times of scheduled tasks. In levelled production, it is important that finished goods reach the warehouse as quickly as possible; the shorter the makespan, the sooner the manufacturing of new products can start. The difference between end times of scheduled tasks is also important; the smaller the difference, the more frequent inflow of goods. Optimizing the utilization of workstations, on the other hand, is one of the key objectives of levelled production.

### 3 Selected Priority Rules

Priority rules are decision rules which permit sequencing jobs processed at particular workstations in a manufacturing unit [20]. According to another definition proposed in the literature of the subject, the priority rule is a function which assigns a value, referred to as the priority ratio, to every pending task. The task with the lowest (or highest) priority ratio is the one, which needs to be completed first [21].

Priority rules are grouped by the scope of information used in the determination of the priority ratio, the relation between the priority ratio and the lapse of time, and the number of task parameters analyzed. Priority rules set on the basis of the scope of information on the tasks carried out in a manufacturing unit can be grouped into local and general. Those whose priority ratio is time- and event-dependent are referred to as static and dynamic. Grouped by the level of complexity of the priority ratio, priority rules are divided into simple, complex, combined and heuristic [22].

In practice, priority rules are most commonly applied for [21–32]:

- shortest task time,
- longest task time,
- longest next task time,
- shortest processing time,
- longest processing time,
- shortest preparation and finishing time,
- nearest task due date,
- longest preparation and finishing time,
- first in first out.

In this paper, research results for five priority rules are presented:

- Shortest task time (STT), a local and static rule that minimizes average task production cycle [33–35].
- Longest task time (LTT), which maximizes average production cycle as well as average number of tasks waiting in queues. However, for job-shop task set it minimizes average workstation-consumption of operations waiting in queues thanks to the fact that the highly workstation-consuming operations are realized faster [21].
- Shortest processing time (SPT), a local and static rule which minimizes average task production cycle and percentage of delayed tasks in job-shop order sets [21, 36].
- Longest processing time (LPT) is a local static rule that has a proven efficiency for production systems with numerous machines and production equipment. LPT also minimizes makespan for simple systems.
- First in first out (FIFO) causes waiting time of operations in queues to extend and, at the same time, extending production cycles times [21].

The scheduling process largely depends on the selection of appropriate priority rules which permit to obtain the assumed criterion. The priority rules presented are most often applied in systems with a fixed set of tasks, as they minimize the production cycle [37, 38]. One of the key drivers of competitiveness and the most important requirement of a levelled production plan is the ability to respond quickly to customer demand.

## 4 Research Methodology

The research was conducted with the use of a scheduling simulator supporting the generation of task sets, developed by the authors.

Each of the generated sets contains from 5 to 10 tasks, each task—from 3 to 20 operations. The duration of operations is generated with equal probability from the set  $\langle 1j, 9j \rangle$ . The machines on which operations are carried out are also selected with equal probability from the set  $(M1, M2, \dots, M10)$ . In order to ensure that an automatically generated set can be later reproduced, the program generates a special

code. The generated set is presented graphically and in a table. The table contains the following information:

- task number,
- duration of operation,
- workstation on which the operation is carried out,
- next operation,
- previous operation.

The scheduling result is generated graphically, in the form of a schedule, and in tables containing information on tasks and machines. Information on tasks is presented in a table of four columns under the following headings:

- task number,
- task start time,
- task finish time,
- aggregate duration of operations in a given task.

Information on machines is presented in a table of five columns under the following headings:

- workstation,
- start time of machine load,
- finish time of machine load,
- aggregate time of machine operation,
- aggregate time of machine downtime.

The research was conducted on 20 task sets. The schedules were assessed in terms of meeting the requirements for levelled production, determined on the basis of three criteria:

- criterion A—makespan, defined as the difference between the time of finishing the last operation and the time of starting the first operation,
- criterion B—standard deviation, defined as the difference between the finish times of particular tasks,
- criterion C—the inverse value of the mean level of utilization of particular machines.

## ***4.1 Research Results***

Twenty automatically generated sets were analyzed. Results for the selected set are presented in the table 1.

Each of the criteria was assigned a weight: (Table 2)

- criterion A—makespan was considered the key criterion of schedule assessment and assigned a weight of 3;

- criterion B—the standard deviation of the difference between the finish times of particular tasks has an impact on the intervals at which finished items reach the warehouse. The criterion was assigned a weight of 2;
- criterion C—the inverse value of the mean level of utilization of machines was assigned a weight of 1. Being the least significant, this criterion must be taken into consideration, since maximum utilization of machines is one of the objectives of levelled production.

Each set was assigned a priority rule which best meets the specified criteria. The assigned priority rule is expressed by the formula below (the minimum total value of products of weights and calculation results for the criteria, presented in Table 1):

$$\min(A * 3 + B * 2 + C * 1)$$

Results for the sets, presenting the priority rule that best meets the criteria taking into consideration the assigned weights, are shown in Table 3 .

**Table 1** Calculation results for each of the criteria—set no. 1

Set no. 1			
	A	B	C
FIFO	78	7.339391	2.098869
STT	71	7.054549	1.723554
LTT	78	5.501515	2.258879
SPT	73	5.501515	1.920805
LPT	80	5.419102	2.014497

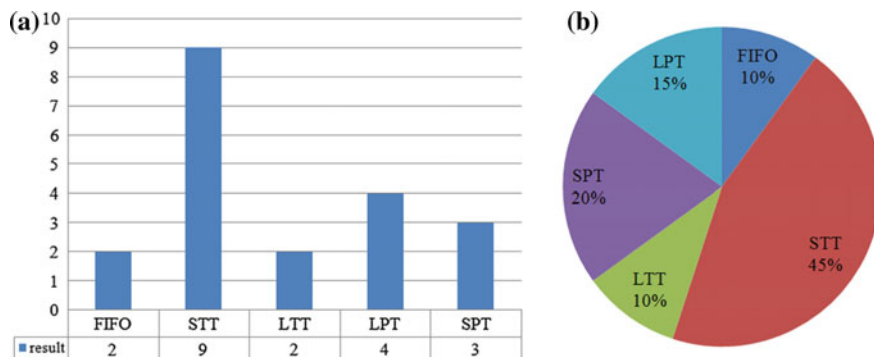
**Table 2** Results for set no. 2 with assigned weights

Set no. 1				
Weights	3	2	1	Results
	A	B	C	
FIFO	78	7.339391	2.098869	250.78
STT	71	7.054549	1.723554	228.83
LTT	78	5.501515	2.258879	247.26
SPT	73	5.501515	1.920805	231.92
LPT	80	5.419102	2.014497	252.85

**Table 3** Research results for the sets

I	II	I	II	I	II	I	II
1	STT	6	STT	11	FIFO	16	STT
2	FIFO	7	STT	12	STP	17	STT
3	LTT	8	STT	13	LPT	18	STT
4	STT	9	SPT	14	SPT	19	LTT
5	STT	10	SPT	15	LPT	20	LPT

*I* set number  
*II* priority rule



**Fig. 2** **a** Number of instances for each priority rule—results for 20 sets. **b** Research results (in percentage terms)

The results are also presented in Fig. 2. Figure 2a showing the number of instances of particular priority rules, while the percentage shares of each priority rule in the research results are presented in Fig. 2b.

The priority rule which best meets the assumed criteria is the shortest task time (STT) priority rule. It provided the best scheduling results for 45% of the sets under analysis. The analysis results confirm that the STT priority rule minimizes the mean production cycle, thus can be successfully applied in the development of a levelled production plan. The priority rules which are least likely to meet the assumed criteria are the longest task time (LTT) and first in first out (FIFO). It is important to notice that this results could be applied to special structures of manufacturing system in which levelling production is reasonable.

## 5 Summary

The results presented in this paper were obtained in the first stage of research on the development of a levelled production plan. It means that impact of complexity of a production order, setup and production times and manufacturing resources availability on the results of the method isn't discussed yet. The research currently in progress seeks to analyze production schedules developed for a larger number of sets of production tasks. Its results will be used for a thorough analysis of the structure of those tasks, in order to identify the priority rules which best meet the criteria adopted for given circumstances. The next stage of the research will focus on other priority rules which may be applied in the development of a levelled production plan. The developed methodology will be verified in selected manufacturing companies.

**Acknowledgements** This work had the financial support of Ministry of Science and Higher Education, Republic of Poland, under the project 02/23/DSPB/7695 Development of production engineering methods and tools and their implementation in the product lifecycle.

## References

1. Hamrol, A.: *Strategies and Practices of Efficient Operation. LEAN SIX SIGMA and other* (in Polish). PWN, Warszawa (2015)
2. Diering, M., Dyczkowski, K.: Assessing the raters agreement in the diagnostic catheter tube connector production process using novel fuzzy similarity coefficient. In: *IEEE International Conference on Industrial Engineering and Engineering Management*, pp. 228–232 (2016)
3. Jasarevic, S., Diering, M., Brdarevic, S.: Opinions of the consultants and certification houses regarding the quality factors and achieved effects of the introduced quality system. *Tehnicki Vjesnik-Technical Gazette* **19**(2), 211–220 (2012)
4. Borkowski, S., Knop, K.: Challenges faced in modern quality inspection. *Manag. Prod. Eng. Rev.* **7**(3), 11–22 (2016)
5. Klos, S., Patalas-Maliszewska, J.: Throughput analysis of automatic production lines based on simulation methods. intelligent data engineering and automated learning—IDEAL. In: Jackowski, K., Burduk, R., Walkowiak, K., Wozniak, M., Yin, H. (eds.) *Lecture Notes in Computer Science*, vol. 9375, pp. 181–190 (2015)
6. Kunz, G., Machado, J., Perondi, E.: Using timed automata for modeling, simulating and verifying networked systems controller’s specifications. In: *Neural Computing and Applications*, pp. 1–11 (2015)
7. Sika, R., Hajkowski, J.: Synergy of modeling processes in the area of soft and hard modeling. In: *8th International Conference on Manufacturing Science and Education (MSE), Trends in New Industrial Revolution* (2017)
8. Sika, R., Rogalewicz, M.: Demerit control chart as a decision support tool in quality control of ductile cast-iron casting process. In: *MATEC Web of Conferences*, vol. 121, p. 05007 (2017). *8th International Conference on Manufacturing Science and Education (MSE 2017)—Trends in new industrial revolution* (2017)
9. Krolczyk, J.B., Krolczyk, G.M., Legutko, S., Napiorkowski, J., Hloch, S., Foltys, J., Tama, E.: Material flow optimization—a case study in automotive industry. *Tehnicki Vjesnik* **22**(6), 1447–1456 (2015)
10. Liker, J.K., Meier, D.P.: *The Toyota Way Fieldbook. A Practical Guide For Implementing Toyota’s 4Ps*. The McGraw-Hill Companies, USA (2006)
11. Andel, T.: Accentuate heijunka, eliminate junk, supply chain flow. *Mater. Handl. Eng.* **54**(8), 77 (1999)
12. Rewers, P., Żywicki, K., Hamrol, A., Chabowski, P.: Methodology of conduct in providing creation of repeatable production plan (in Polish). *Bus. Manage.* **3**, 22–30 (2016)
13. Monden, Y.: *Toyota Management System*. Productivity Press, Portland, OR (1993)
14. Coleman, J.B., Vaghefi, M.: Heijunka: a key to the Toyota production system. *Prod. Invent. Manage. J.* **34**(4), 31–35 (1994)
15. Rinehart, J.: After lean production: evolving employment practices in the world auto industry. *Am. J. Sociol.* **104**(4), 1212–1214 (1997)
16. Yano, C., Rachamadugu, R.: Sequencing to minimize overload in assembly lines with product options. *Manage. Sci.* **37**(5), 572 (1991)
17. Xiaobo, Z., Zhou, Z., Asres, A.: A note on Toyota’s goal of sequencing mixed models on an assembly line. *Comput. Ind. Eng.* **36**, 57–65 (1996)
18. Teece, D.J., Pisano G., Shuen, A.: Dynamic capabilities and strategic management. *Strateg. Manage. J.* **18**(7) (1997)

19. Faccio, M., Gamberi, M., Persona, A.: Kanban number optimisation in a supermarket warehouse feeding a mixed-model assembly system. *Int. J. Prod. Res.* **51**(10), 2997–3017 (2013)
20. Wróblewski, K., Jurecka, A., Krawczyński, R.: Results of a study on the application of priority rules in manufacturing control (in Polish). *Sci. J. Sil. Univ. Technol. Ser. Autom.* **63** (735), 203–214 (1982)
21. Wróblewski, K.J.: Basics of manufacturing flow control (in Polish). WNT, Warszawa (1993)
22. Wróblewski, K.J., Krawczyński, R., Kosieradzka, A., Kasprzyk, S.: Priority rules in manufacturing flow control (in Polish). Wydawnictwo Naukowo-Techniczne, Warszawa (1984)
23. Binchoo, C., Matis, T.I.: A flexible dispatching rule for minimizing tardiness in job shop scheduling. *Int. J. Prod. Econ.* **141**(1), 360–365 (2013)
24. Błażewicz, J., Ecker, K.H., Pesch, E., Schmidt, G., Węglarz, J.: *Scheduling in computer and manufacturing processes*. Springer, Berlin (1996)
25. Coffman, E.G.: Theory of task scheduling (in Polish). WNT, Warszawa (1980)
26. Jardzioch, A., Bulwan, K.: The prioritisation of production orders under the bee colony algorithm. *Adv. Manuf. Sci. Technol.* **37**(4), 49–59 (2013)
27. Jardzioch, A., Skobiej, B.: Application of batch algorithm in sequencing manufacturing tasks. In: Knosala, R. (ed.) *Innovations in Management And Production Engineering*. Polskie Towarzystwo Zarządzania Produkcją, pp. 552–559 (2014)
28. Knosala, R.: Applications of artificial intelligence methods (in Polish). Wydawnictwo Naukowo-Techniczne (2002)
29. Sawik, T.: Discrete optimization in flexible manufacturing systems (in Polish). Wydawnictwo Naukowo-Techniczne, Warszawa (1992)
30. Krenczyk, D., Skołud, B.: Transient states of cyclic production planning and control. *Appl. Mech. Mater.* **657**, 961–965 (2014)
31. Manupati, V.K., Gokula, K.M., Varela, M.L.R., Machado, J.: Telefacturing based distributed manufacturing environment for optimal manufacturing service by enhancing the interoperability in the hubs. *J. Eng.*, 15 p. (2017)
32. Skołud, B.: Multi-range rhythmical manufacturing planning (in Polish). *Zeszyty Naukowe Politechniki Śląskiej, Mechanika*, p. 136 (2000)
33. Conway, R.W.: An Experimental Investigation of Priority Assignment in a Job Shop. Rand Corporation Memorandum, RM-3789-PR, Santa Monica (1964)
34. LeGrande, E.: The development of a factory simulation using actual operating data. *Manage. Technol.* **3**(1), 1–19 (1963)
35. Nelson, R.T.: Simulation of labor efficiency and centralized assignment in a production model. *Manage. Sci.* **17**(2) (1970)
36. Baker, K.R., Dan, Trietsch D.: *Principles of Sequencing and Scheduling*. Wiley, New Jersey (2009)
37. Vieira, G.G., Varela, M.L.R., Putnik, G.D., Machado, J.M., Trojanowska, J.: Integrated platform for real-time control and production and productivity monitoring and analysis. *Romanian Rev. Precis. Mech. Opt. Mechatron.* **50**, 119–127 (2016) (Mecahitech'16)
38. Szuszynski, M., Żurek, J.: Computer aided assembly sequence generation. *Manage. Prod. Eng. Rev.* **6**(3), 83–87 (2015)

# Production Process Analysis in Conditions of Short-Term Raw Materials Expiration Dates and Long Setup Times Using Simulation Method

Adrian Jakobczyk, Kamil Nogaj, Jacek Diakun  
and Reggie Davidrajuh

**Abstract** In the paper, the production process of liquid soap is analyzed using simulation method. The purpose of the study is to assess the impact of production system modernization. First, the liquid soap production process is modeled after studying the characteristics of the processes. Then, two simulation experiments are conducted based on the developed simulation models of the production line. The results of the experiments are presented and discussed.

**Keywords** Production process simulation · Liquid soap production processes  
Flow process simulation · Simulation study

## 1 Introduction

Simulation methods play a significant role in the research of production systems. Effective tools used to improve the performance of production systems at various levels of their operations. They allow a significant degree of elimination of the risk of making the wrong decision about modifying the real (productive) system by analyzing the impact of the proposed changes on its operation. The simulation method can be used for process planning and improvement for discrete or continuous production processes, i.e., in the chemical industry.

The usage of simulation method in production processes may involve various problems, like thorough analysis from the point of view of one measure of

---

A. Jakobczyk · K. Nogaj · J. Diakun (✉)

Chair of Management and Production Engineering, Faculty of Mechanical Engineering  
and Management, Poznan University of Technology, Poznan, Poland  
e-mail: jacek.diakun@put.poznan.pl

R. Davidrajuh

Department of Electrical and Computer Engineering, University of Stavanger, Stavanger,  
Norway

© Springer International Publishing AG 2018

A. Hamrol et al. (eds.), *Advances in Manufacturing*, Lecture Notes in Mechanical  
Engineering, [https://doi.org/10.1007/978-3-319-68619-6\\_12](https://doi.org/10.1007/978-3-319-68619-6_12)



performance, as in [1] and [2], or comparative study of different types of production flow [3]. Except for the most popular type of simulation models nowadays—models built-in commercial simulation software environments, still a lot of researchers and analysts use approaches like Petri nets [4]. Many times simulation study is also supported by another models like UML or BPMN [5].

In the literature, one can find numerous examples of using simulation method for production in chemical industry. In [6] simulation is used for reliability analysis of production system in the chemical plant. Another paper from the same authors describes the usage of simulation for bottleneck analysis of mixed continuous and discrete production process [7]. A complex case study of simulation including the flow of liquids in a pharmaceutical company is presented in [8]. Numerous aspects of the complexity of production processes in chemical industry were highlighted in [9]. An overview of simulation for logistics in the chemical industry is presented in [10] and [11].

## 2 Production Process of Liquid Soap

The simulation study was conducted in the company that deals with the production of liquid soap. The company's business is based on the delivery of individually customized products. The company does not own brands and does not sell at the retail level. The company has its own laboratory, where recipes are created based on the client's guidelines. Nowadays the company has one production line where all the stages of soap production are performed.

The aim of the simulation study is to determine the impact of the proposed modernization of the production line on the production process measures of performance.

The production process of liquid soap starts in a tank with mixers and built-in heating elements. Inside the tank, the soap base is heated to a melting point (temperature depending on the type of base). Then the appropriate amount of water and glycerin is dispensed into the container to prevent the soaking of the soap. The prepared base is enriched with a refreshing concentrate (aromas, essential oils, herbal extracts, natural dyes, pigments, and peels) and a mixing process starts. After mixing the ingredients, the liquid soap is ready for the bottling process.

Prepared liquid soap is pumped through the piping infrastructure to the automatic dispensing line. At this station, the substance is dispensed in the appropriate volume of the bottle and the conveyor belt goes to the dispenser turn-off station. This station is supposed to tighten the dispenser to the bottle in such a way as not to damage the dispenser and not crush the bottle. Adequately positioned dispensers are automatically fed to the tightening torque, which performs linear motion and rotates the dispenser by tightening the dispenser with the corresponding torque to the bottle.

The final stages of the process are bottles labeling, weight control, and packaging. The packaging station consists of four packaging stations for individual product packages and one carton packaging stacker.

Because of frequent changes in product recipes, one of the most important processes is continual inventory control, checking production plans, and ordering the necessary raw materials well in advance. The key factor is the aromas (one of the raw materials used in the production process), because of their very short expiration dates after the opening of the packages. The current shape of production system also enforces the long setup times in the process. The research problem is to analyze the production process in the condition of proposed changes in the production system and process.

### 3 Simulation Model and Its Verification

In the prepared simulation model, all components of the production line were reflected. The model also includes all machine change times, unit throughput capacity and percentage of production barges, 3% of the wrongly labeled product and 2% of wrongly weighted products. The model was created in the FlexSim simulation environment (Fig. 1).

Then simulation model was verified. In order to verify the model the production of 9 kinds of soap was simulated (Table 1).

The production line should produce 14,600 bottles, taking into account the deficiencies of 13,870 pieces of finished product. Also, about 25 L of soap left on the walls of the pipes and in the installation itself should also be deducted from the sum, and so the factory should produce 13,820 pieces of soaps. During the experiment, the value was 13,816 bottles. Based on this, it was assumed that the model reflects the operation of the current production line.

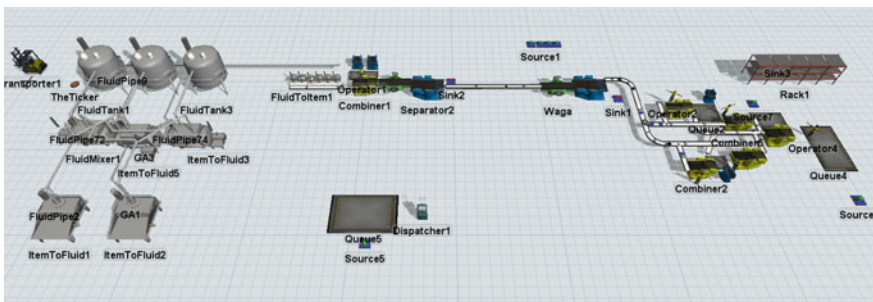


Fig. 1 Simulation model of the liquid soap production line

**Table 1** Production order for the purpose of model verification

Product	Quantity of finished product [l]	Quantity of aroma [l]	Amount of soap base mixture [l]	The amount of glycol and glycerin [l]
1	500	300	170	30
2	800	500	270	30
3	750	450	270	30
4	250	150	70	30
5	1000	630	340	30
6	1000	630	340	30
7	1000	630	340	30
8	1000	630	340	30
9	1000	630	340	30

## 4 Simulation Experiments

Two simulation experiments were conducted in this simulation study. Each of the experiments consisted of five production orders with a different number of products and different batch sizes. The first experiment assumed the use of the currently operating production line. The second experiment was to reflect the process for the modernized line. In both experiments, the productivity was chosen as a measure of performance.

In the first experiment, subsequent production orders reflect the following situations:

- production order 1—production of three types of soap with a relatively large number of ordered pieces of a particular assortment,
- production order 2—production of five different types of medium-sized soap orders,
- production order 3—production of nine types of soap for short batches,
- production order 4—production of large batches of soap no 1 and 2 and smaller lots of soap with numbers 2 and 4 (mixed order),
- production order 5—order a large variety of products for medium-sized batches.

Recipes and quantities of final products for orders 1–5 are presented in Tables 2, 3, 4, 5 and 6.

**Table 2** Recipes and quantities of final products for production order 1 in experiment 1

Product	Quantity of finished product [l]	Quantity of aroma [l]	Mixture ratios	Amount of soap base mixture [l]	The amount of glycol and glycerin [l]
1	6000	150	7:3	4095	1755
2	5000	150	8:2	3880	970
3	4000	100	6:4	2340	1560

**Table 3** Recipes and quantities of final products for production order 2 in experiment 1

Product	Quantity of finished product [l]	Quantity of aroma [l]	Mixture ratios	Amount of soap base mixture [l]	The amount of glycol and glycerin [l]
1	1800	50	8:2	1400	350
2	2000	50	7:3	1365	585
3	1950	50	6:4	1140	760
4	1700	50	7:3	1155	495
5	1800	50	8:2	1400	350

**Table 4** Recipes and quantities of final products for production order 3 in experiment 1

Product	Quantity of finished product [l]	Quantity of aroma [l]	Mixture ratios	Amount of soap base mixture [l]	The amount of glycol and glycerin [l]
1	250	50	6:4	120	80
2	400	50	8:2	280	70
3	500	50	7:3	315	135
4	200	50	7:3	105	45
5	600	50	6:4	330	220
6	500	50	7:3	315	135
7	300	50	8:2	200	50
8	400	50	8:2	280	70
9	350	50	6:4	180	120

**Table 5** Recipes and quantities of final products for production order 4 in experiment 1

Product	Quantity of finished product [l]	Quantity of aroma [l]	Mixture ratios	Amount of soap base mixture [l]	The amount of glycol and glycerin [l]
1	3800	100	6:4	2220	1480
2	250	50	7:3	140	60
3	3500	100	8:2	2720	680
4	500	50	6:4	270	180

The final measure of performance values is shown in Fig. 2.

The second experiment examined the operation of the production process after implementation of the proposed modernization. The modernization relies on dividing six spouting nozzles into three base dispensing nozzles and three nozzles for the dispensing of aroma. There were also an additional nine mobile aroma storage tanks that are connected directly to the three aroma dispensing nozzles.

Thanks to this solution, the bases are prepared in the main tanks, which can be used to produce soaps containing various aromas. Because of the direct dispensing of the aroma to the filled base, it is necessary to mix the entire contents. To solve

**Table 6** Recipes and quantities of final products for production order 5 in experiment 1

Product	Quantity of finished product [l]	Quantity of aroma [l]	Mixture ratios	Amount of soap base mixture [l]	The amount of glycol and glycerin [l]
1	1800	50	6:4	1050	700
2	200	50	7:3	105	45
3	900	50	8:2	680	170
4	1750	50	8:2	1360	340
5	1900	50	6:4	1110	740
6	1000	50	6:4	570	380
7	100	50	8:2	40	10
8	1600	50	7:3	1085	465
9	1500	50	7:3	1015	435

**Fig. 2** Productivity of the production line for orders simulated in experiment 1

this problem, another mixer was added between the dosing station and the weighing station of the product. All of these changes were included in the simulation model.

The modernization of the line reduces the downtime necessary to clean the infrastructure during the manufacture of the product. The solution also has its drawbacks: a twofold slowdown in production and the additional costs incurred for the purchase of nine mobile tanks and mixers.

During the second experiment, simulations of the same orders were performed as in experiment 1. Dosing of a constant volume of aroma directly to each of the products resulted in the need to reduce the concentration of the aromatic concentrate, and the formulas were modified.

Modified recipes of finished products and batch sizes for individual orders are presented in Tables 7, 8, 9, 10 and 11.

The final measure of performance values is shown in Fig. 3.

**Table 7** Recipes and quantities of final products for production order 1 in experiment 2

Product	Quantity of finished product [l]	Quantity of aroma [l]	Mixture ratios	Amount of soap base mixture [l]	The amount of glycol and glycerin [l]
1	6000	360	7:3	3948	1692
2	5000	300	8:2	3760	940
3	4000	240	6:4	2256	1504

**Table 8** Recipes and quantities of final products for production order 2 in experiment 2

Product	Quantity of finished product [l]	Quantity of aroma [l]	Mixture ratios	Amount of soap base mixture [l]	The amount of glycol and glycerin [l]
1	1800	108	8:2	1353.6	338.4
2	2000	120	7:3	1316.0	564.0
3	1950	117	6:4	1099.8	733.2
4	1700	102	7:3	1118.6	479.4
5	1800	108	8:2	1353.6	338.4

**Table 9** Recipes and quantities of final products for production order 3 in experiment 2

Product	Quantity of finished product [l]	Quantity of aroma [l]	Mixture ratios	Amount of soap base mixture [l]	The amount of glycol and glycerin [l]
1	250	15	6:4	141.0	94.0
2	400	24	8:2	300.8	75.2
3	500	30	7:3	329.0	141.0
4	200	12	7:3	131.6	56.4
5	600	36	6:4	338.4	225.6
6	500	30	7:3	329.0	141.0
7	300	18	8:2	225.6	56.4
8	400	24	8:2	300.8	75.2
9	350	21	6:4	197.4	131.6

**Table 10** Recipes and quantities of final products for production order 4 in experiment 2

Product	Quantity of finished product [l]	Quantity of aroma [l]	Mixture ratios	Amount of soap base mixture [l]	The amount of glycol and glycerin [l]
1	3800	228	6:4	2143.2	1428.8
2	250	15	7:3	164.5	70.5
3	3500	210	8:2	2632.0	658.0
4	500	30	6:4	282.0	188.0

**Table 11** Recipes and quantities of final products for production order 5 in experiment 2

Product	Quantity of finished product [l]	Quantity of aroma [l]	Mixture ratios	Amount of soap base mixture [l]	The amount of glycol and glycerin [l]
1	1800	108	6:4	1015.2	676.8
2	200	12	7:3	131.6	56.4
3	900	54	8:2	676.8	169.2
4	1750	105	8:2	1316	329.0
5	1900	114	6:4	1071.6	714.4
6	1000	60	6:4	564.0	376
7	100	6	8:2	75.2	18.8
8	1600	96	7:3	1052.8	451.2
9	1500	90	7:3	987.0	423.0

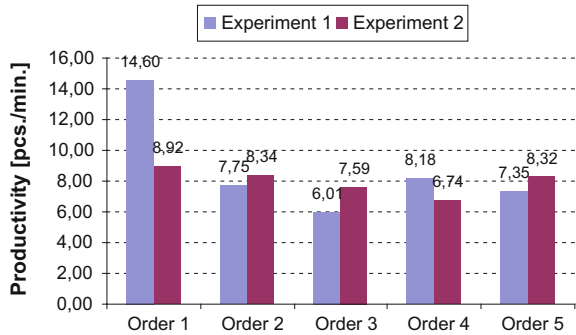
**Fig. 3** Productivity of the production line for orders simulated in experiment 2

## 5 Discussion of Results

For large orders with low diversity, the current line (Experiment 1) shows the highest performance. In the case of frequent changes in the assortment, the time needed to rinse the whole plant and rebuilding machines significantly reduces the production capacity. There is clearly a performance decline, especially for high-volume assortment production at low-volume orders. This is illustrated by the simulation of the third order in experiment 1, during which the yield was just over 6 per minute.

The proposed modernization line (Experiment 2) with respect to the current state performs poorly at higher orders for the same assortment, but less susceptible to changing the type of orders. Line capacity after the proposed upgrade is stable and ranges from 6 to 9 units per minute (for the current line the performance varied between 6 and 15 units per minute). This was achieved by reducing the length of time required for small-scale machine rebuilding and by using the ability to produce different types of soap using a common base.

**Fig. 4** Productivity comparison for orders simulated in both experiments



Comparison of the performance measure for both production line variants is presented in Fig. 4.

In current production conditions, it is highly cost-effective to accept and execute large orders of low diversity, while in the case of a modernized production line, flexibility has been achieved and multi-threaded short series become profitable. This solution alleviates the problem of short-term expiration date raw materials (aromas) storage. Increasing the flexibility of production would allow the company to fill currently unprofitable small orders.

## References

1. Klos, S., Patalas-Maliszewska, J.: Throughput analysis of automatic production lines based on simulation methods. *Lect. Notes Comput. Sci.* **9375**, 181–190 (2015)
2. Kempa, W.M., Paprocka, I., Kalinowski, K., Grabowik, C., Krenczyk, D.: Study on transient queueing delay in a single-channel queueing model with setup and closedown times. *Commun. Comput. Inf. Sci.* **639**, 464–475 (2016)
3. Varela, M.L.R., Trojanowska, J., Carmo-Silva, S., Costa, N.M.L., Machado, J.: Comparative simulation study of production scheduling in the hybrid and the parallel flow. *Manage. Prod. Eng. Rev.* **8**(2), 69–80 (2017)
4. Słota, A., Zajac, J., Uthayakumar, M.: Synthesis of petri net based model of a discrete event manufacturing system for nonlinear process plan. *Manage. Prod. Eng. Rev.* **7**(2), 62–72 (2016)
5. Bohács, G., Kovács, G., Rinkács, A.: Production logistics simulation supported by process description languages. *Manage. Prod. Eng. Rev.* **7**(1), 13–20 (2016)
6. Sharda, B., Bury, S.J.: A discrete event simulation model for reliability modeling of a chemical plant. In: *Winter Simulation Conference*, pp. 1736–1740 (2008)
7. Sharda, B., Bury, S.J.: Bottleneck analysis of a chemical plant using discrete event simulation. In: *Winter Simulation Conference*, pp. 1547–1555 (2010)
8. Kulkarni, N.S.: A modular approach for modeling active pharmaceutical ingredient manufacturing plant: a case study. In: *Winter Simulation Conference*, pp. 2260–2271 (2015)
9. Günther, H.-O., Yang, G.: Integration of simulation and optimization for production scheduling in the chemical industry. In: *Proceedings of the 2nd International Simulation Conference*, Malaga, pp. 205–209 (2004)



10. Schulz, M., Spieckermann, S.: Logistics simulation in the chemical industry. In: Engell, S. (ed.) *Logistic Optimization of Chemical Production Processes*. Wiley-VCH Verlag GmbH & Co. KG (2008)
11. Chaves, I.D.G., López, J.R.G., Zapata, J.L.G., Robayo, A.L., Rodríguez, G.N.: *Process simulation in chemical engineering*. In: *Process Analysis and Simulation in Chemical Engineering*. Springer International Publishing, Switzerland (2016)

# Development of an Intelligent and Automated System for Lean Industrial Production, Adding Maximum Productivity and Efficiency in the Production Process

Adriana F. Araújo, Maria L.R. Varela, Marivan S. Gomes,  
Raissa C.C. Barreto and Justyna Trojanowska

**Abstract** This article is related to the concept of Industry 4.0, both for the automation of manufacturing processes and for the automation of production management processes, in order to allow an improvement of performance and productivity. For its production management, based on “leagile” principles. At the industrial center of Manaus (PIM), there are around 900 companies, many multinational companies, these companies have the same intention: to produce more, by spending less. In general, globalized companies want to invest in innovation, which are technologies, inventions, products, and ideas. In most of the large companies, there are areas dedicated to innovation like research and development laboratories that rely on several researchers. This work is business-centric and it interacts with research institutes such as the Manus Institute of Technology (MIT). In developed countries, the agreement between companies and universities is the center of innovation. It is by means of which technologies, inventions, products, and finally, ideas, arrive at the market. The objective of this work is to identify and make improvements/automation in the factory floor of companies, based on Lean Production, aiming the maximum production and efficiency in the process to increase the quality of the final product. For this matter, a production line with the

---

A.F. Araújo · M.S. Gomes  
Department of Robotics and Automation Manaus,  
Manaus Instituto de Tecnologia, Manaus, Brazil

M.L.R. Varela  
Department of Production and Systems, School of Engineering,  
University of Minho, Guimarães, Portugal

R.C.C. Barreto  
Quality Assurance Department, ADGA Group Consultants Inc., Ottawa, Canada

J. Trojanowska (✉)  
Chair of Management and Production Engineering,  
Poznan University of Technology, Poznan, Poland  
e-mail: justyna.trojanowska@put.poznan.pl

philosophy of lean versus agile production will be developed in this project. This production line will feature an electronic system controlled by ARM high-performance A9 cortex processors that will be responsible for the control of all production line.

**Keywords** Automation · Production process · Production efficiency · Lean production · Agile production

## 1 Introduction

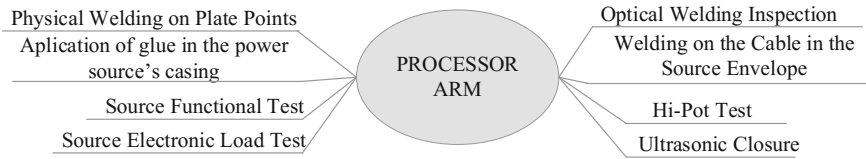
The competitiveness of enterprises depends on the effective production management, which could be supported by, among others, the production improvement methods [1, 2] and decision support methods [3–8]. Lean Production (LP) is essentially used to eliminate or minimize non-value-adding activities to the final product, LP is also known as Toyota Production System (TPS), Lean Manufacturing, or Lean Thinking [9]. Nowadays, this philosophy is widespread and is becoming an essential element in maintaining the competitiveness of companies that, regardless of size, see in this practice an assertive path in the quest for the highest quality and the lowest cost.

Agile or more precisely leagile is an emerging concept, focused on the prompt response to turbulent and dynamic markets. Agility implies integration of all related logistics operations, and from the perspective of the supply chain [10]. Comparison between Lean and Agile Production is the formation of long-term partnerships in the Supply Chain. This works best in stable product and demand situations. However, these partnerships can potentially limit flexibility and the entire Supply Chain [11]. For agile firms, partnerships tend to be more dynamic and focus on relationships in a supplier, rather than the development of lean strategies centered on aligning market needs with the competence of manufacturing firms.

The technological advance provided a modernization of the factories that arose to adapt to the demands and competitiveness of the market. It can be said that automation in a production process, has the purpose of facilitating this process, leading to optimized ones capable of producing goods with lower cost, with more quantity, in a shorter time and with higher quality.

On this project, it will be developed a production line with the philosophy of lean production. This production line will feature an electronic system controlled by ARM high-performance A9 cortex processors that make this project an innovative design. The ARM processor will be responsible for the control of all production line as shown in Fig. 1.

The line will contain machines and equipments that are going to be controlled by a processor. The processor will involve new technologies derived from the use of new knowledge. Innovations in new control techniques involve methods, equipment and/or skills for the performance of new scientific concepts, thus adding value to the research and the Institute.



**Fig. 1** Mind map on ARM processor control

The process of energy source plate requires agility and cadence in the production cycle. It is manually executed in the Power Supply process on Flex Industries SA Company. Due to this matter, some aggravating factors arise during the process, such as the reduction of agility, production efficiency and risk of repetitive strain injury or disease. Close attention is needed to eliminate redundant operations, improve workflow and information, and improve support systems, providing greater efficiency, flexibility, and quality to operations. This set of critical factors points to a viable and timely direction: the automation of the power supply board process, given that the dream of creating an automation that performs all the worker functions, is a reality today. Industrial automation is a strong tool being used to improve the productive processes within the most varied productive fields.

For proper exposure of the main ideas behind this work, this paper was organized with a brief review of the literature on some closely related and similar problems in the real practical example. Therefore, the paper is organized as follows: Sect. 2 presents the review of literature, Sect. 3 puts forward a description of the problem considered in this work, and Sect. 4 presents conclusions.

## 2 Review of Literature

The present work deals with the topic Lean Manufacturing, which began in the 1950s in Japan, more specifically, in Toyota. According to [12], it was Toyota's Eiji Toyoda and Taiichi Ohno who realized that mass manufacturing would not work in Japan and then adopted a new approach to production aimed at eliminating waste. To achieve this goal, techniques such as small batch production, set up reduction, inventory reduction, high-quality focus, and others were used. This new approach came to be known as the Toyota Production System.

Automated production systems have gained space within the factories due to the range of advantages it offers such as minimizing process time, maximizing quality and greater process accuracy, besides these factors, there are others of greater relevance for any company. The reduction of costs with labor and the increase of productivity [13] analyzes a case study about experiences and difficulties of a company in the adoption of management systems aided by computer (type MRP). This means the use of modern machinery, equipment, and software to assist processes even in very complex production areas [14, 15]. The author concludes that

the ME helps in the introduction of such systems. In [16] the authors describe the efforts of the automotive industry to increase productive capacity using ME methods. Mabry and Morrison [17] describe the adoption of some lean techniques in Delphi, while [18] shows the use of lean techniques in a European Mercedes factory that produces the Class “A” model.

Katayama and Bennett [19] compare ME with Agile Manufacturing and Adaptive Manufacturing within the Japanese context. The results show that Japanese companies are trying to achieve adaptability through agile activities. Also in [20], the authors propose a methodology in which some lean and agile principles work together. Detty and Yingling [21] did carry out a work with the simulation to quantify the benefits of adopting several lean techniques. Two studies develop and apply methodologies to evaluate the level of adoption of ME in an industrial sector described [22].

Already Brown [23] conducts a study of multiple cases on the relationship between quality, management commitment, and strategy. This study concludes that a strategic vision and a great commitment of management greatly improve the performance of quality techniques and tools within the ME context. Schuring [24] showing the kaizen, within the ME, in an automobile company. Detty and Yingling [21] did propose a better sequence of ME implementation, making it clear that some activities must be carried out in parallel. And Aydilek et al. [1] perform some studies and proves that each ME deployment is unique, and it is up to the company to choose which principle to emphasize per its strategic objectives.

The evolution in the field of automation brings with it the supplies of industrial needs as well as a range of advantages. The industrial automation has been gaining new horizons inside the companies, in order to perfect the productive process.

Therefore, the proposed solution comes through an automatic system that targets a set of software that will run in real time managed by an ARM processor. These softwares are running in the form of computational processes, concurrently through Thread (small processes that run using the shared time of the processor) with lower cost, higher productive speed, less possibility of failures and with better performance.

### 3 Description of the Problem

A product goes through several stages of construction, especially when it comes to a complex product. It is, therefore, because of the increasing complexity of the products and the means of production that it became necessary to describe the physical means of the project and its design, which were no longer complete in the mind of its creator. In addition, it became increasingly difficult to execute the product directly, since the variables involved were in increasing numbers. Among the alternatives available to improve the efficiency of the products offered by the company, R&D is the improvement of productive process. R&D activity includes: basic research (experimental or theoretical work aimed at acquiring new

knowledge, Without any specific application or use), applied research (experimental or theoretical work aimed at a specific practical objective), experimental development (systematic work based on existing knowledge, obtained through research and practical experience and directed to the installation of new processes and systems, or to substantially improve those already produced or in operation).

From a project development phase and increasing development of new products, through the increasing use of specific methods for the development of products, considering that a large number of variables involved leads to great difficulty for its control. For these reasons, an organization has “design methodologies”, which sought to delineate as ways to facilitate the development of product designs, in order to facilitate the control of its various variables. These methods, according to [25] can be defined as systematic or intuitive, and are used according to the level of complexity of the problem to be solved. Figure 2 shows the proposed automated system model with the main mechanical and pneumatic elements responsible for the execution of the process.

Lean Production Model composed of:

- Optical inspection of solder: welding machine often needs some refinishing or repair in the weld boarders. At this phase of assembling a digital image data’s processing interface (Software Development). A robot with a high-definition camera will check if there is need for repair on the board;
- Two points soldering on the source board: A robot/XYZ manipulator will automatically weld the two wires connected to no wiring source. A system developed in C/C++ language will be responsible for controlling this handler;
- Cable welding in 2 points in the involucro: A robot/manipulator XYZ will weld the two cables of the electrical terminals in the respective pins of the involucro. Software developed in C/C++ language will be responsible for controlling the manipulator;
- A robot/XYZ manipulator will pass the glue in the source’s envelope. The robot has artificial intelligence and it is able to check for the presence of glue in the

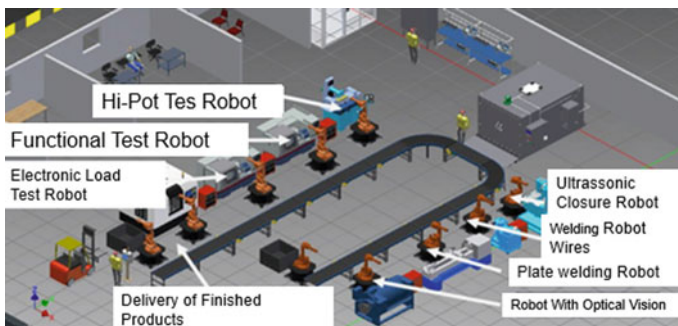


Fig. 2 Lean production model

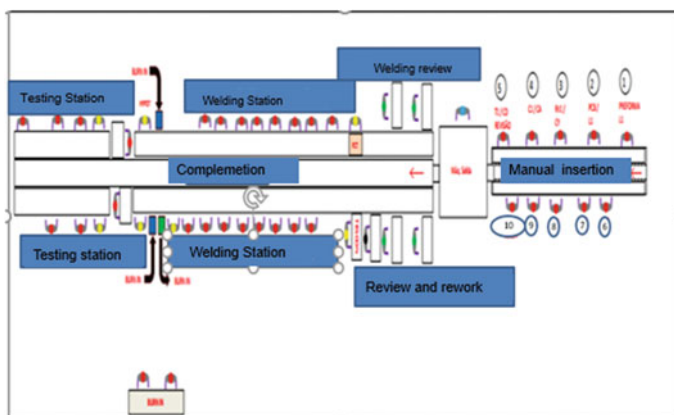
cylinder of the source. Software developed in C/C++ language will be responsible for controlling the manipulator;

- Ultrasonic Closure: A robot/XYZ manipulator will remove the source from the production line leading to the ultrasonic machine.

The production lines of the source plate are flexible and can produce different models of plates for the loaders. For a better understanding of how the productive process of plates for loader source works, Fig. 3 shows the layout and the number of operators involved in this process.

As can be seen in Fig. 3, there are already some machines that perform actions like weld revision and Burn in Anatel. In this conception, 49 operators are used in the whole process, some of them only acting as feeders of the machines. In this process 700 plates/h are manufactured, the amount of plate varies per the model. Throughout the entire productive process of Source Plates for the loaders, ergonomic risk factors can be observed that can cause repetitive strain injuries, especially in the hands and fingers, considered to be ergonomically incorrect, it is the pinch grip. This type of product handling has a great chance of affecting the operator because the activity is performed all the production cycle's time. One of the company's goals is to avoid work diseases and personnel turnover, which is the latter and the main one of this work. Once it is known that the intention of inserting a lean line system to eliminate 90% of the posts to avoid ergonomic problems, increase the production with quality and efficiency and nowadays the cycle is less complex taking only 4 s. It is necessary to develop a system with innovative characteristics to improve the production process, identifying which criteria are required in the design of the proposed system.

The aim of this approach is to ensure that there will be no delay in production or problems as the workforce will be replaced by an automated system and the production will increase for 1000 plates/h.



**Fig. 3** Layout of line 18—power supply

### 3.1 Proposed System

According to [26], the use of flexible and reconfigurable equipment helps companies to be more competitive in the market. The equipment often needs to be redefined and prepared before starting a new task. Thus, it is important to consider the preparation times separately from the processing times when scheduling the jobs on the machines. In addition, setup times are not always known with certainty, and therefore preparation times should be treated as random variables.

The real issue is to determine the production’s tasks schedule and minimal three objectives: delivery time; production cost and production time. This system works with tasks’ scheduling and unrelated parallel machines according to the production demands. The method to be developed aims to demonstrate a set of satisfactory solutions for the manipulation of the productive system and to provide support on production sequencing decisions in an instantaneous way. Figure 4 shows the description of the equipment used in the production line.

Agility is an emerging concept focused on the prompt response to turbulent and dynamic markets. Agility implies integration of all related logistics operations from the perspective of a supply chain. Benefits expected by the company considered an increase in the production of company sources by up to 30%, reduction of labor cost by up to 60% and reduction of company material waste by up to 20%.

### 3.2 Criteria Adopted for the Memory of Calculation

Zandin [27] presents the alternative method of time measurement that succeeded Methods Time Measurement (MTM) techniques from 1975 in the USA. The method consists of a technique oriented to the movement of the object when



Fig. 4 Description of equipment



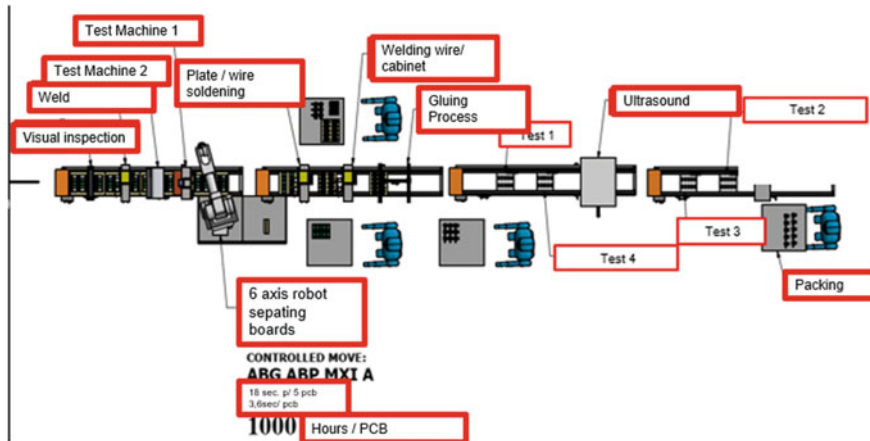


Fig. 5 New automated layout

moving from one referential to the other, free in the space with its trajectory restricted only by the resistance of the air or restricted in only one direction, in the case of contact with a surface.

From the studies of bottleneck points with the MOST technique associated with robot programming techniques, we can deduce point of application of the Robot with six axes for the processes of separation of the plates: 18 s for every 5 plates, 3.6 plates/s, 1000 plates/h. Figure 5 shows the automated lean line.

It was considered that an automated system would perform the same technical actions of the operator correcting the faults and improving the procedural factors involved, guaranteeing a better production efficiency. The project was conceived after a study of probable automated solutions already existing in other industrial processes, in order to generate a viable alternative. Due to the advancement in the automation industry, a diversity of automated elements such as sensors, pneumatic actuators, and integrated PLCs, which are essential for a productive process are being implemented in the market. Given the cycle time from 18 s to 5 plates 3.6 plates/s, the automatic process can produce up to 1000 plates/h, 300 more per hour than the manual process produces in the shortest cycle time. It is extremely important that the automatic process meets this goal because when replacing the operator the system intends to heal the limitations of the manual process while not meeting the demand of the company, the margin of error of productivity should be for more.

## 4 Conclusion

With this proposed automation, it is expected to achieve the main objective of this work: to generate an efficient and definitive solution for a lean line at Flex in Manaus. This proposed project once executed and tested will go through numerous

revisions because it is a virtual concept with probable disagreements of the physical product.

However, it can be ensured that from this idea, what will be built will rather meet expectations, considering that during the development of this work a lot of information was exchanged with automation professionals within the Manaus Institute of Technology and the company Flex that came to physically simulate how this concept addressed here.

**Acknowledgements** This work has been supported by COMPETE: POCI-01-0145-FEDER-007043 and FCT—Fundação para a Ciência e Tecnologia within the Project Scope: UID/CEC/00319/2013. Moreover, the authors would like to thank President Railma Lima and Prof. Marivan and Dr. Marlene Araújo of the Company Manaus Institute of Technology for their support provided for the accomplishment of this work, and also to the Company where this study has been carried out: “Flex Industries SA Company”.

## References

1. Aydılek, A., Aydılek, H., Allahvardi, A.: Increasing the profitability and competitiveness in a production environment with random and bounded setup times. *Int. J. Prod. Res.*, 106–117 (2013)
2. Kolinski, A., Sliwczynski, B., Golinska-Dawson, P.: Evaluation model for production process economic efficiency. *LogForum* **12**(2), 129–145 (2016)
3. Klos, S.: Implementation of the AHP method in ERP-based decision support systems for a new product development. In: Dregvaite, G., Damasevicius, R. (eds.) *Information and Software Technologies: 21st International Conference on ICIST*, pp. 199–207. Springer, Berlin (2015)
4. Klos, S., Patalas-Maliszewska, J.: Throughput analysis of automatic production lines based on simulation methods. In: Jackowski, K., Burduk, R., Walkowiak, K., Woźniak, M., Yin, H.: (eds.) *Intelligent Data Engineering and Automated Learning—IDEAL 2015*. Springer, Berlin (2015)
5. Kujawińska, A., Rogalewicz, M., Diering, M.: Application of expectation maximization method for purchase decision-making support in welding branch. *Manage. Prod. Eng. Rev.* **7** (2), 29–33 (2016)
6. Rogalewicz, M., Sika, R.: Methodologies of knowledge discovery from data and Data mining methods in mechanical engineering. *Manage. Prod. Eng. Rev.* **7**(4), 97–108 (2016)
7. Vieira, G.G., Varela, M.L.R., Putnik, G.D., Machado, J.M., Trojanowska, J.: Integrated platform for real-time control and production and productivity monitoring and analysis. *Romanian Rev. Precis. Mech. Opt. Mechatron.* **50**, 119–127 (2016) (Mecahitech'16; Bucharest)
8. Więcek-Janka, E., Lewandowska, A.: European version of a balanced scorecard in family enterprises (own research). In: *3rd International Conference on Management Science and Management Innovation (MSMI 2016)*. Atlantis Press (2016)
9. James-Moore, S.M., Gibbons, A.: Is lean manufacture universally relevant? An investigate methodology. *Int. J. Oper. Prod. Manage.* **17**(9), 899–911 (1997)
10. Kawa, A., Golinska, P.: Supply chain arrangements in recovery network. In: *KES International Symposium on Agent and Multi-Agent Systems: Technologies and Applications*, pp. 292–301. Springer, Berlin Heidelberg (2010)
11. Kawa, A.: SMART logistics chain. In: *Asian Conference on Intelligent Information and Database Systems*, pp. 432–438. Springer, Berlin, Heidelberg, (2012)

12. Womack, J.P., Jones, D.T., Roos, D.: *A Máquina Que Mudou O Mundo*, 14th ed. Campus, Rio de Janeiro (1992)
13. Johnston, R.B.: Making manufacturing practices tacit: a case study of computer-aided production management and lean production. *J. Oper. Res. Soc.* **46**, 1174–1183 (1999)
14. Ignaszak, Z., Sika, R., Perzyk, M., Kochański, A., Kozłowski, J.: Effectiveness of SCADA systems in control of green sands properties. *Arch. Foundry Eng.* **16**(1), 5–12 (2016)
15. Ignaszak, Z., Popielarski, P., Hajkowski, J., Prunier, J.-B.: Problem of acceptability of internal porosity in semi-finished cast product as new trend—“tolerance of damage”. *Mod. Des. Off. Defect Diffus. Forum* **326–328**, 612–619 (2012)
16. Braiden, B.W., Morrisson, K.R.: Lean manufacturing optimization of automotive motor compartment system. In: 19th International Conference on Computers and Industrial Engineering, vol. 31(1/2), pp. 99–102 (1996)
17. Mabry, B.G., Morrison, N.K.R.: Transformation to lean manufacturing by an automotive component supplier. In: 19th International Conference on Computers and Industrial Engineering, vol. 31(1/2), pp. 95–98 (1996)
18. Kochan, T.A.: Automotive industry looks for lean production. *Assembl. Autom.* **18**(2), 132–137 (1998)
19. Katayama, H., Bennett, D.: Agility, adaptability and leanness: a comparison of concepts and a study of practice. *Int. J. Prod. Econ.* **60–61**, 43–51 (1999)
20. Hampson, I.: Lean production and the Toyota Production System—or, the case of the forgotten production concepts. *Econ. Ind. Democr.* **20**(3), 369–391 (1999)
21. Detty, R.B., Yingling, J.C.: Quantifying benefits of conversion to lean manufacturing with discrete event simulation: a case study. *Int. J. Prod. Res.* **38**(2), 429–445 (2000)
22. Soriano-Meier, H., Forrester, P.L.: A model for evaluating the degree of leanness of manufacturing firms. *Integr. Manuf. Syst.* **13**(2), 104–109 (2012)
23. Brown, S.: New evidence on quality in manufacturing plants: a challenge to lean production. *Prod. Inventory Manage. J.*, 24–29 (1998)
24. Schuring, R.W.: Operational autonomy explains the value of group work in both lean and reflective production. *Int. J. Oper. Prod. Manage.* **16**(2), 171–182 (1996)
25. Medeiros, E.N.: *Uma Proposta de Metodologia para o Desenvolvimento de Projeto de Produto*. Tese de Mestrado, Rio de Janeiro: Kay, J.M. Combining lean and agile characteristics: creation of virtual groups by enhanced production flow analysis. *Int. J. Prod. Econ.* **85**, 305–318 (2003)
26. Allahverdi, A., Aydilek, H.: Algorithms for no-wait flowshops with total completion time subject to makespan. *Int. J. Adv. Manuf. Technol.* **68**, 2237 (2013)
27. Zandin, K.B.: *MOST work measurement systems*, Dekker (1990)

# The Use of Virtual Design to Accommodate a Workplace for a Hearing-Impaired Worker

Karolina Szajkowska and Anna Karwasz

**Abstract** The article describes the possibility to use CAD systems and virtual reality when designing a workplace for a hearing-impaired worker. After a detailed analysis of tasks performed at the given workplace, and the worker's personal characteristics, the authors proposed a project of a cart to transport plated hangers. The design was then evaluated for feasibility and compliance with the requirements of workplace ergonomics.

**Keywords** Disability · Hearing-impaired · Ergonomics · CAD · Virtual reality

## 1 Introduction

The article presents the possibility of using virtual design to accommodate a selected workplace for a worker with hearing impairment.

According to the definition of disability, a disabled person is permanently or temporarily unable to fulfill social functions due to permanent or long-term impairment of their body, resulting in particular in their inability to work.

Disability can be understood as [1] follows:

- (a) the existence of a chronic medical condition, chronic disease,
- (b) the existence of functional limitations,
- (c) inability to work,
- (d) being on sick leave for more than a specified number of days (depending on national regulations),
- (e) being retired because of age or disability.

---

K. Szajkowska (✉) · A. Karwasz (✉)  
Poznan University of Technology, Poznań, Poland  
e-mail: karolina.strykowska@interia.pl

A. Karwasz  
e-mail: anna.karwasz@put.poznan.pl

Hearing impairment causes difficulties in learning a language and speaking, due to the damage to the hearing analyzer. A person with such impairment requires assistance in education and adaptation to social life [2]. The total or partial loss of hearing results in the deprivation of access to sounds originating from the environment, and consequently leads to a worse life situation compared to that of hearing people, e.g., at work, and during cognitive processes [3, 4].

It is necessary to understand the limitations in employment resulting from hearing impairment [5, 6]. Persons with such a disability may suffer from different degrees of hearing loss, have the different educational background, and use different forms of communication. Persons who are deaf or suffer from profound hearing loss communicate and learn primarily through visual methods (sign language, symbols). However, people with mild to severe hearing impairment may use other than visual methods of communication and learning. Such people can also use spoken language [7].

At work, a hearing impairment of a worker requires that accommodation measures be introduced at his/her workstation. The changes affect also daily interactions between the supervisor and subordinate. This is mainly due to the difficulties in communication with a hearing-impaired worker. The problem is caused on the one hand by the disabled person's insufficient knowledge of Polish, and on the other, by the unfamiliarity with the sign language among hearing people, and their inability to understand the limitations faced by the hearing-impaired person. The majority of people with hearing impairment display a low level of competence in Polish: to them, it is a foreign language [8, 9]. Due to their poor skills of reading and writing in Polish, hearing-impaired workers are often unable to effectively communicate in writing [10].

All the above poses a challenge in the professional context when hearing-impaired workers are trained: it is difficult to make sure that they fully understand the information they receive. They may find it difficult to understand the information given in presentations, procedures, or training manuals.

If one does not know the sign language, the simplest methods used in the interaction with a hearing-impaired person involve training by showing how an activity is done, extending the training time, supervising the work to see if all the information has been correctly understood. The whole process is easier if a hearing-impaired worker is familiar with lip-reading techniques.

When a workplace is designed, it is necessary to consider the principles of ergonomics. According to those principles, it is necessary to undertake relevant actions aimed at designing an effective work system which takes into account the well-being of the worker [11]. Such actions include workplace accommodation measures which ensure high efficiency, reduce work discomfort or inconvenience, and result in both physical and psychological comfort of the worker [12–15]. In the case of a hearing-impaired worker, it is also important that the workplace may not pose an additional risk of accident due to the person's inability to receive auditory signals from the environment.

Professional insertion of the disabled improves their self-esteem. They feel they contribute to the economic growth. They are often also socially engaged. We also see greater responsibility for work conditions among employers [16].

Workplace ergonomics principles are particularly vital when the designed workplace will be operated by a hearing-impaired worker. Virtual reality systems may be useful in the process.

Compute-aided design systems (CAD) and virtual reality systems (VR) allow us to create a virtual, three-dimensional environment that can be viewed in real time [17–19]. With CAD or virtual reality, it is possible to design a simulation of a workplace, feel it with the sense of sight and hearing, and interact with objects located at the workplace and in its vicinity [20].

The use of CAD or virtual reality in the process of visualization and interaction brings a number of benefits. First of all, it makes us possible to eliminate errors made during the workplace design process, thus reducing the cost of creating new workplace or accommodating existing workplaces to meet the requirements of ergonomics [21]. It allows you to quickly create and test different options of the designed workplace. It can often be done together with the client, or person working at the given workplace [22]. Through the use of CAD or virtual reality, we can analyze the safety and ergonomics of the workplace [20].

Systems CAD and virtual reality facilitates staff training in various fields; it is not only helpful at the stage of workplace design, but it can be used also in manufacturing, medicine, and education. Therefore, it seems reasonable to use it while training persons with hearing impairments [23–27]. A hearing-impaired person, before starting work at an actual workplace, may be trained using a virtual model.

## **2 Description of a Workplace Operated by a Hearing-Impaired Worker**

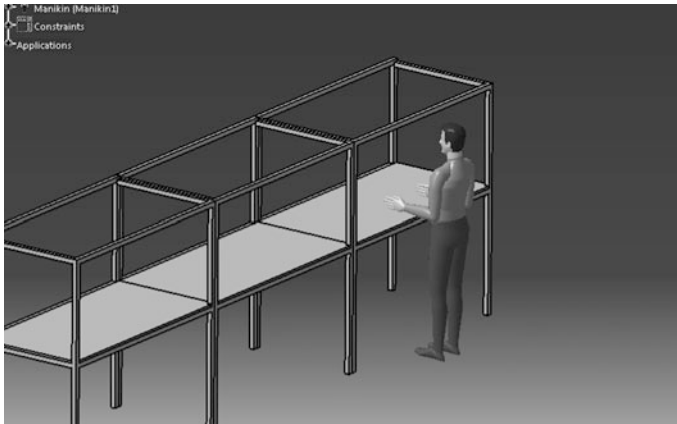
The workplace under discussion is located in the electroplating room and consists of three tables connected to each other, 3 m long and 1.5 m wide. There are also transverse beams located above the tables (Fig. 1). The workplace is operated by hearing-impaired workers.

The worker's job is to place various types of products made of plastic on hangers (Fig. 2).

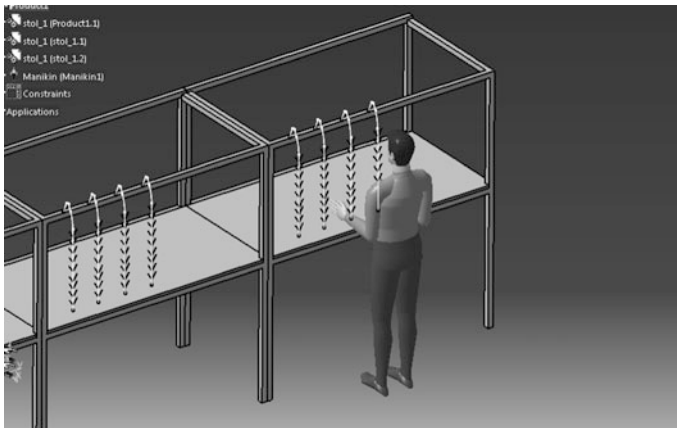
Two types of hangers are used in the electroplating process: single, small Christmas-tree shaped hangers, 100 cm long and 3 cm wide, and rectangular frame-like hangers, 100 cm long and 110 cm wide (Fig. 3).

The two types of hangers are used to hang details from 5–10 mm to 20–100 mm large, respectively, (Fig. 4).

From 20 to 40 elements are placed on one small hanger. On the larger frame-like hangers, from 100 to 200 elements can be placed. The hangers are then put on racks



**Fig. 1** Workplace operated by hearing-impaired workers



**Fig. 2** The job of hanging plastic details on Christmas-tree hangers

and wait until more such hangers with elements are prepared to complete a full load. A complete load consists of a maximum of ten single hangers or one or two frame-like hangers. Four loads of hangers can be loaded into the electroplating machine within one hour. During one shift, the machine can be loaded with 32 loads of hangers.

The next task of the worker is to manually transport the hangers to the loading area of electroplating machine no. 1.

For single hangers, the worker must cover the route between the hanging and loading area maximally five times to prepare one load. In the case of frame-like hangers, they are usually transported in pairs, so it is necessary to walk the route twice to prepare a complete load.

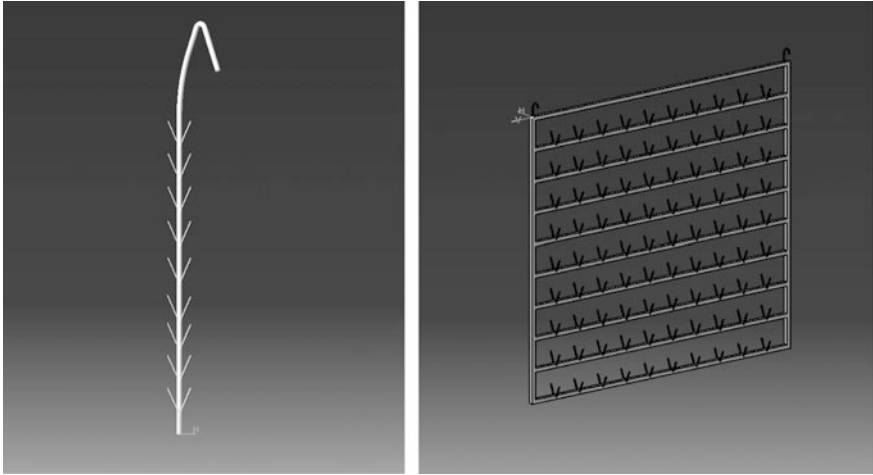


Fig. 3 Small christmas-tree shaped hangers and large, rectangular hangers

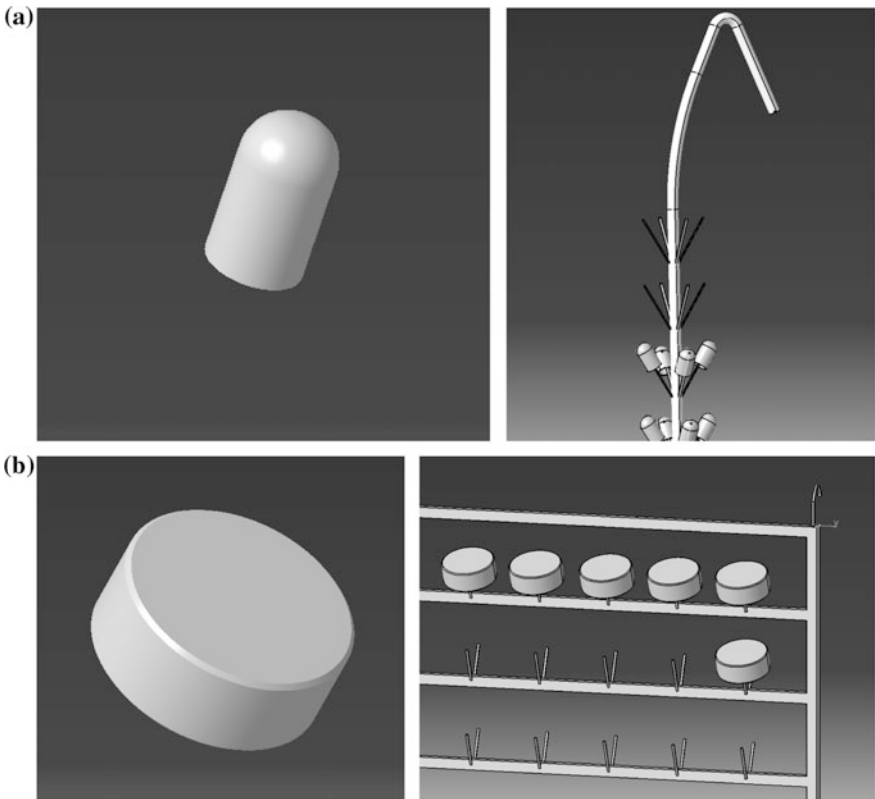


Fig. 4 Details placed on the hangers: a small and b large



### 3 Workplace Analysis

The job performed at the given workplace consists of hanging plastic elements on hangers which are then manually transported to the electroplating machine loading area. The worker moves between the areas of hanging and loading from 32 to 158 times (depending on the type of hangers).

The analysis of work performed at this workplace showed primarily significant monotony, repetitiveness of the work, and the physical load of the worker. The most burdensome activity is the manual transport of hangers to the loading area.

Other workers who perform other tasks on the same floor move near the workplace of the hearing-impaired worker. The hearing-impaired worker repeatedly moves from the hanging station to the loading station, which may cause a risk of collision with other workers. When a frame-like hanger is transported by two persons, the risk of collision is even higher because one of them is moving backward.

Another factor justifying the need to reorganize the workplace is the disability of the worker, and thus risks resulting from having to pass near an electroplating machine, particularly near its moving parts: the chassis, moving with the hangers over the machine. The chassis, after the plating cycle is completed, approaches the unloading station located in front of the machine. The hearing-impaired worker is focused on transporting the hangers and is not able to simultaneously watch the chassis as it crosses his route. While transporting the hangers the worker must be careful not to damage the hanging elements or the hangers.

### 4 Proposed Accommodation of the Existing Workplace

The analysis of tasks performed at the workplace showed that the transport of hangers is the most burdensome and time-consuming activity.

Therefore, we suggested that an improvement can be introduced in the form of a cart to be used to transport hangers between the hanging area and the electroplating machine loading area (Fig. 5).

The cart can be used to transport up to 40 single hangers, which is equal to four complete production loads. The worker will then cover the route not 158 times but 32 times (for single hangers), or 8 times instead of 32 times (for frame-like hangers).

The location of the cart at the workstation is shown in Fig. 6.

The use of the cart significantly reduces the physical burden to the worker, minimizes the risk of collision with other workers, and reduces the time of transport of the hangers to the loading area [27, 28].

Figure 7 shows a top view of the galvanizing department as workstations, hanger's warehouses, galvanizing machine (ABS\_1, ABS\_2, ABS\_3), places of loading and unloading of machine, and planned carts route.

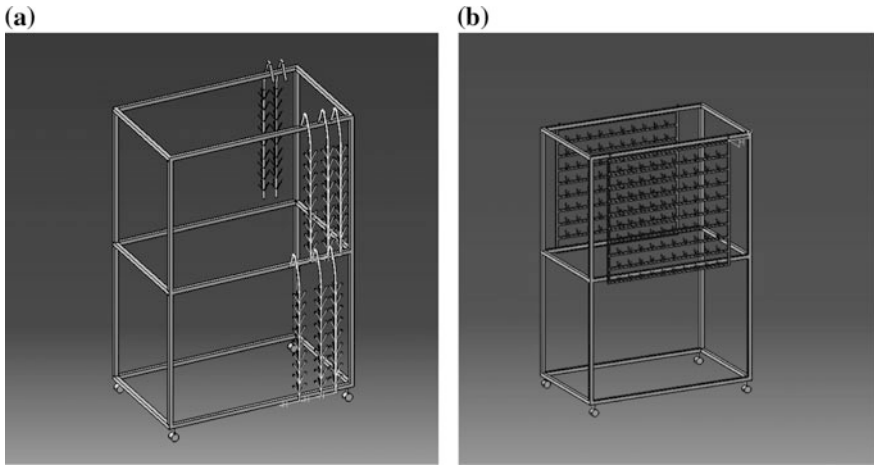


Fig. 5 Design of the cart, a small and b large

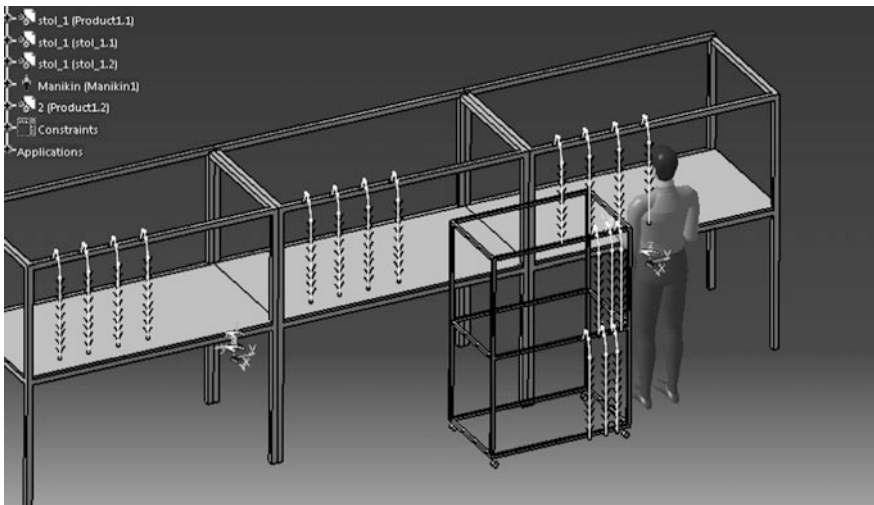


Fig. 6 The location of the cart at the workstation

On the route from the place of loading ABS\_1 to the workstation—hanging the parts on the hangers—there is no other transport movement than this with racks. On each, machine only one employee works, which is responsible for loading and unloading the machine.

The proposed cart has a width of 50 cm, while the transport road in the narrowest place (loading and unloading ABS\_1) has a width of 160 cm. This allows the unloading and loading of the galvanizing machine with the participation of two employees in a way that does not interfere with the work of other persons.

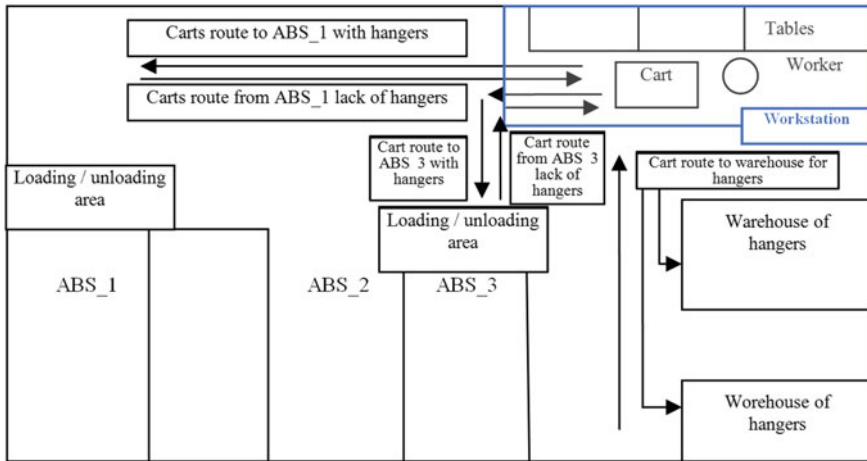


Fig. 7 View of layout of the whole system (galvanizing department and scope of worker's route)

This solution minimizes the possibility of employee collision, which is more likely to occur during manually transporting the hangers to the place of loading.

## 5 Conclusions

CAD and virtual reality systems facilitate the process design work for both product designers and process engineers. The designed virtual model can be tested before its actual implementation. It is, therefore, possible to check different options of the process, e.g., the number of hangers that can be transported, technological, or architectural possibilities on the floor related to the use of the cart. The tool shortens the time needed for the design process and minimizes the cost.

The article demonstrates that such a tool is particularly helpful in accommodating a workplace to the needs of persons with hearing impairments.

## References

1. Declaration on the Rights of Disabled Persons of 1975 (1975)
2. Hoffman, B.: Rehabilitation of the deaf. In: Introduction to Teaching Processes, p. 27. PWN (1979) (in Polish)
3. Grzegorzewska, M.: Special Education, p. 30. PIPS (1964) (in Polish)
4. Bowe, F.G., McMahon, B.T., Chang, T., Louvi, I.: Workplace discrimination, deafness and hearing impairment: the national EEOC ADA research project. *Work* **25**, 19–25 (2015)
5. Starzyńska, B., Kujawińska, A., Grabowska, M., Diakun, J., Więcek-Janka, E., Schnieder, L., Schlueter, N., Nicklas, J.-P.: Requirements elicitation of passengers with reduced mobility for

- the design of high quality, accessible and inclusive public transport services. *Manage. Prod. Eng. Rev.* **6**(3), 70–76 (2015)
6. Strykowska, K., Starzyńska, B.: Accommodating and training hearing-impaired staff at control positions. In: Knosala, R. (ed.) *Innovation in Management and Production Engineering*, vol. 2, pp. 286–299 (2016) (in Polish)
  7. Perkins-Dock, R.E., Battle, T.R., Edgerton, J.M., McNeill, J.N.: A survey of barriers to employment for individuals who are deaf. *JADARA* **49**(2), 66–85 (2015)
  8. Piekot, T.: Report on focus studies—professional identity of hearing-impaired and their problems on the job market (in Polish) (2012)
  9. Smith, J.A.: Managing dual relationships for rehabilitation professionals who work with clients who are deaf or hard of hearing. *Jadara* **49**, 41–52 (2014)
  10. Johnson, V.A.: Factors impacting the job retention and advancement of workers who are deaf. *Volta Rev.* pp. 341–356 (1995)
  11. Article on the website of the Polish Ergonomics Society. [http://ergonomia-polska.com/07\\_03\\_ergonomia.htm](http://ergonomia-polska.com/07_03_ergonomia.htm), 08 Jan 2017
  12. Ejzdys, J., Kobylińska, U., Lulewicz-Sas, A.: *Integrated Systems of Managing Quality, Environment and Work Safety*. Publishing House of the Bialystok Technical University (2012) (in Polish)
  13. Górska, E.: *Ergonomics. Design, Diagnosis, Experiments*. Publishing House of the Warsaw University of Technology (2015) (in Polish)
  14. Górska, E., Lewandowska, J.: *Management and Organization of the Workplace*. Publishing House of the Warsaw University of Technology (2010) (in Polish)
  15. Byrska-Bienias, K., Zemczak, M.: The use of augmented reality in workplace design, innovation in production management and engineering. In: Knosala, R. (ed.) *Innovation in Management and Production Engineering*, vol. 2, pp. 435–446 (2017) (in Polish)
  16. Kujawińska, A., Vogt, K., Wachowiak F.: Ergonomics as significant factor of sustainable production. In: Golińska, P., Kawa, A. (eds.) *Technology Management for Sustainable Production and Logistics*, pp. 193–203. *EcoProduction* (2015)
  17. Burda, G.C., Coiffet, P.: *Virtual Reality Technology*. Wiley, NJ (2003)
  18. Martín-Gutiérrez, J., Mora, E., Añorbe-Díaz, B., González-Marrero, A.: Virtual technologies trends in education. *EURASIA J. Math. Sci. Technol. Educ.* **13**, 469–486 (2017)
  19. Butlewski, M., Sławińska, M., Niedźwiecki, M.: 3D laser models for the ergonomic assessment of the working environment. In: Goossens, R. (eds.) *Advances in Social & Occupational Ergonomics. Advances in Intelligent Systems and Computing*, vol. 487, pp. 15–23. Springer, Cham (2017)
  20. Budziszewski, P., Grabowski, A., Jankowski, J., Kilanowicz, M.: Possibilities of using VR to design workplace for hearing-impaired persons (in Polish). *Saf. Work* **5**, 6–8 (2011)
  21. Górski, F., Wichniarek, R., Zawadzki, P., Buń, P., Rabinek, M.: Building a visual configurator using the engineering knowledge, innovation in production management and engineering. In: Knosala, R. (ed.) *Innovation in Management and Production Engineering*, vol. 2, pp. 168–179 (2017) (in Polish)
  22. Zawadzki, P., Żywicki, K.: Smart product design and production control for effective mass customization in the industry 4.0 concept. *Manage. Prod. Eng. Rev.* **7**, 105–112 (2016)
  23. Górski, F., Buń, P., Wichniarek, R., Zawadzki, P., Hamrol, A.: Effective design of educational virtual reality applications for medicine using knowledge-engineering techniques. *Eurasia J. Math. Sci. Technol. Educ.* **13**, 395–416 (2017)
  24. Buń, P., Wichniarek, R., Górski, F., Grajewski, D., Zawadzki, P., Hamrol, A.: Possibilities and determinants of using low-cost devices in virtual education applications. *Eurasia J. Math. Sci. Technol. Educ.* **13**(2), 381–394 (2017)
  25. Karwasz, A., Trojanowska, J.: Using CAD 3D system in ecodesign—case study. In: Golinska-Dawson, P., Kolinski, A. (eds.) *Efficiency in Sustainable Supply Chain, Part II*. Springer International Publishing, pp. 137–160 (2017)

26. Trojanowska, J., Karwasz, A., Machado, J., Varela, M.L.R.: Virtual reality based ecodesign. In: Golinska-Dawson, P., Kolinski, A. (eds.) *Efficiency in Sustainable Supply Chain, Part II*. Springer International Publishing, pp. 119–135 (2017)
27. Weiss, Z., Diakun, J., Dostatni, E.: Design management in virtual intranet environment. *ISAS/CITSA* **3**, 253–256 (2004)
28. Kowal, E., Gabryelewicz, I.: Diversification of safety culture elements in various professional groups. *Science Journal Poznan University of Technology: Organization and Management*, **65**, 43–53 (2015)

# Intelligent Platform for Supervision and Production Activity Control in Real Time

Gaspar G. Vieira, Maria L.R. Varela, Goran D. Putnik  
and Jose Machado

**Abstract** Nowadays there is a need for platforms, methodologies and tools for enabling to enhance either project or production activity control along with maintenance activities within production companies. In order to help small companies to overcome these difficulties in this paper, we propose a platform that intends to enable these companies to acquire top software tools, at a low cost. Our proposed platform intends to integrate smart objects, able to communicate with central processors and computers, in a network-based environment, including a set of associated input and output devices. These devices enable precise data and information acquisition and processing, in order to better support production management and maintenance decision-making. The proposed platform enables to support decision-making at several distinct hierarchical decision levels within a company, from the shop floor up to higher strategic planning levels. In this paper, a module for supporting the attribution of operations to operators, based on the Hungarian algorithm is presented and briefly discussed.

**Keywords** Production management · Production activity control · Hungarian algorithm

## 1 Introduction

Intelligent platforms have increasingly been proposed during the last years and some important contributions have been put forward, such as, [1–7]. Although there remain some important unsolved issues, for instance regarding a suitable integration

---

G.G. Vieira · M.L.R. Varela · G.D. Putnik  
Department of Production and Systems, School of Engineering,  
University of Minho, Braga, Portugal

J. Machado (✉)  
Department of Mechanical Engineering, School of Engineering,  
University of Minho, Guimarães, Portugal  
e-mail: jmachado@dem.uminho.pt

of input and output devices, along with appropriate methods for reaching better decision-making support regarding manufacturing management and maintenance functions. Therefore, an appropriate, more rigorous, effective and efficient management of production resources and equipments is of utmost importance [8, 9]. In this context, the production planning and control functions play a fundamental role, along with accurate maintenance activities, while reducing waste and costs in order to improve the overall production system performance [10, 11].

Moreover, due to the necessity of the companies to produce in higher quantity, but also with high levels of quality and at reduced prices, the trade-off between these controversial objectives becomes increasingly difficult to reach, becoming even more complicated due to the competition levels arising in the current global market scenario.

In order to help the small companies overcome this difficulty, in this paper, we propose a platform that intends to enable them to acquire top software tools, at a low cost, which is almost impossible nowadays, for instance in Portugal, as this kind of software tools are usually very expensive and require a difficult implementation process in companies with low financial income.

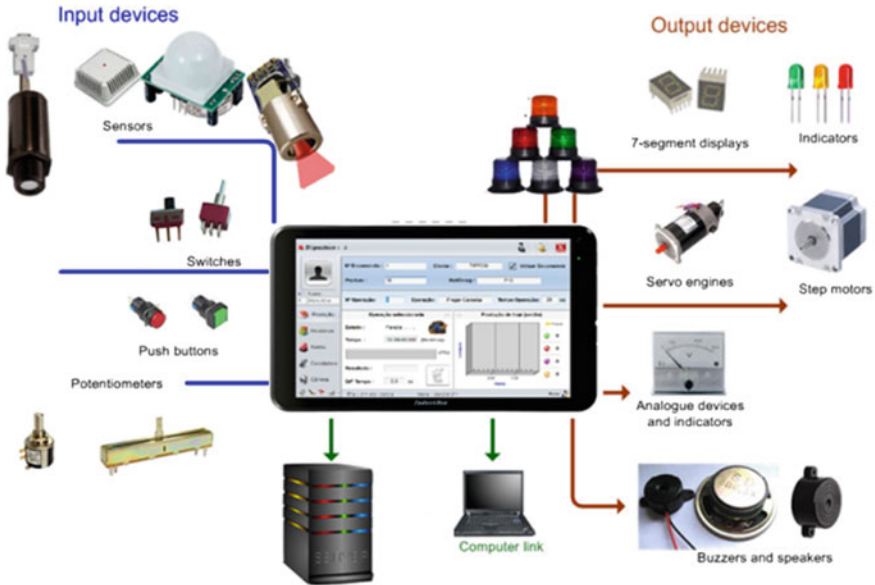
## 2 Proposed Platform

This section presents a proposed intelligent platform for supporting production management, including production planning and control functions, along with production supervision and production activity control.

The proposed platform integrates smart objects, able to communicate with central processors and computers, in a network-based environment, including a set of associated input and output devices, as illustrated in Fig. 1 (e.g. input devices such as, sensors, switches, push buttons, potentiometers and output devices, such as, indicators, segment displays, servo engines, step motors, analogue devices and indicators, buzzers and speakers, among others) for precise data and information acquisition and processing. All these devices are used in order to better support production management and maintenance decision-making, at several distinct hierarchical decision levels within a company, from the shop floor up to higher strategic planning levels.

### 2.1 Platform General Architecture

The proposed platform includes a set of integrated technologies or modules [7], which are mainly based on supervision equipment, data acquisition and processing devices and tools, including smart objects, as illustrated in the platform's architecture shown in Fig. 1. One such core modules integrated within the proposed platform enables to automatically and/or manually collect data from the operating



**Fig. 1** Platform’s input and output devices

manufacturing system, through the smart objects interacting with manufacturing resources or manually through local managers. This data is further inserted in a knowledge base (KB), for being further processed and analyzed through an underlying decision support system (DSS), which integrates several distinct modules, based on distinct kind of decision support algorithms, for instance, based on the Hungarian algorithm, for assigning tasks to operators.

The proposed platform enables automatic monitoring and context perception, which are very important characteristics of several distinct kind of decision support systems, for instance systems for supporting supply chain management, enterprise resource planning and warehouse management [7, 11–15], as they can perform better being automatically updated with dynamically new generated data [7, 14].

## 2.2 Platform’s Main Functionalities

The proposed intelligent platform is integrated and aimsto control and monitor production and evaluation of productivity on a real-time basis via web access. Using hybrid algorithms and scheduling algorithms that allow management and optimized use of production resources and perfect synchronization of production flows, along with high-quality standards, tools and devices, and web-based protocols for communication and data acquisition, processing and presentation [11–14].



This platform aims at fulfilling a gap in the industrial companies on production control on a real-time basis. Therefore, the proposed platform intends to be able to overcome the lack of dynamic information and decision-making support in companies, by enabling to identify and manage the various production processes and report them in an automated and dynamic way. The platform thus enables to provide a centralized system that allows automatic monitoring and supervision, along with a real-time-based production activity control supports the entire production process in a company.

On the other hand, it also allows large companies to add more existing technology in a fast, efficient and compatible way, without ever compromising existing systems, and perfect performance, while running in parallel with other systems.

The intelligent term on the platform arises from the ability that this platform intends to have to perform functions and tasks that, when being carried out by a human being would be considered intelligent. Such capabilities are mainly related to the hybrid algorithms and of multi-criteria analysis connected with Artificial Intelligence that supports the entire platform. This is a broad concept, and it receives as many definitions as we provide different meanings to the word intelligence. We can think of some basic features on this platform, such as reasoning ability (applying logical rules to a set of available data to reach a conclusion), learning (learning from mistakes and correctness in order to act more effectively in the future), among other functionalities. To recognize patterns (data patterns, housed in the database) and inference (ability to apply the reasoning in the quotidian of the industrial company).

This intelligent platform is mainly based on intelligent data acquisition and information processing, based on smart objects, which include two boxes (electronic devices), called IndustBox-Slave and IndustBox-Master that have been developed and are continuing to be improved, for further implementation on other industrial companies. These boxes are used to acquire data of the most diverse equipment or industrial machines, and in the context of this work carried out, particularly regarding equipment used in a clothing company, using a wide range of sensors and actuators, among other devices and tools.

Moreover, another kind of ‘intelligent’ feature of the proposed platform is related to its capability to generate and store new information and knowledge. Each time a decision is made, for instance, each time a task is assigned to a given operator, this information is inserted in the KB for further use, therefore, enhancing the proposed platform’s suitability for better supporting decision-making.

### ***2.3 Platform Usage Scenario for the Allocation of Operations to Operators***

In the proposed platform, the Hungarian algorithm [14] is used for supporting the attribution of operations to operators, according to the operator’s skills.

The information about the operator’s skills is provided not just through the operator’s documentation available in the company, but it is also provided automatically in a continuous and dynamic way through the automatic acquisition of information about them within the shop floor, through smart objects and associated technological devices, including dashboards, for real-time monitoring and control during production activity.

The application of the Hungarian algorithm is quite easy and fast, enabling to obtain high-quality results in terms of operations attribution to operators, for maximizing the overall attribution performance rates. The main steps, along with the main interfaces for its implementation are presented next, through Figs. 2, 3, 4, 5 and 6, which consist in a very intuitive and interactive approach.

These steps for using the Hungarian algorithm to assign operations to operators are illustrated for its use in the context of a clothing company, in Portugal.

The first step is the ‘Order Picking’, which consists of choosing an order along with the list of all the products associated with that order. Figure 2 shows the platform’s interface for supporting to select an order between the existing ones, which in this case are the orders with numbers 10 and 11. While selecting an order the systems do automatic calculation and show the total quantity of products to be produced for that order, and its total contents that are already produced and have to be produced further.

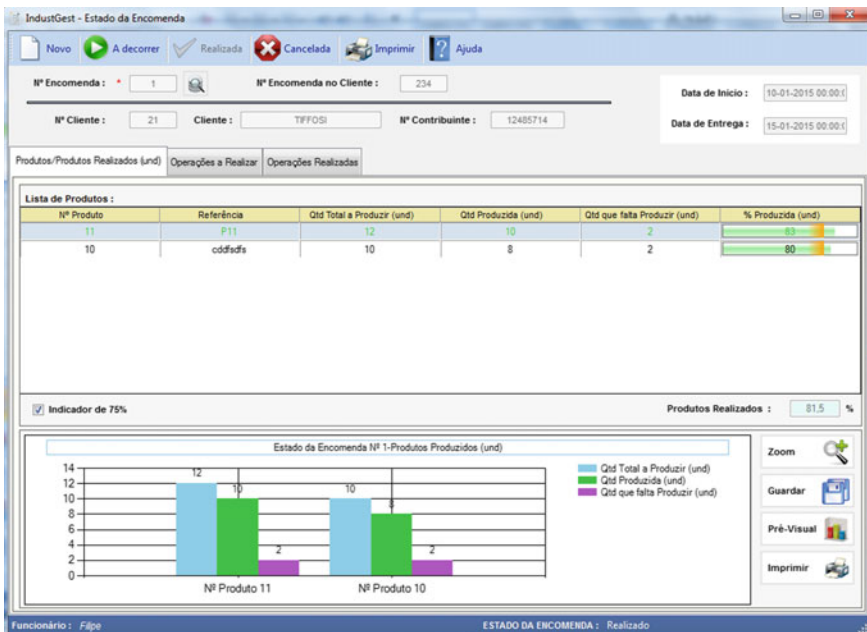


Fig. 2 List of products in an order

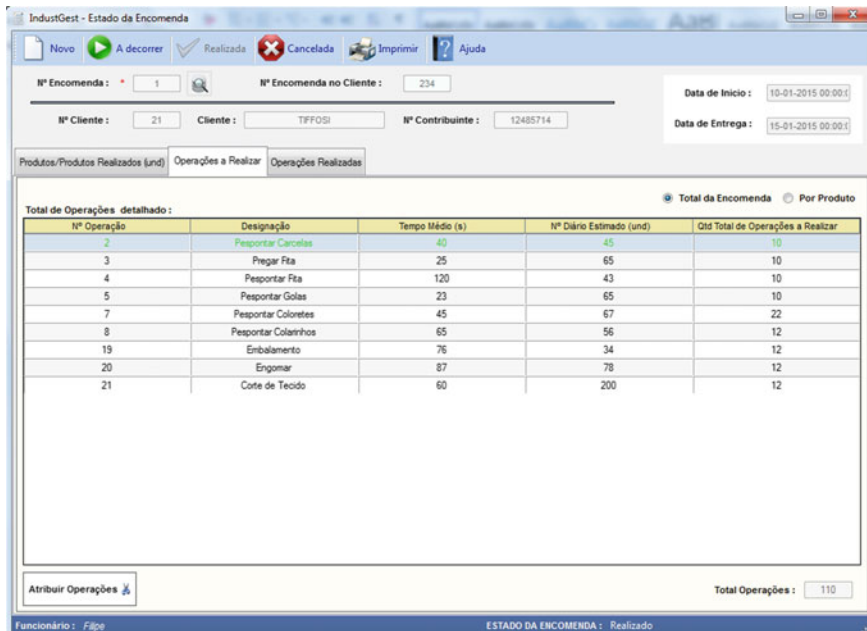


Fig. 3 List of total order's operations

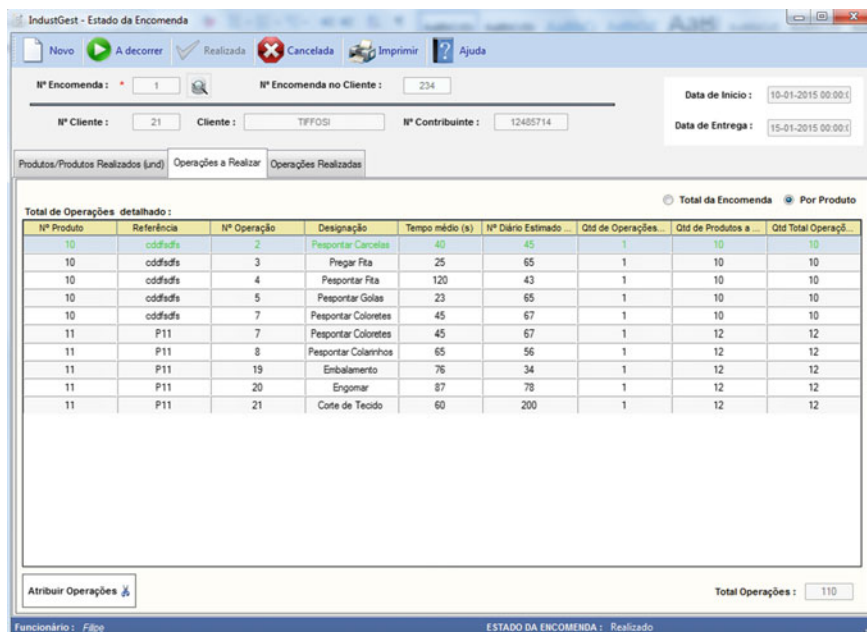


Fig. 4 List of total operations of the order by product

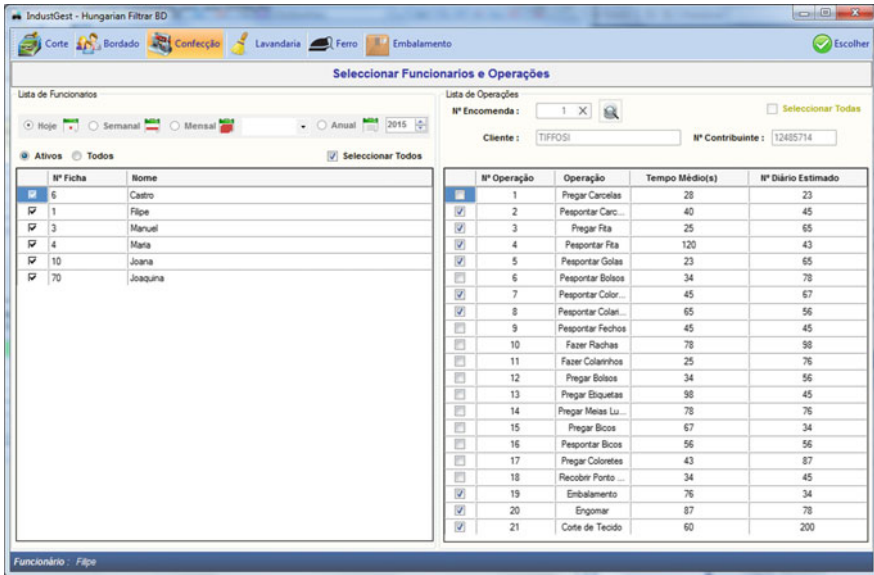


Fig. 5 Select employees per operation and operations

After selecting an order, in step 2, it is possible to verify the total number of operations that have to be executed for the selected order, which is shown in Fig. 3.

Moreover, also the total number of operations of the order per product can also be observed, as illustrated in Fig. 4.

Next, in step 3, the list of the available in the shop floor, for the operations execution, has to be established, by selecting them between the total operations of the company in the corresponding production section, as illustrated through Fig. 5.

Moreover, also the list of the operations that have to be performed from the chosen order, should be selected or automatically confirmed, by default, according to the system’s suggestion provided, by default, including the whole set of operations of that order.

Right after, in the final step (4), the Hungarian algorithm has to be run, in order to get the final result regarding the allocation of operations to the operators, as shown in Fig. 6.

Through this interface shown in Fig. 6 we can observe the list of operations that each operator will have to perform for the production of the chosen order and underlying products for maximizing the total attribution rate and performance levels about the production of the chosen order’s operations.

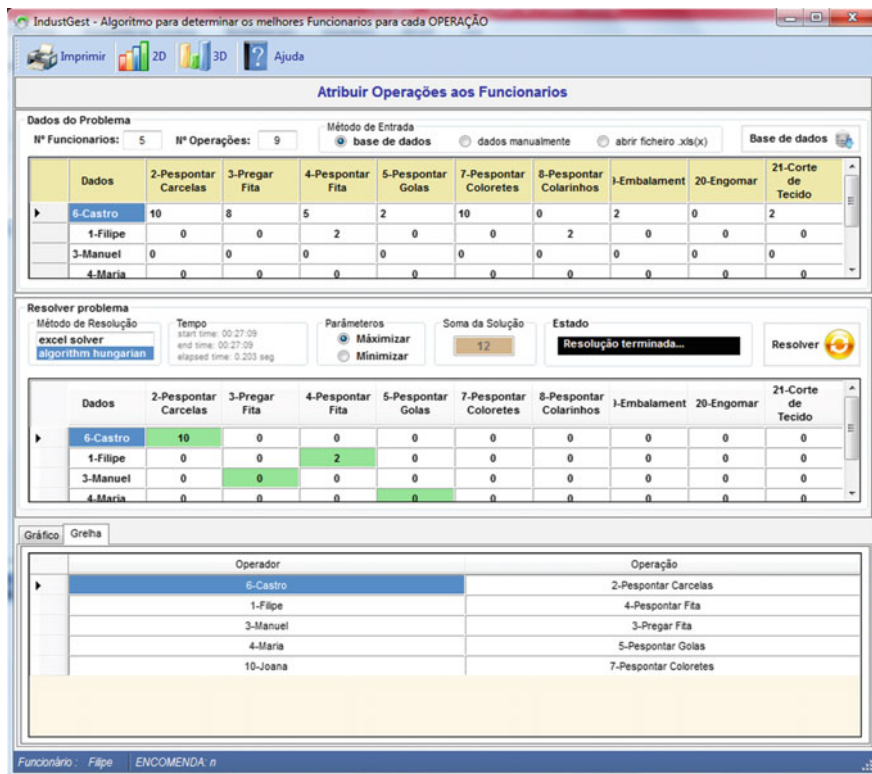


Fig. 6 Results of the Hungarian algorithm

### 3 Conclusions

In this paper, a proposed intelligent platform was briefly described and presented for supporting several production management and maintenance functions, including supervision and production activity control in real-time basis. The proposed platform integrates smart objects, which enable communication with central processors and computers, in a network-based environment, integrating a set of associated input and output devices, such as, sensors, switches, push buttons, potentiometers and output devices; output devices, such as, indicators, segment displays, servo engines, step motors, analogue devices and indicators, buzzers and speakers, among others. The main aim of the proposed platform consists on enabling precise data and information acquisition and processing, for better supporting production management and maintenance decision-making, at several distinct hierarchical decision levels within a company, from the shop floor up to higher strategic planning levels. One such important decision-making task that arises in the context of the companies is the appropriate allocation of operations to operators, in order to maximize the overall manpower performance, along with other

performance measures that have to be optimized, and in this paper, an illustrative usage scenario was provided applied in the context of a Portuguese clothing company.

**Acknowledgements** This work had the financial support of FCT—Fundação para a Ciência e Tecnologia of Portugal under the project PEst2015-2020: UID/CEC/00319/2013.

## References

1. Putnik, G.D., Putnik, Z.: A semiotic framework for manufacturing systems integration—part I: Generative integration model. *Int. J. Comput. Integr. Manuf.* **23**(8), 691–709 (2010)
2. Hashemian, H.M., Bean, W.C.: State-of-the-art predictive maintenance techniques. *IEEE Trans. Instrum. Meas.* **60**(10), 3480–3492 (2011)
3. Meier, H., Roy, R., Seliger, G.: Industrial product-service systems—IPS2. *CIRP Ann. Manuf. Technol.* **59**, 607–627 (2010)
4. Mori Seiki CO., LTD: Service/support von A-Z mit der Sicherheit des Herstellers. Service Brochure published by Mori Seiki
5. Carnap, R.: Introduction to Semantics. Harvard University Press, Cambridge, MA (1942)
6. Jovane, F., Yoshikawa, H., Altng, L., Boer, C.R., Westkamper, E., Williams, D., Tseng, M., Seliger, G., Paci, A.M.: The incoming global technological and industrial revolution towards competitive sustainable manufacturing. *CIRP Ann. Manuf. Technol.* **57**, 641–659 (2008)
7. Vieira, G., Reis, L., Varela, M.L.R., Machado, J., Trojanowska, J.: Integrated platform for real-time control and production and productivity monitoring and analysis. *Rom. Rev. Precis. Mech. Opt. Mechatron.* **50**, 119–127 (2016)
8. Szuszynski, M., Żurek, J.: Computer aided assembly sequence generation. *Manage. Prod. Eng. Rev.* **6**(3), 83–87 (2015)
9. Gapinski, B., Janicki, P., Marciniak-Podsadna, L., Jakubowicz, M.: Application of the computed tomography to control parts made on additive manufacturing process. *Proc. Eng.* **149**, 105–121 (2016)
10. Królczyk, G., Legutko, S., Królczyk, J., Tama, E.: Materials flow analysis in the production process—case study. *Appl. Mech. Mater.* **474**, 97–102 (2014) (Trans Tech Publications, Switzerland)
11. Varela, M.R.L., Trojanowska, J., Carmo-Silva, S., Costa, N.M.L., Machado, J.: Comparative simulation study of production scheduling in the hybrid and the parallel flow. *Manage. Prod. Eng. Rev.* **8**(2), 69–80 (2017)
12. Milgram, P., Kishino, A.F.: Taxonomy of mixed reality visual displays. *IEICE Trans. Inf. Syst.* **E77-D**(12), 1321–1329 (1994)
13. Suri, R.: It's About Time: The Competitive Advantage of Quick Response Manufacturing. Productivity Press (2010)
14. Vieira, G., Varela, M.L.R., Putnik, G.D.: Technologies integration for distributed manufacturing scheduling in a virtual enterprise. In: Putnik, G.D., Cruz-Cunha, M.M. (eds.) 1st International Conference on Virtual and Networked Organizations Emergent Technologies and Tools (ViNOrg 2011). *Communications in Computer and Information Science*, vol. 248, pp. 337–347 (2012)
15. Bajic, E.: A service-based methodology for RFID-smart objects interactions in supply chain. *Int. J. Multimed. Ubiquitous Eng.* **4**(3), 37–54 (2009)

# Definition of Smart Retrofitting: First Steps for a Company to Deploy Aspects of Industry 4.0

**Bruno V. Guerreiro, Romulo G. Lins, Jianing Sun  
and Robert Schmitt**

**Abstract** Nowadays, it is a matter of survival for companies to keep their ability for adapting rapidly to changes. The causes that drive to them are related to external and internal factors. One of the main reasons for these factors is the new possibility that Industry 4.0 brings with it. One of the visions of Industry 4.0 is the production of highly customized products within a mass production line. In addition to it, an intelligent interaction happens between machine–objects–people and this occurs vertically and horizontally within the company. However, most industrial parks are not technologically prepared for the concepts of Industry 4.0; thereby this paper proposes the concept of Smart Retrofitting regarding these challenges. As a result, the methodology proposes to take aspects of Industry 4.0 relevant to a specific process, since this could be the first step for a company to implement the concepts of Industry 4.0. Once these aspects are selected, they will be put into practice with the help of cyber-physical systems. With the application of Smart Retrofitting, it will be possible for companies to adhere in a short time to the requirements of Industry 4.0. In this way, it will be possible to remain competitive in the market. Regarding this paper, there will be a case study for the implementation of Smart Retrofitting. As case study, a drilling process was chosen in a thyssenkrupp manufacturing plant in Brazil to start implementing the Smart Retrofitting, and for this first step it was possible to achieve an improvement of the feed rate reducing it by approximately 9% without reducing the lifetime of the tooling.

**Keywords** Industrial Internet of Things (IIoT) · Industry 4.0 · Smart Retrofitting  
Cyber-physical systems · Smart devices

---

B.V. Guerreiro (✉) · J. Sun  
Fraunhofer Institute for Production Technology—IPT, Aachen, Germany  
e-mail: bruno.guerreiro@ipt.fraunhofer.de

R.G. Lins (✉)  
Federal University of ABC, Santo André, Brazil  
e-mail: romulo.lins@ufabc.edu.br

R. Schmitt  
Laboratory for Machine Tools and Production Engineering of RWTH Aachen University,  
Aachen, Germany

## 1 Introduction

Owing to the competitiveness in a globalized world, the search for new concepts and methods for manufacturing has been highlighted by industries and scientific community. In this incessant search for optimization of production, a new scenario called “Industry 4.0” has been proposed and adopted as part of the “High-Tech Strategy 2020 Action Plan” by the German government [1]. Taking into account this new industrial paradigm, new emerging technologies play an important role in the technology integration at real shop floor, e.g., Industrial Internet of Things [2], wireless sensor networks [3], big data [4], cloud computing [5], embedded system [6], among other technologies. Aforementioned theoretical background, other technology can be highlighted regarding the concepts of industry 4.0, e.g., using Smart Devices in production systems. Smart Devices are electronic equipment, which are wireless, mobile, networked, and shipped with various sensors (geosensors, gyroscopes, temperature, microphone, camera, etc.). To Smart Devices belong, for example, smartphones, tablet PCs and smart wearables, etc. The integration of suitable Smart Devices into the processes of producing company plays an essential role for suppling and motivating workers, by means of providing information and handling instructions everywhere at any time.

In order to deploy these technologies in compliance with “Industry 4.0”, the following three key features must be considered [1]: (1) horizontal integration through value networks, (2) vertical integration and networked manufacturing systems, and (3) end-to-end digital integration of engineering across the entire value chain. Therefore, the production is believed to be able to produce customized and small-lot products efficiently and profitably.

Regarding the equipment’s age used on the production nowadays, some data must be analyzed for the deployment of the proposed methodology. Although France is considered one of the most important industrialized countries of the European Union, it has in average machine tool age of 19 years [7]. That is higher than the Brazilian average age, which is according to ABIMAQ (Brazilian Machinery Builders Association) 17 year. But this scenario is not exclusive in Europe and South America, the United States of America (USA) has machine parks with an average age of 10 years. Thereby, it is the oldest machine park in the history of the USA since the 1932 [8]. Possessing today a technologically outdated industrial park can mean a drastic reduction of the competitiveness of a country in the world market, because the reaction time for change becomes further than for countries that have an industrial park in the state of the art, as is the case of Germany in various industrial segments.

Taking into account the needs of enhancement by industries and the current scenery in terms of machine park age, the use of CNC machines combined with the new concepts of Industrial Internet of Things (IIoT) must open a new front in terms of theory, as well as in terms of practical approach for developing new machines or even for retrofitting systems in operation at existing plant manufactures. Although this new front has a great potential for innovation, the engineers still face some



technical problems and challenges for the deployment of IIoT in real industrial systems already installed. Among these problems, the most important to be highlighted for developing a real project are: (1) the current industrial production lines are mostly based on heterogeneous structures and architectures regarding the used technologies like communication protocols, control systems or electrical and mechanical components, arose from continuous development processes over the last years. As result, the integration of these different technologies is nontrivial and sometimes technically unfeasible; (2) the second challenge is related to human resources, much knowledge is required to cover all the different aspects and peculiarities of the various technologies, thus the integration of them becomes a critical task for updating in-process machining equipment.

This article proposes, describes, and defines the terms for Smart Retrofitting. In addition, a case study has been presented aiming the integration of CNC machines in operation with external embedded system, such as an external tool wear monitoring device, smart devices for in-process data interaction, among others, in order to bring for these machines the capabilities required by this new concept of Industry 4.0. As result, the proposed methodology must bring a robust guide for updating machines in process in compliance with the “Industry 4.0” vision.

This paper begins by describing the related works in Sect. 2. Section 3 introduces the term Smart Retrofitting and its respective definitions. Case study application and its results are described in Sect. 4. Finally, Sect. 5 presents the conclusion.

## 2 Related Work

In this section, the literature survey will be aiming to present a brief overview of the state of the art that will support the paper development in topics related to available retrofitting. The company Bosch Rexroth AG did an excellent use case regarding the retrofitting using their IoT Gateway solution. The use case was accomplished at the test facility for hydraulic valves built in 2007 in Homburg, Germany. The IoT Gateway has been in use at a networking of existing machines and sensory monitoring of the test medium and the formatting unit. The test medium in this case was the oil used in the test facility and the formatting unit was the filters. Thereby, it was possible to automated monitor the ISO purity class of the oil and monitor the status of the filters. In this way, alerts and ordering for the maintenance have to be done automated and not manually like before. With these actions, the maintenance cost has a decrease of 25% and the Overall Equipment Effectiveness (OEE) an increase of 5%. Furthermore, it had a Return of Investment (RIO) of less than 1.5 years.

Working with open software architecture allows the IoT Gateway operating system to use Linux, besides it enables the deployment of customized Java applications. In addition to these two facts, the cloud service will be accomplished through an OSGi framework. Another advantage is that the different Java App will be provided with the IoT Gateway and can be modeled for the individual

requirements. The coordination of hardware and software components happens in three arts of Apps. The Dashboard App allowed through a web-based monitoring of the process data. The conversion of signal into process data happens in the Devices App. Thereby it enables the connections with:

- Analog voltage and current signals,
- Digital voltage signals,
- OPC UA,
- Open Core Interface for Controls,
- Siemens S7,
- RFID and Bluetooth LE.

The Processing App is responsible for the processing and forwarding of the data. The forwarding can happen with the listed Bosch solutions:

- Bosch SI—Production Performance Management,
- Bosch Sensor Cloud,
- Bosch Energy Platform,
- Bosch Rexroth OdiN.

However, this forwarding can also occur through MES Systems and Databases. Consequently, the data processing happened with different method for this scenario [9].

### 3 Definition of Smart Retrofitting

The Smart Retrofitting focuses on machines and processes that were not designed for the Industry 4.0 vision. Thereby, the main purpose of Smart Retrofitting is to transfer the aspects of the Industry 4.0 visions to machines and processes with the least possible financial and time expenditure.

The Smart Retrofitting will occur with the assistance of the Lean Philosophy. The Lean Philosophy seeks continuous improvements of the company through small actions [10–12], and the Smart Retrofitting will seek the same technological improvements of the Industry 4.0 vision to interconnect the company. By following the Lean Philosophy and the application of its tools, it is possible to map the machines and their processes, thereby identifying potential and critical items for which the Smart Retrofitting will provide solutions coming from the Industry 4.0 vision. It is not necessary for companies to bring the entire production to a high level of the Industry 4.0 at the first stage, in order to remain competitive and productive. However, the first step must begin with the involvement and motivation of the employees. Thus, the employees become one of the three main elements of the Smart Retrofitting concept proposed in this paper.

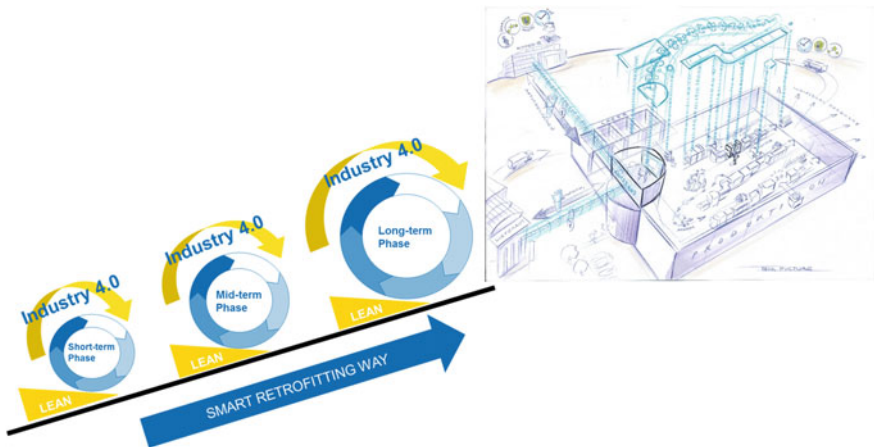
The implementation of the Smart Retrofitting can be better planned in a short, mid and long-term strategy. In this way, at first, the management team will define a

target where they want to be in three years, for instance as a long-term period. On this basis, they build a road map with help of certain Lean tools, for instance a Total Productive Maintenance (TPM) which contributes to an improvement of the OEE. As an example of a first small project of the short-term strategy, it is recommended to start with a Value Stream Mapping (VSM) followed by the addition of elements of the Industry 4.0. The Value Chain mentioned by Porter [13], for the performance and monitoring of the quality and productivity, will be strongly influenced by the application of the Smart Retrofitting in phases.

For the accomplishment of the target established by the management team for the short-term phase, small projects will be required and after the end of these small projects, the results of each one shall be summarized together and then it will be possible to move to the next mid-term phase, and so on. Figure 1 illustrates a sequence-term project, for each phase applying Leans tools for the identification of which Industry 4.0 elements are first necessary and possible to be applied. The Lean sustains the implementation of the Smart Retrofitting on all phases. The number and kind of the activities for all phases vary from case to case.

For the implementation of the Industry 4.0, all three elements of the Fig. 2 are equally important. These elements can be deployed simultaneously but not all of them must necessarily be with the same intensity at the same time, respecting the short-, mid-, and long-term stages. The integration element will always be present in the others elements; this will be explained in the following text.

Like in the Lean, the employee will play a crucial role for the success implementation of Smart Retrofitting inside a company. In this way, it will stimulate a synergetic working atmosphere between shop floor worker and the management team in the several stages of the Smart Retrofitting.



**Fig. 1** Illustration of interactive work between Lean and Industry 4.0 through the Smart Retrofitting trajectory

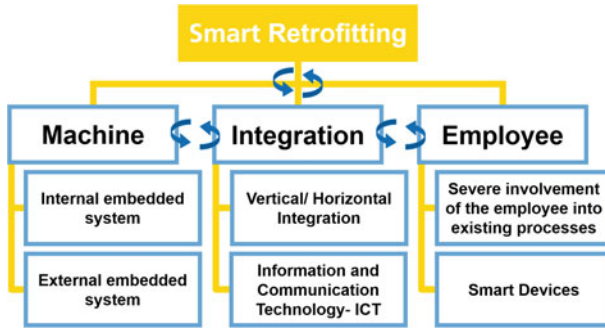


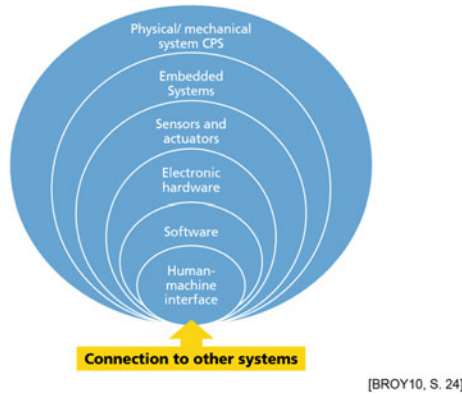
Fig. 2 Action elements of the Smart Retrofitting

Which of the aspects of Industry 4.0 will be chosen and when and where to apply will not be decided by the management team exclusively. Instead, it will be done with the collaboration of the worker. We shall take into account that every department has its priorities and knowledge about the process.

One important factor of the employee element for the Smart Retrofitting is his motivation to do it. Thereby, the employee must be always included in the entire Smart Retrofitting process since the beginning. Thus, Smart Retrofitting will also focus to motivate the employees regarding the Maslow’s hierarchy of needs and two-factor theory from Frederick Herzberg. From the Maslow’s theory [14], Smart Retrofitting will make use of the Esteem part, in that way the employee will note that his opinion is respected within the company and furthermore he will feel motivated to provide contributions for a continuous improvement of the process that he is responsible, constantly.

As Herzberg shows in his Achievement Theory [15], recognition, work itself, responsibility, advancement, and growth play an essential role to motivate the employees, thereby these factors will be stimulated through the Smart Retrofitting in the implementing and running phases. In other words, the employees will receive responsibilities and thereby will feel part of the whole process. The Smart Devices work like a bridge between the employee and the manufacturing process and thereby the employee will be connected in the involved production process too.

Cyber-physical systems (CPS) have a crucial role within the Industry 4.0 and within the machine element of the Smart Retrofitting concept presented in the Fig. 2. In Fig. 3, the onion shell structure of CPS is illustrated as well as the importance of the embedded system [16]. Thereby, the aggregation of internal and external embedded systems to the machine allows collecting data from different source. By the application of IIoT, it will be possible to make the vertical and horizontal integration inside a company. With help of the processing of this data, the integration between machine-to-machine, machine-to-object and machine-to-human will be possible [17]. The integration of machine-to-machine and machine-to-object will occur by acting in the element machine and integration from the Fig. 2. On the other hand, the integration by machine-to-human occurs



**Fig. 3** Illustration of the onion shell structure within CPS

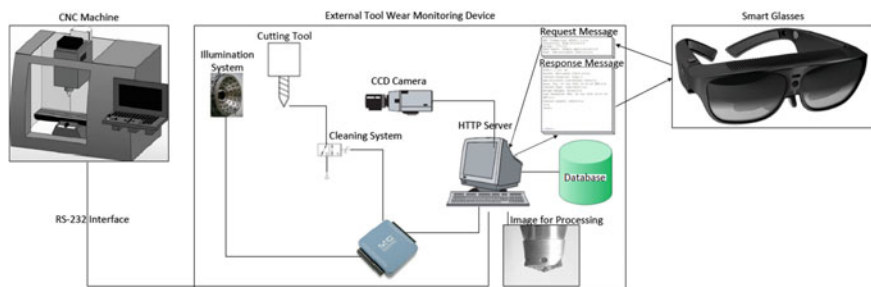
using Smart Devices that will allow the worker to receive real-time information about what is happening in the process. In this way, employee will be able to receive from the system suggestions about what is the next step. Smart Devices will also transmit the final decision to the machine.

Thus, with the use of the embedded system and the collection of data, it is possible to interact between the virtual world and the physical world [16]. Such interaction occurs with the use of sensors that capture what is happening in the physical world, such data will be processed in the virtual world and actions will be put into practice with the use of actuators, for instance. The internal embedded system is already available in the market, thereby they can be easily installed in the machine and enable perhaps the Plug&Produce concept. Instead, the external embedded system is installed in the surroundings of the machine and it can be tailor-made designed for each application. In that way, the combination of the internal and external embedded system and the Information and Communication Technology (ICT) makes vertical and horizontal integration inside the company possible.

Therefore, the Smart Retrofitting differs from the traditional Retrofitting by not only replacing old components in the machine regarding their energy efficiency.

## 4 Case Study

The case study is being developed in progress at thyssenkrupp manufacture plant in Brazil. By applying the Smart Retrofitting concepts defined in this paper, a short-term phase deployment has been chosen and it aims at the installation of internal and external embedded systems for monitoring machining parameters in process. Machining operators are able to receive these data through Smart Devices (for this project a Smart Glasses has been selected), and from them a crucial decision may be



**Fig. 4** Proposed architecture for integration in compliance with Smart Retrofitting

taken, for instance when an insert must be replaced in accordance with its wear boundary. Figure 4 shows the proposed architecture for integration the main devices in compliance with Smart Retrofitting concepts proposed in this paper.

As depicted in the Fig. 4, the installation of an external embedded system for monitoring tool wear has been developed and installed at real shop floor. It consists in the use of a sequence of images for measurement of the in-process tool wear through the processing of an optimized algorithm based on techniques of image processing. Each time when the CNC machine ends a hole machining, the external device is triggered by a digital signal coming from machine panel through RS-232 interface. Then, the drill is cleaned and the tool wear measurement occurs in a maximum of 6 s.

The measurement results are stored into a database in order to create a tool wear history while the production is going on. During the machining operation, a Smart Glasses is integrated through the Hypertext Transfer Protocol (HTTP Protocol) with the other devices that compose the proposed system, then when the algorithm embedded into glasses' core requests a message, the HTTP server sends a response message with all the information required. In this case, HTTP Protocol is technically sufficient for such soft real-time applications. Other communication protocols and frameworks are also possible and will be evaluated in the future works. Finally, the data established by engineer team pops up at Smart Glasses' screen as shown in Fig. 5. In this point, we notice that, although we did not deploy an internal embedded system for monitoring machining parameters, the architecture is capable to be integrated because of the proposed philosophy of Plug&Produce introduced as part of Smart Retrofitting concepts.

Data is updated in an adequate frequency while the production is going on during the day. As result of the deployment of this system, advantages can be featured in comparison with the methodology used nowadays on shop floor, as following:

- From the real-time data available on Smart Glasses' screen, the human machining operator will be able to interpret data parameter faster with more accuracy when it is necessary to make a decision;



**Fig. 5** Monitoring report shown on smart glasses' screen for human machining operator

- Through the proposed architecture, new internal or external devices can be deployed into the machining system, and then new parameters can be monitored in order to improve the machining system management;
- Finally, and most important, the proposed architecture brings a new way for update CNC machines in compliance with Industry 4.0 concepts in such way that is not mandatory the purchase of machines, which must result in a reduction the investment done by corporations when they are looking for an update of their machine park.

Smart Glasses is a practical and powerful auxiliary equipment for realizing Smart Retrofitting, where portability and security of information processing are required. Smart Glasses process has good portability, sensor technology, connectivity, and operational handling, being able to provide information, instruction and tutorial on a head-mounted display while the employee can remain hands on the work. In conjunction with IIoT and cloud-based smart manufacturing platform, Smart Glasses can deliver revolutionary user experiences and great advantage to enhance the employee's competence in future digital factories.

## 5 Conclusion

The proposed paper defines the term Smart Retrofitting in such a way that its theoretical aspects can be used effectively when an update of a machine park is required in compliance with the aspects of Industry 4.0. A real case was presented in order to illustrate how the proposed concepts can be applied for updating machining system in process.

By applying the proposed concepts, an architecture has been defined and developed for deployment of internal and external embedded systems able to monitor machining parameters in real time. As result, the proposed architecture can bring many advantages for machining system management in compliance with Industry 4.0 aspects. Therefore, the concepts presented in this paper can contribute effectively with the state of the art by the upgrade of machining system in process, bringing a robust method for developing future projects.

As practical result of the proposed concepts, through the implementation of a small project belonging to the short-term phase of Smart Retrofitting can be affirmed (with real data) that: With the update of a real machining system, which

consists the use of internal and external embedded system to monitor the feed rate of a drilling tool, it is possible to reduce 9% (measured in thyssenkrupp) in the processing time of this operation and in addition, assuring the final quality of the manufactured product. Future work consists of completing all tests and the implementation of Smart Retrofitting in others process at this thyssenkrupp manufacturing plant in Brazil.

**Acknowledgements** The authors would like to thank the German Research Foundation DFG for the kind support within the Cluster of Excellence “Integrative Production Technology for High-Wage Countries”. The authors are also greatly thankful to thyssenkrupp Brasil Ltd. for the work and accomplishments achieved.

## References

1. Kagermann, H., et al.: Recommendations for implementing the strategic initiative Industry 4.0: securing the future of German manufacturing industry; final report, Industry 4.0 working group. Forschungsunion, Berlin (2013)
2. Jeschke, S., et al.: Industrial Internet of Things. Springer (2017)
3. Huang, P., et al.: The evolution of MAC protocols in wireless sensor networks: a survey. *IEEE Commun. Surv. Tutorials* **15**(1), 101–120 (2013)
4. Ajao, L.A., et al.: Learning of embedded system design, simulation and implementation: a technical approach. *Am. J. Embed. Sys. App.* **3**(3), 35–42 (2016)
5. Oliveira, T., et al.: Assessing the determinants of cloud computing adoption: an analysis of the manufacturing and services sectors. *Inf. Mng* **51**(5), 497–510 (2014)
6. Yin, S., Kaynak, O.: Big data for modern industry: challenges and trends [point of view]. *Proc. IEEE* **103**(2), 143–146 (2015)
7. France is planning the industry of the future, Germany Trade & Invest, (2015)
8. Hagerty, J.: U.S. manufacturing is rolling on aged wheels. *Wall Street J.* (2014)
9. Get ready for Industry 4.0!, Network machines efficiently and optimize processes, Bosch Rexroth AG, (2017)
10. Imai, M.: Kaizen. The Key to Success in the Competition. McGraw-Hill: New York (1986)
11. Pfeifer, T., Schmitt, R. (eds.): Masing Handbook Quality Management. Carl Hanser Verlag GmbH Co KG, Germany (2014)
12. Liker, J.K.: The Toyota Way: 14 Management Principles from the World’s Greatest Manufacturer. McGraw-Hill: New York (2004)
13. Porter, M.: Competitive Advantage: Creating and Sustaining Superior Performance. FreePress, New York (1985)
14. Maslow, A.H.: Motivation and Personality. Harper & Row, New York (1954)
15. Herzberg, F.: One More Time: How Do You Motivate Employees?, pp. 5–16. Harvard Business Review (1987)
16. Broy, M.: Cyber-Physical Systems. Innovation Through Software-Intensive Embedded Systems. Springer-Verlag, Heidelberg, Berlin (2010)
17. Bauernhansl, T., Ten Hompel, M., Vogel-Heuser, B.: Industry 4.0 in Production, Automation and Logistics: Application, Technologies, Migration. Springer-Verlag, Berlin (2014)



# Additive Manufacturing Technologies Cost Calculation as a Crucial Factor in Industry 4.0

Maria Rosienkiewicz, Joanna Gabka, Joanna Helman,  
Arkadiusz Kowalski and Sławomir Susz

**Abstract** The article analyzes the newest trends in the industry and production research. Making insight in the most popular research domains and changes in the industry enabled the authors to formulate a thesis that the manufacturing world strode in the new revolution based on the Additive Manufacturing technologies. It can be stated that a particular gap exists in the field of production engineering that needs to be fulfilled by developing appropriate solutions for the factories integrating AM technologies in their workflow. The paper proves this statement by showing numbers of publications within sub-domains in scope of “individualization of production”. As a basic discouragement on the way to the new production paradigm, it was recognized a deficiency of accurate and versatile cost calculating models. The existing approaches were assessed and assigned to their best application which enabled to indicate a direction of the future research.

**Keywords** New production paradigm · Additive manufacturing  
Cost calculation · Process organization · Industry 4.0

## 1 Introduction

Additive Manufacturing (AM) technologies are becoming more popular which can be observed in intensification of research in this field as well as in the industry and on the market. Current trends indicate that the next revolutionary step in manufacturing will result from using 3D printing technologies on the large scale [1–4]. From the very early stages they were satisfying individual, sophisticated requirement such as customized implants manufacturing [5]. Currently, the level of

---

M. Rosienkiewicz (✉) · J. Gabka (✉) · J. Helman · A. Kowalski · S. Susz  
Faculty of Mechanical Engineering, Wrocław University of Science and Technology, 27  
Wybrzeże Wyspiańskiego, 50-370 Wrocław, Poland  
e-mail: maria.rosienkiewicz@pwr.edu.pl

J. Gabka  
e-mail: joanna.gabka@gmail.com

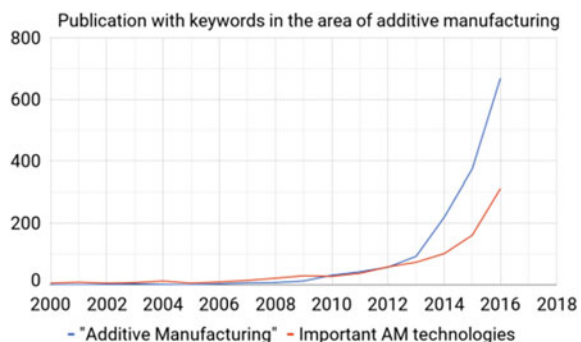
knowledge and excellence in providing repeatability and quality of the processes as well as products enables usage of additive technologies in numerous industries such as aerospace, automotive, consumer goods and medicine [6–10]. Authors of [11] propound that the next industrial revolution may be observed on the basis of Industry 4.0. As experts say one of the pillars of I4.0 is AM. In the ongoing revolution in production processes, AM, which can be called a disruptive technology, is according to the Authors a crucial factor of the Industry 4.0. Therefore, the authors decided to identify the current trends and gaps in the literature related to AM in terms of efficiency. Thus, the main aim of the paper is to analyze existing AM cost models, in particular in scope of cost categories and manufacturing technology used.

## 2 Importance of Cost Calculation in Additive Manufacturing

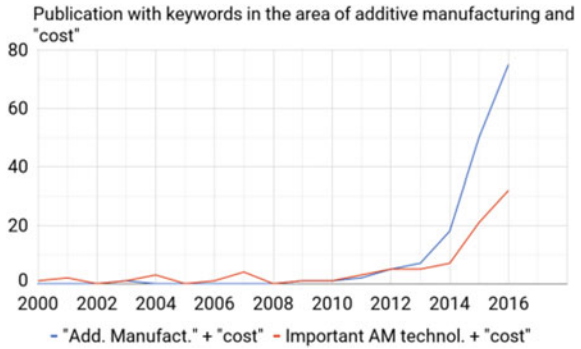
Referring to AM, as one of the Key Enabling Technologies (KETs), is foreseen to shape new approaches to manufacturing products and expanding potential of factories of the future [12]. The increasing number of publications in the area of “additive manufacturing” and important AM technologies are shown in the Figs. 1, 2, 3 and 4, which indicate the growing popularity of these methods.

This is accompanied by a growing number of publications with the keyword “cost” but it rather refers to the cost of equipment or materials as the search for publications dealing with the cost structure, the cost model, effectiveness and analysis returns near to zero results. These findings prove that there exist a certain gap which could be filled in by developing a new, more complex, and flexible models and approaches to the problem of cost analysis referring to the organization of production processes which apply increasing number of AM technologies in their workflow. Literature analysis was made on basis of search from ScienceDirect. The geometric growth of papers published and projects launched within area of AM indicates that we are in the middle of the revolutionary changes—so-called 4th industrial revolution (I4.0).

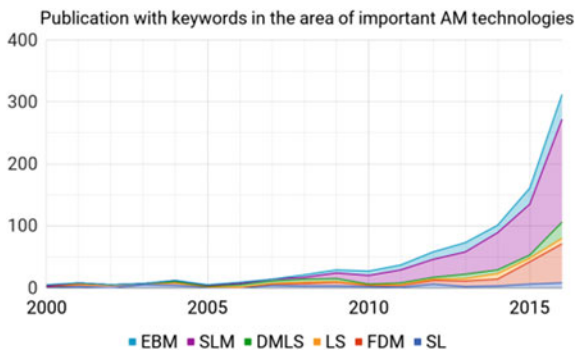
**Fig. 1** Result of search in the ScienceDirect Publications database: keyword “additive manufacturing”



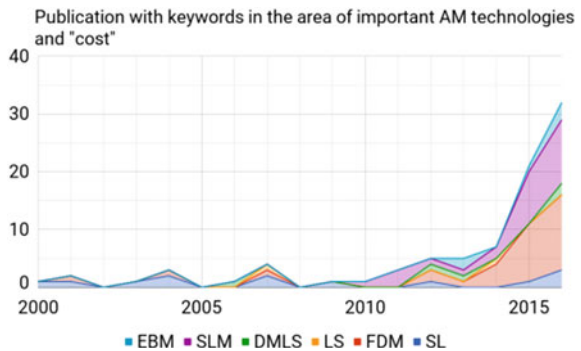
**Fig. 2** Result of search: important AM technologies (EBM, SLM, DMLS, LS, FDM, SL); keywords EBM, SLM, DMLS, LS, FDM, SL alone



**Fig. 3** Result of search: keywords "additive manufacturing" with AM technologies and "cost"



**Fig. 4** Result of search: keywords EBM, SLM, DMLS, LS, FDM, SL alone and "cost"



### 3 Cost Factors in Different Approaches

Bearing in mind that AM technologies are getting more and more popular and that they are either replacing traditional manufacturing in certain cases or are being included into traditional manufacturing processes, the issue of proper cost calculation cannot be overemphasized. According to Young [13], who has proposed the

cost concept including quality and flexibility, there are two major ways of production costs division—“well-structured” and “ill-structured costs”. The first category takes into account cost of labor, material, and machine costs, whereas the second category covers costs of, i.e., build failure, machine setup, and inventory. According to Douglas and Gilbert [14], ill-structured costs, hidden usually in the supply chain, are related to inventory and transportation, consumer’s proximity to production, supply chain management, and vulnerability to supply disruption. For example in the traditional manufacturing high level of stock carries maintenance costs. AM enables the suppliers production of parts directly on demand. This is a great advantage especially in the spares industry, where the demand is usually lumpy and intermittent. Well-structured costs include **material costs, machine cost, build envelope and envelope utilization, energy consumption build time, and labor**. In general, the cost of AM materials is rather higher than the ones used in traditional manufacturing. Different cost models’ authors try to involve somehow **the price of a machine** in the total cost of a part produced with AM technology. Depending on the implemented approach, the final cost of a part may significantly differ. Research performed by Hopkinson and Dickens shows that in the total cost of a metal part, a cost of a machine may vary from 24% (0.52/2.20 Euro) for SLS, to 59% in case of FDM (2.64/4.47 Euro), up to 75% for SL (3.92/5.25 Euro) [15]. Also Lindemann [16] and Atzeni [17] underline the big dispersion when it comes to the machine cost per part. Depreciation rate of a machine also can meaningfully effects the total cost of a part. The build envelope, defined as the maximum area for part production in an AM system [14], can also effect the cost of AM part. Especially the size of the build envelope and its utilization are the factors influencing the cost. Another type of cost which can be distinguished is related to energy consumption. Baumers et al. researched the electricity consumption across selected AM technology variants, analyzing specific energy consumption during the production of dedicated test parts [18]. The impact of capacity utilization on energy was taken into account as well. The authors proposed “a universally applicable methodology for the measurement of the electric energy inputs to additive processes” [18]. Another cost factor is connected with build time. In this case, artificial neural networks (ANN) can be used in order to estimate the time of the parts produced with AM. The authors of this approach state that “a correct prediction of build time is essential to calculate the accurate cost of a layer manufactured object” [19].

## 4 Analysis of Approaches to Cost Calculation in AM

The most common cost estimation approaches were developed by Hopkinson and Dickens [15], Ruffo et al. [20], Ruffo and Hague [21], Allen [22], Xu [23], Atzeni et al. [17] and Piili et al. [24]. Also an important input related to the abovementioned aspect of cost efficiency was considered by Baumers et al. [18].

The methodology of a AM part cost calculation used by Hopkinson and Dickens assumes that a machine produces one part consistently for one year, utilizes maximum volumes, the machine operates for 90% of the time (7884 h per year), and that the machine depreciates after 8 years. In the model, the total cost per part TC<sub>pp</sub> is calculated as the sum of machine cost per part MC<sub>pp</sub>, labor cost per part LC<sub>pp</sub>, and material costs per part MtC<sub>pp</sub>:

$$TC_{pp} = MC_{pp} + LC_{pp} + MtC_{pp}. \quad (1)$$

The detailed elements of each formula can be found in the Table 1. The calculation according to this approach has been applied to stereolithography (SL), fused deposition modeling (FDM) technologies, and selective laser sintering (SLS).

Model developed by Ruffo et al. is related with the activity based costing ABC. It lists several activities associated with AM—material, software, hardware, capital equipment depreciation, labor, maintenance, production overhead, and administration overhead [25]. In their model, only the activity called material was treated as a direct cost.

The total cost of a build ( $C$ ) in the model by Ruffo et al. can be calculated according to a following formula [14]:

$$C = P_{\text{Material}} \cdot M + P_{\text{indirect}} \cdot T, \quad (2)$$

where  $P_{\text{Material}}$ —price of the raw material measured in euros per kilogram,  $M$ —mass in kg,  $T$ —total build time,  $P_{\text{indirect}}$ —cost rate.

Ruffo, Tuck, and Hauge continued their research on the cost efficiency of AM and developed three make or buy scenarios considering (1) when the company has no experience of AM, (2) when the company already has an AM department; and (3) when the company already has an AM function [25]. In the abovementioned models, it was assumed that one part is produced repeatedly, so the cost per part is calculated as the total cost of a build ( $C$ ) divided by the number of parts in the build. Such a situation is however rather rare in AM technologies because these technologies enable producing different parts at the same time. This scenario is more complex, so Ruffo and Hauge performed a comparison analysis on three costing methodologies for assessing the cost of parts produced concurrently (Table 2) [21].

Another approach was proposed in [22], where the research on comparative costs of AM and machine from solid for aero engine parts was performed. In this model a “near net shape” is considered. It is defined “as a part finished component which is ready for finish machining”. The net shape using the machining can be calculated on the basis of the formula [13] (Table 3). In the research, Allen refers to Buy-to-Fly ratio (BtF) and presumes that AM is more cost-effective when BtF is 12-1 in comparison to “more conventional” ratios which tend to be lower [22]. Another interesting approach can be found in the paper Mello et al. [26] where the authors propose a systematic study to formulate the cost of prototypes produced with AM. Their research focuses on FDM technology. They implemented the cost model developed by Xu [23]. In this particular model, a three-stage approach is

**Table 1** Calculation of machine, labor and material costs, model by Hopkinson and Dickens [15]

	Cost factor	Variable	Formula
	<i>Initial data</i>		
	Number per platform	N	Maximum possible in one build
	Platform build time	T	Hours
	Production rate per hour	R	N/T
	Hours per year in operation	HY	$365 \times 24 \times 90\% = 7884$
	Production volume total per year	V	$R \times HY$
	<i>Calculation of machine costs MC<sub>pp</sub></i>		
	Machine and ancillary equipment	E	Machine purchase cost
	Equipment depreciation per year	D	$E/8$
	Machine maintenance per year	M	Most comprehensive package
	Total machine cost per year	MC	$D + M$
	Machine cost per part	MC <sub>pp</sub>	$MC/V$
	<i>Calculation of labor costs LC<sub>pp</sub></i>		
	Machine operator cost per hour	Op	Minimum wage 5.30 euros
	Setup time to control machine	Set	Timed
	Post-processing time per build	Post	Timed
	Labor cost per build	L	$Op \times (Set + Post)$
	Labor cost per part	LC <sub>pp</sub>	$L/N$
	<i>Calculation of material costs M<sub>pp</sub></i>		
SL	Material per part including support (kg)	SLMass	Weighing finished parts
	Material cost per kg	Slcost	Quote = 275.20 euros
	Material cost per SL part	SLMCP	$SLMass \times Slcost$
FDM	Material per part (kg)	FDMPM	Weighing finished parts
	Support material per part (kg)	FDMSM	Weighing finished supports
	Build material cost per kg	FDMPC	Quote = 400.00 euros
	Support material cost per kg	FDMSC	Quote = 216.00 euros
	Material cost per FDM part	FDMCP	$(FDMPM \times FDMPC) + (FDMSM \times FDMSC)$
LS	Material cost per kg	LSC	Quote = 54.00 euros
	Mass of each part	LSM	Weighing finished parts
	Volume of each part	VP	Found with Magics software
	Total build volume	TBV	$34 \times 34 \times 60 \text{ cm}^3$
	Mass of sintered material per build	LSMS	$N \times LSM$
	Mass of unsintered material per build	LSMU	$(TBV - N \times VP) \times 0.475$
	Cost of material used in one build	LSMC	$(LSMU + LSMS) \times LSC$
	Material cost per LS part	LSMCP	$LSMC/N$

**Table 2** A comparison analysis on three costing methodologies [14]

Formula	Where
<i>Method 1—based on parts volume</i>	
$\text{Cost}_{p_i} = \left(\frac{V_{p_i}}{V_B}\right) \cdot \text{Cost}_B$	Cost <sub>p<sub>i</sub></sub> —cost of part <i>i</i> V <sub>p<sub>i</sub></sub> —volume of part <i>i</i> V <sub>B</sub> —volume of the entire build
$\text{Cost}_B = \sum \frac{\text{indirect costs}}{\text{working time}} \cdot (t_{xy} + t_z + t_{\text{HC}}) + \frac{\text{direct cost}}{\text{mass unit}} \cdot m_B$	m <sub>B</sub> —mass of the planned production proportional to the object volumes, and the time to manufacturing the entire build t <sub>xy</sub> —time to laser-scan the section and its border to sinter powder t <sub>z</sub> —time to add layers of powder t <sub>HC</sub> —time to heat the bed before scanning and to cool down after scanning and adding layers of powder <i>i</i> —an index going from one to the number of parts in the build
<i>Method 2—based on building a single part</i>	
$\text{Cost}_{p_i} = \frac{\gamma_i \cdot \text{Cost}_B}{n_i}$ $\gamma_i = \frac{\text{Cost}_{p_i}^* + n_i}{\sum_j (\text{Cost}_{p_j}^* \cdot n_j)}$	<i>i</i> —the index of the part being calculated <i>j</i> —the index for all parts manufactured in the same bed n <sub><i>i</i></sub> —the number of parts identified with <i>i</i> Cost <sub>p<sub>j</sub></sub> <sup>*</sup> —the cost of a single part <i>i</i> estimated using the equation for <i>C</i>
<i>Method 3—based on a part built in high-volume</i>	
$\text{Cost}_{p_i} = \frac{\gamma_i^\infty \cdot \text{Cost}_B}{n_i}$ $\gamma_i^\infty = \frac{\text{Cost}_{p_i}^\infty + n_i}{\sum_j (\text{Cost}_{p_j}^\infty \cdot n_j)}$	Cost <sub>p<sub>i</sub></sub> <sup>∞</sup> is a hypothetical number, which approaches infinity, of manufactured parts <i>i</i>

considered comprising (1) CAD file, (2) processing, execution, and (3) post-processing. The total cost of a prototype *C<sub>fp</sub>* can be estimated according to the following formula:

$$C_{fp} = C_p + C_e + C_m + C_{pp}, \tag{3}$$

where *C<sub>p</sub>* is the processing cost (i.e., PC, software, designer’s cost, PC energy consumption hour rate), *C<sub>e</sub>* the execution cost (i.e., model execution time, machine running cost, machine price and amortization time, taxes), *C<sub>m</sub>* the material cost (i.e., specific cost per model material volume and per support material volume, model and support volume utilized), and *C<sub>pp</sub>* the post-processing cost (i.e., energy consumption rate, average local energy specific cost. The detailed formulas defining each element of the above equation can be found in [26].

The cost-effectiveness of AM has been studied also by Atzeni and Salmi [27] and Aztemi et al. [17]. These researchers state that AM in case of metal parts can

reduce costs if it is combined with part redesign. The research evaluates the production volume for which AM technologies are competitive with respect to traditional manufacturing processes of end-usable metal part. The total cost per assembly ( $TC_{pa}$ )—manufactured with SLS—is based on four factors, according to the following formula [27]:

$$TC_{pa} = M_p + A_p + C_p + B_p. \tag{4}$$

In this approach, the total cost per assembly is a sum of material cost per part MP (based on material cost/kg, part volume, density of the sintered material and mass of material per part), pre-processing cost per part  $A_p$  (including machine operator cost per hour, setup time per build), processing cost per part  $C_p$  (covering depreciation cost per year, hours per year, machine cost per hour, build time, machine cost per build), and post-processing cost per part  $B_p$  (comprising machine operator cost per hour, post-processing time per build, heat treatment cost per build). The detailed formulas defining particular elements of the equation can be found in [27].

Next scenario-based research on manufacturing costs of Laser AM of stainless steel was conducted by Piili et al. [24]. The authors assume that to minimize the cost of the part, it is crucial to shorten time its building. It is also worth mentioning that some research was performed on estimation AM cost based on the artificial neural networks (ANN). Cavalieri, Maccarrone, and Pinto compared parametric and ANN-based cost estimation of a new type of brake disks [28].

**Table 3** Comparative costs of AM and machine from solid for aero engine parts [22]

Formula	Where
<i>The cost of providing a “near net shape” using the machining</i>	
$C_S = (V \cdot \rho \cdot C_f) \cdot (V - v) \cdot \rho \cdot C_m$	$C_S$ = cost of providing a “near net shape” using the machining $V$ = volume of the original billet $\rho$ = density of titanium $v$ = volume of the component $C_m$ = cost of machining
<i>The cost of a “near net shape” using AM</i>	
$C_a = v \cdot \rho \cdot C_d$	$C_a$ = cost of the producing a “near net shape” using AM $v$ = volume of the component $\rho$ = density of titanium $C_d$ = specific cost of deposited titanium



## 5 Discussion

In order to summarize and discuss performed analysis two tables have been developed. Table 4 is built as a result of authors research, presents what kind of crucial cost factors were included in particular cost estimation approaches and used types of cost categories.

Table 5 developed after the conducted analysis, shows which cost estimation approach can be used in order to estimate the cost of a part produced with the particular AM technology. Additionally, it was also marked if the costs were compared with traditional manufacturing.

Analysis of the presented cost models and cost analysis approaches shows that not only each model has some limitations and simplifications, which should be taken into account, but also approaches on cost estimation differ in scope of researched technology. Therefore, not every model is appropriate to estimate cost of any AM. What is also important, the models are based on different cost factors, so estimated cost of a part might differ significantly depending on the approach used.

## 6 Summary

Analyzing current trends in the industry, it is easy to notice the upcoming changes. The approach of the so-called Industry 4.0—the “fourth industrial revolution”—may be also confirmed by reviewing leading domains in publications. Having this thorough picture of the situation, there can be developed a thesis that exists a certain gap in the field of the production engineering solutions dedicated for AM production. The analysis performed in the paper shows that in the literature, there is still missing a versatile cost calculation model that could be used for different AM technologies. Development of such a model is a challenge for the future research. The authors plan to build a hybrid model including variables calculated on the basis ANN—the approach presented in [19] will be implemented. Bearing in mind that currently increasing number of companies is considering changing their production technology from conventional to AM (or implementing hybrid manufacture, where AM is only one of a range of processes used to produce the component [22]), the issue of precise cost estimation is very urgent and important. The problem of efficient identification of the breakeven point for conventional and additive manufacturing is studied deeply regardless type of AM. The comparison of existing cost estimation approaches contained in this paper should be a helpful step towards effective breakeven analysis. Moreover, the paper shows possible paths of future research in field of decision support systems, job specialization, and work organization in the future production system consisting of the AM technologies.

**Table 4** The crucial cost factors versus different cost calculation approaches

Approach by Cost factor	Hopkinson & Dickens	Ruffo et al.	Ruffo and Hauge	Baumers and Tuck <sup>a</sup>	Allen	Mello et al. based on model by Xu et al.	Atzeni and Salmi
Material	•	•	•		•	•	•
Labor	•	•	•		•	•	•
Energy		•	•	•	•	•	
Machine utilization	•	•	•		•	•	•
Production overhead		•	•		•	•	
Administrative overhead		•	•			•	
In the following approaches costs are divided into:	(1) Material (2) Labor (3) Machine	(1) Direct (2) Indirect	(1) Parts volume (2) Building a single part (3) A part built in high-volume production	n/a	(1) Power (2) Labor (3) Depreciation (4) Consumables (5) Material	(1) Processing (2) Execution (3) Material (4) Post-processing	(1) Material (2) Pre-processing (3) Processing (4) Post-processing

<sup>a</sup>Baumers and Tuck focused not on cost estimation but overview of electricity consumption across several major AM technologies

**Table 5** Different cost calculation approaches versus different various AM technologies

Approach by AM technology	Hopkinson & Dickens	Ruffo et al.	Ruffo and Hauge	Baumers and Tuck <sup>a</sup>	Allen	Mello et al. based on model by Xu et al.	Atzeni and Salmi
Stereolithography SL	•						
Fused deposition modeling FDM	•			•		•	
Laser sintering LS	•	•	•	•			•
Direct metal laser sintering DMLS				•			
Selective laser melting SLM				•			
Electron beam melting EBM				•			
Not specified					•		
Traditional manufacturing technology compared:	Injection moulding IM	Injection moulding IM	Injection moulding IM	n/a	Traditional machine from solid using a forged billet	n/a	Highpressure die-casting HPDC

<sup>a</sup>Baumers and Tuck focused not on cost estimation but overview of electricity consumption across several major AM technologies

## References

1. D’Aveni, R.: The 3-D Printing Revolution. *Business Harvard Review* (2015)
2. Ford, S.L.: Additive Manufacturing Technology: Potential Implications for US Manufacturing Competitiveness. *J. Int. Commer. Econ.* (2014)
3. Garrett, B.: 3D printing: new economic paradigms and strategic shifts. *Global Policy* **5**(1), 70–75 (2014)
4. Pierrakakis, K., Gkritzali, C.D., Kandias, M., Gritzalis, D.: 3D Printing: A Paradigm Shift in Political Economy? In: 65th International Studies Association’s Annual Convention (2015)
5. Gubin, A.V., Kuznetsov, V.P., et al.: Challenges and perspectives in the use of additive technologies for making customized implants for traumatology and orthopedics. *Biomed. Eng.* **50**(4), 285–289 (2016)
6. Hansen, R.: Building the future Modeling and Uncertainty Quantification for Accelerated Certification, *Science & Technology Review*, (2015)
7. Pawlak, A., Rosienkiewicz, M., Chlebus, E.: DoE approach in AZ31 powder selective laser melting process optimization. *Arch. Civil Mech. Eng.* **17**(1), 9–18 (2017)
8. Pawlak, A., Szymczyk, P., Ziolkowski, G., Chlebus, E., Dybala, B.: Fabrication of microscaffolds from Ti-6Al-7Nb alloy by SLM. *RP J.* **21**(4), 393–401 (2015)
9. Tapia, G., Elwany, A.: A Review on process monitoring and control in metal-based additive manufacturing. *J. Manuf. Sci. Eng.* **136**(6), 60801 (2014)
10. Wing, I., Gorham, R., Sinderman B.: 3D Opportunity for Quality Assurance and Parts Qualification. *Additive Manufacturing Clears the Bar*. Deloitte University Press (2015)
11. Brettel, M., Friederichsen, N., Keller, M., Rosenberg, M.: How virtualization, decentralization and network building change the manufacturing landscape: an industry 4.0 perspective. *Int. J. Mech. Ind. Sci. Eng.* **8**(1), 37–44 (2014)
12. Living tomorrow. 3D printing—a tool to empower the European economy. Opinion of the European Economic and Social Committee CCMI/131 and CCMI/131, (2015)
13. Son, Y.K.: A cost estimation model for advanced manufacturing systems. *Int. J. Prod. Res.* **29**(3), 441–452 (1991)
14. Thomas, D.S., Gilbert, S.W.: Costs and Cost Effectiveness of Additive Manufacturing. National Institute of Standards and Technology, NIST SP 1176 (2014)
15. Hopkinson, N., Dicknes, P.: Analysis of rapid manufacturing—using layer manufacturing processes for production. *J. Mech. Eng. Sci.* **217**(1), 31–39 (2003)
16. Lindemann, C., Jahnke, U., Moi, M., Koch, R.: Impact and influence factors of additive manufacturing on product lifecycle costs. In: *Solid Freeform Fabrication Symposium*, 2013
17. Atzeni, E., Iuliano, L., Minetola, P., Salmi, A.: Redesign and cost estimation of rapid manufactured plastic parts. *Rapid Prototyping J.* **16**(5), 308–317 (2010)
18. Baumers, M., Tuck, C., Wildman, R., Ashcroft, I., Hague, R.: Energy inputs to additive manufacturing: does capacity utilization matter? *EOS* **1000**(270), 30–40 (2011)
19. Angelo, L.D., Stefano, P.D.: A neural network-based build time estimator for layer manufactured objects. *Int. J. Adv. Manuf. Technol.* **57**(1–4), 215–224 (2011)
20. Ruffo, M., Tuck, C., Hague, R.J.M.: Cost estimation for rapid manufacturing—laser sintering production for low to medium volumes (2006)
21. Ruffo, M., Hague, R.J.M.: Cost estimation for rapid manufacturing—simultaneous production of mixed components using laser sintering (2007)
22. Allen, J.: An investigation into the comparative costs of additive manufacture vs. machine from solid for aero engine parts, DTIC Document (2006)
23. Xu, F., Wong, Y.S., Loh, H.T.: Toward generic models for comparative evaluation and process selection in RP and manufacturing. *J. Manuf. Sys.* **19**(5), 283–296 (2001)
24. Piili, H., Happonen, A. et al.: Cost estimation of laser additive manufacturing of stainless steel. *Phys. Procedia.* **78**, 388–396 (2015).
25. Ruffo, M., Tuck, C., Hague, R.J.M.: Make or buy analysis for rapid manufacturing. *Rapid Prototyping J.* **13**(1), 23–29 (2007)

26. Mello, H.P., Calandrin, Martins R., Gomes, Salgado E., Tavares, Seguso R., et al.: Systematic proposal to calculate price of prototypes manufactured through rapid prototyping an FDM 3D printer in a university lab. *RP J.* **16**(6), 411–416 (2010)
27. Atzeni, E., Salmi, A.: Economics of additive manufacturing for end-usable metal parts. *Int. J. Adv. Manuf. Technol.* **62**(9–12), 1147–1155 (2012)
28. Cavalieri, S., Maccarrone, P., Pinto, R.: Parametric vs. neural network models for the estimation of production costs: A case study in the automotive industry. *Int. J. Prod. Econ.* **91**(2), 165–177 (2004)

# Fulfilling Individual Requirements of Customers in Smart Factory Model

Krzysztof Zywicki and Przemyslaw Zawadzki

**Abstract** The paper presents a concept of integration of modern processes of design of customizable products and production control, in scope of Industry 4.0 idea. Production processes must be constantly adapted, to meet changing customers' requirements. This enforces flexibility on production companies. High quality products, delivered on time, sold with an acceptable price—this is already a standard. The main concepts described in the paper revolve around involving customers into design process by use of various systems based on knowledge. This can lead to competitive advantage and a number of other benefits shown in the paper. Products customization is still a big challenge for production companies, because it demands appropriate planning and production control, which is also presented.

**Keywords** Industry 4.0 · Smart factory · Production planning control · Product design

## 1 Introduction

Smart factory is a concept of manufacturing system featuring the ability of quick response to the needs of customers. It is enabled by automation of manufacturing processes and application of modern IT solutions along the entire manufacturing cycle [1–3]. It results in the development of cyber-physical systems which allow for efficient management of manufacturing resources, yet require smart solutions not only in terms of objects (e.g. The Internet of Things) but also in terms of processes (e.g. Knowledge-Based Engineering) [4]. Due to that [5–8], efficient design of products fulfilling individual requirements of customers, and effective production control should be indispensable components of smart factory of the future [9]. This

---

K. Zywicki (✉) · P. Zawadzki

Chair of Management and Production Engineering, Poznan University of Technology,  
Piotrowo 3 Street, 60-965 Poznan, Poland

e-mail: krzysztof.zywicki@put.poznan.pl; kristov.zywicki@gmail.com

© Springer International Publishing AG 2018

A. Hamrol et al. (eds.), *Advances in Manufacturing*, Lecture Notes in Mechanical Engineering, [https://doi.org/10.1007/978-3-319-68619-6\\_18](https://doi.org/10.1007/978-3-319-68619-6_18)

185

is possible mostly by implementing a strategy of mass customization [10]. Only then will it be possible to utilize the manufacturing potential of an enterprise which owns modern technical resources compliant with Industry 4.0 [11].

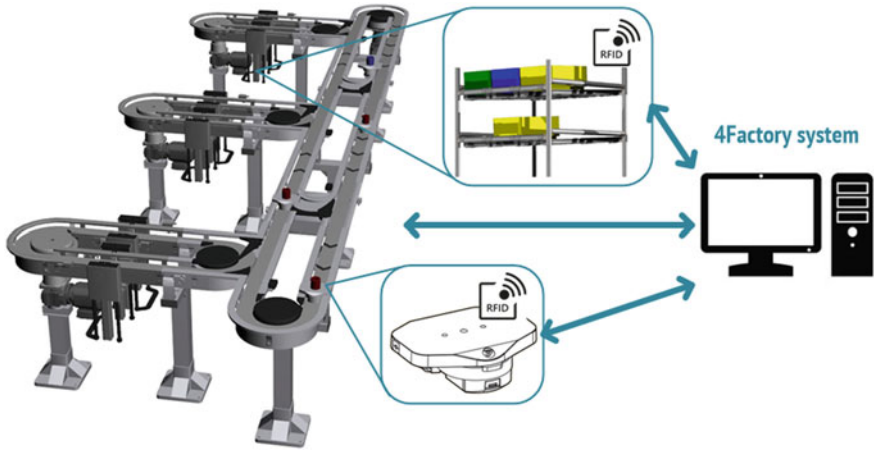
The necessity to take into account individual needs of customers is currently a market standard, although for manufacturers it is a serious organizational challenge [12]. At present, a lot of companies offer the possibility of online configuration of their products. Special applications, called configurators, are becoming more and more popular. They are developed mostly in AR and VR technologies and engage users in the design process [13–15]. On the other hand, in the case of customizable products, designing is mostly made up of routine tasks (ca. 80%), therefore its automation can significantly affect optimization of the entire product lifecycle and savings. This can be achieved by the application of KBE class solutions [16, 17].

Implementing the strategy of manufacturing products in compliance with individual requirements of customers is also a serious challenge for organizing processes of production planning and control. Therefore, it is worth to search for best possible solutions as regards production scheduling, material flow monitoring or decision support. The reason for this is the objective of effective utilization of available resources when meeting individual needs of customers [18–23]. In the necessity of constant adjusting to changes, production scheduling can be referred to as Fast Dynamic Scheduling [24]. One of the elements that should be taken into account while scheduling is preparing variants of material flow. This allows to determine the most efficient production flow with reference to the assumed criteria, e.g. using production resources or shorter delivery time. Bearing in mind the necessity of fulfilling the customers' requirements, the adopted scheduling methods must take into consideration the possibility of producing goods with use of different manufacturing resources. This allows for fast response to new orders or in the event new factors appear which make it impossible to use the resources. It necessitates close integration of production planning and control with product designing [25–27].

This article presents a laboratory model of smart manufacturing system operating to fulfil individual requirements of customer.

## 2 Model of Smart Manufacturing System

A manufacturing system which is part of a SmartFactory lab equipment includes an automated production line made up of four conveyor loops. Production stations are located besides each of the loops. The range of products includes goods manufactured while joining bricks. Products are transported on pallets which can be directed to any production station. The manufacturing system is controlled by original software called 4Factory. It is made up of modules that enable production planning, supervising material flow and production line control.



**Fig. 1** Production system model

The model of a manufacturing system enables mirroring the actual processes connected with fulfilment of client orders in compliance with Industry 4.0 concept (Fig. 1).

Production starts on the basis of a designed product and delivery time approved by customer. Products are designed with use of dedicated software that enables their customization according to individual requirements of customers. Information concerning structure of the product enable generating technological processes to plan the production and thus to define order delivery times (Fig. 2).

Production is planned with use of simulations that show the progress of production, including customer orders, requirements of materials and current resource load. Indexes showing the punctuality of order deliveries and the use of production capabilities were adopted as criteria of evaluation and selection of production plan in the form of production schedule.

### 3 Defining the Configuration of Products

To facilitate the configuration and to provide a broad range of potential variants, a product model is represented by a set of bricks connected in any possible way. The user (customer) can customize the products on his/her own with use of dedicated software. The software’s graphic interface lets users choose predefined parts and visualize the product customization.

It is possible to customize the following: part type, number of parts, part colour, part orientation, part location (Fig. 3).

A product is designed iteratively (step by step). At a given design stage, it is possible to select specific components of the product.



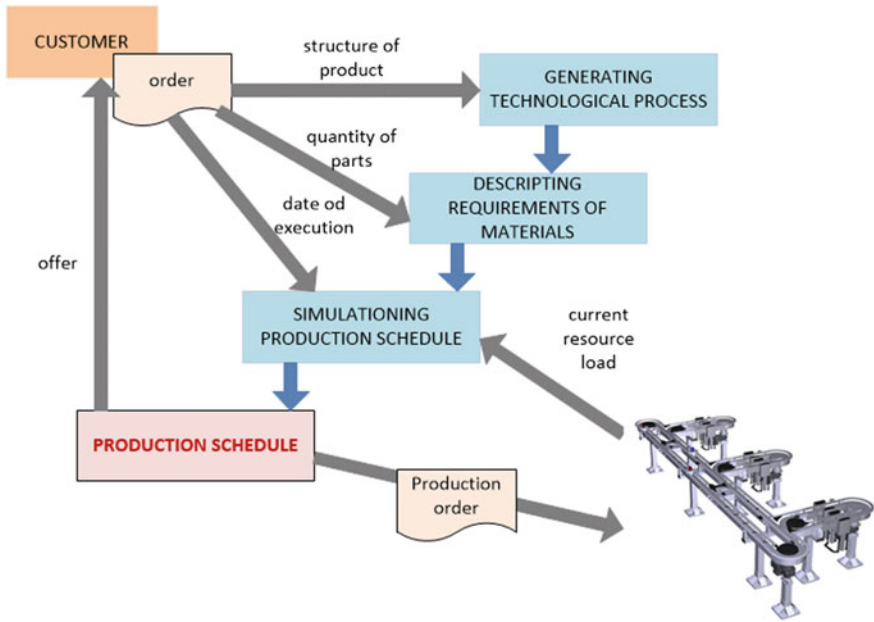


Fig. 2 General order delivery performance model in smart factory model

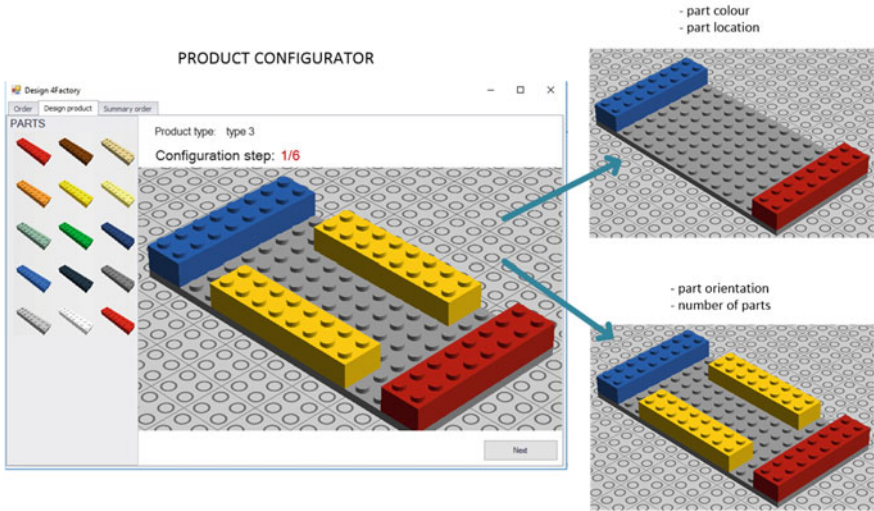


Fig. 3 Product configuration options

Such a product, which can be freely configured by customer, is then analysed with reference to technological processes and demand for materials needed for the

product’s components. This is performed automatically by 4Factory after importing data from the configurator of finished products.

## 4 Defining Technological Processes

In the adopted solution, technological processes are generated automatically based on the given product’s structural design and technological capabilities of the production system.

### 4.1 Technological Capabilities of the Production System

Technological capabilities of the production system are defined as a capability of a given production station to add a specific part that is a component of the finished product. The database of 4Factory was developed based on that assumption. Thereby, a knowledge base with all standard technological processes was developed (Fig. 4).

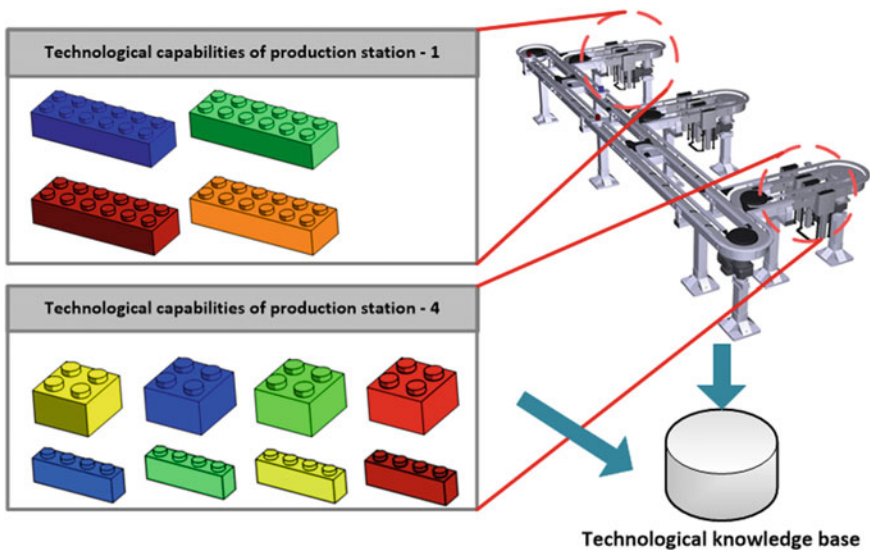


Fig. 4 Technological capabilities of the production system

The technological knowledge base contains information about the dimensions and colours of given parts as well as about unit (standard) times of assembly of given parts in a finished product.

### 4.2 *Generating Technological Processes*

A technological process of product manufacturing is generated automatically based on the structure of products and technological capabilities of the production system. The product structure, in the form of a list of all the product components, is compared to database of technological knowledge about the production system in 4Factory.

This enables to develop a structure of technological process that includes a list of subsequent operations and technological tasks as well as standard time required for performing them, connected with performance of the same at a given production station (Fig. 5).

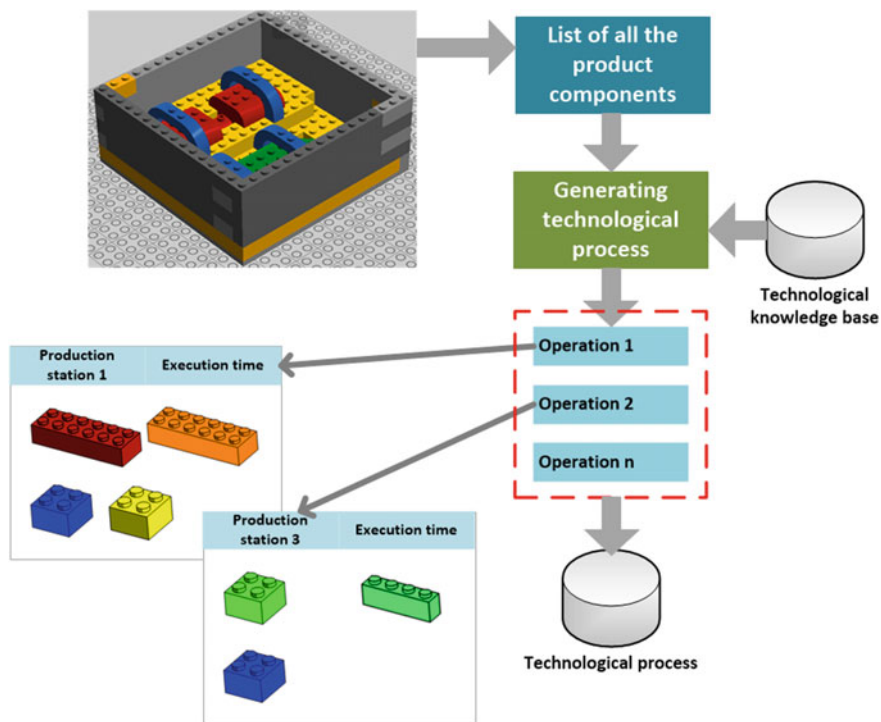


Fig. 5 Generating technological processes

A technological process of manufacturing a product developed in this way serves then as a basis for production planning, including simulating the schedule of resource load.

## 5 Production Planning

Planning in smart factory model is performed under the 4Factory software. The purpose of this function is to develop a production schedule that will determine whether it is possible to perform customer orders with use of given production capabilities within time as required by customers, or what is the nearest feasible order delivery date.

Production planning begins with defining material demand for components of finished products. Next, on the basis of customer orders, production orders are generated for the production system and for individual assembly stations.

Considering the nature of production connected with the necessity of flexible response to variable customer orders, and bearing in mind limited capabilities of production system, planning is performed as a simulation. During the simulation, different variants of production schedules are prepared with reference to various rules of production order allocation (determining the sequence of order performance). The variants are compared to select the optimum one with consideration of the following criteria:

- minimizing the number of orders with exceeded directive delivery time,
- minimizing average delay of order delivery times,
- maximizing the load of production stations.

The scheduling simulation results in development of production station load plan (which is a basis for issuing station orders) and production order performance plan which determines the order delivery times. The production order performance plan indicates whether it is possible to perform production orders, and, as a consequence, whether it is possible to perform customer orders in times as required by customers (Fig. 6).

Such a production schedule serves as a basis for determining times when materials should be delivered to the production system. If the customer accepts the order delivery time, the adopted production plan becomes an implementation plan which controls operation of the production line.

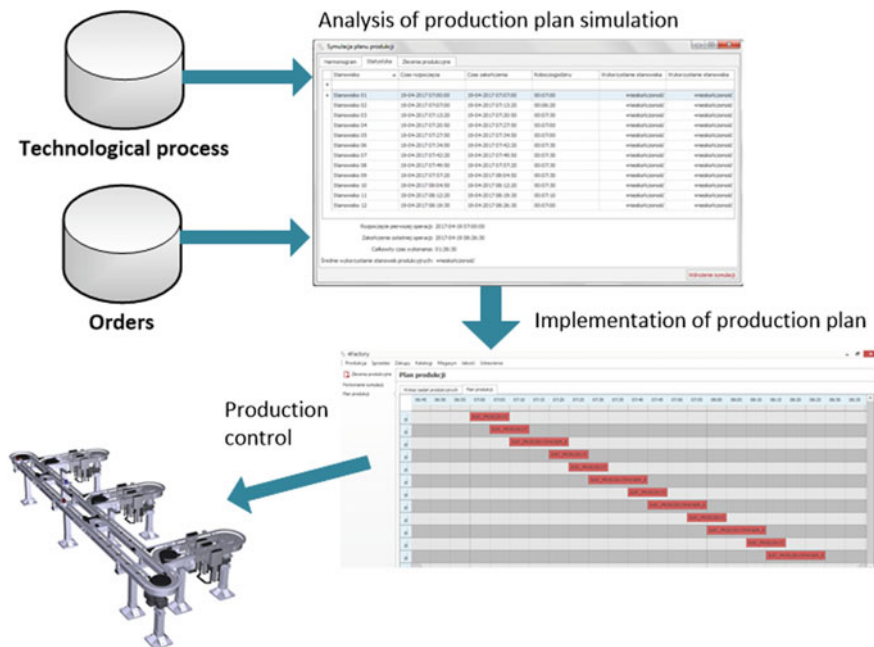


Fig. 6 Production planning process

## 6 Summary

The idea of smart factory enables meeting individual needs of customers with reasonable use of production resources. Planning order delivery must feature close integration as regards exchange of data concerning structural and technological requirements. Only a close integration of those areas will guarantee synchronizing production flow and thus contribute to timely delivery of customer orders.

Functioning of the presented laboratory model of production system is based on the rules of smart factory. The system is managed by original 4Factory software which integrates data concerning all the technical utilities. Thanks to the implemented solutions, it is possible to perform a simulation connected with performance of individual customer orders. These are connected with exchange of data related to product configuration (structural product design), automatic development of technological processes and then production plans.

The production system is subject to development mostly in the area of further integration and automation of data collection (image recognition), and utilizing augmented reality to supervise production processes.

**Acknowledgements** The presented results are derived from a scientific statutory research conducted by Chair of Management and Production Engineering, Faculty of Mechanical Engineering

and Management, Poznan University of Technology, Poland, Poland, supported by the Polish Ministry of Science and Higher Education from the financial means in 2017 (02/23/DSPB/7695).

## References

1. Shrouf, F., Ordieres, J., Miragliotta, G.: Smart factories in industry 4.0: a review of the concept and of energy management approached in production based on the internet of things paradigm. In: IEEE International Conference on Industrial Engineering and Engineering Management (IEEM). IEEE (2014)
2. Brettel, M., Friederichsen, N., Keller, M., Rosenberg, M.: How virtualization, decentralization and network building change the manufacturing landscape: an industry 4.0 perspective. *Int. J. Mech. Aerosp. Ind. Mechatron. Manufact. Eng.* **8**(1) (2014)
3. Kemény, Z., Beregi, R.J., Erdős, G., Nacsa, J.: The MTA SZTAKI smart factory: platform for research and project-oriented skill development in higher education. *Procedia CIRP* **54**, 53–58 (2016)
4. Zawadzki, P., Żywicki, K.: Smart product design and production control for effective mass customization in the Industry 4.0 concept. *Manag. Prod. Eng. Rev.* **7**(3), 105–112 (2016)
5. Colombo, A., Bangemann, T., Karnouskos, S., Delsing, J., Stluka, P., Harrison, R., Jammes, F., Lastra, J.L.: *Industrial Cloud-Based Cyber-Physical Systems: The IMC-AESOP Approach*. Springer, New York (2014)
6. Seitz, K.F., Nyhuis, P.: Cyber-physical production systems combined with logistic models—a learning factory concept for an improved production planning and control. In: The 5th Conference on Learning Factories, *Procedia CIRP*, vol. 32, pp. 92–97 (2015)
7. Veigt, M., Labbe, D., Hribernik, K.A., Scholz-Reiter, B.: Entwicklung eines cyber-physischen logistiksystems. *Ind. Manag.* **1**, 15–18 (2013)
8. Zhang, Y., Xie, F., Dong, Y., Yang, G., Zhou, X.: High fidelity virtualization of cyber-physical systems. *Int. J. Model. Simul. Sci. Comput.* **4**(2) (2013)
9. Ivanov, D., Dolgiu, A., Sokolov, B., Werner, F., Ivanova, M.: A dynamic model and an algorithm for short-term supply chain scheduling in the smart factory industry 4.0. *Int. J. Prod. Res.* **54**(2), 386–402 (2016)
10. Górski, F., Zawadzki, P., Hamrol, A.: Knowledge based engineering as a condition of effective mass production of configurable products by design automation. *J. Mach. Eng.* **16** (2016)
11. Gorecky, D., Schmitt, M., Loskyll, M., Zuhlke, D.: Human-machine-interaction in the industry 4.0 ERA. In: 12th IEEE International Conference on Industrial Informatics (INDIN), pp. 289–294 (2014)
12. Trentin, A., Perin, E., Forza, C.: Product configurator impact on product quality. *Int. J. Prod. Econ.* **135**(2), 850–859 (2012)
13. Górski, F., Buń, P., Wichanierek, R., Zawadzki, P., Hamrol, A.: Immersive city bus configuration system for marketing and sales education. *Procedia Comput. Sci.* **75**, 137–146 (2015)
14. Choi, S., Jung, K., Noh, S.D.: Virtual reality applications in manufacturing industries: past research, present findings, and future directions. *Concurr. Eng.* **23**(1), 40–63 (2015)
15. Górski, F., Buń, P., Wichanierek, R., Zawadzki, P., Hamrol, A.: Design and implementation of a complex virtual reality system for product design with active participation of end user. In: *Advances in Human Factors, Software, and Systems Engineering*, pp. 31–43. Springer (2016)
16. Skarka, W.: Application of MOKA methodology in generative model creation using CATIA. *Engineering Applications of Artificial Intelligence*, vol. 20. Elsevier (2007)
17. Górski, F., Hamrol, A., Kowalski, M., Paszkiewicz, R., Zawadzki, P.: An automatic system for 3D models and technology process design. *Trans. FAMENA* **35**(2), 69–78 (2011)

18. Trojanowska, J., Żywicki, K., Machado, J.M., Varela, L.R.: Shortening changeover time—an industrial study. In: Proceedings of 10th Iberian Conference on Information Systems and Technologies (CISTI), vol. II, pp. 92–97 (2015)
19. Kujawińska, A., Rogalewicz, M., Diering, M.: Application of expectation maximization method for purchase decision-making support in welding branch. *Manag. Prod. Eng. Rev.* **7** (2), 29–33 (2016)
20. Żywicki, K., Rewers, P., Bożek, M.: Data Analysis in Production Levelling Methodology, Advances in Information Systems and Technologies, pp. 519–527 (2017)
21. Trojanowska, J., Varela, M.L.R., Machado J.: The tool supporting decision making process in area of job-shop scheduling. In: Rocha Á., Correia, A., Adeli, H., Reis, L., Costanzo, S. (eds.) Recent Advances in Information Systems and Technologies. WorldCIST, Advances in Intelligent Systems and Computing, vol. 571, pp. 490–498. Springer, Cham (2017)
22. Gangala, C., Modi, M., Manupati, V.K., Varela, M.L.R., Machado, J., Trojanowska, J.: Cycle Time reduction in deck roller assembly production unit with value stream mapping analysis. In: Rocha, Á., Correia, A., Adeli, H., Reis, L., Costanzo, S. (eds.) Recent Advances in Information Systems and Technologies, WorldCIST, Advances in Intelligent Systems and Computing, vol. 571, pp. 509–518. Springer, Cham (2017)
23. Rewers, P., Hamrol, A., Żywicki, K., Kulus, W., Bożek, M.: Production leveling as an effective method for production flow control—experience of polish enterprises. In: *Procedia Engineering*, vol. 182, pp. 619–626 (2017)
24. Piłacińska M., Leśniak K., Kujawińska A., Żywicki K.: The data model of production flow and quality control system. *Studia Inform.* **30**(2B), 109–126, 1642-0489 (2009)
25. Trojanowska, J., Żywicki, K., Pająk, E.: Influence of selected methods of production flow control on environment. *Inf. Technol. Environ. Eng.* **3**, 695–705 (2011)
26. Szuszynski, M., Żurek, J.: Computer aided assembly sequence generation. *Manag. Prod. Eng. Rev.* **6**(3), 83–87 (2015)
27. Żywicki, K., Zawadzki, P., Hamrol, A.: Preparation and production control in smart factory model. In: Advances in Information Systems and Technologies, pp. 519–527 (2017)

# Model of Competency Management in the Network of Production Enterprises in Industry 4.0—Assumptions

Magdalena Graczyk-Kucharska, Maciej Szafranski, Marek Golinski,  
Malgorzata Spychala and Kamila Borsekova

**Abstract** The aim of this paper is to formulate assumptions—the point of departure for a model of competency management in a network of cooperating employers, whose goal is to increase the competitiveness of industry within the concept of Industry 4.0. In a knowledge-based economy, competencies are becoming a key non-material resource, with a significant influence on the development of enterprises, and on skilful use of new technologies, such as the Internet of Things, in order to create competitive advantage. The introduction gives a review of literature dealing with the influence of competencies on creating a smart factory, and the exchange of knowledge and skills within the network of production enterprises. The second part of the paper presents results of the research on key competencies possessed by generation Y. They were then compared to the demand of employers of chosen key enterprises in the region of Wielkopolska for certain skills and with competencies of the future in a smart factory. The final part presents assumptions for the model of knowledge management in production enterprises that aspire to use new technologies in the network, in accordance with the concept of Industry 4.0.

**Keywords** Competency management · Network · Industry 4.0 · Smart factory

---

M. Graczyk-Kucharska · M. Szafranski (✉) · M. Golinski · M. Spychala  
Poznan University of Technology, Poznań, Poland  
e-mail: maciej.szafranski@put.poznan.pl

M. Graczyk-Kucharska  
e-mail: magdalena.graczyk-kucharska@put.poznan.pl

M. Golinski  
e-mail: marek.golinski@put.poznan.pl

M. Spychala  
e-mail: malgorzata.spychala@put.poznan.pl

K. Borsekova  
Matej Bel University, Banska Bystrica, Slovakia  
e-mail: kamila.borsekova@umb.sk



## 1 Introduction

The aim of Industry 4.0 enterprise is to increase effectiveness and efficiency [1], as well as to raise the level of the enterprise's automation. Currently, the omnipresent Internet dominates not only our everyday life, but also enterprises. The fourth revolution caused by the development of the Internet, as well as the Internet of Things, cloud computing, communication between people and machines, including cyber-physical systems (CPS) [2], have a significant influence on the functioning of production enterprises in the competitive market [3].

The scope of Industry 4.0, ever since the first article concerning this concept was published in 2011, has included various approaches. The main ones are [4]: Concept and perspectives of Industry 4.0, CPS-based Industry 4.0, Interoperability of Industry 4.0, Key technologies of Industry 4.0, Applications of Industry 4.0.

Nowadays, smart factories focus mostly on control-centric optimisation and intelligence. Among the areas of fundamental significance for the enterprises in Industry 4.0 [5], listed in the literature, along with technological solutions, are also new values [6], job creation or virtual industrialisation.

Based on the literature [7], the educational level, as well as, the technological infrastructure of the Learning Factory are derived. Currently, in a knowledge-based economy [8], relying on the Resource-Based View of the firm (RVB), it is argued that contemporary enterprises build their competitive advantage mainly on non-material resources, i.e. on knowledge, skills and experience [9]. Thanks to them, they can offer customers a unique bundle of values [10], running organisational excellence as well as the competitive advantage based on quality management system [11] also human factors and ergonomics in manufacturing [12, 13]. In order to create a new value and to use available resources of the enterprises, it is necessary to build a potential of non-material resources of the enterprise, such as competencies of the enterprise.

As a result of the changing environment where the organisation will operate, the role of the employee will evolve towards managing operations which are performed together with cooperating robots. This link of context-related decision-making of man and the precision and regularity of robots will be the source of an abrupt increase of productivity [3]. Employees will be expected to act more on their own initiative, have excellent communication skills and be able to organise their own work [14].

Assuming wider access to human resources, their knowledge and skills within production enterprises in the business network, it is possible to multiply and accelerate processes connected with creating smart factories [15]. One type of business networks are the mutually learning ones [16]. Transfer of knowledge between individual subjects of the network creates opportunities to learn and cooperate between institutions, which can then stimulate new knowledge. At the same time, it facilitates the innovative ability of organisational units [17] that create a network such as a smart factory.

As a result of social and project activities, undertaken by the team of scientists from Poznan University of Technology and Regional Government of Wielkopolska Voivodeship between 2013–2017, an economic-educational network has started to emerge. Its participants focus on creating relationships in order to increase professional competencies (both technical and social) possessed or obtained by future or young employees. They are representatives of the generation, which in the literature of the subject is often—albeit wrongly—identified as generation Y.

The current stage of development of the network, potential advantages of belonging to it, and postulated directions of its development were described by Szafranski et al. [18, 19]. The authors perceive the need to further develop this network, dynamise this development and deepen the identity connected with belonging to the network by subjects that co-create it. Simultaneously, the authors observe that the structure of this network creates a potential, so that subjects belonging to it, especially enterprises, take advantage of it. One of the potential benefits is facilitating management of competencies by subjects cooperating in the network. The network of cooperating production enterprises can act together in order to minimise costs of the enterprises and maximise profits [20]. An innovative solution is the model of competency management in the network of cooperating enterprises. One of the stages preceding the creation and subsequent implementation of such a model is formulating the assumptions necessary for creating it.

## 2 Methodology of Research

Assumptions which are a point of departure for creating a model of competency management in a network of cooperating key employers in Industry 4.0 were based on four stages of research.

The first stage was of quantitative character and consisted in analysing the data available in an IT tool—system.zawodowcy.org. It was designed and implemented for entrepreneurs of Wielkopolska and for students and graduates of secondary schools (generation Y). This stage included the analysis of job offers of more than 1200 employers published between 2013–2015. It was aimed at finding six most frequently sought competencies of employees in the area of personal and social competencies.

The second stage of the research was of qualitative character and consisted in individual interviews in 61 key production enterprises based in one of 19 poviats (counties) of Wielkopolska (total number of poviats in Wielkopolska: 31) and three city-counties (total number of city-counties in Wielkopolska: 4). Individual interviews were carried out with 107 persons in March 2016 and March 2017, in key enterprises that employ at least 150 persons (average number of employees in examined companies is over 300).

The next stages of the research, i.e. third and fourth, were closely connected. The participants were employees of middle and higher level of the organisation, who were responsible for professional education and/or staff, and who understand



**Fig. 1** Outline of research

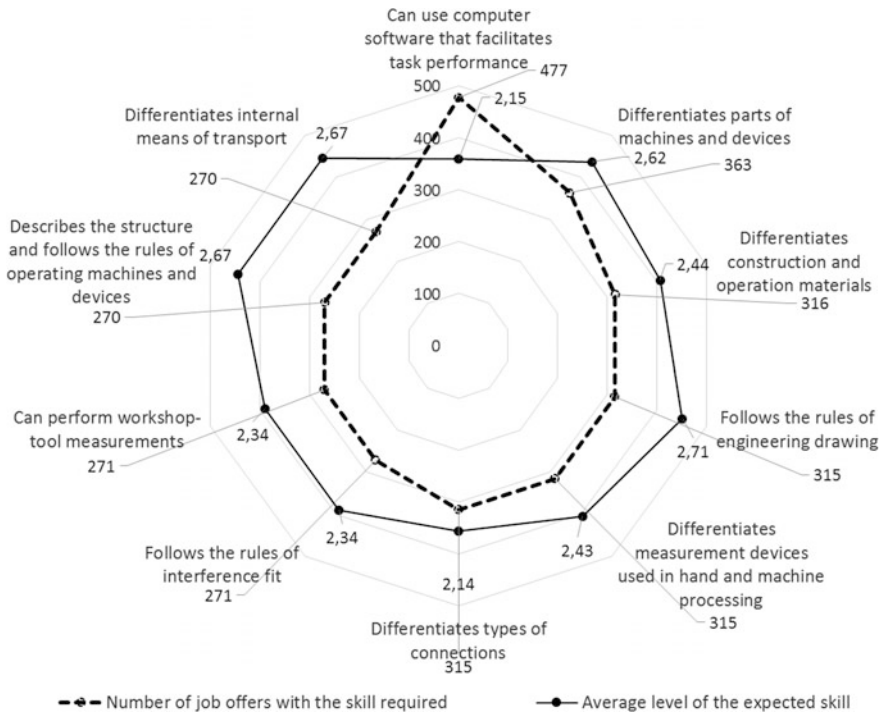
changes taking place in connection with Industry 4.0. An electronic survey was used in the third stage; it took place in the first half of November 2016. The fourth stage—an in-depth group interview—was carried out on 17 November 2016, with participation of nine out of ten enterprises that took part in stage 3 of the research. 17 persons of middle and higher level of the organisation took part in the in-depth group interview. Entrepreneurs represented companies that employ between 150 and 6900 employees (average number of employees is 1450) (Fig. 1).

### 3 Results of the Research

In the first stage, the most frequent competencies pointed by entrepreneurs registered in system.zawodowcy.org (Fig. 2) were analysed. The type of offers addressed to students and graduates of vocational secondary schools (Millennial generation) should be taken into account. As the data analysis shows, the three social skills employers pointed most frequently for young people from the Millennial generation were: can use the computer (477 indications), differentiates parts of machines and devices (363 indications) and differentiates construction and operation materials (316 indications). The highest level of acquisition of a skill was pointed for: follows the rules of engineering drawing (average level of acquisition required: 2.71), differentiates internal means of transport (2.67) and describes the structure and follows the rules of operating machines and devices (2.67). All the skills pointed were assessed on average as 2.45, which may suggest that employers realise the need to train employees in their first job.

In the second stage, based on results of individual interviews, a list of chosen issues and challenges connected with managing competencies in the network of production enterprises in Industry 4.0 was created. The following were among them:

- hard-to-find technical and social competencies, connected with low unemployment rate in Poland and the job market,
- necessity to change work systems, demands for competencies in a workstation and organisation of work connected with a new generation of employees—Millennials,
- increased interest in young employees without experience and required competencies in a given workstation,
- increasing competitiveness of production enterprises,



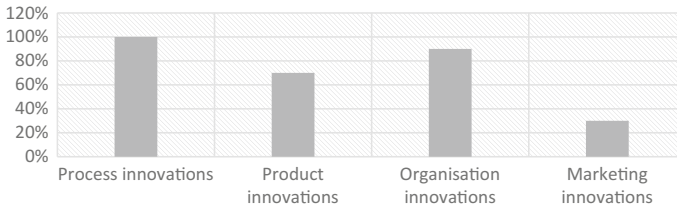
**Fig. 2** Skills—components of professional competencies for a given workstation and the level of acquisition expected by employers. *Source* Own elaboration based on system.zawodowcy.org. [21]

- stress on innovative character of enterprises, especially product innovation,
- the willingness to cooperate within the Educational and Economic network, in order to minimise gaps or scarcity of competencies in the job market,
- exchange of knowledge and learning from one another in the network.

The above challenges for production enterprises are connected with both current operations of enterprises and future ones, not connected with managing competencies in the network, but with the willingness to cooperate in the network of production enterprises.

In stage 3 of the research, during the survey with employees of middle and higher level of the organisation, a preliminary analysis of competencies needs in Industry 4.0 was carried out. The research showed that:

- 7 out of 10 examined key production enterprises in Wielkopolska are planning automation of production processes,
- 7 out of 10 examined key enterprises claim that in recent years automation has had an influence on employment in the company,



**Fig. 3** Planned implementation of innovation in examined production enterprises

- 4 out of 10 companies claim that activities of CSR directed at formal education on the secondary level translates into financial benefits for the enterprise,
- 10 out of 10 examined companies claim that cooperation between school and enterprises in the area of innovation is necessary,
- organisation and process innovation are planned more often than implementation of product or marketing (Fig. 3).

The final stage of the research, before formulating the assumptions for the creation of a model of managing competencies in the network of production enterprises in Industry 4.0, is creating a map of future competencies in a smart factory. This map is created based on opinions of 17 persons from 9 key production enterprises of Wielkopolska. The results of this research is presented below (Fig. 4).

The data analysed show that the biggest change concerning competencies of the future will apply to professional skills connected with machines’ ‘understanding’ and processing data into information and values. It will concern the competency of data analysis (average level of acquisition on level 3, and in the future 5.4), 3D designing (change from 2.5 to 4.1) or widely understood multidisciplinary competency (currently not required, and in the future required on level 5.5). Technical knowledge in production companies will not change and it will be required on the level above 6. Besides creating values based on data, in the future soft competencies will be required, such as team management (currently 3.3, in the future above 6), communication (comparable high level 5.7 both currently and in the future), teamwork (currently 4.7, in the future 5.8), emotional intelligence (currently 4, in the future 5.5). New competencies appear, currently not required: cultural tolerance (on level 5.2), drones steering (3.8) or teleportation (3.8)—pointed by employers, albeit impossible due to technical reasons in wider use. The only competency that lost the importance is mobility (drop from currently required level of 5.1 to 1.8). This can be explained by the use of new communication technologies that allow remote contact with persons from home or another location.

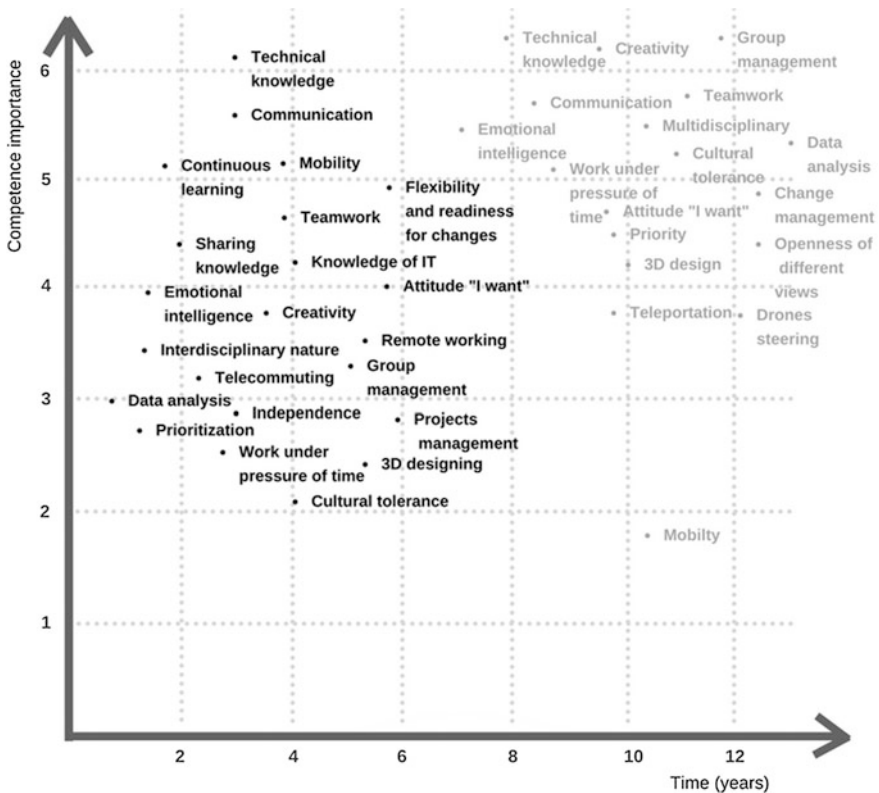
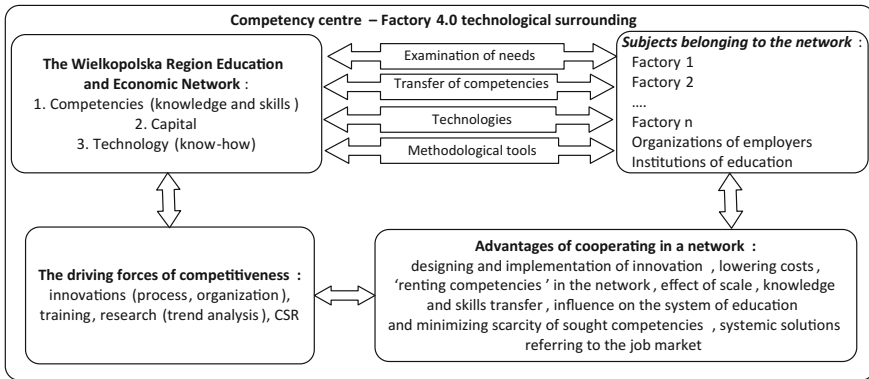


Fig. 4 Future competence map of production enterprises [22]

#### 4 Assumptions for Creating a Model of Managing Competencies in the Network of Production Enterprises in Industry 4.0

The above research results show the demand for key competencies in production enterprises in relation to Industry 4.0. The authors notice the need to manage competencies, including future competencies in the network of production enterprises. The concept of cooperation of the enterprises within the network appeared in 2010, simultaneously with the creation of a system tool that monitors the needs of the market (Wielkopolska System of Monitoring and Forecasting). The research, perfected over 7 years, allowed formulating the assumptions for the model approach of managing competencies in the network of production enterprises (Fig. 5).

The most significant assumption for the functioning of the model is the exchange of information concerning current needs of employers of production enterprises and competencies available in the market, possessed by candidates. It is also vital to



**Fig. 5** Model of managing competencies in the network of production enterprises—assumptions

ensure availability of competencies required by production enterprises in the future. Information about current and future needs for competencies in the job market has an influence on planning. The possibility to analyse these needs by institutions of education (which also belong to the network) plays an educational role as well. Access to information about competencies in the job market facilitates reaction of enterprises to parallel market processes: dynamically changing expectations of customers and continuous development of technologies, with breakthroughs happening in ever-shorter intervals.

Access to information and information exchange in the network increase effectiveness of managing a production enterprise in Industry 4.0. It is mainly connected with managing current and future employees, and as a result—their competencies. Employee’s competencies, expressed in skills and knowledge of employees must be managed flexibly in order to be an effective resource that facilitates realisation of the goals set. Knowledge exchange and human resources exchange between enterprises (declared by research participants—see Chapter ‘Overall Equipment Effectiveness: Analysis of Different Ways of Calculations and Improvements’) facilitates cost minimisation, increases flexibility of competency management, and at the same time—the ability to react quickly to the needs of the market. In order to possess this ability, an enterprise should be supported in the realisation of competency management. An example of such a solution may be innovative, systemic cooperation within the framework of the Wielkopolska Region Education and Economic Network, supported by an IT tool—system.zawodowcy.org. The presented model solution of managing competencies in a network is an attempt at supporting employers in flexible management of employees’ competencies. As the process, which reacts dynamically to the changing needs, the model will also be perfected further.

## 5 Discussion and Conclusions

The development of economy, whose dynamic changes are identified with another industrial revolution, forces enterprises to make revolutionary changes. As a result of global competition, individual enterprises enter into cooperation with other enterprises or organisations of enterprises, local governments (local administration) or institutions of education. What motivates them is minimisation of risk. The basic advantage of cooperation in the network is exchange of knowledge (acceleration of knowledge diffusion). The research, the result of which were presented in this paper, shows that enterprise management is ever more interested in exchanging resources, including the most valuable ones—connected with employee competencies. It refers mainly to enterprises that plan development through implementation of innovation. Realisation of the goals of Industry 4.0 enterprises and gaining market advantage is done through benefits resulting from cooperation. They include cost reduction and increased effectiveness of activities.

The described part of the research process confirms the need to transfer practical engineer knowledge and to manage processes concerning knowledge of employees' competencies. The process, based on the research and perfected over many years, supporting competency management, as well as, the number of users who provide information and test the process (over 1200 employers and more than 22 000 potential employees) also confirms the need of solutions that would enhance the exchange of knowledge about competencies in the job market. The assumptions described in this paper, reflecting the research realised over many years, also confirms the need to manage competencies in a network manner. It would increase competitiveness of enterprises through the ability to react quickly to the needs of the market, and better access to required resources. The use of solutions described in this paper may impose new business models and changes in the organisation's structure, thus fully realising the concept of Industry 4.0.

## References

1. Thames, L., Schaefer, D.: Software-defined cloud manufacturing for industry 4.0. In: *Procedia CIRP*, vol. 52, pp. 12–17 (2016)
2. Lee, J., Behrad, B., Kao, H.A.: A cyber-physical systems architecture for industry 4.0-based manufacturing systems. *Manufact. Lett.* **3**, 18–23 (2015)
3. Brettel, M., Friederichsen, N., Keller, M., Rosenberg, M.: How virtualization, decentralization and network building change the manufacturing landscape: an industry 4.0 perspective. *Int. J. Mech. Ind. Sci. Eng.* **8**(1), 37–44 (2014)
4. Lu, Y.: Industry 4.0: a survey on technologies, applications and open research issues. *J. Ind. Info. Integr.* (2017)
5. Magruk, A.: Uncertainty in the Sphere of the industry 4.0-potential areas to research. *Bus. Manag. Educ.* **14**(2), 275–291 (2016)



6. Graczyk-Kucharska, M.: Big data as a necessity of modern marketing (in Polish). In: *Scientific Quarterly of Szczecin University. Manag. Finan. Mark. Issues.* **41**(2), 265–277 (2015)
7. Tisch, M., Hertle, C., Cachay, J., Abele, E., Metternich, J., Tenberg, R.: A systematic approach on developing action-oriented, competency-based Learning Factories. In: *Procedia CIRP*, vol. 7, pp. 580–585 (2013)
8. Makhmutov, I.I., Isavin, A.G., Karamyshev, S.A.: Classification approach in determination of knowledge in context of organization. *Acad. Strateg. Manag. J.* **15**, 39–45 (2016)
9. Lado, A.A., Wilson, M.C.: Human resource systems and sustained competitive advantage: a competency-based perspective. *Acad. Manag. Rev.* **19**(4), 699–727 (1994)
10. Kunasz, M.: Companies resources in economy theory (in Polish). *Nat. Econ.* **10**, 33–48 (2006)
11. Jašarević, S., Diering, M., Brdarević, S.: Opinions of the consultants and certification house regarding the quality factors and achieved effects of the introduced quality system. *Tech. Gaz.* **19**(2), 211–220 (2012)
12. Hamrol, A., Kowalik, D., Kujawska, A.: Impact of selected work condition factors on quality of manual assembly process. *Hum. Factors Ergon. Manufact. Serv. Ind.* **21**(2), 156–163 (2011)
13. Kujawińska, A., Vogt, K., Wachowiak, F.: Ergonomics as significant factor of sustainable production. In: Golińska, P., Kawa, A. (eds.) *Technology Management for Sustainable Production and Logistics*, Book Series: EcoProduction, pp. 193–203 (2015)
14. Smit, J., Kreutzer, S., Moeller, C., Carlberg, M.: European parliament directorate general for internal policies, policy department A: economic and scientific policy, industry 4.0, 2016, EU. Available at: <http://www.europarl.europa.eu/studies> 25 May 2017
15. Tiwana, A.: Do bridging ties complement strong ties? An empirical examination of alliance ambidexterity. *Strateg. Manag. J.* **29**, 251–272 (2008)
16. Johanson, J., Vahlne, J.E.: Business relationship learning and commitment in the internationalization process. *J. Int. Entrepreneurship* **1**(1), 83–101 (2003)
17. Tsai, W.: Knowledge transfer in intraorganizational networks: effects of network position and absorptive capacity on business unit innovation and performance. *Acad. Manag. J.* **44**(5), 996–1004 (2001)
18. Szafranski, M.: Acceleration of educating as an external factor supporting preventive and improving actions in businesses. In: Ahram, T., Karwowski, W., Schmorow, D. (eds.) *Procedia Manufacturing*, 6th International Conference on Applied Human Factors and Ergonomics and the Affiliated Conferences, AHFE 2015, vol. 3, pp. 4948–4955 (2015)
19. Szafranski, M., Ganowicz, M., Goliński, M.: The development of corporate social responsibility in educational-economic network (in Polish). In: Ejdyś, J. (ed.) *Social Responsibility and Sustainable Development in management. Theoretical and Application Aspects*, Wydawnictwo Dom Organizacji, pp. 99–114 (2016)
20. Medlin, C.J., Törnroos, J.Å.: Exploring and exploiting network relationships to commercialize technology: a biofuel case. *Ind. Mark. Manage.* **49**, 42–52 (2015)
21. Spychała, M., Graczyk-Kucharska, M., Goliński, M., Szafranski, M.: Competency management as the direction of the development of enterprises—based on research, Economic Development and Management Engineering. Wuhan, China (2016)
22. Graczyk-Kucharska, M., Goliński, M., Spychała, M., Szafranski, M.: Future competence as an innovation force, Internal Report after workshops (in Polish) (2017) (time of internal publication—February 2017, planned date of publishing online—October 2017)

# The Benefits of Using Computer Simulation Models to Support Decision-Making

Elzbieta Malec

**Abstract** Improving the efficiency of a manufacturing company is an area of interest for both entrepreneurs and researchers seeking ways to achieve better performance. Among the many ways to support production systems, forecasting and simulation of production systems is one of a great interest. This is because, among other things, in the simulation process, the course of the various stages of production as a function of time can be analyzed in a way that is not practically feasible. This article is based on cooperation between the world of science and business. The aim of the paper is to present new opportunities for improving the efficiency of a viable enterprise. This article describes primarily a different approach to problem solving based on the simulation of the production process using the Vensim program designed to describe diverse environments. The paper is scheduled to be the first in a series that uses Vensim's simulation capabilities. In this article, the focus is on presenting the process of building a simulation model and the overall benefits of this. Already the process of building the model has revealed very interesting areas of analysis, related to lack of tools to support current decisions. The reason for using the simulation methods was the problems observed in the company: the prolonged time of order execution, the risk of losing customers, the risk of negative audits. Thanks to the use of the simulation model in the current activity, the results were also obtained: defining places of delays, streamlining the flow of information, integrating actions and people, and a comprehensive look at the company's activities.

**Keywords** Decision support • Information system • Efficiency • Simulation model

---

E. Malec (✉)

Faculty of Mechanical Engineering, Cracow University of Technology,  
Al. Jana Pawła II 37, 31-864 Kraków, Poland  
e-mail: malec@mech.pk.edu.pl

© Springer International Publishing AG 2018

A. Hamrol et al. (eds.), *Advances in Manufacturing*, Lecture Notes in Mechanical Engineering, [https://doi.org/10.1007/978-3-319-68619-6\\_20](https://doi.org/10.1007/978-3-319-68619-6_20)

205

## 1 Introduction

The desire to have knowledge about the future has long been associated with man. In this complex world, decision support for human operators and information management is a key asset in managing “better-faster-cheaper” competition. Simulation analysis with real data provides forecasts on the basis of the given input values [1]. The Decision Support System (DSS) should be therefore understood as an interactive computer system that helps decision makers use data and models to solve unstructured problems [2]. A Decision Support System is defined as an interactive computer-based information system that is designed to support solutions on decision problems [3]. Whereas DSS primarily serves to directly increase decision-making efficiency rather than organizational productivity [4]. Bank models and analytical techniques are widely used. Model-driven DSS use algebraic, decision analytic, financial, simulation, and optimization models to provide decision support [5]. The ability to accumulate more and more data and perform various analyzes is mainly related to the increase in capacity and power of information systems. Research shows that the implementation of information systems is able to increase the company’s sales by 10–30%, with an increase rate of return on invested capital by up to 100% [6].

Simulation is an approach that is used most commonly in two situations. The first situation is when uncertainty is high due to sparse data and the second is for experimentation in a low-cost, low-risk environment. Both of these applications of simulation are helpful to scientists and researchers, but they come with a set of advantages and disadvantages. Table 1 gives just a brief summary of the advantages and disadvantages of simulation, within the three broad areas related to technology, process, and socialization.

## 2 Research Problem

The essence of a manufacturing company is the production and subsequent sale of manufactured goods. The main content of the production process are the changes taking place in the form of processed object kind of work, but also in the area of economic, social, biological and ecological issues [7]. According to modern business management theories, a company is looking for a compromise between

**Table 1** Advantages and disadvantages of simulation

	Advantage	Disadvantage
Technology	Forecasting under uncertainty Able to answer many questions	Good theories needed No standardized approach
Process	Low data requirements to model Easy what-if scenario analysis	Challenging to validate Potential scope creep in projects
Socialization	Innovative approach	High skepticism

production in line with current demand reported by the market and production capacity [8]. This is not an easy task, especially when there are factors affecting the impossibility of a steady response to the reported demand. Their source can be seen in the limited capacity of the enterprise, but not only due to production capacity, but often from the improper management of these capabilities.

It was the change of theory and thinking from the turn of the 20th and 21st century that companies were forced to adapt to new conditions and situations, and therefore it was necessary to verify and even change the current methods of operation. The competitive edge of companies, whatever their size or sector of activity, basically lies in their ability to mobilize and combine knowledge and skills in order to come up with integrated solutions that meet increasingly complex and differentiated needs [9].

#### Case study—internal transport and storage

Likewise, the problem of efficient management of the enterprise was noticed by a production company with over 20 years of experience in the Polish market.

The company designs and manufactures innovative solutions for improvements to internal transport and storage. Major customers include companies from the automotive industry, which is characterized by high demands of the customers, who often carry the side of their quality audits of suppliers and their criteria themselves tend to be sky-high. Improving production processes has become one of the factors for building a stable market position. Audits conducted in the company and continuous development of cooperation with the automotive industry revealed imperfections and confirmed the conviction, the need to introduce changes that enable efficient management of production processes and streamlined production simultaneously at several points. Figure 1 presents the organization chart of the analyzed enterprise.

Because the production is carried out exclusively on an individual order, it is therefore dependent on the pace of the incoming orders. The first problem noticed in the company was the prolonged period of order fulfillment, which could consequently lead to the loss of customers who were not willing to wait for orders over “reasonable” time (there are competing companies on the market). The situation of excessive accumulation of orders (as well as—in extreme cases—their lack) may have occurred. The company has several options reaction in such a situation: it can determine the priority of orders and determine delivery of finished products, which can be distant and unsatisfactory for the customer. It can increase its production capacity by various methods: employing additional staff, extending the work time, subcontracting some work. It is also possible to streamline processes by eliminating delays. Never before in the analyzed company has the problem of delays been comprehensively addressed to indicate where they originated, to identify causes, to try to eliminate them, and to observe the impact of changes on the behavior of the entire production system. Only in the course of conducted analyzes in the company delays were diagnosed in several areas and revealed “weak” points in the

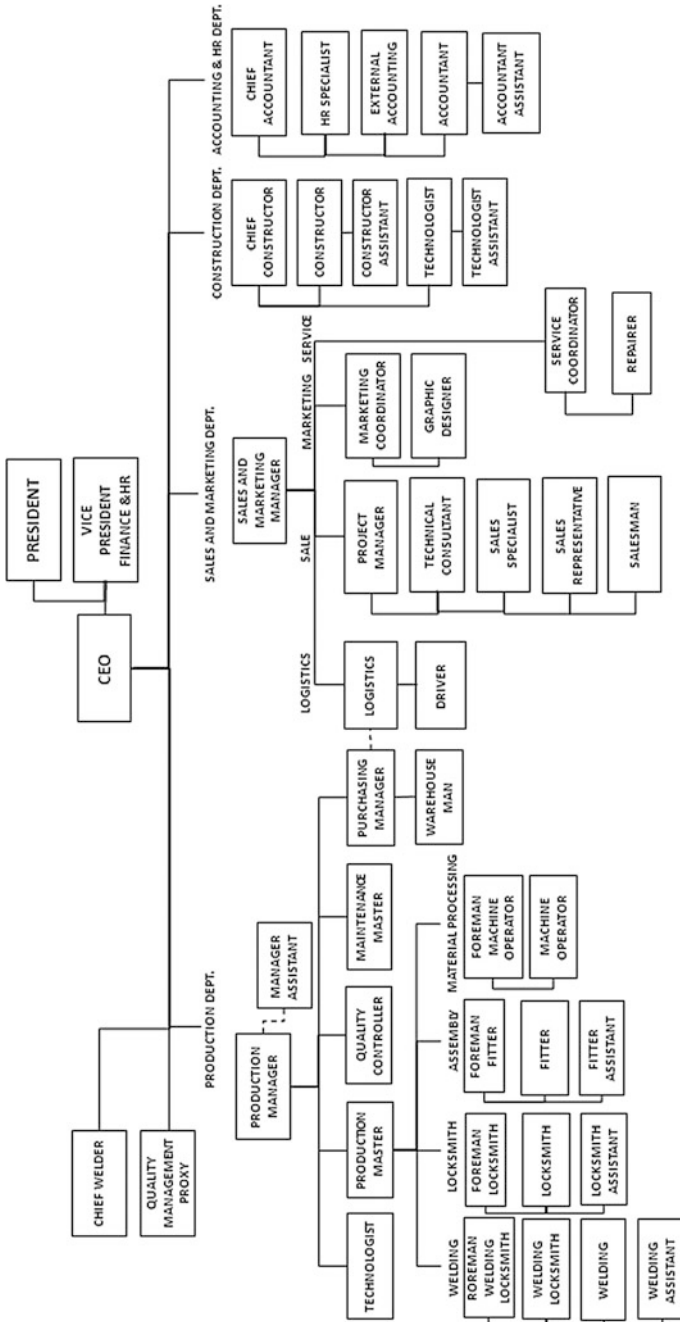


Fig. 1 Organizational chart of analyzed company

company's functioning. Figure 2 shows a model of the main course of production processes in the analyzed production company.

The production system in the company is divided into several successive stages, it is: ironwork, welding, lacquering/galvanizing, assembly. Before there was any awareness of the improvement of the production management process, a lot of information from the manufacturing process was recorded manually (or not recorded at all), and the flow of information was very limited. Unfortunately, these data were processed with a long delay, which most often resulted in an inadequate image and complicate current decision-making. Combined with the need to be cautious in the production planning process, the deadlines for execution of the orders were longer than ever. Difficulties emerged when orders were constantly

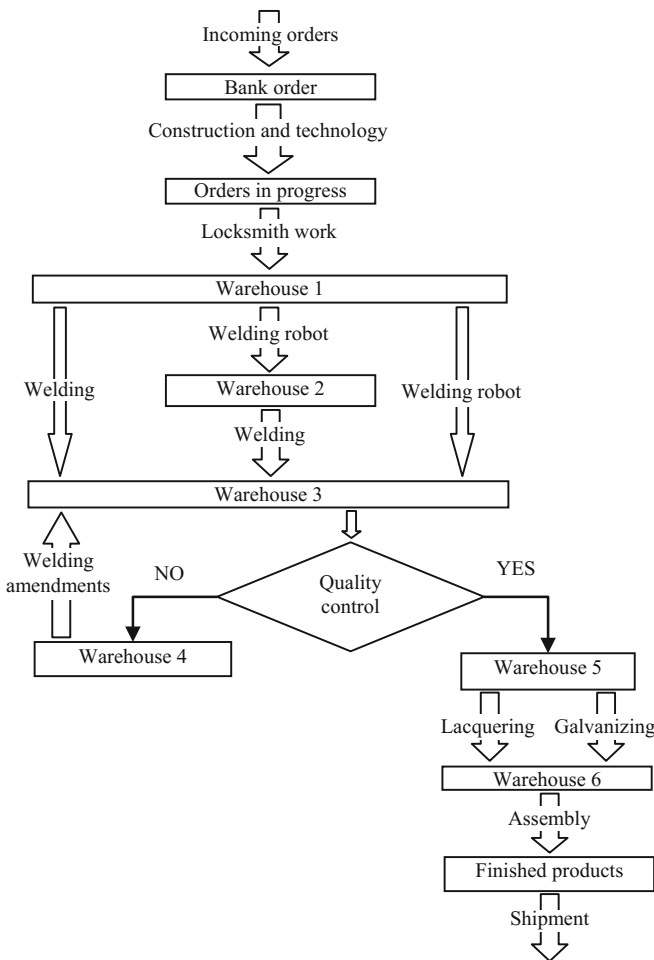


Fig. 2 Model of the main course of production processes in the analyzed production company

coming and the schedule was busy. Customers are not always flexible and are not willing to wait longer for ordered products. In such circumstances, the question of improving the efficiency of production has become the greatest importance and involved a growing number of which directly translate into money.

### 3 Results

In this case, the most important question is how to manage the production process in the context of the pace of orders received? What consequences will decisions arise? Which parameters have the most significant impact on the quality of decisions and the effectiveness of the company? In other words: how will the enterprise respond—the system—on a number of stimuli and what is its sensitivity to particular stimuli?

In order to answer these questions, an attempt was made to build a model of production company. Model of this system relates to the production company, which realizes production functions in a unified manner: acquires means of production such as materials, energy, and human labor, produces certain goods that are then sold. Changes in production levels must take into account changes in the level of demand for manufactured goods. The specificity of “on-demand” production does not allow storage of products. Each batch of products may differ from each other by meeting individual customer requirements. Therefore, it is not possible to use a buffer in the form of a store, which would suppress possible delays in production.

Built model also includes the identification of key sites for delays, one—arising from the realities of the enterprise, due to natural constraints related to the time required for the reaction of the system (e.g., the acquisition and training of new employees), others—resulting from the specificity of the work carried out in the company, company dependent and modelable.

The simulation model was built on the basis of the main processes in the manufacturing company, from the moment the order was received to the dispatch of finished products. Because the described processes are related to temporal changes (dynamic processes), a program for integrating differential equations is needed to describe them in a computer model. The IT tool used in this paper is the dynamic modeling program from Ventana System Inc. called Vensim. Vensim provides a graphical modeling interface with stock and flow and causal loop diagrams, on top of a text-based system of equations in a declarative programming language. It includes a patented method for interactive tracing of behavior through causal links in model structure, as well as a language extension for automating quality control experiments on models called Reality Check. The modeling language supports arrays (subscripts) and permits mapping among dimensions and aggregation. Built-in allocation functions satisfy constraints that are sometimes not met by conventional approaches. It supports discrete delays, queues and a variety of stochastic processes.

There are multiple paths for cross sectional and time series data import and export, including text files, spreadsheets. Models may be calibrated against data using optimization, Kalman Filtering Or Markov chain Monte Carlo methods. Sensitivity analysis options provide a variety of ways to test and sample models, including Monte Carlo simulation with Latin Hypercube sampling.

Vensim model files can be packaged and published in a customizable read-only format that can be executed by a freely available Model Reader. This allows sharing of interactive models with users who do not own the program and/or who the model author does not wish to have access to the model's code base [10].

Vensim is general-purpose software, used in a wide variety of problem domains. Common or high-profile applications include: transportation and energy, business strategy, health, security and terrorism, project management, marketing science in pharmaceuticals and consumer products, logistics, environment.

Vensim has no thematic limitations; used to build and simulate virtually any system whose elements and the relationships between them can be described by mathematical relationships. It provides an easy and smooth way to build system-dynamic models, diagrams cause-and-effect, and structural diagrams, taking into account the feedback [11].

Vensim combines the strengths of automatic data analysis and the simulation results with the visual perception and analysis capabilities of the human user. The use of simulation with an easy-to-use graphical user interface provides the tools and methods that can be used by people with little experience in simulations.

Work on the construction of the model is ongoing. The model has not yet been fully built, inter alia due to the extensive nature of interdependencies in the manufacturing process. Nevertheless, based on the existing part of the model, several areas can be identified, which, by appropriate influence, have an impact on improving the efficiency of the company's functioning. Figure 3 presents a visualization of the hitherto made part of the model.

## 4 Discussion

Works related to the construction of a simulation model required the involvement of employees from different areas of the company. Already during the first meeting, in the course of determining the production process, interdependence, the specifics of individual actions noted the lack of communication within the company. This work highlighted existing gaps in the company in terms of mutual cooperation and understanding of the problems of individual production stages.

Defined many places for delays: the time to prepare construction and technology, the time required to complete the materials, the coordination of the outsourced locksmith work, coordination of welding work, coordination of external work related to galvanizing and lacquering of components, expectation of components and materials for assembly, logistics and different delays associated with human labor.



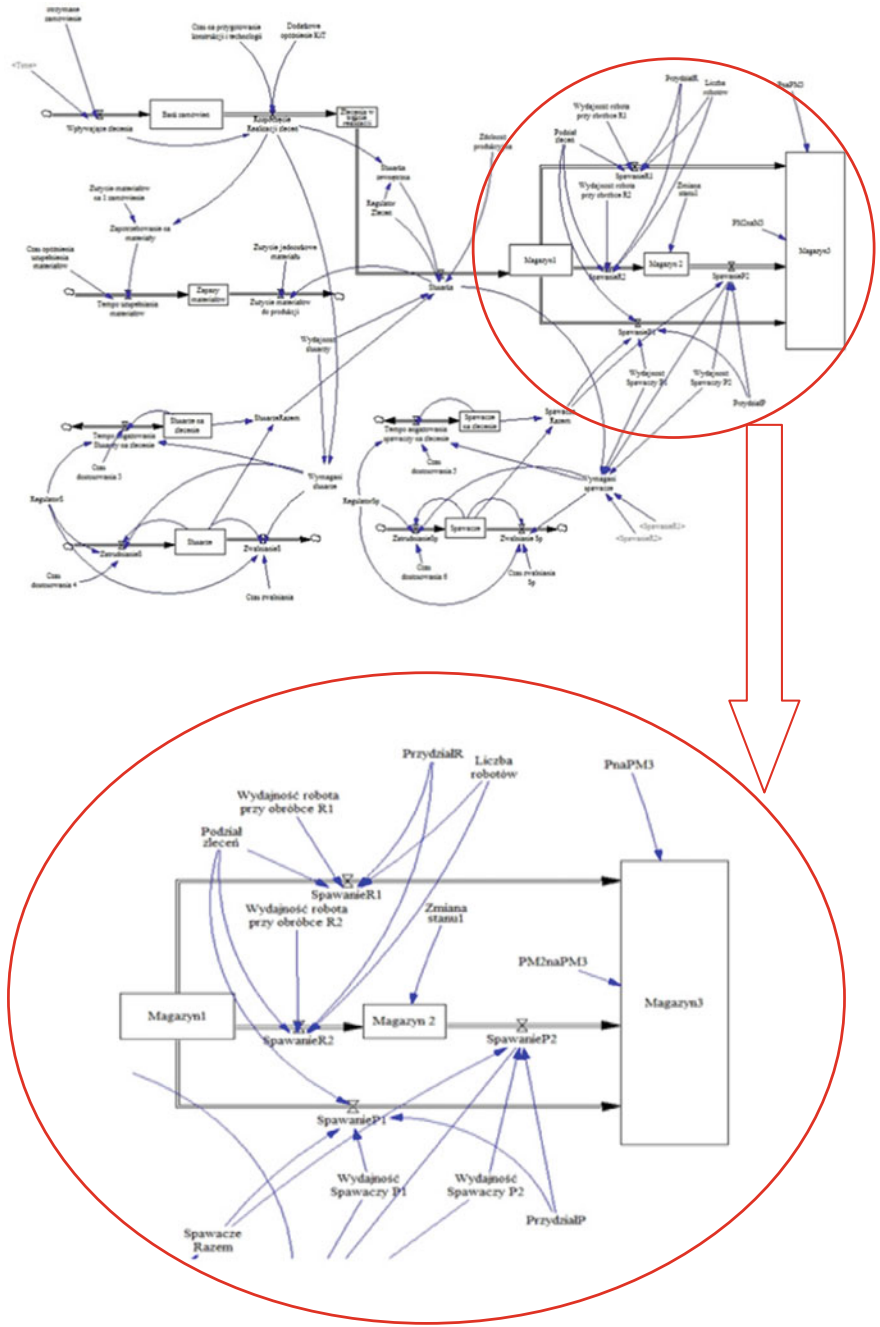


Fig. 3 Visualization of the hitherto made part of the model using Vensim software

The process of preparation for the construction of the model revealed and brought home many other key issues for the efficient production management. There was no current access to information from production processes.

The data were analyzed with the delays and often subject to large errors. They concerned, among others, information about downtime, breakdowns, production fluidity, waste quantities, coordination. In the production there were too often too long downtime. In this situation it was not possible to increase the efficiency and performance of both the machinery and the crew. A large part of the work of people coordinating the company's activities was devoted to monitoring the correctness of the processes, responding to the emerging negative exceptions, which might not have taken place due to better understanding of processes and better planning. In addition, the company was faced with the risk of negative verification in the case of demanding audits conducted by automotive customers. The key problem was excessively lengthening the waiting time for the finished products. It was feared that, in the case of failure to make the necessary changes to the recipient, having noticed problems, they would change the supplier.

As already mentioned, work on defining process flows in an enterprise has helped to understand the need to improve the flow of information within a company. Built simulation model also includes the aspect of human resources management in the enterprise in the context of the efficiency of employees directly related to the production (locksmiths, welders, assemblers).

Detailed simulation-based planning allows for more precise timing of production and delivery in dynamically changing production environments. This is because, in the simulation model, it is possible to accurately reproduce all real random processes that affect production later on. During such planning, possible changes in production conditions are already taken into account. Production jobs are entered into the simulation according to a specific startup list and executed sequentially on the basis of defined rules.

## 5 Conclusion

This article is the first in a planned series of articles on the use of computer simulation models to improve the efficiency of the enterprise. It aims to signal the possibility of achieving the various benefits of implementing a simulation-based model, not only for forecasting future results, but also improving information flow, integrating actions and people, and a comprehensive look at the problems that arise in a company. The built-in model will support the decision-making process and improve the efficiency of the operation, allowing you to define areas where measurable benefits can be derived. In subsequent articles, the discussed issues will be continued and the simulation capabilities of the Vensim model will be presented.

It was noted during the course of the work that often the solution to a single issue is beneficial in several spheres, if several problems are solved immediately, the benefits can be very large. Manufacturers often are trapped in thinking that they

have a well-functioning production, while there is room for significant improvement. Simultaneously, you can save time, improve productivity and streamline scheduling while simulating production. The implementation of simulation methods in the company is an interesting example of the improvement of production at several points at a time. Better planning, greater efficiency and performance, and tighter control of manufacturing processes give the company a specific competitive advantage. In addition, they give the company support during audits, which will help meet the new demands of today's automotive market. This is a very concrete example of strengthening market position by using this type of decision support.

## References

1. Heilala, J., Maantila, M., Montonen, J., Sillanpää, J., Järvinen, P., Jokinen, T., Kivikunnas, S.: Developing simulation-based decision support systems for customerdriven manufacturing operation planning. In: Johansson, B., Jain, S., Montoya-Torres, J., Hukan, J., Yücesan, E. (eds.) *Proceedings of the 2010 Winter Simulation Conference* (2010)
2. Kwiatkowska, A.M.: *Decision support systems. How to use knowledge and information* (2007)
3. Liu, S., Duffy, A.H.B., Whitfield, R.I., Boyle, I.M.: *Integration of decision support systems to improve decision support performance*. Springer-Verlag, London Limited, Knowl Inf Syst (2009)
4. Krupa, K., Wójcik, A., Francik, S.: *Decision support for selected processes in agriculture, based on computer simulation models*, *Logistics-science*, vol. 4 (2014)
5. Power, D.J., Shardab, R.: *Model-driven decision support systems: concepts and research directions*, *Decision Support Systems*, vol. 43 (2007)
6. Unold, J.: *Information Systems for Marketing*. Wroclaw University of Economics, Wroclaw (2001)
7. Liwowski, B., Kozłowski, R.: *Basic issues of production management* (2006)
8. Korotayev, A.V., Tsirel, S.V.: *A spectral analysis of world GDP dynamics: Kondratieff waves, Kuznets swings, Juglar and Kitchin cycles in global economic development, and the 2008–2009 Econ. Crisis* *Struct. Dyn.* **4**(1) (2010)
9. Kefela, G.T.: *Knowledge-based economy and society has become a vital commodity to countries*. *Int. J. Educ. Res. Technol.* **1**(2), (2010)
10. [www.vensim.com](http://www.vensim.com)
11. Krupa, K.: *Modeling, simulation and forecasting*. *Continuous systems* (2008)

# Cyclic Steady-State Approach to Modelling of Multimodal Processes Flow Levelling

Grzegorz Bocewicz, Pawel Pawlewski and Zbigniew Banaszak

**Abstract** The principle of production levelling can be implemented to other areas, such as determining cyclic schedules in: public transport, courier delivery, transport of goods, data transmission, energy transmission, etc. It means that various processes, production tasks, passengers' routes, etc., can be modelled in terms of multimodal processes, i.e. processes composed of segments of local processes implemented by material handling/storing devices, transportation modes, transmission modes and so on. Consequently, it is possible to provide numerous variants of multimodal processes cyclic steady states, which are attainable in the structures of systems of concurrently flowing cyclic processes often occurring in practice. In that context, multiple examples, restricted to production processes that illustrate cyclic steady states flow levelling prototyping, while taking into account the requirements imposed by demand smoothing, load levelling and line balancing are discussed.

**Keywords** Multimodal process · Production levelling · Tact time · Production flow

## 1 Introduction

Cyclic scheduling is one the most effective planning methods in transport systems and an efficient way of operational planning in production systems. The occurrence of cyclic processes is also related with the concept of multimodal processes [1–4],

---

G. Bocewicz

Faculty of Electronics and Computer Science, Koszalin University  
of Technology, Koszalin, Poland

P. Pawlewski (✉)

Faculty of Engineering Management, Poznań University of Technology,  
Poznań, Poland

e-mail: pawel.pawlewski@put.poznan.pl

Z. Banaszak

Department of Mechanical and Manufacturing Engineering,  
Aalborg University, Aalborg East, Denmark

© Springer International Publishing AG 2018

A. Hamrol et al. (eds.), *Advances in Manufacturing*, Lecture Notes in Mechanical  
Engineering, [https://doi.org/10.1007/978-3-319-68619-6\\_21](https://doi.org/10.1007/978-3-319-68619-6_21)

215

which is defined with their help. Multimodal processes, i.e. processes implemented with use of other processes, are observed in everyday practice, e.g. in inter-operational transport subsystems of discrete manufacturing systems, data transmission in computer systems, electrical grids but also in public transport systems, digital communication, etc. It means that the cyclic behaviour of multimodal processes is dependent on the cyclic behaviour of Concurrently Flowing Cyclic Processes (CFCP), which form the platform of local processes. The problems of attainability of cyclic steady states, considered in CFCP environment, squarely correspond with the problems of cyclic scheduling, especially those related with planning the concurrently flowing multimodal processes of various nature. Therefore, they are critical for the quality of production processes, public transport, digital communication, etc. The literature on the subject provides a number of algorithms for determining the optimum schedules of executing operations dedicated to various assumptions and work environments (e.g. in the tasks of setting timetables [1], telecommunication transmissions [5], production planning [2, 6, 7]). Among the problems of cyclic scheduling, the optimisation problems are the primary ones [8]. They include the Basic Cyclic Scheduling Problem (BCSP) [9, 10] and its expansions related with scheduling in manufacturing cells (the so-called manufacturing cell problems), the general Cyclic Jobshop Problem (CJP) [11], Cyclic Flowshop Problem (CFP) [10, 12], Cyclic Open Shop (COP) as well as the problem of enterprise planning CPSP (Cyclic PERT-Shop Problem) [13]. Apart from BCSP, all the problems can be classified as NP-hardness problems, which implies that it is necessary to apply Artificial Intelligence methods to solve them [10, 14]. The market's growing demand for a variety of production generates interest in the models of multi-machine systems of cyclic production. The process optimisation usually means minimising the tact time, yet a certain assortment of products, the so-called Minimum Part Set (MPS) must be guaranteed. Manufacturing products within another MPS begins after all the products from the previous cycle MPS have been manufactured. The concept of production levelling is based on the so-called heijunka box, which generates the schedule of the cyclic production flow. It is a cyclical schedule which is divided into a grid of boxes. The columns represent a specific period of time. Rows represent the product types produced by the subsequent production [15]. In the context of previously presented concepts of cyclic manufacturing and production levelling, the problem of multimodal process flow levelling can be considered by means of determining the acceptable cyclic schedules related with them. The period of each schedule is a multiple of the tact time. From the set of acceptable schedules it is also possible to determine schedules minimising the quantity of production in progress or the size of warehouses of inter-operational storage.

The next chapter presents selected models of multimodal processes, which illustrate exemplary solutions for cyclic manufacturing. In Sect. 3 the problem of prototyping alternative variants of multimodal process flow levelling is formulated. Section 4 provides illustrations of exemplary variants of production levelling. Section 5 includes conclusions prospects for further investigations.

## 2 Cyclic Steady Flows Modelling

Let us consider a production system consisting of five workstations equipped with buffers with capacity of 1. In the system, in the flow mode, there is one order being executed in the workstations  $R_1, R_2, R_3, R_4$ . The times of technological operations executed in the workstations are known, see Fig. 1. It is assumed that the loading and unloading times are included in the times of operations executed in particular workstations. Moreover, processing times = 1 u.t. (unit of time) of inter-operational transport operations (implemented on transport supplies) have been assumed. According to Gantt’s diagram (Fig. 2) illustrating the flow of assigned above production, it is clear that it is executed according to tact time  $TP_1 = 7$  u.t., which equals the period of cyclic schedule ( $T = 7$  u.t.).

As the tact time  $TP_i$  we understand the time between manufacturing two subsequent items of product  $W_i$ . The value of tact time is determined by the workstation  $R_3$ , which is a bottleneck of the production flow and it is determined as the sum of the time of technological operation of this resource (6 u.t.) and the time of transport of the product between workstations (1 u.t. required to release/occupy the resource  $R_3$ ). The other case, which is being considered, refers to the situation when there are two multimodal processes to be executed in the system from Fig. 1. The first one is relevant to the one described above (manufacturing product  $W_2$ ) and the other is related with production of product  $W_2$  implemented in a flowing mode and executed in workstations  $R_5, R_2, R_6, R_7$ . The times of operations executed in these workstations are shown in Fig. 3. According to Gantt’s diagram (Fig. 4) illustrating the production flow of two products, it can be easily seen that it proceeds with tact time  $TP_1 = TP_2 = 9$  u.t. It seems clear that the value of tact time (and thus the period  $T$ ) is determined by the workstation  $R_2$ , which is a bottleneck of the production flow. As in the previous case, the value of tact time is determined by the bottleneck deduced from the sum of times of technological operations  $W_1$  and  $W_2$  from the

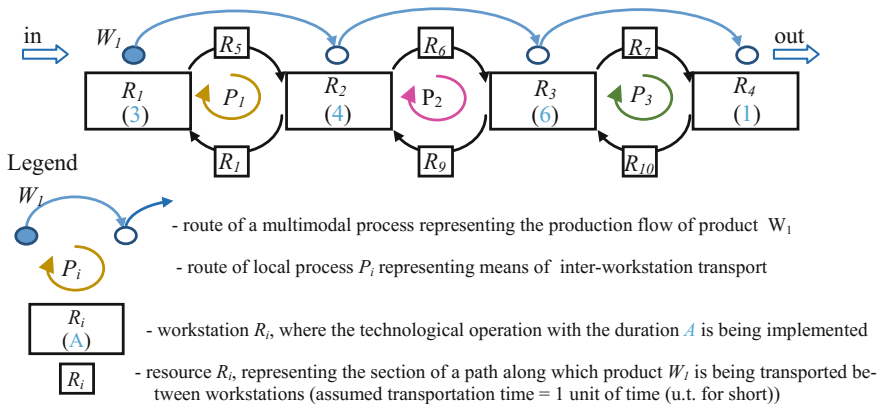
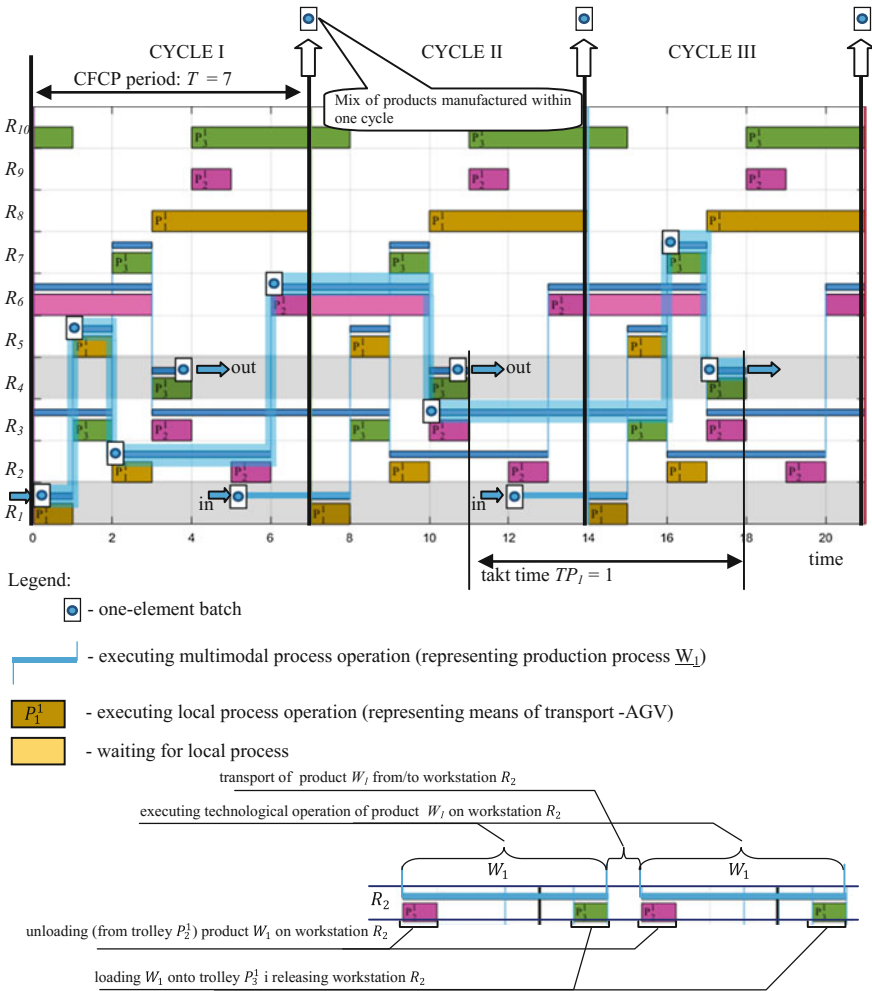


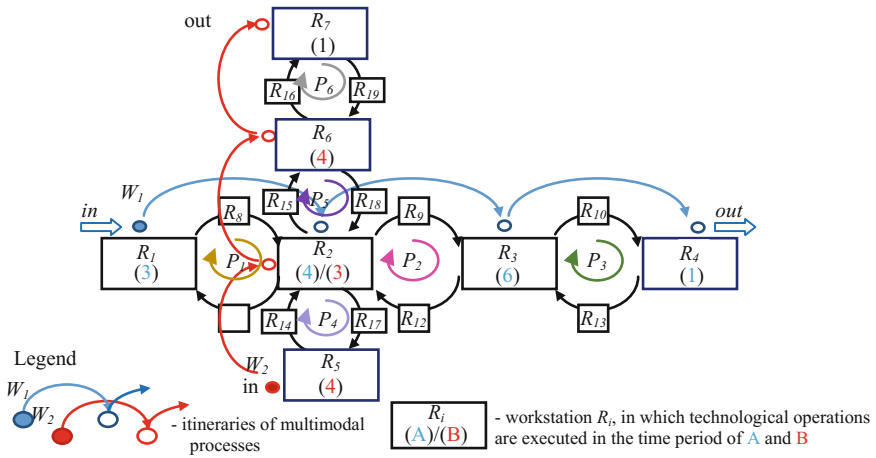
Fig. 1 The diagram of production flow implemented along technological route  $R_1-R_2-R_3-R_4$



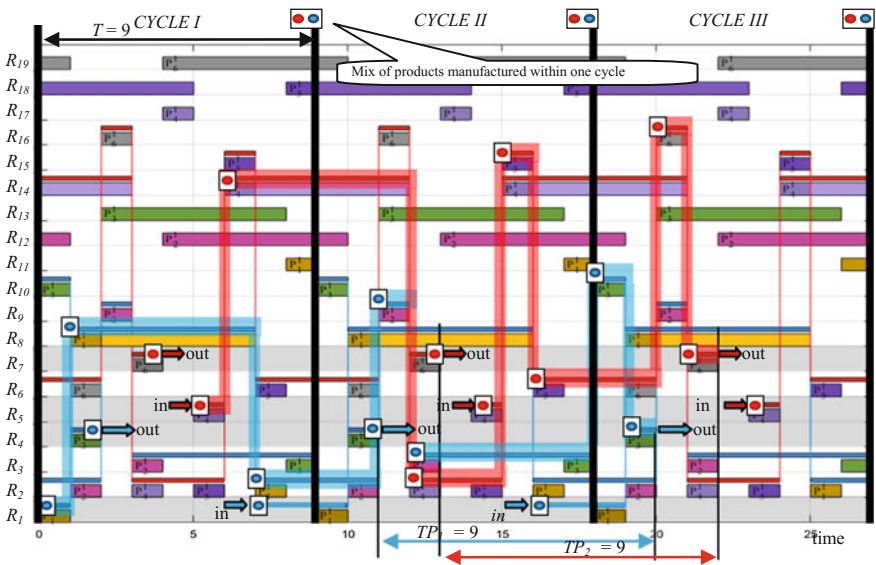
**Fig. 2** Gantt's diagram of production flow in system from Fig. 1

resource (3 + 4 u.t.) and the times of transporting the products between workstations (2 u.t. required to release/occupy resource  $R_2$ ). Moreover, unit capacity of buffers guarantees that it is impossible to introduce more production orders into the system than what the system can handle. The system produces the same total quantity every period equal to the schedule cycle.

It can be easily noticed that the change in tact time results in a delay in completion of the first order. Such a change is caused by the fact that the same workstation is alternately used by the processing of product  $W_1$  and then by the processing of product  $W_2$ . Therefore, the question arises whether it is possible to



**Fig. 3** Schedule of production flow implemented along technological itineraries:  $R_1-R_2-R_3-R_4$  and  $R_5-R_2-R_6-R_7$



**Fig. 4** Gantt's diagram of production flow in the system from Fig. 3



organise simultaneous production of two products, which will not result in a delay in completion of the order related with product  $W_1$ .

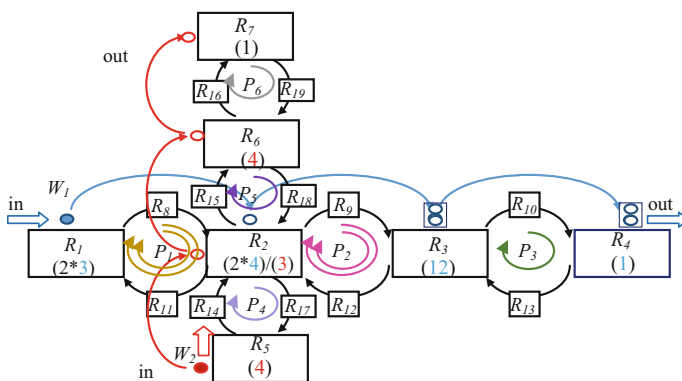
### 3 Problem Statement

In order to answer the question posed above let us consider a reference model of a production system with the mesh structure. In this kind of structure of the production system, it is possible to launch simultaneous production of various products which meets the constraints of arbitrarily made demands. It is assumed that the times of technological operations executed in particular orders are known. The capacity of workstation buffers may change. We seek such solutions for organising the production flow which result in a set course responding to cyclic scheduling that meets customer's requirements in a period coherent with the cycle schedule.

The sought solutions are meant to provide answers to questions concerning two groups of problems corresponding to 'forward' and 'inverse' types of problems, known from the literature on the subject. These types in a natural way correspond with analysis and synthesis tasks [2, 3] known from practical applications.

Below, there is an exemplary question connected with the first group of problem: Are cyclic steady states, which meet customers' demands concerning prompt completion of the ordered batch of products, attainable in the given structure of a production system which executes the multi-assortment flow production?

The other group of problems, the 'inverse' ones, includes the following example: Is there such a structure of a production system that makes it possible to promptly complete a batch of ordered assortment of products, which meets the constraints imposed by the technology?



**Fig. 5** Diagram of the flow of production executed along technological itineraries  $R_1-R_2-R_3-R_4$  and  $R_5-R_2-R_6-R_7$  corresponding to the demand in the form of  $PS = (2, 1)$

The examples illustrating the possibilities of prototyping appropriate cyclic steady states and opportunities for multimodal processes flow levelling resulting from them are discussed in the next chapter.

### 4 Multimodal Processes Flow Levelling

Going back to the previously posed question let us consider the production system shown in Fig. 5. In this system, we seek such organisation of production flow (cyclic schedule) which meets requirements of customers. According to these requirements, two items of product  $W_1$  and one item of product  $W_2$  are to be produced in a time period corresponding to one cycle of the schedule. For the sake of further investigations, an assumption is made that demand is determined by a mix of products (Part Set) defined as a sequence  $PS = (a_1, \dots, a_i, \dots, a_n)$ , in which subsequently occurring elements determine the number of items of products  $W_1, W_2, \dots, W_n$ , delivered in one production cycle. In the considered case demand has the form of  $PS = (2, 1)$ . The diagram of the flow of production executed along technological itineraries  $R_1-R_2-R_3-R_4$  and  $R_5-R_2-R_6-R_7$  is shown in Fig. 6. The assumed capacities of workstation buffers amount to 1, 1, 2 and 2 respectively for workstations  $R_1, R_2, R_3$  and  $R_4$ . The assigned capacity of buffers impose the

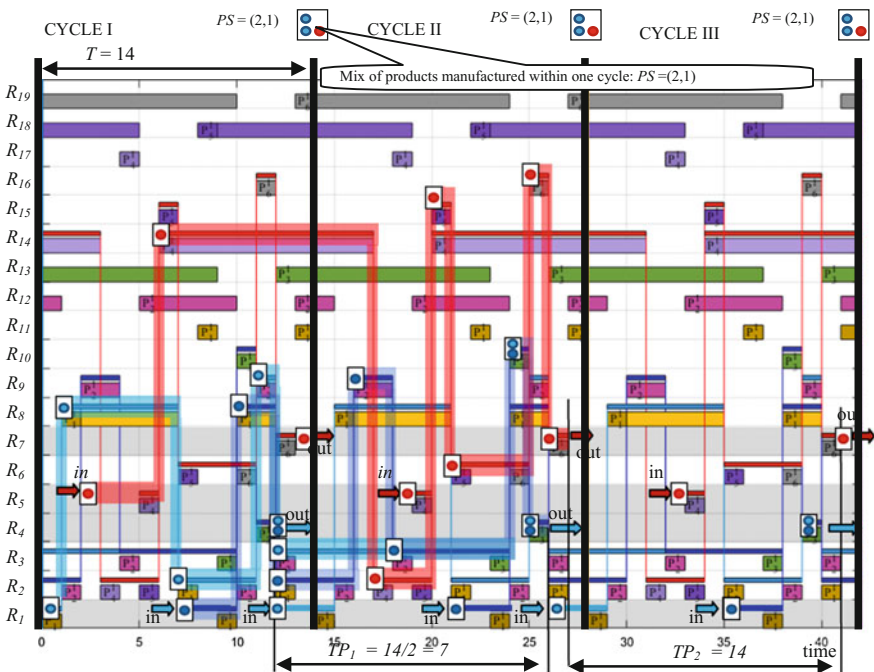
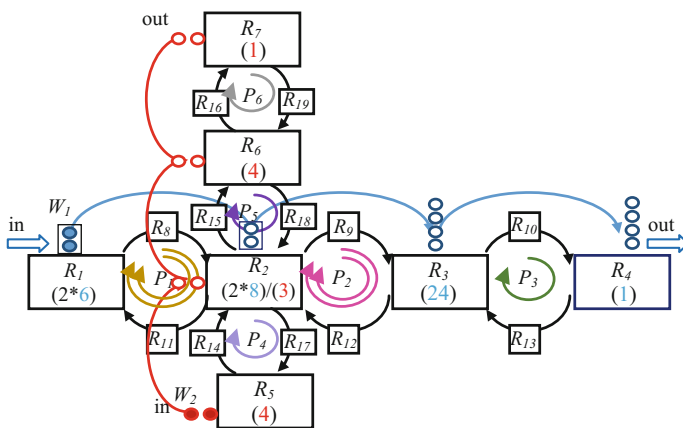


Fig. 6 Gantt's diagram of production flow in the system from Fig. 5

quantity of batches. It is mainly manifested by various quantities of batches that constitute the production flow of product  $W_1$  which corresponds with the demand in the form of  $PS = (2, 1)$ . It can be easily noticed that between workstations  $R_1$  and  $R_2$  and between  $R_2$  and  $R_3$ , the production is executed through batches containing one item of  $W_1$ , and between  $R_2$  and  $R_3$  batches contain two items of  $W_2$ .

According to Gantt's diagram (Fig. 6) illustrating the production flow of two products in the mix in the form of  $PS = (2, 1)$  it is clear that it proceeds cyclically, where the tact time amounts to 14 u.t. In one cycle there two items of product  $W_1$  and one item of product  $W_2$ . It can be easily noticed that tact time is determined by workstation  $R_3$  as it is a bottleneck of the production flow. As in the previous examples, this workstation determines also tact time which, for the products  $W_1$  and  $W_2$  amounts to, respectively,  $TP_1 = 7$  (two items of product per one period)  $TP_2 = 14$  (one item of product per one period). Assuming the capacities of workstation buffers amount to 2, 2, 4 and 4 respectively for workstations  $R_1, R_2, R_3$  and  $R_4$ , let us consider the organisation of production of the mix in the form of  $PS = (4, 2)$ —see Fig. 7. Also in this case, the available capacities of buffers impose the quantity of batches of particular products. It is especially expressed by the varied quantities of batches constituting the production flow of product  $W_1$ . It can be easily noticed that between workstations  $R_1$  and  $R_2$  and between  $R_2$  and  $R_3$  the production is executed through batches containing two items of product  $W_1$ , and between workstations  $R_3$  and  $R_4$  batches include four items of  $W_1$ .

According to Gantt's diagram (Fig. 8) which illustrates the production flow of two products corresponding with the mix  $PS = (4, 2)$ , it can be easily observed that it is of cyclical character, where the period  $T = 25$  u.t. It is clear that the quantity of a cycle is determined by workstation  $R_3$ , which is the bottleneck of the production flow. As in the previous examples, the workstation determines also tact time, which for products  $W_1$  and  $W_2$  amounts to, respectively,  $TP_1 = 6.25$  (four items per one period) and  $TP_2 = 12.5$  (one item per one period).



**Fig. 7** Diagram of the flow of production executed along technological itineraries  $R_1$ – $R_2$ – $R_3$ – $R_4$  and  $R_5$ – $R_2$ – $R_6$ – $R_7$

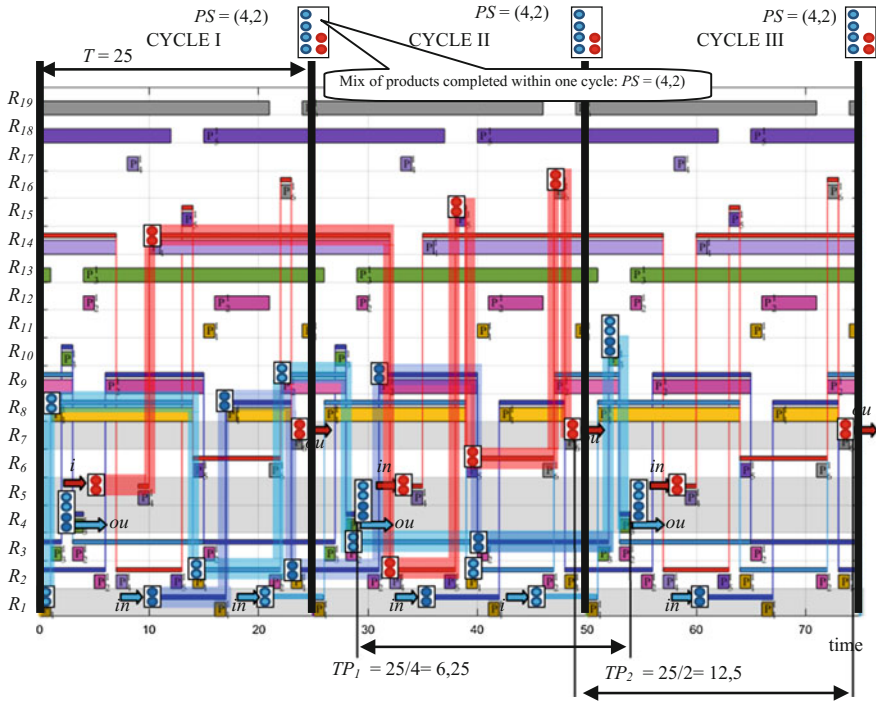


Fig. 8 Gantt's diagram of production flow in the system from Fig. 7

Table 1 Exemplary variants of executing the mix  $PS = (2.1)$  and  $PS = (4.2)$

Mix	$PS = (2.1)$	$PS = (4.2)$	Tact time of $W_1$	$TP_1 = 7$ [u.t.]	$TP_1 = 6.25$ [u.t.]
Period of CFPC	$T = 14$ [u.t.]	$T = 25$ [u.t.]	Tact time of $W_2$	$TP_2 = 14$ [u.t.]	$TP_2 = 12.5$ [u.t.]

Taking into account the notation in which  $T$  means the period of cyclic steady-state flow of multimodal processes and  $TP_i$  means the tact time of the  $i$ -th product the summary of the results of final two examples is presented in Table 1. By analogy with heijunka box, it is easy to see the schedules meeting demand in the form of  $PS = (2.1)$  and  $PS = (4.2)$ . Both customers' demands can be satisfied with the tact time, respectively, 14 and 25 u.t. or with the tact time 7 and 6.25 u.t. for  $W_1$  and 14 and 12.5 u.t. (assuming the ordered products are collected as single items). Obviously, the organisation of the production flow corresponding to the latter case requires changes in both the amount and quantity of batches taking part in the production flow.

## 5 Concluding Remarks

The presented examples illustrate the opportunities of applying CFCP models to modelling and providing variant solutions for cyclic steady states of multimodal processes flow levelling. The presented model assumes implicitly that batches of products manufactured at one workstation should have equal repeatability periods, or the periods should multiply. This restriction can be compensated for by means of combining the demands (a customer's needs) with the capacity of the available production system. In particular, it allows to estimate the possibility of selecting alternatively the amount or quantity of a batch (with the assumed capacity of inter-operational storage buffers) or to select the capacity of buffers (with the assumed amount and quantity of batches). A different research direction is connected with investigating conditions which will allow to reschedule cyclic production according to changeable customers' demands. These changes may comprise both delivery dates and quantities of batches ordered by customers. Except for the mentioned research directions, there are also areas of investigations related with uncertainty of data describing a process itself as well as production tasks executed within it. There also issues connected with determining interference resistant cyclic schedules, which are worth investigating.

**Acknowledgements** This work has been supported by the Logzact S.A. and Faculty of Engineering Management Poznan University of Technology within the project RPWP.01.02.03.00-0064/16-00.

## References

1. Bocewicz, G., Banaszak, Z.: Scheduling for multimodal cyclic transport systems. In: International Conference on Automation, vol. 2, pp. 106–113 (2013)
2. Bocewicz, G., Muszyński, W., Banaszak, Z.: Models of multimodal networks and transport processes. *Bull. PAN Tech. Sci.* **63**(3), 635–650 (2015)
3. Bocewicz, G., Nielsen, I.E., Banaszak, Z.A.: Production flows scheduling subject to fuzzy processing time constraints. *Int. J. Comput. Integr. Manuf.* **29**(10), 1105–1127 (2016)
4. Bocewicz, G., Wójcik, R., Banaszak, Z.A., Pawlewski, P.: Multimodal processes rescheduling: cyclic steady states space approach. *Math. Probl. Eng.* **2013**(407096), 1–24 (2013). doi:[10.1155/2013/407096](https://doi.org/10.1155/2013/407096), see: <https://www.hindawi.com/journals/mpe/2013/407096/cta/>
5. Polak, M., Majdzik, P., Banaszak, Z., et al.: The performance evaluation tool for automated prototyping of concurrent cyclic processes. *Fundam. Inf.* **60**(1–4), 269–289 (2004)
6. Banaszak, Z. (Ed.): *Modelling and Control of FMS: Petri Net Approach*. Wrocław Technical University, Wrocław (1991)
7. Fanti, M.P., Maione, B., Mascolo, S., Turchiano, B.: Low-cost deadlock avoidance policies for flexible production systems. *Int. J. Model. Simul.* **17**(4), 310–316 (1997)
8. Li, J., Meerkov, S.M.: *Production Systems Engineering*, Springer, Berlin (2009)
9. Kampmeyer, T.: *Cyclic Scheduling Problems*. University of Osnabrück, Osnabrück (2006)
10. Levner, E. et al.: Cyclic scheduling in robotic cells: an extension of basic models in machine scheduling theory. In: Levner, E. (ed.) *Multiprocessor Scheduling: Theory and Application*, pp. 1–20 (2007)

11. Błażewicz, J., Ecker, K., Pesch, E., Schmidt, G., Węglarz, J.: Handbook on Scheduling: From Theory to Applications, p. 647. Springer, Berlin (2007)
12. Bożejko, W., Uchroński, M., Wodecki, M.: Block approach to the cyclic flow shop scheduling. *Comput. Ind. Eng.* **81**, 158–166 (2015)
13. Kubale, M., Nadolski, A.: Chromatic scheduling in a cyclic open shop. *Eur. J. Oper. Res.* **164**(3), 585–591 (2005)
14. Munier, A.: The basic cyclic scheduling problem with linear precedence constraints. *Discrete Appl. Math.* **64**(3), 219–238 (1996)
15. Korytkowski, P., Grimaud, F., Dolgui, A.: Exponential smoothing for multi-product lot-sizing with heijunka and varying demand. *MPER* **5**(2), 20–26 (2014)

# Symbolic Representation of Production Knowledge in the Development of Knowledge Management Systems

Alfred Paszek

**Abstract** This paper presents the method of symbolic knowledge representation used for building of knowledge management system in technological production preparation of machine elements. The method is based on symbolic processing of information in the system, and the resources of knowledge were expressed through symbols. Symbolic representation of constructional forms of machine elements to load input data for designing has been elaborated. The designed structure of a technological process has been written in a symbolic way. The description of a technological operation is made according to the method of building of the symbol of an operation that allows to generate the technological process of machine element. Relations between obtained representations are described using decision rules. These rules are stored in the frame structure. With this knowledge, representation is a possible division of the decision problem for partial tasks.

**Keywords** Production · Knowledge · Knowledge representation · Knowledge management system (KMS) · Decision rules

## 1 Introduction

Knowledge is an important resource in the development of manufacturing enterprises. Modern economy should be based on knowledge, which resources and proper management of these resources are seen as the most important source of enterprise's competitive advantage. This applies not only to organizations where employee's intellectual capital is a key resource to be transformed into products such as: expertise's, designs, software. Knowledge management is understood as a set of actions fitting a proper form and the processes direction taking place in the company's knowledge resources. The strategic goal of knowledge management is

---

A. Paszek (✉)  
Department of Knowledge Engineering,  
Opole University of Technology, Opole, Poland  
e-mail: a.paszek@po.opole.pl

the multiplication of intellectual capital and the enlargement of the organization's efficiency. In the case of the knowledge management, key processes are discerned, such as: locating, acquiring, development, distribution, use, and preservation of knowledge [1–4].

A knowledge management system (KMS) is a system for applying and using knowledge management principles. These include data-driven objectives around business productivity, a competitive business model, business intelligence analysis, etc. KMS can help to make critical decisions [5].

Research carried out on artificial intelligence in the range of processing tools of the knowledge determined the emergence of new opportunities [6–8]. Attempts are being made to implement the elements of artificial intelligence in KMS. The research is focused primarily knowledge codification strategy and are based on methods of the expert systems elaboration [9, 10].

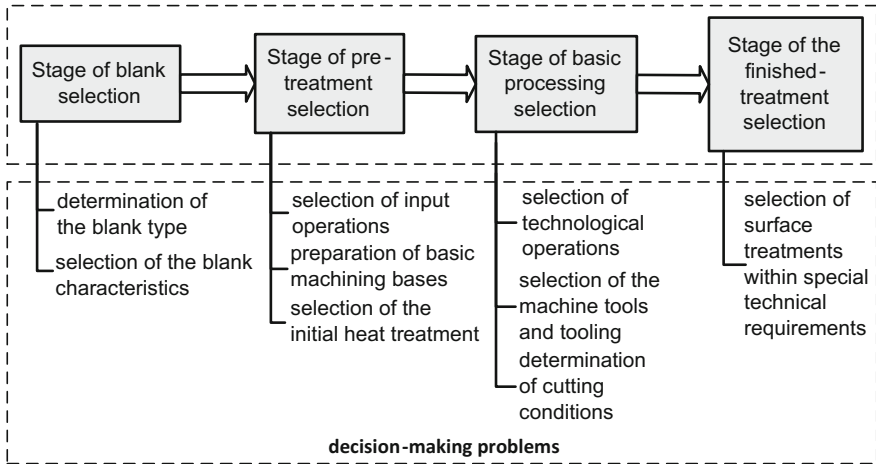
There is a term existing in the manufacturing companies which is called the production knowledge. It contains such sets of information thanks to which the basic objectives of production preparation may be implemented. Production knowledge resources contribute to the improvement of production processes and make the product meet the market requirements. Depending on the sources, the knowledge resources may be divided into basic groups of knowledge about the processes, systems, and products [11, 12]. Knowledge representation means a general formalism of transmission, storage, and collection of any knowledge supplies. It is a combination of data structures and interpretation procedures assigned such that providing that properly used may lead to intelligent behavior and the usage of the computer system [13, 14].

## **2 Analysis of Decision Problems in the Technological Preparation of Production**

The elaboration of a KMS in the enterprise starts with an analysis of the production preparation processes of selected machine elements. This analysis results in the determination of decision-making problems, the solution of which requires specific sets of technological knowledge accumulated in the system. Regarding the elaboration of the knowledge analysis involves [15]:

- construction of machine elements, e.g., the type of material, geometric dimensions, surface net-shape precision, surface roughness, heat treatment, surface hardness, kind of electroplating, etc.,
- technological characteristics of the production system, it means the analysis of the production capacity of the considered company, technical tools, tasks to be performed at a given technological position, the cutting tools base, and technological hardware, etc.
- relationships between the element construction and the process structure, it means determination of technological and technical resources that need to be applied to obtain the required characteristics of the element.





**Fig. 1** Decision-making problems in technological production preparation of machine elements

Preparing of the knowledge sets is based on a multi-stage structure of the technological process of machine parts. The sequence of distinguished decision steps results from the choice of manufacturing operations, in order to increase the net-shape precision and fit desired properties to the treated objects, until the finished product is achieved. In various stages of the design, partial decision problems were picked out, what allowed to organize them according to assumed knowledge sets. Distinguished stages and decision-making problems are highlighted in Fig. 1.

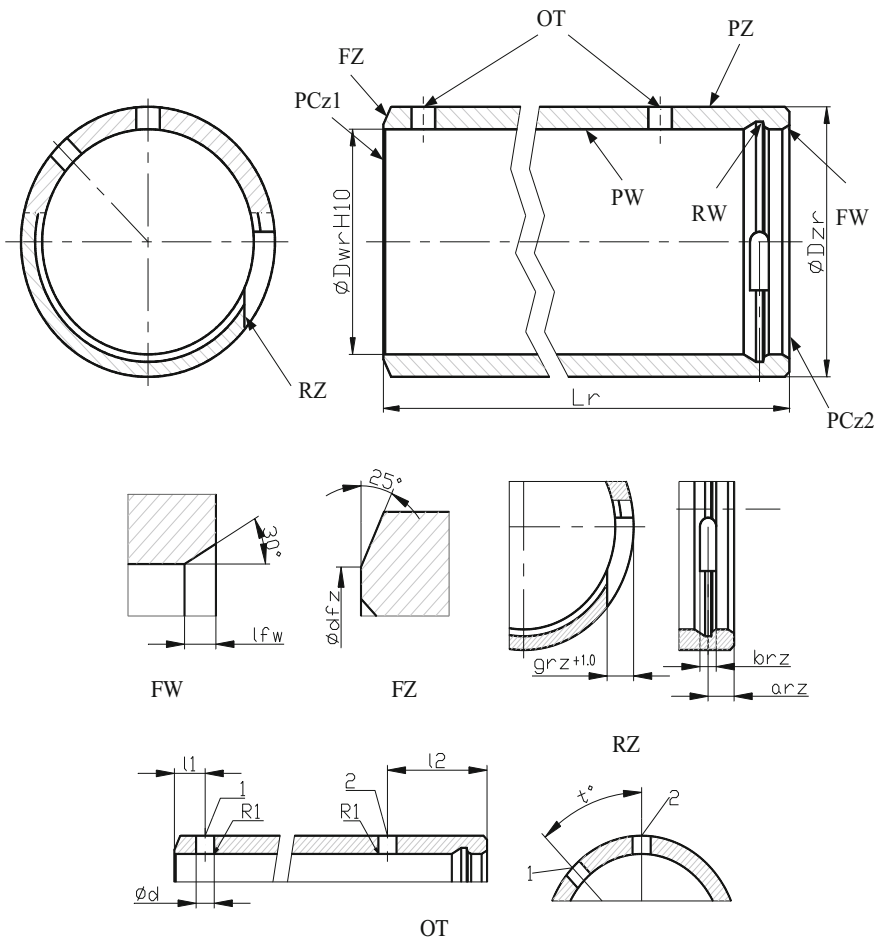
Troubleshooting process of decision-making requires the creation of acceptable alternative solutions from the point of view of the technological capacity of the production system and production profitability in terms of the production costs minimization. A more detailed analysis of decision problems in the technological preparation of production can be found in the papers [15, 16].

### 3 Elaboration of the Method of Knowledge Representation About Structure of Machine Parts

The method of the symbolic knowledge representation is based on the identification of geometric construction features of the machine parts and runs in stages. At the first stage, characteristic dimensions are determined assigning appropriate symbols to them. Characteristic dimensions are the element’s overall dimensions as well as the dimensions of the element’s relevant functional surface, interacting with the other elements surfaces. At the next stage of the construction, a construction division into elementary objects takes place, recording them using symbols.

Elementary objects describe surface groups or an element's individual surfaces. They have been characterized by construction geometrical features. It was assumed that these traits can be permanent and variable. Permanent characteristics are closely associated with the elementary object, and their value is determined in advance and is not changed during the production preparation. While the variable features are determined during consultations with the KMS [15].

The application of the symbolic method for the machine construction representation is shown on the example of the pipes of hydraulic cylinders. Figure 2 shows an exemplary embodiment of a construction component with the selected elementary objects and Table 1 describes their permanent and variable characteristics.



**Fig. 2** Geometric design features of selected pipes elementary objects

**Table 1** Description of the construction features of selected pipes elementary objects

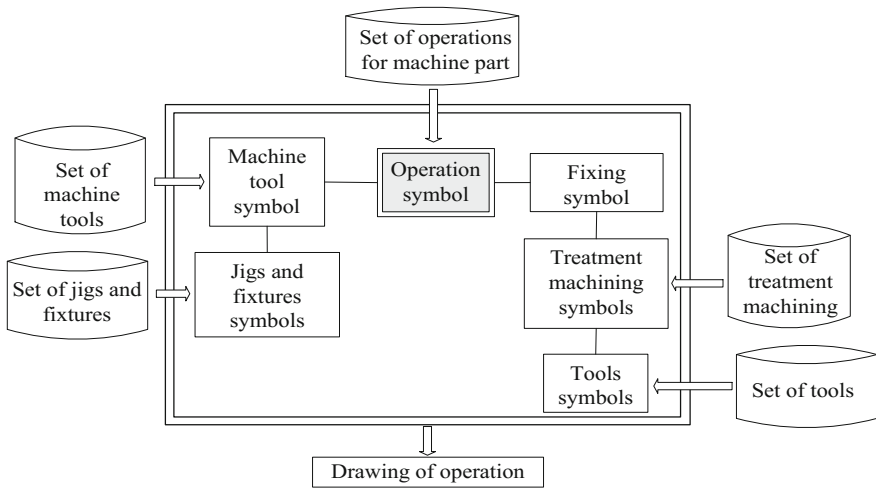
Object symbol	Geometric construction features			
	Variable		Permanent	
	Name	Symbol	Name	Symbol
FW	Length of conical surface	lfw	Chamfer angle	$f = 30^\circ$
			Roughness	Rfw = 10 [μm]
FZ	Diameter of cone base	dfz	Chamfer angle	$f = 25^\circ$
			Roughness	Rfz = 10 [μm]
RZ	Groove distance from the forehead	arz	Value of the tolerance	Tgrz = 1,0 [mm]
	Groove width	brz		
	Groove depth	grz		
OT	Hole diameter	d	Radius of rounding	R = 1[mm]
	Hole 1 distance from the forehead	l1	Roughness	Rot = 10 [μm]
	Hole 2 distance from the forehead	l2		
	Hole spacing	t		

A procedure of assigning values to the variable features in the KMS is introduced, which results in obtaining knowledge about the structure of the selected machine part.

#### 4 Method of the Knowledge Representation About the Structure of the Technological Process

A symbolic knowledge representation about the technological structure in the construction of the KMS should be elaborated. Such representation is constituted by appropriate symbols, which in conjunction with symbols representing the input data and the construction of the machine part allow to generate the technological process for the machine part. The basis for the construction of the representation is to analyze the construction and technological documentation of selected machine elements. This analysis is conducted in order to determine the relationship between construction and the technological process.

In the initial stage, sets of symbols based on the use of the particular variants in technological process designs have been created. Then a method of recording of the symbolic knowledge representation basing on the description of required technological operations in the process has been assumed. The construction scheme and the forming method of the technological symbol has been shown in Fig. 3.



**Fig. 3** The structure of the technological symbol in the knowledge representation

Recording of the technological symbol is based on the following format [15]:

```
{<OPERATION>, <MACHINE TOOL>, <FIXING>, <TREATMENT MACHINING>,
<JIGS AND FIXTURES>, <TOOLS>}
```

Basing on the structure of the operation symbol within the technological process, information is obtained, presented in the form of the description and the operation drawings. An example of the elaboration of a symbolic representation of a technological process for the selected item of a type of pipes is shown in Table 2.

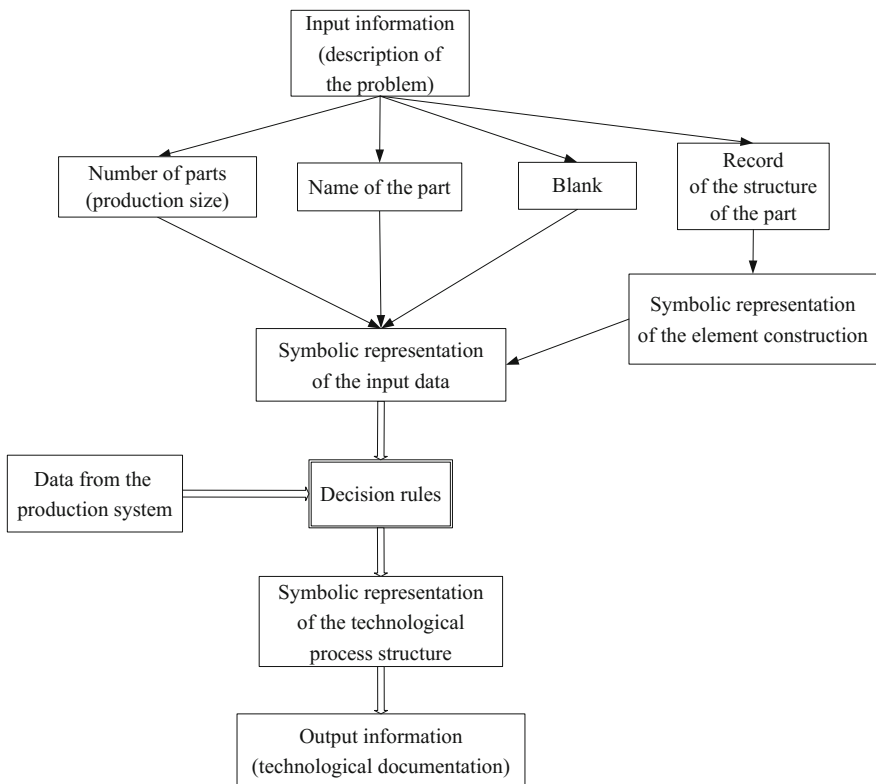
**Table 2** An example of the elaboration of a symbolic representation of a technological process

Operation symbol	Operation drawings
<pre>{&lt;CUTTING&gt;, &lt;SAW300&gt;, &lt;Z1&gt;, &lt;K(Lr1)&gt;, &lt;(PJM-a-200)&gt;, &lt;(BI-M, MLKc-2000, MAUb-150)&gt;}</pre>	
<pre>{&lt;TURNING_1&gt;, &lt;350NC&gt;, &lt;Z1&gt;, &lt;TKPCz2(Lr), WTKRW1(brw1, drw1, arw1), WTLRW1 (t°, drw1), WTP1RW1(crw1, 15°), WTP2RW1(25°), TFW(lfw), TFz(2, 45°)&gt;, &lt;(M-325)&gt;, &lt;(hR111.26 2525//r0.8, N-331, N-691/P, N-335)&gt;}</pre>	

On the basis of the symbol structure of the technological process, information is obtained which is represented in a form of a description and operations drawings, which occur in the technical documentation of the KMS.

### 5 The Use of the Decision-Making Rules in the Designing of Technological Processes

On the essence of the technological processes of machine parts, a close dependence derives between the construction and the structure of the technological process. This dependence is the result of the analysis of the production’s technological preparation of machine parts and research on the selection of technological processes and technical resources required for their implementation. On this basis, a design process using the symbolic knowledge representation about the construction and the technological process structure has been elaborated (Fig. 4).



**Fig. 4** A scheme of the designing process using the symbolic knowledge representation

A key element of the designing process are decision rules. These rules constitute an elementary part of the knowledge base system, and on their basis, the decision problems are solved. The primary objective of the application of the rules is as follows:

- presentation of the dependences between the input information about the decision-making problems, and the knowledge that describes the solutions to these problems,
- record of relationships appearing in the description of the construction element—the rules usually show the arrangement of the description (characteristic dimensions and elementary objects) and the order of assigning values to the variable dimensions,
- the creation of knowledge characterizing the structure of the designed technological process—starting with the record of the highlighted symbol of the structure based on rules describing a symbolic representation of the process structure, it is possible to obtain information about the process according to the assumed level of precision of the description.

Elaborated relationships between symbolic representations of knowledge allow creating the design rules in the following form:

IF *<object symbol>* THEN *<symbol of the process structure>*

On the basis of the form exemplary rules of design procedures in the process structure may be generated e.g.:

- complex rule:

IF  $RW1(arw1, brw1, crw1, drw1, t)$  THEN  $WTKRW1(brw1, drw1, arw)$  and  $WTLRW1(t, drw1)$  and  $WTP1RW1(crw1, 15^\circ)$  and  $WTP2RW1(25^\circ)$

- simple rule:

IF  $FW(lfw)$  THEN  $TFW(lfw)$ .

Introduced symbols of knowledge representation in the conditional and action part of the decision rules are described by information collected in the KMS. Thanks to this, the system supports technological preparation of production by generating proposals for solutions to the decision-making problems in the process designing.

## 6 The Construction of a Framework Representation of the Technological Knowledge

Decision-making problems in the area of technological processes may be very complex and therefore it is often required to elaborate a numerous set of rules in the KMS. It is therefore deliberate to appropriately group rules according to the existent stages of designing. It is required that all rules are recorded in the knowledge system base, which in this case has a modular design. From various methods of knowledge representation, the framework representation has been chosen as the most appropriate method of meeting the requirements of the knowledge base recording.

The base of the presented representation are the frames. The frame is a structure describing the considered object. It consists of so-called substructures—slots, depicting some properties or characteristics of the object. Slots are divided into even smaller knowledge pieces, which are called facets. All frame components have unique names, making them easy to identify and record in the knowledge base. A characteristic feature of the knowledge framework representation is the ability to divide the acquired knowledge into information sets, responding to the stages and decision-making problems in the process design. The advantage of this representation is the possibility to group information concerning selected portion of knowledge in the form of a frame, which facilitates verification and modification of the system’s knowledge base [13]. The scheme of construction of a framework knowledge representation has been shown in Fig. 5.

The presented knowledge representation has a procedural and declarative character. The declarative nature of the representation results from the elaborated

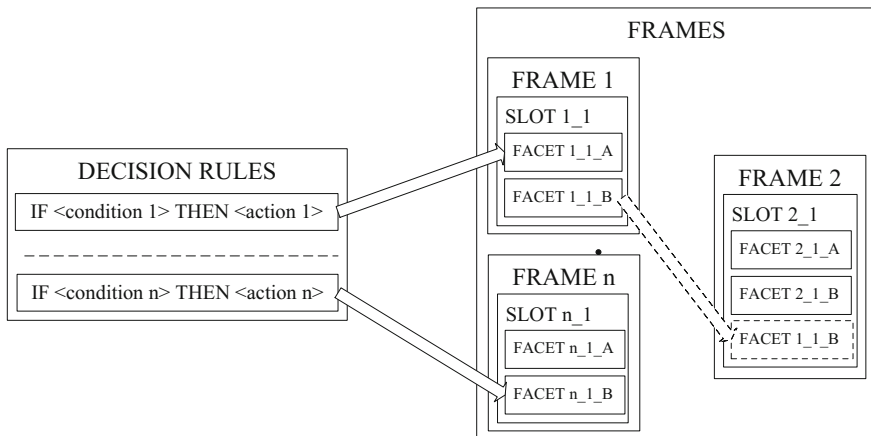


Fig. 5 The scheme of construction of a framework knowledge representation

sets of rules, in which the information has been declared. The procedural representation is based on the frame structure, in which the rules are recorded according to the established procedure of the order of their use [15].

## 7 Conclusion

Elaborated methods of knowledge representation have been aimed at the construction of KMS. It is associated with the processes of knowledge elaboration, from the knowledge acquisition for the sake of the system through the construction of the knowledge representation and recording of the knowledge base system. Presented knowledge structure is introduced to the KMS in the enterprise. This requires the use of an appropriate software tool.

The research related to the elaboration of the construction of the symbolic technological knowledge representation have been based on expert methods. To substantiate the choice of such methods is the nature of the knowledge itself, which is embedded in the realities of the company and includes a set of information about products, processes and production systems. The elaborated method of knowledge representation supports key processes of knowledge management in the production company, hence it is necessary to use in this case, the knowledge of experts in the preparation and execution of production processes. This allows mapping of the experts' reasoning, who solve particular decision problems, which require detailed knowledge resources. Elaborated methods facilitate decision-making related to the technological preparation of the machine parts production.

## References

1. Awad, E.M., Ghaziri, H.M.: Knowledge Management. Dorling Kindersley, London (2008)
2. Dalkir, K.: Knowledge Management in Theory and Practice. Elsevier, Amsterdam (2005)
3. Mertins, K., Heisig, P., Vorbeck, J.: Knowledge Management: Concepts and Practices. Springer, New York (2003)
4. Davenport, T.H., Probst, B.: Knowledge Management Case Book. Best Practices. Publicis Corporate Publishing, Wiley, Berlin, Munich (2002)
5. Maier, R.: Knowledge Management Systems. Springer, Heidelberg (2002)
6. Negnevitsky, M.: Artificial Intelligence. A Guide to Intelligent Systems. Addison-Wesley, Boston (2002)
7. Turban, E., Aronson, J.E.: Decision Support Systems and Intelligent Systems. Prentice Hall, New York (2003)
8. Rutkowski, L.: Computational Intelligence—Methods and Techniques. Springer, Berlin, Heidelberg (2008)
9. Giarratano, J., Riley, G.: Expert Systems. Principles and Programming. Thomson Learning, Beijing (2005)
10. Madanmohan, R.: Knowledge Management Tools and Techniques. Practitioner and Experts Evaluate KM Solutions. Elsevier, Butterworth-Heinemann, New York (2005)



11. Halevi, G., Wang, K.: Knowledge based manufacturing system (KBMS). *J. Intell. Manuf.* **18**, 467–474 (2007)
12. Zhang, L.L., Xu, Q., Helo, P.: A knowledge based system for process family planning. *J. Manuf. Technol. Manag.* **24**(2), 174–196 (2013)
13. Knosala, R.: *Application of Artificial Intelligence Methods in Production Engineering*, (in Polish). WNT, Warsaw (2002)
14. Zhang, Y., Luo, X., Zhang, H., Sutherland, J.W.: A knowledge representation for unit manufacturing processes. *Int. J. Adv. Manuf. Technol.* **73**(5–8), 1011–1031 (2014)
15. Trajer, J., Paszek, A., Iwan, S.: *Knowledge Management* (in Polish). PWE, Warsaw (2012)
16. Paszek, A., Wittbrodt, P.: The method of building a knowledge management system in a manufacturing company. *Int. J. Mod. Manuf. Technol.* **7**(1), 47–52 (2015)

# Methodology of KBE System Development for Automated Design of Multivariant Products

Przemyslaw Zawadzki

**Abstract** The paper presents a methodology of building a KBE system for design automation of product variants. The idea of the system is based on a web-based architecture, assuming that configuration of the product variant is performed by its customer, through a special user interface. Configuration data are transformed in a CAD software automatically, which allows to prepare the technical documentation without participation of qualified engineers. The methodology is presented as a procedure which includes five main stages of KBE system build: identification, acquisition of knowledge, system design, building system components and implementation. The paper presents practical validation of the methodology on the example of plumbing fittings design process.

**Keywords** Knowledge-based engineering • Generative CAD model • Design automation • Product variant design

## 1 Introduction

Manufacturing companies face a number of challenges in the struggle for a strong competitive market position. One such significant challenge is a rise in individual client's requirements as clients expect products better than standard mass-produced products [1]. There is a strategy, named mass customization (MC), which links advantages of piece and mass production [2–4]. MC is a competitive strategy as long as a company can quickly react to expectations and requirements of clients [4]. This can be achieved by using CAx (Computer Aided Systems) in design, which not only support basic engineering tasks but also enable effective use of the knowledge already gathered about the design process of a given product group (knowledge-based engineering systems—KBE) [5–8]. A formal description of rules

---

P. Zawadzki (✉)

Poznan University of Technology, Piotrowo 3 Street, 60-965 Poznan, Poland  
e-mail: Przemyslaw.Zawadzki@put.poznan.pl

© Springer International Publishing AG 2018

A. Hamrol et al. (eds.), *Advances in Manufacturing*, Lecture Notes in Mechanical Engineering, [https://doi.org/10.1007/978-3-319-68619-6\\_23](https://doi.org/10.1007/978-3-319-68619-6_23)

239

used by engineers affects process standardization and enables automation of repeatable design tasks [9–12]. Therefore, creation and implementation of a KBE system in the process of product variant design may for companies be one method of putting mass customization assumptions into practice [13–16].

The essential premise why a KBE system should be taken into account is first and foremost a possibility to rationalize the design process. It is estimated that approximately 80% of design time is spent on routine tasks [15, 16]. Their acceleration might significantly optimize the entire life cycle of products and give substantial savings. Therefore, the basic advantage of KBE systems is the possibility to automate repeated design tasks [9, 15] at the same time enhancing creative capabilities [6].

Although KBE is widely used in practice, approximately 80% of such solutions are temporary [5] as they are built to solve a given problem and are not fit for reuse. This situation continues despite the fact that standards have been developed for years to organize knowledge processing. In this paper two methodologies to support creation of KBE systems are discussed:

- MOKA (Methodology and software tools Oriented to Knowledge-based engineering Applications),
- KADM (Knowledge Aided Design Methodology).

The MOKA methodology was developed in order to support the construction of engineering KBE systems [16] focusing on design construction process. The authors have singled out six stages in the creation of this application although the proper application of this methodology encompasses only two of them: knowledge acquisition and knowledge formalization. MOKA methodology is recognized as a standard in the process of collecting and recording knowledge (with ICARE forms) for the needs of building KBE systems for industrial applications, however, it is not orientated to cooperate with any CAx systems. The KADM methodology offers a different approach which assumes that the ultimate form of representation of design knowledge is a generative model, developed in a given CAx system [17]. However, KADM focuses only on a product and the KBE system becomes in fact an integral part of the CAx system. These solutions are dedicated to experienced designers, well acquainted with the CAx environment. Also, no other tasks carried out in the design process are taken into account.

The following conclusions can be drawn from the analysis above: a majority of approaches to the issue of constructing any KBE system discuss the guidelines for the construction of any KBE system without referring to practical applications. On the one hand, this is an advantage as it enables adaptation of the assumptions to a selected process. On the other hand, however, indispensable modifications may be so numerous that it will be difficult to adapt it to a single approach of choice. Incidentally, this may be the reason why so few implementations follow individual methodological models. Hence, the author, with the above standards in mind, undertook to determine a procedure for automation of product design.

The aim of this paper is to develop a methodology in the form of a procedure which will enable the construction of a KBE system for automation of variant product design process. This methodology should find applications in technical tasks (design documentation) as well as in organizational tasks (automation system service), enabling integration of variant configuration tasks over the Internet (client) and its design in CAD system (manufacturer).

## 2 MDAVP Methodology

Based on their own experience and on literature analysis, the author put forward an original methodology of constructing an automated system of product variant design system. The methodology was given an acronym MDVAP (Methodology of Design Automation of Variant Products), whereas a system based on it was named SAVDP (System for Automatic Variant Product Design). The objective of MDAVP methodology is to support designers and builders of IT systems to enable the users (constructors and manufacturer's clients) to configure a product variant followed by automated, i.e., without resorting to direct CAD operation, development of design documentation.

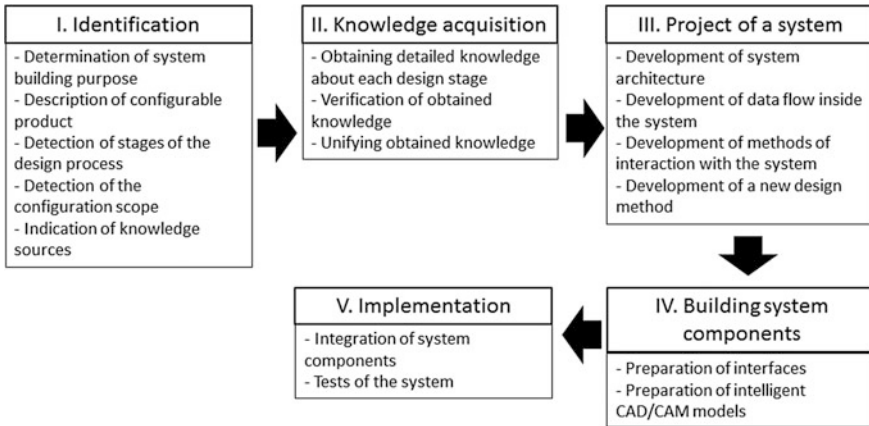
The development of the methodology had the following assumptions:

- it is dedicated to product variant design in situations when each new variant must be accompanied by design documentation,
- configuration of product variant may involve its user,
- methodology should be recorded in the form of a procedure,
- methodology should offer tools indispensable for acquisition of knowledge about design process,
- construction of automated design process requires qualifications in CAD operation (building generative CAD model), in programming (preparation of service interface) as well as in construction of database (building knowledge base).

In MDAVP methodology (Fig. 1), the following phases of building a SAVDP system can be identified:

- identification,
- knowledge acquisition,
- project of a system,
- building system components,
- implementation,

For the phases of the identification and knowledge acquisition stages specially prepared forms, based on the concept of ICARE forms in MOKA methodology, were used, modified and adapted to the requirements of product variant design. MDAVP methodology assumes that five forms will be used (process, phase, task, parameter, relation).



**Fig. 1** Stages in MDAVP methodology

Identification—at this stage of work is carried out by knowledge engineer who interviews the manufacturer’s management. The objective is to obtain basic information for SAVDP designers about:

- description of a product variant,
- description of design process,
- configuration scope of a product variant,
- assumptions of SAVDP system,
- sources of knowledge.

Preparation of a product description ensures unambiguous identification as it involves collecting information about product structure (an individual part, a set of parts), its purpose, manufacture technology, terminology, symbols, etc. Description of design process involves recognition of a cycle that is repeatable for each product variant by indicating its consecutive stages as they are related to the structure of CAD models. The range of product configuration (description of configuration options) is to give information about what and to what extent can be modified by product user. A design brief of a given SAVPD system determines expectations and requirements which must be included in its construction, such as a service system of choice or application (or integration) of selected software used in the given company. The identification stage also includes pointing out knowledge sources, above all selected archived designs of product variants available in the company that will be analyzed at the next stage—knowledge acquisition.

The objective of the knowledge acquisition stage in MDAVP methodology is to find out about various design methods of a given variant product in a manufacturing company and then to record a unified design procedure that will be applicable to every variant of the product. Acquisition of explicit, procedural and declarative knowledge from the resources of documentation available in the company is

assumed (existing CAD models), industrial standards and tacit knowledge gained from expert experience.

Knowledge acquisition is carried out separately for each product variant that is selected for analysis by means of recreation and recording (in forms for each stage, task, parameter, and parameter and relation) of a detailed course of its design (CAD modeling). To that end, information about individual tasks carried out at each, previously identified stage of that process is recognized. This is followed by description of each task by indicating the parameters applied and the relations between them. Knowledge base built in this way will enable recreation of the topology of the analyzed CAD models and verification of the collected data.

Verification facilitates preparation of a unified design procedure that determines standards for the process. It should involve a chronological description of tasks in each stage so that geometry of a CAD model is possible to meet the recognized configuration range. The unified procedure is recorded in forms for stage, task, parameter, and relation.

The method presented here minimizes interactivity of tasks performed later in the process of constructing generative model, and thus contributes to shortening the time needed to construct the entire SAVDP system. The recording of a unified procedure is a result of the second stage of MDAVP methodology.

The next stage—project of a SAVPD system involves:

- preparing the concept of system operation,
- determining and describing individual components of the system,
- preparing the manner of data flow between system components.

In developing a SAVDP system design assumptions described in the identification stage should be taken into account which determine basic requirements and expectations the client wishes to achieve. Therefore, at this stage besides basic components of the SAVDP system, i.e., CAD software and client interface, also other components that perform tasks set by the manufacturer must be included.

The base for development of a generative model in a selected CAD program is a previously prepared unified design procedure. It is recommended to use UML language diagrams that facilitate description of selected actions and ensure universal communication between individuals involved in the construction of the system.

The stage of building system components is divided into programming work to prepare client interface, and engineering to build generative models which, in the context of KADM methodology, refer to a formalization of previously acquired knowledge. Unified design procedure recorded at the stage of acquisition must therefore be implemented with the tools of a selected CAD software package. Most software packages available commercially now have suitable tools.

Practical work on SAVPD also involves construction of the remaining system components including client interface and interface for data exchange between the planned system components. In the course of the above activities tests to check (if possible) functioning of individual system components must be included.

The last stage of launching MDAVP methodology (Implementation) involves integration of SAVDP components as well as testing the operation of the system. This includes programming work in the following areas:

- server preparation and configuration,
- testing data flow structure between client interface and CAD package,
- preparation of macros automating server services,
- preparation of application that manages the system.

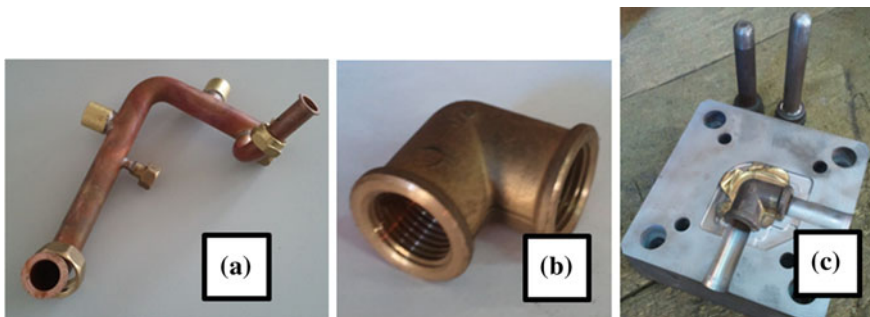
### 3 Case Studies

This chapter presents examples of construction of two different SAVPD systems in accordance with MDAVP methodology. The first one is for designing bent copper pipes (Fig. 2a) used in cold and hot water plumbing systems, heating systems and gas fittings (the scope of producible variants is practically unlimited). The second SAVPD system was prepared for an automation of design of forged couplings (Fig. 2b) and tooling necessary for their production (Fig. 2c).

In both cases, MS Access software package was used, in which database application was prepared to service knowledge processing (five types of forms were prepared) along with CATIA v5 for generative model construction. Client interfaces were prepared using Visual Basic and PHP languages.

#### 3.1 SAVPD System for Bent Copper Pipes

At the identification phase, controlling parameters (pipe diameter, thickness, bending points, two assembly endings, assembly line along the pipe—so-called T-drill) as well as stages in the design process (preparation of a CAD model of pipe



**Fig. 2** a Bent pipes, b forged coupling, c tooling for coupling

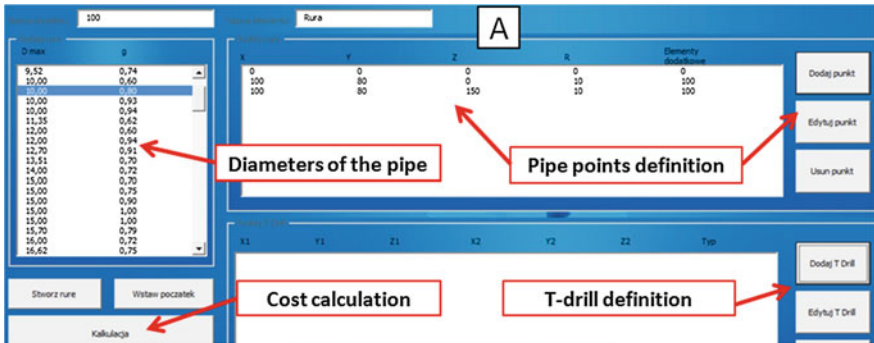


Fig. 3 Interface of developed system

Table 1 Comparison of SAVDP system and conventional design method

Average duration of design stage	Conventional design method (min)	Design in SAVPD (min)	Shortening stage duration (%)
Preparation of pipe model	50	8	84
Cost calculation	15	12	20
Total	65	20	

variants and calculation of manufacture costs of the variant) were recognized. Average time of pipe design was 50 min, and of cost calculation—15 min. Documentation for 10 archived pipe designs of varying geometry was selected. At the stage of knowledge acquisition using the forms of stage, task parameter and relation, different methods of pipe design were described, collected data were compared, then a unified procedure for design process was recorded. A system project was made describing its operation and data flow between client interface and CAD package. At the stage of component construction user interface (Fig. 3) and pipe generative model were made.

At the launch stage server configuration was made to ensure proper reading by CATIA v5 system of new configuration data recorded in design tables at user interface level.

In order to check correct system operation it was tested by comparing pipe design process with an approach conventionally adapted in the specific manufacturing company (Table 1). The results of SADVP system clearly demonstrate a reduction in design time. Coordinate reading from a flat documentation and variant configuration took on average approximately 7 min. Update of configuration data in CAD package did not exceed 1 min. The calculation stage was not significantly shortened because it repeated operations of the conventional design process. Time reduction at this stage resulted from automated retrieval of data about pipe variants from a CAD model.



A significant advantage of the new solution is a simplified estimate preparation for the client as most indispensable tasks do not involve hiring constructors. The entire process of designing new variants may be performed by manufacturer's customers themselves, or by salesmen on location.

### 3.2 SAVPD System for Forged Couplings

In the configuration process of a forged couplings, it is possible to define the thread size, the thread type (internal, external) and dimensions of cylindrical elements on both sides of a product. The design process includes four stages, related with preparation of 3D models of the product, the forging, the punches and the die. At the identification stage documentation for 8 archived projects was selected. At the stage of knowledge acquisition, different design methods were described and compared, which allowed recording a unified design procedure. Consequently, project of a system was prepared, containing detailed description of data flow between a WWW client interface and the CAD package. At the stage of components construction, user interface (Fig. 4a) and generative CAD model (Fig. 4b) were prepared. In the last stage, server configuration and the system tests were performed.

In this case, SAVDP system significantly reduces the design time (Table 2). Configuration of a new product variant using the interface and preparation of a 3D CAD model takes approximately 7 min. Automatic generation of all the necessary models takes approximately one minute for each model.

In this case, SAVDP system significantly reduces the design time (Table 2). Configuration of a new product variant using the interface and preparation of a 3D CAD model takes approximately 7 min. Automatic generation of all the necessary models takes approximately one minute for each model.

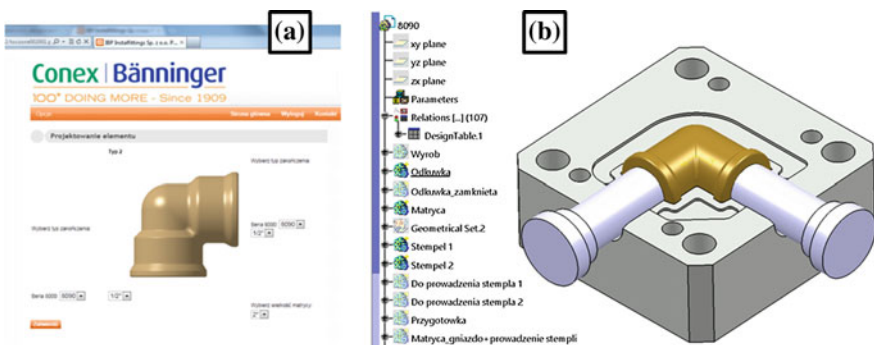


Fig. 4 a User interface, b generative CAD model

**Table 2** Comparison of SAVDP system and conventional design method

Average duration of design stage	Conventional design method (min)	Design in SAVPD (min)	Shortening stage duration (%)
Preparation of product model	300	7	98.7
Preparation of forging model	360	1	99.7
Preparation of punches models	120	1	99.2
Preparation of die model	240	1	99.6
Total	1020	10	

## 4 Conclusions

Many design offices do not take full advantage of the potential that knowledge-based solutions offer, or do not use them at all. One reason might be that the use of KBE tools in CAx systems is not at all easy, requiring engineers to possess experience in design itself and also in programming. Therefore, construction or updating knowledge-based systems requires hiring teams of engineers and programmers. For the manufacturer this is usually connected with investment and it is made even more difficult by continuous changes in products on offer. Another factor limiting construction of this type of systems is that it is time-consuming. It may happen that in the course of knowledge collection and implementation the product completely changes or, even worse, its production is suspended.

Nevertheless, it needs to be emphasized that if mass customization is to be achieved—i.e., delivering individuated products to nearly every client—then the use of automated knowledge-based design systems is unavoidable as it considerably reduces the duration of repeated routine activities of constructors. The author believes that future development of KBE systems for design automation should focus on studies on tools for analysis of automation potential and capabilities of variant products with reference to current market requirements and necessary amount of labor (economic justification of KBE systems development). If configuration assumptions for a variant product are too limited then applicability of the system may expire rather quickly. On the other hand, excessive enlargement of configuration possibilities will result in increased labor and extension of construction duration. If a suitable analysis is not carried out then system construction may not bring anticipated benefits, product life cycle will be short and, with time, constructors will return to conventional design methods.

## References

1. Górski, F., Buń, P., Wichniarek, R., Zawadzki, P., Hamrol, A.: Design and implementation of a complex virtual reality system for product design with active participation of end user. In: *Advances in Human Factors, Software, and Systems Engineering*, pp. 31–43. Springer International Publishing, Switzerland (2016)
2. Fogliatto, F.S., da Silveira, G.J., Borenstein, D.: The mass customization decade: an updated review of the literature. *Int. J. Prod. Econ.* **138**(1), 14–25 (2012)
3. Salvador, F., de Holan, P.M., Piller, F.: Cracking the code of mass customization. *MIT Sloan Manag. Rev.* **50**(3), 71–78 (2009)
4. Górski, F., Zawadzki, P., Hamrol, A.: Knowledge based engineering as a condition of effective mass production of configurable products by design automation. *J. Mach. Eng.* **16**, 5–30 (2016)
5. Reddy, E.J., Sridhar, C.N.V., Rangadu, V.P.: Knowledge based engineering: notion, approaches and future trends. *Am. J. Intell. Syst.* **5**(1), 1–17 (2015)
6. Verhagen, W.J.C., Bermell-Garcia, P., Van Dijk, R.E.C., Curran, R.: A critical review of knowledge-based engineering: an identification of research challenges. *Adv. Eng. Inf.* **26**(1), 5–15 (2012)
7. Van der Laan, A.H.: Knowledge based engineering support for aircraft component design. In: *Design of Aircraft and Rotorcraft*, pp. 254. Faculty of Aerospace Engineering, Delft University of Technology, Delft (2008)
8. Weiss, Z., Diakun, J., Dostatni, E.: Design management in virtual intranet environment. In: *ISAS/CITSA 2004: International Conference on Cybernetics and Information Technologies, Systems and Applications and 10th International Conference on Information Systems Analysis and Synthesis*, vol. 3, pp. 253–256 (2004)
9. Górski, F., Hamrol, A., Kowalski, M., Paszkiewicz, R., Zawadzki, P.: an automatic system for 3d models and technology process design. *Trans. FAMENA.* **35**(2), 69–78 (2011)
10. Chandrasegaran, S.K., Ramani, K., Sriram, R.D., Horváth, I., Bernard, A., Harik, R.F., Gao, W.: The evolution, challenges, and future of knowledge representation in product design systems. *Comput. Aided Des.* **45**(2), 204–228 (2013)
11. Grajewski, D., Diakun, J., Wichniarek, R., Dostatni, E., Buń, P., Górski, F., Karwasz, A.: Improving the skills and knowledge of future designers in the field of ecodesign using virtual reality technologies. (International Conference Virtual and Augmented Reality in Education.) *Proc. Comput. Sci.* **75**, 348–358 (2015). ISSN 1877-0509
12. Dostatni, E., Diakun, J., Grajewski, D., Wichniarek, R., Karwasz, A.: Multi-agent system to support decision-making process in ecodesign. In: *10th International Conference on Soft Computing Models in Industrial and Environmental Applications, Advances in Intelligent Systems and Computing*, vol. 368, pp 415–425. © Springer International Publishing, Switzerland (2015). doi:[10.1007/978-3-319-19719-7\\_40](https://doi.org/10.1007/978-3-319-19719-7_40)
13. Elgh, F., Cederfeldt, M.: Documentation and Management of Product Knowledge in a System for Automated Variant Design: A Case Study, New World Situation: New Directions in Concurrent Engineering, pp. 237–245. Springer, London (2010)
14. Choi, J.W., Kelly, D., Raju, J., Reidsema, C.: Knowledge-based engineering system to estimate manufacturing cost for composite structures. *J. Aircr.* **42**(6), 1396–1402 (2005)
15. Skarka, W.: Application of MOKA methodology in generative model creation using CATIA. *Eng. Appl. Artif. Intell.* **20** (2007) (Elsevier)
16. Stokes, M.: Managing Engineering Knowledge; MOKA: Methodology for Knowledge Based Engineering Applications. Professional Engineering Publishing, London (2001)
17. Skarka, W.: Metodologia procesu projektowo-konstrukcyjnego opartego na wiedzy. Wydawnictwo Politechniki Śląskiej, Gliwice (2007) (in Polish)

# Interacting Manufacturing Features in CAPP Systems

Janusz Pobożniak

**Abstract** Most of computer-aided process planning (CAPP) systems for machining process planning offer the functions for feature recognition. Nevertheless, these functions have limited functionality, restricting the usage of CAPP systems. The research works clearly show that one of the main factors blocking the feature technology is the recognition of interacting features. The paper presents the algorithm for the efficient recognition of interacting features. The starting point is the assumption that manufacturing knowledge plays the crucial role in the feature recognition. The manufacturing knowledge decides how to group the basic geometric entities into the manufacturing features. The presented algorithm uses the feature refinement function, converting the initial set of features into the other set of features based on the manufacturing knowledge and the function for local feature recognition. The algorithm is relatively simple, while taking into account the requirements imposed on the feature recognition systems.

**Keywords** Manufacturing features · Feature recognition · Feature interactions  
CAPP

## 1 Introduction

CAPP (Computer Aided Process Planning) systems form the vital link in Computer Integrated Manufacturing (CIM). These systems are used for process planning. The part model created in CAD system, the manufacturing knowledge database, and several databases of manufacturing equipment (tools, machine tools, fixtures, machining allowances, etc.) are used for the automated process planning. The growing complexity of nowadays manufacturing process used in industry, lack of

---

J. Pobożniak (✉)

Institute of Production Engineering, Cracow University of Technology,  
Al. Jana Pawła II 37, 31-86 Cracow, Poland  
e-mail: pobożniak@mech.pk.edu.pl

© Springer International Publishing AG 2018

A. Hamrol et al. (eds.), *Advances in Manufacturing*, Lecture Notes in Mechanical Engineering, [https://doi.org/10.1007/978-3-319-68619-6\\_24](https://doi.org/10.1007/978-3-319-68619-6_24)

249

qualified engineers staff and other benefits like possibility to store and reuse the company know-how justify the interest in the development of CAPP systems.

Most of the CAPP systems have the machining feature recognition function. This function groups geometrical elements, stored in the CAD drawing database, like faces, edges, points, etc., into the information units significant from the point of view of manufacturing process planning, i.e., manufacturing features like pockets, slots, holes, etc. Then, the machining cycles can be assigned to the recognized manufacturing features. For example, if there is a hole in the part, taking into account its parameters like diameter, length, accuracy of surfaces, type of bottom, thread type, etc., the sequence of machining cycles can be automatically determined, for example, pre-drilling, drilling, rough reaming and final reaming. This task, feature recognition, is one of the basic conditions to automate manufacturing process planning, especially in generative and semi-generative CAPP systems. It should be noted that according to many authors [1–4], one of the main problems blocking the wider feature usage is the limited functionality of the algorithm for the recognition of interacting features. This paper presents the algorithm for dealing with interacting manufacturing features. The next point presents the review of the works on the feature recognition. The main emphasis were put on the drawbacks of these works. Subsequent points describe the algorithm and its advantages. The last part contains the example for the proposed approach.

## 2 Review of the Works on Feature Recognition

The task of manufacturing feature recognition is the grouping of low-level entities like faces, loops, edges. etc. into the manufacturing features. Low-level entities are read from the drawing database of commercial CAD systems. Two dominant model representations in CAD systems are CSG (Constructive Solid Geometry) and B-Rep (Boundary Representation). CSG representation loses its popularity and because of this, the recognition algorithms based on this representation will be not discussed. Three commonly used recognition methods for B-Rep format are graph-based algorithms, volumetric decomposition techniques and hint based geometric reasoning. AAG (Attributed Adjacency Graph) developed by Joshi [5] is the typical representative of the first method. In this method, Joshi uses B-Rep representation of the part transformed into AAG graph. The nodes of this graph represents the surfaces, while the edges represent the angles between the surfaces. If the two adjacent surfaces form the convex angle, the value of 1 is assigned to the edge between the nodes representing these surfaces. If the two adjacent surfaces form the concave angle, the value of 0 is assigned to the edge between the nodes representing these surfaces. The sub-graphs containing only the edges with the value of 0 represent the manufacturing features. The drawback of this method is the fact, the pattern of each manufacturing feature must be represented in the knowledge database. It is not possible to create such patterns for all possible manufacturing features. For example, it is not possible to create the patterns for all possible

closed pocket, differing in the number of side surfaces (rectangular, hexagonal, round pockets, arbitrary shape pockets, etc.). Additionally, this method is not well suited for the recognition of so-called convex features.

Volumetric decomposition algorithms decompose the delta volume into the smaller parts and either directly classify them as features, or combine them into new volumes to be classified. The two main approaches are convex hull decomposition and cell-based decomposition [1]. As noted in this work [1], multiple step reasoning is a common characteristics and drawback of the these approaches. For example, the initial step—ASVP decomposition (in the convex hull decomposition algorithm) and delta volume decomposition into cells (in the cell—based decomposition) are done independently of features and manufacturing process rationale. No robust methods, justifiable from a manufacturing point of view, has been developed to manipulate the intermediate volumes created by these initial steps.

In hint based geometric reasoning, the production rules generate the hints for the presence of manufacturing features [6]. Feature hint may be generated by a characteristic combination of part faces, by a design feature from which a manufacturing feature can be interfered, or by a tolerance or attribute specific specification that can be associated with a certain feature type. These production rules use the fact, that some features should have left the trace in the part geometry even when their geometries are distorted by the interaction (intersection) with other features. The recognition results of this approach depends on the defined hints. Some authors suggests that large number of hints does not lead to the correct manufacturing features. Usually, the hints are heuristic, not based on the mathematic rules. During the development of such hints, the features to be recognized, for example defined in ISO 14649 (STEP-NC) must be taken into account.

The common opinion is that interacting manufacturing features prevent the usage of feature technology [1–4]. Due to the interactions, the features become distorted, for example, some faces are removed. This significantly impedes the feature recognition. The other problem accompanying the recognition of interacting features, not appropriately considered in the research works, is the decomposition of the interacting features. Figure 1a presents the very simple example. The part has two interacting through slots. They can be interpreted as various simple features. For example, these slot can be treated as the open pocket (Fig. 1b), machined with the one machining cycle (Fig. 1e). In the other decomposition, there could be one long, through slot (Fig. 1c) and two shorter through slots. The longer slots is machined first, and then the two shorter slots. The decision, which slot should be selected as the longer one must be taken (Fig. 1c or d). Sometimes, it is very important from the manufacturing point of view. If the interacting slots have different widths, the slot with larger width should be machined first (Fig. 1f). This is because of the basic manufacturing rule, recommending the removal of the larger volume, when the cutting forces are higher, on the beginning of the manufacturing process. So, the slot with the larger width, as having the greater volume, should be machined first. The other reasons is that the machining with the tool having greater diameter is more efficient end economically justified. Because of this, the common part of these two slots should be machined with the tool having the greater

diameter. The personal experience of the author suggests, that manufacturing features cannot be correctly recognized using only the geometrical representation, for example in B-Rep (Boundary Representation) format. Unfortunately, nearly all research works on feature recognition ignore the fact that manufacturing knowledge plays important role in feature recognition. This also limits the usability of the feature technology for practical implementations.

The other problem, which does not have yet the solution, is the recognition of the features occurring in the intermediate states of the part during the machining. Very often such features are not present in the machined part, they occur only in the intermediate part states. For example, during the machining of the part shown on Fig. 2 there is the facing cycle. The cycle uses the plane manufacturing feature. The standard feature recognition systems does not find such plane feature during the recognition process of this part. Similar situation occurs in the case of the profile contouring cycle, which uses the boss feature.

The paper presents the method of manufacturing feature recognition solving the problem of interacting features. The proposed algorithm can convert one manufacturing features in the other feature (or set of features) during the feature

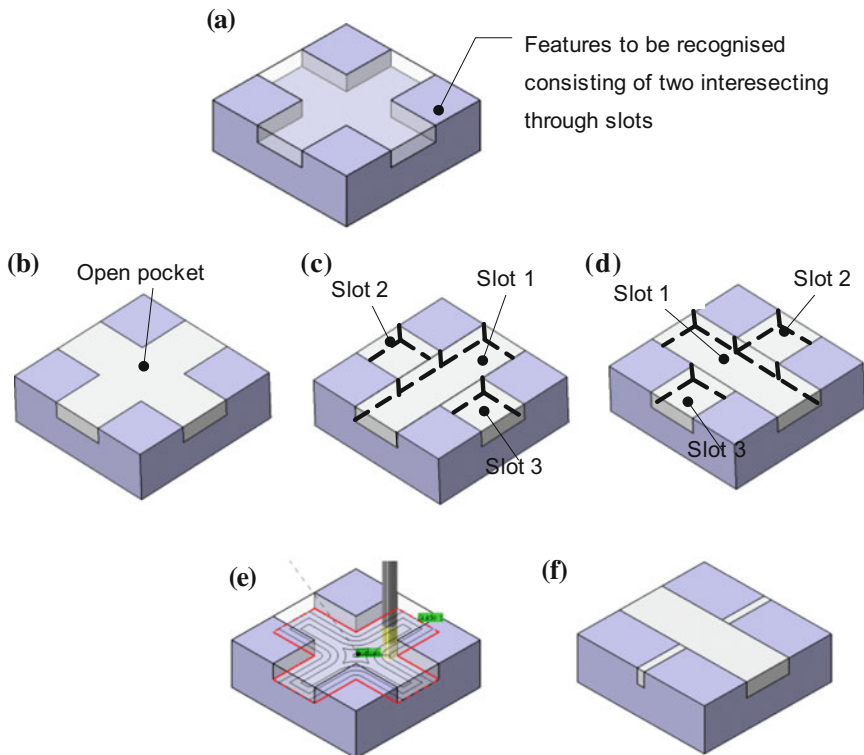


Fig. 1 Different views on interacting features

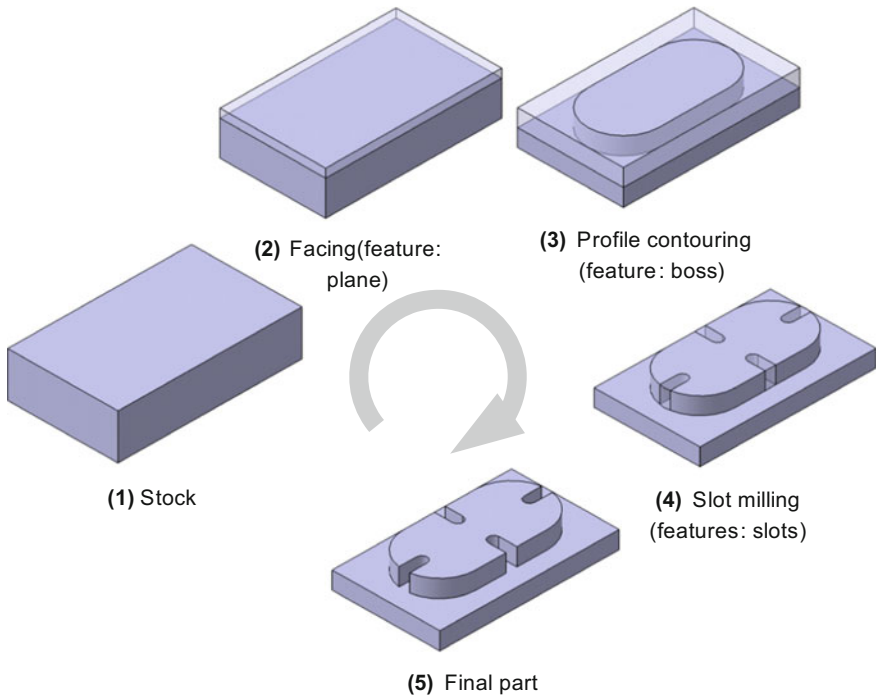


Fig. 2 Features in the intermediate states of the part during the machining

refinement stage [7]. The manufacturing knowledge is used during feature recognition process.

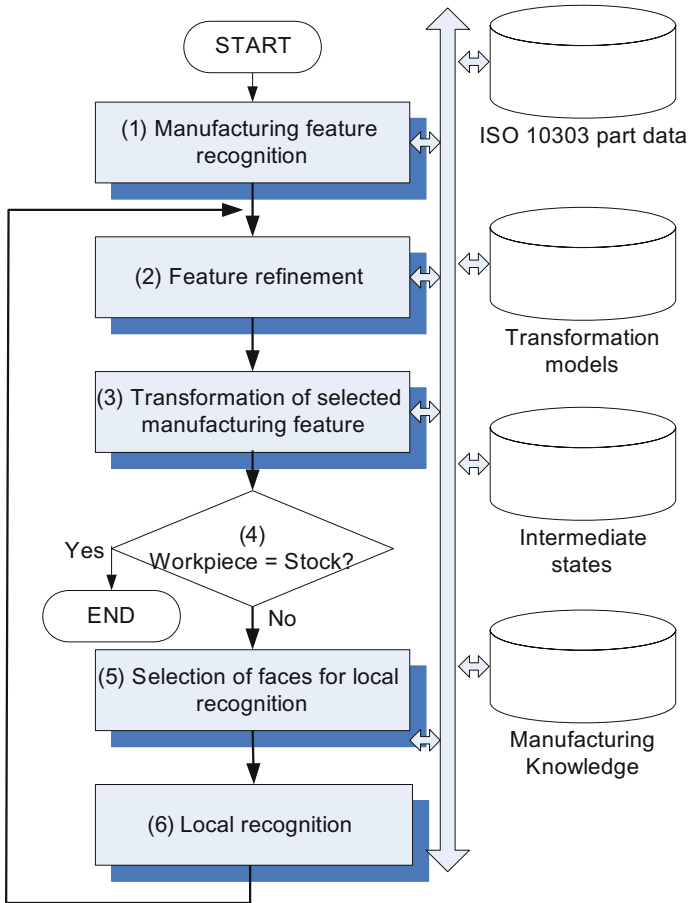
### 3 Algorithm

The part model stored in STEP (ISO 10303 [8, 9]) format with Boundary Representation (B-Rep) is used as the source of input data. Figure 3 presents the steps of the algorithm.

#### (1) Manufacturing feature recognition

The basic manufacturing features defined in STEP-NC standard [9], like closed pockets, open pockets, slots, holes, etc. are recognized using the logic approach and hint based reasoning. For efficient processing, the face adjacency matrix is created and the concavity index developed by author is used [7]. The outcome of this step is the manufacturing feature-oriented part model.





**Fig. 3** The steps of the algorithm

## (2) Feature refinement using manufacturing knowledge

The recognized manufacturing features are then analyzed by the feature refinement functions using the manufacturing knowledge database. This function can convert the initial set of manufacturing features into the other set of manufacturing features, taking into account the processing capabilities of manufacturing system. For example, the outer contour of some rotational parts can be converted into the contour for rough turning and external groove [7].

The contour for rough turning is machined using the rough turning machining cycle with the longitudinal feed, while the external groove is machined with the groove turning cycle. Similarly, open pocket in some parts can be transformed into the closed pocket and through slot. Through slot can be machined using the end mill with the diameter equal to the width of the slot, while the closed pocket can be machined using the end mill with the larger diameter.

### (3) Transformation of selected manufacturing feature

After refinement of manufacturing features, the selected manufacturing feature is transformed by adding the material according to the selected model of transformation. The part transformation proceeds backwards, from the finished part to the stock. The transformation model describes how to add the material. For example, in case of hole reaming, the diameter of reamed hole is decreased (the use of backwards transformation should be noted). In case of drilling, the transformation removes the hole from the set of manufacturing features. To update the part model, the appropriate Boolean operation is performed. The feature to be transformed and the transformation model are selected using the manufacturing knowledge.

The manufacturing knowledge also decides whether it is necessary to store the intermediate state of the part. The intermediate states shall be stored in some situations, for example when changing setup or continuing the machining on the other machine tool. Both B-rep representation as well feature-oriented representation are saved.

### (4) Decision on further processing

This step compares the part and the stock. If the actual state of the part is the same as the state of the stock, the algorithm ends its operation. Otherwise, the processing moves to the point (5).

### (5) Selection of faces for recognition of features in intermediate state

During the transformation of selected manufacturing feature, some faces of the part are changed or even deleted. This necessitates the update of the set of features. All features referencing the changed or deleted faces are removed. The changed or new faces (created during the transformation) are marked as unrecognized.

### (6) Recognition of features in intermediate state

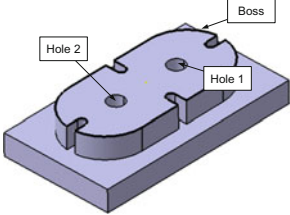
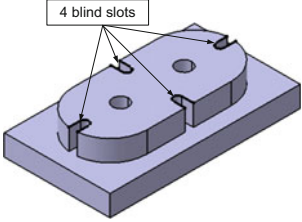
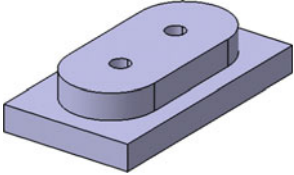
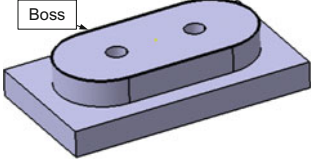
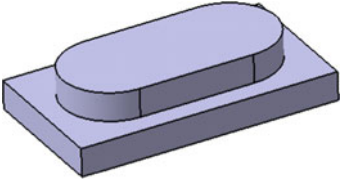
All faces marked as unrecognized in the previous step are subjected to recognition. This is very important step differing this algorithm from the approached proposed in other research works. It shall be noted that the recognition is done on the beginning of the processing as for every intermediate states of the part. After the recognition is finished, the processing moves to the point (2).

## 4 Example of Processing

Table 1 shows the example of the processing.

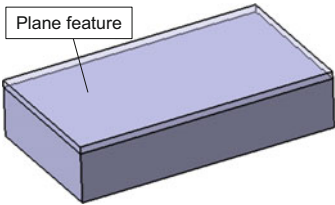
It is not possible to decompose the part into manufacturing features before the process planning. The geometry and topology data of the part do not deliver the information necessary to decide whether to machine the whole boss or first machine the four blind slots and then the resultant boss. The set of features recognized in the part must be changed according to the manufacturing knowledge. In this example

**Table 1** Example of processing

No.	Processing	Illustration
<i>Iteration 1</i>		
1	Step 1 (manufacturing features recognition): Three manufacturing features are recognized: 2 holes and 1 boss	
2	Step 2 (features refinement): The manufacturing knowledge finds that profile of boss features has 4 blind slots. The manufacturing knowledge suggested that the blind slots have so small widths, that the other tool must be used for their machining than the tool for the machining of the boss. These blind slots were not recognized in step 1 (they were treated as the part of the boss)	
3	Step 3: (transformation of selected features): During this step, based on the manufacturing knowledge, the decision to machine four blind slots was taken. The picture on the right shows the part after the transformations	
4	Step 4 (selection of further processing): The processing is continued	
5	Step 5 (selection of faces for local recognition) and Step 6 (Local recognition): Because the faces creating the original boss were changed, the recognition of intermediate states analyzes the part and finds the new boss features	
<i>Iteration 2</i>		
	Step 2: No actions	
	Step 3: Using the manufacturing knowledge, the decision to transform the holes is taken	

(continued)

**Table 1** (continued)

No.	Processing	Illustration
	Step 4: The processing is continued	
	Step 5 and Step 6: As the holes were no interacting features (holes were independent features), no recognition of part intermediate states is done	
<i>Iteration 3 and subsequent...</i>		
	... (Continuation until the stock is reached) ...	

manufacturing knowledge states that first it is necessary to machine the slots and then use the tool with larger diameter to remove the material in a short time. At the end of processing, the plane features is found. This feature is also not visible in the part final state. The advantages of the proposed algorithm grows together with the complexity of the parts.

## 5 Conclusions

The algorithm was partially verified by the development of software. The procedural language Visual C ++ and the geometric kernel ACIS were used.

Base on the results of the work, the following conclusions can be formulated:

- The proposed algorithm seems to be relatively simple in comparison with other algorithms for interacting feature recognition, while it has a good efficiency. The proposed algorithm just recognizes the simple manufacturing features, transforms the selected feature and then recognizes the features in part intermediate states. The transformation just reveals the new simple features, not visible in the part finished state.
- The current state of the part is always subjected to recognition, without predicting the potential shape of the part after the machining of the subsequent machining operations.

The use of manufacturing knowledge significantly increases the practical value of this algorithm. It is not possible to make the correct recognition of manufacturing features without using the manufacturing knowledge. The developed algorithm can also store the intermediate states.

## References

1. Babic, B., Nestic, N., Miljkovic, Z.: A review of automated feature recognition with rule-based pattern recognition. *Comput. Ind.* **59**(4) (2008)
2. Dipper, T., Xu, X., Klemm, P.: Defining, recognizing and representing feature interactions in a feature-based data model. *Robot. Comput. Integr. Manuf.* **27**(1) (2011)
3. Kamrani, A.K., Nasr, E.A.: *Engineering Design and Rapid Prototyping*. Springer, Berlin (2010)
4. Mokhtar, A., Xu, X.: Machining precedence of 2D/3D interacting features in a feature-based data model. *J. Intell. Manuf.* **22**(2) (2011)
5. Joshi, S., Chang, T.C.: Graph based heuristics for recognition of machined features from 3D solid model. *Comput. Aided Des.* **20**(2) (1998)
6. Vandenbrande, J.H., Requicha Aristides, A.G.: Spatial reasoning for the automatic recognition of machinable features in solid models. *IEEE Pattern Anal. Mach. Intell.* **1**(15), 1269–1285 (1993)
7. Pobożniak, J.: Two stage approach to feature recognition for Computer Aided Process Planning. *Adv. Manuf. Sci. Technol.* **29**(4) (2005)
8. ISO 10303-21:2002: Industrial automation systems and integration—Product data representation and exchange—Part 21: Implementation methods: Clear text encoding of the exchange structure
9. ISO 14649-10:2004: Industrial automation systems and integration—Physical device control—Data model for computerized numerical controllers—Part 10: General process data

# Case Studies of the Process-Oriented Approach to Technology Management

Wieslaw Urban and Elzbieta Krawczyk-Dembicka

**Abstract** The article uses the insights of the process approach for research in technology management in companies. The goal set was identification of activities in the area of technology management taking their processual nature into account; the identified research was contrasted with technology management models available in the literature in the field. The case study method was used in the research. Research was conducted in two companies in the metal processing industry. Two technology management processes were identified, sequences of activity as well as dependencies arising between them were described. The gap was shown between the models available in the literature and the actual course of the process of technology management. In the theoretical models, input and output are not defined, attention is not directed at decision points that are key in regard to the success of the process and the development of the company as a whole. In the discussion, the identified processes are evaluated and application recommendations formulated.

**Keywords** Technology management • Business process • Process management Model

## 1 Introduction

The process approach to organizational management is now widely applied in companies. At first, the process approach represented a serious turn in the way of thinking about company management, managers discovered at that time what great losses in efficiency and suboptimization result from the functional view of a company. Despite the passage of time and the accumulation of much experience, transitioning from function to processes is still a kind of challenge, associated among other things with very popular research on the process maturity of an

---

W. Urban · E. Krawczyk-Dembicka (✉)  
Faculty of Management, Białystok University of Technology,  
Wiejska 45A, 15-351 Białystok, Poland  
e-mail: e.dembicka@pb.edu.pl

organization. The study below draws on the insights of the process approach and applies these to the area of technology management in companies. The goal of this research is to identify activities in the area of technology management, taking into consideration their processual nature, and then contrasting the identified processes with the theoretical insights of technology management. Identification of the technology management process was undertaken in two selected companies in the metal processing industry. The study uses the case study method, which allows deep exploration of selected organizational segments as well as multilateral recognition of the course of the processes studied.

## 2 Technology Management Models

Technology itself is a process consisting of the sequencing of many activities, executed in a strictly defined manner. It results in finished products or services meeting the needs of consumers [1]. This process is implemented in a hierarchical production system, based on clearly defined elements that result from both the available theoretical and practical knowledge [2]. In order to be able to order the activities identified in a given technology, the efforts of various researchers to formulate a model of technology management appears to be necessary work.

The pioneer in research into building a model of technology management was Gregory. His generalized model relied on five processes associated with technology management in companies, supplemented by a range of subprocesses characteristic for various analysed industries. The generalized model described topics associated with (I) identification of technologies, (II) their selection, (III) acquisition, (IV) exploitation and (V) protection of knowledge regarding the given technology [3]. Gregory's research was continued by many others who undertook attempts to supplement it with new processes [4], or others to define it [5, 6], to introduce environmental conditions indicating the type of economic activity or they were made dependent on the organizational level of a company [7, 8].

The framework of technology management defined in the literature should support companies in the development of appropriate strategies that would facilitate management of available technologies at the organizational level. With the contemporary dynamic appearance of technological changes, this is extremely difficult, and as a result the models formulated should provide a company with the ability to react quickly to changing conditions [9, 10]. Technology management should not limit itself exclusively to conducting analyses and developing technology, but at the same time should take advantage of means to recognize the mechanisms steering technological processes in organizations [11]. Not insignificant here is still the human factor [12]. A review of the literature in the field reveals that in the available models of technology management, only process frameworks are present, but this research does not take into consideration the precise sequencing of activities or

other characteristics typical of the process approach [13]. Moreover, very little is said about practical courses of action, in other words methods and techniques used in companies having to do with technology management.

### 3 The Business Process

The process view of organizations is very popular among companies because of the numerous advantages it provides. The process approach has its roots in two older and more mature concepts, namely business process reengineering and total quality management [14]. Authors emphasize that what is known as ‘process orientation’ is also embodied in the European Foundation for Quality Management and the Malcolm Baldrige National Quality Award models for business excellence and performance [15]. There are many terms used for this approach to the study of processes, including ‘process simplification’, ‘process improvement’, ‘process re-engineering’ and ‘process redesign’ [15].

The literature provides many definitions of the concept of the organizational/business process. One of the simplest definitions defines a business process as a step-by-step approach to a specific business problem [16]. This definition is interesting because, being very concise, it highlights the most important feature of business processes—the inherent occurrence of the associated sequence of actions in a process. In the popular ISO 9000 standard of Quality Management Systems, the concept of process is defined as a set of interrelated or interrelated actions that transform inputs into outputs [17]. Another quite formalized definition is provided by Workflow Management Coalition, an organization supporting Business Process Management. In this definition, a business process is a set of one or more linked procedures or activities which collectively realize a business objective or policy goal, normally within the context of an organizational structure defining functional roles and relationships [18].

The founders of reengineering understand a business process as a collection of activities which consume one or more inputs and create the output as value for customers [19]. Another definition provided by Palmberg understands a business process as a horizontal sequence of activities that transforms an input (need) to an output (result) to meet the needs of customers or stakeholders [20]. In these definitions, process inputs and outputs as well as process aims are particularly emphasized by the authors. Zellner lists all the elements that can be identified in a business process, which are as follows: trigger (or event), activity, organizational unit (or persons), input, output, control flow, information flow, organizational flow, material flow [21].

A accurate investigation of the processual characteristics of technology management in business entities has not yet been explored rigorously by scholars, although a fairly interesting study of the innovation lifecycle is provided by Milewski et al. [22]. The authors identify the technological changes process as one of a few types of innovation processes. The four standardized phases of the process



of technological change are elaborated, namely ideation, adaptation, preparation, and installation [22]. The empirical in-depth investigation according to this framework revealed the differences between the implementation of externally acquired standard technological solutions and internally developed core technologies. This study tries to deepen the processual nature of technology management in a company. The process approach has great potential for discovering new and fresh views on technology management. As DeToro and McCabe state, the business process approach presents a quite comprehensive array of improvement options [23]; at the same time, this approach is so often practised and well-equipped in proven routines that can be employed without ambiguities for investigating technology management in companies.

## 4 Research Methods

The research process conducted by the authors was qualitative in nature. It was based on the use of the case study method, which was applied to identify and describe the process approach to technology management in companies in the metal processing industry. In accordance with the assumptions of this method, the authors concentrated on recognition and analysis of the regularities occurring in the studied subjects, assuming conditions that would make formulation of generalized results possible [24]. The course of research relied on a script that took into account on the one hand theoretical knowledge demanding empirical verification and on the other research gaps identified in the literature [25].

The research took place during study visits to companies. The script was comprised of three main stages: direct interviews with the management team, heads of production or technological departments as well as with select staff members; analysis of the companies' documentation; observation of the working conditions in particular departments of the company, during which identification of the types of technology used in the production process was made. The main goal of the visits, however, was identification of the technology management process, consisting of analysis of technology from the moment the idea of developing it appears through its full implementation. Identified were the main activities and the relations between them, but also described were decision points influencing the course of the process. In each of the companies studied, one most distinctive technology was described.

As research subjects, two production enterprises in the metal processing industry were selected. In the production process, they use generally available technologies, the introduction of which usually entails the purchase of machines. These technologies they then adapt to their internal needs by making various modifications. In the solutions they create, they introduce innovations that make possible the creation of new production series that are adapted to the individual demands of customers.

For the needs of this study, the names of the companies were replaced with their general characteristics. For the research, two companies in Podlaskie voivodeship were chosen that operate both on the domestic and the foreign markets. These were:

- A company operating in the production of machines and technical devices, for the food industry among others, providing machining services, tooling services, as well as implementing automation of production processes. The company employs 67 people.
- A company operating in the production of farm machinery, specifically mowers, rakes, wire-trap tools, tedders, and snowploughs. The company employs 600 people.

## 5 Case Study of a Company Producing Machines and Technical Devices

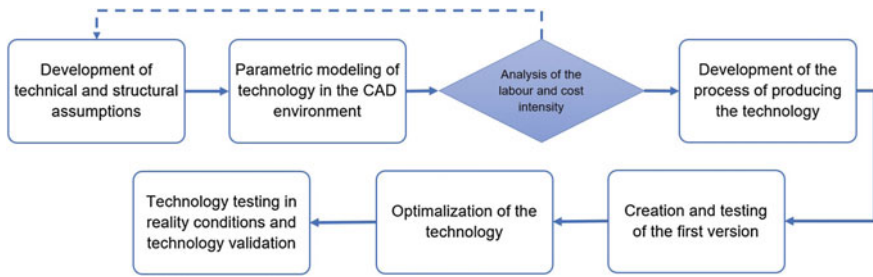
The company studied is engaged in unit production or very small serial production. Its main area of operation is providing customers with individualized machines and technical devices as well as the necessary tools, custom made to a concrete order placed by a customer. This is done based on specifications provided by the customer, or also those worked out by designers in the R&D department.

In the company, the following types of technology were identified as in use in current operations:

- processing technology (processing: machining, plastic working, electroerosive machining, finishing, heat processing),
- materials joining technology (welding: MIG/TIG, laser, electrical),
- assembly technology (machine, hand).

To identify the technology management process, an analysis of the technology of development of devices used for the assembly of fine elements for the company's production needs was performed. The general structure of the implemented process remained constant; however, the company currently uses the principles of this technology to prepare dedicated solutions for individual customer needs. In this case, the technology management process can be linked with the process of technological change, as a variety of the innovation process, stimulated by market demand. The implementation time for the process discussed in this work was around 36 months and allowed the development of procedures that allowed the technology to be adapted to new demands raised by customers. Depending on the stage of development of the technological project, the process of preparing modifications to the technology could take from 3 to 6 months. Specific elements of the process are shown in Fig. 1.

The first step in the implementation process was development of guidelines and technical and structural assumptions. This stage lasted around 5 months, during which specific tasks and functions that the device was to perform were designated, working out the structure as well as the initial selection of appropriate materials and components. Next, on the basis of the developed specifications, the developers created in a CAD environment a parametric model of the designed device. This



**Fig. 1** Diagram of the process of implementing the technology of automated assembly of fine elements

permitted analysis of the labour and cost intensity of the finished solution, which simultaneously governed the decision to proceed to implementation of the given design. Creation of the model also allowed initial testing if the technical and structural assumptions were accurate and correcting them if necessary.

The next stage, based on the results of the modelling work, involved working out the development of the process of producing the technology, which lasted around 9 months. During this stage, available sources (patent records, industry fairs, internet services) were used to identify and check possibilities for producing the technology, and the choice of technological processes required for the execution of particular details was made. Technical specifications were also developed and materials gathered for the next stage.

Creation and testing of the first version of the device lasted about 12 months. This work allowed discovery of previously undetected structural errors and the implementation of necessary corrections to the technical specifications. Testing took place under simulated operating conditions. The goal, aside from detection and elimination of all potential defects, was to evaluate the suitability of the applied technology. The rest results permitted optimalization of the developed technology and creation of the final version of the device. The stage of optimalization and creation of the device, combined with the introduction of required changes in the technical and structural specifications, lasted around 7 months.

The final stage of the implemented process of technology management was activation and testing of the device under real conditions. Positive verification of the achievement of design objectives permitted validation of the technology and its implementation. This stage lasted about 3 months.

The company studied has internally developed procedures regarding the implementation of the technology management process. In this process, an established mode of operation is maintained, owing to which more rapid monitoring and intervention with additional resources (personnel or material) is possible, which in the end significantly shortens the duration of the entire cycle.

Management of the company by a single-member management board ensured that the decision process is clearly defined. The main person who decides about the course of the process of technology management is the Chairman of the Board, who

indirectly participates in the work at every stage. Decisions are made on the basis of information and specifications provided by individual department heads, who are responsible for particular stages. The entire process is completed by a project team, whose members include engineers and technologists from the R&D department.

## 6 Case Study of a Company Producing Farm Machinery

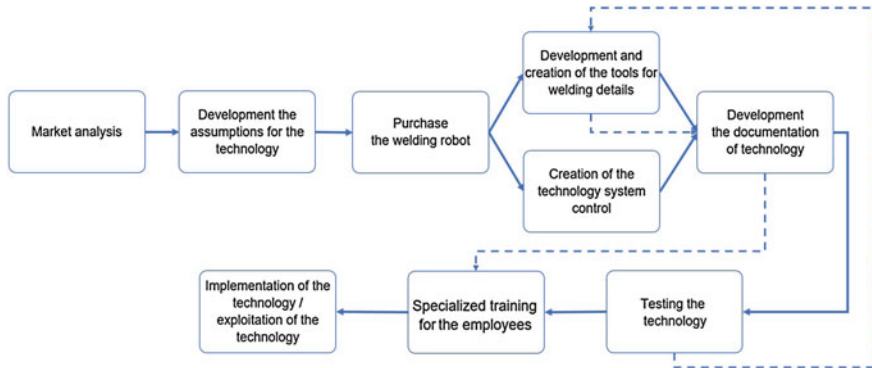
The company classifies its output as small serial production. Because of the character of the machines offered, the vast majority of which (around 90%) are farm machines, production is seasonal in character, the rhythm of seasons changes depending on the purpose of the given type of machine. Technologies available in the company are those associated broadly with steel processing. They can be broken into two main groups, technologies of machine production and processing technologies. The two groups are closely interrelated. Among the processing technologies identified in the company, the following types can be named:

- machine processing (milling, rolling, drilling),
- surface processing (sanding, painting, shot-blasting),
- plastic-cutting processing (cutting, laser cutting, plasma cutting, bending),
- materials joining (welding, assembly).

For the purpose of identification of the technology management process, the technology of materials joining using welding robots was tracked. This technology is used in the company mainly for welding beater shafts and cultivator shafts. The process involving the development and introduction of the technology lasted around 26 months. Implementation of the technology into production caused a reduction in welding time by nearly 60%, which significantly increased the productivity of the manufacturing department, had the beneficial effect of an improvement in the quality of manufactured items and at the same time ensured the maintenance of repeatability and the quality of items. Specific elements of the process are shown in Fig. 2.

The process began with a market analysis, which provided information regarding prevailing trends in the metal processing industry and existing technological possibilities. The content of patent databases was analysed and technological solutions existing in the marketplace were examined. The conclusions drawn and the identification of company resources served to develop the requirements for the technology of materials joining with the use of welding robots. This work was conducted over around 10 months.

The next step was finding a robot on the market that met the established requirements. After it was purchased, it turned out that because of the peculiarities of the items produced, outfitting the station with additional equipment to ensure proper mounting and working conditions was required, which was carried out internally by the company. It was also necessary to create the control system with



**Fig. 2** Diagram of the process of implementing of the technology of joining materials with the use of welding robots

technology that required that an order be placed to the manufacturer of the robot. The work related to development and creation of the tools for welding details and to the creation of the control system was completed simultaneously. This stage concluded with the development of detailed specifications of the technology and sending them for testing after about 10 months of work.

Work related to testing the technology took place under real working conditions for the welding robot. This entailed production of a test series of various kinds of items manufactured for the production needs of the company. During testing, it turned out that in order to fully automate production and exploit the abilities of the robot, it was necessary to equip the station with additional elements. As a result, renewed work associated with the development and production of additional equipment, as well as updating the technical documentations. These activities took about 4 months.

The final stage, associated with the implementation of the technology into the company's current production (exploitation of the technology) was preceded by specialized training for the employees who were to become operators of the robotic station. This work was necessary to ensure work safety and to take full advantage of the abilities offered by the newly developed technology.

In the company studied, for the completion of every process a project team is named, which proceeds in accordance with established regulations and guidelines. At the top is the company board, and team members include also directors and heads of the particular departments taking part in the process as well as the lead engineers. The team organizes weekly meetings, which evaluate the progress and effects of implementing the process, make economic calculations of the profitability of the technology created, and complete decision processes.

## 7 Conclusions

Models of the process of technology management identified in the subject literature do not indicate the typical process approach to the topic analysed. The majority rely on Gregory's generalized model, in which clearly missing is description of the typical sequence of activities and the dependencies existing between them. Equally problematic is determination of the starting point of the process, as well as its conclusion. The identified activities run through each other, which renders impossible delineation of a clear path of the course of process.

More appropriate for the conditions prevailing in companies in the metal processing industry would seem to be issues of the business process, in which technology management is dependent on changing market conditions as well the reaction of the business environment to the creation and implementation to new technologies. The business process is more flexible and reacts more rapidly to the emergence of unexpected changes. It links the idea of development of new technologies with the concrete need to create new products or services in conditions dictated by market demand. This is generated by a dynamic process of technological change, which is an element of the omnipresent processes of innovation.

The processes of technology management identified in the companies studied are clearly different from the process models described in the subject literature. Specific activities are individualized to the concrete needs of the company and are focussed on achieving the desired effects from the implementation of the given technology. Companies place marginal significance on activities related to protecting technology, regarding that as a way to quickly destroy it. In their view, the beginning of the process of protection is simultaneous with its sale, because of the necessity of revealing detailed descriptions. Further work should concentrate on attempts to have the model of the process of technology management take elements of the business process into account. This makes the process sensitive to the emergence of unexpected changes.

**Acknowledgements** The research has been carried out in the framework of the work G/WZ/1/2016 and financed by the National Science Centre (agreement No. 2015/19/N/HS4/02576).

## References

1. Santarek, K. (ed.): *Technology Transfer from Universities to Business. Creating the Technology Transfer Mechanisms*. PARP, Warsaw (2008). (in Polish)
2. Łunarski, J.: *Technology Management. Evaluation and Improvement*, Publishing House of Rzeszów University of Technology, Rzeszów (2009). (in Polish)
3. Gregory, M.J.: *Technology management: a process approach*. *Proc Inst Mech Eng* **209**, 347–356 (1995)
4. Cetindamar, D., Phaal, R., Probert, D.R.: *Technology Management. Activities and Tools*. Palgrave Macmillan, New York (2010)

5. Sumanth, D.J., Sumanth, J.J.: The technology cycle approach to technology management. In: Gaynor, G.H. (ed.) *Handbook of Technology Management*, pp. 3.1–3.17. McGraw-Hill, New York (1996)
6. Jolly, V.J.: *Commercializing New Technologies: Getting from Mind to Market*. HBR Press, Boston, MA (1997)
7. Skilbeck, J.N. Cruickshank, C.M.: A framework for evaluating technology management processes. In: Portland, OR, July 1997, PICMET'97
8. Halicka, K.: Innovative classification of methods of the future-oriented technology analysis. *Technolo Econ Dev Econ* **22**(4), 574–597 (2016)
9. Fellner, B.: *Strategic flexibility in technology strategy. Managing of Technology Turbulence by Incumbent Firms in the Manufacturing Industry*, Graz, Dissertation—Graz University of Technology (2010)
10. Christensen, C.M.: *The Innovator's Dilemma: The Revolutionary Book that Will Change the Way You Do Business* (1st Harper Business pbk). Harper Business, New York (2011)
11. Wipfler, H.: Technology management activities to avoid technological lock-ins. In: *International Association for Management of Technology IAMOT 2017 Conference Proceedings*, Vienna, 2017
12. Urban, W.: Amoeba management system transformation in the light of organisational change literature. *Manag Prod Eng Rev* **8**(1), 16–23 (2017)
13. Krawczyk-Dembicka, E.: Analysis of technology management using the example of the production enterprise from the SME sector. *Procedia Eng* **182**, 359–365 (2017)
14. Niehaves, B., Plattfaut, R.: Collaborative business process management: status quo and quo vadis. *Bus Process Manag J* **17**(3), 384–402 (2011)
15. Lee, R.G., Dale, B.G.: Business process management: a review and evaluation. *Bus Process Manag J* **4**(3), 214–225 (1998)
16. Havey, M.: *Essential Business Process Modelling*. O'Reilly Media, Sebastopol (2005)
17. Norma PN-EN ISO 9000:2015
18. The Workflow Management Coalition Specification. Terminology & Glossary. Workflow Management Coalition, Winchester (1999)
19. Hammer, M., Champy, J.A.: *Reengineering the Corporation: A Manifesto for Business Revolution*. Harper Business Books, Nowy Jork (1993)
20. Palmberg, K.: Exploring process management: are there any widespread models and definitions? *The TQM J* **21**(2), 203–215 (2009)
21. Zellner, G.: Towards a framework for identifying business process redesign patterns. *Bus Process Manag J* **19**(4), 600–623 (2013)
22. Milewski, S.K., Fernandes, K.J., Mount, M.P.: Exploring technological process innovation from a lifecycle perspective. *Int J Oper Prod Manag* **35**(9), 1312–1331 (2015)
23. DeToro, I., McCabe, T.: How to stay flexible and elude fads. *Qual Prog* **30**(3), 55–60 (1997)
24. Czakon, W.: Application of case studies in research in management sciences. In: *Fundamentals of Research Methodology in Management Sciences*, pp. 45–63. Wolters Kluwer Polska Sp. z o.o., Warsaw (2011). (in Polish)
25. Yin, R.K.: *Case Study Research. Design and Methods*. Fifth ed. SAGE Publications, Inc., New Delhi, United States, London (2014)

# Technical Product-Service Systems—A Business Opportunity for Machine Industry

Mariusz Salwin, Bartłomiej Gładysz and Krzysztof Santarek

**Abstract** The aim of this paper is to present an idea of servicization and technical product-service systems. General assumptions, trends, and challenges in business, customer expectations, and manufacturing leading to the need and trend of servicization of economies and production sectors in particular are discussed. Product-service systems characteristics and typologies are discussed. Selected examples of product-service systems are presented. New concept of a technical product-service system was proposed for a manufacturer of moulds. Presented example shows properties that characterize technical product-service systems in relation to a set of services proposed for a manufacturer of moulds. Characteristics of systems were discussed to show possible benefits for a manufacturer of moulds, as well as its customers.

**Keywords** Servicizing · Servicization · Product-service system · Technical product-service system · PSS

## 1 Introduction

Optimization of costs and utilization of assets leads customers to ideas of outsourcing and drives a trend of using assets only when necessary instead of investing in purchasing them. On the other hand, manufacturers want to promote long-term relations with customers, which form a stable basis for a sustainable growth. This leads to a paradigm shift. Products and services are no longer considered separately, but they are considered as closely interdependent and forming product-service systems. Poland recorded a share of services in GDP in 2016 of over 58%, Germany over 69%, and USA over 79%. Trends of increasing service sector share in GDP are observed not only in developed countries and economies [1].

---

M. Salwin · B. Gładysz (✉) · K. Santarek  
Faculty of Production Engineering, Institute of Production  
Systems Organization, Warsaw University of Technology, Warsaw, Poland  
e-mail: b.gladysz@wip.pw.edu.pl



Nevertheless, industry sector is still important in some industrialized countries, e.g., Germany and Japan. Manufacturing plants start the tertiarization of the industry by means of technical product-service systems, which enables new and more stable business-to-business relationships [2]. This paper aims to present an example of such approach for a manufacturer of moulds.

## 2 Product-Service Systems and Servicization

### 2.1 Definitions

Servicizing (servicization) is a transaction that combines the offering of a product and a service by selling them to meet customers’ needs or by increasing service as a part of the product being offered. This concept is based on the belief that customers are not interested in having a product, but rather in the opportunities offered and provided by the product. This means that a provider of servicizing solutions can benefit from a specific feature or product offering, as opposed to traditional product sales [3, 4]. In summary, servicizing involves changes in the treatment of a product in a material way only—the product, together with the set of related services, forms an integral whole, resulting in specific product and service systems [5].

Product-Service System (PSS) is a result of servicizing. PSSs are also called sometimes function-oriented business models. PSSs are “tangible products and intangible services designed and combined so that they jointly are capable of fulfilling specific customer needs” [6]. Baines et al. [7] presented literature review of definitions, characteristics, and concepts of PSS, and presented a concept of PSS (see Fig. 1). PSSs can be considered as a market proposition extending the traditional functionality of a product by including additional services. For these systems, the emphasis is primarily on selling features of products rather than products themselves. In PSSs, customers pay only for using a PSS and not for purchasing the product. An ownership and cost issues are usually moved more to the supplier or the manufacturer of PSS. PSSs are valuable business models primarily for manufacturers, their customers, but also for a society.

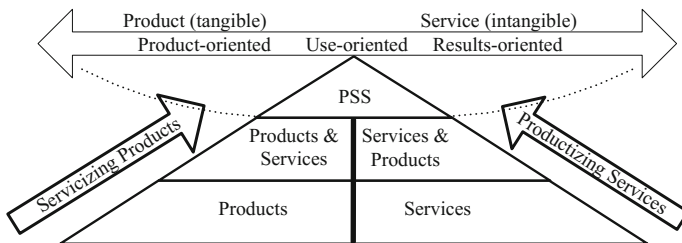


Fig. 1 PSS concept and types based on [6] and [7]

PSSs prolong the life of products, and they can also make the use of products more intense and optimal. The essence of the concept of PSSs is to reduce the use of materials and to shift to the dematerialisation of products and replace them with services. The key challenge here is to explore the relationship between products and services. PSS can be seen also as a market innovation that extends the traditional functionality of the product by offering additional services along with it [8]. The product and service system is just such a solution and in itself is a technical and organizational system providing such solutions. The key here is a systematic approach that defines how tangible and intangible (service) components are combined and delivered to customers. In general, this system is understood to be a combination of products and services into a whole, which provides the user with the required functionality and reduced environmental impact [5].

In many PSSs, technical components are still playing a dominant role. They are called technical product systems. Technical PSS emphasizes the physical product core enhanced and customized by a mainly nonphysical service shell, the investment character of all PSS components, the relatively bigger importance of the physical core of PSS, and the relations between PSS manufacturers and customers [9, 10].

## ***2.2 Types of Product-Service Systems***

There are three general types of PSSs (see Fig. 1; Table 1) [6]. The first type is a product-oriented PSS. Products are sold in a traditional way and the ownership of goods is transferred to customers. Additional services are provided by the manufacturer (seller). The selling company is motivated to introduce a product and service system to minimize the operating costs associated with a long-lasting, well-functioning product, and to design products to last the end of its useful life (reusable products/easily replaceable/reusable parts). The second type is a user-oriented PSS (using only product functionality). A manufacturer (supplier) remains an owner of physical goods. A seller makes available (sells) functions of products to customers through modified distribution systems and payments. In this case, the company has the incentive to create a product and service system to maximize the use of the product to meet demand, prolong the life of the product, and to reduce the consumption of materials for its production. The third type is a result-oriented PSS. Products are replaced by services, e.g., voice-mail replacing an answering machine. Services or its performance (potential) are sold instead of products, e.g., the Internet data replacing directories. Companies offer customized service combinations while retaining ownership of the product. The customer pays only for certain agreed effects (benefits), such as the number of miles traveled by car, etc. [11–13].

**Table 1** Types of product-service systems and their characteristics

Orientation	Product	Use	Results
Role of services	Providing additional services	Modified distribution and payment systems	Replacing products by services
Sales	Traditional (good)	Functions and features	Services
Ownership	Transferred to a customer	Retained by a seller	Retained by a seller
Example	Maintenance and repairs	Leasing of machines	Pay-per-effect, e.g., per copy
Types from [6]	(1) Product-related	(3) Leasing	(6) Activity management
	(2) Advice and consultancy	(4) Renting and sharing	(7) Pay-per-unit use
		(5) Pooling	(8) Functional results

### 2.3 Methodologies and Tools of Products Servicization and Selected Examples of PSS

There is a number of methodologies and tools used to design PSSs. Some examples of them are business ecosystem map, blueprinting model [14, 15], causal loop diagram, cost–benefit analysis, extended activity-based environmental costing [16], IDEF0 [17], life-cycle frameworks [18, 19], scenario planning [20], stakeholder analysis, SWOT analysis, system platforms [17], value framework model [21], and value network analysis [22]. Presented methodologies and tools are also used in other business practices where most of them come from. Business ecosystem map gives the opportunity to identify organizations, and different stakeholder groups in the field of entrepreneurship will be able to collaborate and create relationships in the product-service delivery system. Blueprinting is a tool used to visualize service processes, customer contact points, and physical evidence related to the services from the customer’s point of view [14, 15]. Causal loop diagram is a useful way of representing a business model in which the choices and results of these choices are linked by appropriate arrows depending on causal relationships. Cost–benefit analysis provides a tool to compare the benefits of the project under consideration with its costs to help users identify the available alternatives with maximum net profit (profit minus cost). Extended activity-based environmental costing is a method that allows proper analysis of the flows of products, by-products, and losses (waste) generated by the entire plant or a certain part of the plant [16]. IDEF0 is a method that presents a sequential view of the entire system by analyzing an activity and breaking it down into smaller activities. Such representation enables the designer to analyze the entire system without losing its overall picture [17]. In a case of product-oriented PSS, the appropriate life-cycle model will be the integrated manufacturing and product-service system, for the user-oriented and result-oriented models proposed by [18, 19]. Scenario planning identifies major trends and uncertainties enable to construct different scenarios that will help when a

decision-making error will occur. Scenario planning allows to capture the wealth and diversity of opportunities and draw attention to factors that might otherwise be overlooked [20]. Stakeholder analysis identifies, prioritizes, and allows to understand the needs of different stakeholders in terms of importance. SWOT analysis is a tool to identify the strengths and weaknesses, opportunities, and threats of an enterprise business model, so that it could support the development of PSS. System platform is the result of cooperation between entities of different origins, competences, and cultures, which brings together different actors (manufacturers, service providers, institutional, and end users) and describes the competencies of each, as well as interactions (i.e., material and nonmaterial flows) between them [17]. Value framework model evaluates innovation proposals at different levels and from different value perspectives [21]. Value network analysis represents a tool for exchanging values (good, service, knowledge, and intangible assets) between participants in a given business [22].

PSS design affects social, economic, and environmental issues. It is worth noting that designing PSS is not a linear but interactive process [23]. The design methods developed so far address sustainability issues, include in particular guidelines that help to focus on longevity, product reuse and recycling, analysis, generation of ideas, and phases of PSS implementation. During design, many factors are taken into account, primarily customer satisfaction, environmental protection, and profitability. When designing a PSS, it must be first analyzed, which are strengths and weaknesses, opportunities, and threats that the expansion of the current product portfolio will bring about dedicated services for each of the manufactured products. This is a key activity for an enterprise that wants to implement PSS. Then it comes to generating service ideas for manufactured products. Later, the selection of the most promising ideas is refined. For the best ideas, a detailed project is being implemented, which is aimed at introducing them [24]. PSS design methodology is very similar to traditional product design, including concept development, product design, product detail, prototype building and testing, production preparation, technical services including customer needs identification, feasibility analysis, concept development, service modeling, service planning, testing, and services development [9]. PSSs can also be modularly designed. Modules would consist of stages in product and service design and standard set of tasks to be performed at each phase. This approach can increase the speed of new PSS development, giving new and surprising PSS combinations without the need of design and testing, and thus minimize potential high costs [10]. Some PSS design methods pay attention to the formal and quantitative assessment of customer requirements and technical characteristics, using an optimized nonlinear platform to systematically determine how the combination of products and services maximizes customer satisfaction [25].

Xerox's "pay-per-use model" for photocopiers is an example of result-oriented PSS. The beginning of a transition to PSS was related to the introduction of a new method for printing images by electricity, which avoids the use of wet chemicals. The method was better than others available, but expensive. Xerox tried to find marketing partners for its 914 model, but they constantly rejected the proposal. As a result, the company rather than selling the equipment decided to lease it, at a very

low cost, and then collect a fee for copying over 2000 pages monthly. Xerox provided all the necessary supplies, consumables, services, and supports. Customers used only the effects and could cancel the lease 15 days in advance. Xerox incurred an annual growth rate of 41% in 12 years and has become motivated to develop machines with greater efficiency and availability. It is worth noting that Xerox, to date, has been using this business model for years to come. By using this model, Xerox's customers focus on their core business and do not bother about printing/copying, which is fully (operation, supplies, maintenance, etc.) the duty of Xerox. Customers use devices only when needed, reducing wastes and environmental impacts [26].

Another example is Philips [27] and its “pay-per-lux” model that is result-oriented PSS. The starting point in this model was the concept of the architect Thomas Rau that the customers were not interested lamps themselves, but with the light they produce. Philips provides individual lighting—“floating ceilings”—over each of the jobs that are inexpensive to provide efficient and adjustable lighting in the areas most needed in the workplace. Philips provides an additional integrated sensor and controller system that provides the ability to maintain a satisfactory level of total energy consumption, darken or brighten artificial lighting depending on movement and the presence of daylight. As a result, “pay-per-lux” is not a product but a service: the customer buys a subscription from Philips for a certain amount of light per year. Philips then supplies the lamp, ensures that the energy bill is paid, and takes responsibility for the replacement of the lamp if needed. Philips remains responsible for its products and accompanying energy bills, so the production of durable, energy-efficient lamps is in the interest of the company. When lamps need replacement, raw materials can be reused, thereby reducing the cost of producing new lamps. The design of the lamp ensures that it can easily be used for recycling. In summary, Philips provides access to light, but customers use the intensity they need at the moment. Both the customer and Philips aim to minimize use of an electricity.

Presented above PSS has a significant impact on the environment and resources used in the production of electricity, which is a general feature of PSS in comparison with pure products [7]. Other well-known PSS examples include Rolls-Royce (power-by-the-hour for engines), Atlas Copco (pay-per-m<sup>3</sup> for compressors), Michelin (pay-per-km for tires), Alstom (pay-per-km for trains), Caterpillar (pay-per-hour for machines), and MAN (pay-per-km for trucks) [7, 26].

### **3 Technical Product-Service Systems—A Case of Foundry Moulds**

An example of servicization in manufacturing companies will be introduced using a case of technical PSS of foundry moulds. Schuh et al. [28] proposed a framework for industrial PSS for the tooling industry with a focus on “smart” tools.

This framework was adopted, but limited to conventional tools. Figure 2 and Table 2 depict the evolved concept. It is necessary to discuss the features of moulds, possible additional services, and sales of services provided instead of selling moulds. First assumption is that ownership would not be transferred to the user. It is due to the fact that users struggle with high investment in moulds, which limits their interest into moulds as products. The company supplies moulds to the customer, charging a predetermined fee for the number of pieces made, as well as a monthly subscription charge. A manufacturer provides services related to the operation and professional handling of moulds. A manufacturer also provides maintenance, repairs, cleaning of moulds, as well as help with the filling system. At the request of the user, he also provides training for the safe and effective use of moulds and consulting services related to the whole casting process (technology and organization) or ergonomics of work. For example, a manufacturer consulting services may also include such areas like setup time reduction. It is worth mentioning that the customer needs only to use moulds in their foundry, rather than having foundry moulds and dealing with operations related to its operation and maintenance.

This approach has several benefits for both parties. The customer focuses exclusively on his core business, i.e., the production and sale of casts. The customer is not interested in activities related to the creation of new moulds, the machines used in this process, and also do not need additional designers and operators needed to produce moulds. The company also saves time and resources. With this approach, the customer can increase their production and open an additional casting department in place of a tool shop. A manufacturer of moulds earns from related services and establishes more stable and long-term relation. It is also in his interest to make moulds from high-quality materials, so that the product has a long life cycle. All this is to ensure faultlessness and reduce expenses on potential repairs. The very important benefit for a manufacturer shows up, when it comes to attract new customers. A customer pays only for the amount of castings (pieces) made, which is related to the exploitation of moulds. Thanks to this solution, it has an access to the technology. This also means that manufacturer of moulds has an access to customer’s moulds and collects data on their use, productivity, and failure.

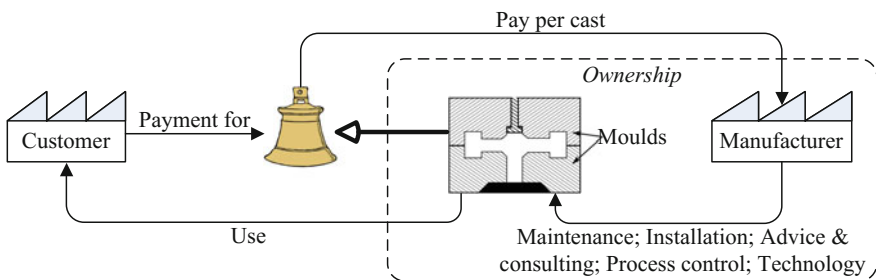


Fig. 2 Moulds as PSS—a concept

**Table 2** Moulds as PSS—a concept

Ownership	Sales	Services	Benefits
Not transferred to a customer	Pay-per-casts and monthly subscriber charge	Start-up	Customer's focus on core processes; outsourcing of supporting processes
	Guaranteed availability rate	Condition monitoring, maintenance and repairs, cleaning	More stable and long-term manufacturer–customer relation
		Support with the filling system, managing tool shop	
		Trainings and consulting—safety, health and ergonomics, technology and organization	Improving quality and design, and decreasing costs of production of moulds

The collected data give an opportunity to improve parameters of moulds, fill systems, and improve foundry process structure. This could also help to develop recommendations on how to use the moulds in a particular company. Data collected in this way could also optimize the maintenance schedule, reduce costs, and reduce environmental impact.

This example serves newly emerging companies, whose resources are severely limited at the initial stage of operation. One important challenge for a manufacturer of mould would be their modularization [29, 30], uniformization, and standardization, so that moulds (or modules) could be interoperable. This would lead to a further increase of utilization of moulds, which is important because moulds are relatively expensive.

## 4 Conclusions

PSSs, and their special case technical PSSs, are interesting alternatives for many companies, looking after new market opportunities, strengthening their competitive position, market share, and new sources of income. The principle of product-service systems does not, however, consist of simply expanding an existing offer range by adding services linked closely or not to manufactured products.

PSSs make a market offer of an enterprise more attractive, widening its scope. PSSs can be significant (and even, as many examples demonstrates it) and very important source of company's income; they can create new workplaces and can be also an important element of sustainable development strategy of an enterprise and industrial sectors, prolonging product life cycle making them more attractive for customers, and last but not least they help to enter new markets. The last can also be a problem for them. Service sector differs significantly from traditional ones oriented mainly on manufactured product. Entering new markets, companies are

facing new players and new rules of a market game. This results in urgent necessity to build and/or to expand existing competencies and resources in many areas: strategy, staff (including managers), service development, costing and accounting, planning, marketing, distribution channels but also several “soft” skills and competencies concerning people behavior, mentality, empathy, communication, etc.

Technical PSSs seem to be very promising for many manufacturers. Practically, there are no constraints in developing services associated with products, adding new value to customers, society, environment and, of course, companies themselves. In this paper, authors explained basic ideas of product-service systems and in particular of technical PSSs using as an example manufacturer of moulds.

## References

1. CIA. The World Factbook. [www.cia.gov/library/publications/the-world-factbook/fields/2012.html](http://www.cia.gov/library/publications/the-world-factbook/fields/2012.html). Accessed 28 Apr 2017
2. Meier, H., Roy, R., Seliger, G.: Industrial product-service systems—IPS2. *CIRP Ann.—Manuf. Technol.* **59**, 607–626 (2010)
3. Toffel, M.W.: Contracting for servicing. [www.hbs.edu/faculty/Publication%20Files/08-063\\_17bf1f50-d901-42e6-8adf-70e832ba49a7.pdf](http://www.hbs.edu/faculty/Publication%20Files/08-063_17bf1f50-d901-42e6-8adf-70e832ba49a7.pdf). Accessed 28 Apr 2017; (Harvard Business School)
4. Stahel, W.: The utilisation-focused service economy: resource efficiency and product-life extension. In: *The Greening of Industrial Ecosystems*, pp. 178–190. National Academy Press, Washington DC (1994)
5. Santarek, K., Salwin, M.: Product-service systems (in Polish: Systemy produktowo-usługowe). In: *Innovations in Management and Production Engineering* (in Polish: Innowacje w Zarządzaniu i Inżynierii Produkcji), vol. 1, pp. 863–873. OW PTZP, Opole (2017)
6. Tukker, A.: Eight types of product–service system: eight ways to sustainability? Experiences from SUSPRONET. *Bus. Strateg. Environ.* **13**, 246–260 (2004)
7. Baines, T.S., Lightfoot, H.W., Evans, S., Neely, A., Greenough, R., et al.: State-of-the-art in product-service systems. *Proc. Inst. Mech. Eng. Part B: J. Eng. Manuf.* **221**(10), 1543–1552 (2007)
8. Morelli, N.: Product service-systems, a perspective shift for designers: a case study—the design of a telecentre. *Des. Stud.* **24**(1), 73–99 (2003)
9. Aurich, J.C., Fuchs, C., Wagenknecht, C.: Life cycle oriented design of technical product-service systems. *J. Clean. Prod.* **14**(17), 1480–1494 (2006)
10. Aurich, J.C., Fuchs, C., Wagenknecht, C.: Modular design of technical product-service systems. In: *Brissaud, D., Tichkiewitch, S., Zwolinski, P. (eds.) Innovation in Life Cycle Engineering and Sustainable Development*, pp. 303–320. Springer, Dordrecht (2006)
11. Cook, M.B.: Understanding the potential opportunities provided by service-orientated concepts to improve resource productivity, In: *Bhamra, T., Hon, B. (eds.) Design and Manufacture for Sustainable Development*, pp. 123–134. Professional Engineering Publishing, Bury St. Edmonds (UK) (2004)
12. Tukker, A., van Halen, C.: *Innovation Scan Product Service Combinations Manual*. PWC, Delft/Utrecht. [www.score-network.org/files/827\\_17.pdf](http://www.score-network.org/files/827_17.pdf) (2003). Accessed 28 Apr 2017
13. van Ostaeyen, J., van Horenbeek, A., Pintelon, L., Dufloy, J.R.: A refined typology of product-service systems based on functional hierarchy modeling. *J. Clean. Prod.* **51**, 261–276 (2013)



14. Fliess, S., Becker, U.: Supplier integration: controlling of co-development processes. *Ind. Mark. Manage.* **35**(1), 28–44 (2006)
15. Bitner, M.J., Ostrom, A.L., Morgan, F.L.: Service blueprinting: a practical technique for service innovation. *Calif. Manag. Rev.* **50**(3), 66–94 (2008)
16. Cagno, E.: Eco-efficiency for sustainable manufacturing: an extended environmental costing method. *Prod. Plan. Control* **23**(2–3), 134–144 (2012)
17. Morelli, N., Tollestrup, C.: New representation techniques for designing in a systemic perspective. In: *International Conference on Engineering and Product Design Education Conference, E&DPE'06, Salzburg, 2006*, pp. 81–86 (FH-Salzburg)
18. Mien, L.H., Feng, L.W., Gay, R., Leng, K.: An integrated manufacturing and product services system (IMPSS) concept for sustainable product development. In: *International Symposium on Environmentally Conscious Design and Inverse Manufacturing, EcoDesign'05, Tokyo, 2005*, pp. 656–662 (IEEE)
19. Lujing, Y., Xing, K., Lee, S.H.: Framework for PSS from service' perspective. In: *International MultiConference of Engineers and Computer Scientists, IMECS'10, vol. 3, Hong Kong, 2010*, pp. 1656–1661 (IAENG)
20. Schoemaker, P.J.H.: Scenario planning: a tool for strategic thinking. *Sloan Manag. Rev.* **36**(2), 25–40 (1995)
21. den Ouden, E.: *Innovation Design: Creating Value for People, Organizations and Society*. Springer, London (2012)
22. Allee, V.: Reconfiguring the value network. *J. Bus. Strateg.* **21**(4), 36–39 (2000)
23. Tukker, A., Tischner, U.: Product-services as a research field: past, present and future. Reflections from a decade of research. *J. Clean. Prod.* **14**(17), 1552–1556 (2006)
24. Tukker, A.: Product services for a resource-efficient and circular economy—a review. *J. Clean. Prod.* **97**, 76–91 (2015)
25. Geng, X., Chu, X., Xue, D., Zhang, Z.: A systematic decision-making approach for the optimal product-service system planning. *Expert Syst. Appl.* **38**(9), 11849–11858 (2011)
26. Baines, T.S., Lightfoot, H.: *Made to Serve: How Manufacturers Can Compete Through Servitization and Product Service Systems*. Wiley, Chichester (UK) (2013)
27. Philips. Case study RAU Architects. [faculty.som.yale.edu/florianederer/behavioral/Pay-per-Lux.pdf](http://faculty.som.yale.edu/florianederer/behavioral/Pay-per-Lux.pdf). Accessed 30 Apr 2017
28. Schuh, G., Potentme, T., Schittny, B., Wittek, A.: Industrial product-service-systems for the tooling industry. In: *International Conference on Concurrent Enterprising, ICE'11, Aachen, 2011*, pp. 1–8 (RWTH Aachen)
29. Michaeli, W., Neuss, A., Wunderle, J.: Integrative process and product development for hybrid plastic-metal components. In: Brecher, C. (ed.) *Integrative Production Technology for High-Wage Countries*. Springer, Berlin Heidelberg (2012)
30. Henriksen, B., Røstad, C.C.: Paths for modularization. In: *IFIP International Conference on Advances Production Management Systems, APMS'14, vol. 3, Ajaccio, 2014*, pp. 272–279 (Springer)

# Development of a Speech System Using BCI Based on ERD/ERS for Patients Suffering from Amyotrophic Lateral Sclerosis

Arkadiusz Kubacki and Dominik Rybarczyk

**Abstract** The article describes the design process for a speech synthesis system based on ERD/ERS for patients suffering from amyotrophic lateral sclerosis (ALS) and for other patients with significantly reduced mobility. The authors performed a literature overview concerning the disease and the systems currently supporting speaking. The method described here is based on ERD/ERS technology. The system was built with the use of bioactive sensors mounted on the head, triggered by a signal known as MI- tasks. The raw signals are transmitted to the external application via VRPN server and, after filtering, is allowed to build the words and phrases. The device has been tested so that the optimal location of the sensor on the head could be chosen.

**Keywords** EEG · Electroencephalography · BCI · Brain-computer interface ERD/ERS · Amyo-trophic lateral sclerosis · ALS · Speech helping system

## 1 Introduction

Amyotrophic lateral sclerosis (ALS, Lou Gehrig's disease or motor neuron disease) is a motor system disease that primarily affects the final common motor pathways in the spinal cord and brain. ALS is characterized by muscle twitching and stiffness which gradually worsens (muscles decreasing in size). The main problems for the patient are difficulty in moving, swallowing and breathing (in the advanced stages of the disease) [1–3].

Only a few clinics around the World conduct research which focuses on ALS treatment. Research focuses on the rehabilitation issues and the restoration of the patient's motor functions. From the patient's point of view, there is also the financial limitations which do not allow attempts at treatment in clinics abroad [4–6].

---

A. Kubacki (✉) · D. Rybarczyk  
Institute of Mechanical Technology, Poznan University of Technology,  
Skłodowska-Curie Square 5, 60-965 Poznan, Poland  
e-mail: arkadiusz.j.kubacki@doctorate.put.poznan.pl

One of the most important problems for patients suffering from ALS (especially from the social perspective) is the speaking issue. Patients with an advanced form of the disease speak or form words with great difficulty which are unclear and vague. From the medical point of view, this problem is referred to as dysarthria. Patients are almost unable to pronounce long complex phrases. This significantly reduces mental comfort. In Poland, there are currently 2500 people suffering from ALS.

Considering the above-mentioned reasons, it is advisable to search for another way to allow patients to properly express their words. In the presented article, the authors propose the construction of a system which enables patients suffering from ALS to pronounce words based on brain activity.

Help for ALS sufferers can be provided by building devices that improve the quality of their lives. Therefore, there is a need to build a low-cost system which will be provided as open source. In this article, the authors propose the construction of such a low-cost device enabling the pronouncing of words by patients suffering from ALS based on Electroencephalography. Electroencephalography is a non-invasive method used to record the activity of the brain from the examined person's skull via electrodes [7]. A brain-computer interface based on ERD/ERS technique was proposed and to record EEG signals, the authors used an Emotiv EPOC+ headset. This headset has 14 electrodes situated in the "10–20" system—nowadays, it is the most popular and most commonly used [8]. Finally, in this method, the distance between electrodes is calculated as a percentage of skull size.

## *1.1 Literature Overview*

Authors of previous articles [9] propose a mobile sensing system for capturing and recognizing a diverse range of non-speech body sounds, one example is a system called BodyBeat. This consists of a piezoelectric microphone, ARM microcontroller, and a smartphone with the Android operating system. Because of the problems with muscle control in people with ALS, the method described in [9] is not suitable.

In another article [10], the authors detailed crosscutting knowledge about speech problems in an ALS context. They focused on acoustic measurements of phonatory instability (amplitude, frequency, shimmer, jitter, harmonics-to-noise ratio coefficients), phonatory limits, and the nasal-oral amplitude ratio.

The authors of the presented article proposed a low-cost system as detailed in [11]. The system is based on piezo sensors, which are triggered by mimicking face movements. The signal is then transmitted to the external application via USB interface, allowing the patient to construct words and phrases. Research was also conducted to find the optimal location of the sensors on the head.

In article [12], the authors presented a brain-computer interface based on ERD/ERS, using this interface to control a wheelchair. The main aim for the patient was to drive the wheelchair on a figure-8 course. For the test, the authors used a JW active model wheelchair from the Yamaha Motor Co. which is rear-wheel drive.

The patients achieved a success rate of over 90% in the conducted experiments and one patient achieved a 95% success rate.

In the next article [13], the authors used ERD/ERS to control a virtual helicopter. They made a virtual room in which the tested person had the task of flying through appearing rings. During the investigations, when the person imagined raising their right hand the helicopter flew to the right, when raising their left hand, the helicopter flew to the left. Raising both hands simultaneously resulted in the ascent of the vehicle.

A similar topic is touched on in article [14]. Authors of this article used real UAV. Using ERD/ERS they gave commands allowing them to control a vehicle in an indoor environment. In all experiments conducted, the researcher achieved a 94.36% success rate.

In article [15], authors used one of the passive methods to build BCI. They used blinking screens as stimulation in a Steady state visually evoked potential (SSVEP) method. Recognizing the frequency nearby the O electrode, the authors were able to determine which screen the subject looked at.

## 2 System Structure

### 2.1 ERD/ERS Method

The method used by the authors is based on the alpha rhythm (8–13 Hz) and beta rhythm (14–30 Hz) of brain activity. During the body's preparation for physical motion, alpha and beta oscillations decrease which is called event-related desynchronization (ERD). After the occurrence of the motion, the oscillations will increase. This situation is called event-related synchronization (ERS). For example, when a person's left hand motion is visualized, the ERD occurs on the right side of the sensorimotor cortex. For the thought process of right hand motion, ERD results in the appearance of the left side of the sensorimotor cortex. The thought process of lifting up both feet causes an ERD to appear in the vicinity of the Cz electrode (Fig. 1). Using this phenomenon, it is possible to control an object by extracting commands from brain signals [12]. This method belongs to the group of active methods. This means that the patient is not subjected to any stimulation by the external element. Taking into account that the authors used ERD/ERS, only the idea of lifting feet was tested.

The method described above can be implemented in Emotive EPOC+ devices with external software. The headset with electrodes can be mounted easily on the patient's head (Fig. 2). This method requires looking at the monitor screen with a dedicated application (presented in the next chapter).

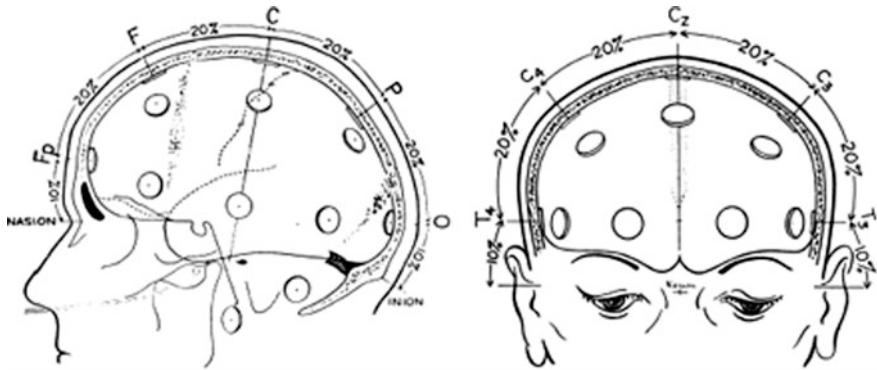


Fig. 1 Electrode placement in accordance with the “10–20” system [8]

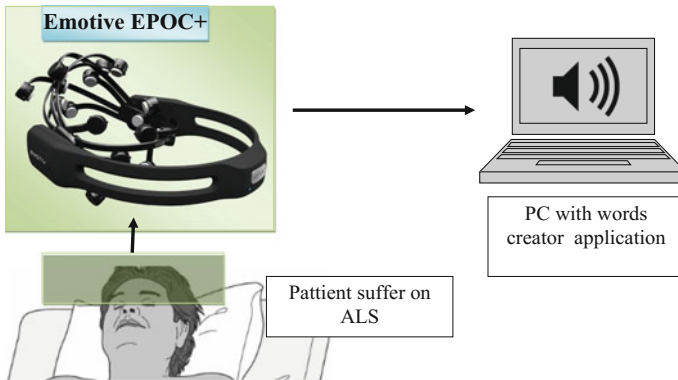
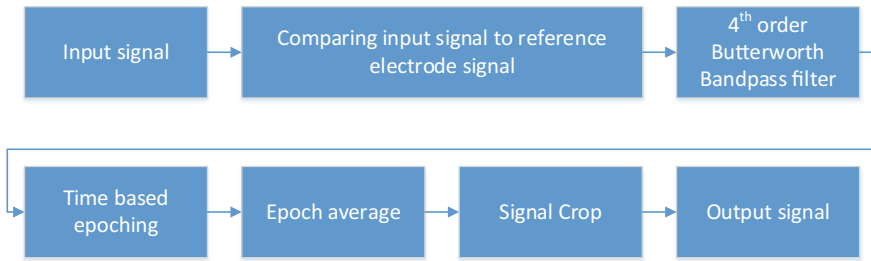


Fig. 2 System structure

### 2.2 Algorithm

The program in OpenVibe collects the EEG signal from all electrodes using Emotiv EPOC+. The recorded signal goes to a block comparing the input signal to the signal from the referenced electrode. The next block is a 4th order Butterworth Bandpass filter which transmits the signal only on the frequency of oscillation before and after movement of feet (16–24 Hz). Another block divides the signal into epochs, which subsequently are averaged. The averaged signal goes to the next block which crops information into a suitable compartment. The output signal is sent via VPRN server to an application described below.

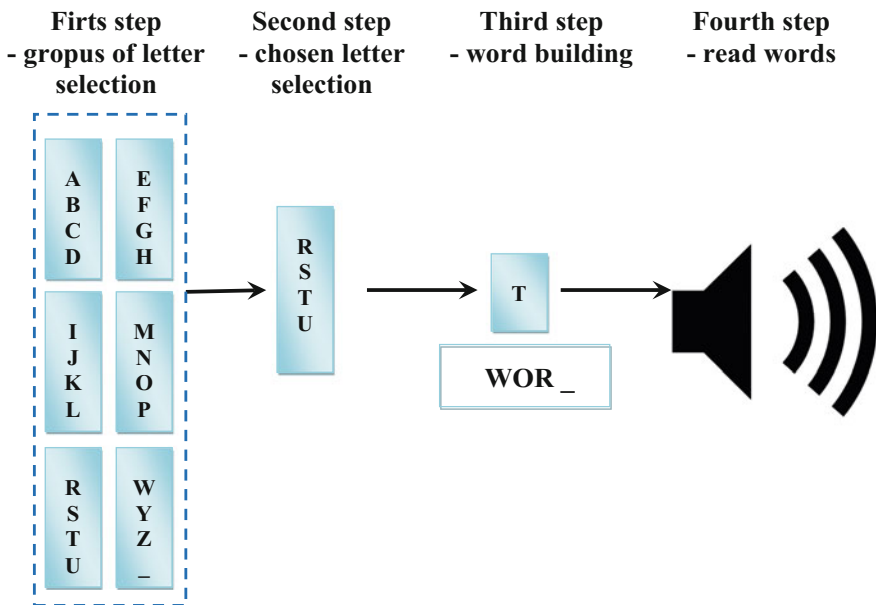
Typing the words and the letters proceeds in several steps. An algorithm used for this is presented in Fig. 3. The groups of letters are displayed in several independent groups, for ex. “A, B, C, D”. After selecting the appropriate group, it becomes



**Fig. 3** Flow diagram for the command recognition by ERD/ERS

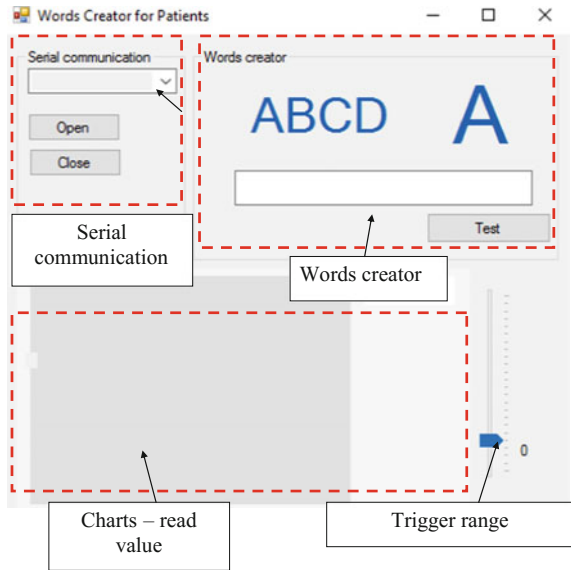
possible to select letters directly from the chosen group. Reading the whole formed phrase is possible by underscore mark selection. The triggered signal is taken from outside the application it is prepared in.

For expressing words and machine speaking, the authors prepared a dedicated application (Fig. 4) and used the Microsoft Speech Platform SDK [16], which provides a comprehensive set of development tools for managing the Speech Platform Runtime in voice-enabled applications, such as recognizing spoken words (speech recognition) and generating synthesized speech (text-to-speech system). The library has support for different languages and does not require connection to the Internet (important for convenient usage). In the case of wrongly entered phrases, the system doesn't crash but, rather, it reads each letter separately (Fig. 5).



**Fig. 4** Typing words—algorithm

Fig. 5 Application form



A prototype of the system as described here is presented in Fig. 6. The system requires further clinical tests (upon receiving of the relevant permits).

### 3 Results and Discussion

The aim of the performed experiments was to investigate the possibility of using the ERD/ERS technique for typing letters and words. The authors tested the system reliability and ease of use. They tested this system on two people and results were similar for both.

After putting on the head set with electrodes and running the application, the task was to write given words. Groups of letters were displayed according to the algorithm described in Sect. 2.2 and selecting of the letters was realized when the tested person thought of moving their foot. Data collected after 4th order Butterworth Bandpass filter, which transmits the signal only on the frequency of oscillation before and after movement of feet (16–24 Hz), is shown in Fig. 7. According to the theory, motion or imagination of foot motion results in the appearance of oscillations in the 16–24 Hz band. After the filtration process described in Sect. 2.2, the received signal (Fig. 8) acts as the trigger and allows selection of the letter. The signal after averaging over epochs is ideally suited to the applications described by the authors. In addition, the ability to set a threshold for a command allows the system to be adapted to many people. It should also be kept in mind that the use of ERD/ERS is related to the training of the subjects. While triggering of the signal by physical foot movement is not a problem, the ability to call commands through the imagery itself is developed through training.



Fig. 6 View of built system

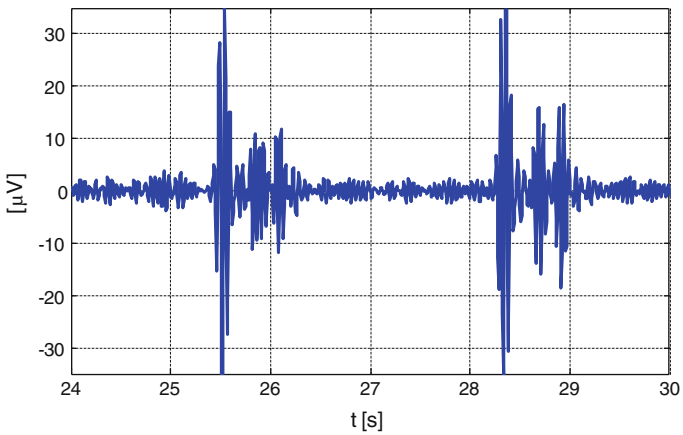
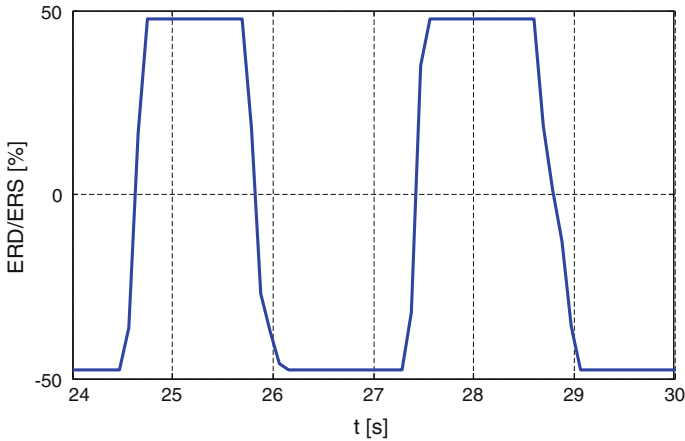
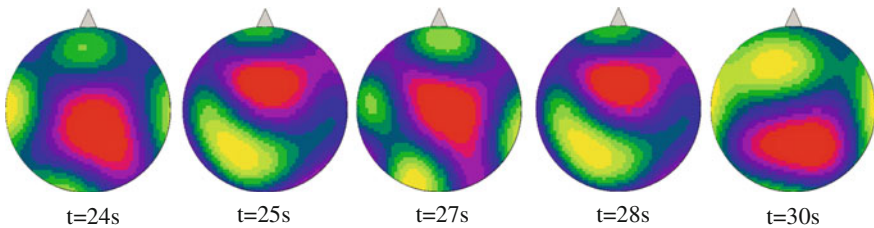


Fig. 7 Raw data after 4th order Butterworth Bandpass filter (16–24 Hz)





**Fig. 8** Output signal after filtration



**Fig. 9** Graphical representation of brain activity during test (top view)

In addition, the collected information was presented in graphical form representing changing brain activity (Fig. 9). The task as described required some training of the patient. The picture clearly shows that brain activity increases in the neighborhood of the electrode Cz cell while stimulating the brain by imagining the movement of the feet. Unfortunately, the number of electrodes in the Emotiv EPOC+ set clearly limits the spatial resolution of the brain map. Better results can certainly be obtained by using more elaborate sets. Unfortunately, there are no sets of high numbers of electrodes in this region. Another way would be to use medical kits, however, their price does not allow for the construction of cheap and portable kits for ALS patients.

## 4 Conclusion

The article described construction of a speaking help system based on ERD/ERS techniques for patients suffering from amyotrophic lateral sclerosis (ALS) and for patients with significant reduction in mobility. The first part focused on the disease and development of systems to support speaking. Based on set assumptions, the system described here was based on the ERD/ERS technique using bioactive sensors mounted on the head, which were triggered by a signal called MI- tasks. The raw signals were transmitted to the external application via VRPN server and, after filtering, allowed for building of words and phrases. Currently, it is not expected to conduct clinical trials of the device due to the work still being carried out on it. This type of system can be used in the future for setting process parameters and triggers.

The described work is an extension of the research described in the publication [11]. Data read was based on small mimic motions registered by low-cost piezo sensors. The advantage of the method presented here is there is no need for any physical movement (which is very important in the case of illnesses like ALS).

The authors also pointed out some disadvantages of the device presented here, such as speed of entering letters and forming words. Depending on the amount of time spent on training regarding operation of the device, these values are within roughly 40 s for less than 10—letter words. In the case of building complex phrases, this value may be too high. For this reason, it is important to conduct further research.

**Acknowledgements** The work described in this paper was funded from 02/22/DSPB/1389.

## References

1. Kiernan, M.C., et al.: Amyotrophic lateral sclerosis. *Lancet*. **377**(9769), 942–955 (2011)
2. Rowland, L.P., Shneider, N.A.: Amyotrophic lateral sclerosis. *N. Engl. J. Med.* **344**(22), 1688–1700 (2001)
3. Wijesekera, L.C., Nigel, Leigh P.: Amyotrophic lateral sclerosis. *Orphanet J Rare Dis.* **4**, 3 (2009)
4. Van den Berg, J.P., et al.: Multidisciplinary ALS care improves quality of life in patients with ALS. *Neurology* **65**(8), 1264–1267 (2005)
5. Van den Berg, J.P., Kalmijn, S., Lindeman, E., Wokke, J.H., van den Berg, L.H.: Reha-bilitation care for patients with ALS in the Netherlands. *Amyotrophic Lateral Scler. Other Mot. Neuron Disord.* **4**(3), 186–190 (2003)
6. Ottenbacher, K.J., Jannell, S.: The results of clinical trials in stroke rehabilitation re-search. *Arch. Neurol.* **50**(1), 37–44 (1993)
7. Fiscon, G., Weitschek, E., Felici, G., Bertolazzi, P., Salvo, S.D., Bramanti, P., Cola, M.C.D.: Alzheimers disease patients classification through EEG signals processing, In: *IEEE Symposium on Computational Intelligence and Data Mining (CIDM)*, 2014
8. Zyss, T.: Application of 10–20 system in placing electrodes into EEG (in Polish). *ELMIKO company, Poland* (2007)

9. Happ, M., Roesch, T., Kagan, S.: Patient communication following head and neck cancer surgery: a pilot study using electronic speech-generating devices. *Oncol. Nurs. Forum* **32**(6), 1179–1187 (2005)
10. Ramig, L.O., Scherer, R.C., Klasner, E.R., Titze, I.R., Horii, Y.: Acoustic analysis of voice in amyotrophic lateral sclerosis a longitudinal case study. *J. Speech Hear. Disord.* **55**, 2–14 (1990)
11. Rybarczyk, D., Kubacki, A.: Development of low cost speech system for patient suffer on the amyotrophic lateral sclerosis, pp. 441–449. Springer, New York (2017)
12. Choi, K.: Control of a vehicle with EEG signals in real-time and system evaluation. *Eur. J. Appl. Physiol.* **112**(2), 755–766 (2011)
13. Royer, A.S., Doud, A.J., Rose, M.L., He, B.: EEG control of a virtual helicopter in 3-dimensional space using intelligent control strategies. *IEEE Trans. Neural. Syst. Rehabil. Eng.* **18**(6), 581–589 (2010)
14. Shi, T., Wang, H., Zhang, C.: Brain Computer interface system based on indoor semi-autonomous navigation and motor imagery for unmanned aerial vehicle control. *Expert Syst. Appl.* **42**(9), 4196–4206 (2015)
15. Bi, L., Fan, X., Jie, K., Teng, T., Ding, H., Liu, Y.: Using a head-up display-based steady-state visually evoked potential brain-computer interface to control a simulated vehicle. *IEEE Trans. Intell. Transp. Syst.* **15**(3), 959–966 (2014)
16. Microsoft web page with SDK documentation: <https://www.microsoft.com/>. Available 1 Oct 2016

# GPenSIM for Performance Evaluation of Event Graphs

Reggie Davidrajuh, Bozena Skolud and Damian Krenczyk

**Abstract** Performance evaluation of a manufacturing system is to find out some useful information about the behavior of the system. Usually, Petri nets are very useful tool for modeling and performance evaluation of manufacturing systems. Literature review reveals that the Petri net models of manufacturing systems are most frequently event graphs, a special type of Petri nets; in addition, they are strongly connected event graphs. Literature review also reveals that there are some simple yet powerful methods for performance evaluation of strongly connected event graphs. General-purpose Petri net simulator (GPenSIM) is a new tool for modeling, simulation, and performance analysis of discrete event systems. This paper is about implementation and application of event graphs in GPenSIM, for performance analysis of real-world manufacturing systems.

**Keywords** Petri nets · Event graphs · GPenSIM · Performance evaluation  
Manufacturing systems

## 1 Introduction

Performance evaluation of a manufacturing system is to find out some useful information about the behavior of the system such as the productivity (flow rate), the existence of bottlenecks and deadlocks, etc. Usually, Petri nets are very useful for performance evaluation of manufacturing systems because of its very useful properties such as self-documenting, simple yet powerful mathematical background, and explicit stateful information. Literature review reveals that the Petri net models of manufacturing systems are most frequently event graphs, a special type of Petri nets; in addition, they are strongly connected event graphs. The literature

---

R. Davidrajuh (✉)

Faculty of Science and Technology, University of Stavanger, Stavanger, Norway  
e-mail: Reggie.Davidrajuh@uis.no

B. Skolud · D. Krenczyk

Faculty of Mechanical Engineering, Silesian University of Technology, Gliwice, Poland

© Springer International Publishing AG 2018

A. Hamrol et al. (eds.), *Advances in Manufacturing*, Lecture Notes in Mechanical Engineering, [https://doi.org/10.1007/978-3-319-68619-6\\_28](https://doi.org/10.1007/978-3-319-68619-6_28)

289

review also reveals that there are some simple yet powerful methods for performance evaluation and that these methods are only applicable for strongly connected event graphs.

General-purpose Petri net simulator (GPenSIM) is a new tool for modeling, simulation, and performance analysis of discrete event systems. GPenSIM, developed by the first author of this paper, is being used by many universities around the world. The aim and scope of this paper are implementation and application of event graphs in GPenSIM, for solving real-world manufacturing problems.

In this paper, Sect. 2 introduces event graphs. Section 3 introduces GPenSIM. Section 4 presents an application example.

## 2 Event Graphs: Definition and Properties

An event graph is an ordinary Petri net in which each place has exactly one input and one output transition.

### 2.1 Definitions [1, 2]

#### Definition: Classic Petri Net (PN)

A classic Petri net is a four-tuple  $PN = (P, T, A, m_0)$ , where

$P$  is the set of places,  $P = [p_1, p_2, \dots, p_n]$ ,

$T$  is the set of transitions,  $T = [t_1, t_2, \dots, t_m]$ ,

$A$  is the set of arcs (from places to transitions and from transitions to places),

$$A \subseteq (P \times T) \cup (T \times P), \text{ and}$$

$m$  is the row vector of markings (tokens) on the set of places;

$m = [m(p_1), m(p_2), \dots, m(p_n)] \in N^n$ ,  $m_0$  is the initial marking.

#### Definition: input and output sets of a place

It is convenient to use  $\bullet p_j$  to represent the set of input transitions of a place and  $p_j \bullet$  to represent the set of output transitions of  $p_j$ .

$$\bullet p_j = \{t_i \in T : (t_i, p_j) \in A\}, p_j \bullet = \{t_i \in T : (p_j, t_i) \in A\}.$$

#### Definition: Timed Petri Net (TPN)

Timed Petri net is a 4-tuple  $TPN = (P, T, A, m_0, D)$ , where

$PN = (P, T, A, m_0)$  is a classic Petri net and

$D: T \rightarrow R^+$  is the duration function, a mapping of each transition into a positive rational number, meaning firing of each transition  $t_i$  takes  $dt_i$  time units.

**Definition: Event Graph (EG)**

Event graph is a classic Petri net  $EG = (P, T, A, m_0)$ , where the sets of input and output transitions of every place have only one member.  $|\bullet p_j| = |p_j \bullet| = 1$ .

**Definition: Strongly Connected Graph**

A directed graph is strongly connected if there is a directed path joining any two nodes of the graph. In a strongly connected graph, there will be cycles (circuits).

**Definition: Elementary Circuit**

An elementary circuit in a strongly connected graph has a directed path that goes from one node and comes back to the same node, while no other node is not repeatedly visited in the path.

## 2.2 Properties of Strongly Connected Event Graphs

Given below are some of the properties of *strongly connected event graph (SCEG)*. These properties are very useful for performance evaluation of discrete event systems. In an SCEG,

- Property-1: The number of tokens in an elementary circuit is invariant, meaning the number of tokens does not change with the firings of the transitions [1, 3].
- Property-2: Performance is bounded by its critical circuit [1, 4]. The critical circuit is the elementary circuit that has the lowest flowrate  $r$ .  $r^* = \min \Sigma(m(p_n))/\Sigma(dt_i)$ , where  $\Sigma(dt_i)$  is the sum of firing times of the transitions in the circuit and  $\Sigma(m(p_n))$  is the sum of all tokens in that circuit.
- Property-3: Under the assumption that a transition fire as soon as it is enabled, the firing rate of each transition in steady state (the same as the current token flow rate at any point in the circuit) is given by  $r = r^*$  [4].
- Property-4: Deadlock-free if and only if every elementary circuit contains at least one token [1].

Based on the properties mentioned above, there are many tools available for performance evaluation of SCEG. However, the General-Purpose Petri Net Simulator (GPenSIM) is considered as the ideal tool for working with event graphs [5], and for interacting with other MATLAB toolboxes [6]. The following section describes the functions of GPenSIM for working with SCEG.

## 3 GPenSIM

In GPenSIM, a discrete system can be modeled either as [7, 8]

- A classic Petri net: firing times are not assigned to any of the transitions, meaning all the transitions are primitive [2], or
- A timed Petri net: firing times are assigned to all the transitions, meaning all the transitions are non-primitive.

### 3.1 Modeling Timed Petri Nets in GPenSIM

In GPenSIM, it is not acceptable to assign firing times to some of the transitions and let the other transitions take zero value; we may assign very small values close to zero, but not zero, to transitions that are very fast compared to the other transitions [GPenSIM]. GPenSIM interprets timed Petri net in the following manner [7, 8]:

- No variable duration of events: the transitions representing events are assigned firing time beforehand. The preassigned firing time can be deterministic (e.g., firing time  $d_{ti} = 5$  TU) or stochastic (e.g., firing time  $d_{ti}$  is normally distributed with mean value 10 TU and standard deviation 2 TU). However, variable firing times are not possible.
- Maximal-step firing policy: Timed Petri Net operates with the maximal-step firing policy; this means, if more than one transition is collectively enabled and are not in conflict with each other at a point of time, then all of them fire at the same time.
- Enabled transition starts firing immediately: enabled transition can start firing immediately as long as there is no (forcibly) induced delay between the time a transition became enabled and the time it is allowed to fire.

### 3.2 The Functions for Performance Evaluation of Event Graphs

Table 1 lists some of the GPenSIM functions that are exclusively for performance evaluation of strongly connected event graph (SCEG).

The “*pnclass*” function: this function checks the class of a Petri net. This function returns a vector of flags representing the following information.

- Flag-1: Whether the Petri net is a binary Petri net or not (0 = not a binary Petri net).  
 Flag-2: Whether the Petri net is a state machine or not (0 = not a state machine).  
 Flag-3: Whether the Petri net is an event graph or not (0 = not an event graph).  
 Flag-4: Whether the Petri net is a timed Petri net or not (0 = not a timed Petri net).  
 Flag-5: Number of strongly connected components in the Petri net.

**Table 1** GPenSIM functions for performance evaluation of SCEG

GPenSIM function	Purpose
<i>pnclass</i>	Find out the class of Petri net
<i>stronglyconn</i>	Find out the number of strongly connected components in the Petri net
<i>mincycetime</i>	Finding the performance bottleneck in an SCEG
<i>Cycles</i>	Extract the elementary circuits in a Petri net

The “*stronglyconn*” function: this function returns the number of strongly connected components in a Petri net. If the returned value is a singleton, then the Petri net is strongly connected. There are several algorithms for finding strongly connected components, e.g., a simple two-pass depth-first-search algorithm [9] and the recent and more efficient Rader’s method [10]. In GPenSIM, the Rader’s method is implemented. In Rader’s method, first the connection matrix  $D$  is computed,  $D = (I - \alpha A)^{-1}$ , where  $\alpha$  (convergence value) is a small value, usually between zero and one. Then, the SCC matrix which has a row for each connected component is computed,  $SCC = D \times DT$ .

The “*mincycetime*” function: this function returns the performance bottleneck (critical elementary circuit) of an SCEG. For finding the elementary circuits, this function makes use of the function “cycles”. The function *mincycetime* also suggests flow rate improvement, if the optional input parameter “expected flowrate” is given. Since current flowrate  $r^* = [\Sigma(m(p_n))/\Sigma(dt_i)]^{\text{critical circuit}}$ , expected flowrate (efr) can be achieved by either:

- Increasing the token count the critical circuit by  $\Delta m0$ ,

$$\Delta m0 = [\text{efr} \times \Sigma(dt_i)] - \Sigma(m(p_n)), \text{ or}$$

- Reducing the delay (total firing times) of the circuit by  $\Delta ft$ ,

$$\Delta ft = \Sigma(dt_i) - [\Sigma(m(p_n))/\text{efr}]$$

The “*cycles*” function: this function finds the elementary circuits in a Petri net. There are several algorithms available for finding the elementary circuits, e.g., Tiernan & Tarjan’s method [11] and Johnson’s method [12]. However, the algorithm that is implemented in GPenSIM is a simple variant of depth-first-search technique. Even though this algorithm is not the most efficient, it is chosen because of its easiness for implementation.

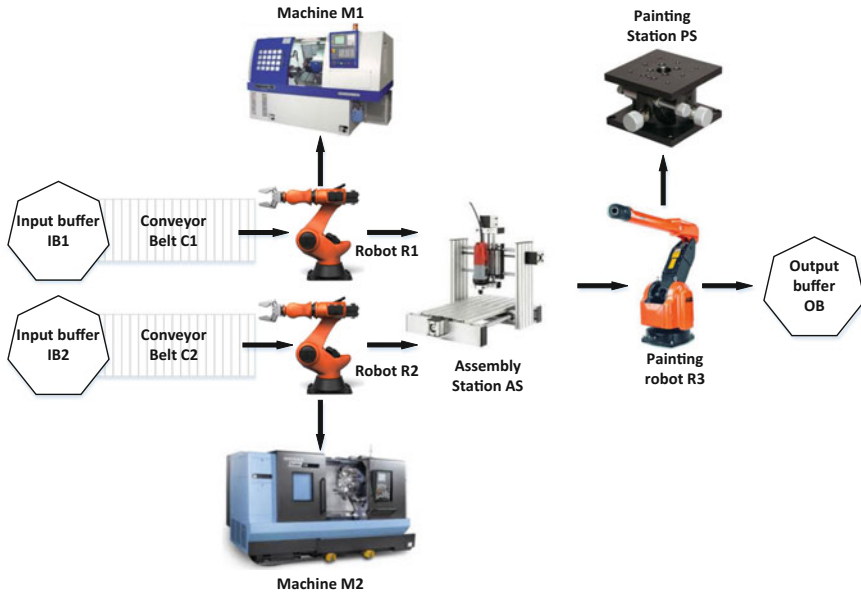
## 4 Application Example

A simple Flexible Manufacturing System (FMS) is shown in Fig. 1 which is to make only one product.

In this FMS,

- The input raw material of type-1 arrives on the conveyor belt C1. Robot R1 picks the raw material type-1 and places into the machine M1. Similarly, robot R2 picks the raw material from conveyor belt C2 and places into the machine M2.





**Fig. 1** The flexible manufacturing system

- Machine M1 makes the part P1, and M2 makes the part P2. When the parts are made by the machine M1 and M2, they are placed on the assembly station by the robots R1 and R2, respectively.
- An assembly station AS joins the two parts P1 and P2 together to form the product. The robot R2 does the part assembly at AS.
- Robot R3 picks the product from the assembly station and places it on the painting (and polishing) station PS. Robot R3 performs the painting and then put the completed product into the output buffer (cartridge) OB.

The following activities explain the FMS operations (“*t*” stand for transition):

- *t*C1: conveyor belt C1 brings the input material type-1 into the FMS.
- *t*C2: conveyor belt C2 brings the input material type-2 into the FMS.
- *t*C1M1: robot R1 moves raw material from conveyor belt C1 to M1.
- *t*C2M2: robot R2 moves raw material from conveyor belt C2 to M2.
- *t*M1: machining of Part-1 at machine M1.
- *t*M2: machining of Part-2 at machine M2.
- *t*MA: robot R1 moves part-1 from M1 and R2 moves part-2 from M2 into assembly station AS.
- *t*AS: robot R2 assembles parts P1 and P2 together at the assembly station AS.
- *t*AP: robot R3 picks the product from the assembly station and places on the painting station PS.
- *t*PS: robot R3 performs painting and surface polishing on the product. When the job is finished, R3 places the product into the output buffer OB.

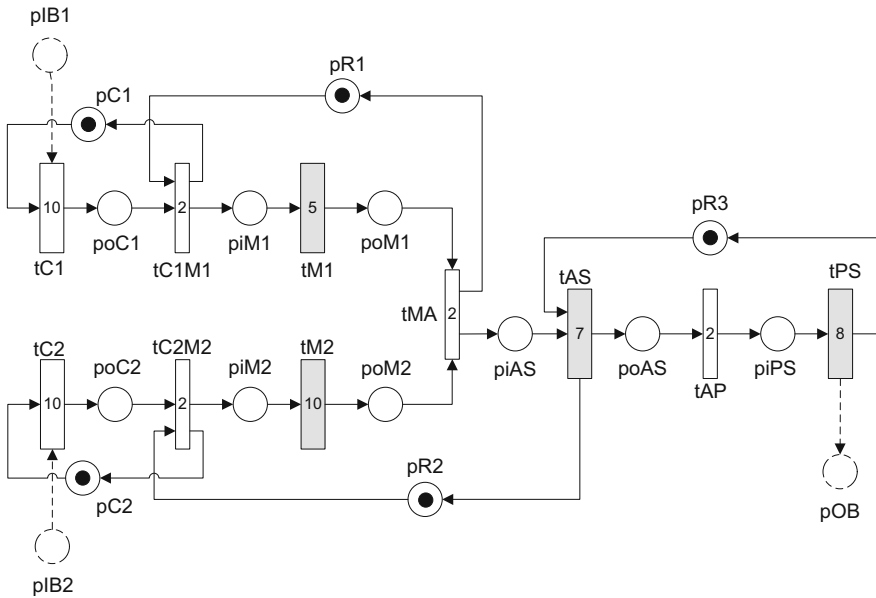


Fig. 2 Petri net model of the FMS

### 4.1 The Petri Net Model

The Petri net model of the FMS is shown in Fig. 2. The Petri net model is obtained by serially connecting the operations listed above; the time taken by the operations are shown in Fig. 2 as the firing times of the transitions.

The input buffers IB1 and IB2 (represented by the places pIB1 and pIB2) and the output buffer (place pOB) are for testing purpose only. These three places will be omitted in the final model, to make it as an SCEG. The presence of the three places will destroy the strongly connectedness property, and the Petri net will not be an event graph. It is safe to neglect the three buffers with the following assumptions:

1. The supply of raw materials from the input buffers (IB1 and IB2) is never exhausted;
2. The finished product will be placed into the output buffer OB that has no capacity restraints.

### 4.2 GPenSIM Code for Simulation

We usually need four files to code (implement) a Petri net model in GPenSIM:

1. Petri Net Definition File (PDF): this is the coding of the static Petri net (the structure of the Petri net defined by the sets of places, transitions, and arcs).
2. Main Simulation File (MSF): In this file, the initial dynamics (e.g., initial tokens in places pC1, pC2, pR1, pR2, and pR3, and the firing times of transitions) are declared.
3. COMMON\_PRE: In this file, the conditions for the enabled transitions to start firing are coded. However, in this FMS example, there are no additional conditions for the transitions as they start firing whenever they become enabled.
4. COMMON\_POST: the post-firing actions of the transitions are coded in this file. Again, this file is not necessary for the FMS example, as there are no post-actions needed to be carried out.

Given below is the PDF in which the sets of places, transitions, and the arcs declared:

```
function [png] = fms_pdf()
png.PN_name = 'Event Graph model of FMS';
%%%%%%%%%%%%%%%%%%%%%%%%%%%%%%%%%%%%%%%%%%%%%%%%%%%%%%%%%%%%%%%% set of places
png.set_of_Ps = {'pC1','pC2', 'pR1','pR2','pR3', ...
                'poC1','poC2','piM1','poM1', 'piM2',...
                'poM2','piAS','poAS', 'piPS'};
%%%%%%%%%%%%%%%%%%%%%%%%%%%%%%%%%%%%%%%%%%%%%%%%%%%%%%%%%%%%%%%% set of transitions
png.set_of_Ts = {'tC1','tC2','tM1','tM2','tAS','tPS',...
                'tC1M1','tC2M2','tMA', 'tAP'};
%%%%%%%%%%%%%%%%%%%%%%%%%%%%%%%%%%%%%%%%%%%%%%%%%%%%%%%%%%%%%%%% set of arcs
png.set_of_As = {'pC1','tC1',1, 'tC1','poC1',1, ... %tC1
                'pR1','tC1M1',1, 'poC1','tC1M1',1,...%tC1M1
                'tC1M1','piM1',1, 'tC1M1','pC1',1, ... %tC1M1
                'piM1','tM1',1, 'tM1','poM1',1, ... %tM1
                'pC2','tC2',1, 'tC2','poC2',1, ... %tC2
                'pR2','tC2M2',1, 'poC2','tC2M2',1,...%tC2M2
                'tC2M2','piM2',1, 'tC2M2','pC2',1,... %tC2M2
                'piM2','tM2',1, 'tM2','poM2',1, ... %tM2
                'poM1','tMA',1, 'poM2','tMA',1, ... %tMA
                'tMA','piAS',1, 'tMA','pR1',1, ... %tMA
                'piAS','tAS',1, 'pR3','tAS',1,... %tAS
                'tAS','poAS',1, 'tAS','pR2',1, ... %tAS
                'poAS','tAP',1, 'tAP','piPS',1, ... %tAP
                'piPS','tPS',1, 'tPS','pR3',1}; % tPS
```

The main simulation file is given below:

```
clear all; clc;
global global_info
global_info.STOP_AT = 100; % stop simulation after 100 TU
pns = pnstruct('fms_pdf'); % declare the PDF
% declare the firing times of the transistons
dyn.ft = {'tC1',10,'tC2',10, 'tC1M1',2,'tC2M2',2,...
          'tM1',5,'tM2',10,'tMA',2, 'tAS',7, 'tAP',2, 'tPS',8};
% declare the initial markings
dyn.m0 = {'pC1',1,'pC2',1, 'pR1',1,'pR2',1,'pR3',1};
% combine static and dynamic parts to form the Petri net
pni = initialdynamics(pns, dyn);
mincyctime(pni); % find the minimum cycle of event graph
```

### 4.3 The Simulation Results

The simulation results show that there are five elementary circuits (“cycles” in the results shown below) in the event graph.

```
This is a Strongly Connected Petri net.
This is an Event Graph (Marked Graph).
Cycle-1:-> pC1 -> tC1 -> poC1 -> tC1M1
TotalTD = 12 TokenSum = 1 CycleTime = 12
Cycle-2:-> pR1 -> tC1M1 -> piM1 -> tM1 -> poM1 -> tMA
TotalTD = 9 TokenSum = 1 CycleTime = 9
Cycle-3:-> pC2 -> tC2 -> poC2 -> tC2M2
TotalTD = 12 TokenSum = 1 CycleTime = 12
Cycle-4:-> tMA-> piAS-> tAS-> pR2-> tC2M2 -> piM2 -> tM2 -> poM2
TotalTD = 21 TokenSum = 1 CycleTime = 21
Cycle-5:-> poAS -> tAP -> piPS -> tPS -> pR3 -> tAS
TotalTD = 17 TokenSum = 1 CycleTime = 17
*** Minimum-cycle-time is: 21, in cycle number-4 ***
*** Token Flow Rate: *** In steady state, the firing rate of each
transition:1/C* = 0.047619 meaning, on average, 0.047619 tokens
pass through any node in the Petri net, per unit period of time.
*** We can increase the current flow rate to 0.058824 tokens/TU, by
improving the critical circuit alone ...
```

In the circuit-4 either: 1. increase the sum of tokens by 1 tokens, or, 2. decrease the total delay (firing times) by 4 TU.

\*\*\* Deadlocks: NO \*\*\* (each elementary circuit has at least one tokens each)

The results show that the elementary circuit number-4 is the bottleneck as it has highest cycle time (=21), which means the flow rate of the circuit is  $1/21 = 0.0476$  tokens per TU. The second highest cycle time (=17) belongs to the circuit number-5, having a flow rate of  $1/17 = 0.0588$ . Thus, we can improve the performance (flow rate) by 23.52% by enhancing the bottleneck (circuit number-4). The proposed enhancements are (1) increase the sum of tokens by one (meaning add one more robot/machine in parallel), and (2) decrease the total delay by 4 TU (meaning reduce the firing times of the robot/machine involved in circuit-4 by 4 TUs).

The results also show that there are no deadlocks (the Petri net is live) as every elementary circuit has at least one token each.

## 5 Discussion

General-Purpose Petri Net Simulator (GPenSIM) is a software for modeling, simulation, performance analysis, and control of discrete event systems. GPenSIM, developed by the first author of this paper, runs on MATLAB platform. Though GPenSIM is new, it has been accepted by many universities around the world because of its simplicity, flexibility, and for the possibilities to interact with the other MATLAB toolboxes and the external environment. GPenSIM (current version 9) can be freely downloaded from the website [7]. GPenSIM is being used to solve diverse problems within manufacturing, e.g., Solving Repetitive Production Planning Problems [13], Assembly Line Balancing Problems [14], Gameplay for manufacturing [15], and logical control system of a marine diesel engine [16]. In this paper, we focus on how GPenSIM can help performance analysis of discrete manufacturing systems if they can be modeled as event graphs.

**Acknowledgements** This paper was written when the first author was staying at the Silesian University of Technology, Poland, for his sabbatical leave. The first author wants to thank the Institute of Engineering Processes Automation and Integrated Manufacturing Systems of the Faculty of Mechanical Engineering, for hosting him.

## References

1. Peterson, J.L.: Petri nets. *ACM Comput. Surv. (CSUR)* **9**(3), 223–252 (1977)
2. Proth J.M.: Performance evaluation of manufacturing systems. In: *Practice of Petri Nets in Manufacturing*, pp. 147–183. Springer, Dordrecht (1993)
3. Commoner, F., Holt, A.W., Even, S., Pnueli, A.: Marked directed graphs. *J. Comput. Syst. Sci.* **5**(5), 511–523 (1971)
4. Chretienne, P.: Exécutions controlées des réseaux de Petri temporisés. *TSI. Technique et science informatiques* **3**(1), 23–31 (1984)
5. Cameron, A., Stumpfner, M., Nandagopal, N., Mayer, W., Mansell, T.: Rule-based peer-to-peer framework for decentralised real-time service oriented architectures. *Sci. Comput. Program* **97**, 202–234 (2015)
6. Lopez, F., Barton, K., Tilbury, D.: Simulation of discrete manufacturing systems with attributed hybrid dynamical nets. Submitted to CASE 2017, Xi'an, China
7. Davidrajuh, R.: GPenSIM: a general purpose Petri net simulator, URL: <http://www.davidrajuh.net/gpensim>
8. Davidrajuh R.: Developing a new Petri net tool for simulation of discrete event systems. *Modeling & Simulation, IEEE Second Asia International Conference*, pp. 861–866 (2008)
9. Cormen, T.H.: *Introduction to algorithms*. MIT press, Cambridge (2009)
10. Rader, C.M.: Connected components and minimum paths. *Graph Algorithms Lang Linear Algebra* **22**, 19 (2011)
11. Tiernan, J.C.: An efficient search algorithm to find the elementary circuits of a graph. *Commun. ACM* **13**(12), 722–726 (1970)
12. Johnson, D.B.: Finding all the elementary circuits of a directed graph. *SIAM J. Comput.* **4**(1), 77–84 (1975)
13. Skolud, B., Krenczyk, D., Davidrajuh, R.: Solving repetitive production planning problems. an approach based on activity-oriented petri nets. *Adv Intell Syst Comput.* **527**, 397–407. Springer, Cham (2016)
14. Davidrajuh R.: Solving assembly line balancing problems with emphasis on cost calculations: a petri nets based approach. *IEEE Eur. Model. Symp. (EMS)*, 99–104 (2014)
15. Chang, H.: A method of gameplay analysis by petri net model simulation. *J. Korea Game Soc.* **15**(5), 49–56 (2015)
16. Pan, X.L., He, G., Zhang, C.J., Ming, T.F., Wang, X.C.: Research on modeling and simulating of discrete event system based on petri net. *Adv. Eng. Forum* **4**, 80–85 (2012)

# Analysis of the Environmental Costs in Manufacturing Companies in the SME Sector in Poland

Lukasz Grudzien, Filip Osinski and Sabahudin Jasarevic

**Abstract** The article presents typical environmental aspects and costs related to those aspects in production companies in the SME sector in Poland. The study aimed to show what standard fees, charges, and other responsibilities enterprises have and what costs should be heard to minimize the environmental impact of the organization. Despite the low impact of a single manufacturing company from this sector, their quantity causes cumulative effects on the environment and should be considered significant. For this reason, it is important to build conscious, sustainable business, which besides of profit will be responsible for the state of the environment. For most companies, achieving that goal is possible through bearing all of the administrative and operative costs of environmental protection.

**Keywords** Environmental cost · Environmental fee · Use of environment · SME

## 1 Introduction

At present, we are witnessing dynamic economic development which in addition to its undoubted benefits also has negative effects, for example, in terms of its impact on the environment. Therefore, man undertakes many initiatives to reduce this negative impact. Increasingly often, companies use decision-making support methods for support production process [1, 2], quality tools [3, 4], or methods that help to minimize losses [5–7]. In the 1990s, the idea of sustainable development [8] was developed. It assumes such human activities that will satisfy current needs, while paying attention to the possibility of meeting these needs in the future generations. The idea of sustainable development has a special reference to companies

---

L. Grudzien (✉) · F. Osinski  
Management and Production Engineering,  
Poznan University of Technology, Poznan, Poland  
e-mail: lukasz.grudzien@put.poznan.pl

S. Jasarevic  
University of Zenica, Zenica, Bosnia and Herzegovina

that use elements of the environment to meet their own needs. On the one hand, it is drawing on the resources (stock consumption, water, etc.) on the other, causing environmental burden (emissions, waste generation, etc.). The above effect is mainly a domain of manufacturing companies that need specific resources to produce a particular product and must implement processes, which are also products of output side, which is almost always a burden for the environment. In order to reduce the negative impact on the environment in recent years, a number of solutions have been introduced to help entrepreneurs to carry out environmental protection activities and to build environmental awareness. These include standards for environmental management systems (ISO 14001, EMAS) corporate social responsibility standards (ISO 26000) or carbon dioxide reduction. Despite many of these initiatives, the level of ecological awareness among Polish SMEs is still insufficient [9]. It is clear that the conscious pursuit of a business that falls within sustainability standards entails additional costs that have not yet appeared in corporate balance sheets. It is still a rare approach of SMEs, which takes into account planning future spending and budgeting current costs associated with environmental management.

The aim of this paper is to show the average cost of environmental activities of enterprises in the SME sector and to focus on the importance of increasing share of these costs in corporate budgets. The article also aims to raise awareness that incurring the costs of environmental activities is a natural element and obligation of business and that it is a result of the environmental use and not just another tax imposed by the legislator.

## **2 Typical Environmental Aspects of Manufacturing Companies**

Environmental aspects of manufacturing companies are mainly related to the type of manufacturing processes being carried out. The specifics of a company's business determines the environmental aspects of resource consumption, gaseous and atmospheric emissions, wastewater production, waste management, and packaging. There is a large correlation between the PKD code (Polish statistical classification of economic activity, similar to NACE) of individual companies and their impact on the environment [10]. For the purpose of verifying this thesis, the authors examined 66 manufacturing enterprises from the SME sector. Data collection was based on audit reports, carried out by environmental management experts during the implementation of the EMS in these companies.

It is important to point out that despite the relatively small environmental impact of individual companies, this impact is compounded by the large market share of SMEs [11]. In 2015, over 1914 thousand companies were registered in Poland, including over 1910 thousand in SME sector enterprises [12]. It is estimated that companies in this sector are responsible for 64% of all industrial pollution in



Europe [13]. Below are shown the main environmental aspects of SMEs, like raw material consumption, air pollution, water, and waste management.

In the surveyed group, the water and sewage management was a minor problem. Aspects related to water intake directly by the organization (own groundwater footage) appeared only in one company. All other companies used water supplied by external suppliers (water companies). In technological processes, water was mainly used for cooling purposes (closed circuits) or for cleaning of technological equipment.

Wastewater in the SME sector group is over 66% classified as social-living sewage [9]. Main sources of industrial sewage are surfactants contaminated water (cleaning agents used in industrial conditions), water used in galvanizing processes, and laboratory effluents contaminated with various chemical reagents.

The use of raw materials in the SME sector does not pose a significant environmental burden [9]. In this area, mainly nonrenewable raw materials are used, but those whose acquisition, use, and recycling are not significantly harmful to the environment (for example, metals and simple chemicals). Only for companies classified in Group C-20 Production of chemicals, which accounted for 4.6% of the enterprises, the risks of a potential raw material release into the environment are significant. This is mainly due to the high toxicity of substances used in these companies for living organisms. In addition, there is a large group of companies that utilize waste from other processes as raw material for production. Companies that professionally recycle or use recycled products should be considered to have a positive environmental impact on the use of raw materials. Currently, over 63% of manufacturing companies declare their willingness to reduce the consumption of natural resources. In most cases, the main reason for this is the desire to reduce production costs, but this is still a big reduction on the environmental impact of the company [14].

The growing problem of air pollution in Poland causes that the environmental aspects related to the emission of gases or dust into the atmosphere are now of particular importance. The vast majority of industrial emissions are related to activities such as follows:

- Fuel combustion (both in internal combustion engines as well as in heating and technological boilers);
- Emissions of volatile organic compounds (related to the use of paints, solvents and certain cleaning and preserving agents);
- Dust and fume emissions related to metalworking (welding, grinding).

Nearly 55% of the companies participating in the study had an organized form of emission. It means that emissions into the air took place through adapted equipment (mechanical ventilation, local exhausts). This suggests that production processes causing emissions into the air were so important that they required the removal of pollutants of the workstation.

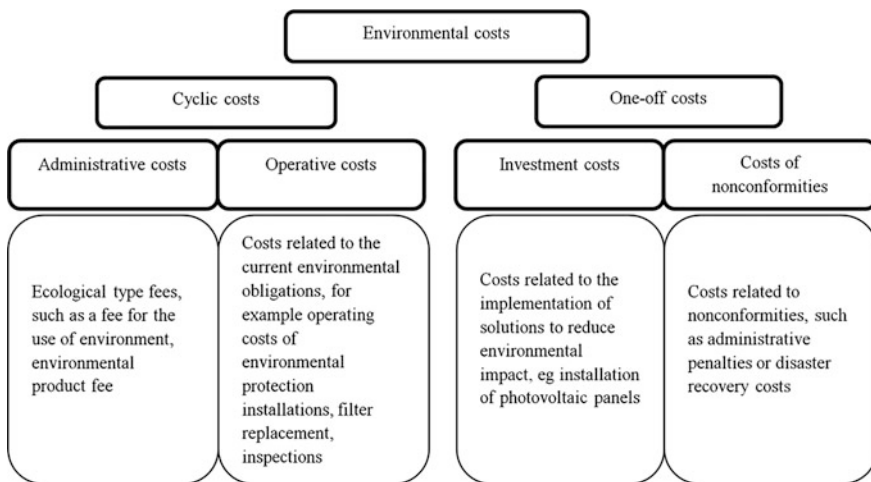
One of the most important and most problematic areas of environmental activity of SME is waste management [15]. Companies in this sector are producing both

nonhazardous and hazardous waste. The amount of nonhazardous waste normally forces the entrepreneurs to selective collection and transmission to professional waste management operators. Most problematic waste in this sector is usually hazardous waste, mainly due to their small amounts. In addition, problems with their proper classification and subsequent management make the waste largely to end up in unsorted municipal waste. Taking into account the accumulation of all the waste generated in this sector, over 7.5 thousand tons of hazardous waste per year can be mixed with unsorted municipal waste.

### 3 Classification of Environmental Protection Costs in Companies

In European countries (EU and OECD), some of the basic fiscal tools include various taxes, for example, in the form of environmental fees [16]. However, to carry out an analysis of the total environmental costs of an enterprise, the cost of ongoing maintenance of equipment and installations designed to reduce pollution (equipment services, filter replacement, etc.), investment costs to reduce environmental impacts, and costs of nonconformities, that is, both the administrative penalties for not keeping up to date legal requirements and the cost of removal of possible emergency situations. The structure of costs suggested by the authors is shown in Fig. 1.

Costs inherent in the implementation of environmental tasks, both active (egg assembly of environmental protection equipment) and passive (egg development of environmental documentation, including reporting), is the staff cost of employees. Regardless of whether these tasks are carried out by designated company



**Fig. 1** Classification of environmental protection costs

employees or outsourced to specialized companies, this cost is necessary. Staff costs are not included in the chart below, as difficult to estimate. The wages of employees, depending on the tasks assigned to them, the competence of staff, etc., vary considerably among the surveyed companies.

Administrative costs are mainly taxes, including environmental fees. They can take on a variety of forms, but the most commonly paid by SMEs are as follows:

- payment for the economic use of the environment,
- payment for the placing on the market products in packaging, including import and intracommunity supply,
- the charge for placing on the market products that are particularly hazardous to the environment (batteries, accumulators, oils, tires, etc.).

Other cyclical environmental costs in manufacturing companies are defined as operating environmental costs. All of these costs include elements such as follows:

- costs of waste management;
- costs of cleaning separators and filters;
- service and maintenance of air conditioning, mechanical ventilation, and fire protection installations;
- purchase of sorbents and cleaners;
- cost of wastewater treatment (both industrial and social);
- participation in maintenance costs of rainwater and melting water receiver (egg drainage ditches); and
- fees for the measurement of emissions (air, composition, and volume of effluents).

Besides to the cyclical environmental costs, one-off costs should be highlighted. These are the costs and expenses associated with individual business incidents. They can be divided into investment costs, for example, all expenditure incurred on investments that can directly or indirectly reduce the environmental impact of the business, like

- building thermo-modernization,
- purchase of renewable energy technologies,
- purchase of more energy efficient machines (including hybrid cars),
- construction or modernization of sewage treatment plant, and
- use of ecodesign technologies to reduce raw material consumption and waste generation [17, 18].

The second group of one-off costs is the costs of nonconformities, which may also be related to the removal of inconsistencies. Any incompliance of legal requirements and the occurrence of accidents that may affect the environment (like fire or the release of dangerous substances into the environment) are considered incompatible. As a consequence, the environmental costs of sanctions, fines, and surcharges imposed by the state administration should be considered as a result of overstepping or unlawful activity.

## 4 Analysis of Environmental Costs in the Manufacturing Company

Studies in the group of SME companies have shown that environmental costs are underestimated in most of them. In the 66 companies surveyed, only two had 100% of their fees due to the implementation of legal requirements related to particular environmental aspects. Most of the times the result was not so much the reluctance of entrepreneurs to incur costs as a lack of awareness of the need to bear them. There was also a situation of deliberate undercutting, for example, the amount of waste generated to reduce the fees.

To better illustrate the amount of environmental costs borne by manufacturing companies in the SME sector, it was decided to make accurate calculations based on the average company from the surveyed group. For this purpose, a summary is showing the unit costs associated with the cost group (Tables 1 and 2).

Only cyclical costs are included in the statement, as one-offs are an individual business and cannot be generalized. Cyclical costs, however, are in most cases a

**Table 1** List of administrative environmental costs

Cost group	Cost type	Cost description	Unit cost
Packaging utilization fee	Recycling fee	Paper and cardboard packages	0.0015 (PLN/kg)
		Plastic packaging	0.0025 (PLN/kg)
		Glass packaging	0.04 (PLN/kg)
		Wooden packaging	0.0012 (PLN/kg)
		Steel packaging	0.0018 (PLN/kg)
		Aluminum packaging	0.03 (PLN/kg)
	Products in packages fee	Paper and cardboard packages	0.65 (PLN/kg)
		Plastic packaging	2.73 (PLN/kg)
		Glass packaging	0.26 (PLN/kg)
		Wooden packaging	0.33 (PLN/kg)
		Steel packaging	0.82 (PLN/kg)
		Aluminum packaging	0.65 (PLN/kg)
Use of the environment		100 liters of solvent consumption (Nitro)	110 (PLN/year)
		100 kg of paint consumption	52 (PLN/year)
		Charge for 100l use of gasoline in an old passenger car (before 1992)	5.8 (PLN/100 l)
		Charge for 100 l use of gasoline in new passenger car (Euro 5)	0.44 (PLN/100 l)
		1000 kg of welding wire use	1.17 (PLN/1000 kg)
		Usage of 1 Mg of coal	1780–3451 (zł/Mg/year)
		Usage of 1 Mg of wood	4.55 (PLN/Mg/year)
	Usage of 1000 m <sup>3</sup> of natural gas	1.34 (PLN/m <sup>3</sup> /year)	

**Table 2** List of operational environmental costs

Cost type	Cost description	Unit cost
Municipal waste management	Standard container 1.1 m <sup>3</sup> —selectively collected	95 (PLN/month)
	Standard container 1.1 m <sup>3</sup> —mixed	119 (PLN/month)
Industrial waste	Hazardous waste (hazardous substances packaging)	500 (PLN/Mg)
	Hazardous waste (oils)	3000 (PLN/Mg)
	Nonhazardous waste	200–600 (PLN/Mg)
Replacement of mechanical filters	Standard nonwoven filter	250 (PLN/unit)
Fire protection installations maintenance	Installation	500 (PLN)
	Fire extinguishers	5–30 (PLN/unit)
	Hydrants	25.0 (PLN/unit)
Inspections of buildings (including environmental protection installations)		<1000 (PLN)
Separators cleaning		250.0 (PLN/unit)
Air conditioning maintenance		200.0 (PLN/unit)
Purchase of cleaners	Surface cleaning paper	8.0 (PLN/unit)
	Cotton cleaners	30.0 (PLN/kg)

multiple of the rates set by the legislator, such as the cost of environmental charges or market rates, resulting from price lists for specific services, such as collection and management of waste.

Tables 1 and 2 show that there are many types of environmental charges for manufacturing companies. Every production company has to remember about the costs of using the environment.

The calculation of exact environmental costs was made on the basis of Alfa company, employing 40 employees (average employment of the companies surveyed). Alfa, in its manufacturing processes, performs welding, machining (cutting, grinding), lacquering, and assembly operations. The quantities of raw materials consumed by the company in the processes and other data necessary to calculate the environmental fee associated with a given aspect are summarized in Table 3.

Additionally, manufacturing and maintenance processes are forming side-classified products which consist of hazardous and nonhazardous waste in annual quantities of, respectively, 3200 and 15,200 kg (including 8000 kg of municipal waste and 5100 kg of scrap metal).

As part of its infrastructure operation, the company uses natural gas for heating installations in buildings with a combined volume of 2250 m<sup>3</sup>. The annual consumption of natural gas is 39,423 m<sup>3</sup>. Alfa company owns a car fleet of 6 passenger cars and 2 trucks, which use 14,400 kg of diesel annually. In addition, the company manages a hardened maneuvering yard and a parking with a total area of 300 m<sup>2</sup>, which drains rainwater into the drainage ditch. Based on the information provided

**Table 3** Quantities of raw materials and other components consumed/produced by Alfa processes

Cost type	Stock	Quantity (unit)
Gases and dusts emission	Solvent usage	191 (dm <sup>3</sup> )
	Lacquer usage	211 (dm <sup>3</sup> )
	Paint usage	215 (kg)
	Fuel consumption	14.4 (Mg)
	Welding wire consumption	2520 (Mg)
	Machining stations work time	3120 (h/year)
	Natural gas consumption	39,423 (m <sup>3</sup> )
Water and sewage	Parking area	300 (m <sup>2</sup> )
	Sewage	876 (m <sup>3</sup> /year)
Waste	Municipal waste	8 (Mg)
	Hazardous waste	2.1 (Mg)
	Other industrial waste	3.2 (Mg)
	Scrap metal	5.1 (Mg)

**Table 4** Summary of annual cyclical environmental costs for an exemplary SME company

Cost group	Cost type	Value (PLN)
Administrative cost	Gases and dusts emissions	840
	Parking drainage	87
Operational cost	Waste management	13,740
	Sewage management	11,400
	Ventilation maintenance	1200
	Fire installations maintenance	1500
	Ventilation filters replacement	600
Total		29,367

in Table 3 and the unit costs contained in Tables 1 and 2, the annual environmental costs borne by Alfa company were compiled. This summary is shown in Table 4.

As can be seen from the statement, the total cost of cyclic environmental charges is 29,367 PLN and at the annual turnover of the company at level 1250 thousand is the share of 2.35%. This proves that it is a cost that cannot be marginalized and it is necessary to include it in the enterprise's budget and in the calculation of revenue structure. As previously described, this is the average value of SMEs' environmental costs. With the increase in scale of production, increasing the number of available infrastructure, etc., these costs will increase proportionately. The size of that costs and their share in turnover illustrates why they are so often avoided by entrepreneurs, where price competition is always strong. It is obvious that enterprise that does not incur environmental costs will be more competitive than the one that borne them. Only honest payment of environmental fees by all entrepreneurs can exclude it as a factor causing a decrease in competitiveness.

## 5 Summary and Conclusions

At the present level of civilization development, further development must take place with respecting the idea of sustainable development. It is possible by balancing between economic growth, environmental care (both natural and man-made), and the quality of human life. Companies, especially the production ones, play a large part in this idea. Manufacturing companies in the SME sector, despite generating, would appear to be a single, small-scale environmental problem, but due to the amount of them on the market, they make a significant contribution to environmental impacts. It is necessary to build conscious business, not only for profit, but also for respect for the environment. This trend is already recognized among global corporations and large organizations. In the small and medium business sector, it is still necessary to spread this idea.

Environmental costs cannot currently be marginalized. The example given in this article shows that for an average manufacturing company in the SME sector, annual environmental management expenditure can fluctuate within 2–5% of a company's turnover. It is very important to build awareness that environmental costs are not just another tax, but the cost of using the environment, which can be compared to the purchase of a particular service from another entity. These costs should be a natural thing in everyday business. It is also important to look at environmental costs, especially investment ones, in the long perspective as part of the environmental costs currently being incurred to reduce future costs. This is true with all environmental investments, which are related to the reduction of energy or material use. These investments in the future should reduce other costs related to operation, energy use and environmental costs due to reduced emissions, etc. Every entrepreneur is obliged to bear these costs and negate the avoidance of environmental charges in order to gain price advantage over other entities.

**Acknowledgements** The results presented in the paper come from a scientific statutory research conducted at the Chair of Management and Production Engineering, Faculty of Mechanical Engineering and Management, Poznan University of Technology, Poland, supported by the Polish Ministry of Science and Higher Education from the financial means in 2017: 02/23/DSPB/7695.

## References

1. Diering, M., Dyczkowski, K.: Assessing the raters agreement in the diagnostic catheter tube connector production process using novel fuzzy similarity coefficient. In: IEEE International Conference on Industrial Engineering and Engineering Management, pp. 228–232, (2016)
2. Kujawińska, A., Rogalewicz, M., Diering, M., Hamrol, A.: Statistical approach to making decisions in manufacturing process of floorboard. In: Rocha Á., Correia A., et al. (eds.) Recent Advances in Information Systems and Technologies, WorldCIST. Advances in Intelligent Systems and Computing, vol. 571, pp. 499–508. Springer, Heidelberg (2017)

3. Starzyńska, B., Grabowska, M., Hamrol, A.: Effective management of practitioners' knowledge—development of a system for quality tool selection. In: 3rd International Conference on Social Science (ICSS 2016), pp. 859–865. China, (2016)
4. Starzyńska, B., Hamrol, A.: Excellence toolbox: decision support system for quality tools and techniques selection and application. *TQM&BE* **24**(5–6), 577–595 (2013)
5. Gangala, C., Modi, M., Manupati, V.K., Varela, M.L.R., Machado, J., Trojanowska, J.: Cycle time reduction in deck roller assembly production unit with value stream mapping analysis. In: Rocha, Á., Correia, A., Adeli, H., Reis, L., Costanzo, S. (eds.) *Recent Advances in Information Systems and Technologies, WorldCIST. Advances in Intelligent Systems and Computing*, vol. 571, pp. 509–518. Springer, Heidelberg (2017)
6. Królczyk, G., Legutko, S., Królczyk, J., Tama, E.: Materials flow analysis in the production process—case study. *Appl. Mech. Mater.* **474**, 97–102 (2014)
7. Varela, M.R.L., Trojanowska, J., Carmo-Silva, S., Costa, N.M.L., Machado, J.: Comparative simulation study of production scheduling in the hybrid and the parallel flow. *J. MPER* **8**(2), 69–80 (2017)
8. Challenges of sustainable development in Poland (in Polish). In: Kronenberg, J., Bergier, T. (eds.) *Fundacja Sędzimir*, (2010)
9. Osiński F., Grudzień Ł. Hamrol A.: Environmental awareness of the SME sector on the project “Implementation of environmental management systems” (in Polish). In: Knosala, R. (ed.) *Innovation in Management and Production Engineering PTZP*, pp. 461–471, (2016)
10. Rozporządzenie Rady Ministrów z dnia 24.12.2007 r. w sprawie Polskiej Klasyfikacji Działalności (PKD) (Dz. U. z 2007 r. nr 251, poz. 1885 z późn. zm.)
11. *Small Businesses And Environmental Compliance*, OECD (2007)
12. *Non-financial corporations activity in 2015* (in Polish). GUS, Warszawa (2015)
13. Calogirou C. et al.: SMEs and the environment in the European Union, Planet SA and Danish Technological Institute, European Commission, DG Enterprise and Industry (2010)
14. EC, Green Action Plan for SMEs: Enabling SMEs to turn environmental challenges into business opportunities, Communication from the Commission to the European Parliament, The Council, The European Economic and Social Committee and The Committee of the Regions, COM(2014)440 Final, Brussels, 2 July 2014
15. *Environmental Policy Toolkit for Greening SME's in the EU Eastern Partnership Countries*. OECD (2015)
16. Małecki, P.: Taxes and ecological fees (in Polish). AE (2006)
17. Grajewski D., Diakun J. et al.: Improving the skills and knowledge of future designers in the field of ecodesign using virtual reality technologies. In: *International Conference Virtual and Augmented Reality in Education, Procedia Computer Science*, vol. 75, pp. 348–358 (2015)
18. Dostatni, E., Diakun, J. et al.: Multi-agent system to support decision-making process in ecodesign. In: *10th International Conference on Soft Computing Models in Industrial and Environmental Applications, Advances in Intelligent Systems and Computing*, vol. 368, pp. 415–425. Springer, Heidelberg (2015)



# Product Variants Recycling Cost Estimation with the Use of Multi-agent Support System

Ewa Dostatni, Jacek Diakun, Radoslaw Wichniarek, Anna Karwasz and Damian Grajewski

**Abstract** The article describes research on recycling-oriented analysis during product ecodesign. The study was conducted using a proprietary agent system operating based on the recycling-oriented product model. The analysis focused on a household appliance: an electric kettle. The authors developed a project of a new appliance and then created its geometric model in a CAD 3D system. Next, analyses were conducted to compare the recyclability of the appliance with different material and joint combinations. A total of 16 different variants of the appliance were designed within the project. Each of them was evaluated for its recycling parameters and cost of recycling.

**Keywords** Recycling · Recycling cost · Ecodesign · CAD 3D

## 1 Introduction

Rapid development of IT solutions and increase in household wealth contributed to the modernization and continuous improvement of household appliances. As a result, households make more frequent purchases of household appliances, which in turn requires that waste electrical and electronic equipment be withdrawn [1, 2]. If the withdrawn appliances were not collected, disposed of, and/or reused in a controlled manner, it would quickly threaten environment. Therefore, legal acts have been introduced to regulate the recycling and reuse of such equipment [3]. The laws force manufacturers to consider recyclability in their manufacturing processes. Some companies are themselves involved in recycling, and others outsource these services to external agencies [4, 5]. One of the most important tasks of recycling is

---

E. Dostatni (✉) · J. Diakun · R. Wichniarek · A. Karwasz · D. Grajewski  
Faculty of Mechanical Engineering and Management,  
Poznan University of Technology, Poznan, Poland  
e-mail: ewa.dostatni@put.poznan.pl

to protect resources. Waste household appliances are among the most difficult waste in terms of recycling [6]. The production and recovery of electrical and electronic waste are focused on the following aspects: increasing amounts of waste equipment, hazardous material content, and recycling cost [7]. The actual recovery of materials is exposed to economic effects, which are affected by the prices of materials [8, 9]. Therefore, it is necessary to consider recycling-related aspects already at the product design stage, among others design criteria like product mechanical properties [10]. Taking into account recycling issues may also influence on more positive product image among customers [11]. When a product is designed, it is not only the manner of recycling that should be taken into account, but also the profitability of the process. Recent years have seen a considerable development of IT tools that support product designer in the recycling-oriented product assessment. One such tool is the author's own system of recycling-oriented product assessment during the design stage [12, 13]. This tool may be also considered as the extension of tools used for quality design of a product [14]. This paper presents the studies on the profitability of recycling of a sample product. The studies were conducted for different variants of the same appliance—electric kettle.

## 2 A System for Recycling-Oriented Product Assessment

The authors' original system for recycling-oriented product assessment is based on the recycling product model (RpM) which was implemented into the CAD 3D system and in the agent system. Into the agent system, the authors implemented the recycling-oriented product assessment including the feature allowing for recycling cost estimation. Agents follow the work of the designer in the 3D CAD system, monitor the changes made in the design, assess their impact on the parameters relevant to recycling, and provide suggestions for product improvements to facilitate recycling. The use of the agent technology and RpM in the application enabled automatic support for the recycling aspect of designing, without having to reexamine the product structure, manually aggregate the parameters relevant for the adopted method of product recyclability evaluation, and to reintroduce them to third-party systems [15]. The functioning of the system is based on original methods of recycling-oriented assessment of a designed product, recycling cost estimations, and tips and suggestions for product designer that are based on knowledge derived from the implementation of previous projects [16]. The method for recycling-oriented product assessment is based on recyclability ratio CWR (total recycling ratio). It is the sum of three sub-indices (1). The sub-indices are mini-mants (the lower their value, the easier the recycling):

- material diversity—WRM
- joint diversity—WRP
- recycling rate—WPR.

$$CWR = WRM + WRP + WPR \tag{1}$$

The percentage of material diversity (WRM) is calculated according to formula (2), and then its value is taken from Table 1:

$$WRM [\%] = (1 - M1)/MW, \tag{2}$$

where *M1* is the number of occurrences of material most common in the product. *MW* is the number of occurrences of other materials used in the product. The WRP ratio is calculated in a similar manner.

The percentage of recycling rate WPR is calculated by the following formula:

$$WPR [\%] = MR/MW, \tag{3}$$

where *MR*—total weight of all recycled elements; *MW*—total weight of the product.

To learn the percentage of recycling target WPR[%], one can find the value of recycling target WPR in Table 2. For example, if the product weighs 5, 4 kg of which are suitable for recycling, the recycling rate is  $[4/5] = 80\%$ . The value of recycling rate weight coefficient WPR depends on the group of household appliances the designed product belongs to. The appliance analyzed in the study is a small-sized household appliance type 2, whose WPR, following the WEEE directive.

The method of estimating recycling cost takes into account two basic factors which affect the recycling cost: the first is the cost of disassembly, and the other is the cost of disposal and recycling of materials used in the product. A negative result means a loss, a positive result—a profit. The authors assumed that the total recycling cost is the total profit on materials which may be sold after disassembly, and the cost is the total cost incurred for disassembly, disposal of hazardous waste, and transport to waste disposal landfill:

**Table 1** The conversion of WRM/WRP [%] to WRM /WRP

WRM/WRP [%]	≤ 10	≤ 20	≤ 30	≤ 40	≤ 50	≤ 60	≤ 70	≤ 80	≤ 90	≤ 100
WRM/WRP	0.5	1	1.05	2	2.5	3	3.5	4	4.5	5

**Table 2** Conversion of WPR [%] to WPR for small-sized household appliances

WPR [%]	<0–75)	<75–80)	<80–85)	<85–90)	<90–95)	<95–100)	100
WPR	15	5	4	3	2	1	0.5

$$K_{RW} = \sum_{i=1}^n K_{MD} - \left( \sum_{i=1}^n K_{UMN} + \sum_{i=1}^n K_{Odpad} + \sum_{i=1}^n K_{Dem} \right), \quad (4)$$

where  $K_{RW}$ —product recycling cost;  $K_{MD}$ —cost of good materials (suitable for recycling and reuse);  $K_{UMN}$ —cost of hazardous waste treatment;  $K_{Odpad}$ —cost of waste;  $K_{Dem}$ —disassembly cost; and  $n$ —number of materials in a given product.

### 3 Recycling-Oriented Assessment of a Selected Product

The research described in the paper is an analysis of a designed product in terms of its recycling, with a particular focus on the estimate of recycling cost. The recycling-oriented product assessment was conducted based on the agent system integrated with RmW developed in CAD 3D. The system provides the means to determine the degree of recyclability of the designed kettle. Calculations in the system, determining the degree of recyclability, are made on the basis of ratios, developed in accordance with the applicable standards and directives on ecodesign. In order to conduct the analysis, apart from the 3D model, it is necessary to define all the materials used to produce the appliance together with the joints connecting all the parts [17].

In the first stage, it was necessary to create a geometric 3D model in the CAD system. The designed product model consists of 12 parts. The construction of the appliance is shown in Fig. 1. Next, after creating the 3D model, a material database was defined to be used by the agent system during the recycling-oriented analysis. For this purpose, the authors used an original tool, Materials And Tools Editor. The application defines groups of materials, individual materials, and tools [18].

Next, the basic materials were defined and assigned to relevant material groups. Each material defined in the database was described by the basic material attributes

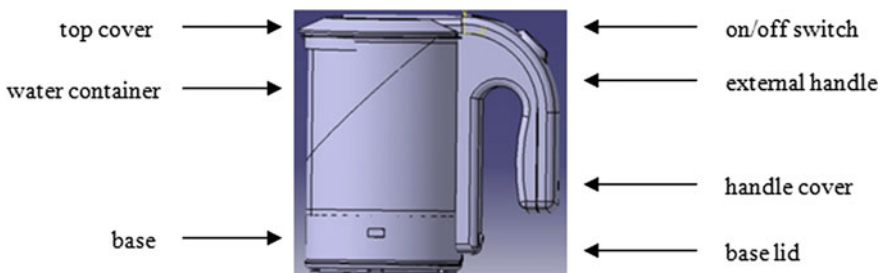


Fig. 1 Electric kettle modeled in the CAD system [14]

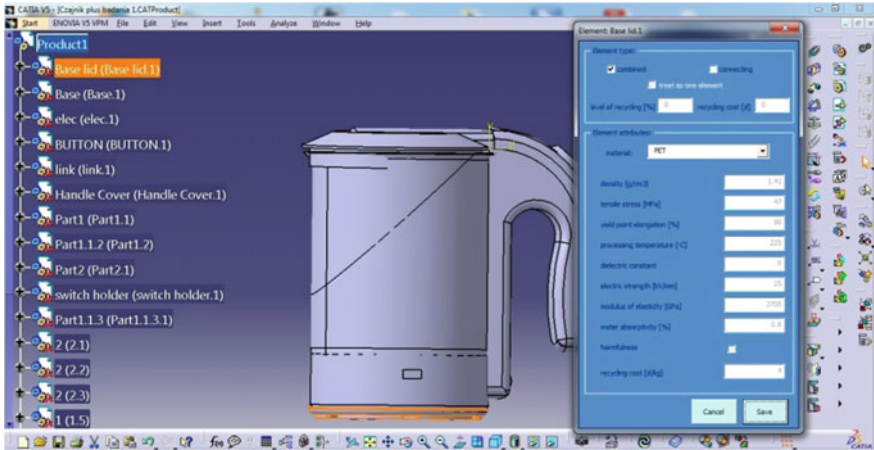


Fig. 2 Defining the materials for all the elements [14]

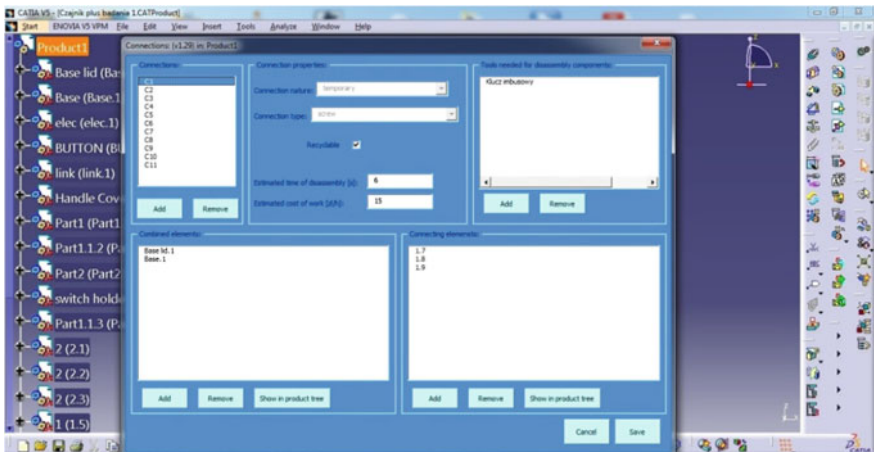


Fig. 3 Joints between the kettle elements and the assigned disassembly tools [14]

and properties. Ten different materials were used in the study. The information about tools for disassemble was also added. The database with all the information was then loaded into the CAD 3D system. The next step was to assign to each part of the kettle, the material from which it could be made, and determine the type of the element (combined or connecting). During the project, materials were changed in the different variants of the designed appliance. Figure 2 shows the material selection interface. The joints between the parts of the kettle were also defined in the model. During the recycling-oriented product assessment, the joints used in the different variants of the designed kettle changed. Also at this stage, we assigned the tools needed to disassemble the joint (Fig. 3).

As a result of the work, two XML files were generated: one was the material database, and the other was a 3D model with materials and joints. The files were then uploaded to the agent system. A total of 16 analyses were conducted, with different material, joint, and disassembly configurations. First, six analyses focused on different materials, and each of them included variants of the joints used and disassembly level. In each analysis, with various materials, two cases were analyzed: the first one, with only push-in joints, screw joints, and welding joints. The second case consisted of all the above plus the riveted joint. It was assumed that the disassembly will be non-destructive. The data concerning the price of purchase and recycling of all the materials was taken from the current price lists of recycling companies. Table 3 shows the basic configuration of product variants with different materials. Table 4 in turn shows the different tests conducted in the analyses.

In Table 3, the symbols represent the following: ABS acrylonitrile–butadiene–styrene copolymer; PE polyethylene; PET polyethylene terephthalate; PP polypropylene; PVC polyvinyl chloride; X12CrMnNiN17-7-5 austenitic stainless steel; X2CrNiMoCuN25-6-3 duplex stainless steel; X6Cr17 ferritic stainless steel; St235 mild steel; and St335 mild steel.

Example results image (for Analysis 1a) from the agent system is shown in Fig. 4. The research revealed that the CWR rate was 7 with WPR = 1, WRM = 3 and WRP = 3, the time of disassembly (TD) was estimated at 40 s, the number of different materials (LM) was 4, the number of different joints (LP) was 4, and the number of tools needed for the disassembly (LN) was 2. Recycling costs ( $K_{RW}$ ) were estimated at 1.03 PLN. The cost includes the disassembly costs ( $K_{DEM}$ ) of 0.09 PLN, and the profit from the disassembled materials ( $K_{MD}$ ) of about 1.12 PLN. The recycling rate (WPR%) amounted to approximately 100%. Therefore, it can be concluded that the appliance is recyclable and meets the standards.

Table 5 presents the summary of results for the selected analyses.

## 4 Research Conclusions and Summary

The summary given in Table 5 shows that in cases when the entire appliance was subject to disassembly, the recycling rate was around 100%. In all these cases, selling the materials obtained from the disassembly brought a profit, which means that recycling was profitable. The profit from the sale of materials was greater when stainless steel was used in the kettle (purchase price of such steel is higher than the price of regular steel). When certain groups of elements were not disassembled, so-called material mixes were obtained, which reduced the profit from selling disassembled elements of the appliance. The kettle did not reach the legally required recycling rate, which would in turn result in additional fees. In all cases, the cost of disassembly was comparable, because disassembly time of all the product variants was similar. Recycling of the kettle (designed according to the variant A.2c) generates costs, as it would be required to pay for the materials to be recycled. The weight of the designed appliance ranged from 0.395 to 0.507 kg,

**Table 3** List of analyses

Component/analysis	1	2	3	4	5	6
Base lid	PP	PE	PVC	PET	PE	ABS
Base	PP	PE	PVC	PET	PE	ABS
Heating element	X12CrMnNiN17-7-5	X2CrNiMoCuN25-6-3	X6Cr17	X6Cr17	X2CrNiMoCuN25-6-3	X12CrMnNiN17-7-5
Button	PE	PP	ABS	ABS	PE	PET
Connection between external and internal handle	PE	PP	ABS	ABS	PE	PET
Handle cover	PE	PP	ABS	ABS	PE	PET
External part of the handle	PP	PE	PVC	PVC	PE	ABS
Water container	PP	PE	PVC	PVC	PE	ABS
Hole plug	PP	PE	PVC	PVC	PE	PET
Switch	PP	PE	PVC	PVC	PE	PET
Top cover	PP	PE	PVC	PVC	PE	ABS
Bolt	Si235	Si335	Si235	Si335	Si235	Si335
Rivet	X12CrMnNiN17-7-5	X2CrNiMoCuN25-6-3	X6Cr17	X6Cr17	X2CrNiMoCuN25-6-3	Si335

**Table 4** Variants of different analyses

	Variant (a)	Variant (b)	Variant (c)	Variant (d)
Analysis 1	With bolted joint	With riveted joint	–	–
Analysis 2	With bolted joint without disassembly of the electrics	With bolted joint with a disassembly of the electrics	With riveted joint without disassembly of the electrics	With riveted joint with a disassembly of the electrics
Analysis 3	With bolted joint	With riveted joint	–	–
Analysis 4	With bolted joint without disassembly of the water container with the heating element and electrics	With bolted joint with disassembly of the water container with the heating element and electrics	With riveted joint without disassembly of the water container with the heating element and electrics	With riveted joint with disassembly of the water container with the heating element and electrics
Analysis 5	With bolted joint	With riveted joint	–	–
Analysis 6	With bolted joint	With riveted joint	–	–

Recycling level			
Required	75.00%	Achieved	100.00%

General information	
Recovery level	100.00%
Mass	0.398
Disassembly time	00:00:40
Recycling cost	1.03
Number of materials	4
Number of tools	2

**Fig. 4** Analysis 1a study results

depending on the type of materials and joints used in the product. The purchase price of used household appliance (not disassembled) is ca. 0.10 PLN/kg, so the price for selling the designed product would range from 0.30 to 0.50 PLN. We can conclude that research has shown that in the case of total disassembly of the device its recycling is cost-effective, particularly if it concerns a greater number of appliances. The results of analyses conducted within this research are only estimates and they showcases when recycling may be profitable. However, recycling should not be avoided even if the disassembly and resale of parts result in a loss; otherwise, paying fines provided for in laws and regulations would be unavoidable. The amount of the fine may be higher than the cost of product disassembly and recycling. The electric kettle used in the study was the most common on the market, and it was mainly made from plastic. For this reason, it is also the most common type of the kettle delivered to companies involved in recycling. Their popularity is



**Table 5** Results of the selected analyses made in the agent system

	A.1b	A.2a	A.2b	A.2c	A.2d	A.3a	A.3b	A.4a	A.4b	A.4c	A.4d
CWR	7.5	21	7	21.5	7.5	7	7.5	21	7	21.5	7.5
WPR	1	15	1	15	1	1	1	15	1	15	1
WRM	3.5	3	3	3.5	3.5	3	3.5	3	3	3.5	3.5
WRP	3	3	3	3	3	3	3	3	3	3	3
TD [s]	46	38	40	43	46	40	46	30	40	36	46
LM	4	4	4	5	4	4	4	6	5	6	5
LP	4	3	3	4	4	3	4	2	3	3	4
$K_{Dem}$	0.06	0.05	0.06	0.06	0.06	0.06	0.06	0.04	0.06	0.05	0.06
$K_{MD}$	1.06	0.09	1.17	-0.31	1.20	1.15	1.17	0.90	1.25	0.88	1.23
$K_{RW}$	1.00	0.04	1.11	-0.37	1.14	1.09	1.11	0.86	1.19	0.84	1.17
WPR%	100	41	100	40	100	100	100	72	100	72	100

mainly due to their price which is lower than the price of electric kettles made of metal, glass, or ceramic. The cheapest kettles are made mostly of polyethylene, while the more expensive are made of polypropylene and ABS. Theoretically, the same material may vary widely between two different kettles in terms of its price and properties. Copper used in the electrical wires would be identical in each kettle. It has been omitted in the calculations, and the same applies to other elements, which can be found in such appliances in trace amounts. Obviously, the presence of copper would have a positive influence on the total cost of recycling of all product variants. The use of bolts made of ordinary carbon steel in the kettle could cause their rapid corrosion, but it is nevertheless a common solution among the manufacturers of the least expensive appliances.

**Acknowledgements** The results presented in the paper come from a scientific statutory research conducted at the Chair of Management and Production Engineering, Faculty of Mechanical Engineering and Management, Poznan University of Technology, Poland, supported by the Polish Ministry of Science and Higher Education from the financial means in 2017: 02/23/DSPB/7695.

## References

1. Lipan, F., Kannan, G., Chunfa, L.: Strategic planning: design and coordination for dual-recycling channel reverse supply chain considering consumer behavior. *Eur. J. Oper. Res.* **260**(2), 601–612 (2017)
2. Yu, J., Williams, E., Ju, M.: Analysis of material and energy consumption of mobile phones in China. *Energy Policy* **38**(8), 4135–4141 (2010)
3. European Parliament and Council, Directive 2012/19/EU of the European Parliament and of the Council of 4 July 2012 on waste electrical and electronic equipment (WEEE). *Off. J. Eur. Union* (2012)
4. Govindan, K., Popiuc, M.N.: Reverse supply chain coordination by revenue sharing contract: a case for the personal computers industry. *Eur. J. Oper. Res.* **233**(2), 326–336 (2014)

5. Kannan, D., Govindan, K., Shankar, M.: India: formalize recycling of electronic waste. *Nature* **530**(7590), 281 (2016)
6. Movilla, N.A., Zwolinski, P., Dewulf, J., Mathieux, F.: A method for manual disassembly analysis to support the ecodesign of electronic displays. *Resour. Conserv. Recycl.* **114**, 42–58 (2016)
7. McCann D., Wittmann A.: Solving the E-waste problem (Step) green paper. In: *E-waste Prevention, Take-back System Design and Policy Approaches*, Bonn, United Nations University—Institute for the Advanced Study of Sustainability (2015)
8. Goodship V., Stevels A.: *Waste Electrical and Electronic Equipment (WEEE) Handbook*. Elsevier, Amsterdam (2012)
9. Jasiulewicz-Kaczmarek M.: Integrating lean and green paradigms in maintenance management. In: *Proceedings of the 19th IFAC World Congress, Cape Town*, vol. 47(3), pp. 4471–4476 (2014) (IFAC PapersOnLine)
10. Górski F., Wichniarek R., Zawadzki P., Hamrol A.: Computation of mechanical properties of parts manufactured by fused deposition modeling using finite element method. In: *10th International Conference on Soft Computing Models in Industrial and Environmental Applications, Advances in Intelligent Systems and Computing*, vol. 368, pp. 403–413 (2015)
11. Jasarevic, S., Diering, M., Brdarevic, S.: Opinions of the consultants and certification houses regarding the quality factors and achieved effects of the introduced quality system. *Tehnicki Vjesnik-Technical Gazette* **19**(2), 211–220 (2012)
12. Dostatni, E., Diakun, J., Grajewski, D., Wichniarek, R., Karwasz, A.: Multi-agent system to support decision-making process in design for recycling. *Soft. Comput.* **20**(11), 4347–4361 (2016)
13. Dostatni, E., Diakun, J., Hamrol, A., Mazur, W.: Application of agent technology for recycling-oriented product assessment. *Ind. Manage. Data Syst.* **113**(6), 817–839 (2013)
14. Starzynska, B., Hamrol, A.: Excellence toolbox: decision support system for quality tools and techniques selection and application. *Total Q. Manage. Bus. Excellence* **24**(5–6), 577–595 (2013)
15. Grajewski D., Diakun J., Wichniarek R., Dostatni E., Buń P., Górski F., Karwasz A.: Improving the skills and knowledge of future designers in the field of ecodesign using virtual reality technologies. In: *Proceedings of International Conference Virtual and Augmented Reality in Education, Monterrey*, pp. 348–358 (2015)
16. Karwasz, A., Dostatni, E., Diakun, J., Grajewski, D., Wichniarek, R., Stachura, M.: Estimating the cost of product recycling with the use of ecodesign support system. *Manage. Prod. Eng. Rev.* **7**(1), 33–39 (2016)
17. Borkowski B.: *The impact of ecodesign on the quality and cost of a product (in Polish)*. M.Sc. thesis, Poznań University of Technology (2016)
18. Dostatni E., Diakun J., Grajewski D., Wichniarek R., Karwasz A.: Multi-agent system to support decision-making process in ecodesign, In: *10th International conference on soft computing models in industrial and environmental applications, advances in intelligent systems and computing*, vol. 368, pp. 463–474 (2015)

# The Use of Machine Learning Method in Concurrent Ecodesign of Products and Technological Processes

Ewa Dostatni, Izabela Rojek and Adam Hamrol

**Abstract** The article describes a new, original approach to integrated ecodesign of products and technological processes, ensuring appropriate selection of materials and connections from the point of view of recyclability. The method was implemented in an expert system. The decision tree induction method was used as the system tool. The expert system offers a practical solution which makes it possible to change a material or connection without having to consult the product designer. It is consistent with concurrent engineering (CE) design.

**Keywords** Decision tree · Expert system · Ecodesign · Technological processes

## 1 Introduction

Product design is a process where the features of the product are gradually defined from general to more and more specific. Decisions made in the design stage affect the manufacturing costs [1–5], the functional properties of the product and its performance, and determine actions that will have to be made in the final phase of the product's life cycle, particularly in relation to the recycling of recovered materials. Such approach to design is called ecodesign. Ecodesign is an additional dimension of traditional design [6, 7]. It involves tasks consisting in a systematic analysis of the effects that mutual interactions of raw materials, manufacturing processes, and the final product have on the environment, and in suggesting improvements in the designed technological processes [8, 9]. In concurrent

---

E. Dostatni · A. Hamrol  
Department of Management and Production Engineering,  
Poznan University of Technology, Poznan, Poland  
e-mail: ewa.dostatni@put.poznan.pl

I. Rojek (✉)  
Institute of Mechanics and Applied Computer Science,  
Kazimierz Wielki University, Bydgoszcz, Poland  
e-mail: izarojek@ukw.edu.pl

engineering (CE), the integration of environmental requirements is a new challenge for design engineers [10]. CE approach is used to develop a product which will be optimal in terms of functionality, cost, quality, and environmental impact.

The solution presented in this paper is a new dimension of ecodesign, consistent with concurrent engineering. The combination is the basic research problem described in the paper. The main aim of this paper is to develop an applicable method for an effective use of ecodesign principles, combining the work of the product designer and engineering process designer.

For this purpose, the authors analyzed the current methods of product ecodesign and indicated the possibilities of extending the methods in the technology engineering process. Based on the literature review and experience of the authors (resulting from their cooperation with business and previous research), it was found that at the time there was no tool to combine the two stages of design within concurrent engineering. In this way, an expert system was developed, which supports process engineers when they cannot consult product designers but must select alternative materials. This may result in a possible new connection with another material, resulting in a connection which is not included in the design documentation. The expert system has been called ESWEW (in Polish: Ekspercki System Wspomagania Ekoprojektowania Wyrobu—CAPECOD, Computer-Aided Product ECODesign). It was implemented using the AI SPHINX (PCShell and Detreex) package.

## 2 Literature Review

Regulations implemented in the European Union require that designers and engineers take appropriate actions related to ecodesign [11]. However, insufficient knowledge of ecodesign often limits their effectiveness [12]. The tools supporting ecodesign include also solutions dedicated, e.g., specifically to product designers [13], based on the automation of the design process taking into account environmental concerns, or solutions made for a particular group of products [14]. However, the large number and complexity of some of the solutions discourage potential users. The tools that work best are simple, easy to use, and dedicated to specific users and purposes [15]. The authors of this paper have long researched ecodesign [2, 16, 17] and computer-aided technological process design based on expert systems. Their earlier work in the area of sustainable product design was aimed at developing a method for product recyclability evaluation at the design stage, based on the recycling product model (implemented into a CAD system) and agent technology. Their efforts in the area of support tools for designing technological processes were related to the development of a method and system to facilitate the engineering process design. The machine learning method was used to develop such a system [18–20]. The method proposed by the authors is also included in the design for environment, which is widely described in the literature [21–23].

### 3 Methods

#### 3.1 The Principle of Integrating Product Ecodesign and Technology Engineering

Ecodesign focuses on recycling relates primarily to activities related to the selection of construction materials and methods of connecting them. When we consider the materials, the product should be designed to include the largest possible number of standardized and recyclable materials. This has a positive impact on the environment in the last stages of the product’s life cycle, such as maintenance or withdrawal of the product from use [24]. When selecting product materials, we should also consider their compatibility: materials used in a product should allow for their recycling at the end of the product’s life cycle without having to be separated [25]. Recycling parameters are shaped primarily by the chemical composition of the materials. Matrices of material compatibility have been developed [26]. The matrices list the compatibility of materials regarding, among others, their recyclability. Figure 1 shows the matrix for selected plastics, which compares material compatibility regarding their recycling. The proposed method offers two ways of selecting materials. In the first one, the material of one product element is defined, and then the material for the second element of the product is selected. The system provides information to what extent the materials of the two elements are compatible. In the second method, the user defines the material selected for an element (part) of the product, and the required degree of compatibility, and the system provides advice which other material should be added. The degree of material compatibility means that they can be reprocessed for reuse. Compatible materials are those that can be reprocessed (without prior separation). Limited compatibility

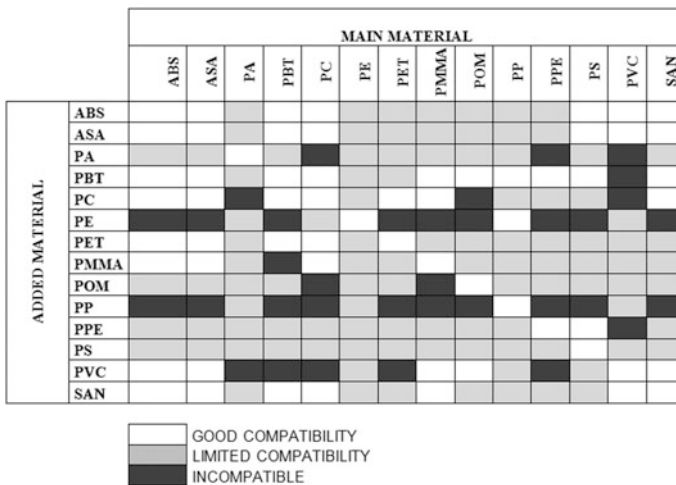


Fig. 1 Matrix of compatible materials [3, 26]

materials are those that exhibit low compatibility and incompatible components that cannot be recycled together.

Material connections should be designed to ensure quick and smooth disassembly, particularly when the use of incompatible or hazardous materials is unavoidable due to functional reasons [2]. In the case of good compatibility, both separable and inseparable connections may be used. However, if material compatibility is low or if materials are incompatible, only separable connections should be used.

The essence of the solution is the development of a communication platform to be used in the design process by the designers of both the product and engineering process. Figure 2 shows a diagram of the solution that supports decision-making in the selection of materials and connections for the designed products. The developed method allows the cooperation of the product designer and process engineer at the stage of the selection and/or verification of materials and connections designed for recycling.

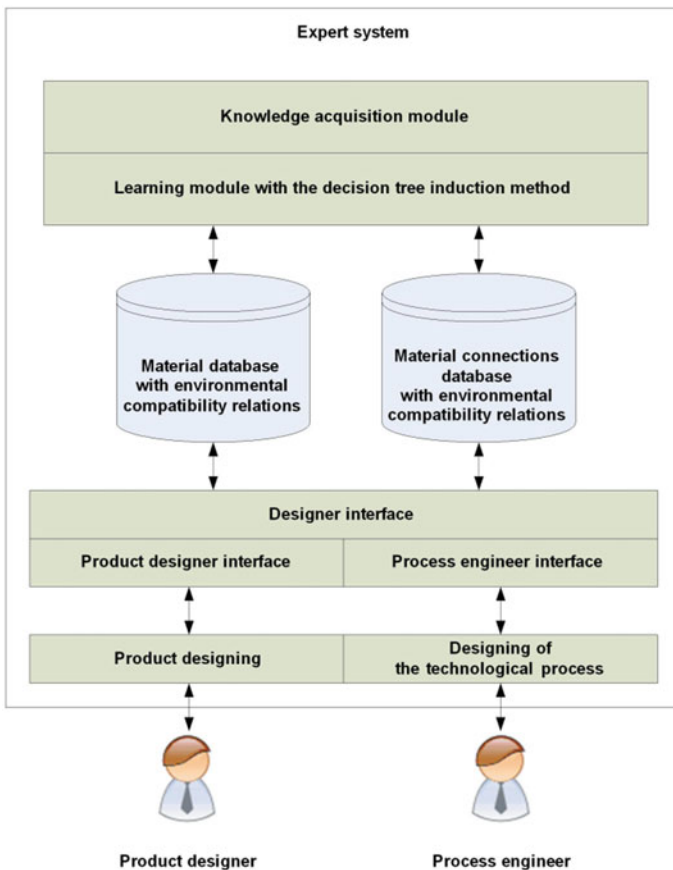


Fig. 2 Diagram of the computer-aided product Ecodesign system

### ***3.2 Decision Tree Induction Method***

In order to build the Computer-Aided Product ECODesign system (CAPECOD), the authors used the machine learning method based on decision tree induction. Machine learning makes it possible to acquire knowledge based on experimental data or learning examples. Knowledge obtained through machine learning methods may be better than knowledge directly deducted by people. It is often the only way to build decision-making support models, if knowledge is lacking or if it cannot be acquired directly from experts.

In this paper, the decision tree induction method was chosen. The choice was made due to the complex problem of material and connection selection (simpler IT tools are sufficient when there are only a few selection options and they can be shown in a simple table). The decision tree induction method based on a set of examples of already made choices, proven throughout the entire life cycle of a product, makes automatic generalizations of such examples to decision rules, which are then implemented into an expert system. Expert system equipped with such rules is an appropriate tool supporting the work of a less-experienced employee.

The choice of the decision tree induction method was also motivated by such advantages as speed of classification, intelligibility, “mature methodology”, and numerous practical implementations [27]. The authors also took into account the many available examples of material and connection selection. Additionally, this method makes it possible to process data as symbols, and not only numbers.

### ***3.3 The Method of Material and Connection Selection for Ecodesign***

#### **3.3.1 General Description**

The method of material and connection selection proposed in this paper has been implemented to be used for environmental design of household appliance. The development of the method started with collecting examples of materials and connections used in such appliance designs. It was also necessary to acquire data concerning the compatibility of all materials used in household appliance production, including in particular plastics. Plastics pose the greatest threat to the environment and it is extremely important to recycle them appropriately. The collected data were used as learning files. Next, decision trees were generated and decision rules were developed. The last stage concerned the creation of the user interface. Data were collected in a real enterprise.

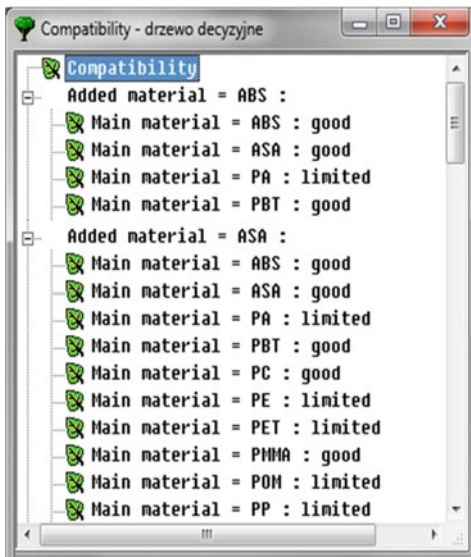
### 3.3.2 Selection of Materials According to Their Compatibility

The first decision tree applies to the selection of materials. It compares materials due to their compatibility. The materials which are to be used in the designed product are defined in the input learning file. The first one is the material chosen by the designer during the construction design (the so-called main material). The other one is the material modified by the process engineer during the design of the engineering process (the so-called added material). The output is the recycling compatibility of the two materials. Compatibility of the materials is defined using the data from compatibility matrices (Fig. 1) and expert knowledge. Decision trees and rules are generated based on such learning data. Figure 3 shows a fragment of a generated decision tree (a) and decision rules (b).

Rules generated in this manner allow us to use the method to compare compatibility of materials used in the product. When the input materials are set, the output is the generated information about the compatibility of the materials.

### 3.3.3 Selecting Additional Material with Regard to Compatibility

The next stage consists in defining learning files. The input is the information about the material already chosen by the designer for the given part, together with the level of product compatibility which the process engineer needs to reach after



(a) Decision tree

Examples of rules:

- 0001 : compatibility = "good" if  
added\_material = "ABS",  
main\_material = "ABS";
- 0002 : compatibility = "good" if  
added\_material = "ABS",  
main\_material = "ASA";
- 0003 : compatibility = "limited" if  
added\_material = "ABS",  
main\_material = "PA";
- 0004 : compatibility = "good" if  
added\_material = "ABS",  
main\_material = "PBT";
- 0005 : compatibility = "good" if  
added\_material = "ABS",  
main\_material = "PC";
- 0006 : compatibility = "limited" if  
added\_material = "ABS",  
main\_material = "PE";

(b) Decision rules

**Fig. 3** The generated decision tree (a) and decision rules (b) for selecting materials according to their compatibility



adding or changing a material in the next part of the product. The output is the information containing data on materials which meet the level of compatibility required by the process engineer. Based on such defined learning data, the next decision tree is generated.

In this case, the generated rules help us select materials, when one material is known and it is necessary to choose another one to achieve the required product compatibility. It is also checked how to select the material for another designed (or modified) part while maintaining the predefined compatibility. The rules make it possible to check what material should not be combined with the originally chosen one.

If the initial setting is “no compatibility”, the system generates a list of materials which should not be chosen.

### **3.3.4 Choosing Material Connections**

Learning data for the method of selecting connections in the product are developed similarly. Depending on the materials and their compatibility, either separable or inseparable connections can be chosen.

Similarly, as in previous cases, a decision tree is generated with rules of selection of material connection. The most important attribute of classification is material compatibility, regardless of the main and additional material. It offers the largest information gain. With the generated rules, it is possible to select the type of connection, depending on the materials used in the product.

## **4 Expert System Supporting Ecodesign with the Use of the CE Approach**

The rules described above have been implemented into an expert system. The expert system consists of a generating module and user interface. The menu of the expert system, used by both the product designer and the process engineer, is shown in Fig. 4a. When choosing the materials according to their compatibility, the process engineer inputs the symbols of the main material and the additional material to the expert system. The system will then advise the compatibility between the materials (e.g., good, limited, or incompatible) (Fig. 4b). In the second option (selection of additional material according to compatibility), the process engineer provides the symbol of the material and indicates the desired degree of compatibility, e.g., good compatibility. The system will then respond by providing symbols of materials which may be added to the main material to maintain the required level of compatibility. The third function of the expert system offers the possibility to select connections between materials. Depending on the required level of compatibility, the system suggests the appropriate type of connections (separable,

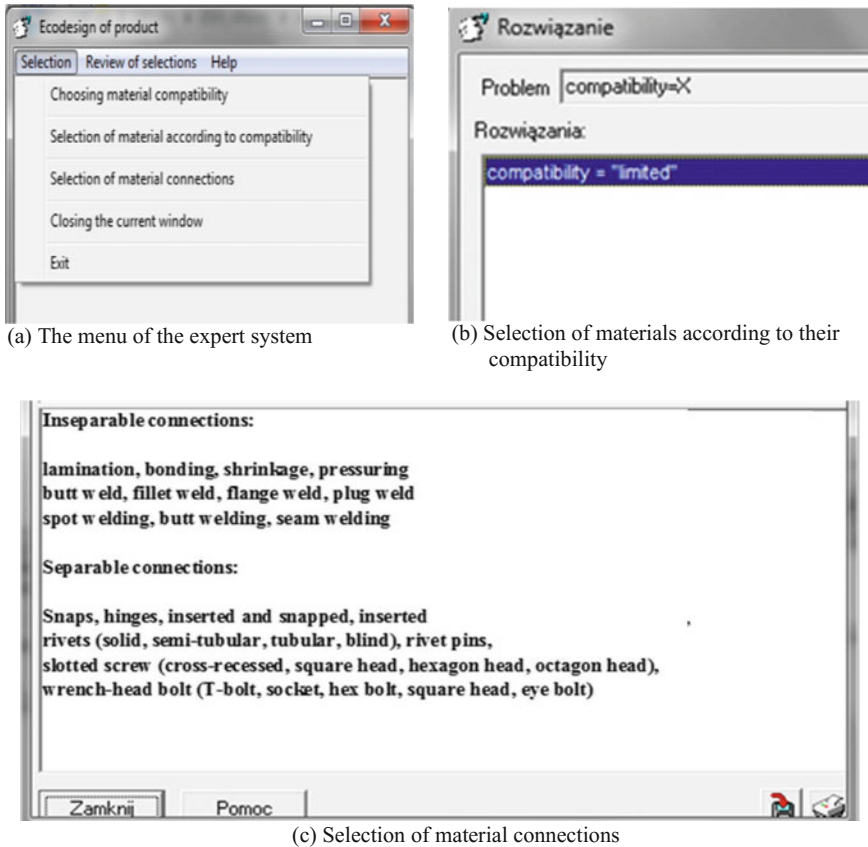


Fig. 4 Examples of expert system screens

inseparable). Additionally, a further, detailed breakdown of separable and inseparable connections has been implemented in the system (Fig. 4c).

The article shows examples of selecting two materials and their connections. However, after expanding the knowledge bases by other materials and connections, and increasing the number of decision rules, the system may be used to select three, four, or even more materials.

## 5 Conclusion and Future Research

The developed system which supports the ecodesign of products and engineering processes may be helpful in sustainable product design according to the CE principle. It is particularly useful in situations where the knowledge of the conditions of green design is difficult to formalize, uncertain and incomplete, or not available.

The use of the machine learning method used in the system proved to be a very valuable tool for acquiring knowledge on the possibilities of selecting materials and connections in the designed product. It turns out that the designer often makes decisions intuitively and cannot explain precisely the rules behind his choices. By acquiring his knowledge, the method may be used to automatically create classic rules found in expert systems. In the case of sustainable product design, it is appropriate to use the decision tree induction as the classification method due to the large number of input data represented in a symbolic form. Rules generated based on decision trees are more concise and the time needed for drawing conclusions is significantly reduced. During further work, the system will be expanded to include not only the compatibility of materials but also their strength and rigidity.

Next stages of the research will involve the integration of the tool with a system supporting the design of technological processes developed and tested in manufacturing companies. It is also planned to include other elements affecting the environmental evaluation of products, e.g., to minimize the number of tools needed for product disassembly, eliminate materials with a negative impact on the environment.

## References

1. Newnes, L.B., Mileham, A.R., Hosseini-Nasab, H.: On-screen real-time cost estimating. *Int. J. Prod. Res.* **45**(7), 1577–1594 (2007)
2. Karwasz, A., Dostatni, E., Diakun, J., Grajewski, D., Wichniarek, R., Stachura, M.: Estimating the cost of product recycling with the use of ecodesign support system. *Manage. Prod. Eng. Rev.* **7**(1), 33–39 (2016)
3. Dostatni, E., Diakun, J., Grajewski, D., Karwasz, A., Wichniarek, R.: *Ecodesign of products in CAD 3D environment with the use of agent technology* (in Polish). Publishing house of Poznan University of Technology, Poznań (2014)
4. AENOR: *Environmental Management of design and development process, design for environment*, UNE 150301 Standards (2003)
5. Flizikowski, J., Macko, M.: Competitive design of shredder for plastic in recycling. *Tools Methods Competitive Eng.* **1–2**, 1147–1148 (2004)
6. Czerniak, J.M., Macko, M., Ewald, D.: The CutMAG as a new hybrid method for multi-edge grinder design optimization. *Adv. Intell. Syst. Comput.* **401**, 327–337 (2016)
7. Gehin, A., Zwolinski, P., Brissaud, D.: Integrated design of product lifecycles—the fridge case study. *CIRP J. Manufact. Sci. Technol.* **1**(4), 214–220 (2009)
8. Burduk, A.: Assessment of risk in a production system with the use of the FMEA analysis and linguistic variables. *Lect. Notes Artif. Intell.* **7209**, 250–258 (2012)
9. Burduk, A.: Evaluation of the risk in production systems with a parallel reliability structure taking into account its acceptance level. *Lect. Notes Artif. Intell.* **6679**, 389–396 (2011)
10. Zhuc, Y.A., Zedtwitz, M., Assimakopoulos, D., Fernandes, K.: The impact of organizational culture on concurrent engineering, design-for-safety, and product safety performance. *Int. J. Prod. Econ.* **176**, 69–81 (2016)
11. Govindan, K., Khodaverdi, R., Vafadarnikjoo, A.: Intuitionistic fuzzy based DEMATEL method for developing green practices and performances in a green supply chain. *Expert Syst. Appl.* **42**(20), 7207–7220 (2015)

12. Yang, Jung Ch., Lewis Chen, J.: Forecasting the design of eco-products by integrating TRIZ evolution patterns with CBR and Simple LCA methods. *Expert Syst. Appl.* **39**(3), 2884–2892 (2012)
13. Dostatni, E., Diakun, J., Hamrol, A., Mazur, W.: Application of agent technology for recycling-oriented product assessment. *Ind. Manage. Data Syst.* **113**(6), 817–839 (2013)
14. Platcheck, E.R., Schaeffer, L., Kindlein Jr., W., Candido, L.H.A.: Methodology of ecodesign for the development of more sustainable electro-electronic equipments. *J. Clean. Prod.* **16**(1), 75–86 (2008)
15. Bovea, M.D., Pérez-Belis, V.: A taxonomy of ecodesign tools for integrating environmental requirements into the product design process. *Int. J. Clean. Prod.* **20**, 61–71 (2012)
16. Dostatni, E., Diakun, J., Grajewski, D., Wichniarek, R., Karwasz, A.: Functionality assessment of ecodesign support system. *Manage. Prod. Eng. Rev.* **6**(1), 10–15 (2015)
17. Grajewski, D., Diakun, J., Wichniarek, R., Dostatni, E., Buń, P., Górski, F., Karwasz, A.: Improving the skills and knowledge of future designers in the field of ecodesign using virtual reality technologies. In: *International Conference Virtual and Augmented Reality in Education*, Monterrey, pp. 348–358 (2015)
18. Rojek, I.: Classifier models in intelligent capp systems. In: Cyran, K.A., Kozielski S., Peters, J.F., Stańczyk U., Wakulicz-Deja A. (eds.) *Advances in Intelligent and Soft Computing*, vol. 59, pp. 311–319. Springer, Berlin (2009)
19. Rojek, I., Jagodziński, M.: Hybrid artificial intelligence system in constraint based scheduling of integrated manufacturing ERP systems. *Lecture notes in artificial intelligence, LNAI*, vol. 7209, pp. 229–240. Springer, Berlin (2012)
20. Rojek, I.: Technological process planning by the use of neural networks. *Artif. Intell. Eng. Des. Anal. Manuf.* **31**(1), 1–15 (2017)
21. Low, J. S. C., Lu, W. F., Song, B., Methodology for an integrated life cycle approach to design for environment. In: Su, D., Zhu, S. (eds.) *Key Engineering Materials*, vol. 572, pp. 20–23 (2014)
22. Broch, F., Warsen, J., Krinke, S.: Implementing life cycle engineering in automotive development as a helpful management tool to support design for environment. In: Sonnemann, G., Margni, M. (eds.) *Life Cycle Management*, pp. 319–329 (2015)
23. Birch, A., Hon, K.K.B., Short, T.: Structure and output mechanisms in design for environment (DfE) tools. *J. Clean. Prod.* **35**, 50–58 (2012)
24. Saniuk, A., Jasiulewicz-Kaczmarek, M., Samolejova, A., Saniuk, S., Lenort, R.: Environmental favourable foundries through maintenance activities. *Metalurgija* **54**(4), 725–728 (2015)
25. Sabaghi, M., Mascle, C., Baptiste, P.: Evaluation of products at design phase for an efficient disassembly at end-of-life. *J. Clean. Prod.* **116**, 177–186 (2016)
26. Chemical Compatibility Chart Plastics: [http://www.terrauniversal.com/appendi-cies/plastics\\_material\\_compatibility.php/](http://www.terrauniversal.com/appendi-cies/plastics_material_compatibility.php/). Accessed 14 April 2016
27. Wu, X., Kumar, V., Quinlan, J.R., Ghosh, J., Yang, Q., Motoda, H., McLachlan, G.J., Ng, A., Liu, B., Yu, P.S., Zhou, Z.-H., Steinbach, M., Hand, D.J., Steinberg, D.: Top 10 algorithms in data mining. *Knowl. Inf. Syst.* **14**(1), 1–37 (2008)

**Part II**  
**Design, Building and Research**  
**of Machines and Devices**

# Intelligent Materials Application in Mechatronic Devices

Andrzej Milecki

**Abstract** The paper covers at first a few different definitions of mechatronics, illustrated with figures and schemes. Furthermore, main research areas of mechatronics are sketched, among which there are the applications of new, so-called, “intelligent” materials and new control and communication methods to be used by human operators. The main goal of these works is to obtain mechatronic devices smart in mechanics and intelligent in communication with the user. In this paper, the basic properties of such “smart” materials like piezoelectric crystals, magnetic shape memory alloys, and magnetorheological fluids are presented. Theoretical review is followed with practical examples of mechatronic devices developed in Division of Mechatronic Devices at Poznan University of Technology (PUT), in which the abovementioned materials are used and applied in new type of actuators.

**Keywords** Mechatronics · Smart materials · Piezo actuator · MSMA  
Magnetorheological fluids

## 1 Introduction

The word “mechatronics” was created in 1969 in Japanese Corporation Yaskawa Electric. This company started to use electronic elements in their mechanical products and wanted to name them using a new technical term. The Corporation Yaskawa Electric has registered this new word as a brand and has got the rights to it in 1972. In the beginning of 1980s, this word has received broad acceptance in academia and then in industry. So, in order to allow its free use, the Yaskawa Corporation decided in 1982 to abandon its rights to term “mechatronics”. The word “mechatronics” is now used as a description of almost every mechanical device in which electronics is used. Across the years, a number of definitions of mechatronics have been proposed by different authors [1–4], either as a text, a logo,

---

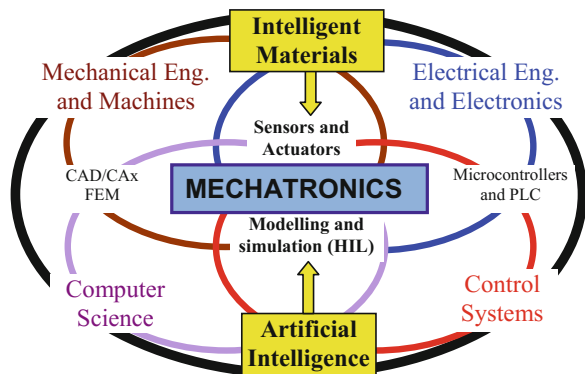
A. Milecki (✉)  
Poznan University of Technology, Poznan, Poland  
e-mail: andrzej.milecki@put.poznan.pl

or pictures. On a web page [5], there are over 20 definitions of mechatronics, which conclude that mechatronics means the integration of the core disciplines of mechanical engineering (mechanical elements, machines, robot arms, etc.), electronics (microelectronics, power electronics, sensors, and actuators), and information technology (control and automation, software engineering, and artificial intelligence). In many commonly used definitions, the synergistic advantages of mechanical engineering with electronic engineering integration are emphasized. In other definitions, the application of intelligent computer control in the mechatronic products is the main point. An overview of general aspects of mechatronics, as well as design and development of mechatronic products, is described in [6–8].

Mechatronics has a variety of applications as products in the area of “manufacturing”. These applications are, for example, computer numerical control machines, tool monitoring systems, flexible manufacturing system, industrial robots, machine vision, etc. The developed by mechantronics drives with piezo actuators or dampers with magnetorheological fluid found application in different production machines. An example is a newly designed adaptronic component with a piezo-stack actuator for active damping of machine vibrations [9].

Nowadays, the application area of mechatronics is extremely broad. It is used in the automation of devices and processes, servo-drives, industrial machines, medical systems, home equipment, energy and power systems, vehicles, military equipment, data communication systems, medical equipment, and many others. The aim of mechatronics is to improve the functioning of systems and devices by transforming them into one automatic and intelligent system. The term mechatronics is described by many graphics and schemes as shown in Fig. 1 [10]. In this figure, two relatively new research areas in mechatronics are also shown: intelligent control and intelligent materials application. They are used in order to create human-like mechatronic devices. In this paper, the chosen investigation results of so-called “smart” materials are presented. The choice of right material is becoming increasingly important in relation to the assumed device tasks. Intelligent materials have itself made it possible to develop the mechatronic actuators which are similar to man muscles. These materials support the general mechatronic concept of integration of smart

Fig. 1 The graphical definition of mechatronics



mechanical drives with intelligent controllers. The intelligent materials are piezo actuators, different shape memory alloys, electro- and magnetorheological fluids and elastomers, as well as pneumatic muscles and smart fabrics. The oldest “smart” material is the piezoelectric crystal, which may act as actuator, converting electrical energy into mechanical energy. They are attractive due to their fast response, large output forces, and high resolution. Piezoelectric actuators have been widely used so far in common rail direct fuel injection systems for petrol and diesel engines. However, these actuators may be also applied as smart drives in small robots, valves, precise devices, etc. Other smart materials applied nowadays in mechatronic drives are magnetostrictive materials, like Terfenol-D, which change their geometry in the presence of magnetic field. Other smart materials are shape memory alloys (SMAs), which respond to temperature change with deformations. Similar materials are magnetic shape memory alloys (MSMAs), which change their properties, i.e., shape, in the presence of external magnetic field. Another group is formed with smart fluids and elastomers, like electro- or magnetorheological or ferrofluids.

## 2 Piezo Actuators Control Electronics

Nanopositioning and nanofabrication tasks [11, 12], with assurance of high frequency of work, are often important requirements for manufacturing devices. In such cases, piezo actuators may be applied. They are able to move mechanical elements with forces reaching kN and with frequencies ranging up to many kHz. Such high resonance frequency of piezoelectric actuators enables them to drive high-frequency mechatronic devices. There are two main types of piezo actuators: stack and bimorph actuators. The first type is linear actuators that can generate forces up to 100 kN and displacement up to a fraction of a mm. However, the stack actuators have to be supplied with controllable voltages in a range of kVs, which can be present as a serious challenge. Bimorph actuator like piezo bender consists of two layers and can be used to elongate, twist, or bend. When supplying, one layer expands while the other layer contracts and as a result, the bending of the actuator is produced. The motion in the range of fraction of millimetres and forces to a few N is typical. The bending actuators can be supplied with voltages ranging from  $\pm 30$  to  $\pm 100$  V and are able to produce forces to a few N. Therefore, piezo bender actuators can be successfully applied in many mechatronic devices, requiring low forces. Their electronic amplifier plays a crucial role in the mechanical behaviours of a piezo bending actuator. Therefore, in Division of Mechatronic Devices at Poznan University of Technology, the investigations on development of amplifier have been undertaken. They have been focused on amplifiers used for the two-layer piezo bending actuators. The main task was to design a low-cost amplifier, which would be based on the typical operational amplifier (OA).

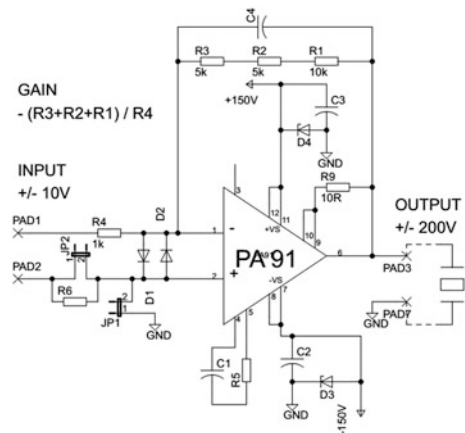
Several companies are producing high-power and high-voltage amplifiers, which may be used as controllers for piezo bender actuators. The examples are as follows:

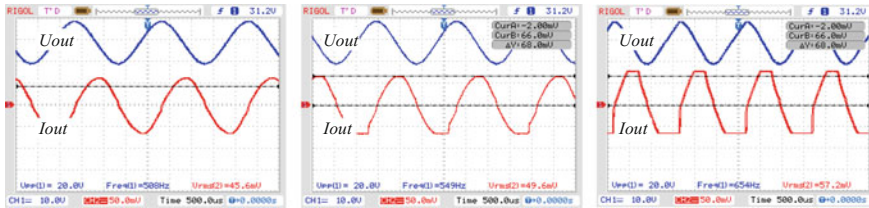


- PAD129; parameters: slow rate 37 V/ $\mu$ s, output voltage up to  $\pm 90$  V, continuous output current of 15 A, cost 210 USD;
- MSK 163; parameters: slow rate 20 V/ $\mu$ s, output voltage up to  $\pm 141$  V, current output of 120 mA;
- PA341; parameters: slow rate 30 V/ $\mu$ s, supply voltage equal to 350 V, current output 120 mA, cost 140 USD; and
- PA91 Parameters: slow rate 300 V/ $\mu$ s, minimum supply voltage  $\pm 40$  V, supply voltage 450 V or  $\pm 225$  V, output current up to 200 mA, pulse currents up to 350 mA, cost 167 USD [13].

After a review of high-voltage power amplifiers available on the market, PA91 is chosen to tests. In the research presented in this paper, a multilayer piezo bender actuator type PL112.10 (Physik Instrumente GmbH & Co. KG, Germany) was used. Its parameters are nominal displacement:  $\pm 80$   $\mu$ m; blocking force: 2 N; resonant frequency: 1 kHz; operating voltage:  $\pm 30$  V; and capacitance:  $2 \times 1.1$   $\mu$ F. From the electrical point of view, the piezoelectric actuator is a non-linear capacitor. Due to this fact, the used amplifiers must be able to generate as much high current when the voltage changes. When the control signal changes in step-like manner, the piezo actuator behaves like a short circuit. The scheme of an amplifier circuit supply based on PA91 designed and built at PUT is shown in Fig. 2 [14]. The resistors used in a circuit established the voltage amplification to 20 V/V. Unfortunately, the cost of such this circuit is about 170 USD, which is rather high in comparison with other ordinary high-power operational amplifiers. Therefore, in the next step, the use of an ordinary, low-cost audio amplifier is proposed. The investigation results are shown in Fig. 3. For supply voltages in a range of 20 Vpp, for frequencies about 500 Hz, both signal voltage and current behave in the same manner. However, for higher frequencies, i.e., above 550 Hz, the amplifier PA91 reduces the maximum current. The maximum current is set using resistor R9. By this way, the OA PA91 and the piezo actuator are protected.

**Fig. 2** Supply circuit based on PA91





**Fig. 3** Investigation results of signals supplying the piezo bender actuator PL112.11 controlled by PA91; *U<sub>out</sub>*—output voltage (blue curve), *I<sub>out</sub>*—output current (red curve)

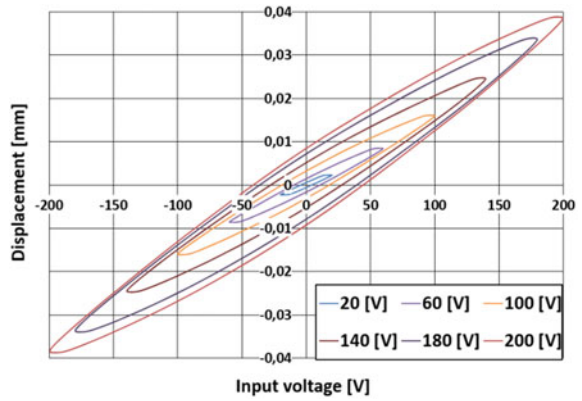
This reduction, i.e., protection is not possible when low-cost (5 USD) audio power amplifier like LM3886 is used. Research results of the application of this circuit to control of piezo actuator are presented in [14].

### 3 Piezo Actuators Hysteresis Modelling and Compensation

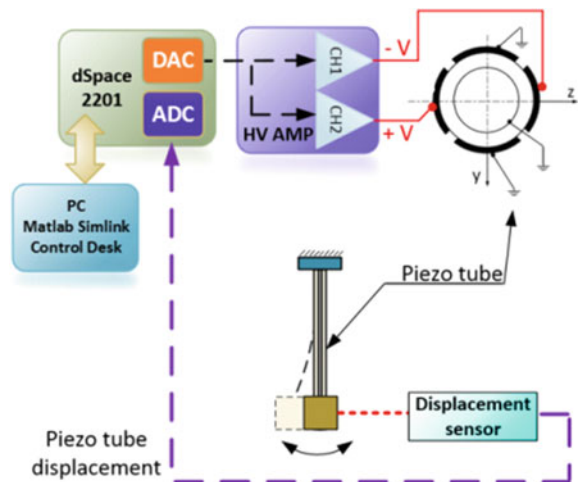
In the next work made at PUT, the offered by PI ceramic piezoelectric PT230 tube actuator was investigated [15]. The geometrical parameters of the tube are length  $l = 40$  mm, outer diameter  $d_o = 3.2$  mm, and inner diameter  $d_i = 2.2$  mm. The maximal operating voltage was  $\pm 250$  V. Depending on different electrical connections and electrode configurations, the tube can change its radius dimension, bend the free end, and elongate along the longest axis. This actuator was at first tested using sinusoidal signal with growing amplitude. In Fig. 4, the relationship between input voltage and actuator displacement is shown. In the obtained characteristic, the significant symmetric hysteresis of approximately 20% is visible.

In the next step of the research, the positioning control of the piezo tube actuator was proposed. For this purpose, the classic PID control algorithm with closed-loop feedback was applied. The feedback signal is generated by laser displacement sensor. The controller was implemented in Matlab Simulink environment. In addition, the dSPACE hardware was used (Fig. 6), which allowed fast parameters modification and testing. The tube could be supplied using five electrodes, one inner and four distributed on the outer surface (circumference of the tube), but in the first research only two outer opposite electrodes were energized and the remaining electrodes were connected to ground. The electrical connection is shown in Fig. 5. In this configuration, the free end of the tube could bend along the  $x$ -axis. The aim of the application of PID controller was to reduce the hysteresis behaviour in positioning. The PID control algorithm was tuned using manual tuning method under real-time work in dSPACE software Control Desk. The results obtained in laboratory investigations have proven that the applied classical PID controller was effective and allowed the reduction of the hysteresis and thus the tracking error in a range of  $\pm 1$   $\mu$ m (Fig. 6).

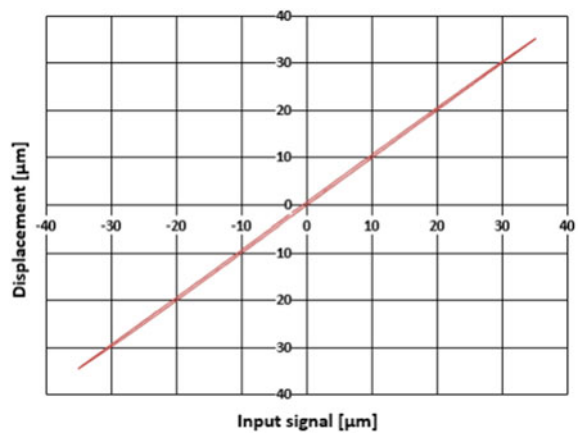
**Fig. 4** Piezo tube actuator characteristics



**Fig. 5** The scheme of control with PID



**Fig. 6** The hysteresis compensation results



However, in many applications of piezo actuators, it is not possible to use position measuring elements, mainly due to the lack of space. One of the possible solutions to reduce the hysteresis is the application of the inverse compensation in a controller system. In the controller, the inversed hysteresis model is used [16]. To describe the hysteresis phenomena, many different models are proposed in the literature. One of them is the generalized Prandtl–Ishlinskii model (GPIM) which allows to model asymmetric hysteresis loops and their saturation. Thus, the GPI model is sufficient for modelling of transducers based on piezo, magnetostrictive, or shape memory alloys. The output signal of GPIM is the sum of generalized play operators output signals, which are additionally increased or reduced by weights. GPIM is preferred for modelling of characteristics with asymmetric shapes. Description and the idea of generalized version of operator is presented in [17]. Ease of creation of analytical inversion is the most important feature of GPIM application. This is an important advantage, which significantly reduces computation time and allows its application in real-time control systems. The parameters of the generalized Prandtl–Ishlinskii model should be estimated based on characteristic obtained in laboratory tests. Therefore, at first, the piezo tube characteristic is measured using input signal  $v(t) = V_m \cos(2\pi/6 \cdot t)$  [V], where amplitude is increased linearly from 0 to 190 V. Thanks to this, the major and several minor hysteresis loops are recorded. The output characteristic of the piezoceramic tube is presented in Fig. 7. In the same figure, the GPIM responses are added. The results show that the GPIM can be used as accurate hysteresis model of the piezoelectric tube. The presented model output curve follows with a good precision the shape of the major as well as minor piezo tube hysteresis loops. The biggest model error is approximately 3.3% relative to the whole displacement range.

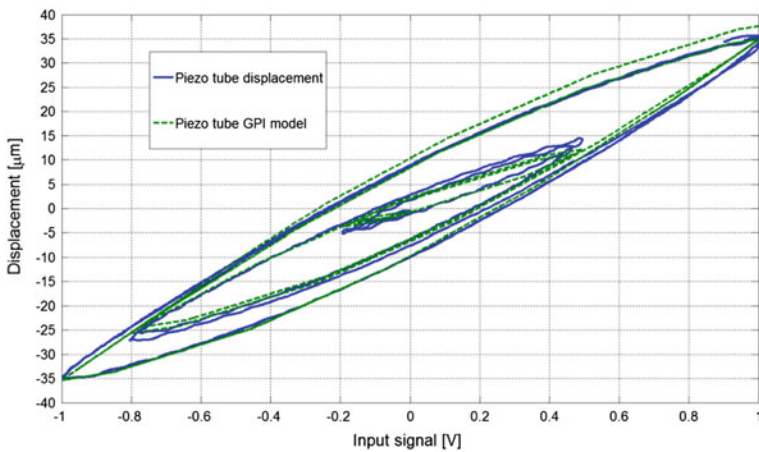


Fig. 7 Piezo tube and GPI model displacement responses

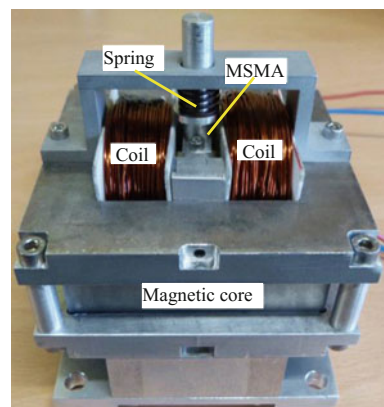
## 4 Magnetic Shape Memory Actuators Investigations

Another smart materials suitable for positioning devices are magnetostrictive (magnetic field stimulation) and shape memory alloys (SMA), which can be activated by temperature (using Joule effect) or by magnetic fields. The last materials are called magnetic shape memory alloys (MSMA). At PUT, the actuator with crystal Ni<sub>2</sub>MnGa alloy of dimensions  $3 \times 10 \times 32$  mm (produced by the AdaptaMat Ltd.) was designed and built (Fig. 8).

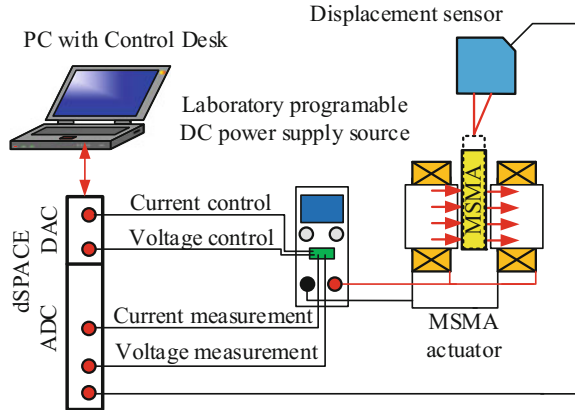
It was based on the spring returned operating mode [18]. Because the shape memory effect in these materials is self-supporting, a source of compressive force is needed. To produce this force, a coil spring placed above the material is used. Without the spring, after the application of the external magnetic field, the material will stay in the elongated state. The spring stiffness is chosen as 6.93 N/mm. The spring has been pre-tensioned to generate 30 N of reaction force at zero position. The magnetomotive force is generated by two coils connected parallel. The magnetic core is divided into two E-shape parts, which are made of low-carbon soft magnetic steel. The magnetic induction in air gap for 4 A coils current equals 0.65 T. The designed actuator displacement is 1000  $\mu$ m.

The test stand was based on a dSPACE 1104 control card equipped with DAC and ADC (Fig. 9). The position of the actuator rod was measured by a Micro-Epsilon laser sensor characterized with the precision of 0.5  $\mu$ m and maximum frequency of 2.5 kHz. The input current was measured by a Hall effect sensor. The ControlDesk software was used to perform different tests and parameters of the control algorithms changes. For investigation purpose, special current input signal was prepared. It was a damped sine function with 1.5 A amplitude with added 1.5 A constant current, which was biased. Thus, the current was changing from 0 to 3 A. Additionally, it was symmetrically damped to the middle value.

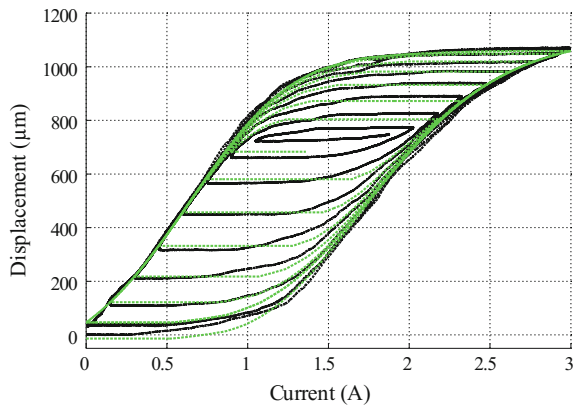
**Fig. 8** The actuator with MSMA



**Fig. 9** Scheme of the control stand

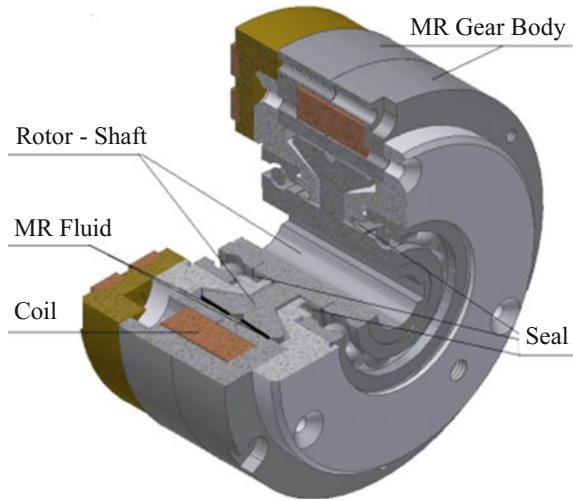


**Fig. 10** MSMA investigations and modelling results



Result of this measurement is presented in Fig. 10, where the black curve is the measured displacement of MSMA actuator with spring. The investigation results showed that MSMA is characterized by saturated hysteresis. In order to control the actuator in open loop, at PUT the adaptation of GPIM and its inversion to compensate hysteresis nonlinearity in actuator with MSMA is made [19]. In this work, we used GPIM which is almost the same as used in modelling of piezo tube. The dashed green line is the generalized Prandtl–Ishlinskii model output signal. The registered data were used for hysteresis model parameters estimation. The fitting of model to measured data was performed using nonlinear least square method. The result of modelling and measurement is shown in Fig. 10. Maximum modelling error was less than 4%.

**Fig. 11** The gear with MR fluid



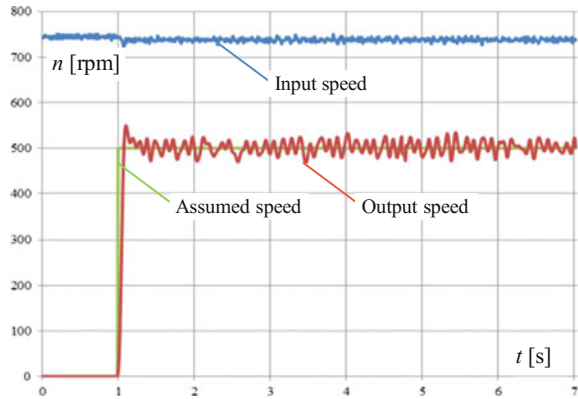
## 5 Gear with Magnetorheological Fluid

Magnetorheological (MR) fluids are suspensions of magnetically polarizable particles in a carrier liquid like oil or water. When a magnetic field is applied, the particles become magnetic dipoles and create chains in the fluid. As a result, the MR fluid apparent viscosity is changing (stiffening of the material). This effect is fast and reversible. MR fluids have found applications in adaptive vibration damping, particularly in automotive shock absorbers, used in multitude of vehicle models in semi-active suspension systems. In order to expand the application of MR fluids, the development of cylindrical MR gear was researched at PUT. Initially, the possibilities of implementation of MR fluid in the clutch were shown [20] and then the gear with MR fluid was proposed and applied (Fig. 11) [21]. Special control system was also implemented. In the research, a step-like assumed signal corresponding to velocity 600 rpm was given to the controller input. The input shaft rotary speed was relatively constant and was equal to about 730 rpm. The output speed reached the desired value within 100 ms and oscillated with the amplitude of less than 5% of the desired value (Fig. 12).

## 6 Summary

Nowadays, the influence of mechatronics on the intelligent device development used in many manufacturing devices is very important. However, these materials suffer for important nonlinearities which may be reduced by applications of special control methods, as shown in this paper. The new “smart” or “functioning” materials introduced have resulted in next generation of mechatronic devices.

**Fig. 12** Velocity step response



In this generation, a deeper integration of advanced, smart materials with intelligent controllers enable the improved functioning of complex mechatronic machines and systems used in the manufacturing sector. Thanks to this, the new mechatronic devices will be so designed to be able to perform also intelligent functions, which so far have been reserved for humans. The mechatronics goal for now and for the future is to develop autonomous, self-learning devices. These devices will be a part of INDUSTRY 4.0 approach.

**Acknowledgements** The research work reported here was supported by the Polish Ministry of Science and Education grants no. 02/22/DSPB/1389.

## References

- Bradley, D., Dawson, D., Burd, D., Loader, A.: *Mechatronics electronics in products and processes*. Chapman & Hall, London (1991)
- Cetinkunt, S.: *Mechatronics*. Wiley, New York (2007)
- Tomizuka, M.: *Mechatronics: from the 20th to the 21th century*. In *First IFAC Conference on Mechatronic Systems* (pp. 1–10), Germany. Elsevier, Oxford (2000)
- Bishop, C.: *The Mechatronics Handbook*. CRC Press, Boca Raton (2002)
- [www.mechatronics.colostate.edu/definitions.html](http://www.mechatronics.colostate.edu/definitions.html). Accessed 19 April 2017
- Bradley, D.: *Mechatronics—more questions than answers*. *Mechatronics* **20**, 827–841 (2010)
- Isermann, R.: *Modeling and design methodology of mechatronic systems*. *IEEE/ASME Trans. Mechatron.* **1**, 16–28 (1996)
- Gausemeier, J., Brexel, D., Frank, T., Humpert, A.: *Integrated product development*. In: *Third Conference on Mechatronics and Robotics*, Germany (1995)
- Ast, A., Braun, S., Heisel, U.: *Adaptronic vibration damping for machine tools*. *CIRP Ann. Manuf. Technol.* **56**(1), 379–382 (2007)
- Milecki, A.: *45 years of mechatronics—history and future*. In: Szewczyk, R., Zieliński, C., Kaliczyńska, M. (eds.) *Progress in Automation, Robotics and Measuring Techniques. Advances in Intelligent Systems and Computing*, vol. 350. Springer, Cham (2015)
- Tsenga, A.A., Notargiacomob, A., Chen, T.P.: *Nanofabrication by scanning probe microscope lithography*. *J. Vac. Sci. Technol.* **23**, 877–894 (2005)



12. Rubio-Sierra, F.J., Heckle, W.M., Stark, R.W.: Nanomanipulation by atomic force microscopy. *Adv. Eng. Mater.* **4**(7), 193–196 (2005)
13. <https://apexanalog-public.sharepoint.com/Resources/PA91U.pdf>
14. Milecki, A., Regulski, R.: Investigations of electronic amplifiers supplying a piezobimorph actuator. *Mech. Syst. Signal Process.* **78**, 43–54 (2016)
15. Regulski, R., Stefański, F., Minorowicz, B., Sędziak, D.: Research of basic parameters of piezoelectric tube actuator. In: Szewczyk, R., Zieliński, C., Kaliczyńska, M. (eds.) *Progress in Automation, Robotics and Measuring Techniques. Advances in Intelligent Systems and Computing*, vol. 350. Springer, Cham (2015)
16. Stefański, F., Minorowicz, B., Nowak, A.: Hysteresis modelling of a piezoelectric tube actuator. In: Szewczyk, R., Zieliński, C., Kaliczyńska, M. (eds.) *Progress in Automation, Robotics and Measuring Techniques. Advances in Intelligent Systems and Computing*, vol. 350. Springer, Cham (2015)
17. Janaideh, M., Mao, J., Rakheja, S., Xie, W., Su, C.: Generalized Prandtl–Ishlinskii hysteresis model: hysteresis modelling and its inverse for compensation in smart actuators. In: *Proceedings of the 47th IEEE Conference on Decision and Control*, Mexico (2008)
18. Riccardi, L., Holz, B., Janocha, H.: Exploiting hysteresis in position control: the magnetic shape memory push-push actuator *Innovative Small Drives Micro-Motor Systems. GMM/ETG Symposium* (2013)
19. Minorowicz, B., Stefanski, F., Sedziak, D.: Hysteresis modeling and position control of actuator with magnetic shape memory alloy. In: *17th International Carpathian Control Conference (ICCC)*, pp. 505–510. IEEE (2016)
20. Rosiakowski, A.: Research on clutch with magnetorheological fluid. *Arch. Mech. Technol. Autom.* **324**(1) (2012)
21. Rosiakowski, A., Owczarek, P., Rybarczyk, D.: Research on speed control by means of a clutch with magnetorheological fluid. *Arch. Mech. Technol. Autom.* **34**(1) (2014)

# Development of Force Feedback Controller For the Loader Crane

Dominik Rybarczyk, Piotr Owczarek and Adam Myszkowski

**Abstract** The publication describes development process of the haptic joystick electronic controller design. The system proposed here was used for positioning of an electrohydraulic manipulator (laboratory model of the loader crane). Authors built controller basis on the 32-bits microcontroller type STM32f407 equipped with DMA controller (Direct Memory Access). The joystick prototype was equipped with DC motor and incremental encoder. Authors implemented an on–off current regulator for DC motor. This allows to control motors torque and therefore the force generated at the end of the joystick effector. The actual current value for on–off regulator was taken from the hall effect sensor. The haptic joystick with its controller was tested with use of an electrohydraulic manipulator equipped with proportional valves.

**Keywords** Current value controller · On–off controller · Haptic joystick  
Electrohydraulic manipulator · Loader crane

## 1 Introduction

During the development of the technical documentation and design of haptic joystick controller, the first step is to define the type of actuators—brake or motors and after that, what type of feedback (sensors) will be used. On this basis, it is possible to select suitable electronic circuits. The driver described here should allow to control the torque generated by the DC motor (active brake) and resistive brake generated by the magnetorheological fluid. In both cases, the regulation amounts to

---

D. Rybarczyk (✉) · P. Owczarek · A. Myszkowski  
Department of Mechanical Engineering and Management,  
Division of Mechatronic Devices, Poznan University of Technology,  
pl. Skłodowskiej-Curie 5, 60-965 Poznań, Poland  
e-mail: dominik.rybarczyk@put.poznan.pl

P. Owczarek  
e-mail: piotr.owczarek@put.poznan.pl

control the current value. This can be achieved in several ways, e.g., operational amplifiers working as a current source configuration.

Authors of presented here publication decided to use an on-off current controller. Implementation of such a controller required the use of, respectively, high-speed microcontroller, additionally equipped with special a DMA controller (Direct Memory Access).

Communication between haptic joystick controller and master (hydraulic manipulator) controller was realized in two ways:

- Digital—interface CAN2.0,
- Analog—encoder and analog inputs of the microcontroller.

The main idea behind presented here project was to build modular electronic controller, which allow to easy reconfiguration and a potential quick repair.

## ***1.1 State of the Art***

The publication [1] focused on the use of Lyapunov theory for control of hydraulic actuators. As the haptic joystick, author use PHANTOM haptic interface. The actuator interacts with the environment emulated by a spring. Effectiveness of the proposed controller is verified by simulation and experimental studies.

Phd thesis [2] described the haptic teleoperation of hydraulic manipulator. Individual theoretical stability of all control schemes was thoroughly investigated considering nonlinear hydraulic functions, servovalve dynamics, haptic device dynamics, human operator dynamics, and dynamics of the task environment in the analysis. All control schemes were individually tested experimentally on a hydraulic test rig to verify their practicality and effectiveness in real applications.

Authors [3] introduce a novel force scheme for master-slave setups operating under a delayed network. The method proposed here reduces the position errors at the slave end-effector, caused by the delay and packet loss (reduced tracking error about 92%). System was experimentally validated effectiveness by testing on a teleoperated hydraulic manipulator.

Article [4] describes the problem of tactile sensor-based object recognition and complete six degrees of freedom (DOF) localization in structured underwater environments. Algorithm based on the recognition of static objects is from a pre-known database. Authors described the construction of deep-sea-capable hydraulic gripper with tactile sensing units which were used for tests.

Authors of [5] described system which is based on this collision vector generated virtual reflection force to avoid the obstacles, and then the reflection force is transferred to the operator who is holding the joystick used to control the mobile robot. Authors claimed that based on this reflection force, the operator can control the mobile robot more smoothly and safely. For this bidirectional teleoperation, a master joystick system using a two-axis hall sensor was designed to eliminate the

nonlinear region, which exists in a general joystick with two motors and potentiometers. The effectiveness of the collision vector and force-reflection joystick is verified by comparing two vision-based teleoperation experiments, with and without force reflection.

The publication [6] describes the manual control system of the manipulator using the haptic joystick with magnetorheological brakes, during which the operator observed the robot work with the limited visibility. The constructions of the investigations stand, system kinematics, and control algorithm were described. Authors compared two control variants: the classical one and with use of the haptic joystick (force feedback).

In article [7], authors proposed a control algorithm to create the force feedback torque for steer by wire system. The direct current measurement approach is used to estimate torque at the steering wheel and front axle motor as elements to the feedback torque.

Described in the above literature, overview examples are concerned with the use of haptic joysticks in different types of industry and research devices. Based on the collected information, authors concluded that there are no detailed information about electronic controller structure in the haptic joystick. Publications focus on the implementation of ready-made joystick for the various operations. In reference articles, there is also a lack of information regarding the use of a on-off regulator to control the current value and—based on it—torque is generated by the motor in the haptic joystick.

## 2 Modeling

The DC motor can be described using the following equations:

$$u(t) = e(t) + R \cdot i(t) + L \frac{di(t)}{dt} \quad (1)$$

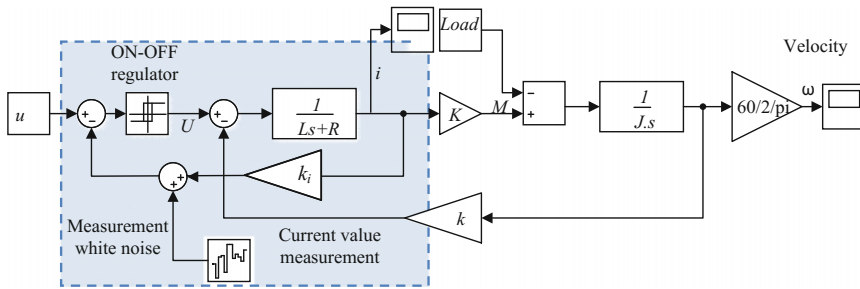
$$M(t) = K \cdot i(t) \quad (2)$$

$$M(t) = M_l(t) + J \cdot \frac{d\omega(t)}{dt} \quad (3)$$

$$e(t) = k_l \cdot \omega(t) \quad (4)$$

where  $u$ —supply voltages,  $e$ —electromotive force,  $i$ —rotor windings current,  $M$ —torque,  $M_l$ —load torque,  $K$ —load coefficient,  $k_l$ —electromotive force coefficient,  $J$ —moment of inertia, and  $\omega$ —angular velocity.

After Laplace transformation of Eqs. (1)–(4), their combination can be obtained as



**Fig. 1** Simulation model of DC motor with the on–off current regulator

$$\frac{I(s)}{U(s) - E(s)} = \frac{1}{s \cdot L + R} \quad (5)$$

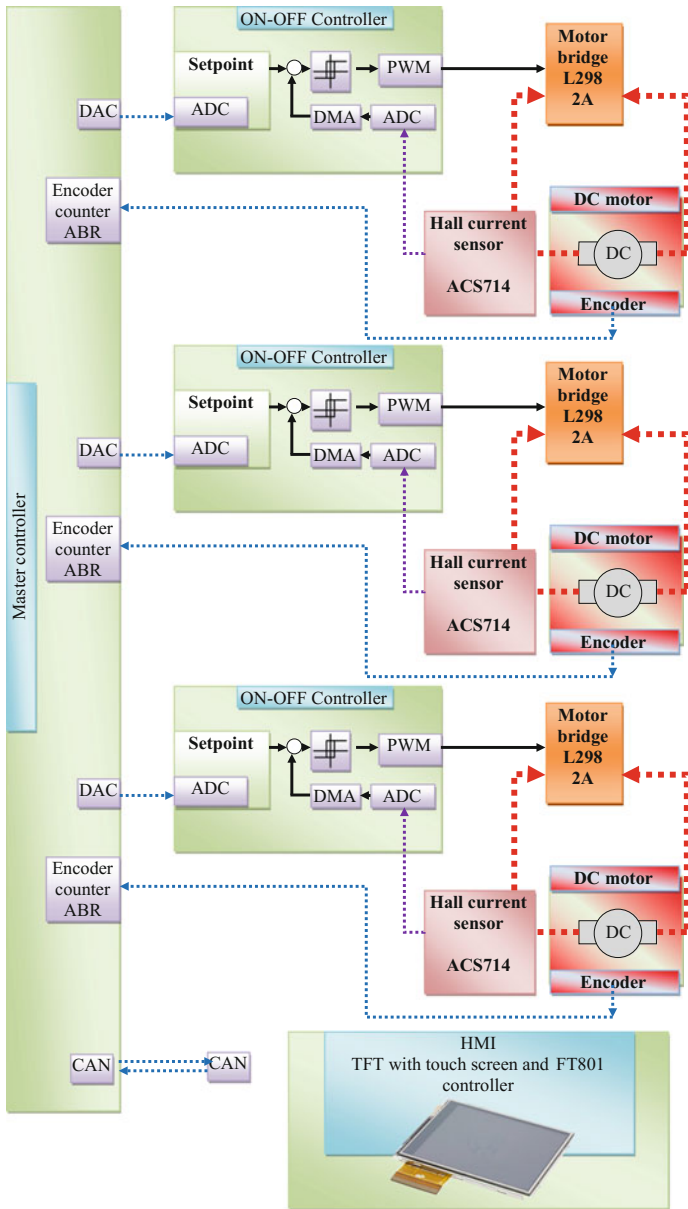
$$\frac{\omega(s)}{M(s) - M_t(s)} = \frac{1}{s \cdot J} \quad (6)$$

Based on Eqs. (5) and (6), a simple (sufficient to the project) simulation model DC motor is prepared in Matlab–Simulink software (Fig. 1). It includes on–off current regulator. In described system here, it was not necessary to add hysteresis to the regulator. In the feedback loop, authors add measurement noise signal which is present in the real controller (for the better reflect reality). The simulation results obtained from the presented here model were compared to the data obtained from the experimental research (real object) and are shown in Fig. 6.

### 3 Electronic Components

A wiring diagram was divided into the several parts, according to the functionality. The central point was the microcontroller as described below. In the project, authors decided to use the modular construction, based on the evaluation board-type STM32f407 discovery. A schematic diagram of the control system is shown in Fig. 2. The control system has been divided into the following parts:

- three independent on–off current value regulators consisting of a Hall effect sensors and the motors drivers (H-bridges),
- digital communication interface-type CAN2.0,
- analog interface: encoders and analog inputs of microcontroller,
- buttons on/off control actuators manipulator,
- HMI user interface based on TFT display with touch panel, and
- supply system.



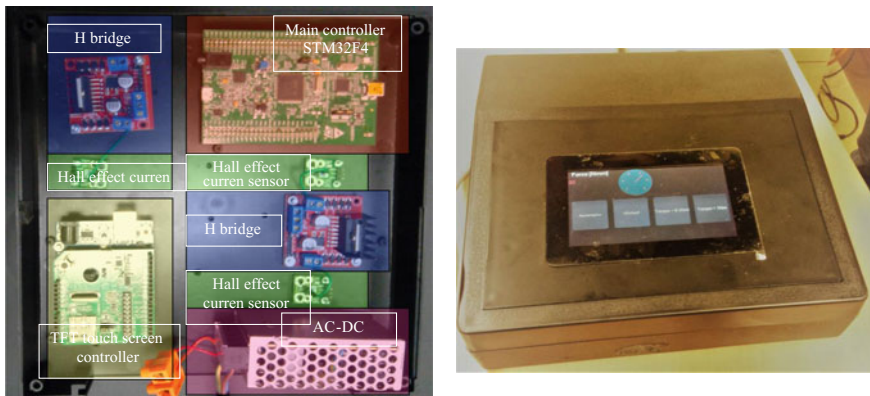
**Fig. 2** An electronic controller structure (analog and digital interfaces, HMI, three on-off current controllers)

STM32f407 microcontroller is performed in 90 nm process and based on the Cortex M4F 32-architecture core, 32-bit architecture. The master clock was set on 168 MHz. The microcontroller is equipped in the following communication interfaces: USART, SPI 18Mbit/s, I<sup>2</sup>C, USB Full Speed, CAN 2.0. The power supply works in the range of 1.8–3.6 V DC (in the described here system was 3.3 V).

For the current measurement feedback, authors used Hall effect sensor-type ACS714. The sensor allows to read current value in the range of  $\pm 5A$  and it was connected in series with the motor circuit. The read current value goes directly to the ADC input of the microcontroller. The most important advantage of the described sensor presented here is that the application is not putting an extra load to the circuit in which it is applied. In addition, the measurement itself not covers such a large degree of noise, which may have to occur in a situation in which the measurement took place by reading a voltage drop across the resistor.

STM32 microcontrollers series are equipped with DMA controllers (Direct Memory Access) [8], to ensure the transfer of data between the microprocessor system memory and a peripheral device without the participation of the central unit. The advantage of DMA is that a single-word transfer is done in a single memory access cycle. At the same time, the processor can execute the main control program. Particularly, large increase in processor performance can be achieved in case of sending more data packets. Each channel is operated independently and is connected to register memory addressing and counter words left to send.

All electronics elements were closed in the dedicated casing. The touchscreen was placed on the upper part of the case (Fig. 3).



**Fig. 3** View of built prototype (electronic module inside box: mainboard with microcontroller, H-bridge, hall effect current sensor, power supply; view on the touchscreen during work)

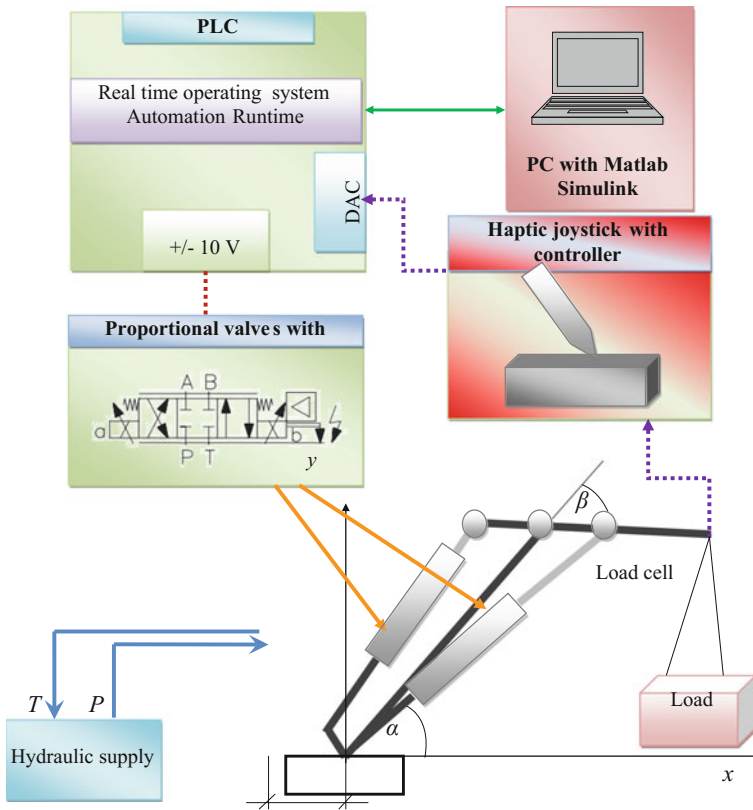
## 4 Experimental Verification

### 4.1 Test Stand

The central point of the test stand is a hydraulic manipulator, which is a laboratory model of the real load crane (HIAB company). Schematic structure of the test stand is shown in Figs. 4 and 5. Manipulator construction presented in the article is based on parallel kinematics. It has been equipped with two cylinders (stroke = 300 mm), controlled by the two independent proportional valves.

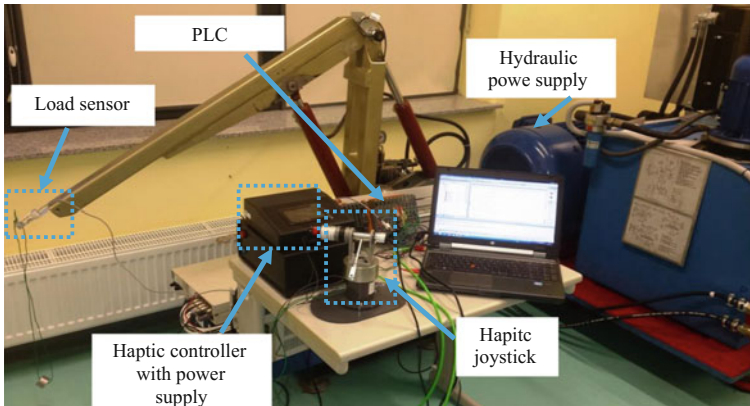
### 4.2 Experimental Tests

In order to verify system with assumptions, authors conducted initial tests of the controller prototype. The first step was to test the step response of the current



**Fig. 4** Test stand structure (hydraulic manipulator with load cell, haptic joystick with its controller, manipulator controller)



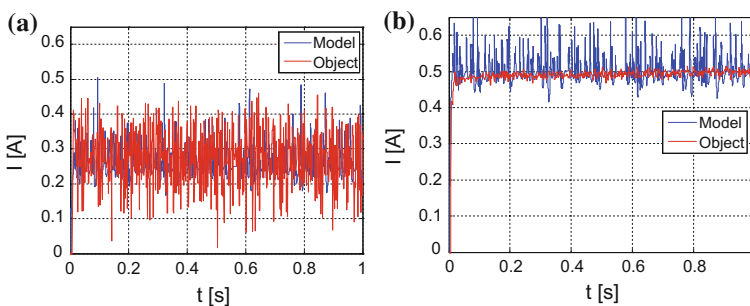


**Fig. 5** Test stand view (hydraulic manipulator with haptic joystick, controllers, hydraulic power supply)

regulator. Selected charts are shown in Fig. 6. The current time constant value was under  $200 \mu\text{s}$  for the current  $0.5 \text{ A}$ . Given the limitations of a human perception (joystick) and the parameters of mechanical components (hydraulic cylinder, HDS manipulator), received value was acceptable.

The next step was to verify the control unit cooperation with the hydraulic manipulator. In Fig. 7, authors show the behavior of the system during the swinging (hanging) load. The observed oscillations were the results of the force vector changing. The force on the load cell is translated directly to the current value in the motor windings.

The last task was to perform a lift test. The load was lifted on the flexible line. The supply pressure was equal to  $p_0 = 8 \text{ MPa}$ . The results are shown in Fig. 8. Tests have shown the transport delay of manipulators hydraulic drives equal to  $100 \text{ ms}$ . The reason is placed in dynamic parameters of the proportional valves (the dominant time constant was equal to  $100 \text{ ms}$ ) and the delays in communication



**Fig. 6** Current step response for **a**  $0.25 \text{ A}$ , **b**  $0.5 \text{ A}$

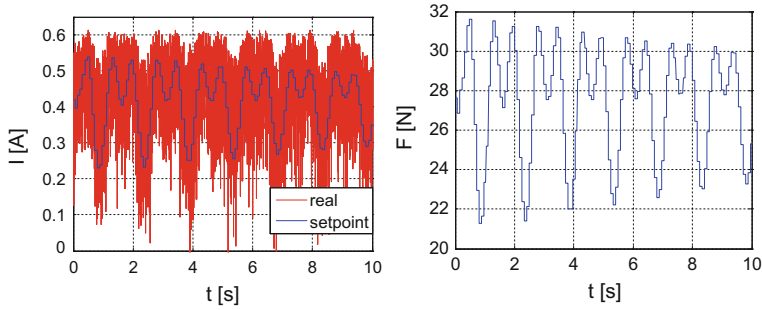


Fig. 7 Current and force value during hanging (swinging) of the load

between the controller joystick control unit and the control card. However, this value does not effect on the physical experience of joystick usage.

Based on the collected data, authors concluded that the torque generated on the motor shaft is directly proportional to the force measured by the load cell sensor placed on the electrohydraulic manipulator effector. For example, the value of 30 N is equal to the DC motor current 0.5 A.

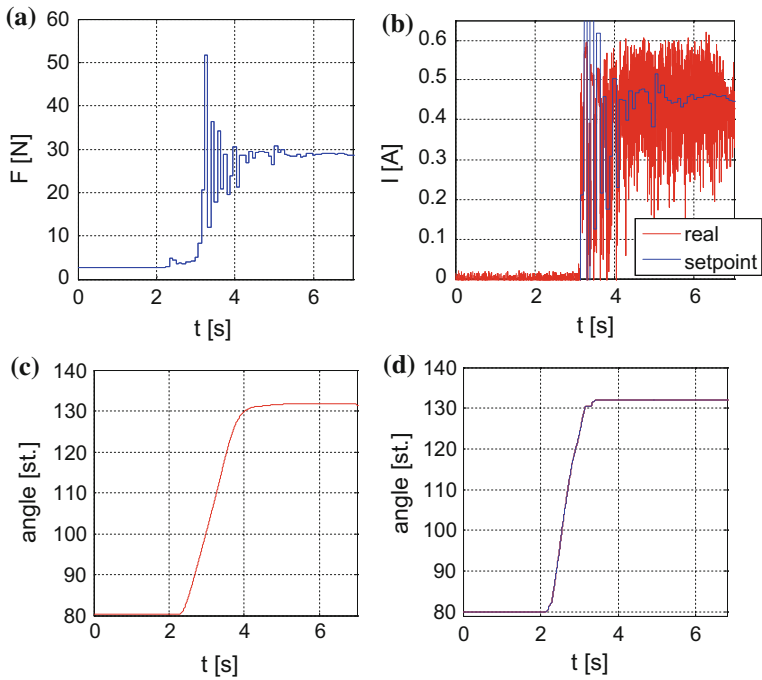


Fig. 8 Step response: a force 30 N, b current value, c manipulator axis displacement, d haptic joystick displacement

## 5 Conclusion

The article includes information about the prototype of the haptic joystick controller, like the description of the wiring diagram and system structure, electronic components, and used algorithms for the control. The system was tested using the haptic joystick and a hydraulic manipulator equipped with proportional valves, which was the laboratory model of the loader crane. Built system fulfilled its assumptions, by given smooth and proportional current regulation and therefore the force on joystick grip. During the experimental test, authors show the force oscillation during hanging the load, which influenced the actual current value and force on the joystick. It increases the system immersion and it is useful in HDS loader crane applications, especially operated in the limited visibility environment.

In the further research, authors will focus on checking the behavior of the controller described here on the real loader crane.

**Acknowledgements** The work described in this paper was funded from PBS3/A6/28/2015.

## References

1. Zareinia, K., Sepehri, N., Wu, Q.: A Lyapunov controller for stable haptic manipulation of hydraulic actuators. *Int. J. Robust Nonlinear Control* **22**(3), 241–261 (2012)
2. Zareinia, K.: Haptic-enabled teleoperation of hydraulic manipulators: theory and application [Online], Available: <http://mspace.lib.umanitoba.ca/handle/1993/5113/>. Accessed: 09 Feb 2017
3. Maddahi, Y., Liao, S., Fung, W., Sepehri, N.: Position referenced force augmentation in teleoperated hydraulic manipulators operating under delayed and lossy networks: A pilot study. *Robot. Auton. Syst.* **83**, 231–242 (2016)
4. Aggarwal, A., Kampmann, P., Lemburg, J., Kirchner, F.: Haptic object recognition in underwater and deep-sea environments. *J. Field Robot.* **32**(1), 167–185 (2015)
5. Cho, S.K., Jin, H.Z., Lee, J.M., Yao, B.: Teleoperation of a mobile robot using a force-reflection joystick with sensing mechanism of rotating magnetic field. *IEEE/ASME Trans. Mechatron.* **15**(1), 17–26 (2010)
6. Chciuk, M., Milecki, A., Bachman, P.: Comparison of a traditional control and a force feedback control of the robot arm during teleoperation. In: Szewczyk, R., Zieliński, C., Kaliczńska, M. (eds.) *Automation, ICA, Advances in Intelligent Systems and Computing*, p. 550. Springer, Berlin (2017)
7. Fahami, S.M.H., Zamzuri, H., Mazlan, S.A.: Development of estimation force feedback torque control algorithm for driver steering feel in vehicle steer by wire system: hardware in the loop. *Int. J. Veh. Technol.* (2015)
8. Technical documentation of STM32F4 microcontrollers series: [www.st.com](http://www.st.com). Accessed: Feb 2017

# Analysing and Optimizing 2.5D Circular Pocket Machining Strategies

Adam Jacso and Tibor Szalay

**Abstract** Though the circular pocket milling seems to be an old manufacturing task, it is nice to have thorough investigation among the different machining strategies, because in spare part production a frequent repeatable shape behaviour. As usual, at pocket milling the roughing operation is critical, because the excess material is in a closed area to the shape thus not possible to fix optimal cutting parameters for the whole area. In this exercise, we will deal with how the NC operational cycles and CAM systems could organize tool paths for circular pockets. This question is very important for the users because the selected strategy will influence the machining time and the tool life which determines the machining cost. In this article, several strategies were been compared through simulation and metal cutting experiments. During experiments, the material removal rate, the cutter engagement, and the cutting force were investigated alongside the tool path. At optimal tool paths, these parameters should be constant, because thus the cutting tool could provide maximum efficiency. It is found during experiments that the pocketing strategies used nowadays are far away from the optimal, and only the CAM-generated tool path strategies can execute the acceptable. The reason is because the tool path generation methods are made based on the part geometry without considering the technological aspects. In this article analysis of current, available strategies were been made, but over that two own-developed algorithms based on technological parameters were been discussed focused on optimal tool path to achieve maximum productivity.

**Keywords** 2.5D milling · Pocket machining · Tool path · Cutter engagement  
Material removal rate

---

A. Jacso (✉) · T. Szalay  
Department of Manufacturing Sciences and Engineering, Budapest University of Technology  
and Economics, Budapest, Hungary  
e-mail: jacso@manuf.bme.hu

T. Szalay  
e-mail: szalay@manuf.bme.hu

# 1 Introduction

The pocket milling process planning could be considered as a complex and diversified task. In this article, we will stay strictly with the investigation of circular pocket milling. It does not mean a big challenge, if we reach close to a suboptimal solution. During selection of theme, one of the main reasons was that at the production of mechanical parts, we frequently face circular pockets with different depths, and thus it is worth researching a perfect solution.

## 1.1 Technological Challenges at Pocket Milling Task

At pocket milling task, the geometry of pocket, the technological goal, and limits are given. Based on these, it must determine the correct cutting tool, correct tool path, and acceptable technological parameters [1]. Though all three factors are important, in this article, we will deal only with generating the optimal tool path. As the tool path generation strategy influences the cutting cost mainly in rough cutting, the theme is focused on this area. The specialty of pocket milling appears during cutting the internal arcs and corners because cutting parameters basically differs if the tool moves along a straight line or it moves along an arc. Thus, it is a serious challenge to adjust optimal cutting parameters through the whole length of tool path [2]. This occurrence is illustrated in Table 1.

The relation between the symbols:  $\theta$  is the cutter engagement,  $r$  is the tool radius,  $s$  is the stepover,  $\rho$  is the path arc radius, MRR is the material removal rate,  $a_p$  and  $a_e$  are the axial and the radial depths of cut, and the  $v_f$  and  $v_{fc}$  are the feed rates at the centre of the cutting tool and through the contour. The formulas were known from the connected literature [3, 4]. Well visible that the tool load at internal arc is higher than the straight milling operation, thus during pocket milling the tool may face excessive tool load and danger of vibration.

**Table 1** The cutter engagement and the material removal rate at straight and arc milling

$\theta = \cos^{-1}\left(\frac{r-s}{r}\right)$	(1)	
$\theta_{arc} = \pi - \cos^{-1}\left(\frac{2r^2 + 2\rho(s-r) - s^2}{2r(\rho-r)}\right)$	(2)	
$MRR = \frac{a_p \cdot a_e \cdot v_f}{1000} \left[ \frac{cm^3}{min} \right]$	(3)	
$MRR_{arc} = \frac{a_p \cdot s \cdot v_f}{1000} \cdot \frac{\rho - s/2}{\rho - r} \left[ \frac{cm^3}{min} \right]$	(4)	
$v_f = v_{fc} \cdot \rho / (\rho + r)$	(5)	

## 2 The Pocket Milling Strategy Evaluation Aspects and Experimental Methods

The quality of tool path could be evaluated in two major aspects: according to tool path smoothness and according to handling of tool load. The smooth continuity of path curve is essential, because the tool can move with a programmed feed rate only if there is no sudden sharp change of direction. If the tool requires slow down due to sharp change of direction, it will negatively influence both the cutting time and the tool life [5]. To handle the change in tool load, the simplest way is to control the feed rate. But with this solution, the danger of vibration and heat load is still remaining [6, 7]. For this reason, it is necessary to think of the tool load during the planning the shape of the tool path. The economical machining is possible only with handling the tool load, the material removal rate, and the cutter engagement due to optimal tool path [8]. Expecting that the process parameters could be constant during circular pocket milling, thus comparing different strategies, the focus was on the level of tool load. Simulation and cutting experiments were been done to evaluate the outcome. It is worth to note that simulation approach has recently received great attention and can be applied to many aspects of manufacturing systems [9, 10].

### 2.1 Simulation Inspection and Metal Cutting Experiments

The material removal rate and the cutter engagement inspection are not possible to explain the explicit correlation, because the neighbour tool path segments interact with each other. Thus, the experiments were been executed through an own-developed pixel-based software.

During cutting experiments, different strategies were taken into consideration to evaluate the force and the surface roughness at the bottom. In order to ensure the appropriate comparability, the cutting time ( $t = 50$  s), the cutting speed ( $v_c = 150$  m/min), and the nominal value of stepover ( $s = 0.5 \cdot r$ ) were similar, when a 10-mm-deep and 40-mm-diameter circular pocket has been made with a starting hole diameter of 12.5 mm. The feed rate was given out from these parameters. Each tool path was also been inspected without any feed rate correction, but at each occasion 20–25% higher peak values noticed at measured force; thus in further discussion, only these samples will be highlighted when the controller modified the feed at tool centre according to Eq. (5). A 10-mm-diameter hard metal cutting tool with two cutting edges was in use during the experiment (tool metal K600, geometry to DIN 6527L, 45° helix). The workpiece material was Al6082. The cutting force was measured by a Kistler 9257B-type piezoelectric force measuring sensor, and then the evaluation was made after filtering the maximum value to one revolution of the tool. The bottom surface roughness was measured by a Mahr Pocket Surf IV type diamond head touch through radial

**Table 2** The simulation cutting experiment results

No.	Strategy	Length	$F_{\max}$	$MRR_{\max}$	$\theta_{\max}$	Ra
		(mm)	(N)	( $\text{cm}^3/\text{min}$ )	( $^\circ$ )	( $\mu\text{m}$ )
1.	Contour parallel	392	258	17.2	163	1.37
2.	Spiral-like	408	254	17.0	90	1.38
3.	Fanuc/Haas	397	286	18.8	96	1.32
4.	Siemens	391	325	21.6	120	1.31
5.	Volumill	443	246	17.0	86	1.42
6.	Waveform	369	258	17.3	78	1.45
7.	Advanced spiral-like I	398	249	16.2	75	1.33
8.	Advanced spiral-like II	377	255	18.6	78	1.32

direction. But it is found that the strategy selected influences very minimum on the roughness of the surface, and thus the outcome is placed only in Table 2.

### 3 The Strategies Used During the Circular Pocket Milling

There are several methods of milling to rough cut of circular pocket. The best economical and promising strategy is starting the cut at an initial hole with an end mill, because of the even distribution of tool load and tool wear along the entire cutting edge length. But for this, a starting hole is required, which could be made by drilling, or even with a flat end mill due to linear or helical ramping. Now keeping aside these, we will deal only with rough cutting. Further, the most significant NC cycles and CAM solutions will be discussed.

#### 3.1 NC Cycles for Circular Pocket Milling

The NC cycle solutions are generally made using concentric arcs or spiral-like tool paths. These solutions generally exclude all types of technical aspects, that is why the speed parameters and stepover are constant. Thus, as was seen in the introduction, the tool load will increase alongside the internal arcs.

The fundamental strategy could be named as **contour parallel strategy** (Fig. 1). In this solution, the tool path is formed by offsetting the external contour. The distance between the offset arcs is the same as the stepover nominal value. At radial direction linking of offset arcs, the path contains sharp edges. In these areas, a reduced feed rate should be used similar to slot milling. A harmful effect of these appears at material removal rate and also at cutter engagement development. The offset curves could be linked through arcs too. The CAM system provides such possibilities, but the experiments showed that a visually better solution is achievable, but the strong tool load variations are still remaining.

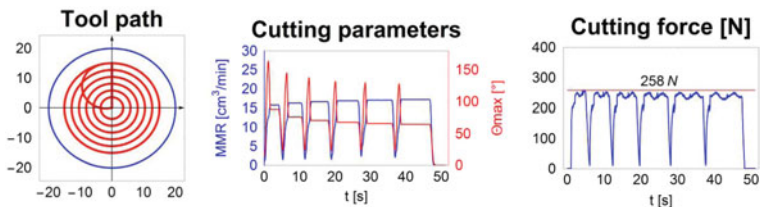


Fig. 1 The contour parallel tool path

The another very widely used method is **spiral-like strategy** (Fig. 2). The tool moves along an Archimedean spiral, where the distance between the neighbour tool path segments is the same as the stepover’s nominal value. This strategy of machining beside its simplicity could be marked as the best among the NC cycles. The only disadvantage is that the cutter engagement in internal sector grows up due to small path curvature, which in case of hard material creates vibration, influencing the tool life.

The **FANUC** and the **HAAS** controllers also use a spiral-like strategy, nevertheless not Archimedean spiral, but uses half circles with shifted centre points to generate the tool path (Fig. 3). It is seen at simulation and at force measuring that the load peak is during the starting of cut, and also the change of cutter engagement is not solved in that case.

The **Siemens** controller cycle follows the contour parallel strategy, nevertheless not through full circle, but builds up with quarter and three-quarter arcs, which are linked to each other by straight tangents (Fig. 4). The big advantage of this against

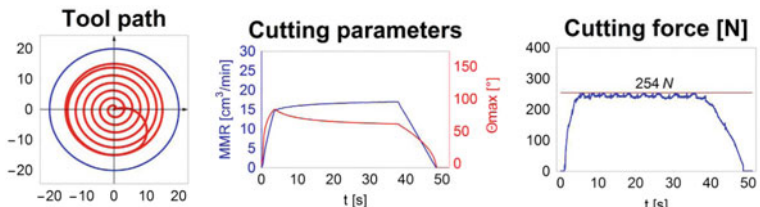


Fig. 2 The spiral-like tool path

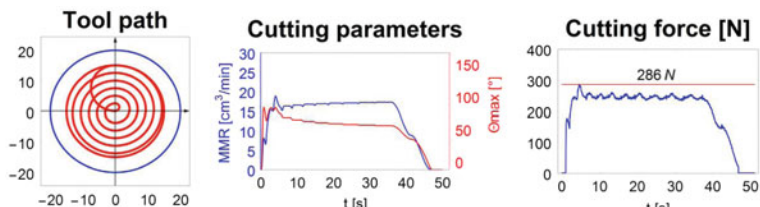


Fig. 3 The Fanuc/Haas tool path



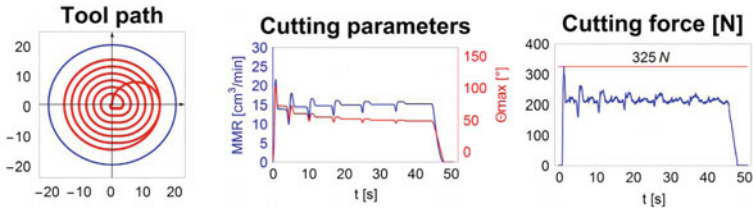


Fig. 4 The Siemens tool path

the conventional contour parallel strategy is that there is no slot milling section. But the varying tool load and the cutter engagement problem remains unsolved.

### 3.2 CAM Systems for Circular Pocket Milling

The CAM system generally provides modern methods to generate the tool path, where during tool path generation different factors are considered to avoid the excessive tool load. These modern considerations are previously placed into, achieve a solution close to optimal. This idea is to keep constant the metal removal rate and/or the cutter engagement. These modern strategies solve these through tool path generation algorithm where spiral-like and trochoidal strategies are used as hybrid. But in case of circular pocketing, the spiral-like strategy will lead due to geometrical nature.

The **VoluMill** rough cutting **strategy** is available in several CAM systems as built-in module (Fig. 5). It seems that the tool path goes along an Archimedean spiral, but as the strategy was made for arbitrary-shaped geometries, but as the strategy was made for arbitrary-shaped geometries, thus the tool path was built in stages step by step. The base strategy is that the material removal rate should remain constant. The algorithm achieves this by controlling the feed rate. For the proper function of strategy, so as to keep constant, the metal removal rate was identified by simulation and also by metal cutting experiments. However, the cutter engagement variation is still unsolved in this solution.

Against the VoluMill strategy, the **Waveform strategy** does not deal with material removal rate but concentrates to keep the cutter engagement at a constant value (Fig. 6). To achieve this, the spiral is made starting from the centre of the pocket with continuously increasing stepover according to the change of path curvature. This results that without controlling the feed rate, the material removal rate remains constant.

The simulation and cutting experiments prove that the strategy properly controls the material removal rate, the cutter engagement, and the cutting force limit. Only one thing is absent from the algorithm; when the tool reaches the pocket contour, then a full circulation is required to eliminate the press mark of the spiral. In this time, the algorithm is not able to control the decreasing material removal rate by controlling the feed rate.

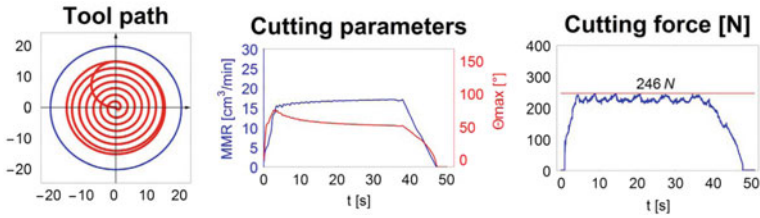


Fig. 5 The Volumill tool path

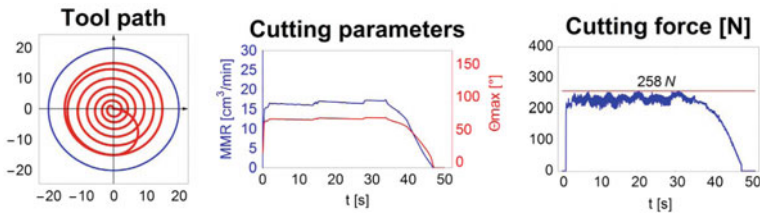


Fig. 6 The Waveform tool path

### 3.3 Evaluation

Evaluating the strategies as discussed above, it was found that in all solutions something was missing. The most favourable could be spiral-like tool path and the CAM system solutions. But these favourable tool path strategies could also be developed further, for example, the VoluMill and the Archimedean spiral-like strategies by avoiding the cutter engagement change, and the Waveform strategy by adjusting the feed rate at the end part of tool path.

## 4 Suggested Circular Pocket Milling Strategies

During proposing the circular pocket milling strategy at the worked out optimizing equation, the machining time minimizing was taken as a goal. The nature of modern tool path is that the tool load is well controlled, because in that case optimal cutting parameters can be provided throughout the whole machining operation achieving maximum efficiency. Thus, based on this the tool, load control to constant is the optimization limit. During our work, two different algorithms were developed to achieve same outcome, but in a different way. The goal was to keep the material removal rate and the cutter engagement simultaneously at a constant value, combining the advantages of VoluMill and Waveform strategies behaviour.

### 4.1 *Advanced Spiral-like Strategy I*

The first solution meets the determined viewpoints (well-controlled cutter engagement and material removal rate) perfectly, but requires a complex calculation that depends on the simulation algorithm. At simulation evaluation, there are path optimization examples to control the feed rate [2]. But our goal was not the feed rate, but the stepover value should be influenced to keep the tool load constant in order to avoid the cutter engagement change too. This was worked by a spiral-like path giving polar coordinate points moving from into out, where for each point it was determined using a section half algorithm to find the radial coordinate maximum  $R(\varphi_i)$ , at which according to simulation the material removal rate will not be bigger than the calculated value made using average depth of cut and speed parameters (Eq. 3). After this, linking the point series besides constant feed rate, the metal removal speed and cutter engagement remain constant.

But at the end section, where the tool travels along the pocket contour with constant speed parameters, both the chip thickness and the metal removal speed decrease. Because it is difficult to change the cutting speed during cutting, thus to keep the tool load constant, it is wise to increase the feed rate to achieve maximum efficiency according to Eq. 6. The adjusted feed rate could be determined by simply arranging of Eq. (4):

$$v_f = \frac{1000 \cdot \text{MRR} \cdot (\rho - r)}{a_p \cdot s \cdot (\rho - s/2)}. \quad (6)$$

The simulation results reflect that material removal rate controlling and cutter engagement balance are solved (Fig. 7). Thus the algorithm achieved the goal perfectly beside keeping limits. Furthermore, the cutting force is developed here to the lowest in our experiments.

### 4.2 *Advanced Spiral-like Strategy II*

The second solution just remains back only for a pinstripe from the first solution, but compensates due to use of a simple algorithm. The base of the strategy is that the increasing stepover is built by simple Archimedean spiral sections to keep the cutter engagement constant. The development of cutter engagement relation to the side step and path is written in Eq. (2). If we want to express the acceptable stepover from this equation, then we will face a complex connection. But as we seen in the previous strategy, it is found that in spite of constant feed rate the constant material removal rate was ensured, thanks to proper tool path shape. Thus, we used material removal rate defined by Eq. (4). After rearranging and simplifying the following simple equation found:

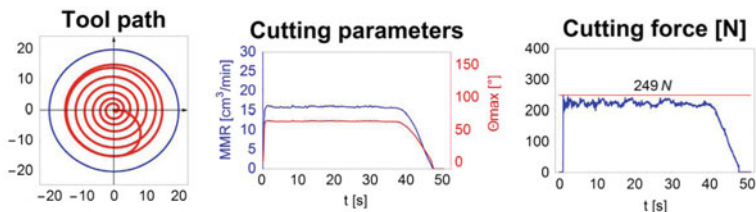


Fig. 7 The advanced spiral-like strategy I

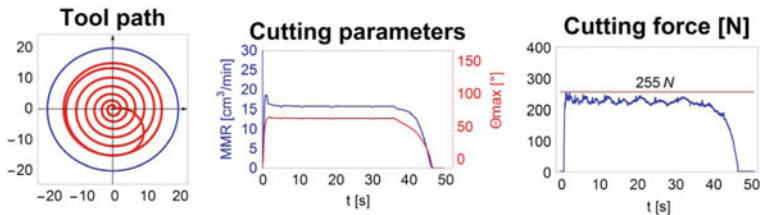


Fig. 8 The advanced spiral-like strategy II

$$s(\rho) = a_e - \rho + \sqrt{a_e^2 - 2a_e \cdot \rho + \rho^2}, \tag{7}$$

where  $s(\rho)$  is the allowed stepover according to path curvature, and  $a_e = r(1 - \cos \theta)$  is the nominal depth of cut according to Eq. 1. From this, as in the previous strategy, a  $\{R(\varphi_i)\}$  polar coordinate point series was built as  $R(\varphi_i) = R(\varphi_i - 2\pi) + s(R(\varphi_i - 2\pi))$  relation with  $\Delta\varphi$  steps. Naturally, this equation can only be used at the middle section of the spiral. At entrance section beside continuously increasing spiral with a full rotation, when at end section of the contour, a full circle would be needed at the internal boundary. In these sections, the feed rate control happens according to Eq. (6), as in the previous strategy.

Evaluating the experimental results (Fig. 8), it is seen that the algorithm functions effectively. The only deficiency is in development of material removal rate where a jump is discovered at the point when the tool path ends the first circular rotation, because the spiral rises sharply compared to the starting section. The solution could be to decrease the feed rate, because there was no jump at cutter engagement. Thus, besides simple path generation, the worked out algorithm provides a fully efficient solution.

## 5 Summary

Evaluating the existing circular pocket machining strategies, it was found that in all solutions something was missing. Because of this, we introduced two newly developed algorithms focused on optimal tool path to achieve maximum

productivity. Table 2 contains the results of the simulation and metal cutting experiments. At the first glance, it may seem to be only a little improvement achieved, but the importance of this should not be downgraded. At series production due to high volume, a small percentage improvement will result in higher productivity assuring a higher profit.

In summary, it can be stated that worked out algorithms were capable to provide an optimal tool path to achieve the predefined goal, the well-controlled material removal rate, and cutter engagement. Furthermore, the second solution could be easily adopted to NC cycles too.

**Acknowledgements** The authors would like to acknowledge the support provided by the CEEPUS III HR 0108 project. This research was partly supported by the EU H2020-WIDESPREAD-01-2016-2017-TeamingPhase2-739592 project “Centre of Excellence in Production Informatics and Control” (EPIC).

## References

1. Held, M.: *On the Computational Geometry of Pocket Machinig*. Springer, Berlin (1991)
2. Kim, H.C.: Optimum tool path generation for 2.5D direction-parallel milling with incomplete mesh model. *J. Mech. Sci. Technol.* **24**(5), 1019–1027 (2010)
3. Chan, K.W., Choy, H.S.: Machining tactics for interior corners of pockets. *Int. J. Adv. Manuf. Technol.* **20**(10), 741–748 (2002)
4. Kramer, T.R.: Pocket milling with tool engagement detection. *J. Manuf. Syst.* **11**(2), 114–123 (1992)
5. Pateloup, V., Duc, E., Ray, P.: Corner optimization for pocket machining. *Int. J. Mach. Tools Manuf.* **44**(12–13), 1343–1353 (2004)
6. Xu, J., Sun, Y., Zhang, X.: A mapping-based spiral cutting strategy for pocket machining. *Int. J. Adv. Manuf. Technol.* **67**(9–12), 2489–2500 (2012)
7. Biertman, M.B., Sandstrom, D.R.: A curvilinear tool-path method for pocket machining. *J. Manuf. Sci. Eng.* **125**(4), 709–715 (2003)
8. Stori, J.A., Wright, P.K.: Constant engagement tool path generation for convex geometries. *J. Manuf. Syst.* **19**(3), 172–184 (2000)
9. Diering, M., Dyczkowski, K.: Assessing the raters agreement in the diagnostic catheter tube connector production process using novel fuzzy similarity coefficient. In: *IEEE International Conference on Industrial Engineering and Engineering Management*, pp. 228–232 (2016)
10. Varela, M.R.L., Trojanowska, J., Carmo-Silva, S., Costa, N.M.L., Machado, J.: Comparative simulation study of production scheduling in the hybrid and the parallel flow. *Manage. Prod. Eng. Rev.* **8**(2), 69–80 (2017)

# Study on Mechanical Characteristics in Electromechanical Disengaging Damper

Grzegorz Pittner, Bartosz Minorowicz and Roman Regulski

**Abstract** The paper is focused on study of new type of vibration control damper which has been designed, machined, assembled, and calibrated by authors. In typical oil dampers, attenuation force is generated by fixed orifices, where oil passes from one chamber to another. More advanced designs include variable orifices, where it is possible to regulate precisely flow area, e.g., by proportional valve. Thus, these solutions are so-called valve mode, also very popular in whole group of magnetorheological dampers. Another known in engineering type of dampers is based on viscous friction. Steel rod passed through cylinder head, where interference fit creates movement resistance. This paper proposes novel design of damper, where in order to control damping force, simple direct current motor and special mechanism, similar to wedge, has been proposed. To perform basic research on damper's characteristics, special test stand was designed. Crankshaft mechanism was used to generate reciprocating movement. During tests, one end fixed damper was connected to slider by force transducer. To describe phenomenon of variable damping force, force–displacement and force–velocity characteristics have been registered and described.

**Keywords** Damper · Semi-active vibration control · Electromechanical damper  
Disengaging damper

---

G. Pittner (✉) · B. Minorowicz · R. Regulski  
Faculty of Mechanical Engineering and Management,  
Institute of Mechanical Technology, Poznan University of Technology,  
Piotrowo Street 3, 60-965 Poznan, Poland  
e-mail: grzegorz.pittner@put.poznan.pl

B. Minorowicz  
e-mail: bartosz.minorowicz@put.poznan.pl

## 1 Introduction

Dampers are a popular solution in engineering for reducing vibration transmission between two bodies. Commonly used typical passive dampers have the ability to dissipate energy from of kinetic vibration into other forms of energy, mostly heat. One of the greatest disadvantages of such passive dampers is constant damping force. Therefore, without possibility of tuning attenuation in vibration system, it is not possible to adapt the system to the variable conditions which cause vibration generation. Quite often damper is necessary to dissipate energy only when rotational system passes through resonance frequency range. Good example of such system is a domestic washing machine, because wet laundry creates a big imbalance in the drum, especially when drum starts acceleration to spin-drying cycle. If drum and its suspension are described by mass-spring-damper model, it was proven numerically and experimentally in [1, 2] that turning off damper for rotational speeds above 1000 rpm is safe and causes a decrease of RMS acceleration in measuring points placed on washing machine housing.

Promising technology used to adapt vibration system to the various conditions is by using semi-active dampers which can change its attenuation properties in response to the control signal. There are many different strategies to control damping force in semi-active way. One of the most popular technologies of semi-active dampers is based on using magnetorheological fluids (MR fluids) [3–6]. Such fluid consists of ferromagnetic particles, with diameters typically from 3 to 10  $\mu\text{m}$ , surrounded by mineral or synthetic oil. Principle of operation of these fluids is based on the ability for formulation particles chains in external magnetic field. This disturbs oil flow and increases shear force. Such dampers consist of coils (as MMF sources) and magnetic cores. Electrically controlled magnetic field causes different shear forces in MR fluid (shear mode) or disturbs flow between two chambers (valve mode). In valve mode, oil can passes from one chamber to another by holes in piston or by bypass line where it is easier to install orifices, which throttles flow. In many cases, MR dampers fulfill their task, however, with this technology is associated also some disadvantages like high costs of maintenance, special-type fluids, high-energy consumption used by control signal and heat generated not only from attenuation phenomenon but also by control signal energy used in coil to generate magnetic field. Another disadvantage of dampers with oil is leakage risk, which practically eliminates them from application in food or pharmacy industry. This problem was solved by MR dampers, which work in shear mode. Piston with coil has on circumference sponge or fiber soaked with MR fluid [7, 8]. Experiments show that such dampers work properly but obtained force is significantly lower than in valve mode dampers. Recently, authors described [2] a new type of damper which involves simple electromechanical technology to control damping force in semi-active way. New type of electromechanical disengaging damper has been verified practically in series of experiments about washing machine drum and chassis vibration reduction. Performed research proved that it could be the promising technology.

The main contribution of this paper is description damping characteristics of new type of damper where damping force is associated with different preloads of friction sleeve. Description of electromechanical damper [2] was focused on implementation of this technology to control washing machine drum vibration during spinning cycle. During work authors used new type damper in off/on way where damper attenuation force was neither fully engaged nor fully disengaged. The transient states of electromechanical damper were neglected. This article is an attempt to study its force–displacement and force–velocity characteristics in control signal states between fully engaged and fully disengaged states. Results of measurements can be useful in the future implementation of more accurate methods of damping force controlling using this new type electromechanical disengaged-type damper.

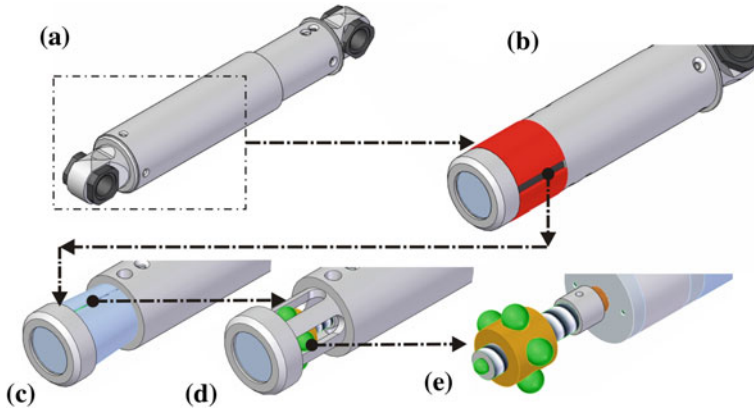
## 2 Electromechanical Semi-active Disengaging Damper

The design of electromechanical damper has been described in detail in paper [2]. This chapter provides only general idea, which has been evoked and presented. Analyzed damper as shown in Fig. 1 consists of cylinder sliding periodically on the fixed shaft. The friction between inner surface of cylinder and outer surface of shaft creates attenuation force, which dissipates energy accumulated in vibrations. In order to control damping force, various frictions need to be generated. To apply variable friction, the normal pressure force needs to be changed in some range. To achieve that goal, the cylindrical C-type sleeve is presented in Fig. 2, as an assembly of a flexible sleeve (5), conical sleeve (6), and frictional sleeve (7) changes its diameter because of steel ball (8) movement along threaded axis. By controlling position of the steel balls and torque of electric DC motor which rotates the thread, it is possible to control friction force between sleeve and cylinder. More details about methods of controlling damping force in such technology have been presented in [2]. As a summary, it can be stated that in order to simplify numerical description between damping force and control signal, the electrical current limit in DC motor circuit, called  $i$  in this paper, needs to be given. Comparison of viscous damper from washing machine and new design is presented in Fig. 3.

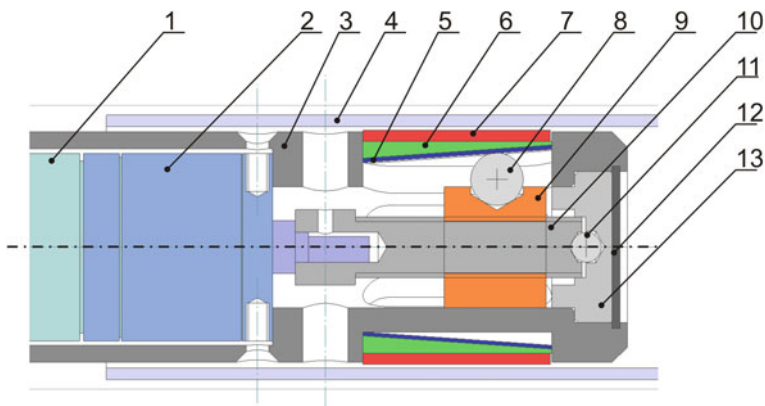
## 3 Experimental Studies

The main contribution of research was experimental designation of characteristics: force–velocity and force–displacement characteristic measurement in various control signal conditions. To perform this task, experimental stand has been constructed. Diagram, which presents the structure of this stand is presented in Fig. 4. The idea of the stand was to enforce periodical relative stroke movement of the damper's mandrel. The enforcement has been done using electrical AC motor (no



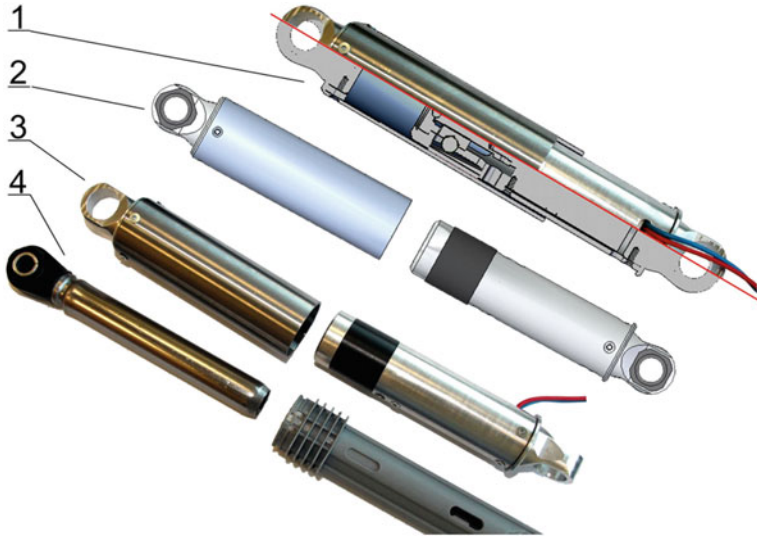


**Fig. 1** **a** External view of electromechanical damper, **b** presentation of frictional sleeve, **c** internal C-shaped conical sleeve made of flexible steel, **d** the socket with steel balls placed under the conical sleeve, **e** the movable nut with the balls [2]

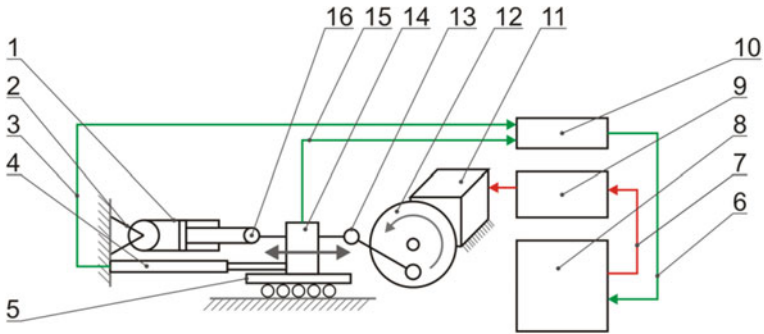


**Fig. 2** Longitudinal section of the damper: (1) DC motor, (2) planetary gear embedded in the motor, (3) the frame of the immovable mandrel, (4) the frame of the moving mandrel, (5) flexible sleeve, (6) conical sleeve, (7) frictional sleeve, (8) steel ball, (9) nut, (10) screw, (11) steel bearing ball, (12) retainer ring, (13) bottom [2]

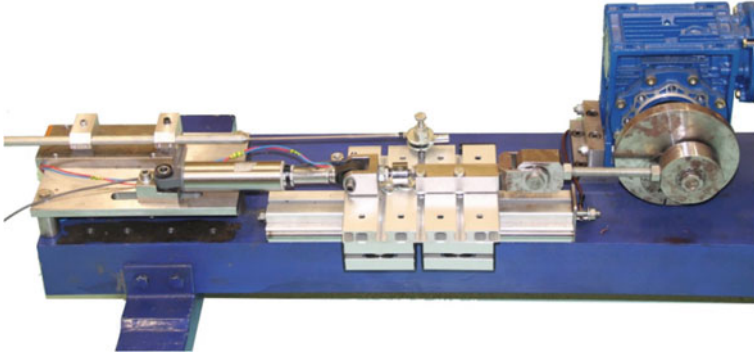
11) and the crankshaft mechanism (no 12), which provides reciprocating movement of slider. Full-bridge HBM 9CU force transducer (measuring range  $\pm 1$  kN) was used as a joint between moving slider and piston (no 16). Measurement process of the damping force was correlated with relative movement of the damper's mandrels measured with the LVDT displacement sensor (4). The information about relative velocity of stroke has been calculated using computation of displacement derivative. The construction of the experimental stand has been presented in detail in Fig. 5.



**Fig. 3** Comparison of dampers: (1) electromechanical damper half section internal view, (2) electromechanical damper CAD project, (3) electromechanical damper real photo, (4) classic constant force friction damper with similar damping force and stroke



**Fig. 4** Experimental stand diagram: 1—damper, 2—fixed joint, 3—displacement signal  $s(t)$ , 4—displacement sensor LVDT WA-100, 5—sliding support, 6—synchronized measurement signals  $s(t)$  and  $F(t)$ , 7—signal of set rotatory speed for motor driver, 8—PC with DAQ CatMan pro, 9—motor driver, 10—DAQ equipment Spider8, 11—electric motor, 12—crankshaft mechanism 13—crankshaft mechanism joint, 14—force sensor HBM 9CU-1kN, 15—Force measurement signal  $F(t)$ , 16—damper joint



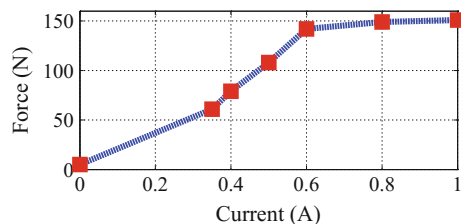
**Fig. 5** Experimental stand used to measure damping force

### 3.1 Measurement Results

During an experiment, the dependence force–displacement has been measured under various signal conditions. The rotatory AC motor, which drives the crankshaft mechanism, has been set to constant value, which ensures maintenance of repeatable speed in the range of  $\pm 115$  mm/s. Current limit  $i$  of the damper mechanism has been set in range from  $i = 0$  A (damper fully disengaged) to  $i = 1$  A (damper fully engaged) in the following sequence  $i = [0; 0.35; 0.4; 0.5; 0.6; 0.8; 1]$  A. In the first step, maximum amplitudes of damping force were registered, which is shown in (Fig. 6). Subsequently, force–displacement characteristics was prepared (Fig. 7).

The static resistance of thread mechanism allows to start mechanism movement just above current limit about 0.35 A, so there is an empty gap in measured data between  $i = 0$  A (damper fully disengaged) and  $i = 0.35$  A, where damper mechanism starts engaging process with its minimum engaged damping force. Next step after force–displacement characteristics has been measured was to calculate force–velocity characteristics of the damper for each condition (Fig. 8).

**Fig. 6** Damping force as function of current



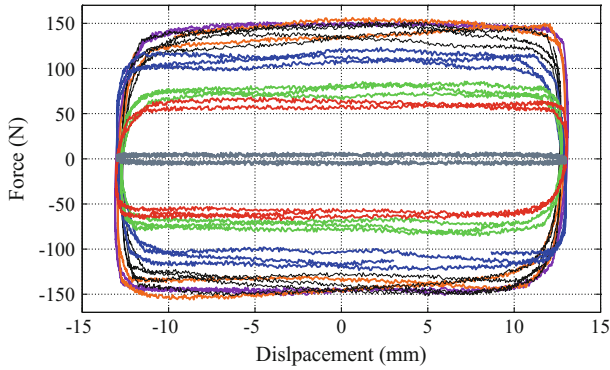


Fig. 7 Force versus displacement characteristics (legend and colors as in Fig. 8.)

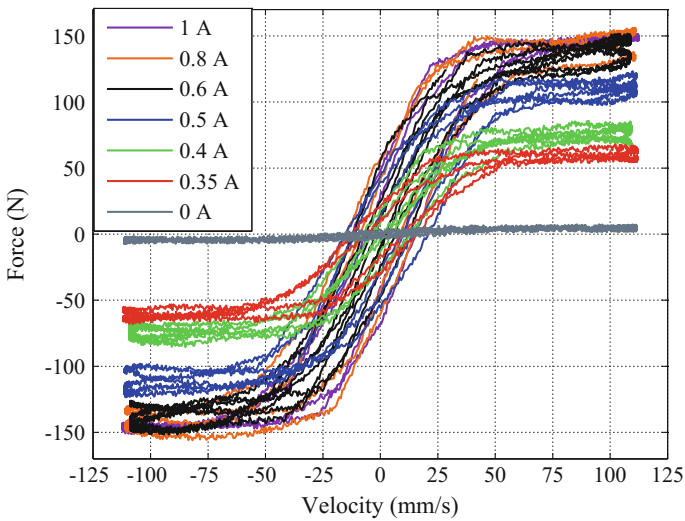


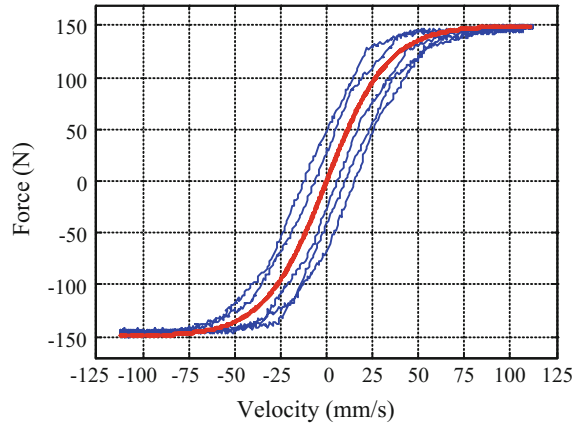
Fig. 8 Force versus velocity characteristics

### 4 Discussion

In the past, many different models of damper’s force characteristics have been presented. The simple way to describe damper behavior is by using bipolar sigma function described as

$$F(t) = \frac{1}{1 + e^{-\lambda t}} - 1. \tag{1}$$

**Fig. 9** Force versus velocity characteristics for 1 A supply current (blue line) and model based on hyperbolic tangent function (red line)



Also, it is possible to use simple hyperbolic tangent function described as

$$F(t) = a_0 \tanh(a_1 v(t) + a_2) + a_3, \quad (2)$$

where  $a_0$ ,  $a_1$ ,  $a_2$ , and  $a_3$  are the parameters of function,  $v$  is the velocity, and  $F$  is the force.

However, such simple approach (2) does not represent hysteretic phenomenon as shown in Fig. 9. Authors estimated the model parameters as  $a_0 = 150$  and  $a_1 = 0.03$ . Other parameters  $a_2$  and  $a_3$  equal to 0 because force characteristics is not biased.

For this reason, more complex approach can also to be taken. In 1967, Bouc introduced mathematical description used to describe nonlinear hysteretic systems [9, 10] and it has been extended by Wen [11] in 1976 who demonstrated its versatility by producing a variety of hysteretic patterns. This model can capture, in analytical form, a range of hysteretic cycle shapes matching the behavior of a wide class of hysteretic systems. Due to its versatility and mathematical tractability, the Bouc–Wen model is often used to model MR fluid dampers behavior [4–6]. However, measured characteristics and simple model presented in this paper show that average error between these two curves could be negligible in mechanical systems where there is no need for precise modeling and damping force control.

## 5 Conclusions

This paper shows a new type of electromechanical damper which has been designed, described, and tested. Presented damper uses friction attenuation phenomenon to generate damping force and its force characteristics shows some similarity in comparison with another type of dampers with variable damping force and some amount of hysteretic such as popular magnetorheological fluid dampers

[1, 3]. Based on the results presented in Fig. 6, it can be concluded that relation between damping force and supply current is nonlinear, which affects the degree of complexity of mathematical model. Source of this nonlinearity can be changing friction factor between sleeve and inner cylinder surface, which is a task for further research. The aim of the work was to perform a study of force–velocity characteristics of a new type of damper. To describe damper characteristics, hyperbolic tangent has been selected. Process of model parameters identification was based on real object measurement in an experimental way. To perform an experiment, the measurement stand has been constructed with the ability to the synchronous measurement of force and mandrel's relative displacement. Relative speed of mandrels has been calculated using displacement–time signal derivative. The experiment has been performed for some range of damper's DC motor current limit responding to various attenuation forces from fully disengaged, through partially engaged ending on fully engaged damping force.

Attempt to describe characteristics of electromechanical dampers using Bouc–Wen model indicated that identification of parameters for that type of dampers is possible and the resulted errors between theoretical model and real object measurement can be similar in comparison with MR fluid dampers [1, 3–5].

Results show that damper and test rig were not free of mechanical backlash; this is the reason why curves of damping force do not create one solid line. Authors consider for further research another test rig with hydraulic drive.

Authors hope that presented study will be useful in further modeling behavior of new type damper and can be the foundation for the development of more accurate damping force controlling methods for electromechanical DC motor-controlled type of dampers.

**Acknowledgements** The presented research results, executed under the subject of 02/22/DSPB/1389, were funded with grants for education allocated by the Ministry of Science and Higher Education in Poland.

## References

1. Minorowicz, B., Stefański, F., Pittner, G., Regulski, R.: Share mode magnetorheological dampers for vibration attenuation in domestic washing machines. *Progr. Autom. Robot. Measur. Tech. Adv. Intell. Syst. Comput.* **350**, 147–156 (2015)
2. Buśkiewicz, J., Pittner, G.: Reduction in vibration of a washing machine by means of a disengaging damper. *Mechatronics* **33**, 121–135 (2016)
3. Bajkowski, J., Pyrz, M., Zalewski, R.: Modelowe Badania Prototypu Tłumika Magnetoreologicznego. *Modelowanie Inżynierskie* **40**, 7–14 (2010)
4. Braz Cesar, M., Carneiro de Barros, R.: Properties and numerical modeling of MR dampers. In: 15th International Conference on Experimental Mechanics (2012)
5. Talatahari, S., Kaveh, A., Mohajer, Rahbari N.: Parameter identification of Bouc–Wen model for MR fluid dampers using adaptive charged system search optimization. *J. Mech. Sci. Technol.* **26**(8), 2523–2534 (2012)

6. Song, J., Der Kiureghian, A.: Generalized Bouc–Wen model for highly asymmetric hysteresis. *J. Eng. Mech.* **132**(6), 610–618 (2006)
7. Minorowicz, B., Stefański, F.: Proposal of a new group of magnetorheological dampers. *Przegląd Elektrotechniczny* **7**, 263–267 (2014)
8. Nguyen, Q.H., Choi, S.B., Woo, J.K.: Optimal design of magnetorheological fluid-based dampers for front-loaded washing machines. *J. Mech. Eng. Sci.* **228**, 294–306 (2014)
9. Bouc, R.: *Modèle mathématique d’hystérésis: application aux systèmes à un degré de liberté*. Doctoral dissertation (1969)
10. Bouc, R.: Forced vibration of mechanical systems with hysteresis. In: *Proceedings of the Fourth Conference on Nonlinear Oscillation, Prague, Czechoslovakia* (1967)
11. Wen, Y.K.: Method for random vibration of hysteretic systems. *J. Eng. Mech.* **102**(2), 249–263 (1976)

# Modeling and 3D Simulation of an Electro-hydraulic Manipulator Controlled by Vision System with Kalman Filter

Piotr Owczarek, Jaroslaw Goslinski, Dominik Rybarczyk, Arkadiusz Kubacki, Arkadiusz Jakubowski and Lukasz Sawicki

**Abstract** In this paper, the modeling and 3D simulation of electro-hydraulic manipulator are presented. In the research, a typical model of electro-hydraulic servo drives is implemented. The output value in the model is a position of a drive; this information is used to compute tilt angles in manipulator's joints. Proposed simulation environment is used to testing new control algorithms. *Online* controlling and 3D visualization can precisely reflect manipulator trajectory. Data from camera is used and three algorithms of estimation of marker position are tested; these are circle fitting method, center of mass, and Kalman filter (KF). The virtual manipulator data is compared with real manipulator data and error analysis is given. The proposed method yields good results with positioning error of tool center point less than 0.5 cm.

**Keywords** Vision system · Electro-hydraulic manipulator · Hydraulic system Simulation model

## 1 Introduction

Nowadays, electro-hydraulic devices are commonly used in industry or in daily life. Electro-hydraulic can be found in applications, where the big ratio of dimension to force is required, e.g., cranes [1], lifts [2], and working machines or manipulators [3]. Also, it is very popular in car parts controlled by electro-hydraulic valve, e.g., suspension, automatic gearboxes, etc. [4, 5]. Therefore, it is important to carry out proper simulations of these devices before their construction. This is possible,

---

P. Owczarek (✉) · D. Rybarczyk · A. Kubacki · A. Jakubowski · L. Sawicki  
Institute of Mechanical Technology, Poznan University of Technology,  
Poznań, Poland  
e-mail: piotr.owczarek@put.poznan.pl

J. Goslinski  
Institute of Control and Information Engineering, Poznan University of Technology,  
Skłodowska-Curie Square 5, 60-965 Poznań, Poland



thanks to simulation models. It reduces prototyping time and, what is more, it is cheaper than preparing new test stands. Many topics in the modeling of electro-hydraulic servo drives were described in the literature. Some papers rise issue of controlling hydraulic drives when using multiple cylinders [6]. In other, authors propose to create a simulation model of hydraulic drive [7]. The simulation model is created in SimulationX program, which provides block diagrams similar to Matlab/Simulink. Interesting work about large hydraulic excavator to simulate a crawler driving system was presented in [8]. In that approach, a RecurDyn software was used in dynamic modeling of the object. The main aim of this work is to prepare dynamic model with faster operational speed than SimulationX.

Preparation and tests of modern devices are very expensive. In the first part of work, authors are concentrating on parameters of the studied device and preparing its CAD model. Before building a prototype, it is important to prepare dynamic simulation model. This model can be used in testing of new control algorithms on a virtual machine. When one has a real device, the simulation can be carried out on a virtual machine, avoiding errors, faults, and failures in the first step of a new program, which is much safer.

Thus, it is important to create new 3D environment to work on simulation model without danger of risking people's life. The presented study is a continuation of a research given in [9, 10]. The authors proved that in the problem of marker's position tracking, the Kalman filter turned out to be accurate. Therefore, here, only the previously estimated data will be used to compare simulated manipulator with real electro-hydraulic manipulator data. In this work, also a new approach in creating a discrete model in C++ and real-time 3D application is presented.

## 2 The Test Bed

In the paper, the aim is to create a virtual model of an electro-hydraulic manipulator in a 3D simulation environment. This is important, because working with real manipulator during tests of new algorithms is dangerous, especially for an operator who is located within the working area of a manipulator. The object of research consists of two electro-hydraulic proportional valves connected with hydraulic cylinders (Fig. 1a).

The hydraulic proportional valves (Fig. 1b) are controlled by dedicated cards. Input voltage in cards is proportional to liquid flow in valves. The input signal is ranging from  $-10$  to  $+10$  V. The set signal is provided by PLC controller (B&R company), where it is equipped with dedicated DAC cards, encoder cards, and I/O cards. Absolute position of angles is measured by incremental encoders with a resolution of 3600 puls/rev. In PLC, a PID controllers are implemented to control the position of manipulator's arms.

The set position of drive is generated by a master application (Vision system). PLC serves here only as positioning controller of electro-hydraulic drives. Data with coordinates are exchanged via TCP/IP protocol with frequency up to 250 Hz.

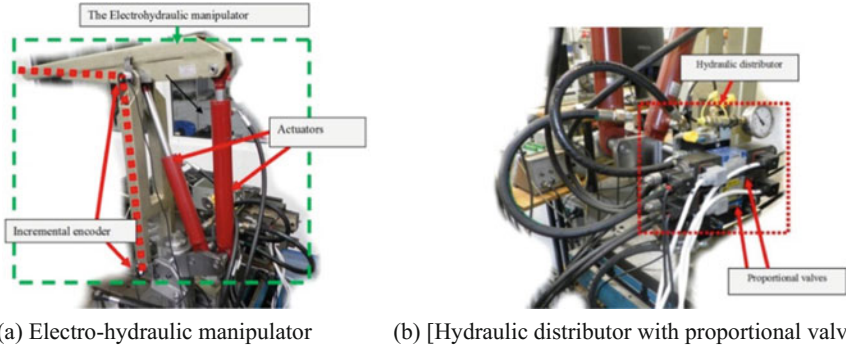


Fig. 1 Research stand

Fig. 2 Research stand



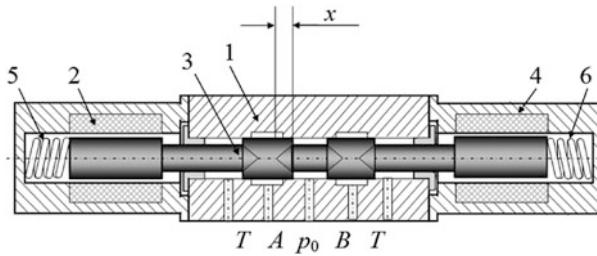
The experiments were carried out on a vision system formed of a fast CMOS camera 3iCube IC1500CU (Fig. 2) [11] and a special software Adaptive Vision Studio, which uses SEE multicore instruction [12]. The focal length of the camera lens was 3.5 mm. The max resolution was equal to  $2592 \times 1944$  px yielding 15 fps. The camera was connected with PC computer via USB 3.0. For the current research, the camera’s resolution was reduced to  $640 \times 480$  px.

### 3 Mathematical Background

In Fig. 3, technical construction of proportional valve is presented. The main parts are numbered 1–6. To change velocity of fluid flow in valve, the position of slider (3) in housing (1) must be changed by the magnetic flux generated by a coil around a permanent magnet (2, 4). The proportional solenoids are supplied by DC voltage [13]. A central position of the slider is set by two springs (5, 6) placed on both sides of slider. A measurement of position  $x$  is made by precise induction sensor (LVDT).

Symbols given in Fig. 3 are commonly known in the literature, and can be explained as follows:

- $p_0$  is a supply pressure,
- $A$  is an output of the valve, connected to the first input of the piston rod,
- $B$  is an output of the valve, connected to the second input of the piston rod,
- $T$  is the return to the main fluid tank.



**Fig. 3** Scheme of proportional valve

These kinds of proportional (Fig. 3) valves are described by mathematical equations, which create a mathematical model of a valve:

$$Q_a(t) = Q_{sa}(t) + Q_{ha}(t) \tag{1}$$

$$Q_b(t) = Q_{sb}(t) + Q_{hb}(t) \tag{2}$$

$$Q_a(t) = K_Q x(t), \quad Q_b(t) = K_Q x(t) \tag{3}$$

$$A_a = A, \quad A_b = Aa, \quad (a < 1), \tag{4}$$

$$Q_{ha}(t) = A \frac{dy(t)}{dt}, \quad Q_{hb}(t) = aA \frac{dy(t)}{dt} \tag{5}$$

$$Q_{sa}(t) = \frac{V_a dp_a(t)}{E_o dt}, \quad Q_{sb}(t) = -\frac{V_b dp_b(t)}{E_o dt} \tag{6}$$

$$m \frac{d^2y(t)}{dt^2} + D_w \frac{dy(t)}{dt} = F_{obc} + A[p_a(t) - ap_b(t)], \tag{7}$$

where

- $Q_a, Q_b$  flows,
- $Q_{ha}, Q_{hb}$  absorption of the actuator chambers,
- $Q_{sa}, Q_{sb}$  flow of the covering losses due to compressibility,
- $p_a, p_b$  the pressure in the chambers of the actuator,
- $A_a, A_b$  active surfaces of the piston,
- $V_a, V_b$  the volume of liquid in the chambers of the actuator, and
- $E_o = 1, 2 \times 10^9 \text{ N/m}^2$ —the modulus of elasticity.

The stroke of the hydraulic actuator is 300 mm. The diameters of the piston and the piston rod, respectively, are  $A = 40 \text{ mm}$  and  $Aa = 63 \text{ mm}$ . The simulation includes linear stiffness and a linear coefficient of kinetic friction coulomb rate of  $D = 100,000 \text{ [Ns/m]}$ . The value of the reduced mass is  $m = 18.3 \text{ [kg]}$  (mass of the

piston and piston rod). The values of the coefficients given in Eq. 6 are as follows:  $E_o/V_a = 9.63 \times 10^{12} \text{ Pa/m}^3$  and  $E_o/V_b = 1,28 \times 10^{12} \text{ a/m}^3$  (in the middle position of the piston).

To prepare discrete simulation in Visual Studio and C++ language, it is necessary to derive equations of proportional valve with hydraulic cylinder, where the output signal of model is a position of the piston rod. In the first step, Eqs. 6 and 1 are combined, yielding the following:

$$Q_a(t) - Q_{ha}(t) = Q_{sa}(t) = \frac{V_a}{E_o} \frac{dp_a(t)}{dt}. \tag{8}$$

Next, Eqs. (3) and (5) are used:

$$K_Q x(t) - A \frac{dy(t)}{dt} = Q_{sa}(t) = \frac{V_a}{E_o} \frac{dp_a(t)}{dt}. \tag{9}$$

Now it is possible to determine time derivative of pressure  $p_a(t)$  and  $p_b(t)$ :

$$\frac{dp_a(t)}{dt} = \frac{V_a}{E_o} \cdot \left( K_Q x(t) - A \frac{dy(t)}{dt} \right) \tag{10}$$

$$\frac{dp_b(t)}{dt} = -\frac{V_a}{E_o} \cdot \left( K_Q x(t) - Aa \frac{dy(t)}{dt} \right). \tag{11}$$

To compute a pressure, integral operation must be applied:

$$p_a(t) = \int \dot{p}_a(dt), \quad p_b(t) = \int \dot{p}_b(dt). \tag{12}$$

Last part is to compute the position of piston rod in the dynamic model. It boils down to the determination of  $y$  based on Eq. (7):

$$\frac{d^2y(t)}{dt^2} + = \frac{F_{obc} + A[p_a(t) - ap_b(t)] - D_w \frac{dy(t)}{dt}}{m}. \tag{16}$$

To simplify Eq. (16), two forces can be written as

$$F_a = Ap_a(t), \quad F_b = Aa \cdot p_b(t). \tag{17}$$

Finally, the equation of acceleration in hydraulic cylinder can be obtained:

$$\frac{d^2y(t)}{dt^2} + = \frac{F_{obc} + F_a - F_b - D_w \frac{dy(t)}{dt}}{m}. \tag{18}$$

## 4 Implementation of Kalman Filter

The Kalman filter is a well-known recursive algorithm, which was originally used for linear problems [14]. During the last 50 years, the KF evaluated to deal with nonlinear models; however, here the classic type of the KF is used. The overall framework of the KF assumes two-stage process. In the first one, namely prediction, the model data is exploited. During that stage, some forecasts on state vector behavior are made. In the next stage, the corrections are being imposed. The KF operates on process model which can be written in a state-space representation:

$$\begin{aligned} x_k &= Ax_{k-1} + Bu_k \\ y_k &= Cx_k, \end{aligned} \quad (19)$$

where  $x_k$  denotes state vector; **A**, **B**, and **C** refer to process, input, and output matrices, respectively. In the fusion process proposed by the authors, the state vector contains positions ( $x$ ,  $y$ ) and velocities ( $v_x$ ,  $v_y$ ) of a central of the marker:

$$\underline{x}_k = \begin{bmatrix} x \\ v_x \\ y \\ v_y \end{bmatrix}. \quad (20)$$

Matrices **A** and **B** are time-variant and thus they are extended with subscripts. The main process is incorporated in  $A_k$  and  $B_k$ . It simply reflects the dynamics of the central point and it is given by

$$A_k = \begin{bmatrix} A_k^z & 0_{2 \times 2} \\ 0_{2 \times 2} & A_k^z \end{bmatrix}, \quad B_k = \begin{bmatrix} B_k^z & 0_{2 \times 1} \\ 0_{2 \times 2} & B_k^z \end{bmatrix}, \quad (21)$$

where  $A_k^z = \begin{bmatrix} 1 & dt \\ -\frac{1}{dt} & 0 \end{bmatrix}$ ,  $B_k^z = \begin{bmatrix} 0 \\ \frac{1}{dt} \end{bmatrix}$ .

The output matrix  $C_k$  directly transfers the state vector to the output vector:

$$C = I_{4 \times 4}. \quad (22)$$

The Kalman filter equations are divided into two stages: The first is state prediction, which yields the a priori state vector  $\hat{x}_k^-$ ; next, it is necessary to compute a priori covariance matrix  $P_k^-$ . One will notice that by applying the first estimation of central point positions in  $k-1$ , the a priori estimation of velocities will be obtained. The KF is prepared in that way, so it can estimate the velocity of point coordinates ( $x$ - and  $y$ -axes) based on the previous ( $k-1$ ) *a posteriori* positions and the input. Also, the positions are upgraded by integrating the *a posteriori* velocities.

In the second stage of Kalman filter, namely correction, three main tasks are being executed. The first one is the Kalman gain  $\mathbf{K}_k$  calculation, and then the prior state vector  $\hat{\mathbf{x}}_k^-$  is corrected with measurement innovation. Finally, the covariance matrix  $\mathbf{P}_k^-$  is updated, obtaining the *a posteriori* covariance  $\mathbf{P}_k$ .

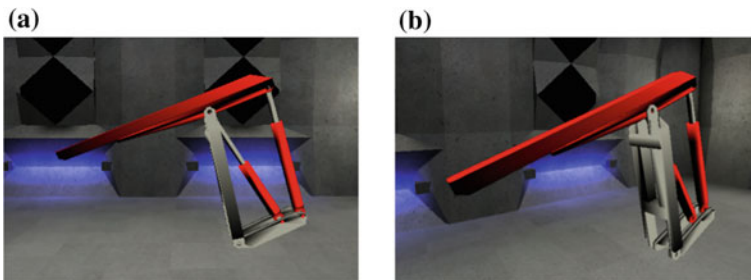
The Kalman filter is tuned via the  $\mathbf{Q}_k$  and  $\mathbf{R}_k$  matrices. The  $\mathbf{Q}_k$  refers to process noise covariance, while the  $\mathbf{R}_k$  stand for measurement noise covariance.

## 5 The Experiment

The research was carried out using a virtual manipulator. To prepare a visualization, a real electro-hydraulic manipulator was used. CAD models were converted into “\*.obj” which is a geometry definition file format. These files of all parts of manipulator were used to present full kinematics, i.e., movements of manipulator. Visualization was made in Visual Studio 2012 in C++ language and OpenGL library supported by Irrlicht 1.8.1 engine (Fig. 4).

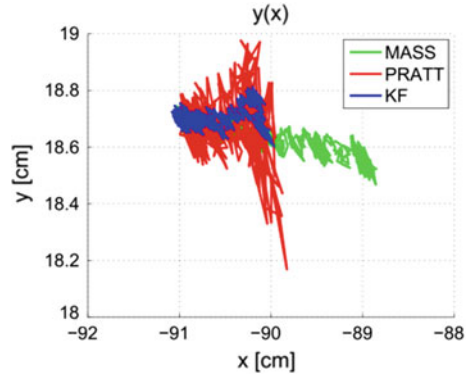
In Irrlicht engine, the user needs to determine absolute position and rotation only one time. Thus, it was necessary to prepare a position and orientation of all parts directly using a cosine theorem and trigonometric operation to compute all angles and positions of objects. These results of visualization are shown in Fig. 4a. The view of visualization can be changed directly from keyboard and mouse. It is possible to look at manipulator from all sides (Fig. 4b).

The research was performed using data from camera. Marker was in static position and only some parts of it were covered to 50% of all dimensions. The trajectory of movement should be a static point in the best case. But when camera loses some important parts of marker, a detection of central position can occur with an error. The main aim was to test algorithms and error positioning for real and simulation manipulator. The first step was to show results of measured positions for endpoint of the manipulator. The results are little fluctuating, because the light in laboratory was changing with the frequency of supply AC voltage. In Fig. 5 measurement data is shown. Data from three different algorithms are compared in



**Fig. 4** Visualization of electro-hydraulic manipulator

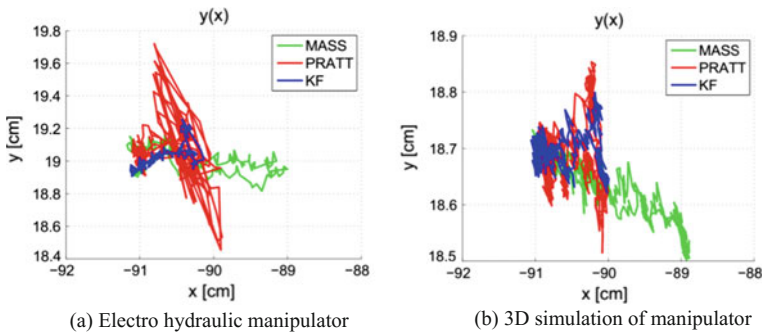
**Fig. 5** Visualization of electro-hydraulic manipulator



case of hiding some parts of marker held in hand of the operator. The most important was to achieve the lowest error of end position. The best result can be obtained via the Kalman filter.

When that test was performed using the electro-hydraulic manipulator, dangerous movements were observed. The problem was with preparing application and settings of gain parameters in controlling algorithms. After proper setup of all settings of PID controllers, the final results are shown in Fig. 6a. The virtual model of a manipulator was built in 3D software. This is more safety when testing a new algorithm on a virtual machine. Software manipulator uses complete model described in this article and a PID controllers, same as in the real manipulator running on PLC (the same implementation of control algorithms).

In Fig. 6b, the results of controlling are shown. The total error of fluctuating position between set point (static marker) and desired point (when marker was covered with 50% of surface) is about 0.5 cm. Having in mind that two arms of the manipulator were equal to 79.5 and 71.5 cm, one can deduce that the overall error is small. Differences between real manipulator and 3D simulation are caused by simple model of hydraulic drive without nonlinearity of square-root pressure



**Fig. 6** Data of positions

characteristic and dead zone of valve spool. The connection with both applications, i.e., Vision and Simulation, was stable and provided by internal TCP/IP protocol. This application can work on with two computers in the same net with PC or PLC.

## 6 Conclusion

In the article, the modeling and controlling of virtual manipulator were presented. All data are compared with real manipulator. The first part of the article recalls state of the art. In the next section, the test bed about controlling a real electro-hydraulic manipulator was presented. This manipulator was built by the authors. The research was undertaken with vision system used to capture an image with markers and recognized their positions. The images were captured from the camera with frequency up to 50 Hz and the resolution of  $640 \times 480$ . In the third section, the mathematical equations which were used in the simulation of electro-hydraulic servo drives were described. In the fourth section, a signal filtering and the implementation of KF were described. In the fifth section, the results of the experiment were shown. In the first part of the fifth section, visualization of manipulator in Irrlicht engine was presented. Next part consists of image processing results. Input image with three red markers was used. One of the markers was disturbed by hiding some small parts of it. The estimation algorithms were tested on the manipulator and on the visualization. Therefore, electro-hydraulic manipulator trajectory and the virtual manipulator trajectory were compared. The main aim of the research was to create a new visualization environment to simulate the behavior of an electro-hydraulic manipulator. When using 3D Cad models of a real manipulator, it is important to refer to real dimensions of the manipulator. A typical equation of electro-hydraulic servo drive was implemented in C++ application. This allows to visualize movements of manipulator's arms. This is very important in case of testing new control algorithm or new filter in the vision system. The researchers were focused on control movement of manipulator when some parts of the marker are hidden. This can occur when the operator rotates on plane and covered marker using some parts of body. The final results with simple model provide maximum error of positioning manipulator of about 0.5 cm with KF algorithms. In the worst case, the position of end point of manipulator was 1 cm in wrong place for algorithms with fitting circle to markers. The similar results occurred with the real manipulator. These results are sufficient to prepare a new trajectory for manipulator while working with people in the close area without danger of their life.

**Acknowledgements** The presented research results were funded with grants for education allocated by the Ministry of Science and Higher Education in Poland. Grant no. 02/22/DSMK/1406 and 02/22/DSPB/1389 Poland.



## References

1. Electro-hydraulic rear-axle steering for mobile cranes. *IEEE Control Syst.* **24**(5), 16–17 (2004)
2. Yan, T.: Notice of retraction analysis and design on air controlled hydraulic system about dump truck lifting mechanisms. In: 2nd International Conference on Artificial Intelligence, Management Science and Electronic Commerce (AIMSEC), 2011, pp. 5405–5408
3. Ahn, K.K., Yang, S.Y.: Robust force control of a 6 link electro-hydraulic manipulator. In: 4th Korea-Russia International Symposium on Science and Technology, KORUS, 2000, vol. 3, pp. 78–83
4. Lazar, C. Caruntu, C.F. Balau, A.E.: Modelling and predictive control of an electro hydraulic actuated wet clutch for automatic transmission. In: 2010 IEEE International Symposium on Industrial Electronics (ISIE), 2010, pp. 256–261
5. Razintsev, V.I., Kulikov, S.N., Volkov, S.V., Razintseva, L.A.: Microprocessor-controlled electrohydraulic power amplifiers. *Russ. Engin. Res.* **33**(7), 385–388 (2013)
6. Nikitin, O.F.: Machine regulation volume hydraulic drive with reciprocating motion of hydraulic motors. In: International Conference on Fluid Power and Mechatronics (FPM), 2015, pp. 593–595
7. Chengbin, W., Long, Q.: Study on simulation and experiment of hydraulic excavators work device based on simulation X. In: International Conference on Electric Information and Control Engineering (ICEICE), 2011, pp. 1742–1745
8. Zhixin, D. Long, Q.: Modeling and simulation of driving system for large hydraulic excavator. In: International Conference on Fluid Power and Mechatronics (FPM), 2011, pp. 669–674
9. Owczarek, P., Goslinski, J.: An estimation of central points of circle markers in a vision system by using Kalman filter and complementary filter. In: 20th International Conference on Methods and Models in Automation and Robotics (MMAR), 2015, pp. 940–945
10. Owczarek, P., Goslinski, J., Rybarczyk, D., Kubacki, A.: Control of an electro-hydraulic manipulator by vision system using central point of a marker estimated via Kalman filter. In: Szewczyk, R., Zieliski, C., Kaliczyska, M. (eds.) *Challenges in Automation, Robotics and Measurement Techniques*, pp. 587–596. Springer, Berlin (2016)
11. Net New Electronic Technology GMBH. <http://net-gmbh.com/>
12. Adaptive Vision Studio. <https://www.adaptive-vision.com/en/home/>
13. Osiecki, A.: *Hydrostatic Drive of Machines*. 2nd ed. WNT, Warsaw (2004). (in Polish)
14. Kalman, R.E.: A new approach to linear filtering and prediction problems. *Trans. ASME J. Basic Eng., Ser. D* **82**, 35–45 (1960)
15. Shimomura, K., Morita, T., Electro-hydraulic Two-Axle Steering System for City Crane. *Kobelco Technology Review*. pp. 41–46, (2013)

# Trends in the Development of Rotary Tables with Different Types of Gears

Kamil Wojtko and Piotr Frackowiak

**Abstract** The paper presents the special solutions of rotary table drive with hybrid spiroid gear drive. The construction solutions of rotary tables were reviewed and the various construction solutions, most frequently encountered on the market, were described. Rotary table solutions are discussed for the application in numerical control machines that are the fifth axis or can be used as an independent positioning device. Many different types of rotary table solutions are available on the market where direct drive or mechanical gear transmissions of different types are used, i.e.: worm gear drive or spiroid gear drive. One of the directions for the development of the rotary table drive are the new hybrid solutions, in which different types of mechanical gear transmissions are used. The article presents the construction and the operating principles of new gear units, in which the cylindrical or conical gear with helical line of the tooth work together with the face gear. The presented solutions are protected by patent applications.

**Keywords** Rotary table · Spiroid gear · Worm gear · Hybrid drive · Positioning

## 1 Introduction

Manufacturers of rotary tables and numerical control machines offer more and more solutions in order to achieve the most efficient transmission, the ability to carry high loads while retaining their self-locking. These requirements are of the utmost importance due to the use of rotary tables in numerically controlled machines, where high precision and repetition of positioning is required, as well as the dynamics of movement of particular machine components during high speed machining [1–3]. It is important to eliminate the backlash and its adjustment, to obtain the appropriate dynamics during the rotation of the rotary table. Nowadays,

---

K. Wojtko (✉) · P. Frackowiak  
Plastic Forging Plant, Institute of Materials Technology,  
Poznan University of Technology, Poznań, Poland  
e-mail: kamil.wojtko@put.poznan.pl

the aim is to achieve high performance rotary tables (over 50%), the ability to carry high loads while maintaining minimum dimensions and high mechanical life [4, 5]. In order to increase durability and positioning accuracy, more and more new solutions that differ in power transmission and gearing, have been proposed by designers [3, 6].

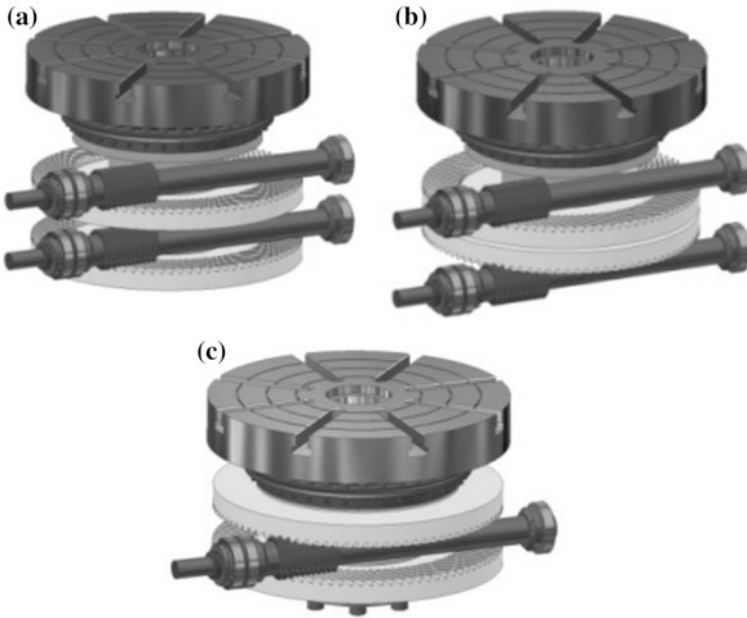
In precision positioning devices and rotary tables for continuous angular division, different gears are used which use a direct drive or mechanical transmission system. Rotary tables based on mechanical gearwheels: worm gear and spiroid are known, depending on the design solution, gear size, gear geometry and the materials from which the individual components are made determine the permissible radial and axial loads that gear drive or rotary table can carry [3]. Spiroid gear drives for use in rotary tables consist of a cylindrical or conical worm gear that work together with face gear or conical face gear [5, 7, 8]. Computing and shaping methods of specific parts of spiroid gear used in rotary tables were described in other works [9–11]. These methods assume that gears will be shaped by worm milling cutter [11], milling head [9] and disc cutter. Rotary tables using worm gear drives where worm gear usually made of alloy steel, works together with bronze face gear (BA10), are manufactured by companies such as Hass Automation and Nikken. There are known methods of structural design in rotary tables where a helical worm gear is used to drive the table disc, works with two face gears according to the invention P.396825 (Fig. 1c).

Various solutions and construction variants of rotary tables have been presented in the present work, which were developed within the research and development projects at the Poznan University of Technology. These solutions are protected by the following patent applications: P.416461, P.416462, P.416463, P.420058, P.420059, P.420060, P.420061.

## **2 Requirements for Rotary Tables and Precision Gearboxes**

The rotary table solutions presented in this article are primarily intended for numerically controlled machines as work tables or as additional precision positioning devices. Due to the fact that they are sub-assemblies, the most responsible and most influential of the precision and repeatability of machining are placed next to the drive units. They are subject to high quality requirements [1, 4].

Spiroid or worm gear drives are highly reducing transmissions, so their accuracy depends mainly on the drive type and used control system. But beyond these elements, the entire transmission system, i.e. the gearbox and its components, is affected by accuracy. The quality of the entire construction and the elements of the gear drive affects the accuracy of the machine movements. One of the most important requirements for rotary tables is no backlash in reverse movements. This results in a direct transfer of movement from the drive element to the rotary table.



**Fig. 1** Rotary table disc driven by a spiroid gear duplex type, in which: **a** two worm gears work together with two separate face gears with the same direction tilt line of the teeth; **b** two worm gears work together with opposite direction tilt line of the teeth; **c** one worm gear works together with two face gears with an opposite direction tilt line of the teeth [6]

When machining an object placed on the rotary table disc, as a result of the forces coming from the cutting process, the object must not be displaced. Therefore, another important requirement for the gear drives in rotary tables is its self-locking. There are known solutions of positioning devices in which the locking of the table disc in a given position is realized by means of additional mechanisms or pneumatic and hydraulic systems. Another possible solution to the problem of self-locking is the use of worm or spiroid gear drives, which are designed as self-locking. Another important issue is the capacity of the turntable and the ability to carry heavy loads. These loads can be derived either from the weight of the element placed on the rotary table or from the process forces. Carry capacity in worm and spiroid gear drives depends on the surface of interface between the gear teeth, the geometry of the gearing and the material from which the gear elements are made. In the case of a worm gear, it is a worm wheel (usually made of bronze) and a steel worm gear, while in the case of spiroid gear a worm gear and face gear. The increase in carrying capacity for these transmissions is achieved by the appropriate selection of cooperating teeth (convex-convex) and by increasing the co-operation surface (worm wheel-worm gear or worm gear-face gear). This problem can be solved by using bigger amount of worm gears, worm wheels and face gears.

### 3 Rotary Tables with Spiroid Gears Duplex Type

As a result of the research and work carried out within the research project, new designs of hybrid rotary tables have been proposed and implemented. Presented solutions are already known and have been described [6].

These solutions are the development of traditional spiroid gear drives. The first of the results of the research and development work was the development of duplex spiroid gear drive, in which the worm gear works together with two face gears, or two worm gears work together with two face gears (Fig. 1a, b).

The presented solutions have been extended with additional face gear or additional worm gears. The purpose of this operation was to increase the surface of the spiroid gearing. Greater surface of co-operation can also be achieved by increasing the amount of face gears working together with one worm gear (Fig. 1c), but also by using two worm gears and two face gears. In one of these variants, the two worms placed on the two separate drive shafts cooperate with the two face gears on the spindle-disk (Fig. 1a). The second variant contains two worm gears placed on separate drive shafts that work together with two face gears with opposite tilted tooth lines. The solutions of these tables were put into production at Loader Company in Środa Wielkopolska.

### 4 Rotary Tables with Hybrid Gearbox

The development of rotary table drives with mechanical transmissions has led to the development of hybrid gear drives in which various gear combinations have been combined: worm gear, helical gear, spiroid gear.

The structures shown below, due to the use of two types of gears, combine the features of each. Each of these drives ensures self-locking, eliminating the need for additional systems (mechanical, hydraulic or pneumatic) to lock the table wheel in the set position and allow the table work by continuous division method.

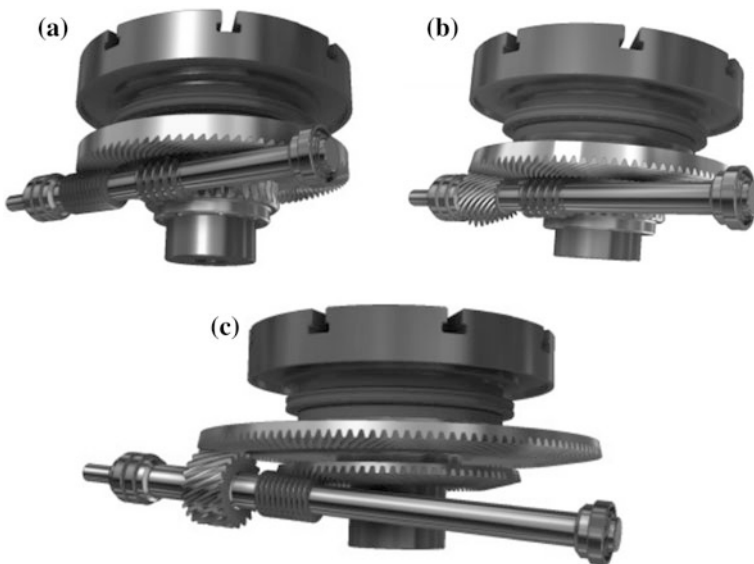
The advantage of these solutions is to increase the surface area of gearing, which translates into greater load carrying capacity. For rotary tables, this feature allows the objects to be machined with greater weight but also in machining where there is greater force from the cutting process. Increasing the gearing surface of the gears also improves the stability and dynamics of the rotary table so that they can be used for heavy duty work where frequent changes of direction of movement and accelerations occur. It should be noticed that, presented gear drives, through the larger contact surface area of the tooth and using the appropriately selected materials can be characterized by greater durability and less wear on the teeth compared to conventional gear units in the rotary tables.

## 5 Rotary Tables with Cylindrical Helical Gears and Flat Face Gears

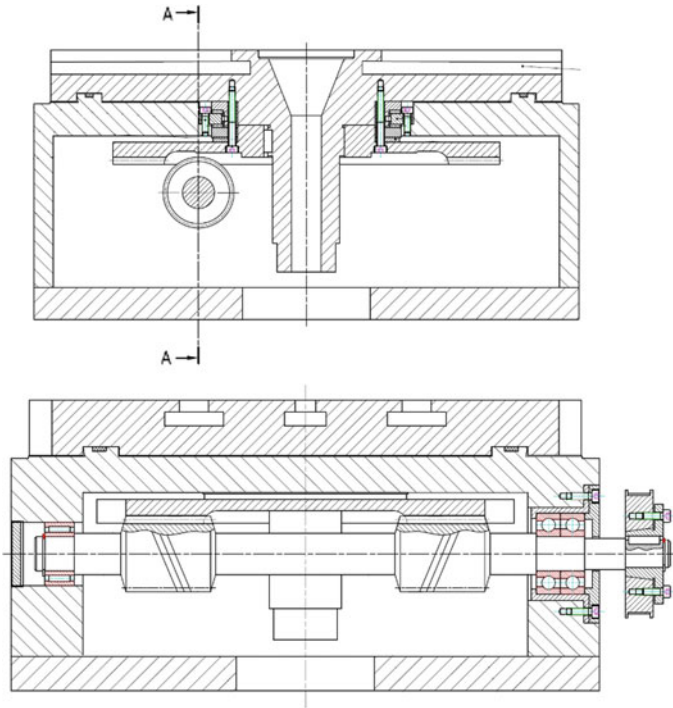
In the latest solutions of drives for rotary table with spiroid gears, two worm gears with opposite cutted teeth (right and left) are placed on one shaft, which work together with the face gear. These solutions have several variants, on the drive shaft, two worm gears (right and left), which work together with one or two face gears [12–15]. The first solution is the construction shown in Fig. 2. The rotary table is driven by two cylindrical worm gears (right and left) which work together with the face gear mounted on the spindle-disk. Worm gear teeth can be cutted on the drive shaft or placed as separate component on the shaft [12].

A second variant of the spiroid gearbox with two cylindrical worm gears mounted on one shaft is a gear drive in which the worm gears work together with the two face gears (Fig. 4). Worm gearing cooperate at the same time with the lower and upper face gear, thus increasing the gearing surface. The upper and lower face gear are located on the spindle-disc and the distance between them is controlled by means of a sleeve and a washer (method of adjusting the gearing clearance).

As shown in Fig. 4, the solution with two face gears is the development of the solution shown in Fig. 3. In order to increase the load capacity of the rotary table (Fig. 3), the lower face gear can be fitted to the spindle-disk as illustrated on Fig. 4,



**Fig. 2** Rotary table drive with hybrid gearbox consisting of: **a** a helical gear that cooperates with face gear and worm gearbox; **b** spiroid gearbox and worm gearbox; **c** a helical gear that cooperates with face gear and spiroid gearbox [6]

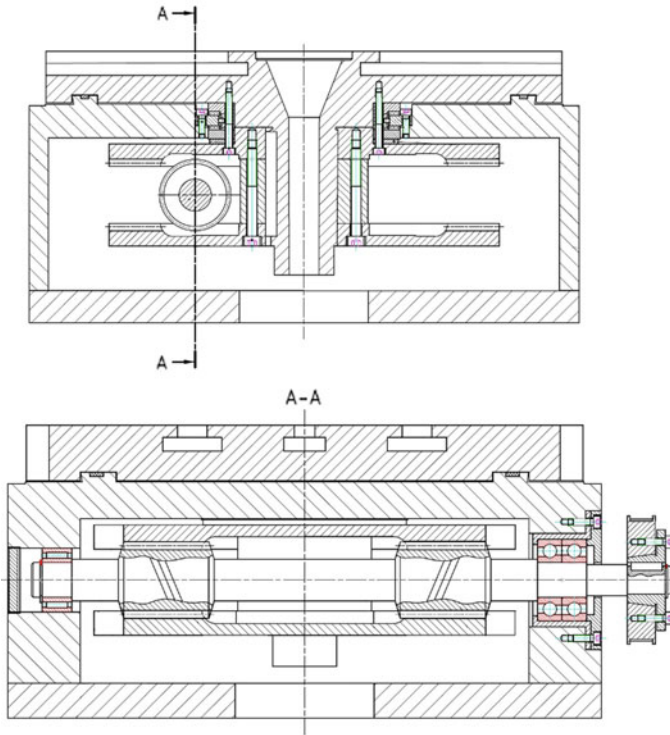


**Fig. 3** Rotary table disc driven by the two helical gears attached to the same shaft, that work together with one flat face gear

which will increase the area of cooperation of the gearing. This operation can also be easily automated by using special electrical, pneumatic or hydraulic systems, where in certain cases it will be possible to axially move the lower face gear and to connect it with the worm gears placed on the drive shaft.

## 6 Rotary Tables with Conical Helical Gears and Conical Face Gears

Further variants of the mentioned constructions are rotary tables in which the two conical worm gears work together with the conical face gear (Fig. 5). The principle of operation and other elements of this construction (except for gearing) are identical to those in the rotary table shown in Fig. 3.



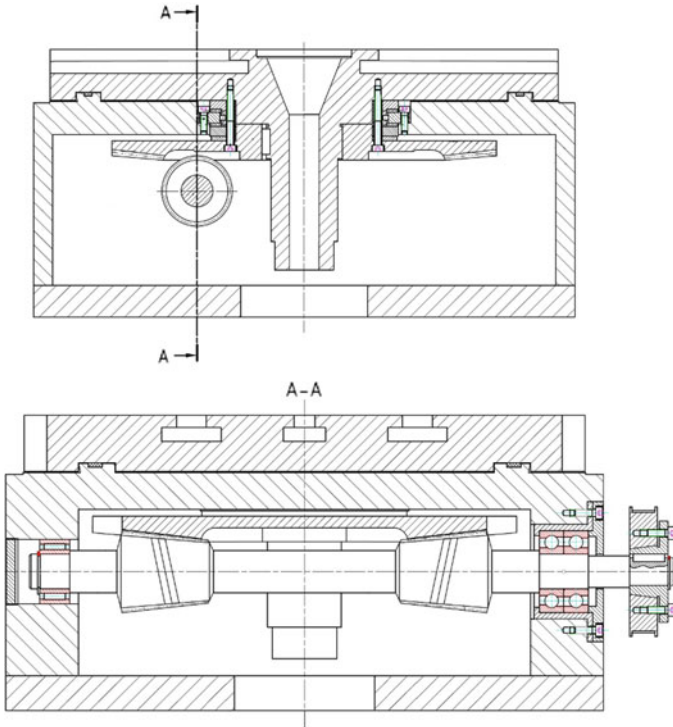
**Fig. 4** Rotary table disc driven by the two helical gears attached to the same shaft, that work together with two face gears with opposite tilted teeth line

In turn a second solution based on conical worm gears, similar to the structure shown in Fig. 4. It is based on co-operation of two conical worm gears with two conical face gears, as shown in Fig. 6.

## 7 Summary

The most recent rotary table drives solutions are characterized by the largest surface area of the gearing at minimum dimensions of the whole rotary table. The table drive solutions shown in Figs. 4 and 6 provide the greatest durability and load capacity of the rotary table. These solutions in rotary table applications have several

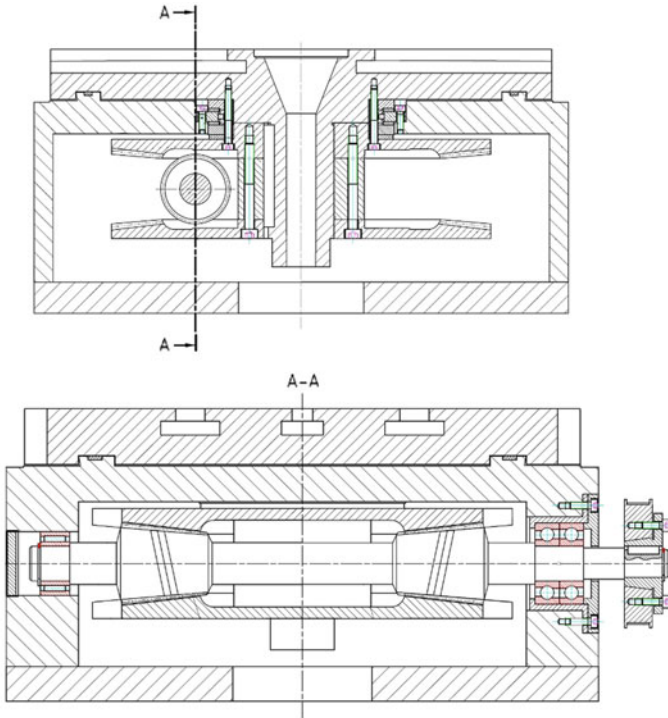




**Fig. 5** Rotary table disc driven by the two conical gears attached to the same shaft, that work together with one conical face gear

times the capacity compared to conventional worm gear units of the same dimensions. This is due to the increased surface area of the cooperation of the teeth and it also helps to improve the stress strength of the gear teeth.

Compared to the currently available solutions, the proposed rotary table drive construction seem to be more advantageous due to the increased surface area of the



**Fig. 6** Rotary table disc driven by the two conical gears attached to the same shaft, that work together with two conical face gears with opposite tilted teeth line

tooth engagement and hence the achievement of other previously mentioned advantages and benefits, most of all load capacity.

In further research, it is envisaged to make the gear elements by means of forging processing.

## References

1. Honczarenko, J.: Numerically Controlled Machines, WNT, Warszawa (2008)
2. Wrotny, L.T.: Anticipating the direction of development of machine tools for removal machining in Poland. *Mechanic* **9**(10), 297–302 (1990)
3. Staniek, R.: Numerically Controlled Rotary Tables. Theoretical Basics, Construction, Technology and Research, Poznan (2005)
4. Funaru, M., Mihaila, L., Pascu, M., Andrioaia, D.: Rotary index table used on multi-axis machining centers. In: 23rd International DAAAM Symposium, vol. 1, pp. 1131–1134 (2012)
5. Litvin, F.L., Gonzalez-Perez, I., Yukishima, K., Fuentes, A., Hayasaka, K.: Design, simulation of meshing, and contact stresses for an improved worm gear drive. *Mech. Mach. Theor.* **42**, 940–959 (2007)

6. Czajka, P., Frackowiak, P.: New solutions of gear drive in mechanism of NC rotary table. *Eng. Model.* **29**(60), 5–10 (2016)
7. Frackowiak, P.: Development of a new geometry and gear shaping technology in which the cylindrical worm gear works together with two face gears and studies about its application in new generation of precision series and heavily loaded NC tables, Research development project nr 0910/R/T02/2010/10, unpublished materials (2014)
8. Frackowiak, P.: Modelling face worm gear drive with cone worm. *Eng. Model.* **24**(55), 27–33 (2015)
9. Litwin, F.L., Nava, A., Fan, Q., Fuentes, A.: New geometry of worm gear drives with conical and cylindrical worm: generation, simulation of meshing, and stress analysis. *Comput. Methods Appl. Mech. Eng.* **191**, 3035–3054 (2002)
10. Frackowiak, P., Ptaszyński, W., Stoić, A.: New geometry and technology forming face-gear with circle line of teeth on CNC milling machine. *Metalurgija* **51**(1), 109–112 (2012)
11. Dudas, I.: The theory and practice of worm gear drives. Penton Press, London (2000)
12. Wojtko, K., Frackowiak, P.: Polish patent application, P. 420058, December 30, 2016
13. Wojtko, K., Frackowiak, P.: Polish patent application, P. 420059, December 30, 2016
14. Wojtko, K., Frackowiak, P.: Polish patent application, P. 420060, December 30, 2016
15. Wojtko, K., Frackowiak, P.: Polish patent application, P. 420061, December 30, 2016

# Survey on Design and Development of Hexapod Walking Robot, Automated Guided Vehicle and Drone

Bartosz Minorowicz, Mariusz Palubicki, Natan Stec,  
Jakub Bartoszek, Lukasz Antczak and Jakub Matyszczyk

**Abstract** This paper presents scope of work performed by Students in R&D Group “Mechatron”, where student can develop own ideas under supervision of experienced tutors. The work carried out mostly on autonomous machines and issues related with their control. In recent years, few interesting designs have been developed by Students, three chosen are presented in this paper. In the first section, two designs were presented and it means automated guided vehicle and drone. Presented line follower and its designer participate successfully in nationwide competitions. This vehicle is a result of three years of learning and gaining experience, which allowed for fabrication such complex design. Next described project is a drone, where students prepared 3D printed reinforced lightweight frame. The purpose of this drone is to carriage, e.g., first aid or rescue equipment like ropes. The following and the biggest part of the paper is focused on walking robot. Authors analyzed different kinematics for movement generation and finally, it was decided to perform legs like a cockroach. Based on a kinematic chain, inverse kinematic approach and oscillators Authors successfully evaluated control algorithm which was used for walking generation.

**Keywords** Hexapod walking robot · Design · Modeling · Line follower UAV · UGV

---

B. Minorowicz (✉)

Faculty of Mechanical Engineering and Management, Institute of Mechanical Technology,  
Poznan University of Technology, Piotrowo Street 3, 60-965 Poznan, Poland  
e-mail: bartosz.minorowicz@put.poznan.pl

M. Palubicki · N. Stec · J. Bartoszek · L. Antczak · J. Matyszczyk  
Faculty of Mechanical Engineering and Management, KNM Mechatron, Poznan, Poland

© Springer International Publishing AG 2018

A. Hamrol et al. (eds.), *Advances in Manufacturing*, Lecture Notes in Mechanical Engineering, [https://doi.org/10.1007/978-3-319-68619-6\\_38](https://doi.org/10.1007/978-3-319-68619-6_38)

# 1 Introduction

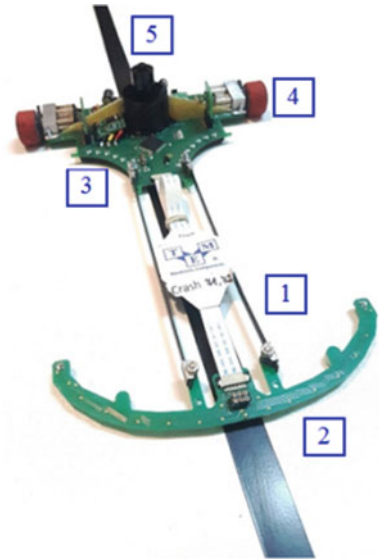
Authors of this paper are students of mechatronics at Poznan University of Technology and their Tutor, they are members of the R&D Group “Mechatron.” The main purpose of work in such organization is enlargement of theoretical knowledge from university courses and realization of own engineering and scientific ideas. For the purpose of this paper, three the most interesting and advanced projects have been selected, thus main contributions can be formulated as follows: description and presentation of own designs, where components selection is based on own calculations and modeling. Selected projects are: (1) hexapod walking robot, (2) automated guided vehicle so-called line follower, and (3) unmanned aerial vehicle so-called drone. Devices number 2 and 3 are described briefly in the introduction part of this paper, remaining part is focused on hexapod design and development. Main motivation to take up these topics is the desire of men to replicate animal’s movements, e.g., to reach inaccessible places.

## 1.1 Line Follower Design and Development

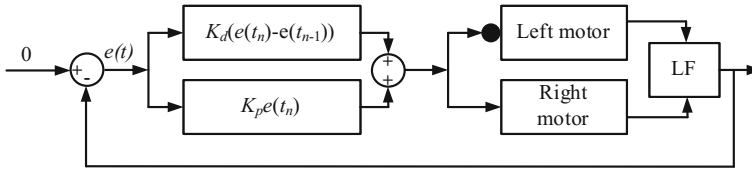
Line followers are a part of a group of AGV (automated guided vehicles). Such vehicles can be used in automated warehouses for goods distribution [1]. At Institute of Mechanical Technology project related with line, followers design has been running for four years since 2013. First designs were only objects for the training of student’s skills including mechanical design, motors, and sensors selection, assembling, and programming. After the stage of development and testing of first prototypes at laboratory conditions, it was decided to participate nationwide competitions, which are organized cyclically in many Polish cities (mostly at universities of technology, e.g., Warsaw, Krakow, Gdansk, Wroclaw, Poznan, etc.). Category of line followers assumes that the main goal of the designed device is to run the special track as fast as this vehicle can. The track is designated by black insulation tape on a white plate. Line follower’s competitions are divided into two categories: standard and turbo. Turbo works in the same way as a diffuser in racing cars. The additional fan sucks an air from the bottom of a line follower, that makes pressure difference whereby what increases speed in turns.

Authors of this paper focused on line follower *Crash* (Fig. 1), which is the most advanced design that has been made so far by Mechatron members. Line follower designer must take into account many factors, because very often time differences between competitors on finish line can be expressed in milliseconds. Key design issues are: mechanical design, proper balancing, drive unit, control algorithm, and PCB which is also frame for all components. Dimensions are limited, the design of line follower cannot exceed A4 sheet area ( $297 \times 210 \text{ mm}^2$ ). Presented in this paper robot *Crash* is distinguished by modular design connected by two rigid carbon link rods (no 1). The front part (no 2) is equipped with a row of sensors,

**Fig. 1** Line follower *Crash*  
—description in text



where high sensitivity photointerrupters KTIR0711S are used, sensors are directed toward the floor. Mass (moment of inertia) of the front part has a significant impact on robot dynamics, thus the main assumption was to design this section as light as possible. The optional robot can be equipped with the proximity sensor, which is necessary for another category “*Linefollower Enhanced*” where obstacles, e.g., the wall can be placed on the route. The main part of the robot is backside (no 3) where microcontroller, driving unit and battery are placed. Used microcontroller (STM32F103VCT6) is distinguished by high computing power (compared to similar robots), thus advanced control algorithm can be implemented. This algorithm analyses not only data from photointerrupters but also uses the gyroscope, accelerometers, and encoders. Traction is provided by two wheels with polyurethane rubber tires (hardness—30 in Shore A scale). Each wheel is linked to brushed DC motor, equipped with gearbox (10:1 ratio), which provides sufficient torque (no 4). Even though motors work on 6 V power supply, a higher voltage is given (11.1 V). This is due to three cell lithium-polymer battery. Motors have for this purpose reinforced brushes, whereby nominal rotational speed increases. This line follower has special turbofan (no 5), which sucks air from chassis. Pressure difference makes that speed can be increased up to 3 m/s in corners and tight turns. The special gasket is mounted under back chassis, which intensifies sub-pressure generation. This solution makes that frame needs reinforcements and additional ribs to increase stiffness and avoid breaking. Central placement of heaviest components helps in reduction of moment of inertia, which low value is significant for fast direction changing. Algorithm for line tracking utilizes classical PD regulator (Fig. 2) [2]. Mechanical parts are distinguished by very high dimensional accuracy obtained on WEDM process (Wire Electrical Discharge Machining). Detailed



**Fig. 2** Implemented control algorithm, where LF is vehicle drive

description and research online follower parameters will be described in another paper.

## 1.2 Drone Design and Development

Unmanned aerial vehicles (so-called UAVs) noted a significant increase in popularity in last two decades. UAVs initially used in military applications quickly found civil applications such as local area monitoring, filming documentaries, search and rescue, drone racing or 3d mapping applications [3, 4]. Undoubted advantage of these devices is the ability to reach inaccessible places preserving a high level of flexibility and maneuverability. Despite these facts, very poor flight range should be mentioned. Also, the mass of payload is limited by the necessity of using heavy batteries. Drone presented in this paper is equipped with eight rotors arranged in X. The mechanical structure combines parts made of machined carbon fiber (stiff and lightweight) connected by 3d printed elements (yellow parts). Quite often when designers want to increase lifting capacity they increase arms with motors. In this case, designers solve this problem by mounting two BLDC motors on each arm, which work antagonistically. Presented in Fig. 3 drone has completed mechanical structure, currently designers are focused on the control system and research on drag force generated by a pair of propellers.

## 2 Hexapod

The main objective of this project was to develop walking robot based on based on arthropod kinematics, which extends the ability to move in heavy terrain [5]. During designing process, few conceptions were considered, e.g., shape and leg's kinematics, a number of legs and their lengths [6]. Finally, it was decided to design six legs robot where kinematics is like cockroach where length proportions between next sections are as follows 1:4:5 [7]. The similar design concept is presented in paper [8], where authors implemented control algorithm for wall-following.

The first stage of this project was mechanical design. Frame and legs were made of aluminum plate, 3 mm thickness and motor flanges where the thickness is 8 mm.



**Fig. 3** Photograph of drone after assembly

Each leg has two degrees of freedom. Smooth work between moving parts was provided by sliding bearings. Drive system is based on twelve servomotors frequently used in hobby constructions, e.g., helicopters. Chosen motors were made by Hitec with serial number HS-645MG (mass 55.2 g), where required voltage supply is 5 V thus generated torque is 0.75 Nm. During first tests, it was realized that motors can overheat, so it was decided to use thermally conductive paste on the motor side where electronics are placed. As a power supply for robot lithium-polymer battery with two cells was used (7.6 V and 6000 mAh capacity). To decrease voltage supply from 7.6 to 5 V (required on motors), two step-down voltage converters were used. First voltage converter generates 5 A of maximum current and it was used for electronics and control systems, the second one generates 9 A and this current was used in servomotors. Converters were placed in plastic housing with switches, average battery life is about 2 h. The main part of control system was Raspberry Pi 2 computer, which uses UART for communication with MiniMaestro. This component has 24 channels and it was responsible precise positioning of each servodrive. Even though Raspberry works on 3.3 V and MiniMaestro work on 5 V, these two plates were connected via logic level converter. Control board has also gyroscope with accelerometer and magnetometer, which send signals via I<sup>2</sup>C interface. In next step legs design was changed by addition of another joint controlled by servomotor, thus total number of motors increased to 18 (Fig. 4).

The control program was written in high-level programming language C++. This is console application works under Linux operating system.

The program executes following sequence:





**Fig. 4** Modified design of hexapod walking robot

1. Check logic conditions for walking mode and way.
2. Calculation of new point of space for leg's end.
3. Rescaling of calculated position.
4. Inverse kinematics calculation.
5. Sending for each servomotor information with the new position.

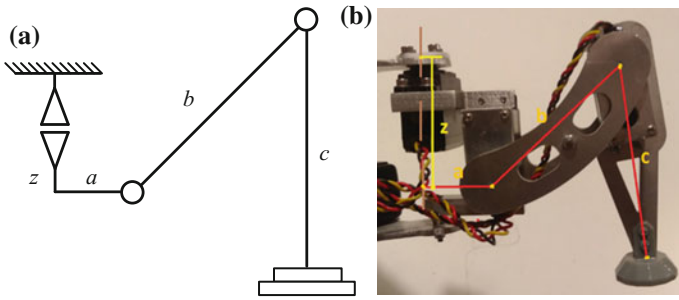
In a performed robot, tripod gait walk is implemented. Six legs are divided into two groups, which works antagonistically in each time interval. When three legs do not touch the ground the other three push the robot forward. For such operating mode, inverse kinematics calculation is necessary. Calculations are based on mechanical design and adopted geometry, including all ambiguities implemented by trigonometric functions [9].

According to Fig. 4, kinematics of each leg can be drawn as presented in Fig. 5a, b, where lengths of indicated parts are as follows:  $a = 30$  mm,  $b = 70$  mm,  $c = 90$  mm,  $z = 55$  mm. Based on this scheme, schemes for inverse kinematics calculations were prepared (Fig. 6).

Proper operation of walking robot needs inverse kinematics. Values are calculated by following mathematical formulations:

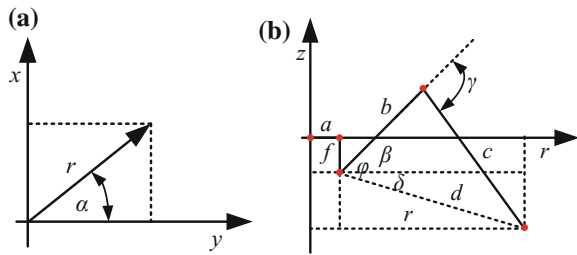
$$r = \sqrt{x^2 + y^2} \quad (1)$$

$$d = \sqrt{(z - f)^2 + (r - a)^2} \quad (2)$$



**Fig. 5** Robot leg's kinematics with characteristics parts, where  $a, b, c, z$  are characteristics dimensions of robot's leg

**Fig. 6** Robot leg's kinematics with characteristics parts



$$\varphi = \cos^{-1} \left( \frac{c^2 - b^2 - d^2}{-2bd} \right) \tag{3}$$

$$\delta = \tan^{-1} \left( \frac{z - f}{r - a} \right) \tag{4}$$

$$\alpha = \tan^{-1} \left( \frac{x}{y} \right) \tag{5}$$

$$\beta = \begin{cases} \delta + \varphi, & r - a \geq 0 \\ \varphi - (\pi - \delta), & r - a < 0 \end{cases} \tag{6}$$

$$\gamma = \cos^{-1} \left( \frac{d^2 - b^2 - c^2}{2bc} \right) \tag{7}$$

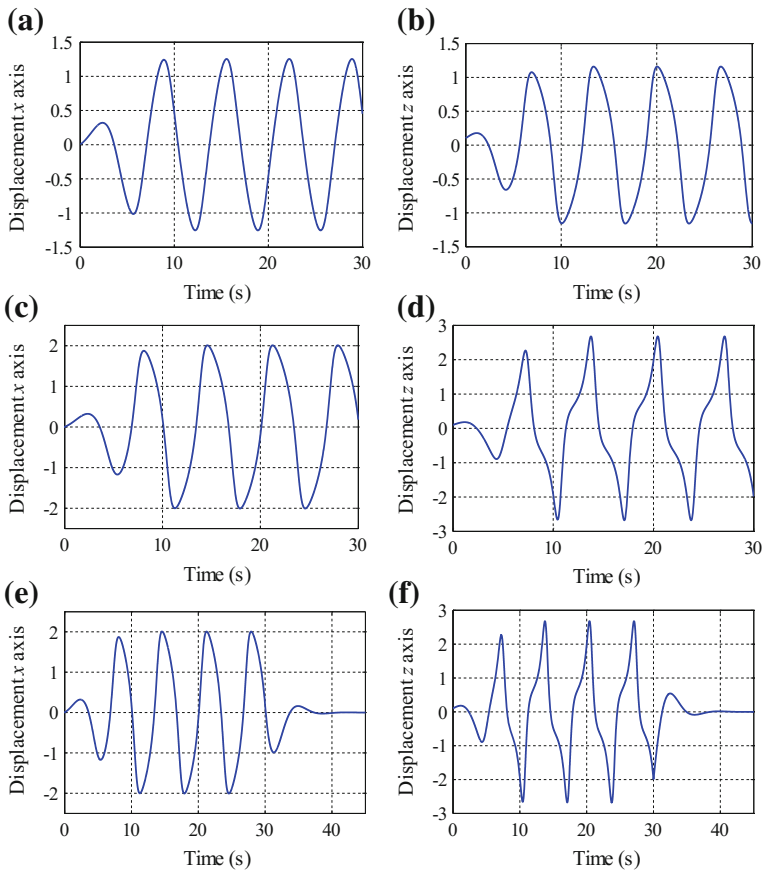
Implemented walk generator was based on three differential equations, namely: Rayleigh oscillator (Eq. 8), van der Pol oscillator (Eq. 9), and damped oscillator (Eq. 10) [9, 10].

$$\ddot{y} - \mu(1 - \dot{y}^2)\dot{y} + \omega^2 y = 0 \tag{8}$$

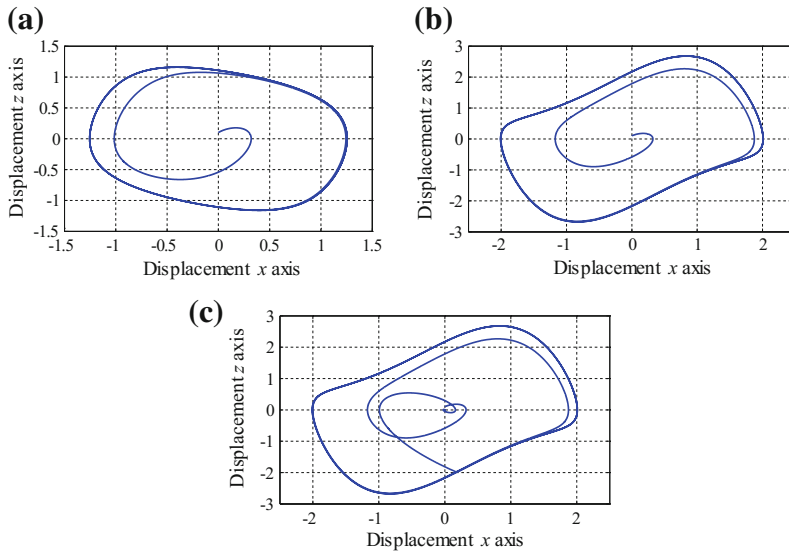
$$\ddot{y} - \mu(1 - y^2)\dot{y} + \omega^2 y = 0 \tag{9}$$

$$\ddot{y} - 2\zeta\omega_0\dot{y} + \omega_0^2 y = 0 \tag{10}$$

The Runge–Kutta fourth order method was chosen for solving the equations, which makes that during walking sequence generation leg position changes as it is shown in Fig. 7a–f. It was assumed that in Eqs. (8–10)  $\dot{y} = z$ . The solution for this assumption gives displacement in the vertical  $z$  axis, while the result of solving the same equations for  $y = x$  gives displacement in the horizontal  $x$  axis. Figures, where  $z(x)$  dependence is shown, are so-called phase portrait of oscillators (Fig. 8a–c).



**Fig. 7** Trajectories calculated based on Eqs. (8–10): **a, b** Rayleigh oscillator, **c, d** van der Pol oscillator and **e, f** damped harmonic oscillator—relative values



**Fig. 8** Phase portraits of: **a** Rayleigh oscillator, **b** van der Pol oscillator **c** damped harmonic oscillator—relative values

### 3 Summary and Discussion

This paper summarized work that has been performed by Students, all projects will be continued. Authors have following ideas for further research and development, some of the projects are already underway. Thus, in such projects students can enrich their theoretical knowledge by new practical skills.

Line follower will be enhanced with an algorithm which registers track. This implementation should help in better velocity profile optimization, and finally velocity in corners or turns will be higher. Powers supply of DC motors also will be increased up to 14.8 V at the same time with this modification new softer tires will be tested. Authors will focus also on the rigidity of follower's frame.

Application of inverse kinematics in walking hexapod gives unequivocal relation between position of leg's end in cartesian coordinate system and coordinate system, which is associated joint of this leg to robot's frame. It makes that it is easier to control foot position, because used servomotors have angular control of output shaft (no necessity to recalculate these positions). Another advantage of this kinematics is easy to walk generation where coordinates from nonlinear oscillators are used. Nonlinearities, which are in oscillators, makes that leg movement is very smooth and it is much closer to natural walk. Each step has starts and finishes at the same point, through application of combination of two oscillators: Rayleigh and van der Pol. Authors currently develop new design of 3D printed foot with embedded force sense resistor. With this foot, robot will be able to walk in rough terrain. Measurements of forces will let for better movement control-it will be an

additional feedback loop for leg position. It is expected, that this solution will compensate servomotor's positions errors caused by gearbox backlash and potentiometer inaccuracy. The second advantage of the described foot's improvement will be embedded spring, which is very important part of this mechanism. The spring has two functions: first is preload generation for force sensor, which improves measurement accuracy. Spring behaves as mechanical low-pass filter, which additionally protects servomotors from impulse loads, which is second function. The spring in foot will change the character of the actuator from conventional to primitive kind of series elastic actuator (SEA). Spring natural frequency with value 650 Hz should protect gearbox efficiently. Parallel work with the installation of stereovision camera 2.5 d mapping is being carried out, which should improve the autonomous behavior of robot in an unknown environment.

## References

1. Cardarelli, E., et al.: Cooperative cloud robotics architecture for the coordination of multi-AGV systems in industrial warehouses. *Mechatronics* **45**, 1–13 (2017)
2. Osorio, R., Romero, J., Peña, M., López-Juárez, I.: Intelligent line follower mini-robot system. *Int. J. Comput. Commun. Control* **1**(2), 73–83 (2006)
3. Siebert, S., Teizer, J.: Mobile 3D mapping for surveying earthwork projects using an Unmanned Aerial Vehicle (UAV) system. *Autom. Constr.* **41**, 1–14 (2014)
4. Nex, F., Remondino, F.: UAV for 3D mapping applications: a review. *Appl. Geomatics* **6**(1), 1–15 (2014)
5. Zielinska, T., Heng, J.: Development of a walking machine: mechanical design and control problems. *Mechatronics* **12**(5), 737–754 (2002)
6. Gonzalez-Rodriguez, A.G., Gonzalez-Rodriguez, A., Castillo-Garcia, F.: Improving the energy efficiency and speed of walking robots. *Mechatronics* **24**(5), 476–488 (2014)
7. Zielińska, T.: *Maszyny kroczące. Podstawy, projektowanie, sterowanie i wzorce biologiczne*. Warszawa (Wydawnictwo Naukowe PWN) (2003)
8. Juang, C.F., Chen, Y.H., Jhan, Y.H.: Wall-following control of a hexapod robot using a data-driven fuzzy controller learned through differential evolution. *IEEE Trans. Industr. Electron.* **62**(1), 611–619 (2015)
9. Piątek, M.: *Problemy sterowania robotami kroczącymi - generatory chodu hexapoda*. Kraków (Doctoral dissertation—in Polish) (2012)
10. Grzelczyk, D., Stańczyk, B., Awrejcewicz, J.: Prototype, control system architecture and controlling of the hexapod legs with nonlinear stick-slip vibrations. *Mechatronics* **37**, 63–78 (2016)

# Development of Conical Face Gear Technology Cooperation with Conical Worm in Spiroid Gear Drive

Piotr Frackowiak and Kamil Wojtko

**Abstract** Generation of a modification involute line of a conical face gear is performed on a CNC milling machine. The method of forming conical face gear proposed in this article is based on the application of the disc tool with a single blade tool (grinding tool) and CNC milling machine with a special programme. The article presents the problems connected with projecting and forming of conical face gear with modification involute line. In the paper, the new method of forming the cone face gear with an involute line on CNC milling machine with continuous divide and the scheme of the process kinematics have been presented. The geometrical design model and the special algorithm for sharpening a conical face gear on CNC milling machine with continuous divide have been used for forming conical face gear. The developed theory is presented in this work has been confirmed by experimental researches.

**Keywords** Face gear · Spiroid gear · CNC milling machine · Disc tool

## 1 Introduction

Face gear with involute teeth line can be cut with conical or cylindrical hob cutter [1–4]. There is also a possibility of cutting an involute teeth line with the use of a disc tool with a single blade tool. The authors of the paper [5] point out some big problems with sharpening hobbing cutters with small radius blades used for cutting face gear and hob scale error that are transferred onto the gear. The development tendency of forming face gear with an involute teeth line is to use numerically controlled machine tools and tools with carbide blades. First studies of forming possibilities of cutting teeth with an involute line were carried out by the author [5, 6] with the application for spiroid gear with a cylindrical worm.

---

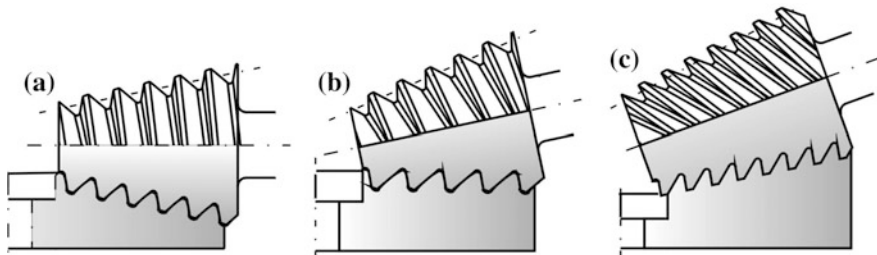
P. Frackowiak (✉) · K. Wojtko  
Institute Technology of Materials, Poznan University of Technology, Poznan, Poland  
e-mail: piotr.frackowiak@put.poznan.pl

Known methods forming conical face gear are based on the kinematics of conventional machine tools. The generation of a conical worm gear of all types of existing design is based on the application of a hob [1–4] for generation of the conical face gear or other method based on application tilted head-cutter for manufacturing a conical face gear [7]. The new technology of cutting a conical face gear on a CNC machine tool based on the application of disc tool with a single blade tool [6, 8, 9]. For generation conical face gear were used the 5-axis vertical CNC milling machine incorporates a rotary table and a NC spindle. The process needs general purpose machine like CNC vertical machining. The generations are performed by a tilted tool edge with straight line profiles of blades. The process gives better results with the use of the newly developed technique to generate a conical face gear. Due to addition, two rotational axes in 5-axis machining enables forming conical face gear and taken high surface quality. For numerically controlled universal milling machine a conical face gear can be shaped with different front lines of teeth. While notching the teeth, workgroups of machine perform movements at a constant speed and the tracks are rectilinear or rotary (NC rotary table, spindle tool). One way to sharp conical face gear is the use of a disc tool with single blade tool in the form of a carbide insert.

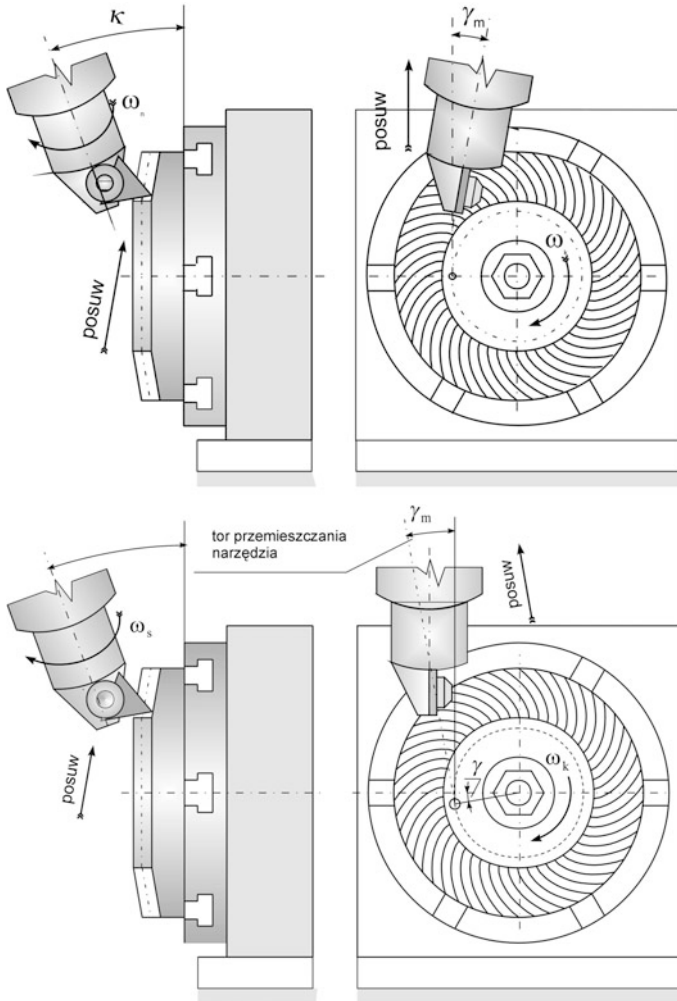
## 2 Technology of Forming of a Conical Face Gear with an Involute Gear Line

The Company Tool Works in Illinois—the USA is manufacturing different types of spiroid gears. The conical worm gear on the application of cylindrical or conical hobs. One of the types based on a conical worm gear with conical worms. Figure 1 illustrates the idea of construction of a conical worm with face gear.

In order to avoid edge contact in the spiroid gear with an involute teeth line [8], the proper setting of the tool and the direction of its movement is used during teeth



**Fig. 1** The view of different types of conical spiroid gears drives with face gear (b) and conical faces gears (a, c)



**Fig. 2** Tool orientation during chasing of gearing with a left direction of inclination resulting from the requirement of obtaining a common normal of the trace defined by the cutting blade's edges and a gearing teeth line [6].  $\omega_k$  Rotational speed of conical face gear,  $\omega_s$  Rotational speed of tools,  $\gamma_m$  Twist angle of the spindle,  $\kappa$  Inclination angle of the spindle to conical face gear,  $P$  Settings point tools

line formation. The tool and its movement should be selected in such way, as to achieve the required teeth line modification, allowing to avoid edge contact.

Avoiding edge contact in spiroid gear with involute teeth line of face gears is possible only in the cases of conical face gear with involute line modification.



The general principle of modified involute line teeth of conical face gear is to set the conformity of the track described by the edges of blade's curve radius and the teeth line of conical face gear in the calculated point and with rolling from a ring with a smaller diameter [6]. The selection of the radius of the ring circumscribes the involute and influences the modification size of line conical face gear (the smaller the rolling ring, the bigger the modification).

In Fig. 1 was presented exemplary orientation of the disc tool on the space of machine tool in relation to the conical face gear installed on the rotation table [6].

During formation, the machine tool's control system couples the spindle rotations with the table's rotations with conical face gear in order to ensure continuous index. The rolling movement (forming of the involute teeth line) is implemented through connecting the SN rotation table movement with the movement of the tool along the axis of conical face gear in a rotated coordinate system by an angle  $\gamma_m$  in the plane of the conical face gear. The rotation of the machine tool's coordinates, with the use of standard machining cycles, is carried out in order to ensure a common normal of the trace marked by the cutting blade's edges and the conical face gear teeth line. The angle  $\gamma_m$  depends on the type of the assumed involute ( $\gamma_m$ —positive values for elongated involute, negative for shortened involute and zero in the case of normal involute). A universal, numerically controlled milling machine, equipped with a twist tool head allows any inclination of the tool axis toward the machined rim.

The main chipping movement is realizing by the disc tool (rotation around its own axis as well as the tangential feed to the generating line of a conical face gear). Due to the tangential feed to a generating line of conical face gear, a compensation of the circular movement of workpiece must be performed in order to realize of a geometrical parameter of a conical face gear. The tangential movement of the disc tool lasts until the calibrating teeth of the disc tool covered the teathed surface. The technology model with penetration advance parallel and next penetration advance perpendicular to the axis of the conical worm gear illustrated in Fig. 3. The blade of the disc tool is a straight line and profile angle  $\alpha_1$  is determined from the conditions that the straight line is a tangent to the cross-section of the conical worm gear at point P (Fig. 3). Figure 3 explains the next positions between tool and workpiece as well as the necessary movements in order to realize the forming involute line in a conical face gear. Finally, complete content and organizational editing before formatting.

In the following methods of shaping conical worm gears with the involute line, are acting on these assumptions:

- a tooth line is shaped by disc tool with a single blade,
- n incision tooth line is rigidly linked to the machined teeth crown,
- a beginning of the system of coordinates is located at the intersection of the axis of symmetry shaped toothing,
- the location of the curve, part of which is tooth lines, is set in relation to the theoretical rolling circle,

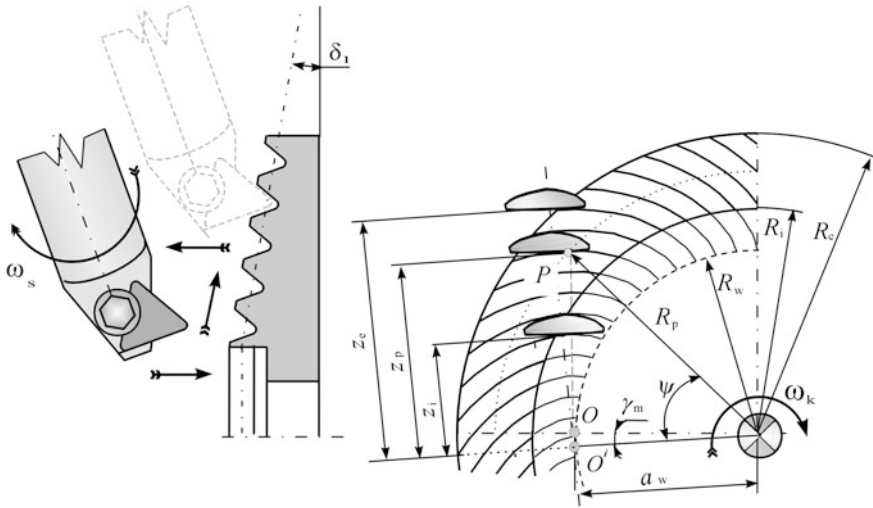
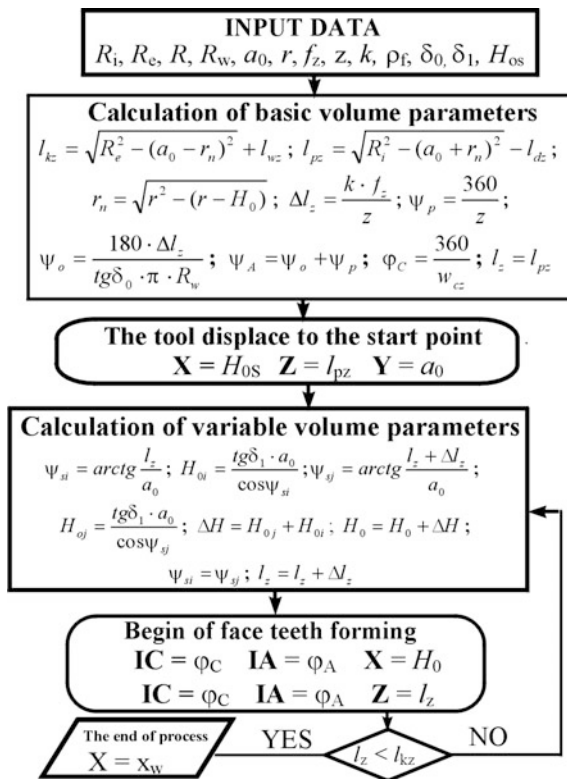


Fig. 3 The technology design of forming of involute line in conical face gear

Fig. 4 The control algorithm of forming a conical worm gear on CNC milling machine



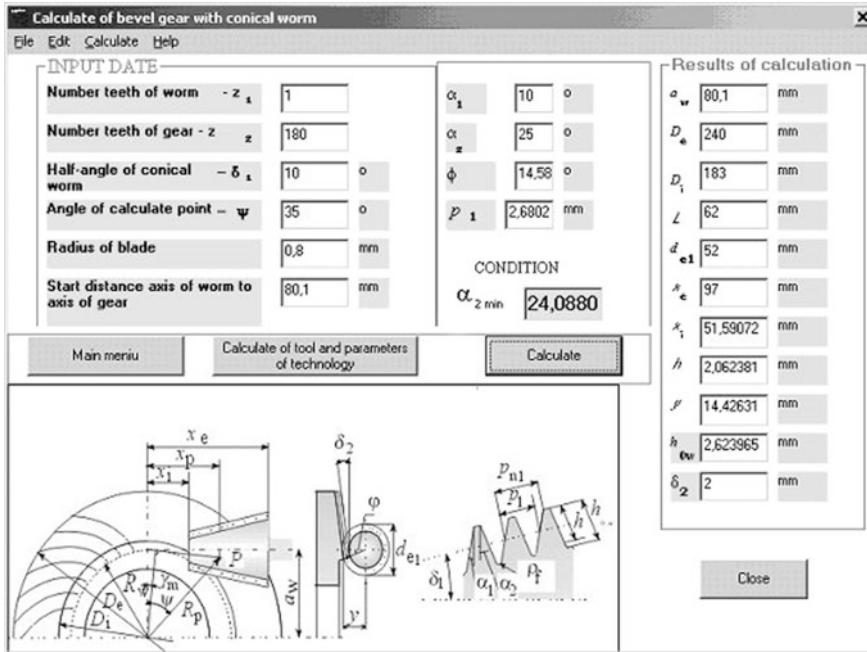


Fig. 5 View the widow of calculation a computer programme parameters of the conical worm gear drive with conical worm

- a trace location of the blade of the tool is described by the blade cutting edge it is so located in relation to the shaped surface in order to have a common normal with the shaped line of the tooth.

On the base technology design, (Fig. 3) described the algorithm with could be worked out also in system control such as HEIDENHAIN or any other. The CNC milling machine must have a 5-axis numeric control. Machine controller reads enough NC blocks prior to the current position to operate with interpolated commands. The control algorithm of forming a conical worm gear is presented in Fig. 4.

A computer programme has been developed to simplify the calculations parameters used in the reassertion of conical worm gears. A method of calculation of parameters of conical worm gear can be found in references [10]. The results of the calculations conical worm gear drive with conical worms are presented in Fig. 5.

The view of the widow of calculations a computer programme of technical parameters of the cone worm gear with the conical worm is illustrated in Fig. 6.

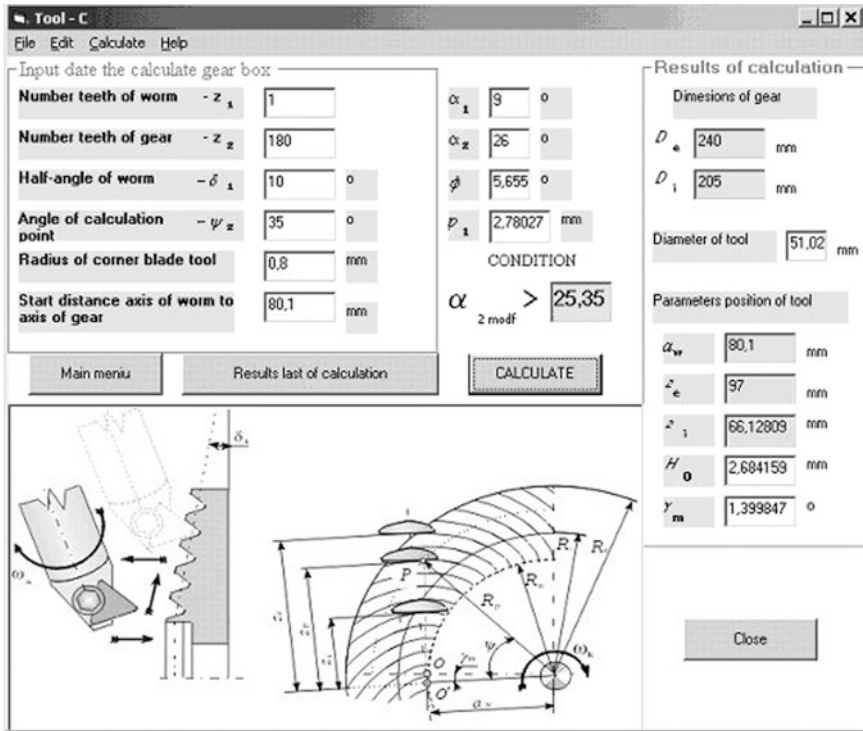
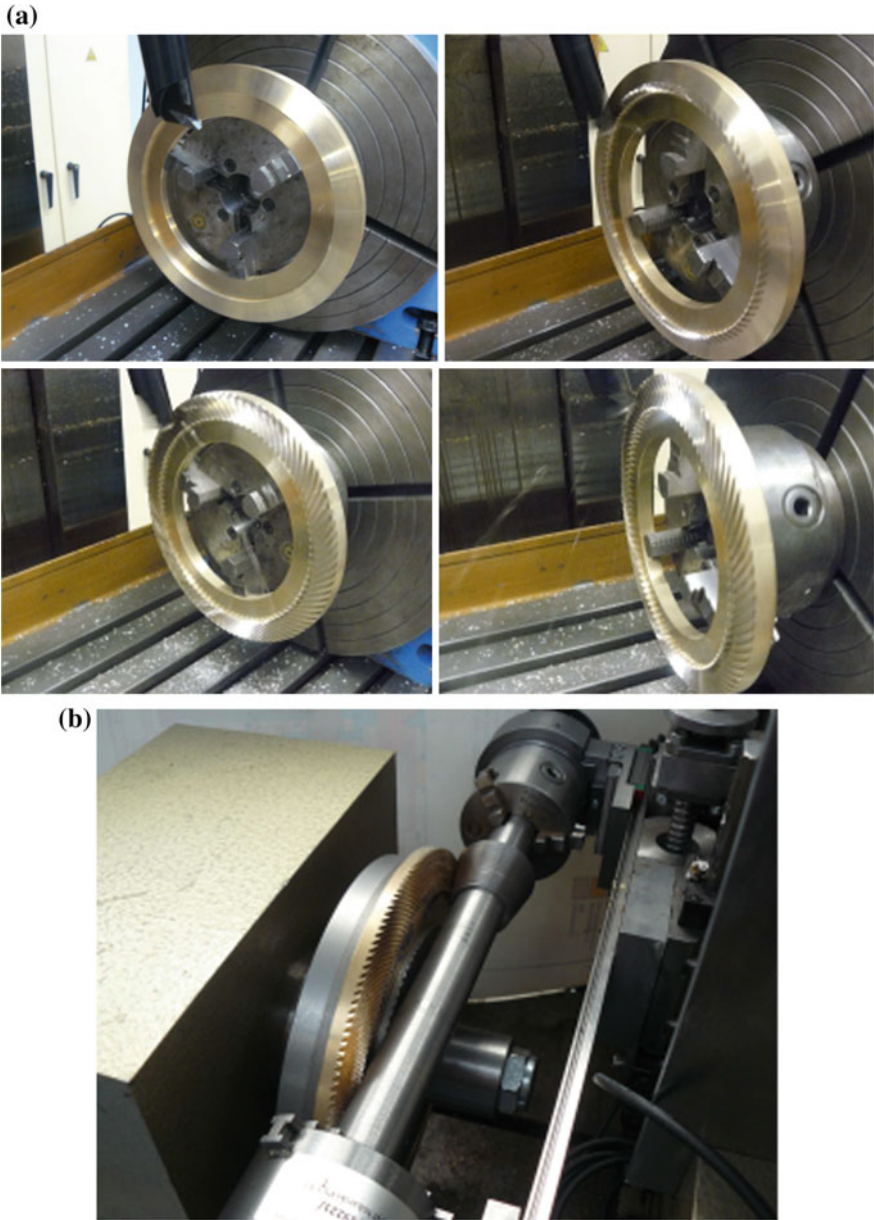


Fig. 6 View the widow of calculation a computer programme of technology parameters of the conical worm gear with conical worm

### 3 Examples of Cutting Conical Face Gears with an Involute Gear Line

Theoretical principles of a teeth forming, which are presented in this paper has been confirmed by experimental researches. View of the examples of conical face gear during cutting on a CNC milling machine is presented in Fig. 7.

Attempts to shape conical face gear were conducted on the milling machine FYN—50Nd type, equipped with the numerically controlled rotary table. The milling machine is holding the control system of the TNC 407 type of the Heidenhain. Heidenhain 407 controller enables simultaneous interpolation in three axes (linear or circular in three-dimensional space). Steering of processing of the outline is held with digital speed control. Servo systems in each axis servo are position regulated type, controlled by deviation signals. Feed the axes X, Y, Z and A are carried out by four independent pulse-controlled AC motors. The drive of the



**Fig. 7** View: **a** investigations stand during cutting a conical face gear (view next position of tool and conical face gear) **b** investigations stand during research of trace of meshing

spindle is equipped with a system for continuously variable speed transmission. A rotational-pulse sensor was fastened in the axis of the spindle of the milling machine, which signals are transmitted to the control system of the machine tool what allows to control spindle as a rotational axis (C).

Design parameters of conical face gear

Inner radius of the theoretical face gear $R_i$	-120 mm
Outer radius of the theoretical face gear $R_e$	-102.5 mm
Number of teeth of the conical face gear $z$	-90
Tooth height (groove depth) $h$	-2.02 mm
Twist angle of the spindle $\gamma_m$	-1.3999°
Concave profiles angle of the conical face gear $\alpha_1$	-9°
Convex profiles angle of the conical face gear $\alpha_2$	-26°
Distance from the axis of the tool axis of conical face gear $a_w$	-80.1 mm

### Legend of Symbols

$R_i$	inner radius of the theoretical face gear
$R_w$	the theoretical radius of the rolling circle
$R_e$	outer radius of the theoretical face gear
$a_w$	the distance between the axis of the tool and the axis of conical face gear
$h$	tooth height (groove depth)
$P$	contact point of sufaces tooth and grinding tool (Fig. 3)
$z$	number of teeth of the conical face gear
$\alpha_1$	concave profiles angle of the conical face gear
$\alpha_2$	convex profiles angle of the conical face gear
$\varphi$	tool rotation parameter
$\psi$	conical face gear rotation parameter
$\Delta l_z$	additional move motion of the grinding tool during conical face gear rotational motion
$\gamma_m$	twist angle of the spindle
X, Y, Z	coordinate system connected to machine tool
x, y, z	coordinate system rigidly connected to conical face gear

## 4 Conclusions

Described the method of forming of modification the involute teeth line of conical face gear on CNC milling machine with disc tool basis of the kinematics that has been mentioned above (Fig. 2) took place in normal conditions without causing reductions of the cost production. The performed investigations presented main directions of improving a cost reduction of cutting the conical face gear for different

kinds of conical spiroid gears. The method is possible only on a machine with the numeric control system and minimum 5-axes numeric control.

Presented possibilities of cutting conical face gear with an involute teeth line allow to execute them on the milling machines with different kinematics.

Discussed methods of forming gear teeth based on contemporary machining offered by modern CNC machine tools. Technological solutions of cutting teeth of gear take advantage of a parametric control programme for moving working units of the CNC machine tool.

## References

1. Litwin, F.L.: Development of gear technology and theory of gearing, NASA, Reference Publication 1406, ARL-TR-1500 (1998)
2. Litwin, F.L., Fuentes, A., Matthew Hawkins, J., Handschuh, R.F.: Design, generation and Tooth contact, Analysis (TCA) of asymmetric face gear drive with modified geometry, NASA/TM-2001-21614 (2001)
3. Litwin, F.L., Fuentes, A., Zanzi, C., Pontiggia, M.: Face gear drive with spur involute pinion, geometry, generation by a worm, stress analysis, NASA/ CR-2002-211362 (2002)
4. Dudas, I.: The theory and practice of worm gear drives. Penton Press, London (2000)
5. Grajdek, R.: Uzębienia czołowe. Podstawy teoretyczne kształtowania i nowe zastosowania, Wydawnictwo Politechniki Poznańskiej (2000)
6. Frackowiak, P.: Cutting face worm gear drives with conical worm on CNC milling machine. In: International Conference Technology, pp. 167–171, Bratislava (2009)
7. Litwin, F.L., Nava, A., Fan, Q., Fuentes, A.: New geometry of worm gear drives with conical and cylindrical worm: generation, simulation of meshing, and stress analysis. *Comput. Methods Appl. Mech. Eng.* **191**, 3035–3054 (2002)
8. Frackowiak, P.: Teeth contact area of face worm gear drives with cylindrical worm. *Arch. Mech. Technol. Autom.* **29**, 59–71 (2006)
9. Frackowiak, P., Ptaszyński, W., Stoić, A.: New geometry and technology forming face-gear with circle line of teeth on CNC milling machine. *Metalurgija* **51**(1), 109–112 (2012)
10. Frackowiak, P.: New method of forming bevel gear of spiroid transmissions with one-blade tool on CNC milling machine and its research, 2010–2012. Research project no. 3398/B/TO2/2009/36, Poznan

# Unilateral Hydraulic Telemanipulation System for Operation in Machining Work Area

Mateusz Sakow, Arkadiusz Parus, Mirosław Pajor  
and Karol Miadlicki

**Abstract** The paper is focused on the minimization of the time transport delay effect which is present in the communication channel of a telemanipulation system. For the minimization of the time transport delay, a prediction block was proposed. The prediction block is characterized by a unitary gain and positive-linear phase shift in a useful frequency spectrum of the system operation. These features allow the block to predict the signal with a constant time and minimizes the gain to a unity level. The use of prediction blocks in the communication channel strongly improved the position tracking abilities of the unilateral system which feature was confirmed in experiments.

**Keywords** Remote control · Telemanipulation · Signal prediction · Hydraulic telemanipulator · Time delay

## 1 Introduction

Teleoperation systems are playing an important role nowadays because they have been applied in almost all of branches in the industry. It is hard to find a factory without a device being controlled by a joystick, a keyboard or other type of remote or automatic control [1]. However, the remotely controlled device does not need to be limited only to perform a simple set of commands [2]. From the early 1960s of the previous century research has been carried out to obtain remote control operation [3–5]. Unfortunately, a continuous control system usually becomes unstable when loop delay exceeds one-half cycle at any signal frequency for which loop gain exceeds unity [6]. However, the transmission delay is not the only component of an aggregate delay in whole teleoperation system. The aggregate delay consists a

---

M. Sakow (✉) · A. Parus · M. Pajor · K. Miadlicki  
Faculty of Mechanical Engineering and Mechatronics, Institute of Mechanical Technology,  
West Pomeranian University of Technology, Szczecin, Poland  
e-mail: mateusz.sakow@zut.edu.pl



processing time of an analog-digital converter, a time of calculation completion by a controller and a processing time of a digital-analog converter [6].

The problem of stability and a counteract of the effect of the delay in the communication channel are addressed by many scientific papers [4, 7, 8]. First methods maintaining the stability were the move-and-wait strategy and the deliberate slowdown of operator motion when approaching the environmental object presented by Ferrell [4]. Later, sensor-based control schemes presented in [4], was redesigned and equipped with a shared compliant control method by Kim [8], which included susceptible bodies in a structure of a Master manipulator. Kim also proposed a control scheme of bilateral force control based on a position error between Master and Slave manipulators, which control scheme has improved the accuracy of a force in the force-feedback communication channel [8].

However, none of these control schemes could guarantee the stability of the entire system when large delays are expected in the communication channel. Only after the modification of the communication channel based on a wave variables allowed bilateral teleoperation systems to maintain stability regardless of the delay in the communication channel [9]. During further research wave variables were extended with the passivity formalism [10]. However, a significant improvement of a force projection in the force-feedback communication channel was an introduction of a new architecture of the communication channel; the four-channel architecture [11, 12] which replaced the two-channel architecture [3, 4, 8, 13]. The four-channel architecture is characterized by a two-way force and position transfer between subsystems Master and Slave. And finally, the four-channel communication architecture was equipped with the adaptive controller which estimated control parameters of force and position channels simultaneously [14].

XXI century is a domain of control schemes implementation based on: sliding mode controllers [15–17], fuzzy logic controllers [18], force-feedback communication channel frequency separation techniques [19, 20], special methods for discretization of a sensor resolution [21], artificial neural networks [22], and adaptive controllers dedicated to variable and asymmetric time delays which are complemented using adaptive filtering methods [23, 24].

It is important to pay attention that bilateral teleoperation systems feature three types of feedback with the operator: vision feedback [6, 13], force-feedback [4] and the combination of vision feedback and force-feedback [8, 12, 22, 25–27]. Remotely controlled devices can be controlled by operator's motion scanners [3, 4, 6, 8, 13, 28] which in a special case are exoskeletons for upper limb [28] and palm [25], by gesture control techniques [29, 30] or by voice control methods [31, 32]. However, the use of a voice control or a gesture control allows to apply only the vision feedback between the operator and remotely controlled device.

Also an important classification of bilateral teleoperation systems with force-feedback is systems which are using force sensor [4, 8, 19, 20] and devices without force sensors also known as a sensor-less or self-sensing techniques in the telemanipulation field [22, 28, 33–35].

The sensor-less teleoperation systems group usually is based on impedance control methods [15] and the inverse modeling techniques to obtain the correct

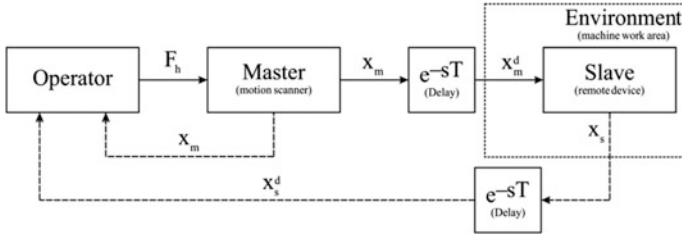
value of force in the force-feedback communication channel [28, 33, 36]. Inverse models are represented frequently by artificial neural networks [22], a nonlinear autoregressive model with exogenous inputs (NARX) [28, 37] and by micromanipulators which are using reversal processes that occur in piezocrystals [34, 35].

Bilateral and unilateral teleoperation systems with or without force-feedback, undoubtedly are the future of development of the robotics next to autonomous systems because many of new scientific papers are addressing the problem of telerobotics and solving its issues.

The paper is focused on the minimization of the constant time transport delay which is present in the communication channel. For the minimization of the transport delay a prediction block was proposed which is a phase shifter with very desirable properties [36]. The prediction block is characterized by a unitary gain and positive-linear phase shift in the useful frequency spectrum of system operation. These features allow the block to predict the signal with a constant time and minimize the gain to a unity level in contrast to a use of constant phase shift and model-free prediction [38]. But, the frequency spectrum of the system operation must be limited depending on the value of the time prediction. However, the frequency limitations of system operation usually are far from the human motion frequency limit expected when the operator needs to wear a motion scanner. The use of prediction blocks in the communication channel strongly improved the position tracking abilities of the unilateral system what is confirmed in simulations and experiments.

## 2 Problem Statement

One of the most notorious problems of the teleoperation is a time delay in the communication channel. The impact of the time delay in the communication channel in the terms of stability and behavior of telerobots is well know and studied in the literature [11]. However, the value of the time delay is not always affecting the remotely controlled system [22]. In the case of the considered unilateral teleoperation system the time delay has a significant impact on a position tracking ability by the Slave manipulator, which was transferred by the motion scanner—subsystem Master. Control scheme of unilateral teleoperation system is presented in Fig. 1. The system consists four basic objects. The operator which is the primary element and controls the position of the subsystem Master (motion scanner) by the force interaction  $F_h$ . One of feedbacks used in the system is the vision feedback provided by the motion scanner  $x_m$  which allows the operator to control its position. The measured position  $x_m$  which is transferred in the communication channel is the basic objective of the motion scanner in a unilateral teleoperation system. However, the information is transferred with the time delay  $T$  to the subsystem Slave. Finally when the information will reach the subsystem Slave, the manipulator will pretend to reflect received data describing the motion.

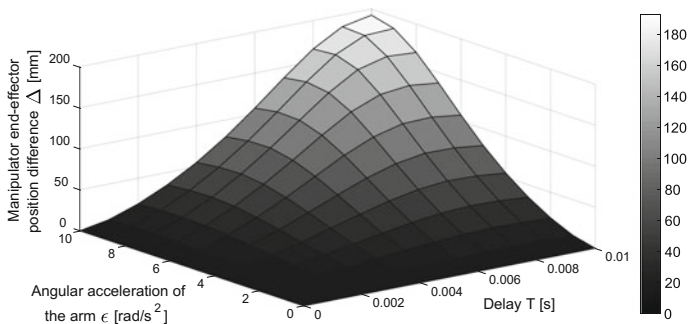


**Fig. 1** Control scheme of unilateral Master-Slave teleoperation system

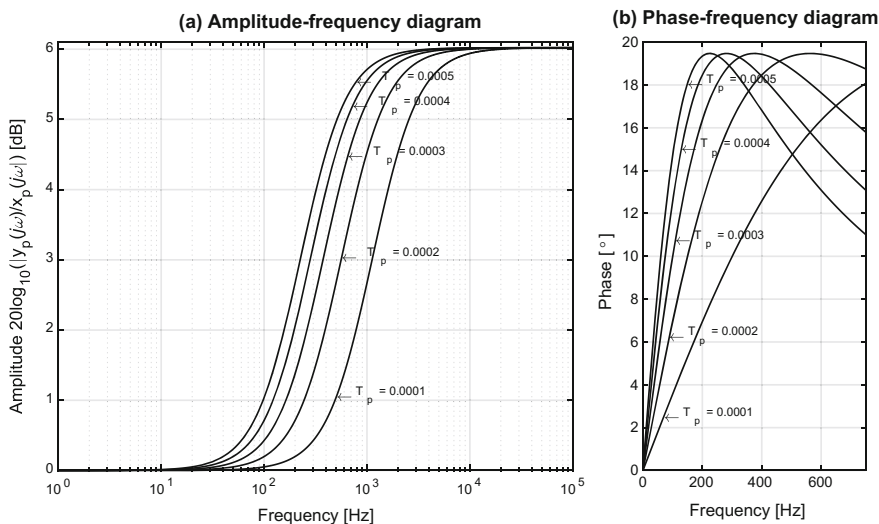
The subsystem Slave usually is a manipulator of similar kinematics as the subsystem Master and is operating in a distant place. This is why the behavior feedback of the manipulator’s Slave motion  $x_s$  is only reachable by a vision feedback, also affected by the time delay. In the case of small size machines the effect of the time delay in the communication channel could be considered as insignificant because of their overall dimensions. But, in the case of bigger size machines such as cranes the time delay can affect the error of the end-effectors’ position to such an extent that the task completion could be impossible. This feature leads to collisions between the manipulator and the environment, which are catastrophic and expensive.

The example of the time delay problem in the positioning of the manipulator’s end effector is a simple 1-DOF rotary joint. Arm range of  $d = 1.5$  m while the angular error of the arm is at  $\varphi = 1$ , is a cause of end effector position error of over  $\Delta = 26$  mm. Without a consideration of a dynamic position error caused by a control unit and actuators. The same situation with a 17 m long crane causes an error of  $\Delta = 0.3$  m. Also, without a consideration of dynamic position error caused by a control unit, actuators and the deflection of mechanical construction. The simple example concerns only the situation when the manipulator performs the movement with a constant velocity. It is important to pay attention to the problem of a variable acceleration and time delay during system operation. In this case, the end effector’s position error also is not a constant value, but it changes according to the manipulators acceleration and the value of the time delay in the communication channel—Fig. 2.

The diagram in the Fig. 2 illustrates how strongly the position error is affected by the time delay during motion with variable acceleration. The variable acceleration is a cause of a variable position error between the motion scanner and the remotely controlled device. The position error additionally is multiplied by the always presented time transport delay in the communication channel. The always present time transport delay feature is strongly affecting the bigger size machines like cranes or bigger manipulators. Telemanipulation in a remote environment, in this case, is much more difficult and it often leads to unwanted collisions. This feature is a motivation for research conducted on remote manipulators which were equipped with prediction blocks in the communication channel.



**Fig. 2** The test stand manipulator end effector position error as a function of a joint angular acceleration and the time delay in the communication channel



**Fig. 3 a** Amplitude-frequency diagram, **b** phase-frequency diagram of the prediction block

### 3 The Prediction Block

During the analysis of the previously presented control schemes based on the prediction techniques used in inverse modeling method [36], in the paper a prediction block with its time constants  $T_p$  was placed directly in the communication channel. The prediction block and its structure were developed during the analysis of the Smith predictive control schemes [39]. The transmittance characterizing the automation structure is described by a ratio of an output signal  $y_p(s)$  and an input signal  $x_p(s)$  and is given by  $y_p(s)/x_p(s) = (2T_p s + 1)/(T_p s + 1)$ , where  $s$  is the Laplace operator—Fig. 3.

While examining the transmittance in the frequency domain, an attention has to be paid to the amplitude (Fig. 3a) and phase diagram (Fig. 3b) of the prediction block presented in Fig. 3. Frequency diagrams confirm a differential character of the proposed prediction block. The prediction block depending on the  $T_p$  constant is able to linearly shift a phase of an input signal, resulting in a constant time shift in useful frequency spectrum—Fig. 3b. Unfortunately, the prediction block like any phase shifter is a cause of a gain of the input signal amplitude, but in the useful frequency spectrum, the gain is close to a unity—Fig. 3a. The useful frequency spectrum is understood to be achievable for a human motion. Scientific literature gives a limit of 6 Hz [40] but for the proper system functioning, it was decided to increase the limit to 10 Hz to leave a bigger margin of error.

The prediction block in a time domain is a “signal predictor” of the input signal  $x_p(t)$ , where predicted time depends only on the  $T_p$  constant. The prediction ability was confirmed by the frequency diagrams of the transport delay, the prediction block and the product of both transmittances presented in the Fig. 4.

Both frequency diagrams in Figs. 3 and 4 are the proof of predictive capabilities of the prediction block. But it is important to note that the prediction block is sensitive to a noise and changes of a signal derivative  $\text{sign } x_p(t)$ . An amplitude of a noise will be increased twice when using only one prediction block. When using more of prediction blocks the gain depends on a number of prediction blocks used in the series configuration by 2 to the power of the number of prediction blocks.

### 4 The Experiment

During the tests carried out at the test stand, in the communication channel of unilateral teleoperation system a time transport delay  $e^{-Ts}$  was included, where

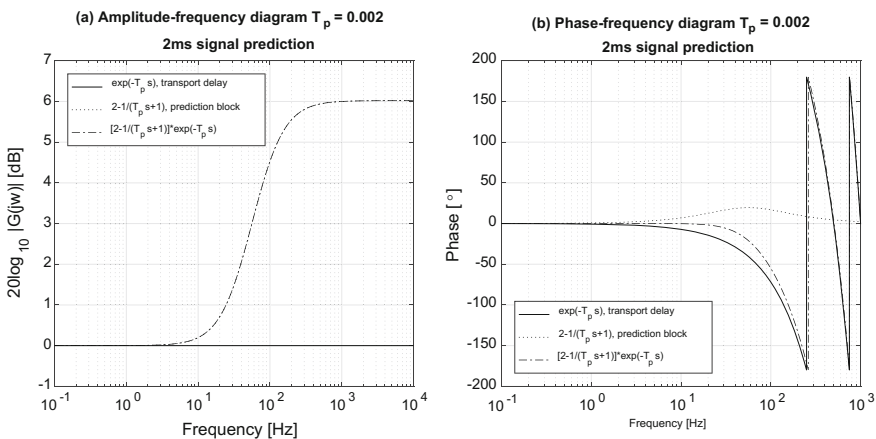
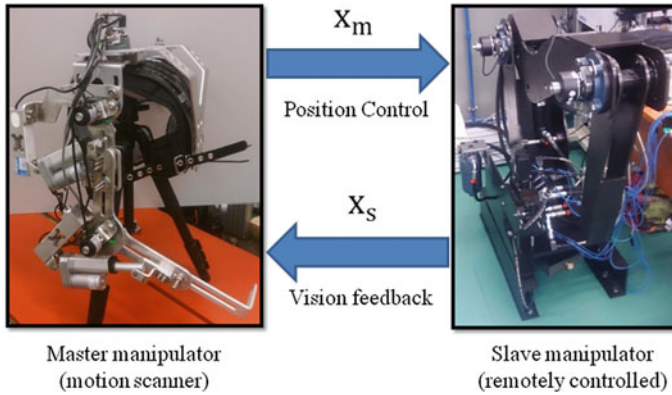


Fig. 4 The prediction block scheme

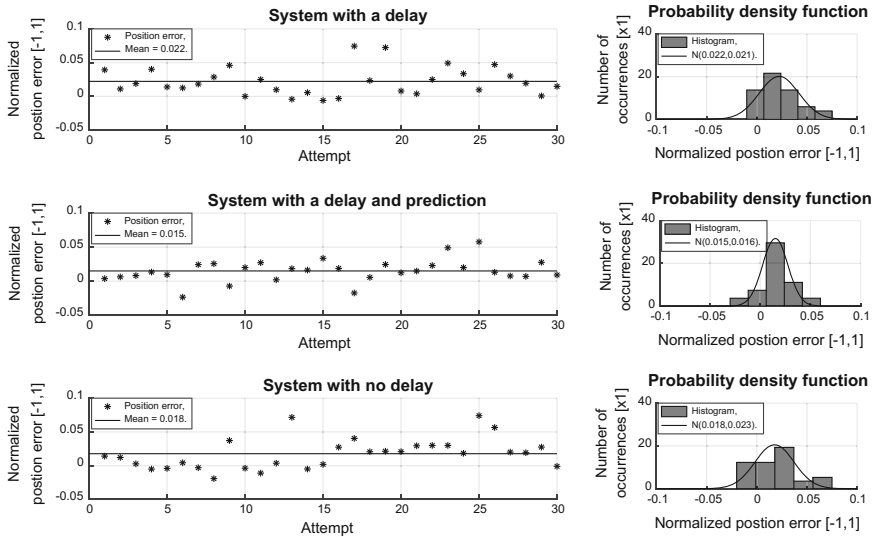


**Fig. 5** Unilateral teleoperation test stand

$T = 0.020$ . The value  $T$  means that the information in the communication channel is transferred with the 20 ms fixed delay. The time delay  $T$  describes only the one-directional delay in the system. Unfortunately, in both ways, the system vision feedback is transferred with a doubled value of the delay  $T$  according to the operator's motion. The predictions blocks were validated at the prepared test stand presented in the Fig. 5.

The system consists of two independent manipulators: the motion scanner and the remotely controllable device. Both systems are similar in kinematic features, but the Slave manipulator is driven by hydraulic actuators. Both systems are capable of transferring the operator's motion from an elbow and a shoulder by consisting of 2-DOFs. During tests, system operator was obliged to perform a simple line in space which included an end effector positioning task. Operator moved the end effector by 0.4 m to the virtual obstruction (which was visible only at the screen) and moved back the end effector to the starting position in a limited time of 10 s. The operator was informed that is required to position the end effector as close as possible to the obstruction. The vision feedback was provided by a movable dot at a screen which described the position of the manipulator end effector. For the test, six operators who were not familiarized with the system tried to position the end effector as close as possible to the obstruction. Each operator had 5 attempts with three types of control unit which included a communication channel with a delay, without a delay and with a delay and a prediction block. Unfortunately, each operator was unaware of the type of a control unit, a delay value and had not any practice before any run of the test. The comparison results of the three types of control (delay, delay, and prediction, no delay) are normalized to  $[-1,1]$  section, where  $-1$  is a  $-0.40$  m position error,  $1$  is a  $+0.40$  m position error. The results are presented in the Fig. 6.

Experimental results clearly showed that system with no delay is easier in the positioning task than the system with the delay. However, the system with the delay and prediction based communication channel was characterized by a higher



**Fig. 6** Unilateral teleoperation test stand's experimental results

accuracy and repeatability relative to other control schemes. This is testified by the mean error and standard deviation which is lower than in other cases. Operator equipped with a prediction based control unit was able to reach higher accuracy because of the increased prediction time from 20 to 25 ms. The prediction allowed the operator to see the position on the screen even before it was reached by the manipulator. However, this fact was a main reason of faster decision making when it came to slow down, when the obstruction was being approached.

It is important to note that six operators did not train with the system before the test, so it clear that after some exercise their abilities could be improved for each of the control unit. A key factor to the measurement results was the time limit which forced the operator to move faster and to make decisions in limited time which has caused multiple overshoot of the position. The equally important factor was the ability to handle the motion scanner which showed that the device did not suit for some operators.

## 5 Conclusions

The paper has been focused on the minimization of the time transport delay which is present in the communication channel by using a prediction block. The prediction block is characterized by a unitary gain and positive-linear phase shift. Experimental results showed that the system with the delay and prediction based communication channel is characterized by a higher accuracy and repeatability

relative to other control schemes—without a time delay, and with a time delay only. The prediction allowed the operator to see the position on the screen even before it was reached by the manipulator. This feature caused an increase of a time for decision making and minimized the positioning error. The prediction block is dedicated to the close to constant time delay effect, and its goal is to minimize that effect directly in the system. The solution is an alternative to methods dedicated to networks control which are based on a constant positive phase shift presented in [38].

**Acknowledgements** The work was carried out as part of the PBS3/A6/28/2015 project, “The use of augmented reality, interactive voice systems and operator interface to control a crane”, financed by NCBiR.

## References

1. Miądlicki, K., Pajor, M.: Overview of user interfaces used in load lifting devices. *Int. J. Sci. Eng. Res.* **6**(9), 1215–1220 (2015)
2. Myszkowski, A., Bartkowiak, T., Gessner, A.: Kinematics of a novel type positioning table for cast alignment on machine tool. In: ASME International Design Engineering Technical Conferences and Computers and Information in Engineering Conference, American Society of Mechanical Engineers, USA (2015)
3. Ferrell, W.R.: Remote manipulation with transmission delay. *Hum. Factors Electron. IEEE Trans. HFE* **6**(1), 24–32 (1965)
4. Ferrell, W.R.: Delayed force feedback. *Hum. Factors J. Hum. Factors Ergon. Soc.* **8**(5), 449–455 (1966)
5. Tomovic, R., Boni, G.: An adaptive artificial hand. *IRE Trans. Autom. Control* **7**(3), 3–10 (1962)
6. Sheridan, T.B., Ferrell, W.R.: Human control of remote computer-manipulators. In: *Proceedings of the 1st International Joint Conference on Artificial intelligence*, pp. 483–494, Morgan Kaufmann Publishers Inc., Washington, DC (1969)
7. Niemeyer, G., Slotine, J.J.E.: Stable adaptive teleoperation. *IEEE Trans. Oceanic Eng.* **16**(1), 152–162 (1991)
8. Kim, W.S., Hannaford, B., Fejczy, A.K.: Force-reflection and shared compliant control in operating telemanipulators with time delay. *IEEE Trans. Robot. Autom.* **8**(2), 176–185 (1992)
9. Sheridan, T.B.: Space teleoperation through time delay: review and prognosis. *IEEE Trans. Robot. Autom.* **9**(5), 592–606 (1993)
10. Arcara, P., Melchiorri, C., Stramigioli, S.: Intrinsically passive control in bilateral teleoperation mimo systems. In: *Control Conference (ECC)* (2001)
11. Lawrence, D.A.: Stability and transparency in bilateral teleoperation. *IEEE Trans. Robot. Autom.* **9**(5), 624–637 (1993)
12. Hastrudi-Zaad, K., Salcudean, S.E.: On the use of local force feedback for transparent teleoperation. In: *IEEE International Conference on Robotics and Automation* (1999)
13. Ferrell, W.R., Sheridan, T.B.: Supervisory control of remote manipulation. *IEEE Spectr.* **4**(10), 81–88 (1967)
14. Wen-Hong, Z., Salcudean, S.E.: Stability guaranteed teleoperation: an adaptive motion/force control approach. *IEEE Trans. Autom. Control* **45**(11), 1951–1969 (2000)
15. Hyun Chul, C., et al.: Sliding-mode-based impedance controller for bilateral teleoperation under varying time-delay. In: *IEEE International Conference on Robotics and Automation* (2001)



16. Moreau, R., et al.: Sliding-mode bilateral teleoperation control design for master–slave pneumatic servo systems. *Control Eng. Pract.* **20**(6), 584–597 (2012)
17. Nguyen, T., et al.: Accurate sliding-mode control of pneumatic systems using low-cost solenoid valves. *IEEE/ASME Trans. Mechatron.* **12**(2), 216–219 (2007)
18. Chang, M.-K.: An adaptive self-organizing fuzzy sliding mode controller for a 2-DOF rehabilitation robot actuated by pneumatic muscle actuators. *Control Eng. Pract.* **18**(1), 13–22 (2010)
19. Polushin, I.G., Takhmar, A., Patel, R.V.: Projection-based force-reflection algorithms with frequency separation for bilateral teleoperation. *IEEE/ASME Trans. Mechatron.* **20**(1), 143–154 (2015)
20. Atashzar, S.F., Polushin, I.G., Patel, R.V.: Projection-based force reflection algorithms for teleoperated rehabilitation therapy. In: *IEEE/RSJ International Conference on Intelligent Robots and Systems* (2013)
21. Hulin, T., Abu-Schäffer, A., Hirzinger, G.: Passivity and stability boundaries for haptic systems with time delay. *IEEE Trans. Control Syst. Technol.* **22**(4), 1297–1309 (2014)
22. Tadano, K., Kawashima, K.: Development of 4-DOFs forceps with force sensing using pneumatic servo system. In: *IEEE International Conference on Robotics and Automation, ICRA* (2006)
23. Zhai, D.H., Xia, Y.: Adaptive control of semi-autonomous teleoperation system with asymmetric time-varying delays and input uncertainties. *IEEE Trans. Cybern.* (99), 1–13 (2016)
24. Zhai, D.H., Xia, Y.: Adaptive control for teleoperation system with varying time delays and input saturation constraints. *IEEE Trans. Industr. Electron.* **63**(11), 6921–6929 (2016)
25. Zhou, M., Ben-Tzvi, P.: RML glove—an exoskeleton glove mechanism with haptics feedback. *IEEE/ASME Trans. Mechatron.* **20**(2), 641–652 (2015)
26. Ben-Dov, D., Salcudean, S.E.: A force-controlled pneumatic actuator for use in teleoperation masters. In: *IEEE International Conference on Robotics and Automation* (1993)
27. Tavakoli, M., Patel, R.V., Moallem, M.: A force reflective master-slave system for minimally invasive surgery. In: *IEEE/RSJ International Conference on Intelligent Robots and Systems* (2003)
28. Saków, M., Pajor, M., Parus, A.: Estymacja siły oddziaływania środowiska na układ zdalnie sterowany ze sprzężeniem siłowym zwrotnym o kinematyce kończyny górnej. *Modelowanie Inżynierskie* **58**, 113–122 (2016)
29. Miądlicki, K., Pajor, M.: Real-time gesture control of a CNC machine tool with the use microsoft kinect sensor. *Int. J. Sci. Eng. Res.* **6**(9), 538–543 (2015)
30. Pajor, M., Miądlicki, K., Saków, M.: Kinect sensor implementation in FANUC robot manipulation. *Arch. Mech. Technol. Autom.* **34**(3), 35–44 (2014)
31. Stuart, K.D., Majewski, M., Trelis, A.B.: Intelligent semantic-based system for corpus analysis through hybrid probabilistic neural networks. In: *International Symposium on Neural Networks*, Springer, Berlin (2011)
32. Stuart, K.D., Majewski, M.: Intelligent opinion mining and sentiment analysis using artificial neural networks. In: *International Conference on Neural Information Processing*, Springer, Berlin (2015)
33. Wei, Tech A., Khosla, P.K., Riviere, C.N.: Feedforward controller with inverse rate-dependent model for piezoelectric actuators in trajectory-tracking applications. *IEEE/ASME Trans. Mechatron.* **12**(2), 134–142 (2007)
34. Rakotondrabe, M., et al.: Simultaneous displacement/force self-sensing in piezoelectric actuators and applications to robust control. *IEEE/ASME Trans. Mechatron.* **20**(2), 519–531 (2015)

35. Khadraoui, S., Rakotondrabe, M., Lutz, P.: Interval modeling and robust control of piezoelectric microactuators. *IEEE Trans. Control Syst. Technol.* **20**(2), 486–494 (2012)
36. Saków, M., Parus, A.: Sensorless control scheme for teleoperation with force-feedback, based on a hydraulic servo-mechanism, theory and experiment. *Meas. Autom. Monit.* **62**(12) (2016)
37. Saków, M., Miądlicki, K., Parus, A.: Self-sensing teleoperation system based on 1-dof pneumatic manipulator. *J. Autom. Mob. Robot. Intell. Syst.* **11**(1), 64–76 (2017)
38. Ge, X. et al.: Analysis of a model-free predictor for delay compensation in networked systems. In: *Time Delay Systems*, pp. 201–215, Springer, Berlin (2017)
39. Kaya, I.: Obtaining controller parameters for a new PI-PD Smith predictor using autotuning. *J. Process Control* **13**(5), 465–472 (2003)
40. Lichiardopol, S., Wouw, N. v. d., Nijmeijer, H.: Control scheme for human-robot co-manipulation of uncertain, time-varying loads, in *2009 American Control Conference*, 1485–1490 (2009)

# Effect of Different Electrolytes on Material Removal Rate, Diameter of Hole, and Spark in Electrochemical Discharge Machining

Mukund L. Harugade and Sachin D. Waigaonkar

**Abstract** Advanced materials like glass, quartz, and composites have high potential for their applications in different fields of engineering due to their favorable properties like hardness, chemical inertness, electrical insulation, low thermal conductivity. The recent analytical and experimental work have opened the avenue of machining nonconductive materials like glass, alumina, etc., using an integrated process of electrochemical discharge machining (ECDM). ECDM is a nonconventional machining process which is an integrated process of electrochemical machining (ECM) and electro discharge machining (EDM). In this paper, ECDM has been investigated for drilling operation in glass. This study reports effect of different electrolytes on material removal rate, entrance and exit diameter of the hole, and sparking difference at the machining junction. Three different electrolytic solutions (NaOH, NaNO<sub>3</sub>, and H<sub>2</sub>SO<sub>4</sub>) have been used for ECDM. The performance of three different electrolyte solutions is compared among themselves based on the process performance based on above parameters. The conditions for the maximum material removal rate, less difference in entrance and exit diameter with better sparking stability have been established from the experimental findings.

**Keywords** Electrochemical discharge machining · Material removal rate (MRR) Diameter of hole · Spark stability

## 1 Introduction

Advanced glass, quartz, and composites are suitable for engineering applications like micro-electromechanical systems (MEMS), aerospace engineering and biomedical field, however machining of these materials is difficult. Machining of

---

M.L. Harugade (✉) · S.D. Waigaonkar (✉)  
BITS Pilani, K. K. Birla Goa Campus, Pilani 403726, Goa, India  
e-mail: p20160026@goa.bits-pilani.ac.in; mukundharugade86@gmail.com

S.D. Waigaonkar  
e-mail: sdw@goa.bits-pilani.ac.in

glass is difficult due to its hardness and brittle nature and also being nonconductive in nature, it cannot be machined using EDM or ECM. The recent experimentations have shown that machining of nonconductive materials like glass, alumina, etc., using an integrated process of ECDM is possible [1]. Electrochemical discharge machining process consists of two electrodes which are submerged in an electrolytic solution. One is the tool electrode (cathode) and the other is the auxiliary electrode (anode). Workpiece is situated below the tool electrode. Electrolysis starts when direct current (DC) power supply is applied between the tool electrode and the auxiliary electrode. This phenomenon leads to spark generation at the tip of tool electrode and when the workpiece is kept near to tool electrode the spark generation results into erosion of workpiece. Sarkar et al. [2] have developed mathematical model to determine material removal rate. They concluded applied voltage is a most significant parameter for improved material removal rate. Chak et al. [3] experimentally observed that electrolyte conductivity is another important parameter for MRR in ECDM process, with increase in thermal conductivity material removal rate increases. Gupta et al. [4] investigated the effect of different electrolytes like NaCl, KOH, and NaOH on the quality of glass work after drilling by the ECDM process. In this work, it is observed that NaOH gives highest material removal rate compared to NaCl and KOH. Goud et al. [5] analyzed material removal in ECDM. They used two electrolytes NaOH and KOH for two different workpiece materials for the experimentation. They found that material removal rate more improves with electrolyte concentration for soda lime glass compared to alumina. Kolhekar et al. [6] observed the effect of electrolyte concentration on surface roughness and surface hardness, at low concentration surface wrinkles are observed on the workpiece. Zang et al. [7] studied the use of the low-conductivity salt solution in tube electrode for electrochemical discharge drilling. It is observed that low-conductivity salt solution increases material removal rate. Paul et al. [8] studied the ECDM process by generating response modeling of microholes. It is observed that MRR increases with increase in voltage, electrolyte concentration, and duty factor.

This paper discusses the effect of different electrolyte solutions on the workpiece during ECDM. From the available literature on this process, it is evident that the electrolyte plays a crucial role in the performance of the process. In this paper, three electrolytes NaOH, H<sub>2</sub>SO<sub>4</sub>, and NaNO<sub>3</sub> are used to study their effect on MRR; as NaOH represents strong base, H<sub>2</sub>SO<sub>4</sub> represents strong acid and NaNO<sub>3</sub> represents strong acid-base salt, respectively. Their performance characteristics like material removal rate, entrance and exit diameter of the hole, and sparking difference are compared.

## 2 Experimentation

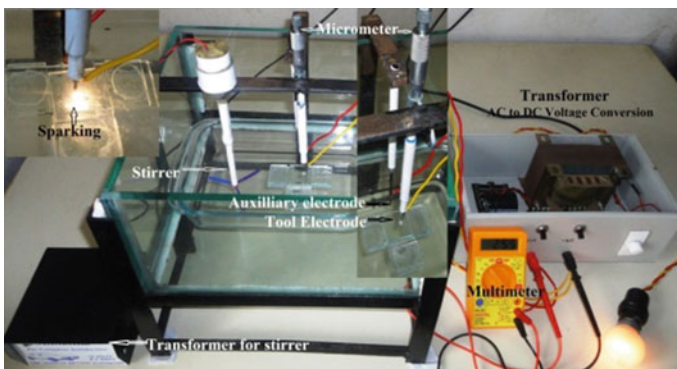
In the present work, ECDM was performed on a workpiece of the soda lime glass (Chemical composition: SiO<sub>2</sub>—74.42%, CaO—11.27%, Na<sub>2</sub>O—12.9%, Al<sub>2</sub>O<sub>3</sub>—0.75%, MgO—0.30%). To decide the levels of process parameters, a few

preliminary experiments were conducted by changing the voltage, electrolyte concentration and inter-electrode gap. Based on this, the envelope of process parameters is selected as applied voltage 40–60 V, electrolyte concentration based on weight 10–30% and inter-electrode gap 10–30 mm. In this experimental work, the performance of ECM process with three different electrolytes NaOH, NaNO<sub>3</sub>, and H<sub>2</sub>SO<sub>4</sub> is also studied. These electrolytes have different electrical conductivity due to which the performance of ECM will be different for different electrolytes. In order to study the effect of these electrolytes on performance characteristics of the ECM, the weight-based concentration with water (10–30%) is used in experimentation.

## 2.1 Experimental Setup

A functional setup of the ECM process has been designed and developed as shown in Fig. 1 the main components of the ECM setup are machining chamber, tool feeding mechanism, and power supply system.

The machining chamber having dimensions of 150 mm × 100 mm × 30 mm is made up of glass in order to facilitate the observation of the process. At the center of machining chamber, there is a provision of mounting the workpiece. A vertical scale is attached with one of the channel pieces to measure the height of the electrolyte. The glass workpiece of 3 mm thickness is selected for machining. Copper is used as material for both tools as well as auxiliary electrodes. A tool electrode is fitted in micrometer with help of tool holder and this micrometer is mounted on steel strap. Auxiliary electrode was mounted at the top of the steel frame. A stirrer driven by the geared motor is used to ensure adequate electrolyte circulation. The level of electrolyte solution was maintained at 1 mm above the workpiece material throughout the experiments. The special transformer was



**Fig. 1** Experimental setup of electrochemical discharge machining

**Table 1** Machining conditions for ECDM

Parameter	Condition
Current	3 A
Tool electrode diameter	Ø700 µm
Auxiliary electrode diameter	3 mm
Machining time	30 min
Electrolyte concentration	10–30%
Applied voltage	30–50 V
Inter-electrode gap	10–30 mm

designed and developed to provide low voltage conditions of 10–100 V and 3 A current.

## 2.2 Selection of the Process Parameter and Machining Conditions

The process parameters of the experimental investigation were categorized as electrical and nonelectrical parameters. Major electrical parameters were discharged voltage, current and electrolyte concentration and nonelectrical process parameters were a gap between tool electrode and workpiece, tool feed rate, tool rotation speed, and inter-electrode gap. The electrolyte concentration is considered as an electrical parameter as it acts as a conductor for the electric current and change in concentration directly affects the flow of current which also affects the spark generation. Based upon the initial experimental work for this setup, three parameters voltage, electrolyte concentration and inter-electrode gap (gap between the tool electrode and auxiliary electrode) were selected as variants in experimentation. The machining conditions for experimentation are shown in Table 1.

## 3 Result and Discussion

Experiments were conducted and drilling of the glass was carried out using ECDM. For each set of process variables, the experiments were conducted for the three electrolytes chosen and material removal rate was found. Table 2 shows the MRR values for this experimentation.

### 3.1 Effect of Electrolytes on Material Removal Rate

Regression analysis for material removal rate was conducted using MINITAB16. The related experimental data for these equations is taken from the Table 2. The

**Table 2** Material removal rate for different electrolyte solutions

(A) Voltage (V)	(B) Electrolyte concentration (%)	(C) Inter-electrode gap in (mm)	Material removal rate (mg/min)		
			For NaOH	For NaNO <sub>3</sub>	For H <sub>2</sub> SO <sub>4</sub>
40	10	20	1.0013	0.4933	0.2997
40	20	30	1.0908	0.5828	0.3102
40	30	40	1.3795	0.6515	0.6984
50	10	30	1.3745	0.6665	0.4834
50	20	40	1.0735	0.5655	0.3724
50	30	20	2.1815	1.4735	1.0404
60	10	40	1.5578	1.0498	1.0875
60	20	20	1.9978	1.2998	1.1702
60	30	30	2.0566	1.3986	1.0113

regression equation was developed to evaluate the effect of process parameters on the material removal rate.

The regression equation for material removal rate for NaOH electrolyte is shown in Eq. (1). The voltage, electrolyte concentration, and inter-electrode gap are the considered process parameters.

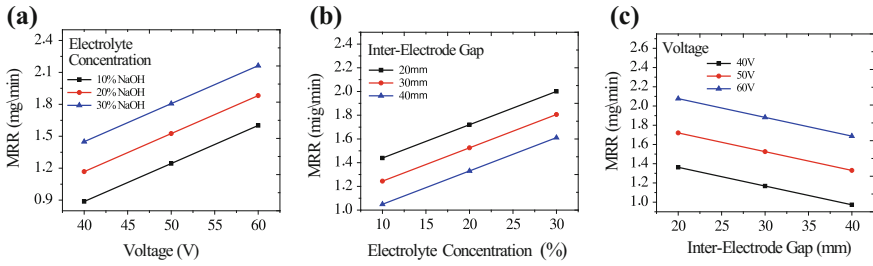
$$MRR_{(NaOH)} = -0.237 + 0.0357 \times A + 0.0281 \times B - 0.0195 \times C \quad (1)$$

Similarly, the regression equation for material removal rate for NaNO<sub>3</sub> and H<sub>2</sub>SO<sub>4</sub> electrolytes are shown in Eqs. (2) and (3).

$$MRR_{(NaNO_3)} = -0.713 + 0.0337 \times A + 0.0219 \times B - 0.0167 \times C \quad (2)$$

$$MRR_{(H_2SO_4)} = -1.03 + 0.0327 \times A + 0.0147 \times B - 0.00587 \times C \quad (3)$$

The variation in material removal rate with the voltage provided in between tool electrode and the auxiliary electrode, electrolyte concentration, and the inter-electrode gap is shown in Figs. 2, 3 and 4. It is observed that a voltage of 60 V and 30% electrolyte concentration the material removal rate was maximum and it decreased for increasing inter-electrode gap at 40 mm. As the workpiece contains the 74.42% silica which is higher than the other constituent of glass, i.e., Na<sub>2</sub>O (12.9%) and CaO (11.27%), these three constituents are chemically reactive with the NaOH electrolyte solution causing the improved material removal rate. According to Arrhenius theory in base electrolytes, OH<sup>-</sup> are donors of electrons in its aqueous solution and according to Lowry and Bronsted theory H<sup>+</sup> are acceptor of electron. Hence, whenever the electric charge is passed through the electrolyte solution the bubble generation and hydrogen gas layer formation phenomenon takes place at tool electrode which results in erosion helping in constant desired material removal rate at the same time oxygen or oxides are also formed near the auxiliary

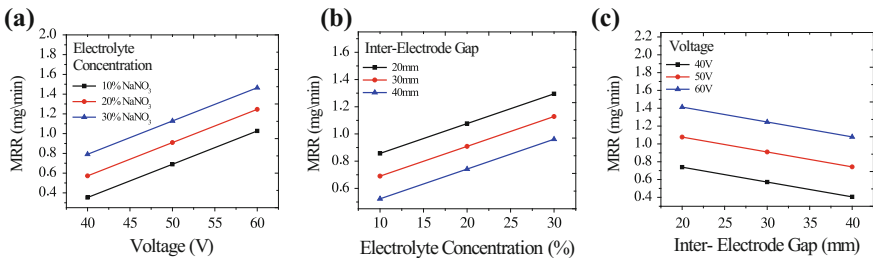


**Fig. 2** Effects of process variables on material removal rate (MRR), NaOH as electrolyte solution. **a** Effects of voltage on material removal for different concentration, inter-electrode Gap = 30 mm. **b** Effects of concentration on material removal for different inter-electrode gap, voltage = 50 V. **c** Effects of inter-electrode gap on material removal for different voltages, concentration = 20%

electrode. The potential differences between the two electrodes are responsible for sparking phenomena.

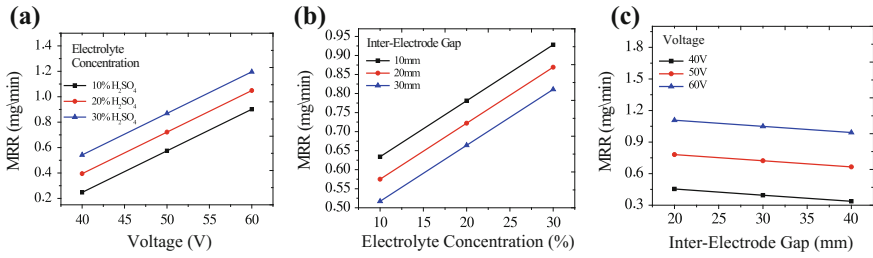
To study the contribution of the process parameters of the electrochemical discharge machining process pie chart analysis is conducted. Pie chart analysis of variance is a simple method for analyzing the results for the NaOH, NaNO<sub>3</sub>, and H<sub>2</sub>SO<sub>4</sub>. Pie chart analysis of NaOH, NaNO<sub>3</sub>, and H<sub>2</sub>SO<sub>4</sub> are shown in Figs. 5, 6 and 7. These pie chart diagrams show the contribution of parameters like voltage, electrolyte concentration, inter-electrode gap, and error on material removal rate. The error shown in the diagram is a deviation occurred from actual result due to experimental error, variation in room temperature, humidity, tool movement, etc.

In Fig. 5, NaOH is used as electrolyte solution; the voltage contribution in material removal rate is 49.16% and is highest compared to other parameters. Electrolyte concentration also plays an important role and contributes in MRR 32.53%. The inter-electrode gap and error are to be 9.56% and 8.75%, respectively. The pie chart Fig. 6 for NaNO<sub>3</sub> shows that the voltage contributes in MRR at about 59.65%, also electrolyte concentration, inter-electrode gap, and error contribute



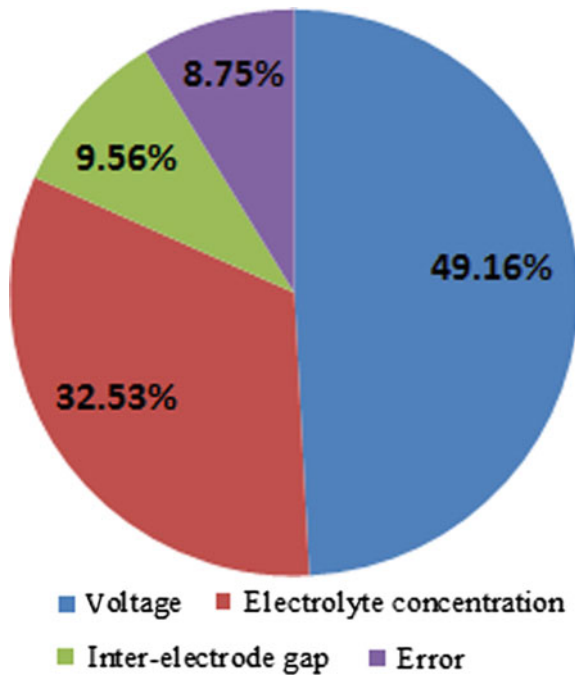
**Fig. 3** Effects of process variables on material removal rate (MRR), NaNO<sub>3</sub> as electrolyte solution. **a** Effects of voltage on material removal for different concentration, inter-electrode gap = 30 mm. **b** Effects of concentration on material removal for different inter-electrode gap, voltage = 50 V. **c** Effects of inter-electrode gap on material removal for different voltages, concentration = 20%



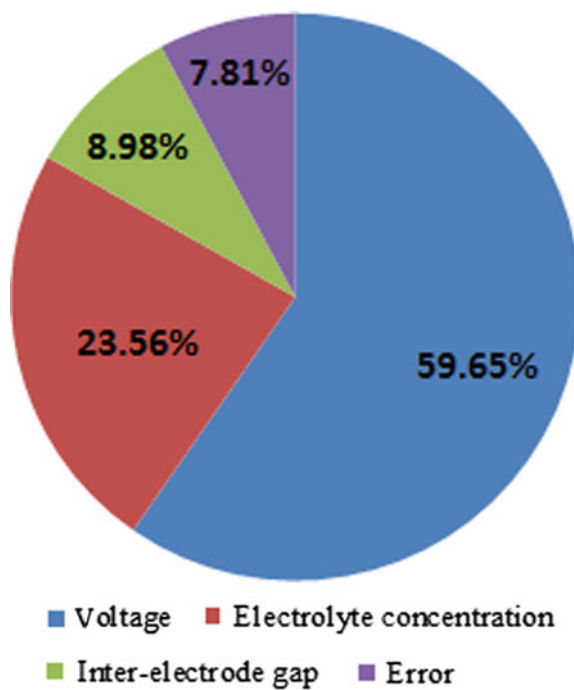
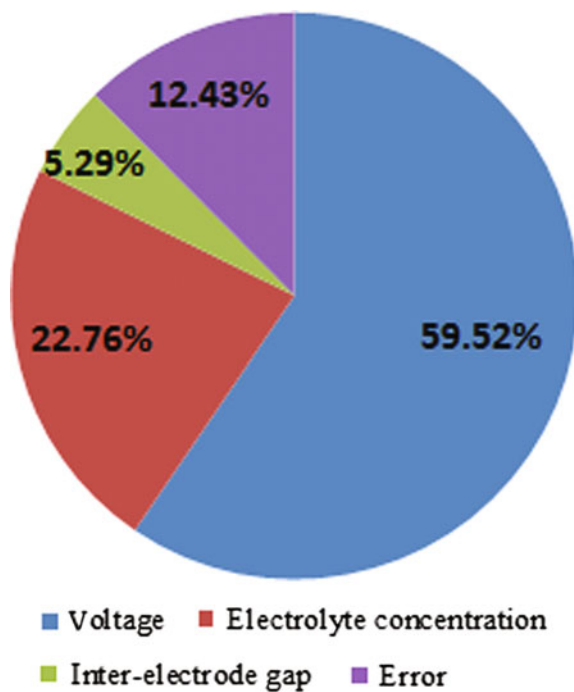


**Fig. 4** Effects of process variables on material removal rate (MRR), H<sub>2</sub>SO<sub>4</sub> as electrolyte solution. **a** Effects of voltage on material removal for different concentration, inter-electrode gap = 30 mm. **b** Effects of concentration on material removal for different inter-electrode gap, voltage = 50 V. **c** Effects of inter-electrode gap on material removal for different voltages, concentration = 20%

**Fig. 5** NaOH as electrolyte



23.56, 8.98 and 7.81%, respectively, in MRR. The pie chart Fig. 7 for H<sub>2</sub>SO<sub>4</sub> shows that the voltage contribution to material removal rate 59.52% and other parameters like electrolyte concentration, inter-electrode gap and error has the contribution of 22.76, 5.29, and 12.43% respectively.

Fig. 6  $\text{NaNO}_3$  as electrolyteFig. 7  $\text{H}_2\text{SO}_4$  as electrolyte

### 3.2 *Effect of Electrolytes on Entrance and Exit Diameter of Hole*

The entrance and the exit diameter of the hole for different electrolyte solutions are shown in the Figs. 8, 9 and 10. It was seen that the difference in diameter of the holes machined was less with NaOH. Table 3 presented that overall comparison of three different electrolyte solutions. From Table 3, it can be clearly seen that NaOH gives the ratio of the entrance and exit diameter near to unity with stable spark generation and through the hole. When H<sub>2</sub>SO<sub>4</sub> is used as an electrolyte solution, the tool cannot penetrate workpiece. As workpiece get cracked because of unstable spark, due to this exit diameter in H<sub>2</sub>SO<sub>4</sub> cannot be determined.

### 3.3 *Spark Color and Spark Stability*

NaOH is a strong base and it has good ion mobility compared to the NaNO<sub>3</sub> and H<sub>2</sub>SO<sub>4</sub> electrolyte solutions. NaOH gives constant bubble generation, stable

Fig. 8 Drilled using NaOH

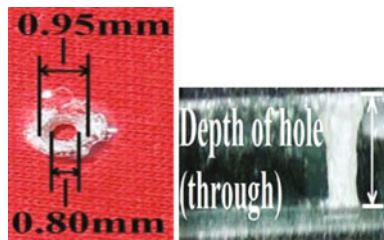


Fig. 9 Drilled using NaNO<sub>3</sub>

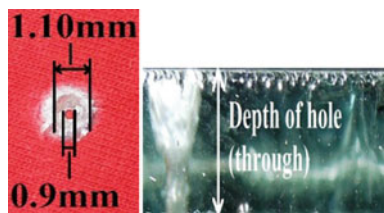
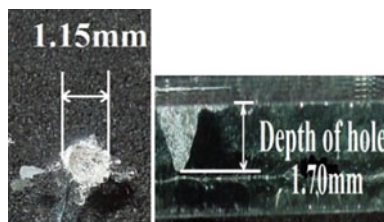
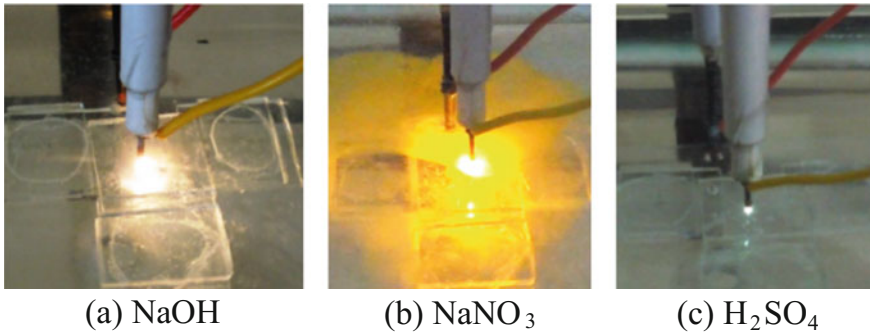


Fig. 10 Drilled using H<sub>2</sub>SO<sub>4</sub>



**Table 3** Comparative of the three electrolyte solution

Electrolyte solution	Depth of hole	Entrance diameter in mm	Exit diameter in mm	Spark color	Spark stability
NaOH	Through	0.95	0.80	Orange	Constant
NaNO <sub>3</sub>	Through	1.10	0.90	Yellow	Constant
H <sub>2</sub> SO <sub>4</sub>	Blind	1.15	–	Blue	Fluctuated

**Fig. 11** Difference in spark stability [9]

sparkling condition which is helpful for the machining. This type of stable sparking is mostly seen in the strong base electrolytes.

Figure 11a shows the color of spark generated during the ECDM process using NaOH solution. This spark is stable and its color is orange-yellow. Figure 11b shows spark generation in NaNO<sub>3</sub> electrolyte solution, NaNO<sub>3</sub> is strong acid and strong base combination. The base part of NaNO<sub>3</sub> tries to generate bubble while acid part of NaNO<sub>3</sub> opposes the bubble generation due to this exactly opposite phenomenon in single solution so bubble generation is less with NaNO<sub>3</sub>. Bubble generation in H<sub>2</sub>SO<sub>4</sub> electrolyte solution is also at negligible level. Hence, with H<sub>2</sub>SO<sub>4</sub> electrolyte solution the fluctuated sparking is observed which results into cracking of workpiece material. The color of fluctuated sparking is blue and is shown in Fig. 11c and cracked workpiece are shown in Fig. 10.

## 4 Conclusion

In this paper, an attempt has been made to study the effect of different electrolytes on MRR of a typical ECDM process of different electrolyte solutions. For the experimentation three electrolyte solutions were used; NaOH, NaNO<sub>3</sub>, and H<sub>2</sub>SO<sub>4</sub>. It was found that NaOH had the most substantial effect on material removal rate, entrance and exit diameter of the hole, and spark stability. The difference of

entrance and exit diameter of the hole was less for NaOH than NaNO<sub>3</sub> and H<sub>2</sub>SO<sub>4</sub>. Entrance and an exit diameter of the hole and spark stability are different for different electrolyte solutions. With the use of 0.7 mm tool diameter the entrance diameter obtain in workpiece varies with electrolyte solutions for NaOH the entrance diameter is 0.95 mm for NaNO<sub>3</sub> it is 1.1 mm and for H<sub>2</sub>SO<sub>4</sub> is 1.15 mm. It was also observed that MRR was higher for NaOH and it decreases for NaNO<sub>3</sub> and H<sub>2</sub>SO<sub>4</sub>, respectively. With H<sub>2</sub>SO<sub>4</sub> the workpiece material got cracked due to unstable spark generation hence, it can be concluded that H<sub>2</sub>SO<sub>4</sub> cannot be used to machine soda lime glass until a feasible solution to control unstable spark is find out.

## References

1. Wuthricha, R., Fasciob, V.: Machining of non-conducting materials using electrochemical discharge phenomenon An overview. *Int. J. Mach. Tools Manuf* **45**, 1095–1108 (2005)
2. Sarkar, B.R., Doloi, B., Bhattacharyya, B.: Parametric analysis on electrochemical discharge machining of silicon nitride ceramics. *Int. J. Adv. Manuf. Technol.* **28**, 873–881 (2006)
3. Chak, S.K., Rao, P.V.: Trepanning of Al<sub>2</sub>O<sub>3</sub> by electro-chemical discharge machining (ECDM) process using abrasive electrode with pulsed DC supply. *Int. J. Mach. Tools Manuf* **47**, 2061–2070 (2007)
4. Gupta, P.K., Dvivedi, A., Kumar, P.: Effect of electrolytes on quality characteristics of glass during ECDM. *Trans. Tech. Publ., Switz.* **658**, 141–145 (2015)
5. Goud, M., Sharma, A.K.: A three-dimensional finite element simulation approach to analyze material removal in electrochemical discharge machining. *J. Mech. Eng. Sci.* 1–12 (2016)
6. Kolhekar, K.R., Sundaram, M.: A study on the effect of electrolyte concentration on surface integrity in micro electrochemical discharge machining. In: 3rd CIRP Conference on Surface Integrity (CIRP CSI), **45**, 355–358 (2016)
7. Zhang, Y., Xu, Z., Zhu, D., Xing, J.: Tube electrode high-speed electrochemical discharge drilling using low-conductivity salt solution. *Int. J. Mach. Tools Manuf.* (2016)
8. Paul, L., Hiremath, S.S.: response surface modeling of micro holes in electrochemical discharge machining process. *Int. Conf. Des. Manuf., IConDM* **64**, 1395–1404 (2013)
9. Harugade, M.L., Hargude, N.V., Shrotri, A.P., Shinde, S.P.: A comparative study for selection of effective electrolyte solution for electrochemical discharge machining. *Int. J. Mech. Eng. Technol.* **6**, 98–10 (2015)

# ExoArm 7-DOF (Interactive 7-DOF Motion Controller of the Operator Arm) Master Device for Control of Loading Crane

Pawel Herbin and Miroslaw Pajor

**Abstract** Control of loading crane using conventional control methods is a difficult task, demanding adequate training and practice. Developed algorithms for crane controlling in Cartesian coordinates much facilitate the material reloading process. We propose an innovative method of machine control that uses the basic way of human interacting with the world, which is the sense of touch. Through the movement of the human upper limb and its contact with the control device bilateral teleoperation will be carried out between the operator and the crane. Interactive 7-DOF Motion controller of the operator arm (ExoArm 7-DOF) increases operator's ability to interact with the machine. The designed device for scanning operator movement provides information to the operator about the load limits and crane movement range by force feedback. The article presents the ExoArm 7-DOF kinematics structure correlated with kinematic of human upper limb, as well as the mechanical model of the solution.

**Keywords** Wearable robot · Master device · Exoskeleton · Dynamics model

## 1 Introduction

Machine control is a rapidly growing field of science. The current technologies of machine control much facilitate the work with cranes, but also they increase the worker safety during the operation. A typical loading crane is constructed of two kind of joints: rotary and sliding. Due to a specific construction, controlling cranes is not a simple issue. Thus, the realization of rectilinear motion requires the motion of all the joints, which is practically impossible using classical control methods. Therefore, we propose an innovative control system for the loading crane using the inverse kinematic model [1]. Using the inverse kinematics model and measuring

---

P. Herbin (✉) · M. Pajor  
Faculty of Mechanical Engineering and Mechatronics West,  
Pomeranian University of Technology Szczecin, Szczecin, Poland  
e-mail: pawel.herbin@zut.edu.pl

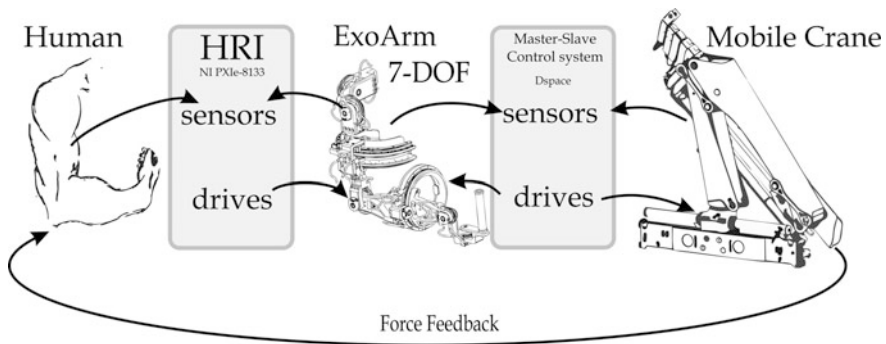
systems for the position of crane components, it is possible to control the crane in Cartesian coordinates. For controlling the crane in the Cartesian coordinate system you can use voice control [2], haptic systems [3], manual programming [4] and control systems with force feedback [5]. Design and implementation of intelligent human-machine interfaces is an important field of applied research. This study is part of the activities relating to the implementation Augmented Reality, Interactive Systems, and Operator’s Speech Interface for Controlling Lifting Devices.

The article focuses on kinematics structure and the mechanical solution of master device for controlling the loading crane using force feedback. The designed device, an exoskeleton, is used for scanning the position of the operator’s arm and interacting with it by contact force. The control method and communication between the devices, crane and ExoArm 7-DOF, is shown in Fig. 1.

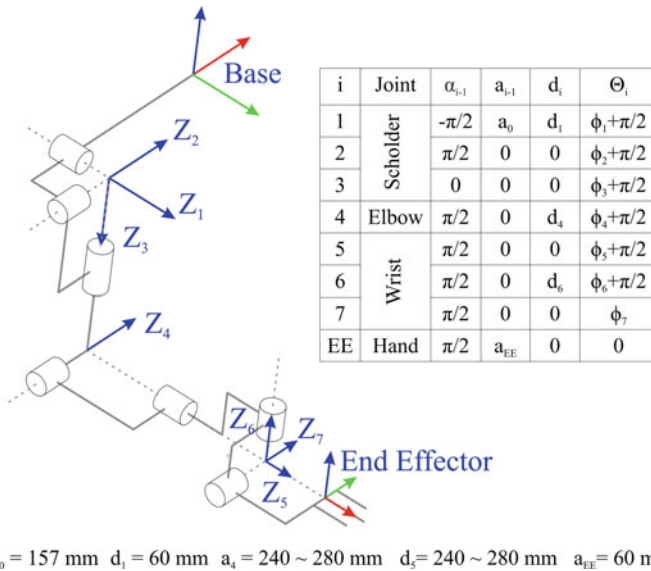
Scanning of the operator’s upper limb movement requires compatibility of the device specific points moving with the movement of the upper limb parts such as the arm, forearm and hand. To maintain the compatibility of displacements, it is necessary to develop a kinematic structure corresponding to the biomechanical kinematical model of the operator’s upper limb. Due to the complex kinematic structure of the human arm, the designed device has seven rotary joints. The Exoarm 7-DOF consists of 3 DOF shoulder joints, 1 DOF elbow joint and 3 DOF wrist joints. Figure 2 presents the kinematic structure and Denavit–Hartenberg (D–H) parameters of the proposed master device.

## 2 The Mechanical Design

In order to ensure maximum operator safety and minimize the risk of machine—operator collision, the structure of Exoarm 7-DOF is anthropomorphic and includes all the degrees of freedom of the human upper limb. The proposed master device is



**Fig. 1** Control scheme of loading crane and Interactive 7-DOF motion controller of the operator arm taking into account the force feedback



**Fig. 2** Kinematic structure and Denavit–Hartenberg (D–H) parameters of ExoArm 7-DOF

a complex mechatronic device equipped with 7 actuators and 30 different sensors i.e. encoders, strain gauge torque sensors, motor controllers.

To reduce the weight of ExoArm 7-DOF, the drivers are placed outside the structure. The device used a closed loop Bowden cable conduit system for transmitting the movement of the actuators to the ExoArm 7-DOF joints. This system ensures a constant ratio of generated torque at the ExoArm 7-DOF joints to the force generated by the actuators. The DC actuators used in the device are equipped with a ball screw and are characterized by a high speed of motion with high force generated by the piston. Table 1 shows the parameters of the designed device. Table 2 shows the angular range of joint movement. The mobility of exoskeleton joints corresponds to angular ranges of human joints presented in [6].

### 2.1 The Closed Loop Bowden Cable Conduit System

All rotary joints (1–7) are coupled with a DC linear motor by the closed loop Bowden cable conduit system shown in Fig. 3. The use of the conduit system

**Table 1** Hardware specification

Symbol	Value (unit)
Volume	$475 \times 390 \times 260 \text{ (mm}^3\text{)}$
Mass	6.3 kg
Power source	12 V DC/125 A
Degree of Freedom	7

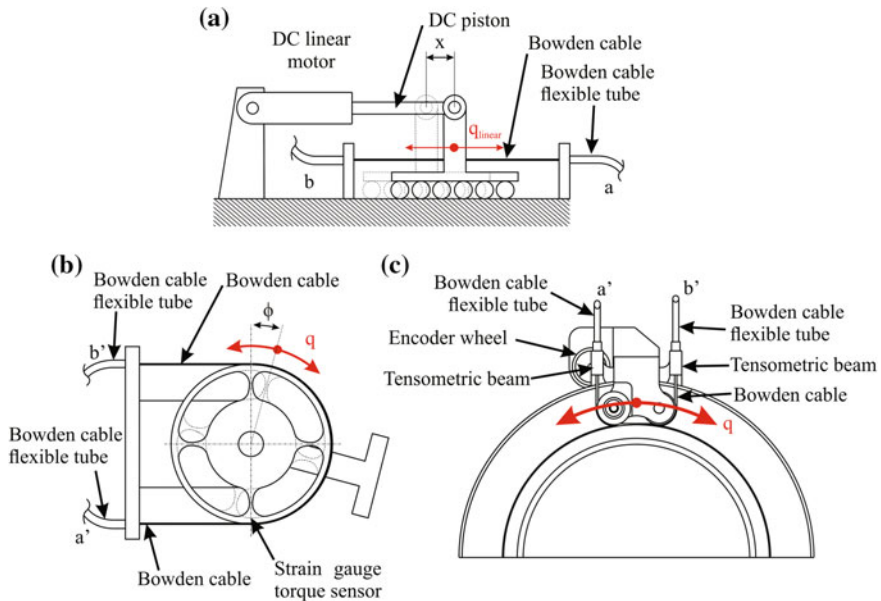


**Table 2** Designed joints working ranges

Joint number	Angle	Range
1	$-3 \leq \Theta_1 \leq 130^\circ$	133°
2	$-50 \leq \Theta_2 \leq 170^\circ$	220°
3	$-60 \leq \Theta_3 \leq 70^\circ$	130°
4	$0 \leq \Theta_4 \leq 100^\circ$	100°
5	$-90 \leq \Theta_5 \leq 80^\circ$	170°
6	$-20 \leq \Theta_6 \leq 30^\circ$	50°
7	$-50 \leq \Theta_7 \leq 50^\circ$	100°

allows to transfer the drives into a fixed stand and therefore also the weight of ExoArm 7-DOF moving parts is significantly reduced. On the other hand, we had to deal with variable friction force between the wrapping connector and the Bowden cable flexible tube. This force depends on the angle and the radius of flexible tube deflection. Moreover, the mentioned conduit system is characterized by backlash depending on initial tension of wrapping connectors. It is the main disadvantage of this implemented solution, because it induces nonlinearity in drive system. However, the use of torque measuring system and joint angular position measuring system directly on the joint, minimizes the impact of conduit system defects.

The Exoarm 7-DOF has two different types of closed loop Bowden cable conduit system, shown in Fig. 3b, c. Construction of all joints, except 3rd and 5th, is based



**Fig. 3** The scheme of two joint constructions: **a** the first type of joint, **b** the second type of joint; and **c** linear motor stand

on cable wheel integrated with a torque sensor (called a cable strain gauge torque sensor) specially designed for Exoarm 7-DOF. Each joint is equipped with two wrapping-connectors for movement in two directions (see Fig. 3b). The 3rd and 5th joints, responsible for shoulder interior/exterior rotation and elbow supination/pronation, respectively, were built according to the second conduit system solution (see Fig. 3c). In 3rd and 5th joints, it was difficult to apply the cable wheel integrated with torque sensor, due to the fact that these device components are built around the human arm and forearm, respectively. Therefore, instead of the torque sensor, we used two strain gauge beams to measure forces transferred by wrapping connectors. They pass through the holes in the strain gauge beams and then run after the groove sheave. Both types of conduit system provide a constant dependence of the driving torque on the force generated by the DC actuator, which is undoubtedly a great advantage of these solutions.

## 2.2 The 3 DOF Shoulder Joint

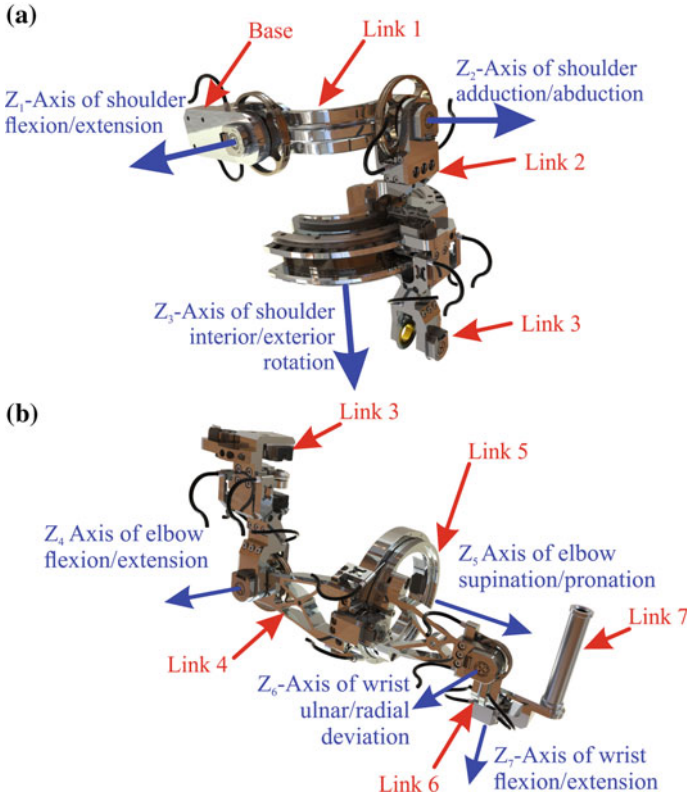
According to the biomechanical model, shoulder is a 3 degree of freedom ball joint. In designed device, the functionality of this joint is achieved by using 3 rotary joints with one degree of freedom. The position of the joints is shown in Fig. 4a. The shoulder joint of ExoArm 7-DOF has 3 orthogonal rotation axes that realize: adduction/abduction movements (axis 1), flexion/extension movements (axis 2) and interior/exterior rotation movements (axis 3). The first two joints were fitted with cable wheels for measuring torque. These wheels have a diameter of 80 mm and the maximal design torque value is 60 Nm. The third joint is equipped with two strain gauge beams for measuring forces transferred by wrapping connectors. Then the values of measured forces are converted to torque using Formula (1), where  $R_3$ , the radius of fairlead sheave, is equal 88 mm.

$$M_3 = F_{31} \times R_3 - F_{32} \times R_3 \quad (1)$$

The maximum design force transfer by wrapping connector is 454 N, therefore the maximum torque value is 40 Nm. The revolution of the 1st and 2nd joint is performed with slide bearings, whereas the rotation of 3rd joint is realized by an arc ball guide. The maximum rotation speed of the 1st and 2nd joint is 28°/s, and of the 3rd joint is 57°/s.

## 2.3 The 1 DOF Elbow Joint

The functionality of the human elbow joint is realized by a rotary joint (the 4th joint according to Fig. 2). The rotation axes of this rotary joint and the 3rd joint are mutually perpendicular. The position of the elbow flexion/extension joint is shown



**Fig. 4** a 3-DOF shoulder joints, b 1-DOF elbow and 3-DOF wrist joints

in Fig. 4. The movement range of this joint is  $100^\circ$ . The maximum design torque of the joint drive is 35 Nm and the maximum rotation speed of elbow joint is  $56^\circ/\text{s}$ . The revolution of the 4th joint is performed with slide bearings made of brass.

## 2.4 The 3 DOF Wrist Joint

The ExoArm 7-DOF wrist joints (5th, 6th and 7th according to Fig. 2) have 3 orthogonal rotation axes that perform the following movements: human elbow supination/pronation, human wrist ulnar/radial deviation and human wrist flexion/extension. The position of the joints is shown in Fig. 4b. The 5th joint responsible for elbow supination/pronation is based on a cross-roller bearing, whereas the construction of the other two joints, i.e. 6th and 7th, responsible for wrist ulnar/radial deviation and wrist flexion/extension, respectively, is based on slide bearings. The measurement of 6th and 7th joint torque is realized using cable

wheels integrated with a torque sensor, as was mentioned in Sect. 2.1. These wheels have a diameter of 42 mm and the maximum design torque value is 15 Nm. The maximum rotation speed of the 6th and 7th joint is 38°/s and 44°/s, respectively. The 5th joint is equipped with two strain gauge beams for measuring forces transferred by wrapping connectors. The value of torque is obtained from Formula (2), where  $R_5$ , the radius of fairlead sheave, is 75 mm.

$$M_5 = F_{51} \times R_5 - F_{52} \times R_5 \quad (2)$$

The maximum design force, transferred by wrapping connector, is 346 N, therefore the maximum torque value is 26 Nm. The maximum rotation speed of the 5th joint is 56°/s.

### 3 The Prototype

We have developed a complex mechatronic device, called Interactive 7-DOF Motion Controller Of The Operator Arm. The designed device has 30 different sensors, listed in Table 3. Figure 5 shows location of the sensors, as well as the type of bearings i.e. slide, cross roller bearings and arc ball guide used to ensure required movements. Elements of the designed exoskeleton were made of aluminum alloy 7075, Ti6Al4V and 1.7225 steel. These materials have been selected to ensure both the lowest possible weight and also proper safety factor. In order to make possible testing the device by a wide group of operators, it has adjustable length of individual parts, so that it is possible to adapt the device to the dimensions of the arm, forearm and hand of the potential operator. The adjustment of the distance between the Z2–Z4 and Z4–Z6 axles is performed by exchangeable spacers placed between the part of the second and fifth link. The device is in contact with the operator only in five areas for the arm, four for the forearm and one for the palm. Figure 6 shows a photo of the device before connecting drives.

### 4 Dynamic Loads of Closed Loop Bowden Cable Conduit System

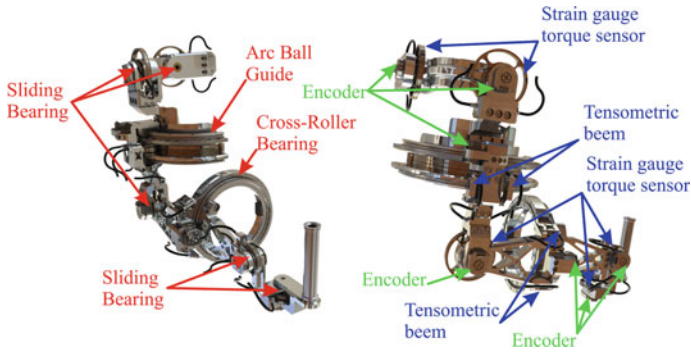
For the developed geometric models, the analysis of the forces and moments acting on the ExoArm 7-DOF joints during movement was conducted. The calculations were performed using the dynamics model, described by Eq. 3:

$$M(q)\ddot{q} + C(q, \dot{q})\dot{q} + D(q) = F \quad (3)$$

where:

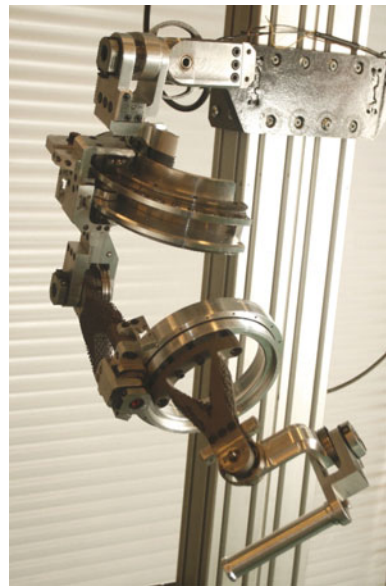
**Table 3** Sensors specification

No.	Sensor/actuator	Type	Quantity	Value (unit)
1	Motor controller	Pololu Simple High-Power Motor Controller 24v23	7 (1 per joint)	$5.49 * 10^{-5}$ (V) 16 bit
2	Ammeter	ACS712ELCTR-30A-T	7 (1 per motor)	$7.23 * 10^{-3}$ (A) 12 bit
3	Strain gauge torque sensor	Self-design sensor based on HBM -LY13-1.5/120	9 (2 per 3,4 joint and 1 per other)	$9.16 * 10^{-4}$ (Nm) 16 bit
4	Encoder	CUI AMT203-V	7 (1 per axis)	5.27" (12 bit/rev)
5	Force sensing resistor	FSR 400 Short	10	$7.81 * 10^{-2}$ (N) 8 bit



**Fig. 5** Mechanical design

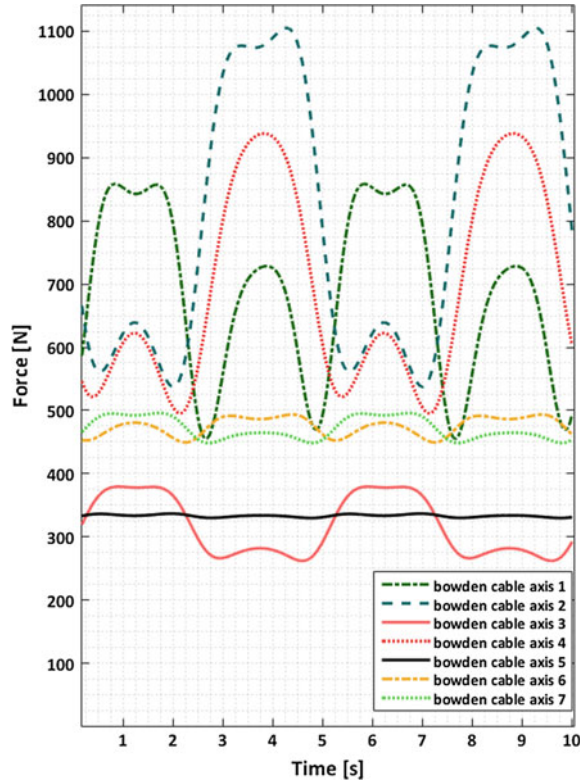
**Fig. 6** Prototype of the ExoArm 7-DOF



- $q, \dot{q}, \ddot{q}$  position, velocity and acceleration in joint space,
- $M(q)$  matrix of inertia,
- $C(q, \dot{q})$  Coriolis and centrifugal force matrix,
- $D(q)$  gravity matrix,
- $F$  forces acting on the system.

We conducted simulation tests for the movement presented in [5]. As a result of the analysis, we received the maximum force acting on Bowden cables, that may occur in the device during the operation movement. The construction optimization, aimed at reduction of mass, was also performed. As a result, we also obtained a

**Fig. 7** Load of closed loop Bowden cable conduit system



significant reduction of torque and force acting on Bowden cables. The load on the Bowden cables, during movements from [5], is shown in Fig. 7.

## 5 Conclusions

In the presented study, an exoskeleton (ExoArm 7-DOF) was developed. The device will be applied to teleoperation with a load-handling crane using a force feedback. The apparatus has seven degrees of freedom in sequence responsible for: adduction/abduction movements (axis 1), flexion/extension movements (axis 2) and interior/exterior rotation movements (axis 3), elbow flexion/extension (axis 4), elbow supination/pronation (axis 5), wrist ulnar/radial deviation (axis 6) and wrist flexion/extension (axis 7). The presented kinematic structure and mechanical solutions used during prototype construction ensure convenience and unlimited operator motion. We have received great fit in terms of mobility between the simulation model and the real object. In further study, sensor calibration, as well as a test of Bowden cable conduit system are planned.

**Acknowledgements** This project is financed by the National Centre for Research and Development, Poland (NCBiR), under the Applied Research Programme—Grant agreement No. PBS3/A6/28/2015.

## References

1. Herbin, P., Pajor, M.: Modeling direct and inverse kinematics of loading crane with redundant degrees of freedom structure using matlab. *Modelowanie inżynierskie*, 44–50 (2016)
2. Majewski, M., Kacalak, W.: Conceptual Design of Innovative Speech Interfaces with Augmented Reality and Interactive Systems for Controlling Loader Cranes, *Artificial Intelligence Perspectives in Intelligent Systems*, pp. 237–247. Springer International Publishing, Berlin (2016)
3. Milecki, A., Bachman, P.: Admittance and impedance control in the electrohydraulic drive system of haptic joystick. *Pomiary Automatyka Robotyka* **17**, 456–460 (2013)
4. Herbin, P., Pajor, M., Stateczny, K.: Six-axis control joystick based on tensometric beam. *Adv. Manuf. Sci. Technol.* **40**(4), 33–41 (2016)
5. Herbin, P., Pajor, M.: Exoskeleton of upper limb—model using real movement parameters. *Modelowanie inżynierskie*, 40–46 (2015)
6. Bochenek, A., Reicher, M., Bilikiewicz, M.: *General Anatomy: Bones, Joints and Ligaments, muscles*, PZWL (2007)



# Influence of Selected Factors on Static Friction for Combination of Expanded Graphite-Steel

Aleksandra Rewolinska and Karolina Perz

**Abstract** The article presents the results of tests of the static friction coefficient of cooperating material sets. The tests were made on two graphite materials—pure expanded graphite and expandable graphite with PTFE—cooperated with a steel surface. The device, on which the friction coefficient was tested, enables the study to be conducted in the reciprocating motion. Measurements were made at different unit pressures (0.5; 2 and 5 MPa) and for different work cycles (0, 500, 1500, and 3000). Based on the obtained results, it has been found that the set with pure expanded graphite has a higher static friction coefficient than the set of the graphite with PTFE. In addition, the influence of load and number of cycles on the coefficients of friction of the examined material combinations is noticeable. Also, the fact of the film formed on the combination steel surface also requires noticing.

**Keywords** Expanded graphite · PTFE material · Static friction coefficient  
Graphite film

## 1 Introduction

Material combination of expanded graphite-steel is commonly found in motion seals in valves and pumps. The static friction tests [1] for the above combination have shown that this friction can significantly affect the operation of machines and equipment, especially those operating in the motion-resting system. This effect can be adverse, for example, when it is the cause of vibration that causes a disturbance in the movement of the scattering element, it is so-called stick-slip phenomenon [2]. Also starting the machine can be difficult, especially when the contact time between the cooperating surfaces is longer. At that time, diffusion processes of atoms on

---

A. Rewolinska (✉) · K. Perz  
Institute of Machines and Motor Vehicles, Poznań University of Technology,  
Poznań, Poland  
e-mail: aleksandra.rewolinska@put.poznan.pl

elemental contact surfaces intensify increasing the strength of adhesive joints over time [3].

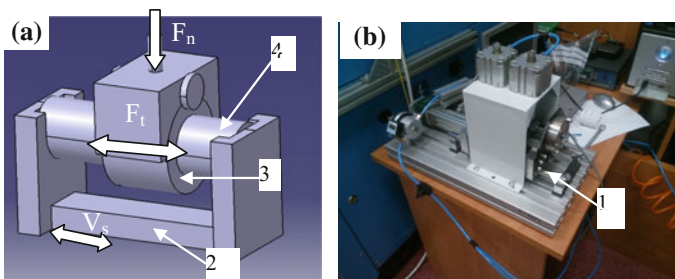
Literature of the subject presents numerous studies on the mentioned tribological phenomena occurring in the polymer–steel combination [4–6]. Graphite in these studies is often an addition to a polymer that is introduced in various forms and amounts [7–11]. In general, the published research results [12–14] report that graphite improves the wear resistance of a cooperating material, lowers frictional temperature, stabilizes friction coefficient, and reduces noise. However, these studies do not concern extended graphite. Whereas in practice, there are combinations in which expanded graphite—pure or with a dopant of plastic—cooperates with the steel surface. However, there are no tests on such combinations. Therefore, one should recognize the phenomenon of static friction occurring in the aforementioned combinations. An additional factor indicating the need to perform the above tests are the problems associated with the start-up of the graphite–steel combination, as the manufacturers and users of the seals say. Knowledge of the above issues will allow to better design and select seals for specific application in the future, which will allow minimizing losses caused by negative friction results.

The purpose of the work is to determine the value of static friction coefficient for selected graphite materials cooperating with steel mandrel.

## 2 Test Subject

The view of a rig and the scheme of a cooperating combination are shown in Fig. 1.

The device, on which the tests were carried out, makes possible to conduct sliding friction tests in reciprocating motion. During the tests, a ring-shaped sample, attached to the handle, was clamped with a  $F_n$  force to the steel counter-sample. The samples were made of pressed expanded graphite rings with industrial cleanliness (GRAFMET<sup>®</sup>950) and expanded graphite with PTFE (GRAFMET<sup>®</sup>950TF). The density of the tested materials was 1.8 g/cm<sup>3</sup>. The counter-sample was made of



**Fig. 1** The test rig used to determine the static friction force in reciprocating motion; **a** schema, **b** view; 1 bottom carriage, 2 upper carriage, 3 sample (graphite ring), 4 counter-sample (steel mandrel),  $F_n$  pressure force,  $F_t$  friction force,  $V_s$  average speed

stainless steel with a hardness of 40 HRC in the form of a mandrel with a roughness  $R_a = 0.98\text{--}1.12 \mu\text{m}$ . The system moving the counter-sample consisted of two carriages mounted on each other so that they could move in the same direction. The slip force  $F_t(t)$  was recorded at 100 Hz. Based on the course of changes in the frictional force during the start-up, the value of the static friction force  $F_{st}$  was determined, and on its basis—the friction factor  $\mu_{st}$ .

### 3 Motion Tests of the Combination

#### 3.1 Test Conditions

Test conditions are shown in Table 1. Prior to the commencement of proper measurements, the paired material was break-in until the expanded graphite sample touched the entire steel surface of the counter-sample.

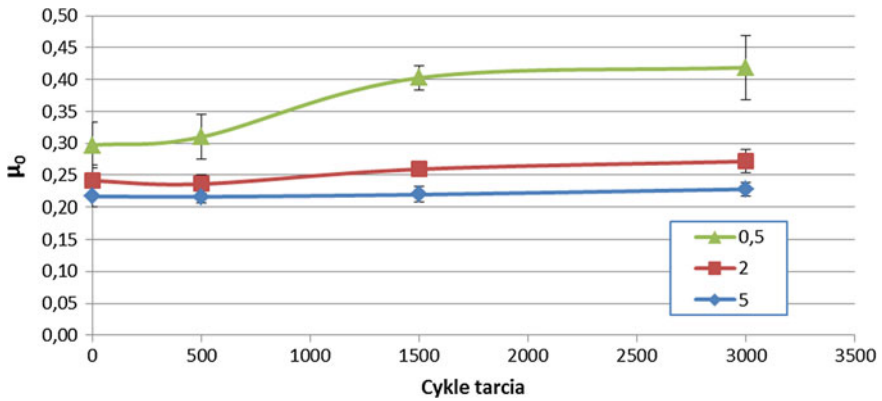
The experiment was performed with a 3 times repetition for each material set. After each of the three series of tests, the samples were weighed. Measurements were made to the nearest 0.01 g.

#### 3.2 Test Results

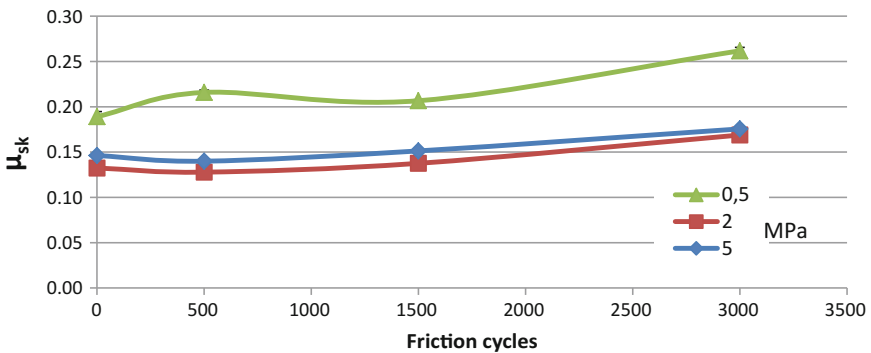
As a result of the tribological cooperation of the steel mandrel with samples made of pure expanded graphite noticed the friction coefficient decrease with an increase in pressures (Fig. 2).

**Table 1** Test conditions

Stage	Pressure (MPa)	Cycles	Average speed (mm/s)
Breaking-in	1	100	20
1	0.5	0	20
		500	
		1500	
		3000	
2	2	0	20
		500	
		1500	
		3000	
3	5	0	20
		500	
		1500	
		3000	



**Fig. 2** Dependence of static friction coefficient on friction cycles and load for the material set of pure expanded graphite—steel



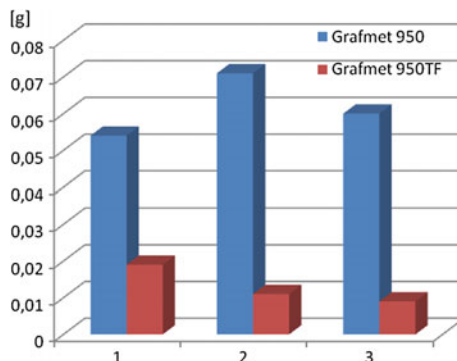
**Fig. 3** Dependence of static friction coefficient on friction cycles and load for the material set of expanded graphite with an addition of PTFE—steel

The results of the tests for the material set of expanded graphite with PTFE—steel are shown in Fig. 3.

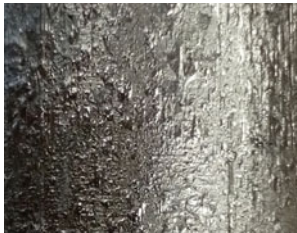

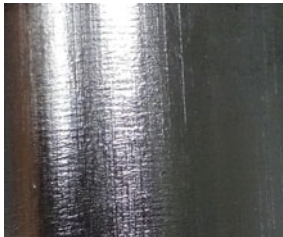
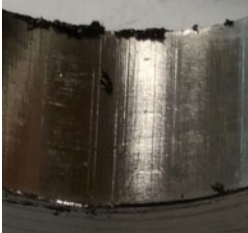
The results of samples mass consumption of individual batches after 3000 cycles are shown in Fig. 4.

After examining each material combination in a given series, pictures of the mandrel and rings were made. Both the appearance of the mandrel and the rings differed for the materials tested (Table 2).

**Fig. 4** Mass consumption of samples of selected material sets after 3000 cycles for each series (1, 2, 3)



**Table 2** Photos of steel mandrel and graphite rings after 3000 cycles of work

Set of materials	Steel mandrel	Graphite ring
Grafmet 950		
Grafmet 950TF		

## 4 Summary and Conclusions

The results obtained during the tribological tests allowed to formulate the following conclusions and observations:

- it was found that the difference in static friction coefficient for the tested material sets was noticeable; the set with pure expanded graphite has a higher friction coefficient than the expanded graphite with PTFE,

- the impact of the load on the static friction coefficient is noticeable; as the load increases, the coefficient decreases, with low pressures—0.5 MPa—high friction coefficient (especially for pure graphite) is visible,
- as the number of cycles increases, the static friction coefficient increases, especially at a load of 0.5 MPa,
- greater mass consumption of rings made of pure expanded graphite is visible; at a load of 5 MPa these rings were severely damaged,
- also the fact should be noted of the film formed on the steel surface which is characteristic for the cooperation of steel with graphite; the film formed by cooperation of graphite with PTFE with a steel mandrel is thinner and smoother; literary research is not unequivocal as to the factors that influence its origins and the tribological processes that are taking place in its formation which encourages further research in this direction [15].

## References

1. Rewolińska, A., Kowalewski, P., Perz, K., Paczkowska, M.: A study of friction in reciprocating movement of slipping pair steel-expanded graphite. *Tribologia* **6**, 131–138 (2016)
2. Nosal, S.: *Tribologia, Introduction to the Issues of Friction, Wear and Lubrication*. WPP, Poznań (2016)
3. Norbert, D., Kusznierevicz, Z., Rymuza, Z.: Measurement of resting friction in miniature polymeric-polymer slide bearings. *Measur. Autom. Control* **57**(7), 760–763 (2011)
4. Tabor, D., Bowden, F.P.: *Introduction to Tribology*. WNT, Warszawa (1980)
5. Dobrowolska, A.: Influence of unit pressure on the coefficient of static friction of selected biomaterials. *Curr. Prob. Biomech.* **6**, 27–30 (2012)
6. Liping, T., Xiaohua, Z.: Effects of the difference between the static and the kinetic friction coefficients on a drill string vibration linear approach, research article, mechanical engineering. *Arab. J. Sci. Eng.* **40**, 3723–3729 (2015)
7. Zhanga, G., Rashevaa, Z., Schlarbb, A.K.: Friction and wear variations of short carbon fiber (SCF)/PTFE/graphite (10 vol.%) filled PEEK: effects of fiber orientation and nominal contact pressure. *Wear* **268**, 893–899 (2010)
8. Zhang, X.R., Pei, X.Q., Wang, Q.H.: Friction and wear studies of polyimide composites filled with short carbon fibers and graphite and micro SiO<sub>2</sub>. *Mater. Des.* **30**, 4414–4420 (2009)
9. El-Tayeb, N.S.M.: A study on the potential of sugarcane fibers/polyester composite for tribological applications. *Wear* **265**(1–2), 223–235 (2008)
10. Slavič, J., Boltežar, M.: Measuring the dynamic forces to identify the friction of a graphite-copper contact for variable temperature and current. *Wear* **260**(9–10), 1136–1144 (2006)
11. Gachot, C., Rosenkranz, A., Hsu, S.M., Costa, H.L.: A critical assessment of surface texturing for friction and wear improvement. *Wear* **372–373**, 21–41 (2017)
12. Jaworski, J.: *Friction Linings for Brakes and Clutches of Motor Vehicles* WKŁ, Warsaw, 1984
13. Ścieszka, S.: *Friction Brakes. Material, Construction and Tribological Issues*. ITE Radom, Gliwice, 1998
14. Nosal, S., Orłowski, T.: Influence of the type of graphite and coke used on the friction-friction properties of friction materials. *Tribologia* **5**, 85–93 (2010)
15. Rewolińska, A., Stachowiak, A., Kinal, G., Paczkowska, M., Perz, K.: The phenomenon of material transfer in combination expanded-steel graphite. *Tribologia* **4**, 167–175 (2015)

# Development of Experimental Design for Hydraulic Active Heave Compensation Systems

Arkadiusz Jakubowski, Arkadiusz Kubacki and Piotr Owczarek

**Abstract** The article presented here describes the development of test stand for hydraulic active heave compensation system. For measurements, actual position of hydraulic cylinder was used displacement sensors by the authors. They measured actual position of hydraulic motor by means incremental encoder. The test stand was built with the use of force sensor and 3 DOF accelerometer and gyroscope. During experimental tests force, acceleration and rotations (Pitch and Roll) were measured. Authors used two servo valves for the controlled position of hydraulic cylinder and hydraulic motor. The control system was based on PLC controller type Power Panel 500. The performed test included step response of hydraulic motor and hydraulic cylinder for sine signal.

**Keywords** Heave compensation · Offshore operation · Active heave · Servo valve · Hydraulic system · Winch system

## 1 Introduction

In the last few decades, maritime industry has shown a growth in interest the development of presented day maritime technologies. The focus is on control new ships and their devices that are supposed to meet high requirements. Operation on the ships is dangerous because of human factor and occurrence of a failure. Due to demanding maritime environment, winch and sea crane are very important devices [1–3].

---

A. Jakubowski (✉) · A. Kubacki · P. Owczarek  
Institute of Mechanical Technology, Poznan University of Technology,  
Skłodowska-Curie Square 5, 60-965 Poznań, Poland  
e-mail: arkadiusz.z.jakubowski@doctorate.put.poznan.pl

A. Kubacki  
e-mail: dominik.rybarczyk@put.poznan.pl

P. Owczarek  
e-mail: piotr.owczarek@put.poznan.pl

There are three types of heave compensation. The first one is a passive heave compensation. In this method, pneumatic cylinder is used which is connected to air accumulator. The second type of heave compensation is semi-active heave compensation (SAHC). This method combines an active and passive heave compensation (PHC). In this method, active element and a several passive elements are implemented such as pneumatic cylinders. The last type of heave compensation is active heave compensation (AHC). The AHC is the most popular method and is the most commonly used. In the active heave compensation, controlled hydraulic drivers are used such as hydraulic cylinders, hydraulic motors. Based on the sensors placed on board, the ship control system controls hydraulic drivers [4, 5, 6, 7].

In the last few years, many scientists have put emphasis on the development of the active heave compensation systems and its implementation. They also focused on development of the new control systems and its implementation such as Model Predictive Control (MPC), PID, fuzzy logic, and other [8, 9, 6].

The paper is organized as follows. Design of heave compensation system is given in Sect. 2. In Sect. 3, we focus on presentation experimental results. Conclusion and future works are shown outlined in Sect. 4.

## 2 Design of Heave Compensation System

### 2.1 *Experimental Test Stand*

In order to perform experimental research, authors developed the test rig. The new test stand is presented in Fig. 1. The test stand consists hydraulic cylinder which is used to realized waves simulation. The hydraulic motor is fixed at the end of the piston rod of the hydraulic cylinder. The hydraulic cylinder and hydraulic motor were controlled by electrohydraulic servo valves. Steel load is fixed at the end of steel cable. The force sensor is implemented between steel cable and the steel load. Accelerometer and gyroscope are mounted on the top of the steel load. The stroke of the double acting hydraulic cylinder was equal to 400 mm. The diameter of the piston was equal to 100 mm and the diameter of piston rod was equal to 60 mm. Max rotary speed of the hydraulic motor was equal to 810 rpm. Max output power of the hydraulic motor was equal to 16 kW.

Authors used a hydraulic power supply which is characterized by the parameters: maximus flow rate = 100 dm<sup>3</sup>/min, maximum pressure  $p_o = 40$  MPa and electric motor power is equal to: 37 kW.



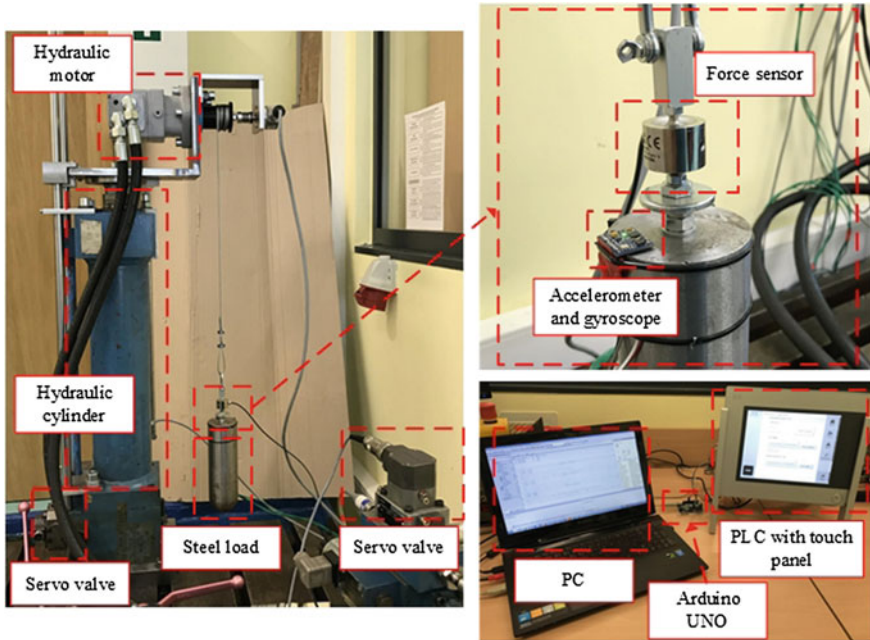


Fig. 1 View of the experimental test stand for active heave compensation

## 2.2 Control Design

The control system schematic is presented in Fig. 2. The control system was based on PLC controller type Power Panel 500. The PLC is equipped with a touch panel. The electrohydraulic valves were controlled by dedicated valves amplifier (control card) which were connected to PLC. A Displacement sensor is used to measure actual position of a double acting hydraulic cylinder. For measured displacement Authors used inductive displacement transducer WFS/500 HBM company with range 500 mm. The actual position of the shaft of the hydraulic motor is measuring via incremental encoder. The range of incremental encoder is equal to 1000 pulse rate. During movement, force is created between the steel load and the steel cable.

The created force is measured using the force sensor U9C HBM company with range 1 kN. During the experimental tests, authors measured acceleration in Z-axis and rotation in X-axis and Y-axis via GY-87 electronic module. The GY-87 devices combine a three-axis gyroscope and three-axis accelerometer with an onboard Digital Motion Processor (DMP). The GY-87 module is connected to Arduino UNO by means I2C serial bus. Size of the GY-87 is equal to  $2.2 \times 1.7$  cm and weight: 6 g. The control system for Arduino UNO was based on PC. The acceleration and rotation from GY-87 module were sent to PLC via RS 232 to RS 485 converter. The hydraulic motor and double acting hydraulic cylinder were

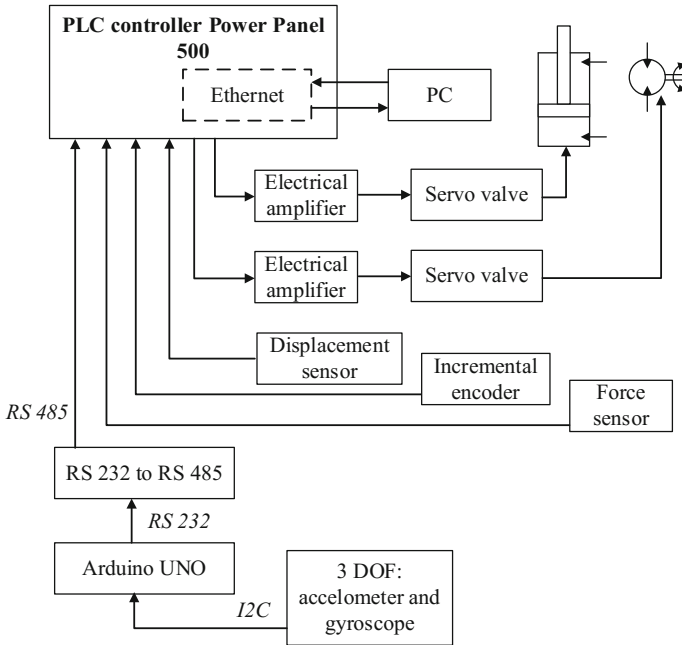


Fig. 2 The control system schematic

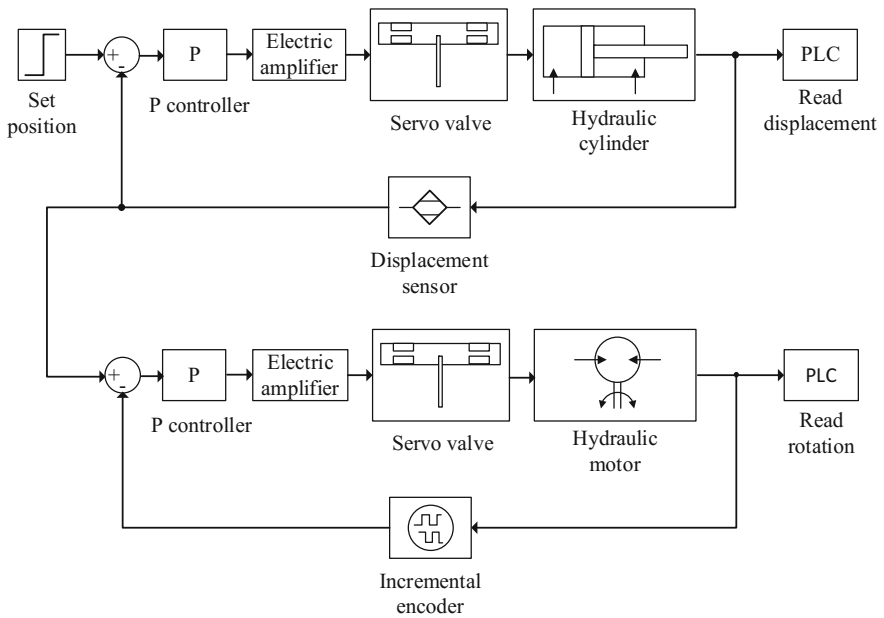


Fig. 3 The test stand controller scheme

controlled via the proportional regulator. The schematic of the test stand controller is presented in Fig. 3.

### 3 Experimental Results

The aim of the first performed experiments was to check the force which is created between steel cable and steel load during movement of the hydraulic cylinder. The experimental tests were performed for a different period of the sine signal. The displacement of the hydraulic cylinder was compensated by means hydraulic motor. The hydraulic motor followed hydraulic cylinder. All of the experiments were performed for the supply pressure  $p_o$  equal to 8 MPa.

The first experimental test was performed for the period of the sine signal which was equal to  $T = 4$  s. The gain value for hydraulic cylinder was  $k_p = 40$  and for the hydraulic motor was  $k_p = 80$ . The double acting hydraulic actuator was existed by used of the step-type signal with a range of 100 mm for all of the experiments. The collected data was shown on Fig. 4.

The second step has checked the force for different parameters of sine signal. The period of the sine signal was  $T = 2$  s. For the second step the gain value for hydraulic actuator was  $k_p = 20$  and for the hydraulic motor was  $k_p = 50$ . The result is shown in Fig. 5.

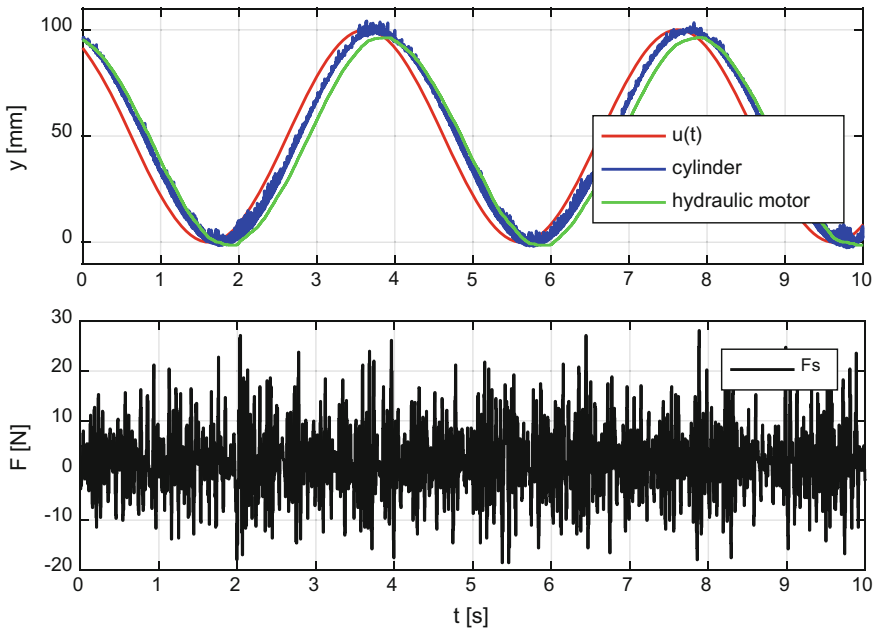
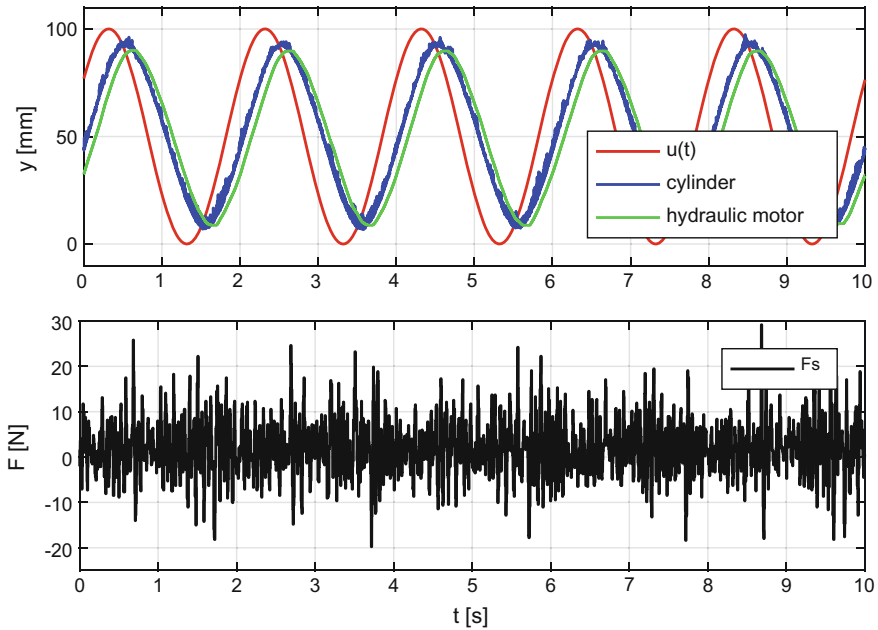


Fig. 4 The experimental results. The effect of force changed



**Fig. 5** The effect of force change for different sine signal parameters

In the last step, the authors measured acceleration and rotation of the steel load. For the last step experimental test was performed for the same period of sine signal as the first step and was equal to  $T = 4$  s. The gain value for both hydraulic drives was the same as the first step. The results of the last experiment are shown in Fig. 5.

The measured rotations were collected for two axis:  $X$ -axis (Roll) and  $Y$ -axis (Pitch). The  $Z$ -axis acceleration was measured via accelerometer with range  $\pm 2$  g. In the Fig. 6 they showed the results for the rotations with forced motion and during movement of the two hydraulic drivers (without forced motion). In motion (during tests), there is no rotation in both axes. The effect is that the steel load has not moved.

## 4 Conclusion

The article describes the development of test stand for hydraulic active heave compensation system. The system was tested for different parameters of the controller. The authors checked the motion of the load by means force sensor, accelerometer, and gyroscope. The force is changed during movement with range 30 N. For different parameters of sine signal the force change not too much. The results of measured the rotations shown that the steel load in both axes has not moved.

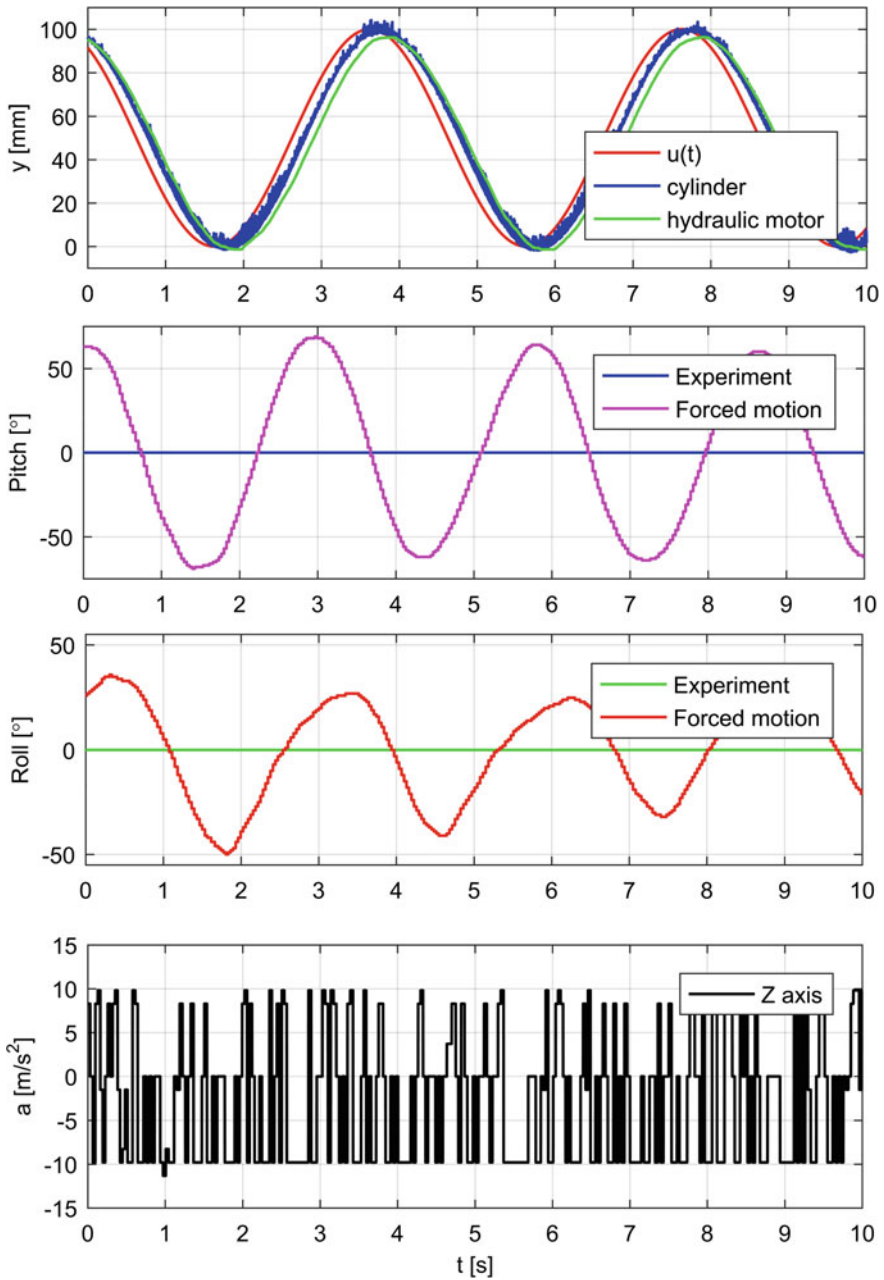


Fig. 6 The rotations in X, Y-axes and acceleration in Z-axis

The developed test stand was possible to measured acceleration, rotation, and force in motion. Further research aims to reduce acceleration in Z-axis and created force by means another controller such as PD and Model Predictive Control (MPC).

**Acknowledgements** The work described in this paper was funded from 02/22/DSPB/1389.

## References

1. Messineo, S., Celani, F., Egeland, O.: Crane feedback control in offshore moonpool operations. *Control Eng. Pract.* **16**, 356–364 (2008)
2. Huser, A., Bergstrom, H., Gosior, J., White D.: Design and operational performance of a standalone passive heave compensation system for a work class ROV. In: *OCEANS 2009*, pp. 1–8 (2009)
3. Sun, Y., Li, W., Dong, D., Mei, X., Qiang, H.: Dynamics analysis and active control of a floating crane. *Tehnicki vjesnik - Technical Gazette* **22**(6) (2015)
4. Sanfilippo, F., Hatledal, L.I., Zhang, H., Rekdalsbakken, W., Pettersen, K.Y.: A Wave Simulator and Active Heave Compensation Framework for Demanding Offshore Crane Operations, pp. 1588–1593 (2015)
5. Sun, Y., Qiang, H., Yang, K., Chen, Q., Dai, G., Dong, M.: Experimental design and development of heave compensation system for marine crane. *Math. Model. Eng. Prob.* **1**(1), 15–20 (2014)
6. Walid, A.A., Gu, P., Hansen, M.R., Hovland, G., Iskandarani, Y.: Modeling and simulation of an active heave compensated draw-works. *Recent Adv. Manuf. Eng.*
7. Das-han, D., You-gang, S., Long, L.: Simulation studies on dynamic characters of floating cranes. *Sci. Technol. Eng.* (2013)
8. Kimiaghalam, B., Homaifar, A.: An application of model predictive control for shipboard crane. In: *Proceedings of the American Control Conferences*, Arlington, vol. 2, pp. 929–934 (2001)
9. Richter, M., Arnold, E., Schneider, K., Eberharter, J.K., Sawodny, O.: Model predictive trajectory planning with fallback-strategy for an active Heave Compensation system, pp. 1919–1924. *American control conference*, USA (2014)
10. El-Hawary, F.: Compensation for source heave by use of a Kalman filter. *IEEE J. Oceanic Eng.* **7**(2), 89–96 (1982)
11. Woodacre, J.K., Bauer, R.J., Irani, R.A.: A review of vertical motion heave compensation systems. *Ocean Eng.* **104**, 140–154 (2015) (Sierpie 2015)

# Loader Crane Working Area Monitoring System Based on LIDAR Scanner

Karol Miadlicki, Mirosław Pajor and Mateusz Sakow

**Abstract** Segmentation and analysis of the environment using 3D data (point clouds) in real time are dynamically developing the area. Falling prices of depth sensors based on technologies: LIDAR, ToF, RADAR, increasing computing power, growing interest in autonomous vehicles and robots, favor this trend. This paper presents test studies of loader crane working area monitoring system based on the Velodyne VLP-16 LIDAR scanner. Developed system use ground plane estimation and surroundings segmentation algorithms. The ground points filtering algorithm is based on the dot product of vectors as well as interpolation using the RANSAC method. Segmentation algorithm uses angle threshold between points and breadth-first search (BFS) method for determine neighborhood. The proposed system was adapted to operate with sparse LIDAR data in real time. Described system allows for detects human bodies, environmental elements, and monitors changes in the loader crane work area. The effectiveness of developed algorithms was tested on data obtained from loader crane test bench. An experiment showed that segmentation and monitoring loader crane working area in real time even with sparse data is possible. Moreover, the authors discuss other methods used to segmentation sparse point cloud in real time, describe the Velodyne VLP-16 scanner, and presents an outline of current research into HMI interfaces for loader cranes.

**Keywords** Work zone segmentation · Ground filtration · Loader crane · Mobile crane · LIDAR · VLP-16 · RANSAC · Dot product

---

K. Miadlicki (✉) · M. Pajor · M. Sakow  
Faculty of Mechanical Engineering and Mechatronics,  
Institute of Mechanical Technology, West Pomeranian University  
of Technology, Szczecin, Poland  
e-mail: karol.miadlicki@zut.edu.pl

© Springer International Publishing AG 2018  
A. Hamrol et al. (eds.), *Advances in Manufacturing*, Lecture Notes in Mechanical Engineering, [https://doi.org/10.1007/978-3-319-68619-6\\_45](https://doi.org/10.1007/978-3-319-68619-6_45)

465

## 1 Introduction

A loader crane is a hydraulically powered, articulated arm fitted to a truck or trailer. The pressure source is a hydraulic pump connected to the propulsion system of the vehicle on which it is fixed. These cranes are often called HDS, knuckle-boom crane, or articulating crane. Loader cranes are used for loading/unloading vehicles, handling the heavy loads on construction sites or in harbors. Even though they have an important role in the industry, the development of control systems and support systems used in them, it is not as dynamic as in the sector of industrial robots and automotive. Currently, to control the cranes are usually used hydraulic levers or control panels. The standard also become joysticks, electronic levers, buttons, switches, LEDs and LCD displays. All these factors influence on control precision, comfort of performing complex movements, and setting multiple parameters of the crane without entering the cabin or going to the control panel.

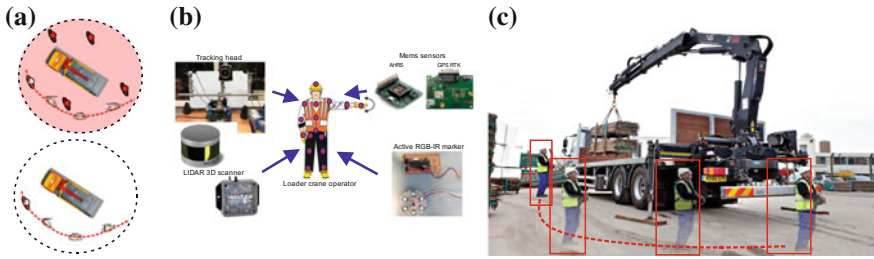
Problems of development control interfaces and support systems for cranes are studied in several academic centers. In [1–3], researchers present implementation of augmented reality interactive system with voice control for loader cranes. In addition, to present the main principles of the system they focused on intelligent voice interface. The system proposed by them allows to use voice commands and even natural language to control the crane. However, in [4] method using simple gestures, recognized by the Microsoft Kinect sensor for controlling loader crane has been proposed. In [5, 6], researchers presented a different approach to controlling loader crane. They used augmented reality and environment scanning (using stereovision and structural light). Also, cranes manufacturers are continuously improving their control systems. In 2016 Hiab introduced a HiVision control system for forestry cranes. The system allows the operator to see all around the crane without leaving the cabin. This effect was achieved by using a 270 degrees' field of view camera mounted on the boom and augmented reality helmet Oculus Rift used by the crane operator. A review of the available literature, especially works about the systems for monitoring the loader crane working area or tracking operator position using sensor-fusion has shown that there is little work on this subject.

Therefore, following the trends of the dynamically growing markets with the Cargotec company, it was decided to develop a modern control and monitoring system for loader crane (Fig. 1).

The proposed system is designed to allow tracking the operator's position in real time and controlling the crane using gestures. The system described in this article involves the use of real-time depth information about the environment around the crane. The developed system will consist of many sensors. That sensor-fusion system for the loader crane uses operator tracking head with two RGB cameras and two NIR cameras, a thermal imager, active LED markers, AHRS and GPS sensors, and a LIDAR scanner. The algorithm proposed in this work is part of a subsystem which uses LIDAR scanner to monitor the working area of the loader crane.

After analyzing the literature [7–9] it was decided to use a depth laser scanner Velodyne LIDAR VLP-16. The depth points generated by the sensor will be used





**Fig. 1** Concept of control and monitoring system for loader crane. **a** Unauthorized intrusion detection, **b** sensor-fusion concept, **c** real-time operator tracking

for monitoring the crane working area and tracking operator. For this purpose, it is necessary to perform conversion and segmentation of the received data. Segmentation is difficult because the VLP-16 is the lowest scanner model offered by Veldyne. Therefore, point cloud obtained from the scan is sparse (low resolution). The algorithm proposed in this work uses LIDAR scanner to monitor the working area of the loader crane. The main aim of this subsystem is the segmentation of loader crane working area, monitoring movements in the area, tracking the operator’s position, and allow to map crane environment in virtual reality. The applied algorithm analyzes sixteen points from each VLP-16 sensor scan. Points are projected onto the YZ plane. After received full 360 scans, the ground points are filtered based on dot product and the ground plane is fitted using RANSAC algorithm. Next segmentation based on angle threshold between points using breadth-first search (BFS) method for determine neighborhood is performed.

The rest of paper is organized as follows. In the next paragraph, the previous works on the sparse LIDAR data problem have been discussed. Then the Velodyne VLP-16 scanner and the method of data reading and interpretation received has been described. In Sect. 4 proposed ground filtration and segmentation algorithm were described. Finally, a conclusion of this paper and an outline of the future work are given in Sect. 5.

## 2 Related Work

Data obtained from various types of depth sensors are usually represented by point cloud-oriented in three-dimensional space. Segmentation objects form 3D points clouds is a relatively well-researched topic. In a lot of works, researchers are focused on the offline segmentation of large cloud points. These segmentation methods have been used on different data such as 3D range sensors or 2D lasers in push-broom mode. However, for this study, particularly interesting was methods for real-time sparse data segmentation, customized to scanners providing 360-degree data in one scan. Segmentation methods, appropriate to the task discussed in this

article can be divided into three groups. The first group segmentation techniques are focused on data segmentation in a 3D domain. In these methods, the entire space must be divided into small cubes called Voxels, that form the grid [10, 11]. Then, using methods such as RANSAC [12], GP-INSAC [13], PROSAC [14] or different varieties of the nearest-neighbor algorithm, algorithms for detecting sophisticated features for data segmentation. Feature-based methods, although allow for accurate segmentation large cloud points, are often very complex and computationally intensive, thus not suitable for real-time applications. Furthermore, the best results are achieved for density depth data.

Methods from the second group focus on the projection of 3D point cloud to the 2D plane (most commonly ground plane) divided with the special grid (squares or circles) [15]. These methods are fast and can be used for real-time tasks, but have a tendency to under-segmentation (multiple objects can be grouped as one). This error often occurs, when objects are close to each other or grid parameters are mismatched.

The third group of segmentation methods uses only the raw depth data, i.e., measured distance from the sensor to objects. These data are presented on range images, wherein the intensity of the point indicates the distance from the sensor. Then, using the relations between points or small point groups segmentation is performed. Compared to other methods, this approach is most effective for applications requiring segmentation in real time. Performance boost in these methods is achieved using only one parameter. No raw data conversion to the point cloud or grid discretization is required. After the literature review, method from third group presented in [16], was used in the application described in this article. Selected method is optimized for segmentation sparse data (low resolution) from LIDAR sensor in real time and will be shortly described in next section.

In all described methods, ground plane should be removed before segmentation. Single ground points or sets of points generate errors during segmentation. Removing these points simplify segmentation process. Simple methods of removing ground plane, classify all points below a certain height as ground points. However, these approaches do not work well for rough ground because they can misclassify points near the ground.

### 3 LIDAR Scanner

Laser distance sensors, LIDAR (Light Detection and Ranging) measures distance by illuminating a target with a laser and analyzing the reflected light. Due to the decreasing price and improving measurement parameters they gain more and more popularity. LIDAR sensors are used in many applications: autonomous cars [17], robots [18], drones [19], submarines [20]. Control systems of these devices are suitable to analyze the environment [21, 22], recognize the human bodies [23], recognize objects and obstacles [24], or even find the right paths [25]. In all these applications, proper segmentation and classification based on sensor data are crucial.

In the segmentation process, typically the first step is filtration of ground points. The result of this process has a direct impact on the classification results. Used in the described system VLP-16 scanner is the third generation of laser scanners produced by Velodyne. The scanner is composed of 16 individual laser-detector pairs which are individually aimed in 2-degree increments on the laser head. That sensor configuration provides a 30° field of view (−15° to 15°), which results in 300,000 depth points per second. Based on research conducted at the University of Houston [26], where researchers evaluate the sensor for long-term stability, geometric calibration and the effect of temperature variations. We can conclude that the information about sensor accuracy for the factory calibration is true (±30 mm). Moreover, after the local calibration is even possible to increase the sensor accuracy to ±10 mm. The raw data from VLP-16 is in the standard 3D polar coordinate  $(\rho_i, \theta_i, \gamma_i)$ , where  $\rho_i$  is a spatial distance from the sensor to a point,  $\theta_i$  and  $\gamma_i$  are the horizontal and vertical angle with respect to the sensor coordinate system. To represent sensor readings in Cartesian coordinate as a set of points  $(x_i, y_i, z_i)$  in space is necessary to convert the received data considering the position of the laser sensor pairs and the current head position (encoder measurement). Conversion from polar coordinates to cartesian coordinates are calculated based on the simplified Eq. (1).

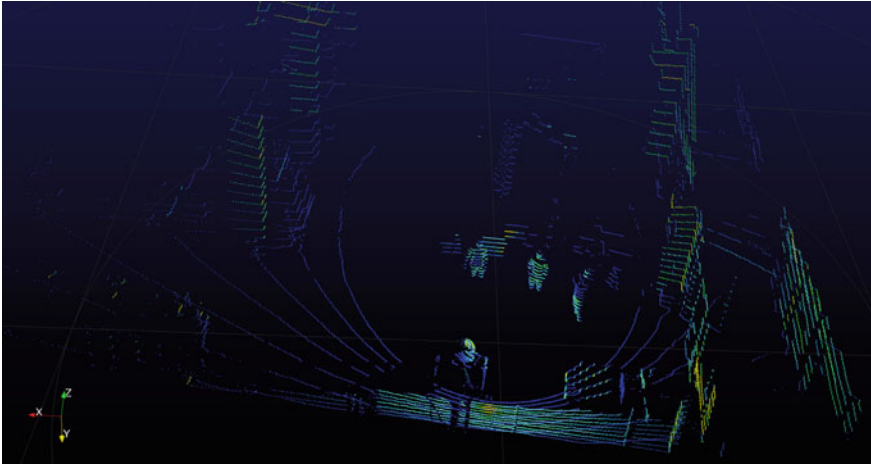
$$r^s - \begin{bmatrix} (s^i * \rho_i + D_o^i) * \cos(\gamma_i) * [\sin(\theta_i) * \cos(\beta_i) - \cos(\theta_i) * \sin(\beta_i)] \\ -H_o^i * [\cos(\theta_i) * \cos(\beta_i) + \sin(\theta_i) * \sin(\beta_i)] \\ (s^i * \rho_i + D_o^i) * \cos(\gamma_i) * [\cos(\theta_i) * \cos(\beta_i) + \sin(\theta_i) * \sin(\beta_i)] \\ -H_o^i * [\sin(\theta_i) * \cos(\beta_i) - \cos(\theta_i) * \sin(\beta_i)] \\ (s^i * \rho_i + D_o^i) * \sin(\gamma_i) + V_o^i \end{bmatrix} \quad (1)$$

where

- $s^i$  distance scale factor
- $D_o^i$  distance offset
- $\beta_i$  horizontal rotation correction
- $H_o^i$  horizontal offset from scanner frame origin
- $V_o^i$  vertical offset from scanner frame origin
- $\gamma_i$  vertical rotation correction (vertical sensor position)
- $\rho_i$  raw distance measurement (encoder readings)
- $\theta_i$  encoder angle measurement (spatial distance from sensor).

$$\begin{cases} x_i = \rho_i \cos(\gamma_i) \sin(\theta_i) \\ y_i = \rho_i \cos(\gamma_i) \cos(\theta_i) \\ z_i = \rho_i \sin(\gamma_i) \end{cases}$$

The simplification is allowed because the first six parameters of the equation are internal sensor calibration constants. These constants are defined by the manufacturer during the production calibration process of the device at the production stage. Only the last two parameters  $(\rho_i, \theta_i)$  that are measured by the sensor in real time

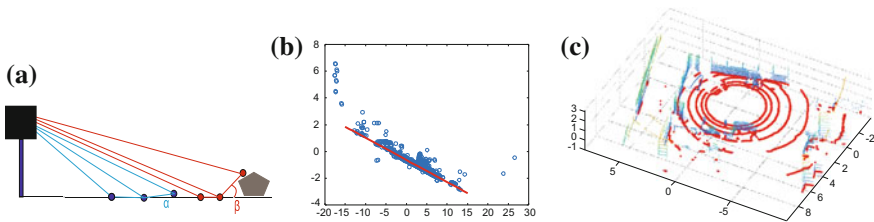


**Fig. 2** Loader crane working area scanned by VLP-16 sensor

determine the location of points in space. If the constant of Eq. (1) will be ignored, the equation will be simplified. The final equation (Eq. 2) for each of the coordinates and their geometric representation are shown in Fig. 4c. Figure 2 shows the points cloud obtained after converting raw data from the sensor. Sparse lines visible on image are caused by only 16 laser sensors in VLP-16. Despite the low resolution in Fig. 2 are clearly visible: three human bodies, loader crane, room walls and other environment elements (hydraulic pump, test stand).

## 4 Ground Filtration and Segmentation Algorithm

In this study, the loader crane working area shown in Fig. 3 has been scanned and segmented. The aim of the experiment was the segmentation of the environment, with emphasis on human bodies. During the experiment, the sensor VLP-16 and modified algorithm developed by Bogoslavskyi and Stachniss [16] were used.

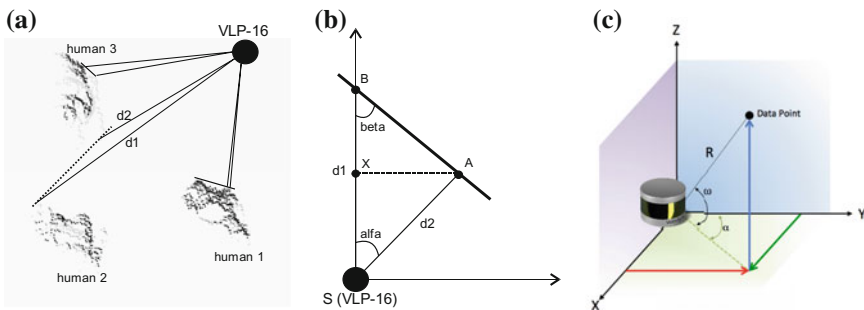


**Fig. 3** A graphic algorithm explanation ground filtering algorithm. **a** Vector dot product, **b** RANSAC model fitting, **c** filtration results

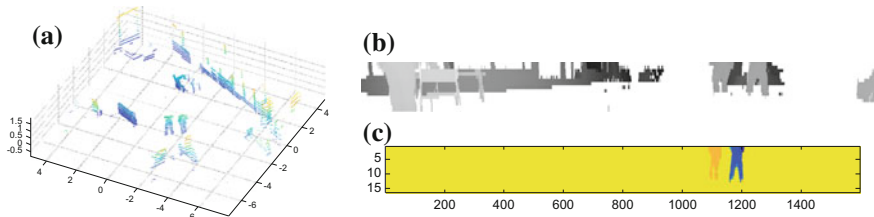
The algorithm was divided into several stages. In the first stage, ground plane was removed. The algorithm that we propose to filtrate ground points is similar to the solutions presented in the work [10, 13, 17]. However, in our solution we use dot product of vectors (Fig. 3a) as well as interpolation using the RANSAC method (Fig. 3b). In the presented algorithm, we analyze a single scan from 16 laser sensors. Then the points are projected onto the YZ plane. Starting with the point with the smallest value of the Z coordinate, we create two vectors from three successive points. If the angle between the vectors DE and EF is zero, the points are probably lying on the ground plane. To determine this condition, we use dot product of the DE and EF vectors whose value should be close to 1. In the next step, we select points D, F, G. That operation is repeated until all points have been analyzed. Since each point is involved in computing the scalar product of vectors, three times we store all three values in the array. This helps to avoid misclassifying points near obstacles or if the terrain is uneven because the threshold is based on two maximum values from dot product array. In addition, the use of this matrix allows to extract the edges of the image, i.e., the place where obstacles or walls begin. Additionally, to avoid the detection of walls as a ground plane, the thresholds for differences in X coordinate are observed. The last step in the algorithm is to determine the ground plane. For this purpose, we used the RANSAC method. The linear function is fitted to the filtered ground points projected on the plane YZ.

The next step is segmentation the non-ground points from the cloud. The used algorithm has been described in [13] in detail. Moreover, the principle of its operation was graphically illustrated in Fig. 4a, b, where the part of a scene from Fig. 2 has been analyzed. Figure 4a shows a view of 3 persons (top-view) with marked laser beams coming from the sensor VLP-16, Fig. 4b explains a geometrical interpretation of Eq. (3).

$$\beta = \frac{\arctan AX}{XB} = \frac{\arctan(d_2 \sin(\alpha))}{d_1 - d_2 \cos(\alpha)} \tag{3}$$



**Fig. 4** a, b Graphic algorithm explanation based on the part of scene from Fig. 2, c geometric interpretation of VLP-16 polar coordinates to X, Y, Z coordinates conversion



**Fig. 5** Segmentation results, **a** 3D data, **b** depth map, **c** segmentation results

Based on Eq. (3), angle  $\beta$  between points was calculated. That angle determines if the point is a part of object. (label) The threshold value for angle  $\beta < 10^\circ$  was established during the research. Every point below  $10^\circ$  was assigned to the new object. The same thresholding (based on  $\beta$  angle) can be performed by projecting points on the other two planes  $X$ - $Y$ . To determine the neighborhood of the points with the same labels, breadth-first search method was used. After tests with another 3D data set (Fig. 5a) transformed to depth map (Fig. 5b), bodies of two people were detected (Fig. 5c). The developed algorithm had problems with segmentation when the distance between objects was less than 150 mm. Then the two objects were classified into one. The application was run on a PC with a processor i7 4700K and 8 GB of ram memory. On this hardware and poorly optimized code in MATLAB segmentation frequency of 50 Hz was achieved. Because the movement speed of the crane is not high, that value is reasonable.

## 5 Conclusions

In this article, a method for real-time scanning and segmentation of the loader crane working area using LIDAR system had been presented and implemented. Assessed the performed studies it can be stated, that both the LIDAR scanner and the proposed method are appropriate for real-time monitoring loader crane working area. The algorithm used in our approach allows the correct segmentation and separation of human bodies, using sparse depth data from VLP-16. Despite the problems with the segmentation of objects which are close to each other, the proposed approach should be regarded as promising. After algorithm optimization and applying thresholding (based of the angle  $\beta$ ) in all three dimensions ( $XYZ$ ), the effectiveness of the method should increase. Using a large number of sensors or sensors with higher resolution (HDL-32 or HDL-64) is another way to improve the system. As a part of further research the system is planned to expand with several algorithms: motion detection in crane operation area, operator tracking, and identification. In addition, it is planned to implement simple safety features that will detect potential collisions of transferred cargo with surrounding elements.

**Acknowledgements** The work was carried out as part of PBS3/A6/28/2015 project, “The use of augmented reality, interactive voice systems and operator interface to control a crane”, financed by NCBiR.

## References

1. Majewski, M., Kacalak, W.: Smart control of lifting devices using patterns and antipatterns. In: Silhavy, R., Senkerik, R., et al. (eds.) *Artificial Intelligence Trends in Intelligent Systems: Proceedings of the 6th Computer Science On-line Conference (CSOC)*, vol. 1, pp. 486–493. Springer, Berlin (2017)
2. Majewski, M., Kacalak, W.: Human-machine speech-based interfaces with augmented reality and interactive systems for controlling mobile cranes. In: Ronzhin, A., Rigoll, G., Meshcheryakov, R. (eds.) *Interactive Collaborative Robotics, 1st International Conference, ICR*, 89–98. Springer, Berlin (2016)
3. Majewski, M., Kacalak, W.: Innovative intelligent interaction systems of loader cranes and their human operators. In: Silhavy, R., Senkerik, R., et al. (eds.) *Artificial Intelligence Trends in Intelligent Systems, Proceedings of the 6th Computer Science On-line Conference (CSOC)*, vol. 1, pp. 474–485. Springer, Berlin (2017)
4. Pietruszewicz, K., Miądlicki, K.: Gestures can control cranes. *Control Eng.* **61**(2), 14 (2014)
5. Westerberg, S., Manchester, I.R., Mettin, U., Hera, P.L., Shiriaev, A.: Virtual environment teleoperation of a hydraulic forestry crane. In: *IEEE International Conference on Robotics and Automation*, pp. 4049–4054 (2008)
6. Westerberg, S., Shiriaev, A.: Virtual environment-based teleoperation of forestry machines: designing future interaction methods. *J. Hum. Robot Interact.* **2**(3), 84–110 (2013)
7. Horaud, R., Hansard, M., Evangelidis, G., Menier, C.: An overview of depth cameras and range scanners based on time-of-flight technologies. *Mach. Vis. Appl.* **27**(7), 1005–1020 (2016)
8. Blais, F.: Review of 20 years of range sensor development. *J. Electr. Imaging Rev.* **13**(1), 231–243 (2004)
9. Panda, S.S., Rao, M.N., Thenkabail, P.S., Fitzgerald, J.E.: *Remote Sensing Systems-Platforms and Sensors: Aerial, Satellite, UAV, Optical, Radar, and LiDAR (Remotely Sensed Data Characterization, Classification, and Accuracies)*, pp. 3–57. CRC Press-Taylor & Francis Group, Boca Raton (2016)
10. Himmelsbach, M., Luettel, T., Wuensche, H.J.: Real-time object classification in 3D point clouds using point feature histograms. In: *IEEE/RSJ International Conference on Intelligent Robots and Systems*, pp. 994–1000 (2009)
11. Himmelsbach, M., Hundelshausen, F.v., Wuensche, H.J.: Fast segmentation of 3D point clouds for ground vehicles. *Intell. Vehicles Symp. (IV)*, 560–565 (2010) (IEEE)
12. Meng, X., Cao, Z., Zhang, L., Wang, S., Zhou, C.: A slope detection method based on 3D LiDAR suitable for quadruped robots. In: *12th World Congress on Intelligent Control and Automation (WCICA)*, pp. 1398–1402 (2016)
13. Chen, T., Dai, B., Liu, D., Zhang, B., Liu, Q.: 3D LIDAR-based ground segmentation. In: *1st Asian Conference on Pattern Recognition*, pp. 446–450 (2011)
14. Meng, X., Zhou, C., Cao, Z., Zhang, L., Liu, X., Wang, S.: A slope location and orientation estimation method based on 3D LiDAR suitable for quadruped robots. In: *IEEE International Conference on Robotics and Biomimetics (ROBIO)*, pp. 197–201 (2016)
15. Yin, H., Yang, X., He, C.: Spherical coordinates based methods of ground extraction and objects segmentation using 3-D LiDAR sensor. *IEEE Intell. Transp. Syst. Mag.* **8**(1), 61–68 (2016)

16. Bogoslavskiy, I., Stachniss, C.: Fast range image-based segmentation of sparse 3D laser scans for online operation. In: IEEE/RSJ International Conference on Intelligent Robots and Systems (IROS), pp. 163–169 (2016)
17. Petrovskaya, A., Thrun, S.: Model based vehicle detection and tracking for autonomous urban driving. *Auton. Robots* **26**(2–3), 123–139 (2009)
18. Lima, T.A., Forte, M.D.d.N., Nogueira, F.G., Torrico, B.C., Paula A.R.d.: Trajectory tracking control of a mobile robot using lidar sensor for position and orientation estimation. In: 12th IEEE International Conference on Industry Applications (INDUSCON), pp. 1–6 (2016)
19. Haag, M.U.d., Bartone, C.G., Braasch, M.S.: Flight-test evaluation of small form-factor LiDAR and radar sensors for sUAS detect-and-avoid applications. In: IEEE/AIAA 35th Digital Avionics Systems Conference (DASC), pp. 1–11 (2016)
20. McLeod, D., Jacobson, J., Hardy, M., Embry, C.: Autonomous inspection using an underwater 3D LiDAR. In: OCEANS, pp. 1–8 (2013)
21. Opromolla, R., Fasano, G., Rufino, G., Grassi, M., Savvaris, A.: LIDAR-inertial integration for UAV localization and mapping in complex environments. In: International Conference on Unmanned Aircraft Systems (ICUAS), pp. 649–656 (2016)
22. Dewan, A., Caselitz, T., Tipaldi, G.D., Burgard, W.: Motion-based detection and tracking in 3D LiDAR scans. In: IEEE International Conference on Robotics and Automation (ICRA), pp. 4508–4513 (2016)
23. Shackleton, J., VanVoorst, B., Hesch, J.: Tracking People with a 360-degree LIDAR. In: 7th IEEE International Conference on Advanced Video and Signal Based Surveillance (AVSS), pp. 420–426 (2010)
24. Han, J., Kim, D., Lee, M., Sunwoo, M.: Enhanced road boundary and obstacle detection using a downward-looking LIDAR sensor. *IEEE Trans. Veh. Technol.* **61**(3), 971–985 (2012)
25. Kim, J.K., et al.: Experimental studies of autonomous driving of a vehicle on the road using LiDAR and DGPS. In: 15th International Conference on Control, Automation and Systems (ICCAS), pp. 1366–1369 (2015)
26. Glennie, C.L., Kusari, A., Facchin, A.: Calibration and stability analysis of the VLP-16 laser scanner. *Int. Arch. Photogramm. Remote Sens. Spatial Inf. Sci.* **XL-3/W4**, 55–60 (2016)



# Optimization of the Movement Trajectory of Mobile Crane Working Elements

Wojciech Kacalak, Zbigniew Budniak and Maciej Majewski

**Abstract** The article presents simulation testing of the optimization of the cargo trajectory in the mobile crane handling system, whose purpose was to determine the function that minimizes the total length of the path, and thus an increase of efficiency, with stability conditions being maintained. In order to perform a movement analysis and an optimization of the handling assignment, a parametric crane system model built and a simulation model developed in the integrated CAD/CAE environment were used.

**Keywords** Crane safety · Mobile crane · Crane stability · Trajectory optimization

## 1 Introduction

When planning the movement trajectory, safe and fast transport of the cargo, one needs to ensure that the planned points of the path, including the accuracy of the final positioning of the cargo, are reached. It is important that at the same time the minimization of the path length of the cargo transported and the minimization of the handling assignment time are ensured.

Defining of the load transport trajectory is always done taking into account the stability of the crane and of the environment where it works. This is due to the fact that transporting large loads with mobile truck cranes may, in certain condition, lead to the loss of stability [1–9]. The needs of an absolute fulfilment of stability conditions and the requirement of collision free movement forces one to use various bypass paths, which frequently eliminates the geometrically shortest path.

The study presents simulation testing of the optimization of the mobile crane handling system cargo trajectory based on the methodology developed with the use of a simulation model built in the integrated CAD/CAE environment. The model

---

W. Kacalak (✉) · Z. Budniak · M. Majewski  
Faculty of Mechanical Engineering, Koszalin University of Technology,  
Raclawicka 15-17, 75-620 Koszalin, Poland  
e-mail: wojciech.kacalak@tu.koszalin.pl

proposed consists of the main crane assemblies coupled together: the truck with outrigger system and the base, the slewing column, the inner and outer arms, the six-member telescopic boom, the hook with lifting sling and the transported load. In the modelling of the crane system, the masses of the majority of the equipment and the assemblies that load the system were taken into account.

An example of the application of the method proposed to determine an optimal trajectory of the handling assignment being performed was presented as the results of simulation testing.

## 2 Methodology of the Optimization of the Handling Assignment

In the simulation testing of the optimization of the trajectory of the cargo of the handling assignment being performed by the mobile crane, the methodology presented in the following articles [2, 10, 11] was used. The following are the basic elements of the method implemented:

- parametric modelling of the elements and the entire crane system in the CAD system for the defined configuration;
- determination of the system stability conditions (a notation of equations that constitute a mathematical model to calculate the following: the trajectory of the mass centres of the elements of the crane system, the reaction of the base on the crane outrigger system, the stabilizing torque  $M_u$  and the overturning torque  $M_w$ , as well as the safety indicator);
- building of a kinematic model of the crane and carrying out simulation testing in the integrated CAD/CAE system;
- an analysis of the kinematic and dynamic quantities of the crane system during handling in connection with maintaining constant balance (loader crane stability);
- optimization of the trajectory of the displacements of the crane working elements for specified assignments taking limiting conditions into account.

Integrated CAD—SolidWorks software as well as the module for computations and engineering analyses: CAE—SolidWorks Motion was used for the purpose of the modelling and numeric tests of the crane handling system.

## 3 Model of the Handling Crane

The assemblies of the truck crane type HDS HIAB XS (Cargotec Poland) in relation to which the voice control system was proposed [12–15], include the design of all the main parts and sub-assemblies as well as other important elements of the construction [2, 11], shown in Fig. 1.

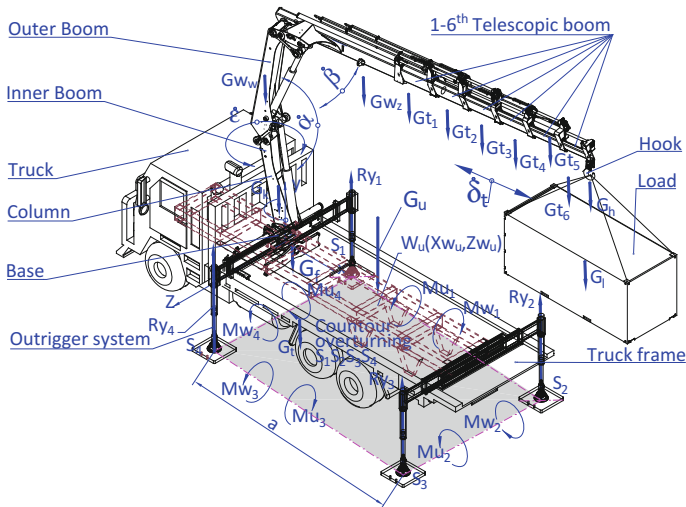


Fig. 1 Handling system of mobile crane type HDS HIAB XS 111

The model of the support system is composed of the following crane assemblies that are coupled together: the truck frame, the outrigger system placed in the crane base frame connected with the frame of the truck chassis, the crane base, the slewing column, the inner and outer boom with the installed six-member telescopic boom and the hook including lifting slings loaded with the transported cargo. All the geometric quantities as well as all the properties of the constructional elements used of the constructional models were entered to the file of the programme in a parametric manner. This manner allows for a complete control of changes to the geometric dimensions of the crane elements. The possibility to select any reciprocal position of the main crane assemblies with a selected accuracy is important, as well.

The modelling takes into account the masses of the elements of the equipment and the assemblies that load the system [2, 11]. A change to the configuration of the crane system is connected with its working movements. An analytical description of the configuration of the crane kinematic system involves strenuous conversions of vector-matrix equations [2], until explicit dependences have been obtained that determine the variable angular and linear quantities. Knowledge of these dependences is very desirable. It needs to be emphasized, however, that it is very difficult to obtain explicit dependences for the crane handling system. The integrated CAD/CAE system was therefore used to determine vectors that specify the configuration of the crane system.

## 4 Kinematic Model of the Handling System

In simulation testing, a kinematic model was used of the mobile crane handling system with four degrees of freedom, which is presented in the following articles [2, 10, 16]. In the kinematic model (Fig. 1):

- mass, whose centre of gravity coincides with the gravity centre of the solid model, was ascribed to the individual elements of the system,
- the geometric dimensions of the elements of the rigging and solid models of the crane are identical.

In the model developed, drives were defined that perform the rotary motion of the crane column with velocity  $\dot{\epsilon}$  and linear drives that force the rotary motion of the inner and outer arms with velocities  $\dot{\alpha}$  and  $\dot{\beta}$  as well as sliding out of the six-member telescopic boom with velocity  $\dot{\delta}t$ .

## 5 Optimization of Cargo Displacement Trajectory

Owing to the performance of simulation testing in line with the methodology proposed and presented in the articles [2, 10, 11], it is possible to determine the optimum trajectory of cargo displacements for a selected handling assignment.

### 5.1 Criteria and Limitations of Optimization

When planning the trajectory of the movement, safe and fast transport of the cargo, one needs to ensure that the planned points of the path are reached and to ensure the accuracy of the final cargo positioning. It is important to ensure at the same time the minimization of the path length of the cargo transported and of the execution time of the handling assignment. In a general case, the optimization problem consisted in seeking the vector of decision variables, for which the defined objective function reaches the minimum:

$$\min L_l = f(x)_t \quad (1)$$

where:

- $L_l$  path length of the cargo transported,
- $x$  vector of decision variables that contains the configuration parameters of the crane handling system [2],
- $t, s$  handling assignment cycle time.

The length of path  $L_l$  was calculated from the following formulas (2) and (3):

$$L_l = \sum_{j=0}^{n-1} (L_{j-1} + \Delta L_j) \tag{2}$$

$$\Delta L_j = \sqrt{(x_{L_j} - x_{L_{j-1}})^2 + (y_{L_j} - y_{L_{j-1}})^2 + (z_{L_j} - z_{L_{j-1}})^2} \tag{3}$$

where:

$\Delta L_j$  increment of the path of the cargo transported in time  $\Delta t$ ,  
 $x_{L_j}, y_{L_j}, z_{L_j}$  current coordinates of the cargo location.

The developed crane simulation model and numerical applications were used for the calculations. Inequality constraints were imposed on the decision variables. They follow from the stability conditions of the crane system (Fig. 1), which are as follows:

1. According to international standards [17] and PN [18] it is accepted that the crane is stable if at any position of the boom loaded with lifting capacity with an adequate extension, the stabilizing torque  $M_u$  is greater than the overturning torque  $M_w$  by the value of  $\Delta M$  (4):

$$\Delta M = M_u - M_w > 0 \tag{4}$$

2. The value of the pressure on the base of the least loaded crane support and the value of the changes of this force in time [1, 11, 19];
3. The location of the symmetric mass centre of the handling system of the crane in relation to the support points [1, 2]. The system is stable if, in the projection on the horizontal plane, the mass centre is located inside the quadrangle that is established by the support points of the crane outrigger system;
4. Safety indicator  $W_b$  as the stability criterion of the crane system, which was defined as (5):

$$W_b = \min \in \left\{ \frac{\min(Ry_i)_t}{G_u \cdot k_1 \cdot (1 - k_2)} - \frac{k_2}{1 - k_2} \right\}_t \tag{5}$$

where:

$i = 1-4$  number of the outrigger,  
 $j$  number of the elementary fragment of the trajectory,  
 $\min(Ry_i), \text{ kN}$  the smallest of the vertical reactions of the base on the outrigger  $i$ ,  
 $G_u, \text{ kN}$  total weight of the crane system,  
 $k_1$  index of the maximum load of the crane outrigger,  
 $Ry_{\max} = G_u \cdot k_1$ , where:  $k_1 \leq 0.25$ —for a crane with four outriggers,

- $k_2$  index that determines the minimum load of the crane outrigger,  $Ry_{\min} = G_u \cdot k_2$ ,
- $t, s$  time of the working cycle of the handling assignment.

In order to guarantee the stability of the crane system, the value of the indicator  $W_b$  should be greater than zero when  $\min (Ry_i) > k_1 \cdot k_2$ . The value of the indicator  $k_2$  is determined considering safety on the level that depends from the crane working conditions. It was accepted that the value of this index takes into account the wind speed as well as the velocities, accelerations and pulls in the crane kinematic pairs. Pulls may be the result of the cargo frozen to the ground being torn off, the cargo being broken off, sudden breaking, hitting an obstacle etc.

### 5.2 Optimization Assignment

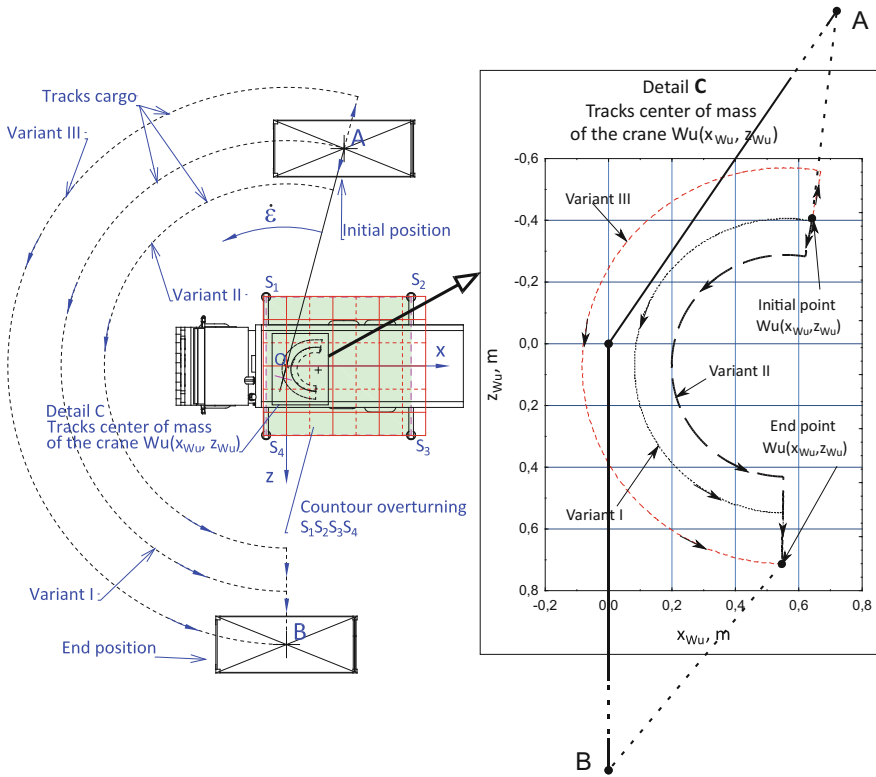
Optimization of the handling task was performed for an example mobile crane type HDS HIAB XS 111. The configuration of the movement of the working mechanisms of the crane during the execution of the three variants of the handling assignment is presented in Table 1, where the denotations of the location parameters were accepted according to Fig. 1. The cargo located in position A was to be transported and positioned in location B (Fig. 2).

The integrated CAD/CAE system with an additional computational application was used in simulation testing, which permitted the following among others:

- an accurate determination of the coordinates of any point of the crane system based on the mathematical model that describes its configuration—[2],
- establishing the trajectory of the gravity centre of the crane  $W_u(x_{Wu}, z_{Wu})$ ,
- calculation of the path length of the cargo transported,
- calculation of the reaction in the outriggers ( $Ry_1, Ry_2, Ry_3, Ry_4$ );  $Ry_i = f\{G_l, W_u(x_{Wu}, z_{Wu}), t\}$ —[11],
- calculation of the difference of the torques  $\Delta M = M_u - M_w = f\{G_l, W_u(x_{Wu}, z_{Wu}), t\}$ ,
- calculation of the safety indicator  $W_b = f\{G_l, W_u(x_{Wu}, z_{Wu}), t\}$ ,

**Table 1** Parameters of sequential movements for three variants of handling assignment

Movement sequence	1st variant of cargo displacements (I)	2nd variant of cargo displacements (II)	3rd variant of cargo displacements (III)
1	$\Delta = 7.2$	$\Delta = 7.2$	$\Delta = 7.2$
2	$\Delta\varepsilon = -189^\circ$	$\Delta\delta t = -1.5$ m	$\Delta\delta t = 2.1$ m
3	$\Delta\delta t = 2.1$ m	$\Delta\varepsilon = -189^\circ$	$\Delta\varepsilon = -189^\circ$
4	$\Delta = -5.2^\circ$	$\Delta\delta t = 3.6$ m	$\Delta = -5.2^\circ$
5	–	$\Delta = -5.2^\circ$	

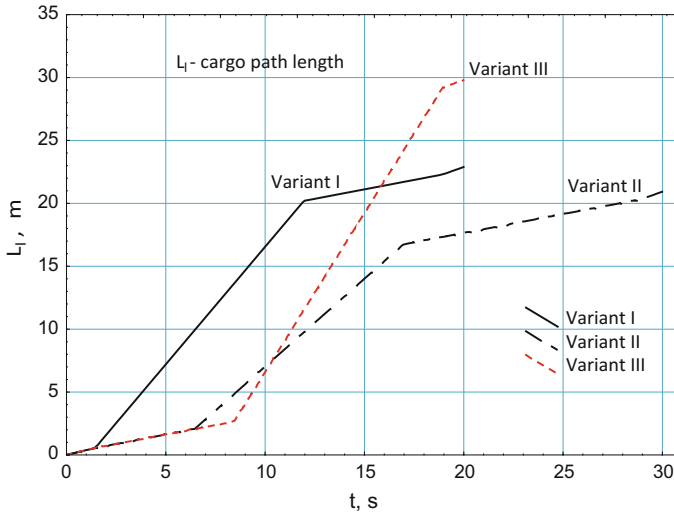


**Fig. 2** Handling assignment consisting in carrying the cargo from its initial position A to position in point B, for three displacement variants

- determination of the values of the working loads and the crane lift curves,
- determination of the crane stability conditions in the function of its working load and extension,
- evaluation of the stability of the performance of the entire loader crane handling cycle,
- optimization of the movement trajectory of the crane working elements for the accepted optimization criterion  $\min L_l$ .

### 5.3 Simulation Testing Results

Simulation testing results are presented in Fig. 3 which presents changes in the cargo paths for the three variants of the handling assignment. Variant II, for which  $L_l = 20.92$  m, is the most optimal solution from the perspective of the minimization of the path length of the cargo transported. In this variant, in spite of the shortest



**Fig. 3** Change of cargo path length for three handling assignment variants

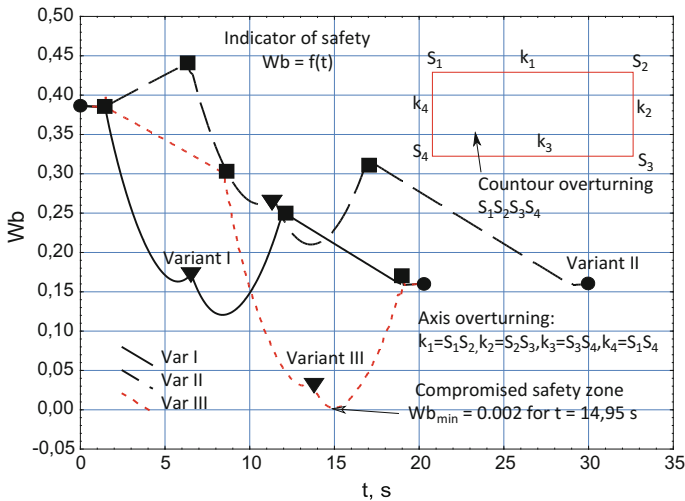
path length, the execution time of the handling assignment takes as much as 29.92 s; therefore, it is substantially longer than for variant I. Hence, variant I is an alternative solution, where the cargo path length is  $L_l = 22.89$  m, the execution time of the handling assignment is only 19.99 s, and it is significantly shorter than in variant II.

The inequality constraints imposed in the optimization task that follow from the crane stability conditions are fulfilled. This is confirmed with the graphs presented in Figs. 2 and 4.

The trajectories presented in Fig. 2 that are determined by the gravity centres  $W_u(x_{Wu}, z_{Wu})$  of the crane system are located inside the tip-over outline  $S_1S_2S_3S_4$  (detail C); hence, stability conditions are met.

This is confirmed by the courses of the formation of the value of the safety indicator  $W_b$  that are presented in Fig. 4. It is evident for the handling assignment example presented that the minimum value of the safety indicator for all of the three cases is greater than 0; hence, the crane system is stable over the whole range. For the third variant of the handling assignment, however, the value of this indicator  $W_b = 0.002$  is very small. This means that for the trajectory of the load carried  $\tau_H$  the working conditions are the least favourable as there is a risk of a loss of the crane system stability.





**Fig. 4** Courses of the value of the safety indicator  $W_b$  for the three variants of the handling assignment, where: filled circle—start and end of movement, filled square—start and end of circular motion, inverted filled triangle—change of the tip-over axis from  $k_1$  to  $k_4$

## 6 Conclusion

The article presents the use of the optimization method of the cargo trajectory of the mobile crane handling system, whose purpose was to determine a function to minimize the total path length, and thereby to increase the efficiency while maintaining stability conditions. The fact needs to be emphasized in the method presented that modern CAD/CAE computer technologies were used on the example of a mobile crane type HDS HIAB XS 111.

Owing to the results of numerical simulation that meet stability conditions, it is possible to determine the optimum trajectory of the cargo displacements for the selected handling assignment. The use of the corrections of the displacements of the moving elements of the crane may prevent the outriggers from being broken off, and hence it allows fully safe operation in any conditions.

The method developed may prove to be useful in the optimization of the trajectory of the handling task performed. In optimization procedures, where the minimization of the path or handling time is the objective function, the values that determine the crane stability are constraining conditions. In another case, when the maximisation of  $W_b$  index is the objective function, the constraining conditions are related to the execution time of the assignment or the path length of the cargo.

**Acknowledgements** This project is financed by the National Centre for Research and Development, Poland (NCBiR), under the Applied Research Programme—Grant agreement No. PBS3/A6/28/2015.

## References

1. Janusz, J., Kłosiński, J.: Influence of the selected control strategies of mobile crane motions on its stability. *Acta Mech. Autom.* **10**(2), 74–80 (2010)
2. Kacalak, W., Budniak, Z., Majewski, M.: Crane stability for various load conditions and trajectories of load translocation. *Mechanik* **12**, 1820–1823 (2016)
3. Posiadała, B., Waryś, P., Cekus, D., Tomala, M.: The dynamics of the forest crane during the load carrying. *J. Struct. Stab. Dynam.* **13**(7), 1340013 (2013)
4. Posiadała, B., Waryś, P.: Modeling and simulation research of forest crane in operating cycle. *Model. Eng.* **10**(41), 331–338 (2011)
5. Rauch, A., Singhose, W., Fujioka, D., Jones, T.: Tip-over stability analysis of mobile boom cranes with swinging payloads. *J. Dyn. Syst. Meas. Contr.* **135**(3), 031008 (2013)
6. Aneziris, O.N., et al.: Towards risk assessment for crane activities. *Saf. Sci.* **46**(6), 872–884 (2008)
7. Sochacki, W.: The dynamic stability of a laboratory model of a truck crane. *Thin Walled Struct.* **45**(10–11), 927–930 (2007)
8. Kłosiński, J., Janusz, J.: Control of operational motions of a mobile crane under a threat of loss of stability. *Solid State Phenom.* **144**, 77–82 (2009)
9. Lei, Z., Taghaddos, H., Han, S., Bouferguene, A., Al-Hussein, M., Hermann, U.: From AutoCAD to 3ds Max: an automated approach for animating heavy lifting studies. *Can. J. Civ. Eng.* **42**(3), 190–198 (2015)
10. Kacalak, W., Budniak, Z., Majewski, M.: Simulation model of a mobile crane with ensuring its stability. *Model. Eng.* **29**(60), 35–43 (2016)
11. Kacalak, W., Budniak, Z., Majewski, M.: Support system reactions in the assessment of mobile crane stability. *Buses Tech. Exploit. Trans. Syst.* **12**, 1014–1019 (2016)
12. Majewski, M., Kacalak, W.: Intelligent speech interaction of devices and human operators. *Adv. Intell. Syst. Comput.* **465**, 471–482 (2016)
13. Majewski, M., Kacalak, W.: Intelligent speech-based interactive communication between mobile cranes and their human operators. *Lect. Notes Comput. Sci.* **9887**, 523–530 (2016)
14. Majewski, M., Kacalak, W.: Building innovative speech interfaces using patterns and antipatterns of commands for controlling loader cranes. *IEEE Xplore Digital Library*, pp. 525–530 (2016)
15. Majewski, M., Kacalak, W.: Smart control of lifting devices using patterns and antipatterns. *Adv. Intell. Syst. Comput.* **573**, 486–493 (2017)
16. Herbin, P., Pajor, M.: Modeling direct and inverse kinematics of loading crane with redundant degrees of freedom structure using Matlab. *Model. Eng.* **27**(58), 44–50 (2016)
17. ISO 4305:2014: Mobile cranes—determination of stability
18. PN-ISO 4305:1998: Mobile cranes—determination of stability
19. Rupa, D., Hladnik, J., Jerman, B.: Loader crane inertial forces. *FME Trans.* **44**(3), 291–297 (2016)

# Design, Manufacture, and Application of Chamber for the Magnetohydrodynamic Deposition Made of PP

Jeremiasz K. Koper

**Abstract** Magnetohydrodynamic deposition can allow deposition of layers or particles that are difficult or impossible to obtain by other methods. This is related to the presence of additional forces during electrochemical processes. Due to the complexity of the method, it is necessary to properly design and manufacture the chamber with all parameters in mind. The paper presents the design process and the chamber manufacture. It is included a detailed description of the method of 3D printing using PP filament. A test was performed in the chamber, confirm the significant effect of magnetic field on the iron corrosion processes. The silver particles deposited on the surface of the titanium at different magnetic field parameters showed different morphology. Occurrence of the magnetic field has a significant effect on the current density during of silver deposition process.

**Keywords** 3D printing · Polypropylene · Magnetohydrodynamic deposition MHD · Silver nanoparticles · Titanium

## 1 Introduction

Many available coatings and particles deposition techniques such as chemical vapor deposition (CVD), physical vapor deposition (PVD), and plasma enhanced chemical vapor deposition (PECVD) are existing for use on ceramic and metallic substrates [1]. One of the most commonly used methods is deposition of pure metals on conducting surface by electrolytic methods [2]. Various techniques are used to obtain different morphologies and structures of the deposition coating.

An alternative may be the deposition of metals and their particles from the electrolytes by the magnetohydrodynamic method (MHD). In a time of depositing by this method, additional ionic force occurs. This force supports the deposition process according to Lorentz's generally accepted force [3]. This force acts on the

---

J.K. Koper (✉)  
Poznan University of Technology, Poznan, Poland  
e-mail: jeremiasz.koper@put.poznan.pl

moving charge by accelerating it in a direction perpendicular to the current and thus leading to electrolyte mixing. This effect can lead to increased mass transfer during cathode deposition [4, 5]. Another strength is the strength of the field gradient. This is the force acting on paramagnetic ions in regions with high-density magnetic flux and diamagnetic ions in regions with low magnetic flux density [3]. This strength is insignificant in homogeneous magnetic fields, but its effect can counter Lorentz's power when there are high magnetic flux density gradients [6]. Force balancing is expected to be dependent on the concentration of paramagnetic ions in the homogeneous magnetic field and directed toward higher concentration gradients indicating the same direction as the diffusion in the electrolyte [7, 8]. However, some authors indicate that this force has no measurable effect on electrochemical processes [3, 9].

The effect of magnetic field on corrosion of metals such as iron is important for technology. It has been shown that the potential of passivation is lower as for more noble materials. Magnetic field is applied when its flow is perpendicular to the flow of current [10]. Explaining this phenomenon is the effect of MHD powered by the Lorentz Force.

The effect of a constant magnetic field with magnetic induction values ranging from zero to 1 T was investigated in various configurations with respect to the electrode surface [11]. It was observed that the homogeneous magnetic field applied parallel to the surface of the electrodes increased the current density and deposition rate. The obtained results show that the use of homogeneous magnetic field causes changes the kinetics of the deposition of alloys, change in chemical composition of deposited alloys, and their surface morphology as well as changes in crystallographic parameters of alloys [12].

Observations of mass transport measurement were increased by diamagnetic elements ( $\text{Ag}^+$ ,  $\text{Zn}^{2+}$ ,  $\text{Bi}^{3+}$ ) and paramagnetic ( $\text{Cu}^{2+}$ ,  $\text{Ni}^{2+}$ ). Theoretical models of hydrodynamics of magnetic field influence on electrochemical processes have been developed [13]. Microscopic images confirmed magnetohydrodynamic flow in the electrolyte and that it is more intense when the direction of vector ( $B$ ) is parallel to the electrode's working surface than when it is perpendicular to the electrode's working surface [14].

Presented research gives hope to change the dynamics of deposition for metals. It may have a significant impact on the applicability of the produced layers by this method. However, it is necessary to properly design a chamber that enables the deposition of metal in the additional magnetic field.

## 2 Design

*Design chamber assumptions:*

1. Use of electromagnet JARZMO BH-2 with the VoltCraft PS1440 power supply;
2. Magnetic field minimum 1 T;
3. Minimum samples size  $\text{Ø}10$  mm;
4. Possibility of placing samples in a perpendicular and parallel position to the

magnetic field force lines; **5.** Chemical resistant for acid and temperature up to 100 °C; **6.** Electrolyte mixing; **7.** Measurement current density by standard reference electrode through Lugin's capillar; **8.** Volume of chamber minimum 50 ml.

*Design constraints:*

Ad. 1 and 2—Extend of magnets up to a distance of 20 mm give 1 T magnetic field in the working space (measurement by halothrometer ASONIK SMS 102).

Ad. 3 and 4—Maximum extended magnets (20 mm) give a possibility of using 4 mm chamber construction wall. Such maximum wall thickness will allow sample placement perpendicular and parallel position to the magnetic field force lines. 12 mm wide will also allow using a standard reference electrode inside the chamber without the risk of shielding the part.

Ad. 5—due to the aggressive environment and high temperature, the best materials will be PTFE, PP, PE.

Ad 6—due to the presence of a strong magnetic field, it is not possible to mix the electrolyte with a magnetic stirrer. Will be used mechanical stirrer with a blade diameter of Ø45 mm, ChemL and AG20-S. In order to use such a mixer, the design of the electrolysis chamber must be brought out of the working area and extended to the correct dimension.

Ad. 7—designed chamber must be brought out from the opposite side of the stirrer for the reference electrode. Part of the chamber for the reference electrode will be in contact with the rest of the cell space only through a Lugin capillary.

Ad. 8—application of extended space for mixer give more space for electrolyte (<100 ml). Such modification additionally allows easying modify electrolyte in time of experiments.

*Design:*

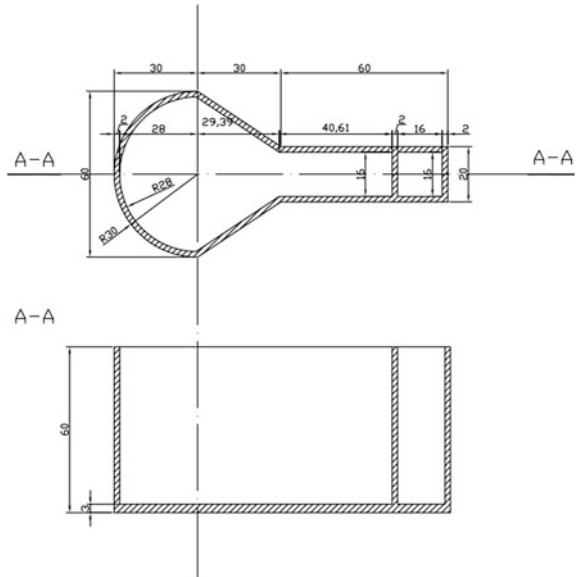
Presented project meet all of the presented design assumptions (Fig. 1). Development of the project in the final version was preceded by the production many models of the chamber. In order to enable the electrolysis of the available manufacturing techniques, the 3D model was designed (Fig. 2).

### **3 Manufacture**

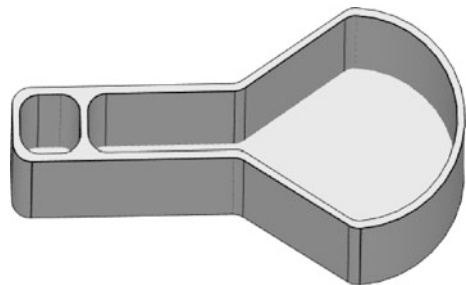
Due to lack of access to raw PTFE material in the form of a 60 mm thick board or a 80 mm shaft, start searching another available material meeting the assumed requirements of chemical resistance.

Another material that meets the requirement is PP. PP is much easier to obtain but slightly worse chemical resistance and much worse temperature resistance, however, in an acceptable range of strength. After consultation with the manufacturer's dealing with the machining of plastic and metal materials, it turned out that shape of the chamber is difficult to perform.

**Fig. 1** Chamber project according to design principles



**Fig. 2** 3D model designed chamber



This has led to change technology from machining to 3D printing. PTFE due to its properties and the high melting temperature is not suitable for 3D printing. 3D printing from PP is also not easy and popular due to the properties of this material but possible. Only one manufacturer in Europe (Filament PM) produce filament from specially modified Polypropylene possible to use in 3D printer [15].

The 3D printing was realized using the MakerBot Replicator 2X machine. This is a machine, which realizes the Fused Deposition Modeling (FDM) process. This process consists in the layered deposition of heated thermoplastic material in form of a filament, fed through a nozzle in an extruder directly on a model table.

The polypropylene filament is a difficult material for the FDM technology, due to its specific mechanical and thermal properties. The main problem during the presented studies was a selection of proper print parameters for this material, to obtain stability of the process, enabling its finishing and obtaining a defect-free product. This was achieved only partially. The following controllable process

parameters decide about the FDM process stability: temperature of material extrusion, temperature of modeling table, speed of extrusion, and head movement and layer thickness.

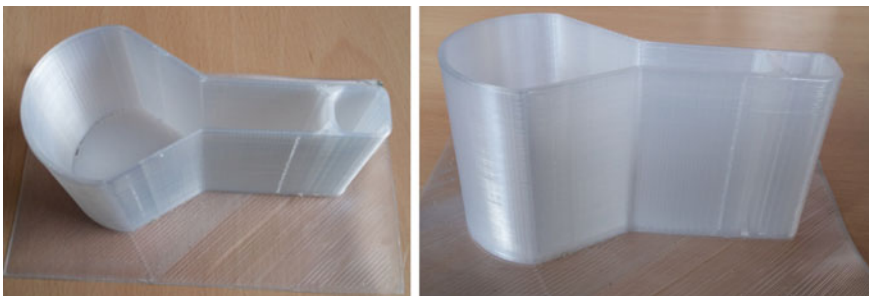
The parameters above were tested in different ranges. The temperature of 220 °C was attempted and proper, continuous extrusion was achieved in the nozzle test mode (launched in the machine control panel by use of the “Load” command, which activates material feeding and heating process without a table and head movement).

The speed of extrusion and head movement was initially set as a standard for the ABS material, which is 40 mm/s for the layer contours and 90 mm/s for the internal filling (infill). This was proven to be not suitable for the PP filament, because of its different properties after heating (polypropylene is much more elastic, so it needs more time to be extruded properly). After a number of experiments by trial & error, this was reduced to 15 mm/s for both contour and infill. This setting significantly increases the time of manufacturing, but any speed higher than 20 mm/s results in holes and other disqualifying material discontinuities present in the final product. The layer thickness was arbitrarily set to 0.3 mm allows to The MakerBot Replicator 2X allows obtaining stable 3D prints.

The table temperature was set between 70 and 110 °C. This parameter decides about sticking the material to the model table. In general, the higher table temperature is recommended for materials with higher processing shrinkage (such as ABS). The recommended temperature for this filament is between 70 and 90 °C. Unfortunately, none of the selected values (5 test prints were made, with the step of 10 °C) ensured proper stability of the 3D print. The most acceptable stability was achieved at 90 °C, so this temperature was selected for the final print (Fig. 3).

The main problems and observations related to the process stability problem while printing out of the PP filament are:

- mechanical properties during layer finishing—closing the layer contour was not possible to do. It is performed by a rapid movement of the machine head, to snap the heated filament; as PP has elongation at break near 500%, so the remaining filament stuck to the nozzle and later caused visual and shape errors;



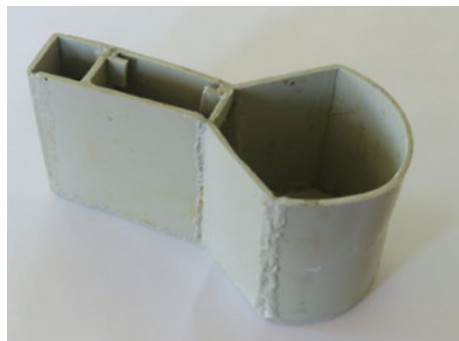
**Fig. 3** Photos of the chamber made by PP filament printed on a MakrerBocie 3D printer

- extrusion defects—typical 3D printing materials, such as ABS or PLA, tend to extrude in an ordered manner and the extrusion can be easily stopped with no excess material remaining at the nozzle; the PP tends to form droplets at the end of the nozzle, these droplets are then left somewhere inside the layer contour; the layers are uneven and during forming of the next layer, the nozzle collides with the leftover droplet from the previous layer, causing mechanical defects inside the part;
- thermal properties—in general, the PP has lower thermal conductivity than the standard ABS material used in the FDM processes, it also has higher coefficient of thermal expansion; combined with only partial heating of the working space (the table is heated, but the ambient temperature during the 3D printing process is approx. 23 °C), this causes the upper layers of any 3D printed part more prone to thermal deformations, as the temperature in upper layers is lower than in the layers closer to the heated table; these deformations cause further shape and dimensional defects, as well as decrease of process stability.

Finally, after several unsuccessful prints, the part was manufactured repeatedly two times in a row, with stability and full shape representation achieved (see Fig. 3). The print took 5 h in total. Unfortunately, there were certain defects, causing leakage in between spaces of the designed chamber. These defects caused the authors to try an alternative approach.

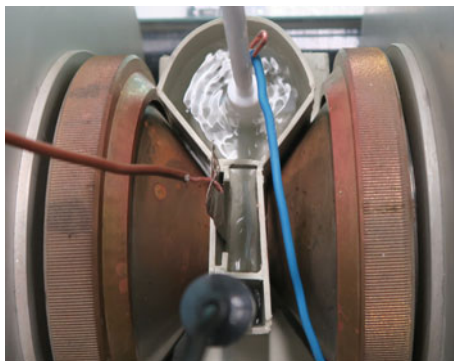
The PP chamber was alternatively made by a plastic welding method. For this purpose, a 2 mm thick polypropylene plate was used. After numerous attempts, the chamber produced by this method proved to be fully tight and meets the requirements (see Fig. 4). At the end of the production stage, the ready-to-use chamber was placed in the electromagnetic working area (see Fig. 5). The first tests of the chamber were then performed.

**Fig. 4** Pictures of the chamber made of 2 mm thick PP boards by welding methods





**Fig. 5** Picture of the chamber in the working space of electromagnet with mechanical stirrer mounted



## 4 Experimental Details

Preliminary attempt to measure the influence of Lorentz force on electrochemical processes. A 99.7% Titanium sample (0.25 mm foil) was used as a working electrode, with 99.8% iron (0.1 mm foil) as a counter electrode, and Ag/AgCl reference electrode. During the test was used electrolyte contains 0.01 M  $\text{HNO}_3$  Without mixing, constant voltage  $-1$  V, variable magnetic field 1 T (perpendicular to sample surface).

Studies have been conducted on the basis of previous silver deposition studies on anodized oxidized titanium [16]. Because of small working space in the chamber the samples were made of titanium foil (0.25 mm, 99.7%). Sample before use was sanded on 1500-gage water paper and then polished.

Prior to the silver deposition process, samples were purified with distilled water. Samples were placed in an electrolyte contains silver and nitrogen ions with concentration 0.01 M with additional mixing. In a time of deposition, set DC voltage  $-1$  V, according to the OCP, using the low voltage SOLARTRON 1285 potentiostat and Ag/AgCl reference electrode. The deposition process was carried out under different magnetic conditions.

The use of a counter electrode in the form of a silver plate allowed for the constant concentration of silver ions. After the process, the samples were dried. After the deposition process samples were characterized by the SEM and XRD.

## 5 Results and Discussion

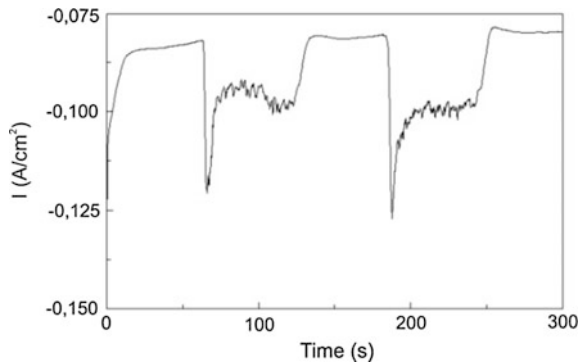
Test with pure iron as a counter electrode without additional electrolyte mixing. Lorentz's influence on the behavior of the electrolyte was observed. When the voltage is applied to the electromagnet (up to 1 T magnetic field), the electrolyte is automatically mixed by Lorentz's force, facilitating or hindering the flow of electrical current.

In the initial stage, the process went without an additional magnetic field, which for obvious reasons (corrosion processes) caused a rapid decrease in current density and the establishment of a relatively constant level. After 60 s and 180 s, the voltage was applied to the electromagnet which influenced the measurement itself (strong decrease in the measured current density caused by physical phenomena and electrical induction on the wires). While the magnetic field was involved, the corrosion process of the iron electrode was accelerated while the electrolyte itself swirled, accelerating the ions by repelling them from the electrode. After 60 s of magnetic field, the voltage of the electromagnets was disconnected, resulting in a small rise of the measured current density. After complete disconnection of the magnetic field, the corrosion processes proceeded in a fixed manner at the level established at the initial stage of the test (Fig. 6).

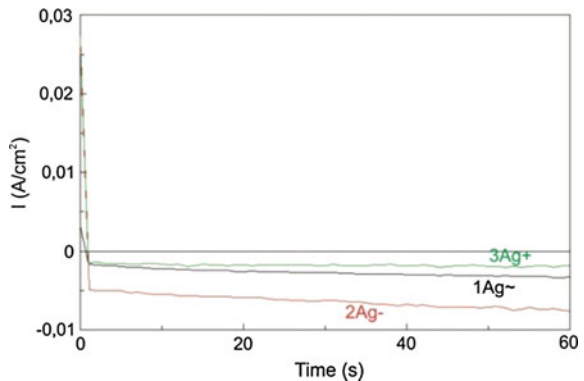
*Test with silver deposition*

The nature of the current density curves is the same as for anodized oxidized titanium surfaces—with the deposition time of the silver particles a slow increase in deposition velocity is associated with the larger surface area of the conductivity deposited (silver particles) (Fig. 7).

**Fig. 6** Preservation of electric current density flowing through an iron sample during a 1 V potentiometer test, with a variable magnetic field with a negative polarity of 60 s

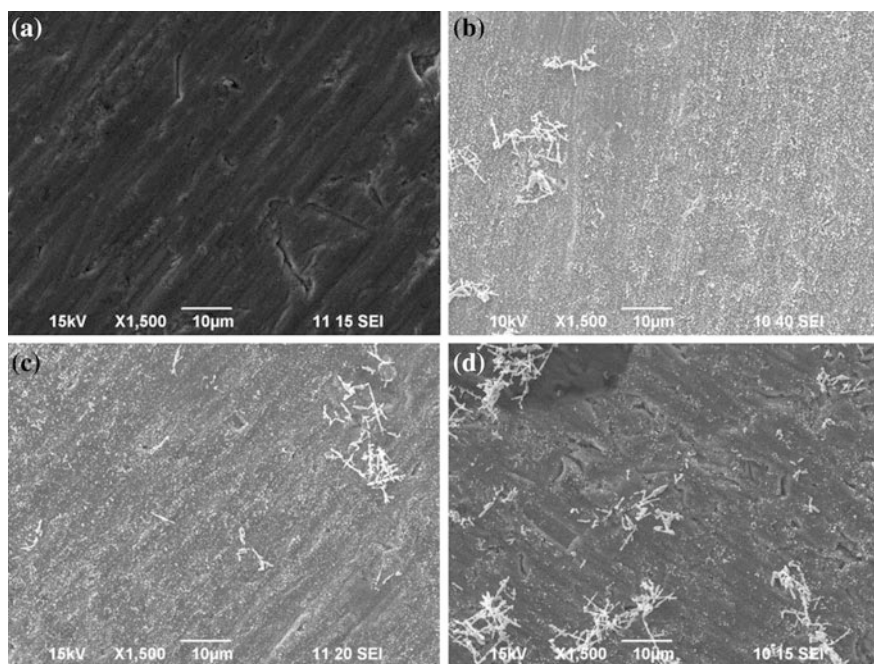


**Fig. 7** Graphs of current density when depositing silver particles on titanium surfaces of samples



**Table 1** Values of the electrical charge flowed through the samples during silver deposition process

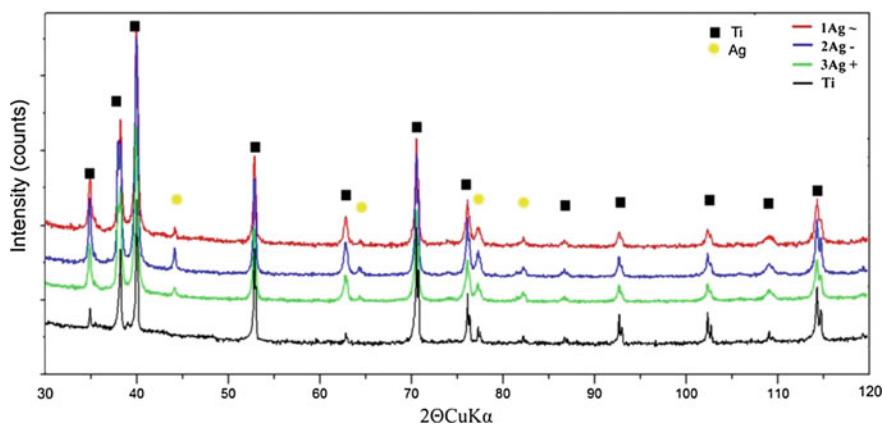
Magn. field	0	Negative	Positive
Sample	1Ag~	2Ag <sup>-</sup>	3Ag <sup>+</sup>
Charge $Q$	0.16 C	0.38 C	0.11 C



**Fig. 8** SEM image of sample surface after OCP test (a) after silver deposition (b) silver deposition in negative magnetic field (c) silver deposition in positive magnetic field (d)

However, the measured values of the electrical charge passing through the surface are significantly lowered to similar values observed for depositing silver particles by the positive polarization of the 1 T magnetic field (Table 1). As in previous studies, it can be stated that when depositing silver in a positive magnetic field, the electrolyte flowed in a lower electrical charge. The use of negative magnetic fields has significantly increased the flow of electricity. With such a substrate, the lowest current was observed during deposition of silver particles without an additional magnetic field.

The morphology of the titanium specimen after silver deposition without additional magnetic field 1Ag ~ was characterized by numerous very fine particles of silver about 100 nm (see Fig. 8b). These distributions were characterized by small size scattering and a crystalline structure which can be determined by the shape of



**Fig. 9** XRD spectra of titanium and samples after silver deposition in electrolyte contains 0.01 M  $\text{HNO}_3$  and  $\text{AgNO}_3$  1Ag $\sim$ , with addition negative magnetic field 2Ag $^-$ , and positive magnetic field 3Ag $^+$

the particles. They are spread at regular intervals throughout the sample. In a few places, there are visible expansions in the form of bands of irregular shape.

The morphology of the titanium specimen after deposition of silver with an additional magnetic field with negative polarity 2Ag $^-$  was characterized by numerous very fine particles of silver about 100–400 nm (Fig. 8c). These distributions were characterized by small size scattering and a crystalline structure which can be determined by the shape of the particles. They are spread at regular intervals throughout the sample. In a few places, there are visible divergences in the form of irregularly shaped dendrites. The increased current density for this sample was sufficient for the deposition of deposited silver particles.

The morphology of the titanium sample after silver deposition with an additional magnetic field of positive polarization 3Ag $^+$  was characterized by numerous very fine particles of silver about 100–300 nm (Fig. 8d). These distributions were characterized by small scattering of size and crystalline structure. In a few places, there are visible divergences in the form of irregularly shaped dendrites.

X-ray deposition of silver specimens was characterized by the presence of titanium and silver peaks (Fig. 9). No additional peaks or anomalies were found in any of the samples.

## 6 Summary

The designed chamber fulfilled its task and allowed for proper deposition of silver particles on the titanium surface. The 3D printing process was proven to be not fully suitable for manufacturing this type of part, due to numerous issues with process

stability and shape defects, causing leakages between spaces of the 3D printed chamber. However, the 3D printing can be used for preliminary testing and prototyping of such parts, for visual evaluation and initial tests. The studies allowed obtaining a satisfying combination of process parameters for the polypropylene material. However, a working, fully functional part had to be made using an alternative approach of plastic welding.

The designed chamber allowed to observe the influence of the magnetic field on the corrosive phenomena. During the operation of the magnetic field, increase electron flow through the electrolyte was measurement. Also electrolyte was automatically stirring caused by Lorentz force. Both phenomena are not observed without the action of an additional magnetic field.

The magnetic field affected by the deposition of silver particles on the titanium surface. Negative magnetic polarization (1 T) caused the acceleration of the deposition process. On the surface was observed larger particles of silver crystals compared to silver deposit without an additional magnetic field. Positive magnetic polarization slowed the deposition process. In this case, the appearance of silver dendrite was observed with a small amount of crystal deposits.

## References

1. Kawata, K., et al.: Effects of Chlorine on Tribological Properties of TiN Films Prepared by pulsed d.c. plasma-enhanced chemical vapor deposition. *TSF* **407**, 38–44 (2002)
2. Lahiri, A., Kobayashi, S.I.: Electroless deposition of gold on silicon and its potential applications: Review. *Surf. Eng.* **32**(5), 321–337 (2016)
3. Hinds, G., Coey, J.M.D., Lyons, M.E.G.: Influence of magnetic forces on electrochemical mass transport. *Electrochem. Commun.* **3**, 215–218 (2001)
4. Tacken, R.A., et al.: Applications of magnetoelectrolysis. *J. Appl. El.* **25**, 1–5 (1995)
5. Coey, J.M.D., Hinds, G. J.: Magnetic electrodeposition. *Alloys Compds.* **326**, 238 (2001)
6. Pullins, M.D., Grant, K.M., White, H.S.J.: Microscale confinement of paramagnetic molecules in magnetic field. *Phys. Chem. B* **105**, 8989–8994 (2001)
7. O'Brien, R.N., Santhanam, K.S.V.J.: Magnetic field assisted convection in an electrolyte of nonuniform magnetic susceptibility. *Appl. Electrochem* **27**, 573–578 (1997)
8. Leventis, N., Dass, A.J.: Isolation and demonstration of the elusive concentration-gradient paramagnetic force. *Am. Chem. Soc.* **127**, 4988–4989 (2005)
9. Coey, J.M.D., Rhen, F.M.F., Dunne, P., McMurphy, S.J.: The magnetic concentration gradient force—Is it real? *Solid State Electrochem.* **11**, 711–717 (2007)
10. Tang, Y.C., Davenport, A.J.J.: Magnetic field effects on the corrosion of artificial pit electrodes and pits in thin films. *Electrochem. Soc.* **154**, C362–C370 (2007)
11. Koza, J.A., Uhlemann, M., Gebert, A., Shultz, L.: The effect of magnetic fields on the electrodeposition of CoFe alloys. *Electrochim. Acta* **53**, 5344 (2008)
12. Zieliński, M.: Influence of constant magnetic field on the electrodeposition of cobalt and cobalt alloys. *Int. J. Electrochem. Sci.* **8**, 12192–12204 (2013)
13. Coey, J.M.D., Hinds, G.J.: Magnetic electrodeposition. *Alloy Compd.* **326**, 238–245 (2001)
14. Ragsdale, S.R., White, H.S.: Analysis of voltammetric currents in concentrated organic redox solutions. *Anal. Chem.* **71**, 1923–1927 (1999)

15. Górski, F., et al., Computation of mechanical properties of parts manufactured by fused deposition modeling using finite element method. *Adv. Int. Sys. Comp.* **368**, 403–413 (2015) (Springer)
16. Jakubowicz, J., et al.: Silver nano-trees deposited in the pores of anodically oxidized titanium and Ti scaffold. *Int. J. Electrochem. Sci.* **10**, 4165–4172 (2015)

# Testing of Tight Crimped Joint Made on a Prototype Stand

Nikodem Wrobel, Michal Rejek, Grzegorz Krolczyk and Sergej Hloch

**Abstract** The paper presents a project of a prototype solution of a device for making inseparable crimped joints consisting in forming the material of two elements to be joined to each other with the use of punches. The work contains the assessment and analysis of the joints made in the stand with the use of various forming tools. Furthermore, the paper presents the analysis of the characteristic features of the new joints, as well as dependences in strength tests. The elements joined on the machine had been made of 5754 aluminium. This material and the presented joint are used in the construction of heat exchangers, such as water, oil coolers or condensers in the automotive or aircraft branch.

**Keywords** Prototype stand · Inseparable tight joints · Crimped joints · Bent joints

## 1 Introduction

Reliable and economical operation of various devices strongly depends on many factors, such as the type and condition of the material [1–3], components geometry [4, 5] or type of work conditions [6, 7]. Industry expects more accurate methods for manufacturing quality products [8–10] to face the challenges related to technological progress. Construction elements of industrial applications can be subjected to aggressive influence of the cooperating medium, high pressure or high temperature gradients. Those factors lead to shorter operating time of particular applica-

---

N. Wrobel · M. Rejek  
PRO-ZAP Grupa Introl, 47a Grabowska Street, 63-400 Ostrów, Wlkp, Poland

G. Krolczyk (✉)  
Department of Manufacturing Engineering and Production Automation,  
Opole University of Technology, 76 Proszkowska Street, 45-758 Opole, Poland  
e-mail: g.krolczyk@po.opole.pl

S. Hloch  
Faculty of Manufacturing Technologies, Technical University of Kosice,  
080 01 Presov, Slovakia

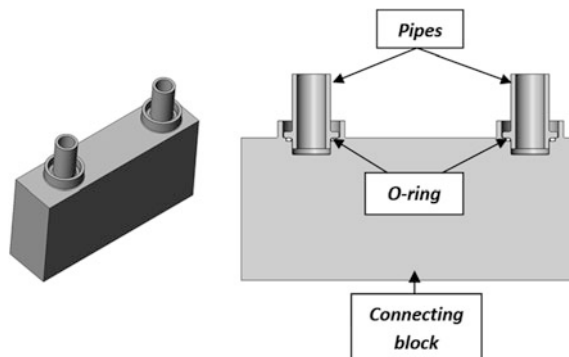
tions and possible failures [11]. The automotive and aircraft industry, with the assumed rate of development of new projects and principles related to the sequence of manufacturing the construction of the individual vehicle or aircraft parts, determine the possibilities of creating smaller sub-assemblies, as well as the mode of manufacturing them and possible mounting [12]. The difficulties resulting from the above aspects determine physical values, such as forces or torques to be set to the given product via the machine in order to obtain satisfactory results in the form of properly tight joint with adequate tightness. The design actions in the above-mentioned area, however, are constrained by the limited mounting possibilities which can be used in order to supply the demanded energy to the system.

## 2 Materials and Method

The prepared device is intended for simultaneous forming two identical joints, at a distance of 45 mm from each other, for the same tube diameters and sizes of sockets in which they are seated. Figure 1 shows the tested case of joint before the execution of it.

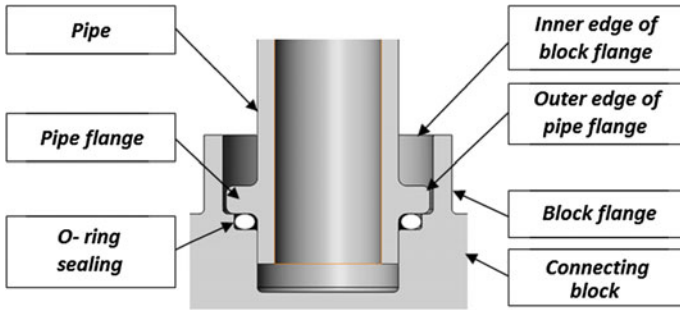
Tight joints used by the automotive and aircraft industry in manufacturing heat exchangers are based particularly on soldering details contacting each other or on the use of various kinds of seals out in or cast on the material. In the manufactured and described joint (Fig. 2), static sealing in the form of an o-ring has been applied. It allows the connection block to be added to the already soldered exchanger. The material selected for the execution of the joints was aluminium alloy 5754.

In order to make an inseparable joint between the pipe and the block, it has been assumed that the block flange with the wall thickness of 1.2 mm will be bent towards the pipe flange so that, in the first phase, the inner part of the block flange contacts the outer rounding and, in the second phase, the upper part of the flange contacts the upper part of the pipe. It is assumed in the connection that, when the joint is being formed, the pipe should be pressed to the socket for initial

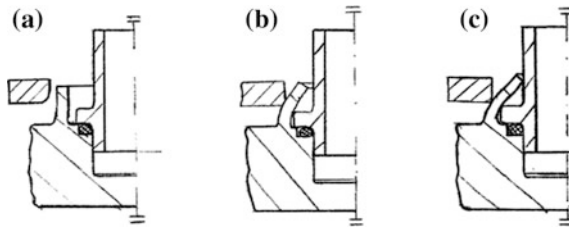


**Fig. 1** A view of connection block with the pipe and o-ring





**Fig. 2** A 3D view of the connection block cross section with the explanation of the individual element parts



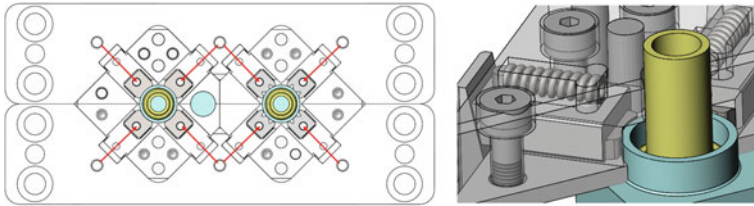
**Fig. 3** Joint formation: the system before the punch coming in (a); first phase—contact of the flanges (b); second phase—the block flange contact with the pipe (c)

compression of the o-ring. This eliminates the risk of “catching” and as result execution of a defective joint has been avoided. A diagram of manufacturing the connection has been shown in three steps (Fig. 3).

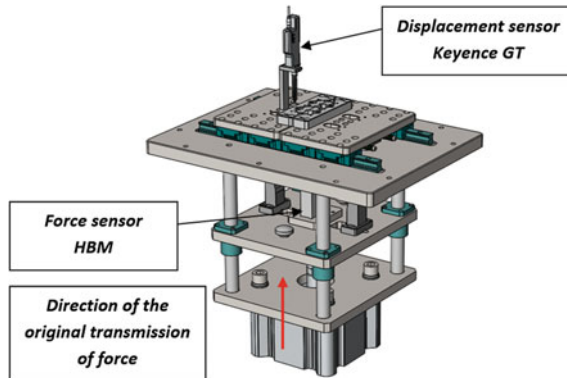
Plastic deformations of the described joint result in the material consolidation in the forming area, which positively influences its strength. In the construction of prototype tools for manufacturing various types of joints, in the case of aluminium, materials whose main destination is injection moulds are often used. In this case, material 1.2311 with the hardness of 32 HRC has been used.

### 3 The Stand Concept

Each device or machine must meet the predetermined assumptions. Therefore, it is important to design according to strictly defined principle and standards of creating a construction and to keep in mind the financial balance of the project. In prototyping, the critical issue, prior to the proper work, is to select the best concept and to learn the values of the physical magnitudes required for correct modelling of the technological process. The concept of the stand has been based on the assessment of



**Fig. 4** A view of the method of applying forces to the joint



**Fig. 5** A view of the main unit of the force generating machine

the forces to be applied to the system to execute the joint, possibilities of mounting, time of execution and quality of the joint, as well as the work ergonomics. The role of the stand is reliable execution of joints formed by the punch perpendicular entering the pipe flange and bending it on the pipe planes. Due to that two details will be joined to each other without an additional bond, just with the use of the native material. A diagram of force application to the joint via the device can be seen in Fig. 4.

Limited access has necessitated basing the machine design on mechanical transmissions in the form of two wedges for each of the punches. The conversion is effected from the vertical motion generated by the servomotor to the horizontal motion of the punch socket. Figure 5 shows a 3D view of the stand with the indication of the elements of acting and sensing.

The measurement system for data collection has been based on a PC provided with a PC LAB transducer which allows for collecting signals during the test, in the form of current values (4–20 mA—displacement sensor) and voltage values (0–10 V—force sensor).

### 4 Methodology of the Experiment

Six connection blocks have been prepared for the tests; there are two sockets in each of them for 12 pipes. The test has been performed for two pipe diameters, and each of them had also two values of the flange diameter. Ten samples have been provided with sealings in the form of o-rings, and two had no sealing rings. A view of the joint with the dimensions has been shown in Fig. 6 and Table 1; the experiment design in Table 2.

In order to make the joint, four kinds of punches have been used with two kinds of shapes matched to various diameters (Table 3). The execution of each joint has been recorded by the system of data collection and presented in two dependences: force as a function of time and force as a function of the path. The test results are to serve for learning the forces necessary to obtain proper quality of the joint. The joint is supposed to have proper tightness and strength. The executed joints have been subjected to destructive and non-destructive tests. A test verifying a joint in industrial conditions is measurement of tightness in which air helium is used. In the case under discussion, air device, ASTEQ F520 has been used. The sealings have been based on elastic hoses clamped on the outer diameter of the pipe. The samples have been subjected to tensile tests with the use of the testing machine.

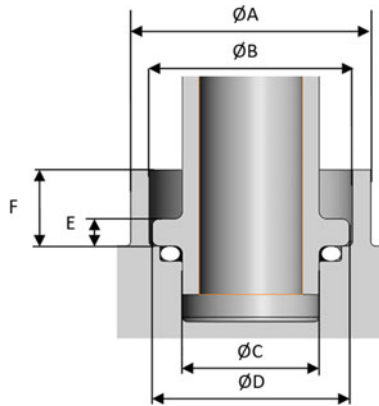


Fig. 6 A view of the joint with dimensions

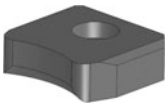
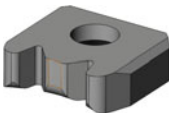
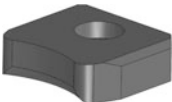
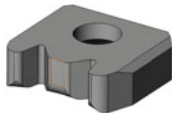
Table 1 Dimension description of the joint

No	Case	ØA	ØB	C	ØD	E	F	O-ring
1	A	15.8h7	13.4H7	9h7/H6	13h13	1.7h13	5	Ø8 × 1.5
2	B	14.8h7	12.4H7	8h7/H6	12h13	1.7h13	5	Ø7 × 1.5

**Table 2** Design of the experiment

No	Case	Tool	Test 1 tightness	Test 2 tensile strength	Micrography	Notes
1	A	S2	X		X	
2	A	S1	X		X	
3	A	S2	X	X		
4	A	S1	X	X		
5	A	S2	X		X	No O-ring
6	A	S1	X		X	No O-ring
7	B	S4	X		X	
8	B	S3	X		X	
9	B	S4	X	X		
10	B	S3	X	X		
11	B	S4	X		X	No O-ring
12	B	S3	X		X	No O-ring

**Table 3** The punches used in the tests

	S1	S2
Case "A"		
Case "B"		

The force has been applied by means of a precision ball screw. For the tensile test, internal threads have been made in the connection blocks; the pipes had internal threads for case "A" and external ones for case "B" (Table 2).

## 5 Results and Discussion

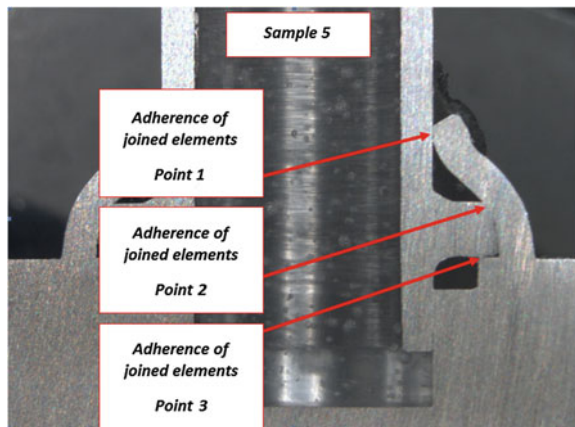
Each of the 12 samples has been subjected to an analysis of tightness. Expectations concerning the joints were as follows: with the pressure of 0.6 MPa, the admissible leakage has been determined at the level of 4 [(Pa l)/s]. The magnitude meets the requirements of the present automotive branch for heat exchangers in the form of oil and water coolers. In order to adapt to the tested object such test parameters as the time of filling, stabilisation or test have been selected in trials. The results indicate that each of the joints has the desired test parameters. The results have been shown in Table 4.

The obtained results show small differences between the leakage magnitudes. The reason of the described fluctuations is the relatively small volume of compressed air in the test system. The consequence of the fact is the influence of temperature on the result related, among others, to the thermal expansion of the detail and its variable volume resulting in the pressure drop. It has also been found that the result deteriorates with the number of tests performed on one sample. The changes can also be caused by delivering compressed air to the joint, which is likened to labour which changes into heat in accordance with the first principle of thermodynamics. During the selection of the test parameters consisting, among others, in increasing the pressure from 0.1 to 0.6 MPa, the set pressure of 0.175 MPa has been found to maintain for the test case no. 5. The sample had no sealing. This means that it is possible to obtain tightness with a lower range of requirements even with the absence of o-ring. This phenomenon implies that, in series production, if lower requirements are adopted, an incomplete joint can be qualified as a good one. Micrography of that sample can be seen in Fig. 7; very good adherence of the joined elements is noticeable which can occur within the three characteristic points. On the other hand, the acquisition of the described tightness was influenced by point 2. The first one is the upper part of the pipe flange, this means that local embossing of the flange on the pipe flange radius has occurred at that place. Due to that, on the described circumference, surface roughness has been smoothed. The sample has been made by means of S3 tool which makes joint by even shape in the whole pressure surface.

**Table 4** Description of joint dependence and the tests performed on the joint

Test no	1	2	3	4	5	6	7	8	9	10	11	12
Pressure (MPa)	0.6	0.6	0.6	0.12	X	X	0.6	0.6	0.6	0.6	X	X
Leak (Pa l)/s	3	4	3	X	X	X	2	3	3	4	X	X

**Fig. 7** Microsection of joint number 5



Constructional joints made by forming a socket flange on the pipe flange are loaded mainly with tensile forces. However, they must be resistant, too, to the operator's actions during transport of the exchanger. The tested samples have been analysed while applying the forces.

Analysis of the test results shown in Fig. 8 has allowed us to formulate the following dependences:

- Dependence of the arisen reaction force on the tool shape. The results were characteristic and analogous between samples 1 and 2, as well as between samples 7 and 8.
- Dependence of the arisen reaction force on the diameter of the connection block flange.

Description of those dependences has been executed basing on the diagrams made for cases 1 and 2 as well as 7 and 8. The first samples 1 and 7 have been formed by means of a punch with the same shape type, and the situation with samples 2 and 8 was similar. It has been observed that the force necessary to form a joint by means of punches S2 and S4 is smaller than that for punches S1 and S3. Its total value for the first case was 60.5 kN, for the second case 65.0 kN, for the

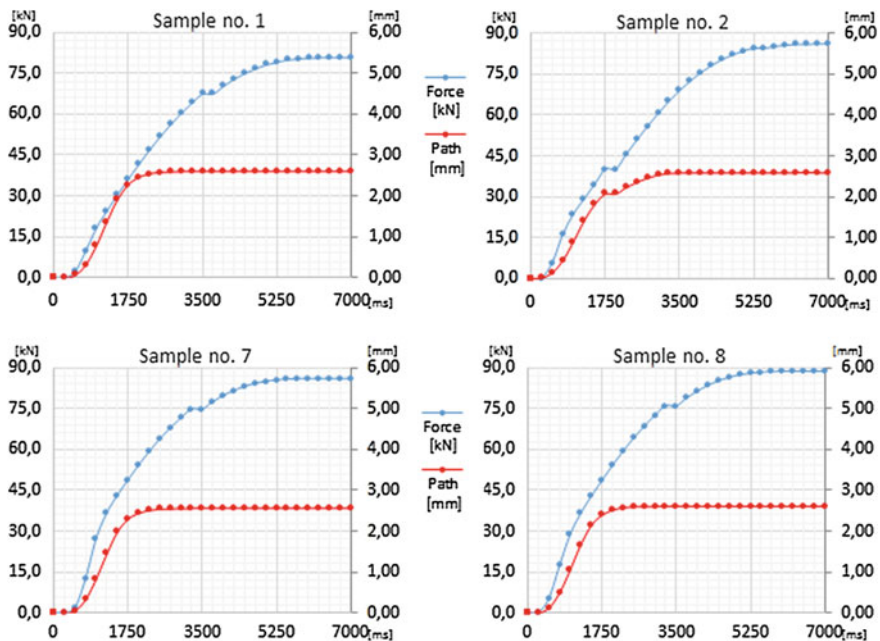


Fig. 8 Diagram of the dependence of the force on time and force on the path for sample 1,2,7,8

seventh one 67.8 kN and for the eighth one 68.6 kN. The differences are less perceptible for smaller diameter or for cases “A”. This is due to matching the punches to the smaller flange diameters and, consequently, for punch S3 the distance between the teeth is less, which influences the closeness of the contact surfaces. During plastic forming, local hardening of the material occurs, reduction of the distance of the contact points causes increase of the force.

Samples 3, 4, 9 and 10 have been subjected to a tensile test. The purpose was to check the joint with the minimum force of 1.56 kN. This magnitude corresponds to the application of a pressure of 10 MPa to the flange.

The tests whose results have been shown in Fig. 9 have proved that, with the force applied, the joint has not been destroyed. Only the connection pipe has been broken. For cases “A”, the values have oscillated around 5 kN; for cases “B”, they amounted about 3 kN. The differences were due to the execution of thread in the pipe (Fig. 10).

Joints are significantly influenced by the parameter of the bending angle of the support flange, as well as its thickness and girding on the pipe radius. Samples 2 and 8 have been made by the same kind of jaws, and the angle values are close to each other (Fig. 11).

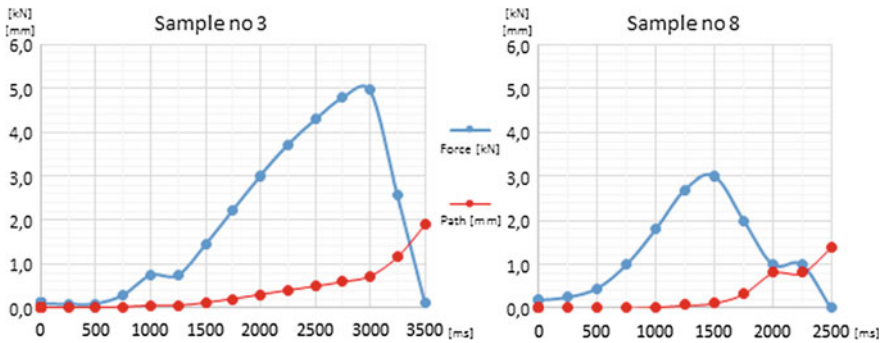


Fig. 9 Diagram of the joint stretching in the dependence of force on time and path on time for sample 3 and 8



Fig. 10 Photographs of the samples after the execution of the joint and after the strength test

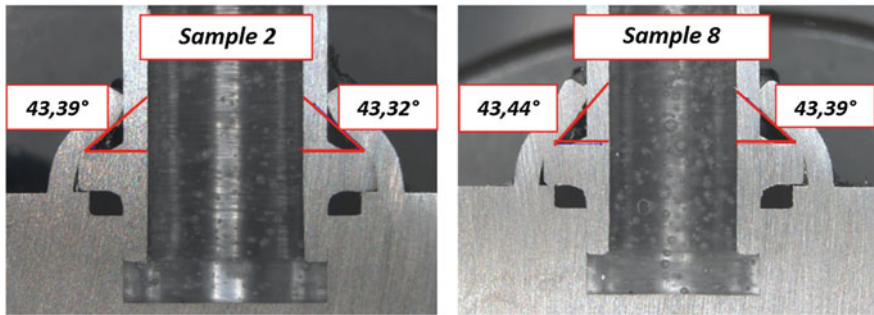


Fig. 11 A photograph of the microsection made for joint no. 2 and 8

## 6 Conclusions

The performed tests of inseparable constructional joint have allowed us to formulate the following conclusions:

- I. Application of punch kinds S2 and S4 has reduced the forces necessary for forming the joint,
- II. Smaller flange diameter with the applied S3 and S4 punches has resulted in an increase of the forces used to make the joint,
- III. Non-destructive examination in the form of the test of air tightness has shown that adequate selection of parameters and the temperature influence are very important,
- IV. As regards the aspect of strength, each of the tested joints can work in any kind of heat exchangers, water or oil, coolers or condensers,
- V. In the prototype machine, the best solution for force application is electric servo drive; it allows for full control of the process of the joint execution.

## References

1. Nieslony, P., Cichosz, P., Krolczyk, G.M., Legutko, S., Smyczek, D., Kolodziej, M.: Experimental studies of the cutting force and surface morphology of explosively clad Ti—steel plates. *Measurement* **78**, 129–137 (2016)
2. Zaleski, K.: Study on the properties of surface—active fluids used in burnishing and shot peening processes. *Adv. Sci. Technol. Res. J.* **10**, 235–239 (2016)
3. Maruda, R.W., Krolczyk, G.M., Nieslony, P., Wojciechowski, S., Michalski, M., Legutko, S.: The influence of the cooling conditions on the cutting tool wear and the chip formation mechanism. *J. Manuf. Proc.* **24**, 107–115 (2016)
4. Zhang, C., Li, Z., Hu, C., Chen, S., Wang, J., Zhang, X.: An optimized ensemble local mean decomposition method for fault detection of mechanical components. *Meas. Sci. Technol.* **28**, 35102 (2017)



5. Niemczewska-Wojcik, M.: Multi-sensor measurements of titanium alloy surface texture formed at subsequent operations of precision machining process. *Measurement* **96**, 8–17 (2017)
6. Krolczyk, G., Królczyk, J., Legutko, S., Hunjet, A.: Effect of the disc processing technology on the vibration level of the chipper during operations process: *Tehnički Vjesnik—Technical Gazette* **21**(2), 447–450 (2014)
7. Krolczyk, J.B., Gapinski, B., Krolczyk, G.M., Samardzic, I., Maruda, R.W., Soucek, K., Javadi, Y., Legutko, S., Nieslony, P., Stas, L.: Topographic inspection as a method of weld joint diagnostic. *Tehnički Vjesnik—Technical Gazette* **23**(1), 301–306 (2016)
8. Jašarević, S., Diering, M., Brdarević, S.: Opinions of the consultants and certification houses regarding the quality factors and achieved effects of the introduced quality system: *Tehnički Vjesnik—Technical Gazette* **19**(2), 211–220 (2012)
9. Krolczyk, J., Krolczyk, G., Legutko, S., Napiorkowski, J., Hloch, S., Foltys, J., Tama, E.: Material flow optimization—a case study in automotive industry. *Tehnički Vjesnik—Technical Gazette* **22**(6), 1447–1456 (2015)
10. Kujawińska, A., Rogalewicz, M., Diering, M.: Application of expectation maximization method for purchase decision-making support in welding branch. *Manage. Prod. Eng. Rev.* **7**(2), 29–33 (2016)
11. Glowacz, A., Glowacz, Z.: Diagnostics of stator faults of the single-phase induction motor using thermal images, MoASoS and selected classifiers. *Measurement* **93**, 86–93 (2016)
12. Arghir, G., Bere, P.: Utilisation of composite materials in the model aircraft construction. *Acta Tech. Napoc. Ser. Appl. Math. Mech. Eng.* **60**(1), 19–24 (2017)

**Part III**  
**Cutting Machining & Technological**  
**and Assembly Processes**

# Computer Simulation of the Process of Regenerating the Adsorbent Using Microwave Radiation in Compressed Air Dryers

Sergey S. Dobrotvorskiy, Ludmila G. Dobrovolska  
and Borys A. Aleksenko

**Abstract** The issues of improving the design of adsorption dryers for compressed air are considered, by using the energy of microwave radiation in the process of regeneration of the adsorbent. The expediency of moving the adsorbent layer relative to the source of microwave radiation during the desorption is proved in order to achieve better uniformity of heating of the desorbed material. The expediency of using software products using the finite element method is shown with the aim of modeling the heating process of the adsorbent in the cavity of the adsorption column.

**Keywords** Regeneration · Adsorption · Dryer · Modeling · Waveguide  
Microwaves

## 1 Introduction

The use of compressed air has become widespread in machine-building enterprises, in metallurgical and pipe production, in cases of increased flammability of technological processes inherent in the chemical and woodworking industries. The energy of compressed air is used in pneumatic equipment drives, pneumatic transport, in monitoring systems for the purpose of blowing cameras and sensors, in instrumentation, in the preparation of surfaces, the application of paint and special protective coatings, and so on.

---

S.S. Dobrotvorskiy (✉) · L.G. Dobrovolska (✉) · B.A. Aleksenko (✉)  
Kharkov Polytechnic Institute, National Technical University,  
Kharkiv 61002, Ukraine  
e-mail: ttm777@ukr.net

L.G. Dobrovolska  
e-mail: lyudmyla@ukr.net

B.A. Aleksenko  
e-mail: commerage@list.ru

A pneumatic system using compressed air energy also has a significant advantage compared to a hydraulic one, as it is more environmentally friendly and is practically safe in case of leakage of the working environment.

There is a consistent tendency to expand the use of pneumatic actuators, pneumatic control systems, and pneumatic logic in modern machine tool construction. The new, in particular, metallurgical, equipment, includes more and more components, units and drives using the energy of compressed air. In Europe, the production of compressed air accounts for 3% of electricity consumed by industry. At the same time, the payment for electricity consumed by the compressor is the largest share in the structure of the company's costs.

## 2 Research Problem

The reason for the significant consumption of electricity by compressors is due to the laws of thermodynamics. Thus, the work (adiabatic) stage of the compressor can be expressed as [1]:

$$\begin{aligned} L_{\text{ad}} &= i_{2\text{ad}} - i_1 = (k/(k-1))R(T_{2\text{ad}} - T_1) \\ &= (k/(k-1))RT_1(P_{\text{cp}}^{(k-1)/k} - 1) \\ &= C_p(T_{2\text{ad}} - T_1) \end{aligned} \quad (1)$$

where  $i = C_vT + PV$ —enthalpy ( $P$ —pressure,  $V$ —volume,  $T$ —temperature absolute);  $C_v$ —heat capacity of the gas at a constant volume;  $C_p$ —heat capacity of the gas at a constant pressure;  $R = C_pC_v$ —universal gas constant (for air = 286[J/kg K]);  $k = C_p/C_v$ —the adiabatic exponent (for air = 1.4);  $P_{\text{cp}} = P_2/P_1$ —pressure difference after and before compression.

The work, supplied to the gas during the compressor working, increases its enthalpy. With adiabatic compression, occurring in practically all compressors, into the internal energy of the air transmits (in the first approximation):

$$u = C_v(T_{2\text{ad}} - T_1) \quad (2)$$

Thus, the share of heat produced in the compressor operation in the ideal case is as follows:  $u/L_{\text{ad}} = C_v/C_p = 1/k = 0.71$  from the supplied working. In real compressors, the amount lost of air heating energy can reach up to 80%. In fact, taking into account other items of costs, the total cost of 1 m<sup>3</sup> of compressed air exceeds the “electrical” component by a factor of 1.5–2.

Thus, the production of compressed air is a power-consuming process, which requires close attention to its economical use. One of the areas of energy saving is to improve the quality of air preparation equipment, in particular, to increase the energy efficiency of this type of device such as adsorption dryers for compressed air.

The present study is devoted to the study of the processes taking place in the adsorption dryer with microwave regeneration of the adsorbent and to study the effect of the configuration and mutual arrangement of the waveguide and adsorbent on the propagation of microwave energy in the volume of the adsorbent in the cavity of the adsorption column of the dryer.

Adsorption dryers with cold regeneration used in production lose some of the already dried compressed air at a proportion of 15–18% of the nominal capacity of the dryer. Dehumidifiers with hot regeneration of the adsorbent consume a minimum of the dried compressed air. Dryers with this principle of operation are currently the most economical means of producing dried air, and developing the design of this type of equipment is the most important direction to improve the energy efficiency of industrial production.

The main attention of developers of drying equipment with hot regeneration is focused on the problems of heat energy recovery, which is used in the desorption process. Also, engineers are striving to maximally reduce the unproductive costs of thermal energy for heating the combined components of the equipment, up to the transfer of the heating source directly to the cavity of the adsorption columns.

Meanwhile, the use of alternative types of energy can become a serious alternative to traditional technologies of regenerating adsorbents.

### 3 Results and Discussion

Hot regeneration assumes the heating of the drying convecting air to a temperature of the order of 200 °C; thus, the volume of the adsorbent during the drying process is heated up to 190–180 °C.

The inability of the hot adsorbent to absorb moisture presupposes an additional phase of preparation of the adsorbent to the subsequent adsorption cycle by cooling it to a temperature of no higher than 30–35 °C, and the cooling process must proceed intensively. Since if the duration of the regeneration cycle exceeds the duration adsorption in the second column of the desiccant, the dried air at the output of the plant will not be obtained. To cool the heated adsorbent, the previously dried compressed air is used (as in adsorption plants with cold regeneration), which, along with the heating costs, also accounts for a significant share in the total energy consumption of the dryer.

In the process of desorption with hot purge air, the entire volume of the adsorbent is heated. Meanwhile, the adsorbent absorbs moisture only by an external microporous layer with a thickness of 100–500 Å at the granule size (the most common in air drying technology is adsorbent type KSMG) in 3–7 mm. In addition, the scavenged warm air also serves as a carrier of thermal energy, which transfers heat from heaters to the adsorbent with all the inevitable losses of heat, with which extensive struggle is waged with the use of thermal insulation and plate heat recuperators.

If the energy, used for the drying of the adsorbent, will act directly and only on the water molecules in the outer microporous layer of silica gel, in a volume that is necessary and sufficient for the molecules to leave the micropores and effectively evaporates from the surface of the adsorbent, then the desorption energy consumption will be minimal. At the same time, some of the thermal energy, which has passed from water molecules to the drying air used to purge the adsorbent layer, can be recovered using a recuperation technology. In the described technology, the heated air supplied is not used as a drying agent, but for transporting vaporized water vapor out of the adsorption column. The air is heated to the drying temperature of silica gel (60–80 °C, which is 100 °C below the heating temperature with the existing technology). Thus, the purpose of warming up of air consists exclusively in increase in its moisture capacity.

Since such a desorption technology is known to be less energy-intensive, from here comes a significant reduction in the loss of the pre-dried compressed air used to cool the adsorbent heated during the drying time.

The main task that should be solved for the practical implementation of the technology of microwave regeneration (see Fig. 1) is to create conditions for uniform heating of the entire volume of adsorbent material in the cavity of the adsorption column. To solve this problem, computer simulation using software is used, which, using the finite element method, allows modeling the propagation of the electromagnetic field intensity in space. From the formula (3) of the dependence of the microwave radiation power on the intensity of the electromagnetic field, we are able to simulate the propagation of thermal energy in the volume of the adsorbent and visualize the results (see Fig. 2).

$$P = E^2 \omega \varepsilon_r \varepsilon_0 t g \sigma \quad (3)$$

The pattern of the traveling wave field inside the waveguide can be determined by solving the Maxwell equation [2]. The following equation, which is solved by a two-dimensional solving device, was obtained directly from the Maxwell equation [3].

$$\nabla \times \left( \frac{1}{\mu_\gamma} \nabla \times E(x, y) \right) - k_0^2 \varepsilon_\gamma E(x, y) = 0 \quad (4)$$

where  $\mu_\gamma(x, y)$ —complex relative permeability;  $E(x, y)$ —complex amplitude representing an oscillating electric field;  $\varepsilon_\gamma(x, y)$ —complex relative dielectric permeability;  $k_0$ —phase constant of free space, equal to

$$k_0 = \omega \sqrt{\mu_0 \varepsilon_0} \quad (5)$$

where  $\omega$ —circular (angular) frequency at  $\omega = 2\pi f$ , where  $f$ —frequency [Hz];  $\mu_0$ —magnetic permeability of the medium;  $\varepsilon_0$ —dielectric permittivity of the medium.

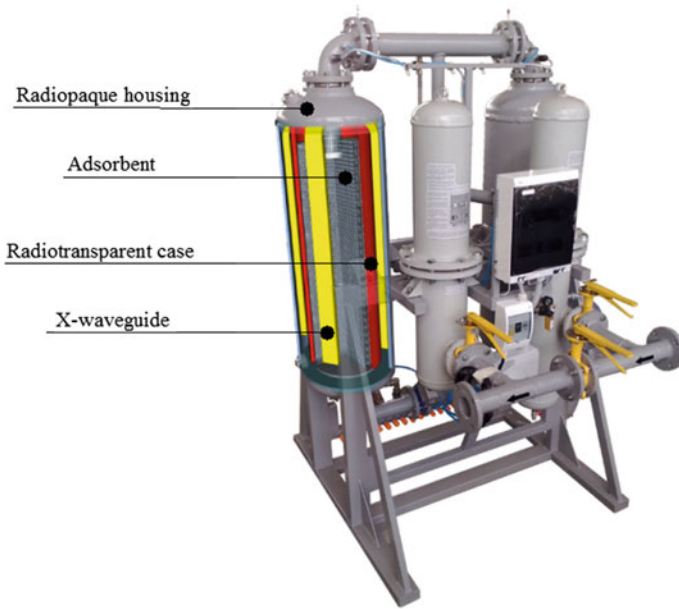


Fig. 1 Section of the adsorption column of the dryer TDS-10-RGM with the technology of microwave regeneration of the adsorbent

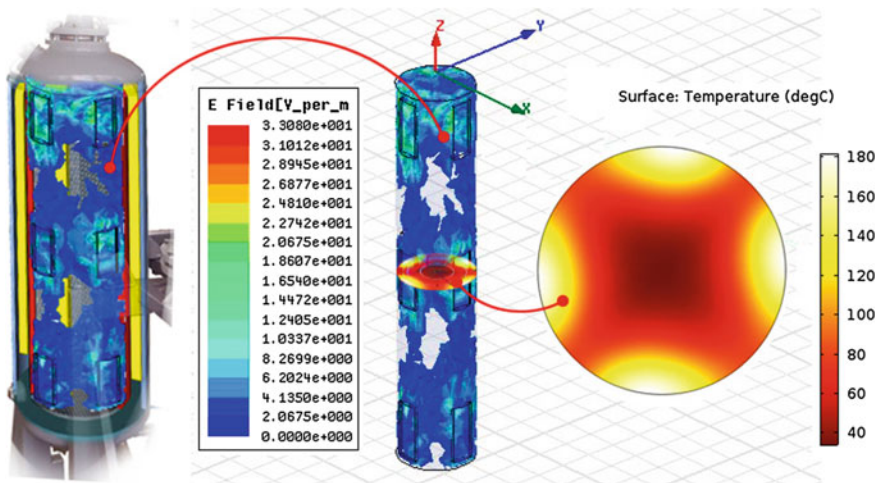


Fig. 2 Computer model of the intensity of the electromagnetic field and the face of the heating of the adsorbent in the cavity of the adsorption column

In the process of solving this equation, a two-dimensional solving device obtains a picture of the field for the complex amplitude  $E(x, y)$ . This solution is independent of  $z$  and  $t$ ; After multiplying by  $e^{-\gamma z}$  (where  $\gamma = \alpha + j\beta$  is the complex propagation constant, where  $\alpha$  is the damping coefficient of the wave,  $\beta$  the propagation constant associated with the wave, which determines the dependence of the phase angle from  $z$  on the given time  $t$ ), they will become traveling waves.

Since the calculated field pattern is valid only for one frequency, different field patterns are computed for each frequency point. For a waveguide or transmission line with a given cross section, there are a number of base field patterns (modes) that satisfy Maxwell equations at a particular frequency. Any linear combination of these modes can exist in a waveguide. If these higher-order modes are reflected back to the excitation port or transferred to another port without much loss, then the S-parameters associated with these modes can be calculated.

When calculating the total solution for the 3D field, the following wave equation is solved:

$$\nabla \times \left( \frac{1}{\mu_\gamma} \nabla \times E(x, y, z) \right) - k_0^2 \varepsilon_\gamma E(x, y, z) = 0 \quad (6)$$

where  $\mu_\gamma$ —complex relative permeability;  $E(x, y, z)$ —a complex vector representing the electric field;  $\varepsilon_\gamma$ —complex relative permittivity;  $k_0$ —phase constant of free space;

This equation is analogous to the equation used in the computation of the two-dimensional field pattern in each of the ports by a two-dimensional solver. The difference is that the 3D solver does not accept that the electric field is a traveling wave propagating in a single direction. It is assumed that the vector  $E$  is a function of  $x$ ,  $y$ , and  $z$ . A real electric field is a real part of the complex amplitude, and  $e^{j\omega t}$ [4]:

$$E(r, t) = \Re \{ E(r) e^{j\omega t} \} \quad (7)$$

where  $e^{j\omega t} = \cos(\omega t) + j \sin(\omega t)$ —Euler's formula;  $t$ —time;  $j$ —Is an imaginary unit.

Thus, the formula for calculating the field pattern becomes:

$$E(x, y, z, t) = \Re \{ E(x, y, z) e^{j\omega t} \} \quad (8)$$

The obtaining waveguide of the maximum level of the electromagnetic field is not a sufficient condition for achieving the maximum efficiency of the microwave heater. The most important task of stabilizing the heat treatment regime is to increase the uniformity of the distribution of microwave energy inside the heating chamber, which is facilitated by a change in the overall structure of the electric field. It is possible to improve the uniformity of heating, if the available modes of oscillations or some of them are switched in turn. The addition or, conversely, the



removal of any mode leads to a change in the overall structure of the electric field. The same happens when the ratio of the amplitudes of different modes is changed. Areas with the maximum and minimum amplitude are displaced in space and can change places. As a result, each part of the column volume is alternately affected by fields of different configuration and intensity. It is with a large number of combinations that the effect of microwave influence can be fairly uniform. Also, the uniformity of the distribution of thermal energy in the volume of adsorbent is facilitated by a change in the relative location of the source of microwave energy and the material, which is heated.

Taking into account the dependence (3), the uneven heating of the volume of the heated material was determined by the formula:

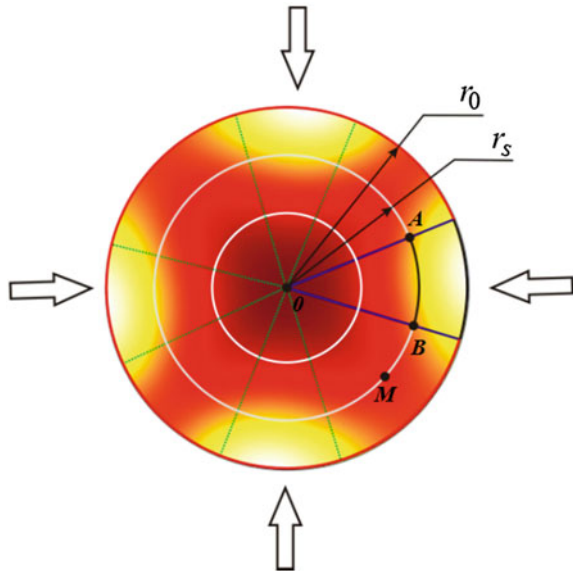
$$\Delta E = \int_n \left( \frac{E^2(x_H, y_H, z_n, t) - E^2(x_M, y_M, z_n, t)}{E^2(x_H, y_H, z_n, t)} \right) dn \tag{9}$$

where  $(x, y, z)$  are the coordinates of the points in the heating  $H$  and convection  $M$  sectors (see Fig. 4) in the space of the cylindrical volume of the heated material (see Fig. 3).

The circumferential speed of rotation was calculated by the formula:

$$v_{rot} = \frac{2\pi r_0}{KtL_{re}n(m_a C_a / m_s C_p)} \tag{10}$$

**Fig. 3** Picture of the propagation of thermal energy in the plane of the cross section of the volume of the adsorption column with a fixed volume of the adsorbent and with a stationary waveguide is presented. The arrows show the effects of microwave energy sources



where  $m_s$ —the mass of the material being heated;  $C_p$ —the heat capacity of the heated material;  $m_a$ —the mass of the purge air,  $C_a$ —the heat capacity of the blowing air;  $\alpha$ —the angle formed by the radiuses  $OA$  and  $OB$ ,  $r_0$ —the radius of the volume of the adsorbent (see Fig. 3);  $L_{re} = \frac{\pi r_s \alpha}{180}$ —the length of the arc  $\widehat{AB}$ , formed by a circle with a radius  $r_s$  and points  $A$  and  $B$  with the calculated value of the electromagnetic field strength  $E(x, y, z)$ , see Eq. (8);  $K$ —the coefficient expressing the ratio  $r_0$  to  $r_s$ ;  $n$ —the number of arms of the waveguide (see Fig. 4).

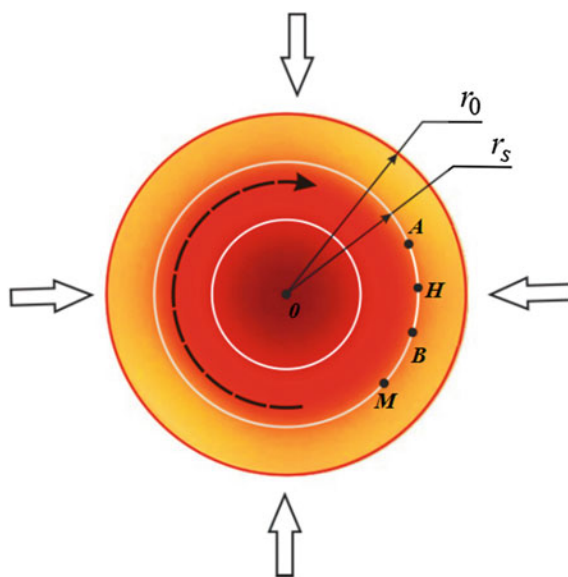
In the course of this study, two computer models of an adsorption column with an internal 4-arm x-shaped waveguide, installed in the cavity of the desiccant adsorption column and excited by a coaxial cable were developed and compared.

The first model under consideration was a model with a fixed position of adsorbent and with a stationary waveguide. In the described model, the mutual arrangement of the source of microwave energy and the material to be desorbed did not change.

The second model in question was a model with a movable volume of adsorbent and a stationary waveguide. In this model, the mutual arrangement of the source of microwave energy and the material to be dried continuously changed due to the rotation of the volume of the absorbing substance around the vertical axis of symmetry with variable circumferential velocity.

During the comparison of the studied models, it was shown that the change in the mutual location of the source of microwave radiation and the volume of the material, which is heated, promotes more uniform heating and prevents local overheating of the material, which is especially important for the process of desorption of industrial adsorbents [5, 6].

**Fig. 4** Picture of the propagation of thermal energy in the plane of the cross section of the volume of the adsorption column with a fixed waveguide and with the volume of the adsorbent, which is rotated about a vertical axis of symmetry with an optimum circumferential velocity, is presented. The arrows show the effects of microwave energy sources



Modeling using the described technique was used in the design of the equipment produced.

## 4 Conclusions

The performed work has shown the possibility of achieving the goal of reducing energy costs by using the energy of microwave radiation during the regeneration of adsorbents of compressed air dehumidifiers.

The technique for calculating the designs of adsorption dryers with microwave regeneration of the adsorbent is improved.

It is proved that is expedient to move the adsorbent layer relative to the source of microwave radiation during the desorption process in order to achieve better uniformity of heating of the material, which is desorbed.

The expediency that the using software products using the finite element method is shown to simulate the heating during the adsorbent regeneration in the cavity of the desiccant adsorption column.

**Acknowledgements** The authors of this study would like to thank to National Aerospace University “KhAI” for their technical support and to prof. Gennadiy I. Kostuyk for his valuable recommendations.

## References

1. XuMuK/Lecture course on heating engineering/Chapter 17.1. Volumetric compressor—URL: <http://www.xumuk.ru/teplotehnika/054.html> (date of request: 24.03.2017)
2. Bankov, S.E., Kurushin, A.A., Razevig, V.D.: Analiz i optimizatsiya trehmernyih SVCh struktur s pomoschyu HFSS. Red. d.t.n., prof. Bankova S.E.—M., SOLON-Press, 208 s (2008)
3. HFSS—High Frequency Structure Simulation. Manuals, Ansoft. URL: [www.ansoft.com](http://www.ansoft.com) (date of request: 10.02.2017) (2004)
4. Balanis, K.A.: Antenna Theory: Analysis and Design, 942, 2nd edn. Wiley, USA (1997)
5. Auerbach, S.M., Carrado, K.A., Dutta, P.K.: Handbook of Zeolite Science and Technology. Marcel Dekker Inc, NY (2003)
6. Farooq, S., Ruthven, D.M.: Heat effects in adsorption column dynamics. 1. Comparison of one and two-dimensional models. *Ind. Eng. Chem. Res.* **29**(6), 1076–1084 (1990)

# Spatial Adjusting of the Industrial Robot Program with Matrix Codes

Jakub Wojciechowski and Olaf Ciszak

**Abstract** The study presents a method to modify the program of industrial robots related to the change of the position of objects in the workspace. The aim is to increase the flexibility of the station and to reduce the need for expensive tooling, such as precision, large-size positioners. The object to be processed can be placed in any position on the table. The location and the orientation are determined by a camera detecting tags in the form of a matrix code. Methods for the calibration of the system and the transformations performed in the preparation and execution of the program were presented. Repeatability of the method has been investigated experimentally.

**Keywords** Robotics · Machine vision · Calibration · Matrix codes

## 1 Introduction

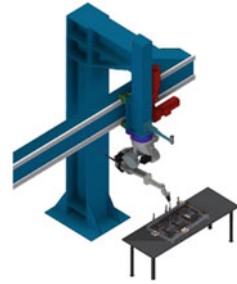
Tooling for robotized stations is expensive, and transition for the production of another product is problematic. In order to facilitate SMEs' access to robotics, extra effort should be reduced. It is proposed to abandon the current method of constructing a rigid framework instrumentation attached to the ground or using expensive and requiring significant space rotary positioners. This type of tooling could be replaced by light frames, placed by the operator on the table (Fig. 1).

Rigid position of the object frame fixing is not necessary, because of the matrix codes. The camera located near the station recognizes the codes and determines their position in space. Information about the type of the tooling and its location in space is transmitted to the robot controller. The coordinate system is adapted to the current position of the object on the table.

---

J. Wojciechowski (✉) · O. Ciszak  
Faculty of Mechanical Engineering and Management,  
Poznan University of Technology, Poznan, Poland  
e-mail: jakub.wojciechowski@put.poznan.pl

**Fig. 1** Idea of system matching the program to the location of objects



## 2 Related Work

In the literature, many varieties of machine vision locating objects have been described. Most of them are systems based on tags or additional components that are easy to identify and distinguish on images. Markers often take the form of a set of spatially disposed balls, flat circles of coded shapes. More information can be provided by the matrix data. The matrix contains the fields of light and dark; the amount of data depends on the number of fields [1]. An extension of this concept is the use of the matrix QR code described in this paper. The position and the orientation of the pattern relative to the camera, that is, displacement and rotations, can be determined if the size of the code is known, which extends the approach given in the [2].

Matrix codes are a popular way of marking items. With their help, words, links to Web sites, and e-mail addresses can be encoded. Assuming a strictly defined size of code, it can specify not only the encrypted data, but also the position of the code relative to the camera. These characteristics of matrix codes have already been used in robotics.

In [3] QR codes are used as guideposts for a mobile robot. The encrypted data give guidance to the movement of the mobile platform. Closer to this publication is the solution [4]. Industrial robot on the mobile platform is positioned relative to the station using the matrix codes and a vision sensor, transmitting also the object distance from the camera. In this study, the tooling position detection based only on the plain image is considered.

## 3 Approach

The proposed method is based on solving the perspective-three-point problem (P3P). This task consists of determining the position and the orientation of the camera based on three points at a known position in three-dimensional space projected onto the image plane of the camera. This is one of the basic tasks of photogrammetry; the solution of which is essential to calibrate the camera, object

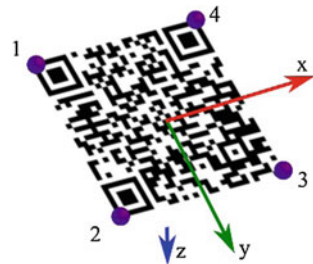
tracking, and determining camera motion based on consecutive shots [5–8]. Great practical importance led to the development of many methods to solve this task. They can be divided into two groups. Iterative methods are typically computationally more complex, but they are more accurate and resistant to disruption in the data than non-iterative methods, based on closed systems of equations. Most methods allow to specify the position of the camera on the basis of more than three points, which improves accuracy [9]. In order to achieve the assumed stability and precision of the results, the combination of two methods was used. The first approximation is obtained with the approach described in [10], in which location is the solution of closed equation system based on the analysis of orthography and scaling. This initial solution is transferred to the iterative method which relies upon the virtual servo described in [11]. The described algorithms were implemented in C++ using software libraries. Ready recognition method for the matrix code and the reconstruction of the position on the basis of points can be found, among others, in the software package ViSP [12].

## 4 Detection of Matrix Codes

The primary function of the matrix codes is to store data. Rotation of the code, scaling, or even placing it on a flexible, deformable surface still allows reading the data. However, if the code is applied on a plane and its dimensions are known, it is possible to read also the position relative to the calibrated camera. This property, simultaneously storing text data, identifying objects and geometric data for determining the position of the label in the space, prompted the authors to use just such a marker.

Reconstruction of the label position relative to the camera is based on the corners of the matrix code found in the image. Due to the popularity of QR matrix codes, the ready-to-use methods of solving this task are available. The input to the program is a picture of an industrial robot station, and the output is a vector containing data decoded from all recognized labels and the location of the corners on the image. Figure 2 shows the code corners numbering and placing the coordinate system convention.

**Fig. 2** Reference system of the matrix code and the numbering of the corners

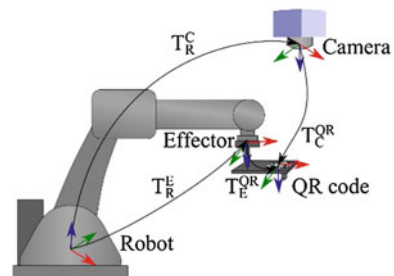


## 5 System Calibration

Knowing the location of markers in a camera coordinate system is not enough. Calibration is required, that is, the procedure to determine the relative positions of the coordinate systems of the robot and the camera, to be able to manipulate objects. In the described solution, a pattern identical to those used to identify objects was used, that is, a label with a QR code applied to the gripper. It is possible to apply a number of markers in a particular area of the tool. Transformations between coordinate systems including rotation and translation are represented by  $4 \times 4$  homogeneous matrices. The relation between the coordinate systems is shown in Fig. 3.

The calibration of the system, consisting of a camera, a pattern, and the robot, can be performed using the solutions provided for the problem of eye-hand calibration; the task of calibrating a camera mounted on a movable arm. The problem can be solved by classical methods of linear algebra [13], but newer, improved methods may provide greater accuracy and stability of the solution [14–17]. In the case of robots with low accuracy, which do not pass calibration using specialized equipment or in case of the use of cameras with low resolution and high distortion difficulties in calibrating the robot, camera system can often be encountered. Deviations in the position of the robot and camera readings are so large that methods solving systems of equations become unstable and do not generate the correct results. This phenomenon can be observed especially for methods which use the methods of linear algebra [18] and closed systems of equations based on quaternions [19]. To a lesser extent, it applies to iterative methods, which are considered more stable and thus useful for calibrating cameras in endoscopes [20]. The experience of the authors indicates, however, that regardless of the method you can get incorrect results, which can lead to malfunctioning robot system. Certainly, there is a possibility of careful calibration algorithm design, development of validation methods, and determination of the position of the robot that do not lead to ill-conditioned equations [21]. However, in this study, a different approach, a simplified method of calibration is presented. It assumes the possibility of execution of the specific program of robot motions, in contrast to the classical method of determining the position of the camera relative to the robot based on a set of arbitrary positions.

**Fig. 3** Relationship between coordinate systems for system calibration



The developed calibration method consists of two steps. The first is to determine the direction of the base of the robot coordinate system relative to the camera. For this purpose, a program in which the robot moves only in the direction of the base is written. The marker in the form of the QR code is placed on the effector, as shown in Fig. 4.

Image processing program, running on a computer connected to the camera, reads the position of the code in each of the stop positions of the arm. Having saved the position of the marker on each node of the grid in both the robot and the camera coordinate system, the sum of shifts in the main direction of the robot can be presented in the camera coordinate system. The rows of the matrix are vectors representing the displacement of the marker in a camera coordinates when moving robot in each main direction:

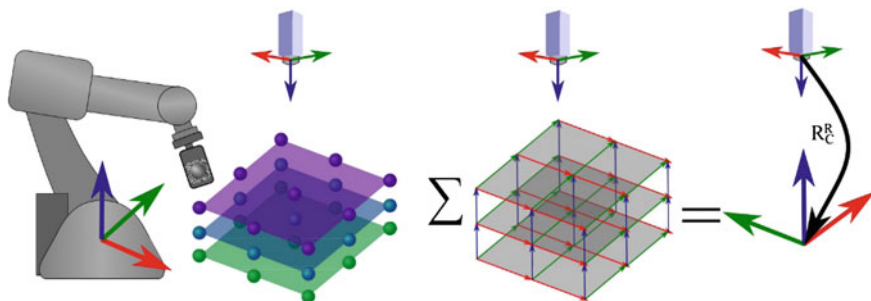
$$M_C^R = \begin{bmatrix} Xx & Xy & Xz \\ Yx & Yy & Yz \\ Zx & Zy & Zz \end{bmatrix} \tag{1}$$

The resulting matrix does not have the characteristics of the rotation matrix. Normalization of individual vectors also may not produce the desired results, as it may be, that the vectors will not be perpendicular to each other. The closest corresponding rotation matrix can be obtained by the SVD decomposition as in the equations:

$$[U, S, V] = SVD(M_C^R) \tag{2}$$

$$R_C^R = U \cdot V^T \tag{3}$$

After this operation, the matrix  $R_C^R$  is orthogonal. The results of this method are not affected by the position of the QR code relative to the robot. It is also not essential to know the position of the marker in relation to the default tool coordinate system of the robot.



**Fig. 4** Procedure for determining the direction of the robot relative to the camera coordinate system



Position calibration is done by contact. A tool with the tip is mounted in the robot's wrist. It must be defined by setting the operating point. Sufficient for that purpose is standard tool calibration procedure implemented in the robot's controller. A marker, which can be a matrix code applied to the plane, is placed in the shared workspace of the robot and the camera. The position of the marker relative to the camera coordinate system  $T_C^S$  is determined on the basis of image, as shown in Fig. 5.

Next, the tool is moved to contact the tip with the middle of the code, and its coordinates are read in the robot's coordinate system. The tool orientation at a contact point is not essential. Translation vector between the camera and the model should be provided in the robot coordinate system, using previously designated directions.

$${}^R t_C^S = (R_C^R)^T \cdot {}_C t_C^S \quad (4)$$

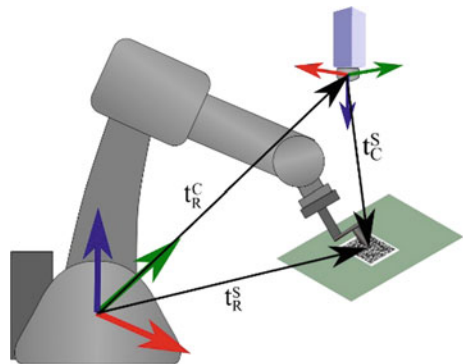
After bringing the two translation vectors to a common coordinate system, that is, the base of the robot R, the offset between the robot and the camera can be expressed as in Eq. 5.

$${}^R t_R^C = {}^R t_R^S - {}^R t_C^S \quad (5)$$

The transformation between the robot system and the coordinate system of the camera can be saved as a single, homogeneous matrix transformation  $T_C^R$ .

$$T_C^R = \begin{bmatrix} (R_C^R)^T & & & \\ 0 & 0 & 0 & 1 \end{bmatrix} \quad (6)$$

**Fig. 5** Determining shifts between the robot and the camera



## 6 Dynamic Adjusting of the Program

Development of a program which dynamically adjusts to the position of objects in the workspace of the robot is not more difficult than to write a typical program for an object placed in a rigid tooling. The programmer puts the object anywhere in the common area of the operation of the robot and the camera. Own coordinate systems to facilitate the writing of the program can be defined, as shown in Fig. 6.

After completion of the program development, the procedure for saving the program is started. An image of an object in the workspace is saved along with the instructions. The transformation matrix between the QR code and a user coordinate system (UCS) can be determined on the basis of images and data from earlier calibration. If the programmer has defined more than one coordinate system, the calculation is repeated.

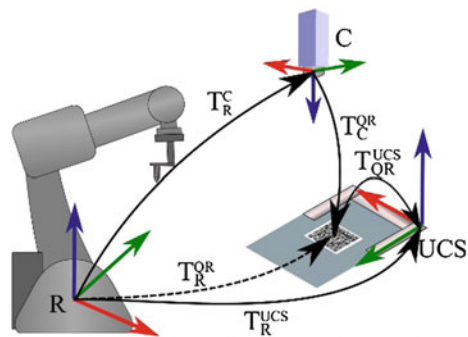
$$T_{QRi}^{UCS} = (T_C^{QR})^{-1} \cdot (T_R^K)^{-1} \cdot T_{Ri}^{UCS} \tag{7}$$

Transformation  $T_R^C$  is the result of calibration; as described in Sect. 5,  $T_C^{QR}$  is the result of the algorithm determining the position and the orientation of the marker relative to the camera based on the location of the code corners on the image; and  $T_R^{UCS}$  is shift and rotation of the user coordinate system relative to the robot's base.

In the system developed by the authors, these calculations are carried out on the PC. Communication with a camera and a robot, that is, the transmission of images and parameters of coordinate systems, is carried out via TCP/IP.

The tooling keeping the processed object in stable position can be marked with a few code matrices. It is proposed to arbitrarily select virtual markers coordinate system to replace several real systems. During the development phase, the program performs the image of the tooling and determines the position of the markers relative to the virtual coordinate system. During the program execution, the location of the virtual coordinate system can be determined even if a single marker is

**Fig. 6** Development of the program aligning to the position of an object



detected. If more than one marker is detected, the position of the virtual coordinate system is determined for each of the detected markers separately.

$$T_{Ci}^{QR} = T_C^{QRi} \cdot T_{QRi}^{QR} \quad (8)$$

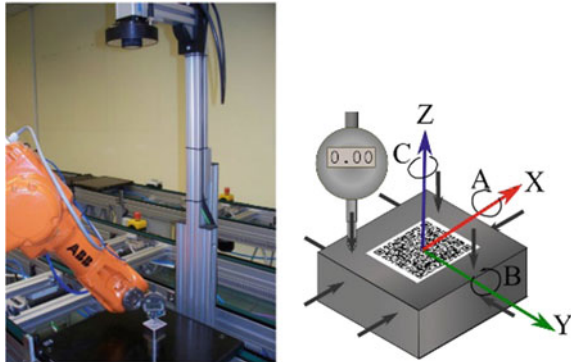
Next, the transformation  $T_C^{QR}$  is averaged using the approach described in [22]. If only one marker is used, the virtual markers coordinate system is identical to the system of a single used tag. The solution developed by the authors does not require the involvement of the operator. It automates the running program with a variable position of the object.

The industrial robot activated by the operator is directed toward a base position which does not lead to shading image of the workspace. Readiness of robot is indicated by setting the digital output signal. Triggered camera takes a picture and sends it to be processed on a PC. There the position of the QR code is found, and the coded information about the type of the tooling located on the work table is read. Then, the problem of perspective with four points for each of the detected code is solved, which results in a transformation that represents the position of the matrix codes relative to the camera. Based on the data from the camera calibration and transformation  $T_{QR}^{UCS}$ , which are defined in Eq. (8), location for the new, transformed user coordinate system according to the following formula can be specified.

$$T_R^{newUCS} = T_R^C \cdot T_C^{QR} \cdot T_{QR}^{UCS} \quad (9)$$

The new coordinate system, along with the information about the type of instrumentation located in the working space, is sent to the robot controller. There the right program is chosen and executed with the new, modified, coordinate system. Calculation and data transmission time do not exceed a second and are negligible at typical industrial robot technology programs.

**Fig. 7** Repeatability test of determining position using a vision system



**Table 1** Standard deviation in the static repeatability test

sx, sy [mm]	sz [mm]	sA, sB [°]	sC [°]
0.32	1.77	2.23	0.50

## 7 Experimental Verification

In order to verify the applied solutions, experiment, as shown in Fig. 7, was planned.

A cube object with dimensions of 40 mm by 40 mm is marked with the matrix code printed on standard paper using an office laser printer. The test of repeatability in the normal direction to the plane of the code and in direction parallel to the marker's plane is separated. Their values differ significantly due to the methodology used to determine the position of the object. Program for the robot according to the procedure described in Sect. 6 was developed. In the robot's wrist, adapter allowing to mount the sensor is fixed. Digital dial indicator allows to directly measure the deviation with respect to the base of the program. Ten static attempts were made. The measurements were carried out using a camera equipped with a sensor with resolution of 1600 by 1200 pixels. The field of view in the plane of the measurement range is 340 by 250 mm. Reproducibility of obtaining each position in the object's coordinate system is illustrated as standard deviation of sensor readings. Variability in consecutive directions is summarized in Table 1.

Variation of positioning in the direction normal to the marker is greater, but in practical problems, often the precision required in this direction is lower. This can be seen in the case of manipulating the objects, wherein variations are compensated by the gripper. If vacuum gripper is used, inaccuracy can be compensated due to the elasticity of the suction cup. In the case of welding, the inaccuracy of the position in the direction normal to the QR code, and thus in the direction of welding nozzle, usually can be compensated by automatic regulation of the arc length and the automatic adjustment of the welding parameters.

## 8 Conclusions

The paper presents a method for dynamic modification of the programs of industrial robots. The use of coded tags to mark objects enables selecting the appropriate program and adjusting the coordinate system to object location in the robot's working space. The algorithms required for determining the position of objects using matrix codes, recognized by the stationary camera, cooperating with the industrial robot are presented. Simplified, stable calibration for robots and cameras with low accuracy was proposed. Geometrical relationships, which should be calculated when the program of industrial robots is developed and executed, were presented. The results of repeatability test of solutions were collected and discussed.

Proposed by the authors, solution is a simple, inexpensive way to increase the universality of robotized stations. Further research should be done to improve the accuracy and repeatability of the system, so that the proposed method for the optical determination of the position of objects could replace the use of expensive rigid positioners in the working space of industrial robots.

**Acknowledgements** The presented research results were funded with grants for education allocated by the Ministry of Science and Higher Education in Poland.

## References

1. Rekimoto, J.: Matrix: a realtime object identification and registration method for augmented reality. In: 3rd Asia Pacific Computer Human Interaction, pp. 63–68. (1998)
2. Rostkowska, M., Topolski, M.: On the Application of QR codes for robust self-localization of mobile robots in various application scenarios. In: Szewczyk, R., Zieliński, C., Kaliczyńska, M. (eds.) *Progress in Automation, Robotics and Measuring Techniques*, pp. 243–252. Springer, Germany (2015)
3. Suriyon, T., Keisuke, H., Choompol, B.: Development of guide robot by using QR code recognition. In: 2nd TSME International Conference on Mechanical Engineering, pp. 1–6 2011
4. Andersen, R.S., Damgaard, J.S., Madsen, O., Moeslund, T.B.: Fast calibration of industrial mobile robots to workstations using QR codes. In: IEEE ISR, pp. 1–6 2013
5. Yuan, J.S.-C.: A general photogrammetric method for determining object position and orientation. *IEEE Trans. Robot. Autom.* **5**(2), 129–142 (1989)
6. Oberkampf, D., DeMenthon, D.F.: Iterative pose estimation using coplanar feature points. *Comput. Vis. Image Underst.* **63**(3), 495–511 (1996)
7. Quan, L., Lan, Z.: Linear N-point camera pose determination. *IEEE Trans. Pattern Anal. Mach. Intell.* **21**(8), 774–780 (1999)
8. Negahdaripour, S., Prados, R., Garcia, R.: Planar homography: accuracy analysis and applications. In: IEEE International Conference on Image Processing, I–1089. (2005)
9. Lepetit, V., Moreno-Noguer, F., Fua, P.: EPnP: an accurate O(n) solution to the PnP problem. *Int. J. Comput. Vis.* **81**(2), 155–166 (2009)
10. Dementhon, D.F., Davis, L.S.: Model-based object pose in 25 lines of code. *Int. J. Comput. Vis.* **15**(1–2), 123–141 (1995)
11. Marchand, E., Chaumette, F.: Virtual visual servoing: a framework for real-time augmented reality. *Eurographics* **21**(3), 289–298 (2002)
12. Marchand, E., Spindler, F., Chaumette, F.: ViSP for visual servoing: a generic software platform with a wide class of robot control skills. *IEEE Robot. Autom. Mag.* **12**(4), 40–52 (2005)
13. Tsai, R.Y., Lenz, R.K.: New technique for fully autonomous and efficient 3D robotics hand/eye calibration. *IEEE Trans. Robot. Autom.* **5**(3), 345–358 (1989)
14. Horaud, R., Dornaika, F.: Hand-Eye Calibration. *Int. J. Rob. Res.* **14**(3), 195–210 (1995)
15. Strobl, K., Hirzinger, G.: Optimal hand-eye calibration. In: IEEE/RSJ International Conference on Intelligent Robots and Systems, vol. 3, pp. 4647–4653. 2006
16. Liang, R., Mao, J.: Hand-eye calibration with a new linear decomposition algorithm. *J. Zhejiang Univ. Sci. A* **9**(10), 1363–1368 (2008)
17. Ruland, T., Pajdla, T., Kruger, L.: Globally optimal hand-eye calibration. In: IEEE Computer Society Conference on Computer Vision and Pattern Recognition, vol. 2, pp. 1035–1042. 2012

18. Tsai, R.Y., Lenz, R.K.: Real time versatile robotics hand/eye calibration using 3D machinevision. In: IEEE International Conference on Robotics and Automation, pp. 554–561. 1988
19. Daniilidis, K.: Hand-Eye calibration using dual quaternions. *Int. J. Rob. Res.* **18**(3), 286–298 (1999)
20. Schmidt, J., Vogt, F., Niemann, H.: Robust hand-eye calibration of an endoscopic surgery robot using dual quaternions, *Pattern Recognition*. In: 25th DAGM Symposium, vol. 2781, pp. 548–556. 2003
21. Zhang, J., Shi, F., Liu, Y.: An adaptive selection of motion for online hand-eye calibration. *AI Adv. Artif. Intell.* 520–529 (2005)
22. Curtis, W.D., Janin, A.L., Zikan, K.: A note on averaging rotations. In: IEEE Virtual Reality Annual International Symposium vol. 2, pp. 377–385. 1993

# Topology Optimisation Aimed at Additive—SLM Manufacturing of Metal Parts of ExoArm 7-DOF

Pawel Herbin, Dariusz Grzesiak and Marcin A. Krolikowski

**Abstract** Topology optimisation of mechatronic scanner arm components is presented in this chapter. Optimisation was carried out after static, linear FEM analysis of parts. Von Mises stress map was applied for topological optimisation (TO). Topological optimisation was performed by removal of body's volumes. Optimised parts after removal remained partially perforated. Only functional areas of the parts remained unchanged. In order to fulfil outer part functional dimensions, cell lattice structures were applied. Cell structures were prepared in CAD/CAM system, fully parameterised. Boolean operations on optimised parts were applied to fill empty volumes. Parts were then generated with application of selective laser melting (SLM) technique. After SLM, machining of matching surfaces of corresponding elements was applied.

**Keywords** Selective laser melting · SLM · FEM · Topology optimisation  
Lattice structures

## 1 Introduction

Selective laser melting (SLM<sup>TM</sup>) is a generative technique grouped in rapid manufacturing range derived from rapid prototyping technologies. During SLM, metal (or alloy) powder is selectively melted in horizontal areas, slice by slice. “Selective” means that melting process is realised only in areas included for scanning. The element is manufactured slice by slice. Virtual model is generated from CAD system, as an STL file; prepared for melting by a special, dedicated software; and then uploaded to a machine controller. Preparation for melting process includes generation of support structures and division of the element vertically into slices. Selective laser melting is getting to be a common manufacturing technique, used in

---

P. Herbin · D. Grzesiak · M.A. Krolikowski (✉)  
Faculty of Mechanical Engineering and Mechatronics, West Pomeranian University  
of Technology, Piastów Av. 19, 70-310 Szczecin, Poland  
e-mail: marcin.krolikowski@zut.edu.pl

the wide spectrum of scientific and industrial applications. Research on SLM process focuses on following main areas: manufacturing of implants from biocompatible alloys and personalised medical equipment [1–7], manufacturing of composites and nanocomposites [8, 9], generating the fully controlled lattice ultralightweight structures [10]. SLM is applied as well to the production of special tools used in different manufacturing techniques, like conformal cooling systems for injection moulds and punches & dies for plastic working [11]. The possibility to manufacture almost all geometric structures and shapes creates opportunities to use it in combination with models of parts resulting from the optimisation of the topology.

Topology optimisation (TO) [12] is a mathematical method that optimises material layout for a given set of loads, boundary conditions and constraints within a given design space, with the desired goal, for example, maximising the performance of the system. TO is different from shape optimisation in the sense that the design can attain any shape within the design space, instead of dealing with pre-defined configurations.

The conventional TO formulation uses a finite element method (FEM) to evaluate the design performance. Nonlinear programming techniques such as the method of moving asymptotes, genetic algorithms and optimality criteria are typically used for the design optimisation. Another method of solving TO is the use of level sets [13] and topological derivatives.

Topology optimisation is mostly used at the initial level of the design process to arrive at a design proposal that is then fine-tuned for performance and manufacturability. This replaces time-consuming and costly design iterations while improving design performance.

In some cases, results from a topology optimisation, although optimised, may be expensive or infeasible to manufacture by traditional technologies. These challenges can be overcome through the use of manufacturing constraints in the problem formulation or through the use of additive manufacturing technology.

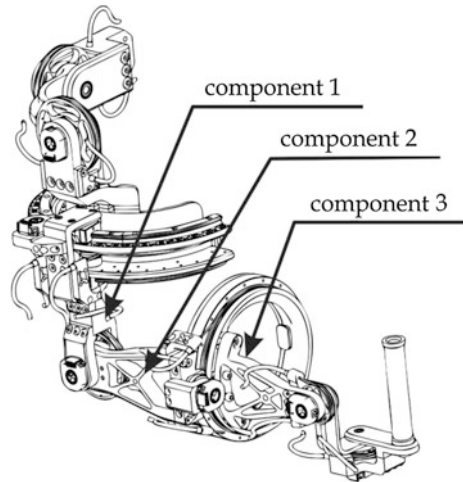
## 2 Research Objective

The subject of the optimisation process was elements of an ExoArm 7-DOF (interactive 7-DOF motion controller of the operator arm) in the form of exoskeleton. Interactive operator arm motion scanner is a mechatronic device [14]. Its task is to allow the realisation of control of virtual and real equipment with force feedback.

Designed device is equipped with a variety of sensors such as sensors of torque moments and operator force interaction as well as drives with tension gear. Device drives have to synchronise the movement of a scanner with the movement of the arm of operator together with the realisation of force feedback. Therefore, the drive power is dependent on the maximum forces interacting with the operator and the moments resulting from dynamic motion. Research on simulation shows that the strength of the interaction with operator slightly affects the power of drives. Much



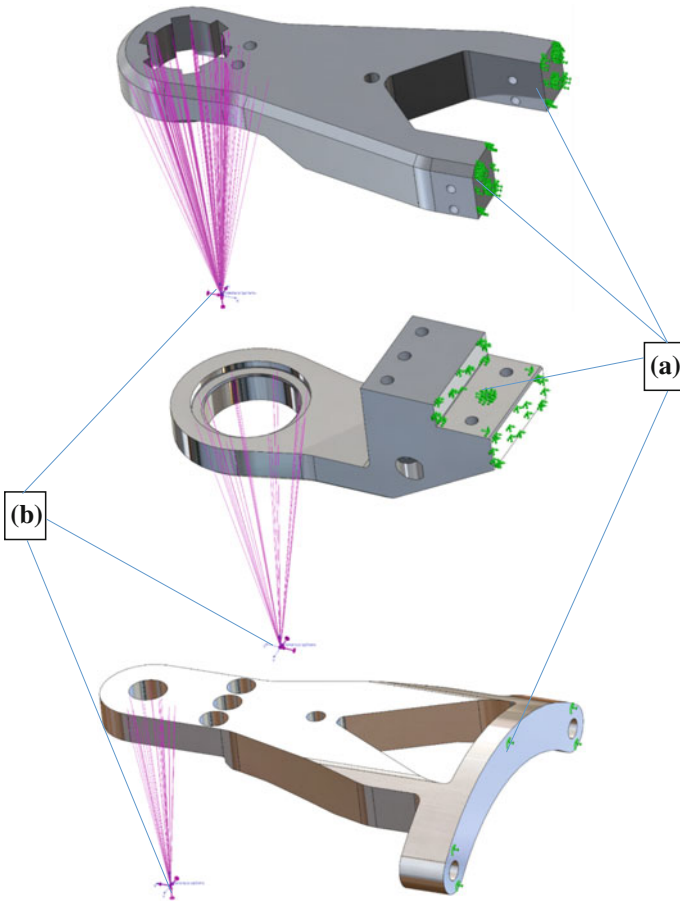
**Fig. 1** ExoArm 7-DOF together with the indicated items foreseen to be manufactured by AM (Additive Manufacturing)



more impact has inertia forces and the influence of gravity. Therefore, it is necessary to reduce the mass of the moving components. As a result, weight of the unit was reduced by removal of the drives from the parts and application of cable transmission along with the measurement of torque. Weight of the operator arm movement scanner mechanism had to be reduced also by the reduction of parts weight. Assembly elements up to now are made of 7075 aluminium alloy and steel. In order to further reduce weight, three parts (marked as 1, 2 and 3—Fig. 1) were selected to be topologically optimised and manufactured with the application of selective laser melting of Ti6Al4 V titanium alloy [15] in order to reduce the weight while maintaining the specified strength. Figure 1 shows the interactive operator arm movement scanner with the indicated items foreseen for additive manufacturing.

### 3 Research Methodology

Process optimisation was preceded by using the finite element method—linear static structural analysis. The parts were discretised using linear tetrahedral finite elements. Each of the analysed parts was clamped in corresponding areas where the target will be in contact with the other elements of the scanner. Clamp fixed translational degrees of freedom on selected walls (Fig. 2a). Then, each of the parts has been loaded with the concentrated force and torque moment in reference point (Fig. 2b), which has been correlated with the real loads in a complete kinematic assembly of movement scanner (Fig. 1). The values of the forces for individual components are shown in Table 1.



**Fig. 2** Clamp areas (a) and loads (b) of exoskeleton elements

**Table 1** Forces and torque moments for each part

No.	Part no.	X Force (N)	Y Force (N)	Z Force (N)	X Torque moment (Nm)	Y Torque moment (Nm)	Z Torque moment (Nm)
1	1	21.03	17.32	21.81	25.77	4.79	50.83
2	2	21.03	17.32	21.81	25.77	4.79	50.83
3	3	4.55	3.92	4.61	0.22	19.79	15.28

The results of the analysis are shown in Figs. 3 and 4. Reduced von Mises stress distribution is shown in Fig. 3. Figure 4 shows the distribution of the nodal displacements.

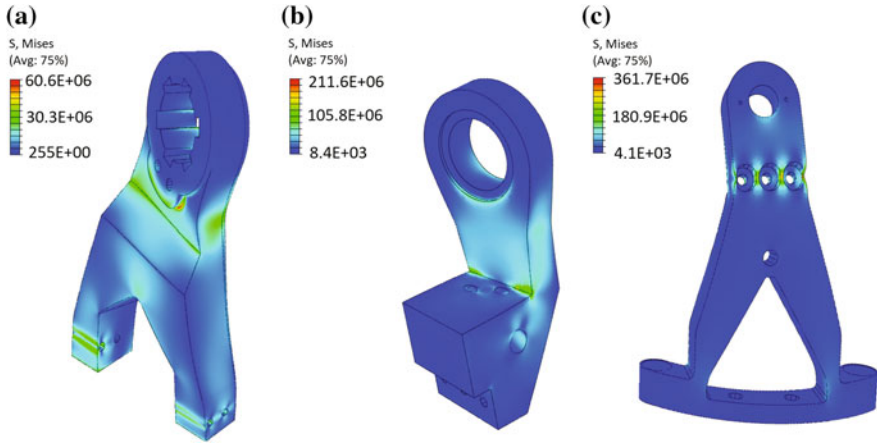


Fig. 3 Von Mises stress distribution

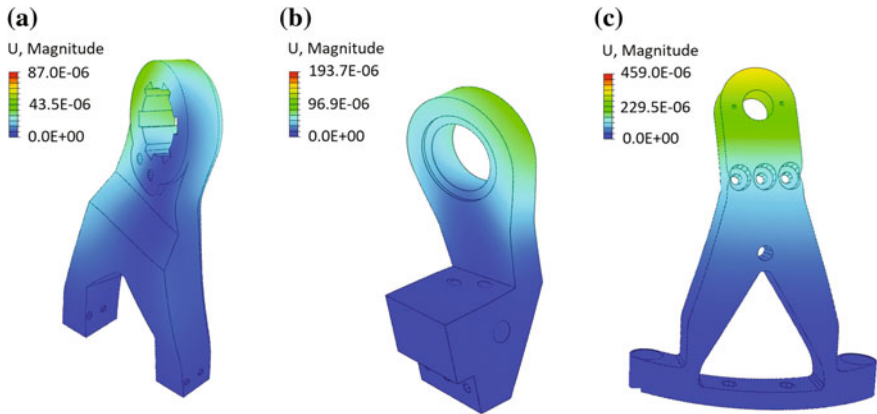


Fig. 4 Distribution of the nodal displacements

As an objective function of the optimisation process, a minimum volume of material parts was assumed, while applying restrictions in the form of the maximum stress focused with a value of 560 MPa. This value results from the values of yield strength ( $R_p 0.2$ ) of the final material of the parts (Ti6Al4 V- $R_p 0.2 = 1120$  MPa [14]), divided by 2, which was the result of the safety factor application.

In order to preserve the functionality of the optimised part, selected areas were excluded from the analysis. These areas are in contact with either other corresponding parts or the connectors placement. Comparison of part geometry obtained in the process of the geometry optimisation is shown in Figs. 5, 6 and 7, respectively, for part No. 1, 2 and 3 of exoskeleton.

Optimisation resulted in significant reduction in the analysed parts volume. The exact values of the volume of each part before and after the optimisation are presented in Table 2.

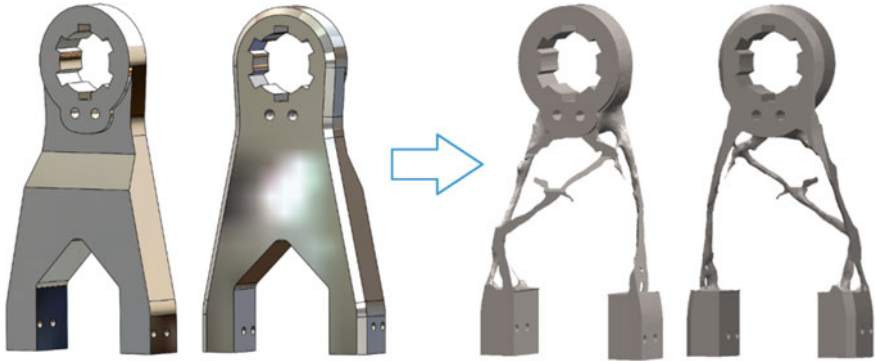


Fig. 5 Optimisation volume “morphing” for part No 1

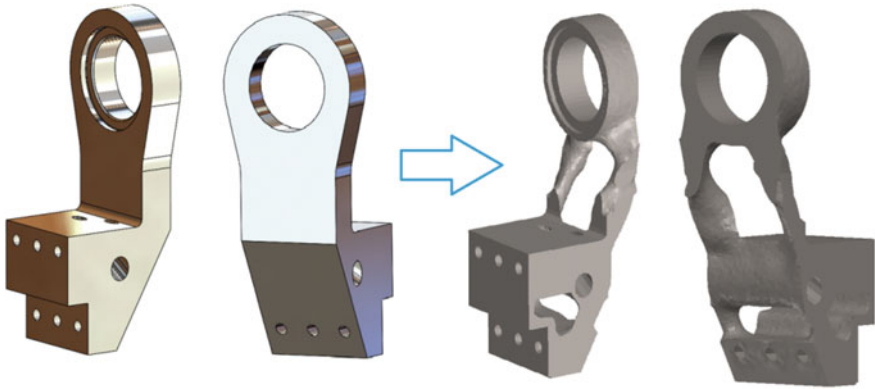


Fig. 6 Optimisation volume “morphing” for part No 2

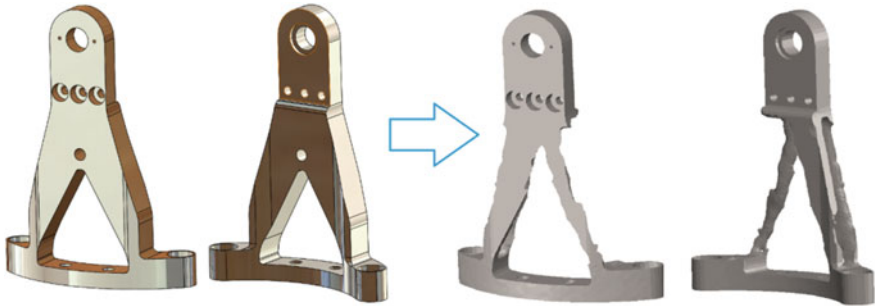


Fig. 7 Optimisation volume “morphing” for part No 3

## 4 Post Processing—Application of Lightweight Lattice Structures

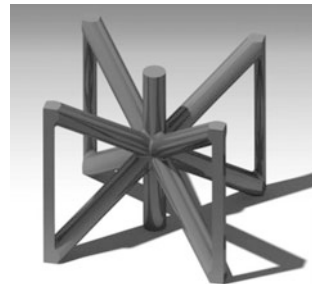
Empty space of components left after optimisation had to be filled with some body. Ultralightweight matrix was applied because of further SLM manufacturing process. Manufacturing of parametric ultralightweight lattice structures is possible only with the application of additive manufacturing, for example, SLM technique.

Aimed at this, structure type XLo (Fig. 8) was selected. Figure 8 presents view of the cell element. Cell dimensions are  $5 \times 5 \times 5$  mm with round bridges of dia. 1 mm. Matrix was prepared in CAD/CAM system CATIA v5. Technology known as “PowerCopy” was applied to generate single cell. Cell is fully parameterised to be patterned then across the parts. To prevent functional areas contacting with the corresponding moveable parts of the sensor, Boolean operators were applied. Such approach generated solid elements in functional parts and ultralightweight structure around optimised bridges after material removal. Figures 9, 10 and 11 show,

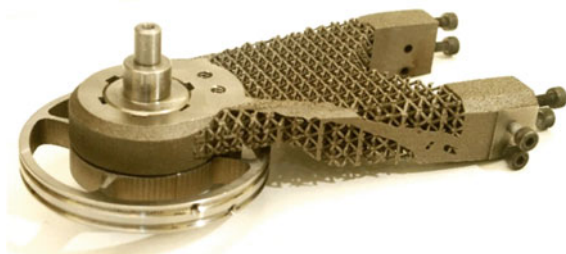
**Table 2** Results of the optimisation

Part	Volume before optimisation (cm <sup>3</sup> )	Volume after optimisation (cm <sup>3</sup> )	Percentage reduction (%)
1	85.703	19.29	77.5
2	38.408	22.13	42.4
3	61.64	33.61	45.5

**Fig. 8** Structure cell with code name XLo  $5 \times 5$  mm



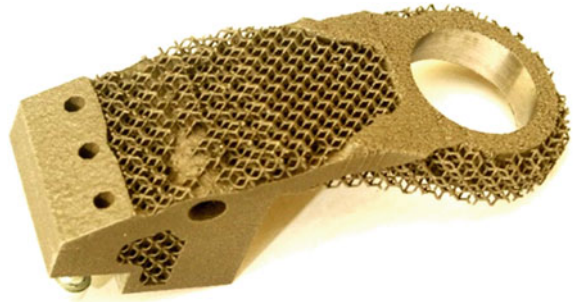
**Fig. 9** Part No. 1 ready for assembly



**Fig. 10** Part No. 2 ready for assembly



**Fig. 11** Part No. 3 ready for final assembly



respectively, parts 1, 2 and 3 photos, after SLM manufacturing with lattice structures filling the part bodies. Parts are presented after machining process, ready for assembly.

## 5 Summary

Topology optimisation caused significant removal of part volume; therefore, insertion of lattice structure to fill parts dimensions was essential. Cells coded XLo with small bridge diameters were applied. Some deformations of structures, caused by residual thermal stresses were, however, observed after a couple of months. Additional thermal processing—heat treatment—is essential for removal of residual stresses of complex lattice structures after SLM manufacturing. Alternative cell types are also taken into account for further research.

Additional and further research is foreseen to predict the effects of residual stresses versus the type of cell element and type of geometrical bodies. Analytical prediction finally could be very useful although needs a lot of experimental research.

Experiments with new materials with anti-stress additives or even experiments with alloys for lattice cell structures are foreseen as well.

A dedicated scientific project would be essential to solve above issues.

**Acknowledgements** This project is financed by the National Centre for Research and Development, Poland (NCBiR), under the Applied Research Programme—Grant Agreement No. PBS3/A6/28/2015.

## References

1. Wehmoller, M., Warnke, P.H., Zilian, C., Eufinger, H.: Implant design and production—a new approach by selective laser melting. *Inter. Congr. Ser.* **5**, 690–699 (2005)
2. Lin, C.Y., Wirtz, T., Lamarca, F., Hollister, S.J.: Structural and mechanical evaluations of a topology optimised titanium interbody fusion cage fabricated by selective laser melting process. *J. Biomed. Mater. Res. Part A* **88**, 272–279 (2007)
3. Mullen, L., Stamp, R.C., Brooks, W.K., Jones, E., Sutcliffe, C.J.: Selective laser melting: a regular unit cell approach for the manufacture of porous, titanium, bone in-growth constructs, suitable for orthopaedic applications. *J. Biomed. Mater. Res. B Appl. Biomater.* **89**, 325–334 (2008)
4. Mullen, L., Stamp, R.C., Fox, P., Jones, E., Ngo, C., Sutcliffe, C.J.: Selective laser melting: a unit cell approach for the manufacture of porous, titanium, bone in-growth constructs. *J. Biomed. Mater. Res. B Appl. Biomater.* **90**, 178–188 (2009)
5. Uklejewski, R., Winiecki, M., Rogala, P., Mielniczuk, J.: Selective laser melted prototype of original minimally invasive hip endoprosthesis. *Rapid Prototyping J.* **17**(1), 76–78 (2011)
6. Uklejewski, R., Rogala, P., Winiecki, M., Kędzia, A., Ruskowski, P.: Preliminary results of implantation in animal model and osteoblast culture evaluation of prototypes of biomimetic multipiked connecting scaffold for noncemented stemless resurfacing hip arthroplasty endoprostheses. *BioMed Res. Int.* (formerly titled *Journal of Biomedicine and Biotechnology*), ID 689089 (2013)
7. Uklejewski, R., Rogala, P., Winiecki, M., Mielniczuk, J.: Prototype of minimally invasive hip resurfacing endoprosthesis—bioengineering design and manufacturing. *Acta Bioeng Biomech.* **11**(2), 65–70 (2009)
8. Lu, L., Fuh, J.Y.H., Chen, Z.D., Leong, C.C., Wong, Y.S.: In situ formation of TiC composite using selective laser melting. *Mater. Res. Bull.* **35**, 1555–1561 (2000)
9. Gu, D., Hagedorn, Y.C., Meiners, W., Wissenbach, K., Poprawe, R.: Nanocrystalline TiC reinforced Ti matrix bulk-form nanocomposites by selective laser melting (SLM): densification, growth mechanism and wear behaviour. *Compos. Sci. Technol.* **71**, 1612–1620 (2011)
10. Santorinaios, M., Brooks, W., Sutcliffe, C.J., Mines, A.W.: Crush behaviour of open cellular lattice structures manufactured using selective laser melting. *High Perform. Struct. Mater.* **3**, 481–490 (1985)
11. Abe, F., Osakada, K., Shiomi, M., Uematsu, K., Matsumoto, M.: The manufacturing of hard tools from metallic powders by selective laser melting. *J. Mater. Process. Technol.* **111**, 210–213 (2001)
12. [https://en.wikipedia.org/wiki/Topology\\_optimisation](https://en.wikipedia.org/wiki/Topology_optimisation)
13. Bendsoe, M.P., Sigmund, O.: *Topology optimisation: theory, methods, and applications*. Springer Science & Business Media, Berlin (2013)
14. Herbin, P., Pajor, M.: Exoskeleton of upper limb—model with application of real movement measurement, *Engineering modelling*, pp. 40–46 (2015)
15. EOS Titanium Ti64 material datasheet

# Applications of Optomechatronic Technologies in Innovative Industry

Tomasz Giesko and Adam Mazurkiewicz

**Abstract** This paper presents a review of the recent progress of optomechatronics for innovative industry. In identifying the direction of further development of optomechatronic technologies, the authors have used their own extensive experience in implementing numerous high-end vision systems for monitoring the technological processes and product inspection as well as unique research equipment. During the analysis of the literature, reports and case studies, the authors indicate future trends in the area of optomechatronic technologies that involve hybrid inspection methods that use 2D and 3D imaging methods and terahertz spectroscopy, which increases the resolution of camera sensors. Observed problems and limitations of optomechatronic technologies are discussed. This chapter presents selected examples of implementations with the authors' participation of automated optical systems in industry. The system for visual inspection and qualitative selection of shafts in the automotive industry and the hybrid system for online monitoring the plastic forming processes are described. The original hybrid inspection method of the aluminium extrusion process demonstrates the ability to detect defects in the material structure that are not visible in the visible range. A new important direction of research planned in the authors' scientific activity is the use of terahertz imaging for the inspection of materials and products.

**Keywords** Innovative industry · Optomechatronic technologies · Knowledge transfer

## 1 Introduction

Increasing the productivity of industrial enterprises is a key priority in maintaining market competitiveness. The effectiveness of production processes, the quality of the manufactured products and the cost of production are crucial to its level. These

---

T. Giesko (✉) · A. Mazurkiewicz  
Institute for Sustainable Technologies, National Research Institute, Radom, Poland  
e-mail: tomasz.giesko@itee.radom.pl



factors depend directly on the level and intensity of the implementation of innovative technologies in enterprises in the fields of robotics, automation and the computerization of production processes. Complementary action to increase the production efficiency is to increase the flexibility of production lines by reconfiguring and adapting them to a variety of tasks with a focus on the future development of intelligent modular production systems [1]. A comprehensive and systematic approach to the organization and operation of innovative enterprises using smart technologies represents the features of *Factories of the Future* [2].

Innovative solutions for improving the quality and efficiency of manufacturing processes in industry are the result of research and development combining technologies from different areas of intelligent specialization. The integration of various areas of research and development is a key to the development of new incremental or breakthrough technologies. A particularly interesting example of the process of shaping new multidisciplinary research and technological development areas is optomechatronics, which is a synergic integration of mechatronics and optoelectronics [3, 4]. For several years, the growing role of optomechatronic technology in enhancing the level of innovation in the economy is indicated in the priorities of the strategy for the development of research and industry [5]. The key importance of advanced pro-development and industrial technologies is reflected in the priorities of the EU Framework Programme “Horizon 2020”, which is a programme oriented towards the development of enterprises [6]. Issues in the area of optomechatronics have been included in the R & D priorities within the scope of “National Smart Specializations in Poland”. Responding to the growing demand of industry for modern technologies are strategic programmes that provide solutions to the problems of the development of system innovativeness in a systematic way and consolidate and integrate the potential of research and development institutions [7]. The articles prepared on the base of achieved results discuss the main trends in the development of optomechatronic technologies for industry and present selected examples of innovative optomechatronic systems developed at ITeE-PIB and implemented in industrial companies [8].

## **2 The Area of Research and Main Directions for the Development of Optomechatronic Technologies for Industry**

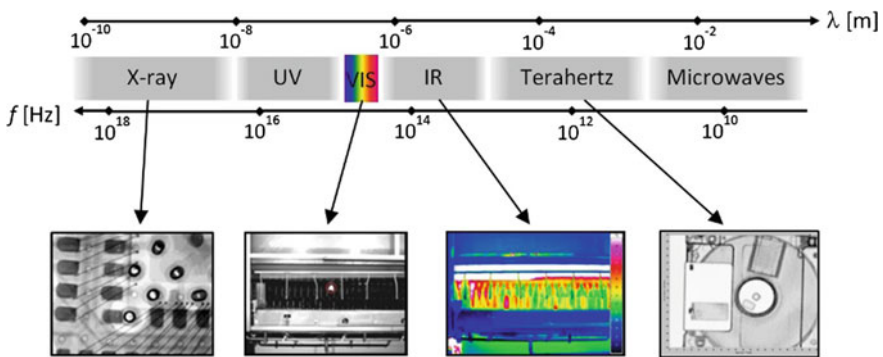
An overview of vision systems and their applications in a variety of industrial branches during the previous decade was presented in [9]. The author points out the following as the most significant challenges to the modern vision systems applied in industry: the flexibility of the vision systems and their ability of adaptation to evolving tasks, and the development of image processing sensor and human-computer interfacing. The prevailing group of solutions used in industry are the systems for automated optical inspection used in production. Selected examples of

progress in optomechatronic technologies, including laser and fibre optics, machine vision, micro-optoelectro-mechanical systems and optomechatronics for manufacturing applications, are presented in [10].

The specificity of optomechatronic systems primarily originates from the principles of the interaction of optical radiation with matter and the change of the attributes of radiation occurring as a result of reflection, diffusion, transmission and deflection. Optical sensors are used to enable imaging in different spectral ranges that extend beyond the visible spectrum (Fig. 1). A breakthrough in industrial inspection methods is a terahertz technology with a radiation range of approx. 0.1–10 THz [11]. Wide use of terahertz technology will be fully possible in the future with the further development of sources and radiation detectors. In the design of measuring systems, the direct dependence of optical resolution and the accuracy of measurements taken from the wavelength of the applied optical radiation determine the application capabilities of the system.

The use of computer technology to analyse these phenomena in integration with mechatronic technologies allowed new functionalities, which are characteristic of the breakthrough of optomechatronic technology. Optomechatronic systems show significant features, such as the ability to use non-contact measurement, the use of information encoded in a vision image for object evaluation, high immunity to interference, the ability to detect signals in an extended range of electromagnetic spectrum, and integration in automation systems for technological processes. The most common feature of optomechatronic systems is the modularization of the structure, which integrates optoelectronic sensors that perform specialized tasks, dedicated microcomputers and mechatronic modules.

In the general structure of the optical inspection system (Fig. 2), the following basic components are distinguished:



**Fig. 1** Spectrum of electromagnetic radiation and sample images recorded in selected radiation ranges

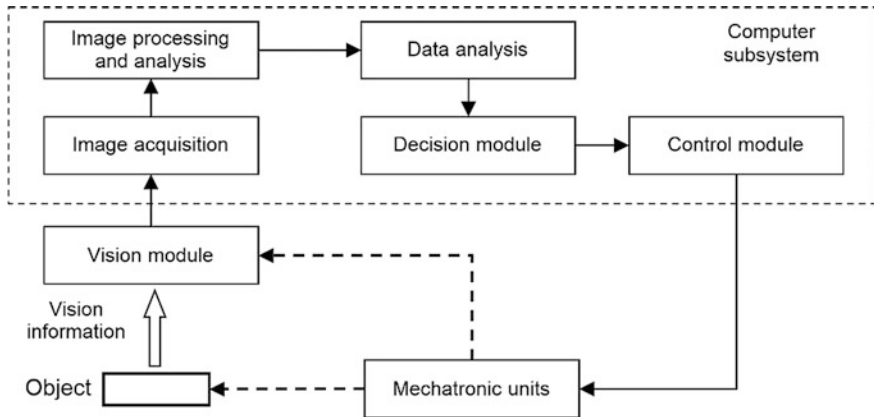


Fig. 2 Diagram of the structure of the optical inspection system in a general

- a vision module that records an image of an object;
- a computer system that performs the tasks of recording, processing and analysing images and the obtained measurement results, as well as controlling the monitoring process; and
- mechatronic executive systems.

The optical signal that reaches the camera sensor is converted to an analogue signal and then to digital signal and finally stored in the computer's memory. The image is digitally processed using appropriate algorithms to distinguish features that may be relevant for the object's monitoring and inspection process. In the process of digital image analysis, the detection and quantification of the features make it possible to identify and classify them.

In the optical inspection system, there exists a feedback loop in which the optical information of the object converted into a quality inspection result is the basis for the activation of control processes for mechatronic units. Basic tasks of units include the transportation of inspected products with their positioning in the measuring zone and the selection of products after quality inspection. Other functions performed by mechatronic systems may include cleaning the products before inspection, changing the position of the vision module relative to the controlled object and changing the configuration of the vision module (e.g. lighting positions).

The following key factors determine the level of technical sophistication and the innovation of optical inspection systems:

- Camera parameters, including resolution of the sensor, spectral sensitivity, rate of image acquisition and data transfer;
- Parameters of lenses, including optical resolution and image distortion level;
- Used lighting methods and parameters of illuminators;

- The performance and efficiency of image processing and analysis algorithms; and,
- Operational features, including immunity to interference, producing reliability.

Advanced optomechatronic systems enable the achievement of high measurement accuracy, providing the repeatability and stability of automated measurement processes. An important problem in the design of industrial inspection systems is often the necessity of adjusting the speed of operation to the efficiency of the production line.

Due to the specifics and often high innovative level of the developed optomechatronic systems, the methodology of design and implementation of optomechatronic solutions, in particular unique optomechatronic systems, must take into account the systematic approach to addressing the problems that arise with the involvement of multidisciplinary teams of scientists and engineers and using advanced modelling and simulation methods [12]. Therefore, the design and implementation processes of optomechatronic systems vary considerably from typical engineering projects. Selected key issues in the design and implementation of optomechatronic systems, as observed in R & D and application projects, are presented in Table 1.

As the main directions for the development of optomechatronic technologies for the needs of innovative industry, the following should be noted:

- Increasing the resolution of camera sensors;
- Increasing acquisition and transfer rates for images recorded in computer memory (introduction of 10 GigE cameras);
- The development of hyperspectral and multispectral cameras;
- The development of terahertz imaging technology;
- The development of hybrid methods and systems that combine different methods (e.g. fusion of images recorded in different electromagnetic spectrum ranges);
- The development of 3D imaging methods;
- The development of adaptive optical systems, including liquid lenses; and
- The development of micro-optoelectro-mechanical systems technology.

The results of the research work show a wide range of possibilities for the use of inspection systems based on the analysis of radiation reflected from objects as well as the emission of materials subjected to terahertz radiation [13].

An analysis of available reports and market forecasts for optomechatronic technologies indicates a steady increase in their share in industrial production. The global market value of machine vision systems will increase from around \$19 billion in 2016 is estimated at \$30 billion in 2021 [14].

**Table 1** Selected issues occurring during the design and implementation of optomechatronic systems

Issue	Applied approach and actions
Utilization of phenomena of light interacting with matter and effects of changes in radiation characteristics as a result of reflection, deflection, dispersion and transmission within the developed solutions	Application of specialized apparatus and software for data analysis; Application of specialized methods of modelling and simulation intended for the area of photonics
Methods of encoding information using: – coherent radiation (attributes: amplitude, frequency, radiation phase, direction of polarization); – non-coherent radiation (attributes: intensity distribution, spectral range, polarization)	Modelling and simulations Selection of sampling and quantization parameters for optical signals by analysis and experiments
Integration of mechatronic and optoelectronic components and systems	The application of a method of simultaneous implementation of tasks
The high accuracy of optomechatronic systems The influence of the accuracy of construction and mechanical disturbance factors (strokes, vibrations) on optomechatronic systems	Detailed analysis and identification of disturbing factors and the application of methods to eliminate or reduce their effect The application of specialized mounting technology The application of appropriate calibration methods
The uniqueness of the solution Limited range or no other available components providing analogous parameters	Growing database for components available on the market; The development of alternative concepts and design projects
Sensitivity of optoelectronic systems to environmental factors	The need for detailed analysis and identification of disturbing factors and for taking into account effective methods to eliminate or limit them; Taking into account the increase in project costs

### 3 Examples of Applications of Optomechatronic Technologies in Innovative Industry

The main directions of research in the field of optomechatronic technologies implemented at the Institute for Sustainable Technologies—NRI, with the author's participation correspond to the latest world trends in this field. The results of research and development works are several dozen innovative specialized solutions for many industries, including metal, automotive, tobacco, glass, as well as special production areas. The systems presented below are only some selected examples of effective cooperation between the Institute and industry.

### 3.1 *System for Visual Inspection and Qualitative Selection of Shafts*

The developed system is intended for automated optical inspection of metal shafts and their qualitative selection [15]. The system enables the inspection of the following features: thread, knurls, grooves and measurements of the shaft length. The principle of the operation of the device consists in the use of three CCD cameras vision system for acquisition of images of inspected shafts (Fig. 3). The solution allows the detection of defects in subregions with a high optical resolution. To ensure proper lightning of the inspected shaft, specialized front-light and back-light LED illuminators were developed.

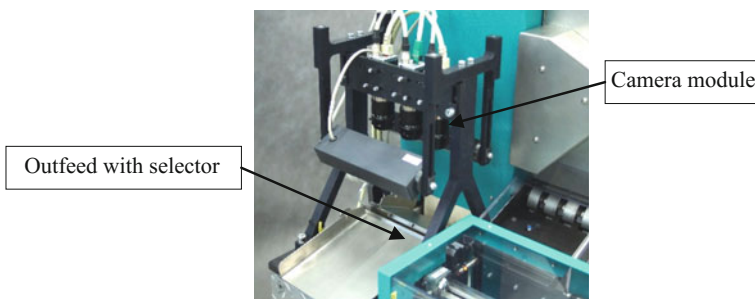
The image processing is performed by original software with the use of the following operations: filtering, morphology operations (dilation and erosion) and edge identification (Fig. 4). Various shaft measurements are checked and calculated, and features of the shaft are detected (thread, knurls, grooves).

The shaft measurement is calculated based on the position of the shaft ends presented in images with use of the “Look-up Table” (Fig. 5). The two-dimensional Look-up Table was created in order to calculate a correct shaft length considering perspective errors. The system allows shaft length measurements with an accuracy of 0.1 mm.

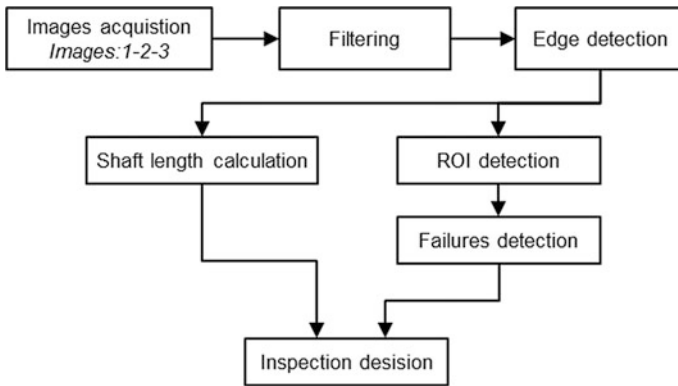
The developed system was implemented in a company producing products in large scale, delivered to the recipients who are global automotive companies.

### 3.2 *Hybrid System for Monitoring the Plastic Forming Processes*

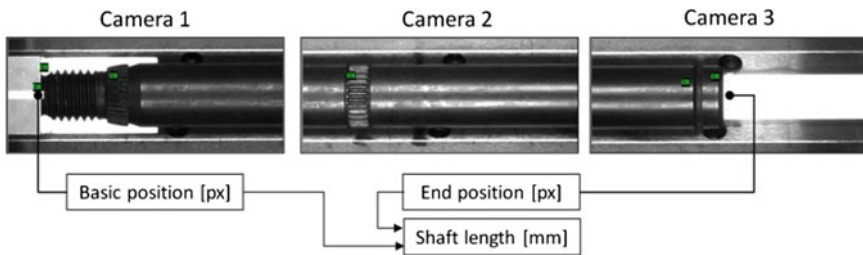
The result of the research project is a method and hybrid system for monitoring industrial processes of hot extrusion and automated online inspection of extruded profiles [16]. The innovative hybrid monitoring method developed is based on the



**Fig. 3** Visual inspection and qualitative selection module in the developed device

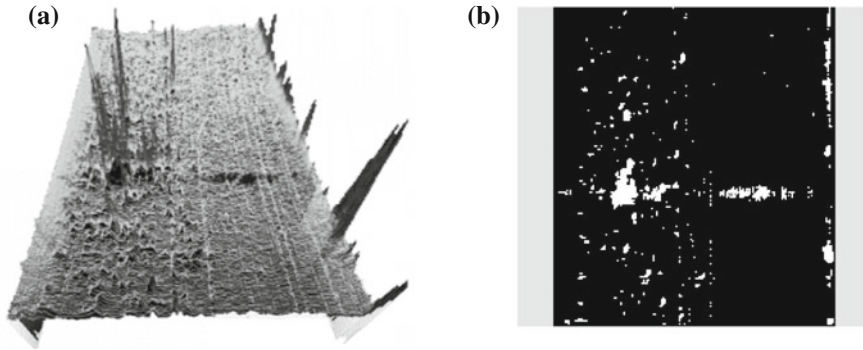


**Fig. 4** Scheme of inspection procedure

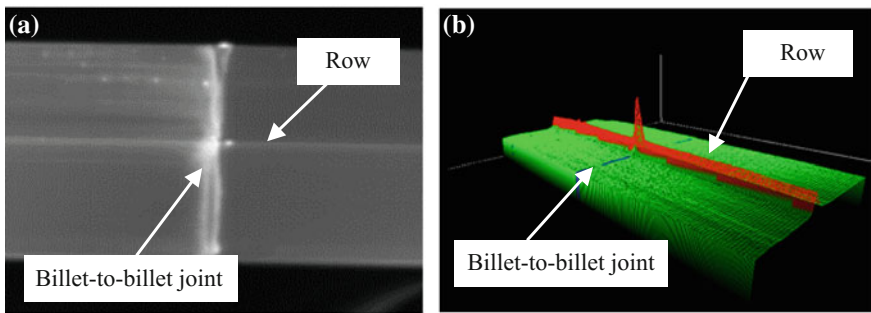


**Fig. 5** Shaft length measurement

use of combined techniques for surface observation in the infrared and visible bands and the computerized analysis of recorded images. Applied algorithms enable the detection of various types of defects of the products and the identification of irregularities in the technological process based on the analysis of thermograms presenting the temperature distribution on the surface of the product. The following defects can be identified: streaks, grooves, cracks, recesses, blisters, bonding lines, dimensional defects and shape defects [17, 18]. The authors' special achievement is the developed hybrid method that enables the detection of an uncontrolled local increase in temperature, which results in streak defects that manifest themselves only after anodizing or painting of the aluminium profile. For observation of the surface of aluminium at high temperatures up to approx. 600 °C, a NIR sensor camera with a spectrum of 0.9–1.7 microns was selected. The proposed solution provides the most favourable conditions of temperature measurement due to the characteristics of the emissivity. The accuracy of temperature measurement by the camera is  $\pm 1$  °C. The 3D visualization of the temperature distribution on the surface of the profile is shown in Fig. 6a. Each temperature deviation from the assumed level is marked by the white colour on the image after the binarization process (Fig. 6b).



**Fig. 6** Visualization of experimental results: **a** 3D visualization of temperature distribution on the surface, **b** thermal image after the process of binarization



**Fig. 7** Examples of defects observed on the surface of profile: **a** thermogram after thresholding operation **b** 3D thermogram after erosion and dilation operations

The developed system enables the detection and identification of various types of aluminium profile defects (Fig. 7). The potential uses of the hybrid method and developed system include the monitoring of high temperature processing, such as hot rolling, hot forging and extrusion.

Continued work involves the application of high-resolution infrared cameras and multispectral cameras, and developing advanced algorithms for image processing and analysing.

## 4 Conclusion

This paper presents a state of the art review on the recent progress of optomechatronics for innovative industry. In identifying the direction of further development of optomechatronic technologies, the authors have used their own



extensive experience in implementing numerous high-end vision systems for monitoring the technological processes and product inspection as well as unique research equipment. This chapter presents only selected examples of developed solutions. The original hybrid inspection method of the aluminium extrusion process demonstrates the ability to detect defects in the material structure that are not visible in the visible range. The research works carried out by the authors utilize the latest achievements of optomechatronic technologies, such as an imaging method in terahertz band. Previous research confirms the potential for use of terahertz imaging for the inspection of materials and products in industry. The key determinant of the future use of terahertz spectrometry will be an increase in imaging resolution. The major challenge in optical inspection systems for the innovative industry is to increase the functionality and elasticity that allow modification and adaptation of the system to a variety of tasks in the production lines. Optomechatronic systems are now becoming indispensable in many industries, including automotive, aviation and special production. Trends in the further development of optomechatronic technology result from the industrial revolution strategy of “Industry 4.0” and new business needs. The main directions of R & D work include the further development of advanced photonic sensors and the use of hybrid methods, including 3D imaging.

## References

1. Daschenko, A.: *Manufacturing technologies for machines of the future*, Springer-Verlag, Berlin (2003)
2. European Commission: *Research&Innovation. Factories of the Future*. [http://ec.europa.eu/research/industrial\\_technologies/factories-of-the-future\\_en.html](http://ec.europa.eu/research/industrial_technologies/factories-of-the-future_en.html) (2014)
3. Cho, H.: *Optomechatronic: fusion of optical and mechatronic engineering*, CRC Press Taylor & Francis Group (2006)
4. Cho, H., Kim, M.Y.: *Optomechatronic technology: the characteristic and perspectives*. *Trans. Ind. Electron.* **52**(4), 932–943 (2005)
5. Mazurkiewicz, A.: *Technical support for sustainable development. Research and application directions*. (in Polish). Instytut Technologii Eksploatacji—Państwowy Instytut Badawczy, Radom (2011)
6. European Commission: *Horizon 2020, The EU Framework Programme for Research and Innovation*. <http://ec.europa.eu/programmes/horizon2020/en> (2014)
7. Mazurkiewicz, A.: *Strategic programme “Innovative Systems of Technical Support for Sustainable Development of Economy”, Final Report* (in Polish). Instytut Technologii Eksploatacji—Państwowy Instytut Badawczy, Radom (2015)
8. Mazurkiewicz, A., Giesko, T.: *Advanced mechatronic technologies to improve maintenance and manufacturing processes of technical objects*, (in Polish). Instytut Technologii Eksploatacji—Państwowy Instytut Badawczy, Radom (2015)
9. Malamas, E.N., Petrakis, E.G.M., Zervakis, M., Petit, L., Legat, J.D.: *A survey on industrial vision systems, applications and tools*. *Image Vis. Comput.* **21**, 171–188 (2003)
10. Tutsch, R., Cho, Y.-J., Wang, W.-C., Cho, H.: *Progress in optomechatronic technologies*, Springer (2013)
11. Jepsen, P.U., Cooke, D.G., Koch, M.: *Terahertz spectroscopy and imaging—modern techniques and applications*. *Laser Photonics Rev.* **5**(1), 124–166 (2011)

12. Giesko, T.: Design and implementation methodology of innovative optomechatronic systems (in Polish). Wydawnictwo Naukowe Instytutu Technologii Eksploatacji—PIB, Radom (2013)
13. Peiponen, K-E., Zeitler, A., Kuwata-Gonokami, M. (eds.): Terahertz Spectroscopy and Imaging, Springer (2013)
14. Research and Markets, Global Markets for Machine Vision Technologies. <http://www.researchandmarkets.com/reports/3979159/global-markets-for-machine-vision-technologies#pos-39> (2016)
15. Garbacz, P., Giesko, T.: Multi-camera vision system for the inspection of metal shafts. In: Challenges in Automation, Robotics and Measurement Techniques, Series of Advances in Intelligent Systems and Computing, vol. 440, pp. 743–752 (2016)
16. Garbacz, P., Giesko, T., Mazurkiewicz, A.: Inspection method of aluminium extrusion process. Arch. Civil Mech. Eng. **15**, 631–638 (2015)
17. Zhu, H., Zhang, X., Couper, M., Dahle, A.: Effect of initial microstructure on surface appearance of anodized aluminum extrusions. Metall. Mater. Trans. **40A**, 3264–3275 (2009)
18. Saha, K.: Aluminum Extrusion Technology, ASM International (2000)

# Case Study of Thermal Stress Distribution Within Coating Applied on Aluminum Plain Clutch Plate by Thermal Spray Coating Technique

Piotr Jablonski, Piotr Czajka, Adam Patalas, Rafal Talar and Michal Regus

**Abstract** In this paper, information about the durability of friction clutches under high heat conditions was described. As a way to extend their life and performance, thermal spray coating method is proposed. Process of modeling and conducting simulation in FEA (finite element analysis) environment was described. The thermal stress distribution in coating system in relation to the thickness of applied coating was investigated. Conducted simulation allowed to obtain data that presented strong correlation between coating thickness and both maximum value of Huber-Mises reduced stress and stress distribution characteristics within coating. Collected data allowed to evaluate the possibility of application of such coating on an aluminum plain clutch plate that works under high heat and dry conditions. Presented research has proven that design of such coating should especially consider coating thickness and thermal stress conditions, as these factors may have strong influence on reliability of clutch plates.

**Keywords** Thermal stress · Finite element analysis · Thermal spray  
Wear · Friction

## 1 Introduction

Friction clutches belong to the group of mechanical units which purpose is to couple driving part of the machine to driven part in the way that allows for the transmission of power and motion. Therefore, friction clutches are commonly applied in automotive, aerospace, and machine industry [1]. Increasing demands on

---

P. Jablonski (✉) · P. Czajka · A. Patalas · R. Talar (✉) · M. Regus  
Faculty of Mechanical Engineering and Management,  
Poznan University of Technology, Poznań, Poland  
e-mail: piotr.le.jablonski@doctorate.put.poznan.pl

R. Talar  
e-mail: rafal.talar@put.poznan.pl

performance and durability of clutch components require their continuous development in the field of wear and heat resistance.

Engagement of clutch plates is connected with the increase of contact pressure between these plates. Increasing value of this pressure combined with high relative slide velocity results in the generation of significant frictional heat which leads to high temperature rise on the clutch plate surfaces. This phenomenon is significant issue that must be taken into consideration, because it might cause meaningful thermomechanical problems such as occurrence of thermal deformations or thermoelastic instability that result in thermal cracking and high rate of wear [1, 2]. For these reasons, it is clear that during clutch components designing process, one of the most important issues that must be thought about is the choice of material for friction pair combined with optimal coating technology. Vast studies connected with increasing demands on product quality and performance have been concentrated on the extensive investigations in which empirical studies have been published [3–5].

Surface and coatings technology take important part on the field of machine components life extension, together with the increase of their performance. Over the last years, constant development of surface engineering has contributed to the creation of numerous methods of coating technology that are capable of significant change in surface properties of the processed object without changing its substrate [6, 7].

Among these methods, one of the most versatile applications to protect components from corrosion and abrasive or adhesive wear is thermal spray coating technique. Thermal spraying is the term that defines a group of processes in which both metallic and nonmetallic materials are sprayed on the substrate in the form of fine particles in molten or semi-molten conditions or even in some cases in the solid state to form coating [8, 9]. Coating material includes pure metals, metal alloys, hard metals (i.e., carbides and cement), ceramics, polymers, and combination of these materials. Depending on used technique—defined by the tool which can be special gun or torch—feedstock material can be delivered in the form of powder, wire, or rod shape.

As main advantages of thermal spray processes in comparison with other coating technologies can be stated as follows [8]:

- extremely wide range of materials that can be used to make a coating;
- the heat input to the coated component is noticeable low; therefore, application of thermal spray coating has relatively small effect on the substrate properties;
- significant change in substrate surface properties and functionalities can be obtained, for instance, in its hardness and wear resistance, and also chemical corrosion and heat resistance;
- cost efficiency;
- ability in most cases to strip and recoat worn or damaged coatings without changing the properties and dimensions of the part; and
- thermal spraying is regarded as green technology.

However, this technology is not free of drawback. Major disadvantages are size limitations that prohibit the coating of small objects and also the line-of-sight nature

of the deposition process—meaning that only what the torch or gun can actually “see” can be coated [9].

During the deposition process, torch or gun does multiple passes over the surface of the coated object. The structure of sprayed deposit is characterized by lamellar nature. What is more, properties of the deposit are significantly influenced by the parameters that were used in spraying process [7, 8]. According to the state of the art on the field of thermally sprayed coatings [7, 10], residual stresses that are generated within the coating have serious influence on its performance. The phenomenon of these stresses is quite complex to predict depend largely on thermal conditions of spraying process. As it is presented in [7], residual stresses which develop in coating are the combination of quenching stresses that generate during deposition and cooling stresses which occur after the process. The quenching stresses have always tensile nature and are the result of rapid cooling of sprayed particles from their melting temperature to the temperature of substrate after they reach its surface [10, 11]. The cooling stresses occur in phase called secondary cooling when the temperature of applied deposit drops from the temperature that was reached during the process to the room temperature. These stresses are induced by mismatch in thermal shrinkage of substrate and coating as a result of the difference in coefficients of thermal expansion (CTE).

Depending on the sign of quenching and cooling stresses values, residual stresses in coating could be of tensile or compressive nature [10–12]. According to [7, 10, 13, 14], the presence of compressive residual stresses is generally more favorable than tensile ones, as they not only may not harm the coating system but also can contribute to improvement of adhesion bonding and inhibit formation of cracks in coating layers. Occurrence of tensile nature of residual stresses usually leads to problems such as initiation and propagation of cracks which result in interface delamination, loss of adhesion, and fatigue failure [7, 10, 11, 15].

The present research introduces finite element modeling (FEM) technique to study thermal stress generation and distribution on thermal spray coatings on clutch plain plates. Obtained data is expected to be a useful knowledge in future development of wear resistant coatings that are exposed to high temperature conditions.

## 2 Research Problem

The aim of present study was to designate distribution and magnitude of thermal stress in thermal spray coatings manufactured on clutch plain plates. This research considered application of  $\text{Cr}_3\text{C}_2$ -NiCr coating on aluminum alloy plain plate. Such coating can be applied on motorcycle clutch components to increase their wear resistance, especially in high temperatures. As some high performance applications involve dry conditions of clutch operation, excessive wear and increased temperature may occur. Because of that, application of functional coatings should be considered as promising way of increasing durability and performance of motorcycle dry clutches. As proposed coating material has different (lower) coefficient of

thermal expansion than substrate material, under conditions of increased temperatures, thermal stresses in coating occurrence are expected. To better increase correlations between coating thickness and stress distribution within coating, authors decided to conduct several finite element simulations.

## 2.1 Simulation Model Preparation

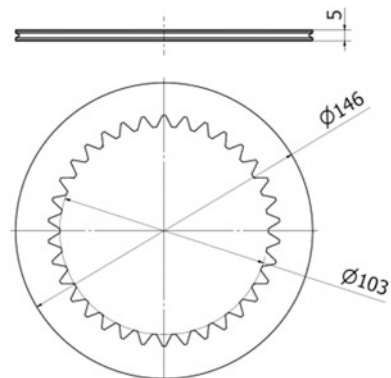
Single plain aluminum clutch plate was assumed as input geometry for simulation. Design of tested clutch plate with its dimensions was presented in Fig. 1. Thin coating was applied to both load bearing surfaces of clutch plate.

Thickness of coating was defined as 0.1, 0.2, 0.4, and 0.5 mm. Simulations were conducted as 3D, static, and structural type.

Model for finite element analyses was multibody. Material properties were applied separately for different bodies. In Table 1, material properties assigned to different bodies included in simulation were presented.

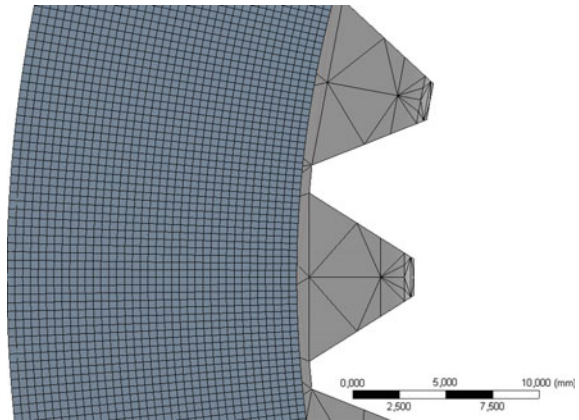
Boundary conditions assumed application of frictionless support on surfaces of plate that stays in contact with engine shaft in real conditions. As well, the symmetry of developed model was assumed. Model was described as symmetrical with symmetry plane perpendicular to main axis of the model and placed in center of a model. Also, axial symmetrical of problem was assumed. Loads in described problem assumed only thermal conditions for all bodies. Applied temperature was equal to 300 °C. Reference temperature was equal to 22 °C. Relation between substrate and coating model was defined as bonded contact type. Contact problem formulation included augmented Lagrange method. Finite element mesh was applied to a model. Size for meshing of the coating was set as 0.05 mm maximum and for meshing substrate as 1 mm. Difference in element size for different bodies resulted because of the fact that study was aimed to designate stress in coating, rather than in substrate. Finite element mesh was presented in Fig. 2.

**Fig. 1** Geometry of clutch plate



**Table 1** Material properties and its assignment

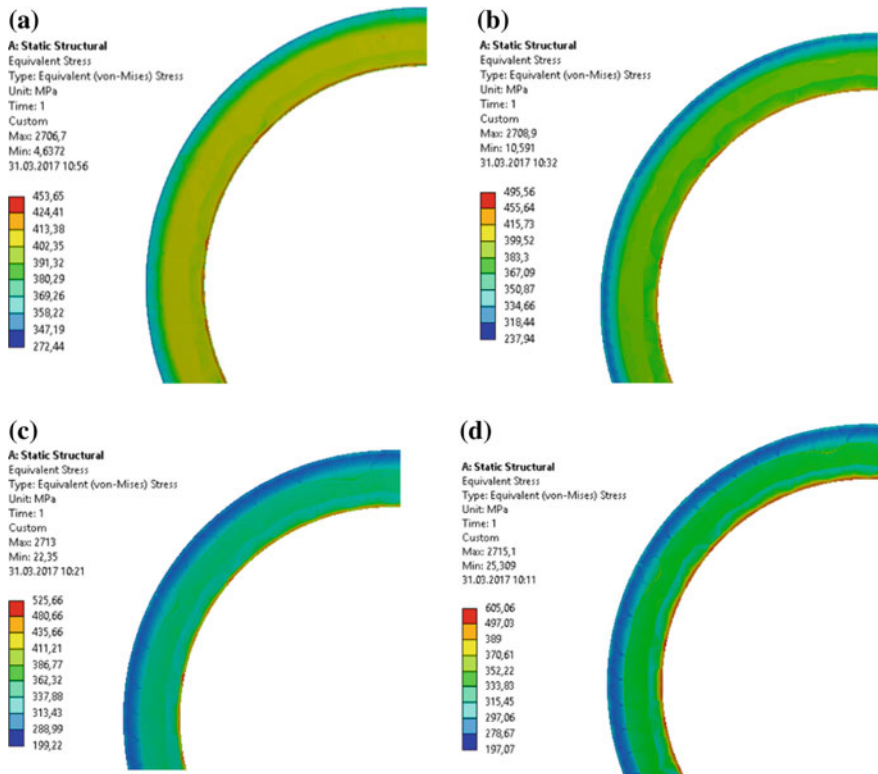
Material	Young modulus (GPa)	CTE ( $10^{-6} \text{ K}^{-1}$ )	Density ( $\text{kg/m}^3$ )	Assignment
EN AW 7075	82	23.1	2810	Substrate (clutch plate)
$\text{Cr}_3\text{C}_2\text{-NiCr}$	260	10.5	6800	Coating

**Fig. 2** Finite element mesh on studied model

### 3 Results

Presented research included four tests, conducted with different coating thickness varying from 0.1 mm to 0.5 mm. All simulations were conducted under the conditions of temperature equal to 300 °C. In order to determine the behavior of applied coating under assumed temperature and its influence on stress distribution within studied coating system, the maximum value of Huber-Mises reduced stress and uniformity of stress distribution in coatings were adopted as the evaluation criteria.

All presented figures show stress distribution in cross section close to the boundary between substrate and coating, as maximum magnitude was observed there. Reduced stress distribution for case with lowest coating thickness equal to 0.1 mm was presented in Fig. 3a. As one can be seen, maximum stress zone was placed in inner boundary of coating and achieved the value of 453 MPa. In case of coating thickness 0.2 mm, slight increase of stress magnitude was noted. Stress magnitude in that case reached 496 MPa. Stress distribution for this case can be observed in Fig. 3b. Simulation results for coating thickness equal to 0.4 and 0.5 mm were presented in Fig. 3c and d. In case of coating thickness 0.4 mm, maximum observed stress reached 526 MPa. Simulation with maximum coating thickness equal to 0.5 mm resulted in stress magnitude over 605 MPa.



**Fig. 3** Stress distribution for coating thickness: **a** 0.1 mm, **b** 0.2 mm, **c** 0.4 mm, and **d** 0.5 mm

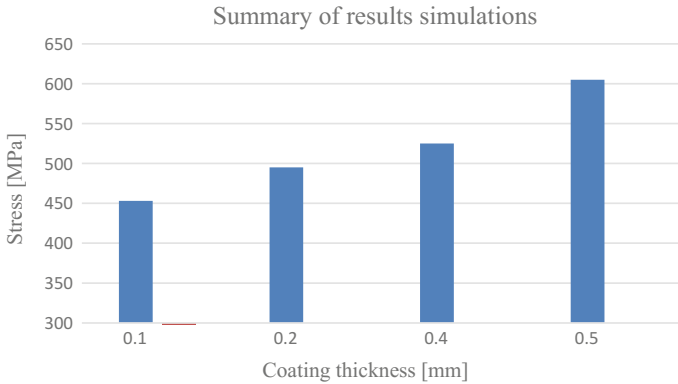
## 4 Discussion

Based on the results that were presented in Fig. 3, change in characteristics of distribution can be seen. In case of lower coating thickness, calculated stress distribution was more uniform than in case of coating thickness with greater thickness. It can be noticed that increase of coating thickness resulted in shift of the maximum stress close to inner coating diameter.

Comparative chart of obtained maximum stress magnitudes for each simulation was presented in Fig. 4. One can be observed the significant change in maximum stress magnitude. Analysis of the obtained results showed the nonlinear correlations between the thickness of the coating and the maximum stress value.

Change in stress value and its distribution can be explained by the differences between CTE of substrate and deposit material. What is more, change in stress distribution and its shift with increase of coating thickness should be explained by notch effect. This information is all the more important considering lamellar nature of the coating deposited with thermal spray technique.





**Fig. 4** Summary chart of resulted magnitude of maximum reduced stress in coatings

## 5 Conclusions

The thermal stress distribution in coating system in relation to the thickness of applied coating was investigated. Conducted simulation allowed to obtain data that presented strong correlation between coating thickness and both maximum value of Huber-Mises reduced stress and stress distribution characteristics within coating. As it was expected, these maximum values occurred at the interface of substrate and deposit material. Reason for this is a big difference in substrate and deposit material CTE (coefficient of thermal expansion) value. This difference contributed to thermal deformation of substrate while thermal stress occurrence. Thin coating, because of the significantly lower coefficient of thermal expansion, experiences stretching stress. This kind of stress is strongly unwanted in ceramic-based materials, as such kind of materials is capable of bearing higher compressive stresses.

Analysis of stress distribution allowed to notice increase of this distribution toward inner boundary of coating with increase of coating thickness. What is more, significant increase in the value of stress also was observed. Explanation of this phenomenon might be by the increase of notch effect. This is very important data, especially if taken into account lamellar nature of thermal spray coating.

Correlations between observed stress magnitudes and coating thickness were nonlinear. Because of that, optimization of coating thickness should be considered while designing coating application. One can observe that in case of coating thickness change from 0.4 to 0.5 mm, increase in obtained maximum stress value is approximately two times greater than in case of thickness change from 0.2 to 0.4 mm. Knowledge of this correlation can be useful in best coating thickness determination.

Presented coatings besides superior wear resistance and frictional properties show some drawbacks when exposed to some conditions. Nickel-based composite coating tends to present lower values of coefficient of thermal expansion than metallic substrates. Especially, application of such coatings on an aluminum alloy

substrate causes significant differences in thermal deformation of substrate and coating. In case of steel substrates, differences in coefficient of thermal expansion are lower, so the influence of thermal stress is expected to be less significant.

The results of described research allowed to formulate following conclusion that the success of coating that was deposited with thermal spray technique depends on many factors. Among these factors, correct selection of materials which are going to form the coating system is particularly important. In the analyzed case, it was shown that, although presented coatings should contribute to extend life and performance of aluminum plate clutches in fact may cause accelerated wear and damage due to material mismatch—especially in case of CTE value.

**Acknowledgements** The authors wish to acknowledge that research presented in this paper was funded by Institute of Mechanical Technology, part of Faculty of Mechanical Engineering and Management at Poznan University of Technology. Described research was conducted thanks to Institute's scientific resources and was a part of author's work for the Institute.

## References

1. Abdullah, O.I., Schlattmann, J.: Contact analysis of a dry friction clutch system. *ISRN Mechanical Engineering*, vol. 9 (2013). doi:[10.1155/2013/495918](https://doi.org/10.1155/2013/495918)
2. Khamlichia, A., Bezzazia, M., Parrón Vera, M.A.: Optimizing the thermal properties of clutch facings. *J. Mater. Process. Technol.* **142**, 634–642 (2003)
3. Maruda, R.W., Krolczyk, G.M., Nieslony, P., Wojciechowski, S., Michalski, M., Legutko, S.: The influence of the cooling conditions on the cutting tool wear and the chip formation mechanism. *J. Manufac. Process.* **24**, 107–115 (2016)
4. Krolczyk, G.M., Nieslony, P., Krolczyk, J.B., Samardzic, I., Legutko, S., Hloch, S., Barrans, S., Maruda, R.W.: Influence of argon pollution on the weld Surface Morphology. *Measurement* **70**, 203–213 (2015)
5. Królczyk, G., Legutko, S., Raos, P.: Cutting wedge wear examination during turning of duplex stainless steel. *Tehnički Vjesn. Tech. Gaz.* **20**, 413–418 (2013)
6. Matikainen, V., Bolelli, G., Koivuluoto, H., Sassatelli, P., Lusvardi, L., Vuoristo, P.: Sliding wear behaviour of HVOF and HVOF sprayed Cr<sub>3</sub>C<sub>2</sub>-based coatings. *Wear* (2017). doi:[10.1016/j.wear.2017.04.001](https://doi.org/10.1016/j.wear.2017.04.001)
7. Stokes, J., Looney, L.: Residual stress in HVOF thermally sprayed thick deposits. *Surf. Coat. Technol.* **177–178**, 18–23 (2004)
8. Vuoristo, P.: Thermal spray coating processes. *Compr. Mater. Process.* **4**, 229–279 (2014). doi:[10.1016/B978-0-08-096532-1.00407-6](https://doi.org/10.1016/B978-0-08-096532-1.00407-6)
9. Tucker, R.C.: Thermal Spray Coatings. *ASM Handb. Surf. Eng.* **5**, 497–509 (1994)
10. Arif, A.F.M., Al-Athel, K.S., Mostaghimi, J.: Residual stresses in thermal spray coating. *Compr. Mater. Finish.* **3**, 56–70 (2016). doi:[10.1016/B978-0-12-803581-8.09199-2](https://doi.org/10.1016/B978-0-12-803581-8.09199-2)
11. Azizpour, M., Norouzi, S., Majd, H., Sajedipour, D., Sadr, R., Mehr, M., Shoabi, S., Mohammadi, R.: Development trend in investigation of residual stresses in WC-Co coating by HVOF thermal spraying. *Int. J. Chem. Mol. Nucl. Mater. Metall. Eng.* **5**(6), 473–476 (2011)
12. Davis, C.L., Krousgrill, C.M.: Effect of temperature on thermoelastic instability in thin disks. *J. Tribol.* **124**(3), 429–437 (2002)

13. Oladijo, O.P., Sacks, N., Cornish, L.A., Venter, A.M.: Effect of substrate on the 3 body abrasion wear of HVOF WC-17wt.% Co coatings. *Int. J. Refract Metal Hard Mater.* **35**, 288–294 (2012)
14. Jen, T.C., Nemecek, D.J.: Thermal analysis of a wet-disk clutch subjected to a constant energy engagement. *Int. J. Heat Mass Transf.* **51**(7–8), 1757–1769 (2008)
15. Abdullah, O.I., Schlattmann, J.: Finite element analysis of temperature field in automotive dry friction clutch. *Tribol. Ind.* **34**(4), 206–216 (2012)

# Augmented Reality in Training of Fused Deposition Modelling Process

Filip Gorski, Radoslaw Wichniarek, Wieslaw Kuczko, Pawel Bun and John A. Erkoyuncu

**Abstract** The paper presents results of a pilot study using Augmented Reality techniques for learning and training of 3D printing process of Fused Deposition Modelling (FDM). The authors created a mobile, tablet-based Augmented Reality solution for learning of basic operations performed on a 3D printer during preparation and realization of a process of Fused Deposition Modelling. Then, two groups of novice students were tested for efficiency in realizing these processes: one group was taught using traditional learning method and the other—without any traditional training whatsoever, only basing on the Augmented Reality application for the process guidance (self-learning). The obtained process realization times were compared with reference times obtained by expert process engineers. The results are promising, but there is a high need of expert consulting for students using only the Augmented Reality.

**Keywords** Augmented reality · Fused deposition modelling · Engineering training · Learning

## 1 Introduction

Modern design and process engineers have many technologies and methods aiding their daily work and decision-making at their disposal. Among these methods, there are plenty of traditional ones, such as statistical methods [1], as well as a whole bunch of new technologies, such as agent computing and artificial intelligence [2]. Another

---

F. Gorski (✉) · R. Wichniarek · W. Kuczko · P. Bun  
Chair of Management and Production Engineering,  
Poznań University of Technology, Poznań, Poland  
e-mail: filip.gorski@put.poznan.pl

J.A. Erkoyuncu  
Through-Life Engineering Services Institute,  
Cranfield University, Cranfield, UK

important new technologies, which can be used both for decision-making and directly in design or training processes are Virtual Reality and Augmented Reality.

The Augmented Reality (AR) technology is used for displaying dynamic spatial and flat visualizations overlaid on real-world objects. The AR definition by Azuma [3] includes constant bond between real-world and digital objects as well as an interaction between the user and the virtual objects. The AR solutions can be based on headsets [4], such as Microsoft HoloLens, as well as on mobile devices, such as cell phones or tablets [5, 6]. Augmented Reality is widely used in engineering processes, such as manufacturing [7] or maintenance [8].

Augmented Reality and related technology of Virtual Reality (VR) both use similar visualization techniques and hardware, although VR is focused on obtaining a feeling of immersion [9] through placing a user in a computer-generated environment, e.g. for better educational effect [10]. The AR and VR applications are often used for training and education [11], in engineering [12–14], medicine [4] and standard education processes [15]. Both technologies allow enclosing of human knowledge inside a computer application and visualization with high level of interaction [16], thus enabling high efficiency in training performed without supervision and self-learning. The AR is also one of the key elements of the so-called Industry 4.0 concept [17].

The paper presents a pilot study using Augmented Reality application used on a mobile device for self-learning of operations performed in a 3D printing process of Fused Deposition Modelling. Efficiency of self-learning based on AR is compared with traditional learning methods and results of experts.

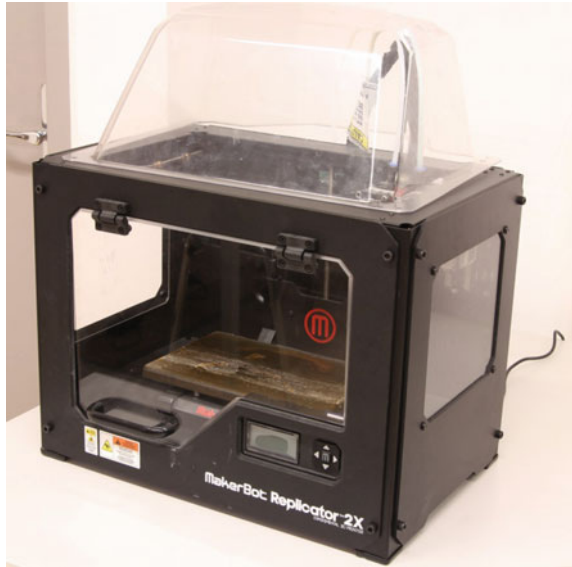
## 2 Materials and Methods

### 2.1 *Fused Deposition Modelling Technology*

The Fused Deposition Modelling (FDM) technology is one of the less complex technologies of additive manufacturing (3D printing), regarding both the process and machine design. As a consequence, FDM machines come in all size and cost variants, with the cheapest ones being economically acceptable even for personal use [18]. In the FDM process, material in form of a filament made out of a thermoplastic polymer is supplied to an extruder, moving in XY (horizontal) plane. The material is heated and extruded into a modelling platform, where it solidifies. After a given layer is completed, the platform (table) moves in the Z (vertical) axis, to continue extruding material in a subsequent layer. This process is repeated until the whole model is obtained [19]. Two types of materials are used: basic material for the product (model) and support material for the support structures, which are removed after the process is finished.

The FDM technology, especially regarding the low-cost machines or semi-professional devices, such as the MakerBot Replicator 2X by Stratasys

**Fig. 1** MakerBot replicator 2X machine for fused deposition modelling



company (Fig. 1), requires specific preparations before the process is started and supervision during its realization. It is related to possibilities of thermal deformations, caused by shrinkage of material after it is deposited [20]. The platform or the chamber can be heated, to partially prevent this. Nonetheless, disjoining the semi-finished part from the modelling platform is a frequent problem of many FDM machines including the Replicator 2X [21]. It can be prevented also by proper preparation of the modelling table—using specific materials to cover it, to ensure proper adhesion of extruded polymer.

Other stages of machine preparation include loading of material filament into the nozzle, cleaning the modelling space and ensuring that material flows properly out of the nozzle. The process itself must be supervised—when certain defects occur, their early spotting can save the whole part or at least allow quick restarting of the process without too high time and material loss.

All the above-mentioned factors make the FDM process engineers obtain specific manual skills and experience in visual evaluation of the material, modelling table and the process course. These skills must be taught accordingly. The aim of the studies presented in this paper was to find out if it is possible to self-learn the basic stages of the FDM process preparation using the Augmented Reality technology.

## **2.2 Operating Procedure of MakerBot Replicator 2X**

The authors formalized the expert knowledge regarding basic operations of 3D print process preparation using the MakerBot Replicator machine into a descriptive form

of a single procedure, divided into tasks, further divided into subtasks. The procedure, written as a text and image document, covers all the basic stages of machine preparation and making of a test part. It was used as a basis for further research activities—it was slightly modified and digitized into an AR app (see next chapter) and in its basic form it was used as a manual for students trained using a traditional approach.

The procedure consists of the following tasks and subtasks:

- Task 1. Check machine status and turn it on
  - Subtask 1.1 Locate the machine
  - Subtask 1.2 Check machine completeness
  - Subtask 1.3 Check if the modelling table is empty
  - Subtask 1.4 Turn on the machine
- Task 2. Prepare table for manufacturing
  - Subtask 2.1 Make general visual evaluation of the table
  - Subtask 2.2 Check kapton tape
  - Subtask 2.3 Prepare kapton
  - Subtask 2.4 Coat table with ABS solution
- Task 3. Prepare extruders
  - Subtask 3.1 Run preheat mode
  - Subtask 3.2 Check material spools
  - Subtask 3.3 Load material
- Task 4. Make test print
  - Subtask 4.1 Prepare machine
  - Subtask 4.2 Start test print
  - Subtask 4.3 Supervise the print
  - Subtask 4.4 Remove print

The procedure usually is presented to students of the Production Engineering program, over the course of 3-h. The authors perform this training in person on a yearly basis. The exemplary test print is a model of a bracelet (Fig. 2), supplied with the machine software. It is manufactured out of ABS material, and the 3D print time is approx. 17 min.

### ***2.3 Augmented Reality Application***

The Augmented Reality application was created using the Unity 3D engine and Vuforia package for Augmented Reality purposes. Destination platform of the application is the Android operating system, making it available for use on generic



Fig. 2 Test print model—ABS bracelet

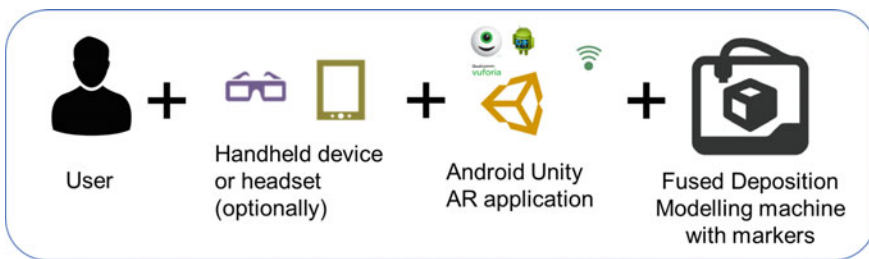


Fig. 3 Scheme of AR application for learning of FDM process

cell phones or tablets with this system. General scheme of use of the application is presented in Fig. 3.

The procedure described in Sect. 2.2 was digitized for display and task flow. Each task has its description and image displayed for the user. Each subtask has an image, a description and an additional 3D animation, displayed when user points camera of a mobile device in the direction of a specific marker, which is a square black and white pattern, printed on a regular paper. The animations are displayed only for a current subtask and are attached to specific marker numbers, meaning that they are effectively bound to the real-world coordinates (markers are placed around the working space of the machine), see Fig. 4 for an example. Animations show specific activities which should be performed by the user at the given moment, such as turning on the machine, removing the print from the table, placing the material spool in a correct place etc.

Interaction with the application is based on a graphical user interface, which allows reviewing the current task and subtask, as well as going to next task and subtask after certain activities are finished. The application does not check if the user physically performed the subtask—he is only obliged to go near the marker and display the appropriate animation linked to it before he is allowed to confirm





**Fig. 4** Example of animation displayed for the user, visible markers around the machine

that the subtask is done. Course of the procedure is recorded in a log file for a current session, so the times of tasks can be retrieved for further analysis.

## **2.4 Research Outline**

The efficiency of learning of 3D printing on the MakerBot Replicator 2X machine was tested by comparison of two groups of students. The two groups of 10 people—adults, students of Production Engineering program, aged in between 25 and 30 years old—were taught using two different methods. The first group—named the reference group—was taught using a traditional method. A 3-h standard training was performed by a 3D printing expert. The training consisted both in lectures (depiction of machine and process, machine parts, operations in the process) and practical work under supervision of an expert. The second group was given no standard training whatsoever and no interaction with an expert beforehand; they only had a loose idea and common knowledge about the realized process and general aim of the exercise. Their only source of knowledge was the AR application, prepared by the authors. Persons from both groups were tested individually—they were presented with a task, described in the AR application, presented for the reference group in a printed form. The participants were asked to perform it themselves, with no supervision. The time of operation until success (meaning fully printed test part with acceptable quality, arbitrarily evaluated by an expert) was recorded, as well as number of times of consultations with an expert. An expert was always present in the 3D printing laboratory, but was not actively participating or

supervising, unless asked by particular students, which was allowed. The participants were not aware that they are taking part in a scientific experiment, as it was included in their normal course of studies, so there was no bias.

### 3 Results and Discussion

The results of both test groups, along with time of operation reached by experts, are presented in Table 1. Only mean and standard deviation are presented, for a general overview. Time of manufacturing of part is not included, as it is constant for all participants. A number of expert interventions were also recorded for both groups and then divided by a number of persons in both groups to obtain a coefficient.

The following observations were made during the studies:

- the time of the reference group is better than the time achieved by the self-learning group, which was expected; however, the difference is not that significant (approx. 10%), meaning that the self-learning process is effective,
- all the participants managed to finish all the operations with success (meaning they succeeded in manufacturing a test part), although in 3 cases of the self-taught group the 3D printing process had to be repeated after expert intervention—this can be explained by a lack of knowledge of how the proper process should look like and what are the possible symptoms of the process going wrong (which was also expected); this did not happen in the reference group,
- the number of expert interventions is almost twice as high in the self-taught group (15 interventions in total, each student needed direct help on at least one occasion), while in the reference group some students did not need expert assistance at all,
- the self-taught students lost lots of time while exploring structure of the machine and the process, they were also less confident while performing physical tasks (like removing the part from the table), as they did not see it before on their own eyes,
- time achieved by both groups of students is not near the time obtained by experts—many more repetitions would be required to achieve this level of practical experience.

**Table 1** Results of studies

Statistics	Reference group (traditional learning)	AR self-learning group	Experts
Mean time	45.3	49.5	28.3
Std. deviation time	3.1	5.2	1.1
No. of interventions/person	0.8	1.5	n/a

To sum up—the times and results obtained by the group, which was self-taught using the AR application and did not have previous experience nor training on the process are, obviously, significantly worse. However, all the participants managed to perform all the operations with success, without threatening integrity of machine or their own safety (the FDM technology can be evaluated as a relatively safe manufacturing process for the novice users, only basic safety information is required). Therefore, it is much more economically justified to use the AR technology for training, as 3-h course is not needed to get into the basics of the process. It would be interesting to observe the learning curve after numerous repetitions of the same procedure—the authors think that standardization of procedure contained in the application would allow to make the curve more beneficial for the self-taught group.

The participants from the self-taught group, after interviewing them, formulated certain guidelines for improvement of the AR application, which will be considered by authors in their further studies:

- the expert intervention could be done on a remote level, meaning no physical presence of an expert would be required, just a communication channel to exchange text, image and voice messages—this would allow eliminating need of expert presence in the room, as he was mostly unoccupied during the studies,
- the animations should be more detailed, presenting the whole scope of a given activity performed by an animated character, rather than simple animations of objects—this would help increasing confidence of performing physical activities, replacing physical demonstration of a given activity by an expert during a standard course.

## 4 Summary

The authors managed to compare two methods of engineering training on example of a 3D printing process of Fused Deposition Modelling. Traditional training performed in person by a skilled expert in form of a theoretical and a practical course was confronted with an approach of equipping users with an Augmented Reality application, containing all the knowledge they need to have at a given moment of time while performing a certain process on a machine. There is a lot to do in terms of improvement of the AR-based training, but it serves its purpose—all the students did manage to perform the procedure successfully. It must be noted, however, that their efficiency was lower and they all needed help by expert on one or more occasions. The next step in development of the prepared solution will be enabling of remote guidance by expert and exchange of messages, in order to get rid of necessity of expert's physical presence in site, where a certain manufacturing procedure is performed by an unskilled operator. If the authors will succeed in this approach, this could mean a huge step towards self-taught processes with minimal engagement of experts, meaning better use of given resources in a company and increasing its efficiency of manufacturing and maintenance operations.

The authors plan to develop the concept further and perform more studies, with remote experts and on different procedures, including inspection and maintenance procedures. It can be concluded that the Augmented Reality has a large potential in training operators, especially when they are unskilled in the process—this may be useful in terms of Industry 4.0 concept, where manufacturing processes are flexible and can be changed at any time. The AR technology should be therefore very useful in a factory of the future.

## References

1. Kujawińska, A., Rogalewicz, M., Diering, M., Hamrol, A.: Statistical approach to making decisions in manufacturing process of floorboard. In: Proceedings of 5th World Conference on Information Systems and Technologies, Recent Advances in Information Systems and Technologies, vol. 3, pp. 499–508. Springer (2017) doi:[10.1007/978-3-319-56541-5\\_51](https://doi.org/10.1007/978-3-319-56541-5_51)
2. Dostatni, E., Diakun, J., Hamrol, A., Mazur, W.: Application of agent technology for recycling-oriented product assessment. *Ind. Manag. Data Syst.* **113**(6), 817–839. <http://dx.doi.org/10.1108/IMDS-02-2013-0062>
3. Azuma, R.T.: A survey of augmented reality. *Presence Teleoperators Virtual Environ* **6**(4), 355–385 (1997)
4. Hamacher, A., et al.: Application of virtual augmented, and mixed reality to urology. *Int. Neurourol. J.* **20**(3), 172–181 (2016)
5. Ramirez, H., Mendivil, E.G., Flores, P.R., Gonzalez, M.C.: Authoring software for augmented reality applications for the use of maintenance and training process. *Procedia Comput. Sci.* **25**, 189–193 (2013)
6. Rumiński, D., Walczak K.: Creation of interactive AR content on mobile devices, in: lecture notes in business information processing. In: van der Aalst, W., Mylopoulos, J., Rosemann, M., Shaw, M.J., Szyperski, C. (eds.) International Conference on Business Information Systems, Poznań, Poland, 19–20 June 2013, vol. 160, pp. 258–269. Springer (2013)
7. Ong, S.K., Nee, A.Y.C.: Virtual and augmented reality applications in manufacturing. Springer, Singapore (2004)
8. Palmirini, R., Erkoyuncu, J.A., Roy, R.: An innovative process to select augmented reality (AR) technology for maintenance. *Procedia CIRP* **59**, 23–28 (2017)
9. Bowman, D.A., McMahan, R.P.: Virtual reality: how much immersion is enough? *Computer* **40**(7), 36–43 (2007)
10. Wu, F., Liu, Z., Wang, J., Zhao, Y.: Establishment virtual maintenance environment based on VIRTTOOLS to effectively enhance the sense of immersion of teaching equipment. In: Proceedings of the 2015 International Conference on Education Technology, Management and Humanities Science (ETMHS 2015). Atlantis Press. doi:[10.2991/etmhs-15.2015.93](https://doi.org/10.2991/etmhs-15.2015.93)
11. Martín-Gutiérrez, J., Mora, C.E., Añorbe-Díaz, B., González-Marrero, A.: Virtual technologies trends in education. *EURASIA J. Math. Sci. Technol. Educ.* **13**(2), 469–486 (2017)
12. Torres, F., Tovar, L.A.N., del Rio, M.S.: A learning evaluation for an immersive virtual laboratory for technical training applied into a welding workshop. *EURASIA J. Math. Sci. Technol. Educ.* **13**(2), 521–532 (2017)
13. Gorski, F., Bun, P., Wichniarek, R., Zawadzki, P., Hamrol, A.: Immersive city bus configuration system for marketing and sales education. *Procedia Comput. Sci.* **75**, 137–146 (2015)
14. Trojanowska, J., Karwasz, A., Machado, J., Varela, M.L.R.: Virtual reality based ecodesign. In: Golinska-Dawson, P., Kolinski, A. (eds.) Efficiency in Sustainable Supply Chain, Part II, pp. 119–135. Springer International Publishing (2017). doi:[10.1007/978-3-319-46451-0\\_8](https://doi.org/10.1007/978-3-319-46451-0_8)

15. Martín-Gutiérrez, J., Fabiani, P., Benesova, W., Meneses, M.D., Mora, C.E.: Augmented reality to promote collaborative and autonomous learning in higher education. *Comput. Hum. Behav.* **51**, 752–761 (2015)
16. Gorski, F., Bun, P., Wichniarek, R., Zawadzki, P., Hamrol, A.: Effective design of educational virtual reality applications for medicine using knowledge-engineering techniques. *EURASIA J. Math. Sci. Technol. Educ.* **13**(2), 395–416 (2017)
17. Zawadzki, P., Żywicki, K.: Smart product design and production control for effective mass customization in the industry 4.0 concept. *Manag. Prod. Eng. Rev.* **7**(3) (2016)
18. Gajdoš, I., Slota, J., Spišák, E., Jachowicz, T., Tor-Świątek, A.: Structure and tensile properties evaluation of samples produced by Fused Deposition Modeling. *Open Eng.* **6**(1), 86–89 (2016)
19. Górski, F., Wichniarek, R., Kuczko, W., Zawadzki, P., Buń, P.: Strength of ABS parts produced by fused deposition modelling technology—a critical orientation problem. *Adv. Sci. Technol. Res. J.* **9**(26), 12–19 (2015)
20. Sooda, A.K., Ohdarb, R.K., Mahapatra, S.S.: Improving dimensional accuracy of fused deposition modelling processed part using grey Taguchi method. *Mater. Des.* **30**(10), 4243–4252 (2009)
21. Nickel, A.H., Barnett, D.M., Prinz, F.B.: Thermal stresses and deposition patterns in layered manufacturing. *Mater. Sci. Eng. A* **317**, 59–64 (2001)

# Complex Control Method of Degreasing Process

Michal Zoubek, Jan Kudlacek, Petr Chabera and Andrey Abramov

**Abstract** This chapter deals with possibilities of complex control of the degreasing process in industrial applications, i.e., especially the possibilities of checking the state of the surface of the product before and after the degreasing process and checking the condition of degreasing liquids using UV-Vis spectroscopy.

**Keywords** Degreasing · Surface treatment · Grease detection · UV-VIS  
Recognoil

## 1 Introduction

The surface degreasing process is crucial for achieving a high quality and functional finish. The clear majority of defects and surface treatment failure result from insufficient or unmanaged pre-treatment of the surface of the component. When considering high demands placed on the coating maker, it is necessary to address the complex ways of controlling this process. The aim of research and development realized at the Faculty of Mechanical Engineering of CTU in Prague in cooperation with industrial partners is the development of methodology and equipment enabling continuous control of the degreasing process. The aim is not only the surface condition control of the object before and after the degreasing process, but also to monitor the contamination of the individual process liquids of the surface finish.

---

M. Zoubek (✉) · J. Kudlacek  
Department of Manufacturing Technology, Faculty of Mechanical Engineering,  
CTU in Prague, Technická 4, 166 07 Prague 6, Czech Republic  
e-mail: [michal.zoubek@fs.cvut.cz](mailto:michal.zoubek@fs.cvut.cz)

P. Chabera  
TechTest, s.r.o., Na Studankach 782, 551 01 Jaroměř, Czech Republic

A. Abramov  
Department of Mechatronic Systems, Kalashnikov Izhevsk State  
Technical University, 30 let Pobedy Str. 2, 426033 Izhevsk, Russia

## 2 Degreasing Quality Control

Contemporary technology development and increased demands on production quality require that the control methods used make it possible to obtain accurate and reliable values in real time, in a simple and repeatable way, without the possibility of distortion due to improper handling, with easy interpretations and documentation. The neglect of the pre-treatment quality control process can lead to defects apparent immediately after the surface treatment—e.g., fisheye in organic coatings or the no coloring of the aluminum oxide layer in the anodic oxidation of aluminum [1], or they may occur during the exposure of the segment in a corrosive environment because of the failure of the protective function of the coating [2–4]. From the above method, it is clear that extended subjective methods of assessing the surface condition of a component with respect to the occurrence of greasy impurities by detecting chalks, inks, or fixings are totally unsuitable for use in automated serial production operations [4]. Likewise, the control of degreasing and rinsing liquids needs to be automated to achieve continuous online control for optimization of the entire process and thereby to reach economy and high efficiency of the pre-treatment process. User and time-consuming control processes such as titration or determination of the proportion of petroleum substances by demulsifiers need to be replaced by automated methods with sufficient proficiency [5].

### 2.1 Grease Detection on Product Surface

For direct detection of oily impurities on the surface of objects in cooperation with the Institute of Engineering and Technology CTU in Prague, TechTest company developed a device allowing quantitative assessment of the degree of contamination, including visualization of the distribution of these impurities. Detection of grease consists in exciting the fluorescence of the contaminant by means of UV radiation, its registering, and SW evaluation. The developed Recognoil (recognize oil) handheld device allows the surface to be described by a fluorescence map of impurity decomposition, fluorescence intensity determination, and determination of thickness and area contamination concentration Fig. 1. Recalculating the fluorescence value to layer thickness [nm], respectively, the area concentration [ $\text{mg m}^{-2}$ ] is subject to laboratory calibration to create a physico-mathematical oil model. The SW output and the device itself are shown in Fig. 1. The evaluation of the surface condition itself is carried out by attaching the detector to the surface, irradiating it, and generating a fluorescence map with the determination of the fluorescence value and its comparison with the standard value. For example, this can be the fluorescence of the base material after the degreasing process, where the subsequent coating reaches the desired adhesion values. The size of the evaluated area is  $12 \times 18$  mm, and the detection range is from about  $15 \text{ mg m}^{-2}$  (17 nm) to about  $6000 \text{ mg m}^{-2}$  (6  $\mu\text{m}$ ). Due to the different fluorescence values of different

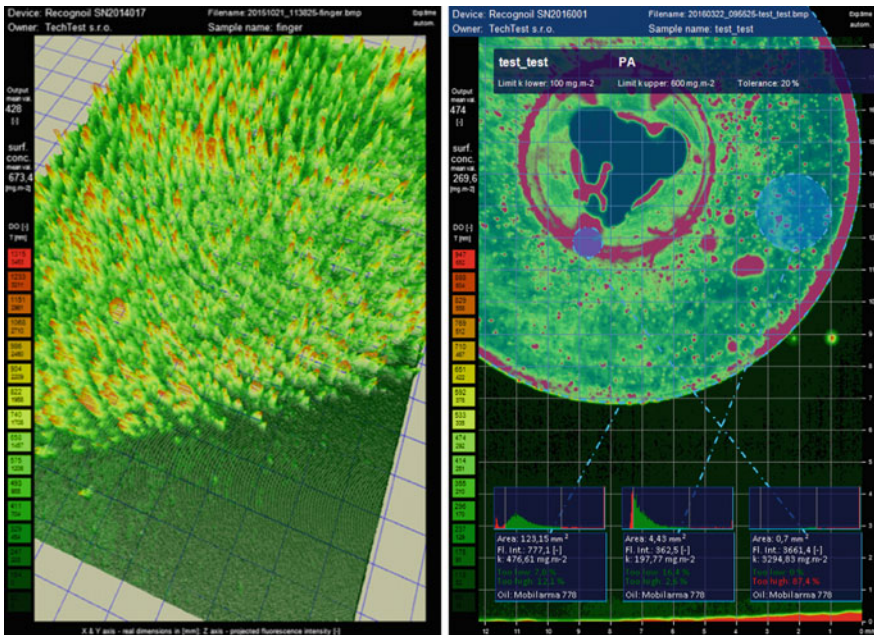


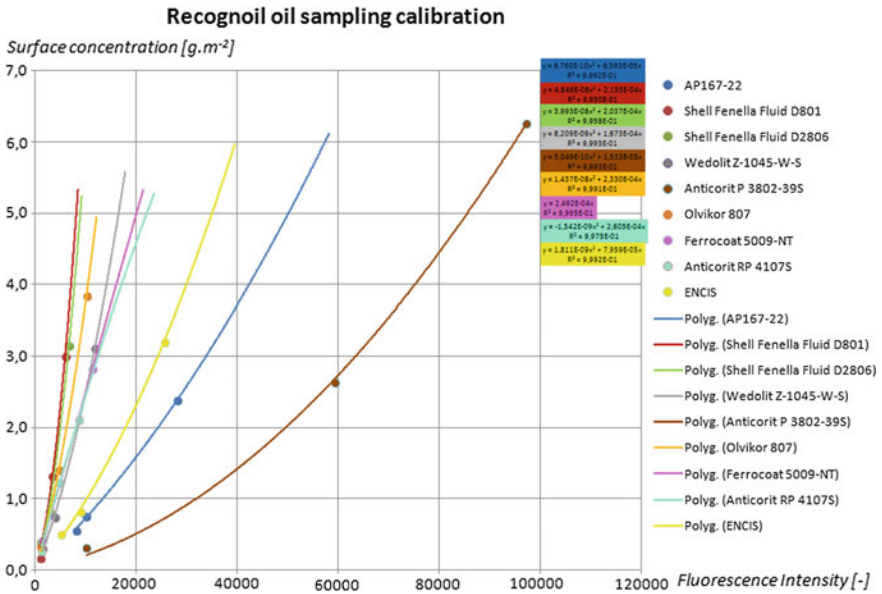
Fig. 1 Fluorescence maps of greasy dirt distribution—photo mode output of Recognoil device

types of oils, depending on the thickness of the applied layer, Fig. 2, given their nature (mineral, synthetic) and composition (additives), it is necessary to determine the permissible fluorescence values individually for each operation [6, 7]. This method of detection can also be used in processes of mechanical pre-treatment (blasting, tumbling, grinding, etc.), where it also enables the control of grease of abrasives. In the same way, the device can be used to check the application of oil layers when preserving the surface or in forming operations. For fast component control, the device also allows real-time measurement in the so-called live mode. It is therefore possible to check the workpiece and, in the event of an abnormality, to perform a full evaluation of the contaminated area [8, 9].

## 2.2 Sequential Scanning of Objects

As already mentioned, the Recognoil device lets you go beyond standard mode, with live previews to quickly check the entire surface of the product. However, this control method is only suitable for the detection of contamination itself or for indicative measurement. If it is necessary to precisely document the entire part (i.e., an area larger than  $12 \times 18$  mm), it is necessary to perform automated sequential scanning. This is accomplished by placing the object in a dark box and scanned





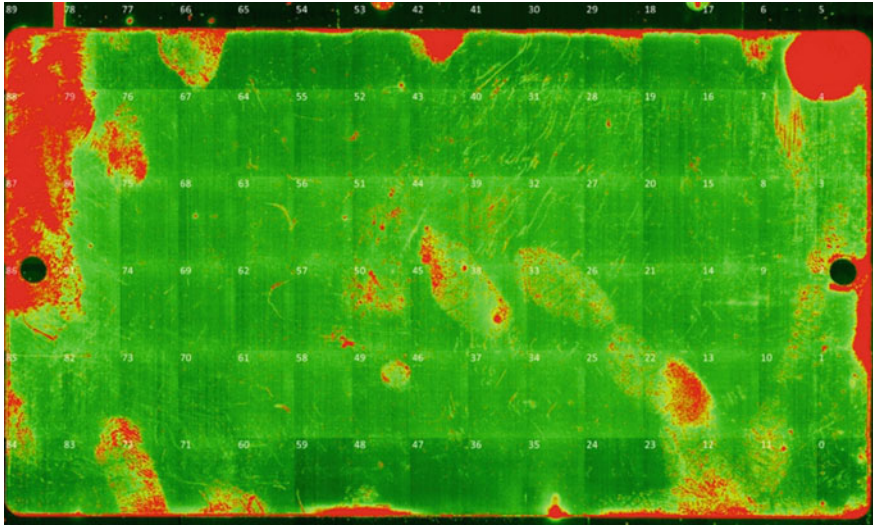
**Fig. 2** Different waveforms of fluorescence depending on the thickness of the surface concentration (film) of different oils

using a detector clamped on a computer-controlled portal. The entire area is gradually measured in the grid, and the output is a SW composite image of the individual fluorescent maps of the product. Distribution of greasy impurities is shown in Fig. 3.

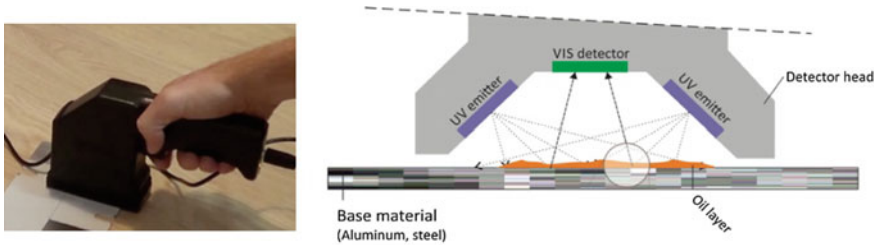
Measurement of defined areas can be done by using negative shaped cover or again by placing the device in a measuring box (where the detector is not affected by an external light source). Special cover can be made using the rapid prototyping method, which means that the variability of the measured surfaces can be ensured, as shown in Fig. 4.

### 2.3 Inspection of Internal Surfaces of the Tubes

To control internal and difficult-to-access areas where the detector cannot be inserted, a special device has been developed that exploits the same principles and functions on a similar SW platform Recognoil—TubeScanner. The device measures only one point compared to the previous model. The minimum inner diameter of the tube is 10 mm, and the device can determine the quality of a degreasing process, even with very long products see Fig. 5.



**Fig. 3** Distribution of greasy impurities on the area of 270 mm × 72 mm obtained by sequential scanning



**Fig. 4** Detection of greasy dirt on a plane (left), detector scheme (right)

### 3 Selecting a Degreasing Agent

In the process of chemical surface pre-treatment, the choice of an effective odorizing agent is crucial to ensure a stable quality and process economy. The Recognoil device enables you with quickly and objectively selecting the appropriate degreasing technology, degreaser, or setting the degreasing process parameters (temperature, concentration). In the case of an evaluation of the efficiency of the degreasing process, the fluorescence value, ideally close to the fluorescence value of the treated material, can be considered as a suitable process quality indicator. Table 1 lists the results of the experiment in order to select the appropriate means for the immersion degreasing process. The measurement procedure itself was carried out as follows: preparation of samples for application of oil film (manual degreasing by solvent,

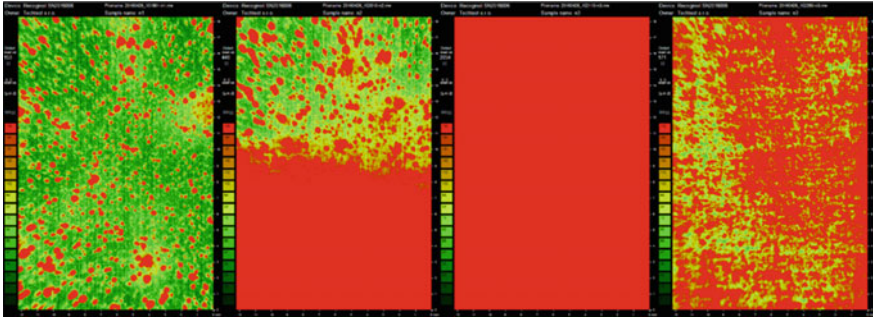


**Fig. 5** Measuring of greasy contamination of inner tube surfaces

**Table 1** Fluorescence [-] and weight loss [g] depending on immersion time using different types of degreasing baths (baseline fluorescence 15,000)

Time [min]	A	B	C	D	E	F
<i>Fluorescence [-] depending on degreasing time for A–F</i>						
1	11,010	8119	13,977	13,805	14,251	11,272
2	9883	6295	13,144	13,794	13,911	5183
3	6693	6104	11,696	12,181	13,772	2097
5	6253	5898	11,287	12,175	13,497	1769
7	4606	4927	11,162	11,979	13,014	1420
10	4546	4538	10,879	11,164	12,967	922
15	4484	3024	9552	9075	12,920	669
20	4228	2769	7252	7094	11,632	619
<i>The course of weight loss [g] depending on the degreasing time</i>						
1	-0.0164	-0.0164	-0.0114	-0.0048	-0.0047	-0.0175
2	-0.0181	-0.0285	-0.0129	-0.0054	-0.0056	-0.0215
3	-0.0222	-0.0294	-0.0134	-0.0086	-0.0058	-0.0258
5	-0.0224	-0.0300	-0.0162	-0.0118	-0.0060	-0.0280
7	-0.0274	-0.0314	-0.0170	-0.0120	-0.0069	-0.0280
10	-0.0275	-0.0317	-0.0179	-0.0129	-0.0087	-0.0314

ultrasonic degreasing in tenside, rinsing in distilled water, drying, detection of fluorescence values, and determination of sample weight), application of a continuous oil film, finding out weight and fluorescence of oil film, degreasing in test medium, rinsing, drying, determination of mass loss of greasy impurities, and detection of fluorescence change. To reduce the measurement uncertainty, only samples with approximately the same initial oil film fluorescence were included in the experiment to achieve the same starting conditions for the individual measurements. Determination of weight loss and fluorescence values was performed three



**Fig. 6** Quick visual visualization of surface contamination when setting a limit

times for each time of degreasing. In order to ensure a minimum of pollution in the bath, a new bath was created once the five of the samples were degreased. In the table, for the protection of third parties, individual products are marked A–F. If coatings are prepared for such samples and tests are carried out, for example, to determine the adhesion of coatings to the parent material, the allowable fluorescence limit can be defined from the test results for use in the process. The operator can then evaluate the surface condition very easily by the visual evaluation of the image after the limit value is set up—in the SW interface all red parts of fluorescence map after exposure are over limit and therefore inadmissible, see Fig. 6.

A similar experiment can of course compare the efficiency of individual methods or process parameters, to achieve the required degree of surface cleanliness for the type of surface treatment.

## 4 Detection of Contamination of Liquids

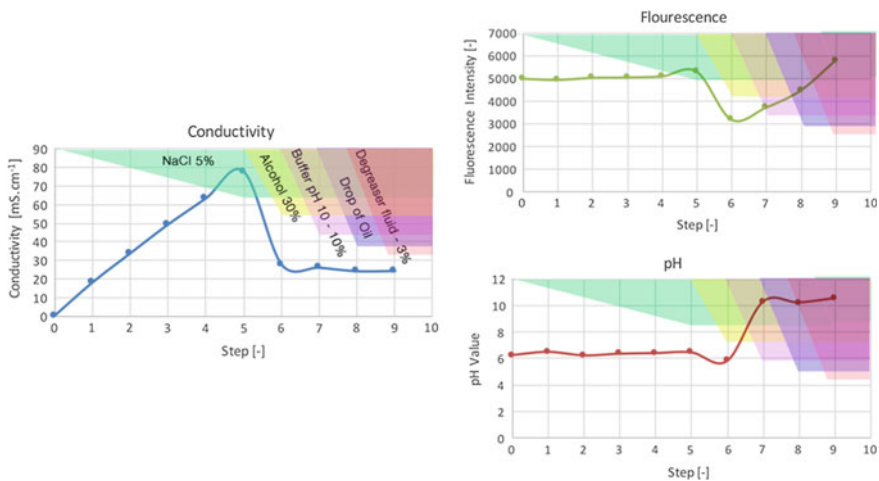
Just as it is important to monitor the condition of the surface of the product before and after the degreasing process, it is important to monitor the condition of the media to which the sample is exposed. This is mainly the condition of the degreasing bath, where loss of degreasing capacity due to the high oil content or the low proportion of unbound surfactants, of course, will negatively affect the grease condition of the surface of the products. Excessive effort to keep the degreasing bath in a workable condition without sufficient control on the other side leads to uneconomic operation and increased ecological onus. Likewise, the control of rinses and other process liquids is crucial to achieving stable production quality. The aim of the cooperation between the Faculty of Mechanical Engineering CTU in Prague, the Department of Manufacturing Technology, TechTest, s.r.o., and the manufacturer of degreasing agents EVERSTAR, s.r.o., is the development of a device for automated continuous detection of liquids to minimize or eliminate user-demanding control methods. The fully automated continuous detection system

also allows the operator to respond flexibly to abnormalities and thereby mitigate possible negative effects on the quality of production.

The process of developing an automated device is currently at an early stage when individual measurement methods and their reaction capabilities are verified. At the same time, the goal of realized experiments is the correct interpretation of the results in relation to the individual components of the working media from the point of view of influence on the value of the measured quantity.

Commonly used degreasing bath pollution detection methods include pH value, electrical conductivity, and titration. The measurement of the fluorescence of liquids is also expected for the device being developed. From the knowledge gained so far, it is clear that for a sufficiently broad description of the working media behavior it is necessary to combine several automated methods and to assign individual trends of the measured quantities to a certain phenomenon (increase in the concentration of oil, surfactants, dilution of the bath, etc.). One of the simple experiments focused on the measuring methods responsiveness is illustrated in Fig. 7. One liter of distilled water was contaminated in each step. pH value, conductivity, and fluorescence were measured as seen; it is important to watch composition of the fluid with different types of devices to get the quick reaction on tiny changes.

In addition, laboratory experiments use analytical methods to evaluate bath contamination for a wider spectrum of information gathered. The measurement itself is realized in a simple measuring circuit simulating the circulation of the working media, see Fig. 8. The fluorescence measurement itself is realized using the Reconoil device, which is placed in a sight glass that is equipped with a soda-lime glass. For the comparison of laboratory tests and simulations, the device was installed into real operation to extend the existing methods of detection and verification of the detection and usability of the device, see Fig. 9. In this case, the



**Fig. 7** Reaction ability of various measuring methods for contamination of 1 L of demineralized water



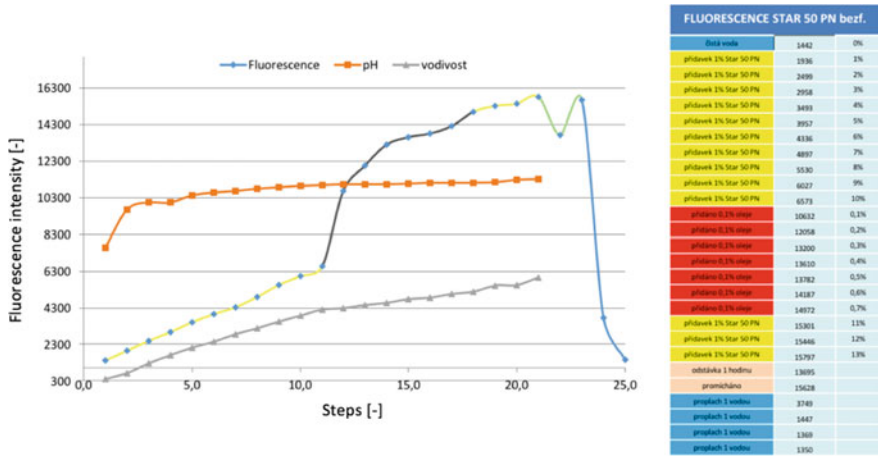
**Fig. 8** Laboratory loop for measurement of contamination of working fluids (EVERSTAR, s.r.o.)



**Fig. 9** Fluorescence measuring in bypass manufacturing (left), model of cover for field measurements of collected fluid samples (center), measurement outputs (right)

device is placed on a bypass with a desoldering unit before entering the supply tank. The measured fluorescence values are then compared with the results of the routine control tests performed during the shift. The operator can also perform laboratory sampling using a handheld surface condition monitoring device by means of a special cover that allows the sample to be placed with a sample of the liquid, see Fig. 9.

Figure 10 shows the progress of the individual measured quantities when diluting the STAR 50 PN aqueous solution of the degreasing agent (yellow in the table) and the ability of the individual methods to react to oil droplets (in the table red). The graph shows a surge in the value of fluorescence due to the addition of oil.



**Fig. 10** Reaction ability of various measuring methods for diluting and contamination of STAR 50 PN aqueous solution of the degreasing agent (EVERSTAR, s.r.o.)

### 5 Conclusion

From these findings and results, it can be stated that in order to ensure the quality of the surface pre-treatment technology, it is necessary not only to control the parts themselves before and after the pre-treatment process, but also to continuously check the working media used. Thanks to the continuous development of electronic components and the capabilities of SW solutions, the technique based on the use of an electronic fluorescence analyzer as a surface condition monitoring device is a suitable method for assessing the acceptability of the surface condition of the object for further operations in the process. In addition, this method can be easily used on fully automated lines, including the use of various communication protocols to inform operators or executives about the current status of the process, or when the limit values are exceeded. The use of this device is of course also possible in the opposite way—for controlling the application of continuous layers, whether passivation, preservatives, or lubricants.

When developing a new device for continuous detection of contamination of liquids, it will be necessary to introduce additional quantities measurements for more detailed documentation of the behavior of the individual components of the bath and to choose sensitive methods, i.e., ones which will allow flexibility to respond to even changes in the composition of the bath.

**Acknowledgements** The research work reported here was made possible by SGS16/217/OHK2/3T/12—Sustainable Research and Development in the Field of Manufacturing Technology.

## References

1. Short, T.: The Identification and Prevention of Defects on Anodized Aluminium Parts [online]. Metal Finishing Information Services (2003) 200 [cit. 2017-04-12]. Available from: <http://www.fot.de/uploads/docs/fehlermoeglichkeiten.pdf>
2. Talbert, R.: Paint Technology Handbook. CRC Press, Boca Raton. ISBN 1574447033 (2008)
3. Fitzsimons, B.: Fitz's Atlas of Coating Defects. In: Weatherhead, R., Morgan, P., Wintney, H. (eds.) MPI Group, 19, Hampshire (2000). ISBN 0951394029
4. Koleske, J.V.: Paint and Coating Testing Manual: Fifteenth Edition of the Gardner-Sward Handbook. ASTM International, West Conshohocken (2012). ISBN 978-0-8031-7017-9
5. Menta, M., Frayret, J., Gleyzes, C., Castetbon, A., Potin-Gautier, M.: Development of an analytical method to monitor industrial degreasing and rinsing baths. *J. Clean. Prod.* **20**, 161–169 (2012)
6. Kudláček, J., Chábera, P., Šikulec, L.: Luminescence method—instrument used for detection of surface cleanliness. *Technical Gazette* **22**(4), 1051–1055 (2015). ISSN 1330-3651
7. Kudláček, J., Chábera, P., Pepelnjak, T., Car, Z.: Mathematical modelling of surface grease deposits. In: Proceedings of International Conference on Innovative Technologies IN-TECH 2012, pp. 335–338. Faculty of Engineering University of Rijeka, Rijeka (2012)
8. Pacák, I., Kudláček, J.: The calibration of a device used for the detection of surface cleanliness. In: CO-MAT-TECH 2005. STU, Bratislava, p. 133 (2005). ISBN 80-227-2286-3
9. Plankovskiy, S., Trifinov, O., Shypul, O., Kozlov, V., Szalay, T.: Simulation of removing mechanism of free particles from surface by detonable gaseous mixtures, pp. 1–8. Manufacturing 2012. Budapest, Hungary (2012)



# Hybrid Processing by Turning and Burnishing of Machine Components

Włodzimierz Przybylski and Stefan Dzionk

**Abstract** The paper presents a method of hybrid manufacturing process of long shafts and deep holes by simultaneous turning and burnishing method. The technological results of the research focus on the influence of the basic technological parameters of this process on the surface roughness of piston rods of hydraulic cylinders. Research results are presented in the graphs as well as mathematical formula. Set of samples were made of steel (C45) as a rod with slenderness ratio ( $l/d$ ) 5–20 and a diameter 56 mm. It shows as well the original CNC machine, which can perform hybrid process (turning and burnishing) of rods and shafts which diameters are in the range 20–100 mm and maximum length 1750 mm.

**Keywords** Hybrid processing · Rolling burnishing process

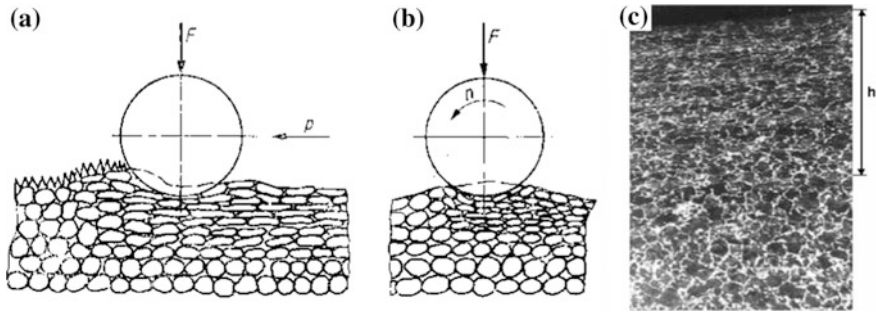
## 1 Introduction

Burnishing process is most popular as the finishing process of plastic deformation of elements surface used for long shafts and piston rod [1–4]. It is an ecological process with great view for the future development of a forming method of defining and profitable operating factors of surface of the elements [5]. Burnishing is the cheap, finishing, cold machining of the surface. Usually the tools for rolling burnishing can be effectively applied to: steel, cast steel, copper alloys, aluminum alloys, cast iron and other materials, whose initial hardness  $HRC < 40$  and the value of relative elongation  $A_5 > 6\%$  [6–8], but in the special cases burnishing of hard surfaces also are used [9, 10]. Burnishing is a form of surface plastic process (Fig. 1) where the burnishing elements are rollers or sliders. The surface is

---

W. Przybylski · S. Dzionk (✉)  
Faculty of Mechanical Engineering, Gdańsk University of Technology,  
G. Narutowicza Street, 11/12, 80-933 Gdańsk, Poland  
e-mail: sdzionk@pg.gda.pl

W. Przybylski  
e-mail: wprzybyl@pg.gda.pl



**Fig. 1** Scheme of plastic deformation in the surface layer of ball-rolled shaft: **a** axial section, **b** scheme of the longitudinal section, **c** cross section of surface layer mag. apx.  $50\times$ ,  $h$ —zone of deformation

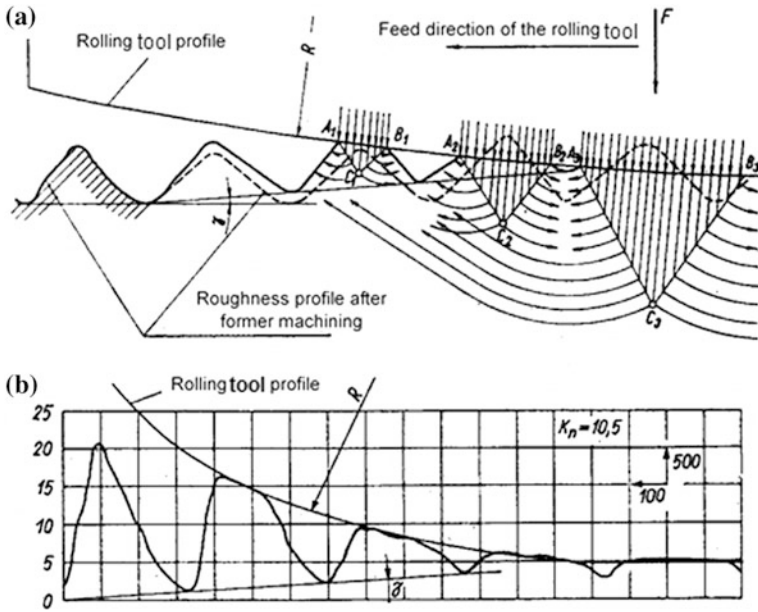
deformed by these elements and results of this process are reduction irregularities of surface and strengthening surface layer. This process may be used after rough machining, for example, turning, milling. The degree of deformation surface irregularities create in these processes depends on pressure of the tool  $F$  and machining parameters such as feed  $f$  and burnishing speed  $v$ . The burnishing technology principle is based on the application of a pressing force to a very stiff burnishing element which rolls on the workpiece and induces plastic deformations into this surface layer along a reduction of the grain size and orientation of the material structure [1, 11, 12]. As a result, strain hardening occurs in the working zone as a consequence of permanent plastic deformation [13–15] (Fig. 2).

## 2 Roughness Deformations in Rolling Burnishing Process

For rolling process, various tools and different kinds of applying pressure to the workpiece are used. It can be imposed mechanically by use of springs or by pneumatic or hydraulic system.

Determined manufacturing process conditions considered here are highly influenced by factors imposed by a specific combination of process variables resulting from the objective of the process (smoothing, dimensional and smoothing or strengthening burnishing), the manner of exerting pressure of burnishing to the workpiece surface (stiff or elastic pressure) and the type of contact of burnishing elements with surface worked (rolling or sliding burnishing). The shape of the rolling burnishing elements depends on used method and other parameters of the process. These are usually sets of: rolls, balls, disks, barrels, cylinders, etc.

Hence, in the research course, the range of corresponding analysis has been limited and the focus put on the pressure rolling burnishing of cylindrical external surfaces, performed in the hybrid (integrated) systems.



**Fig. 2** Scheme of the deformation in the rolling process: **a** scheme of force distribution and roughness formation, **b** profilograph of plastically deformed roughness in the rolling zone (after tool reverse)

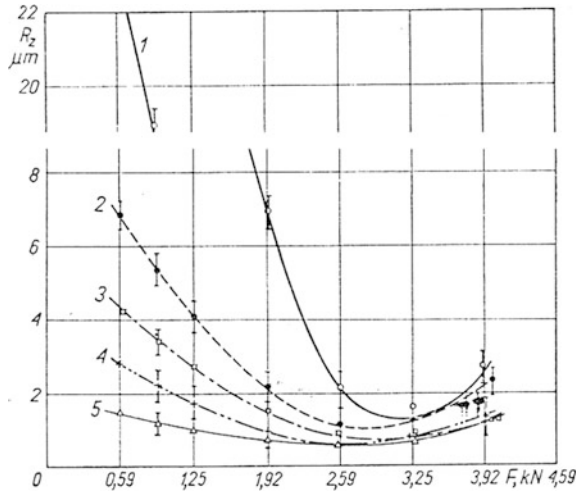
Using the burnishing tools on precision CNC machines and turning-burnishing centres allows to concentrate all shape and finishing processes at one working area. The sliding operation which is normally placed at different working area is not required, and consequently, production cost is reduced. Figure 3 presents the influence burnishing force on the surface roughness of steel rolling shafts (C45) (hardness 30HRC) feed = 0.005 mm/rev  $R = 30$ . Before rolling the surface, roughness of shafts was  $R_{z1} = 8.2\text{--}68.5 \mu\text{m}$ . The curves present a significant impact on roughness after burnishing has a roughness from the previous process. Next conclusion is that if previous process creates lower irregularity, expected parameters of surface are obtained using less pressure of the burnishing roller. The optimum value of the roughness parameter is obtained, when the force magnitude is in the range:  $F = 2,59\text{--}3,25 \text{ kN}$ . Shapes of curves are typical for the rolling burnishing process.

An approximate formula for the roughness  $R_z$  after burnishing is as follows: [1]

$$R_z \cong 10^3 \left( R - \frac{1}{2} \sqrt{4R^2 - f^2} \right) [\mu\text{m}] \tag{1}$$

where  $R_z$ —roughness parameter,  $R$ —roller profile radius of burnishing tool [mm],  $f$ —feed of burnishing process [mm/rev].

**Fig. 3** Dependence surface roughness parameter  $R_z$  on the strength of burnishing ( $F$ ) for different parameters after turning: 1–5  $R_z$  parameters after turning form range 8.2 (5)–68.5 (1)  $\mu\text{m}$



Pressing force for burnishing smoothing can be estimated by the experimental formula which includes length ( $l_c$ ) of the surface's contact of the tool and workpiece and diameter of tool ( $D_t$  and diameter of workpiece  $d_w$ )

$$F \cong 0.001kl_c d_e \text{ [kN]} \tag{2}$$

where  $k$ —preferred pressing unit of burnishing as a function of material strength in MPa (it gives a linear dependence for  $R_m = 600$  MPa,  $k = 40$  MPa or for  $R_m = 1200$  MPa,  $k = 80$  MPa),  $d_e$ —equivalent diameter for burnishing, which is calculated as a proportion  $d_e = D_t d_w / (D_t + d_w)$ ,  $l_c$  [mm].

Permitted longitudinal feed of burnishing  $f$  when using roller (pulley) can be evaluated from approximated formula

$$f \cong 2.87 \sqrt{RR_z} \text{ [mm/rev]} \tag{3}$$

where  $R$ —radius of curvature of the roller [mm],  $R_z$ —height of surface roughness [mm].

Burnishing feed has to be smaller than length of contact ( $l_c$ ) of burnishing element and workpiece. This feed is commonly placed inside range  $f = (0.2-0.3)l_c$  [mm/rev]. Burnishing is the surface plastic working in which element is rolling along work surface deforming and diminishing irregularities of surface left by previous machining, for example, turning. The degree of deformation of those irregularities depends on pressing of the tool  $F$  and machining parameters: feed  $f$  and burnishing speed  $v$ . Burnishing does not have a significant influence on the shape of a workpiece from previous operation. It slightly (by a few microns) diminishes the dimension of the workpiece (plastic deformation).

### 3 Hybrid Machining and Burnishing Process

For the time reduction of treatment, it is possible to carry out processing of turning and burnishing in the same time, applying the same longitudinal feed. For processing integrated in this way, one should use the special instrumentation or special machine tools, called turning-burnishing machine [16, 17].

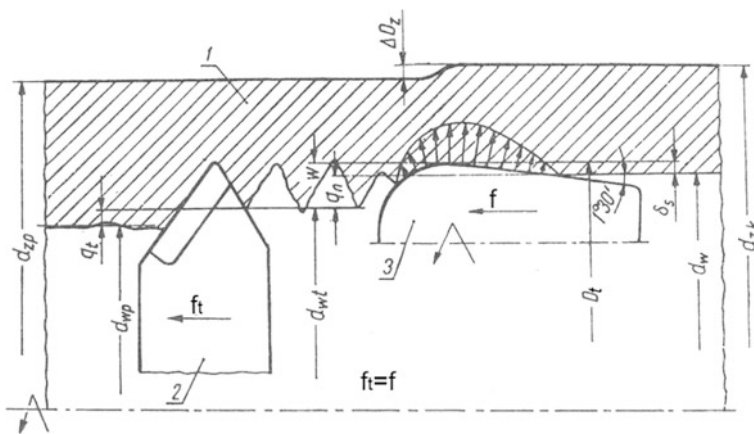
When you are machining thin-walled tube deformation, it is expected to increase the value of external diameter  $\Delta D_z$  and of decreased internal diameter of the value  $\delta_s$  in relation to the setting burnishing head. Scheme of this process presents Fig. 4.

In case of integrated processing of cylinders through chamfering with hybrid burnishing, the special chamfering-burnishing head is used. In this tool head, the setting of cutting tools to finishing should take into account the increase the cylinder diameter as a result of the burnishing process.

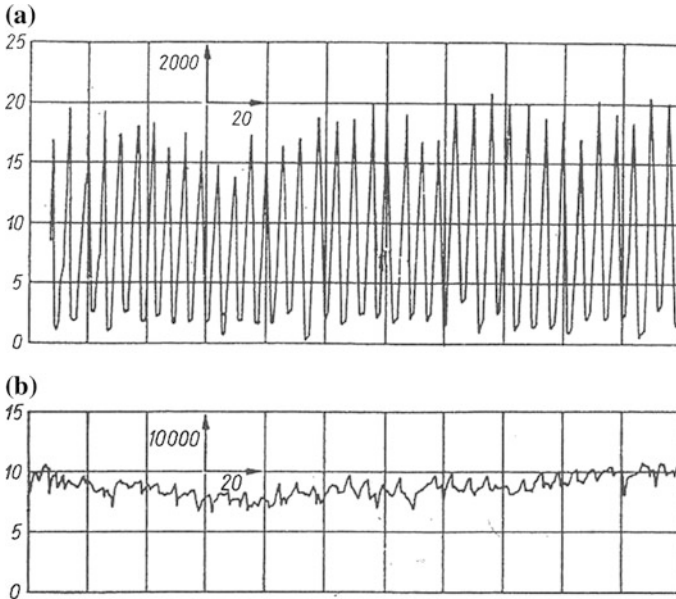
Roughness of surface of the hydraulic cylinder  $\phi 180$  mm is shown in Fig. 5. The sleeves were made of steel C45 and processed with turning-burnishing tool.

As the result of research works conducted at the Gdańsk University of Technology in cooperation with FAT PONAR Wrocław, the TUR 50 CNC-N machine was built (Fig. 6) for processing accomplishment integrated for shafts through turning and burnishing [17]. The machine is equipped with the CNC driver of Sinumerik type 810 T and two measuring probes LP2H Renishaw for measurements of the workpiece and putting position of the lathe tool.

After starting the turning process of shaft tree, burnishing rolls are automatically pushed near to shaft's surface (Fig. 6). Next two of them are staying jammed by devices (5), and one stays under the influence of the plumbing pressure. In this way, an arrangement is being created steady movable for the worked roller which is simultaneously turned and burnished. It enables processing of every diameter of



**Fig. 4** Plastic deformation in the workpiece as a result of hybrid cutting and burnishing process: 1 —machined cylinder, 2—cutting tool, 3—burnishing rolls

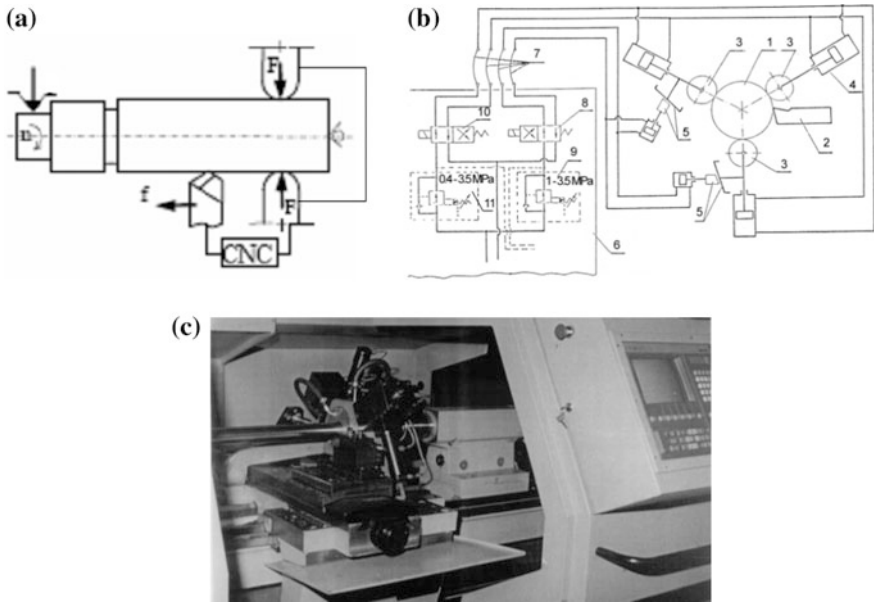


**Fig. 5** Profilographs of surface's roughness of the hydraulic cylinders  $\phi 180$  mm of sleeve made of C45 steel processed with turning-burnishing too: **a** surface roughness after turning, **b** surface roughness after burnishing: processing parameters: processing speed  $v = 2$  m/s, feed  $f = 0.2$  mm/rev, burnishing interference  $w = 0.08$  mm

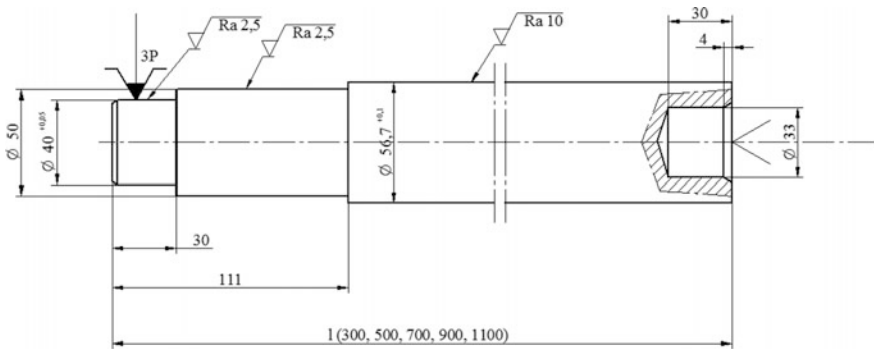
slender shafts in scope 20–100 mm and lengths up to 1750 mm without resetting the machine tool.

To protect against ingress of chips into the burnishing zone, a compressed air stream directed towards to the spindle between the cutting and burnishing zone was applied. The stream of this air is also delivers cooling liquid and the object during processing is being very well cooled. Technological examinations for burnishing shafts and piston rods, which slenderness was  $l/d < 20$  were conducted as an aim of confirming the usefulness of integrated processing system. They conducted research on samples (piston rods) of steel C45 about diameter  $\phi 56$  mm and lengths 700–1000 mm Fig. 7.

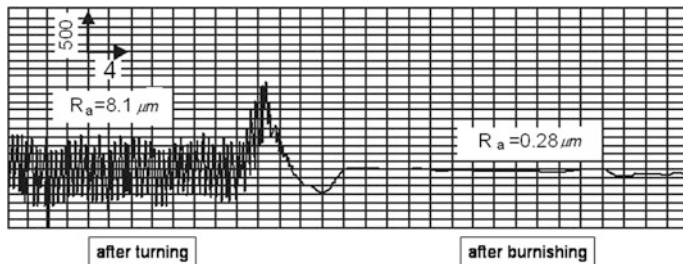
These samples were machined on turning-burnishing machine TUR 50 CNC-N in following technological conditions (established in preliminary examinations):  $n = 560$  rev/min,  $f_t = 0,22$  mm/rev,  $a_p = 0,35$  mm,  $F = 2,1$  kN, diameter of tool  $D_t = 60$  mm, radius of circles  $R = 30$  mm, TNMG 160404 TC 35 lathe tool, at one processing operation by the head with abundant cooling with liquid and air.



**Fig. 6** Schematic arrangement of turning and burnishing machine TUR 50 CNC-N: **a** scheme of processing, **b** scheme of hydraulic control system, 1—processed element (shaft), 2—cutter, 3—burnishing rollers, 4—working hydraulic cylinder, 5—blocking wedge, 6—oil supply unit, 8, 10—control valves, 9, 11—reducing valves [17], **c** special type TUR 50 CNC-N for long shafts manufacturing in one pass simultaneous turning and burnishing process, equipped with the control system Sinumeric 810T



**Fig. 7** Sample drawing used in the research



**Fig. 8** Profilograph of the piston rod surface  $\phi 56$  mm and  $l = 100$  mm after turning combined with burnishing operation rollers  $D_t = 60$  mm,  $R = 30$  mm, machining conditions: roller pressure  $F = 4$  kN, feed  $f = 0.18$  mm/rev

The roughness of the surface after turning was  $Ra_t = 5\text{--}10$   $\mu\text{m}$ , however after burnishing process the value of roughness parameter was in the range  $Ra = 0,13\text{--}0,28$   $\mu\text{m}$ , exemplary profilograph of surface presents Fig. 8. They were five repetitions for each set parameters being tested. Results are presented in Table 1.

A study plan was developed, and based on the results of the research, the relationships between the input parameters and the  $Ra$  parameter of the geometric surface structure were determined. The second-order polynomial was used to determine the relationship between the input parameters and the  $Ra$  roughness parameter. Approximated dependency is represented by formula (4).

$$Ra_c = 0.00028x_1^2 - 0.00385x_2^2 + 1.945x_3^2 - 0.00000107x_4^2 - 0.00845x_1 - 0.01255x_2 - 0.60614x_3 + 0.00121x_4 \quad (4)$$

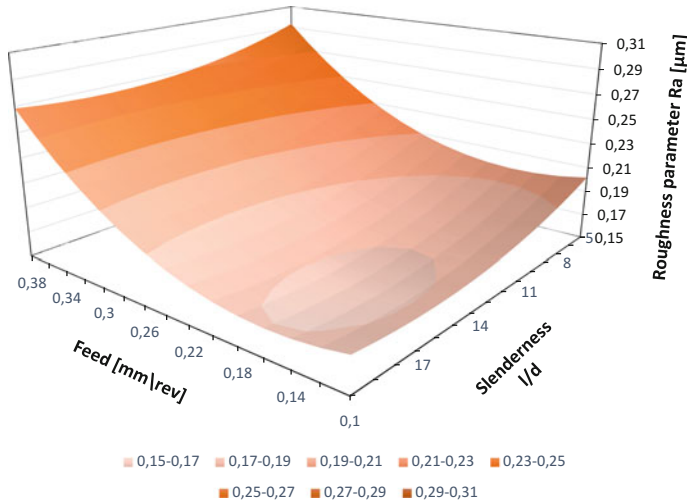
where  $Ra_c$ —calculates  $Ra$  parameter [ $\mu\text{m}$ ],  $x_1$ —slenderness of shaft  $L/d$  [dimensionless],  $x_2$ —burnishing force [kN],  $x_3$ —feed [mm/rev],  $x_4$ — rotational speed [rev/min].

Figure 9 presents the relation between the slenderness of the machined shaft and the burnishing feed on the  $Ra$  parameter of the roughness after burnishing. It can be noted here that in this machining system where the shaft is based between the burnishing rollers in the closed circuit processing force, the slenderness of the shaft slightly influences on the output parameters of the process. Figure 10 presents relationship between feed rate, burnishing force and surface roughness  $Ra$  parameter. Within the scope of the presented parameters, both parameters have an influence on the value of the output parameter. With high forces (about 4 kN) and small feeds, you should expect a material outflow which may slightly worsen the roughness of the surface. According on the graph in this process the optimal feed value consists in range  $0,14\div 0,18$  mm/rev

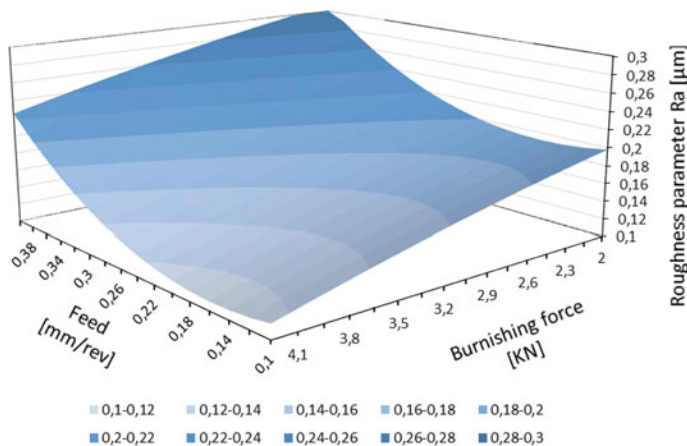


**Table 1** Experimental results of turning and burnishing of hydraulic piston rods on the turning-burnishing lathe TUR 50 CNC-N

No	Slenderness	Burnishing force	Feed	Rotational speed	Roughness parameter $Ra$					Average value	Middle value
					1	2	3	4	5		
	$l/d_w$	kN	mm/rev	rev/min	$\mu\text{m}$	$\mu\text{m}$	$\mu\text{m}$	$\mu\text{m}$	$\mu\text{m}$	$\mu\text{m}$	$\mu\text{m}$
1	5.36	2.7	0.22	560	0.2	0.19	0.24	0.21	0.15	0.198	0.2
2	19.6	2.7	0.22	560	0.21	0.18	0.17	0.21	0.18	0.19	0.18
3	12.5	1.5	0.22	560	0.28	0.21	0.14	0.22	0.21	0.212	0.21
4	12.5	3.9	0.22	560	0.14	0.13	0.13	0.16	0.11	0.134	0.13
5	12.5	2.7	0.12	560	0.13	0.2	0.17	0.2	0.16	0.172	0.17
6	12.5	2.7	0.32	560	0.17	0.23	0.23	0.22	0.21	0.212	0.22
7	12.5	2.7	0.22	440	0.15	0.21	0.19	0.14	0.16	0.17	0.16
8	12.5	2.7	0.22	680	0.18	0.16	0.16	0.17	0.13	0.16	0.16
9	12.5	2.7	0.22	560	0.17	0.21	0.18	0.18	0.17	0.182	0.18



**Fig. 9** Relationship between the  $R_a$  parameter, feed rate, slenderness of the machining shafts for burnishing force 2.75 kN and rotational speed 580 rev/min



**Fig. 10** Graph of the relationship between the  $R_a$  parameter and the feed rate and burnishing force of the machining shafts for slenderness 12.5 and rotational speed 580 rev/min

## 4 Conclusion

The paper shows the process of burnishing rolling as a method of finishing machine components. Particular attention was paid to the new innovative method of hybrid manufacturing by turning and burnishing. The paper discusses the complex turning (boring) and burnishing of long shafts and hydraulic cylinders. Construction and

setting of hybrid cutting and burnishing tool head and the special burnishing- lathe with CNC controller is explained. Analyses show that the greatest impact on the surface state determined by parameter  $Ra$  has the burnishing feed, and next is the burnishing force, slenderness and speed burnishing. In the burnishing system used, the smallest roughness of the treated piston rod was obtained for shaft slenderness  $l/D$  in the range of 12–16 and the feed rate of 0.14–0.16 mm/rev. Feed should not be less than 0.15 mm/rev because it increases roughness parameter  $Ra$ . Furthermore, the effects of burnishing rolling operation are as follows: increase the hardness and residual stress as well as wear and fatigue strength of burnished components.

## References

1. Przybylski, W.: Surface Plastic Working, 1–480. Publishing Home-Metallurgy, Moscow (1991) (in Russian)
2. Przybylski, W.: Special tools and attachment for turning and burnishing process on CNC lathes. In: 10th International Conference on Tools, University of Miskolc (2000)
3. Przybylski, W., Siemiątkowski, M.: Creating manufacturing alternatives of axially symmetric parts incorporating burnishing technologies. In: Proceedings (CD-ROM) of 16th International Conference on Production Research ICPR, pp. 1–15 (2001)
4. Przybylski, W., Siemiątkowski, M.: Deeming manufacturing conditions in integrated CNC turning-burnishing process planning. Annals of DAAM Symposium (1998)
5. Griffings, B.: Manufacturing Surface Technology. Penton press, London (2001)
6. Dzionk, S., Przybylski, W.: Surface waviness of components machined by burnishing method, archives of mechanical technology and automation. Polish Acad. Sci. **32**(2) (2012)
7. Grzesik, W., Żak, K.: Charakterisation of surface integrity by sequential dry hard turning and ball burnishing operations. J. Manuf. Sci. Eng. **136**(03), 1017–1019 (2014)
8. Kukielka, L.: Incremental Material Model and Its Application in the Modeling of the Burnishing Rolling Operation, p. 34. Scientific Book of the Department of Mechanical Engineering, Koszalin University of Technology (2004)
9. Klocke, F., Liermann J.: Roller burnishing of hard turned surfaces. Int. J. Machine Tools Manuf. **38** (1998)
10. Grzesik, W., Żak, K.: Modification of surface finish produced by hard turning using super finish and burnishing operations. J. Mater. Proc. Technol. **212**, 315–322 (2012)
11. Kaczmarek, J., Przybylski, W.: The surface contact characteristics after sliding and rolling burnishing. Adv. Manuf. Sci. Technol. Q. PAN **26**(1), 29–52 (2002)
12. Schiou, F.J., Chen, C.H., Li, W.T.: Automated surface finishing of plastic injection mold steel with spherical grinding and ball burnishing process. Int. J. Adv. Manuf. Technol. **20**, 61–66 (2006)
13. Kukielka, L., Kułakowska, A., Patyk, R., Numerical modeling and simulation of movable contact tool-workpiece and application in technological process. J. System. Cybern. Inform. **8** (5) (2010)
14. Skalski, K., Morawski, A., Przybylski, W.: Analysis of contact elastic-plastic strains during the process of burnishing. Int. J. Mech. Sci. **37**(5), 461–472 (1995)

15. Grzesik, W.: *Advanced Machining Processes of Metallic Materials*. Elsevier, Amsterdam (2008)
16. Przybylski, W.: Development perspectives of machine tools and equipment for burnishing. *Mach. Eng.* **6**(2) (2001)
17. Przybylski, W., Scisławski, J., Zieliński, J.: *Method and Equipment for Shafts Burnishing*, Patent PL nr 161449, Warsaw (1987)

# Virtual Reality and CAD Systems Integration for Quick Product Variant Design

Przemyslaw Zawadzki, Filip Gorski, Pawel Bun,  
Radoslaw Wichniarek and Karina Szalanska

**Abstract** The paper describes an integrated process of design of configurable products, on example of a city bus, comprising of two stages: configuration of a product variant with client participation and preparation of appropriate technical documentation in the design division of a company. The configuration stage is realized in a special, VR-class system—Virtual Design Studio (VDS). The technical documentation preparation stage is automated, by use of intelligent, generative CAD models, developed in the Autodesk Inventor software. They allow to save time of engineering design. The paper presents operation of the VDS system, process of building generative CAD models and integration of both stages.

**Keywords** Virtual reality systems · Generative CAD models · Mass customization · Product variant design · Knowledge based engineering

## 1 Introduction

A need of fulfilling individual needs of clients is today stronger than ever before. It concerns not only the consumer market, but also relations between companies. Expectations of recipients more and more often go beyond a standard offer by the producers [1–3]. The clients expect higher flexibility in field of applied technical solutions, as well as adjustment in scope of functional and visual features of products. What is attractive for a client, is problematic for a producer, as according to the Mass Customization (MC) strategy, products adjusted to a specific recipient should not be significantly more expensive than the standard products [4]. That is because the clients do not want to pay for the customization possibility alone, but only for a value of a customized product.

The idea of mass customization was described as early as in 80s of the twentieth century, but it is still up-to-date, especially in context of a developing concept of

---

P. Zawadzki (✉) · F. Gorski · P. Bun · R. Wichniarek · K. Szalanska  
Poznan University of Technology, Piotrowo 3 Street, 60-965 Poznan, Poland  
e-mail: Przemyslaw.Zawadzki@put.poznan.pl

Industry 4.0 [5, 6]. Mass customization becomes prominent in almost each branch, starting from advertising gadgets, through clothing design, electronics, architecture and automotive—it significantly contributes to competitiveness of companies [7, 8]. Development of the mass customization strategy over the last ten years was heavily influenced by, among other things, popularization of computer applications, known as the product configurators, allowing recipients to “design” a new variant of a product by themselves [9, 10]. Nowadays, many companies allow configuring their products via the Internet, and the market is full of IT solutions, which make preparation of such applications easier and easier. Moreover, dynamic development of Virtual Reality systems contributed to more and more frequent creation of immersive product configurators, that utilize this technology [11–13].

However, integration of advantages of mass and piece production requires changes also in scope of organization of a production system, especially including the design process. It is necessary to develop dedicated solutions, improving and coordinating design of configurable products in a way to shorten the time of this process and ensure its appropriate quality [14]. Modern CAx systems (Computer Aided Technologies), can be used for that purpose, allowing, among other things, enrichment of geometrical CAD (Computer Aided Design) models with a formal recording of engineering knowledge. The so-called generative product models, created this way, are a basis of Knowledge Based Engineering (KBE) systems.

This paper focuses on integration of VR and CAD systems, used in a process of design of variant products. On example of a VR application for configuration of a city bus, a solution is presented, aimed at automation of preparation of technical documentation (concerning arrangement of seats and handrails) of a designed variant of a product in a CAD system.

## 2 Product Variant Design Using VR and CAD Systems

The VR technologies in engineering design are usually associated with the notion of virtual prototyping. Using interactive and immersive projection systems, they help engineers in rapid variant change of new structures and in the decision making [15, 16]. Unfortunately, such solutions are usually niche, applied mostly by very large companies or research institutions, mostly because of significant costs of their development. Their integration with CAD systems is ensured, among other things, by the VRML standard, but this concerns only one-directional data exchange (from a CAD system to a VR system).

The VR systems are more popular in field of building applications for configuration of variant products. This type of software is focused on aiding of sales activities, focusing on visual representation of a product variant and preparation of an offer for a client. The VR is very popular in automotive branch, as well as in architecture, as it improves communication between a producer and a recipient. These solutions improve precision of defining needs and allow avoiding mistakes, related to incompatibility of client’s imagination of the real product.

The tools aiding engineers in process of design of variant products are usually developed using CAX systems. Scope of configuration of a designed product, meaning certain features and degree of their changeability, are admittedly dependent on expectations of recipients, but still, it is estimated, that 80% of design time is consumed by routine tasks [17, 18]. Their acceleration may therefore significantly influence optimization of the whole product lifecycle and allow certain savings. One of methods of automation of this type of work is development of generative models in CAD systems—this type of models is an example of a solution of KBE class [14, 18, 19]. In the KBE-class systems, identified and gathered expert knowledge about what needs to be done and how, is processed by a computer system, allowing its easier use in new projects. Formal description of rules applied by the design engineers influences standardization of the design process and accelerates development of new prototypes.

### 3 Virtual Design Studio for City Buses Configuration

The Virtual Design Studio is a multimodal, complex system for visual, real-time configuration of city buses, developed in Poznan University of Technology (Fig. 1) [20]. The system is focused on cooperative work with the clients, for effective selection of visual and technical features of city buses. It consists of several subsystems, using various VR solutions to accelerate and facilitate selection of a client-centered optimal variant of a product, in agreement with the producing company.

The subsystems are based on hardware for stereoscopic image projection and intuitive interaction with objects placed in a virtual environment. Application of realistic visualizations and immersive environment, allowing testing of a selected variant in a way similar to testing of a real product (i.e., virtual walk, interaction with the bus elements) allows to avoid problems and mistakes related to differences between the real product and requirements of clients. Using only text configurators and basic visual aids (such as physical material samples)—a traditional way—is a cause of many mistakes, as results from practical experience of the company. These problems generate costs, because there is a need of adjusting product features even after production, when inconsistencies are detected. The system is currently implemented in the company and is available for the clients during the sales negotiation process, as well as for internal use.

The main features of the system are as following:

- Free configuration of selected features of a city bus (more than 100 options).
- Stage 1 (pre-configuration)—visualization on a touch table.
- Stages 2 and 3 (synchronized in real-time)—displaying the product on a large screen with full interaction and configuration possibilities (stage 2) and using immersive devices such as a Head-Mounted Display (Fig. 2) to give client a possibility of virtual walk.



**Fig. 1** Virtual Design Studio—interface of the pre-configuration module

- The configuration and all the functions of the system based on graphical user interfaces, standard peripheral devices such as mouse, keyboard and joystick, as well as gestures and movement recognized by devices such as optical tracking systems and contact gesture recognition devices.
- Interactivity of bus elements (possibility of opening doors, animations, etc.).
- Free navigation: predefined and free camera views in two modes: Orbit and Walk (for external and internal vehicle exploration, correspondingly).
- Special set of visualization functions—hiding/showing groups of elements, dynamic sectioning etc.
- Full synchronization between configuration stages in real time.

The VDS system can be summed up as a solution, where knowledge about the visual aspects of the product and their logical connections is aggregated and it is possible to easily access this knowledge via graphical interface and VR peripherals. From the company's side, one of the biggest advantages of the VDS system is its



**Fig. 2** Virtual walk with HMD device



open architecture. By principle, it operates as a framework, built over a commercial 3D engine (the EON Studio software), with easy access to all the functions, requiring virtually zero programming activities while adjusting or adding new contents. Readiness for integration with other tools used in the company (PLM, CAD systems) was one of the crucial assumptions while the system was built. That is why data describing a variant selected by a particular user (known as the V-BOM—virtual Bill of Material, which is a list of selected options and their values, linked to active components and their positions) may be exported by the system to a number of formats (including plain text file and PDF). It allows creating a connection to a CAD system.

The integrated VDS system consists of several main modules:

- (1) Visualization module—which displays a city bus and holds all the logic responsible for configuration and visualization. It was created using EON Studio software.
- (2) Main graphical user interface—it is usually launched together with the main module. It contains all the functions for configuration and visualization and it is also dynamically created on the basis of library assignments.
- (3) Auxiliary GUI—it is a simplified interface based on web technologies, so it can be launched on any device with a web browser, for example on a tablet or laptop.
- (4) Administrative application—it works independently of the basic modules and is used to manage contents of the library and process data exchange between the VDS system and other tools, like PLM and CAD systems. It is also a special,

dedicated application, which allows modification and adding of 3D and 2D content to the system without need of programming.

- (5) Minor modules—there is a number of supporting modules, such as the system launcher, report generator, etc.
- (6) Library—a set of data, consisting of 3D data (meshes), 2D data (textures, photographs, movies etc.) and logical and metadata (virtual BOMs—bills of material for defined products, connections between options, special conditions, animation paths etc.)

Relations between the system elements are presented in a structural diagram, shown in Fig. 3.

Because of high complexity of the city bus interior model, VR-CAD integration was initially planned only for the seat and handrail arrangement (Fig. 4). The input data for the CAD system is configuration of a given variant, prepared by a user of the VDS system, comprising of number of seats, their type and position: direction (4 possible angular positions: towards front, back, left or right side of the bus) and location in the interior space, selected from the physically possible locations, within a predefined range.

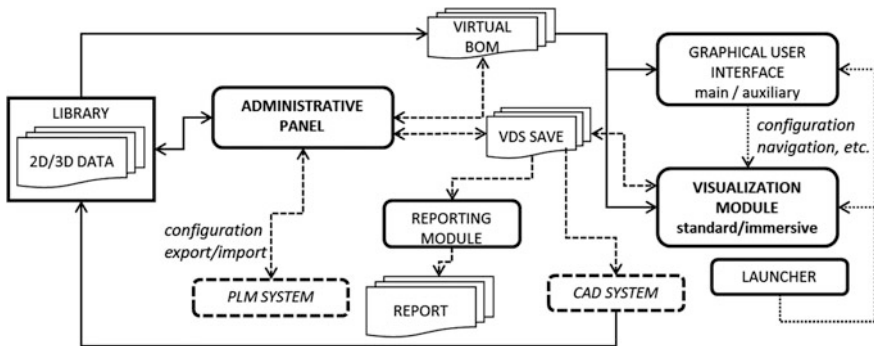


Fig. 3 Structure of the VDS system with indication of data flow directions

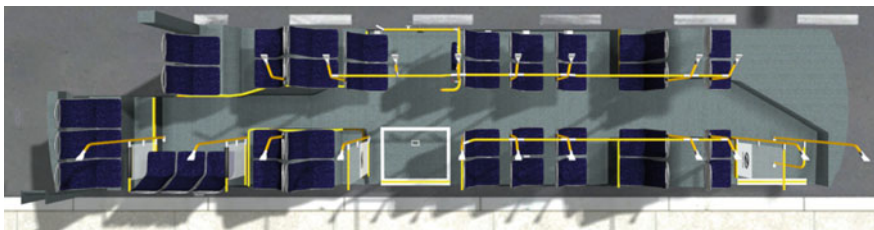


Fig. 4 Configuration of seats position in the VDS system

### 4 Generative CAD Model of Bus Interior

High level of freedom during the seats configuration process is a huge problem for the design engineers. For each consecutive variant, they must prepare appropriate documentation, considering technical conditions of the arrangement (mounting, spaces between seats etc.) and shaping of handrails. The VDS system allows users to configure seat positions, but the handrail arrangement is decided by the engineers.

To accelerate work of engineers, an appropriate generative CAD model was prepared in the Autodesk Inventor system. This model allows representation of each possible configuration prepared in the VDS system. It was assumed, that a basis for adjustment of geometry of a given variant of city bus interior will be automatically called design rules (Fig. 5a), describing a method of modeling of handrails, depending on a number and location of seats in a bus. Knowledge about methods of handrail modelling applied in the company, as well as conditions of their occurrence (shape of a handrail is dependent on location and direction of a particular seat) were gathered from experienced design engineers working in the company. Information about a particular arrangement desired by a client was automatically sent from the VDS system, by import of data saved to a special design table, linked to the CAD model (Fig. 5b).

The design rules were prepared in a way to first build a model of seat arrangement corresponding to the arrangement saved in the VDS system. For each possible seat, a separate rule was prepared, checking its presence and then direction and location coordinates. Then, for each seat, possible variants of handrail mounting are analyzed in the model. The consecutive rules verify location of a seat

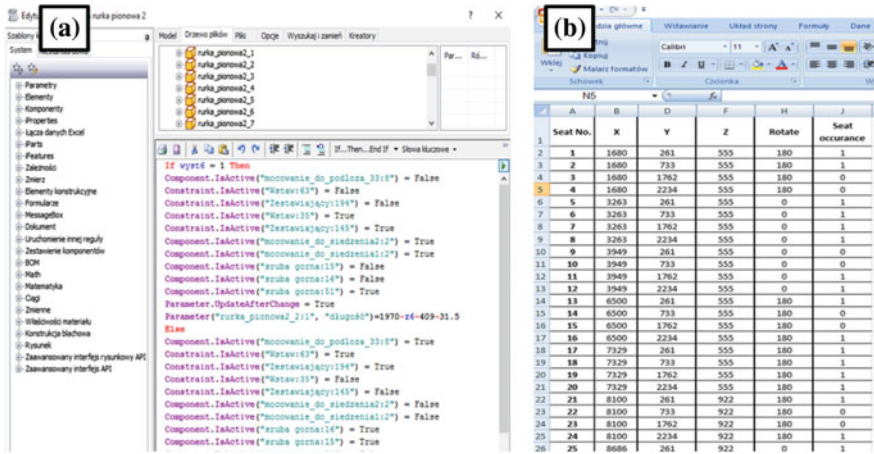
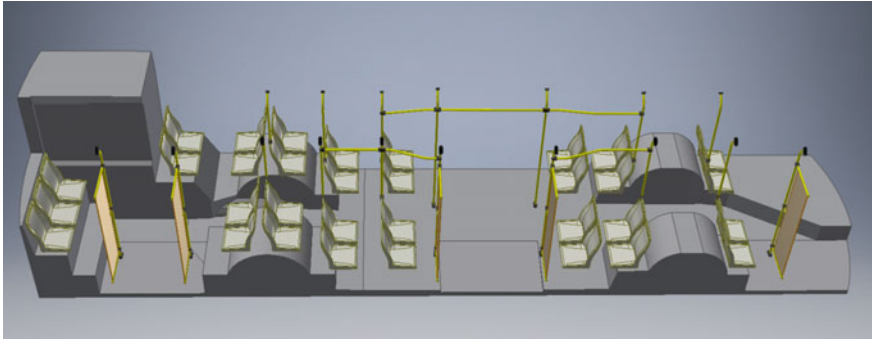


Fig. 5 a Example of a design rule in the generative CAD model, b design table for the CAD model



**Fig. 6** Generative CAD model of bus interior

and its surroundings (e.g., wheel house shell, wheelchair bay, doors), to properly select a handrail arrangement appropriate for a given bus.

The generative CAD model of the bus interior (Fig. 6) was described by more than 40 design rules and approximately 900 geometrical parameters, both dimensional and logical. Only 132 of them are taken directly from the VDS system. The developed CAD model, enriched with the engineering knowledge, is capable of automatic generation of documentation of hundreds of thousands of correct combinations of handrails, without participation of a design engineer.

## 5 Conclusions

Tests of the VDS system confirm possibility of integration of various systems, where the CAD system is not only a source of data for the VR system, but its recipient as well. The most important advantage of the developed solution is shortening of time needed for preparation of technical documentation of a new variant of product. In a traditional design process, preparation of a technical documentation (preparation of a CAD model of handrails for a new bus variant), despite high repeatability of work, is always realized nearly from the scratch. It is, obviously, aided by templates of typical connections and shapes of handrails. However, considering individual requirements of clients requires manual adjustment of CAD models. This work can take average of several hours per one variant. Thanks to application of a generative CAD model, this time was shortened to several minutes in the presented solution. The generated variant data does not need to be re-interpreted and thoroughly verified in the CAD system, as they are automatically imported from the VR configurator. It can be therefore concluded, that intelligent VR/CAD solutions allow better realization of the mass customization strategy in a company. They also contribute to more smooth knowledge flow and allow recording and storing human knowledge, for easier access (no high

qualifications nor knowledge is required to operate both the VDS system and the generative CAD model).

One clear disadvantage of the prepared solution is lack of the real-time feedback from the CAD system to the VR system. The VDS system user can manipulate seats (within scope of physical possibilities), but there will not be an automatic visual adjustment of handrail shape, as it is done afterwards in the CAD system—it will be visible for an engineer, but not immediately for the client. A rapid way of sending the generated geometry back from the CAD system will have to be developed in order to overcome this disadvantage. The authors focused on improving the design engineers work, so this was not a primary issue while building the presented solution.

Additionally, it must be noted that insofar as the application of generative CAD models and their integration with the VR system shortens absolute configuration and design time for a new product variant (involving client in the process and considering his requirements), the process of building the system itself is very time consuming. All the above mentioned work on building of the VDS system took more than a dozen months by a team of developers. Despite existence and use of certain methodical patterns (e.g., MOKA—its assumptions were used extensively), very helpful in build of KBE solutions, development is still difficult to realize in practice and that is the most probable reason why such solutions are so rarely seen implemented in industrial practice. The further work should be therefore directed at looking for methods improving gathering and implementation of knowledge used in design, as well as building of generative models, to allow economic justification of building of this type of solutions.

## References

1. Starzyńska, B., Kujawińska, A., Grabowska, M., Diakun, J., Więcek-Janka, E., Schnieder, L., Schlueter, N., Nicklas, J.-P.: Requirements elicitation of passengers with reduced mobility for the design of high quality, accessible and inclusive public transport services. *Manage. Prod. Eng. Rev.* **6**(3), 70–76 (2015)
2. Hamrol, A., Kowalik, D., Kujawinska, A.: Impact of selected work condition factors on quality of manual assembly process. *Hum. Fact. Ergon. Manuf. Serv. Ind.* **21**(2), 156–163 (2011). doi:[10.1002/hfm.20233](https://doi.org/10.1002/hfm.20233)
3. Kujawińska, A., Vogt, K., Wachowiak, F.: Ergonomics as significant factor of sustainable production. In: Golińska, P., Kawa, A. (eds.) *Technology Management for Sustainable Production and Logistics*. *EcoProduction*, pp. 193–203 (2015). doi:[10.1007/978-3-642-33935-6\\_10](https://doi.org/10.1007/978-3-642-33935-6_10)
4. Tseng, M.M., Hu, S.J.: Mass customization. In: *CIRP Encyclopedia of Production Engineering*, pp. 836–843. Springer, Berlin, Heidelberg (2014)
5. Brettel, M., Friederichsen, N., Keller, M., Rosenberg, M.: How virtualization, decentralization and network building change the manufacturing landscape: an Industry 4.0 perspective. *Int. J. Mech. Aerosp. Ind. Mech. Manuf. Eng.* **8**(1) (2014)
6. Zawadzki, P., Żywicki, K.: Smart product design and production control for effective mass customization in the Industry 4.0 concept. *Manage. Prod. Eng. Rev.* **7**(3), 105–112, (2016)

7. Salvador, F., de Holan, P.M., Piller, F.: Cracking the code of mass customization. *MIT Sloan Manage. Rev.* **50** (3) (2009)
8. McIntosh, R.I., Matthews, J., Mullineux, G., Medland, A.J.: Late customisation: issues of mass customisation the food industry. *Int. J. Prod. Res.* **48**(6), 1557–1574 (2010)
9. Fogliatto, F.S., da Silveira, G.J., Borenstein, D.: The mass customization decade: an updated review of the literature. *Int. J. Prod. Econ.* **138**(1), 14–25 (2012)
10. Trentin, A., Perin, E., Forza, C.: Product configurator impact on product quality. *Int. J. Prod. Econ.* **135**(2), 850–859 (2012)
11. Górski, F., Buń, P., Wichniarek, R., Zawadzki, P., Hamrol, A.: Immersive city bus configuration system for marketing and sales education. *Proc. Comput. Sci.* **75**, 137–146 (2015)
12. Choi, S., Jung, K., Noh, S.D.: Virtual reality applications in manufacturing industries: past research, present findings, and future directions. *Concurr. Eng.* **23**(1), 40–63 (2015)
13. Chandrasegaran, S.K., Ramani, K., Sriram, R.D., Horváth, I., Bernard, A., Harik, R.F., Gao, W.: The evolution, challenges, and future of knowledge representation in product design systems. *Comput. Aided Des.* **45**(2), 204–228 (2013)
14. Górski, F., Zawadzki, P., Hamrol, A.: Knowledge based engineering as a condition of effective mass production of configurable products by design automation. *J. Mach. Eng.* **16** (2016)
15. Grajewski, D., Diakun, J., Wichniarek, R., Dostatni, E., Buń, P., Górski, F., Karwasz, A.: Improving the skills and knowledge of future designers in the field of ecodesign using virtual reality technologies. In: *International Conference Virtual and Augmented Reality in Education*. *Procedia Computer Science*, vol. 75, pp. 348–358 (2015). ISSN 1877-0509
16. Pandilov, Z., Milecki, A., Nowak, A., Górski, F., Grajewski, D., Ciglar, D., Mulc, T., Klaić, M.: Virtual modelling and simulation of a CNC machine feed drive system. *Trans. FAMENA* **39**(4), 37–54 (2015)
17. Stokes, M.: *Managing Engineering Knowledge; MOKA: Methodology for Knowledge Based Engineering Applications*. Professional Engineering Publishing, London (2001)
18. Skarka, W.: *Application of MOKA methodology in generative model creation using CATIA*. In: *Engineering Applications of Artificial Intelligence*, vol. 20. Elsevier (2007)
19. Górski, F., Hamrol, A., Kowalski, M., Paszkiewicz, R., Zawadzki, P.: An automatic system for 3D models and technology process design. *Trans. FAMENA* **35**(2), 69–78 (2011)
20. Górski, F., Buń, P., Wichniarek, R., Zawadzki, P., Hamrol, A.: Design and implementation of a complex virtual reality system for product design with active participation of end user. In: *Advances in Human Factors, Software, and Systems Engineering*, pp. 31–43. Springer International Publishing (2016)

# An Approach to Modeling and Simulation of a Complex Conveyor System Using Delmia Quest—A Case Study

Waldemar Malopolski and Adam Wiercioch

**Abstract** In this paper an appropriate method for modeling and simulation of a complex conveyor system based on Delmia Quest is presented. The described model is similar to a real system in which work-pieces are transported on pallets. The transportation subsystem consists of linked conveyors. In this system, pallets are moved between many conveyors. The presented method of modeling prevents collisions between pallets and can be used to perform simulation experiment. Using this solution, the efficiency of the transportation subsystem based on simulation experiment was examined.

**Keywords** Modeling · Simulation · Complex conveyor system · Delmia quest

## 1 Introduction

The globalization of the world economy and economic developments in many countries, have led to a large increasing in competition among manufacturers of consumer goods of all kinds. The means of survival for many companies is to reduce production costs. In many cases, the only way to achieve this goal is to introduce an automation of production processes. Particularly large savings are possible to achieve in terms of minimizing the cost of transport operations. This is because the transport activities do not generate added value. Transportation sub-systems usually generate nothing but additional cost. Therefore, cost minimization in this area is very often assumed as an objective function in optimization process. Computer modeling and simulation is very favorable way to achieve this goal.

---

W. Malopolski (✉)

Faculty of Mechanical Engineering, Production Engineering Institute,  
Cracow University of Technology, Kraków, Poland  
e-mail: malopolski@mech.pk.edu.pl

A. Wiercioch

Faculty of Mechanical Engineering, Cracow University of Technology,  
Kraków, Poland

© Springer International Publishing AG 2018

A. Hamrol et al. (eds.), *Advances in Manufacturing*, Lecture Notes in Mechanical Engineering, [https://doi.org/10.1007/978-3-319-68619-6\\_58](https://doi.org/10.1007/978-3-319-68619-6_58)

609

Very often, the automation of transportation subsystem is carried out by automated guided vehicles (AGV) or conveyors. Transportation subsystems based on AGVs are flexible. But there are many problems with mechanical, safety and positioning aspects of design of AGV [1, 2]. Moreover, appropriate pathfinding, collision-free and deadlock-free algorithms must be implemented [3]. In case of transportation subsystems with AGVs an approach to optimization based on simulation can be very effective [4].

Transportation subsystems based on conveyors are very popular and efficient. This type of transport is simple and relatively inexpensive. Depending on the applications, there are many types of conveyors. Very important types of conveyors are high tonnage conveyors. This type needs a special approach to design because of effect of dynamics (starts and stops). In the past, it was very significant problem. However, drive technology has been highly improved recently and therefore main attention can be focusing on analysis of emergency stops and ‘what if’ scenarios. A practical verification of solutions with these types of conveyors is very important [5]. Another area of application of conveyors is the transport within production lines. Very often, this type of transportation subsystem is built of many linked conveyors. In this case, a proper coordination of activities among all conveyors is essential, especially to prevent collisions between work-pieces. At the design stage of the transportation subsystem, it is very important to ensure its efficiency. This can be achieved using computer simulation.

There are many different tools and languages for modeling and simulation [6]. One of the most popular simulation tools is Delmia Quest. It is the powerful tool for discrete event process modeling. It has many functions and features of process modeling [7]. Therefore simulation based on this tool is effective and it can be used to produce an objective decision support in a real factory [8]. The possibilities of Quest are increased by embedded Simulation Control Language (SCL). Therefore the effectiveness of this tool is very high [9].

Delmia Quest software can be used for material flow simulation and optimization of manufacturing line. In this case, based on simulation experiment, e.g., bottlenecks, conveyors utilization or new manufacturing strategies can be found and manufacturing line can be improved [10–12]. In other words, simulation can be used to improve material flow and operation of manufacturing systems [13, 14]. For example, 3D simulation can be used as a tool for effective design of an assembly line, by taking into consideration among others: work measurement, line balancing and ergonomic problems [15, 16].

However, simulation efficiency depends on the correctness of model creation. For this reason this paper presents an appropriate methodology of building simulation models. It focuses primarily on complex conveyor systems. The main purpose of the paper is presentation of the correct method of modeling and simulation of complex conveyor systems.

Section 2 of this paper a production line with transportation subsystem is described. This line is an academic example but it is similar to a real line. Section 3 model building of a complex conveyor system using Delmia Quest is presented.



Section 4 simulation experiment and results are described. Section 5 includes conclusions.

## 2 Description of the Production Line

Manufacturing system with transportation subsystem based on conveyors, described in this paper, is similar to a real system. The manufacturing system consists of eleven production lines. Each line produces different type of product. A cycle time for each line is presented in Table 1.

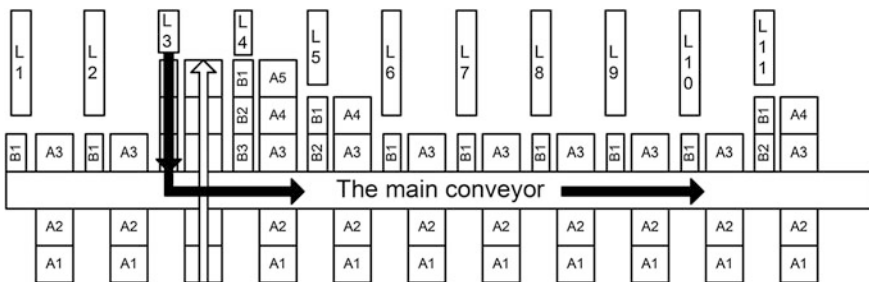
### 2.1 Transportation Subsystem Description

All finished products are packaged on main pallets and moved to buffers. The transportation subsystem layout is shown in Fig. 1. Dimensions of the main pallet are 1/2/2 m (width/length/height). Each line has own buffer, which can accommodate: 1, 2 or 3 pallets. All buffers are simple accumulated conveyors. There is a second type of pallet with dimensions 2/2/1 m. These pallets include accessories, which are consumed in the production processes on lines (L1–L11). These pallets are transported across the main conveyor to each production line. There are eleven conveyors which transport pallets with accessories, one for each production line.

The main task of transportation subsystem is picking up all pallets from production lines (L1–L11). In the first step, pallets are moved from production lines to buffers (conveyors). After that, each pallet should be moved on the main conveyor,

**Table 1** Production lines cycle time (s)

L1	L2	L3	L4	L5	L6	L7	L8	L9	L10	L11
300	293	276	200	346	372	372	276	372	372	287



**Fig. 1** The layout of transportation subsystem

which transports all pallets to the next station. The main conveyor is constantly in motion. Therefore, pallet can move on the main conveyor if there is an appropriate space on it. In the first step a pallet is moved on the main conveyor (exactly under it) and after that, in the second step it is put down on the main conveyor and moved to the next station. When main pallets are transported on the main conveyor, pallets with accessories should move cross the main conveyor between main pallets. There must be a suitable distance between main pallets for a process to succeed. Before building simulation model the precise analysis of pallets movement should be done.

## 2.2 Pallets Movement Analysis

There are two cases related to pallet movement. First, when the main pallet is moved from the buffer on the main conveyor. Dimensions of the main pallet are 1 m width and 2 m length. Width of the main conveyor is 2 m. We can assume, that velocity of the main conveyor  $V_m$  (m/s) and buffer conveyors with accessories  $V_a$  (m/s) are the same. When the main pallet starts from buffer conveyor, it has to cover a distance of 2 m. After that it will be exactly under the main conveyor. At the same time, the main conveyor covers the same distance. Therefore, a minimum required space on the main conveyor is 2 m plus 1 m for the main pallet width. It means, that minimum distance  $lm_{min}$  between two other pallets on the main conveyor should be equal 3 m. Under this condition the main pallet theoretically can be placed on the main conveyor between two other main pallets. This minimum distance should be increased about additional safety distance before and after the main pallet, see Fig. 2. The value of safety distance is set to 0.1 m after the main pallet and to 0.3 m before it. Therefore  $lm_{min} = 0.3 \text{ m} + 2 \text{ m} + 1 \text{ m} + 0.1 \text{ m} = 3.4 \text{ m}$ .

We need to consider second case, when pallet with accessories is about to cross the main conveyor. This pallet width and length are 2 m. It has to overcome the distance 4 m to cross by the main conveyor. In this case the minimum distance  $la_{min}$  between two main pallets on main conveyor is 4 m plus 2 m (width of the pallet with accessories). For safety reasons we have to add additional distance before and after main pallet. The value of safety distance is set to 0.1 m after the main pallet and to 0.3 m before it. The total distance  $la_{min} = 0.3 \text{ m} + 4 \text{ m} + 2 \text{ m} + 0.1 \text{ m} = 6.4 \text{ m}$ . The value of  $la_{min}$  distance depends on velocity of conveyors. Finally  $l_{min} = \max(lm_{min}, la_{min})$  The values of  $l_{min}$  distance for different values of velocity of the main conveyor  $V_m$  (m/s) and conveyor with accessories  $V_a$  (m/s) are presented in Table 2.

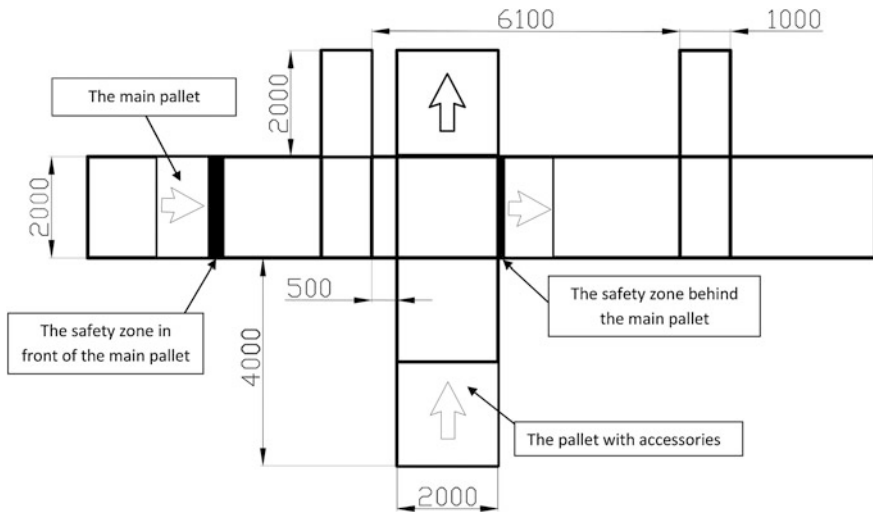


Fig. 2 Description of the pallets movement

Table 2 Values of  $l_{min}$  (m) distance for selected values of velocity

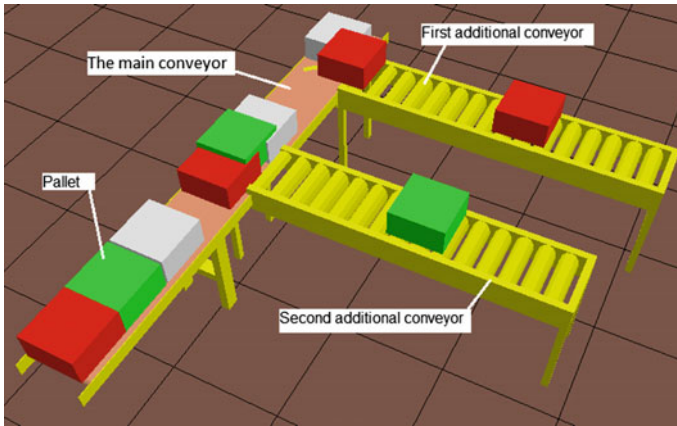
$V_m$	$V_a$		
	0.33	0.42	0.50
0.20	4.80	4.32	4.00
0.25	4.40	4.80	5.40
0.30	6.00	5.28	4.80

### 3 Conveyors Modeling with Delmia Quest

Delmia Quest has dedicated powerful tools for conveyors modeling. These tools are easy to use for modeling simple and stand-alone conveyors. In the production systems there are very often more than one conveyor. Transportation subsystems usually consist from many linked conveyors. In this case, when work-pieces are moved from one to other conveyor, building of the model is not easy.

#### 3.1 Model Building of a Complex Conveyor System

Figure 3, three linked conveyors are presented. The first one (widest) is a main conveyor. Two additional conveyors are linked to the main conveyor. First additional conveyor touches to the border of the main conveyor. Therefore the work-piece being moved will jump from the end of the first additional conveyor to the center of the main conveyor. This kind of operation is impossible in reality. An appropriate solution is introduced with the second additional conveyor. In this case



**Fig. 3** An example of complex conveyor system

the end of the second conveyor is moved to the center of the main conveyor. When the work piece reaches the end of the second additional conveyor it will be exactly in the center of the main conveyor. It can start travel on the main conveyor if it can take enough space on it.

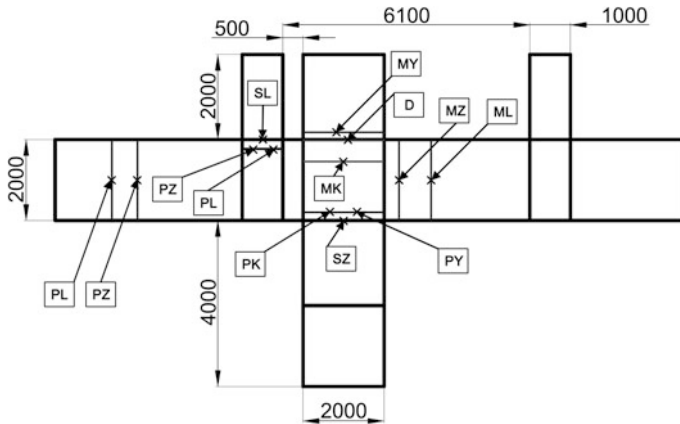
This solution is not sufficient because of possibility of collisions. The basic problem is how to correctly model the movement of pallets from one conveyor to another. What is needed, this is the correct method of modeling. The proposed method is described below.

In this case special decision points have to be introduced to avoid the collisions between work-pieces. Decision points are usually used in Delmia Quest to creation additional input or output places along a conveyor. Moreover these points can be used for detection a work-pieces which travel on a conveyor. They can detect: leading edge, origin or trailing edge of work-pieces. Delmia Quest has a large number of built-in logics, which are used to make a decision and control of individual objects in a simulation. Moreover, the user can compose custom logics based on SCL.

In this way user can control behavior of any object. SCL is a procedural language similar to other high-level computer languages. It has several data types that allow getting specific information about each object.

### **3.2 Additional Decision Points**

In order to fully control the flow of pallets additional decision points have to be entered. These points are presented in Fig. 4. The unit of measure is (mm). First *SL* decision point is dedicated to the main pallet. It checks an available space on the main conveyor. This point permits the main pallet to entry on the main conveyor if



**Fig. 4** Description of additional decision points. Decision points: *SL*, *PL*, *ML*, *PK* and *MK* are used by the main pallet. Decision points: *SZ*, *PZ* and *MZ* are used by the pallet with accessories. Points: *D*, *PY* and *MY* are used by the pallet with accessories too

there is a required distance  $l_{min}$  before and after other main pallets on the main conveyor and if there is not pallet with accessories on the main conveyor. This point cooperates with four points: *PL*, *ML*, *PK* and *MK*. There are exactly two points of type *PL*. First two points check for other main pallet on the main conveyor. The second two points check for the pallet with accessories on the main conveyor. *SL* point cannot permit the main pallet to entry on the main conveyor if there is other main pallet between points: *PL* and *ML* or if the pallet with accessories is crossing through the main conveyor and it is between points: *PK* and *MK*.

*SZ* decision point is dedicated to pallet with accessories. This point cooperates with points: *PZ* and *MZ*. There are exactly two points of type *PZ*. They forbid the pallet with accessories to cross the main conveyor if there is a main pallet between *PZ* point and *MZ* point on the main conveyor. This is because the distance between main pallets is smaller than  $l_{min}$ . The pallet with accessories cannot cross the main conveyor if its destination place is not free too. To do this *D* decision point was introduced. This point cooperates with points: *PY* and *MY*.

To each point a procedure in SCL language was added. These procedures use four variables: *K*, *Y* and *L*, *Z*.

For example the procedure in one of the two *PL* points adds (*Plus*) a value '1' to the variable *L*. The procedure in *ML* point subtracts (*Minus*) a value '1' from the variable *L*. If the value of *L* and *K* variable is equal zero, than the procedure in *SL* point can permit the main pallet to entry on the main conveyor. An example of procedure in *SL* decision point is shown below. Procedures like this are assigned to all *SL<sub>i</sub>* points, where  $i = 1, \dots, 11$ . An example of procedure in SCL is shown below.

```

Var
Li :Integer % variable L for buffer #i
Ki :Integer % variable K for buffer #i
Procedure SLi()
Begin
While (True) Do
if(Li==0 AND Ki==0) then
resume_travel
endif
delay 0.01
Endwhile
End

```

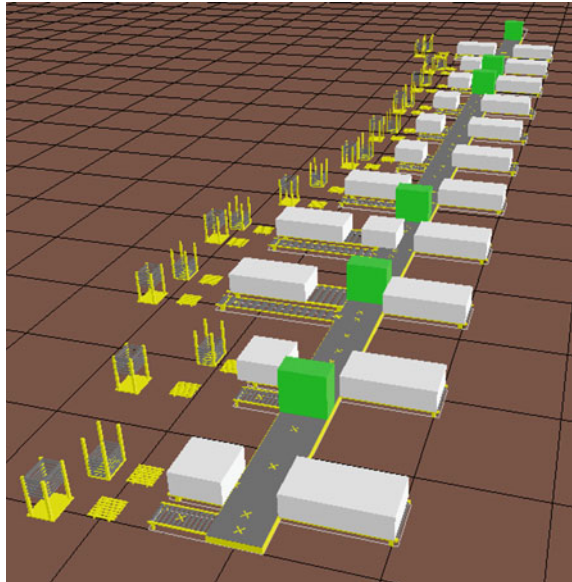
Based on decision points, described above, the control rules for pallets movement were created. These rules were implemented to the model with Simulation Control Language.

### 3.3 Model of Production Lines

The model of whole production system is presented in Fig. 5. This model consists among others from: one main conveyor, eleven accumulated conveyors (buffers) linked to production lines and eleven conveyors for pallets with accessories (crossed with the main conveyor). Decision points, described above, were added to the model to all conveyors linked with production lines.

After that, all control rules were implemented to the model. In this way, moving of all pallets in this model was under control. Thus, the behavior of the model was

**Fig. 5** The model of whole production system



the same as the real system. There were not collisions between all pallets and pallets were properly deployed on conveyors. After building the model, the validation of its correctness was carried out. The operation of the model was analyzed with the various parameters. After checking the correctness of the model, simulation experiments were carried out.

### 4 Simulation Experiment and Results

After verifying the correctness of the model, simulation experiments were performed under different velocities of the conveyors. The simulation time was set to 8 h. Stochastic factors were added to production lines cycle time. To verify that the transportation subsystem fulfils its task, statistics have been collected from the additional buffers, that were placed before the accumulated conveyors (buffers). In this way the number of pallets, that downtime was not equal to zero for each line was counted. The tests were performed for different values of the speed of conveyors. The results are shown in Table 3. The values in the table show the number of pallets which exceeded the acceptable waiting time. For conveyor speeds 0.25 and 0.5 m/s, there was only one pallet, which was waiting too long to enter on the conveyor. The waiting time was very small. Therefore this configuration of speeds was taken into account as acceptable solution. Table 4 shows the results of the simulation.

Configurations that meet requirements are denoted by ‘O’. Others, not satisfactory configurations are denoted by ‘X’. The simulation experiments indicate that the production line can work with three configurations of conveyor speeds. In these cases, the transportation subsystem is efficient. In the way presented above we can find the best (smallest) values of conveyors velocity.

**Table 3** The number of pallets waiting too long for entrants

$V_m$ (m/s)	0.20	0.25	0.25	0.30	0.30	0.30
$V_a$ (m/s)	0.50	0.42	0.50	0.33	0.42	0.50
Buffer 1	0	0	0	0	0	0
...						
Buffer 9	6	1	0	3	0	0
Buffer 10	73	9	1	12	0	0
Buffer 11	95	2	0	1	0	0

**Table 4** The result of simulation experiment

$V_m$ (m/s)	$V_a$ (m/s)		
	0.33	0.42	0.50
0.20	X	X	X
0.25	X	X	O
0.30	X	O	O

## 5 Conclusions

The article describes the basic capabilities of Delmia Quest for modeling simple transportation subsystems. The problems with complex conveyor system modeling associated with capabilities of collisions were discussed. In order to correct modeling of such systems, the method based on the introduction of additional decision points to the model was proposed. The full control of the flow of pallets between the conveyors was possible by adding to the model procedures written in SCL. These procedures are based on the decision points. With the proposed method, it was possible to build a properly functioning model. The simulation experiments were carried out using this collision-free model. Based on these experiments, configurations of conveyor speeds that ensure its efficient operation have been determined. This would not be possible without using the method described in the article. The presented method can be applied by all Delmia Quest users to the similar issues with complex conveyor system modeling.

## References

1. Zajac, J., Słota, A., Krupa, K., Więk, T., Chwajół, G., Małopolski, W.: Some aspects of design and construction of an automated guided vehicle. *Appl. Mech. Mater.* **282**, 59–65 (2013)
2. Wójcik, K.: Observation as learning methods in simple visual system of vehicle control. *Appl. Mech. Mater.* **613**, 144–150 (2014)
3. Zajac, J., Chwajół, G., Więk, T., Krupa, K., Małopolski, W., Słota, A.: Automated guided vehicle system for work-in-process movement. *Solid State Phenom.* **196**, 181–188 (2013)
4. Małopolski, W.: Cost optimization in manufacturing system with unidirectional AGVs. *Appl. Mech. Mater.* **555**, 822–828 (2014)
5. Lodewijks, G.: Two decades dynamics of belt conveyor systems. *Bulk Solids Hand.* **22**, 124–132 (2002)
6. Bohacs, G., Kovacs, G., Rinkacs, A.: Production logistics simulation supported by process description languages. *Manage. Prod. Eng. Rev.* **7**(1), 13–20 (2016)
7. Donald, D.L.: A tutorial on ergonomic and process modeling using QUEST and IGRIP. In: *Winter Simulation Conference. Proceedings*, vol. 1, pp. 297–302 (1998)
8. Nilsson, P., Nordberg, G.: Discrete-event simulation of conveyor systems—providing decision support for Saab automobile AB. Master of Science Thesis in the Master Degree Programme, Production Engineering, Department of Product and Production Development, Division of Production Systems. Chalmers University of Technology, Gothenburg, Sweden (2012)
9. Wang, C., Qiu, C.: Virtual simulation of the job shop scheduling system based on Delmia/QUEST. In: *Asia Simulation Conference—7th International Conference on System Simulation and Scientific Computing*, pp. 1129–1132 (2008)
10. Gingu, E.I., Zapciu, M., Sindile, M.: Balancing of production line using discrete event simulation model. *Proc. Manufact. Syst.* **9**(4), 227–232 (2014)
11. Krajcova, K., Pechacek, F., Velisek, K.: Material flow design and simulation of part production in the free machines layout. In: *Proceedings of the 22nd International DAAAM Symposium*, **22**(1), 1303–1304 (2011)



12. Mohora, C., Anania, D., Calin, O.A.: Simulations strategies using DELMIA QUEST. In: Proceedings of the 20th International DAAAM Symposium, **20**(1), 335–336 (2009)
13. Klos, S., Trebuna, P.: Using computer simulation method to improve throughput of production systems by buffers and workers allocation. *Manag. Prod. Eng. Rev.* **6**(4), 60–69 (2015)
14. Gregor, M., Skorik, P.: Simulation and emulation of manufacturing systems behaviour. *Manage. Prod. Eng. Rev.* **1**(2), 11–21 (2010)
15. Longo, F., Mirabelli, G.: Effective design of an assembly line using modelling and simulation. *J. Simul.* **3**(1), 50–60 (2009)
16. Rekiek, B., Dolgui, A., Delchambre, A., Bratcu, A.: State of art of optimization methods for assembly line design. *Ann. Rev. Control* **26**(2), 163–174 (2002)

# Prediction of HPDC Casting Properties Made of AlSi9Cu3 Alloy

Jakub Hajkowski, Pawel Popielarski and Robert Sika

**Abstract** The paper describes the influence of type of structure and its parameters on mechanical properties of high-pressure die-casting (HPDC) products out of AlSi9Cu3 alloy. The dendritic structure was described using the DAS parameter—a distance between branches of dendrites of a solid  $\alpha$  solution (silicon in aluminium), which is a measure of microstructure refinement. According to the Hall–Petch law, the smaller grain causes the better strength. The finest grained structure can be obtained by increasing the rate of heat extraction from a casting to a mould. The best results, considering the classical methods, can be achieved using the high-pressure die-casting method. Therefore, results of studies of mechanical properties of sample castings, made using the above-mentioned casting method, are presented. The sample castings (cast-on samples) were subjected to tensile tests to determine mechanical properties (tensile strength, yield strength and elongation), as well as microstructure studies, considering the DAS. Experimental-simulation validation was performed using the Procast code with the application of a micro-model in the scope of compatibility of the DAS value and yield strength.

**Keywords** High-pressure die-casting · Aluminium alloys · Mechanical properties · Dendrite arm spacing · Micromodel

## 1 Introduction

Operational properties of cast products are dependent on the technology of their manufacturing [1, 2]. These properties are affected mainly by solidification rate of particular casting zones [2–4]. Extraction heat rate out of a casting may be controlled by the use of materials of diversified thermal parameters, such as thermal conductivity ( $\lambda$ ), specific heat ( $c$ ) and density ( $\rho$ ). A mould can be made out of a homogeneous material (mould sand with a quartz sand matrix, metal mould for

---

J. Hajkowski (✉) · P. Popielarski · R. Sika  
Poznan University of Technology, Poznań, Poland  
e-mail: jakub.hajkowski@put.poznan.pl

gravity or pressure casting) [2, 3]. In industrial conditions, hybrid, combined moulds are often used (mould sand with chills, permanent metal moulds with sand or salt cores), as well as pressure moulds with insets made out of a different material, usually of a higher capacity of heat transfer than the mould material. At the same time, it must be remembered that the selection of an appropriate technology of manufacturing a casting, as well as methods of its further processing, has very high impact on the state of its surface quality and its capability of maintaining proper operational properties [5].

In the case of high-pressure die-casting, formulation of the crystal structure, meaning its refining [6–8], is greatly affected by the multiplication pressure (exerted in the last, third phase of casting), interacting on an alloy during the solidification process and causing several times higher refinement of structural phases in relation to solidification carried out in atmospheric pressure conditions (as in a gravity metal mould). Additionally, solidification rate influences on morphology of the forming the intermetallic phases [9, 10]. In specific conditions these phases will never form.. This paper focuses on the validation of the selected mechanical and plastic properties, as well as degree of microstructure refinement, using the DAS (dendrite arm spacing) parameter.

Procedures of design with the use of virtualization of processes bring wider possibilities of both qualitative and quantitative prediction of locality of structure and mechanical properties. Nowadays, there is a trend towards expectations of the modern approach to design and operation of castings, mostly in link with applications for modelling and virtual prototyping of new products [11, 12] and production processes [13]. It is also related to a design rule, which is more and more often applied, concerning defect tolerance. It is a new direction in design and optimization of castings. This rule responds to applications of cast products, and directions of this development are enforced by increase of technical and operational requirements.

Professional systems, such as NovaFlow&Solid, Magmasoft or Procast, allow the prediction of local properties of castings, but it is done using simplified principles (soft modelling—an empirical approach, basing on temperature fields calculated on the basis of processes simulation) or through micromodelling (so-called deterministic modelling) [14].

This paper describes experimental and simulation studies of cast-on samples, manufactured in conditions of high-pressure die-casting. The studies were conducted using the most widespread alloy for automotive industry parts [15], manufactured using the above-mentioned method, with designation of AlSi9Cu3.

## 2 State of the Art

Quality of castings is influenced, apart from processing conditions, by the chemical composition of a used alloy. Even if it is compatible with tolerance limits assumed in the standards, mechanical properties of cast products (such as tensile strength, hardness) may differ even by several dozen per cent.

The most important elements influencing the properties of aluminium alloys are Si, Cu, Mg, Mn and Fe. All these elements have a specific influence on forming structure of a casting [2, 16]. The silicon improves castability, feeding of shrinkage discontinuities and resistance to hot tear defects. Copper increases tensile strength and hardness, improves machinability and thermal load resistance, and simultaneously, it reduces corrosive resistance and worsening of elongation. Iron increases tensile strength and yield strength but reduces plasticity. Magnesium enables heat treatment, which influences tensile strength and yield strength. Manganese neutralizes negative influence of iron (it minimizes worsening of plastic properties) [16].

Elements contained in the aluminium alloys influence the creation of intermetallic phases. Thus, except basic phases like solid solution of a silicon in aluminium and eutectic ( $\alpha + \text{Si}$ ), there are also intermetallic phases (because of other elements in an alloy apart from aluminium and silicon, such as Fe, Cu, Mg, Mn, they may have an influence on decreasing of mechanical properties). The intermetallic phases that occur most frequently are as follows: Al<sub>2</sub>Cu, Mg<sub>2</sub>Si, Al<sub>3</sub>FeSi, Al<sub>15</sub>(MnFe)<sub>3</sub>Si<sub>2</sub>, Al<sub>5</sub>Mg<sub>8</sub>Cu<sub>2</sub>Si<sub>6</sub>, Al<sub>8</sub>Si<sub>6</sub>Mg<sub>3</sub>Fe [9, 10, 17]. The intermetallic phases may form below and above the temperature of silicon eutectic solidification. It is worth emphasizing that the introduction of alloy admixtures influences synergy of properties. An example may be a multi-element alloy AlSiCu.

The AlSi9Cu3 (other designations: A226, AC-46000) is the most frequently used aluminium alloy in foundry by HPDC casting. It is estimated that approximately 70% of parts manufactured using this method are made out of this particular alloy [18]. The alloy, because of its small tendency to create shrinkage cavities and good machinability, is often used for the production of castings of a high degree of complexity, mostly in the automotive industry. The chemical composition AlSi9Cu3 alloy is presented in Table 1.

The AlSiCu alloys are used in automotive and aeronautical branches, mostly for loaded elements, such as cylinder heads, crank boxes of combustion engines, pistons of diesel and petrol engines, subassemblies of turbocharger, frames of gear-boxes or parts of aeronautical pumps [16, 19]. The best material properties (tensile strength, yield strength and elongation) are obtained using the cold-chamber pressure casting. There are two types of these machines: with a horizontal chamber (Fig. 1)—the most frequently used—and with a vertical chamber. Depending on the piston movement in a chamber and its location, there are three phases of filling the mould cavity, described below.

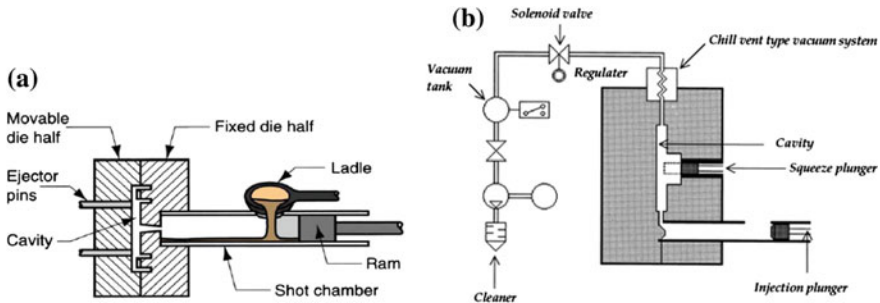
The first phase consists of filling channels of a gating system, up to height of inflow crevices. Stroke of the piston is realized with low velocity (0.3–0.5 m/s), and

**Table 1** Standard chemical composition of AlSi<sub>9</sub>Cu<sub>3</sub> all—EN 1676 standard

Element	Si	Fe	Cu	Mn	Mg	Cr	Ni	Zn	Pb	Sn	Ti
(%)											
Min	8	–	2	–	0.05	–	–	–	–	–	–
Max	11	1.3	4	0.55	0.55	0.15	0.55	1.2	0.35	0.25	0.25

**Table 2** Values of parameters assumed for the simulation tests

Parameter	Name	Value	Unit
$n_{\max}$	Maximum grain nuclei density (first nucleation parameter of the dendritic primary phase. Maximum density of nuclei of the Gaussian distribution)	9e6	1/cm <sup>3</sup>
$\Delta T_{\delta}$	Standard deviation undercooling (second nucleation parameter of the dendritic primary phase. Standard deviation of the Gaussian distribution)	3	K
$\Delta T_n$	Average undercooling (third nucleation parameter of the dendritic primary phase. Average undercooling of the Gaussian distribution)	10	K
$A_e$	Nucleation constants (first nucleation parameter of the eutectic phase. Nucleation factor)	9e6	K <sup>-n</sup> /cm <sup>3</sup>
$n$	Nucleation constants (second nucleation parameter of the eutectic phase. Nucleation exponent)	2	–
$\mu_e$	Eutectic growth coefficient (eutectic growth kinetics constant)	5e-6	cm/sK <sup>2</sup>

**Fig. 1** Scheme of high-pressure die-casting with a cold chamber: **a** without the vacuum system [19], **b** vacuum process and additional module for local squeeze casting [21]

it transports metal to a place near the inflow crevices [20]. Low velocity of the piston stroke results in out of time of metal solidification in machine shot chamber. Wrong values of the stroke movement in this phase lead to danger of waviness of a free surface of a liquid alloy. This may lead to air entrapment and introducing it to the mould cavity, together with an alloy. This may cause air occlusions in the final casting, if all the air will not be evacuated by the venting channel system.

The second phase is filling the mould cavity. Stroke of the piston is realized with a higher velocity (usually 1.5–4.0 m/s, max. 8 m/s) [20]. This phase is characterized by higher dynamics of the piston movement. Therefore the higher pressure is exerted on an alloy, thanks to this, time of mould cavity filling is shorter than solidification time of the thinnest walls of a casting.

The last, third phase is repressing of an alloy inside the mould cavity, known as the multiplication. Further rapid increase of piston on alloy occurs, and the growth of pressure on transition between phase II and phase III does not exceed 0.02–

0.03 s [20]. The phase is ended when the casting solidifies. The multiplication has a significant impact on quality of a casting, it influences the refinement of its structure, mechanical properties, and it reduces dimensions of gas bubbles and, above all, limits shrinkage porosity and increases the accuracy of casting shape representation.

The pressure casting process allows obtaining significant efficiency—30–60 injections per hour, high accuracy and dimensional quality of castings, as well as precise representation of their shapes, connected to high yield of metal (approximately 95% when casting metal in the cold chamber machines) and better physical properties of castings thanks to their fine-grained structure [20].

To limit the occurrence of porosities, which helps improving the quality of castings, certain supporting methods are used, not present in the classic method of pressure casting. The methods are as follows: pressure–vacuum system in the pressure mould cavity (the vacuum process), local interaction on a local alloy pressure in the liquid and solid–liquid state (local squeeze casting) [21].

High-pressure die-casting technology causes high cooling rate and leading to refinement of grains (low DAS parameters) and better mechanical properties of casting. The authors [15] obtained DAS parameter from 5 to 13  $\mu\text{m}$  to the contact with mould and in the centre, respectively (6 mm diameter sample) and ultimate strength approx. 270 MPa and yield strength approx. 150 MPa. In [7], the average value for ultimate strength is 250 MPa and yield strength is approx. 160 MPa.

Because of high cost of manufacturing of casting moulds for the high-pressure die-casting, the simulation systems are widely used for the optimization of the casting process, especially concerning filling of the mould cavity. Commercial simulation codes, apart from basic phenomena of flow and heat exchange (hard modelling), are also able to predict structural properties, e.g. DAS (dendrite arm spacing), portions of particular structure phases, mechanical properties (tensile strength, yield strength and elongation). Quality of calculations using the simulation systems, regarding the course of the casting process, is dependent on the accuracy of used material data. Only the data that appropriately characterize materials and phenomena, referring to a real process, guarantee obtaining right conclusions and predictions regarding the behaviour of the casting–mould system. In the commercial simulation codes (NovaFlow&Solid, Magmasoft, Procast), typical physical models describe particular stages of forming of a casting (filling the mould cavity, solidification and cooling of an alloy, heating the mould). The problem of material data concerns each of these stages.

Creators of these simulation systems ensure the completeness of the material databases. They cannot be always treated as sure and tested in industrial conditions. Quality of available databases must be estimated, considering a number of issues. Among others, they are as follows: source of data and conditions of its determination, accuracy, comparison with time and temperature characterizing the casting process, criteria and selection of the best dataset for a problem being solved, sensitivity of simulation results to errors of coefficients, which are impossible to identify and are caused by static and dynamic phenomena.

The authors undertook an attempt at such a reverse comparison. On the basis of obtained empirical (experimental) data and simulation results, comparison of basic mechanical properties and degree of structure refinement was made. The trial castings were made of the AlSi9Cu3 alloy.

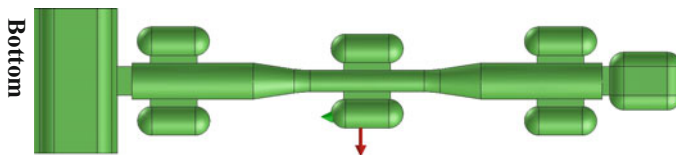
### 3 Methodology of Studies

The experimental studies were performed in a selected high-pressure die-casting foundry. It consisted the complex studies of metallurgical quality of an alloy, which was assigned for manufacturing of castings for parts for the automotive industry. Control and measurement apparatus were used, to determine parameters of metallurgical quality: density index—DI, chemical composition tests (spectrometer) [22]. These studies were performed for each ladle after refining process with a rotor, four ladles in total, to fill the whole preheating furnace, out of which an alloy was taken directly for the casting process.

The preheating furnace was filled with a liquid AlSi<sub>9</sub>Cu<sub>3</sub> alloy, of known metallurgical quality. The density index was below 2.6% (the acceptable upper limit is 3%). The applied average casting process parameters were as follows: pressure during filling—120 MPa, velocity of mould filling—3.3 m/s and pressure in third phase—300 bar. Studies of mechanical properties (tensile strength, yield strength and elongation) were conducted on high-pressure die-cast samples (cast-on) of shape compatible with the PN-83-H-83500 standard. The tests were carried out on raw samples, without machining, using a strength testing machine Instron. Randomly selected pressure-cast samples were subjected to tests. Finally, out of 425 samples, 54 pieces were randomly chosen, and representative values were then estimated by statistical methods.

The basic structure phases in the examined alloy are  $\alpha$  solid solution and the eutectics ( $\alpha + \text{Si}$ ). The refinement of precipitations of the solid solution  $\alpha$  was described using an intermediate parameter of average distance between last arms of well-developed parts of dendrites observed in the microstructure (DAS).

Results of the static tensile test using the above-mentioned samples were referred to results of simulation in the Procast system (the micromodel). The geometry of a sample is presented in Fig. 2.



**Fig. 2** CAD geometry of test sample—with part of the gating system. Vertical pouring position

## 4 Results and Discussion

The simulation eventually allowed to obtain the  $R_e$  parameter value to compare it with results of a real sample. In the scope of the studies, 54 samples were randomly chosen; for each of them, the mechanical properties—tensile strength, yield strength and elongation—were determined. To select a representative value of the yield strength parameter, it was proposed to estimate the outliers in the first place, using the Grubbs test, according to the formula (1).

$$G = \frac{\max|Y_i - \bar{Y}|}{s}, \quad (1)$$

where

- $G$  value of statistics of the Grubbs test,
- $Y_i$  subsequent value from the set,
- $\bar{Y}$  average value from the set,
- $s$  standard deviation.

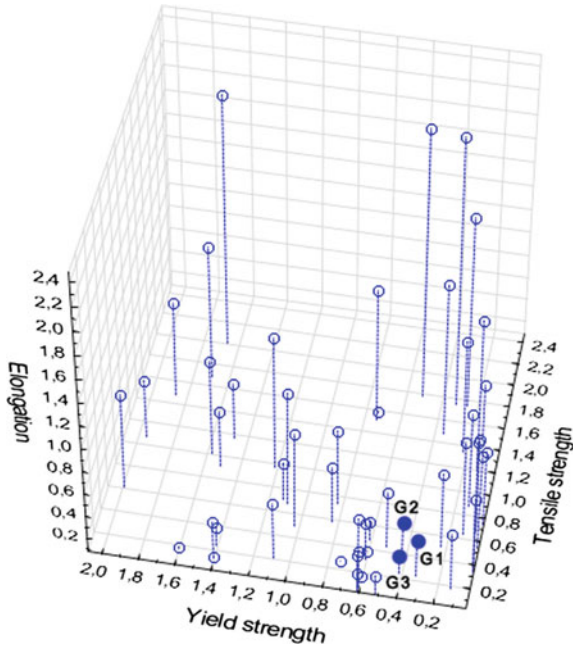
This way it is possible to identify distant values in a randomly selected set of samples. It turned out that for the assumed sample size ( $N = 54$ ) and significance level  $\alpha = 5\%$ , the critical value of the test (Critical Z) is 3.21 and no value of the yield strength parameter is distant enough to discard it from the set.

According to the above-mentioned facts, a statistical method was proposed for the estimation of the most representative yield strength value, which will take too higher deviations from the mean value into account. It was decided that the yield strength representative value should be contained within the representative sample described simultaneously by three mentioned parameters—apart from the tensile strength, yield strength and elongation, as well. Such three values of a sample allow better representation of repeatability of results of single specimen mechanical tests than the yield strength parameter value itself. For each group of parameters out of all the randomly selected samples, statistical value of the Grubbs test was calculated. Then, samples for which all the three parameters describing mechanical properties had Grubbs test value lower than 0.5 were selected (statistics on this level determines values of a parameter being relatively close to the most frequently occurring values). See Fig. 3.

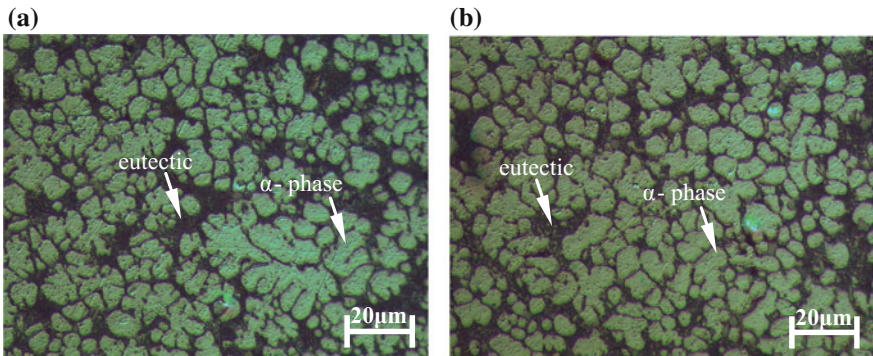
Figure 4 shows the representative real microstructure for the validation of the DAS parameter (dendrite arm spacing). Obtained values of DAS parameter varied on the cross section. The measured values near the edge of a sample were approx. 9  $\mu\text{m}$ , and they increased in function of distance to sample axis, up to value of 11  $\mu\text{m}$ . It is caused by various heat extraction rates (heat flux) on the casting–mould interface.

As a result of simulation, a virtual map of yield strength property was obtained (Fig. 5). The virtual YS prediction does not include occurrence of porosity which can appear in experimental castings.



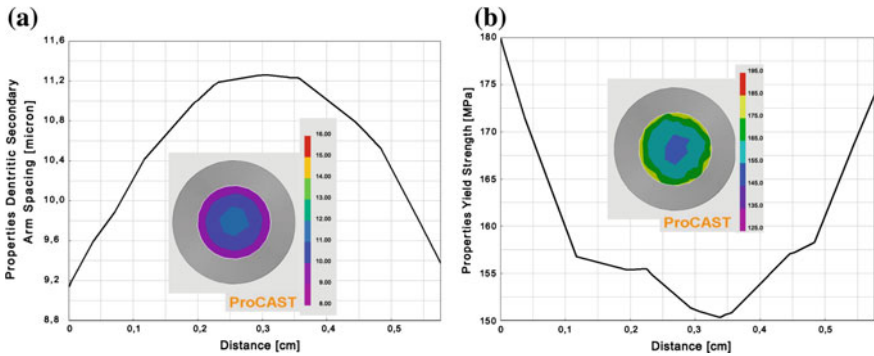


**Fig. 3** Results of the Grubbs test for parameters describing mechanical properties of samples—for three samples, compatibility on the Grubbs test level below 0.5 was obtained



**Fig. 4** Microstructure of a representative sample for testing of mechanical properties: **a** edge of a sample, **b** centre of a sample

The experimental-simulation validation, considering the DAS size and average value of the yield strength, was conducted. Values obtained experimentally were confirmed by simulation in the Procast code and they were approximately 9.2  $\mu\text{m}$  near the edge of a sample and they increased in function of distance to sample axis,



**Fig. 5** Results of simulation tests obtained using the Procast code: **a** DAS—dendrite arm spacing. **b** Yield strength. For parameters shown in Table 2

up to value of 11.2  $\mu\text{m}$ , while the yield strength decreased from 180 to 150 MPa (Fig. 5).

High refinement of grains of the  $\alpha$  phase (low DAS values, approx. 9  $\mu\text{m}$  in the near-surface layer, from the side in contact with the mould, and 11  $\mu\text{m}$  in the central part) in the pressure-cast products (the test sample), as well as low porosity, ensures better structure compactness in comparison with gravity castings. It let to obtain better strength with good plastic properties.

## 5 Summary

The carried out experimental-simulation tests allow to draw the following conclusions:

- Obtained experimental results for DAS and mechanical parameters are comparable with literature ones,
- The database applied in the Procast code concerning the micromodel (nucleation and growth crystal parameters) for AlSi<sub>9</sub>Cu<sub>3</sub> alloy applies to gravity die-casting. For high-pressure die-casting process (tests made under actual industrial conditions), these values were increased by four orders of magnitude due to better contact at the casting–mould interface (smaller air gap) and consequently a greater heat flux thus achieving the DAS parameter on level of values derived from the experiment, while maintaining the experimental values of the yield strength,
- Statistical analysis of the experimental results (tensile strength, yield strength and elongation) using the modified Grubbs method was required to determine the most representative value of the yield strength parameter from the sample,

- There is the limitation of direct usage of basic database (standard values parameters) of particular simulation codes in the case of HPDC case. Each simulation code should be validated concerning dynamic of casting process,
- The described research has enabled the Procast code database to be adapted to include values for high-pressure die-casting.

**Acknowledgements** The research work reported here was made possible by 02/25/DSPB/4412 projects.

## References

1. Kujawińska, A., Rogalewicz, M., Piłacińska, M., Kochański, A., Hamrol, A., Diering, M.: Application of dominance-based rough set approach (DRSA) for quality prediction in a casting process. *Metalurgija* **55**(4), 821–824 (2016)
2. Campbell, J.: *Complete Casting Handbook*, 2nd ed. Butterworth-Heinemann (2015)
3. Kurz, W., Fisher, D.J.: *Fundamentals of Solidification*. Trans Tech Publications (1992)
4. Dantzig, J.A., Rappaz, M.: *Solidification*. EPFL Press Lausanne, Switzerland (2009)
5. Legutko, S., Žak, K., Kudlacek, J.: Characteristics of geometric structure of the surface after grinding. In: *The 4th International Conference on Computing and Solutions in Manufacturing Engineering 2016—CoSME'16*, p. 94 (2017)
6. Hurtalova, L., Tillov, E., Chalupov, M.: Optical and electron microscopy study of the mechanical properties improvement on recycled AlSi9Cu3 cast alloy along the hardening. *Int. Virtual J. Sci. Techn. Innov. Ind. MTM* **7**, 48–51 (2011)
7. Leal dos Santos, S., Antunes, R.A., Santos, S.F.: Influence of injection temperature and pressure on the microstructure, mechanical and corrosion properties of a AlSiCu alloy processed by HPDC. *Mater. Des.* **88**, 1071–1081 (2015)
8. Niu, X.P., et al.: Vacuum assisted high pressure die casting of aluminium alloys. *J. Mater. Process. Technol.* **105**, 119–127 (2000)
9. Dash, M., Makhlof, M.: Effect of key alloying elements on the feeding characteristics of aluminum-silicon casting alloys. *J. Light Met.*, pp. 251–265 (2001)
10. Martinez, E.J.D., Cisneros, M.A.G., Valtierra, S., Lacaze, J.: Effect of strontium and cooling rate upon eutectic temperatures of A319 aluminum alloy. *Scr. Mater.* **52**, 439–443 (2005)
11. Trojanowska, J., Varela, M.L.R., Machado, J.: The tool supporting decision making process in area of job-shop scheduling, recent advances in information systems and technologies. In: Rocha, Á., Correia, A., Adeli, H., Reis, L., Costanzo S.: (eds.) *WorldCIST, Advances in Intelligent Systems and Computing*, vol. 571. Springer, pp. 490–498 (2017)
12. Pandilov, Z., Milecki, A., Nowak, A., Górski, F., Grajewski, D., Ciglar, D., Klaić, M., Mulc, T.: Virtual modelling and simulation of a CNC machine feed drive system. *Trans. FAMENA* **39**(4) (2016)
13. Gorski, F., Zawadzki, P., Hamrol, A.: Knowledge based engineering as a condition of effective mass production of configurable products by design automation. *J. Mach. Eng.* **16** (4), 5–30 (2016)
14. Szczerbicki, E. (ed.): *Cybernetics and Systems, Special issue on Soft Computing and Intelligent Systems for Industry*, p. 33 (2002)
15. Sanna, F., Fabrizi, A., Ferraro, S., Timelli, G., Ferro, P., Bonollo, F.: Multiscale characterisation of AlSi<sub>9</sub>Cu<sub>3</sub>(Fe) die casting alloys after Cu, Mg, Zn and Sr addition. *La Metall. Ital.*, 4 (2013)
16. Pietrowski, S.: *Silumins*. Publ. House of Lodz University of Technology, Lodz (2001)

17. Anza, I., Sáenz de Tejada, F.: Development of New Al-Si<sub>9</sub>Cu<sub>3</sub> alloys for HPDC components with tailored properties. In: World Foundry Congress in Bilbao (2014)
18. Dobrzanski, L.A., Engineering Materials and Materials Project, WNT (2006)
19. Talat Lectures. <http://core.materials.ac.uk/>
20. Waszkiewicz, S., Fic, M., Perzyk, M., Szczepanik, J.: Dies and High-Pressure Die-Casting Moulds (in Polish), WNT (1983)
21. Kima, E.S., Leeb, K.H., Moon, Y.H.: A feasibility study of the partial squeeze and vacuum die casting process. *J. Mater. Process. Technol.* **105**, 42–48 (2000)
22. Ignaszak, Z., Hajkowski, J.: Contribution to the identification of porosity type in AlSiCu high-pressure-die-castings by experimental and virtual way. *Arch. Foundry. Eng.* **15**, 143–151 (2015)

# Internal Stresses Analysis in the Shrink-Fitted Joints of the Assembled Crankshafts

Zbigniew Siemiatkowski, Mirosław Rucki and Jan Kudlacek

**Abstract** The paper describes investigation results aimed to the assessment of the shrink-fitting of the marine diesel crankshaft elements. Since the crankshafts are of the large size (above 20 m) and weight (above 300 tons), the models were made in scale 1:5, keeping the same technical conditions. The measurement of internal stresses was made by a non-destructive ultrasonic method. The obtained results confirmed the existence of the zones where stresses had crossed the yield points, which meant the plastic deformation and weakening of the interference fit.

**Keywords** Shrink-fitting · Tightness · Internal stress · Ultrasonic measurement

## 1 Introduction

One of the technologies used for the crankshaft fabrication is to assemble it out of the separated elements (cranks and journals) joint usually by the shrink-fitting [1]. The reliability of the joint depends on its tightness (interference) and on the internal stresses generated during the cooling process. The residual stresses and their distribution in mechanical components may cause them to fail at a load level significantly lower than expected [2], which is true for the shrink-fitted couplings. Moreover, in the assembled crankshafts, the hub must be axially positioned on the shaft and resist the moments and forces generated by misalignments [3].

In case of the large-size assembled crankshafts manufactured for the marine engines, it is difficult to perform a series of investigations, because the weight of such a crankshaft is up to 313 tons, its length is up to 22.5 m, and the maximal

---

Z. Siemiatkowski · M. Rucki (✉)

Faculty of Mechanical Engineering, Kazimierz Pułaski University of Technology  
and Humanities in Radom, 54 Krasickiego Str., 26-600 Radom, Poland  
e-mail: m.rucki@uthrad.pl

J. Kudlacek

Faculty of Mechanical Engineering, Czech Technical University in Prague,  
Technická 4, 166 07 Praha 6, Czech Republic

© Springer International Publishing AG 2018

A. Hamrol et al. (eds.), *Advances in Manufacturing*, Lecture Notes in Mechanical  
Engineering, [https://doi.org/10.1007/978-3-319-68619-6\\_60](https://doi.org/10.1007/978-3-319-68619-6_60)

633

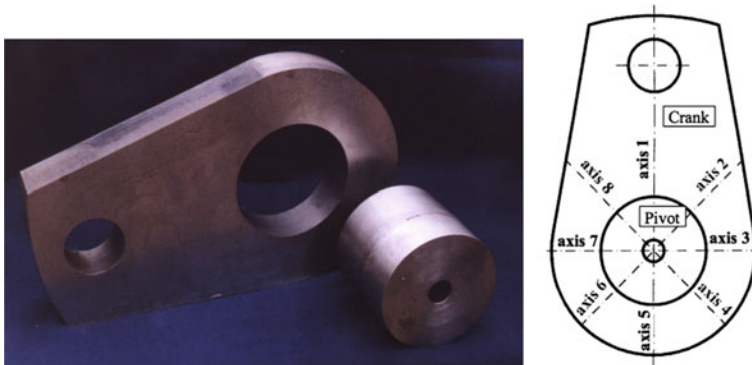
radius reaches ca. 1500 mm [4]. Fabrication of a crankshaft or a joint of huge dimensions for just experimental purposes is too expensive, so it was decided to prepare a number of the models of joints. Thus, the models were made in scale 1:5, keeping the technical conditions close to the ones kept in the CELSA Huta Ostrowiec factory's production lines for the marine diesel engine assembled crankshafts.

The present study focused on the non-destructive stresses measurement in the joints. It does not address to the heat transfer and the evolution of the contact pressure. In fact, the publications on this topic of the assembled marine crankshafts are relatively few, and they focus more on the fatigue issues than on the tightness of the joints [5]. The comprehensive study on the contact behavior during the shrink-fitting process was performed by Sun et al. [6], which did not, however, present any measurement of the stresses. On the other hand, Otsuki with co-authors used a destructive method for the stress measurement [7].

## 2 Experimental Conditions

The internal stresses in the shrink-fitted elements were measured using the ultrasonic measurement device Debro (laboratory of the Institute of Fundamental Technological Research, Polish Academy of Sciences). The models of the crank and pivot before assembling are shown in the Fig. 1 (left), while the Fig. 1 (right) presents the positioning of the measurement axes in the assembled joint. In fact, they were radial semi-axes marked by numbers from 1 to 8, because non-symmetrical distribution was expected.

The probing points were assigned along each axis with the step of 10 mm. Close to the contact border between crank and pivot, the additional measuring point was added. Thus, the first measurement was made on each axis at the distance



**Fig. 1** Crank and pivot models before assembling (left) and the axes of stress measurement (right)

$r_c = 5$  mm away from the border between the coupled details. For each crank–pivot couple, the measurement was made before they were joined together and afterward.

The measured value was in fact the ultrasonic wave passing time, polarized along the marked axis and perpendicular to it. Here,  $t_{R0}$  and  $t_{R1}$  mean the passing time in nanoseconds in the direction coaxial to the radius  $R$ , before and after assembling, respectively. Similarly,  $t_{\text{tang}0}$  and  $t_{\text{tang}1}$  mean the passing time in nanoseconds in the circumferential direction (perpendicular to the radius). The acoustic anisotropy  $t_{R\text{-tang}}$  was calculated as follows:

$$t_{R\text{-tang}} = \frac{t_R - t_{\text{tang}}}{0.5(t_R + t_{\text{tang}})}, \quad (1)$$

for the crank and pivot before assembling (indexed with 0) and after it (indexed with 1), respectively. Table 1 contains the example of the obtained time values and respective stresses  $\sigma_r$  (radial) and  $\sigma_\theta$  (circumferential) in the material along the axis 1.  $\Delta\sigma$  was the differences between  $\sigma_\theta$  and  $\sigma_r$ , and so-called reduced stress  $\sigma_{\text{red}}$  was calculated as their sum square:

$$\sigma_{\text{red}} = \sqrt{\sigma_r^2 + \sigma_\theta^2}. \quad (2)$$

Since the axis 1 was the longest axis of the crank (see Fig. 1), there were 19 measuring points, but only 4 are presented in the Table 1 as an example. The measurement results should be treated as the stresses averaged along the material thickness. In case they were performed close to the border between the details, they meant average along the joint.

### 3 Results and Discussion

Figure 2 presents the graphs of stresses differences  $\Delta\sigma$  measurement results along all 8 axes for the crank–pivot coupling example given in the Table 1. The points of different shapes represent the measuring results, while the curves represent the polynomials based on the measured values. The relative tightness of the shrink-fitting was  $W_w = 2.35\%$ . The reduced stresses  $\sigma_{\text{red}}$  for the same joint are presented in the Fig. 3.

It should be noted that at the distance of 5 mm from the crank edge, four axes reveal the stresses above the yield point, and along the axis 7, the yield point is crossed throughout the distance of 25 mm. The results thus confirm that in case of high tightness of the shrink-fitting, some plastic deformation takes place and weakens the joint loadability.

In order to check the obtained results, the residual stresses near the surface were measured using the hole-drilling strain-gage method [8]. The graphs of the tangential and radial stresses are shown in the Fig. 4. It is seen from the graph that the

**Table 1** Ultrasonic measurement of the internal stresses

$r_c$ (mm)	$t_{R0}$ (ns)	$t_{R1}$ (ns)	$t_{\text{ang}0}$ (ns)	$t_{\text{ang}1}$ (ns)	Acoustic $t_{R-\text{tang}0}$ (ns)	Anisotropy $t_{R-\text{tang}1}$ (ns)	$\Delta\sigma$ (MPa)	$\sigma_r$ (MPa)	$\sigma_0$ (MPa)	$\sigma_{\text{red}}$ (MPa)
5	45,393	45,343	45,443	45,458	-0.0011	-0.0025	-181.3	151.6	332.9	365.8
10	45,380	45,370	45,416	45,476	-0.0008	-0.0023	-195.0	110.9	305.9	325.4
15	45,463	45,363	45,443	45,458	0.0004	-0.0021	-320.5	-50.1	270.4	275.0
20	45,474	45,341	45,453	45,432	0.0005	-0.0020	-312.3	-53.3	259.0	264.4



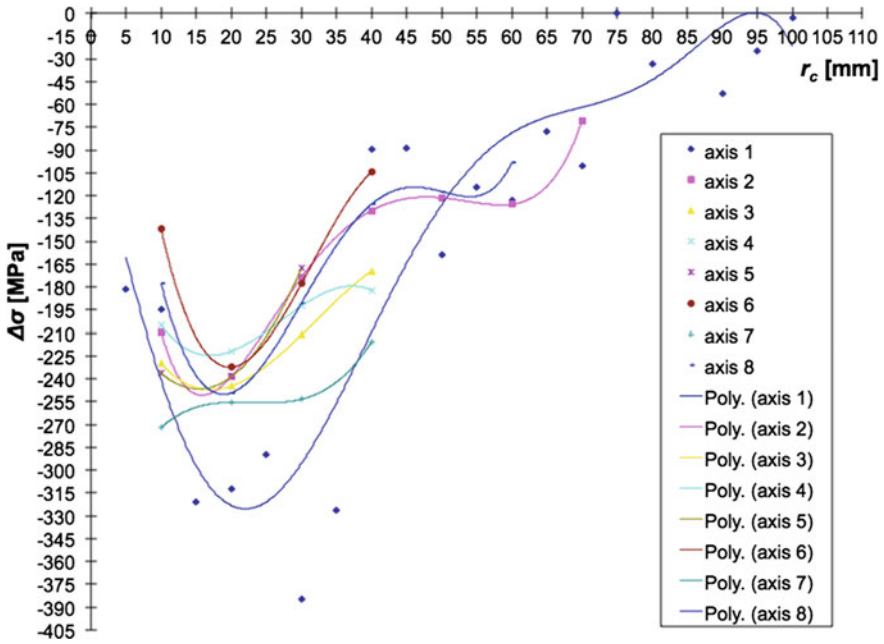


Fig. 2 Measured stresses differences  $\Delta\sigma$  and their approximations with polynomials

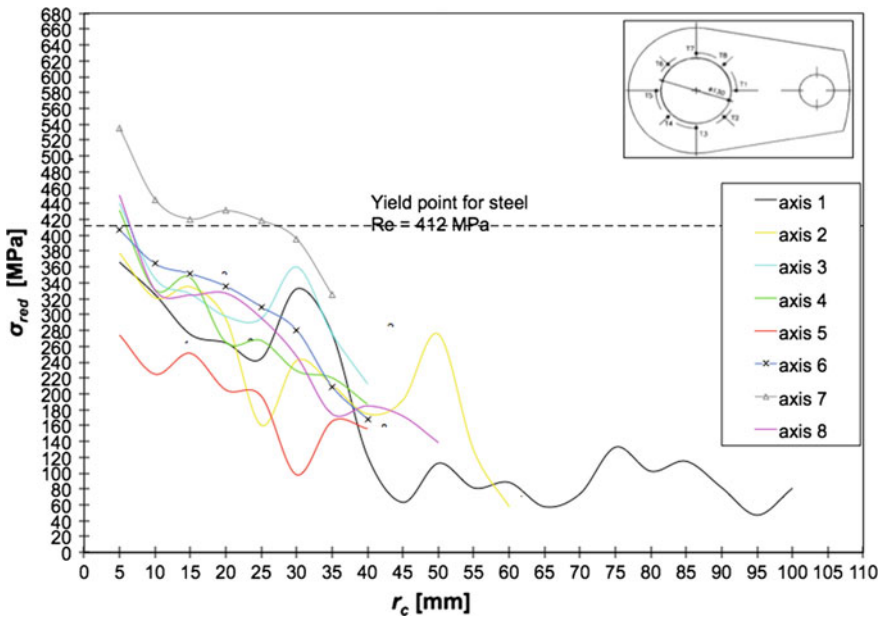


Fig. 3 Reduced stresses  $\sigma_{red}$  for the shrink-fitted joint of relative tightness  $W_w = 2.35\%$

differences between points 3 and 4 in case of both stresses  $\sigma_A$  and  $\sigma_T$  are ca. 40%. Such irregularity may be responsible for the possible failure, especially under the overload conditions.

Symmetrical differences between the internal stresses in axes 1–5 and 7–3 are reflected in the pivot stress distribution, too. Figure 5 presents the example of the pivot stress distribution, where maximal modules of stresses (i.e., both negative and positive extremes) are concentrated around the pivot orifice. The analysis was made using the finite element approach [9].

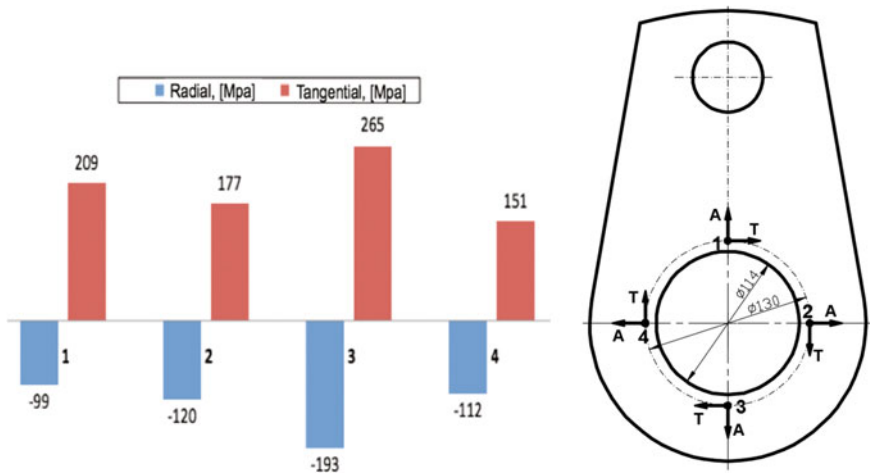
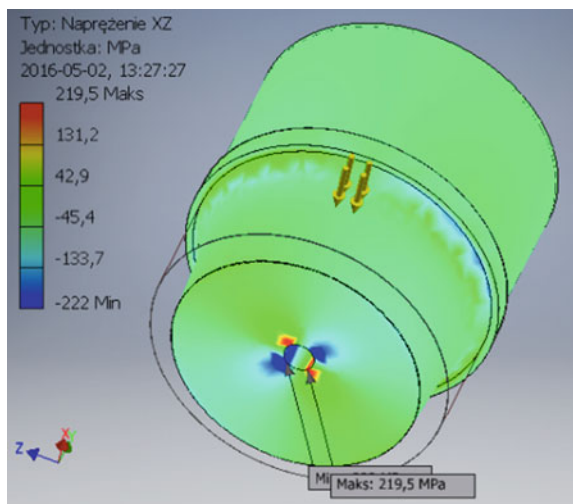


Fig. 4 Residual stresses in the shrink-fitted joint of relative tightness  $W_w = 2.37\%$

Fig. 5 Stresses distribution in the pivot



The models of the joints enabled to assess the real internal stresses that take place after the shrink-fitting of the crank and pivot. However, for the entire assembled crankshaft, the stress calculation is relatively complicated task because of many multi-coaxial components [10]. The future researches should challenge this issue.

## 4 Conclusions

The investigations were made on the models of the crankshafts produced in the conditions similar to the ones for the large-sized diesel marine engine crankshafts. The internal stresses were measured with a non-destructive ultrasonic method. The results of stress measurement lead to the conclusion that they should be analyzed in 3-D terms, and it is insufficient to model the complicated stress network with the 2-D ones, especially it is unacceptable to simplify it in terms of linear squeeze or stretch.

The stress distribution is non-uniform, and for the large relative tightness, plastic deformations may take place. In fact, for the relative tightness  $W_w > 2.2\%$ , the yield point is usually crossed. The radial stresses are negative in values, and their modules are smaller than those of the circumferential stresses. Thus, in industrial practice, it is not recommended to project the shrink-fittings of the tightness above 2.2%, because the plastic deformation caused by high stresses may weaken the joint.

In the future researches, the issue of the stresses in the entire assembled crankshaft should be addressed, emphasizing their impact on the coaxiality of its elements.

**Acknowledgements** The research work was not supported by any specific funds. Authors express their gratitude to the company CELSA Huta Ostrowiec for the cooperation.

## References

1. Yamagata, H.: The Science and Technology of Materials in Automotive Engines. Woodhead Publishing Ltd., Cambridge (2005)
2. Baldi, A.: Using optical interferometry to restart the ring-core method. *Exp. Mech.* **56**, 1191–1202 (2016)
3. Mancuso, J.R.: *Couplings and Joints: Design, Selection & Application*, 179, Marcel Dekker, Inc., New York, Basel (1999)
4. *Products and Services Information* KOBEL Steel Ltd., Kobe (1994)
5. Fonte, M., Duarte, P., Anes, V., Freitas, M., Reis, L.: On the assessment of fatigue life of marine diesel engine crankshafts. *Eng. Fail. Anal.* **56**, 51–57 (2015)
6. Sun, M.Y., Lu, S.P., Li, D.Z., Li, Y.Y., Lang, X.G., Wang, S.Q.: Three-dimensional finite element method simulation and optimization of shrink fitting process for a large marine crankshaft. *Mater. Des.* **31**, 4155–4164 (2010)

7. Otsuki, E., Kajihara, Sh., Hanawa, Y., Hamada, T., Kubo, H.: Stress assessment of crankshaft of low speed diesel engines considering residual stress in manufacturing process. *J. Jpn. Inst. Mar. Eng.* **42**(2), 136–141 (2007)
8. ASTM E837-13a. Standard Test Method for Determining Residual Stresses by the Hole-Drilling Strain-Gage Method. <https://www.astm.org/Standards/E837.htm>
9. Mathapati, N.C., Dhamejani, C.L.: FEA of a crankshaft in crank-pin web fillet region for improving fatigue life. *Int. J. Innov. Eng. Res. Technol.* **2**(6) (2015). Paper ID: IJIERT-P15-223
10. Qiu, J., Zhou, M.: Analytical solution for interference fit for multi-layer thick-walled cylinders and the application in crankshaft bearing design. *Appl. Sci.* **6**, 167–187 (2016)

# The Influence of Composition Chemical of Nanofluids on Hardness and Wear Resistance of Laser-Treated C20 Steel

Wojciech Gestwa

**Abstract** The utilization of nanofluids in the hardening processes of steel elements contributed to the improvement of the exchange of warmth among the quenching mediums and cooling element. There is still, however, the agglomeration phenomenon which leads to the deprivation of the significant influence nanoparts on the created structure in hardened elements what influences on the mechanical proprieties of these factors in the event of this type of quenching mediums. It can get the assurance of the constant nanosize on the way of the influence of ultrasounds or changes in the chemical composition of quenching mediums dissolving nanoparticles. Within the framework of this research, it was undertaken the test of the modification of composition chemical nanofluids uses 1% the water solution nanoparts  $Al_2O_3$ . At the base of the analysis of cooling curve, the obtained quenching mediums showed the intensification of the warmth receipt in relation to the quenching mediums no modified. The maintenance of the nanosized particles contributed to the improvement of the wear abrasive resistance of elements with the produced surface layer as the result of laser alloying with utilization of the carburizing paste. In these quenching mediums, the obtained hardness on the section of hardened elements showed higher value and softly fall from the surface to the core in the relation to the others heat-treatable samples. The profitable changes of propriety are the effect of the arrangement changes of phase in forming structure of elements from constructional steels after hardening.

**Keywords** Hardening · Nanofluids · Laser alloying · Carburizing · Wear abrasive resistance

---

W. Gestwa (✉)

Institute of Materials Engineering, Poznań University of Technology,

Poznań, Poland

e-mail: wojciech.gestwa@put.poznan.pl

© Springer International Publishing AG 2018

A. Hamrol et al. (eds.), *Advances in Manufacturing*, Lecture Notes in Mechanical Engineering, [https://doi.org/10.1007/978-3-319-68619-6\\_61](https://doi.org/10.1007/978-3-319-68619-6_61)

641

## 1 Introduction

This study presents the research with the use of nanofluids to change some properties of layer's surface, which created in laser carburizing (alloying). The fluidized bed for many years make up the significant center in the cooling process, which produces in the controlled way the definite structure connected with suitable mechanical proprieties in the element quenching. The appearance of the solid body particles of nanosize resulted in the possibility of their use in fluidized bed, and it changes the cooling proprieties of the traditional hardening mediums. This study [1–11] presents the possibilities of the proprietary changes of the physico-chemical mediums that modified nanoparticles. The authors of these works used nanoparticles in the spheroidal shape of the particle size below 50 nm and especially nanoparticles  $\text{Al}_2\text{O}_3$ . By investigating, the authors obtained the change in the method of the heat exchange among the centers from the nanofluidized group and quenching elements in the range of the occurrence temperature of the particular cooling phase. The authors further suggest two methods of the maintenance of applied nanosized particles. First method is the utilization of ultrasounds to break agglomerates, which were formed from nanoparticles after their introduction to the solution. The second method is the use of suitable solvent, which blocks the agglomerates of nanoparticles. In the quenching mediums, the stoppage of suitable nanosized particles has the meaning for the heat transfer coefficient and zeta potential. This effect can be observed in the works [2, 3, 7], which show the growth value of these parameters with the growth of the nanosized particles of the  $\text{Al}_2\text{O}_3$  and  $\text{SiO}_2$  type. The offence of certain values of nanoparticles stabilized the zeta potential. Authors for this effect burden not to the end conducted with breaking ultrasounds joint nanoparticles. They believe that in addition nanoparticles should not cross the 0.5% value of the volumetric part to obtain the most profitable effects of quenching. The modification of the chemical composition of thinner can contribute to tendencies decrease of nanoparticles to the agglomeration according to them, what improve the proprieties in the final effect cooling nanofluid. The new possibilities got when hardening with the use of nanofluids can be more enlarged by the development the surface cooled. The work [12] shows change in the possibility of tensions and surface topography in surface layer of materials sandblasted from their chemical composition independently. The laser modifications can use in connection with the processes of the quenching in nanofluids in the formation of the propriety of the surface layer except to exchanged the process above. The changes in the examples of the surface layer propriety in the result of laser modification can be found in [13–15] work. The information from the literature about possibilities nanofluidów and laser processing on the propriety change of elements, they made up the point of the exit to preliminary investigations in this subject matter. The obtained results were presented in the present study.

## 2 Methods of Research

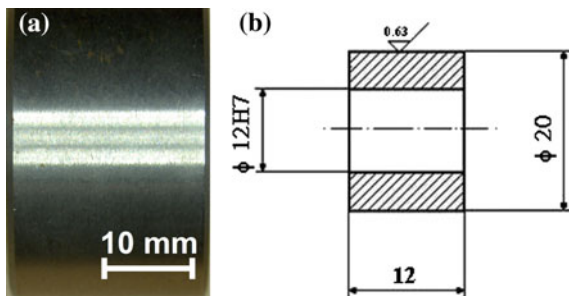
Three quenching mediums were applied in investigations; their chemical composition and work parameters are presented in Table 1.

The assessment of cooling intensity was realized in accordance with the standard of ASTM D6200-97: The Standard Test Method for Determination of Cooling Characteristics of Quench Oils Cooling Curve Analysis (Tensy Method). In this method, the probe used is cooled in the Tensy method. The sampler has the diameter of 12.5 mm and length 60 mm in applied probe as well as it is made from INCONEL 600 alloy, which in geometrical center is located in the type K thermocouple. This sampler was warmed in the resistance furnace vertical, which ensures the temperature of  $850\text{ }^{\circ}\text{C} \pm 2.5\text{ }^{\circ}\text{C}$  on the length 120 mm in the furnace retort. The data obtained in the temperature–time arrangement are subjected to mathematical analysis using the Fourier series [16]. The specimen of C20 steel was applied in the investigations of structure and the propriety of hardened elements. This steel is designed on elements subjected toughen or hardening thermal. This steel executes from the small machine parts, collars and elements cooperating with sheet metals to work in temperature not exceeding  $450\text{ }^{\circ}\text{C}$ . However, this steel quickly loses its proprieties after crossing  $200\text{ }^{\circ}\text{C}$ . The chemical composition on the basis of spectral analysis (0.2% C; 0.4% Mn; 0.24% Si) is according to norm PN-EN 10083-1:2008. The surface photo and the dimensions of samples created

**Table 1** Kind of nanofluid used

The kind of medium	The chemical composition of medium	The work temperature of medium ( $^{\circ}\text{C}$ )	The sonic time (h)
I	The distilled water	20	0.0 (no sonic)
II	The distilled water + 1% water solution of $\text{Al}_2\text{O}_3$ nanoparticles	20	0.5
III	The distilled water + 1% water solution of $\text{Al}_2\text{O}_3$ nanoparticles + 10% ammonia water	20	0.0 (no sonic)

**Fig. 1** Surface photos (a) and picture (b) of sample used in research



with C20 steel are presented in Fig. 1. The rough surface of samples before the realization of laser modification processes was increased. For that purpose, the samples were subjected to the jet abrasive processing with utilization of the abrasive material on the base of usual aloxite brown about the F16 granularity in the FEPA standard. The machine was applied to sandblasting, which uses the ejector method of feed abrasive materials. This test characterizes constant parameters: the working pressure of gas  $p = 0.7$  MPa; the incidence angle of abrasive materials on the sample surfaces amount to  $\theta = 90^\circ$ ; the working time of the abrasive material on the sample,  $t = 300$  s; the internal diameter of the nozzle in the server of abrasive materials,  $\varnothing_{in} = 7$  mm ( $7 \times 10^{-3}$  m); the distance between the nozzle and the surface worked,  $l = 100$  mm (0.1 m). The working gas (air), abrasive materials and sample have an ambient temperature, carrying out  $20^\circ\text{C}$  during the processes. The covering of external surface was total (100%) on the whole circuit of sample.

The diffusive paste was material used to change the chemical composition of the layer in the consequence of the laser modification. The carburizing paste was used in the present work, which consisted of graphite and polyvinyl alcohol with smooth consistency. The paste was coated on the oval samples by hand. The sample with modifying paste was dried in the surrounding temperature.

The measurements of the thickness of the put on paste were executed the Posi Tector 6000 Advance meter, which equipped in the simple probe of F type. The measurement results showed the paste thickness in the range from 160 to 176  $\mu\text{m}$ . The presented results of paste thickness are average arithmetical from ten measurements, which obtained on single sample with the put on paste. In this way, prepared samples were subjected to stopping process with the aid of  $\text{CO}_2$  molecular laser. The process parameters of laser alloying were as follows: the use of laser power (45%):  $1.17 \div 1.18$  (kW); the scanning speed of head over sample: 2.88 (m/min); the rotary speed of sample: 45.85 (rot/min); the feed of laser head: 0.28 (mm/rot); the diameter of laser beam: 2 (mm); the path kind: helical; the degree of path overlap (overlapping): 86%. The samples after the stopping processing were subjected additionally hardening from austenitizing temperature amount to  $860^\circ\text{C}$ . The austenitizing time carried out was 0.5 h. In hardening process, it uses the quenching mediums about the definite work parameters which were described earlier. Samples during the process were safe before the oxygenation and decarburization by the use of the protective atmosphere which was produced from nitrogen. The hardened samples were tempered in the temperature of  $150^\circ\text{C}$  by 1 h. The realization of all assumption processes on samples generated three variants, which are given in Table 2. The macroscopic assessment of the sample surface was conducted: the unarmed eye in scratch, roughness, burn, changes of tinges, and cracks of the activity. In the aim of the filing of macroscopic investigations, the registrations of the samples surface were conducted the digital apparatus before and after the stopping laser process. The hardness investigations of hardened elements were conducted by the utilization of the Vickers method to weight 0.981 N (0.1 kg), in accordance with norm PN-EN ISO 6507-1:2007 on the hardness testing machine of the Zwick firm. The hardness measurement was executed in parallel to the action of laser bundle that is on the transverse section of sample.



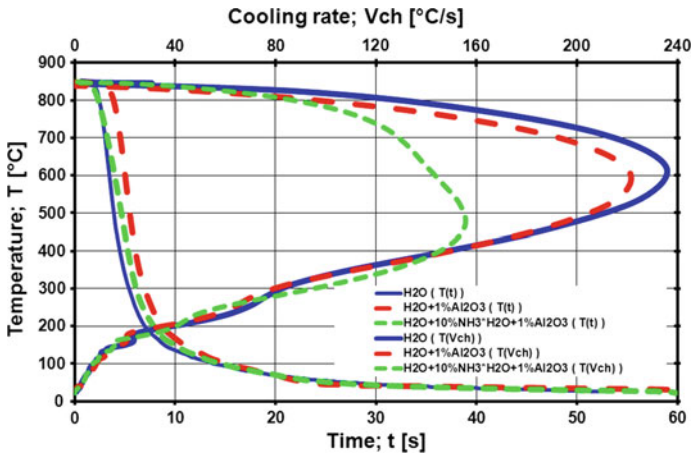
**Table 2** Process kind realized on samples

The variant of process	The method of surface modification	The kind of past	The modification layer	Hardening $T$ (°C)/ $t$ (h) (quenchant)	Tempering $T$ (°C)/ $t$ (h)
I	The sand-blast cleaning	The carburizing paste	The laser	860/0.5 (medium I)	150/1
II	The sand-blast cleaning	The carburizing paste	The laser	860/0.5 (medium II)	150/1
III	The sand-blast cleaning	The carburizing paste	The laser	860/0.5 (medium III)	150/1

The investigations of abrasion resistance were conducted for assistance of the frictional machine, type AMSLER in accordance with norm PN-H-04332:1982 on the basis of the mass (weight) wear in the arrangement: the sample in the form of the turning disc from thermal dressed steel (diameter 20 mm, thickness 12 mm) and counter-sample in the form of plate from carbide parched (S20S). The investigations were realized to the constant weight  $F = 147$  N and the sample speed  $v = 0.26$  m/s ( $n = 250$  r.p.m.). The friction tests were carried out in the condition of friction on dry. During investigations, the temperature of rubbing elements on their point of contact did not cross 100 °C (373 K), so there was lower than the tempering temperature samples. The temperature was measured by the contact thermometer and pyrometer on the sample surface. The method and obtained results were peaceable with the work [17]. Three to five samples for every variant of process were applied. The assessment of structure was realized on the light microscope model Neophot 32 of Carl Zeiss Jen firm with the digital registration with 1000 $\times$ . The samples were digested to the 2% of nitric alcohol solution for the structure observation.

### 3 Results of Research

The analysis of used quenching mediums with nanofluids groups was begun from breaking of Al<sub>2</sub>O<sub>3</sub> nanoparts, which was in solutions used by ultrasonic. The Tyndall effect was used in the assessment of ultrasonic break degree of agglomerate, which forms with nanoparticles in II medium. In the same method of particles size appraised in III medium, which included ammonia water and didn't put to ultrasonic. The obtained Tyndall effect after breaking of agglomerate nanoparticles was in accordance with the show that results in work [2, 3]. In these preparation of quenching mediums realized the investigation of cooling intensity, which the results present Fig. 2 in the form of the cooling curve. On the basis of the obtained cooling curves (Fig. 2), we can affirm that addition to water of 1% nanoparticles of the solid body from Al<sub>2</sub>O<sub>3</sub> and ammoniac water reduced the cooling intensities in the steam jacket phase and



**Fig. 2** Quenching curve of water and water with 1% addition of  $\text{Al}_2\text{O}_3$  nanoparticles as well as water with 10% ammonia and 1% addition of  $\text{Al}_2\text{O}_3$  nanoparticles

convective heat transfer exchange phase imperceptibly.. The largest differences are observed in the nucleate boiling phase, where adding only  $\text{Al}_2\text{O}_3$  nanoparticles minimally reduced the cooling speed. However, the addition of ammonia water causes significant lowering of cooling speed in this phase with the simultaneous lowering of the temperature of occurrence of the maximum cooling speed.

On the basis of these curves, we can also affirm that the maximum cooling speed in the case of water (the I medium) and II medium occurred in range of the temperatures 590–610 °C and for III medium in range of temperatures 400–550 °C. In the effect of the modification nanoparticles, the value of maximum cooling speed got smaller about 12 °C/s, and additionally, ammoniac water lowered this value about 85 °C/s. In the quenching mediums, the slight change in warmth reception was in the consequence of modification nanoparticles of solid body, but in the larger degree near the addition of ammoniac water. On this basis, we can affirm that the modified quenchant will let get smaller tensions in hardened sample at simultaneous obtainment of propriety on the same level as in the case of hardened sample in no modified quenchant. The research showed that it got the profitable effect of quenching in nanofluids, because the introduction of nanoparticles to the cooling medium unreels the surfaces of contact point between factor cooling and element cooled. The development of surface can be increased by the growth of surface roughness (on the example by sandblasting) during hardening, too. The similar effect got in the result of the modification laser of the surface layer, where the surface roughness also grows up. The samples with the laser modified of layer additionally hardened in three various cooling mediums and low tempering. The subjected three various processes of structure formation of samples submitted the investigations of wear resistance. The analysis of the wear resistance coefficient showed, in the case of studying surfaces, the smaller value in the reference to the

surface only modified by laser. The differentiation of the surface roughness with carburizing paste in the result of the laser processing improved the imperceptibly wear resistance. The execution of hardened and tempering on carburizing samples by laser stopping raised the significantly wear resistance in the relation to samples only after laser processing or carburizing by laser stopping. The kind of applied cooling mediums not considerably differentiated got the results of wear resistance coefficient of hardened samples. However, analysis of samples after all variants of realizing processes shows that carburized sample by laser stopping and hardened in the cooling mediums including ammoniac water has the best wear resistance. The profitable growth of wear resistance can be caused the better heat transfer coefficient resulting from the blocking of the agglomeration of particles about size nano by the introduction to the solution of ammoniac water. This effect can also try accounted for the smaller total surface of the contact point (bearing capacity), which has however in the case of the single points of contact point the larger value between elements rubbing in the case when the element is characterized the higher roughness coefficient. The results put in the work [15] are confirmation this. The possible influence of sandblasting on the consolidation of surface layer was liquidated done in the result conducted on these samples of the laser and heat treatment processes (hardened and tempering low). The hardness investigations presented in Fig. 3 showed that the largest hardness had got the sample subjected to processing according to the V variant that is sandblasted, carburized by laser stopping and hardened in III cooling mediums and tempering low.

The smallest values of hardness were obtained on sample sandblasted and subjected laser thermal processing. The hardness investigation by weight 0.98 N (0.1 kg) was also found inn the full section of samples that were hardened in different degrees. The hardness results correlate with the wear resistance results,

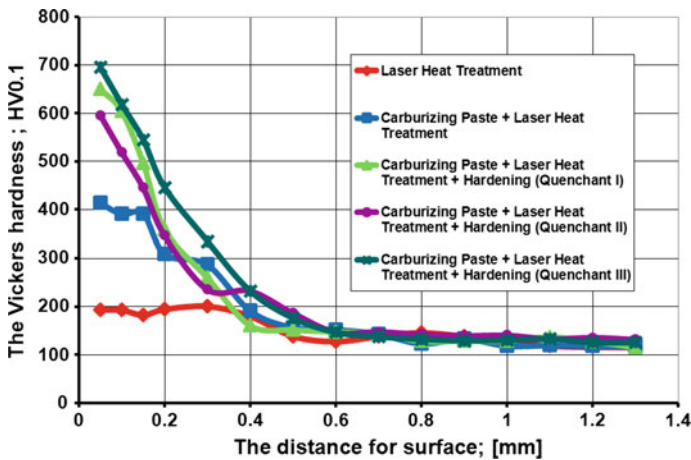
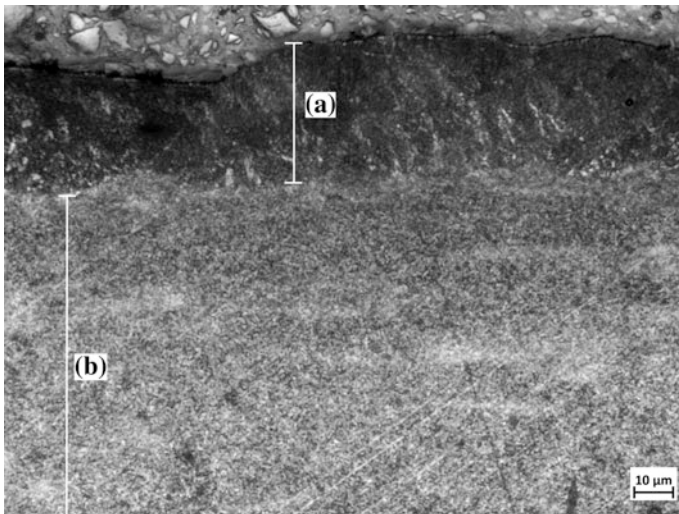


Fig. 3 Hardness changes of sample after different surface treatment created with C20 steel, which hardened in nanofluids

where this sample alone got the best result in investigations. The obtained results of investigations show that changes occurred in their structure on studying samples. All samples in the exit state had the ferrite–pearlite structure. The realized processes of hardening allowed to obtainment of hardened structure on the whole section of the sample, what confirms got hardness on the section of sample as well as it lets assume the large cooling intensity of the used quenching mediums

The samples after laser heat treatment without the paste show in the layer of the fine-grained structure approximate to bainite and in the core of ferrite–pearlite structures approximate to the exit state. This sample can also observe the heat-affected zone. The martensitic structure occurred in the surface layer of samples which were carburized by laser stopping, but also areas demonstrative on not melting the paste with bases. The cores of this sample are also the ferrite–pearlite structure. In this sample, the heat-affected zone resulting from the laser processing, but about the smaller thickness than in the previous sample can also be observed. The carburized sample by laser stopping and hardened in nanofluids lets get after therealized processes in the layer and the core the hardened structure (Fig. 4). In the layer of the sample, the structure is the phase mixture of martensitic and bainite, and in the case of sampel core it is the phase mixture of bainite and ferrite supersaturated.

The influence of warmth zone is not observed in this sample, which was removed by heat treatment. The obtained structure changes included size and distribution of such phase components, how martensitic, bainite, and ferrite supersaturated on the section samples of carburized, hardened, and tempered low.



**Fig. 4** Structure of sample after the III variant of process, where **a** the hardened melted zone, **b** the hardened base materials zone

In the result of the laser processing of surface layer, the additional surface development caused increase in surface having of direct contact with the cooling mediums. In the nanofluids case, every hollow causes the so-called shadow effect. The settling down of nanoparticles in hollow caused the reduction in cooling intensity of element, which contributes to the slowing down of phase transformation occurred especially in the superficial zone.

The analysis of microstructure after hardening in III medium and tempering shows the larger fraction of martensitic in the structure of the surface layer sample.

## 4 Summary

1. Introduction of nanoparts in the solid body of  $Al_2O_3$  type to the quenching mediums reduces its cooling intensity, especially in the steam jacket phase and bubble boiling phase.
2. The utilization of 10% addition of ammoniac water allows for maintenance of the nanosize in quenching mediums cooling down without the additional influence of ultrasounds.
3. The cooling in nanofluids including ammoniac water allows to the more profitable of the cooling phase distribution during quenching the element.
4. The assurance of occurrence of the larger quantity of nanosized particles in nanofluids by the addition of ammoniac water contributes to the growth of hardness as well as wear resistance.
5. The surface development of samples in the result of carburizing by laser stopping also contributes to the obtained values of hardness and wear resistance.
6. The realized processes of hardening allowed to obtainment of hardened structure on the whole section of the sample, what confirms got hardness on the section of sample as well as it lets assume the large cooling intensity of the used quenching mediums.
7. In samples, the obtain structure consisted of phase: martensite, bainite, and supersaturated ferrite.

In the present stage of conducted research, it was found that the use of nanofluids including factors stabilizing the nanosize (ammoniac water) and development of the surface cooled during hardening obtained the increase in hardness and wear resistance in the relation to elements hardened in traditionally quenching mediums. The results give bases to further research in this range.

**Acknowledgements** This work has been financially supported by Ministry of Science and Higher Education in Poland as a part of the 02/24/DSPB project.

## References

1. Bahiraei, M., Hosseinalipour, S.M., Saeedan, M.: Prediction of Nusselt number and friction factor of water- $\text{Al}_2\text{O}_3$  nanofluid flow in shell-and-tube heat exchanger with Helical Baffles. *Chem. Eng. Communications* **202**, 260–268 (2015)
2. Changwei, P., Jung-Yeul, J., Jae, Won L., Yong, Tae K.: Thermal conductivity measurement of methanol-based nanofluids with  $\text{Al}_2\text{O}_3$  and  $\text{SiO}_2$  nanoparticles. *Int. J. Heat Mass. Transfer.* **55**, 5597–5602 (2012)
3. Changwei, P., Jung-Yeul, J., Yong, Tae K.: Thermal conductivity enhancement of  $\text{Al}_2\text{O}_3$  nanofluids based on the mixtures of aqueous NaCl solution and  $\text{CH}_3\text{OH}$ . *Int. J. Heat. Mass. Transfer.* **56**, 94–100 (2013)
4. Durga Prasad, P.V., Gupta, A.V.S.S.K.S., Sreeramulu, M., et al.: Experimental study of heat transfer and friction factor of  $\text{Al}_2\text{O}_3$  nanofluid in U-tube heat exchanger with helical tape inserts. *Exp. Therm. Fluid Sci.* **62**, 141–150 (2015)
5. Ghalambaz, M., Behseresht, A., Behseresht, J., Chamkha, A.: Effects of nanoparticles diameter and concentration on natural convection of the  $\text{Al}_2\text{O}_3$ -water nanofluids considering variable thermal conductivity around a vertical cone in porous media. *Adv. Powder Techn.* **26**, 224–235 (2015)
6. Ho, C.J., Chung, Y.N., Lai, C.-M.: Thermal performance of  $\text{Al}_2\text{O}_3$ /water nanofluid in a natural circulation loop with a mini-channel heat sink and heat source. *Energy Convers. Manag.* **87**, 848–858 (2014)
7. Kurzydłowski, K., Lewandowska, M.: *The Engineering, Constructional and Functional Nanomaterials* (in Polish), PWN (2010)
8. Mahbubul, I.M., Chong, T.H., Khaleduzzaman, S.S., et al.: Effect of ultrasonication duration on colloidal structure and viscosity of alumina-water nanofluid. *Ind. Eng. Chem. Res.* **53**, 6677–6684 (2014)
9. Malvandi, A., Safaei, M.R., Kaffash, M.H., Ganji, D.D.: MHD mixed convection in a vertical annulus filled with  $\text{Al}_2\text{O}_3$ -water nanofluid considering nanoparticle migration. *J. Magn. Mater.* **382**, 296–306 (2015)
10. Narayan Prabhhu, K., Fernandes, P.: Heat transfer during quenching and assessment of quench severity—a review. *J. ASTM Int.* 16–39 (2010)
11. Zakaria, I., Azmi, W.H., Mohamed, W.A.N.W., Mamat, R., Najafi, G.: Experimental investigation of thermal conductivity and electrical conductivity of  $\text{Al}_2\text{O}_3$  nanofluid in water—ethylene glycol mixture for proton exchange membrane fuel cell application. *Int. Commun. Heat Mass Transfer* **61**, 61–68 (2015)
12. Kucharski, S., Starzynski, G.: Study of contact of rough surfaces: modeling and experiment. *Wear* **311**, 167–179 (2014)
13. Radziejewska, J.: *The laser modification of the top layer propriety helped pressing* (in Polish), The works of Institute of Fundamental Technological Research Polish Academy of Sciences, p. 325 (2011)
14. Gęstwa, W.: The influence of paste type as well as laser beam on some properties of elements from constructional steel. *Mater. Eng.* **5**(201), 370–373 (2014)
15. Gęstwa, W., Kinal, G.: The influence of surface roughness on microstructure and some properties of steel elements hardened in nanofluid. *Mater. Eng.* **6**(208), 428–432 (2015)
16. Felde, I., Reti, T. Chen, X.L.: Efficient data encoding and filtering for quenching analysis. In: 3rd International of Conferences on Quenching and Control of Distortion, pp. 208–215 (1999)
17. Przyłęcka, M., Kulka, M., Gęstwa, W.: Carburizing and carbonitriding bearing steel (ŁH15–52100), International of Heat Treating Conferences on Equipment and Processes, pp. 233–238 (1994)

# Application of Correlation Function for Analysis of Surface Structure Shaping by Hybrid Manufacturing Technology

Sara Dudzinska, Michal Szydowski, Daniel Grochala  
and Emilia Bachtiaak-Radka

**Abstract** The article is focused on determining the optimal parameters of surface treatment using hybrid machining—milling and burnishing. Optimal SGP 3D conditions may be achieved on a previously milled surface using specific parameters in the technological burnishing process. The authors present a method of evaluating the differences in surface topography of milled and then burnished surfaces using cross correlation. This approach can be used for optimizing hybrid technology as well as to track surface texture changes (e.g. analysis of regeneration of machining marks during cutting).

**Keywords** Surface topography · Surface metrology · 3D surface parameters  
Confocal microscopy · Surface technology

## 1 Introduction

Currently manufactured surface types of machine parts are the effect of several treatment operations [1, 2]. Owing to a wider production range of modern technological machines, operations from different areas of manufacturing technology can be combined into one operation [1–6]. Integration of plastic shaping of the workpiece with finishing treatment of removal machining is called hybrid technology. Surface texture of a ready product is the effect of several surface processing operations conducted on the earlier-formed surface. Geometric product specification (GPS) changes are dependent on the type of successive treatments that comprise hybrid operations and on the values of applied technological parameters. Therefore, final assessment of GPS is problematic [7–9]. The analysis of 3D GPS poses challenges in selection and setting of surface roughness parameters. Another challenge is to determine the effect of successive technological treatments comprising hybrid operations on surface roughness parameters.

---

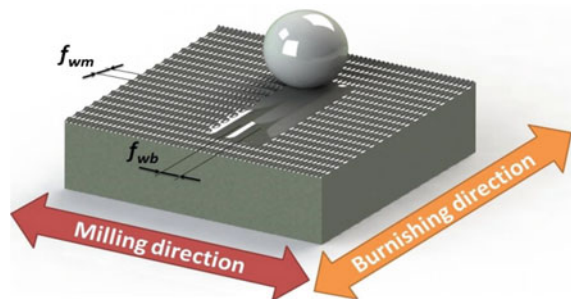
S. Dudzinska (✉) · M. Szydowski · D. Grochala · E. Bachtiaak-Radka  
West Pomeranian University of Technology, Szczecin, Poland  
e-mail: sara.dudzinska@zut.edu.pl

The surface of a ready product often shows traces of both shaping and surface finish treatment. It is difficult to establish the effect of the two treatment methods on the proportion of texture share in the surface of a ready product [9–12]. If the surface finish operation has not been conducted appropriately, the initially shaped irregularities and texture left by rough pre-machining cannot be removed [11, 12]. Striving for GPS improvement in surface finish operations may end in rough handling of tools and machines and their excessive wear and tear. Should this be the case, technological parameters of successive operations should be correlated, thus creating the so-called synergistic effect—roughness minimization on the surface of a ready product. The correlation function can be used for assessment of hybrid operations conducted in this way (selection of technological parameters of treatment) as it can differentiate the status of GPS after each individual operation. The surface after rough machining is the reference surface, relative to which the correlation of coordinates of points recorded for surface after finishing treatment is determined. The use of correlation function in GPS analysis can help to select synergistic parameters of combined operations. Minimization of correlation function of surface points becomes a criterion of the objective function for multi-criterion optimization of all technological parameters. The minimum of correlation function of surface points will occur, regardless of changes in texture, isotropy and 3D GPS high values.

## 2 Burnishing of Complex Spatial Surfaces After Milling

All modern manufacturing technologies are required to shorten production time, reduce production costs and meet high requirements of precision and shape. Therefore, hybrid treatment methods have become so popular. Integration of shaping milling with finish burnishing [1–4] is such a method. Since two different treatments have been combined into one technological operation, it is possible to obtain a smooth surface with significantly reduced surface roughness height [5–8]. The final effect depends not only on the applied technological parameters but also on the mutual trajectory of tools used in shaping and surface finish treatments [9–11] (Fig. 1).

**Fig. 1** Kinematics of hybrid surface treatment:  $f_{wm}$ —milling interval,  $f_{wb}$ —burnishing interval [11]





There exists a large body of literature on integration of plastic surface treatment with shaping milling. The fundamental criterion of how to select treatment parameters is based, according to many authors, on minimum 2D surface geometry height parameters [1, 2, 7–10]. More recent papers define the fundamental criterion as 3D SG parameters relative to changes of surface geometric structure [12], degree of isotropy [11, 12] or 3D SG spatial parameters based on surface autocorrelation functions, such as Sal, Str or Std [11].

No paper published to date on hybrid removal machining with plastic surface treatment discussed the changes of surface roughness height while at the same time considering shape changes and direction and type of surface texture on a ready product compared to the surface obtained in forming machining. Research on 3D surface geometry status after forming machining is difficult to conduct. You have to halt the process after forming machining, scan the surface and transfer the sample back on the multi-axis machining centre to perform finish machining. After finish burnishing, the surface of the ready product must be scanned again.

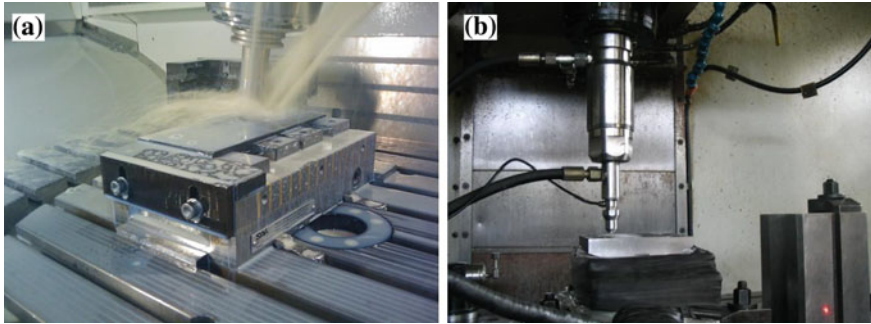
Technological challenges of workpiece positioning arising during machining interrupted with measurements can be overcome through appropriate sample preparation. The same surfaces should be analyzed in workpiece reference positioning during machining and measurements.

### 3 Materials and Methods

#### 3.1 Sample Preparation

To validate the use of cross-correlation function of surface points after shaping milling and  $F_b$  finish burnishing, a series of experiments was conducted (Fig. 2). 42CrMo4 steel,  $100 \times 100 \times 20$  mm samples were prepared. They were then thermally improved to  $35 \pm 2$ HRC. In the first step, shaping milling was conducted on DMG DMU 60MONOBLOCK machining centre, with spindle angle of  $15^\circ$  (Fig. 2a). A WNT R1000G.42.6.M16. IK torus with six inserts—diameter of  $d_p = 10$  mm (RD.X1003 MOT—WTN1205) was used. Samples were machined with velocity  $v_c = 1$  m/min, cutting tip feed  $f_z = 0.1$  mm and milling depth of  $a_p = 0.5$ . Two values of transverse feed of 0.3 and 0.5 mm were selected for further analysis.

Samples were finish burnished on 3-axis MIKRON VCE 500 machining centre (Fig. 2b). As a tool was applied ball burnishing tool with bellows actuator [10], with a ZrO<sub>2</sub> ceramic tip with a diameter of  $d_b = 10$  mm. Burnishing velocity  $v_b$  was 8 m/min and transverse feed was  $f_{vb} = 0.12$  mm. Burnishing was conducted with forces  $F_b$  of 200, 500 and 800 N. Each burnished area was 11 mm wide.



**Fig. 2** Sample preparation **a** shaping milling with spindle at an angle on DMG DMU 60 MONOBLOCK machining centre, **b** finish burnishing on 3-axis MIKRON VCE 500 machining centre

**Table 1** Selected 3D SG parameters after hybrid milling and burnishing

SG data		After milling		Burnishing force $f_b$ (N)					
				200 N		500 N		800 N	
$f_{wm}$	0.3 mm	0.5 mm	0.3 mm	0.5 mm	0.3 mm	0.5 mm	0.3 mm	0.5 mm	
Sq	1.9	3.46	1.23	2.8	0.39	1.11	0.304	0.296	
Sz	10.2	18.3	6.68	11.6	3.13	5.58	4.58	5	
Sal	0.118	0.187	0.149	0.211	0.326	0.217	0.14	0.193	
Str	0.117	0.185	0.159	0.219	0.316	0.213	0.141	0.194	
Std	90.3	90.3	90	90	0.343	90.5	0.337	0.334	

### 3.2 Surface Measurements

GPS measurements were conducted on  $2 \times 2$  mm areas with an AltiSurf A520 multisensor, manufactured by Altimet, for surface topography analysis. It was fitted with a chromatic confocal CL1 sensor, with a range up to  $130 \mu\text{m}$  and resolution of  $8 \text{ nm}$  in Z optical axis. Scanning resolution along X and Y axes was  $0.5 \mu\text{m}$ . The generated point clouds were processed with AltiMap PREMIUM 6.2. Point clouds for each recorded surface were generated in the same way:

- a threshold level was determined to delete unreliable surface point data
  - surface levelling (with mean area) was conducted,
  - some 3D SG parameters were determined in compliance with ISO 25178
- Table 1 presents some selected 3D SG parameters.

Experiments showed that a significant reduction of Sq and Sz roughness height parameters was not correlated with a radical change of surface texture (Fig. 3). The surface of all samples machined differently is isotropic in character. This is due to predetermined shape of milling and burnishing tools and their rectilinear motion trajectory. Another piece of evidence is provided by low values of Sal and Str

parameters which never exceeded 0.6. In all the series, samples burnished with  $F_b = 500$  N force looked best. Their Sal and Str parameters varied depending on milling interval from 0.3 at  $f_{wm} = 0.3$  mm to approximately 0.2 at  $f_{wm} = 0.5$  mm. Maximum Sal and Str parameters are due to marks left on the surface after milling and deep marks left by the burnishing tool (Fig. 3e, f).

Burnishing with a force of 800 N in both cases managed to change the direction of dominating texture, from milling to burnishing texture, as evidenced by Std parameter—the value of dominating direction of 3D SG structure (Fig. 3g, h). Figure 3 shows surfaces obtained in the experiments.

### 3.3 Data Processing—Normalized Cross Correlation

The cross correlation is a measure of similarity of two data series displaced relatively one to the other. One can calculate the cross correlation using formula (1).

$$C(\tau) = \int f^*(t)g(t + \tau)dt \tag{1}$$

where  $f^*$  is a complex conjugate of signal  $f$ ,  $g(t - \tau)$  is the displaced signal  $g$  and  $\tau$  is the displacement. Given that the surface measurements are two dimensional and discrete, the cross correlation can be calculated using Eq. (2):

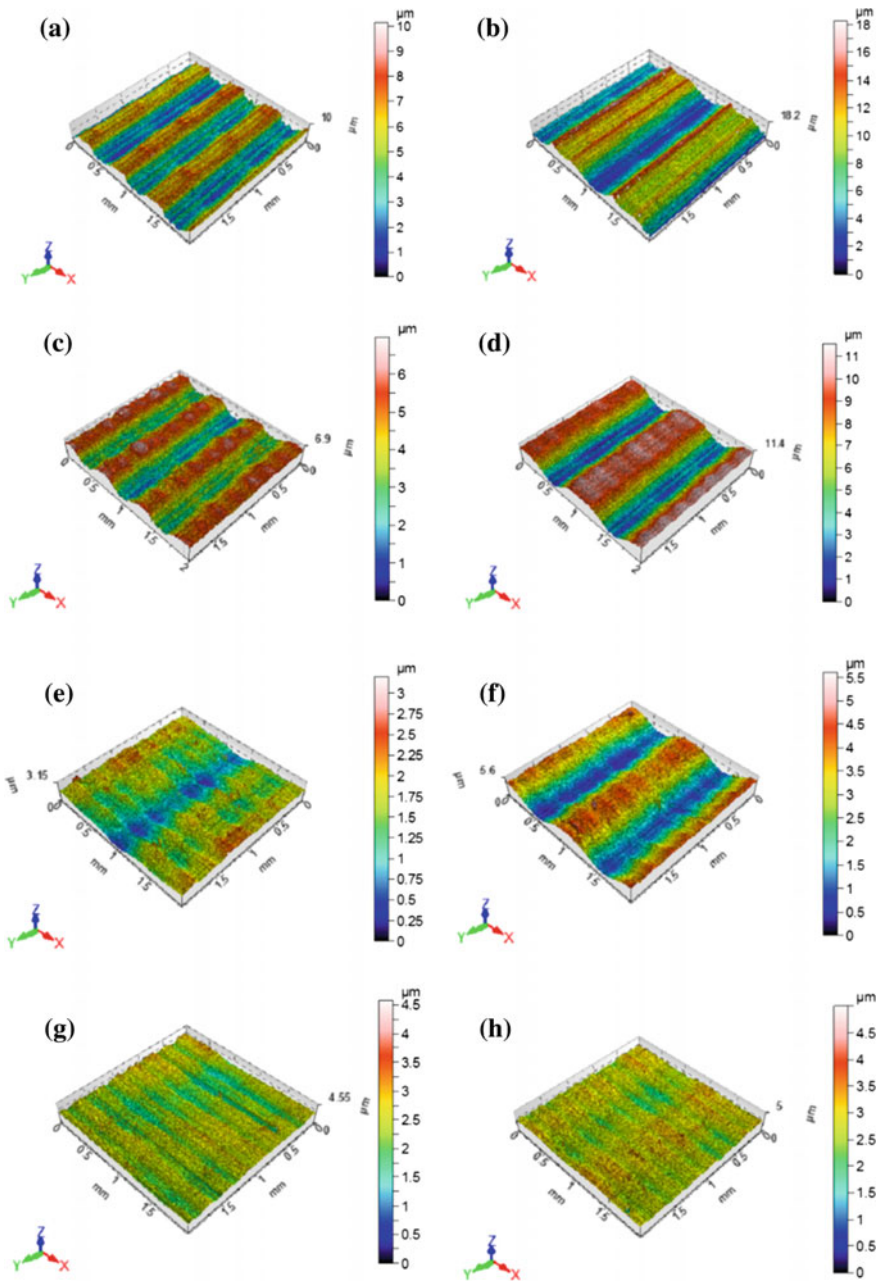
$$C(k, l) = \sum_{m=0}^{M-1} \sum_{n=0}^{N-1} S_1(m, n)S_2^*(m - k, n - l), \tag{2}$$

$$\begin{cases} -(W - 1) \leq k \leq M - 1 \\ -(V - 1) \leq l \leq N - 1 \end{cases}$$

where  $S_1$  is  $M$ -by- $N$ ,  $S_2$  and  $W$ -by- $V$  matrixes containing surface measurements,  $S_2^*$  is considered a complex conjugate and  $k$  and  $l$  are the displacements in both directions.

Unfortunately, if energy of the signal varies relative to position, the interpretation of  $C(k, l)$  could be flawed. Therefore, normalization is needed as proposed by Lewis [13]. Given  $\overline{S_1}$  that  $\overline{S_2}$  and are the means of their respective signals one can evaluate the normalized cross correlation using Eq. (3).

$$C_n(k, l) = \frac{\sum_{m=0}^{M-1} \sum_{n=0}^{N-1} (S_1(m, n) - \overline{S_1})(S_2(m - k, n - l) - \overline{S_2})}{\sum_{m=0}^{M-1} \sum_{n=0}^{N-1} (S_1(m, n) - \overline{S_1})^2 \sum_{m=0}^{M-1} \sum_{n=0}^{N-1} (S_2(m - k, n - 1) - \overline{S_2})^2} \tag{3}$$



**Fig. 3** Surface obtained after milling: **a**  $f_{\text{wm}}$  of 0.3 mm, **b**  $f_{\text{wm}}$  of 0.5 mm, after hybrid milling and burnishing **c**  $f_{\text{wm}}$  of 0.3 mm,  $F_b = 200$  N; **d**  $f_{\text{wm}}$  of 0.5 mm,  $F_b = 200$  N; **e**  $f_{\text{wm}}$  of 0.3 mm,  $F_b = 500$  N; **f**  $f_{\text{wm}}$  of 0.5 mm,  $F_b = 500$  N; **g**  $f_{\text{wm}}$  of 0.3 mm,  $F_b = 800$  N; **h**  $f_{\text{wm}}$  of 0.5 mm,  $F_b = 800$  N

The values  $C_n$  can be taken from  $-1$  to  $1$ . The closer the value to  $1$  or  $-1$  the more similar the signals are. Zero denotes no similarity. The position of the correlation peak might suggest a spatial shift within the compared signals.

## 4 Results

Comparing the signal with itself would result in a peak equal to  $1$  in the centre of the 2D correlation function response. A comparison of two surface pairs is shown in Fig. 4. The top row represents surfaces before the second operation. The middle row represents surfaces after the second operation.

The last row shows the calculated cross-correlation functions. One can see that for the surfaces on the right-hand side the max  $C_n$  value was higher— $0.4190$ —in comparison with  $0.5832$ . Table 2 shows max and min values of the normalized correlation function for all the compared surfaces.

## 5 Summary and Conclusions

Based on the conducted experiments, the following conclusions can be formulated.

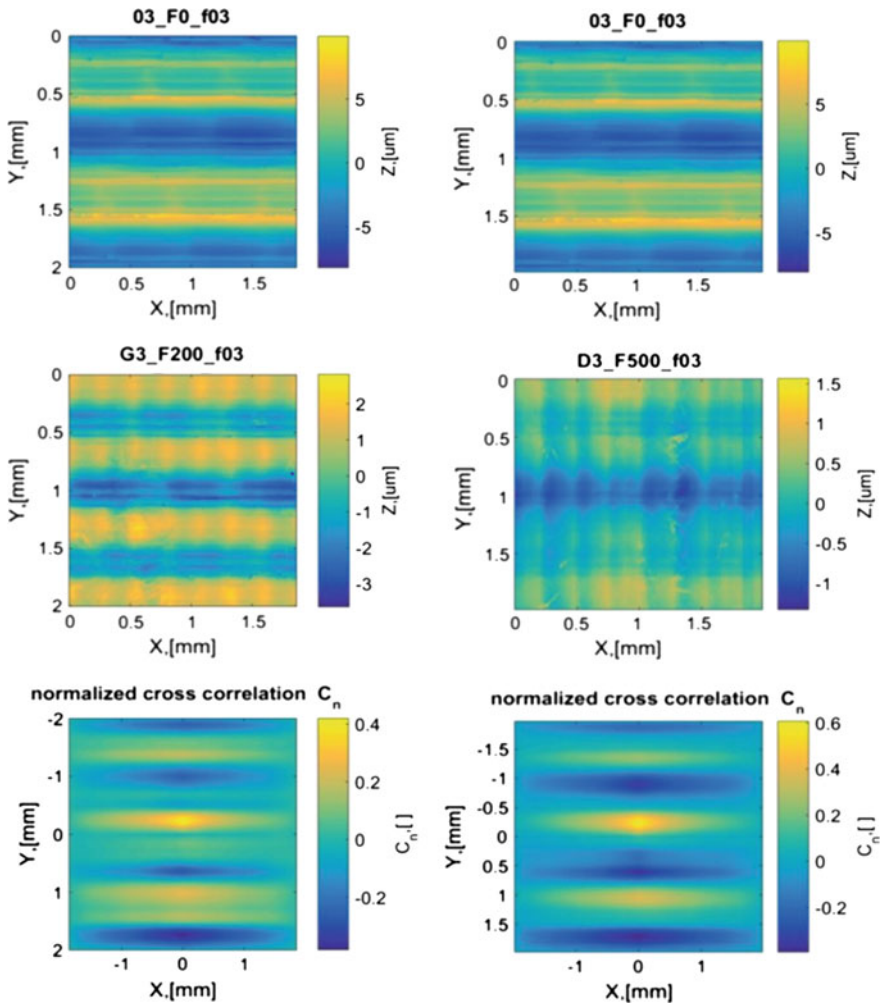
Burnishing with forces in the range of  $200$ – $500$  N is low effective. Significant marks left after milling are visible. It is more effective to burnish low irregularities resulting from milling with small interval  $f_{wm}$ . For small burnishing forces  $F_b$ , large dispersion of cross-correlation space parameters of max  $C_n$  and min  $C_n$  is observed. Furthermore, milling with small interval  $f_{wm}$  is labour intensive which results in high cost of the operation. To maintain high efficiency of the hybrid technology, it is more effective to burnish with higher levels of force  $F_b$ .

The use of  $800$  N force reversed the direction of surface texture. The main trace observed on the surface was left by the burnishing tool. Although the texture changed from milling into burnishing in character, the change from anisotropic (directional) surface texture to isotropic (non-directional) texture was not achieved. Additionally, it was impossible to completely eliminate the influence of initial surface structure obtained after milling, as evidenced by other than zero values of cross-correlation function of max  $C_n$  and min  $C_n$ .

From the technological point of view, the use of high values of burnishing force may result in obtaining a certain optimal 3D GPS state. It means that regardless of surface condition after shaping milling, 3D GPS with texture and height parameters similar to all cases of arbitrary forming machining will be created in the finish treatment.

It can be seen in the determined parameters of cross correlation, for which the spread of max  $C_n$  and min  $C_n$  is the smallest relative to milling interval  $f_{wm}$ .

Mutual correlation of real surfaces obtained in measurements of material surface of the workpiece may be difficult to use in industrial practice. It may require



**Fig. 4** Comparison of two surface pairs

examination of surface topography with portable instruments in the cabin of a multi-axis machine tool. In some situations, if measurement is impossible to make, reference surface can be modelled with a surface meeting the technological parameters and geometric-kinematic characteristics of forming machining.

Cross correlation is a new and original tool in surface topography analysis. It can be used to optimize hybrid technological operations, to analyze changes in surface texture following successive paint layers and to examine regeneration of machining marks. Our ongoing research into the use and improvement of the tool will be continued in a wider scope on the selection and optimization of technological parameters of shaping milling and finish burnishing.

**Table 2** Max and min values of the cross correlation

Surfaces compared	max $C_n$ [-]	min $C_n$ [-]
(c) $f_{wm} = 0.3$ mm versus $f_{wm} = 0.3$ mm $f_b = 200$ N	0.4190	-0.3813
(d) $f_{wm} = 0.5$ mm versus $f_{wm} = 0.5$ mm $f_b = 200$ N	0.596	-0.7803
(e) $f_{wm} = 0.3$ mm versus $f_{wm} = 0.3$ mm $f_b = 500$ N	0.6071	-0.3938
(f) $f_{wm} = 0.5$ mm versus $f_{wm} = 0.5$ mm $f_b = 500$ N	0.5832	-0.7757
(g) $f_{wm} = 0.3$ mm versus $f_{wm} = 0.3$ mm $f_b = 800$ N	0.4548	-0.3862
(h) $f_{wm} = 0.5$ mm versus $f_{wm} = 0.5$ mm $f_b = 800$ N	0.5082	-0.3853

## References

1. Lopez de Lacalle, L.N., Lamikiz A., Munoa, J., Sanchez, J.A.: Quality improvement of ball-end milled sculptured surfaces by ball burnishing, *Int. J. Mach. Tools Manuf.* **45**, 1659–1668 (2005)
2. Lopez de Lacalle, L.N., Lamikiz, A., Sanchez, J.A., Arana, J.L.: The effect of ball burnishing on heat-treated steel and inconel 718 milled surfaces. *Int. J. Adv. Manuf. Technol.* **32**, 958–968 (2007)
3. El-Taweel, T.A., El-Axir, M.H.: Analysis and optimization of the ball burnishing process through the Taguchi technique. *Int. J. Adv. Manuf. Technol.* **41**, 301–310 (2009)
4. Grochała, D., Berczyński, S., Grządziel, Z.: Stress in the surface layer of objects burnished after milling. *Int. J. Adv. Manuf. Technol.* **71**, 9–12 (2014)
5. Tadic, B., Randjelovic, S., Todorovic, P., Zivkovic, J., Kocovic, V., Budak, I., Vukelic, D.: Using a high-stiffness burnishing tool for increased dimensional and geometrical accuracies of openings. *Precis. Eng.* **43**, 335–344 (2016)
6. Patyk, R., Kukielka, L.: Optimization of geometrical parameters of regular triangular asperities of surface put to smooth burnishing, In: 12th International Conference Metalforming, AGH, International Special Edition, Publishing Company Verlag Stahleisen, vol. 2, pp. 642–647 (2008)
7. Shiou, F.J., Chen, C.H.: Ultra-precision surface finish of NAK80 mould tool steel using sequential ball burnishing and ball polishing processes. *J. Mater. Process. Technol.* **201**, 554–559 (2008)
8. Shiou, F.J., Chuang, C.H.: Precision surface finish of the mold steel PDS5 using an innovative ball burnishing tool embedded with a load cell. *Precis. Eng.* **34**(76), 84 (2010)
9. Rodríguez, A., López de Lacalle, L.N., Celaya, A., Lamikiz, A., Albizuri, J.: Surface improvement of shafts by the deep ball-burnishing technique. *Surf. Coat. Technol.* **206**, 2817–2824 (2012)
10. Grochała, D., Sosnowski, M.: The problems of burnishing complex spatial surfaces on machining centres (in Polish). *MECHANIC* **1**, 14–18 (2011)
11. Bachtiaak-Radka, E., Dudzińska, S., Grochała, D., Berczyński, S., Olszak, W.: The influence of CNC milling and ball burnishing on shaping complex 3D surfaces. In: *Surface Topography: Metrology and Properties*, vol. 5 (2017)
12. Bachtiaak-Radka, E., Grochała, D., Chmielewski, K., Olszak, W.: The isotropy tests of a milled and hard-burnished surface of the X160CrMoV121 steel (in Polish). *MECHANIC* **8–9**, 641–653 (2015)
13. Lewis J.P.: Fast template matching. In: *Vision Interface*, pp. 120–123 (1995)

# Investigation of Heat Distribution in Coated Indexable Tool Inserts

Marta Bogdan-Chudy, Piotr Nieslony and Grzegorz Krolczyk

**Abstract** Article presents the results of temperature changes and heat distribution in a cemented carbide indexable tool insert with a TiAlN coating. The study presented in the article focused on heat distribution in a cutting tool–chip interface in two special cases: when a heat source is in contact with the TiAlN tool coating and when the heat source is in direct contact with a substrate plate. The thermophysical formulas were applied to both of them. The change of heat flux as a function of the distance from the heat source contact point along with experimental data was examined. The experimental data for the heat propagation in the cutting tool point have been gathered using an authors' test stand.

**Keywords** Heat distribution · Tool coating · Tool protection · Machining

## 1 Introduction

WC-based cemented carbides are among the most commonly used materials for cutting inserts, especially for milling and turning operations. Coated cemented carbide currently corresponds to 80% of all cutting tool inserts [1]. Its widespread use as a tool material is due to the combination of cutting and mechanical properties [2, 3]. Thin hard coatings are widely used to substantially improve the performance of cemented carbide tools in metal cutting. Titanium nitride (TiAlN) is a material widely used as a protective coating due to its good mechanical and tribological properties, including high hardness [4], good wear resistance [5] and excellent thermal stability [6]. This type of coating increases the stability of the cutting tool, mainly by reducing the intensity of heat transfer to the tool material [7, 8]. Machining generates high cutting temperature, which increases tool wear and reduces cutting tool life, thus leading to impairs of the surface quality [9].

---

M. Bogdan-Chudy · P. Nieslony · G. Krolczyk (✉)  
Department of Manufacturing Engineering and Production Automation,  
Opole University of Technology, 76 Proszkowska Street, 45-758 Opole, Poland  
e-mail: g.krolczyk@po.opole.pl



Challenges associated with machining are directly related to high cutting tool temperatures due to low thermal conductivity and the heat generated in the primary shear zone and on the tool–chip interface [10]. Vast studies concerning temperature in the cutting zone were focused on the investigations in which empirical and numerical models have been published [11–14]. Santhanakrishnan et al. [11] present the effect of geometrical and machining parameters such as the rake angle, nose radius, cutting speed, feed rate and depth of cut on the increase in temperature during an end-milling operation. The temperature rise while machining was measured using a Type K thermocouple, which was coupled with a thermal indicator. Mia and Dhar [12] present the effects of material hardness and a high-pressure coolant jet in respect of surface roughness and a cutting temperature using a Taguchi L36 orthogonal array. The statistical analysis presented in the paper showed that workpiece hardness is the most significant factor for cutting temperature and surface roughness. Zhang et al. [13] proposed a thermal error modelling approach by using the thermal error transfer function of the machine tool. Malakizadi et al. [14] present a FEM-based approach to predict the rate of flank wear evolution for uncoated cemented carbide tools in longitudinal turning processes. The results presented in the paper were used to establish the quadratic relation between the input variables and the responses required for tool wear prediction such as interface temperature.

## 2 Theoretical Background

Heat flux is the sum of the stream associated with radiation and convection of heat transfer

$$Q = Q_k + Q_r \quad (1)$$

where  $Q_k$  is the heat flux of convection and  $Q_r$  is the heat flux of radiation. The individual heat flows define relationships (2) and (3).

$$Q_k = A_z \alpha_k (T_z - T_{ot}) \quad (2)$$

where

- $A_z$  the exterior surface of the heat transfer,
- $\alpha_k$  convective heat transfer coefficients,
- $T_z$  temperature of the wall exterior surface heat transfer,
- $T_{ot}$  ambient temperature.

$$Q_r = A_z \varepsilon C_c (T_z^4 - T_{ot}^4) \quad (3)$$

where

$\varepsilon$ —emissivity of the exterior surface of the heat transfer; in our application,  $C_c = 5.67 \times 10^{-8} \text{ W}/(\text{m}^2 \cdot \text{K}^4)$  was adopted.

After the transformation of Eq. (3) in relation to temperature, the following is obtained

$$Q_r = A_z \varepsilon C_c (T_z^2 - T_{ot}^2)(T_z^2 + T_{ot}^2) = A_z \varepsilon C_c (T_z - T_{ot})(T_z + T_{ot})(T_z^2 + T_{ot}^2) \quad (4)$$

and next

$$Q_r = A_z [\varepsilon C_c (T_z + T_{ot})(T_z^2 + T_{ot}^2)] (T_z - T_{ot}) \quad (5)$$

$$Q_r = A_z \alpha_r (T_z - T_{ot}) \quad (6)$$

where  $\alpha_r$  is the radiation heat transfer coefficient defined in (7)

$$\alpha_r = \varepsilon C_c (T_z + T_{ot})(T_z^2 + T_{ot}^2) \quad (7)$$

Taking into account the identity of Eqs. (3) and (6), the radiative heat transfer coefficient can also be calculated with formula (8a)

$$\alpha_r = \frac{\varepsilon C_c}{T_z - T_{ot}} (T_z^4 - T_{ot}^4) = \frac{\varepsilon C_c}{T_z - T_{ot}} \times 10^8 \left( \left( \frac{T_z}{100} \right)^4 - \left( \frac{T_{ot}}{100} \right)^4 \right) \quad (8a)$$

Considering the value of the Stephen-Boltzmann constant ( $C_c = 5.67 \times 10^{-8} \text{ W}/(\text{m}^2 \text{ K}^4)$ ), the equation for the calculation of the radiation heat transfer coefficient  $\alpha_r$  can be defined as follows (8b):

$$\alpha_r = \frac{5.67 \varepsilon}{T_z - T_{ot}} \left( \left( \frac{T_z}{100} \right)^4 - \left( \frac{T_{ot}}{100} \right)^4 \right) \quad (8b)$$

It should be noted that the adoption of the constant emissivity of the outer surface of heat transfer  $\varepsilon$  in Eqs. (8a) and (8b) is a simplification which assumes that  $\varepsilon = \varepsilon_{1-2} = \varepsilon_1$ . This is the result of the general Eq. (9). In this case, for flat or convex surfaces with area of  $A_1$  and  $\varepsilon_1$  exchanging radiation energy to surface  $A_2$  with emissivity  $\varepsilon_2$ , the resultant emissivity can be defined as:

$$\frac{1}{\varepsilon} = \frac{1}{\varepsilon_{1-2}} = \frac{1}{\varepsilon_1} + \frac{A_1}{A_2} \left( \frac{1}{\varepsilon_2} - 1 \right) \quad (9)$$

Based on Eq. (9) and on the assumption that cutting insert surface  $A_1$  is much smaller than area  $A_2$ , and so  $A_1/A_2 \cong 0$ , the emissivity of the outer surface of heat transfer is  $\varepsilon = \varepsilon_{1-2} = \varepsilon_1$ . Finally, the total heat flux based on Eqs. (1), (2) and (6) can be calculated with formula (10)

$$Q = A_z(\alpha_k + \alpha_r)(T_z - T_{ot}) [\text{W}] \quad (10)$$

Similarly, heat flux density  $q = Q/A_z$  corresponds to Eq. (11).

$$q = (\alpha_k + \alpha_r)(T_z - T_{ot}) [\text{W}/\text{m}^2] \quad (11)$$

$\alpha_r$  can be determined using Eqs. (7) or (8a and 8b). The value of convective heat transfer coefficient  $\alpha_k$  must be defined with regard to the fluid flow conditions (with specific physicochemical properties), the heat sink and the geometry of the system.

For the conditions of washing out the air from the corners of the “rhombus” insert geometry, the criterial equation (determined experimentally) takes form (12)

$$\text{Nu} = C\text{Re}^n\text{Pr}^{0.333} \quad (12)$$

where

Nusselt number

$$\text{Nu} = \frac{\alpha_k l}{\lambda_p} \quad (12a)$$

Reynolds number

$$\text{Re} = \frac{w_p l \rho_p}{\eta_p} \quad (13)$$

Prandtl number

$$\text{Pr} = \frac{c_p \eta_p}{\lambda_p} \quad (14)$$

The values of constant  $C$  and index  $n$  depend on the Reynolds number defined by characteristic dimension  $l = 4a/\pi$  where  $a$  is the dimension of the side length of the tool insert. In this case, for

$$\begin{aligned} 2500 < \text{Re} < 7500 & \quad C = 0.261, \quad n = 0.625, \\ 5000 < \text{Re} < 100,000 & \quad C = 0.222, \quad n = 0.588, \end{aligned}$$

**Table 1** Air property at atmospheric pressure

Temperature (°C)	Temperature (K)	Density $\rho_p$ , kg/m <sup>3</sup>	Viscosity $\eta_p \times 10^6$ , Pa·s	Thermal conductivity $\lambda_p \times 10^2$ W/(m K)	Prandtl number
10	283.15	1.206	17.751	2.448	0.722
20	293.15	1.164	18.224	2.518	0.722
30	300.15	1.127	18.660	2.575	0.722
40	310.15	1.092	19.224	2.645	0.722
50	320.15	1.056	19.613	2.714	0.722

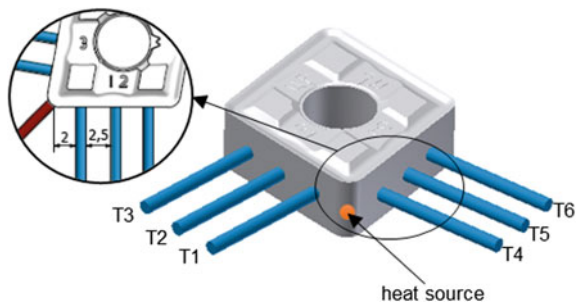
- $w_p$  air linear velocity m/s,
- $\rho_p$  air density kg/m<sup>3</sup>,
- $\eta_p$  coefficient of air dynamic viscosity Pa s,
- $\alpha_k$  convection heat transfer coefficient W/(m<sup>2</sup> K),
- $\lambda_p$  air thermal conductivity W/(m K).

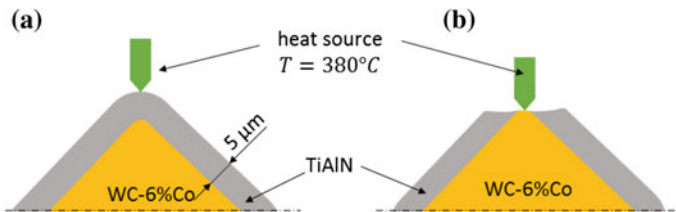
The property of air as a function of temperature and at atmospheric pressure is summarised in Table 1.

### 3 Materials and Method

The aim of experimental tests was to determine temperature changes at constant points of an indexable insert when a heat source is in contact with the TiAlN coating and when it is in direct contact with a carbide substrate. The studies were carried out on authors' own test stand, which enabled the measurement of temperature with Type K thermocouples at the same points on the side lengths of the tool insert. The location of the heat source and thermocouples is presented in Fig. 1. For the tests, carbide insert CNMG 120412-UP KC5010 by KENNAMETAL was used. It was made of WC-6%Co cemented carbide and covered with a TiAlN coating using physical vapour deposition. The average thickness of the coating was 5 µm for machining of, among others, titanium alloys.

**Fig. 1** Scheme of measuring points on the tool insert





**Fig. 2** Scheme for heat source contact with the tool insert. Heat source contacting with external TiAlN coating (a) and heat source contacting directly with substrate (b)

It was assumed that the heat source has a constant temperature of 380 °C, which corresponds to an average temperature in the range of cutting zone temperatures for selected machining conditions [15]. The tests were carried out at an ambient temperature of 20 °C. Two cases of the contact between the heat source and the insert were considered. In the first case, the heat source is in contact with the TiAlN coating (Fig. 2a), and in the other, the heat is distributed to the insert substrate directly; thus, a thermal barrier is omitted (Fig. 2b).

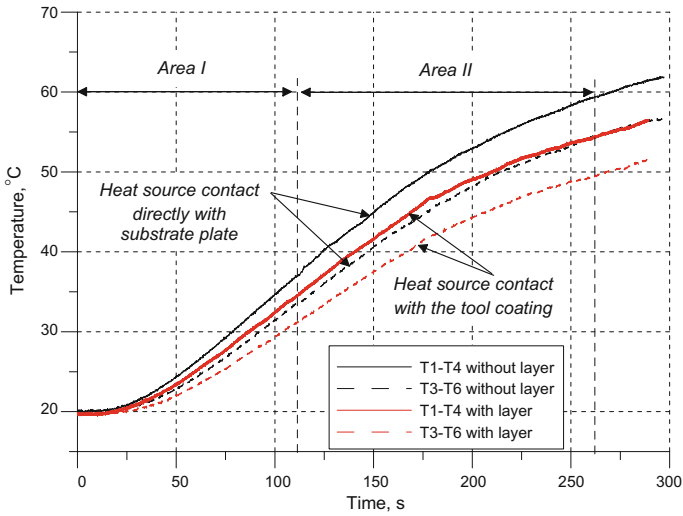
## 4 Results and Discussion

The measurements of the temperature changes while heating the TiAlN-coated cutting insert for both cases of heat source contact  $Q$  with the sample are shown in Fig. 3.

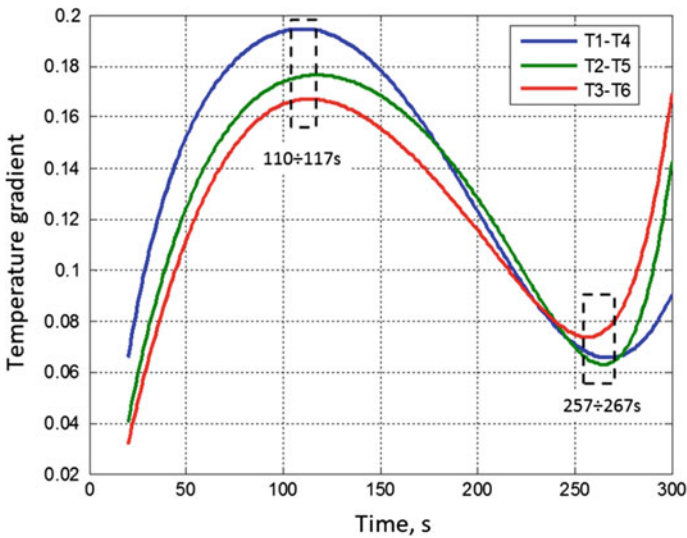
The measurement of the temperature changes while heating the cutting insert with the TiAlN coating for both cases of heat source contact  $Q$  with the sample are shown in Fig. 3. For both cases, the nature of temperature changes over time is similar. From the very beginning of the test, the material of the insert clearly absorbed heat more quickly, thus increasing the temperature value at the measurement point for the case when heat source  $Q$  is in direct contact with the substrate (Fig. 3).

On the basis of Fig. 4, it was observed that irrespective of the location of the thermocouple measurement (T1–T4 or, e.g. T3–T6), the gradients increased until measurement time was 110–117 s and reached the highest values of 0.18°/s on average. This period is marked as Area I in Fig. 3. It was followed by a monotonous decrease in the gradients until measurement time was 257–267 s—Area II in Fig. 3. In this case, the extreme value of the gradient was 0.07°/s. It should be assumed that some reduction followed the first period of fast insert heating. This may be associated with the heat accumulation on the substrate–coating interface and the stabilization of heat transfer conditions.

The gradient characteristics for the contact of  $Q$  directly with the substrate are similar. In order to compare the values of the temperatures at control points, the



**Fig. 3** Temperature changes during heating tool insert for two special cases of heat source contact for T1–T4 and T3–T6 pair of thermocouples



**Fig. 4** The gradient characteristics for the contact of heat source  $Q$  with the TiAlN coating

evaluation was made for the time corresponding to the end of Area II ( $t = 260$  s) in which the lowest values of the gradient were reached.

On the basis of the results gathered in Table 2, it may be assessed that higher temperatures on the surface of the insert were achieved for heat source  $Q$  being in

**Table 2** Temperature during the heating tool insert for time  $t = 260$  s

	Measured temperature when heat source $Q$ contact with	
	Tool coating TiAlN (°C)	Substrate plate (°C)
T1–T4	54.7	60.0
T2–T5	52.2	56.1
T3–T6	49.1	55.9

contact with the substrate. Based on the equations in Sect. 2, heat flux density depending on the distance from the heat source can be calculated. The heat flux density for the cutting tool insert for both cases of heat source contact was calculated for the data presented in Table 3.

Based on the data from Table 3 and Eqs. (12) and (13), the Reynolds and Nusselt numbers were calculated.

$$Re = 1251.0702, Nu = 20.0557 \text{ for } C = 0.261 \text{ and } n = 0.624.$$

In the next step, the radiative and convection heat transfer coefficients were calculated. The convection heat transfer is constant for the tested range of temperature = 30.83 W/(m<sup>2</sup> K). The values of radiative heat transfer coefficients as a function of temperature and its slight increase were presented in Table 4.

The impact of the state of the cutting insert on the value of the heat flux density as a function of distance from the heat point can be analysed based on the data included in Table 4.

It was found that the TiAlN coating significantly affects the distribution of heat flux in the carbide insert. The intensity of heat flux clearly increases when the heat source is not in contact with the coating. In this case, heat flux being absorbed by the cemented carbide did not have to penetrate through the tool coating with a small  $\lambda$  and, additionally, did not have to travel through the TiAlN and WC interface. For  $Q$  being in contact with the coating, heat flux has to travel through the thermal barrier associated with the TiAlN coating twice. This resulted in heat flux density being lower by 200 W/m<sup>2</sup> on average at measurement points.

**Table 3** Basic data for calculating the heat flux density

Ambient temperature	$t_a$	21.17	°C
Air velocity	$w_p$	1.2	m/s
Side length of the rhomboidal cutting tool inserts	$a$	12.9	mm
Characteristic dimension	$l$	16.42	mm
Emissivity	$\varepsilon$	0.8	
<i>Air properties for ambient temperature</i>			
Density	$\rho_p$	1.16	kg/m <sup>3</sup>
Coefficient of air dynamic viscosity	$\eta_p$	1.83E-05	Pa·s
Thermal conductivity	$\lambda_p$	0.02525	W/(m·K)
Prandtl No.	$Pr$	0.722	

**Table 4** Heat flux density in a function of distance of heat point for two cases of heat source contact

	Heat source $Q$ contact with						Heat source $Q$
	Tool coating TiAlN			Substrate plate			
	T1–T4	T2–T5	T3–T6	T1–T4	T2–T5	T3–T6	
Temperature, °C	54.7	52.2	49.1	60	56.1	55.9	380
Temperature, K	327.85	325.35	322.25	333.15	329.25	329.05	653.15
Convective heat transfer coefficient, $\alpha_c$ , W/(m <sup>2</sup> K)	30.83	30.83	30.83	30.83	30.83	30.83	30.83
Radiative heat transfer coefficient, $\alpha_r$ , W/(m <sup>2</sup> K)	5.48	5.41	5.33	5.62	5.52	5.51	22.06
$\alpha_r + \alpha_c$	36.31	36.24	36.16	36.46	36.35	36.34	52.89
$q$ , W/m <sup>2</sup>	1217.47	1124.59	1009.91	1415.60	1269.64	1262.18	18978.1

With these data, it is possible to take them into account while FEM modelling of the insert in the cutting zone. Only the coating or substrate is subject to the evaluation of thermal properties [7, 8]. However, in case of chemical compounds that are deposited using PVD or CVD, and during which the chemical interaction between a coating and material occurs, synergy may gain high importance. Therefore, a scientific approach seems rational, in which the evaluation of such a coating will be made in conjunction with a substrate material on which it was deposited, along with the preservation of the conditions required for its production.

## 5 Conclusions

This experimental study of distribution of heat in PVD-TiAlN-coated carbide confirmed the existence of a thermal barrier on a coating–substrate interface.

- It was observed that the increase in temperature at control points of the insert is not constant. Within the period of 100 s, an intense increase in temperature occurs with a gradient of 0.18°/s. After this period to around 260 s, the gradient of the increase in temperature decreases and reaches only 0.07°/s.
- The stand-based tests of the distribution of heat in the carbide insert with a tool coating confirmed the existence of a thermal barrier on a coating–substrate interface. It was assessed that the TiAlN coating limits the intensity of heat flux density by about 200 W/m<sup>2</sup>.
- The test stand with a known configuration of measuring elements enables experimental data to be obtained in order to determine thermophysical properties of a tool coating.



- It was initially determined that on the basis of these tests, the thermal properties of a coating may be calculated, with regard to a synergistic effect using reverse engineering and by use of classical thermophysical equations. These data will enable a better description of thermal effects in the cutting zone while modelling of this process with numerical methods.

## References

1. Kupczyk, M.J.: Cutting edges with high hardness made of nanocrystalline cemented carbides. *Int. J. Refract. Met. Hard Mater.* **49**, 249–255 (2015)
2. Wojciechowski, S., Twardowski, P., Pelic, M., Maruda, R.W., Barrans, S., Krolczyk, G.M.: Precision surface characterization for finish cylindrical milling with dynamic tool displacements model. *Precis. Eng.* **46**, 158–165 (2016)
3. Maruda, R.W., Krolczyk, G.M., Nieslony, P., Wojciechowski, S., Michalski, M., Legutko, S.: The influence of the cooling conditions on the cutting tool wear and the chip formation mechanism. *J. Manuf. Process.* **24**(P1), 107–115 (2016)
4. Wojciechowski, S., Twardowski, P., Wieczorowski, M.: Surface texture analysis after ball end milling with various surface inclination of hardened steel. *Metrol. Meas. Syst.* **21**, 145–156 (2014)
5. Zaleski, K.: Study on the properties of surface—active fluids used in burnishing and shot peening processes. *Adv. Sci. Technol. Res. J.* **10**, 235–239 (2016)
6. Feldshtein, E., Jozwik, J., Legutko, S.: The influence of the conditions of emulsion mist formation on the surface roughness of AISI 1045 steel after finish turning. *Adv. Sci. Technol. Res. J.* **10**, 144–149 (2016)
7. Maruda, R.W., Krolczyk, G.M., Feldshtein, E., Nieslony, P., Tyliczyczak, B., Pusavec, F.: Tool wear characterizations in finish turning of AISI 1045 carbon steel for MQCL conditions. *Wear* **372–373**, 54–67 (2017)
8. Merola, M., Ruggiero, A., De Mattia, J.S., Affatato, S.: On the tribological behavior of retrieved hip femoral heads affected by metallic debris. A comparative investigation by stylus and optical profilometer for a new roughness measurement protocol. *Measurement* **90**, 365–371 (2016)
9. Mrkvica, I., Neslušán, M., Čep, R., Sléha, V.: Properties and comparison of PVD coatings. *Tehnicki Vjesnik* **23**(2), 569–574 (2016)
10. Heigel, J.C., Whintont, E., Lane, B., Donmez, M.A., Madhavan, V., Moscoso-Kingsley, W.: Infrared measurement of the temperature at the tool–chip interface while machining Ti–6Al–4 V. *J. Mater. Process. Technol.* **243**, 123–130 (2017)
11. Santhanakrishnan, M., Sivasakthivel, P.S., Sudhakaran, R.: Modeling of geometrical and machining parameters on temperature rise while machining Al 6351 using response surface methodology and genetic algorithm. *J. Braz. Soc. Mech. Sci. Eng.* **39**(2), 487–496 (2017)
12. Mia, M., Dhar, N.R.: Optimization of surface roughness and cutting temperature in high-pressure coolant-assisted hard turning using Taguchi method. *Int. J. Adv. Manuf. Technol.* **88**(1–4), 739–753 (2017)
13. Zhang, C., Gao, F., Yan, L.: Thermal error characteristic analysis and modeling for machine tools due to time-varying environmental temperature. *Precis. Eng.* **47**, 231–238 (2017)
14. Malakizadi, A., Gruber, H., Sadik, I., Nyborg, L.: An FEM-based approach for tool wear estimation in machining. *Wear* **368–369**, 10–24 (2016)
15. Nieslony, P., Grzesik, W., Habrat, W.: Experimental and simulation investigations of face milling process of Ti-6Al-4V titanium alloy. *Adv. Manuf. Sci. Technol.* **39**, 39–52 (2015)

# Assessment of the Accuracy of High-Speed Machining of Thin-Walled EN AW-2024 Aluminium Alloy Elements Using Carbide Milling Cutter and with PCD Blades

Jozef Kuczmaszewski, Waldemar Login, Pawel Piesko  
and Magdalena Zawada-Michalowska

**Abstract** The paper presents an assessment of the accuracy of high-speed machining of thin-walled elements made of the EN AW-2024 aluminium alloy using two different tools: a milling cutter with carbide blades and a milling cutter with PCD blades. Additionally, the impact of so-called technological history effect on machining accuracy is also analysed. In the studied case, the rolling direction of the semi-finished product, longitudinal or transversal, is taken into account. The degree of post-machining deformations and the quality of sample surface after HSM are adopted as indicators describing machining accuracy. Based on the obtained results, it can be stated that depending on the adopted accuracy assessment criteria, i.e. shape error or machined surface quality, it is recommended to use carbide tools or tools with PCD blades.

**Keywords** Aluminium alloy · HSM · Thin-walled elements · Execution accuracy

## 1 Introduction

Currently, thin-walled elements are commonly used in industry, especially in aerospace, marine and automotive. Technologies such as riveting and welding are increasingly more often avoided during their production, while the produced so-called integral elements are fabricated entirely by machining, wherein up to 90% of the material is removed as chips [1–3].

One technology of thin-walled element production is high-speed machining (HSM), which—in comparison with conventional machining—is characterised primarily by increased cutting speed  $v_c$  and low depth of cut  $a_p$ . The values of the

---

J. Kuczmaszewski · P. Piesko · M. Zawada-Michalowska (✉)  
Department of Production Engineering, Faculty of Mechanical Engineering, Lublin  
University of Technology, Nadbystrzycka 36, 20-618 Lublin, Poland  
e-mail: m.michalowska@pollub.pl

W. Login  
PZL Mielec a Sikorsky Company, Wojska Polskiego 3, 39-300 Mielec, Poland

applied technological parameters depend on numerous factors, e.g. machined material grade, operation type and tool construction [4–7].

It is important that under HSM, the cutting force drops as machining speed  $v_c$  increases. Consequently, there are no clearly defined process parameters that delineate the boundary between conventional and high-speed machining, noticeable reduction in cutting force is assumed as the moment where HSM range begins. Additionally, an increase in machined surface quality can be noticed, as well as accelerated tool wear correlated with the increased machining speed  $v_c$  [4, 7].

The HSM process enables marked shortening of the proper machining time and consequently an increase in its effectiveness, which allows for a major reduction in production costs [4].

The disadvantages of thin-walled elements include increased roughness, resulting from the lower rigidity of machine-grip-workpiece-tool systems, and difficulties in maintaining dimension as well as shape accuracy, manifesting as, for example, deformations caused by “lingering” of residual stresses in the material’s surface layer [1–3, 8, 9].

Surface roughness is one of the indicators that determine the material’s machinability. It depends on many factors, e.g. machining parameters, machined material, used tool and other external features related to the system’s stability. Presently, modern tool materials enable achieving increasingly improved surface quality [5, 10–12].

Manufacture of thin-walled elements meets a range of problems linked to elastic and plastic deformations, forming during the machining and after its completion. Elastic deformations generate shape errors and vibrations, which adversely affect the accuracy and quality of processing. Plastic deformations cause residual stresses, difficult to remove from the element’s surface layer. They lead to permanent changes in shapes and dimensions, increasing costs and extending production time, for example, due to the need of using additional heat treatment [3, 7, 10, 13].

## 2 Methodology

The aim of the study was to assess the accuracy of high-speed machining (HSM) of thin-walled elements made of EN AW-2024 aluminium alloy using two different tools: a milling cutter with carbide blades and a milling cutter with PCD blades. Additionally, the impact of rolling direction, longitudinal or transversal (so-called technological history effect), on machining quality was analysed.

Machining tests were performed on Avia VMC 800HS vertical machining centre. Samples were made of EN AW-2024 T351 aluminium alloy, commonly utilised especially in the aircraft industry. Its chemical composition and selected mechanical properties are presented in Table 1.

**Table 1** Chemical composition and mechanical properties of EN AW-2024 T351 [14, 15]

Chemical composition [%]	Si	Fe	Cu	Mn	Mg	Cr	Zn	Ti
	0.5	0.5	3.8–4.9	0.3–0.9	1.2–1.8	0.1	0.25	0.15
Mechanical properties	Density, $\rho$	Young’s modulus, $E$		Tensile strength, $R_m$		Yield strength, $R_{p0.2}$		Brinell hardness
	2.78 g/cm <sup>3</sup>	73 GPa		430 MPa		290 MPa		122 HB

Three milling cutters were used in the experiments:

- Kennametal (25A03R044B25SED14) indexable end milling cutter with milling inserts (EDCT140416PDFRLDJ)—HPC—rough machining,
- Sandvik (R216.33-16040-AC32U H10F) carbide milling cutter—HSM—finish machining, and
- Bryk (D10.1603) milling cutter with PCD (polycrystalline diamond) blades—HSM—finish machining.

High performance cutting (HPC) technology was used for roughing, while high-speed machining (HSM) was employed for finishing. Table 2 summarises the values of technological parameters of both methods.

The degree of post-machining deformation (deflection values when clamping forces were removed) and surface quality of samples after HSM were taken as indicators of machining accuracy.

Sample deflection was measured using the Sylvac CL44 L = 36.5 digital sensor with low measurement pressure of 0.07 N ( $\pm 15\%$ ). This station included three main elements: said measuring instrument mounted in magnetic grip and fixed to the headstock of machining centre. The use of the SylConnect B1.072 software enabled measuring deflections of samples along with their entire length ( $l = 160$  mm) in three planes.

Surface roughness was measured with the Hommel Tester T1000 contact profilometer. Ra parameter—the arithmetic average of the absolute values of the roughness profile ordinates—was used to analyse surface quality.

**Table 2** Technological parameter values of both technologies

Technological parameters	Strategy	
	HPC	HSM
Depth of cut $a_p$ (mm)	4.3	0.4
Milling width $a_e$ (mm)	18.75	12
Cutting speed $v_c$ (m/min)	1000	1200
Feed per blade $f_z$ (mm/blade)	0.1	0.02
Rotational speed $n$ (rpm)	12,732	23,873
Feed rate $v_f$ (mm/min)	3820	1432
No. of passes $i$ [-]	2	1

**Fig. 1** Sample with measurement planes marked

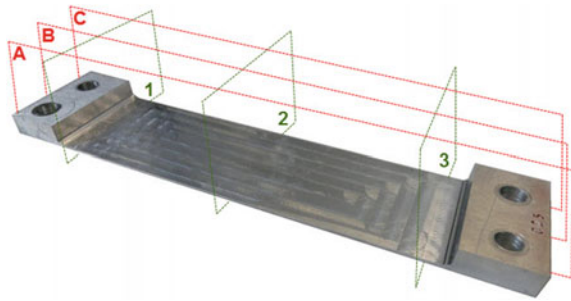


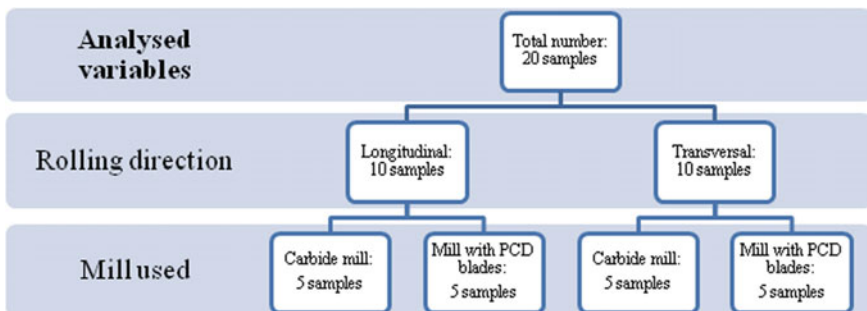
Figure 1 presents a sample after milling, with measurement planes marked. For deformation measurement purposes, they were designated with the following letters: A, B and C, while for roughness with the digits: 1, 2 and 3. Sample dimensions were length 210 mm, width 45 mm and thickness before machining 10 mm, while after milling—1 mm.

The total number of tested samples was 20. Ten samples were analysed for each of the two rolling directions, i.e. longitudinal and transversal, of which five samples were machined with a carbide milling cutter and five with a milling cutter with PCD blades (Fig. 2).

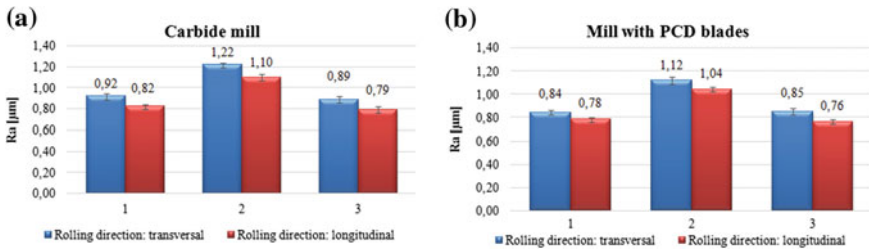
For each plane, measurements were made three times, for both deflection and roughness.

### 3 Results

The first part of the study concerned the comparison of quality of the obtained surfaces after high-speed machining (HSM) using two tools and for the following rolling directions: longitudinal and transversal (technological history effect). The analysis was performed based on Ra parameter. Figure 3 presents the values of Ra

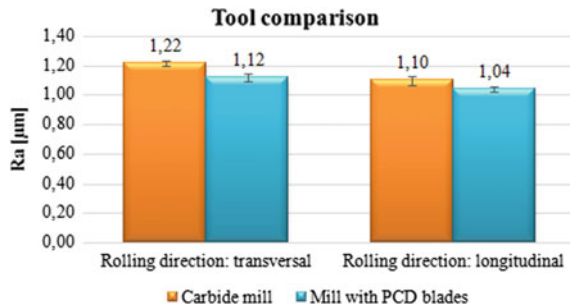


**Fig. 2** Variable analysis pattern



**Fig. 3** Values of Ra roughness parameter, obtained in three studied measurement planes for: **a** carbide milling cutter, **b** milling cutter with PCD blades and two rolling directions

**Fig. 4** Comparison of Ra roughness parameter values obtained in the central measurement plane (2) for the two rolling directions and tested milling cutters



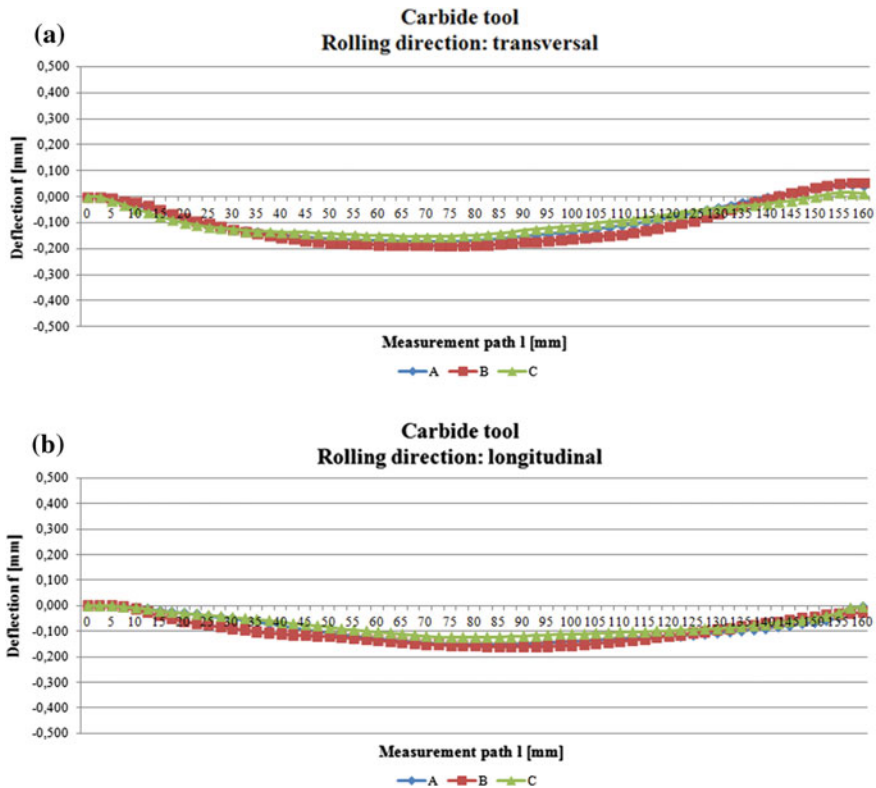
roughness parameter, obtained in the three measurement planes, 1, 2 and 3, for the carbide milling cutter (Fig. 3a) and for PCD blades (Fig. 3b), and for the two rolling directions. In both analysed cases, the highest values of Ra roughness parameter were obtained in the central measurement plane (2), for the carbide milling cutter,  $Ra = 1.22 \mu\text{m}$  (transversal direction) and  $Ra = 1.10 \mu\text{m}$  (longitudinal direction), and for the milling cutter with PCD blades,  $Ra = 1.12 \mu\text{m}$  (transversal direction) and  $Ra = 1.04 \mu\text{m}$  (longitudinal direction). Lower values of this parameter, and with smaller differences, were obtained for the extreme planes (1 and 3). Additionally, greater values of the Ra parameter were observed in samples subjected to the transversal rolling direction.

Figure 4 shows a comparison of Ra roughness parameter values measured on the central measurement plane (2) for the two rolling directions and tested tools. For this roughness parameter, higher values were obtained for carbide milling cutter, for both longitudinal and transversal rolling direction. Consequently, it was confirmed that HSM using a milling cutter with PCD blades is characterised by better surface quality.

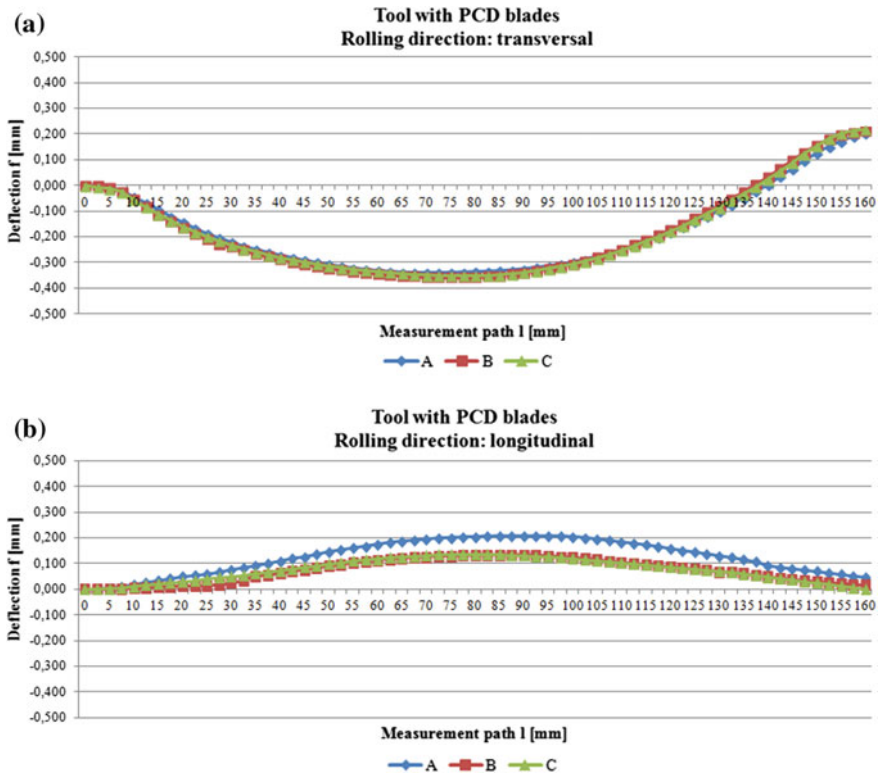
During the next stage of the study, post-machining deformations, which for the executed samples take the form of deflections, were measured and analysed. Deflection values  $f$  for samples machined with the carbide milling cutter, as a function of measurement path  $l$ , are presented in a graphical form in Fig. 5. The measurements were taken in three measurement planes: A, B and C (according to

Fig. 1) and the two rolling directions: transversal (Fig. 5a) and longitudinal (Fig. 5b). In every analysed case, the maximum deflection occurred in the middle of the sample's length, at  $l = 80$  mm. Additionally, only slight differences were noted between the measurement results for the three discussed planes. However, there are differences visible in deflection values for samples with transversal and longitudinal rolling directions. In the central plane B, the following were obtained:  $f_{\max} = -0.189$  mm (transversal direction) and  $f_{\max} = -0.160$  mm (longitudinal direction). The minus sign denotes deviation below the “zero” line connecting the ends of the sample.

Next, post-machining deformations of samples machined with the milling cutter with PCD blades were analysed. Figure 6 presents sample deflection  $f$  as a function of measurement path  $l$  obtained in the three tested areas: A, B and C, for the transversal (Fig. 6a) and longitudinal (Fig. 6b) rolling directions. Also for this tool, the maximum deflection was obtained in the middle of the sample's length, at  $l = 80$  mm. Furthermore, greater deformation values were observed for the front plane A, which



**Fig. 5** Sample deflection  $f$  as a function of measurement path  $l$ —obtained in three measurement planes, for the carbide milling cutter and the following rolling directions: **a** transversal, **b** longitudinal



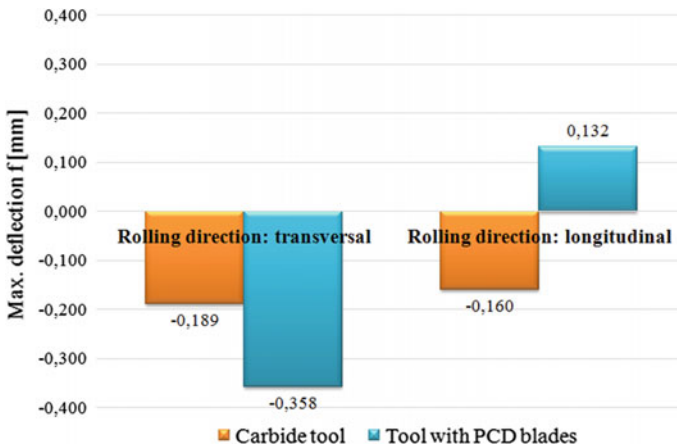
**Fig. 6** Sample deflection  $f$  as a function of measurement path  $l$ —obtained in three measurement planes, for the milling cutter with PCD blades and the following rolling directions: **a** transversal, **b** longitudinal

may indicate that the studied element has been twisted. Differences between the other two areas were insignificant. Additionally, the use of a milling cutter with PCD blades caused a “positive” deflection (deviation located above the “zero” line) to occur for longitudinal rolling direction. The maximum deflection in the central area B was  $f_{max} = -0.358$  mm (transversal direction) and  $f_{max} = 0.132$  mm (longitudinal direction).

A summary of the maximum deflection values  $f_{max}$  in the central measurement plane (B), with all analysed variables taken into account, is presented in Fig. 7.

The results summary (Fig. 7) confirms that greater post-machining deformations were obtained for the milling cutter with PCD blades. Additionally, a significant impact of the rolling direction was observed. For both tools, greater deflection values were obtained for the transversal rolling direction.





**Fig. 7** Summary of maximum deflection values  $f_{\max}$  in the central measurement plane for two rolling directions and the tested tools

## 4 Conclusion

The experimental test results allow for formulating the following conclusions:

- Surface quality
  1. The highest values of Ra roughness parameter were obtained in the central measurement area. This is mostly the result of the longest distance of plane B from the element mounting points during processing; in that place, the material is exposed to greater effects of vibrations.
  2. Inferior surface quality was observed for transversal rolling direction; this may be caused by phenomena caused by cutting of grains, elongated in the rolling process, during the machining process. This also demonstrates that a relation between rolling direction and roughness exists.
  3. Higher values of Ra roughness parameter were obtained for the carbide tool. This means that better surface quality can be achieved using milling cutter with PCD blades.
- Post-machining deformations
  4. The fabricated thin-walled elements underwent significant deformations, which resulted from the occurrence of residual and post-machining stresses in the surface layer.
  5. In every analysed case, the maximum deflection was noted in the middle of the sample's length, at  $l = 80$  mm.
  6. For both tools, greater deflection values were obtained for transversal rolling direction.

7. For the milling cutter with PCD blades, the highest deformation value (compared to other areas) was observed in the front plane A. This may indicate twisting of the tested elements.
8. For tool with PCD blades and longitudinal rolling direction, a different deflection form was obtained that in all other cases, namely it has a positive value.
9. Greater post-machining deformations were observed with the milling cutter with PCD blades.

The obtained results are not conclusive, as elements fabricated using the carbide tool underwent lesser deformations, compared to ones processed with the milling cutter with PCD blades, but at the same time had inferior surface quality. Depending on the adopted accuracy assessment criteria, i.e. shape error or machined surface quality, it is recommended to use carbide tools or tools with PCD blades.

### Acknowledgements



Study conducted as part of the INNOLOT sector project (Acronym BloStEr) titled “Development of innovative mechanical connections for the purpose of replacing conventional connections in aircraft structures” (“Opracowanie innowacyjnych połączeń mechanicznych celem zastąpienia konwencjonalnych połączeń w strukturach lotniczych”), coordinated by PZL Mielec Sp. z o.o., subsidised from National Research and Development Centre and European Union funds under the European Regional Development Fund within the scope of the Innovative Economy Operational Programme. Priority I, Action 1.5 IE OP., agreement no. INNOLOT/I/5/NCBR/2013

### References

1. Ab-Kadir, A.R., Osman, M.H., Shamsuddin, K.A.: A comparison of milling cutting path strategies for thin-walled aluminium alloys fabrication. *Int. J. Eng. Sci.* **2**(3), 1–8 (2013)
2. Agrawal, A., Singh, A.: Comparison of deforming forces, residual stresses and geometrical accuracy of deformation machining with conventional bending and forming. *J. Mater. Process. Technol.* **234**, 259–271 (2016)
3. Awan, W.S., Mabrouki, T.: Numerical and experimental investigations of post-machining distortions in thin machined structures considering material-induced residual stress. *J. Braz. Soc. Mech. Sci. Eng.* **39**(2), 509–521 (2017)
4. Erdel, B.P.: *High speed machining*, Dearborn (2003) (SME)
5. Kuczmaszewski, J., Pieško, P., Zawada-Michałowska, M.: Surface roughness of thin-walled components made of aluminium alloy EN AW-2024 following different milling strategies. *Adv. Sci. Technol. Res. J.* **10**(30), 150–158 (2016)
6. Twardowski, P.: Influence of dynamics process milling of hardened steel on machined surface roughness in HSM conditions (in Polish). *Archiwum Technologii Maszyn i Automatykacji* **40**(2), 183–192 (2008)

7. Zębala, W.: Errors minimalisation of thin-walled parts machining (in Polish). *InżynieriaMaszyn* **15**(3), 45–54 (2010)
8. Chen, B., Luo, M., Ma, J., Wu, B., Zhang, D.: Vibration suppression of thin-walled workpiece machining considering external damping properties based on magnetorheological fluids flexible fixture. *Chin. J. Aeronaut.* **29**(4), 1074–1083 (2016)
9. Ding, H., Wu, Y., Yuan, Y., Zhang, H.T., Zhu, T.: Bayesian learning-based model-predictive vibration control for thin-walled workpiece machining processes. *IEEE/ASME Trans. Mechatron.* **22**(1), 509–520 (2017)
10. Becker, A.A., Liu, S., Ratchev, S.: Error compensation strategy in milling flexible thin-wall parts. *J. Mater. Process. Technol.* **162–163**, 673–681 (2005)
11. Cellary, A., Chajda, J., Wieczorowski, W.: Guidebook to measurement of surface irregularity, i.e.: roughness and not Orly (in Polish), Poznań (2003) (Politechnika Poznańska)
12. Oczos, K.E., Kawalec, A.: Processing of light metal (in Polish), Warszawa (2012) (PWN)
13. Kuczmaszewski, J., Pieško, P., Zawada-Michałowska, M.: Analysis of cutting speed influence on the deformation of thin-walled elements made of aluminium alloy EN AW-2024 after milling (in Polish). *Mechanik* **8–9**, 1066–1067 (2016)
14. PN-EN 573-3:2014-02. Aluminium and aluminium alloys. Chemical composition and form of wrought products. Part 3: Chemical composition and form of products
15. PN-EN 485-2:2016-10. Aluminium and aluminium alloys. Sheet, strip and plate. Part 2: Mechanical properties

# Effect of Heat Treatment on Mechanical Properties of Inconel 625/Steel P355NH Bimetal Clad Plate Manufactured by Explosive Welding

Robert Kosturek, Michal Najwer, Piotr Nieslony  
and Marcin Wachowski

**Abstract** In this investigation, steel P355NH was successfully clad with Inconel 625 through the method of explosive welding. Explosively welded bimetal was subjected to the two separated heat treatment processes: stress relief annealing (at 620 °C for 90 min) and normalizing (at 910 °C for 30 min). In order to examine the quality of joint and effects of heat treatments, the mechanical properties of the obtained samples were evaluated by tensile test, shear test, Charpy impact test and bend test. It was found that tensile strength of explosively welded bimetal is higher than tensile strength of the base material in the as-received state. Compared to the bimetal clad plate without heat treatment, bimetal subjected to the stress relief annealing has improved mechanical properties. It was stated that stress relief annealing is recommended heat treatment for Inconel 625/steel P355NH bimetal clad plate obtained by explosive welding.

**Keywords** Heat treatment · Explosive welding · Steel P355NH  
Inconel 625 · Mechanical properties

## 1 Introduction

P355NH is a non-alloy elevated temperature quality steel, commonly used in construction of pressure vessel tanks. Unfortunately, the corrosion susceptibility of this steel limits its applications in the chemical industry. This problem can be solved by cladding P355NH steel plate with layer of Inconel 625, which is nickel-based superalloy having excellent corrosion and oxidation resistance [1]. Explosive

---

R. Kosturek · M. Wachowski  
Military University of Technology in Warsaw, Warsaw, Poland

M. Najwer · P. Nieslony  
Opole University of Technology, Opole, Poland

M. Najwer (✉)  
EXPLOMET High-Energy Techniques Works, Opole, Poland  
e-mail: [michal.najwer@explomet.pl](mailto:michal.najwer@explomet.pl)

welding is appropriate technology to produce such bimetal clad plate. In this solid state, welding process materials are joined during high-velocity collision caused by detonation of high-explosive material [2–4]. Due to very high pressure and dynamics of the explosive welding process, the mechanical properties and structure of the joining materials in the bond area change significantly. As an effect of the plastic deformation during collision, the materials are subjected to the high strain hardening, which not only improves their strength and hardness, but also causes residual stress in the joint. In order to decrease those effects, the obtained joint should be subjected to the heat treatment [5–7].

## 2 Results of the Research

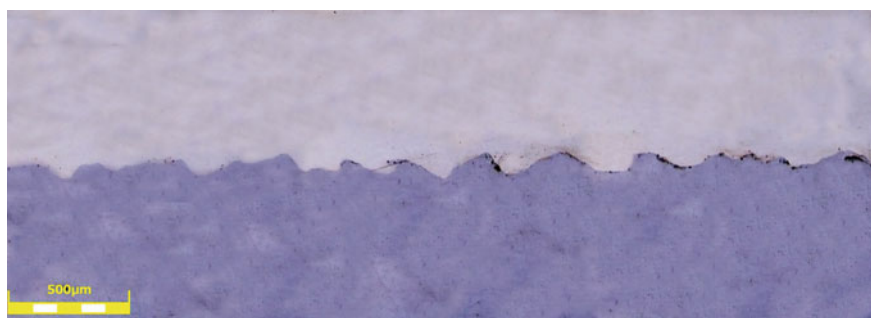
Mechanical properties of Inconel 625 and steel P355NH in the as-received state are presented in Table 1.

Inconel 625/steel P355NH bimetal clad plate was obtained by explosive welding process. In this research, three kinds of samples were examined in terms of their mechanical properties: 3/5, 3/5 OCO and 3/5 OCN. Sample 3/5 was not subjected to any heat treatment, sample 3/5 OCO was subjected to the stress relief annealing, and sample 3/5 OCN was subjected to the normalizing. Welding interface of the explosively obtained joint is shown in Fig. 1. Parameters of the heat treatments are presented in Table 2.

**Table 1** Mechanical properties of Inconel 625 and steel P355NH in the as-received state

Material	$R_e$ (MPa)	$R_m$ (MPa)	A (%)	KV, J (avg.)
Inconel 625	476	872	50	–
P355NH	445	551	30	77

$R_m$  tensile strength,  $R_e$  yield strength, A elongation, KV impact toughness



**Fig. 1** Light microscopy image of the bond area showing the wavy shape of the interface

**Table 2** Parameters of the heat treatments: stress relief annealing (3/5 OCO) and normalizing (3/5 OCN)

Sample	Heating		Soaking		Cooling
	Temp. (°C)	Rate (°C/h)	Temp. (°C)	Time (min)	Rate (°C/h)
3/5 OCO	300	100	620	90	100, from 300 °C cooling in still air
3/5 OCN	100	100	910	30	Cooling in still air

**Table 3** Results of the tensile test

Sample	R <sub>e</sub> (MPa)	R <sub>m</sub> (MPa)	A (%)
		≥ 355	490–630
3/5	479	567	31
3/5 OCO	383	543	32
3/5 OCN	308	522	32

R<sub>e</sub> yield strength, R<sub>m</sub> tensile strength, A elongation

## 2.1 Tensile Test

Tensile test allows to establish mechanical properties such as yield strength, tensile strength and elongation of a material. According to PN-EN 13445:2014, the test was conducted only on base plate material [8]. Results and acceptable ranges are presented in Table 3.

## 2.2 Charpy Impact Test

Charpy impact test measures the amount of energy absorbed by a material during fracture. For each kind of sample, the test was conducted three times in temperature –20 °C. Similarly to tensile test, Charpy impact test is also performed only on base plate material. Results and acceptable range are presented in Table 4.

**Table 4** Results of the Charpy impact test

Sample	1, J (min. 16 J)	2, J (min. 16 J)	3, J (min. 16 J)	$\bar{x}$ , J (min. 23 J)
3/5	119	145	132	132
3/5 OCO	137	142	138	139
3/5 OCN	53	101	103	86

1, 2, 3 number of test,  $\bar{x}$  average value



Fig. 2 Specimen with technological set prepared for shear test

Table 5 Results of the shear test and bend test

Sample	$R_s$ (MPa)	Shear	Bend test
3/5	572	In joint	Positive
3/5 OCO	591	In joint	Positive
3/5 OCN	383	In joint	Positive

$R_s$  shear strength

### 2.3 Shear Test and Bend Test

The aim of shear test and bend test is to evaluate the quality of joint. Bend test is performed by the side bending of a sample by angle  $180^\circ$  and the examination of joint for any defects. In shear test, according to PN-EN13445:2014, the minimum shear strength of material must be equal to 140 MPa. The specimen with technological set is presented in Fig. 2. Results of the both test are presented in Table 5.

## 3 Discussion

Inconel 625/steel P355NH bimetal clad plate was successfully obtained in explosive welding process. The welding interface has characteristic wavy shape. Comparing to the as-received state, the mechanical properties of base plate material have increased slightly due to explosive welding process. High velocity collision during explosive welding process results in the strain hardening of the base plate material, which increases its yield strength by 35 MPa and its tensile strength by about 15 MPa. Although the mechanical properties of bimetal clad plate in as-welded condition contains within the acceptable range according to PN-EN 13445:2014, in order to eliminate residual stress the bimetal clad plate was subjected to the two different types of the heat treatment. The first proposed heat treatment was stress relief annealing, in which a material was heated to the temperature  $610^\circ\text{C}$  and soaked for 90 min. Due to this heat treatment, yield strength of

base plate material was decreased by about 100 MPa and tensile strength by about 25 MPa. At the same time, results of the Charpy impact test and shear test were changed slightly. Bimetal clad plate after normalizing at 910 °C for 30 min has decreased its mechanical properties significantly compared to joint in as-welded state. The results of tensile test show increasing of base plate material plasticity after normalization, its yield strength is lower than in as-welded state by about 170 MPa and is equal to 308 MPa which does not meet the standards according to PN-EN 13445:2014. The softening of base plate material and reduction of joint strength after normalization have been observed in decreasing of impact toughness and shear strength. The results of shear test and bend test show good quality of joint in all samples.

## 4 Conclusions

- (1) Stress relief annealing of Inconel 625/steel P355NH bimetal clad plate decreases yield strength of base plate material by about 100 MPa compared to as-welded state.
- (2) Bimetal clad plate after normalization at 910 °C for 30 min has lower yield strength of base plate material than base plate material in as-received state. Based on the results of tensile test, further research will be undertaken in order to examine effects of normalization on the bimetal clad plate structure.
- (3) Stress relief annealing at 620 °C for 90 min of Inconel 625/steel P355NH clad plate gives a positive effect of decreasing yield strength and retaining other mechanical properties such as tensile strength, impact toughness and shear strength. Lower yield strength compared to as-welded state is important in terms of further plastic working of bimetal, e.g. forming of dished ends and vessel heads for chemical industry.

**Acknowledgements** This work uses results of the research from the project M-Era.net “Novel explosive welded corrosion resistant clad materials for geothermal plants”, co-financed from The National Centre for Research and Development of Poland (No DZP/M-ERA.NET-2013/2309/2014).

## References

1. Dobrzański, L.: Metal engineering materials. WNT, Warsaw (2004)
2. Nieslony, P., Cichosz, P., Krolczyk, G.M., Legutko, S., Smyczek, D., Kolodziej, M.: Experimental studies of the cutting force and surface morphology of explosively clad Ti–steel plates. *Measurement* **78**, 129–137 (2016)
3. Nieslony, P., Krolczyk, G.M., Zak, K., Maruda, R.W., Legutko, S.: Comparative assessment of the mechanical and electromagnetic surfaces of explosively clad Ti-steel plates after drilling process. *Precis. Eng.* **47**, 104–110 (2017)



4. Gałka, A., Najwer, M.: Explosive cladding of titanium and aluminium alloys on the example of Ti6Al4 V—AA2519. *Arch. Metall. Mater.* **60**, 2985–2991 (2015)
5. Prażmowski, M., Paul, H., Žok, F.: The effect of heat treatment on the properties of zirconium—carbon steel bimetal produced by explosion welding. *Arch. Metall. Mater.* **59**(3), 1143–1149 (2014)
6. Findik, F., Yilmaz, R., Somyurek, T.: The effects of heat treatment on the microstructure and microhardness of explosive welding. *Sci. Res. Essays* **6**, 4141–4151 (2011)
7. Manesh, H.D., Taheri, A.K.: The effect of annealing treatment on mechanical properties of aluminum clad steel sheet. *Mater. Des.* **24**, 617–622 (2003)
8. PN-EN 13445:2014, Technical delivery conditions for clad products for pressure purposes

# Alternative Methods of Chemical Pre-Treatment on Hot-Dip Galvanization Surface for Adhesion Organic Coatings

Jakub Svoboda, Jan Kudlacek, Viktor Kreibich  
and Stanislav Legutko

**Abstract** The first part of this paper deals about chemical surface pre-treatments of zinc and the impact of alternative pre-treatments for adhesion of organic coating. The second part is devoted to the experimental part, and there was created several surface pre-treatments of hot-dip galvanization and subsequently applied two kinds of organic coatings. The objective was a comparison of chemical pre-treatments, mechanical pre-treatment and the effect each of them on the adhesion of the organic coating. It was created seven variants pre-treatment of hot-dip galvanization surfaces. Adhesion of these systems was investigated by pull-off test according to ČSN EN ISO 4624, adhesion test with X-cut tape test according to ASTM D 3359, adhesion crosscut test according to ČSN EN ISO 2409. In this work was investigated two coating systems at six chemical and one mechanical pre-treatment of the surface of the hot-dip galvanization.

**Keywords** Conversion layers · Adhesive · Zinc coating · Organic coating  
Chemical pre-treatment

---

J. Svoboda (✉) · J. Kudlacek (✉) · V. Kreibich  
Department of Manufacturing Technology, CTU in Prague,  
Faculty of Mechanical Engineering, Technická 4, Praha 6, Czech Republic  
e-mail: jakub.svoboda1@fs.cvut.cz

J. Kudlacek  
e-mail: jan.kudlacek@fs.cvut.cz

S. Legutko  
Institute of Mechanical Technology, Poznan University of Technology,  
M. Sklodowskiej-Curie 5, 60-965 Poznan, Poland

## 1 Introduction

Duplex system is one type of surface treatment material, where the total protection system consists of a zinc coating and coating paints. These systems are frequent technology corrosion protection. With the highest life is then a method for protection of steel structures, especially in atmospheric conditions.

Concentration of the coating system and the zinc coating to prolong the lifetime of the system up to 100 years, but depending on the aggressive corrosive environments, and many other factors [1, 2].

Galvanized sheets are usually protected from the corrosive environment conversion coatings (phosphate, chromate, etc.) and are provided with organic coatings which provide barrier protection against corrosion. The conversion layer is created particularly for higher corrosion resistance, but also to improve the adhesion of organic coatings, provides sufficient porosity and roughness for adhesion of organic coatings [3]. However, there are many methods for producing conversion layers on the basis on phosphate, chromate, modified types of ferrous phosphate, Ti–Zr conversion layers, etc. Each of the above-mentioned chemical surfaces pre-treatment has own effect on the adhesion of organic coatings, which is also the subject of investigation of this work.

## 2 Conversion Layers

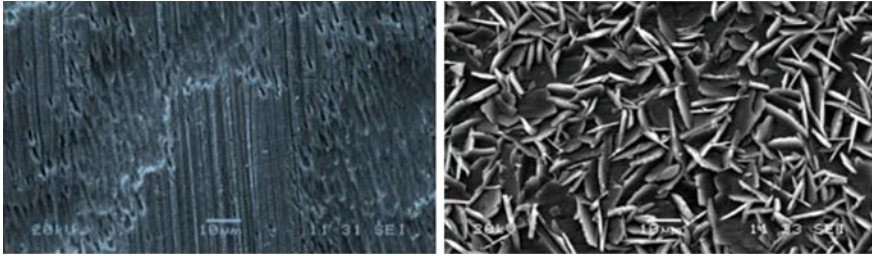
### 2.1 Phosphating

It is the most chemical treatment of steel in which are formed on the surface of the tertiary phosphates of zinc, calcium, and manganese. Other capabilities of these layers are binding certain organic substances on their surface. These include petrolatum, impregnating oils, but especially paints. Phosphate coatings are also used to form the insulating properties at the surface of transformer sheets to reduce friction of the moving parts [4, 5].

Using phosphates under organic coatings increases the corrosion resistance of the whole system. Phosphate layer prevents corrosion of paint systems and increases the adhesion to the metal surface. To increase adhesion is required fine grained layers of individual crystals ( $10\text{--}60\text{ mg dm}^{-2}$ ), because thick layers of phosphate lead to the release of the individual crystals (Fig. 1).

### 2.2 Chromating

It is a widely used method of passivation is used to improve the corrosion resistance and adhesion of organic coatings especially for nonferrous metals, for example, zinc, aluminum, and cadmium coatings.



**Fig. 1** Left: SEM image an amorphous of ferrous phosphate, Right: SEM image hopeite crystals of zinc phosphate [12]

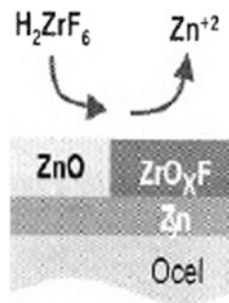
Electrolytic galvanizing and subsequent treatment of the zinc surface with chromate conversion layers is now very widespread, but it is an effort to replace these conversion layers with new alternative chemical pre-treatments. Chromate coatings provide improved corrosion resistance of zinc coatings mainly due passivation effect of chromium compounds present in the coating [4]. Chromate bath may be alkaline or acidic type.

### ***2.3 Alternative Technologies for the Ferrous Phosphating and Chromating***

Chemical pre-treatment is an essential step process for producing conversion layers, in particular, steel, aluminum, and zinc materials. With these surface pre-treatments, we achieve increase adhesion of the coating system and the overall corrosion resistance. Traditional surface preparation before application of organic paints is now turned into those more environmentally friendly. However, it was proved that some alternative conversion layers are not able to have a corrosion resistance, such as is the case of conversion layers on the basis of Cr [6], although certain sources describe an almost identical or even higher corrosion resistance of these alternative chemical surface pre-treatment of low carbon steel, particularly  $\text{TiO}_2$  and  $\text{ZrO}_2$  [7, 8].

Conversion layer based on Ti or Zr in recent years becomes a major alternative to the chemical pre-treatment based on chromium. Pre-treatment of Ti/Zr has not been studied as extensively as chromium pre-treatment, and their effects are less well known [6]. For these applications, the most commonly used coatings based on zirconium and titanium secreted from solutions containing fluorozirconate (Bonderite NT 1 TecTalis) but also coatings hydrolyzed organosilicate (Dynasilan Degussa ff.) [9]. The phosphate conversion coatings are increasingly replacing various alternatives, mainly because of environmental friendliness, energy, and other procedural aspects [10].

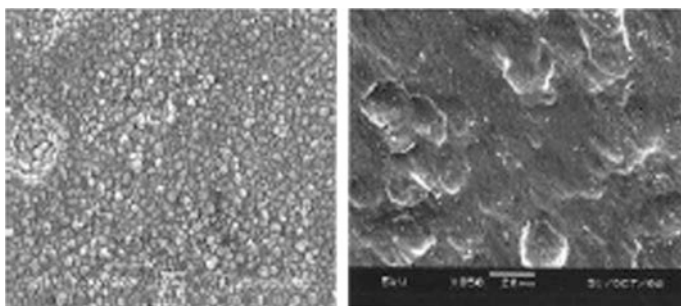
**Fig. 2** Reactions in the formation of layers [9]



In the current time, other promising technologies have emerged that can fairly well to replace phosphates and trivalent chromates. In particular, the use of zirconium oxide on the surface using the sol—gel method, or immersion in acid H<sub>2</sub>ZrF<sub>6</sub>. It has been found that coatings ZrO<sub>2</sub>, thicknesses of 18–30 nm provide a higher corrosion resistance compared to conventional phosphates. These methods are also commonly used for chemical pre-treatment of hot-dip galvanized coating. Zircon absorbed in surface layers most often occurs as a zirconia (ZrO<sub>2</sub>).

It was found that zirconium oxide layers 50 nm or less have comparable resistance to conventional chromate and phosphate [8].

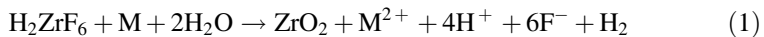
Today, new TecTalis® surface pre-treatment, which is commercially available, is based on acid H<sub>2</sub>ZrF<sub>6</sub> and fully replaces the phosphating process. This product can be applied by spraying or by immersion at room temperature does not require sealed with chromic acid and can be used on a variety of metal surfaces (steel, aluminum, zinc). The bath is based on dilute H<sub>2</sub>ZrF<sub>6</sub> (Zr < 200 mg l<sup>-1</sup>) with a small amount of Si and Cu for improved long-term performance bath [7] (Figs. 2, 3).



**Fig. 3** Appearance of the coating Zn phosphate (left) TecTalis (right) [9]

**TecTalis reaction during layer formation**

pH = 3.8–4.8,  $T = 10\text{--}50\text{ }^{\circ}\text{C}$ , Time = 30–180 s, reaction:



M = basic material

### 3 Experimental Part

In the experimental part were used two paints: ZINOREX (S2211—Acrylic semi-gloss single layer paint for steel and zinc) and AXAPUR (U2218—polyurethane semi-gloss two component single layer paint). These coatings were applied to pretreated zinc surfaces. Another objective of the experimental part was to verify the physical–mechanical properties of coating systems.

For experimental section was created seven variants of the pre-treatment hot-dip galvanized samples, six chemical and one mechanical surface preparation:

1. SurTec678, 2. Pragokor BP, 3. Nanotech cs-one, 4. Interlox 5705, 5. Activation with  $\text{HNO}_3$ , 6. Light blasting, 7. Degrease of hot-dipped galvanized samples.

**SurTec 678**

Trivalent passivation for zinc and alloys of zinc/nickel, is a highly concentrated product, containing Cr (III) and cobalt salts.

**Pragokor BP**

This is a composition that does not contain chromate ions, chromium, or other environmentally harmful substances. The passivation effect of this product is higher than the range of compositions based on chromate ion. Furthermore, it can be used to passivate the active surfaces of non-phosphated steel, aluminum and magnesium alloys, zinc and tin coatings, zinc castings after degreasing, or other activated surface.

**Nanotech cs-one**

Nanotech cs-one product is supplied from a Turkish company CHEMSOLL—chemical laboratories solution, it is an alternative method of phosphating iron and zinc. Eliminates the disadvantages of the use of phosphate baths and according to the manufacturer should provide effective adhesion and long life of the coating versus phosphate. On the surface material are formed transparent nano-ceramic surface [11].

**Interlox 5705**

Interlox 5705 contains a two-component bath free of chromium, which creates a conversion layer on aluminum, aluminum alloys, magnesium, zinc, and steel. This is a composition which enhances the corrosion protection of parts of a cast and

wrought aluminum alloys. It provides a basic layer on aluminum, zinc, and steel before wet and powder coating, and its Qualicoat approved pre-treatment (A-65).

This product is not recommended for steel passivation without subsequent painting.

#### **Activation with HNO<sub>3</sub>**

In this case, the chemical pre-treatment of the surface of the zinc was the activation of the zinc coating with an alkaline degreasing and nitric acid (HNO<sub>3</sub>). This chemical pre-treatment is useful for activation of surface, without the thin oxide layers.

#### **Light blasting**

For comparison, mechanical and chemical pre-treatments were selected mechanical pre-treatment using light blasting. Light blasting technology in the pre-treatment of zinc coatings is still very popular and effective pre-treatment prior to application of organic coating systems. The main objective of this pre-treatment is to achieve a perfectly clean surface, free from corrosion products of zinc, and a rough surface for the subsequent application of other finishes. The experimental part was chosen abrasive resource (brown artificial corundum).

Light blast zinc coating should ensure a minimum consumption of zinc layer, mostly in terms of removing the surface layer up to 10 microns. Samples were blasted by a pneumatic blasting equipment PTZ 100 I by S.A.F. setting the nozzle pressure of 0.5 MPa.

#### **The degreased hot-dipped galvanized samples**

For comparison of the various pre-treatments of the hot-dip galvanization, samples were prepared only alkali-degreased using a degreasing product Simple Green in a concentration of 1:30.

### ***3.1 Verification Physico-Mechanical Properties of the Coating Systems***

They were investigated various test procedures for the determination of physico-mechanical properties of coating systems.

- (a) Determine the thickness of coatings according to DIN EN ISO 2808 nondestructive electromagnetic method. The type Elcometer 456.
- (b) Determine the adhesion of coatings cut test according to DIN EN ISO 2409.
- (c) Determine the adhesion of paint tear test according to DIN EN ISO 4624.
- (d) Determination of adhesion and crosscut according to ASTM D 3359.

### 3.2 Comparison of Various Pre-Treatments

The results show that good adhesive strength reached with use a coating system AXAPUR (U2218), which was formed by the paint itself AXAPUR and hardener C 7002. These are polyurethane coatings which were applied with a ruler. In all applications of this, coating system was applied one layer, which was achieved excellent result in terms of adhesion and coating quality after curing the coating system. In the case of an acrylate coating system ZINOREX (S2211) in many applications low adhesive strengths were achieved. Reasons for the poor quality of the coating can be different; it could be an unsatisfactory application temperature or temperature curing paint shop also inadequate moisture for the application of paints or poor mixing of the individual components of the coating system. Finally, it could be a chemical reaction of the zinc surface pre-treatment with the ZINOREX (S2211). The causes will be investigated further (Table 1).

## 4 Experimental Part

It is obvious that some alternative method of passivating the surface of hot-dip galvanized parts can compete with today trivalent passivation in the adhesion of paint systems. Particularly in comparison product SurTec 678, which is a trivalent

**Table 1** Summary of test results for individual adhesion of surface preparation the hot galvanization zinc

Pre-treatment + Coating system Zinorex (S2211)	The average adhesive strength [MPa]
Surtec 678	0.34
Pragokor BP	0.59
Nanotech cs-one	0.15
Interlox 5705	2.13
HNO <sub>3</sub>	4.63
Light blasting	3.27
Degreased samples	2.69
Pre-treatment + Coating system AXAPUR (U2218)	
Surtec 678	12.46
Pragokor BP	7.37
Nanotech cs-one	7.42
Interlox 5705	15.63
HNO <sub>3</sub>	18.13
Light blasting	18.53
Degreased samples	14.12

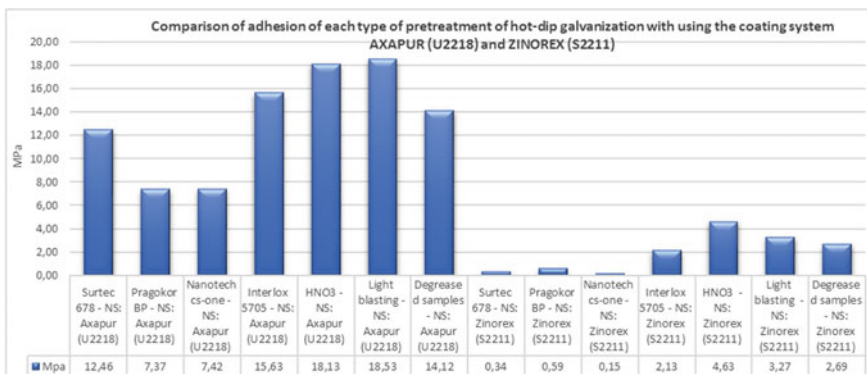


transparent passivation to zinc and alloys of Zn/Ni achieved tension using coating system AXAPUR (U2218) values of adhesive strength on average 12.46 MPa, whereas the alternative methods Interlox 5705, which constitute a two-component spa containing chromium, which produces the conversion coating on aluminum, aluminum alloys, magnesium, zinc, and steel, reached values adhesive strength of coating system AXAPUR (U2218) on average 15.63 MPa. When using other alternative methods of surface passivation of hot-dip galvanized components Pragokor BP, which is free chromate passivating based on agents containing hexafluorozirconates and ammonium hydrogen difluoride. When CS AXAPUR (U2218) was used the adhesive strengths on average 7.37 MPa were achieved. AXAPUR (U2218) values adhesive strength on average 7.37 MPa. It should be noted that this is still an adhesive strength, which corresponds with according of the internal regulations for the protection of hot-dip galvanized structures, more than 5 MPa. Another alternative method was investigated by Nanotech cs-one, which is a new generation of nano-ceramic coatings. In this application, using the coating system AXAPUR (U2218) was achieved adhesive strength on average 7.42 MPa, and the main advantage of this product is low-temperature applications without necessarily degreasing.

The best results in terms of adhesion of the chemical pre-treatment the zinc reached degreasing and subsequent activation of the surface using HNO<sub>3</sub> with coating system AXAPUR (U2218). The adhesive strengths are in average 18.13 MPa. This chemical pre-treatment is from an economic point of view very interesting, but the problem is the high toxicity and the dangers of handling this acid, there is a problem with many European regulations. Under regulation European directive no. 1272/2008, the substance is classified as dangerous.

When activating the surface using HNO<sub>3</sub> is achieved comparable adhesive strength, as when using a mechanical pre-treatment light blasting, adhesive strength 18.53 MPa.

The results of the experimental part are obvious that some alternative chemical pre-treatment of the surface of the zinc are comparable with today trivalent



**Fig. 4** Comparison of adhesion of each type of pre-treatment of hot-dip galvanization with using the coating system AXAPUR (U2218) and ZINOREX (S2211)

passivation, and many of them can cope even the most commonly used mechanical pre-treatment of the surface of the zinc, a light blasting. Use of these methods will be further examined (Fig. 4).

**Acknowledgements** The research was financed by The Technology Agency of the Czech Republic (TACR), Competence Centre (CVPÚ)—Research Centre Of Surface Treatment TE02000011.

## References

1. Povrchová úprava. Aktuální problémy vytváření povlaku typu duplex na podkladech zinkovaných ponorem [online] [cit. 2015-03-14]. Available from: <http://povrchovauprava.cz/clanek/49/aktualni-problemy-vytvareni-povlaku-typu-duplex-na-podkladech-zinkovanych-ponorem>
2. Časopis Povrcháři. Duplexní povlaky ocelových konstrukcí [online] [cit. 2015-03-14]. Available from: [http://www.povrchari.cz/kestazeni/201201\\_povrchari.pdf](http://www.povrchari.cz/kestazeni/201201_povrchari.pdf)
3. Bajat, J.B., Mišković-Stanković, V.B., Popić, J.P., Dražić, D.M.: Adhesion characteristics and corrosion stability of epoxy coatings electrodeposited on phosphated hot-dip galvanized steel. *Prog. Org. Coat.* **63**(2), 201–208 (2008)
4. Kreibich, V.: *Teorie a technologie povrchových úprav*, Ed. 1, Praha: České vysoké učení technické, 1996. ISBN 800101472X
5. Xu, L., Zhang, E., Yang, K.: Phosphating treatment and corrosion properties of mg-mn-zn alloy for biomedical application. *J. Mater. Sci. - Mater. Med.* **20**(4), 859–867 (2009)
6. Saarimaa, V., Kauppinen, E., Markkula, A., Juhanoja, J., Skrifvars, B.J., Steen, P.: Microscale distribution of Ti-based conversion layer on hot dip galvanized steel. *Surf. Coat. Technol.* **206** (19–20), 4173–4179 (2012)
7. Zhou, J., Chen, X., Duan, H., Ma, J.: Synthesis and characterization of organic fluorine and nano-SiO<sub>2</sub> modified polyacrylate emulsifier-free latex. *Prog. Org. Coat.* **89**, 192–198 (2015)
8. Adhikari, S., Unocic, K.A., Zhai, Y., Frankel, G.S., Zimmerman, J., Fristad, W.: Hexafluorozirconic acid based surface pretreatments: characterization and performance assessment. *Electrochim. Acta* **56**(4), 1912–1924 (2011)
9. Szelag P., Pragochema, spol. s.r.o.—internal pdf document for teaching. Železnaté fosfátování [cit. 2016-04-29]
10. Ooij, W.J., Sabata, A.: Chemical stability of phosphate conversion coatings on cold-rolled and electrogalvanized steels. *Surf. Coat. Technol.* **39–40**(2), 667–674 (1989)
11. Chemsoll.com—internet source. Nanotech CS-ONE. [online] [cit. 2016-06-07]. Available from: <http://www.chemsoll.com/kategori/nanotech-cs-one>
12. Pokomy, P., Mejta, V., Szelag, P.: Povrchová úprava: Příspěvek k teoretickým základům tvorby fosfátového povlaku [online]. Hradec Králové: IMPEA, s. r. o., 2011, VII [cit. 2012-05-01]. ISSN 1801-707X

# Influence of Machining Conditions on the Energy Consumption and Productivity in Finish Hard Turning

Roman Chudy, Wit Grzesik and Krzysztof Zak

**Abstract** In this paper such mechanical characteristics as cutting forces, cutting energy, specific cutting energy and volumetric machining rate were selected for finish turning of hardened 41Cr4 alloy steel with variable cutting speed and feed rate using commercial CBN tools. In addition, a specific energetic characteristic of the hard machining process was performed, and the machine tool used was taken into account. This approach is focused on the prediction of the relation between the specific cutting energy and the volumetric machining removal rate and comparison of hard machining process with other machining processes in terms of their productivity.

**Keywords** Hardened steel · Machining parameters · Cutting forces · Cutting energy · Specific cutting energy

## 1 Introduction

Hard machining is typically used for finish shaping of different highly loaded machine components made of hardened steels, such as geared shafts, bearing and hydraulic components, dies and moulds with high dimensional and shape accuracy and special requirements regarding surface finish and functional performance [1–3]. In general, hard machining process is characterized by specific cutting mechanics, chip formation, tool wear, surface integrity and part accuracy and energy consumption [1, 2]. As a result, many technological problems including unacceptable surface finish and insufficient part form accuracy occur due to the specific action of the cutting edge with a high negative rake angle, aggressive thermal influences, excessive friction, rapid tool wear and higher energy consumption [1, 4]. It is also distinguished by a lower productivity resulting from a low machining removal rate.

---

R. Chudy · W. Grzesik (✉) · K. Zak  
Faculty of Mechanical Engineering, Opole University of Technology,  
5th Mikołajczyka Str., 45-271 Opole, Poland  
e-mail: w.grzesik@po.opole.pl

It is obviously known that the energy consumption increases distinctly due to extreme high hardness of the material which is machined using CBN cutting tools with a high negative rake angle. Moreover, total energy consumption increases due to intensive ploughing effect [5]. This specific effect becomes more important when machining with CBN cutting inserts with the tool nose radius larger than 800 (1200)  $\mu\text{m}$  [6, 7]. It is important from a mechanical point of view that hard machining is performed with dominating passive force in comparison with conventional turning. In general, the ratio of the passive force to the cutting force is distinctly higher than 1, whereas in conventional cutting, it is lower than 1 and typically equal to  $F_p = (0.3-0.5)F_c$ . As a result, the excessive passive force changes the dynamic behaviour of the machining system and causes the tendency to process instabilities such as chatter [3].

In this study, three components of the resultant cutting force, cutting and specific cutting energy and corresponding machining removal rate were determined under the variable cutting speed and feed rate in turning of a 41Cr4 hardened steel. In addition, the unique cutting characteristic which relates the specific cutting energy to the machining removal rate was determined for the CNC lathe used.

## 2 Experimental Details

### 2.1 Workpiece Materials and Machining Conditions

This experimental study includes a number of hard turning tests in which hardened EN 41Cr4 alloy steel (equivalent DIN 41Cr4 grade and AISI 5140 grade) with  $55 \pm 1$  HRC hardness was machined using fresh CBN cutting tools under variable machining conditions. Chemical compositions and mechanical properties of the hard alloy steel machined are specified in Tables 1 and 2, respectively.

**Table 1** Chemical compositions of the workpiece materials used in comparative study

Steel grade	C %	Si %	Mn %	P %	S %	Cr %	Mo %	Al %	Cu %
EN 41Cr4	0.38–0.45	max 0.40	0.60–0.90	max 0.025	max 0.035	0.90–1.20	max 0.10	max 0.050	max 0.30

<http://www.lucefin.com/en/siderurgia/acciai-speciali-e-al-carbonio>

**Table 2** Mechanical properties of the workpiece materials used in comparative study

Steel grade	HRC	UTS in $\text{N/mm}^2$	Rp <sub>0.2</sub> in $\text{N/mm}^2$	Y in GPa
EN 41Cr4	55	2080	1590	210

<http://www.lucefin.com/en/siderurgia/acciai-speciali-e-al-carbonio>

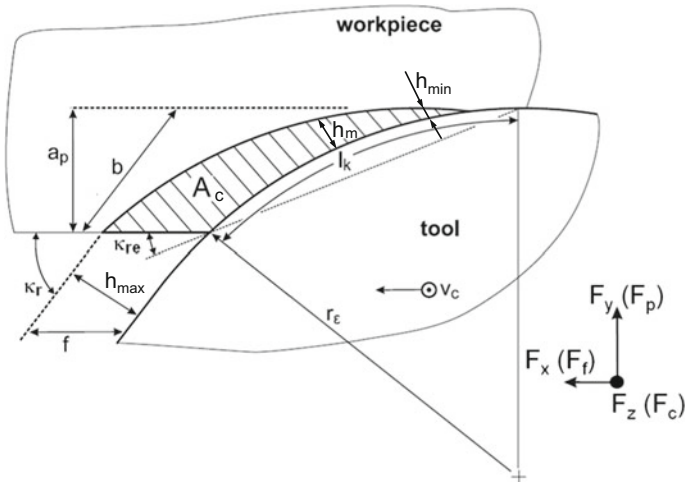
**Table 3** Specification of machining conditions employed in comparative study

Steel grade	Cutting speed, $v_c$ in m/min	Feed rate, $f$ in mm/rev	Depth of cut, $a_p$ in mm	Tool corner radius, $r_\epsilon$ in $\mu\text{m}$
EN 41Cr4	150, 200, 250, 300	0.05, 0.075, 0.1, 0.125, 0.15, 0.175, 0.2	0.2	800

CBN cutting tools of CB 7015 grade produced by Sandvik Coromant were equipped with chamfered TNGA inserts with the corner radius of  $r_\epsilon = 800 \mu\text{m}$ . For this geometrical configuration, the chamfer rake angle  $\gamma_{cf} = -30^\circ$  and the average cutting edge radius  $r_n = 10 \mu\text{m}$ . Cutting parameters selected for hard turning passes are specified in Table 3. They were performed on a three-axis CNC turning centre, Okuma Genos model L200E-M.

### 2.2 Measurements of Cutting Forces and Cutting Energy

Three components  $F_c$ ,  $F_f$  and  $F_p$  of the resultant cutting force (see Fig. 1) were measured using a three-component Kistler dynamometer (model 9129A). Concurrently, consumed power/energy was measured using special recording system installed on the CNC lathe [4]. The measured signals were processed with a sampling rate of  $f = 1 \text{ kHz}$  and a low-pass filter with a cut-off frequency of  $f_c = 300 \text{ Hz}$ . In addition, the cutting energy  $E_c$  was recorded along with other energy components using a special multichannel measurement system and DAQ system [4].



**Fig. 1** Typical cross section of the uncut chip layer for finish hard turning [5]

### 2.3 Computations of the Cutting and Specific Cutting Energy

Cutting energy was determined using the well-known Eq. (1), and in this study, it was automatically recorded using Labview software [4]. The relevant Eq. (1) is as follows [2]:

$$E_c = F_c v_c \Delta t \quad (1)$$

where  $F_c$  is the cutting force, and  $v_c$  is the cutting speed. The time increment  $\Delta t$  was determined as the ratio of the cutting length  $l_c$  to the feed rate applied. In this study, the cylindrical workpieces were prepared with the same length of about 50 mm.

Specific cutting energy  $e_c$  was calculated as the ratio of the measured value of the cutting energy force  $E_c$  and the volume of the removed layer  $V$  or equivalently the cutting energy force  $F_c$  and the cross-sectional area of cut  $A_c$  which is calculated as the product of the equivalent cutting edge of the length  $l_k$  and the mean uncut thickness  $h_m$  shown in Fig. 1. The relevant Eq. (2) is as follows:

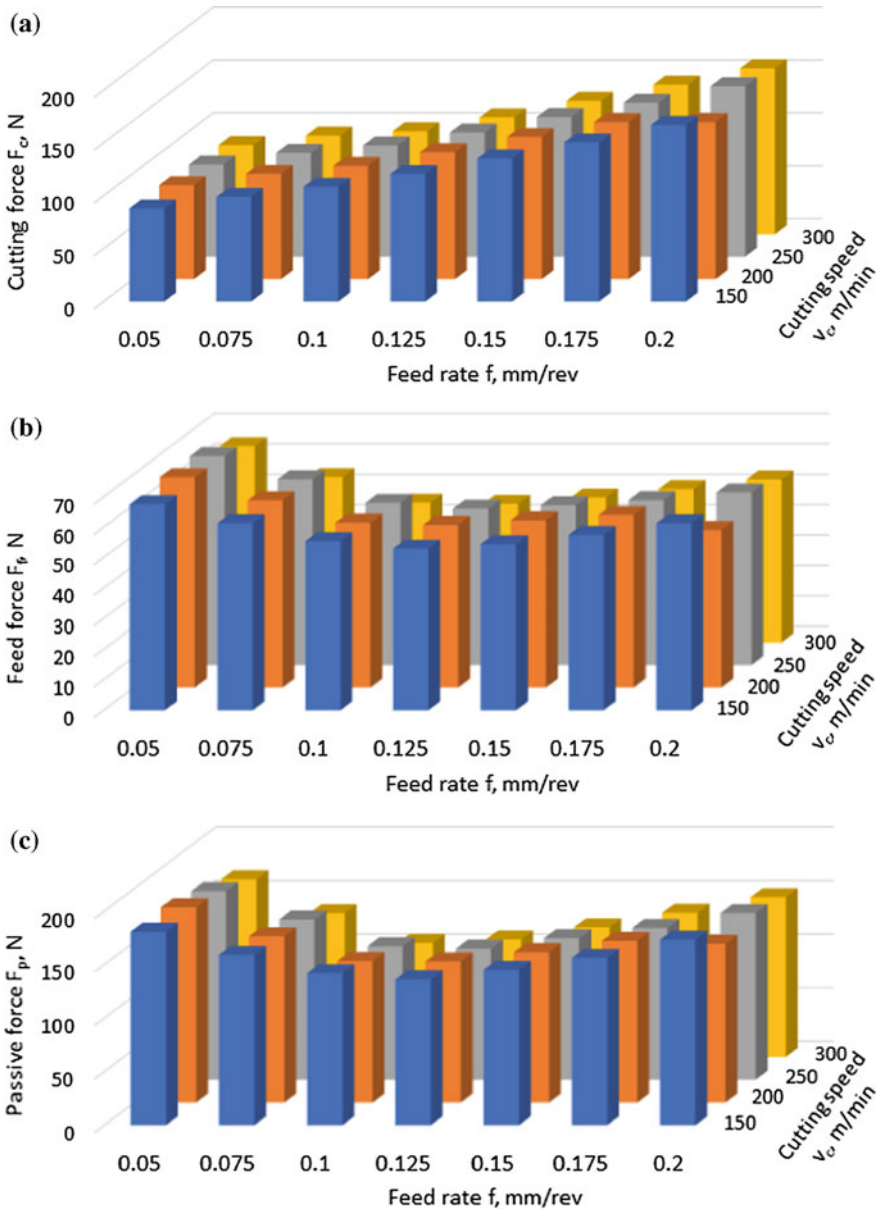
$$e_c = \frac{E_c}{V} = F_c / A_c \quad (2)$$

where  $V$  is the material volume removed in one turning pass ( $V = l_c \times f \times a_p$ ).

## 3 Experimental Results and Discussion

### 3.1 Cutting Forces and Their Relationships

As reported in Sect. 2.2, three components  $F_c$ ,  $F_f$  and  $F_p$  of the resultant cutting force were recorded during hard turning passes for several variable cutting speeds and feed rate (see Table 3). In total, 21 different turning passes were performed with three repetitions for each pass. Simultaneously, the cutting energy  $E_c$  was measured in a real-time mode using a special measurement system [4]. The changes of three force components resulting from variations of the feed rate and the cutting speed are presented in Fig. 2. As shown in Fig. 2a, the minimum values of the cutting force  $F_c$  were obtained for the minimum feed rate of 0.05 mm/rev independently of the cutting speed applied. It is important to note that the relationship between the cutting force and the feed rate is approximately linear. On the other hand, the changes of both feed and passive forces are not linear with a visible minimum value observed at the feed rate of 0.125 mm/rev (Fig. 2b and c). It should be noted based on Fig. 2a and c that the values of the passive force recorded in the turning of DIN

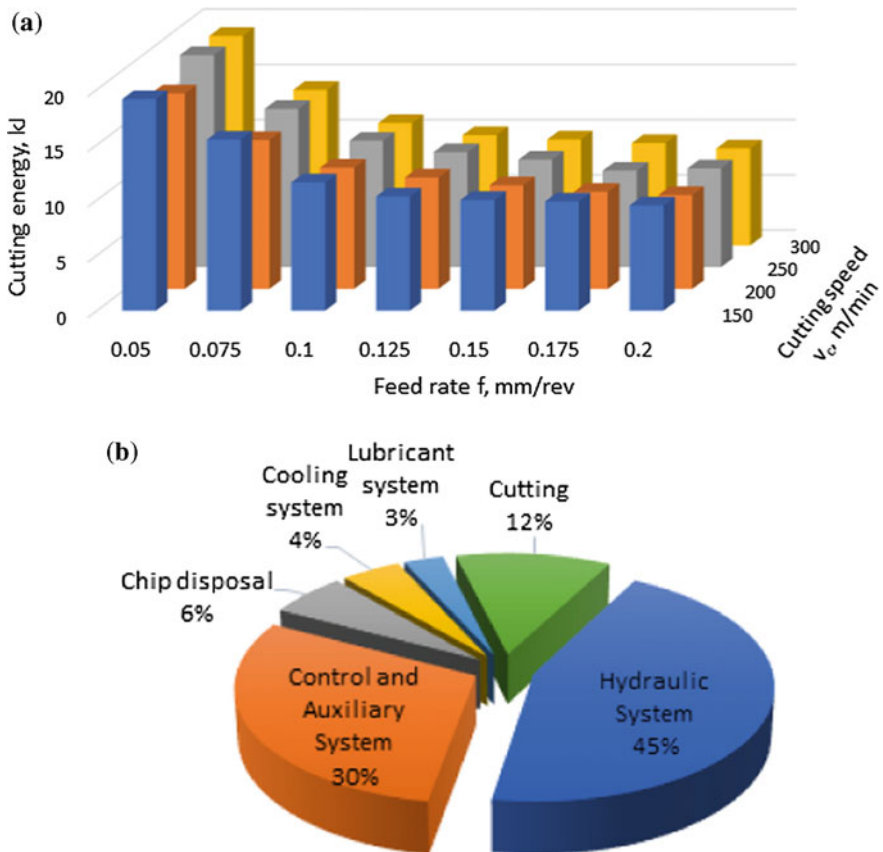


**Fig. 2** Influence of feed rate and cutting speed on the three components of the resultant cutting force: **a** cutting, **b** feed and **c** passive forces for 41Cr4 alloy steel at the depth of cut  $a_p = 0.2$  mm

41Cr4 hardened steel are higher than the corresponding values of the cutting force  $F_c$ . In particular, at the lowest feed rate of 0.05 mm/rev, the ratio  $F_p/F_c$  is about 2, but it tends to decrease down to about 1 when the maximum feed rate of 0.2 mm/rev was selected.

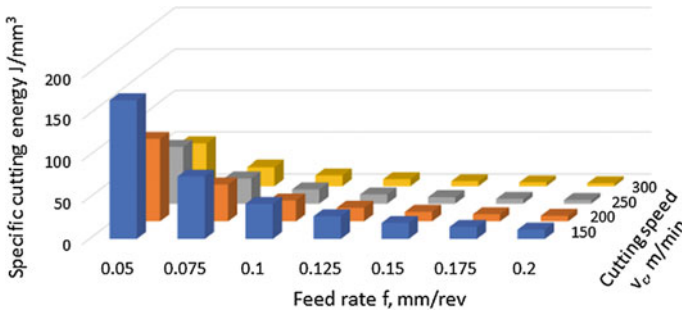
### 3.2 Changes of Cutting Energy Resulting from Variable Machining Conditions

The changes of the cutting energy  $E_c$  defined by Eq. (1) and the specific cutting energy (SCE)  $e_c$  defined by Eq. (2) obtained for variable machining conditions are presented in Figs. 3 and 4, respectively.



**Fig. 3** Changes of cutting energy for variable feed rate and cutting speed (a) and pie diagram of energy distribution (b) for a three-axis CNC turning centre, Okuma Genos model L200E-M for  $v_c = 200$  m/min,  $f = 0.1$  mm/rev,  $a_p = 0.2$  mm [4]





**Fig. 4** Influence of feed rate and cutting speed on the specific cutting energy for 41Cr4 alloy steel at the depth of cut  $a_p = 0.2$  mm

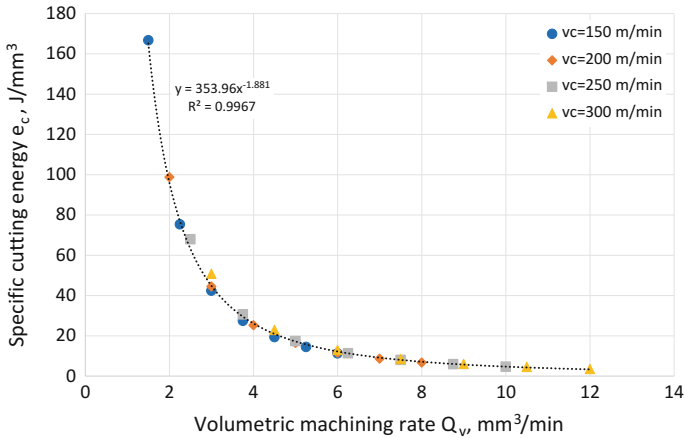
As shown in Fig. 3a, the cutting energy decreases from about 19 kJ to about 8–9 kJ when the feed rate increases from 0.05 to 0.2 mm/rev. Only small difference of about 5–10% in energy consumption was recorded for the cutting speed of 200 m/min. Probably for this cutting speed, the thermal softening of the machined hard steel seems to have predominant influence on the process behaviour.

The pie diagram presented in Fig. 3b shows that in finish hard machining, the energy consumption strictly for the cutting performance is about 12% of the total energy recorded, and this percentage is practically independent of the machining conditions employed. On the other hand, 75% of the electrical energy is consumed by hydraulic system and control and auxiliary system.

Figure 4 shows that values of SCE depend on both feed rate and cutting speed selected with a more distinct influence of the feed rate. Typically, its highest values are determined for lower feed rates, but the increase of cutting speed results in decreasing of the SCE value. For instance, for the lowest cutting speed of 150 m/min, the specific cutting energy decreases distinctly from about 170 J/mm<sup>3</sup> down to about 10 J/mm<sup>3</sup> when the feed rate increases from 0.05 to 0.2 mm/rev. On the other hand, the increase of cutting speed causes that the SCE decreases due to the thermal softening effect. It is the most intensive (on average the reduction by 3 times, i.e. from 170 to 50 J/mm<sup>3</sup>) for the lowest feed rate of 0.05 m/min applied. As a result, as shown in Fig. 4, the minimum specific energy of 3.5 J/mm<sup>3</sup> was determined for the combination of the maximum cutting speed of 300 m/min and the maximum feed rate of 0.2 mm/rev.

### 3.3 Relationship Between Cutting Energy and Machinability Rate

Figure 5 shows the unique relationships between the SCE and the volumetric material removal rate  $Q_v$ , obtained for a number of machining condition sets specific for the CNC lathe used. The function of SCE versus  $Q_v$  has a typical hyperbolic



**Fig. 5** Specific cutting energy versus volumetric machining rate obtained for 41Cr4 alloy steel and a three-axis CNC lathe, Okuma Genos model L200E-M at cutting speed  $v_c = 150\text{--}300$  m/min, feed rate  $f = 0.05\text{--}0.2$  mm/rev and the depth of cut  $a_p = 0.2$  mm

shape due to a strong dependence of the SCE on the uncut chip thickness (UCT) and equivalently on the feed rate [3]. It should be noted that the machining removal rate increases from  $1.5$  mm<sup>3</sup>/min (for  $v_c = 150$  m/min and  $f = 0.05$  mm/rev) to  $12$  mm<sup>3</sup>/min (for  $v_c = 300$  m/min and  $f = 0.2$  mm/rev). Its mathematical model which satisfies all feed rates and cutting speeds applied ( $f = 0.05\text{--}0.2$  mm/rev and  $v_c = 150\text{--}300$  m/min) with the regression coefficient  $R^2 = 0.9967$  is as follows:

$$e_c = 353.96 \cdot Q_v^{-1.881} \tag{3}$$

where the volumetric machining removal rate can be determined as  $Q_v = v_c \cdot f \cdot a_p$

Equation (3) is a very practical model which allows manufacturers determining the energy consumption for a range of machining operations with variable machining parameters performing on a selected CNC machine tool. It is efficiently used in the energetic analysis of machining processes performed for sustainable manufacturing [8, 9].

## 4 Conclusions

1. In this experimental study, the performance of hard machining process was characterized by cutting characteristics such as components of the resulting cutting force, specific cutting energy and cutting energy consumption and material removal rate. This set of cutting characteristic seems to be optimal for energetic characterization of the machining process.

2. In hard turning, the passive force ( $F_p$ ) overestimates both cutting ( $F_c$ ) and feed ( $F_f$ ) forces. For the CBN cutting tool with the corner radius of 800  $\mu\text{m}$ , the ratio of  $F_p/F_c$  changes between 1 and 2 depending on the combination of the cutting speed and feed rate. It is also influenced by the thermal softening effect.
3. Under the machining conditions used, the energy consumption varies from 8(9) to 19 kJ depending mainly on the feed rate applied. The main trend is that lower energy consumption corresponds with higher feed rates.
4. The specific cutting energy (SCE) decreases distinctly from about 170  $\text{J}/\text{mm}^3$  down to about 10  $\text{J}/\text{mm}^3$  when the feed rate increases from 0.05 to 0.2  $\text{mm}/\text{rev}$ . Similarly, the lowest value of SCE corresponds to higher feed rate due to higher values of the UCT.
5. It is possible to visualize the energetic process index for the machining conditions and the machine tool used incorporating the SCE and the material removal rate. For these hard machining tests performed on a Okuma CNC lathe, this unique mathematical model is expressed in the form of exponential function  $e_c = Q_v^{-1.881}$ .

## References

1. Davim, J.P. (ed.): Machining of Hard Materials. Springer, London (2011)
2. Grzesik, W.: Advanced Machining Processes of Metallic Materials. Elsevier, Amsterdam (2017)
3. Grzesik, W.: Prediction of the functional performance of machined components based on surface topography: State of the art. J. Mater. Eng. Perform. **25**, 4460–4468 (2016)
4. Chudy, R., Grzesik, W.: Comparison of power and energy consumption for hard turning and burnishing operations of 41Cr4 steel. J. Mach. Eng. **14**, 113–120 (2015)
5. Grzesik, W., Denkena, B., Żak, K., Grove, T., Bergmann, B.: Energy consumption characterization in precision hard machining. Int. J. Adv. Manuf. Technol. **85**, 2839–2845 (2016)
6. Chou, Y.K., Song, H.: Tool nose effects on finish hard turning. J. Mater. Process. Technol. **148**, 259–268 (2004)
7. Bartarya, G., Choudhury, S.K.: State of the art in hard turning. Int. J. Mach. Tools Manuf **53**, 1–14 (2012)
8. Grzesik, W.: Energy consumption optimization in machining processes. In: Metal Cutting Technologies, Progress and Current Trends, pp. 36–59. De Gruyter Oldenbourg (2016)
9. Duffou, J.R., Sutherland, J.W., Dornfeld, D., Herrmann, Ch., Jeswiet, J., Kara, S., Hauschild, M., Kellens, K.: Towards energy and resource efficient manufacturing: A processes and systems approach. CIRP Ann. Manuf. Technol. **61**(2), 587–609 (2012)

# Application of Principal Component Analysis and Decision Trees in Diagnostics of Cylindrical Plunge Grinding Process

Pawel Lajmert, Malgorzata Sikora, Bogdan Kruszynski  
and Dariusz Ostrowski

**Abstract** In the grinding process, information about the process state may be derived from many measurement signals. As a result of these signals preprocessing, it is possible to obtain a high number of features of which only a part is related to the monitored process. This paper deals with the feature selection problem and modeling of relationships of selected features with grinding process states and grinding results. Firstly, time–frequency signal processing techniques are analyzed. Using the Hilbert-Huang transform, force, vibration, and acoustic emission signals are decomposed into separate intrinsic mode functions, and then the statistical features are extracted from these functions. Next, principal component analysis is used to select the most relevant features and to remove redundant data. Finally, decision trees are applied to additionally decrease the number of features and to model the grinding process. Using the proposed approach, it is possible to automate the feature selection process and to effectively diagnose the process state and predict final part quality parameters.

**Keywords** Plunge grinding · Diagnostics · Data mining · Classification

## 1 Introduction

Efficient supervision of any machining process requires an analysis of a number of measurements signals, containing information about the process and tool state. These signals may originate from many sensors measuring various physical quantities related to the machining process, such as machining power, force components, vibration, or acoustic emission (AE) [1–3]. As a result of appropriate signal processing in time and frequency domain, it is possible to obtain data patterns of very high dimensionality. This means that individual groups of data, such

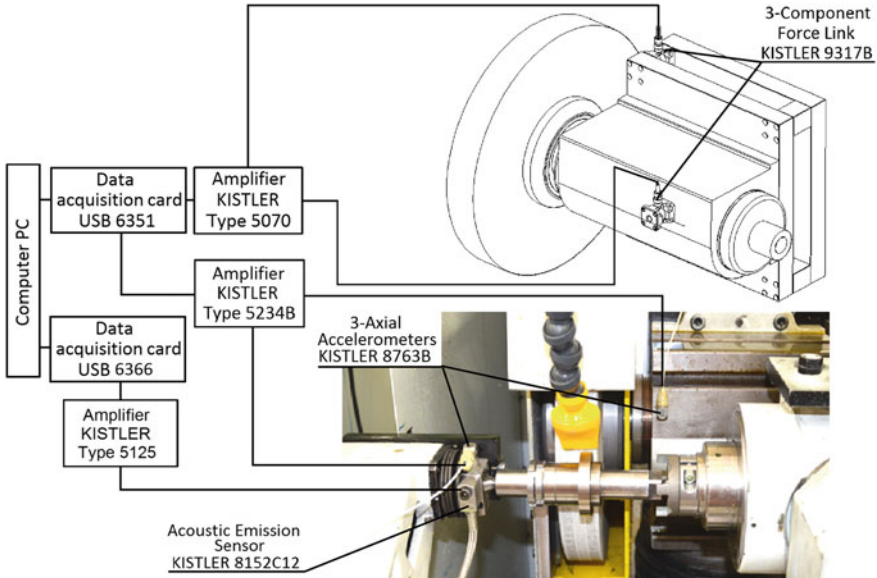
---

P. Lajmert (✉) · M. Sikora · B. Kruszynski · D. Ostrowski  
Institute of Machine Tools and Production Engineering,  
Technical University of Lodz, Lodz, Poland  
e-mail: pawel.lajmert@p.lodz.pl

as vibration or AE measurements have a very large number of attributes. In practice, it turns out that many of these attributes are quite closely correlated with other attributes or with the machining kinematic parameters, leading to a redundancy of information contained in the analyzed dataset. Therefore, to obtain a complete description of the analyzed phenomena, it is sufficient to consider only a small subset of the original set of attributes. Since high dimensionality degrades the effectiveness of many learning algorithms and makes the learning process computationally intensive, there is a need to use dimensionality reduction methods, which allow selecting the most relevant attributes that would be useful in the decision process about machining process and tool state. Correctly diagnosed process and tool state are the basis for the adaptive control system to make decisions concerning tool regeneration or an adjustment of machining kinematic parameters to maintain the process within the optimal working region and, as a consequence, meet part quality parameters [4, 5]. In grinding, the need for such data reduction techniques is even stronger because grinding is stochastic, very complex process for which still no accurate models can be created [2, 5]. This is also due to the high cost of super-abrasive wheels, which state has to be properly diagnosed to make practical and effective use of their cutting abilities [1, 2]. Many approaches to the diagnostics of the grinding process have been proposed in the literature, among which the artificial intelligence techniques are the most popular, including genetic algorithms, neural networks, fuzzy logic, or the rough sets theory [4–7]. These techniques may be used in modeling and attributes selection tasks. However, their modeling and attributes extraction abilities significantly decrease with the increase of a number of model input variables when the correlation between input variables exists [8]. Additionally, in general, they need a human expert during the attributes selection process and knowledge discovery.

## **2 Hardware Setup and Conditions of Experimental Research**

To obtain symptoms of different undesired process states, experimental research has been carried out for a wide range of grinding conditions, using different cylindrical grinding machines [3, 9]. These machines were equipped with sensors for the measurement of grinding force components, vibration, and AE signal. Force components were measured on the basis of oil pressure changes in the pockets of grinding wheel spindle hydrostatic bearing [10] or using Kistler piezoelectric sensors mounted between the body of the wheel headstock and the housing of the wheel spindle, see Fig. 1. Vibration signals were acquired using piezoelectric sensors mounted on the grinding wheel headstock and the tailstock center. Raw AE signal and its RMS value were measured using the piezoelectric sensor mounted on the tailstock center. After each grinding test, workpiece surface roughness and waviness errors were measured using a roughness measurement device and a laser triangulation sensor.



**Fig. 1** General view of the test stand with measurement sensors

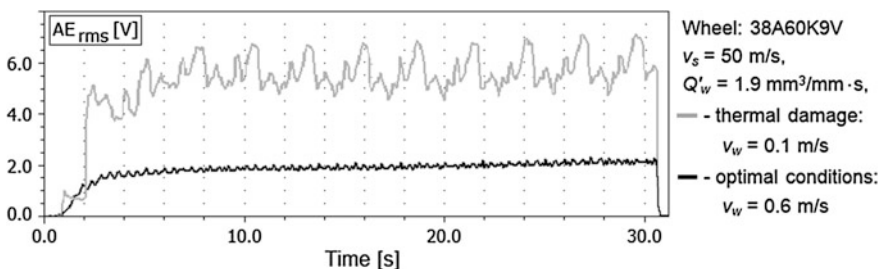
All these measurements were made by means of specially developed control and data acquisition software written using the C++ programming environment. The data acquisition frequency rate and preliminary antialiasing filtering were chosen in such a way as to measure the signals frequency content up to 2 kHz for force components, up to 10 kHz for vibration and AERMS signal and ranging from 50 to 500 kHz for raw AE signal. During the tests, 41CrAlMo7-10 (38HMJ) steel hardened to 50 HRC in the form of 100 mm diameter rings mounted on the shaft was grounded using 38A60K9V and 38A80K5V grinding wheels. The test was carried out for different working conditions related to the workpiece thermal damage and the development of chatter vibrations. Each cycle consisted of 50–150  $\mu\text{m}$  infeed without spark-out and with rapid wheel retraction. This cycle was repeated until the end of the wheel life. The material removal rate  $Q'_w$  was in the 0.5–3  $\text{mm}^3/\text{mm s}$  range and the workpiece peripheral speed  $v_w$  varied in the range from 0.1 to 2 m/s.

### 3 Discrete Time Series Analysis Methods

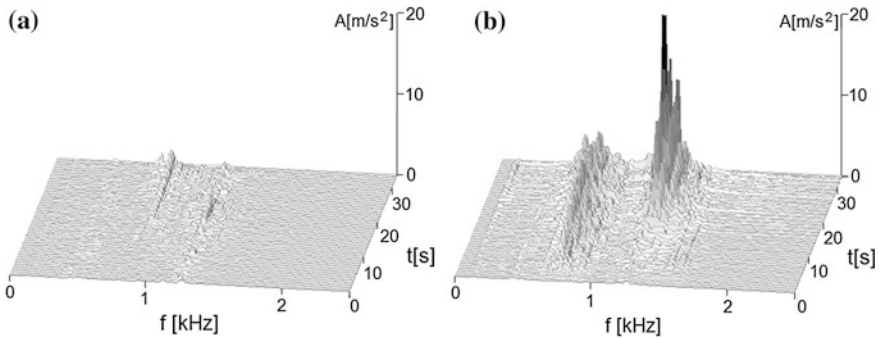
Signals acquired in data acquisition systems take the form of discrete time series and require their further preprocessing to find the information related to the analyzed phenomena. The analyzed signals may contain important information in the time, frequency, or time–frequency domains. In the case of processing in time

domain, determination of attributes (features) may be based on signal statistical measures, such as the mean value, root mean square value (RMS), standard deviation, kurtosis, skewness [1–3, 5, 6]. These measures may be used to diagnose the state of the grinding wheel [1, 3, 11], the identification of the workpiece burn or to estimate residual stress in the surface layer of the workpiece [6, 12]. Signal attributes identified this way, although partially correlated with the analyzed phenomena, may contain information coming from many other sources of information occurring in various frequency ranges of the analyzed signals. In Fig. 2, changes of RMS value of AE signal are presented for grinding in the workpiece thermal damage zone and in the range of optimal grinding conditions. It may be seen that  $AE_{RMS}$  value as well as the variance of this measure increases significantly for operation in the workpiece thermal damage zone.

In the case of frequency decomposition methods, fast Fourier transform (FFT) is the basic method [1, 3, 13]. It is based on the use of periodic sinusoidal functions, representing one frequency. This results in a loss of information about the time of occurrence of individual frequency incidents, since values of signal amplitude are averaged. To overcome this drawback, the short-time Fourier transform (STFT) or wavelet transform (WT) is used. In STFT, the Fourier transform is used on a windowed signal within the frame of the analyzed timer series, whereby the window is moved along the time axis. This allows the observation of short-term changes of signal in subsequent periods of time. The sensitivity of the STFT method mainly depends on the window width. Nevertheless, the resolution of the method is constant in the time domain. A method which is devoid of the mentioned disadvantage is the discrete or continuous wavelet transform (WT) [14]. In the both methods, the window width decreases with the increase of the analyzed frequencies, which theoretically makes them more sensitive than the STFT. The main area of application of STFT and WT covers vibration or AE signal analysis to identify grinding burns or identification of the grinding wheel wear [3, 14]. In Fig. 3, exemplified STFT spectra of vibration signal are presented during grinding using sharp and worn grinding wheel due to the regenerative effect on the wheel surface [15]. However, the above mentioned methods are not well suited for analyzing of nonlinear signals and do not provide explicit information about signal frequency components.



**Fig. 2** Changes of  $AE_{RMS}$  value at grinding in the workpiece thermal damage zone and within the optimal grinding conditions

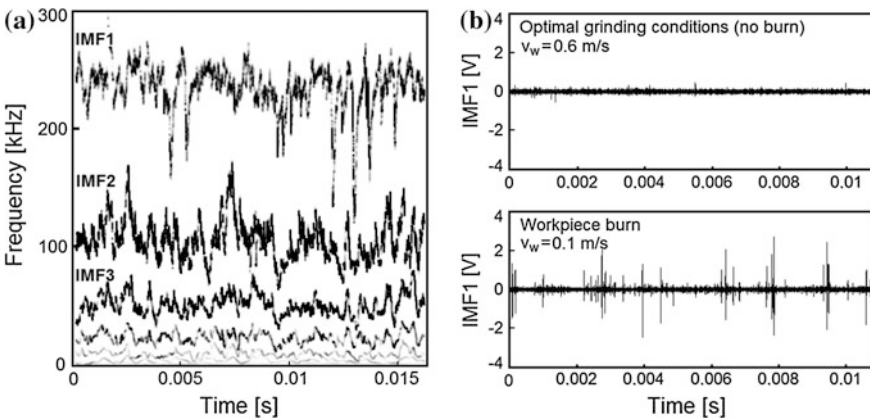


**Fig. 3** Short time Fourier spectrum of vibration signal measured on grinding wheel headstock for: **a** first grinding cycle, **b** fourth grinding cycle after removing of about  $V'_w = 230 \text{ mm}^3/\text{mm}$  (38A60K6V,  $v_s = 35 \text{ m/s}$ ,  $v_w = 0.3 \text{ m/s}$ )

A very promising method is the Hilbert-Huang transform (HHT), which is an adaptive method designed particularly for analyzing non-stationary and nonlinear signals changing even within one oscillation cycle [16]. It uses two signal processing techniques:

- Empirical mode decomposition, i.e., signal decomposition into a set of intrinsic mode functions (IMFs) representing oscillatory modes, which can have variable amplitude and frequency in the time domain.
- Hilbert transform, which determines variations in the amplitude and frequency for individual IMF functions in time domain.

Figure 4 presents an application of the method for decomposing a raw AE signal into IMFs to identify the symptoms of the workpiece thermal damage.



**Fig. 4** Application of HHT to raw AE signal analysis: **a** an exemplified HHT spectrum, **b** course of first IMF1 component for optimal grinding conditions (no workpiece burn) and for conditions when there is workpiece burn (38A60K9V,  $v_s = 40 \text{ m/s}$ ,  $Q'_w = 2 \text{ mm}^3/\text{mms}$ )



When grinding is performed at workpiece peripheral speed too low, a large number of spikes in the first IMF1 component can be observed in Fig. 4b, being the evidence of the workpiece thermal damage or abrasive grains fracture due to the high thermal load of the grinding wheel [6].

## 4 Feature Selection and Data Modeling Methods

A number of techniques can be used for the grinding process modeling, covering statistical, and artificial intelligence methods. The first group includes multiple linear and nonlinear regression methods, correlation analysis methods as well as discriminant and factor analysis methods [8]. The latter cover neural networks, fuzzy logic methods, decision tree induction methods, or rough set methods [5–7]. However, it is known that the use of knowledge induction algorithms with the data containing a large number of correlated input variables does not guarantee to obtain the most appropriate models [8]. Therefore, one of the stages of knowledge acquisition from the analyzed datasets is a process of input variables selection or transformation into a new subspace of reduced size, where new variables are independent of one another.

In the case of feature selection methods, one of the approaches may be the method called filter approach, which is based on the application of certain measures (such as correlation, information entropy) to provide statistical information about significance of the relationship between the predicted output variable and the subset of the model input variables, selected with the use of an adequate searching algorithm.

Another approach known as the selection with the use of knowledge induction algorithms, in the selection process, utilizes such learning algorithms like neural networks or support vector machines [5, 11] to evaluate the different subsets of input variables. The currently analyzed subset of input variables is evaluated by determination of quality factors of model functioning. The method was used in the paper [17] to select the most significant features of AE signal to identify the grinding wheel condition. However, in many cases, these methods are impractical from the point of view of designing automatic systems for grinding process supervision.

A different approach is the use of decision tree learning algorithms for the best feature subset selection [18]. At each node of the tree, the learning algorithm chooses the feature of the dataset that most effectively splits its set of samples into subsets enriching in one class or the other. The feature with the highest normalized information gain is chosen to make the decision.










If a very large number of features are analyzed, a much better approach is to use feature transformation methods which transform the original dataset of features to a new subspace of reduced size without the loss of information contained in the original dataset. In this case, the basic algorithm is the principal component analysis method (PCA) [8]. It is a statistical procedure that uses orthogonal transformation to



convert a set of observations of possibly correlated variables into a set of values of linearly uncorrelated variables called principal components. The number of principal components is usually much lower than the number of original variables. This transformation is defined in such a way that the first principal component has the largest possible variance and each succeeding component in turn has the highest variance possible under the constraint that it is orthogonal to the preceding components.

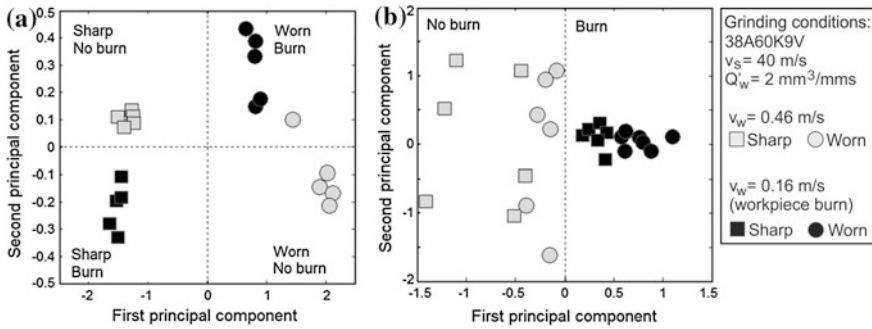
The effectiveness of the PCA method was evaluated on the basis of vibration and AE signal measurements. A principal component analysis method was applied. In order to compute principal component matrixes for vibration and AE signals, a set of statistical features was created for different grinding conditions involving states for sharp and worn grinding wheel due to the waviness development on the wheel surface as well as for high and low workpiece peripheral speeds where workpiece burn occurs. The feature vector was composed of maximum, mean value, standard deviation, kurtosis, and skewness of real value, instantaneous amplitude and frequency of selected vibration and AE IMF components of HHT transform. Due to the large size of the feature vector (15 features for each IMF component), a principal component analysis was carried out to reduce the dimensionality of data without any significant loss of information. As a result, the feature vector was reduced by more than 83% for the vibration data, while for the AE data by 40%. The selected features and its average weight are shown in Table 1. As may be seen for the AE signal standard deviation, kurtosis, and skewness of real IMF and IMF amplitude are potentially the most important features. For vibration signal, mean value of IMF amplitude and IMF frequency which decreases with the increase of grinding wheel waviness development is the most important.

In Fig. 5, scatter plots of the scores of the first two principal components for vibration and AE signal are shown. As may be seen, when using the first two principal components, almost all the grinding conditions were separated correctly. The presented results imply that the grinding wheel wears due to the wheel waviness development as well as process state related to the workpiece thermal damage or grinding wheel thermal load may be effectively detected using the features resulting from the HHT.

**Table 1** Selected features and its relative importance

	<i>Max. value</i>	<i>Mean value</i>	<i>Standard deviation</i>	<i>Kurtosis</i>	<i>Skewness</i>
Real IMF					
IMF amplitude					
IMF frequency					

—Vibration signal, —acoustic emission signal

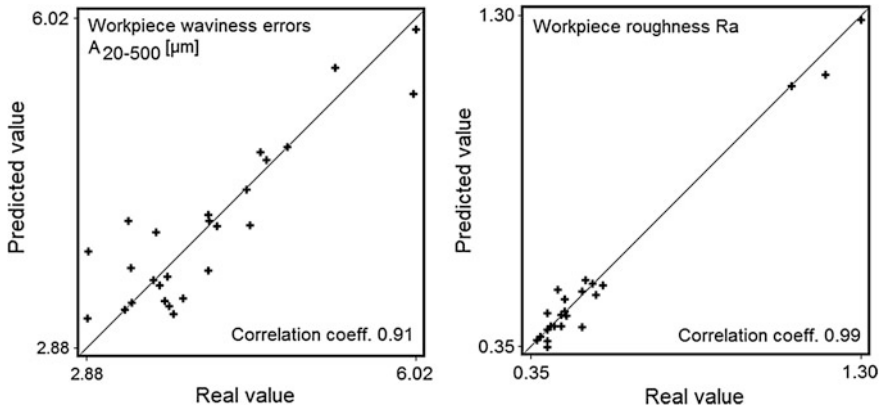


**Fig. 5** Principal component scatter plots for the first two principal components obtained from: **a** vibration and **b** raw AE signal IMF features

For classification in the principal component space or the reduced space of original features a number of methods can be applicable. In the case of decision trees, classification is performed by recursive partitioning of the data into categories in successive tree nodes. At each node, the remaining attributes with the greatest entropy reduction or highest information gain are selected and used to categorize data as the next partitioning step in the following nodes of the tree. At the last node, the data are assigned to one of several data categories which may correspond to different process or grinding wheel wear states. In the paper, the C5.0 decision tree learning algorithm and the hybrid approach proposed by Quinlan (Rulequest Cubist) [18] were used, which combines the C5.0 decision tree algorithm with regression method. In this method, a linear regression equation for attributes partitioned in a given tree branch is determined in the last node of the tree. Using this algorithm, regression equations were estimated to predict the workpiece quality parameters, i.e., workpiece waviness errors and surface roughness. Diagnostic rules were generated using the dataset composed of grinding kinematic parameters and initially selected features (using PCA) including force components, grinding wheel cutting ability, mean and sum of amplitudes, standard deviation, energy of force, vibration, raw AE and AE<sub>RMS</sub> signals. Two datasets were created for training and verification of the decision tree algorithm. For the waviness errors  $A_{20-500}$  (sum of amplitudes in the frequency range from 20 to 500 waves on the workpiece circumference), the following rules were found:

- RULE 1: IF** ( $\sum A_{VIB(600-1100\text{ Hz})}$  is Low) **THEN**  $A_{20-500} = 6.45 - 0.52 Q'_w - 2.6 v_w - 3 \sum A_{RMS EA(10-250\text{ Hz})} - 1.2 \sum A_{VIB(600-1100\text{ Hz})}$
- RULE 2: IF** ( $\sum A_{VIB(600-1100\text{ Hz})}$  is Medium or High) **THEN**  $A_{20-500} = 1.84 + 2.56 v_w + 3.3 \sum A_{VIB(600-1100\text{ Hz})}$

The most important is the second rule, for medium and high level of vibrations, which states that the waviness errors increase with the increase of workpiece peripheral speed and with the increase of sum of vibration amplitudes  $\sum A_{VIB(600-1100\text{ Hz})}$  in the frequency range from 600 to 1100 Hz. In Fig. 6, the



**Fig. 6** Distribution of real and estimated values of workpiece waviness errors and workpiece surface roughness

distribution of real and estimated values of workpiece waviness errors  $A_{20-500}$  and workpiece surface roughness  $Ra$  with the use of this method is presented.

For workpiece thermal damage, classical C5.0 decision tree algorithm was used. Two classes were set, i.e., for no burn and workpiece burn. Only one rule was generated, which explains all grinding cases:

**RULE 1: IF** ( $E_{IMF1,RMS-EA} > 3.4$ ) **THEN WORKPIECE BURN**

From this rule, it follows that the energy  $E_{IMF1,AE-RMS}$  of first IMF component resulting from  $AE_{RMS}$  signal is the most important feature.

## 5 Conclusions

Statistical features of individual measurement signals may have a great potential in grinding process diagnostics. However, due to the nonlinear nature of the analyzed signals and the extensive number of resultant signals features, advanced time–frequency signal decomposition techniques are required, e.g., HHT, and feature selection methods to expose the most important subsets of features. Based on the theoretical and experimental analysis, it can be concluded that:

- Hilbert-Huang transform is highly productive as for the separation of continuous and transient components from force, vibration, and especially AE measurements.
- The use of PCA allows for a significant reduction in the number of features and for the identification of grinding wheel wear and workpiece burn using the inconsiderable number of components in the reduced principal component space.

- The application of decision tree algorithms allows for further reduction in the number of features and to establish the minimal set of features necessary to diagnose the considered phenomena.

The presented approach, which combines the use of the PCA method with decision trees, seems to be a very promising solution for the feature selection tasks, the identification of process states and the prediction of grinding results.

## References

1. Tönshoff, H.K., Friemuth, T., Becker, J.C.: Process monitoring in grinding. *Ann. CIRP*. **51** (2), 551–571 (2002)
2. Teti, R., Jemielniak, K., O'Donnell, G., Dornfeld, D.: Advanced monitoring of machining operations. *Ann. CIRP* **59**(2), 717–739 (2010)
3. Lajmert, P., Leżański, P.: Monitoring of the cylindrical plunge grinding process. *Arch. Mech. Technol. Autom.* **33**(3), 3–15 (2013)
4. Kruszyński, B.W., Lajmert, P.: An intelligent system for online optimization of the cylindrical traverse grinding operation. *Proc. Ins. Mech. Eng. Part B J. Eng. Manuf.* **3**, 355–363 (2006)
5. Kacalak W., Lipiński D., Krzyżyński T.: On the hybrid system of quality supervising in the automated grinding process. In: *Proceedings of the 2nd International Conference—Modern Trends in Manufacturing*, Wrocław, pp. 167–174. (2003)
6. Wang, Z., Willet, P., Deaguiar, P.R., Webster, J.: Neural network detection of grinding burn from acoustic emission. *Int. J. Mach. Tools Manuf.* **41**, 283–309 (2001)
7. Bi, J., He, P., He, X., Wang, H.: Research for on-line diagnostic system for intelligent roll grinding. In: *IEEE Control and Decision Conference*, pp. 5248–5252. (2008)
8. Jolliffe, I.T.: *Principal Component Analysis*. Springer, New York (2002)
9. Lajmert, P., Kruszyński, B., Wrąbel, D., Sikora, M.: A stand for multifaceted examination of the cylindrical OD grinding process (in Polish). *Mechanic*. **8–9**, 273–282 (2013)
10. Lewandowski D.: Pressure measurement of loads (in Polish). In: *Drives and Hydraulic Control*, Wrocław, pp. 144–150. (2002)
11. Chen, X., Limchimchol, T.: Monitoring grinding wheel redress-life using support vector machines. *Int. J. Autom. Comput.* **1**, 56–62 (2006)
12. Webster, J., Marinescu, I.: Acoustic emission for process control and monitoring of surface integrity during grinding. *Ann. CIRP* **43**(1), 299–304 (1994)
13. Hundt, W., Leuenberger, D., Rehsteiner, F., Gygax, P.: An approach to monitoring of the grinding process using acoustic emission (AE) technique. *Ann. CIRP* **43**(1), 295–298 (1994)
14. Liao, T.W., Ting, C., Qu, J., Blau, P.J.: A wavelet-based methodology for grinding wheel condition monitoring. *Int. J. Mach. Tools Manuf* **47**, 580–592 (2007)
15. Inasaki, I., Karpuszewski, B., Lee, H.-S.: Grinding chatter—origin and suppression. *Ann. CIRP* **50**(2), 515–534 (2001)
16. Huang N.E., et al.: The empirical mode decomposition and the Hilbert spectrum for non-linear and non-stationary time series analysis. In: *Proceedings of the Royal Society of London Series A*, pp. 903–995. (1998)
17. Liao, T.W.: Feature extraction and selection from acoustic emission signals with an application in grinding wheel condition monitoring. *Eng. Appl. Artif. Intell.* **23**(1), 74–84 (2010)
18. Quinlan R.J.: Learning with continuous classes, In: *Proceedings of the 5th Australian Joint Conference On Artificial Intelligence* (World Scientific), pp. 343–348. (1992)

# Assessment of Deformation Characteristics on CW004A Copper Influenced by Acoustically Enhanced Water Jet

Dominika Lehocka, Vladimir Simkulet and Stanislaw Legutko

**Abstract** Paper deals with copper CW004A deformation characteristics evaluation after pulsating water jet disintegration. Experimental samples were prepared from copper CW004A with marking A, B, and C. As variable factors were selected combinations of pressure of pump pressure and nozzle diameter: A ( $p = 65$  MPa;  $d = 1.067$  mm), B ( $p = 49$  MPa;  $d = 1.321$  mm), C ( $p = 38$  MPa;  $d = 1.600$  mm). Surface topography was evaluated using optical profilometry. Microhardness measurement was measured using Vickers indenter. Hardness measurement was performed on seventeen points under disintegrated area in distance from 0.1 to 3 mm. Measured values indicate slight increase of strain hardening undercutting area.

**Keywords** Pulsating water jet · Strain hardening · Microhardness · Copper

## 1 Introduction

Destructive effect of water on various materials is recognized in long-term view Cook [1]. Clean water jet (WJ) or abrasive water jet (AWJ) [2–6] is currently used for cutting of wide range of materials. High-pressure WJ and AWJ reach technological and economical limits. Nowadays is known material destruction [7, 8] using lower pressure, fortified by additional device. Pulsating water jet (PWJ) can by

---

D. Lehocka · V. Simkulet  
Faculty of Manufacturing Technologies with a Seat in Presov,  
Technical University of Kosice, 1 Bayerova St., 08001 Presov, Slovak Republic

D. Lehocka (✉)  
Institute of Geonics of the CAS, v. v. i., 1768 Studentska St.,  
70800 Ostrava, Poruba, Czech Republic  
e-mail: dominika.lehocka@tuke.sk

S. Legutko  
Poznan University of Technology, Pl. Marii Skłodowskiej-Curie 5,  
60-965 Poznan, Poland

applied in various industry sectors. Numerous ways of approach to create discontinual flow are recognized. Modulation of continual flow, which subsequently starts to form into pulses, is considered as most perspective [9].

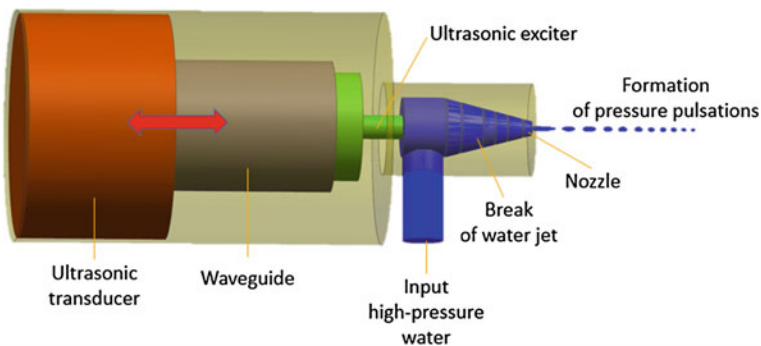
Technological modification principle of acoustically excited pulsating water jet is based in generating of pressure pulses, which affect incoming pressurized water in resonance chamber. Pressurized pulses cause liquid outflow through the nozzle with variable speed [10]. Wave formation (liquid clusters) cause speed difference of water flowing through nozzle. Part of water jet accelerated by ultrasonic exciter shortens distance between continually flowing liquid, which causes pulses creation. Authors dealing with possibilities of water jet ultrasound modulation were Vijay et al. [11, 12], who described principle of pulse generating in pressurized liquid. Principle consists in vibration generating in ultrasound transducer (Fig. 1), which is supplied into water inside nozzle by waveguide and ultrasonic tool [12, 13]. Water jet exits nozzle as continual flow and in specific distance starts creating individual liquid clusters (Fig. 1). Material is subsequently disintegrated by impacts of water clusters with high kinetic energy (Fig. 1). It is proven that PWJ disintegration is more efficient in comparison to continual jet [14, 15].

Destruction potential can be fully used in building industry for disintegration of rock materials and remediation of concrete constructions Sitek et al. [16, 17], in mining industry for breaking mineral materials Dekhoda and Hood [18] and for surface treatment of ornamental stones Bortolussi et al. [19]. Last research indicates possibility of PWJ application in orthopedic field for the removal of bone cement during reimplantation of weight-carrying joints [20].

Experimental investigation described in this paper follows research of authors Foldyna et al. [14, 15] and Lehocka, et al. [21, 22].

Presented research was focused on the assumption of copper CW004A sub-surface reinforcement after pulsating water jet disintegration. For verification, were used the evaluation of deformation characteristics, measured by static method using Vickers indenter.

Presented results are a part of large research which deals with a new approach to disintegration metal materials by acoustically enhanced pulsating water jet.



**Fig. 1** Acoustically enhanced PWJ technological setup

Research is focused on examining a various set of factors and technological setup. The main aim of research is to apply pulsating water jet technology to practice.

Experiment was held in cooperation with the Faculty of Manufacturing Technologies in Presov with Institute of Geonics of the CAS, v.v.i. in Ostrava–Poruba Experimental part of research was realized in Institute of Geonics of the CAS, v.v.i. in Ostrava and microhardness measurement was performed in the laboratory of Faculty of Manufacturing Technologies with a seat in Presov and surface topography identification was performed in the laboratory of Faculty of Mechanical Engineering and Management, Poznan University of Technology.

## 2 Experimental Conditions

### 2.1 Experimental Material

A sample of copper identified as CW004A (CuETP or ECu-57) in the group of electrically conductive copper. It is characterized by high conductivity, relative high resistance against erosion, and has high temperature coefficient. It is used for electrical and electronic applications, by default for the manufacture of thermocouples, compensating cables, and for bimetallic heaters. Mechanical properties and chemical composition of copper CW004A are shown in Table 1.

### 2.2 Experimental Investigation

Technological conditions of disintegration were chosen based on experiments described in [21, 22]. Pressure and round nozzle diameter were selected as changing factors. For determination of significance factor influence on effectiveness PWJ disintegration was selected combination of higher pressure and smaller nozzle diameter.

In research [22] was demonstrated slightly subsurface reinforcement of copper alloy (brass) with using nanoindentation measurements. For verification of this fact,

**Table 1** Mechanical properties and chemical composition of copper CW004A

Mechanical properties				Chemical composition [%]	
Tensile strength $R_m$ [MPa]	Yield strength $R_{p0.2}$ [MPa]	Elongation $L_0 = 100 \text{ mm A}$ [%]	Hardness HB	Cu + Ag	O
395	365	4	114	>99.90	<0.04



measurements of microhardness under the groove of CW004A copper were performed in this research.

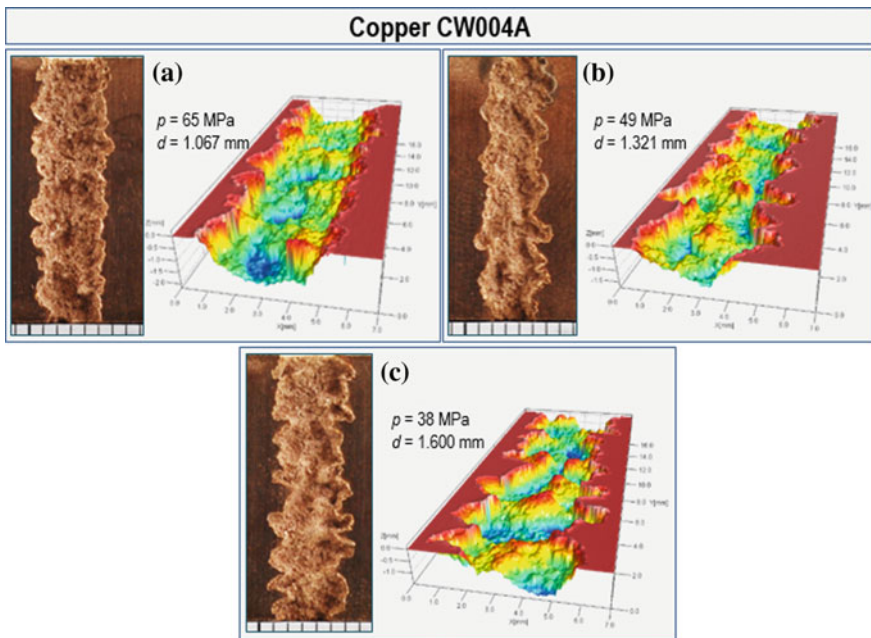
Experiment was realized using cutting head, circular nozzles Stone Age with required equivalent diameter, hydraulic high-pressure pump Hammelmann HDP 253 (max. operational pressure 160 MPa, maximal flow rate  $67 \text{ l min}^{-1}$ ), ultrasonic device Ecoson WJ-UG\_630-40 for pulse generation and industrial robot ABB IRB 6640-180//2.55 for cutting head manipulation. Technological conditions of disintegration are shown in Table 2.

Three experimental samples of rectangular shape with dimensions  $(1 \times w \times t)$   $50 \times 20 \times 5 \text{ mm}$  were prepared. The samples were disintegrated with using technological conditions listed in Table 2.

Topography measurement was realized using optical profilometry with contactless optical profilometer MicroProf FRT operating with white light. Subsequently, topography and grooves surface (Fig. 2) were evaluated in software SPIP 6.5.2.

**Table 2** Technological conditions of experiment

Sample	$v$ [mm/s]	$P$ [W]	$f$ [kHz]	$p$ [MPa]	$d$ [mm]
A	0.5	410	20.29	65	1.067
B		380		49	1.321
C		510		38	1.600



**Fig. 2** Comparison grooves topography of samples A, B, C with using circular nozzle

**Table 3** Measured microhardness values HV 0.2

No.	Distance from the cut (mm)	A	B	C
		$p = 65 \text{ MPa};$ $d = 1.067 \text{ mm}$	$p = 49 \text{ MPa};$ $d = 1.321 \text{ mm}$	$p = 38 \text{ MPa};$ $d = 1.600 \text{ mm}$
1	0.1	192.8	187.8	179.6
2	0.2	178.0	180.1	175.2
3	0.3	171.5	171.0	172.3
4	0.4	169.4	169.3	170.6
5	0.5	173.5	166.7	177.7
6	0.6	175.2	159.2	168.8
7	0.7	155.6	166.6	174.3
8	0.8	161.2	166.9	167.4
9	0.9	156.1	160.0	173.2
10	1.0	159.7	161.3	167.1
11	1.1	159.0	158.5	168.3
12	1.2	159.9	165.0	175.2
13	1.3	162.2	155.7	173.8
14	1.4	162.6	164.3	164.4
15	1.5	160.1	160.4	161.8
16	2.0	166.6	156.8	162.7
17	3.0	159.3	161.8	162.4

Measured samples were cut on smaller parts and poured into cold acrylic resin. Subsequently were samples grinded and polished manually using device MTH KOMPAKT 1031.

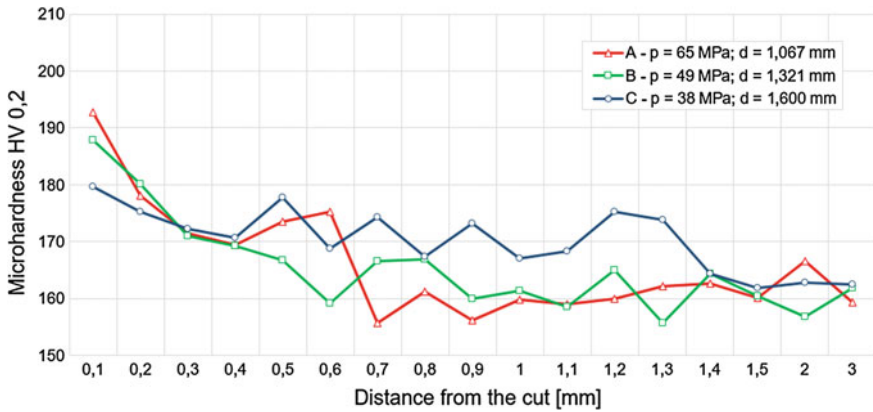
Microhardness measurement was performed on microhardness tester CV 400 DAT set to 200 g load for 10 s (HV 0.2). Measurements were realized in increasing distance below disintegrated surface in one line. First measurement was at a distance 0.1 mm below disintegrated surface. Each further measurement was displaced by 0.1 mm in y-axis till distance 1.5 mm (15 measurements). At the end were realized 2 measurements at a distance 2 and 3 mm (Table 3).

### 3 Results

Figure 2 shows 2D and 3D profiles of individual grooves of samples A, B, C. (Figure 2).

According to surface topography (Fig. 2) is shape of grooves inconsistent, but some shared properties can be find as:

- Absence of strict boundaries of grooves,
- Most of grooves edges have rounded character,
- Contoured surface with protrusions and depressions in random shapes and destinations,



**Fig. 3** Measured values of microhardness HV 0.2; samples A, B, C

- The predominant sharp characteristics of protrusions and depressions,
- Extrusion of material above upper level of the groove.

Graphical dependence shown on Fig. 3 describes measured values of microhardness HV 0.2. Significant changes were observed at small distance below A and B grooves. Hardness measured in first indent (distance 0.1 mm under disintegrated area) is 21% higher in comparison to base material for sample A ( $p = 65$  MPa;  $d = 1.067$  mm) and for sample B ( $p = 49$  MPa;  $d = 1.321$  mm) 17% higher. Not significant change of hardness was indicated for sample C ( $p = 38$  MPa;  $d = 1.600$  mm).

Graphical dependence (Fig. 3) shows initial slight increase of hardness HV 0.2 and stabilization of values from certain distance. This indicates formation of subsurface reinforcement of material. Slight subsurface reinforcement is indicated to distance 0.6 mm for sample A and to distance 0.4 mm for sample B. Not significant subsurface reinforcement was indicated for sample C.

Each sample was disintegrated with different combination of pressure of pump  $p$  [MPa] and nozzle diameter  $d$  [mm]. Considering this fact different local strain hardening was detected. The highest strain hardening was indicated in sample A (192.8 HV), disintegrated using highest pressure of pump pressure  $p$  [MPa] and the smallest nozzle diameter  $d$  [mm]. These findings indicated a significant influence of higher pressure of pump  $p$  [MPa] on strain hardening of copper CW004A.

## 4 Conclusions

Objective of experimental investigation was to assess the impact of factors acoustically enhanced PWJ on subsurface reinforcement of copper CW004A. It was found significantly influences of higher pressure of pump  $p$  [MPa] on deformation

reinforcement under disintegrated groove. Experimental results obtained using lower pressure of pump  $p$  [MPa] shows only mechanical removal of copper CW004A, without significant influence on subsurface reinforcement. In the fact of this can be assumed that using lower pressure  $p$  [MPa] causes only material removal on roughness level. If this assumption is confirmed, it would be possible to find application of pulsating water jet in practice, for example as a surface treatment before protective layers application. In this area, a slight surface roughening could allow better adhesion of applied substances. Cleaning surface from coatings, dirt, rust, or paints is other area of pulsating water jet possible usage. In future, it is planned to test of influence of lower pressure of pump  $p$  [MPa] on various types of materials.

**Acknowledgements** This work was supported by the Slovak Research and Development Agency under Contract No. APVV-207-12. Experiments were carried out with the support of the Institute of Clean Technologies for Mining and Utilization of Raw Materials for Energy Use–Sustainability Program, reg. no. LO1406 financed by Ministry of Education, Youth, and Sports of the Czech Republic, and with support for the long-term conceptual development of the research institution RVO: 68145535.

## References

1. Kumar, R., Chattopadhyaya, S., Dixit, A.R., Bora, B., Zelenak, M., Foldyna, J., et al.: Surface integrity analysis of abrasive water jet-cut surfaces of friction stir welded joints. *Int J Adv Manuf Technol.* **88**, ISSN 1687–1701 (2017)
2. Hlaváček, P., Cárach, J., Hloch, S., Vasilko, K., Klichová, D., Klich, J., et al.: Sandstone turning by abrasive waterjet. *Rock Mech. Rock Eng.* **48**, ISSN 2489–93 (2015)
3. Hloch, S., Hlaváček, J., Vasilko, K., Cárach, J., Samardžić, I., Kozak, D., et al.: Abrasive waterjet (AWJ) titanium tangential turning evaluation. *Metalurgija.* **53**, 537–540 (2014)
4. Zhong, Z.W., Han, Z.Z.: Turning of glass with abrasive waterjet. *Mater Manuf. Process.* **17**, 339–349 (2002)
5. Yue, Z., Huang, C., Zhu, H., Wang, J., Yao, P., Liu, Z.: Optimization of machining parameters in the abrasive waterjet turning of alumina ceramic based on the response surface methodology. *Int. J. Adv. Manuf. Technol.* **71**, 2107–2114 (2014)
6. Lissek, F., Kaufeld, M., Tegas, J., Hloch, S.: Online-monitoring for abrasive waterjet cutting of CFRP via acoustic emission: Evaluation of machining parameters and work piece quality due to burst analysis. *Proced. Eng.* **149**, 67–76 (2016)
7. Botko, F., Hatala, M., Kormoš, M., Ungureanu, N., Šoltés, P.: Using Edgcam for creating CNC programs in education process. In: SAMI 2015. Danvers: IEEE, pp. 255–259, ISBN 978-1-4799-8220-2 (2015)
8. Duplak, J., Hatala, M., Botko, F., Kormos, M.: Analysis of cutting tools durability importance in turning process of steel C60. In: *Key Engineering Materials: Operation and Diagnostics of Machines And Production Systems Operational States 3.*, Vol. 669, pp. 319–326 (2016)
9. Kušnerová, M., Foldyna, J., Sitek, L., Valíček, J., Hloch, S., Harničárová, M., et al.: Innovative approach to advanced modulated waterjet technology. *Inovativni pristup naprednoj moduliranoj tehnologiji vodenog mlaza. Teh Vjesn* **19**, 475–480 (2012)
10. Zelenak, M., Foldyna, J., Scucka, J., Hloch, S., Riha, Z.: Visualisation and measurement of high-speed pulsating and continuous water jets. *Meas J Int Meas Confed.* **71**, 1–8 (2015)

11. Vijay M.M., Foldyna J., Remisz J.: Ultrasonic modulation of high-speed water jets. *Int Conf: Geomech.* **93**, 327–332 (1994)
12. Říha, Z., Foldyna, J., Ultrasonic pulsations of pressure in a water jet cutting tool. *Ultrasvučne pulzacije tlaka u alatu za rezanje vodenim mlazom. Teh Vjesn* **19**, 487–491 (2012)
13. Foldyna, J., Sitek, L., Švehla, B., Švehla, S., Utilization of ultrasound to enhance high-speed water jet effects. *Ultrason Sonochem* **11**, 131–137 (2004)
14. Foldyna, J., Klich, J., Hlavacek, P., Zelenak, M., Scucka, J.: Erosion of Metals by Pulsating Water Jet. *Teh Vjesn Gaz* **19**, 381–386 (2012)
15. Foldyna, J., Sitek, L., Ščučka, J., Martinec, P., Valíček, J., Páleníková, K.: Effects of pulsating water jet impact on aluminium surface. *J. Mater Process Technol.* **209**, 6174–6180 (2009)
16. Sitek, L., Foldyna, J., Souček, K.: Shaping of rock specimens for testing of uniaxial tensile strength by high speed abrasive water jet: First experience. In: *Impact of Human Activity on the Geological Environment—Proceedings of International Symposium International Society for Rock Mechanics Eurock 2005* (2005)
17. Sitek, L., Foldyna, J., Martinec, P., Ščučka, J., Bodnárová, L., Hela, R.: Use of pulsating water jet technology for removal of concrete in repair of concrete structures. *Baltic J. Road Bridge Eng.* **6**, 235–242 (2011)
18. Dehkhoda, S., Hood, M.: An experimental study of surface and sub-surface damage in pulsed water-jet breakage of rocks. *Int. J. Rock Mech. Min. Sci.* **63**, 138–147 (2013)
19. Bortolussi A., et al.: Ornamental stones surface finishing by pulsating jet: A project for an industrial application. In: *Water Jet 2013—Research, Development, Applications*, pp. 17–24, ISBN 978-80-86407-43-2 (2013)
20. Hloch, S., Foldyna, J., Pude, F., Kl'oc, J., Zelenák, M., Hvizdoš, P., et al.: Experimental in-vitro bone cements disintegration with ultrasonic pulsating water jet for revision arthroplasty. *Teh Vjesn Tech Gaz* **22**, 1609–1615 (2015)
21. Lehocka, D., Klich, J., Foldyna, J., Hloch, S., Krolczyk, J.B., Carach, J., et al.: Copper alloys disintegration using pulsating water jet. *Meas J. Int. Meas Confed.* **82**, 375–383 (2016)
22. Lehocka, D., Klich, J., Foldyna, J., Hloch, S., Hvizdoš, P., Fides, M., et al.: Surface integrity evaluation of brass CW614N after impact of acoustically excited pulsating water jet. *Procedia Eng.* **149**, 236–244 (2016)

**Part IV**  
**Measurement Systems and Quality**  
**Engineering**

# Measuring the Punching Profile of a Punch And Bind Machine

Joao Sousa, Luis Figueiredo, Jose Machado and Joao P. Mendonca

**Abstract** In the design process of a manual or electrically actuated punch and bind machine, the required force to punch a stack of paper sheets is a crucial parameter that affects ergonomics, product design, power requirements, and ultimately product cost. The required punch force profile considered two punch pin geometries, introducing some innovative aspects. Measurements were performed using a tensile/compression machine and the punching force profile of the 21 punching pins arrangement during punching cycle was extracted for both geometries. Results show a smoother force profile for the double shear angle punching pin arrangement as opposed to the concave pin geometry pin arrangement with a lower peak punching force value.

**Keywords** Paper punching · Punching geometry · Punch and bind machine

## 1 Introduction

This paper focuses on the measurement and optimization of a binding machine's paper punching tool geometry. Force profile measurements were performed to demonstrate the reduction of the required punching force, and consequently, the power requirements using a new shear punch geometry improving its efficiency. Results from measurements using common 80 gsm office paper are presented showing the variation of a decisive punching parameter such as shearing angle in punching force requirements.

---

J. Sousa (✉)  
Mechanical Engineering Department,  
School of Engineering, University of Minho, Braga, Portugal  
e-mail: jsousa@dem.uminho.pt

L. Figueiredo · J. Machado · J.P. Mendonca  
MEtRICs Research Center, School of Engineering,  
University of Minho, Braga, Portugal

Other authors show previous studies about the performance of paper punching systems. Previous studies of a 34 holes Punch and bind machine used multi-body dynamics simulation to study the punching system and calculate the total punching force [1].

A previous study using a punching blade, found an estimated optimal solution, making great improvements on the performance of the binding machine [2].

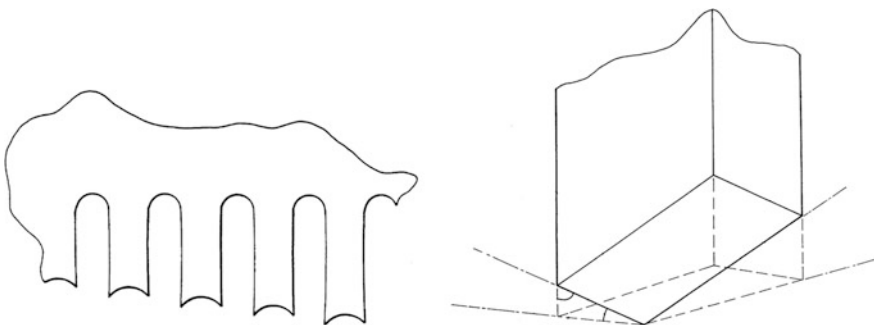
Punch pins used in comb-binding machines were also previously studied evaluating the comb-binding machine's punching performance. The influence of some parameters such as size and depth of the punch in shear forces was also evaluated [3].

Cutting force is affected by numerous factors such as: the shear strength of the workpiece material, thickness, die clearance, length of the cutting line, geometry of the cutting line, tool wear, surface condition of the tools, and guides lubrication [4]. Punch and die radii influence the cutting force as well, according to Bierzer and Schmidt [5] work.

The presented above parameters, valid for a sheet metal punching operation, can be related to a paper punching operation. Parameters like the punched hole profile quality are also affected by the punching operation [6].

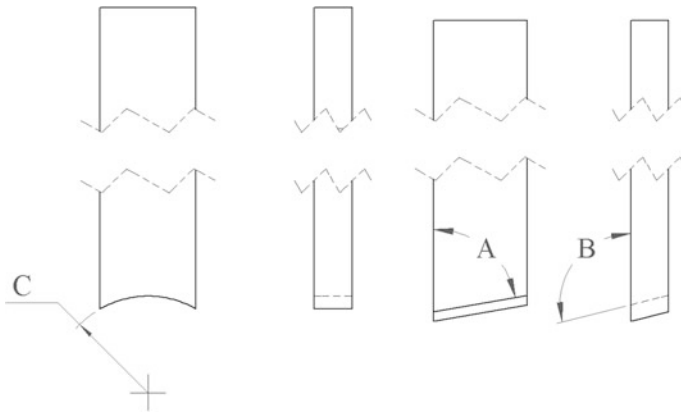
In the vast majority of binding types which require the punch operation, holes can present three different geometries: rectangular, square, and round. The dimensions of each hole, geometry, and the spacing between them are related to the binding spine configuration. To achieve the described punching types, there are several types of punchers with different pin geometry. These different geometries aim to reduce the required force to punch the document along with a quality hole finishing (burr free). This force reduction helps to increase punching capacity, keeping the same required force or equipment cost reduction, lowering power requirements [6].

Among the used punching pin geometries, the most relevant configurations are the concave geometry (Fig. 1) and the double shear angle geometry (Fig. 2). These pin geometries may be used in various types of punching.



**Fig. 1** Concave punching geometry [7] (left), double shear angle geometry [8] (right)





**Fig. 2** Original geometry F2 (left) and optimized geometry F1 (right)

## 2 Experimental Procedures

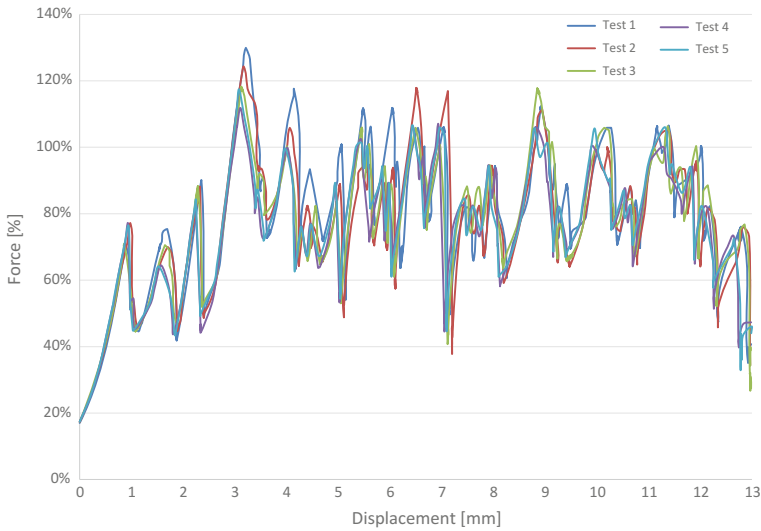
The required force for completely punch a stack of paper sheets was measured using an Instron<sup>®</sup> compression/tensile machine, with a custom support to drive the punching pins. Tested geometries are presented in Fig. 2. The F2 geometry (original) has a concave geometry with a radius “C.” The F1 geometry (optimized) has a double shear angle presented as “A” and “B.” Presented pins result in a rectangular hole and the measured arrangement has a total of twenty-one punch pins, which is a common number for binding machines designed to be used with stacks of A4 paper.

Each pin has a different length. The rationale is that during a punch stroke, only a single pin of the twenty-one pins will initially contact the stack of sheets at a time as the punching system is displaced in the punching direction [6].

The pins arrangement was compressed against a stack of ten paper sheets, in punching direction at a loading rate of 4 mm/s and using a total displacement of 13 mm. The used displacement guarantees that all twenty-one holes are totally achieved/perforated.

## 3 Results and Discussion

Figure 3 shows the punching force profile for the F2 original concave geometry. Presented profile has a very irregular punch stroke, the force and vibration which are transmitted, through the punching system’s actuating handle, to the user provides a disjointed and rough operational feel.



**Fig. 3** Punch profile for F2 original geometry

Figure 4 shows the punching force profile for optimized F1 double shear pin geometry. Presented profile shows a lower peak force to complete the punch stroke, but also shows a punch stroke with a smooth, even force profile. The even force profile results in a more ergonomic touch for the user operating a manual binding machine. Additionally, for motor-actuated applications, [9] the smooth force profile during the punch stroke can offer advantages as well.

As seen in Fig. 3, the punch force firstly increases to a first peak force value. After the initial maximum has been reached, the force value lowers, likely after some of the punch pins have pierced through the stack of paper sheets. Then, the punch profile shows a succession of upper and lower values in force as displacement of the punch pins arrangement continues during the punch stroke until the final maximum peak is reached. After that, the force lowers to zero at the end of the punch stroke with a small variation due to the friction as the punch pins pass through the punched holes in the stack of paper sheets. The smoother punch profile provided by the optimized geometry F1 (Fig. 1—right) is defined by the small percentage change in force between the first peak force value and the final peak force value. This small percentage change results in a smoother feel the user experiences when using a manually actuated binding machine.



Fig. 4 Punch profile for F1 optimized geometry

### 4 Conclusions

The optimized geometry F1 (Fig. 1—right) provides both a lower peak punching force value (30% less), as well as a smoother punch force profile. The total area under the curve in Fig. 3 represents the required energy, by sum of punch pins, to complete the punch stroke. Once the punch force profile is determined, for this particular punch pins arrangement, the transmission mechanisms can be redesigned to provide the appropriate force at the required displacement of the punch pin. This will result in a correspondence between the required force input and the force that the user must provide if a manually actuated machine is used or the required force of the electrical actuator in electrically actuated machines. Adjustments made to the pin’s tip geometry and to the length, orientation, and positioning of the pins can also result in different punch profiles that can be optimized for a specific binding application.

**Acknowledgements** The authors want to acknowledge the support from ACCO Brands Portuguesa, Lda. The authors also would like to thank the University of Minho’s Materials Testing Laboratory for the required testing facilities and support.

## References

1. Ye, Y., Yang, C., Ma, Z.: The test and CAE simulation way in the punching-binding machine design. *Ningxia Eng. Technol.* **4**, 352–354 (2009)
2. Zhang, M., Pan, B., Liang, L.: Multi-objective optimization design of punching blade structures. *Mech. Sci. Technol. Aerosp. Eng.* **12**, 1718–1722 (2010)
3. Jia, S., Liang, L., Pan, B.: Research on working performance of punch pin used in comb binding machines. *Light Ind. Mach.* **1**, 94–97 (2011)
4. Klocke, F.: *Manufacturing Processes 4*. Springer, Heidelberg (2013)
5. Bierzer, F., Schmidt, R.-A.: *Cold Forming and Fineblanking: A Handbook on Cold Processing Steel Material Properties Component Design*. Carl Hanser Verlag GmbH & Co, Germany (2007)
6. Sousa J., Pinho T., Figueiredo L., Mendonça J., Machado J.: Development and optimization of a paper punching system. *Adv Manuf.* **2B**, V02BT02A028 (2015)
7. Felton G., Aries P.A., Kandasamy B.: Punching and binding machine. WO 1999051406 A1, (1998)
8. Szoke E., Coric M.: Binding machine, US 8434987 B2, (2009)
9. Figueiredo L., Sousa J., Monteiro L., Mendonça J., Machado J.: Innovative mechatronic approach to redesign a punch and bind machine. *Adv. Manuf.* **2**, V002T02A043 (2016)

# Influence of the Inlet Nozzle Diameter on the Air Gauge Dynamics

Michal Jakubowicz, Mirosław Rucki, Gyula Varga  
and Radomir Majchrowski

**Abstract** In the paper, the experimental results of the study on the dynamic characteristics of the air gauges are presented. Dynamical properties of the air gauge are dependent mainly on the pressure transducer type and also on the geometry of its flow-through elements. The present investigations focused on the diameter of the inlet nozzle and its impact on the time constant and the frequency at which the dynamic error would not exceed 5%. It was proved that in the most common configurations of the air gauges, those two parameters may vary up to 100%, and the dynamics of the air gauges worsened with smaller inlet nozzles. The results are of high practical importance in industrial measurement systems where the air gauges are applied, because the multiplication of the air gauge is typically set by the adjustment or replacement of the inlet nozzle.

**Keywords** Air · Gauge · Dynamics · Time constant · Sine input response

## 1 Introduction

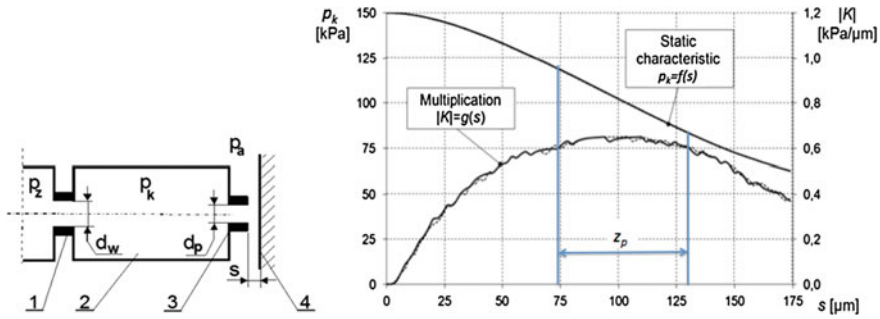
The evolution of machines and methods of their manufacture in the industrial economy is clearly aimed at economic factors [1]. The air gauges as a cheap and precise measurement devices are known for almost a century, and investigations on

---

M. Jakubowicz (✉) · R. Majchrowski  
Division of Metrology and Measurement Systems,  
Institute of Mechanical Technology, Poznan University of Technology,  
Piotrowo 3, 60965 Poznan, Poland  
e-mail: michal.jakubowicz@put.poznan.pl

M. Rucki  
Faculty of Mechanical Engineering, Kazimierz Pulaski University  
of Technology and Humanities in Radom, 54 Krasickiego Str,  
26-600 Radom, Poland

G. Varga  
Institute of Manufacturing Science, University of Miskolc,  
Miskolc – Egyetemváros 3515, Hungary



**Fig. 1** Typical back-pressure air gauge [7] (left) and its static characteristics (right)

the improvement of their dynamic characteristics were undertaken as long ago as in the middle of the twentieth century worldwide [2, 3]. It was commonly assumed that their dynamic characteristics are rather poor, but the recent studies proved that it was almost entirely dependent on the pressure transducers' dynamics [4]. New applications, new pressure transducers [5], and new computational capacities [6] stimulate further investigations on air gauge dynamic characteristics.

At present, most of the working air gauges are of the back-pressure type shown in Fig. 1. The slot width  $s$  between the measuring nozzle 3 (its diameter is  $d_p$ ) and the measured surface 4 is represented by the corresponding change of the back-pressure  $p_k = f(s)$  in the measuring chamber 2 of certain volume  $V_k$ . The inlet flow of the feeding pressure  $p_z$  is restricted by the inlet nozzle 1 of the fixed diameter  $d_w$  or by the adjustable restrictor of any type. After leaving the flapper-nozzle area, the pressure drops down to the atmospheric pressure  $p_a$ . In the certain range  $z_p$ , the function  $p_k = f(s)$  is almost linear, and it is used as a measuring range of the air gauge.

## 2 Dynamic Mass Flow and Back-Pressure in the Air Gauge

Relations between static and dynamic characteristics of the flapper-nozzle type air gauge are presented graphically in Fig. 2.

In the dynamic conditions of measurement, the sudden change of the slot width  $s(t)$  results in a drop or a jump of the measuring chamber pressure  $p_k(t)$ . In Fig. 2, there are graphs of the air gauge dynamic work when the step input  $\Delta s$  (left) causes the step response of the back-pressure  $p_k(t)$  (right) in line with the static characteristics  $p_k = f(s)$ .

When the slot  $s$  becomes smaller, the pressure  $p_k$  rise up, while the mass flow drops down. So it may be written:

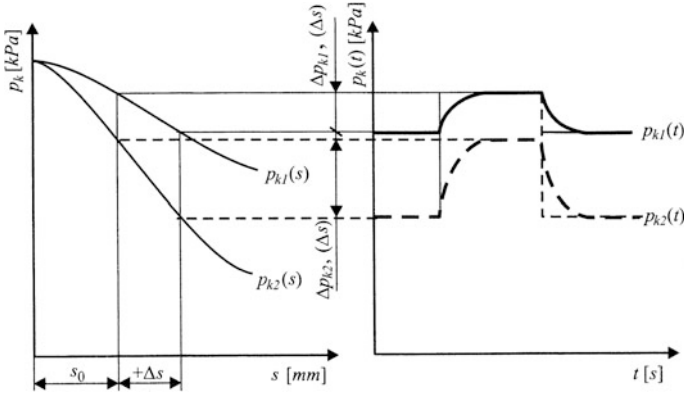


Fig. 2 Step response of the air gauge [8]

$$\dot{m}_w(t) - \dot{m}_p(t) = \frac{d(\dot{m}_k)}{dt} \tag{1}$$

where

- $\dot{m}_w(t)$  mass flow through the inlet nozzle,
- $\dot{m}_p(t)$  mass flow through the measuring nozzle,
- $\dot{m}_k$  mass of the air inside the volume  $V_k$ .

After the introduction of the mean mass flow corresponding with the steady state  $\dot{m}_0$ , the Eq. (1) may be rewritten as follows:

$$\dot{m}_w(t) - \dot{m}_0 + \dot{m}_0 - \dot{m}_p(t) = \frac{d(\dot{m}_k)}{dt}, \tag{2}$$

or in the other form:

$$\Delta\dot{m}_w(t) - \Delta\dot{m}_p(t) = \frac{d(\dot{m}_k)}{dt} \tag{3}$$

where:

$\Delta\dot{m}_w(t) = \dot{m}_w(t) - \dot{m}_0$  and  $\Delta\dot{m}_p(t) = \dot{m}_p(t) - \dot{m}_0$  represent the increase in the mass flow compared to the mean steady stream.

The back-pressure  $p_k(t)$  in the measuring chamber is bound with the mass flow by the following equation:

$$\dot{m}_w(t) = \alpha_w A_w \psi_{c1} \sqrt{\left(\frac{P_k(t)}{P_{zc}}\right)^{\frac{2}{\kappa}} - \left(\frac{P_k(t)}{P_{zc}}\right)^{\frac{\kappa+1}{\kappa}}}, \quad (4)$$

where

$\alpha_w$  flow-through coefficient of the inlet nozzle,  
 $A_w$  flow area of the inlet nozzle,  
 $P_k(t), P_{zc}$  absolute pressures: back-pressure and feeding pressure, respectively,  
 $\psi_{c1}$  auxiliary function that includes the absolute temperature  $\Theta_{zc}$  of feeding air and gas constant  $R$ :

$$\psi_{c1} = \frac{P_{zc}}{\sqrt{\Theta_{zc}}} \sqrt{2 \frac{\kappa}{R(\kappa-1)}}. \quad (5)$$

However, the theoretical unsteady value of the back-pressure  $P_k(t)$  is different from the actually measured one because of the second critical parameters [9]. The stream contraction in the flow-through elements causes certain losses of pressure; therefore, the actual pressure ratio for maximal mass flow differs from the theoretical one. This ratio is called the second critical pressure ratio  $\beta_{kr2}$ . The corresponding flow coefficient is:

$$\alpha_{kr2} = \frac{\dot{m}_{rzmax}}{\dot{m}_{imax}}, \quad (6)$$

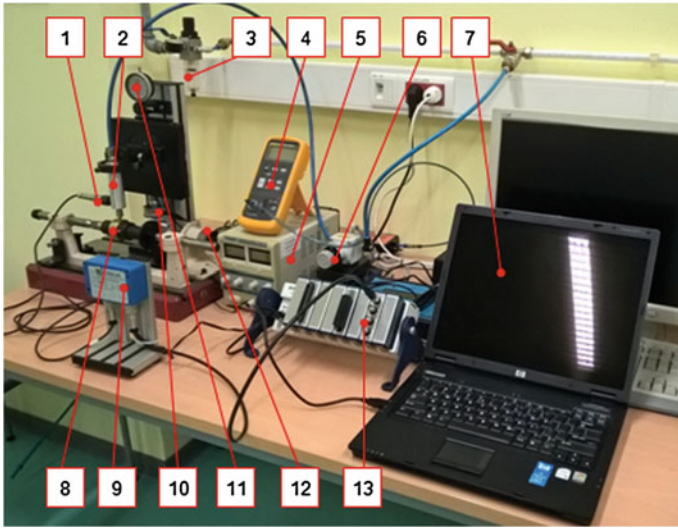
where  $\dot{m}_{rzmax}, \dot{m}_{imax}$  represent maximal values of the mass flow, actual and theoretical ones, respectively.

### 3 Experimental Apparatus

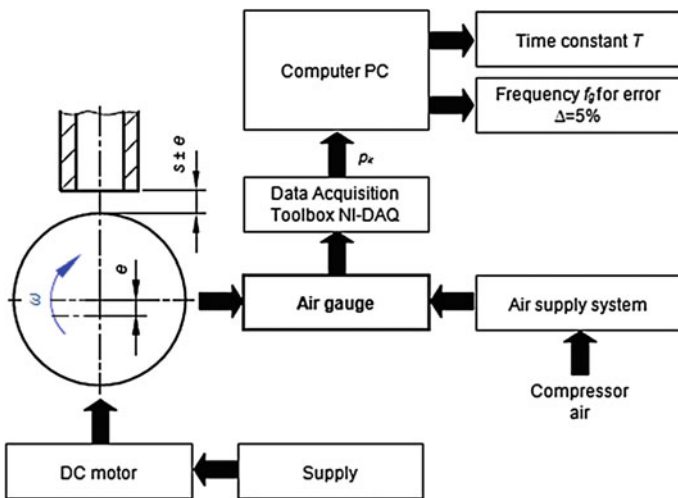
In order to perform the experimental evaluation of the dynamic characteristics of the air gauges, the sine input test rig described in previous works [9–11] was modernized and improved. Figure 3 presents its view, and Fig. 4 shows its block scheme.

The measurement equipment presented in Fig. 3 consists of: 1—piezoresistive pressure transducer Kistler 4043A2; 2—physical model of the air gauge; 3—reducer with the filter SMC AW20-A; 4—pressure calibration unit Fluke 717 30G; 5—power supply PS3003; 6—pressure stabilizer SMC IR2000-F02; 7—computer with the software LabVIEW SignalExpress; 8—eccentric of diameter  $\varnothing 50$  mm and known eccentricity  $e$ ; 9—amplifier Kistler 4618 A2; 10—air gauge positioning screw; 11—position indicator; 12—motor for eccentric rotation Maxon DC; 13—microprocessor system NI-DAQ-9172 with the measurement module NI 9234.





**Fig. 3** Experimental rig for the amplitude–frequency characteristics of the air gauges (described in the text)



**Fig. 4** Scheme of the amplitude–frequency characteristics experimental rig

The flapper surface was chosen because the typical measurement with the air gauges is the assessment of the rounded surfaces (diameters). In fact, usage of flat surface would make it necessary to introduce some correction for the rounded ones [12]. Based on the previous experimental research, it was assumed also that it is unnecessary to perform repetitions for different diameters of the eccentric.

The air gauges of the back-pressure type with the chambers of volume  $V_k$  below  $5 \text{ cm}^3$  perform the characteristics of the inertial first-order dynamic system [13]. Accordingly, its amplitude in a sine input response depends on time constant  $T$  and multiplication  $K$ :

$$A_{pk}(f_i) = \frac{K}{\sqrt{1 + (f_i T)^2}}. \tag{7}$$

During the measurement, for the air gauges with various inlet nozzles, the sine input was generated using a series of frequencies. The registered normalized amplitudes were:

$$A_u(f_i) = \frac{\Delta p_{ki}}{\Delta p_{k(f=0)}}, \tag{8}$$

where

$\Delta p_{ki}$  back-pressure value corresponding with  $i$ th value of applied frequency  $f_i$ ;  
 $\Delta p_{k(f=0)}$  back-pressure value for the static measurement, when  $f_0 = 0 \text{ Hz}$ .

From the obtained data, the time constants were calculated using well-known formula [14]:

$$T = \frac{\sum_{i=1}^n \frac{(1 - A_{ui}^2(f_i))}{A_{ui}^2(f_i)}}{\sum_{i=1}^n f_i \frac{\sqrt{1 - A_{ui}^2(f_i)}}{A_{ui}(f_i)}}. \tag{9}$$

Then, the frequency  $f_{0.95}$  that generates dynamic error 5% was calculated for each set of the collected data.

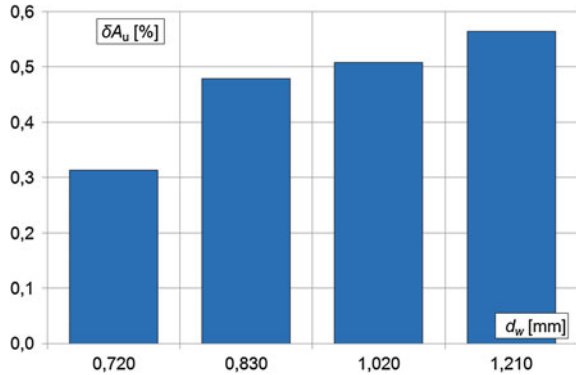
The air gauges with the measuring nozzle  $d_p = 1.391 \text{ mm}$  but with different inlet nozzles ( $d_w = 0.720; 0.830; 1.020$  and  $1.210 \text{ mm}$ ) were tested. In order to assess the approximation error, its mean square value  $\delta A_u$  was calculated from the formula [15]:

$$\delta A_u = \sqrt{\frac{1}{n} \sum_{i=1}^n (A_{ui} - A_{uti})^2} \cdot 100\%, \tag{9}$$

where

$i$ th normalized amplitude of the experimental characteristics,  
 $A_{ui}$   $i$ th normalized amplitude of the experimental characteristics,  
 $A_{uti}$   $i$ th normalized amplitude of the theoretical characteristics.

**Fig. 5** Amplitude approximation error  $\delta A_u$  for the air gauge with different inlet nozzles  $d_w$



**Fig. 6** Amplitude–frequency characteristics of the air gauge with  $d_w = 0.720$

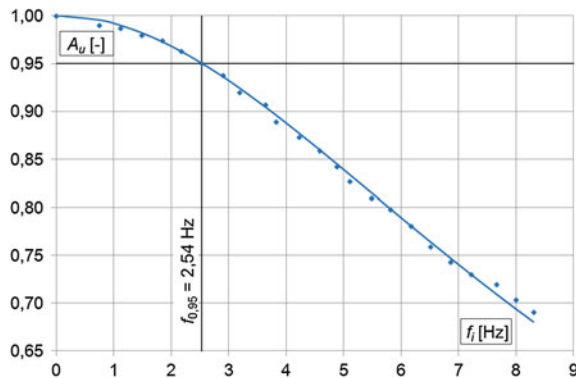


Figure 5 presents the graph of the approximation errors.

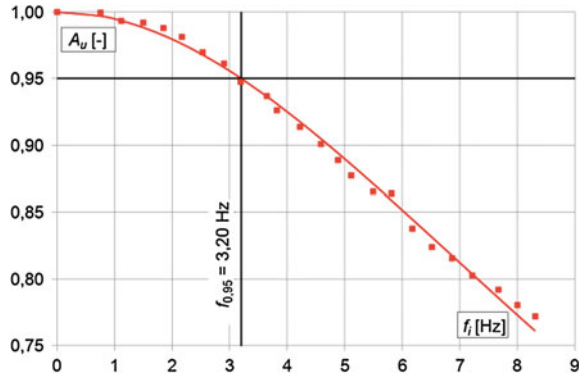
The approximation error for the air gauge with the inlet nozzle  $d_w = 1.210$  mm is almost twice larger than that with the  $d_w = 0.720$  mm. This result is consistent with the expectation on dynamics of the air gauges with larger inlet nozzles.

## 4 Measurement Results and Discussions

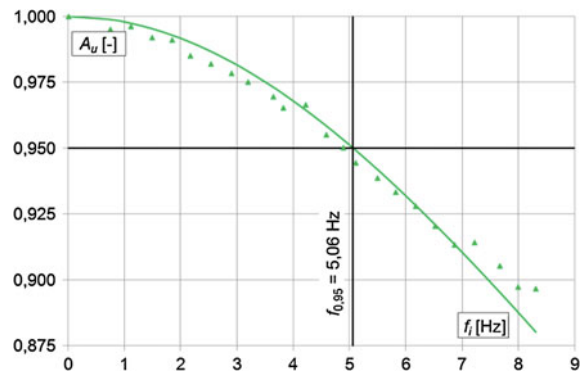
Figures 6, 7, 8, and 9 present the results of the measurement with dots representing the experimentally obtained amplitudes for each frequency, and the curves representing theoretical amplitude–frequency graphs.

From the graphs, it is seen that the experimental results are much more scattered for the larger diameters of inlet nozzles, which explain the rise of the approximation error noted in the previous chapter. For the air gauges with larger inlet nozzles, the 5% dynamic error frequency is larger and reaches the value of  $f_{0,95} = 8$  Hz for the air gauge with  $d_w = 1.210$  mm. Naturally, the time constant should be smaller for the larger inlet nozzles, as it is seen in Fig. 10.

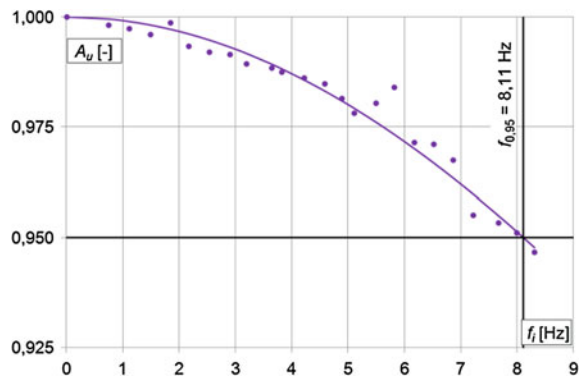
**Fig. 7** Amplitude–frequency characteristics of the air gauge with  $d_w = 0.830$



**Fig. 8** Amplitude–frequency characteristics of the air gauge with  $d_w = 1.020$  mm

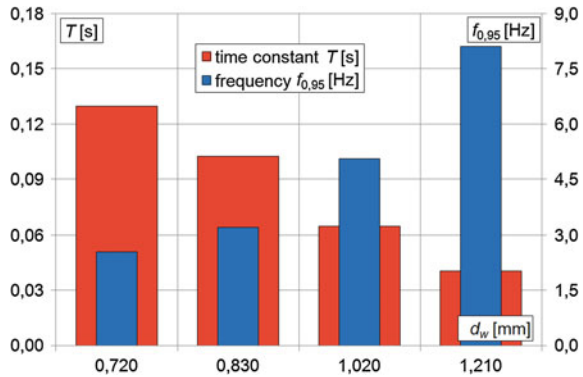


**Fig. 9** Amplitude–frequency characteristics of the air gauge with  $d_w = 1.210$  mm



The influence of inlet nozzle diameter on the static characteristics means that for larger  $d_w$ , the measuring range  $z_p$  becomes longer, but the multiplication  $K$  decreases. The investigations show that the time constant and critical frequency vary substantially, even more than 100%, dependent on the inlet nozzle diameter.

**Fig. 10** Amplitude–frequency characteristics of the air gauge with  $d_w = 1.210$  mm



In the industrial practice, when the dynamic measurement is performed, the response time variations should be taken into consideration. Otherwise, despite the better sensitivity of the air gauge with smaller inlet nozzle, its response time  $T$  could be too long to perform correct measurement.

On the other hand, when the air gauge is exposed to the periodical changes of the measured value, e.g., in the roundness assessment, the critical value of  $f_{0.95}$  should not be crossed. The operator must be aware of its dependence on the respective inlet nozzle diameter.

## 5 Conclusions

Industrial practice demands accurate measurement with high resolution also in the dynamic conditions. The air gauges meet this requirement providing reasonably accurate measurement at relatively small expenses. In the most typical configuration of the back-pressure air gauges, the time constant  $T$  between 0.04 and 0.13 s is reachable, with the 5% dynamic error  $f_{0.95}$  at the frequencies between 8 and 3 Hz, respectively.

However, the study proved that the exchange of the constant diameter inlet nozzle as well as the changes of the regulated inlet restriction unequivocally leads to the substantial changes of its dynamic parameters. Both the time constant  $T$  and the critical frequency  $f_{0.95}$  may be changed even 100% of its previous values.

Increase in the inlet nozzle diameter causes improvement of the dynamic characteristics (shorter  $T$ , larger  $f_{0.95}$ ). The air gauge operator must take it into consideration in the adjustment process, when the inlet restriction diameter is changed. Moreover, this fact must be challenged when the air gauge is projected, in the same degree as the dependence of the measuring range and the multiplication on the inlet nozzle diameter.

## References

1. Młynarski, S.: Evolution of machine reliability and life and economics of operational use. *Manage. Prod. Eng. Rev.* **7**, 76–85 (2016)
2. Mierzejewski, H.: Air gauge quick operation assessment (in Polish). *Mech. Rev.* **13**(4), 110–111 (1954)
3. Joyce, A.H., Rugg, K.E.: Dynamic air gaging reduces cycle time in precision measurement. *Gen. Motors Eng. J.* **5**(5), 32–39 (1958)
4. Rucki, M., Jermak, Cz.J.: Dynamic properties of small chamber air gages. *J. Dyn. Syst. Meas. Contr.* **134**(1), 011001 (2012)
5. Yurish S.: Product news. *Sens. Transducers e-Digest.* **91**(4) (2008). Available online [http://www.sensorsportal.com/HTML/DIGEST/april\\_08/PRECISE.htm](http://www.sensorsportal.com/HTML/DIGEST/april_08/PRECISE.htm)
6. Liu, J., Pan, X., Wang, G., Chen, A.: Design and accuracy analysis of pneumatic gauging for form error of spool valve inner hole. *Flow Meas. Instrum.* **23**, 26–32 (2012)
7. Jermak, Cz.J.: Methods of shaping the metrological characteristics of air gages. *Strojnicki vestnik—J. Mech. Eng.* **6**(56), 385–390 (2010)
8. Zelczak, A.: *Pneumatic Length Measurement* (in Polish). Warsaw (WKŁ) (2015)
9. Jermak, Cz.J., Rucki, M.: *Air Gauging: Static and Dynamic Characteristics*. Barcelona (IFSA) (2012)
10. Jermak, Cz.J.: Measurement equipment for the amplitude-frequency characteristics of the air gauges. *Arch. Mech. Technol. Autom.* **31**(4), 79–85 (2011)
11. Jermak, Cz.J., Majchrowski, R.: Measurement equipment for the amplitude—frequency characteristics of the air gauges. In: *Proceedings of the 13th National and 4th International Conference Metrology in Production Engineering*, Poznan—Zerkow, pp. 201–206 (2009)
12. Jermak, Cz.J., Rucki, M.: Calculation of the outlet surface for measurement by the air gauge. In: *Proceedings of the 4th International Conference Measurement 2003*, Slovak Academy of Sciences, Smolenice, pp. 495–498 (2003)
13. Rucki, M.: Dynamic properties of the back-pressure air gauges with small measuring chambers (in Polish). Poznan (2011)
14. Soboczyński, R.J.: *Investigations on the Metrological Characteristics of the High-Pressure Air Gauges*. doctoral thesis (in Polish), Wrocław (Politechnika Wrocławska) (1977)
15. Zięba, A.: *Analysis of the Measurement Data in Exact Sciences and Technics* (in Polish). Warsaw (PWN) (2014)

# Accuracy of Hysteresis Modeling in Smart Actuator with MSMA

Bartosz Minorowicz, Grzegorz Pittner and Frederik Stefanski

**Abstract** This paper is focused on hysteresis modeling in actuator with magnetic shape memory alloy, briefly MSMA. MSMAs are new group of active materials which change shape in external magnetic field. Active element is made of  $\text{Ni}_2\text{MnGa}$ , and it is very suitable to use in actuators for positioning, because this alloy combines great strains (up to 6%) and good dynamic properties. On the other side, it is distinguished by nonlinear behavior. In this case, it is wide saturated asymmetric hysteresis. Reason for that is a kind of internal friction called twinning stress. Such drawback does not allow to precise position control in open-loop control system. Described in this paper method for hysteresis modeling is based on mathematical formulation, which utilizes so-called phenomenological models. Hysteresis modeling is provided by generalized Prandtl-Ishlinskii model (GPIM) where hyperbolic tangents were used as envelop functions in play operator. This paper describes modeling accuracy for different GPIM structures. Actuator is designed for high-strain applications up to 1 mm. Data acquisition was provided by dSPACE system.

**Keywords** Hysteresis · Generalized Prandtl-Ishlinskii model · Magnetic shape memory alloy · Actuator · Smart materials

## 1 Introduction

Actuators and transducers play very important role in each engineering system. They convert and amplify energy, e.g., hydraulic servo valve converts electrical command signal, which power is expressed in mW into flow rate where power is expressed in kW. Common feature of most devices is their operation principle

---

B. Minorowicz (✉) · G. Pittner · F. Stefanski  
Faculty of Mechanical Engineering and Management,  
Institute of Mechanical Technology, Poznan University of Technology,  
Piotrowo Street 3, 60-965 Poznan, Poland  
e-mail: bartosz.minorowicz@put.poznan.pl

based on electromagnetic force (classical solution). In the other hand, a group of unconventional actuators can be mentioned [1], where movement and force are generated by so-called smart materials. The most interesting feature of these materials is the fact that they actively respond for changing state of surrounding (electric field, magnetic field, temperature, pressure, etc.) Smart materials unlike other materials can convert energy between many physical domains. They provide smaller size, better energy efficiency, better dynamics, better positioning accuracy. It perfectly fits to needs from advanced engineering branches such as aerospace, bioengineering, precision machining.

Significant disadvantage of smart materials is their nonlinear behavior, where hysteresis is strongest one. Sometimes, this hysteresis can be saturated and asymmetrical. All these things make that control issue of smart actuators becomes a big challenge. Practically, open-loop control system is impossible for the implementation in these actuators. For this reason, special techniques of nonlinear control can be adapted. Basic element of compensation system is proper hysteresis model and its inversion. Literature survey shows that phenomenological models, such as Preisach, Krasnoselski-Pokrovskii or group of Prandtl-Ishlinskii models can be effectively used in control systems. Structure of these models consist superposition of weighted operators (mathematical models without consideration of physics phenomenon's). Hysteresis compensation is based on inversion of hysteresis model. If hysteresis model has significant error, it affects accuracy in open-loop control with cascade compensator.

Contribution of this paper is research on accuracy of hysteresis modeling with generalized Prandtl-Ishlinskii model. Structure of this model allows for some modifications because it is assumed that for hysteresis modeling should be used four hyperbolic tangent functions. In this paper, authors check and compare what happens when two external hyperbolic tangent functions will be removed.

## ***1.1 Magnetic Shape Memory Alloys—MSMAs***

In this paper, author presents actuator with magnetic shape memory alloy, described first time by Ullakko et al. in 1996 [2]. This material, similarly to other shape memory alloys such nitinol consists of martensitic structure, but mechanism of shape memory is quite different. In nitinol, shape changes with temperature, which affects internal structure (phase transformation between austenitic and martensitic structures). Because it is thermal stimulation, dynamic properties are very weak, but the scope of possible strain is unusual compared to other active materials, up to 10%. In MSMAs, memory effect occurs only in martensitic phase, where external magnetic field can rearrange structure described as magnetically induced reorientation (crystal lattice deformation), and this results in strain up to 6%. Significant difference is dynamics, because MSMA reacts in milliseconds to a step change in external magnetic field strength. Interesting property of MSMA is its relative



permeability which changes linearly with elongation [3]. Magnetic core combined with permanent magnets and MSMA element as a part of core gives the easiest way to design energy harvester for energy recovery in vibrating systems. MSMA provides variable reluctance which gives alternating magnetic flux. Described properties show that MSMA is multifunctional material which wide range of possible engineering applications. Wider description of MSMA, its properties and rearrangement of crystal lattice in magnetic field can be found in [4, 5].

## 2 Hysteresis Modeling

Generalized Prandtl-Ishlinskii model is the special case of Prandtl-Ishlinskii model (PIM). Structure of PIM and shape of play operator allow only for modeling symmetric unsaturated hysteresis shapes which is very rare in case of active materials characteristics. For this reason, two models based on PI were proposed. First one is modified PI model (MPIM), which is cascade of PIM and scalar, memory-free function described by weighted one-side dead-zone operators [6]. First idea of generalized play operator is shown in [7]. This proposition is deeply investigated by Janaideh [8–10]. GPIM and its inversion are used to compensate hysteresis in thermal shape memory alloys [11], magnetostrictive actuators [9].

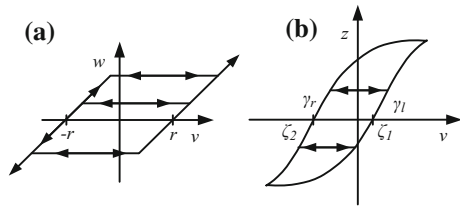
Advantages of models derived from Prandtl-Ishlinskii model are: analytical inversion, simple structure and easy implementation, significantly lower number of operators needed for hysteresis modeling than in case of Preisach and Krasnosel'skii-Pokrovskii models.

### 2.1 Generalized Prandtl-Ishlinskii Model

Classical Prandtl-Ishlinskii model is a superposition of weighted play operators. In contrast to operators from Krasnosel'skii-Pokrovskii and Preisach models, output of play operator is not limited by interval from  $-1$  to  $1$ . Operators presented below in Fig. 1a, b connect input  $v$  with output  $w$  or  $z$ . Distinguished parameter is threshold  $r$ . Total width of operator is expressed as  $2r$ . Elementary Prandtl-Ishlinskii play operator  $F_r$  can be represented as backlash block in Simulink, which is also mechanical clearance in systems such as gear boxes or lead screw drives.

Mathematical description of backlash is (1). Let us consider  $v(t)$  as an input function, which belongs to space  $Q[t_o, t_s]$ . This space represents piecewise monotone functions in range from  $t_o$  to  $t_s$ . Function  $v(t)$  satisfies monotonicity condition in each time interval  $[t_i, t_{i+1}]$ .

**Fig. 1** Play operators for Prandtl-Ishlinskii model and its generalized version



$$F_r[v](t) = \begin{cases} \max(v(t) - r, w(t_i)) & \wedge v(t) > v(t_i) \\ \min(v(t) + r, w(t_i)) & \wedge v(t) < v(t_i) \\ w(t_i), & \wedge v(t) = v(t_i) \end{cases} \quad (1)$$

In generalized case, play operator is defined as  $G_r$  (2). In this new defined operator, it is possible to choose envelope functions to describe better shape of hysteresis. Moreover, it is possible to define two separate functions to describe rising ( $\gamma_l$ ) and decreasing ( $\gamma_r$ ) edges of operator. Generalized operator meets the same conditions as classical play operator.

$$G_r[v](t) = \begin{cases} \max(\gamma_l(t) - r, z(t_i)), & \wedge v(t) > v(t_i) \\ \min(\gamma_r(t) + r, z(t_i)), & \wedge v(t) < v(t_i) \\ z(t_i), & \wedge v(t) = v(t_i) \end{cases} \quad (2)$$

Depending on shape of hysteresis, different functions can be chosen. The most appropriate functions for MSMA characteristics shape are hyperbolic tangent which can describe saturation effects (3) and (4).

$$\gamma_l = a_0 \tan h(a_1 v + a_2) + a_3 \quad (3)$$

$$\gamma_r = b_0 \tan h(b_1 v + b_2) + b_3 \quad (4)$$

Last important parameter is density function  $p(r)$  (5), which depends on the value of  $j$ -th threshold  $r$ . At the same time, threshold is positive multiple described by operator number (6).

$$p(r_j) = \rho e^{-\tau r_j} \quad (5)$$

$$r_j = \alpha j \quad (6)$$

Generalized model output  $Y$  is single integral of threshold function. This can be simplified to finite sum of play operators weighted by density function (7), where  $n$  is number of play operators.

$$Y_{pv}(t) = \Omega[v](t) + \sum_{j=0}^n p(r_j) \cdot G_{r_j}[v](t) dr \quad (7)$$

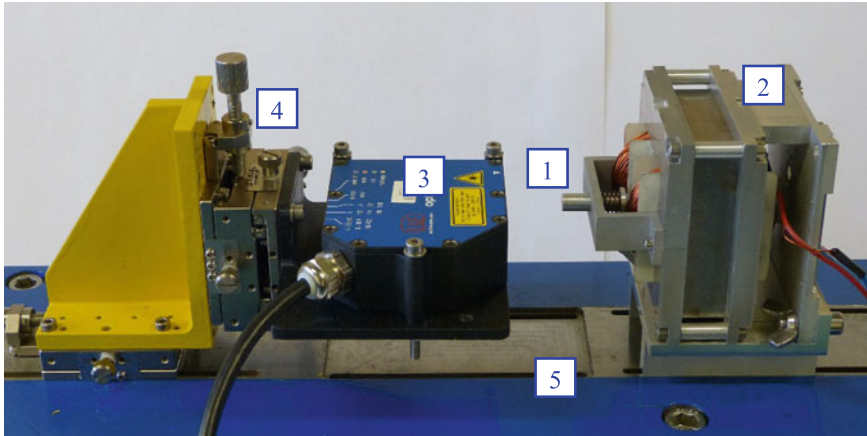
External shape function  $\Omega[v](t)$  consists of two additional functions activated for increasing or decreasing input (8). They can also be hyperbolic tangents [8, 12].

$$\Omega[v](t) = \begin{cases} c_0 \tan h(c_1 v + c_2) + c_3 & \wedge \frac{dv}{dt} \geq 0 \\ d_0 \tan h(d_1 v + d_2) + d_3 & \wedge \frac{dv}{dt} < 0 \end{cases} \quad (8)$$

### 3 Actuator and Test Stand

Examined actuator is a second device with MSMA designed, assembled, and calibrated in the Institute of Mechanical Technology. In this case, magnetomotive force is generated by two coils connected in parallel. Excitation current equals 3 A. MSMA element is distinguished by dimensions:  $3 \times 10 \times 32 \text{ mm}^3$  is placed in air gap in magnetic core. Width of air gap is slightly bigger and equals 3.2 mm. Relative permeability of MSMA when it is fully compressed equals 2. This is the main reason why one of MSMA sides is significantly shorter than another. Core is made of low carbon soft magnetic steel (steel grade 04 J), very similar in chemical composition to ARMCO iron. Magnetic field generated in coils causes martensite variants reorientation and pushes rod to move forward. Actuator works in spring returned mode. It means that backward movement is provided mechanically by spring. Processes of assembling and calibration of MSMA actuator are associated with setting proper value of spring preload by its preliminary compression. It is very important because preload force reduces maximum scope of strain to 3–4%. Alternative solution is actuator with two MSMA samples, which work oppositely. Advantage of this design is keeping by push-push actuator adjusted position without coils excitation. Reason of that is internal friction occurred in crystal lattice on twin boundaries. Negative effects of this friction are hysteresis and heat generation in fast switching systems. Rising temperature causes increase in austenite phase, which decreases max. strain of actuator. MSMA actuator similar to described in this paper is presented in paper [13], where authors proposed magnetic core containing permanent magnets.

Composition of prepared test rig is presented in Fig. 2. The most important parts which are actuator and examined push rod are presented in right part of photograph. Position measurement is provided by  $\mu$ Epsilon triangular laser displacement sensor, which is mounted by adjustable in three-axis tables. Heavy steel plate is a base of test rig; additionally, it is supported on steel legs with damping elastomer. Structure of actuator is separated from steel plate by holder made of aluminum. PC computer is central part of data acquisition and control system. Models are prepared in MATLAB/Simulink software and implemented by Control Desk on dSPACE



**Fig. 2** Test stand and MSMA actuator, where 1—examined push rod, 2—MSMA actuator, 3—triangular laser displacement sensor  $\mu$ Epsilon ILD-1700-10, 4—fast calibration mechanical system, 5—mechanical steel breadboard

board with ADC and DAC connections. Coils are energized by programmable DC power supply.

## 4 Hysteresis Models and Results

First step in hysteresis modeling is static characteristics registration. For this purpose, damped sine function was used. Characteristics features of this function are maximum amplitude of applied current (1.5 A) plus 1.5 A of bias, which gives current changes from 0 to 3 amperes. After two cycles from 0 to 3 A, current asymptotically decreases to 1.5 A. Thanks to this input signal, detailed hysteresis shape can be registered. Obtained results are used in Simulink model, where parameters estimation is made. Hysteresis modeling in this case includes two scenarios. First model is based on Eq. 7, where it can be noticed that four hyperbolic tangent functions were used, and second scenario assumes that Eq. 8 equals 0 so hysteresis model is simplified and shape functions are reduced to two hyperbolic tangent functions.

Response of Simulink models with estimated parameters for the same current input signal is shown in Figs. 3 and 4.

It can be noticed that model with more hyperbolic tangent functions covers better hysteresis shape. For accuracy evaluation, another plot was made, where errors are shown (Fig. 5). Detailed presentation of modeling errors is in Table 1. It is clearly visible that original model is much more precise than reduced one. In next pictures (Figs. 6 and 7), authors indicated places, where maximum positive and negative errors are located.

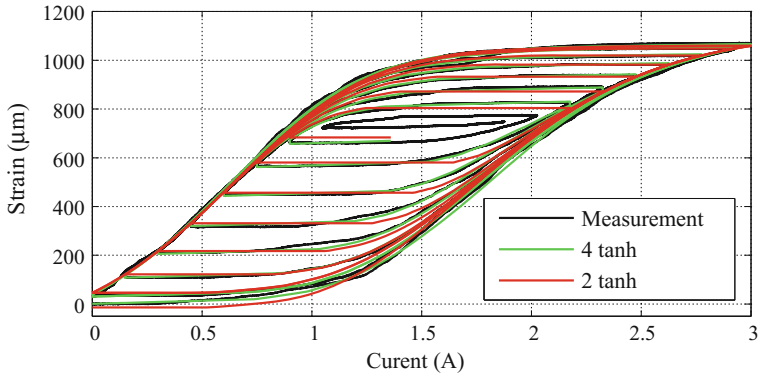


Fig. 3 Major and minor hysteresis loops registered on test rig and obtained in examined models

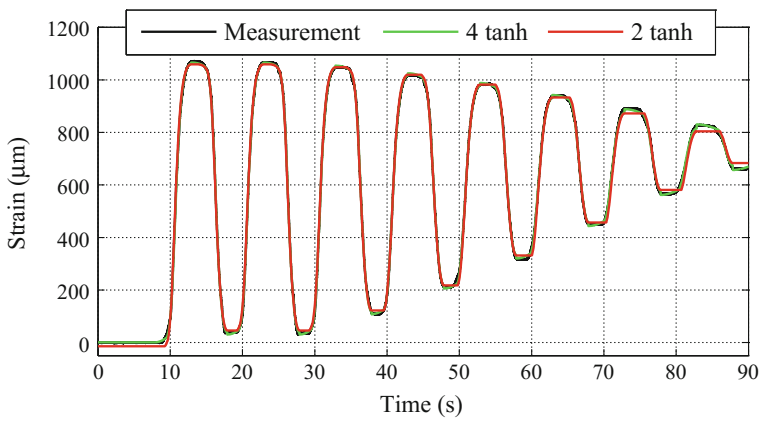


Fig. 4 Measurement and modeling results presented in time domain

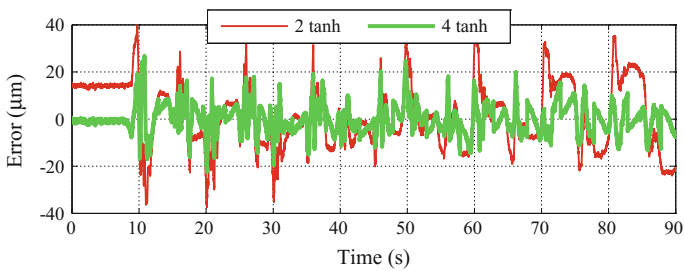
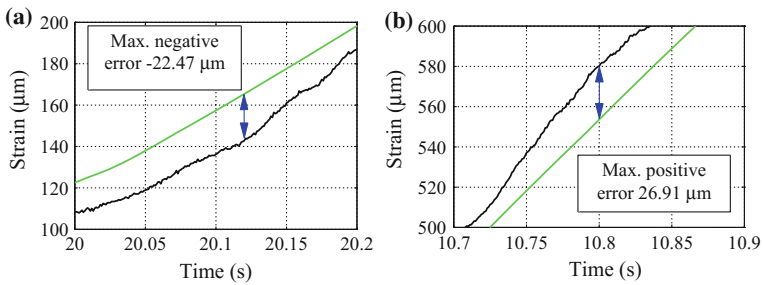


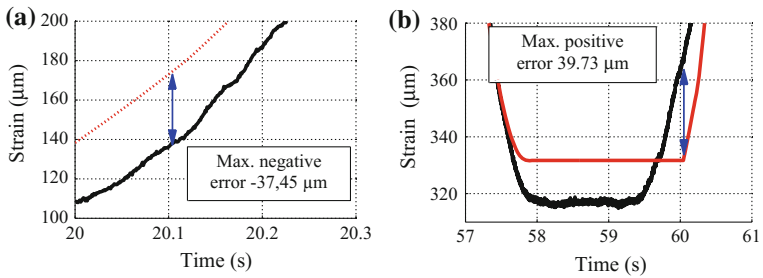
Fig. 5 Modeling errors for GPI original and reduced models

**Table 1** Modeling errors

	Reduced model errors		Original model errors	
	( $\mu\text{m}$ )	%	( $\mu\text{m}$ )	%
Measured strain	1074.5	100	1074.5	100
Max. positive error	39.73	3.70	26.91	2.5
Max. negative error	-37.45	3.49	-22.47	2.09
Max. positive +  Max. negative  errors	77.18	7.18	49.83	4.64
Max. absolute error	39.73	3.70	26.91	2.5
Mean error	2.58	0.24	-0.0533	0.005
Absolute mean error	11.71	1.09	4.37	0.41
RMSE	13.9	1.29	5.99	0.56



**Fig. 6** Indication of places with **a** maximum negative error and **b** maximum positive error for model described in Eq. 7 (four hyperbolic tangents)



**Fig. 7** Indication of places with **a** maximum negative error and **b** maximum positive error for model without external shape functions (two hyperbolic tangents)

## 5 Conclusions and Discussion

Based on the analysis of simulation results, it can be stated that despite which model of hysteresis is used, modeling errors are in acceptable range (shown in Table 1). Model with four hyperbolic tangents needs eight parameters more than simplified one, and it means that estimation time is longer. It is much more complicated to use complex model for hysteresis compensation by inverse model, and whole process needs much more computing power. Compared to the literature in both cases, modelling errors are lower. For example, modified Prandtl-Ishlinskii model has errors 11.2 [14] and 14.5% [15]; in case of Krasnoselskii-Pokrovskii model, this error is also bigger and equals 8.16% [16, 17].

**Acknowledgements** The presented research results, executed under the subject of 02/22/DSPB/1389, were funded with grants for education allocated by the Ministry of Science and Higher Education in Poland.

## References

1. Janocha, H.: *Adaptronics and Smart Structures*. Springer, Berlin (2007)
2. Ullakko, K., Huang, J.K., Kantner, C., O'Handley, R.C., Kokorin, V.V.: Large magnetic-field-induced strains in Ni<sub>2</sub>MnGa single crystals. *Appl. Phys. Lett.* **69**(13), 1966–1968 (1996)
3. Gabdullin N.A., Khan S.H.: Application of change in permeability of magnetic shape memory (MSM) alloys for optimization of magnetic circuit in actuators. In: *Computation in Electromagnetics (CEM 2014)*, 9th IET International Conference on, IET, pp. 1–2. (2014)
4. Schiepp, T., Maier, M., Pagounis, E., Schluter, A., Laufenberg, M.: FEM-simulation of magnetic shape memory actuators. *IEEE Trans. Magn.* **50**(2), 989–992 (2014)
5. Jokinen T., Ullakko K., Suorsa I.: Magnetic Shape Memory materials-new possibilities to create force and movement by magnetic fields. In: *Proceedings of the Fifth International Conference on Electrical Machines and Systems, ICEMS*, vol. 1, pp. 20–23 (2001)
6. Kuhnen, K.: Modeling, identification and compensation of complex hysteretic nonlinearities: A modified Prandtl-Ishlinskii approach. *Eur. J. Control* **9**, 407–418 (2003)
7. Brokate, M., Sprekels, J.: *Hysteresis and Phase Transitions*. Springer, New York (1996)
8. Al, Janaideh M., Rakheja, S., Su, C.Y.: A generalized Prandtl-Ishlinskii model for characterizing the hysteresis and saturation nonlinearities of smart actuators. *Smart Mater. Struct.* **18**(4), 045001 (2009)
9. Al Janaideh, M., Rakheja, S., Su, C.-Y.: An analytical generalized Prandtl-Ishlinskii model inversion for hysteresis compensation in micropositioning control. *IEEE ASME Trans. Mech.* **16**(4), 734–744 (2011)
10. Al, Janaideh M., Rakheja, S., Su, C.Y.: Experimental characterization and modeling of rate-dependent hysteresis of a piezoceramic actuator. *Mechatronics* **19**(5), 656–670 (2009)
11. Sayyaadi, H., Zakerzadeh, M.R.: Position control of shape memory alloy actuator based on the generalized Prandtl-Ishlinskii inverse model. *Mechatronics* **22**(7), 945–957 (2012)
12. Minorowicz, B., Nowak, A., Stefanski, F.: Hysteresis modelling in electromechanical transducer with magnetic shape memory alloy. *Przegląd Elektrotechniczny* **11**, 244–247 (2014)
13. Matsunaga, K., Niguchi, N., Hirata, K.: Study on starting performance of Ni-Mn-Ga magnetic shape memory alloy linear actuator. *IEEE Trans. Magn.* **49**(5), 2225–2228 (2013)

14. Riccardi L., Naso D., Turchiano B., Janocha H.: Adaptive approximation-based control of hysteretic unconventional actuators. In: Decision and Control and European Control Conference (CDC-ECC), IEEE, pp. 958–963 (2011)
15. Riccardi L., Naso D., Turchiano B., Janocha H., Adaptive modified Prandtl-Ishlinskii model for compensation of hysteretic nonlinearities in magnetic shape memory actuators, In: 37th Annual Conference on IEEE Industrial Electronics Society, pp. 56–61 (2011)
16. Riccardi, L., Ciaccia, G., Naso, D., Janocha, H., Turchiano, B.: Position control for a magnetic shape memory actuator. IFAC Proc. Vol. **43**(18), 478–485 (2010)
17. Riccardi, L., Naso, D., Janocha, H., Turchiano, B.: A precise positioning actuator based on feedback-controlled magnetic shape memory alloys. *Mechatronics* **22**(5), 568–576 (2012)



# Application of Scanning Techniques in the Analysis of the Wear Forging Tools

Marek Hawryluk, Jacek Ziemia and Marcin Rychlik

**Abstract** The work concerns the possibility of the use of modern non-contact measurement techniques in a die forges. In particular, the possibility of using measuring arms with integrated linear scanners to analyze wear of forging instrumentation. The research was divided into two phases. The first step was to analyze tool wear based on direct scanning of their surfaces, then develop a wear-loss curve of the geometric material. In the second step, a selected area of cyclic retrieved forgings from the forging process was scanned for use of an intermediate scanning method—reverse 3D scanning. On this basis, an analysis of the progressive material growth on the selected surface of forgings was made, which was also a loss of material on the tools. The performed analyses showed a good agreement of the geometrical properties of the surfaces (of the selected forgings representing the proceeding wear of the tool) and the geometrical defect of the working impression of the tool, based on the direct measurements during the production process. The obtained results allow for a fast analysis of the forging tool life with respect to the quality and the quantity forging instrumentation.

**Keywords** Quality control · Scanning 3D reverse · Forging tools · Durability

---

M. Hawryluk · J. Ziemia (✉)  
Department of Metal Forming and Metrology,  
Wrocław University of Science and Technology,  
Lukasiewicza 7-9, 50-371 Wrocław, Poland  
e-mail: jacek.ziemia@pwr.edu.pl

M. Hawryluk  
e-mail: marek.hawryluk@pwr.edu.pl

M. Rychlik  
Kuźnia Jawor, ul. Kuziennicza 4, 59-400 Jawor, Poland

## 1 Introduction

The digitization of real objects is of fundamental importance in various fields of science and industry. Industrial processes like assembly or product manufacturing are complicated, highly automated, and usually based on CAD data (Computer Aided Design). So, optimal operation of such processes is afforded by the application of various quality assurance systems. This concerns both machines and devices, as well as tools and the product itself. In particular, the geometry of assembled parts and subassemblies or of a manufactured product must be checked thoroughly in order to ensure that the dimensions are correct and other quality specifications are met. Effective measurement and analysis of shape using static and mobile 3D scanners, and more and more frequently, measuring arms with integrated 3D scanners, can provide this [1, 2].

3D scanners on measuring arms serve for performance of precise scans and measurements. They are ideally suited for inspection and comparing point clouds with CAD data, rapid prototyping, reverse engineering, and 3D modeling. They are mounted on rigid arms made from strong and resilient materials like aluminum, titanium, or carbon fiber, as well as on rotating high-accuracy encoders. At the beginning, scanners of this type served solely as measuring arms, using probes for contact measurements, but over time, the range of their capabilities was vastly expanded by functions such as contactless scanning, which meant that these scanners could be successfully applied in reverse engineering. 3D scanning can be performed by means of various technologies; however, each of them has its limitations and advantages. For example, optical technologies make it more difficult to scan glossy or transparent objects. This problem can be solved by covering an object with a matting agent. A well-established classification [3] divides digital technologies for acquiring the shape of a three-dimensional object into two categories: contact and contactless. Contactless solutions can be divided into two additional subcategories: active and passive. Measuring arms with integrated 3D scanners are currently equipped with white light and scanning heads that employ either laser scanning (cheaper version) or structured-light scanning (more expensive version) to capture a three-dimensional image of the entire object. Structured-light scanning is still a very active field of research, with new scientific articles published on this subject every year [4–7].

3D scanners are currently finding applications in many branches of industry, including in construction and civil engineering for building measurements and documentation, in medicine for capturing shape for the purposes of designing orthoses, prostheses, or dental implants, in coordination of product manufacturing—using parts from multiple sources, and within the broad scope of reverse engineering, as well as in quality assurance and industrial metrology. This last field of applications, in particular, is finding the increasing recognition, e.g., in controlling the geometry of forging tools and forgings. Die forging processes are one of the most difficult manufacturing processes to perform. Despite the fact that the technology is relatively well known, proper manufacturing of forgings with complicated shapes,

that will meet requirements concerning accuracy and quality posed by customers, require much experience from process engineers and operators. Wearing of forging tools and other instrumentation causes a change of the manufactured product's geometry, and any surface defects on tools (cracks, losses) are reflected on the forged product, affecting the quality of the ready product [8–10].

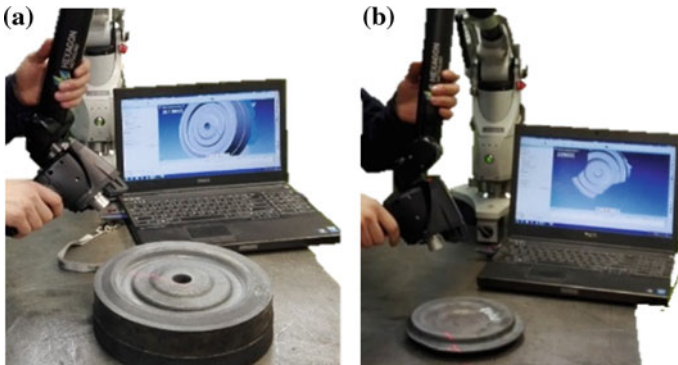
The main and most common destructive mechanisms include abrasive wear, mechanical cracking, plastic deformation, and thermal and thermal-mechanical fatigue [11]. The classical measuring methods applied at forges do not allow for rapid and comprehensive evaluation of the quality and accuracy of an entire object. This is why this situation is changing more and more often, particularly in modern forges, and greater emphasis is now placed on the application of more accurate measuring tools and instruments and on employing new measuring methods, including contactless scanning techniques [2]. 3D scanning technology is mainly used for final quality control of products [12, 13], and decidedly, less frequently used for evaluation of the condition of tools used to manufacture a given product or similar applications [12, 14, 15]. Such measurements are usually based on evaluation of shape errors according to a defined contour and surface [16]. An example of such an application of the 3D scanning method is using an optical scanner to determine shape errors of a defined surface, and then, based on obtained data, determining the geometric specifications for the regenerative padding process [12, 18]. Another application of spatial scanning methods is to use shape error analysis of a defined surface to evaluate the wear of forging tools, nitrided or coated with hybrid coatings [19, 20]. Interest in such applications inclines toward analysis of scanning techniques from the perspective of the possibilities of their application and development in the forging industry, including for analysis of tool geometry changes over the course of the forging process and for continuous assessment of a forging tool's condition based on cyclically acquired and scanned forgings, as well as for more advanced analyses and applications.

### ***1.1 Goal and Scope of the Paper***

The goal of this paper is to design and develop a contactless measuring method—spatial scanning for analysis and assessment of forging tools' wear using a measuring arm with an integrated linear scanner.

## **2 Measuring Method and Description of the Measuring Station**

The ROMER Absolute ARM 7520si with an integrated RS3 scanner and Polyworks software, enabling scanning in Real Time Quality Meshing technology, was selected for tests for applying a contactless measuring method to scan tools and



**Fig. 1** The measuring station with the ROMER Absolute Arm 7520si with an integrated RS3 laser scanner for measurements of: **a** insert die, **b** forging

forgings over the course of the forging process. This machine makes it possible to perform contact measurements using an additional measuring probe as well as contactless measurements using an RS3 laser scanner integrated with the arm, which provides the capability of collecting up to 460,000 points/s for 4600 points on a line at a linear frequency of 100 Hz with the scanning system accuracy SI 0.058 mm in relation to B89.4.2. To conduct measurements for the purposes of the developed measurement technology, a laboratory measuring station was built, as presented in Fig. 1.

Measurements employing contactless techniques, including with the application of a measuring arm and integrated scanner, are most commonly used for two groups of objects: both forgings and ready forged products, as well as for measurements of forging tools and instruments. In the case of mobile measuring equipment (measuring arms and scanners), measurements of forging apparatus are decidedly more popular thanks to their mobility and the capability of measuring large-size and heavy dies, often directly on the production line.

### 3 Scanning of Forging Tools

The authors conducted wear measurements of a selected forging tool after an increasing number of forgings and compared obtained scans of increasingly worn tools with the scanned image of a new tool (Fig. 2).

The presented results of superpositions of the images of worn tools onto the image of a new tool (after an increasing number of forgings) indicate progressing wear. In the initial period, for inserts after a low number of forgings, up to 1850 pieces, no material loss is visible. However, starting from 2500 forgings onward, wear can be observed clearly in the central part and increasingly on the tool's bridge. For an insert that has produced 12,500 forgings, the loss of the face exceeds 1.8 mm, and the loss of the bridge is approx 1.6 mm. It can be seen that for the

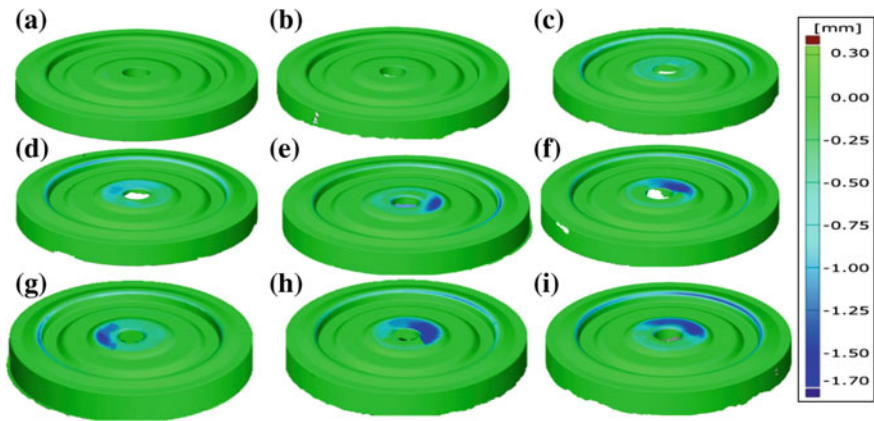


Fig. 2 Tool scanning results after different numbers of manufactured forgings: a 550, b 1850, c 2500, d 4300, e 5000, f 6900, g 9500, h 11,000, i 12,500

majority of tools, wear on the insert's face is clearly asymmetrical, while more uniform loss can be observed on the bridge. The analysis presented in Fig. 2 may prove to be insufficient, so on the basis of collected scans of tools after an increasing number of forgings, a wear characteristic of a given tool can be determined as a function of numbers of forgings from 0 to 12,500 pieces. Based on the presented chart (Fig. 3), resembling a classical wear (Lorenz) curve, interesting dependencies can be observed, and several wear ranges (periods) can be distinguished. However, the presented analysis concerns volume loss on all working surfaces of the selected tools, which may result in certain differences between individual scans in Fig. 3.

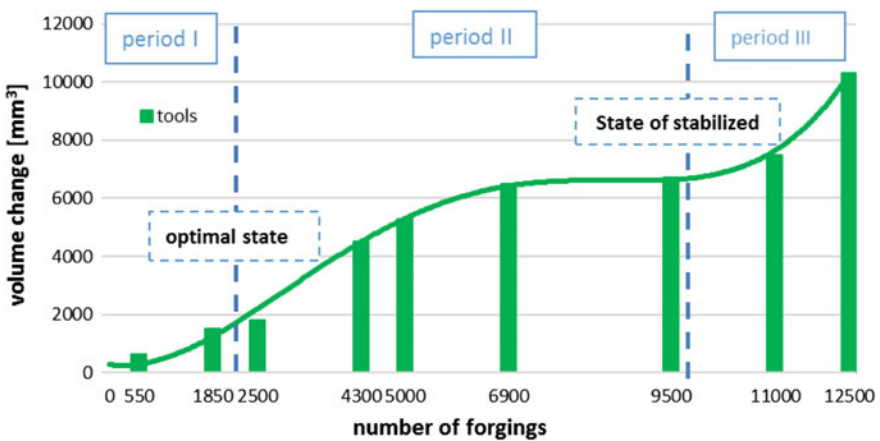


Fig. 3 Material loss (volume change) on dies as a function of the number of forgings

As seen on the chart (Fig. 3), based on analysis of scans, material loss for a given tool/die insert grows very rapidly at the beginning of the forging process, up to about 2000 forgings (period I). This is related to the “adaption” of the entire system, during which the initial condition of the surface layers of contacting elements (tool and forging) is worn down to its optimal condition.

After reaching the optimal condition, meaning more than 3000 pieces, the so-called normal operating condition (period II) begins, characterized in approximation by a stabilized intensity of the aforementioned destructive phenomena, which lasts until approx 9500 pieces in the analyzed case. The volume change in this forging number range spans from 3000 to 6200 mm<sup>3</sup> and starting from 9500 pieces until the end of a tool’s lifetime (over 12,000 pcs.), the volume change reaches up to 4000 mm<sup>3</sup>. On this basis, it can be concluded that the stabilized wear condition can be accepted to last within 3000–9500 forgings, the latter value of which can be accepted as the beginning of wear period III. In the case of the analyzed tool, this condition lasts until the end of lifetime, i.e., 12,000 pcs., and ends when the maximum tool shape change is exceeded, and the tool is withdrawn from further production. A similar situation takes place for the classical Lorenz curve, which usually transitions into an accelerated wear condition at the end of normal operation. It should be clearly stated that the shape of the wear curve may differ for other tools, as confirmed by the authors’ studies, presented in work [1].

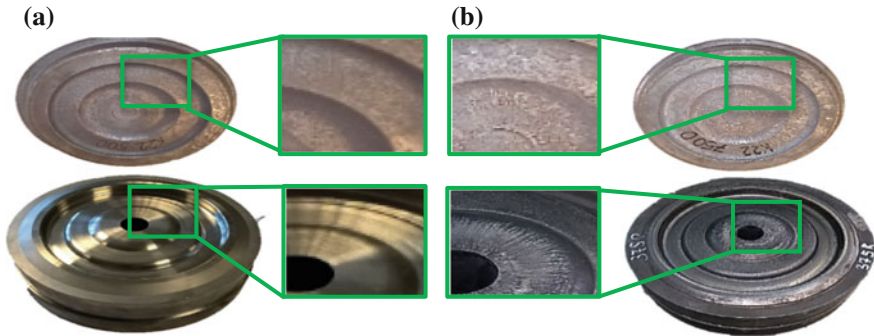
## 4 Development of Reverse 3D Scanning Methods

The next stage of development for tool wear analysis methods was to build a wear characteristic without interfering in the ongoing forging process.

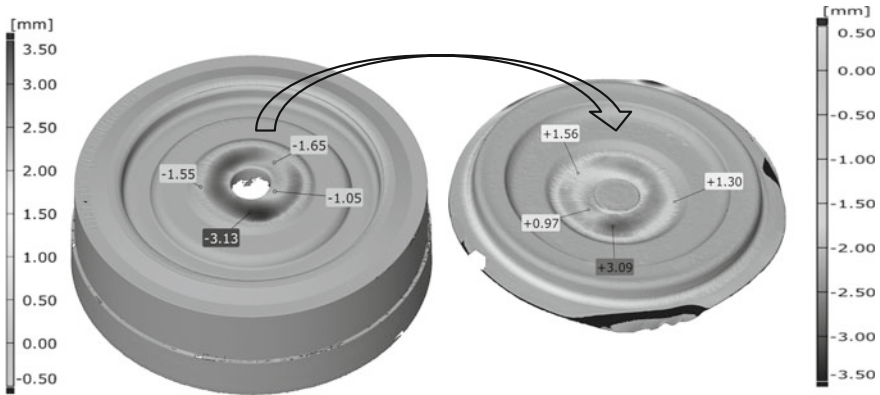
In this case, the 3D scanning method was applied for indirect quality control and monitoring of geometric changes of forging tools (without the need to dismount them) through direct measurement of geometry changes in periodically acquired forgings. On this basis, a wear characteristic with a result comparable to the curve obtained on the basis of tool scans can be determined. The essence of the developed die wear assessment technology is to employ the forging’s shape changes, occurring as a result of die wear over the course of the forging process, in measurements. For this purpose, the observed similarity (reflection) of the tool’s working surface on a selected surface of the forging was employed, by which the decrement of tool material is equal to the increment of material on the forging. Figure 4 presents an example of a die surface before and after operation along with the forging surfaces corresponding to these conditions.

Figure 5 presents measured values of material decrements on the tool and the corresponding material increments on the analyzed forging. The presented reverse 3D scanning concept utilizes the reflection of changes on the tool onto the selected area of the forging.

The developed method is based on measurement of progressing wear of a selected forging tool (in the form of its material loss) using a scanner, on the basis of shape



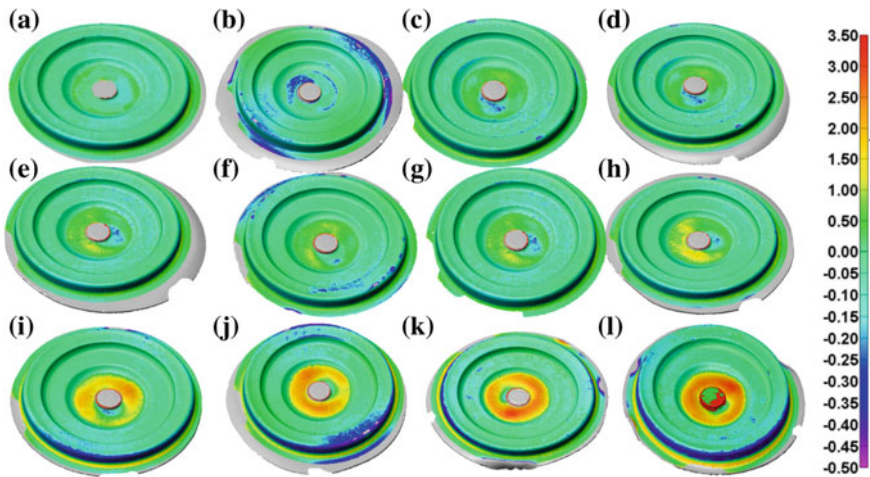
**Fig. 4** Example of a die insert: **a** new—before operation along with forging from the beginning of operation (500 pcs.), **b** worn—after forging 7500 forgings along with the last forging



**Fig. 5** Comparison of scans of the die and final forging, in the form of surface shape change

changes of forgings periodically acquired from the process (in the form of material increments on the forging) (Fig. 5). A color map of deviations on the surface of the forging scan is the result of the comparison, illustrating the deviation of the scanned surface from the nominal dimension given by the scan of the 100th forging. Based on the obtained point cloud, a polygonal surface consisting of elementary triangles was generated, representing the geometry of the measured object. To reconstruct the progression of die wear, forgings selected from a series were scanned (100th pc. and every 1000 pcs.) out of a total of 12,500 pcs. for the selected die.

Figure 6 presents scans of forgings (every 1000 pcs.) in the form of shape change of the defined surface in comparison with the scan of the 100th forging, which was acquired according to the measurement technology described above. The results indicate that progressing tool wear can be observed for as the number of forgings increases thanks to the employment of the reflection of the tool image on the surfaces of successive forgings and comparing it to the “un-worn” 100th forging.



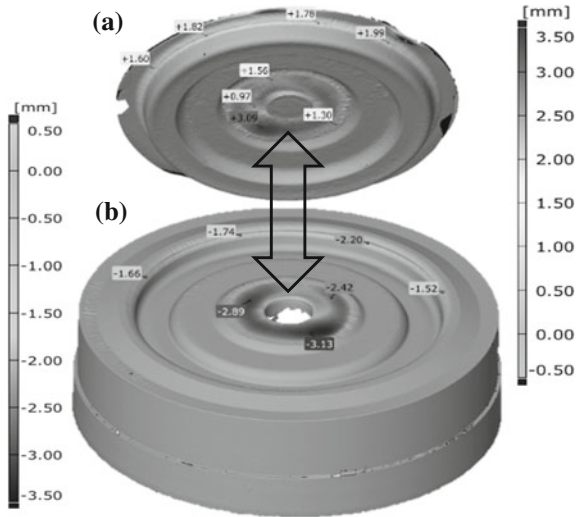
**Fig. 6** Comparison of scans of forgings forged using the die in the form of shape change of the captured surface compared to the 500th forging, after: **a** 1000, **b** 2000, **c** 3000, **d** 4000, **e** 5000, **f** 6000, **g** 7000, **h** 8000, **i** 9000, **j** 10,000, **k** 11,000, **l** 12,000 pieces

Wear is located in the central part, near the pusher hole in the area of the forging's face, and is irregular in the initial phase of the forging process. At the end of the die's lifetime, radial grooves in a deep ring are visible (Fig. 6). Scans also show wear in the area just in the front of the bridge (flash area) in the form of an asymmetrical wear ring. The results presented in the form of the shape error of periodically acquired forgings only allow for simplified analysis. Such analysis makes it possible to determine the areas of the die where wear occurs as well as the sites with the greatest material loss. Such reconstruction of the progression of wear makes it possible to conduct analysis at an interval equal to the frequency of forging acquisition.

The presented results of wear analysis, calculated on the basis of forging analysis, are very similar to the results of typical die wear analysis at the end of the forging process (Fig. 7). So, it can be assumed that employing the reflection of tool changes over the course of the forging process onto periodically acquired forgings yields results that are consistent and allow for wear analysis.



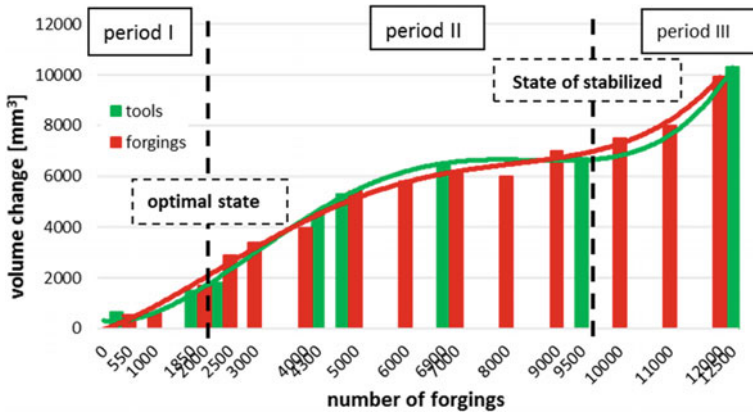
**Fig. 7** Comparison of 3D scanning results: **a** final forging, **b** die at the end of the forging process



### 5 Comparison of the Wear Curve Determined on the Basis of Scanned Tools and Reverse 3D Scanning

Figure 8 presents a comparison of the Lorenz curve determined on the basis of scanned tools after increasing wear (Fig. 3) and on the basis of the reverse 3D scanning method, by measurement of systematically acquired forgings (their scans are presented in Fig. 6).

The comparison of both charts presented in Fig. 8, which allows for determination of dependencies describing tool wear over the course of forging (determination of tool life), indicates high coincidence between their results. The greatest divergences can be observed at the very beginning, i.e., from 0 to 2500 forgings, and within the range from 4500 to 9500 forgings. Differences in the initial range are most probably the result of stabilization of the process (the entire system), meaning stabilization of the proper tool working temperature and of optimal lubricating and cooling conditions—tribological conditions. However, differences in the later period can be explained by the studies conducted by the authors, which demonstrated that in this process, within the range of approx 4000–5000 forgings, destructive mechanisms are intensified, which are linked to detachment of increasingly large particles of the nitrided layer and tool material from the areas under the highest load. Other causes of slight discrepancies between both curves may be the fact that tools selected for wear determination were taken from several, identical processes but after increasing numbers of manufactured forgings. This was dictated by the need to maintain similar process conditions (elimination of tool cooling for scanning analysis and reheating before continuing the production process). Moreover,



**Fig. 8** Comparison of wear curves based on tool scans (green) and forging scans (blue) as a function of number of forgings

every tool was not used again after scanning analysis but rather cut into specimens for further tests: microstructural, SEM, microhardness measurements, etc. Other, less significant causes of slight discrepancies may be the measuring accuracy of the scanner itself ( $\pm 0.035$ ) and oxidation and scaling of measured forgings, which were cleaned before measurement, as well as errors arising from the computation algorithm in volume analysis. With an awareness of the above, the presented comparison confirms that determining wear on the basis of scanned forgings periodically acquired over the course of the production process (without the need to disrupt the process) is an effective and economically justified method. It should also be emphasized that determining wear on the basis of tool scans is an impractical method that generates additional cost, often causing difficulties in production continuity, breaks in production and changes of process and tribological conditions.

## 6 Summary

This paper presents methods for monitoring the wear of a forging tool using contactless 3D scanning techniques, which make it possible to conduct both simple and comprehensive analyses. Based on the research conducted, the most important conclusions were drawn up:

1. Research has shown the use of contactless measurement technology for indirect and direct quality analysis and tool change design (without disassembly of the forging equipment). As a result, a wear analysis of forging tools became possible directly during production.
2. The use of the arm and integrated laser scanner for wear analysis enabled the development of a 3D reverse scanning method based on the measurement of the

- shape changes of subsequent forgings. Analysis of the volume increment of subsequent forgings on the basis of measurements allows to precisely determine the loss of material of the forging tool in subsequent phases of its operation.
3. The innovative approach to assessing the state of the forging tool proposed by the authors allows the decision to prolong or shorten the life of the forging tool based on the actual (current) wear and not on the basis of the rigidly fixed tool life (maximum number of forgings).
  4. The advantages and disadvantages of the tool developed for tool wear analysis using 3D scanners allow for longer tool life and significantly lower production costs.
  5. Further research with the objective of developing and improving the reverse 3D scanning method is currently underway.

**Acknowledgements** The research work reported here was made possible by National Centre for Research and Development, Poland (NCBiR); grant no. POIG.01.04.00-02-056/13.

## References

1. Gronostajski, Z., Hawryluk, M., Kaszuba, M., Ziemia, J.: Application of a measuring arm with an integrated laser scanner in the analysis of the shape changes of forging instrumentation during production. *Maintenance Reliab.* **18**(2), 194–200 (2016)
2. Ratajczyk, E.: Coordinate measuring arms and their accuracy tests (in Polish). *Electrotechnical Rev.* **5**, 181–185 (2008)
3. Curless, B.: From range scans to 3D models. *ACM SIGGRAPH* **33**(4), 38–41 (2000)
4. Dworzak, Ł., Hawryluk, M., Kaszuba, M., Ziemia, J.: Analysis of the approximation of data obtained from scanning of a forging instrument measuring arm under production conditions. In: *IV Manufacturing Conference: Selected Conference Proceeding*, pp. 23–34 (2016)
5. Gąska, A., Olszewska, M.: Evaluation of shape mapping using a coordinate measuring arm equipped with an optical head (in Polish). *Adv. Sci. Technol.* **7**, 37–43 (2011)
6. Derejczyk, K., Siemiński, K.: Accuracy analysis of optical 3D scanning methods (in Polish). *Mechanic* **4**, 312–313 (2016)
7. Juras, B., Szewczyk, D.: Dokładność pomiarów realizowanych skanerem optyczny. *Postępy Nauki i Techniki* **7**, 29–36 (2011)
8. Gronostajski, Z., Hawryluk, M., et al.: Solution examples of selected issues related to die forging. *Arch. Metall. Mater.* **60**(4), 2767–2775 (2015)
9. Hawryluk, M., et al.: Phenomena and degradation mechanisms in the surface layer of die inserts used in the hot forging processes. *Eng. Fail. Anal.* **79**, 313–329 (2017)
10. Hawryluk, M.: Review of selected methods of increasing the life of forging tools in hot die forging processes. *Arch. Civ. Mech. Eng.* **16**, 845–866 (2016)
11. Gronostajski, Z., et al.: A review of the degradation mechanisms of the hot forging tools. *Arch. Civ. Mech. Eng.* **14**(4), 528–539 (2014)
12. Marton, E., Pizzolon, F.: Dimensional control during forging. *Innovative 3d laser measuring systems. Forge Appl.* **1** (2010)
13. Weckenmann, A., Weickmann, J.: Optical inspection of formed sheet metal parts applying fringe projection systems and virtual fixation. *Metrol. MS* **13**(4), 321–334 (2006)
14. Macháček, P., Tomíček, J.: Application of laser scanning in reverse engineering and prototype manufacturing. *WTP* **1**(21), 35–44 (2010)

15. Pachutko, B., Ziólkiewicz, S.: Investigation of the wear processes of dies for forging building anchors basing on metallographic examinations. *OPM* **23**(4), 277–293 (2012)
16. Kuş, A.: Implementation of 3d optical scanning technology for automotive applications. *Sensors* **9**, 1967–1979 (2009)
17. Kontrola jakości odkuwek i matryc – archiwizacja i regeneracja matryc, ITA-Polska
18. Measurement of a forging die for tooling corrections: AICON\_3D\_SYSTEM
19. Gronostajski, Z., et al.: The application of the reverse 3D scanning method to evaluate the wear of forging tools divided on two selected areas. *J. Auto. Tech.* **18**(4), 653–662 (2017)
20. Hawryluk, M., et al.: Analysis of the wear of forging tools surface layer after hybrid surface treatment. *Int. J. Mach. Tools Manuf.* **114**, 60–71 (2017)

# Comparison of Geometrical Accuracy of a Component Manufactured Using Additive and Conventional Methods

Witold Habrat, Maciej Zak, Jolanta Krolczyk and Pawel Turek

**Abstract** This chapter describes three different methods of manufacturing a vacuum cleaner connector made of ABS and NECURON plastic material. Basically, the part is produced on an injection molding machine; however, with the help of manual laser scanner analysis, it is possible to compare two other methods: part manufactured by milling is 0.04 mm and part manufactured by injection molding machine is  $-0.15$  mm and 3D-printed part is  $-0.20$  mm. All the above-mentioned methods of producing the connector have their advantages and disadvantages. The fabrication time of all elements (under 1 min for injection molding machine, 1.5 h for milling machine and ca. 7 h for 3D printing) and costs of machines and tooling are decisive factors for manufacturing technique selection.

**Keywords** Manufacturing technology · Reverse engineering · 3D printing · 3D scanning

## 1 Introduction

The development of CAD and CAM software has become the basis of aiding engineering efforts. This technology has enabled achieving better quality products at lower manufacturing prices, thus contributing to production optimization [1–3]. More and more often finished products are being processed to electronic models. This method is known as reverse engineering. Rapid prototyping enables the creation of physical models and prototypes based on a 3D-CAD model. 3D profilometry as a method of surface geometry inspection enables the monitoring of

---

W. Habrat (✉) · M. Zak  
Faculty of Mechanical Engineering, Rzeszow University of Technology,  
12 Powstancow Warszawy, 35-959 Rzeszow, Poland  
e-mail: witekhab@prz.edu.pl

J. Krolczyk · P. Turek  
Faculty of Mechanical Engineering, Opole University of Technology,  
76 Proszkowska Street, 45-758 Opole, Poland

metrological changes of machine parts or processes [4, 5]. The machine part defects are very often caused by the inappropriately selected input parameters and manufacturing processes [6–8]. Additive manufacturing of components becomes effective in single-piece production or low-volume production [9], and it eliminates the need to use specially designed tooling (e.g., dies or molds). It possesses a big advantage compared to conventional fabrication methods, as well as presents a particular advantage over machining processes [10]. Additive manufacturing methods, however, do not ensure adequate elements accuracy in case of small- and micro-sized components. Rapid prototyping methods in combination with reverse engineering make a good tool for producing prototypes.

Along with industry development, new machines and manufacturing methods being developed. Moreover, the significant increase of application of polymer plastics in production is being observed. The ability to adjust properties to user requirements in particular applications is the main feature of mass and common application in different areas of the economy. In the past decade, the global demand for plastics has grown by 62% while the manufacturing of steel shrunk by 21% [11]. Plastics are characterized by the ease of forming and coloring. Injection molding of plastics is commonly used for manufacturing household articles components, packaging, machine components, tools, prostheses and other models used for serial production. The general property of plastics is their lower density compared to metals, corrosion resistance, moisture resistance and very low heat conductivity as well as very good dielectric properties.

The purpose of this paper is to compare the geometrical accuracy of a selected component manufactured with the use of three basic fabrication methods: machining, injection molding and 3D printing (rapid prototyping). The geometry was verified using manual laser 3D scanner.

## 2 Materials and Methods

The model used for research is a connector used to join the suction nozzle with a telescopic tube of a Zelmer vacuum cleaner (Fig. 1). After creating the geometry in CAD software, it was vital to save the data in a neutral format enabling further data processing in rapid prototyping system.

The file was created in Creo Parametric 2.0 software in PRT format (Fig. 1). Additionally, the generated STL file was analyzed in 3D-Tool software. A relevant density of triangular mesh resembling the surface controls the exported model accuracy. The solid model was generated and described by a triangular mesh of 0.01 resolution (Fig. 2).

The verified model was sent to Insight Stratasys software responsible for preparing the STL model to be fabricated by the 3D printer. Optimum parameters in configurational option are shown below:

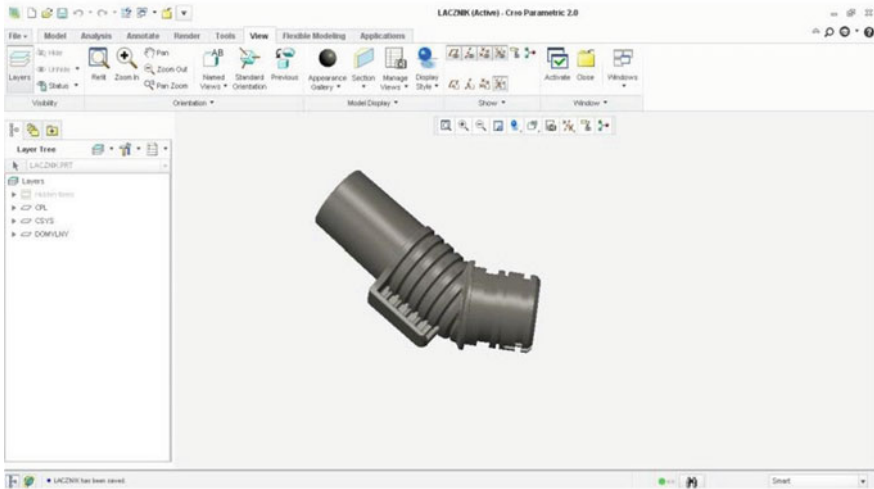


Fig. 1 Surface CAD model of a connector for the vacuum cleaner

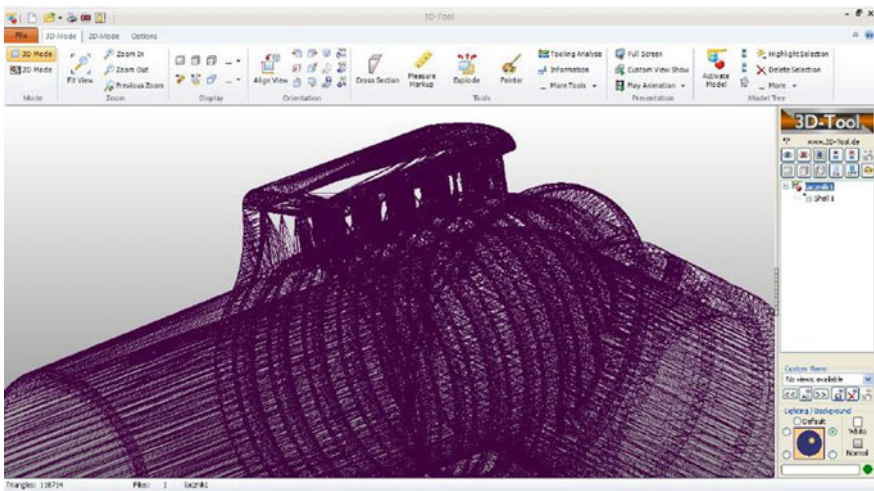


Fig. 2 High-resolution triangular grid of STL model

- 3D printer model—Fortus 360mc Small,
- Single-layer height set to 0.254 mm,
- head model used to build the component—T16,
- modeling material—ABS-M30,
- head model used to build supports—T12,
- support material—SR30,
- interior design—solid—normal,

- visible surface—reinforced,
- support design—columns.

Subsequently, the program performed relevant calculations simulating the view of supports (gray), part (red) and approximate fabrication time. Different settings were selected aiming to achieve lower support material consumption, improved surface finish of the surface used to fit the telescopic tube of the vacuum machine and optimum printing time. Optimum model is depicted in Fig. 3. The verified model was transmitted to software synchronized with the 3D printer. The printer model is Fortus 360mc (Fig. 4), which utilizes the FDM technology to create the prototype. This method consists in applying “liquified” thermoplastic material onto a particular modeling support and self-hardening of the material.

The system is equipped with a  $355 \times 254 \times 254$  mm workspace, two heads and four material feeds—two for model material (ABS-M30) and two for the so-called support (T12SR30). Each layer is 0.254 mm thick. The material feeding nozzle is heated to material melting temperature in order to prevent solidification in the nozzle. Easily melting wax is used as a supporting material for the printing process to enable effortless disposal when the task is finished. It is an easy and safe method which does not damage the model. The supports were dissolved in PADT cleaning device, model SCA-1200. The final view of the printed connector is shown in Fig. 5.

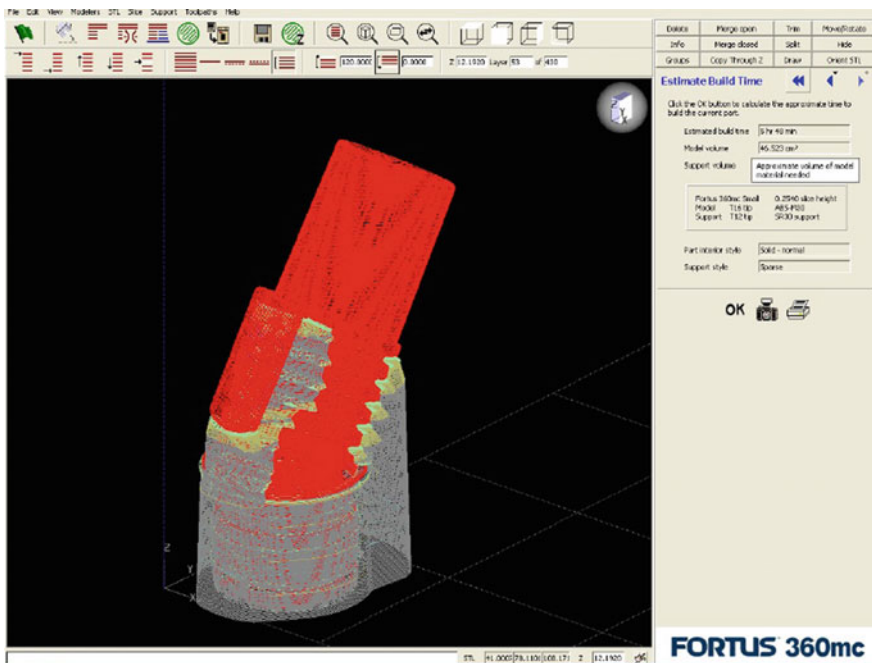


Fig. 3 Model for 3D printing

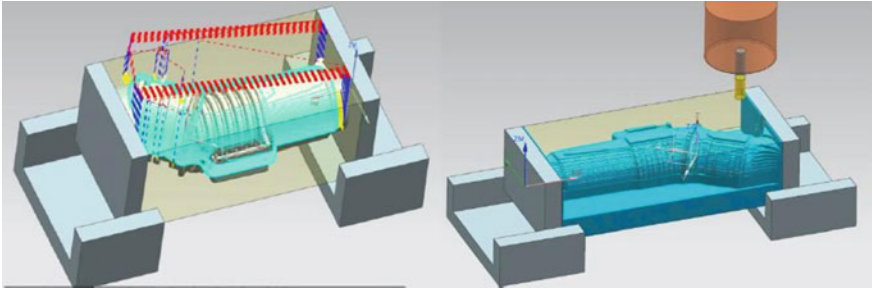




**Fig. 4** 3D printer Fortus 360mc



**Fig. 5** Model of the connector performed on a 3D printer

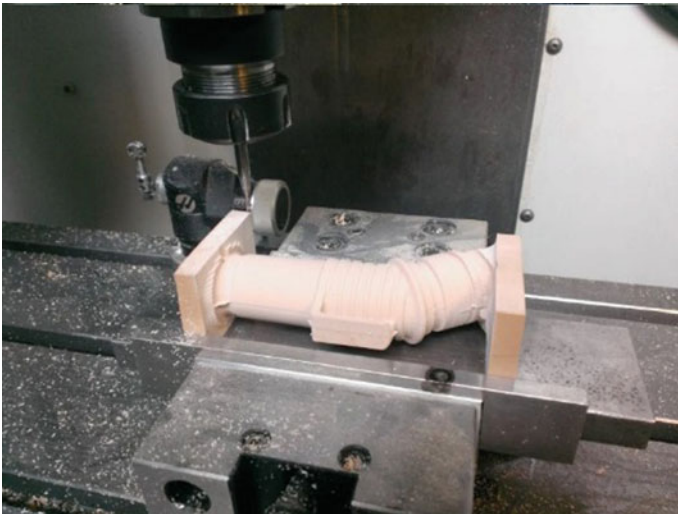


**Fig. 6** View of toolpaths and machined model

The second component used for comparative analysis was processed by machining. A 6-mm-diameter end mill with 40-mm holder length was used. The stock value at sidewalls was set to 0.2 mm, and tolerance values were set to 0.003 mm. Tool paths generated and the machined model are presented in Fig. 6.

Next, a 3-mm-diameter ball end mill with 40-mm holder length was utilized for semi-finish machining of the connector's cavity. The subsequent stock was set to 0, and inner and outer wall tolerances were set to 0.003 mm. Afterward, three other tools were added—12-mm-diameter and 6-mm-diameter end mills and a 3-mm-diameter ball end mill.

Machining was performed on a vertical machining center HAAS Mini Mill on a Necuron material workpiece. Necuron is a polyurethane material possessing a uniform structure and good machinability, taking into account its hardness and strength. The final stage of machining is depicted in Fig. 7.



**Fig. 7** Final machining stage of the connector on the milling machine

**Fig. 8** Station for laser scanning



Last part has been manufactured using injection molding technology, and this is a manufacturing process for producing parts by injecting material into a mold.

The models obtained were subject to dimensional verification using a digital contactless NIKON laser scanner, model K-scan MMD100 mounted on an MCA II measurement arm (Fig. 8) and using Focus Handheld software. The width of the laser beam equals 100 mm, measurement error is 10  $\mu\text{m}$  and a number of scanned line points is 1000 at 33–150 Hz scanning frequency.

### 3 Results

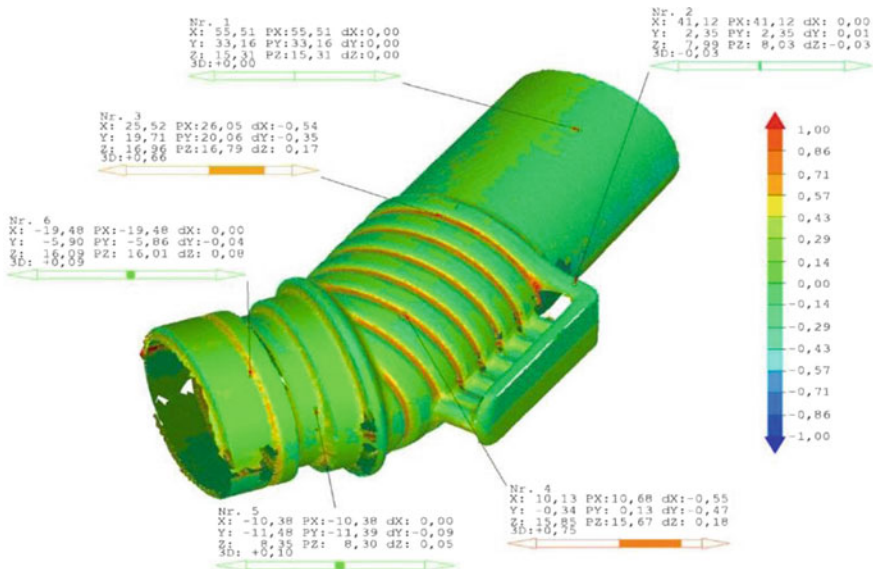
Scanning was performed by adjusting the power of the laser beam to the character of the scanned object surface. For a white, brown and black connector, the power of the laser was consecutively set to 18, 36 and 98. This resulted in best possible resemblance of scanned surface of the model. The scanner enables precise and fast measurements when scanning shiny and polished surfaces. The Focus software ensures data processing with minimal involvement of the operator. The CAD model creation process consists in scanning the surface of the object with the laser beam followed by importing and preprocessing of a cloud of points or a triangular mesh in the program. Subsequently, curves surrounding the scanned component are created and then a mesh is created on the measured part. Before comparing the scanned model with the base CAD model of the connector, undesirable surfaces

**Table 1** Deviation data for model connector created with different processes

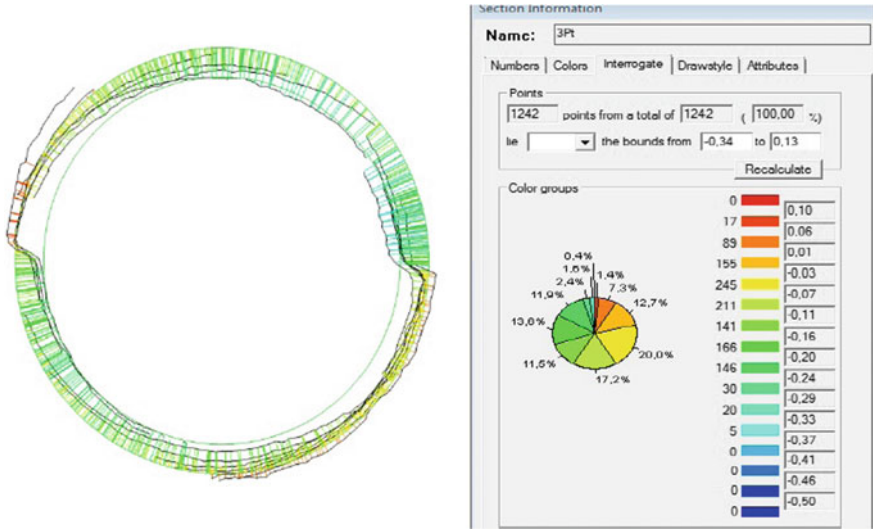
	Milling machine	FDM printing in a 3D printer	Injection molding machine
Number of points	82,271	71,698	51,399
Maximum deviation (mm)	1.59	1.63	1.39
Minimum deviation (mm)	-1.10	0.79	-1.87
Range (mm)	2.69	2.42	3.25
Mean deviation (mm)	0.04	0.20	-0.15

that could interfere with the results of the measurements were cut off. Next both models were opened in Inspection software and overlaid onto each other with “Best Fit” option enabled along with 1- $\mu$ m-fit tolerance. For each component, two reports were presented: a chromatic map of 3D deviations and surface inspection results achieved by cutting the model with a 2D plane. Analysis results are shown in Table 1 and graphically in Figs. 9, 10, 11 and 12. Measurement results are depicted with colors: red—the feature value of the measured component is above tolerance limit, green—the feature value of the measured component is within tolerance, and blue—the feature value of the measured component is below tolerance limit.

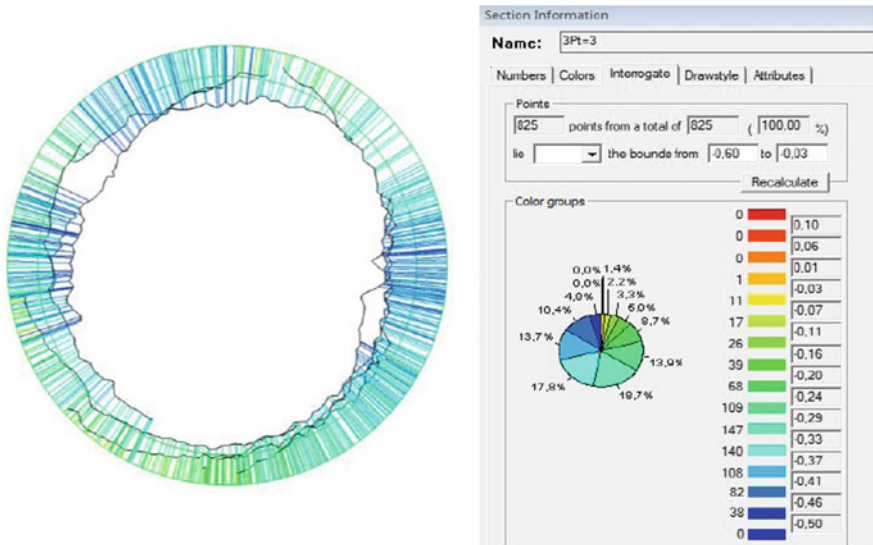
The highest number of points was managed to be collected on the machined part model, i.e., 82,271 points. The maximum positive deviation for all three connectors



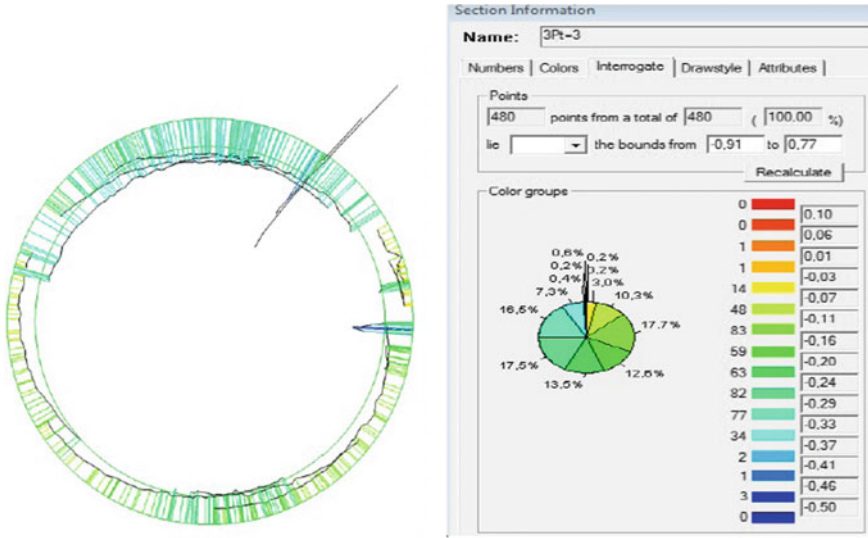
**Fig. 9** Chromatic map of deviations of the connector fabricated using machining on the milling machine, including 6 representative points



**Fig. 10** Cross-section and chromatic deviation map including the number of points within the given range for the connector fabricated using machining on the milling machine



**Fig. 11** Chromatic map of deviations of the connector fabricated using FDM method on the 3D printer, including 5 representative points



**Fig. 12** Cross-section and chromatic deviation map including the number of points within the given range for the connector fabricated using injection molding

equaled approximately the same reaching, and the highest value for 3D-printed part is +1.63 mm, for machined part, the value is +1.59 and the injection molded part has the value of +1.39 mm. The negative deviation was the biggest for injection molded component -1.87 mm, for the machined component, it is -1.10 mm and for the 3D printer, it is -0.79 mm. The most precisely manufactured component was the part with smallest mean deviation of all points measured compared to the base model, i.e., the machined part of 0.04 mm, followed by injection molded part of -0.15 mm and 3D-printed part of -0.20 mm. The injection molded part achieved the highest range of cross-section deviation of 1.68 mm based on 480 points, followed by 3D-printed part with 0.63 mm based on 825 points and the machined part proved again to be the most precisely fabricated part with deviation range of 0.37 mm based on 1242 points.

## 4 Conclusions

1. Model fabricated using 3D printing showed the lowest manufacturing accuracy with a mean deviation of -0.20 mm. However, one has to consider that the print was performed with high accuracy available for the machine, i.e., 0.25 mm, which is in agreement with the result received. In order to achieve more precise results, it is necessary to use a more accurate machine.

2. The connector fabricated on injection molding machine was black with a shiny surface, which was an obstacle in the precise scanning of the model and resulted in a low number of points collected in comparison with other methods i.e., 51,399, about 1/3 points less. It effected in the fact that the injection molding method appeared to be the second least effective with a mean deviation of  $-0.15$  mm. Additionally, the manufacturing inaccuracy could result from problems present during forming, i.e., contaminated mold, too high/too low injection speed, moist granulate.
3. The machined model turned out to be fabricated with the highest quality and a mean deviation of only 0.04 mm. The result could be even better if tools with smaller diameters were utilized—unfortunately, they were not available in the storage room. The color of the printed part (brown and matt) was favorable for laser scanning. This resulted in the collection of a highest number of points and a low number of scanning repetitions which aided achieving trustworthy results for further analysis.
4. All presented methods have their strengths and weaknesses. The connector fabricated on the molding machine presented an average manufacturing precision, and it is adequate, however, for household equipment. Additionally, its main advantage was short-cycle time (under 1 min) for producing a single part. The disadvantage of this method is the cost of injection molding machine and the mold. The connector manufactured with the use of FDM proved to be the less accurate and its time of fabrication reached approximately 7 h, which is disqualifying for high-volume production. The advantage of 3D printing is the low cost of the machine and project preparation and relatively fast fabrication of a prototype. An additional strength of RP technology is the ability to manufacture parts of complex geometry and free surface shapes which cannot be produced using other techniques. The surface of the machined model was the most precise. The fabrication time reached about 1.5 h which is a result by far worse than achieved by injection molding but better than the result presented by the FDM method. Manufacturing of the part involves the purchase of an expensive machine, specialized tooling and preparation of a program to machine the part. Fabrication of a wide spectrum of shapes depends on available cutting tools, fixturing and collision-free access to the machining area which is usually hindered by design complexity.

## References

1. Krolczyk, J., Krolczyk, G., Legutko, S., Napiorkowski, J., Hloch, S., Foltys, J., Tama, E.: Material flow optimization—a case study in automotive industry. *Tehnicki Vjesnik—Techn. Gaz.* **22**(6), 1447–1456 (2015)
2. Kujawińska, A., Rogalewicz, M., Diering, M.: Application of expectation maximization method for purchase decision-making support in welding branch. *Manage. Prod. Eng. Rev.* **7**(2), 29–33 (2016)

3. Kujawińska, A., Rogalewicz, M., Diering, M., Hamrol, A.: Statistical approach to making decisions in manufacturing process of floorboard. In: *World Conference on Information Systems and Technologies*, Springer, Cham, pp. 499–508 (2017)
4. Zhang, C., Li, Z., Hu, C., Chen, S., Wang, J., Zhang, X.: An optimized ensemble local mean decomposition method for fault detection of mechanical components. *Meas. Sci. Technol.* **28**, 35–102 (2017)
5. Krolczyk, G.M., Maruda, R.W., Nieslony, P., Wieczorowski, M.: Surface morphology analysis of duplex stainless steel (DSS) in clean production using the power spectral density. *Measurement* **94**, 464–470 (2016)
6. Glowacz, A.: Recognition of acoustic signals of synchronous motors with the use of MoFS and selected classifiers. *Measur. Sci. Rev.* **15**(4), 167–175 (2015)
7. Krolczyk, J.B.: Metrological changes in the surface morphology of cereal grains in the mixing process. *Int. Agrophys.* **30**, 193–202 (2016)
8. Nieslony, P., Krolczyk, G.M., Zak, K., Maruda, R.W., Legutko, S.: Comparative assessment of the mechanical and electromagnetic surfaces of explosively clad Ti–steel plates after drilling process. *Precis. Eng.* **47**, 104–110 (2017)
9. Sobolak, M., Budzik, G.: Experimental method of tooth contact analysis (TCA) with rapid prototyping (RP) use. *Rapid Prototyping J.* **14**(4), 197–201 (2008)
10. Krolczyk, G., Raos, P., Legutko, S.: Experimental analysis of surface roughness and surface texture of machined and fused deposition modelled parts. *Tehnički Vjesnik—Tech. Gaz.* **21** (1), 217–221 (2014)
11. Rokicki, P., Kozik, B., Budzik, G., Dziubek, T., Bernaczek, J., Przeszlowski, L., Markowska, O., Sobolewski, B., Rzucidlo, A.: Manufacturing of aircraft engine transmission gear with SLS (DMLS) method. *Aircr. Eng. Aerosp. Technol.* **88**, 397–403 (2016)



# Studies of Geometric Accuracy of Polygons Machined by Polygonal Turning Technique

Michal Regus, Bartosz Gapinski, Piotr Czajka and Piotr Jablonski

**Abstract** In this paper, characterization of shape and dimensional accuracy of polygons manufactured by polygonal turning were investigated. The theoretical value of maximum value of outline error was calculated and compared with real sample shape deviation. The data obtained from geometrical measurement of manufactured samples, geometrical characteristics, allowed to evaluate the influence of cutting parameters on machined part accuracy.

**Keywords** Polygons · Polygonal turning · Geometrical accuracy · CNC lathe

## 1 Introduction

Modern machine tools and mechanisms that are used in industry these days consist of components which are frequently characterized by a very complex geometry. Axisymmetric elements with flat or polygonal surfaces, which may be used as a part of shape connection in assembly processes or serve as work surface to operate a device, are good examples of such a complex geometry [1].

In the past, implementation of the flat surface in the axisymmetric components required use of the milling machine equipped with rotary table after turning process [2]. Today, thanks to the great development of technology that has taken place in the last decades in the field of technological machines; manufacturing such parts is possible in one operation with the use of special milling-turning centers. However, it should be noted that manufacturing flat or polygons surfaces using milling technology is still very inefficient and labor-intensive process [3]. Therefore, in case of necessity to manufacture such parts in bulk production, it is worth considering application of polygonal turning technique in machining process.

The technique of polygonal turning (known also as polygon turning) is a machine process that allows for machining non-circular forms like polygons or flat

---

M. Regus (✉) · B. Gapinski · P. Czajka · P. Jablonski  
Poznan University of Technology, Piotrowo 3, 60-965 Poznan, Poland  
e-mail: [michal.j.regus@doctorate.put.poznan.pl](mailto:michal.j.regus@doctorate.put.poznan.pl)

surfaces by use of universal turning machines equipped with C axis and turret with tool drive system. According to the work of art [3], this technique is several times more efficient as compared to conventional milling. The concept of polygonal turning is based on the synchronization of the rotary motion of the tool with lathes spindle. During machining process, this tool makes parallel movements to the spindle axis. The kinematic diagram of this process is shown in Fig. 1.

The shape of polygon manufactured with polygonal turning technique is specified by two factors: ratio of tool rotary speed to spindle speed and the number of cutting edges. Relationship between these factors is described by the following equation [4]:

$$p = z \cdot \frac{n_{\text{tool}}}{n_{\text{spindle}}} \tag{1}$$

where  $p$  stands for the number of machined flat/polygons surfaces,  $z$  is the number of cutting edges, and  $n_{\text{Tool}}$  and  $n_{\text{Spindle}}$  are respectively rotary speed of tool and lathe spindle. Based on this equation it can be stated that obtaining a polygon with a specified number of sides is determined by different combinations of cutting edges and ratio of tool to spindle rotary speed. These two factors have significant influence on accuracy of machined polygons [2]. Therefore, this aspect will be further discussed in next section of this paper.

Although the use of polygonal turning technique in machining polygon surfaces can bring many benefits, it should be emphasized that this technology is not free of drawbacks like component dimension limits and surface shape deviations [5, 6]. As it is described by Razumov in [2], the machined surfaces are not flat, and their outline in cross-section is elliptical. An example of the theoretical shape of a hexagonal obtained by polygonal turning is presented in Fig. 2.

The mathematical basis formulated by Razumov and Grechukhin in [2, 3] allows for calculating the trajectory of the tool and also determines the theoretical shape together with its deviation. In Fig. 2, the maximum deviation of shape is described

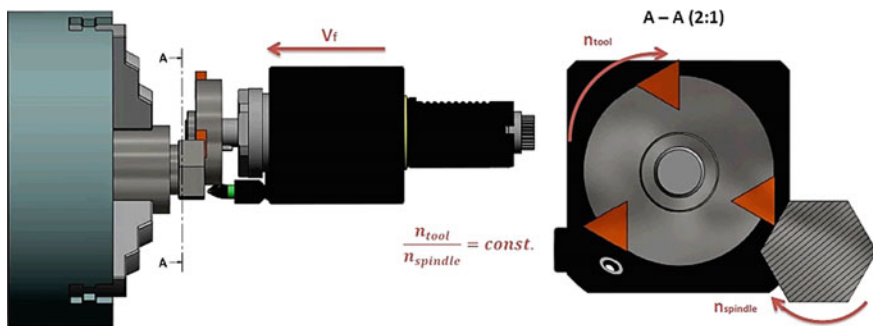
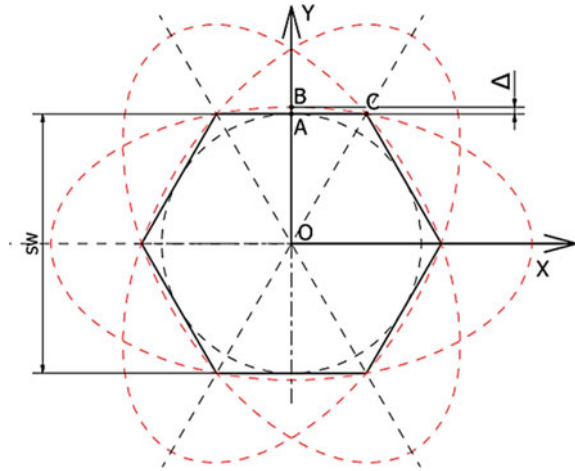


Fig. 1 Kinematic diagram of polygonal turning process

**Fig. 2** Theoretical shape of hexagon machined by polygonal turning technique



as segment  $AB = \Delta$ . The mathematical formula that allows to estimate the maximum deviation ( $\Delta$ ) of shape of any polygon with even number of sides is [2]:

$$\Delta = |r \cdot \left\{ 1 - \sin \left[ \arctg \left( \frac{2A + r}{r} \cdot \text{ctg}(\varphi_0) \right) \right] \right\}| \quad (2)$$

where  $A$  is distance between axes of tool and spindle and  $r$  stands for radius of circle inscribed in a polygon. In the formula (2), the value of  $\varphi_0$  angle is calculated by the following correlation [2]:

$$\varphi_0 = \frac{\pi}{2} : z \quad (3)$$

According to the Eq. (2), it can be noticed that the theoretical value of maximum polygon shape deviation ( $\Delta$ ) is determined by polygon dimensions, tool diameter, ratio of tool speed to spindle speed, and also number of cutting edges. However, it should be noted that the indicated formula (2) is correct only in case of polygons with even number of sides that would be machined with ratio of tool speed to spindle speed equal to 2:1.

In general, it can be stated that accuracy of polygons machined by polygonal turning technique is dependent on both geometrical and technological factors and also occurrence of following error between spindle drive and tool drive [6]. In Fig. 3, the relationship between these factors is shown.

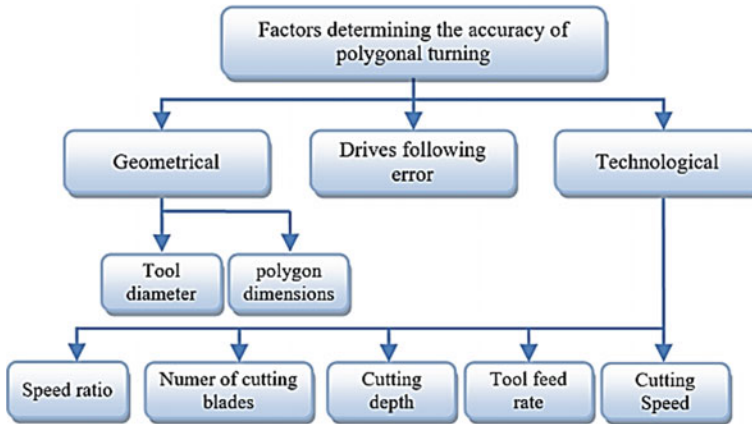


Fig. 3 Factors that determine accuracy of polygons machined by polygonal turning

## 2 Research Problem

Former research on the field of polygonal turning technique was focused on mathematical basis that allows to determine a theoretical shape of polygon. Razumov and Grechukhin in their paper presented such a mathematical model, but they did not verify this theory.

Aim of the presented study was to compare theoretical geometry of polygons calculated with use of Razumov [2] mathematical theory with real characteristic of polygons made by polygonal turning. In order to obtain necessary data, hexagons, tetrahedrons, and samples with two parallel faces were machined with different configurations of speed ratio and number of cutting edges. Measurement of the geometrical features of manufactured samples allowed to:

- compare the theoretical calculated shape of polygons with the real ones,
- evaluate correctness of used mathematical model,
- designate the influence of cutting parameters on polygons shape error.

## 3 Results

Basing on Eq. (2), theoretical profile error for polygonal turned elements, varying in polygon size and tool diameter, was evaluated. Constant ratio of spindle speed to tool speed was assumed, as well as number of cutting edges (depending on polygon type). Results were presented with graphs:  $\Delta = f(D)$ .

Overview of presented graphs proves that profile deviation rises along with increasing polygon size and decreases with increasing tool diameter. Essential observation is that in case of square shape, deviation of profile was nearly 3 times greater than in case of hexagonal shape (Fig. 4).

In order to designate profile errors of polygonal turning under real manufacturing conditions, tests with CLX 350 V3 lathe were conducted. This machine offers possibility of spindle and live tool synchronization. Polygonal cutter L381. G090.22.04 with inserts L314.MK50.20 made by HORN was used [4].

Conducted research covered manufacturing of polygons that are most common in mechanical engineering applications. As a raw material, bars from aluminum alloy EN AW-5083 were used. Constant total cutting speed was assumed during tests. It is important to consider polygonal turning kinematics as consisting of two opposite rotational movements. Because of that, total cutting speed is:

$$v_c = v_{\text{tool}} + v_{\text{spindle}} \left[ \frac{m}{\text{min}} \right] \tag{4}$$

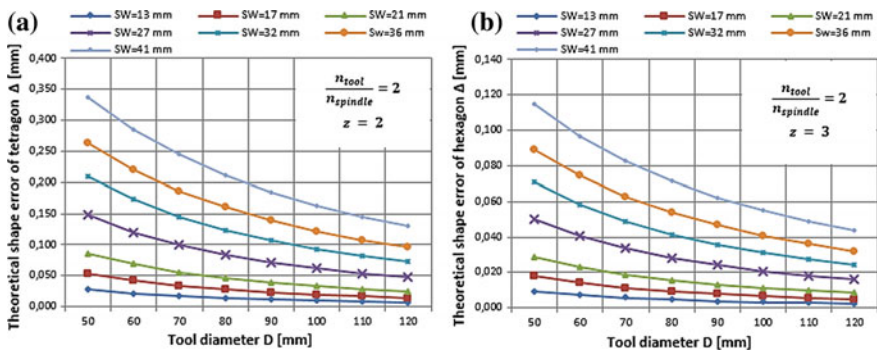
Assuming constant speed ratio:

$$\frac{n_{\text{tool}}}{n_{\text{spindle}}} = \beta \tag{5}$$

Equation (4) can be stated as:




$$v_c = \frac{\pi \cdot n_{\text{tool}}}{1000} \cdot (SW + D \cdot \beta) \left[ \frac{m}{\text{min}} \right] \tag{6}$$

Turning tests were conducted with numerous configurations of speed ratio and number of cutting edges. These data were presented in Table 1. Green color was used to indicate tool manufacturer—recommended specifications [4]. Machined samples were measured with coordinate measuring machine DEA Global Image



**Fig. 4** Theoretical shape error of polygons made by polygonal turning **a** for tetragons and **b** for hexagons

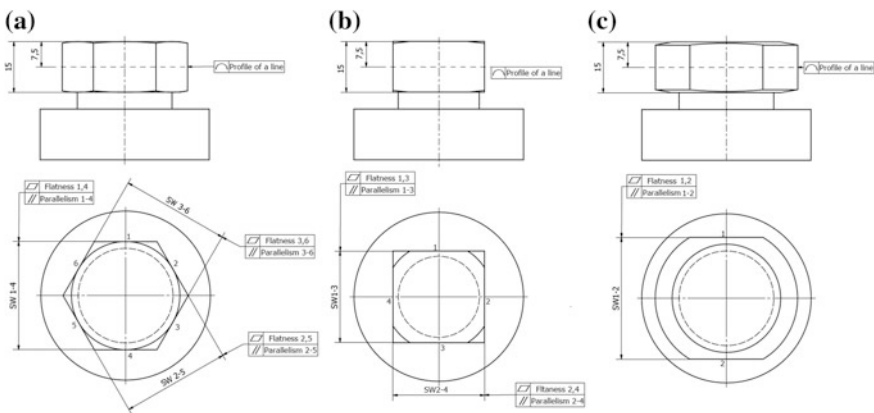
**Table 1** Configurations of speed ratio and number of cutting edges for various polygons

Polygon	$\frac{n_{tool}}{n_{spindle}} = \beta$	Number of cutting edges [z]
	2:1	1
	1:1	2
	2:1	2
	4:1	1
	2:1	3
	3:1	2

Clima 7.7.5 and PC-DMIS 2016 software-equipped computer station. Maximum permissible error of applied measurement equipment is equal to:



$$MPE_E = 1,5 + \frac{L}{333} [\mu m] \tag{7}$$

Tables 2, 3, and 4 present the results of conducted tests. Results of flatness and parallelism included in the tables are equal to averaged measurement data for each profile shape—e.g., in case of hexagonal, presented result is equal to average for measurement of six planes (Fig. 5).





**Fig. 5** Overview of measured dimensions and geometrical features on machined samples. **a** hexagon, **b** tetragon, and **c** two parallel planes



**Table 2** Results of measurement for hexagons made with following configuration  $\beta = 2$  and  $z=3$

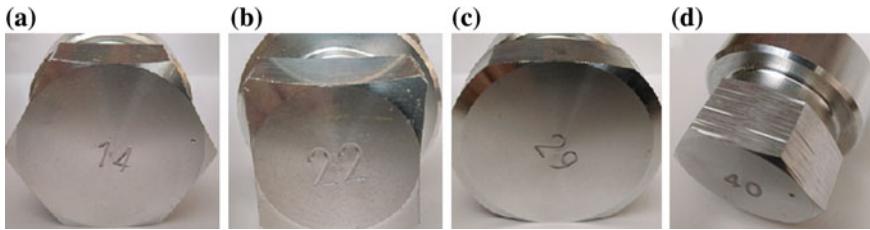
Nominal size	Measured geometric features [mm]						
	SW					//	
	1-4	2-5	3-6	Range			
13	12.961	12.993	13.028	0.067	0.015	0.015	0.062
17	16.947	16.976	17.010	0.063	0.024	0.025	0.092
21	20.934	20.962	20.996	0.062	0.045	0.048	0.141
27	26.921	26.960	26.988	0.067	0.051	0.055	0.206
32	31.890	31.922	31.952	0.062	0.080	0.085	0.273
36	35.852	35.900	35.920	0.068	0.089	0.088	0.322
41	40.850	40.898	40.919	0.069	0.124	0.149	0.430

**Table 3** Results of measurement for tetragons made with following configuration  $\beta = 2$  and  $z=2$

Nominal size	Measured geometric features [mm]					
	SW				//	
	1-3	2-4	Range			
13	12.961	12.971	0.010	0.024	0.024	0.108
17	16.938	16.952	0.014	0.039	0.041	0.177
21	21.162	21.141	0.021	0.102	0.101	0.272
27	26.804	26.847	0.043	0.154	0.127	0.534

**Table 4** Results of measurement for samples with 2 parallel planes made with following configuration  $\beta = 2$  and  $z = 1$

Nominal size	Measured geometric features [mm]			
	SW		//	
13	12.957	0.025	0.026	0.108
17	16.947	0.039	0.037	0.178
21	20.935	0.042	0.042	0.169
27	26.905	0.066	0.066	0.233
32	31.897	0.073	0.074	0.285
36	35.885	0.096	0.097	0.303
41	40.850	0.131	0.138	0.364



**Fig. 6** Shape error of samples made with not recommended configurations of “ $\beta$ ” and “ $z$ ” (a, b, and c) or with too high cutting parameters—lack of finishing turning (d)

It was observed that polygons created with parameters marked on red in Table 1 have significant shape error. It can be seen in Fig. 6a–c.

## 4 Discussion

Analysis of the results presented in the previous section allowed to formulate the conclusion that use of the mathematical formula (2) to determine theoretical shape of machined elements was correct. As expected on the basis of the mathematical model, surfaces of machined polygons were convex; however, the values of occurred deviations were bigger than calculated one. The main reason for these differences was that the used formula did not take into account the influence of machined material deformation during the process and occurrence of following error of drive systems.

The nominal diameter of polygonal cutter was 90 mm. Before the machining process was started, the tool had been measured on the pre-setter. The deviation between three cutting edges—this configuration of edges was used for machining of hexagon—on diameter reached 0.070 mm. The same deviation between the surfaces was observed during the process of measuring distance (SW 1–4, SW 2–5, and SW 3–6).

It was proved that cutting speed, cutting depth, and feed rate are relevant parameters that affect the accuracy of polygons. The producer of the tool which was used during the research recommends the following parameters for the aluminum alloys:  $v_c = 500\text{--}1000$  m/min and  $f = 0.1\text{--}0.2$  mm/tooth. Cutting depth  $a_p$  is not defined by the producer, despite the fact that it plays a significant role in the quality of the obtained polygons. It was observed that to reach an acceptable quality of surfaces, it is necessary to split the machining process into rough and finishing operations. Otherwise, high deformation of the surfaces was observed (Fig. 6d.). To reach good quality of polygons made of EN AW-5083, it is recommended to use the following parameters in the finishing operation:  $v_c = 400\text{--}500$  m/min,  $f = 0.03\text{--}0.05$  mm/tooth, and  $a_p = 0.5\text{--}1.0$  mm.

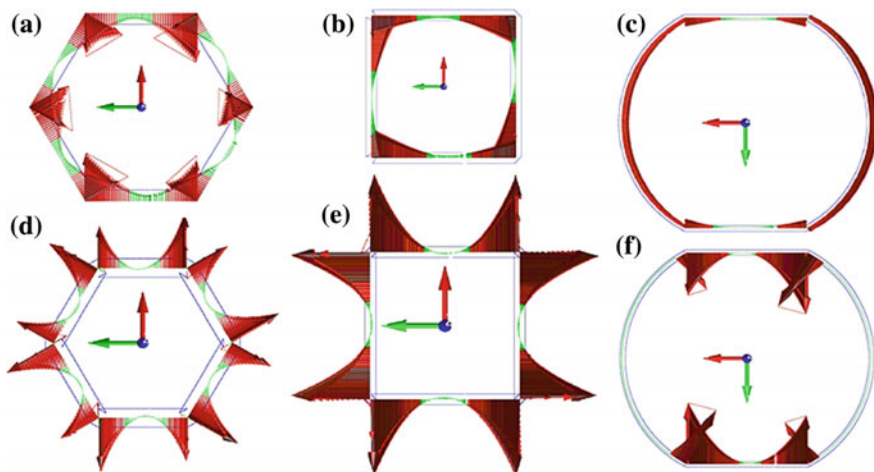


## 5 Conclusions

In this paper, the geometric accuracy of polygons machined by polygonal turning technique was taken under investigation. The data that were obtained during conducted research allowed to compare the calculated theoretical values of maximum deviation ( $\Delta$ ) of polygons shape with the real ones. As a result of the measured parameters analysis, it could be stated that use of the mathematical formula that Razumov had proposed in [2] is correct. However, measured values of the deviations were different from the calculated ones, as Razumov's formula (2) determines the shape deviation only on the basis of the tool trajectory ignoring the influence of machined material deformation during the machining process and occurrence of following errors of drive systems.

Another factor that significantly contributed to the value of observed deviation was application of a tool head which did not have possibility of adjusting the correct radial and axial position of cutting inserts. To improve the accuracy of machined polygons, it is necessary to design the tool head with special positioning cartridges in which the inserts are mounted. The cartridges should be adjusted independently in radial and axial positions.

The intermittent work of the cutting tool was also determined as the factor that caused occurrence of shape error. The reason for this was the influence of cutting resistance on change of cutting speed. When cutting edge got into material, the speed of tool decreased, and when the edge went out of the material, the speed increased to the value which was higher than the nominal one. The impact of cutting speed oscillation on machined surfaces can be seen in Fig. 7b.



**Fig. 7** Shape error of samples made by polygonal turning **a** hexagon:  $\beta = 2$  and  $z = 3$ , **b** tetragon:  $\beta = 2$  and  $z = 2$ , **c** 2 parallel planes:  $\beta = 2$  and  $z = 1$ , **d** hexagon:  $\beta = 3$  and  $z = 2$ , **e** tetragon:  $\beta = 4$  and  $z = 1$ , and **f** 2 parallel planes  $\beta = 1$  and  $z = 2$

In the course of the research, the correlation between machining parameters and machined object was also investigated. It was proved that cutting speed, cutting depth, and feed rate are relevant parameters that affect the accuracy of polygons. According to the research results, split of the machining process into rough and finishing operations was found to be necessary requirement in order to produce high-quality polygons.

The results of conducted research allowed to classify polygonal turning technique as the technology that should be intended for machining polygons, the surfaces of which do not need to fulfill high geometric shape accuracy requirements.

**Acknowledgements** The authors wish to acknowledge that research presented in this paper was founded by Institute of Mechanical Technology, part of Faculty of Mechanical Engineering and Management at Poznan University of Technology. Described research was conducted thanks to Institute scientific resources and was a part of authors' work for the Institute.

## References

1. Ghionea, A., Catrina, D., Predinca, N., Parpala, L.F.: Generation features of polygonal areas on lathes. In: International Conference on Economic Engineering and Manufacturing Systems, Braşov, 2009, pp. 26–27
2. Razumov, M.: Form error calculation during polygonal sharpening of polyhedrons with even number of sides. *Metall. Min. Ind.* (1), 66–69 (2015)
3. Razumov, M., Grechukhin, A., Pykhtin, A.: Determination of shape errors during polygonal turning of polyhedrons with an odd number of faces. *Proced. Eng.* **150**, 844–848 (2016)
4. [www.phorn.de](http://www.phorn.de). Accessed 1 April 2017
5. Jastrzębski, R., Kowalski, T., Osówniak, P.: Possibility of shaping surfaces on CNC lathes by complex technological movements. *Technol. Autom. Assem.* (4), 54–58 (2012). (in Polish)
6. Kowalski, T., Niedbała, M., Soporek, M.: Machining of polygons by turning method. *Technol. Autom. Assem.* (4), 30–32 (2008). (in Polish)

# Ensuring the Reliability of the Car Body Controls by Controlling the Current Inspection of Measuring Machines

Robert Koteras, Michal Wieczorowski, Piotr Znaniński  
and Lidia Marciniak-Podsadna

**Abstract** Coordinate measuring machines are one of the most often used measurement devices in modern industry. Keeping high level of their accuracy parameters becomes then a critical issue. In the paper, some aspects regarding CMM reverification in production conditions and periodical check were discussed. A method of periodical check was elaborated in order to obtain regular information about changes in accuracy parameters. Possible risks and consequences of lack of knowledge regarding current CMM accuracy status were indicated. The results of current research conducted on 6 CMMs with single and double column construction were shown. One common measurement program for all machines working in CNC mode was developed for repeatability. During 6 months, 106 studies were performed and 7326 points were collected. The paper presents also some extreme results of the check together with the discussion. The presented method was adapted to production conditions. Its use is associated with a small 15 min break in a working time of a coordinate measuring machine.

**Keywords** Coordinate · Measuring machine · Calibration · Reverification

## 1 Introduction

Coordinate measuring machines are most often checked once a year. Then a periodic review and calibration are performed. However, the period of one year between CMM calibration is long, especially since many coordinate measuring machines operate in production conditions often in three-shift mode. They are

---

R. Koteras (✉) · P. Znaniński  
Volkswagen Poznań Sp. Z o.o., Poznań, Poland  
e-mail: Robert.Koteras@vw-poznan.pl

M. Wieczorowski (✉) · L. Marciniak-Podsadna  
Faculty of Mechanical Engineering and Management,  
Poznań University of Technology, Poznań, Poland  
e-mail: Michal.Wieczorowski@put.poznan.pl

exposed to accidental collisions which potentially might affect their geometry, and as a consequence also their accuracy. Therefore, in addition to receiving and periodic tests, current checks on used measuring machines should also be carried out. This is to maintain the reliability of the measurements taken. These checks are performed according to user procedures. ISO 10360-2 [1] recommends that current (temporary) inspections were carried out in schedule that takes into consideration all of environmental conditions, the type of measurement task, and any event that may affect CMM performance. In addition, the standard recommends the use of patterns with a thermal expansion coefficient similar to those of typical CMM objects [2]. It is also possible to use items subjected to previous calibration measurements. Comparing results obtained during the calibration of these items with results of the current check, a difference which should be less than the assumed extended uncertainty for such measurement is obtained [3–5]. During the tests, the CMM operator should use the instrument he/she most often uses. The ideal situation would be to check all measuring heads together with their extension cords. However, if this is not possible due to the high workload, it is recommended firstly to check the most used equipment and stay at less frequent interval.

## 2 Aspects of Current Inspections

The most important goal of conducting this type of CMM tests is to maintain a steady and high level of knowledge of the machine operator about its technical condition. Conduction of current checks adequately leads to ability of the operator to prove that the quality of measurements has not deteriorated since the last periodic test. Another important reason for the purpose of these activities is the ability to identify many CMM faults before they can immobilize the machine. If the operator observes a result that is significantly different from the expected result or if the results are successively deteriorating, there is a possibility of preventive repair or adjustment of it.

Current knowledge of the CMM accuracy allows to avoid risks with possible economic or even legal consequences. Its lack can lead to the following potential situations:

- in the case of delivery control, defective items may be allowed for further processes and parts fulfilling requirements—classified as defective. This generates unnecessary costs for fixing or scrapping products;
- in the case of manufactured components, the measurement results are used to control production processes, which may lead to erroneous corrections as a result of defect production;
- in the case of inspection of finished products, there is the risk of giving the customer a faulty product which can lead not only to losing his trust, but also may have legal consequences;

- lack of supervision over the condition of the machine can lead to unexpected failure and downtime for number of information on the production process;
- in extreme cases, it is possible to question the quality management system's compliance.

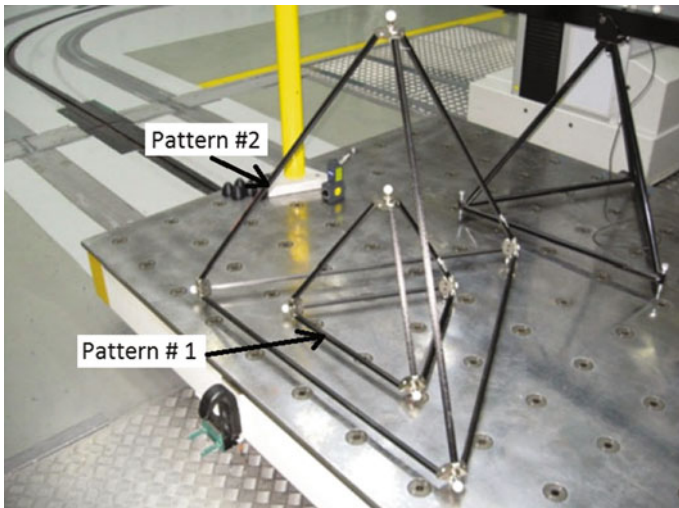
In the case of no proper control at the beginning of the production process, it will have to be prepared to pay for the costs, and manufacturer should be prepared to pay for costs, which would increase adequately to the stage of the process when the problem would be discovered. If such a product leaves the factory and due to its malfunctioning an accident involving a customer will take place, we may also be liable for this.

### 3 Artifacts Applied to Research

This example uses spatial patterns resembling tetrahedron. The tests use models with nominal distances between the centers of balls of 500 and 1000 mm of Unimetrik (Fig. 1).

In each corner of the pattern there is a ceramic research ball situated. Distances between these balls are calibrated and given with the expanded uncertainty  $U$ , what is shown in Table 1.

Frame of the patterns is made of carbon fiber rods, which provide a low linear expansion factor and a small mass of the whole pattern. CMM 4 was tested using pattern # 1, the rest of CMM using pattern # 2 (Fig. 1).



**Fig. 1** Spatial patterns with nominal distances between the centers of balls of 500 mm

**Table 1** Values given in calibration certificate for pattern no 1 and 2

Distance between centers of balls with its numbers	$L$ [mm]	$U$ [ $\mu\text{m}$ ]
<b>Pattern no 1</b>		
$U$ [ $\mu\text{m}$ ] = (1.0000 + 0.0010* $L$ [mm]), $k = 2$ , $\alpha = \pm 1.15 \cdot 10^{-6} \cdot K^{-1}$ , $u(\alpha) = \pm 0.5 \cdot 10^{-6} \cdot K^{-1}$ , $t = 20$ °C $\pm 1$ K		
1-2	495.9557	1.5
1-3	496.5097	1.5
1-4	495.7294	1.5
2-3	495.7412	1.5
2-4	496.0336	1.5
3-4	496.1294	1.5
<b>Pattern no 2</b>		
$U$ [ $\mu\text{m}$ ] = (1.0000 + 0.0010* $L$ [mm]), $k = 2$ , $\alpha = \pm 1.15 \cdot 10^{-6} \cdot K^{-1}$ , $u(\alpha) = \pm 0.5 \cdot 10^{-6} \cdot K^{-1}$ , $t = 20$ °C $\pm 1$ K		
1-2	1000.4593	2.0
1-3	1001.2585	2.0
1-4	999.9936	2.0
2-3	1000.6894	2.0
2-4	1000.5781	2.0
3-4	1000.7625	2.0

**Table 2** Data of checked CMMs [6]

CMM number	Maximum permissible error EL, MPE = $\pm$ minimum from (A + L/K) and B [ $\mu\text{m}$ ]		Measurement volume CMM X/Y/Z [mm]
CMM1	30 + L/50	80	3000/1600/2100
CMM2	25 + L/100	60	6000/1600/3000
CMM3	25 + L/100	60	6000/1600/3000
CMM4	25 + L/50	70	2000/1200/1500
CMM5	60 + L/40	120	7000/1800/2700
CMM6	60 + L/40	120	7000/1800/2700



## 4 Coordinate Measuring Machines

Research was carried out on six CMM with movable column and horizontal arm, of different construction and different sizes of measurement space. CMM1 and CMM4 machines have less measuring space, while pairs of CMM 2 and 3 and CMM 5 and 6 allow to work in dual mode operation. The following is a summary of the data concerning the tested machines (Table 2) [6].



**Fig. 2** Left picture presents RST-P [7], right picture presents TP20 [8]

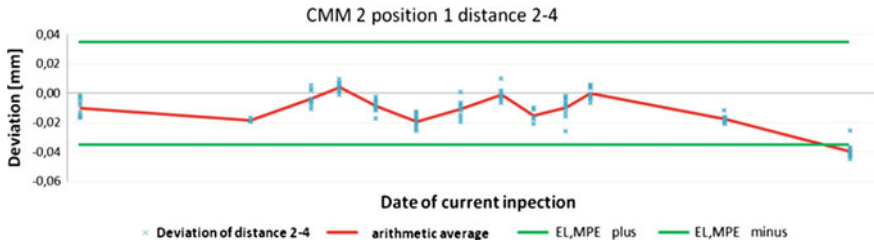
**Table 3** Technical specification of probe with modules MF and EF [8]

Measurement direction	Module	$\pm X, \pm Y, +Z$
Variability of switching path	MF	$\pm 1.00 \mu\text{m}$
	EF	$\pm 2.00 \mu\text{m}$
Unidirectional repeatability	MF	$\pm 0.50 \mu\text{m}$
	EF	$\pm 0.65 \mu\text{m}$
Repeatability of stylus changing	Manual exchange	$\pm 1.00 \mu\text{m}$
Module	Marked with a color	Trigger force
MF—medium force		XY: 0.1 N
		Z: 1.9 N
		Stylus: 25 mm
EF—extended force		XY: 0.1 N
		Z: 3.2 N
		Stylus: 50 mm

All CMMs were equipped with RDS-CAA rotary-tilting heads. Depending on the machine, the TP20 probe system from Renishaw or the Zeiss RST (Fig. 2) was used. Tables 3 and 4 summarize the technical data of the used heads provided by the manufacturers.

**Table 4** Technical specification of probe RST-P [7]

Measurement direction	$\pm X, \pm Y, +Z$
Unidirectional repeatability	$\pm 0.30 \mu\text{m}$



**Fig. 3** Results for machine no. 2

## 5 Measurements

The study was conducted over a period of six months to observe deviations from the patterns dimensions. In total, 106 studies were conducted in which 7326 measurement results were obtained.

According to ISO 15530-3: 2011 [3], in order to maintain consistent conditions of the experiment, the machine should move between the same positions, thus giving the possibility of minimizing the effect of systematic error on the measurement result [9, 10]. For this purpose, one common program for all measuring machines was written. Machines worked in CNC mode, and the probe always had the same angular position which is most commonly used in daily measurements [11].

The aforementioned assumptions of the measurement program have enabled, thanks to the automatic mode, to eliminate the impact of the CMM operator, eliminate the maximum permissible error of the rotary tilt sensor position  $P_{LTE}$  as well as systematic errors due to differences in programs [6, 12].

## 6 Results

A survey of six measuring machines was conducted over 6 months provided a lot of information about their technical condition and behavior during this period. Only two extreme results have been shown in the paper to indicate the validity of such checks.

The tests conducted for machine No. 2 (Fig. 3) showed overrun of  $E_{L, MPE}$  for the distance between balls 2 and 4. The periodic inspection and routine test were carried; however, the deterioration of results has already occurred within 8 weeks and was also noticeable for other distances. Using the spreadsheet trend function,



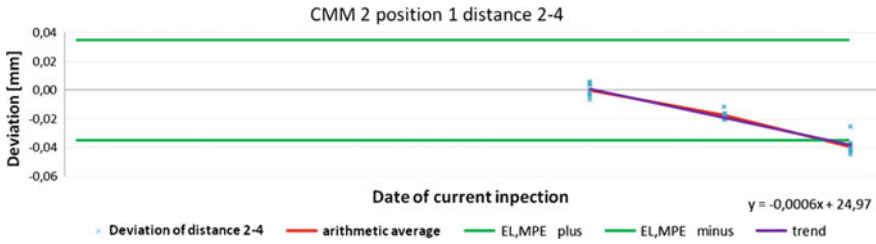


Fig. 4 Determination of CMM no. 2 accuracy loss function

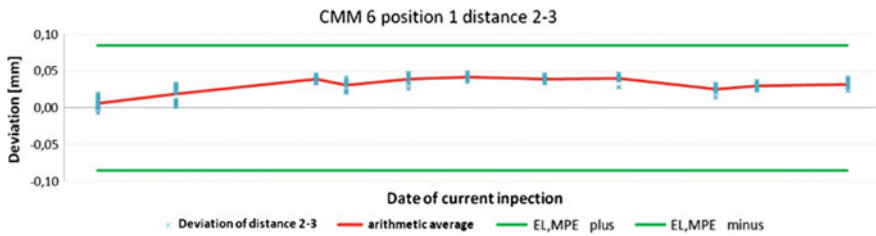


Fig. 5 Results for machine no. 6

the linear function of the trend line ( $y = 0.0006x + 24.97$ ) was determined for the three worst-case series (Fig. 4). The result of prediction in this situation was similar to the change in the arithmetic mean of the series, which would allow us to predict the date of the necessary periodic and routine inspection.

However, some machines have retained their accuracy throughout the test period (Fig. 5).

## 7 Conclusions

Standards do not specify exactly how and how often a user is expected to perform current checks. Therefore, there is a need for practical research to determine the time frames for checking and developing new solutions ready for easy implementation in machines monitoring. The presented method is an idea that considers some limits of the availability of industrial CMMs. So far, researches have confirmed the usefulness of the presented method of current checks in production conditions. In one position, the tetrahedr pattern was measurable in six different directions, both in one-column and multi-column mode. In the tested CMM ten repetitions were realized, the machine performed the tests in one standard position within 15 min. Extension uncertainty  $U$  did not exceed 10% of maximum permissible error  $E_L / MPE$ . This is undoubtedly the greatest advantage of the method, allowing for ongoing checks with negligible effect on the availability of CMM in

production processes. Similar parameters cannot be achieved using, for example, reference plates because of the need to change their positions during the test [6]. Results of the study were analyzed in terms of the possibility of determining models of accuracy loss on examined CMM and their approximation by means of linear functions. This provides the ability to use loss of accuracy models for determining safe periods of technical reviews and periodic inspections. When there is no clear trend regarding the loss of CMM accuracy, there is an option to make a decision whether to perform or to postpone the review and study. However, if there is a systematic error with value similar to  $E_{L, MPE}$  or the machine's indication is too affected by the influence of accidental or unknown factors, the presented method will record the moment of exceeding the tolerance limit.

The method presented along with the measurement programs prepared for its needs are ready to use solution for the CMM for which the extended calibration uncertainty will not exceed 20% of the maximum permissible error. It also allows simultaneously collecting data needed to determine the uncertainty of the measurement process, taking into account the component of error resulting from the inaccuracy of the positioning of the rotary-tilting heads. It should be also noted that this component is not included in the specified parameter  $E_{L, MPE}$ .

Based on the conducted research, it was found that

1. The semi-annual period of the current checks was long enough to make a clear visualization of accuracy changes of the examined CMMs in time. The method complies with the guidelines of the standards and allows for the evaluation of the technical condition of the machines. This allows to determine a model for CMMs accuracy change and to forecast the need for a review and periodic inspection, or record a sudden deterioration of CMM accuracy and close it down for service or repair. Uncertainty of calibration according to the proposed method does not exceed 10% of  $E_{L, MPE}$  which is good result.
2. It has been shown that model of the accuracy loss is unique to each CMM, even in the case of machines capable of working in pairs, operated for the same time period and similarly operated.
3. There were the following cases describing the accuracy of CMM:
  - the use in different degrees tolerance of error  $E$  without a clear trend of loss the accuracy;
  - the use in different degrees tolerance of error  $E$  with a clear trend of loss the accuracy which can be quite easily approximated in 4th or 8th week with linear function;
  - a systematic error near the tolerance limit represented by  $E_{L, MPE}$ , where the overflow is sudden and unpredictable.
4. Determination of fixed time limits for reviews and periodic inspections is incorrect. This is confirmed by the occurrence of  $E_{L, MPE}$  overflow for several machines in the course of the study cycle and the lack of a clear trend in the other CMMs. Only the analysis of the actual technical condition of the CMM

allows for proper planning of the necessary maintenance and designation in economically justified way.

5. In industrial conditions, checks shall be performed at steps that enable to observe the trend of loss of accuracy in at least three series of measurements, but not less frequently than the acceptable time and duration of inadequate measurement results.
6. It is impossible to predict the time after which the  $E_{L, MPE}$  is exceeded, when a systematic error value is close to  $E_{L, MPE}$ . Such prediction is also impossible in the situation of CMM which indication errors are too sensitive to random, unknown disturbances.
7. On the basis of results of tested CMMs, it is concluded that the optimal check frequency once per week will enable determination of a linear function for a trend that goes on at least 4 weeks and at the same time makes a negligible impact on the availability of CMM as well as on the cost of functioning of the entire laboratory.
8. It is possible to develop universal measuring programs dedicated to the used patterns and their application on the CMM for which the size of the measurement volume allows it. It is possible to eliminate the accidental error resulting from an unintentional change in the control file and to use less experienced employees in the CMM test.

## References

1. PN/EN/ISO 10360-1. Geometrical Product Specifications (GPS). Acceptance and Reverification Tests for Coordinate Measuring Machines (CMM). Part 1: Vocabulary (in Polish), PKN, Warsaw (2003)
2. ISO 10360-2:2009. Geometrical Product Specifications (GPS)—Acceptance and Reverification Tests for Coordinate Measuring Machines (CMM)—Part 2: CMMs Used for Measuring Linear Dimensions
3. ISO 15530-3:2011. Geometrical Product Specifications (GPS)—Coordinate Measuring Machines (CMM): Technique for Determining the Uncertainty of Measurement—Part 3: Use of Calibrated Workpieces or Measurement Standards (2011)
4. Śladek, J., Krawczyk, M.: Methods for assessing the accuracy of coordinate measurements. *Meas. Autom. Control* **9**(53), 478–481 (2007)
5. Śladek, J., Krawczyk, M.: Methods for assessing the accuracy of coordinate measurements. *Measur. Autom. Control* **9**(53), 478–481 (2007)
6. Znaniecki P.: The Concept of the Coordinate Measuring Machine Monitoring System, Machine Construction and Operation (in Polish). University of Bielsko-Biala (2012)
7. [www.zeiss.pl](http://www.zeiss.pl). State for the day: 21-03-2017
8. [www.renishaw.com.pl](http://www.renishaw.com.pl). State for the day: 10-12-2016
9. Śladek, J.: Accuracy of Coordinate Measurement (in Polish). Cracow University of Technology, Cracow (2011)
10. Flack D.: CMM verification. Measurement good practice guide 42 (2011)
11. Pachala, A., Grzelka, M.: Program for checking the accuracy of CMMs using a step pattern and PC-DMIS software. *Measur. Autom. Control* **1**(56), 70–72 (2010)
12. Flack D.: CMM measurement strategies. Measurement good practice guide 41 (2014)

# Application of Industrial Robot as a Measuring System

Ksenia Ostrowska, Robert Kupiec, Malgorzata Kowalczyk,  
Pawel Wojakowski, Halszka Skorska and Jerzy Sladek

**Abstract** Robotics is currently one of the fastest developing technical fields. During the last decade, the industry transformed. After the introduction of automated and robotized manufacturing solutions, factories face a new challenge—the Fourth Industrial Revolution. Industry 4.0 is a trend that applies to automatization and exchange of data in manufacturing technologies. Therefore, it was decided by the Laboratory of Coordinate Metrology (Cracow University of Technology)—LMW PK—to use Kawasaki RS10N industrial robot as a coordinate measuring system. Heidenhain’s scanning probe head was installed. Programs and software allowing the use of PC-DMIS measurement software were written.

**Keywords** Industrial robot · Coordinate measuring technique · Database Metrological software · Industrial revolution 4.0

## 1 Introduction

Nowadays, robotics is one of the fastest developing technical fields. The number of robotized stations on production lines is growing on a daily basis. It is assumed that the degree of development of an enterprise depends on the number of robotic and metrological systems installed [1–5]. Industrial robots are currently replacing people at hazardous workplaces or work as their assistants in the machine industry, building industry, transportation, farming, metrology, or even medicine. According to the International Federation of Robotics, the number of industrial robots globally sold in 2014 broke the record—a total of 225,000 units. The developing trend in robotics is establishing safe co-working for both humans and robots at the work place. The number of unconventional applications of robots is still increasing.

---

K. Ostrowska (✉) · J. Sladek

Laboratory of Coordinate Metrology, Cracow University of Technology, Cracow, Poland  
e-mail: kostrowska@mech.pk.edu.pl

R. Kupiec · M. Kowalczyk · P. Wojakowski · H. Skorska  
Institute of Production Engineering, Cracow University of Technology, Cracow, Poland

© Springer International Publishing AG 2018

A. Hamrol et al. (eds.), *Advances in Manufacturing*, Lecture Notes in Mechanical Engineering, [https://doi.org/10.1007/978-3-319-68619-6\\_77](https://doi.org/10.1007/978-3-319-68619-6_77)

797

Single machine can perform many tasks simultaneously. The Kawasaki industrial robot (courtesy of Astor, located in Cracow) was integrated with scanning probe head and metrological software at LMW PK [6, 7]. Introduced system consists of many elements and is the basis for the construction of the virtual measuring robot. The following programming languages and programs are used to integrate the entire system: AS language (language of the robot's driver), KTerm (software that cooperates with the robot), Python programming language (software integration, file transfer, searching the files intended for export), Transact SQL (the language of SQL Server database), Visual Basic (PC-DMIS' collaboration scripts) and metrological software—PC-DMIS. The number of elements used may be considered large but was deemed necessary by the authors.

## 2 The Object of the Research

The Kawasaki RS10N industrial robot is the object of the research. It is a 6-axle robot with a lifting capacity up to 10 kg (Fig. 1-1). The fastest rotary pair of the robot is characterized by the speed of 700°/s. It has 17-bit encoders. Its range is 1450 mm. This robot has kinematic chain and is redundant. The control is done using teach pendant with a touch screen. Direct use of the computer to control the robot is possible with the help of the KTerm software.

**Fig. 1** Redundant measurement system: 1 the Kawasaki measuring robot, 2 the scanning probe head, 3 the driver of the robot, 4 the measured element



The accuracy of unidirectional positioning (linear motion) is the deviation between the set point and the average value of the actual positions reached by the robot when it is approaching the set point from one direction. It equals to 0.024 mm.

Repeatability of unidirectional positioning (linear motion) is the measure of the scattering of the actual positions when approaching the set point for  $n$ -times from the same direction. It equals to 0.036 mm. The given data was determined according to the norm PN-EN ISO 9283—Manipulating Industrial Robots—Performance criteria and related test methods [8]. The laser tracker was used to check the readings from a retroreflector mounted on the last kinematic pair of the robot.

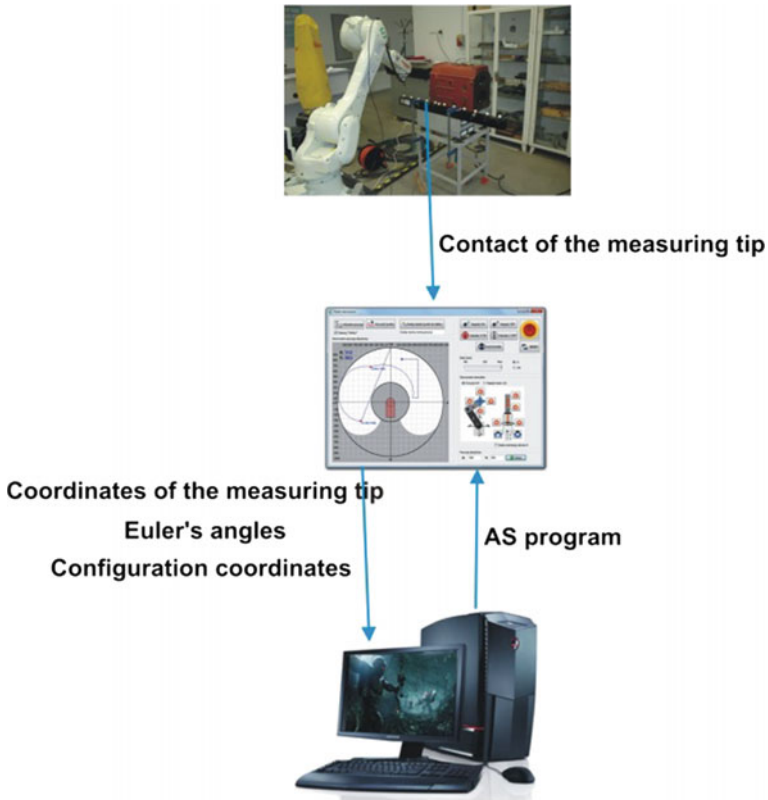
A five-way touch-trigger Heidenhain's probe with Ø8-mm measuring tip made of ruby was attached to the robot (Fig. 1-2). The probe was attached to robot's mechanical interface and connected directly to its driver (Fig. 1-3). Thus, at the moment of detecting the tilt of the stylus, the signal is sent to the input of the driver. The driver informs then that the tip of the measuring head has touched the measured element (Fig. 1-4).

### 3 Modules of the Measurement System

After installing the scanning probe head on the robot, it was necessary to integrate it with the driver device. The basic assumption was made that when the measuring tip touches the measured element the robot should stop in place. This was needed to avoid collision that would cause the destruction of the scanning probe head. Firstly, the program was written in AS Language so it can be understood by the driver and then sent to it. Afterward, the driver reads the coordinates of the measuring tip, the Euler angles, and the configuration coordinates. Those readings were received from the encoders. The data is sent to the computer via TCP/IP Protocols and processed by the KTerm software, responsible for cooperating with the robot. The KTerm software generates a text file with the data (Fig. 2).

The first thing that was necessary for the proper use of the Kawasaki RS010N industrial robot as a measuring device was to determine the coordinate system of the tool. The six-point method was used, as recommended by the manufacturer (Fig. 3). In this method, six positions for the tool are defined in relation to a stationary point (according to certain rules). An inner cone was used to perform this operation. It allowed the reproducibility of the measuring tip's point of contact. This was allowed to determine the displacement and rotation of the scanning probe head in relation to the last pair of the robot.

Another module is based on the Python programming language: it allows the continuous search for changes in the file generated by the robot's software. Changed or overwritten files are recognized as a new measurement. The results are later sorted and exported to a database created by using Microsoft SQL Server.



**Fig. 2** Module responsible for the integration of the scanning head with the robot

At this stage, the basic geometric elements are distinguished, e.g., whether a circle or sphere was measured. This stage was prepared so the needs of the industry were met as the large quantities of measurements need to be stored. *Furthermore, in this stage the elements of the measurement simulation are to be connected using the Monte Carlo method—thus the creation of the Virtual Measuring Robot (Fig. 4).*

Metrological software PC-DMIS runs scripts written in the Visual Basic, so any additional subprograms can only be integrated by using it. The user of the PC-DMIS sees only one additional Integrator icon. The Integrator communicates with the SQL Server database to gain access to the readings of the measurements. Some of those are prepared for the PC-DMIS' evaluation and the rest are measured using PC-DMIS. Both are done separately. This particular layout of the modules allows measurements to take place directly on the production line. Afterward, the processing of the results and reports by the quality engineer is possible. The procedures do not need to be processed at the same place and time.

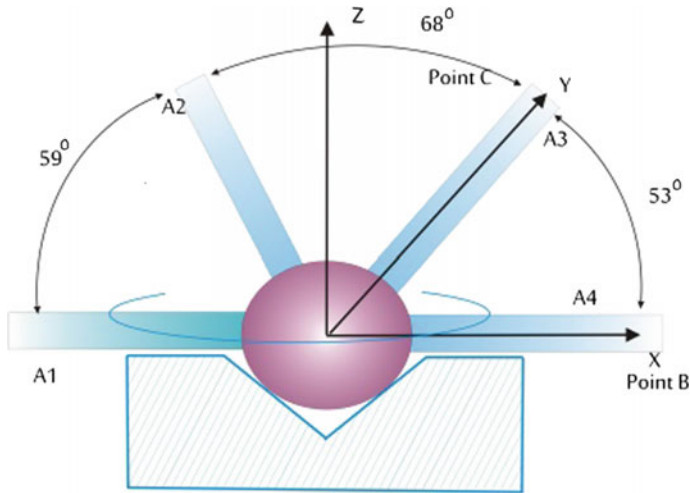


Fig. 3 All six positions of tools in relation to a point [6, 7]

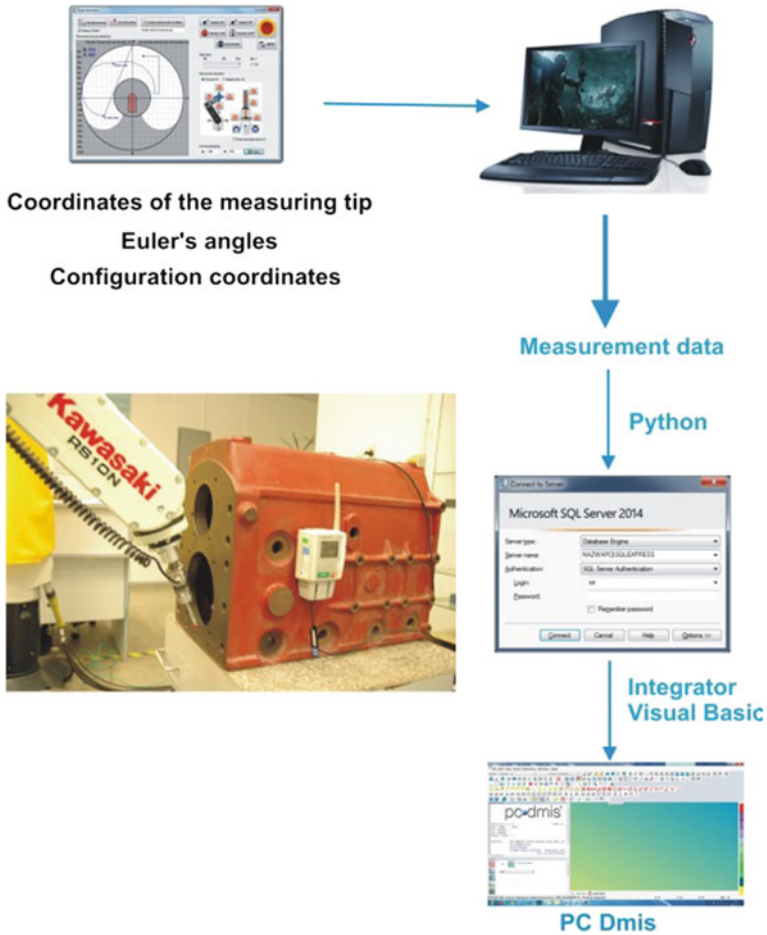
The measurement that uses the presented system can be done in either automatic or manual mode. Unfortunately, the measurement performed in automatic mode requires writing subprograms for a given feature.

#### 4 Execution of Verifying Measurement

To verify the correctness of the presented system, we measured the industrial element according to the multi-position method [9] (Fig. 1). The diameter of the cylinders was measured with the denominations 100,008 mm, 149,998 mm and the distance within planes with the denomination 488,839 mm. Next, we measured the ring gauge and the length gauge (Ball Bar type). In the article [6, 7], robot calibration was performed according to ISO standard 10360- [10]. Maximum permission error (MPE) was set on level  $0.17 \pm 0.25 * 10^{-3}$  L mm [11].

The measurement results were given with the extended uncertainty (for coverage factor  $k = 2.5$ ) and are shown in Table 1 and Fig. 5.





**Fig. 4** Module linking data received from the robot and metrological software PC-DMIS

**Table 1** Measurement results

Measured feature	Diameter of cylinder 100 mm	Diameter of cylinder 150 mm	Distance within planes 489 mm
Average	100.011	149.957	488.645
Uncertainty extended	0.011	0.019	0.036
Difference	0.003	0.041	0.194

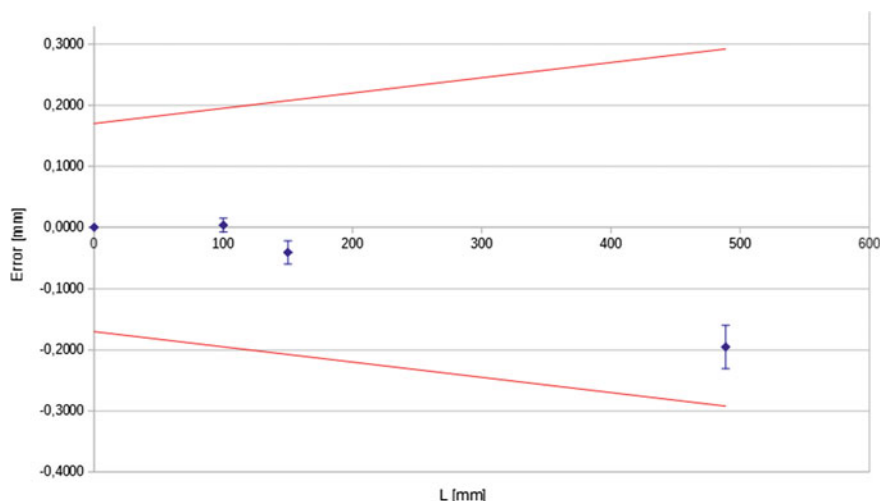


Fig. 5 Measurement results in MPE equation

## 5 Conclusion

The presented measurement system can be used to measure large elements. The results have no correction. The assembled head was the one used for the machine tool measurements. Errors that occurred were due to the deflection of the stylus head and the switching time of the head.

In further research some corrections of the measuring head will be made, using neural networks. All of the robot's errors will be determined and their correction matrix CAA will then be modeled.

**Acknowledgements** Reported research was realized within confines of project financed by Polish National Centre for Research and Development No: LIDER/024/559/L-4/12/NCBR/2013.

## References

1. Gawlik, J., Lekki, Z., Sokal, G.: Realizacja zadań pomiarowych z wykorzystaniem robota COMAU Smart S3, W: Automatyżacja produkcji 2000: wiedza - technika - postęp. T. 2, Referaty sesyjne. - Wrocław: Ofic. Wydaw. PWroc., 2000. - s. 95–102, bibliogr. 4 poz
2. Otko, T., Sokal, G.: Badania dokładności i powtarzalności pozycjonowania robota z wykorzystaniem głowicy wieloczujnikowej, W: Metrologia w technikach wytwarzania maszyn: IX konferencja naukowo-techniczna. T. 2/[red. nauk. Krzysztof Tubielewicz, Henryk Czarniecki]. - Częstochowa: Wydaw. PCzęst., 2001. - s. 487–492, bibliogr. 3 poz
3. Śladek, J.: Coordinate Metrology: Accuracy of Systems and Measurements. Springer Tracts In Mechanical Engineering, ISSN 2195-9862 (2016)

4. Śladek, J., Gawlik, K.: Looking for uncertainty of measurement—virtual machines based on the matrix method using artificial neural networks. In: IV International Congress on Precision Machining 2007, Sandomierz-Kielce (2007)
5. Sokal, G.: Metoda podwyższenia dokładności pomiarów współrzędnościowych dokonywanych przez roboty przemysłowe. doktorat, Politechnika Krakowska
6. Ostrowska, K., Krawczyk, M., Kupiec, R., Śladek, J.: Mathematical errors model of touch-triggerprobe installed on the industrial Robot. In: XIIth International Scientific Conference Coordinate Measuring Technique, Bielsko-Biała, 18–20 April 2016
7. Ostrowska, K., Kupiec, R., Harmatys, W., Gromczak, K., Śladek J.: Determination of the accuracy of the redundant coordinate system consisting of industrial robot with a measuring probe. In: XIIth International Scientific Conference Coordinate Measuring Technique, Bielsko-Biała, 18–20 April 2016
8. [N1] PN-EN ISO 9283 Industrial Robots—Functional Testing Methods
9. [N2] ISO/CD TS 15530-2 GPS—Use of multiple measurement strategy
10. [N3] ISO 10360-12:2016 Geometrical product specifications (GPS)—Acceptance and reverification tests for coordinate measuring systems (CMS)—Part 12: Articulated arm coordinate measurement machines (CMM)
11. Ostrowska, K., Owczarek, D., Gromczak, K., Śladek, J., Kielbus, A.: Methods of calibration of articulated arm coordinate measuring machines. In: Advanced technologies in designing, engineering and manufacturing research problems, str. 109–122, 2015

# Surface Roughness of Graphite and Aluminium Alloy After Hydro-abrasive Machining

Jan Carach, Dominika Lehocka, Stanislaw Legutko, Sergej Hloch, Somnath Chattopadhyaya and Amit R. Dixit

**Abstract** The paper compares the quality of machined surface of graphite and aluminium alloy by abrasive waterjet using the focusing tube with a diameter of  $d_{f1} = 0.5$  mm and  $d_{f2} = 0.78$  mm. The machining was carried out using the technology of rotating workpiece disintegration by abrasive waterjet. Abrasive tangential waterjet was used to carry out the experiment (water pressure  $P = 400$  MPa). Workpieces were clamped in the rotating chucking appliance with rotation frequency  $n = 300 \text{ min}^{-1}$ . The change in focusing tube diameter caused the change in values of roughness parameters and also caused the change of resulting shape of workpieces. Values of roughness parameters were measured using the MicroProf FRT optic profilometer.

**Keywords** Abrasive · Waterjet · Machining · Roughness parameters

## 1 Introduction

Cutting of materials by abrasive waterjet currently represents a very effective and frequently used process for the preparation of flat semi-finished products [1–4]. Hydro-abrasive disintegration of rotating workpieces represents the technology

---

J. Carach · D. Lehocka (✉) · S. Hloch  
Faculty of Manufacturing Technologies with a seat in Presov,  
Technical University of Kosice, 1 Bayerova St., 080 01 Presov, Slovak Republic  
e-mail: dominika.lehocka@tuke.sk

D. Lehocka · S. Hloch  
Institute of Geonics of the CAS, v. v. i, 1768 Studentska St.,  
708 00 Ostrava Poruba, Czech Republic

S. Legutko  
Faculty of Mechanical Engineering and Management, Poznan University of Technology,  
Pl. Marii Skłodowskiej-Curie 5, 60-965 Poznan, Poland

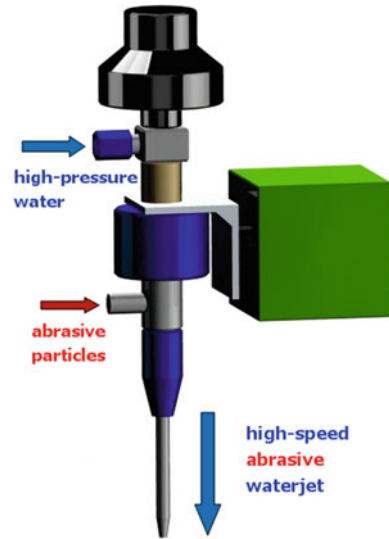
S. Chattopadhyaya · A.R. Dixit  
Indian Institute of Technology, Indian School of Mines, Dhanbad, India

connecting abrasive waterjet (AWJ) and rotation movement of workpiece [5–7]. Hydro-abrasive disintegration of rotating workpieces [8, 9] does not compete with the conventional turning of metals [10] for the time being, but suitable applications can be seen mainly in the machining of composite materials, glass [11], rock materials, abrasive wheels [12] and ceramics [13]. These are represented mainly by very hard and brittle materials causing problems in conventional turning associated with a high degree of wear of the tool and effectiveness of machining. Material removal without thermally affected zone [14, 15] and the option of machining a wide range of materials are advantages, such as cutting flat materials by AWJ [16]. Correct adjustment of values of technological factors plays an important role in AWJ machining from the point of view of achieving high accuracy of shapes and low values of roughness parameters [17]. Correct adjustment of cutting head trajectory and adjustment of movement corrections (disintegration of AWJ with increasing distance from the mouth of the focusing tube) [18] are also very important. The experience of the operator, accuracy and technological parameters of the machine also plays an important role [19, 20]. Low cutting force (approximately 40 N) acting on the material during the material removal process is also an advantage of hydro-abrasive disintegration of rotating workpieces. When cutting and machining materials using AWJ, it is necessary to take into account the contact of abrasive water with material from the point of view of the possible origin of corrosion and clogging functional parts of the machine with abrasive [21]. In this study, circular bars of graphite and aluminium with diameter of  $d_w = 12$  mm were used for the experiment. The objective was to demonstrate the option of machining small diameters of brittle (graphite) and ductile (aluminium alloy) material, using hydro-abrasive disintegration of rotating workpieces. Graphite machining is the process of material removal in the form of very small dust particles. Chips of visible dimensions are not formed like in the case of classical machining of steels using a tool with defined cutting edge. Material properties of graphite deteriorate the manufacture of these shapes, because brittle failures occur when machining them. In contrast, the material properties of aluminium alloys allow its easy machining using conventional technologies. Aluminium alloys are used mainly in the automotive industry due to their low weight and sufficient strength. Graphite machining deteriorates the quality of the working environment and has an unfavourable impact on the human organism. In the case of hydro-abrasive cutting of graphite semi-finished products, dust particles are absorbed by water, so abrasive waterjet could represent an alternative to roughing operations. Graphite is used mainly in the manufacture of electrodes for electro-erosive hollowers.

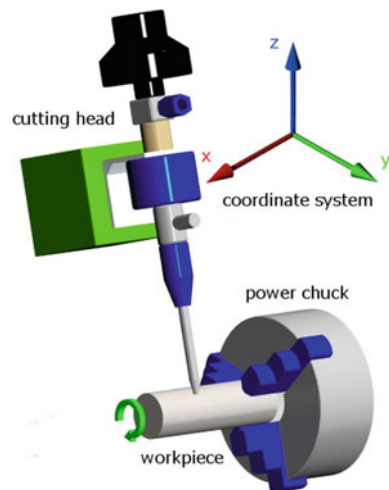
## 2 State of the Art

Material removal (micro-erosion process) in abrasive waterjet technology is carried out by scouring, breaking off and creation of microchips at the point of contact of workpiece with AWJ [22]. Waterjet is generated in the cutting head, where

**Fig. 1** 3D model of cutting head



**Fig. 2** 3D model of technological assembly for hydro-abrasive disintegration of rotating workpieces



high-pressure water ( $P = 400\text{--}600\text{ MPa}$ ) is transformed to high-speed water ( $v = 900\text{--}1000\text{ m s}^{-1}$ ). Abrasive particles are added into the waterjet in the mixing chamber. The resulting abrasive waterjet is formed by passage through the focusing tube (Fig. 1), [23].

The erosion process caused by water and abrasive particles impinging on the workpiece surface is the basic principle of hydro-abrasive disintegration of rotating workpieces. The cutting head performs a translation movement (movement in axes  $X$ ,  $Y$  and  $Z$ ), and the workpiece clamped in the chucking appliance performs a rotating movement (the workpiece can move both in the same direction and opposite direction of the outgoing AWJ) (Fig. 2).

### 3 Experiment

The objective of the experiment was to describe the impact of focusing tube diameter ( $d_{f1} = 0.5$  mm and  $d_{f2} = 0.78$  mm) on the quality of machined surface of workpiece from graphite and aluminium alloy when machining small diameters. Two different materials were selected for comparison of effect AWJ with using same technological factors. Tangential waterjet with the addition of Australian garnet as an abrasive was used for the experiment. Adjustment of values of technological factors is illustrated in Table 1.

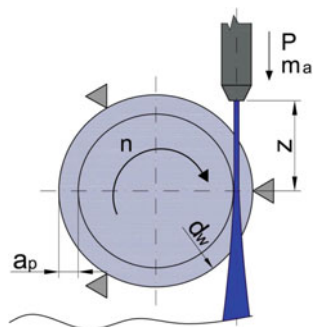
Different values of abrasive mass flow rate are based on the maximum admissible quantity for addition to waterjet of the given orifice. Grain size of abrasive mesh was the same for both diameters of focusing tube. Semi-finished products of graphite and aluminium with the diameter of  $d = 12$  mm were used for the experiment. Figure 3 explains the identification of technological factors.

Rotating shape of workpieces with three diameters was proposed for the experiment. Trajectory for CNC control of machining technological process was developed on the basis of 2D design (Fig. 4). The design takes into account AWJ

**Table 1** Experimental conditions

Factors	Values
Pressure $p$ (MPa)	400
Orifice diameter $d_o$ (mm)	0.2
Size of abrasive particles (MESH)	120
Revolution $n$ (rpm)	300
Standoff distance $z$ (mm)	13
Traverse speed $v$ (mm min <sup>-1</sup> )	10
Focusing tube diameter 1 $d_{f1}$ (mm)	0.5
Focusing tube diameter 2 $d_{f2}$ (mm)	0.78
Abrasive mass flow rate— $d_{f1} m_a$ (kg min <sup>-1</sup> )	0.15
Abrasive mass flow rate— $d_{f2} m_a$ (kg min <sup>-1</sup> )	0.4
Depth of cut $a_p$ (mm)	1–4

**Fig. 3** Graphical identification of technological factors



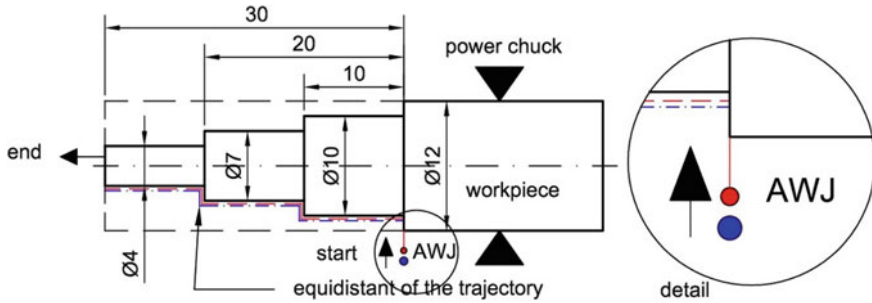


Fig. 4 2D design of workpiece shape with trajectories of cutting head movement

diameter for different diameters of focusing tube in the form of equidistance from required trajectory. Equidistance for focusing tube with the diameter of  $d_{f1} = 0.5$  mm is depicted with the dashes line, and equidistance for focusing tube with the diameter of  $d_{f2} = 0.78$  mm is depicted with the dotted line (Fig. 4). Start, direction and end of machining are depicted in Fig. 4.

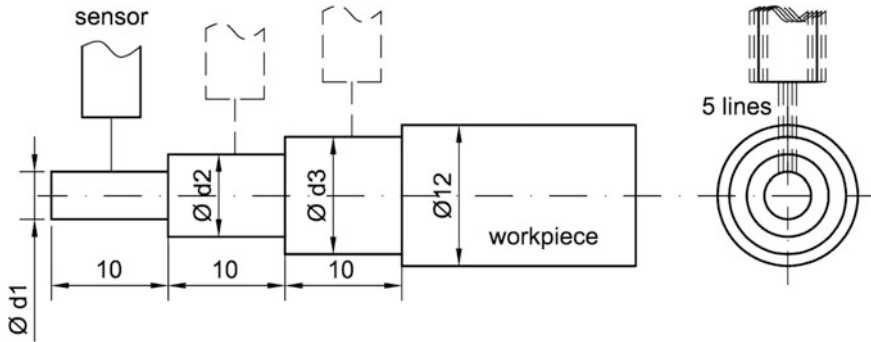
The water pressure was generated by the PTV 75-60 pump with two pressure multipliers (the pump allows operational pressure of  $40 \div 415$  MPa and a maximal water flow of  $7.8 \text{ l min}^{-1}$ ). The machined piece was attached to a power chuck operated by an electric motor that provided the main working movement. This accessory was attached to the technological device for the disintegration of flat materials (2D X-Y cutting table PTV WJ2020-2Z-1xPJ). The experiment was carried out at the Institute of Geonics CAS in Ostrava (Czech Republic), and surface topography identification was performed in the laboratory of Faculty of Mechanical Engineering and Management, Poznan University of Technology, Poland.

## 4 Measurement and Results

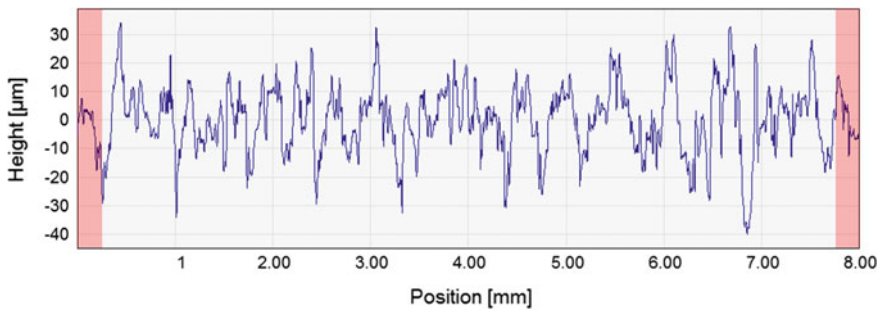
Measurement of values of roughness parameters  $R_a$ ,  $R_z$ ,  $R_q$  was carried out using the MicroProf FRT optic profilometer. Optic measurement was carried out in parallel with the axis of workpiece in sections of 8 mm (for each diameter), because scouring occurred at the boundaries of passages between seats during machining. The sensor carried out measurement on five lines (Fig. 5). Graphs of primary surface profiles were prepared for all lines (Fig. 6) that were used for statistics. The arithmetic average of measured values of roughness parameters was selected for the description of change in surface quality.

The last part of the graphite workpiece with diameter of  $\text{Ø}d_1$  broke off during the experiment (Fig. 5), so it can be stated that the direction of start and end of machining should be reversed. The material properties of aluminium provided sufficient strength, so such breaking off did not occur. Average values of roughness parameters are stated in Tables 2 and 3.





**Fig. 5** Proposal of measurement using the optic MicroProf FRT profilometer



**Fig. 6** Primary profile of aluminium alloy surface, point of measurement— $\text{Ø}d_2$  focusing tube diameter  $d_{j2} = 0.78$  mm

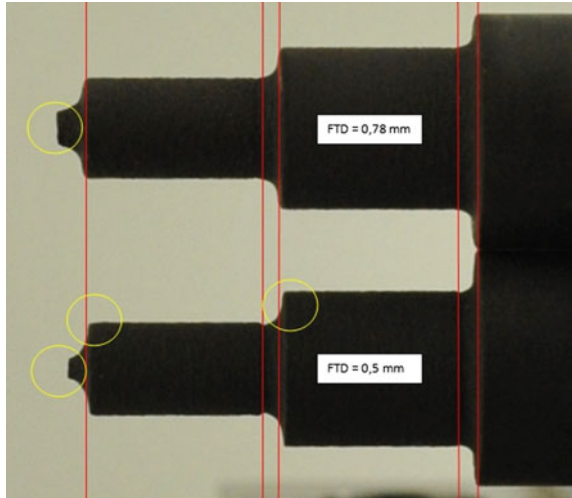
**Table 2** Values of roughness parameters of graphite

Measurement position	Focusing tube diameter $d_{f1} = 0.5$ mm				Focusing tube diameter $d_{f2} = 0.78$ mm			
	Diameter	$R_a$ ( $\mu\text{m}$ )	$R_q$ ( $\mu\text{m}$ )	$R_z$ ( $\mu\text{m}$ )	Diameter	$R_a$ ( $\mu\text{m}$ )	$R_q$ ( $\mu\text{m}$ )	$R_z$ ( $\mu\text{m}$ )
$d_1$	—	—	—	—	—	—	—	—
$d_2$	4.7	13	16	93	5.1	13	17	101
$d_3$	7.9	9	12	73	8.2	9.4	12	74

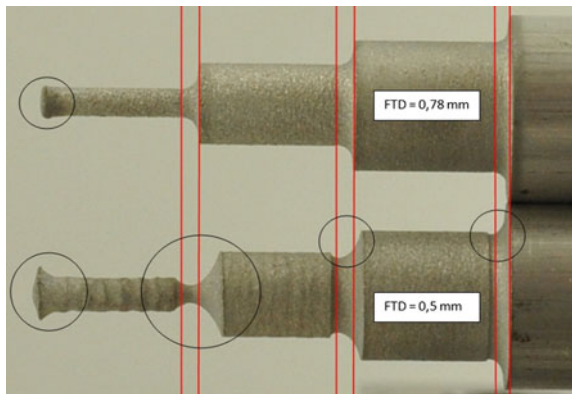
**Table 3** Values of roughness parameters of aluminium

Measurement position	Focusing tube diameter $d_{f1} = 0.5$ mm				Focusing tube diameter $d_{f2} = 0.78$ mm			
	Diameter	$R_a$ ( $\mu\text{m}$ )	$R_q$ ( $\mu\text{m}$ )	$R_z$ ( $\mu\text{m}$ )	Diameter	$R_a$ ( $\mu\text{m}$ )	$R_q$ ( $\mu\text{m}$ )	$R_z$ ( $\mu\text{m}$ )
$d_1$	2.1	40	55	342	1.8	16	21	140
$d_2$	5.5	13	17	113	5.2	10	12	80
$d_3$	8.3	6	8	50	8.3	6	7	50

**Fig. 7** Comparison of graphite samples in the case of change in focusing tube diameter (FTD—focusing tube diameter)



**Fig. 8** Comparison of aluminium alloy samples in the case of change in focusing tube diameter (FTD—focusing tube diameter)



Figures 7 and 8 depict a visual comparison of samples in the case of a change in focusing tube diameter and the given adjustment of technological parameter values.

## 5 Conclusions

From the measured values of roughness parameters, it can be concluded that the change in focusing tube diameter has affected the quality of machined surfaces of graphite and aluminium alloy. During the gradual increasing of depth of cut (during passage along the movement trajectory), values of roughness parameters were increased in the machined graphite. This is valid for the focusing tube with the diameter of  $d_{f1} = 0.5$  mm and  $d_{f2} = 0.78$  mm. A similar condition can also be seen

in the machining of aluminium alloy. Changes in both materials can be seen from the point of view of the values of machined diameters. At focusing tube diameter  $d_{f1} = 0.5$  mm and  $d_{f2} = 0.78$  mm, the precise required diameter was not achieved during machining, which was caused by the disintegration of abrasive waterjet with increasing distance from the orifice mouth. Increasing depth of cut in material removal also caused the reflection of AWJ from the wall of unmachined material. On the basis of a smaller number of abrasive grains (focusing tube with diameter of  $d_{f1} = 0.5$  mm), substantially larger rounding of machined graphite and aluminium alloy can be observed during passages (Figs. 7 and 8). Abrasive waterjet did not have sufficient quantity of abrasive particles for the quick removal of material, so a larger reflection of jet and machined points scouring occurred for a longer period of time. This difference can be observed mainly in the case of aluminium alloy. Differences in shape can be observed mainly in the case of aluminium alloy, so finally it can be stated that properties of machined material and the quantity of abrasive particle dispersed in waterjet mostly affect the resulting shape. For further research, it is necessary to carry out the experiment (machining of brittle, ductile, elastic and hard materials) using focusing tubes of different diameters ( $d_f = 0.5$ ; 0.78 and 1.2 mm) and with equal quantity of abrasive added to waterjet. The end part was broken off during the machining of graphite in both cases, so it can be stated that the direction of start and end of machining was not selected correctly. However, by the suitable adjustment of values of technological parameters, corrections and trajectories of movement, it would be possible to prepare simple shapes of workpieces for subsequent finishing using conventional methods.

**Acknowledgements** This work was supported by the Slovak Research and Development Agency under Contract No. APVV-207-12. Experiments were carried out with the support of the Institute of Clean Technologies for Mining and Utilization of Raw Materials for Energy Use—Sustainability Program, reg. no. LO1406 financed by Ministry of Education, Youth and Sports of the Czech Republic, and with support for the long-term conceptual development of the research institution RVO: 68145535.

## References

1. Sharma, V., Chattopadhyaya, S., Hloch, S.: Multi response optimization of process parameters based on Taguchi-Fuzzy model for coal cutting by water jet technology. *Int. J. Adv. Manuf. Technol.* **56**, 1019–1025 (2011)
2. Hreha, P., Radvanská, A., Hloch, S., Peržel, V., Królczyk, G., Monková, K.: Determination of vibration frequency depending on abrasive mass flow rate during abrasive water jet cutting. *Int. J. Adv. Manuf. Technol.* **77**, 763–774 (2015)
3. Hreha, P., Radvanska, A., Knapčíková, L., Krolczyk, G.M., Legutko, S., Krolczyk, J., et al.: Roughness parameters calculation by means on-line vibration monitoring emerging from AWJ interaction with material. *Metrol. Meas. Syst.* **XXII** **2**, 315–326 (2015)
4. Manu, R., Babu, N.R.: Influence of jet impact angle on part geometry in abrasive waterjet turning of aluminium alloys. *Int. J. Mach. Mach. Mater.* **3** (2008)

5. Cárach, J., Hloch, S., Hlaváček, P., Ščučka, J., Martinec, P., Petřů, J., et al.: Tangential turning of Incoloy alloy 925 using abrasive water jet technology. *Int. J. Adv. Manuf. Technol.* **82**, 1747–1752 (2016)
6. Hloch, S., Hlaváček, J., Vasilko, K., Cárach, J., Samardžić, I., Kozak, D., et al.: Abrasive waterjet (AWJ) titanium tangential turning evaluation. *Metalurgija* **53**, 537–540 (2014)
7. Sitek, L., Foldyna, J., Souček, K., Shaping of rock specimens for testing of uniaxial tensile strength by high speed abrasive water jet: first experience. In: *Impact of Human Activity on the Geological Environment—Proceedings of the International Symposium of the International Society for Rock Mechanics, Eurock (2005)*
8. Hlaváček, P., Cárach, J., Hloch, S., Vasilko, K., Klichová, D., Klich, J., et al.: Sandstone turning by abrasive waterjet. *Rock Mech. Rock Eng.* **48**. ISSN 2489–93 (2015)
9. Hutyrova, Z., Scucka, J., Hloch, S., Hlavacek, P., Zelenak, M.: Turning of wood plastic composites by water jet and abrasive water jet. *Int. J. Adv. Manuf. Technol.* **84**, 1615–1623 (2016)
10. Duplak, J., Hatala, M., Botko, F., Kormos, M.: Analysis of cutting tools durability importance in turning process of steel C60. In: *Key Engineering Materials: Operation and Diagnostics of Machines and Production Systems Operational States 3*, vol. 669, pp. 319–326 (2016)
11. Zhong, Z.W., Han, Z.Z.: Turning of glass with abrasive waterjet. *Mater. Manuf. Process* **17**, 339–349 (2002)
12. Axinte, D.A., Stepanian, J.P., Kong, M.C., McGourlay, J.: Abrasive waterjet turning—An efficient method to profile and dress grinding wheels. *Int. J. Mach. Tools Manuf.* **49**, 1–6 (2009)
13. Liu, D., Huang, C., Wang, J., Zhu, H., Yao, P., Liu, Z.: Modeling and optimization of operating parameters for abrasive waterjet turning alumina ceramics using response surface methodology combined with Box-Behnken design. *Ceram Int.* **40** (2014)
14. den Dunnen, S., Mulder, L., Kerkhoffs, G.M.M.J., Dankelman, J., Tuijthof, G.J.M.: Waterjet drilling in porcine bone: the effect of the nozzle diameter and bone architecture on the hole dimensions. *J. Mech. Behav. Biomed. Mater.* **27**, 84–93 (2013)
15. Hloch, S., Valíček, J., Kozak, D.: Preliminary results of experimental cutting of porcine bones by abrasive waterjet. *Tech. Vjesn.* **18**, 467–470 (2011)
16. Lissek, F., Kaufeld, M., Tegas, J., Hloch, S.: Online-monitoring for abrasive waterjet cutting of CFRP via acoustic emission: Evaluation of machining parameters and work piece quality due to burst analysis. *Proc. Eng.* 67–76 (2016)
17. Hreha, P., Hloch, S.: Potential use of vibration for metrology and detection of surface topography created by abrasive waterjet. *Int. J. Surf. Sci. Eng.* **7**, 135–151 (2013)
18. Hreha, P., Radvanska, A., Carach, J., Lehocka, D., Monkova, K., Krolczyk, G., et al.: Monitoring of focusing tube wear during Abrasive WaterJet (AWJ) cutting of AISI 309. *Metalurgija* **53**, 533–536 (2014)
19. Lehocka, D., Klich, J., Foldyna, J., Hloch, S., Krolczyk, J.B., Carach, J., et al.: Copper alloys disintegration using pulsating water jet. *Measurement* **82**, 375–383 (2016)
20. Lebar, A., Junkar, M., Poredoš, A., Cvjeticanin, M.: Method for online quality monitoring of AWJ cutting by infrared thermography. *CIRP J. Manuf. Sci. Technol.* **2**, 170–175 (2010)
21. Hashish, M., South, A.: Optimization factors in abrasive—waterjet machining. *J. Eng. Ind.* **1** (1991)
22. Dong, Y., Liu, W., Zhang, H., Zhang, H.: On-line recycling of abrasives in abrasive water jet cleaning. *Proc. CIRP* (2014)
23. Arola, D., Ramulu, M.: A study of Kerf characteristics in abrasive waterjet machining of graphite/epoxy composite. *J. Eng. Mater. Technol. Trans. ASME* **118**, 256–265 (1996)

# Measurement of Surface Topography Using Computed Tomography

**Bartosz Gapinski, Michal Wieczorowski, Lidia Marciniak-Podsadna, Alejandro Pereira Domínguez, Lenka Cepova and Anton Martinez Rey**

**Abstract** Computed tomography is a new field of coordinate measuring metrology. For this reason, many areas of its application are not yet completely known. The paper presents reproduction possibilities of geometrical structure of a surface by computer tomography. Results are combined with data from a classical tactile profilometer to measure surface topography. Comparison of the obtained values makes it possible to confirm the usefulness of computer tomography to reconstruct the surface geometry. This is especially important when indoor surfaces are indispensable. Such measurement with any other device than computer tomograph is not possible or requires damage of the element being measured. As a result of the measurement by means of a computer tomograph, from the same measurement data we obtain not only information about the surface and shape of the element, but also—as an additional advantage—ability to evaluate internal structure of material, for example its porosity or fibre distribution in case of composites.

**Keywords** Computed tomography · Surface topography · Accuracy of measurement · Micro-CT

## 1 Introduction

Every object that surrounds us is bounded by surfaces. Their diverse structure is responsible for their appearance and nature of cooperation with another surface. However, in every case, it is necessary to measure the surface and to select the

---

B. Gapinski (✉) · M. Wieczorowski · L. Marciniak-Podsadna  
Faculty of Mechanical Engineering and Management, Poznan University  
of Technology, pl. M. Skłodowskiej-Curie 5, PL-60965 Poznan, Poland  
e-mail: bartosz.gapinski@put.poznan.pl

A. Pereira Domínguez · A. Martinez Rey  
University of Vigo, Vigo, Spain

L. Cepova  
VŠB—Technical University of Ostrava, Ostrava, Czech Republic

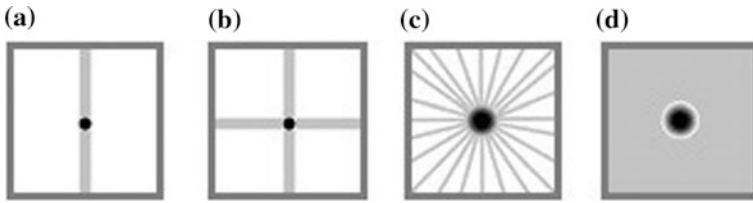
parameters that properly characterize it in order to assess the surface. It is also indispensable to provide appropriate conditions for the measurement of constant temperature, vibration reduction, etc. [1–3], that is to ensure that measurement and/or control system is a reliable source of information [4].

There are two main groups of measurement methods: scanning and surface. Scanning methods can be also divided into profile scanning and image scanning. Profile scanning methods evaluate the roughness on the basis of the set of profiles, while image scanning is based on the sequence of images. Surface methods, on the other hand, measure roughness based on averaging and accepting a model describing measured irregularities [5]. The assessment of surface topography based upon a set of profiles means realizing horizontal scans and traditionally comes down to stylus or optical profilometry including a series of profiles most often in parallel directions. Among the profile methods, those which are especially worth to be pointed are tactile profilometry, self-focusing point profilometry, use of profilometric confocal probes, scanning tunnelling microscopy and atomic force microscopy. When mapping surfaces by means of profile methods, the measuring tip has significant influence on reliability of the obtained result, and whether it is contact made of synthetic diamond or optical is based on interferometry or confocal phenomenon [6].

All of previously mentioned methods are used to reproduce the surface, but have also one additional common attribute. It is necessary to have access to the measured area and physical contact with the surface or to observe it. Unfortunately, in some cases, it would be necessary to destroy the test piece by cutting off the appropriate sample. In recent years, however, an alternative method has appeared—computed tomography. It allows you to evaluate the structure of the surface, including the inner areas closed without destroying the element. Computed tomography, however, has some limitations due to the ability to penetrate the X-rays of the object measured and the effect of radiation power on the accuracy of the measurement [7, 8].

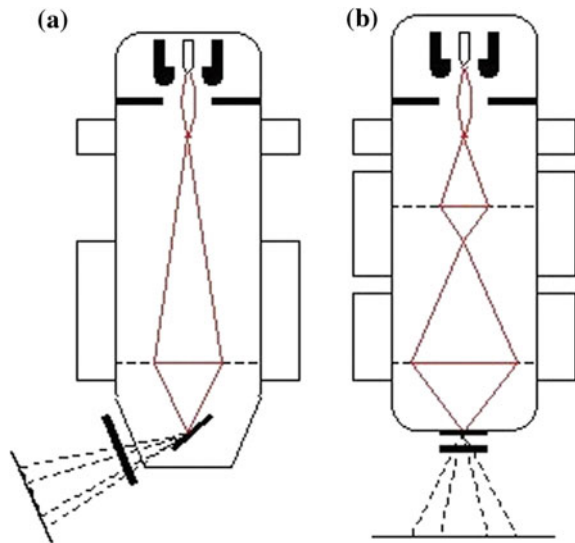
## 2 Computed Tomography

The word tomography comes from the Greek words “tomé” (cross section) and “gráfein” (save). As a result of combining the measured object projections from different directions, it is possible to create cross-sectional (2-D) and spatial (3-D) images. Analysis and processing of individual projections are done using a computer—hence the name computed tomography (CT) [9, 10]. Measurement tomography is a type of X-ray tomography, based on X-rays discovered by Röntgen. The test is performed by directing the X-ray beam to the object and recording its intensity on the detector on the other side. Its intensity is weakening when passing through the object under investigation, what is a function of radiation energy and the type and thickness of the material under investigation [11–13]. The volume of



**Fig. 1** Steps of generating a tomographic image—measurement of a cylinder: **a** one projection; **b** two measurement projections spaced every 90°; **c** multiple measurement projections at different angles of 360° range; **d** final result of the measurement—3-D image—the effect of reconstruction of multiple projections

**Fig. 2** Lamps used in measuring tomograph: **a** directional, **b** transmission [20]



the object is divided into small cells, called voxels, in which the linear absorption coefficient of radiation is the same. Reconstructed cross-sectional image is a quantitative map of the linear absorption coefficient in voxels that are integral with in the scanned layer (Fig. 1) [14, 15].

The source of the X radiation in the tomograph is the X-ray lamp. There are two basic types of lamps: transmission and directional. The transmission lamp allows for a larger magnification, while the directional one allows for possessing the higher directional power (Fig. 2) [16–19]. In order to obtain a better resolution of the measured image in tomograph, microfocus and nanofocus lamps are used [20].

### 3 Equipment Used During the Test

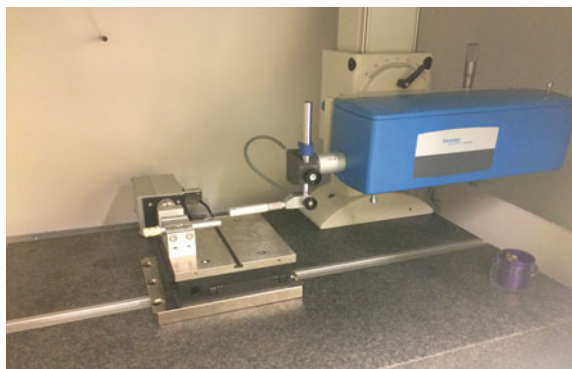
GE Phoenix v|tome|x s240 tomograph is equipped with two X-ray tubes. The high-power directional light allows to operate up to 240 kV and achieve a beam power of 320 W with a maximum magnification of up to 100×. The second one is a transmission-type nanofocus lamp. It is characterized by lower power—up to 15 W, but its design allows for a significantly smaller spot in the focus and magnification up to 200×. This lamp allows for detail detection at the level of 0.5 μm. The measuring volume of the tomograph allows to measure elements whose outer dimensions do not exceed 260 mm in diameter and 420 mm in high. However, it should be taken into consideration that as the density of the material to be measured increases, the thickness of the cross-sectional area is reduced. An example of a CT used in our research is shown on Fig. 3.

Contact profilometer Hommel-Etamic T8000 is equipped with a table for topography measuring surface. It is also equipped with measuring head that allows

**Fig. 3** GE Phoenix v|tome|x s240 tomograph in the laboratory of the Poznań University of Technology



**Fig. 4** Hommel-Etamic Profilometer T8000 in the laboratory of the Poznań University of Technology





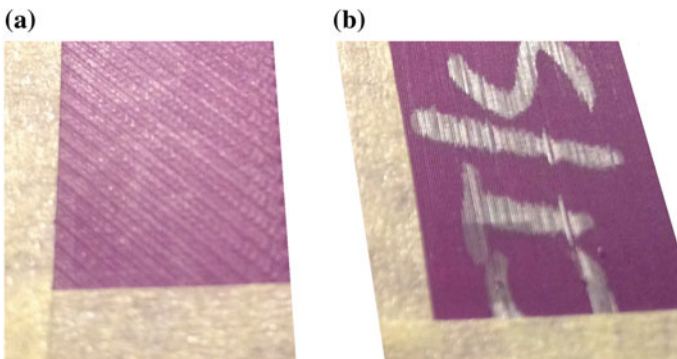
for measurement in a vertical range of 800  $\mu\text{m}$  at 1-nm resolution. The measurement pressure of a diamond tip with a radius of 2  $\mu\text{m}$  and a  $90^\circ$  angle is 1.6 mN (Fig. 4).

## 4 Studied Objects

Two surfaces that were made using a fused deposition modelling (FDM) 3-D printer were subject of analysis. The material used to print the elements was ABS. During printing, the base surface is perpendicular to the axis of the printhead. The first surface (surface A—Fig. 5a) was positioned perpendicularly to the base surface so that further layers of applied material are visible on the surface. The second surface (surface B—Fig. 5b) was located parallel to the base surface. No further layers are visible on it, and since the last applied outer layer is being measured, it has a very regular and repetitive character.

Both samples were tested on a traditional surface topography equipment and CT scanner.

In the case of contact measurement, the area under investigation may be specified very precisely. The study was conducted on a  $5 \times 5$  mm area. For this purpose, 501 profiles of 5 mm length were measured. Such profiling arrangement allows for accurate surface mapping. For its correct location, a marker is affixed to the surface, and the edge of the measuring area is offset by 1 mm in each axis. Measurement carried out on computer tomography also allows to define the area to be measured, and it may be only a slice of the controlled part. However, the exact dimensions and location of the analysed area were only possible at reconstruction and spatial processing of measured data. Computer tomography measurements were made for the transmission light, at a voltage of 100 kV and a current of 300  $\mu\text{A}$ . The voxel size was 40.6  $\mu\text{m}$ , and the geometric magnification was  $4.92\times$ .

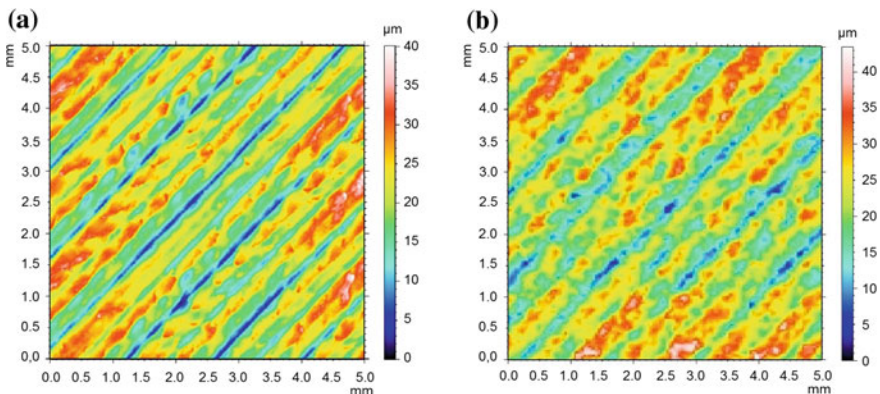


**Fig. 5** Surface made for testing on a 3-D printer: **a** surface A; **b** surface B

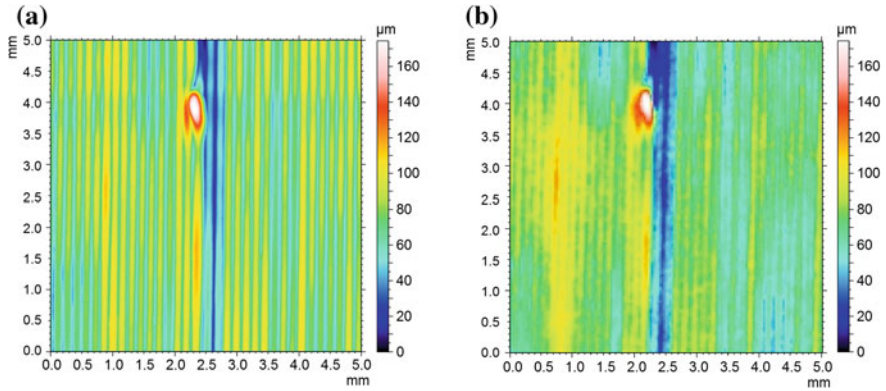
Results of the measurement are two surfaces obtained by two different measuring devices. Processing of measured data leads to obtain corresponding surfaces on both components. Figure 6 shows the surface A measured by the profilometer and the tomograph, and on Fig. 7 the surface B.

On the basis of data presented in Figs. 6 and 7, it can be observed that in this case, data obtained from the CT scanner have lower resolution, and the image of this surface is less accurate. However, while observing the nature of the deviation distribution and the vertical scale, it can be pointed that these data are identical. For the surface B, a peak can be clearly observed that is significantly higher than the surrounding surface. Likewise is the groove running alongside the peak over the entire length of the surface to be tested. In both cases, the distribution of deviations and their values in individual axes are identical.

Further analysis of the measurement result leads to the determination of parameters convergence for individual surfaces. Differences in the resulting numerical value can be noticed but it comes from the lower resolution of the image obtained by the tomograph. This results in a worse acceleration of the sharp edges of the tops. Then, the average line according to which some of the parameters are calculated is shifted, what effects in change of the values. In the case of computer tomography, the spatial image is obtained as a result of the reconstruction of a number of X-ray pictures. The next step is to determine the boundary of the material and the surrounding air. As result of this process, for many cases, the calculated edge is deeper, and the valley is wider at the base than in the case of contact measurements with a specialized tactile device. Those factors as well as worse resolution of the tomograph than the tactile device also reflect problems with the correct mapping of the slope, which can be observed by analysing the  $Sdq$  parameter, which is smaller, which corresponds to the tendency to produce sharper edges of the measured surface. Selected parameters characterizing the measured surfaces are summarized in Tables 1.



**Fig. 6** Measurement result of surface A for profilometer (a) and computed tomograph (b)



**Fig. 7** Measurement result of surface B for profilometer (a) and computed tomograph (b)

**Table 1** Summary of parameters characterizing the topographic parameters for surface A and surface B

Topography parameter	[]	Surface A		Surface B	
		T8000	CT	T8000	CT
Sq	μm	6.11072	6.96361	12.46730	9.96744
Ssk	–	–0.18012	0.03681	–0.15926	0.41488
Sku	–	2.72179	2.69414	3.16372	5.37617
Sp	μm	19.37500	27.18280	62.16300	66.38620
Sv	μm	20.72200	25.41110	53.42100	59.60190
Sz	μm	40.09700	52.59390	115.58400	125.98800
Sa	μm	4.96067	5.65380	10.17790	7.74940
Sk	μm	10.92590	12.58150	27.47520	22.73810
Spk	μm	2.93702	3.14181	8.35668	10.38910
Svk	μm	4.91989	4.24278	12.83620	7.21083
Smr1	%	7.73765	7.30479	5.71747	10.58880
Smr2	%	85.58410	89.76610	80.76120	93.22200
Sal	μm	124.96400	158.00800	38.80260	57.74890
Str	–	0.08859	0.05236	0.01546	0.02302
Std	°	43.50650	47.72610	89.47570	87.98210

Based on the analysis of presented results, significant correlation between the surface measured by the tomograph and the tactile profilometer can be noticed. This is also very well visible on spatial maps of the measured surfaces. Clearly, it can be observed that the surface of a computer tomograph (Fig. 8b) is less regular and that the peaks are not so reproduced as in the case of contact measurements (Fig. 8a).

As for surface A, surface B is also reproduced more irregularly at the peak of the image obtained from the computed tomograph (Fig. 9b) than those obtained from the profilometer (Fig. 9a). However, it can be observed that the nature of the surface

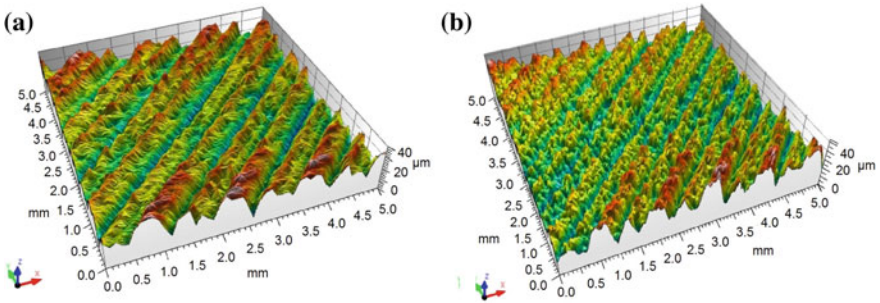


Fig. 8 Measurement result for 3-D surface A on the profilometer (a) and computer tomograph (b)

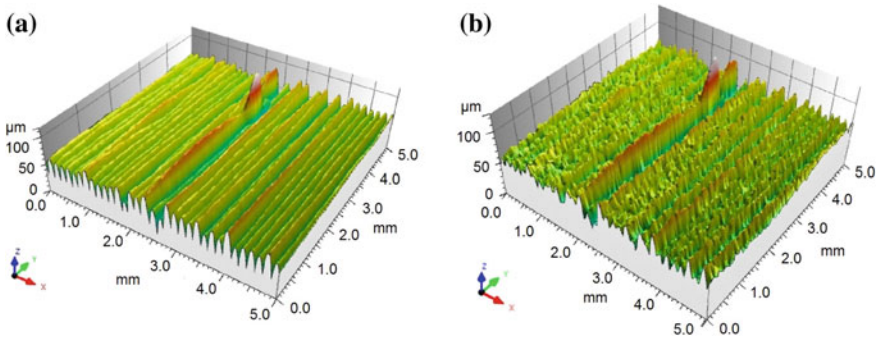


Fig. 9 Measurement result for 3-D surface B on the profilometer (a) and computer tomograph (b)

and the single vertex, as well as the position of the groove on the centre of the surface, has been reconstructed correctly for both surfaces. By analysing in detail both the surface parameters and cross-sectional transverse to the groove, we obtain information that the apex-to-bottom distance is 127.7  $\mu\text{m}$  for the profilometer and 124.8  $\mu\text{m}$  for the CT scanner. These are therefore corresponding values.

### 5 Conclusions

Computer tomography is a new group of measurement methods within the coordinate measuring technique. Technical applications have been used recently. As shown in this paper, it is suitable not only for the qualitative assessment of the tested elements but also for the quantitative assessment.

Surfaces obtained by the CT scan not only are similar to the surfaces obtained using a standard device such as a tactile profilometer, but also are corresponding in terms of the value of the parameters acquired. It can also be observed that the results achieved by computer tomography are worse at resolution, which translates into the

ability and accuracy of mapping of peaks and valleys. This has a direct impact on the value of the calculated parameters.

The results present the high usefulness of the new technique of computed tomography. The ability to use it for topography evaluation is justified, and if it is not possible to access directly to the controlled surface, then it may prove to be an indispensable technique.

Despite different resolution of the two methods described above, one can see quite good correlation between the results obtained from various surfaces. This can be a very important feature in additive manufacturing, when it is necessary to merge surfaces and data files obtained with different measurement devices. Thus, it would be possible to connect macro- and micro (or even nano)-scales for certain features on the same surface and perform a sophisticated multiscale analysis.

**Acknowledgements** The presented research results were funded with grants PBS2/NCBiR (No. PBS2/A6/20/2013) “Research and assessment of the reliability of modern methods of measuring surface topography in micro- and nanoscale”.

The presented research results were funded with grants for education allocated by the Ministry of Science and Higher Education in Poland (No. 02/22/DSPB/1387).

## References

1. Miller, T., Adamczak, S., Świdorski, J., Wieczorowski, M., Łętocha, A., Gapiński, B.: Influence of temperature gradient on surface texture measurements with the use of profilometry. *Bull. Pol. Acad. Sci. Tech. Sci.* **65**(1), 53–61 (2017)
2. Kuczmaszewski, J., Zagórski, I., Zgórnjak, P.: Thermographic study of chip temperature in high-speed dry milling magnesium alloys. *MPER* **7**(2), 86–92 (2016)
3. Grochalski, K., Peta, K., Wieczorowski, M., Jabłoński P.: Climatic chamber for the credibility evaluation of profilometric measurements. Construction and control, 22nd International Conference on Methods and Models in Automation and Robotics (MMAR 2017), IEEE, 2017
4. Diering, M., Hamrol, A., Kujawińska, A.: Measurement system analysis combined with Shewhart’s approach. *Key Eng. Mater.* **637**, 7–11 (2015)
5. Wieczorowski, M., Gapiński, B., Grochalski, K., Miller, T.: Theoretical aspects of analysis of selected sources of errors in profile measurements of surface asperities. *Mechanik* **4**, 335–338 (2017)
6. Wieczorowski, M., Gapiński, B., Grochalski, K., Miller, T.: Experimental research of selected sources of errors in profile measurements of surface asperities. *Mechanik* **4**, 339–343 (2017)
7. Kruth, J-P., Bartscher, M., Carmignato, S., Schmitt, R., De Chiffre, L., Weckenmann, A.: Computed tomography for dimensional metrology. keynote paper, *CIRP Annals* **61**(2) (2011)
8. Kowaluk, T., Wozniak, A.: Methods for verifying the dimensional and material properties on industrial CT scanners according to VDI/VDE 2630 Blatt 1.3. *Advanced Mechatronics SolutionS*, Advances in Intelligent Systems and Computing, 2016, 393, 341–346
9. Ratajczyk E., CT in Industrial Applications, Part. I. Idea of measurements, construction and their functions (in Polish), *Mechanik*, 2011, 2, 112–117
10. Thompson A., Maskery I., Leach RK., X-ray computed tomography for additive manufacturing: a review, *MEASUREMENT SCIENCE AND TECHNOLOGY*, 2016, 27(7)
11. Plessis, A., Yadroitsava, I., Roux, D., Yadroitsev, I., Fieres, J., Reinhart, C., Rossouw, P.: Prediction of mechanical performance of Ti6Al4V cast alloy based on micro-CT based load simulation. *J. Alloy. Compd.* **724**, 267–274 (2017)

12. Woziniak, A., Kowaluk, T.: A new threshold selection method for X-ray computed tomography for dimensional metrology. *Precis. Eng.* (2017)
13. Townsend, A., Pagani, L., Scott, P., Blunt, L.: Areal surface texture data extraction from X-ray computed tomography reconstructions of metal additively manufactured parts. *Precis. Eng.* **48**, 254–264 (2017)
14. Warnett, J.M., Titarenko, V., Kiraci, E., Attridge, A., Lionheart, W., Withers, P., Williams, M.A.: Towards in-process x-ray CT for dimensional metrology. *Meas. Sci. Technol.* **27**(3) 2016
15. Ziolkowski, G., Chlebus, E., Szymczyk, P., Kurzac, J.: Application of X-ray CT method for discontinuity and porosity detection in 316L stainless steel parts produced with SLM technology. *Arch. Civ. Mech. Eng.* **14**(4), 608–614 (2014)
16. Gapinski, B., Janicki, P., Marciniak-Podsadna, L., Jakubowicz, M.: Application of the computed tomography to control parts made on additive manufacturing process. *Procedia Eng.* **149**, 105–121 (2016)
17. Maszybrocka, J., Stwora, A., Gapiński, B., Skrabalak, G., Karolus, M.: Morphology and surface topography of Ti6Al4V lattice structure fabricated by selective laser sintering. *Bull. Pol. Acad. Sci. Tech. Sci.* **65**(1), 85–92 (2017)
18. Gapinski, B., Zachwiej, I.: Kołodziej A. Comparison of different coordinate measuring devices for part geometry control, *Digital Industrial Radiology and Computed Tomography* (2015)
19. Thompson, A., Körner, L., Senin, N., Maskery, I.: X-ray computed tomography of additively manufactured metal parts: the effect of magnification and reconstruction sampling on surface topography measurement. In: *16th International Conference on Metrology and Properties of Engineering Surfaces*, pp. 29–31 (2017)
20. Web site—Amfis X-Ray Co.,Ltd <http://www.amfis.com> (2017.05)

# Cylindricity Measurement on a Coordinate Measuring Machine

Nermina Zaimovic-Uzunovic and Samir Lemes

**Abstract** A set of different parameters affect the measurement of cylindrical profiles on a coordinate measuring machine (CMM). This paper presents the influence of measuring strategy and different types of styli on the results of cylindricity measurement. Experiments with three different styli and three different strategies were performed and the results are presented in this paper. The lowest results were achieved with smaller stylus tips and strategy with lines, while the most stable result, the closest to the reference measurement, is the strategy with parallel circles.

**Keywords** Coordinate measuring machine (CMM) · Cylindricity · Measuring strategy

## 1 Introduction

Some standards (ASME/ANSI, ISO, BS) define how form, location, orientation and runout should be controlled. However, the standards do not define how to actually measure these features. NPL collected the end-user and CMM manufacturer experience on such measurements and recently published them in NPL's Guide of best practices [1]. The guide covers some, but not all, of the deviations that could occur due to poor selection of measuring strategy.

Souza, Arencibia and Costa in [2] discussed the procedures for estimating measurement uncertainty when both circular and cylindrical deviations exist. They concluded that, although procedures are similar, the related mathematical models are different, due to variations in properties and working principles of different systems. Chajda et al. [3] designed a software which could help in strategy selection for cylindrical gear measurement. Adamczak et al. [4] used Legendre–Fourier coefficients to quantitatively compare strategies of cylindricity measurement by approximation of cylindrical surfaces. Dovica and Vegh [5] presented measurement

---

N. Zaimovic-Uzunovic · S. Lemes (✉)  
University of Zenica, Zenica, Bosnia and Herzegovina  
e-mail: slemes@unze.ba

and estimation of cylindrical deviation of rotational symmetrical workpieces, by using standard Gaussian cylinder. Pawlowski et al. [6] used CMM's to analyse cylindricity deviation. They created an expert system to analyse the measurement uncertainty. Simulation was compared with CMM experiments and with reference measurements on specialized measurement devices. Vrba et al. [7] presented the influence of measurement strategy on cylindricity error measured on the CMM. They concluded that the sampling strategy is significantly more influential than the evaluation method. They also observed that the highest error values are present with helix path sampling method and LSQ evaluation method. Danish [8] explained that most standards are based on minimum zone concept, but none of them prescribes the method how to determine the minimum zone. He suggested the new algorithm which provides the minimum deviation.

Adamczak et al. [9–15] performed a number of researches on cylindrical profile measurement. They explained the parametric method of measurement and experimentally verified the concept of reference measurement. Gapinski et al. [16] explained how deviation of roundness is measured on CMM. They analysed the influence of the number of probing points and type of roundness deviation on the final result. They proved that minimum number of probing points is never sufficient for measurement, while too big number of points does not make measurement any better, and they finally gave some recommendations about the number of probing points. Ollison et al. [17] tried to investigate the quality of Rapid Prototypes and came to the conclusion that the results of cylindricity measurement with touch-trigger and scanning probe have different accuracy. Petrò [18] examined a number of strategies for roundness evaluation: blind, adaptive, sample-based, signature-based strategies. He concluded that the uncertainty of measurement largely depends on so-called manufacturing signature; the manufacturing technology largely influences the number and distribution of sampling points. Rossi and Lanzetta [19] optimized the sampling strategy for the roundness evaluation of circular profiles using the minimum zone tolerance method. They concluded that there is an optimal value for the dataset size and the search-space providing the highest accuracy and lowest computation time. Wen et al. [20] used adaptive Monte Carlo and GUM methods for the evaluation of measurement uncertainty of cylindricity error. They established the mathematical model of cylindricity error based on the minimum zone condition and proposed a quasi-particle swarm optimization algorithm (QPSO) for searching the cylindricity error. They found adaptive Monte Carlo method more applicable to evaluate the measurement uncertainty of cylindricity error. Salah [21] used the Flick standard to evaluate the measurement accuracy of dimension and roundness form of a coordinate measuring machine for particular measurement tasks. The author observed that there are proportional relationships between each of uncertainty and error potential of the empirical error formulae in measurement.



## 2 Cylindricity Measuring Strategies

The minimum number of points for cylindricity measurement is defined in ISO 12180-2 [22]. The standard describes four limited measuring strategies: the strategy for measurement of roundness profiles, the strategy for measurement of generatrix lines, the “bird-cage” strategy (which is a combination of measurement of roundness profiles and generatrix lines) and the point strategy. These measuring strategies are shown in Fig. 1.

Measuring strategy using roundness profiles uses the intersections with planes perpendicular to the cylinder axis [23]. The main feature of this method is the high density of points in volume, compared to the density of points per axis. In addition, this method can combine probe angles.

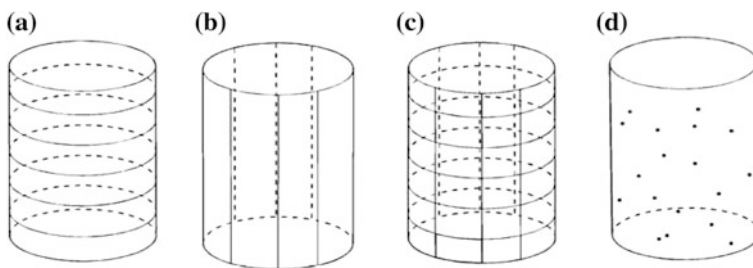
Measuring strategy along lines parallel to the cylinder axis includes a series of straight trajectories set in the vertical direction parallel to the axis of the cylinder. Adjustments can be made, such as the number of lines per cylinder or the density of points on the lines.

Bird-cage measurement is based on a combination of the first two strategies. This strategy informs the operator about the shape of a cylinder. The disadvantage of this strategy is that measurement lasts longer. Cylinders with interruptions in its geometry are not suitable for this measuring strategy.

The points measuring strategy uses arbitrarily taken points across the complete cylinder. The density of points in this method is limited, and therefore, it limits the analysis of the content of harmonic components.

In addition to these strategies, there is another strategy, often used in practice, the measuring along the helix. This measurement strategy includes the helix path around a cylinder with a spiral movement. This method requires the simultaneous movement of the probe in both Z- and X-axes together with spindle-like movement. The adjustable parameter of this measuring strategy is the number of revolutions.

The goal of this research is to compare the results of different measuring strategies, in order to provide recommendations for practical measurements of



**Fig. 1** Standard measuring strategies [22]: **a** strategy for measurement of roundness profiles; **b** strategy for measurement of generatrix lines; **c** “bird-cage” strategy; **d** points strategy

cylindricity when this form is required by technical documentation: which stylus size to use, which strategy, and how many points are optimal for cylindricity measurement.

### 3 Experimental Setup

An experiment was performed in order to analyse the effect of different probes and different measuring strategies on the results of cylindricity measurement. The experiment was carried out on a calibrated cylinder gauge with the following dimensions: nominal diameter  $d = 89.996$  mm, outside diameter  $D = 140$  mm and height  $h = 24$  mm (Fig. 2).

Measurements were performed using probes with different stylus tip radii (Table 1), combined with different measuring strategies (circles, generatrix lines and helix). The experiment was performed on a coordinate measuring machine Zeiss Contura G2 ( $MPE_E = (1.8 + L/300) \mu\text{m}$ ,  $MPE_P = 1.8 \mu\text{m}$ ).

In order to eliminate the influence of scanning resolution and speed, all measurements were performed with step width of 0.1 mm and speed about 25 mm/s. Table 1 summarizes the geometry of the styli probe used. Figures 3, 4 and 5 show how strategy is set-up within the CMM software Zeiss Calypso. Figure 3 shows the example of strategy with set of four parallel circles. Figure 4 shows the example of strategy with 12 parallel vertical lines, and Fig. 5 shows an example of helix with four revolutions.

Figure 6 shows the coordinate measuring machine used for this experiment.

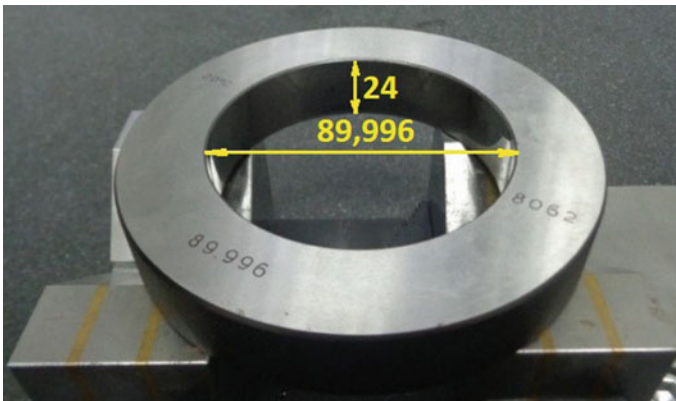
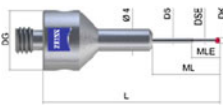
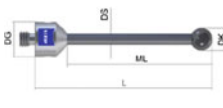
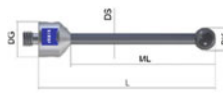
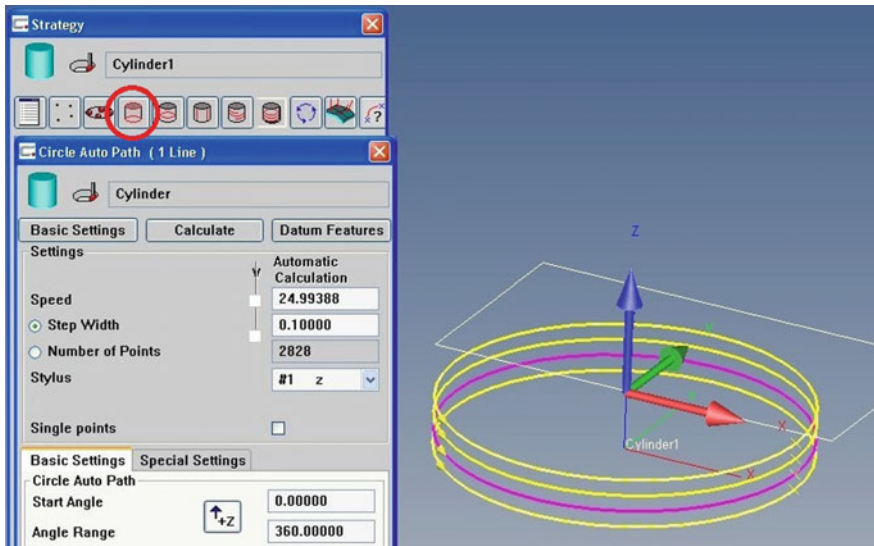


Fig. 2 Calibrated cylinder gauge used for the experiment

**Table 1** Geometry of styli used

	Stylus A	Stylus B	Stylus C
			
DK (mm)	2	5	8
L (mm)	44	75	114
DG (mm)	11	11	11
MG (mm)	19	65	101
DS (mm)	1.5	3.5	6
Weight (g)	5	5	10



**Fig. 3** Setting-up a measuring strategy in CMM software; measuring cylindricity with circles

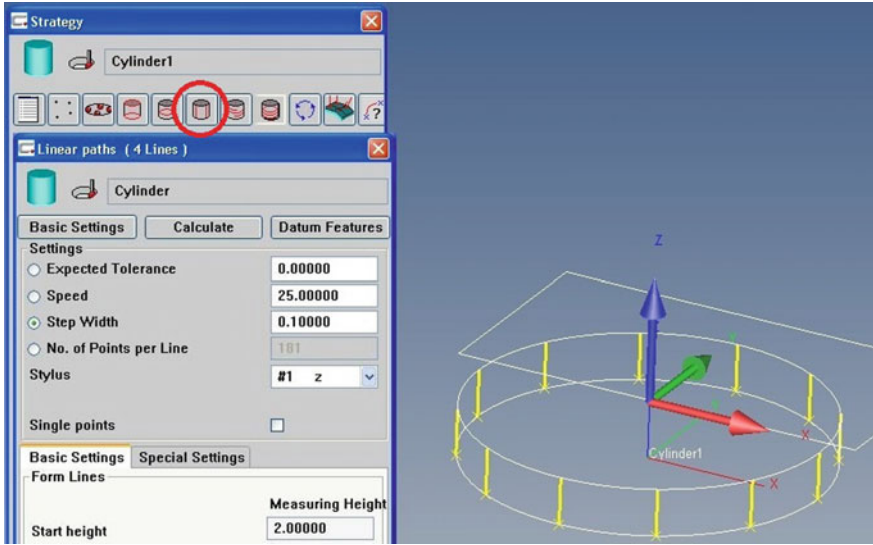


Fig. 4 Setting-up a measuring strategy in CMM software; measuring cylindricity with lines

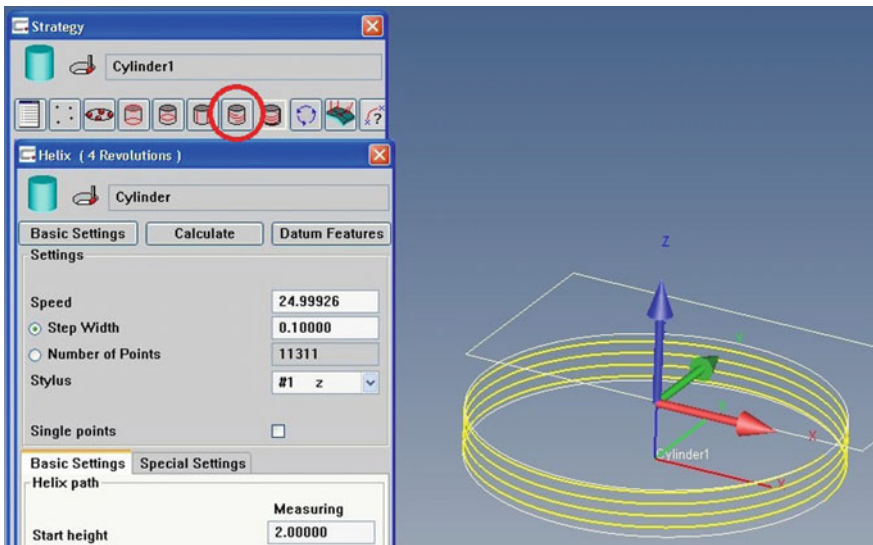


Fig. 5 Setting-up a measuring strategy in CMM software; measuring cylindricity with a helicoid

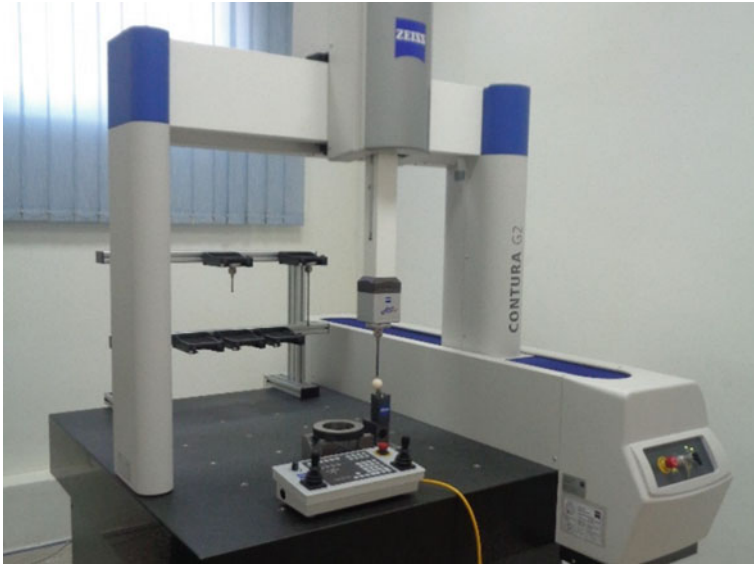


Fig. 6 Coordinate measuring machine zeiss Contura G2

## 4 Results

The results of the experiment are summarized in Table 2 and Fig. 7. The table provides the details of strategies used, the number of points acquired for each case, standard deviation of all measured points and the cylindricities. The final result represents the reference measurement, performed with high resolution (the scanning step is 0.01 mm, measuring speed is 2.5 mm/s, the strategy is helix with 10 revolutions, and the number of points acquired is 257,589). The measuring time varied from 20 s to 2 min, while the reference measurement took about 18 min, due to high number of points and low speed.

The lowest results were achieved when generatrix lines were used, but one should have in mind that the cylinder is rather short, therefore, the probe path was the shortest, and this strategy gives the best result in terms of straightness measurement. In addition, this strategy is the least sensitive to stylus tip size.

If one compares the other two strategies, the strategy with circles seems to be better than the helicoidal strategy. The most probable cause of bigger deviations in helicoidal strategy could be that it combines the influence of both stylus positioning error and stylus leading error in all three coordinate axes.

Concerning the stylus tip size, Table 2 and Fig. 7 surprisingly show that the probe with smallest stylus tip gives the lowest results, while the stylus with the biggest tip has the biggest results. In addition, the smallest stylus tip size also has the smallest standard deviation (0.0003 mm, which is less than maximum permissible error of the machine). One possible explanation is that although larger

**Table 2** Measurement results for combinations of the parameters

Stylus	Measuring strategy	Number of elements	Number of points acquired	Standard deviation	Cylindricity (mm)
Stylus A (Ø 2 mm)	Circles	2 circles	5,879	0.0003	0.0040
		4 circles	11,753	0.0003	0.0055
		7 circles	20,572	0.0003	0.0053
	Lines	4 lines	522	0.0003	0.0020
		8 lines	1,041	0.0003	0.0025
		12 lines	1,562	0.0003	0.0023
	Helix	2 revolutions	5,503	0.0003	0.0031
		4 revolutions	11,065	0.0003	0.0031
		8 revolutions	22,190	0.0003	0.0080
Stylus B (Ø 5 mm)	Circles	2 circles	5,880	0.0008	0.0067
		4 circles	11,756	0.0008	0.0072
		7 circles	20,577	0.0007	0.0086
	Lines	4 lines	521	0.0007	0.0025
		8 lines	1,041	0.0008	0.0029
		12 lines	1,561	0.0006	0.0033
	Helix	2 revolutions	5,289	0.0006	0.0043
		4 revolutions	10,632	0.0006	0.0064
		8 revolutions	21,316	0.0007	0.0165
Stylus C (Ø 8 mm)	Circles	2 circles	5,876	0.0008	0.0116
		4 circles	11,755	0.0008	0.0113
		7 circles	20,569	0.0008	0.0105
	Lines	4 lines	520	0.0006	0.0016
		8 lines	1,041	0.0006	0.0022
		12 lines	1,560	0.0004	0.0036
	Helix	2 revolutions	5,101	0.0008	0.0052
		4 revolutions	10,252	0.0008	0.0071
		8 revolutions	20,558	0.0013	0.0251
Reference	Helix	10 revolutions	257,589	0.0013	0.0106

stylus tip diameter is less sensitive to surface roughness (Fig. 8), it will express larger standard deviation and result in higher values of cylindricity, because it does not reach the most distant points on the surface being measured, which in turn compensate the peaks at the surface. But, anyway, this requires deeper analysis in order to give the proper explanation.

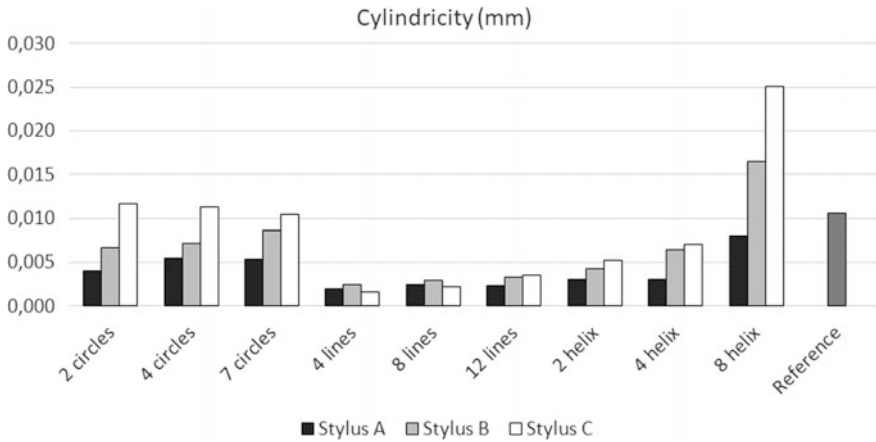


Fig. 7 Graphical representation of the measurement results

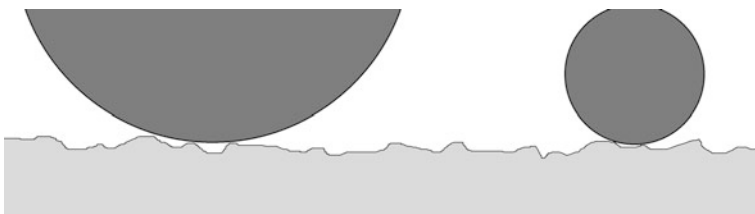


Fig. 8 Stylus tip with larger diameter is less sensitive to surface irregularities

## 5 Conclusions

This experiment showed that the most appropriate method for cylindricity measurement is the circles method, and it is recommended to use the smallest available stylus tip. However, the generatrix lines method is the least sensitive to number of lines used for measurement, while the helicoidal method is very sensitive to changes in parameters and should not be used for cylindricity measurement.

The standard deviation of the results (variations of coordinates of all points being measured) was smallest for stylus with smallest tip diameter, and it did not vary for different strategies. This was an unexpected result, and it should be investigated more in further researches.

## References

1. Flack, D., CMM Measurement Strategies, Measurement Good Practice Guide 41. National Physical Laboratory (2014)
2. Souza, C.C., Arencibia, R.V., Costa, H.L., Piratelli, A.F.: A contribution to the measurement of circularity and cylindricity deviations. *ABCM Symp. Ser. Mechatron.* **5**, 791 (2012)
3. Chajda, J. et al.: Coordinate measurement of complicated parameters like roundness, cylindricity, gear teeth or free-form surface. In: 8th International Conference Advanced Manufacturing Operations, pp. 225–231, Kranevo, Bulgaria (2008)
4. Adamczak, S., Janecki, D., Makiela, W., Stepień, K.: Quantitative comparison of cylindricity profiles measured with different methods using Legendre-Fourier coefficients. *Metrol. Meas. Syst.* **17**(3), 397–403 (2010)
5. Dovica, M., Vegh, A.: Comparison of the cylindricity deviation using different evaluation methods. *Am. J. Mech. Eng.* **1**(7), 339–342 (2013)
6. Pawlowski, M., Gapinski, B., Rucki, M.: Experimental check of the simulated cylinder's geometrical characteristics obtained from the expert program. In: XIX IMEKO World Congress: Fundamental And Applied Metrology, pp. 1838–1840 (2009)
7. Vrba, I., Palencar, R., Hadzistevic, M., Strbac, B., Hodolic, J.: The influence of the sampling strategy and the evaluation method on the cylindricity error on a coordinate measurement machine. *J. Prod. Eng.* **16**(2), 53–56 (2013)
8. Dhanish, P.B.: A simple algorithm for evaluation of minimum zone circularity error from coordinate data. *Int. J. Mach. Tools Manuf.* **42**, 1589–1594 (2002)
9. Adamczak, S., Janecki, D., Stepień, K.: Concept of reference measurements of cylindricity profiles of machine parts. In: XVII IMEKO World Congress: Proceedings, p. 201, Dubrovnik, Croatia (2003)
10. Stepień, K.: Research on influence of angular method parameters on the result of the V-block cylindricity measurement. *Strojarsтво: časopis za teoriju i praksu u strojarstvu* **54**(3), pp. 237–245 (2012)
11. Adamczak, S., Janecki, D., Stepień, K.: The comparison of cylindricity profiles using normalized cross correlation function. In: Proceedings of 5th International Conference Measurement 2005, Smolenice, Slovakia (2005)
12. Stepień, K., Janecki, D., Adamczak, S.: On the cylindricity measurement by the V-block method. In: DAAAM International Scientific Book, pp. 027–044 (2012)
13. Stepień, K.: Research on Influence of the Sensor Position on the Result of the V-block Cylindricity Measurement, Kielce University of Technology, Al. 1000-lecia, p. 7, Kielce, Poland (2010)
14. Stepień K.: An analysis of errors of the cylidnrlicity measurements by the V-block method. PhD dissertation, Kielce University of Technology, Kielce, Poland (2006)
15. Adamczak, S., Janecki, D., Stepień, K.: An analysis of errors of V-block cylindricity measurement with regard to the method parametres. In: XVIII IMEKO World Congress: Metrology for a Sustainable Development, pp. 17–22, Rio de Janeiro, Brazil (2006)
16. Gapinski, B., Grzelka, M., Rucki, M.: The roundness deviation measurement with coordinate measuring machines. *Eng. Rev.* **26**, pp. 1–6, Rijeka, Croatia (2006)
17. Ollison, T.E., Ulmer, J.M., McElroy, R.: Coordinate measurement technology: a comparison of scanning versus touch trigger probe data capture. *Int. J. Eng. Res. Innov.* **4**(1), 60–67 (2012)
18. Petrò, S., Geometric Tolerances Verification: Strategy Optimization for CMM Measurement. PhD dissertation, Politecnico di Milano, D02250 (2007)
19. Rossi, A., Lanzetta, M.: Optimal blind sampling strategy for minimum zone roundness evaluation by metaheuristics. *Precision Eng.* **37**(2), 241–247 (2013)



20. Wen, X., Zhao, Y., Wang, D., Pan, J.: Adaptive Monte Carlo and GUM methods for the evaluation of measurement uncertainty of cylindricity error. *Precision Eng.* **37**(4), 856–864 (2013). doi:[10.1016/j.precisioneng.2013.05.002](https://doi.org/10.1016/j.precisioneng.2013.05.002)
21. Salah, H.R.A.: Performance investigation of CMM measurement quality using flick standard. *J. Qual. Reliab. Eng.* 960649, 1–11 (2014). doi:[10.1155/2014/960649](https://doi.org/10.1155/2014/960649)
22. ISO/DIS 12180-1, 2: 1999, Geometrical Product Specifications (GPS)—Cylindricity (1999)
23. Nugent, P.: *Form measurement fundamentals*. Mahr. Meas. Center (2008)

# Improvement of Acceptance Sampling Inspection for the Operation of Sealing Packages

Agnieszka Kujawska, Michal Rogalewicz, Magdalena Diering,  
Marcin Luczak, Mariusz Bozek and Sachin D. Waigaonkar

**Abstract** One of the many purposes for which data are gathered from manufacturing processes is assessment of these processes against predefined criteria. Assessment results are often used for monitoring and supervising the process based on a developed statistical model. This paper looks at the issue of selection of sample size for sampling inspection in the process of packaging medical products. Packaging is an important stage of manufacturing medical products, since the package ensures safety and sterility of the product. In the process of packaging medical products, the operation of sealing the package is of key importance in terms of following medical procedures. Tensile strength of the seal is the critical feature. This paper presents a case study in which an efficient statistical sampling plan was executed for the process of sealing medical packages which led to the saving of time as well as cost.

**Keywords** Acceptance sampling inspection · Packaging process · Quality improvement

## 1 Introduction

One of many sources of industrial data, used in the monitoring and supervision of manufacturing processes, is the quality inspection. It is defined as assessment of compliance of a product or process with the predefined requirements, on the basis of observation or measurement [1, 2].

---

A. Kujawska (✉) · M. Rogalewicz · M. Diering  
Poznan University of Technology, Poznan, Poland  
e-mail: agnieszka.kujawska@put.poznan.pl

M. Luczak · M. Bozek  
Aesculap Chifa Sp. z o.o, Nowy Tomyśl, Poland

S.D. Waigaonkar  
Department of Mechanical Engineering,  
BITS Pilani, K K Birla Goa Campus, Pilani, India

Considering the method of conducting quality inspection, it can involve assessment of measurable (quantitative) or immeasurable (qualitative, assessed alternatively) features. Measurable features are inspected through direct or indirect measurement. The output of the inspection is a numeric value of the measured feature. Alternative features are assessed—a decision is made to classify the product to one of the possible states [3].

The form of quality inspection depends on the stage at which it is carried out. At the stage of product design, it is in fact verification of the design against designer-predefined requirements (based on expectations of prospective users). At the next stage of designing the manufacturing process, quality inspection comes to verification whether the existing methods or means of manufacturing permits to obtain the manufacturing quality matching the design quality. At the stage of manufacturing, quality inspection permits to assess whether the quality of a semi-product or a part of it meets the requirements specified in the design or technological documentation [2, 4, 5].

At the design stage, quality inspection is usually conducted offline, unlike quality inspection during the manufacturing processes, which is online. Quality inspection of a given operation may be repeated on many occasions, and being well-planned and organized, it permits to monitor the operation in time and alert of situations in which certain corrective, preventive or improvement measures.

The method of quality inspection depends on the characteristics of the manufacturing process [6–8]. In the case of single-unit or low-series production, 100% quality inspection is conducted; i.e., every product is assessed (against the adopted criteria). In mass production, assessment of every product is economically unjustified or even impossible for technical reasons (destructive tests, long duration of the assessment, etc.). Instead, statistical methods are used. On the basis of data gathered from a random sample, conclusions are drawn concerning the entire lot<sup>1</sup> [9].

The most commonly used statistical methods of quality control are the statistical process control, the measurement system analysis and the design of experiments [10, 11]. The literature describes analyses of data collected from manufacturing workstations, artificial intelligence techniques (e.g. artificial neural networks, genetic algorithms, fuzzy logic, grey systems) [11–14].

One of the types to make critical decision based on the data and finally making inferences about the manufacturing process of statistical quality inspection is referred to as sampling inspection. Its main objective is to eliminate from the manufacturing process, any products (materials, semi-products, parts) which do not meet predefined requirements. Considering the method of assessment of sampled items, sampling inspection can be the number of features which do not meet the requirements or the number of non-compliant items in the sample or even a numerical value (where the decisive value is the statistics obtained from measurements of sampled items).

---

<sup>1</sup>However, sometimes long series or mass production requires 100% quality inspection, if delivery of products non-compliant with the requirements may result in serious consequences (e.g. in the food, pharmaceutical, medical or aviation industry).

Acceptance sampling inspection is conducted on a random sample of products from the assessed lot. The sample is 100% tested, and on the basis of the results, a decision is made to accept or reject the entire lot. The inspection permits to assess whether the tested lot of products meets the predefined quality requirements. The lot of products may be, e.g., supplied to the user, received at the warehouse or passed on to the next manufacturing station.

The inspection plan includes the number of sample items  $n$  and the maximum permissible number of incompliant items in the sample  $A_c$ .

One of its flaws is that the manufacturing process cannot be corrected, based on its results, in real time or on an ongoing basis, as the acceptance sampling inspection is usually conducted once the manufacturing process is completed.

Each form of inspection, also the acceptance sampling inspection, generates costs [15]. Improperly planned, quality inspection may generate unnecessary costs of manpower and materials, if the tests are destructive. Results of assessment of acceptance sampling inspection in the operation of packaging of medical products were presented in the following part of the paper.

## 2 Research Problem

Medical package has an important role in the manufacturing of medical products. Safety of medical procedures largely depends on the quality of packages of medical products. Sterile medical instruments which require temporary storage or transportation must be protected by a package which keeps the contents sterile from the moment the sterilization process is completed until the instrument is used.

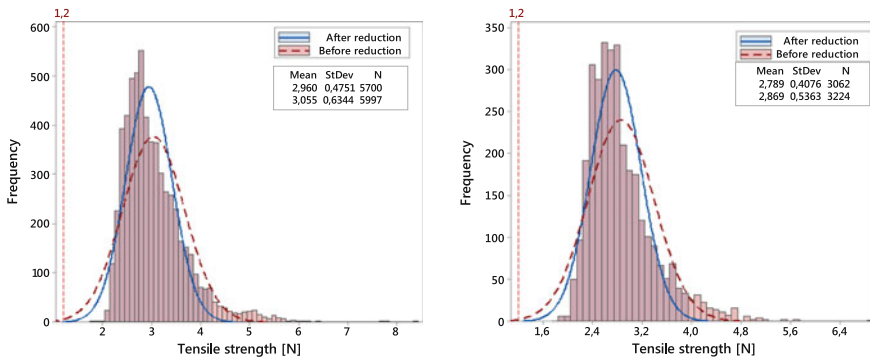
Medical packages which go through the process of sterilization are designed in a way which permits the ingress of the sterilizing agent into the package. They commonly consist of two layers: a foil laminate, which provides barrier protection, and medical paper, which permits the ingress of the sterilizing agent.

A critical factor for maintaining sterilized instruments aseptic is the method of packaging. Medical products must be packaged in a way which prevents damage of the package and facilitates aseptic removal of the contents.

The process of packaging has been analysed at a company manufacturing surgical instruments. One of the final operations of packaging is sealing, and the critical feature of the package is the tensile strength of the seal. Low tensile strength poses a risk of accidental damage to the package, e.g. during transportation.

The company uses two types of packages for the surgical instruments under analysis—"small" and "big", with the size as the only differentiating feature. Both types of packages are made of the same material. "Small" packages are sealed three at a time to form a collective package. "Big" packages are sealed into collective packages of two units.

Within three months, 221,766 items of "small" packages and 91,730 items of "big" packages were sealed at the workstation under analysis, with the average of 41 orders per month. The manufacturer is obliged to control the tensile strength of the seal. Its minimum permissible value is 1.2 N. Having gone through a tensile



**Fig. 1** Distribution of probability of tensile strength for the “small” package (left) and the “big” package (right) before and after reduction

strength test, the product is classified as compliant or non-compliant. The inspection plan provides testing tensile strength of 65 items of each order. Sampling is performed according to the DIN ISO 2859-1 standard, taking into consideration the second control level and the indicator  $AQL = 0.65$ . Application of the above-mentioned control plan is not provided in the contract with the client. The plan ensures that no package of tensile strength lower than required is classified as compliant.

In order to increase efficiency, the process was modified through the purchase of a new sealing machine and implementation of a new sealing technology. However, the technological changes were not accompanied by changes in the organization, and the previously applied quality inspection plan was adapted to the new process. An initial analysis of tensile strength test results suggested that the process efficiency is improved. Action was taken to reduce process inspection.

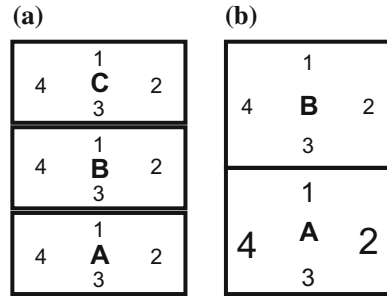
An analysis of the tensile strength volatility model developed for the data collected within three months (5997 samples of the “small” package—2.6% of the lot, and 3224 samples of the “big” package—3.3% of the lot) (Fig. 1—data presented before and after reduction of outliers and errors) leads to a conclusion that there is little risk of a seal which does not meet the requirements.

Considering that the average monthly cost of quality inspection is ca. PLN 4000 (covering mainly the cost of manpower, which is much higher than the cost of material loss in the destructive tensile strength test), the research team verified the quality inspection plan to see whether the decision to minimize the testing was right.

### 3 Research Methodology and Analysis of Results

In order to verify the inspection plan, tensile strength test was carried out on a sample of  $n$  packages.

**Fig. 2** Numbering of areas of tensile strength measurement for **a** “small” packages and **b** “big” packages



**Table 1** Tensile strength test results [N]

Small package	A1	A2	A3	A4	B1	B2	B3	B4	C1	C2	C3	C4
Mean	2.56	2.82	2.43	3.20	2.53	2.62	2.49	2.89	2.58	3.01	2.59	3.21
Standard deviation	0.36	0.44	0.33	0.52	0.29	0.15	0.30	0.23	0.33	0.54	0.39	0.40
Big package	A1	A2	A3	A4	B1	B2	B3	B4				
Mean	2.61	2.96	2.59	2.87	2.70	2.85	2.60	2.88				
Standard deviation	0.32	0.31	0.24	0.39	0.29	0.40	0.25	0.24				

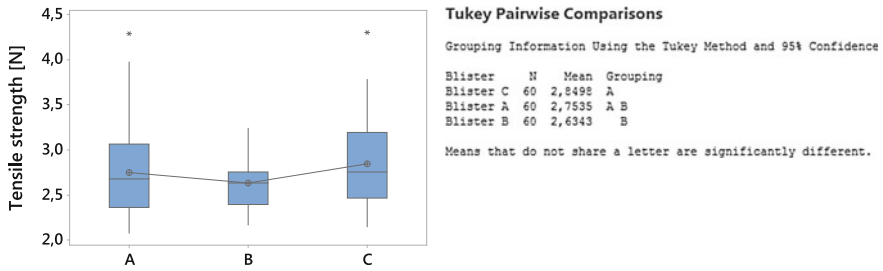
Tensile strength was tested in four areas of the package (Fig. 2), taking into consideration the location of the areas in the collective package.<sup>2</sup> The objective of the test was to verify whether the areas varied significantly in strength. The areas were numbered in the clockwise direction (Fig. 2). Fifteen measurements for each area of the “small” package and eleven measurements for each area of the “big” package were taken. Statistical results of the tensile strength test are shown in Table 1.

On the basis of measurement results, tensile strength of packages A, B and C (for the collective package of “small” packages) and packages A and B (for the collective package of “big” packages), as well as of areas 1, 2, 3 and 4 for both collective packages, was compared.

### 3.1 Analysis of Results for “Small” Packages

An analysis of differences between mean tensile strength of packages A, B and C of a collective package of “small” packages, performed by means of the ANOVA test

<sup>2</sup>The relevant inspection plan did not define areas of assessment or sampling method.



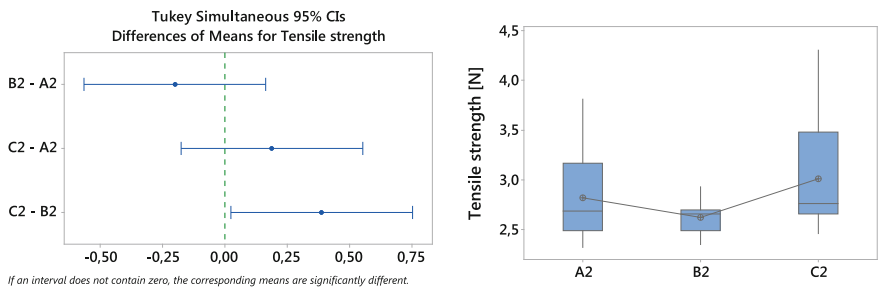
**Fig. 3** Results of comparison of mean tensile strength of packages A, B and C—boxplot and Tukey’s test results

and Tukey’s post hoc test, shows that there are significant differences between the tensile strength of packages B and C (Fig. 3).

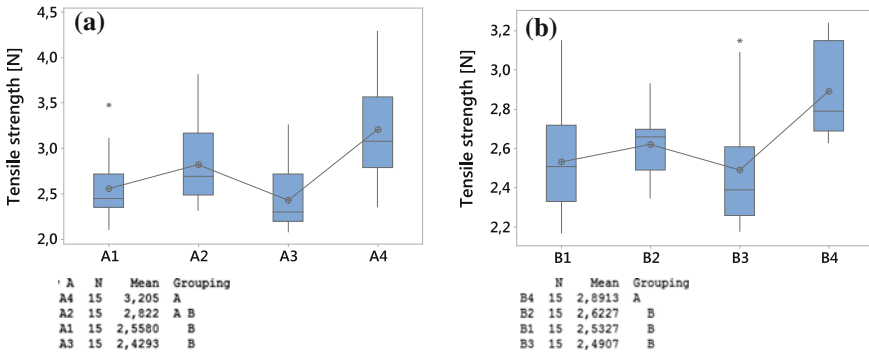
Next, the hypothesis of equal tensile strength within the areas of packages was verified by means of the variance analysis ( $\mu A1 = \mu B1 = \mu C1/\mu A2 = \mu B2 = \mu C2/\mu A3 = \mu B3 = \mu C3/\mu A4 = \mu B4 = \mu C4$ ). It turned out that areas 1, 3 and 4 have equal tensile strength. However, the ANOVA for area 2 showed the occurrence of significant differences between the packages (Table 2). The differences in tensile strength for area 2 are shown in a boxplot and by means of confidence intervals for differences between packages (Fig. 4; Table 2). A material difference between packages B and C for this area is evident.

**Table 2** Variance analysis results for areas 1, 2, 3 and 4 and packages A, B and C

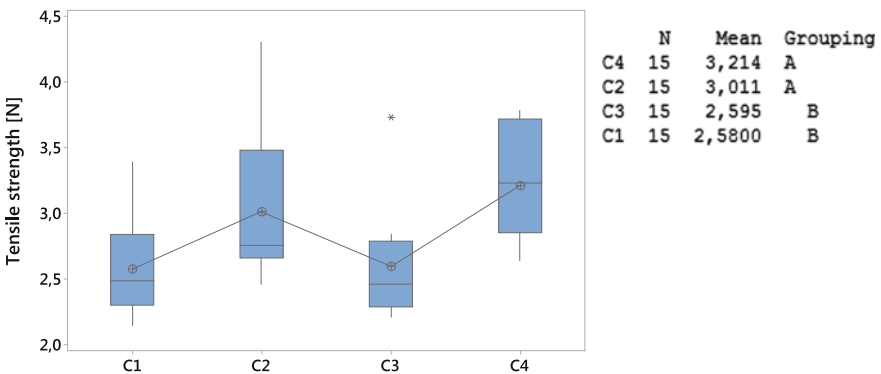
	F value	p-value		F value	p-value
Area 1	0.08	0.925	Package A	10.13	0
Area 2	3.36	0.044	Package B	7.94	0
Area 3	0.91	0.410	Package C	8.36	0
Area 4	3.19	0.051			



**Fig. 4** Confidence intervals for differences in tensile strength between packages in area 2 and boxplot for the tensile strength under analysis



**Fig. 5** Results of comparison of mean tensile strength for areas 1, 2, 3 and 4 of packages: A (a) and B (b)—boxplot and Tukey’s test results



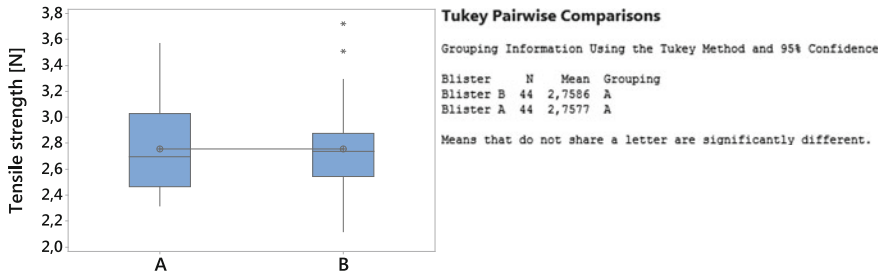
**Fig. 6** Results of comparison of mean tensile strength for areas 1, 2, 3 and 4 of package C—boxplot and Tukey’s test results

At the next stage of the research, differences in tensile strength between areas 1, 2, 3 and 4 for a given package were analysed. It turned out that tensile strength is different in different areas of packages A, B and C (Table 2; Figs. 5 and 6).

### 3.2 Analysis of Results for “Big” Packages

An analysis of the differences between mean tensile strength of packages A and B of a collective package of “big” packages, performed by means of the ANOVA test and Tukey’s post hoc test, shows that there are no significant differences in tensile strength (Fig. 7).





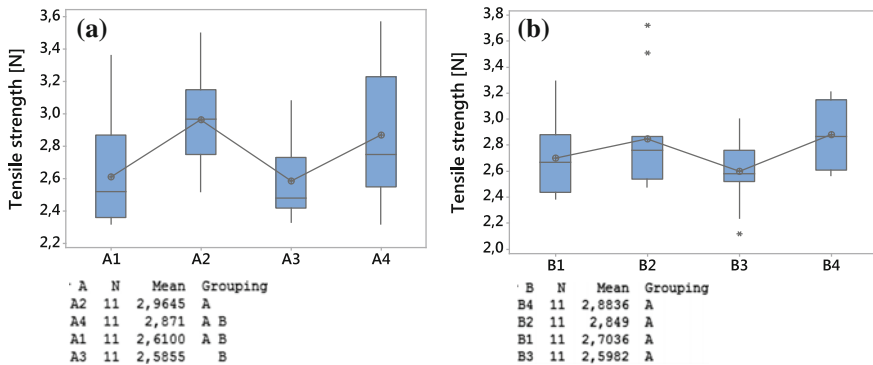
**Fig. 7** Results of comparison of mean tensile strength of packages A and B—boxplot and Tukey’s test results

Next, the hypothesis of equal tensile strength within the areas of packages was verified by means of the variance analysis ( $\mu A1 = \mu B1/\mu A2 = \mu B2/\mu A3 = \mu B3/\mu A4 = \mu B4$ ). It turned out that no statistically significant differences occur between tensile strength of the areas (Table 3).

Similarly as for “small” packages, at the next stage of the research, differences in tensile strength between areas 1, 2, 3 and 4 for a given package were analysed. It turned out that areas of package A have different tensile strength (Table 3; Fig. 8), while no differences were observed for areas of package B (Fig. 8).

**Table 3** Variance analysis results for areas 1, 2, 3 and 4 and packages A and B

	<i>F</i> value	<i>p</i> -value		<i>F</i> value	<i>p</i> -value
Area 1	0.52	0.480	Package A	3.86	0.016
Area 2	0.57	0.458	Package B	2.09	0.116
Area 3	0.01	0.905			
Area 4	0.01	0.928			



**Fig. 8** Results of comparison of mean tensile strength for areas 1, 2, 3 and 4 of package A (a) and B (b)—boxplot and Tukey’s test results

## 4 Conclusions and Recommendations

The results of the experiment were used to determine the parameters of a model of tensile strength volatility in areas 1–4 for “small” packages (A, B, C) and “big” packages (A, B). An analysis of the volatility model for “small” packages led to the following conclusions: the risk of a package of tensile strength smaller than 1.2 N is less than 0.00135 and thus may be considered low for the process under analysis; tensile strength of “small” packages A and B is comparable; however, package C has materially different tensile strength. Tensile strength of area 2 is considerably different from that of other areas. What is more, area C2 shows the highest tensile strength volatility (it has the lowest Cpk indicator of 1.12). Considering the above, the following recommendations were made for “small” packages: reduction of the size of analysed samples from 65 to 15, sampling of packages in equal time intervals and testing packages in the same area—C2.

The risk of a “big” package with tensile strength lower than 1.2 N is ca. 0.00135 and may be considered low. Tensile strength of packages A and B is comparable. What is more, there are no considerable differences in tensile strength of particular areas of packages A and B. Area B2 has the lowest value of the Cpk indicator—1.46 (the highest volatility). Considering the above, the following recommendations were made for “small” packages: reduction of the size of analysed samples from 65 to 15, sampling of packages in equal time intervals and testing packages in the same area—B2.

Implementation of the changes reduced the costs of quality inspection. The main component of the cost was the labour cost of quality inspectors—it constituted more than 95% of the total cost (the remaining 5% was attributed to the cost of destroyed material and electricity used). The cost was reduced by a whopping 75%. What is more, considering the reduction of inspection activities, some employees could be delegated to perform other tasks. The new acceptance sampling inspection was implemented in early April 2017. No complaints, internal or external, have been reported within the last month. In June 2017, effectiveness of the changes will be verified.

**Acknowledgements** The presented results are derived from a scientific statutory research conducted by Chair of Management and Production Engineering, Faculty of Mechanical Engineering and Management, Poznan University of Technology, Poland, supported by the Polish Ministry of Science and Higher Education from the financial means in 2017 (02/23/DSPB/7695).

## References

1. Bożek, M., Hamrol, A., Rogalewicz, M.: Control cost analysis in the production of medical devices—case study (in Polish). In: Knosala, R. (ed.) *Innovation in Management and Production Engineering*, vol. 2, pp. 323–335 (2014)
2. Hamrol, A.: Process diagnostics as a means of improving the efficiency of quality control. *Prod. Plann. Control* **11**(8), 797–805 (2000)

3. Diering, M., Dyczkowski, K.: Assessing the raters agreement in the diagnostic catheter tube connector production process using novel fuzzy similarity coefficient. In: IEEE International Conference on Industrial Engineering and Engineering Management, 228–232 (2016)
4. Vieira, G., Reis, L., Varela, M.L.R., Machado, J., Trojanowska, J.: Integrated platform for real-time control and production and productivity monitoring and analysis. *Rom. Rev. Prec. Mech., Opt. Mechatr.* **50**, 119–127 (2016)
5. Trojanowska, J., Żywicki, K., Pająk, E.: Influence of selected methods of production flow control on environment. In: Golińska, P., Fertsch, M., Marx Gomez, J. (eds.) *Information Technologies in Environmental Engineering*, 695–705. Springer, Berlin (2011)
6. Kłos, S.: A Model of an ERP-based knowledge management system for engineer-to-order enterprises. In: Dregvaite, G., Damasevisius, R. (eds.) *Information and software Technologies, 22nd International Conference, ICIST 2016, Com. In Comp. and Inf. Sc.* Springer, Berlin, vol. 639, pp. 42–52 (2016)
7. Królczyk, G., Legutko, S., Królczyk, J., Tama, E.: Materials flow analysis in the production process—case study. *Appl. Mech. Mat. Trans Tech Publ. Switz.* **474**, 97–102 (2014)
8. Skołod, B., Krenczyk, D.: Rhythmic production planning in the context of flow logic. In: *Proceedings 4th International Scientific-Technical Conf. MANUFACTURING 2014, Selected Conference Proceedings Poznan University of Technology*, 35–43 (2016)
9. Drury, C.G., Sinclair, M.A.: Human and machine performance in an inspection task. *Human Factors Ergon. Manuf.* **25**(4), 391–399 (1983)
10. Hamrol, A.: *Strategies and practices of efficient operation, LEAN SIX SIGMA and other*, Warsaw, (PWN) (2015)
11. Rogalewicz, M., Sika, R.: Methodologies of knowledge discovery from data and data mining methods in mechanical engineering. *Man. Prod. Eng. Rev.* **7**(4), 97–108 (2016)
12. Mahato, S., Dixit, A.R., Agrawal, R.: Application of lean six sigma for cost-optimised solution of a field quality problem: A case study. *J. Eng. Manuf.* **231**(4), 713–729 (2017)
13. Moore, S.S., Murphy, E.: Process visualization in medical device manufacture: an adaption of short run SPC techniques. *Qual. Eng.* **25**(3), 247–265 (2013)
14. Więcek-Janka, E., Mierzwiak, R.: The analysis of successors' competencies in family enterprises with the use of grey system theory. *Grey Sys.: Th. Appl.* **5**(3), 302–312 (2015)
15. Jasiulewicz-Kaczmarek, M., SWOT analysis for planned maintenance strategy—a case study. In: Dolgui, A. et al. (ed.) *IFAC Conference on Manufacturing Modelling, Management and Control (MIM), IFAC PapersOnLine*, vol. 49, no. 12, pp. 674–679 (2016)

# I Spy, with My Little Eye: Quality Standards of Different Target Groups

Beatrice M. Rich, Jane Worlitz, Stefan Peplowsky and Ralf Woll

**Abstract** According to the Kano model, companies would be required to use a continuous adaptation of audit criteria. If the ever-changing customer necessities are not neglected, the relevancy of defined audit criteria and the framework conditions of the production start for product audits cannot be permanently ensured. For this reason, companies should compare and adjust the quality standards of all concerning employees with that of the customer, so that the audit criteria can also be reconciled and adjusted accordingly. In this respect, a procedure for matching quality standards has been developed together with a vehicle manufacturer and a feasibility study has been carried out. The focus of the study was on possible differences regarding the detection of defects between the employees, dealers, and customers, as well as the recording and analysis of the visual focus areas. For the study, the participants had to complete a written questionnaire and make a practical defect detection directly on the vehicle. The study results have shown a variety of potentials for action that can be applied at other companies. These include the regular internal matching of the quality standards, the continuous training of the employees as well as the integration of the customers and their changing product requirements after the start of product production.

**Keywords** Product audit · Quality standards · Feasibility study · Customer requirements

## 1 Introduction

In the introduction and implementation of auditing systems and certification in this context, companies are supported by national and international standards (ISO 9001/ISO 19011/ISO/TS 16949) (eg, AIAG/VDA/SMMT/, etc—national

---

B.M. Rich (✉) · J. Worlitz · S. Peplowsky · R. Woll  
Chair of Quality Management, Brandenburg University of Technology  
Cottbus-Senftenberg, Senftenberg, Germany  
e-mail: BeatriceMonique.Rich@b-tu.de

associations of the supplier auto industry) and guidelines. The information base is particularly diverse in system audits (process/process audits) and certification audits. The product audit is much less noticeable in the literature. A VDA directive of 1983/1998 or the revised requirements deals more closely with the development and implementation of product audits [1–3]. Continuous adjustment of the product audit, due to changing customer requirements, will not be dealt with in detail.

Based on concepts such as the Kano model, it can be assumed that the customer requirements for the same product change over time [4, 5]. In addition, innovations and the continuous development of technology direct the demands on products in new directions. In a past study, the research needs of the subject could be confirmed by literature review and three expert interviews [6].

The current literature of the past years is focused around the credibility and independence of auditors and various corporate settings as well as the corresponding relationship between management and auditors. No publications were found for product audits. The lack of the literature review on product appraisals, and their continuous development, and integration of changing customer needs is an indication of a need for more present research. Rainer Göppel also calls for attention to the lack of support from companies in the implementing of regulations, especially within the field of auditing [7]. VDA and DIN regulations point to the need for continuous development (the What?) but neglect the aspects of implementation (the How?) [6].

This requires the development of a procedure for the adjustment of the product audits at regular intervals in order to ensure the customer relevance of the features tested.

For these reasons, a procedure was developed together with a vehicle manufacturer to compare the current product audits with the current requirements of the customers. The aim is to find out whether the customer requirements correspond to or differ from the audit criteria of a product that has been in production for a long time. The procedure, the implementation, and the resulting findings are presented below. Confidential data is not dealt with in more detail to protect the company.

## **2 Objectives and Research Question of the Feasibility Study**

In relation to the life cycle of a product, indifferent features can create delight, fulfill performance needs, and ultimately become basic needs [8]. A comparison of the change in the customer requirements with the once-defined standard is therefore to be assumed. A vehicle approved by the employee according to the standard does not have to correspond to the quality standard of the customer. In addition to answering the core question, the study also carried out the derivation of recommendations for action in the following areas:

- The product audit,
- The end-of-line (EOL)/production, and
- The interpretation of the company’s standard.

### 3 Methodology

A three-day workshop was held for data collection. Within the framework of the workshop, three vehicles were audited by different target groups. For this, defects were previously made on the vehicles.

The target groups can be roughly differentiated into plant internal and external. The group consisting of workers, auditors, Q-specialists, and EOL employees are grouped together. The plant external group is composed of dealers and customers. In order to ensure statistical evaluation, the minimum number of participants was set to 30 [9]. The composition of the participants can be taken from Fig. 1.

The selection of the vehicles was based on various criteria. The customer complaint rate, the internal complaint rate, and the problem areas in general had an influence. Regarding the latter, particular attention was paid to the various defects in the different life phases of the vehicles. The focus was on optical and haptic defects. Functional defects were not relevant. Subsequently, the defect preparation was carried out. The prepared customer-relevant characteristics (PCCs) were selected, and faulty components were mounted on the respective vehicles. The PCCs were installed in three different visual areas (A, B, C).

The course of the workshop was divided into three parts and is shown in Fig. 2.

Each participant received a briefing at the beginning. Subsequently, each test person individually audited the three vehicles one after the other. Each participant

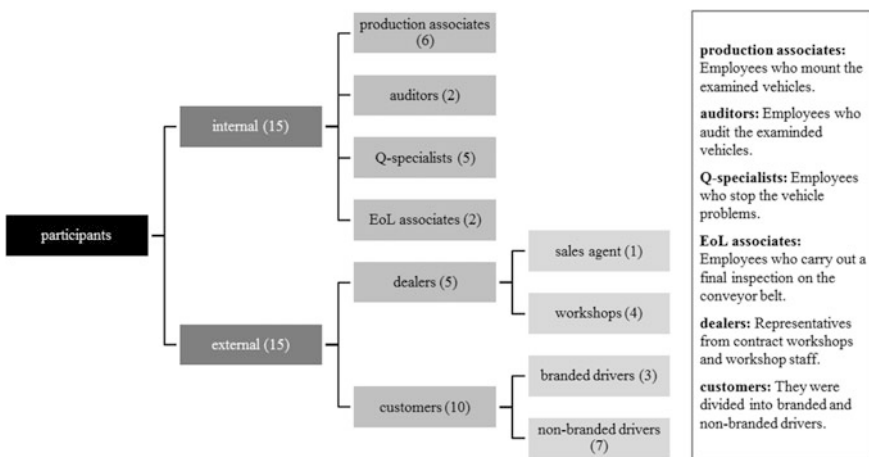


Fig. 1 Composition of the participants

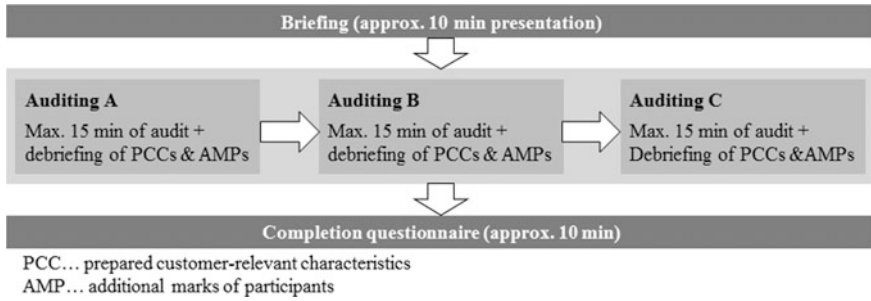


Fig. 2 Course of the workshop

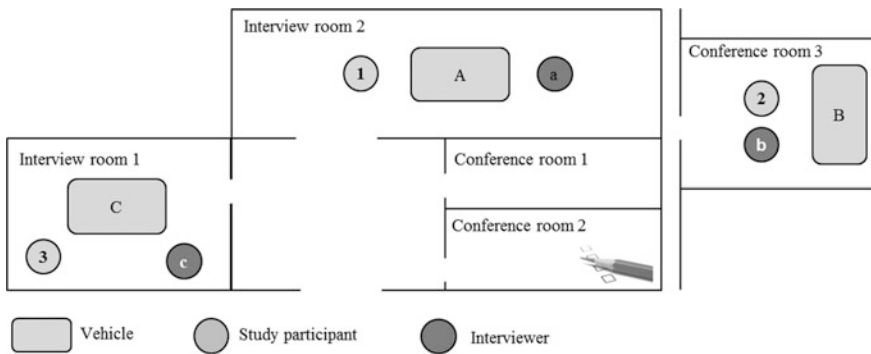


Fig. 3 Spatial structure of the workshop

was allowed to walk around the vehicle, use seating possibilities, and touch it. The participant then marked all noticed defects by sticky notes. An interviewer also recorded the angle of view and the pathway of the subject and noted when a defect was found. Following each of the three audits, the interviewee was asked in a personal interview to evaluate the defect relevance of all recognized and unrecognized PCCs. The rating was on a scale of 1 to 10, where 1 is an “absolute no go.” Defects found by the participant, which were not pre-prepared, were recorded as additional marks of participants (AMPs) and were also evaluated by the test person. Finally, the respondent was asked to answer a questionnaire.

Figure 3 outlines the spatial structure of the workshop.

### 4 Data Analysis and Implications

Three hypotheses were investigated to answer the core question. Table 1 summarizes the null hypotheses with the corresponding alternative hypotheses. It is postulated that H0a–H0c are discarded in favor of alternative hypotheses.

**Table 1** Hypotheses with the corresponding alternative hypotheses

H0a	There is no difference between the target groups (internal/external) with regard to defect detection
H1a	There is a difference between the target groups (internal/external) with regard to defect detection
H0b	There is no difference between the viewing areas with respect to the detection of defects
H1b	There is a difference between the viewing areas with respect to the detection of defects
H0c	There is no difference between the target groups (internal/external) and a given standard with regard to the evaluation of the defects relevance
H1c	There is a difference between the target groups (internal/external) and a given standard with regard to the evaluation of the defects relevance

The results of the data analysis are shown below for H0a–H0c. Based on the results, recommendations were made for the company.

### 4.1 Influence of the Target Group Type on Defect Detection (H0a)

It was analyzed how many of the PCCs were recorded by the different target groups. A Chi-square test was used to determine whether there was a difference between the target groups with respect to the percentage of detected defective units. The test showed a significant difference ( $p < 0.001$ ). Table 2 shows the target groups whose percentages of detected defective units differ from each other. The comparison chart in Fig. 4 shows the results graphically. Red non-overlapping intervals represent differences.

The null hypothesis H0a is rejected in favor of the alternative hypothesis H1a. There is a difference between the target groups regarding error detection.

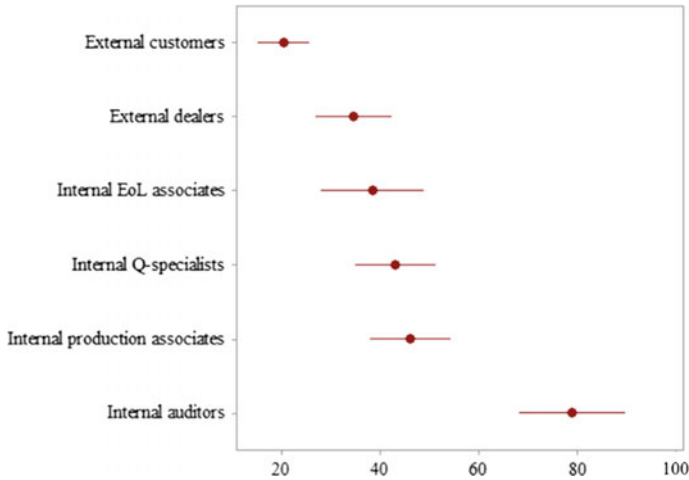
In the interpretation, it should be kept in mind that the time for defect detection was limited to 15 min for all subjects. Furthermore, it should also be kept in mind that the light conditions in the rooms for the subjects could not be kept constant due to solar irradiation.

The following recommendations for action are derived for the company. The internal auditors recognized in 15 min almost 80% of the PCCs. There is no need for training by the auditors. Internal EOL employees, Q-specialists, and assembly

**Table 2** Deviating target groups regarding defect detection (H0a)

Number	Target group	Deviate from
1	External customers	2, 3, 4, 5, 6
2	External dealers	1, 6
3	Internal EOL associates	1, 6
4	Internal Q-specialists	1, 6
5	Internal production associates	1, 6
6	Internal auditors	1, 2, 3, 4, 5





**Fig. 4** Comparison chart—percentage of detected PCCs by target group (H0a)

staff recognize an average of 30% fewer defects. In order to raise awareness by these employees to defects, additional training should be carried out. With a total of 20%, the external customers recognized the fewest PCCs. The relevance of the PCCs for the external customers should be checked. Under certain circumstances, testing and corrective efforts can be reduced.

## 4.2 Influence of Viewing Areas on Defect Detection (H0b)

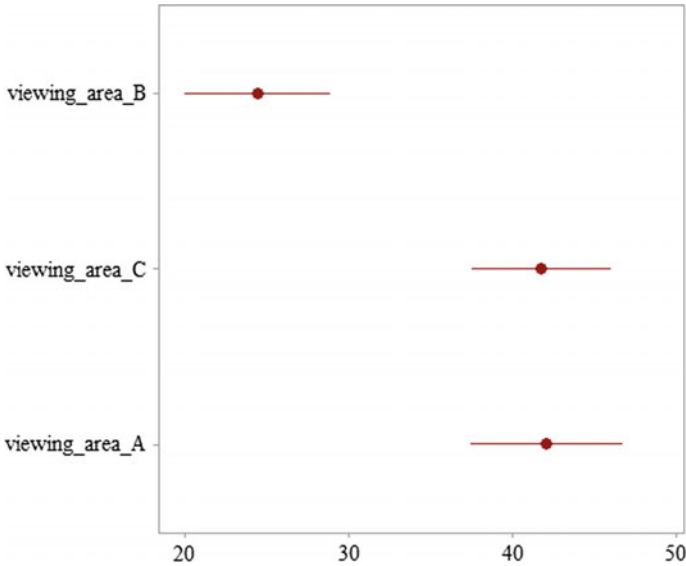
It was analyzed how many of the PCCs were recorded in the different viewing areas. A distinction has been made between the following areas of vision: A—“Main vision range,” B—“Mid-vision range,” C—“Secondary vision range.” From the company side, it is assumed that a defect in the visual field A is perceived as more severe than the same defect in visual field B or C. The Chi-square test was used to examine whether there is a difference between the visual areas with respect to the percentages of detected defective units. The test showed a significant difference ( $p < 0.001$ ).

Table 3 shows the viewing areas whose percentages of detected defective units differ from each other. The comparison diagram in Fig. 5 shows the results graphically. Red non-overlapping intervals represent differences.

Viewing areas A and C do not differ from each other. In both areas, approximately 42% of the errors were discovered. In visual field B, approximately 25% of the defects were discovered. The null hypothesis H0b is discarded in favor of the alternative hypothesis H1b. There is a difference between the viewing areas with regard to defect detection.

**Table 3** Deviating viewing areas regarding defect detection (H0b)

Number	Viewing area	Deviates from
1	Viewing area_B	2, 3
2	Viewing area_C	1
3	Viewing area_A	1



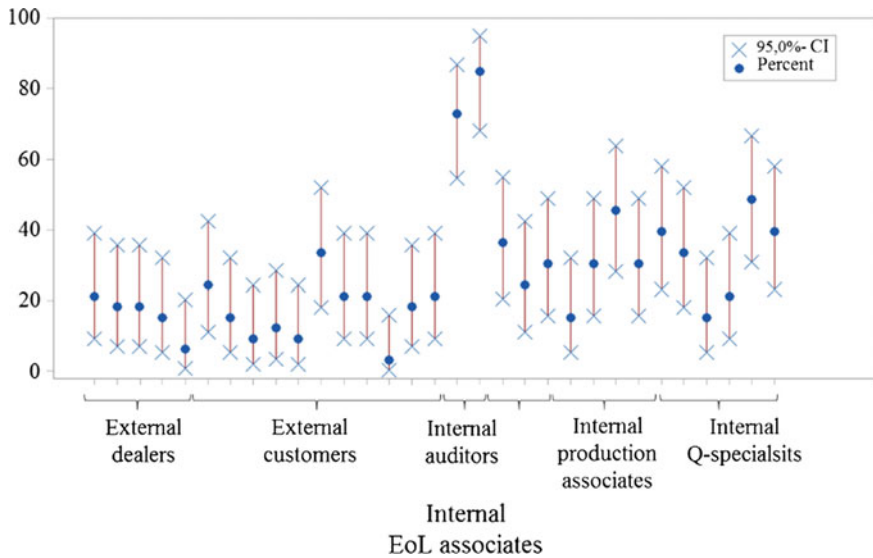
**Fig. 5** Comparison chart—percentage of detected PCCs by viewing areas (H0b)

When interpreting the results, it should be kept in mind that the subjects were specifically looking for defects in the entire vehicle.

The following recommendations for the company are derived for the company. Unexpectedly, there was no difference between vision areas A and C. Thus, not only defects are detected in the defined main vision range. The classification of the visual areas should be considered. The influence of the visual areas on the evaluation of the error irrelevance should be taken into account.

### 4.3 Influence of the Target Group Type on the Evaluation of Defect Relevance Compared to the Standard (H0c)

It was analyzed whether the assessment of the defect relevance by the target groups coincides with the standard. The investigation was carried out by means of attuned coincidence analysis. The evaluation of the defects relevance of the PCCs by the target groups was compared with the company standard.



**Fig. 6** Comparison chart—percentage match of the target groups to the standard (H0c)

The results suggest a low consistency. The total Kendall coefficient between the target groups is 0.397 ( $p < 0.001$ ). The Kendall coefficient for all target groups vs. the standard is 0.411 ( $p < 0.001$ ). The following diagram in Fig. 6 shows the individual results graphically.

Apart from the assessment of the auditors, the assessment of no target group is more than 70% consistent with the standard. The target groups rate on average is more stringent than the standard. The null hypothesis H0c is discarded in favor of the alternative hypothesis H1c. There is a difference between the target groups and a given standard with regard to the evaluation of the defect relevance.

When interpreting the results, it must be taken into account that the subjects may have assumed a more critical attitude by concentrating on the search for defects. The following recommendations for action are derived for the company. In comparison to the standard, the target groups evaluate the defect relevance of the majority of the PCCs on average. An adaptation of the standards of the relevant PCCs should be made. Assuming that the standard coincided with the evaluation of the target groups at the time of product introduction, it can be concluded that a scale adjustment is necessary during the product life cycle.

## 5 Discussion

The present study is a first experimental set-up. For that reason, it is plausible that a number of limitations could have influenced the results. As already mentioned, for further studies, same light conditions for all subjects should be considered to avoid

the possibility of affected perception of surface defects. Furthermore, by focusing the subjects on defect searching, it is assumed that the subjects were more critical regarding the product quality than they would be in everyday life. In this respect, a more realistic framework must be created for further studies.

Future studies should also consider a higher number of participants. This is associated with a higher effort, but could lead to a better validity and more possibilities of evaluation.

Additional experimental investigation needs to be done to establish whether the developed procedure is transferable to other products and industries. Furthermore, based on the present study findings, the usability of rated defects by a scale from 1 to 10 needs to be investigated. One question is whether the chosen interval is too minor or too major.

The current study provides the basis for a range of further investigations. Some of the theme is already in progress.

## 6 Conclusion

The research question: “Do all employees and customers, irrespective of position and work area, apply the same quality standards to the vehicles?” can be answered with “no.”

In order to meet customer requirements as best as possible, companies should periodically reconcile internal quality standards with those of customers. This implies a regular adjustment of the product audits as well as a corresponding training of the employees. The present study shows how a procedure for the identification of quality scale differences can look like. In follow-up studies, it is necessary to investigate the intervals at which a quality scale calibration should be carried out. In order to standardize the procedure for other companies, the procedure is revised, improved, and re-executed on the basis of the experience gained in this study.

## References

1. German Association of the Automotive Industry, Quality control in the automotive industry: product audits for automobile manufacturers and suppliers—implementation, conducting, evaluation, Frankfurt am Main-Schwanheim (1983) (VDA)
2. German Association of the Automotive Industry, Quality Management in the automotive industry—product audit Part 5, Frankfurt am Main (1998)
3. German Association of the Automotive Industry, Quality management in the automotive industry—Product audit Part 5, vol. 2. Berlin (2008)
4. Nilsson-Witell, L., Fundin A.: Dynamics of service attributes: a test of Kano’s theory of attractive quality. *Int. J. Serv. Ind. Manage.* 16, 152–168 (2005)

5. Kano, N., Seraku, N., Takahashi, F., Tsuji, S.: Attractive quality and must-be quality. In: Quality, I.A.f. (ed.) *The Best on Quality—Targets, Improvements, Systems*, München, pp. 165–186 (1984)
6. Rich, B., Goldmann, C., Woll, R.: Product Audits—Why we don't ask the customers? In: *Proceedings of the 19th QMOD Conference on Quality and Service Sciences*, Rom, 2016, pp. 229–244
7. Göppel, R.: Overview of Audit Types, Steinbeis-Transfer Centrum Managementsystems. [Online] Available at: <http://www.tms-ulm.de>, pp. 1–9 (2016)
8. Witell, L., Löfgren, M., Dahlgaard, J.J.: Theory of attractive quality and the Kano methodology—the past, the present, and the future. *Total Qual. Manage. Bus. Excellence* **23**, 1241–1252 (2013)
9. Diekmann, A.: *Empirical Social Research. Basics, Methods, Applications*, Reinbek near Hamburg, p. 403 (Rowohlt) (2009)

# Reduction of Errors of the Conformity Assessment During the Visual Inspection of Electrical Devices

Krzysztof Knop, Manuela Ingaldi and Marta Smilek-Starczynowska

**Abstract** Visual inspection is the quality control with a significant share of human labor, so that it is prone to errors and mistakes during the assessment of compliance of product features with the requirements. In the visual inspection, controllers can commit two types of errors. Type I error means that a controller detects a defect that does not exist. This category is called the risk of the producer, as the producer runs the risk of rejection of good product. Type II error means that control does not detect a defect. This category is called the risk of the supplier, because the customer runs the risk of receiving a defective product. In the paper, results of research for identification and assessment of errors of conformity assessment of the product—electric switch—were presented. In the research to assess a visual inspection, the coefficient Attribute GR&R was used. Corrective actions in order to reduce the possibility of occurrence of these errors in the visual inspection of the device were proposed and implemented.

**Keywords** Visual inspection · Inspection errors · Attribute GR&R · Improvement

## 1 Introduction

As Seneca Elder said “to err is human.” Everyone makes mistakes. Errors and mistakes happen in even the best, the most stable process and among the most experienced and skilled employees. In production processes, the greater the share of human work is, the greater the chance of error is. The same observation applies to

---

K. Knop (✉) · M. Ingaldi

Department of Production Engineering and Safety, Faculty of Management,  
Technical University of Czestochowa, Armii Krajowej 19B,  
42-200 Czestochowa, Poland  
e-mail: krzysztof.knop@wz.pcz.pl

M. Smilek-Starczynowska

Management and Production Engineering, Faculty of Management,  
Technical University of Czestochowa, Czestochowa, Poland

quality control processes. The more “human” in the process of quality control appears, the greater the risk of error is; the greatest risk is in case of an organoleptic control (inspection with the senses, e.g., visual inspection) and manual control (e.g., inspection with the use of go/no go gauges) [1]. The complete elimination of “human” from the control will not guarantee that only good products will be delivered to the customer. In some cases, humans still outperform machines in most attribute inspection tasks [2]. None quality control is free from errors, none control will guarantee that the nonconforming product is delivered to the customer [3, 4]—it is better to accept this fact or to work toward maximizing the risk reduction of errors by undertaking targeted improvement actions.

Quality inspection of attributes is a chronic problem for many organizations [5]. The quality of process of quality control, including alternative control processes, as revealed by studies so far, is affected by many factors including types of nonconformities, workplace organization, monotony, ergonomics of workstation, work shift, environmental factors [6–9]. The influence of these factors and their strength must be taken into account in assessing the quality control process and then in proposing improvement actions. Improvement of the alternative control process can also be a complex, multistage process [10, 11], the result of which should increase the efficiency and effectiveness of such a process [12, 13]. It should be stressed that quality inspections should be a source of considerable value-added activity [14], and activities that do not create added value should be eliminated [15].

In the alternative control, inspectors can make two types of errors in assessing conformity with the requirements of the product features: type I and II errors [16, 17]. Type II error means that the control does not detect a defect. This category is called the risk of the supplier, because the customer runs the risk of receiving a defective product. Type I error means that a controller detects a defect that does not exist. This category is called the risk of the producer, as the producer runs the risk of rejection of good product [18]. These errors can be measured and decreased by using different approaches and indicators [19–23]. For this purpose, the procedures proposed by the automotive industry association called AIAG can be used MSA reference manual [24]. These procedures allow to estimate (among others) the level of type I and II errors, which allow to take targeted actions to improve the alternative inspection system.

## 2 Research Problem

The aim of the research was to identify and to reduce errors of the conformity assessment—type I and type II errors—during the visual inspection and to improve the effectiveness of this inspection in relation to the research product—electric switch. The product comes from the assortment group including automatic switches and switching power supply systems. It is used among others in business plants, sewage treatment plants, hospitals, and in the maritime industry on the ships. Its

task, after adapting the accessory, is to disconnect power supply in case of an overload in the electrical network. It may be installed in switch cabinet.

Quality controls performed by the operator at the electric switch are the visual inspection, combined with manual, with use of a feeler gauge. The operator uses two feeler gauges in case of doubt about the quality of the product, i.e., the feeler gauges 0.05 and 0.3 mm. According to the stand documentation, the operator determines whether the controlled chamber has retained requirements for gaps on the entire surface. According to the requirements described in the technical documentation, in case of every rivet in the proper distance from the center of the rivet, the operator looks for places where halves of casings are in contact over a distance of 2 mm—which means that at the distance of 2 mm the feeler gauges 0.05 cannot fit. In other places, the gap cannot be greater than 0.3 mm. Performing control of the switch, the operator relies on the picture showing controlled zones of the product (Fig. 1).

The reason for research in term of improvement of the visual inspection was to lower the cost of nonconformities by 4%. The major cost was generated by the defective semi-products in form of chambers. The most common cause for the high cost of nonconformity non-quality costs (NQC) was crushed rivet. As a result of conducted analyses, there is a suspicion of inconsistent assessment of the permissible gaps in the chambers. Inconsistent related to (all) three areas of conformity assessment with the requirements: *Compact line*, *Chambers line*, and *quality inspection station*. The consequences of a lack of consistency in the conformity assessment of the gaps were: recognition of correct products to be non-correct, and vice versa, causing false alarms and stopping production, overshoot of the riveting tool, and consequently high NQC.

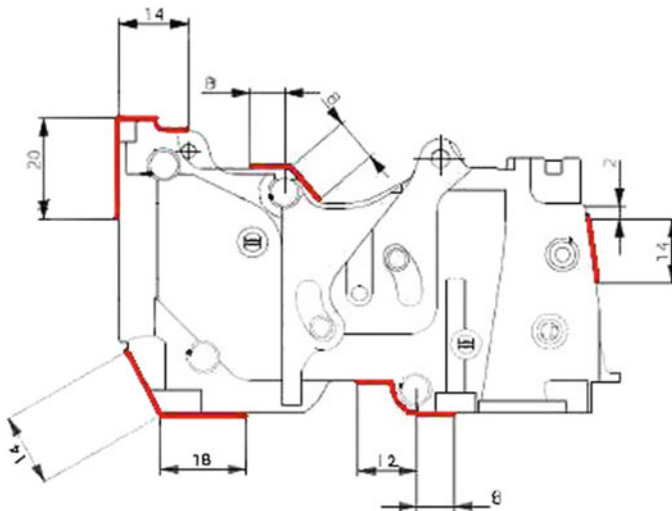


Fig. 1 Range of the permissible gaps verified by the operator



**Fig. 2** Example of chambers:  
**a** correct (without gap) and  
**b** defective (with gap)



The decision was made to perform the research of the gap only in the front part of the chamber, because it was an aspect controlled in each area. Twenty-two samples of the chambers with gaps were prepared, and then they were assessed by operators according to the guidelines set out in the inspection instructions. Between all the chambers, 11 pieces had correct gaps, while another 11 non-correct (Fig. 2).

Each chamber was marked in such a way that it was not visible to the operators. Each of the respondents had at his disposal the documentation and the feeler gauge 0.5 mm. The research involved a total of 40 people. Each of the research operators assessed the chambers in random order, and the results were recorded by the leader of the analysis. The operators repeated twice the series of part measurements, controlling them at random.

In order to determine the number of errors in conformity assessment of the gaps in the chambers, the Attribute GR&R coefficient was chosen to be used [3, 8].

### 3 Results and Discussion

The results of the conducted research of the Gage R&R analysis showed divergence between operator assessments (overall error rate was 11%). The level of the GR&R coefficient was 89%, what indicates the generally high capability of the control system of the correct quality classification of the chambers. The results were presented in Fig. 3.

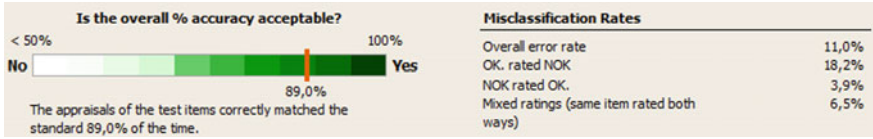


Fig. 3 Overall result of Gage R&R analysis

Percentage of the correct chambers assessed as non-correct was 18.2% (type I errors), percentage of non-correct chambers assessed as correct (type II errors) was 3.9%, while percentage of chambers assessed in different way in two turns was 6.5%.

Analyzing each research group in detail, it turned out that there are people (controllers) who were too restrictive in their assessment (they made too many type I errors) or too hasty (they committed too many type II errors). During the research, it was noted that not all operators were using a feeler gauge in case of any doubt, while those who used the feeler gauge, did it in different way—one group of controllers inserted the feeler gauge gently and at the moment of the emergence of resistance they stopped further evaluation, while other group tried to move the feeler gauge through the entire length of the halves of casings connection. In aim to detailed analysis the research group was divided into: *quality inspectors, leaders of the Compact line, leaders of the Chambers line, trainers of the Compact line, trainers of the Chambers line, and setters of the Chambers line.*

Results of research by the use of Gage R&R coefficient for *quality inspectors* were presented in Fig. 4.

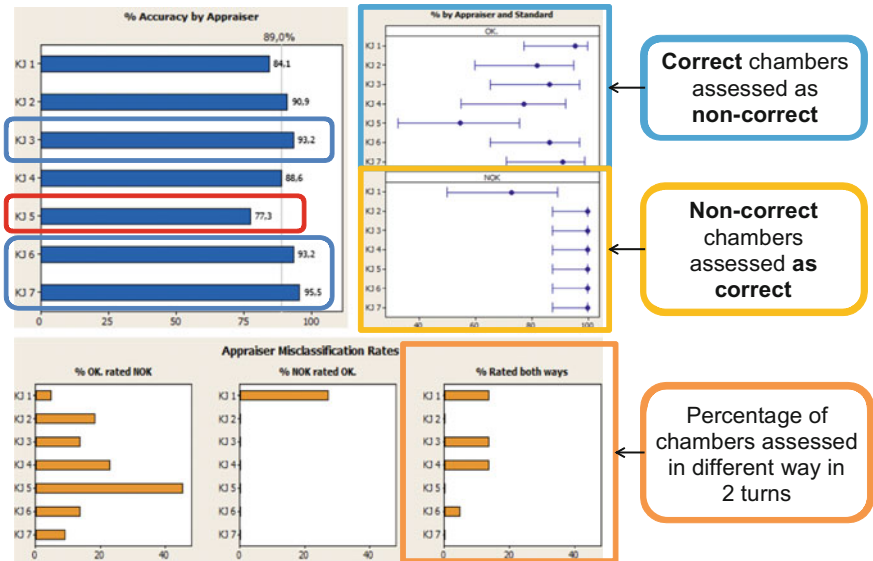


Fig. 4 Results of Gage R&R for quality inspectors

On the basis of the detailed analysis of results from the quality inspectors, it can be concluded that the quality controller No 5 assessed the chambers too restrictively (she rejected correct chambers), while the controller No 1 too hasty (she accepted non-correct chambers). The quality inspectors No 1, 3, and 4 in case of 15% of chambers, and the quality controller No 6 in case of 5% of chambers did not repeat their first qualitative classification. The quality controller 3, 6, and 7 had average accuracy coefficient above 93%, while the quality controller No 5 only at 77.3%. The average result for the whole group of the quality inspectors was **89%**.

Results of research by the use of Gage R&R coefficient for *leaders of the Compact line* were presented in Fig. 5.

On the basis of the detailed analysis of results from leaders of the Compact line, it can be concluded that the leaders treated all control too restrictively. If it comes to the leaders No 8 and 7, lots of chambers were assessed as non-correct, while the rest of leaders made the conformity assessment in too hasty way and the non-correct chambers were assessed as correct. Most of leaders of the Compact line (except leaders No 4 and 8) noted inconsistent assessments between the first and second series of assessments. Between all leaders of the Compact line, one of them, the leader No 3, had average accuracy coefficient at 95.5%. Leaders No 6 and 8 had results at 79.5 and 77.3%. The average result for the whole group of the leaders of the Compact line was **85.9%**.

Results of research by the use of Gage R&R coefficient for *leaders of the Chambers line* were presented in Fig. 6.

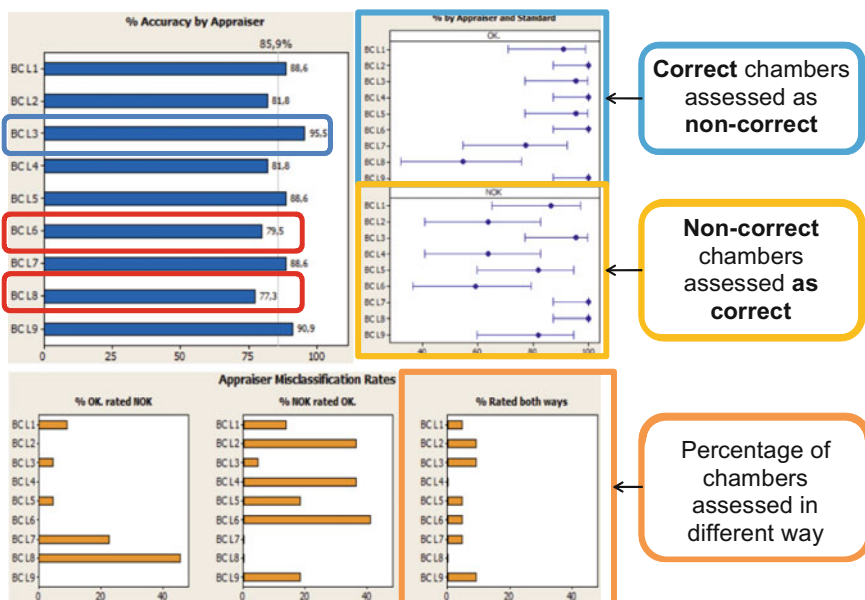


Fig. 5 Results of Gage R&R for leaders of the Compact line

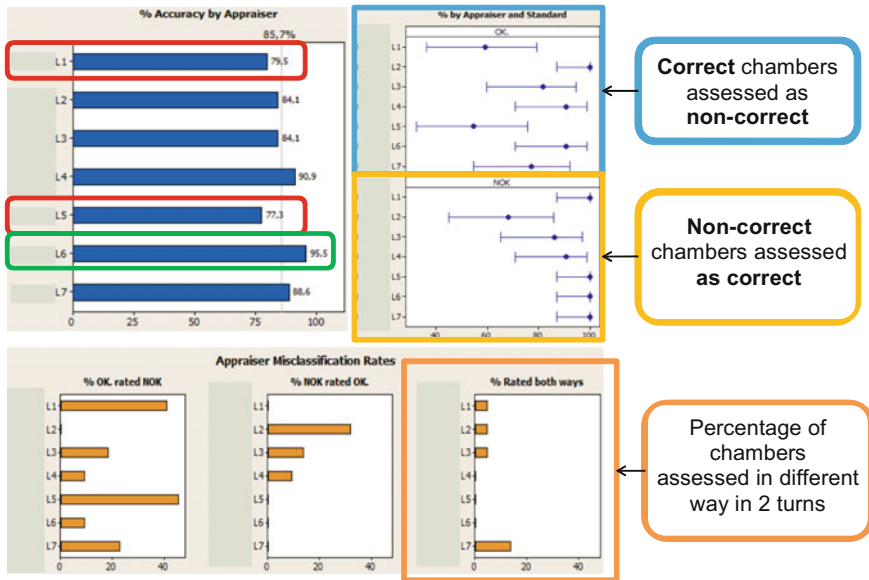


Fig. 6 Results Gage R&R for leaders of the Chambers line

Between leaders of the Chambers line, the leader No 2 was too hasty during the conformity assessment of the chambers, as the only one she assessed all chambers as correct, and at the same time she made more mistakes with serious consequences, i.e., type II errors. The leader No 7 had the biggest differences between the two series of assessments. The most correct and repetitive assessments were given by the leaders No 4, 5, and 6. Taking into consideration the coefficient GR&R, the worst results were noted in case of the leaders No 1 and 5 (below 80%), while the highest results were observed for the leader 6 (95.5%). The average result for Chambers line was **85.7%**.

Results of research by the use of Gage R&R coefficient for *trainers of the Compact line* were presented in Fig. 7.

From the detailed analysis of assessments given by trainers of the Compact line, it results that all the trainers, except the trainer No 7, assessed correct chambers as non-correct. The trainer No 7 had very low inconsistency of assessments, because she assessed most of the chambers as correct. Between all trainers of the Compact line, only the trainer No 6 repeated her assessments in both series. The trainer No 6, as the only one, achieved an overall result below 80%. The trainer No 8 achieved the average accuracy coefficient at 93.2%. The average result for the whole group of the trainers of the Compact line was **87.5%**.

Results of research by the use of Gage R&R coefficient for *trainers of the Chambers line and setters* were presented in Fig. 8.

From the analysis of the last research group, it appears that the trainer No 3, who assessed most of the correct chambers as non-correct, was the most restrictive if it

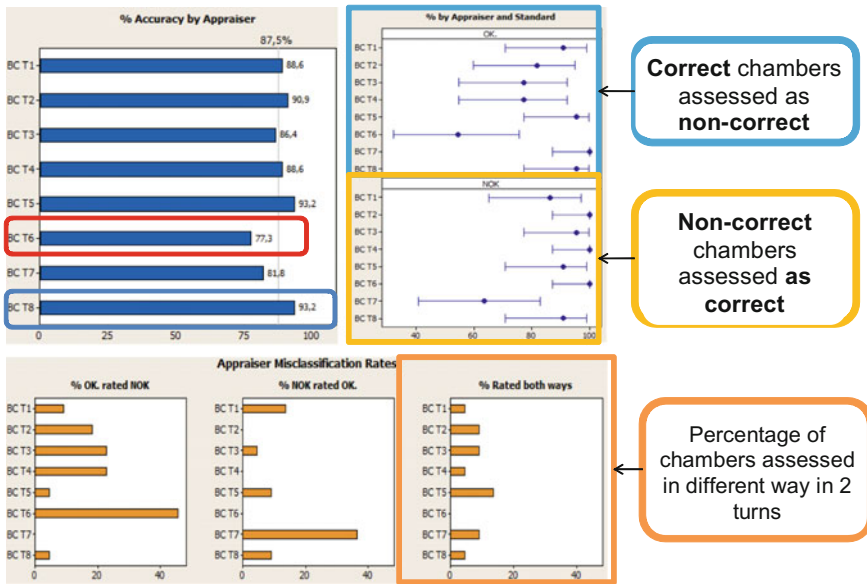


Fig. 7 Result of attribute Gage R&R for trainers of the Compact line

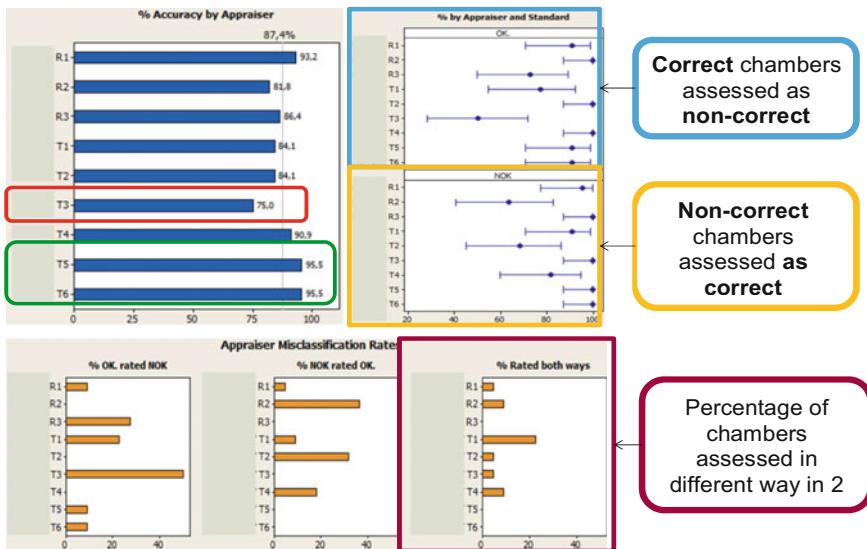


Fig. 8 Results of Gage R&R for trainers of the Chambers line and setters

comes to conformity assessment of the chambers. Only the setter No 2 and the trainer No 4 assessed all correct chambers as correct, but their assessment was too hasty, because they also assessed non-correct chambers as correct. Between all the

groups, only the setter No 3 and the trainers No 5 and 6 gave repetitive assessment in each of attempts. The worst result was observed in case of the trainer No 3 (result at 75%). The best results over 90% were reached by the trainers No 5 and 6. The average result for the whole group was **87.4%**.

Summing up the results of all researches of the coefficient Attribute GR&R, it turned out that in each group, there is the weakest person and people who can in the best way interpret requirements included in the technical documentation. The worst result was observed in case of the leaders of Chambers line, among which 20.8% of correct chambers were assessed as non-correct, thus generating high NQC costs. After the presentation of the results, it turned out that this assessment results from the fear of rejecting the dubious chambers on the main assembly line. While between the leaders from Compact line, the situation was opposite, because up to 18.7% non-correct chambers were assessed as correct, that is, more chambers were allowed for further production than they should.

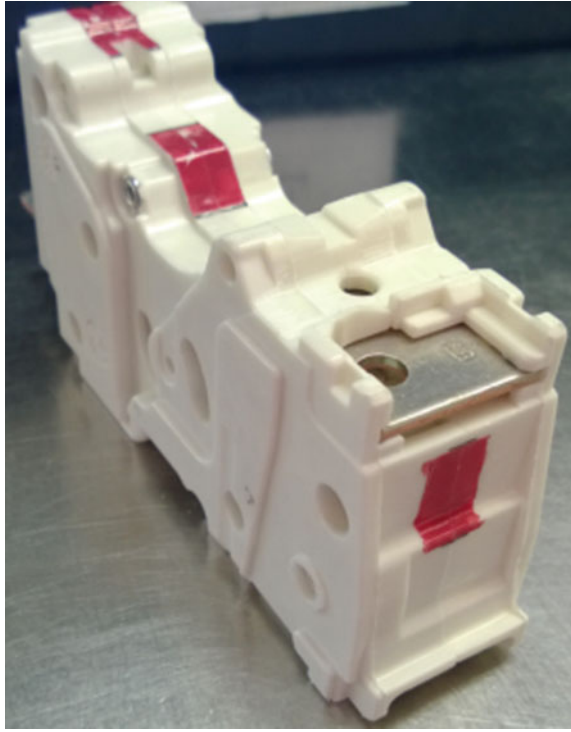
## 4 Conclusion

After the analysis of the results of the Attribute GR&R, in order to standardize assessments in all areas of control, people who took part in the research were interviewed to answer the question: *“What is the most difficult for them to decide whether to assess the chamber as correct or non-correct, according to the guidelines contained in the technical documentation?”*. It turned out that a large group of people could not specify the exact distance where the feeler gauges 0.05 should stop. In addition, the rejection of doubtful chambers was also a result of fear of their rejection at the next stage, so:

- the Chambers line workers were afraid of rejecting the doubtful chamber by the Compact line workers what, after reporting, lowered their score and consequently reduced the value of the quarterly bonus,
- the Compact line workers preferred to reject the doubtful chamber, because were afraid of the negative assessment by the quality controller at the final inspection, which resulted in report as nonconformity device, and then lowering the result in the quarterly bonus. The detection of the error during the final inspection also resulted in obligation of 100% control of the entire pallet with the order, and the same it was resulted in the lowering the quarterly bonus,
- while the quality control workers were afraid of the return of the device by the distribution center, and, as a result of sending nonconformity device to the customer, of the loss of good reputation and effectiveness.

All three groups found it easier to assess the dubious chamber as non-correct and to disassemble it generating losses in NQC. In case of chambers with gaps present already on the Chambers line, operators, to eliminate the gaps, tighten the rivet

**Fig. 9** Model with marked zones for the control with the feeler gauge 0.5 mm



several times, what resulted in cracking of the chambers casings and increased costs of NQC.

In order to reduce the conformity assessment errors during the visual inspection of the switch, preparation of a visual model (Fig. 9) with marked zones in which a length of at least 2 mm long without gap should be found was proposed.

After the preparation of the model for all lines and training of all 40 people on joint training—to avoid the lack of answers to occurring questions, NQC costs have dropped significantly. Also during the training, one principle on the method of performing control with the feeler gauge was established, and people responsible for exchanging used feeler gauges for new ones were chosen.

When the research on the evaluation of the effectiveness of alternative control with coefficient Gage R&R and employees' training were finished, the annual NQC output has been reduced to 0.8% level.

## References

1. Borkowski, S., Knop, K.: Challenges faced in modern quality inspection. *Manag. Prod. Eng. Rev.* 7(3), 11–22 (2016)

2. Jiang, X., Gramopadhye, A.K., Melloy, B.J., Grimes, L.W.: Evaluation of best system performance: human, automated, and hybrid inspection systems. *Hum. Factors Ergon. Manuf. Serv. Ind.* **13**(2), 137–152 (2003)
3. Ulewicz, R.: Quality control system in production of the castings from spheroid cast iron. *Metalurgija* **42**(1), 61 (2003)
4. Webber, L., Wallace M.: *Quality Control for Dummies*. Wiley Publishing Inc., Hoboken (2007)
5. Baird, R.: The Chronic Problem of Quality Inspection of Attributes. Retrieved from <https://www.linkedin.com/pulse/chronic-problem-quality-inspection-attributes-robert-baird> (2016)
6. Kujawińska, A., Vogt, K.: Human factors in visual quality control. *Manag. Prod. Eng. Rev.* **6**(2), 25–31 (2015)
7. Hamrol, A., Kowalik, D., Kujawińska, A.: Impact of chosen work condition factors on quality of manual assembly process. *Hum. Factors Ergon. Manuf.* **21**, 2, 3331, 156–163 (2011)
8. Vogt, K., Kujawińska, A.: Analysis of the effect of the type of nonconformity on the effectiveness of visual inspection (in Polish). In: Knosala R. (eds.) *Innovation in Management and Production Engineering*, vol. 2, pp. 470–480
9. Pesante, J.A., Williges, R.C., Woldstad, J.C.: The effects of multitasking on quality inspection in advanced manufacturing systems. *Hum. Factors Ergon. Manuf. Serv. Ind.* **11**(4), 287–298 (2001)
10. Johnson, L., Geiger, R.: Breakthrough Improvement for your Inspection Process. Retrieved from [https://www.minitab.com/uploadedFiles/Content/News/Published\\_Articles/inspection\\_process\\_improvement\\_breakthrough.pdf](https://www.minitab.com/uploadedFiles/Content/News/Published_Articles/inspection_process_improvement_breakthrough.pdf)
11. Sloma-Williams, T.: Five steps to cutting inspection costs. *Quality Mag.* **4**(1) (2003)
12. Lubicz, M.: Effectiveness and efficiency of product quality inspection processes. *Eng. Costs Prod. Econ.* **8**(3), 215–222 (1984)
13. Varela, M.R.L., Trojanowska, J., Carmo-Silva, S., Costa, N.M.L., Machado, J.: Comparative simulation study of production scheduling in the hybrid and the parallel flow. *Manag. Prod. Eng. Rev.* **8**(2), 69–80 (2017)
14. Majta, M.: Do Quality Inspections Add Value? (2012) Retrieved from <http://www.aprison.com/blog/2012/06/do-quality-inspections-add-value/>
15. Ulewicz, R., Jelonek, D., Mazur, M.: Implementation of logic flow in planning and production control. *Manag. Prod. Eng. Rev.* **7**(1), 89–94 (2016)
16. Diering, M., Kujawińska, A.: *MSA-Measurement System Analysis. Guide to Procedures* (in Polish), Poznan (2012)
17. Feliks, J., Lichota, A.: Computer-aided measurement analysis. *Arch. Foundry Eng.* **3**, 169–174 (2010)
18. Ingaldi, M.: Visual control in production company (in Polish). In: Borkowski S, Ingaldi M. (eds.) *Toyotarity. Control issues in BOST method*, 2014 (Oficyna Wydawnicza Stowarzyszenia Menedżerów Jakości i Produkcji)
19. Johnson, N.L., Kotz, S., Wu, X-Z.: *Inspection Errors for Attributes in Quality Control*. Chapman and Hall/CRC, London, England, United States (1991)
20. Borkowski, S., Knop, K., Mielczarek, K.: The use of six sigma indicators for measurement the process quality of products' conformity assessment in the alternative control. In: Borkowski S., Konstanciak M. (eds.) *Quality Control as Process Improvement Factor*, Czestochowa (2012) (Oficyna Wydawnicza Stowarzyszenia Menedżerów Jakości i Produkcji)
21. Knop, K., Borkowski, S.: The estimation of alternative control efficiency with the use of the Cohen's Kappa coefficient. *Manag. Prod. Eng. Rev.* **2**(3), 19–27 (2011)
22. Borkowski, S., Knop, K.: Evaluation of effectiveness of alternative control from the viewpoint of conformity assessment errors in a signal detection method. *Kvalita a spol'ahlivost technických systemov*, Nitra (2012) (Slovenska pol'nohospodarska univerzita v Nitre)
23. Krenczyk, D., Dobrzanska-Danikiewicz, A.: The deadlock protection method used in the production systems. *J. Mater. Process. Technol.* **164**, 1388–1394 (2005)
24. *Measurement System Analysis (MSA): Reference Manual, Fourth Edition*. AIAG Group (2010)



# Possibilities and Limitations of Passive Experiments Conducted in Industrial Conditions

Michał Rogalewicz, Paweł Smuskiewicz, Adam Hamrol,  
Agnieszka Kujawinska and Luis P. Reis

**Abstract** Experimenting is one of the basic tools for design and improvement of products and manufacturing processes. Experiments conducted in industrial conditions should marginally interfere with course of a studied process. These expectations are fulfilled in the best way by so-called passive experiments, in which data is gathered using records obtained from processes conducted in their natural environment and real conditions, without any alteration of set-up parameters. However, it is difficult to control interference originating from variability of studied factors during course of such experiments. That is why use of passive experiments in practice is limited. It is probably caused by distrust regarding credibility of obtained results. Aim of the paper is to compare results obtained from passive and active experiments, conducted in comparable conditions during a process of manufacturing of a selected product and presentation of guidelines for application of passive experiments, developed on the basis of the obtained results.

**Keywords** Design of experiments · Active experiment · Passive experiment

## 1 Introduction

A set of methods making it possible to prepare and conduct studies aimed at determination of influence of many (usually several, less often—over a dozen) factors, and their mutual interactions are known as the design of experiments (DOE). In industrial applications, experiments may be used, for example, to optimize manufacturing processes, to select the best parameters of a machine and to obtain design processes immune to disturbances [1–3]. In general, they can be considered, similarly to other approaches [4, 5] as a method supporting decision process.

---

M. Rogalewicz (✉) · P. Smuskiewicz · A. Hamrol · A. Kujawinska  
Poznan University of Technology, Poznan, Poland  
e-mail: [michal.rogalewicz@put.poznan.pl](mailto:michal.rogalewicz@put.poznan.pl)

L.P. Reis  
University of Minho, Braga, Portugal

In a specific case, aim of the DOE is to plan an experiment, which allows obtaining as many information about a studied object (a structure, a product, or a process) with the least possible time and expends, thanks to possibility of optimization of a selected property (e.g., accuracy, durability, energy consumption). Developing a plan of an experiment consists mostly in: determination of an output quantity (a criterion of process assessment), selection of input quantities, known as the examined factors, determining a number of combinations in which the examined factors can be present at the input of the process (each combination is a separate sub-experiment), defining a range of variability of the examined factors and levels, at which they will be set in the experiment, and assumption of a number of repetitions (replications) of each sub-experiment [6–8].

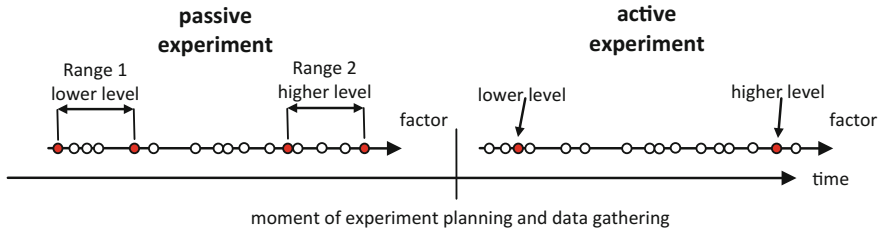
Experiments are usually conducted in a form of active experiments, meaning that examinations are conducted out as in a laboratory and levels of examined factors are set “on purpose” to certain values for the needs of an experiment. The opposite of active experiments is passive experiments, in which the “historical” data is used, obtained from a process not subjected to any operations related to purposeful (planned) change of values of factors. It can be stated that a passive experiment consists in studying a process in its “natural conditions.” Levels and ranges of factors in a passive experiment are selected post-factum, on the basis of results obtained, for example, during “standard” production.

Such approach was suggested by Box [9] who used the evolutionary operation method (EVOP) in the 1950s. It consisted in use of data originating from already realized processes to determine a direction of change of a result of a process and identification of factors, which have an influence on that change. On the basis of this knowledge, Box conducted further experiments using the active approach and, on the basis of results obtained in this part of experiment, changed values of process parameters. Then, he repeated the study cycle—gathering of data occurred, as well as its division, analysis, testing, and improvement. As apparent, such a way of experimenting contained elements of both passive and active experiments.

In analysis of the literature in scope of passive experimenting, the authors who made attempts at optimization of experiment plans [10] to obtain specific benefits, such as decreased labor consumption or accuracy of experiment results, should not be omitted. Such attempts consist of a number of sub-experiments and a number of their repetitions (replications), which should be as high as possible from the statistical point of view and as small as possible for the economic reasons. Chu and Han [11], for example, change a number of tests in the classic EVOP method to decrease time of experiment, with simultaneous increase of number of the considered factors.

Troyanovskyi and Serdyuk [12], on the other hand, emphasize a problem of results of a passive experiment being affected by process disturbances. They underline a possibility of occurring trends and process instability, which may have an impact on incorrect interpretation of results of a passive experiment.

Another group of publications pays specific attention on a way of data preparation for a passive experiment. Holmes and Mergen [13] suggest to analyze the



**Fig. 1** Change of a factor from quantitative into qualitative

examined factors using control charts before experimenting with the EVOP method, to check their stability and observe their variability in time. Measurement system analysis for analyzed factors is also suggested [14].

A key stage of experimenting, both active and passive, is selection of appropriate levels of the studied factors. In the active approach, the quantitative (numerical) factors are assigned determined values. In the passive experimenting, it is necessary to assume levels of numerical factors in a certain range (Fig. 1). It is a result of the historical data (i.e., data obtained from processes realized before designing the experiment) not always containing constant, set point values of input factors. In such cases, a certain level of variability of a given factor is assumed as its level and treated as a kind of label. In other words, a quantitative factor is changed into a qualitative one.

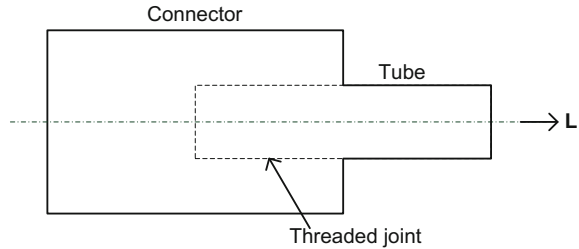
It needs to be noted that during planning of passive experiments, to avoid problems with selection of range of input factors, exact values of their levels are selected instead. However, it limits a number of factors subjected to examination and decreases amount of data possible to use in an experiment.

Conduction of a passive experiment in the “everyday” conditions of a process and acceptance of a certain range of the examined factors (not assuming single point values) causes the experiment results being affected by two kinds of variability: One caused by “instability” of a factor at a given point of experiment and the other—natural variability of the process.

## 2 Comparison of Active and Passive Experiments Results on Example of Industrial Studies

To find out if passive experiments can replace the active ones—as more economically efficient and considering nature of a studied process in a better way—the authors have conducted suitable comparative studies. The studies were conducted in an automotive company, manufacturing gearbox elements. A subject of experiment was a process of building of a subassembly consisting of a tube and a connector, and a premise to conduct it was a problem of low strength of connection of these two elements (Fig. 2). A measure of strength is a force of ripping the connector

**Fig. 2** Scheme of examined subassembly



from the tube. Minimal ripping force defined in requirements by the client is 25 N. Because of high requirements of the client, regarding process capability, the manufacturer strives for finding a process setting which would maximize the ripping force. However, it can be no less than 40 N.

Process of assembling the tube with the connector consists of several stages:

- (1) **Input inspection**—the following values are checked: tube outer diameter, connector internal diameter, batch of material, out of which both elements are produced, as well as connector width and outer diameter,
- (2) **Heating the tube** and drawing a steel cord through it, which is then cut, bent, and kneaded,
- (3) **Screwing the connector onto the tube**—operator sets parameters deciding about course and results of the screwing process (the connector cannot be screwed too hard, as it can damage the tube; it cannot be screwed too weak, either, as it could slide off the tube): machine pressure, which decides about rotary speed of screwing and number of rotations of connector around the tube. Operator also decides about placement and positioning of the connector in the machine,
- (4) **Assembly, cut, bending, and kneading** of the second end of the steel cord,
- (5) **Final inspection and packing**. Destructive measurement of the force ripping the connector off the tube is performed selectively.

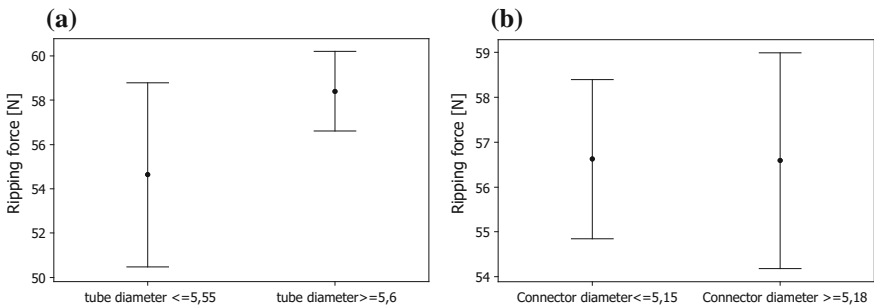
In planning of the experiment, factors related both to parts of the built subassembly and the process settings were taken into consideration. On the basis of knowledge and experience, five factors were eventually selected and given designations of *A*, *B*, *C*, *D*, and *E*: outer tube diameter (*A*—the tube diameter), inner connector diameter (*B*—the connector diameter), number of a mold socket, in which the connector was produced (*C*—the mold socket number), pressure set on the machine (*D*—the machine pressure), number of rotations of the device screwing the connector onto the tube (*E*—the number of rotations).

### 2.1 Experiment 1—Conducted with Passive Approach

In the passive experiment, the historical data was used as the input data (this data was recorded because of client’s requirements). They were gathered in a process realized through three months preceding a moment of developing a plan of the passive experiment.

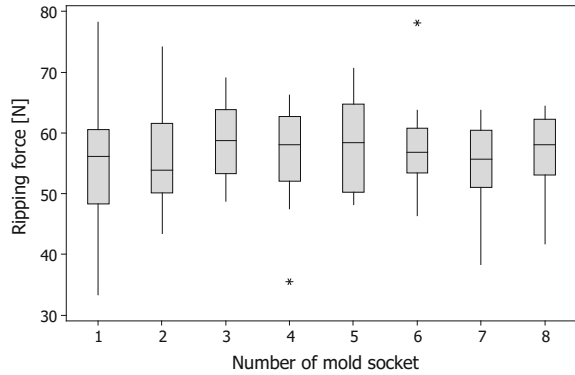
Selection of ranges of quantitative (*A*, *B*, *D*, and *E* factors) and qualitative (*C*) factors was preceded with a preliminary data analysis, in which selection criterion was assumed as ability to differentiate influence of a factor on force of ripping the connector from the tube. They are as follows:

- **Tube diameter (A):** Two ranges were assumed as levels of the A factor:  $A \leq 5.55$  mm (level -1) and  $A \geq 5.6$  mm (level +1). Analyzing data on Fig. 3a, it can be observed that the average ripping force at  $A \leq 5.55$  mm is lower by app. 4 N than the average ripping force for  $B \geq 5.6$  mm (difference of averages is significant on the  $p$  level = 0.096),
- **Connector diameter (B):** Two ranges were assumed:  $B < 5.15$  mm (level -1) and  $B > 5.18$  mm (level +1). Difference between average values for these ranges is 0.03 N (difference of averages is definitely not significant because  $p$  level = 0.981) (see Fig. 3b),
- **Number of the mold socket (C):** On the basis of a box diagram (Fig. 4), it can be stated that the average ripping force for all sockets changes in range of 56.4–58.5 N. Hence, it is of similar values—the ANOVA analysis shows that there is no significant difference between the sockets ( $p$  level = 0.817). Besides, variability of the ripping force is not significantly different between all molds ( $p$  level for the Levene’s test = 0.775). However, two groups of sockets were distinguished to the further analysis. These are the following groups: {6, 8} and {1, 2, 3, 4, 5, 7}. For them, levels of (-1) and (+1) were assumed, respectively,



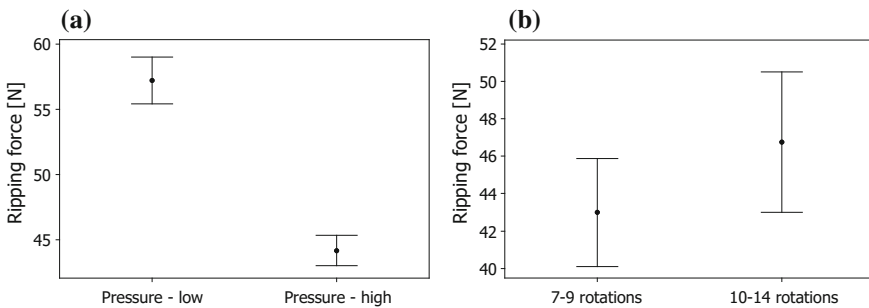
**Fig. 3 a** Interval plot of influence of tube diameter on the ripping force (85 observations). **b** Interval plot of influence of connector diameter on the ripping force (119 observations)

**Fig. 4** Box plot of relation between the average ripping force and the mold socket (15 observations for each socket)



- Pressure on the machine for the connector screwing (D):** It could be set on a continuous scale from the range (1.75; 6.25) but is set in a standard way, according to the instruction manual. That is why it was assumed that this factor is changed on a low level (-1), which is a standard setting, or on a high level (+1). Analyzing data on Fig. 5a, it can be observed that the average ripping force at low level is higher by app. 13 N than at high level (difference of averages is significant on the  $p$  level  $< 0.001$ ),
- Number of connector rotations (E):** It was set for 10–14 rotations (for lower tube diameters—level +1) and 7–9 rotations (for higher diameters—level -1). Difference between average values for these two levels of the factor is 3.82 N (difference is significant on the  $p$  level = 0.112) (see Fig. 5b).

On the basis of the results and assumptions from preliminary analysis, a study plan was developed. Even if some factors seemed to be insignificant, they were left together with set levels to find out if there is any interaction between factors. Considering necessity of conducting an active experiment in the second phase of the studies, requiring more expenditures and time than the passive experiment, the  $2^{5-1}$  fractional design was decided to be used.



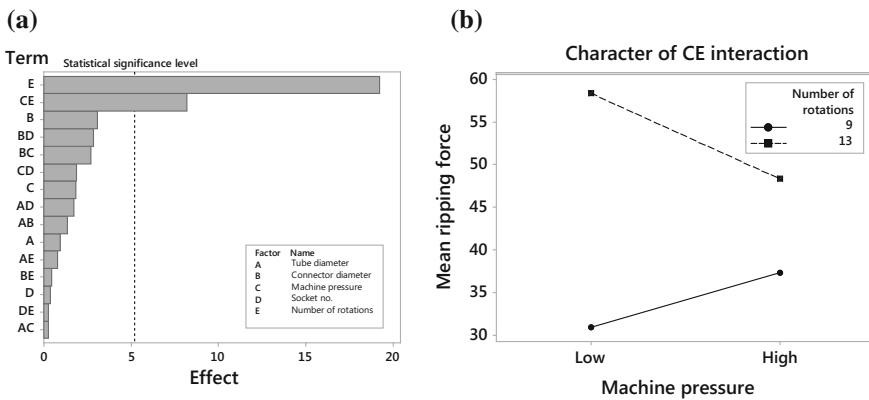
**Fig. 5** **a** Interval plot of influence of pressure on the machine for the connector screwing on the ripping force (300 observations). **b** Interval plot of influence of number of connector rotations on the ripping force (73 observations)

Consequently, out of the data base which stored more than 1000 data records gathered during permitting measurements and tests, a selection was made to find records matching the assumed factor combinations. Thanks to such an approach, for each 16 combinations, 10 to 25 replications were obtained. Presentation of factor levels and average values of the dependent variable is presented in Table 1. Pareto diagram of results is presented in Fig. 6a.

Analysis of results shows that a factor having the decisive influence on the ripping force is the number of rotations (*E*). Change of rotation number from (−1) to (+1) level improves strength of connection by 19 N. The strength is also significantly influenced by the CE interaction, Fig. 6b. Influence of the number of rotations on strength of connection is higher, when the machine pressure is lower. It confirms that the biggest potential for increase of the ripping force of the analyzed product is not in the material, but in setup of the screwing machine and ensuring its appropriate service.

**Table 1** Plan and results of the passive experiment—a fragment

No. of sub-experiment	Factors					Dependent variable	
	Tube diameter "A" [mm]	Connector diameter "B" [mm]	Machine pressure "C" [set level]	Socket no. "D"	Number of rotations "E"	Average ripping force [N]	Standard deviation [N]
1	+	+	−	−	+	55.5	2.42
...	...	...	...	...	...	...	...
16	+	−	+	+	−	33.8	1.87
	−up to 5.55	−up to 5.15	−low	−(6, 8)	−(7–9)		
	+from 5.6	+from 5.18	+high	+(1, 2, 3, 4, 5, 7)	+(10–4)		



**Fig. 6 a** Pareto diagram for main factor significances and interactions—passive experiment. **b** Character of CE interaction

### 2.2 Experiment 2—Conducted with Active Approach

The second experiment was conducted with an active approach—in this case, also the  $2^{5-1}$  fractional design was applied. It needs to be emphasized that the qualitative factors *D* and *E* were changed into quantitative ones.

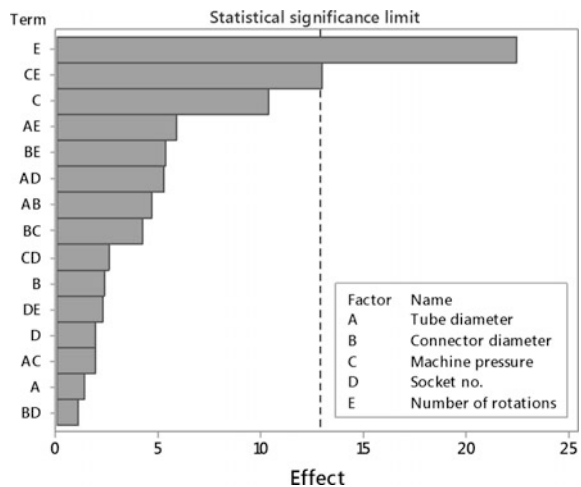
A fragment of the experiment plan and results of the conducted sub-experiments are presented in Table 2. To make it possible to compare the obtained results, selection of the value levels in this experiment is based on the previously conducted passive experiment.

Pareto diagram presenting influence of particular factors on the average ripping force is shown in Fig. 7. It confirms that the most important factor and interaction are, similarly as in the passive experiment, the number of rotations and interaction between it and the machine pressure.

**Table 2** Plan and results of the active experiment—a fragment

No. of sub-experiment	Factors					Dependent variable	
	Tube diameter “A” [mm]	Connector diameter “B” [mm]	Machine pressure “C” [set level]	Socket no. “D”	Number of rotations “E”	Average ripping force [N]	Standard deviation
1	+	+	–	–	+	78.5	2.02
...	...	...	...	...	...	...	...
16	+	–	+	+	–	32.94	1.06
	–5.50 +5.65	–5.15 +5.18	–2.5 +6	–3 +4	–9 +13		

**Fig. 7** Pareto diagram for main factor significances and interactions—active experiment





Results of the both experiments—active and passive—are comparable. Both indicate the same critical factor (*E*) and the same critical CE interaction (it is easy to find out that its effect is the same as in the passive experiment—influence of the *E* factor on the connection strength is higher, when the machine pressure factor —*C*—is lower).

### 3 Summary of the Passive and Active Experiments

The conducted experiments prove the far-reaching equivalence of passive and active experiments. The same critical factors were identified in both, although in the passive experiment, one of them was hidden in an interaction with the other.

To generalize the study results and conducted considerations, it can be concluded that using the historical data to conduct a passive experiment is, admittedly, burdened with some disadvantages, but they are by far compensated by advantages. In particular, the following aspects need to be emphasized:

**Table 3** Comparison between passive and active experiment

Comparison criteria	Passive experiment	Active experiment
Time and labor consumption	“Quick” and cheap. Empirical phase not necessary, as experiment is based on historical data	It is necessary to conduct experiments planned on purpose. It consumes additional time and requires certain expenditures
Process interference	The data is taken from the processes even before developing an experiment plan—no process interference	Requires interfering with a process (usually resulting in excluding it from the current manufacturing process)
Danger of interferences during experiment	Does not allow controlling of conditions, in which the data is created. Susceptible to uncontrolled interferences	Allows controlling the experimental conditions to a large degree
Possibility of selection of factor variability range	Does not allow definition of variations of studied factors outside a range in which a process operates	Allows definition of factors’ levels outside a range, in which a process operates
Accuracy of setting of factor levels	Allows accurate determination of levels of quantitative factors, but lack of certain combinations of the factor levels in the historical data base can be a premise to use ranges of values	Allows accurate determination of levels of quantitative factors, without need of using value ranges
Flexibility	Limits possibility of selection of methods (plan) of experiment and reduction of influence of interferences on a process result	Gives a possibility of selection from a wide range of methods of experimenting and reduction of influence of interferences on a process result

- In passive experiments, it is necessary to select value ranges for the quantitative factors, as it allows to obtain a higher number of “repetitions” from the historical data base.
- Because of selection of ranges for the quantitative factors, possibility of finding an optimal setting of factors in a process through a passive experiment is limited, as labels are used instead of numerical values.
- Passive experimenting is particularly advisable for processes described mainly by the qualitative factors.

Summary of comparisons between passive and active experiments is shown in Table 3.

Limitations of passive experiments mentioned in Table 3 are a probable reason for their infrequent use in industrial practice. Still, it needs to be emphasized that it is a wastage of valuable data gathered while realizing processes in a company. This data could be used for improvement of these processes. Although drawing conclusions on the basis of a passive experiment requires certain level of caution, such approach can be an invaluable tool preceding application of an active experiment and making it possible to use it more effectively.

## References

1. Mead, R., Gilmour, S.G., Mead, A.: *Statistical Principles for the Design of Experiments*. Cambridge University Press, Cambridge (2012)
2. Jiju, A.: *Design for Experiments for Engineers and Scientists*. Elsevier, Amsterdam (2014)
3. Hamrol, A., Kowalik, D., Kujawińska, A.: Impact of chosen work condition factors on quality of manual assembly process. *Hum. Factors Ergon. Manuf.* **21**(2), 156–163 (2011)
4. Dostatni, E., Diakun, J., Hamrol, A., Mazur, W.: Application of agent technology for recycling-oriented product assessment. *Ind. Manag. Data Syst.* **113**(6), 817–839 (2013)
5. Karwasz, A., Dostatni, E., Diakun, J., Grajewski, D., Wichniarek, R., Stachura, M.: Estimating the cost of product recycling with the use of ecodesign support system. *Manag. Prod. Eng. Rev.* **7**(1), 33–39 (2016)
6. Kackar, R.: Off-line quality control, parameter design and the Taguchi method, with discussion. *J. Qual. Technol.* **17**, 176–209 (1985)
7. Smuśkiewicz, P., Taguchi, T.: Design of experiments at manufacturing [in Polish]. *Qual. Manag.* **3–4**, 129–138 (2012)
8. Starzyńska, B., Hamrol, A.: Excellence toolbox: decision support system for quality tools and techniques selection and application. *Total Qual. Manag. Bus. Excell.* **24**(5), 577–595 (2013)
9. Box, G.E.P.: Evolutionary operation: a method for increasing industrial productivity. *Appl. Stat.* **6**, 81–101 (1957)
10. Pinto, J.C.: Impact of EVOP procedures on the optimization and design of experiments. *Can. J. Chem. Eng.* **79**(3), 412–421 (2009)
11. Chu, Y.H., Han, I.S., Han, C.: Improved evolutionary operation based on D-optimal design and response surface method. *Korean J. Chem. Eng.* **19**(4), 535–544 (2002)

12. Troyanovskiy, V., Serdyuk, O.: Some problems of passive experimental data processing. In: Proceedings of the PHYSCON, Leon (2011)
13. Holmes, D.S., Mergen, A.E.: Identifying need for new factors in EVOP. *Qual. Eng.* **18**, 219–224 (2006)
14. Diering, M., Dyczkowski, K., Hamrol, A.: New method for assessment of raters agreement based on fuzzy similarity, In: Book Series: Advances in Intelligent Systems and Computing, vol. 368, pp. 415–425 (2015)

# A Study of Raters Agreement in Quality Inspection with the Participation of Hearing Disabled Employees

Beata Starzynska, Karolina Szajkowska, Magdalena Diering,  
Alvaro Rocha and Luis P. Reis

**Abstract** This paper presents results of a study of the level of agreement of assessments and decisions made by quality controllers in a sensory inspection. The study subjects included persons with hearing disability. The study was conducted in an automotive manufacturing company. The employees with hearing loss perform product quality inspection which includes, among other things, visual inspection of the goods. The measurement system analysis (MSA) procedure for attributes, with the use of Gwet's  $AC_1$  coefficient, was applied to estimate the level of agreement of decisions made by the raters. The study results show that the quality of work performed by employees with hearing disability is at least as good as that of able-bodied employees. Based on the knowledge possessed by the authors, this approach to the problem is characterized by novelty.

**Keywords** Quality control · Sensory inspection · Hearing disability  
Measurement system analysis (MSA) ·  $AC_1$  coefficient

## 1 Introduction

Increasing interest in the problems of disabled people in the workplace has been observed in the last few decades all over the world, and in the last ten or more years in Poland. The way the disabled and their participation in social life are perceived has changed. The major driving force behind the changes is the social policy aimed

---

B. Starzynska · K. Szajkowska (✉) · M. Diering  
Poznan University of Technology, Poznan, Poland  
e-mail: karolina.strykowska@interia.pl

B. Starzynska  
e-mail: beata.starzynska@put.poznan.pl

A. Rocha  
University of Coimbra, Coimbra, Portugal

L.P. Reis  
University of Minho, Minho, Portugal

at breaking down social, economic, and physical barriers to provide employment support for the disabled [1].

In the context of health experience, the World Health Organization (WHO) distinguishes three concepts of chronic disease [2]: impairment, disability, and handicap. An impairment is any loss or abnormality of psychological, physiological, or anatomical structure or function. A disability is any restriction or lack (resulting from an impairment) of ability to perform an activity in the manner or within the range considered normal for a human being. A handicap is a disadvantage for a given individual, resulting from impairment or a disability that limits or prevents the fulfilment of a role that is normal (depending on age, sex, and social and cultural function) for that individual.

In the EU Member States, the issue of employment of the disabled is regulated under the European Employment Strategy [3]. All EU countries are required to apply the policy of equal treatment in employment [4]. The new EU legislation establishes a general framework for equal treatment in employment and occupation, and forbids discrimination based on disability, among other things [5]. Under Directive EU 2000/78/EC and other legal acts on equal opportunities for the disabled [6, 7], the policy of employment activation of the disabled, i.e. providing employment opportunities to the disabled by supported employment enterprises and enterprises without this status, is in effect.

One of the types of disability is hearing loss. According to Hoffman [8], a person with impaired hearing is someone who, due to difficulties in unassisted language and speech acquisition caused by defective auditory analyser, requires special assistance in learning, upbringing, and adoption to social and working life.

According to various sources, there are ca. 4.5 m disabled people in Poland [9], i.e. 12.2% of the total population, of whom ca. 2 m are at working age. An estimated 100,000 have a hearing disability, 44% of whom are at working age [10].

Owing to the efforts made among the wider public to raise awareness of disability and opportunities to reduce or break down the barriers faced by disabled people, knowledge of these issues is increasingly often used when creating jobs or scheduling and organizing the scope of work at organizations employing disabled people. The process concerns employees with hearing disability [11].

The actions mentioned above are also taken in the enterprise where the study presented in this paper was conducted. The study objective was to measure the level of agreement of assessments made by quality controllers in a sensory inspection. The key objective of quality inspection is early detection of irregularities in the process and their causes, and application of corrective and/or preventive actions. Such an approach makes improves the opportunity to maintain the desired quality level [12].

The aim of the study was to verify whether disabled employees are able to provide the same quality of work as their able-bodied colleagues. The study was conducted in an automotive manufacturing company, which has the status of a supported employment enterprise. Employees with hearing disability carry out quality inspections that involve, among other things, visual inspection of goods. In order to assess whether the level of agreement of assessments made by disabled inspectors is

acceptable, the study covered a reference group of able-bodied employees. The level of agreement of decisions made by the inspectors was estimated by the measurement and control system analysis (MSA) procedure for attributes (MSA for attribute system), but with the use of Gwet’s AC<sub>1</sub> coefficient [13, 14].

## 2 Research Problem

The study was conducted in operational conditions, at the final quality inspection workstation. The workers carry out 100% quality inspection of plastic goods with a decorative galvanic coating applied by the electrochemical method. The goods are inspected against templates of acceptable and unacceptable defects, detail inspection instructions, and catalogues of errors and defects. In a visual inspection, the employee classifies the products as: “meeting the requirements” or “not meeting the requirements”, “compliant” or “incompliant”, “good” or “bad”, OK. or NOK. The empirical studies which have been conducted so far usually assess the level of agreement of decisions made in visual inspection processes by able-bodied employees. In the case under analysis, the inspection was performed by able-bodied and hearing disabled employees.

Decisions made by quality inspectors were validated and quality of their work within the scope of inspection processes compared, taking into consideration the characteristics of the inspected items, with the use of MSA procedures for attribute features, with the use of Gwet’s AC<sub>1</sub> coefficient.

AC<sub>1</sub> is applied for determining the level of internal agreement and agreement among decisions of particular raters in the control and measurement system for qualitative characteristics (for attributes).

Internal agreement provides information whether the subjects provide the same assessment of certain products in consecutive assessment series (a study of repeatability). However, there is no reference to the predefined requirements (assessment criteria included e.g. in the catalogue of errors and defects) [13].

Agreement among raters, i.e. reliability of assessments made by various raters, permits to determine the regularity of obtained classifications (assessments) [13].

The value of Gwet’s AC<sub>1</sub> coefficient is determined with the following formula [14]:

$$AC_1 = \frac{P_a - P_e}{1 - P_e},$$

and:

$$P_a = \frac{1}{n} \sum_{i=1}^n \sum_{k=1}^q \frac{r_{ik}(r_{ik} - 1)}{r_i(r_i - 1)}, P_e = \frac{1}{q - 1} \sum_{k=1}^q \pi_k(1 - \pi_k) \text{ and } \pi_k = \frac{1}{n} \sum_{i=1}^n \frac{r_{ik}}{r_i},$$

where:

- $AC_1$  Gwet's coefficient of decision level of agreement,  
 $r$  number of raters,  
 $q$  number of categories,  
 $k$  category,  
 $n$  total number of objects in the study,  
 $n'$  number of objects in the study assessed by at least two raters,  
 $p_a$  share of consistent decisions in the total number of possible decisions by the team of raters,  
 $p_e$  probability of random agreement,  
 $r_{ik}$  number of raters who classified object  $i$  to category  $k$ ,  
 $r_i$  number of raters who assessed object  $i$ ,  
 $\pi_k$  probability of classifying any object to category  $k$  by any rater.

Other approaches for estimating the level of raters agreement can be also found in [13–16].

Regarding the study, a range of 30–50 objects is assembled, representing all the discrepancies described in the catalogue of errors and defects. The study sample contains at least 30% of objects explicitly defective, 30% of objects of explicitly good quality, and at least 30% of objects difficult to assess, with defects that can be acceptable or rejectable [16].

Each object is numbered before the study. The numbers are unique, invisible to the assessors, and visible only to the person in charge of the study.

The study is conducted in conditions most similar to real-life conditions in terms of the lighting, noise level, temperature, and work rate.

Before commencement of the study, each rater is acquainted with the catalogue of acceptable and unacceptable defects. Next, the study is conducted in three series.

After completion of each series, the person in charge of the study changes the sequence of samples to ensure that the rater cannot remember their previous assessment. Pauses between series minimize the effect of tiredness and drop in workers' productivity.

The rater uses the nominal dichotomous scale 0–1 (0—rejectable, 1—acceptable). Prior to each series, expert decisions are taken to determine the reference values for the examined objects.

The results of the study are summarised in a report on the level of agreement (the value of the  $AC_1$  coefficient) (total for all raters, total for all raters with the reference value, internal—for each rater separately, for each rater with the reference value). The data included in the report is obtained based on the acceptance criteria for the level of agreement level (Table 1).

The value of  $AC_1$  coefficient is in the range 0–1. According to the guidelines for the application of the  $AC_1$  coefficient, if the level of agreement is lower than 0.4, it is necessary to implement corrective actions with respect to the inspection process. For higher values of the  $AC_1$  coefficient, preventive and/or improvement actions are recommended. Taking into consideration the objective of the study, it is especially

**Table 1** Acceptance criteria for the level of agreement among the raters [13]

AC <sub>1</sub> value	Level of agreement	Recommendations
$0 < AC_1 < 0.4$	Low (insignificant)	Corrective actions are necessary
$0.4 \leq AC_1 < 0.75$	Good	Preventive and improvement actions should be taken
$0.75 \leq AC_1 \leq 1$	Very good	Improvement actions are recommended

interesting for the authors to compare the values of the AC<sub>1</sub> coefficient for the distinguished groups of raters.

### 3 Results

The study, aimed at validating the measurement and control system for non-measurable characteristics (attributes), covered three hearing disabled employees, marked as Inspector A(ON), Inspector B(ON), and Inspector C (ON), three able-bodied employees, marked as Inspector D, Inspector E, and Inspector F, and the Expert (manager of the Quality Assurance department).

The employees assessed the quality of plastic goods with galvanized coating. To minimize the impact of such factors as job seniority, experience, or age, the study was conducted on employees of similar competences (with their consent). The hearing disabled employees participating in the study had a similar degree of hearing loss. Additionally, support of a sign language interpreter was used in the preparation of the disabled employees for the study.

Prior to the study, the employees familiarized themselves with the catalogue of product defects. The catalogue contains a list of all possible product defects that may occur, together with their assessment (OK or NOK).

The study sample included 45 knobs, selected in compliance with the methodology described above.

On the basis of the obtained results, first the internal level of agreement between the raters made by the expert and the inspectors was estimated (Table 2).

It results from calculations based on the criteria described in Table 2 that internal level of agreement for the disabled inspectors A (ON), B (ON) and C (ON) was good (in the range of 0.68–0.74). The level of internal level of agreement for able-bodied raters D, E, F was also good, although lower than that for the disabled raters.

Next, the level of agreement of the decisions made by the raters and the expert was estimated. The level of agreement with the reference value (REF), obtained for the disabled inspectors A (ON), B (ON) and C (ON), was good or very good: 0.77 for A (ON) with the Expert, 0.74 for B (ON) with the Expert, and 0.69 for C (ON) with the Expert. For the able-bodied inspectors (D, E, and F), the level of



**Table 2** Study results—consistency among assessors

Rater (inspector)	Internal level of agreement	Level of raters agreement with REF	Total level of agreement (with REF)
A (ON)	0.68	0.77	0.59
B (ON)	0.74	0.74	
C (ON)	0.74	0.69	
D	0.55	0.62	
E	0.63	0.65	
F	0.47	0.65	
Expert (REF)	1.00	–	

agreement was lower and amounted to: 0.62 for D with the Expert, and 0.65 for E with the Expert and F with the Expert. Here, the level of agreement for the able-bodied inspectors is also lower than that for the disabled employees.

## 4 Discussion

The study was aimed to verify whether the quality of work performed by disabled employees is the same as that performed by their able-bodied colleagues. A comparison of the results obtained for the group of raters under analysis show that the level of agreement for the decisions made by hearing disabled employees is good and higher than that for decisions made by able-bodied employees.

The results may follow from the training system dedicated to disabled employees, among other things. Experience in working with hearing disabled people shows that they are faced with various difficulties in the working environment caused by impeded communication and understanding with able-bodied employees [17]. For this reason, hearing disabled and able-bodied employees receive training in different training systems. The main difference is the duration of training. Training on product quality assessment provided to hearing disabled employees is longer, as well as their preparation for carrying out tasks related to inspection operations in the company under analysis. All types of defects and their degrees of acceptability must be explained on examples (approved templates), with the participation of a sign language interpreter. All the contents of presentations, procedures, and training instructions must be presented in sign language. Training able-bodied employees does not require explanation of defects on examples, as they obviously understand the spoken language and voice communication (in speaking and writing).

The same difficulties may occur in any new situations, such as starting a new job or new product introduction, etc. Communication problems may isolate hearing disabled people or even impede their ability to work [18]. Persons with hearing

disability must have a clear understanding of their job requirements so that they are able to meet the expectations of their superiors [19].

## 5 Conclusions

This paper presents results of a study of the level of agreement of assessments made by raters in a sensory inspection. The study subjects included able-bodied and hearing disabled employees. Employees with hearing loss perform product quality inspection that includes, among other things, visual inspection of goods. The MSA procedure for attributes, with the use of  $AC_1$  coefficient, was applied to estimate the level of agreement of decisions made by raters.

The study results show that the quality of work performed by hearing disabled employees is at least as good as that of able-bodied employees.

Keeping in mind the study results, it is worthwhile to develop quality engineering and work organization methods and tools [20] for the creation of working conditions for disabled people, for example dedicated control charts [21] or Virtual Reality programs and applications [22], as they facilitate employment activation of this social group.

Therefore, further study on other factors that have an impact on adequacy and effectiveness of quality inspection [23–25], as well as on improvement of working conditions of employees with disability, would be recommendable. Such factors include training systems, job aptitude, skills of interpreting results and drawing conclusions, perceptiveness, ability to focus, and personality features. Moreover, environmental factors related to workstations of hearing disabled employees are also worth analysing. Based on the knowledge possessed by the authors, this approach to the problem is characterized by novelty.

**Acknowledgements** The results presented in the paper come from a scientific statutory research conducted at the Chair of Management and Production Engineering, Faculty of Mechanical Engineering and Management, Poznan University of Technology, Poland, supported by the Polish Ministry of Science and Higher Education from the financial means in 2017: 02/23/DSPB/7695.

## References

1. Strykowska, K., Starzyńska, B.: The process of implementing on quality inspection workplace person with a hearing impairment (in Polish). In: Knosala, R. (ed.) *Innovation in Management and Production Engineering*, vol. 2, pp. 286–299 (2016)
2. World Health Organisation: *International Classification of Impairments Disabilities and Handicaps*. World Health Organisation, Geneva (1980)
3. Majewski, T.: Employment systems for people with disabilities in the European Union (in Polish). *Bezpieczeństwo Pracy* **5**, 7–9 (2003)
4. European Commission: *European employment strategy*. Retrieved from <http://ec.europa.eu/social/main.jsp?catId=158&langId=pl>. 24 April 2017

5. Council Directive 2000/78/EC of November 2000 establishing a general framework for equal treatment in employment and occupation. Retrieved from <http://eur-lex.europa.eu/LexUriServ/LexUriServ.do?uri=CELEX:32000L0078:en:HTML> (2017)
6. Resolution of the Council and the Representatives of the Governments of the Member States meeting within the Council of 20 December 1996 on equality of opportunity for people with disabilities (97/C 12/01)
7. Council Resolution of 17 June 1999 on equal employment opportunities for people with disabilities (1999/C 186/01)
8. Hoffman, B.: Revalidation of deaf people (in Polish), Basics of pedagogical conduct, p. 27. PWN, Warsaw (1979)
9. The National Census of Population 2011: Population of the disabled. Retrieved from <http://www.niepelnospawni.gov.pl/index.php?c=page&id=78>. 24 April 2017
10. Piekot, T.: Focused research report—occupational identity of the deaf and their problems on the labor market (in Polish). Centrum badawczo-szkolenowe Dobre Kadry, Wrocław (2012)
11. Starzyńska, B., Kujawińska, A., Grabowska, M., Diakun, J., Więcek-Janka, E., Schneider, L., Schlueter, N., Nicklas, J.-P.: Requirements elicitation of passengers with reduced mobility for the design of high quality, accessible and inclusive public transport services. *Manage. Prod. Eng. Rev.* **6**(3), 70–76 (2015)
12. Hamrol, A.: Process diagnostics as a means of improving the efficiency of quality control. *Prod. Plann. Control* **11**(8), 797–805 (2000)
13. Diering, M.: Measurement system analysis for attributes with the use of Cohen's Kappa and Gwet's AC<sub>1</sub> coefficients (in Polish). In: Knosala R. (ed.) *Innovation in Management and Production Engineering*, vol. 2, pp. 196–205. Opole (2016)
14. Gwet, K.L.: *Handbook of Inter-Rater Reliability. The Definitive Guide to Measuring the Extent of Agreement Among Multiple Raters*, 3rd ed. LLC, Gaithersburg (2012)
15. Diering, M., Dyczkowski, K.: Assessing the raters agreement in the diagnostic catheter tube connector production process using novel fuzzy similarity coefficient. In: *IEEE International Conference on Industrial Engineering and Engineering Management*, pp. 228–232 (2016)
16. *Measurement Systems Analysis*, 4th ed., Reference manual, AIAG-Work Group, Daimler Chrysler Corporation, Ford Motor Company, GM Corporation (2010)
17. PFRON: Satisfaction with the work of people with disabilities (in Polish), Warszawa (2010)
18. Foster, S., MacLeod, J.: Deaf people at work: assessment of communication among deaf and hearing persons in work settings. *Int. J. Audiol.* **42**(Supplement 1), 128–139 (2003)
19. Johnson, V.A.: Factors impacting the job retention and advancement of workers who are deaf. *Volta Rev.* **95**, 341–356 (1993)
20. Grudzień, Ł., Hamrol, A.: Information quality in design process documentation of quality management systems. *Int. J. Inf. Manage.* **36**, 599–606 (2016)
21. Sika, R., Rogalewicz, M.: Demerit control chart as a decision support tool in quality control of ductile cast-iron casting process. In: *MATEC Web of Conferences 121, 05007, 8th International Conference on Manufacturing Science and Education (MSE 2017)—Trends in New Industrial Revolution* (2017)
22. Górski, F., Bun, P., Wichniarek, R., Zawadzki, P., Hamrol, A.: Effective design of educational virtual reality applications for medicine using knowledge-engineering techniques. *Eurasia J. Math. Sci. Technol. Educ.* **13**(2), 395–416 (2017)
23. Hamrol, A., Kowalik, D., Kujawińska, A.: Impact of selected work condition factors on quality of manual assembly process. *Hum. Factors Ergon. Manufact. Serv. Ind.* **21**(2), 156–163 (2011)
24. Kujawińska, A., Vogt, K., Hamrol, A.: The role of human motivation in quality inspection of production processes. *Adv. Intell. Syst. Comput.* **490**, 569–579 (2016)
25. Trojanowska, J., Varela, M.L.R., Machado, J.: The tool supporting decision making process in area of job-shop scheduling. In: Rocha, Á., Correia, A., Adeli, H., Reis, L., Costanzo, S. (eds.) *Recent Advances in Information Systems and Technologies, Advances in Intelligent Systems and Computing*, WorldCIST, vol. 571, pp. 490–498, Springer, Berlin (2017)

# Assessment of Quality Management System Maturity

Marta Grabowska and Josu Takala

**Abstract** Quality management in a manufacturing company is manifested by specific activities, which can be less or more efficient. The authors of this paper assume that level of efficiency is an indicator of the maturity [1] of a quality management system (QMS). The aim of this paper is to present a technique developed by the authors to assess the maturity of a quality management system. The technique is based on an original, generalized model of quality costs in which the QMS maturity is a variable and quality costs are an output quantity. This procedure provides a strategy to assess the maturity of processes and indicate areas and potential of improvement.

**Keywords** Quality management · Maturity of quality management system  
Quality costs

## 1 Introduction

Quality management in a manufacturing company is manifested by specific activities, which can be less or more efficient. The authors of this paper assume that level of efficiency is an indicator of the maturity [1] of a quality management system (QMS). Quality management processes are characterized by maturity—a certain level of development, which is manifested by a range of activities related to prevention and assurance of quality. Maturity manifests itself through a range of quality assurance activities as well as prevention and correction of non-conformances. The higher the ratio between the level of efficiency and any indications of non-conformance are, the high the class of maturity is. In the top class, activities to assure product quality that aligns with the client's requirements

---

M. Grabowska (✉)  
Poznan University of Technology, Poznan, Poland  
e-mail: marta.grabowska@put.poznan.pl

J. Takala  
University of Vaasa, Vaasa, Finland

are an inherent element of employees' daily routine. In contrast, the least mature quality management processes are characterized by continual attention to product and process quality control as well as correction of any non-conformances with resulting higher non-conformance and evaluation costs.

## 2 Maturity of Quality Management System

The relations between different activities between company management and priorities initiated by clients and/or by managers have been changing over many years. The authors have assumed that it is possible to indicate areas of management, processes, or groups of activities (further named collectively "aspects of company operation"—ACO), features of which correlate well with dependencies characterizing the particular class of maturity of quality management systems. On the basis of the TQM philosophy and own observations, the following ACOs were selected for juxtaposition (Table 1):

- leadership/engagement of top management,
- engagement of employees, tools, and methods of management,
- character of manufacturing processes,
- client relations (client-centered approach to management),
- relations with stakeholders, including suppliers,
- revision of operation effects, decision-making process, communication, continuous improvement,
- inspection processes, including inspection and measuring equipment,
- material resources for realization of processes.

The least mature processes of quality management are characterized by a dominance of actions related to product quality control (Table 1). Such a situation is manifested by high costs of incompatibility and evaluation.

The mature quality management processes consist mostly of activities related to ensuring compatibility of products with customers' requirements. These activities are elements of daily tasks of employees and are realized throughout the whole product lifecycle. Monitoring of the quality costs boils down to analysis of causes of incompatibility occurrence [2].

Symptoms of maturity of the quality management processes in a company can be evaluated by values and relations between costs of:

- conformance (compatibility)—understood as expenditures,
- non-conformance (incompatibility)—understood as losses resulting from improper realization of tasks [3].

**Table 1** Maturity of quality management processes

QMS maturity ACO	Class I	Class II	Class III
	Immature processes	Processes of average maturity	Mature processes
Engagement of top management	Top management does not or begins to use rules of quality management and promote continuous improvement	The Top Management applies rules of quality management and promotes prevention	Engagement of the Top Management present, ability to formulate mission statement based on quality
Engagement of employees, tools, and methods of management	Concentration on quantity of produced goods starts to be replaced by striving for assuring their quality. Training focuses on possibilities of processes improvement	There is an awareness of client’s meaning for the organization. Training focuses on possibilities of process improvement, aimed at increase of awareness	Possibility of integration of personal goals with the organizational culture. Modern management methods are applied, training sessions are used to raise awareness, qualification, and skills
Character of manufacturing processes	Processes related with assessment and monitoring of quality are mostly automated	Processes are monitored and stable	All stages in the product lifecycle are based on the rule of prevention and are aimed at generation of added value
Client relations (client-centered approach to management)	Large amount of discards and complaints, beginning of introduction of actions related to assurance of fulfillment of client’s requirements, their motive being a wish of avoiding losses	Client at the center of attention—at the input to the system, client’s requirements are investigated, with his satisfaction checked at the output	Striving for fulfilling requirements of widely understood client (also stakeholders)
Relations with stakeholders, including suppliers	Purchase is decided mostly by price, but partnership relations with suppliers and other contractors are beginning to be built	Wide definition of a client, taking employees and suppliers into account as internal clients. Relations with suppliers realized according to standards for other internal processes	Processes of management of external relations (e.g., with suppliers, influence on natural environment and society) and internal resources are realized. Suppliers are stakeholders of a company

(continued)

**Table 1** (continued)

Revision of operation effects, decision-making process, communication, continuous improvement	Quality assessed on the basis of data about number and types of complaints. Gathering and analysis of data about manufacturing processes. Information in form of orders, without interpretation and influence of employees	Gathering and analysis of data about internal processes. Determination of common aims on that basis	Results assessed on the basis of financial indexes, including quality costs, as well as non-financial indexes, built on the basis of stakeholders satisfaction. Analysis of changes in environment. Determination of problem-solving procedures
Inspection processes, including inspection and measuring equipment	Possible final inspection, gradual implementation of procedures of interoperation inspection	Monitoring in the whole product lifecycle, feedback present	Self-control processes dominating, awareness of responsibility for the product is present
Material resources for realization of processes	Lack or unfulfilled procedures of supervision of material resources, resources inadequate, or insufficient for effective realization of processes	Analysis of adequacy of resources and measuring and inspection equipment for effective process realization	Resources adequate to realized processes. Conducted analysis of risk and possibilities of implementation of newer solutions, monitoring critical points of processes

### 3 Quality Costs in the Context of Company Operation—ACO

There are different definitions of quality costs in the literature, eg.:

- narrow view - quality costs are limited to the cost of non-conformance,
- quality costs are the sum of the costs of compliance and non-compliance.
- broad interpretation, quality costs are higher than those ones recorded in the accounting system [4].

Therefore, an overview of definitions, classifications, and models of quality costs was made [5–9].

One of the first quality cost models, proposed by Juran and Gryna (1974) [10], described manufacturing processes which conformed to standards from the 1950s to the 1970s. In this model, value of quality costs per a qualified unit of product was defined by conformance with requirements.

The basis of this model was the assumption that manufacturing processes, though automated to some degree, were still dominated by human labor. Because a

human is unreliable by nature and is not able to maintain concentration and full psychophysical capability, he/she makes mistakes. Thus, the highest costs are costs of evaluation, i.e., detection of non-conformances. This model illustrated a model based on evaluation costs. It should be emphasized that this model was developed in a time when quantity of supplied goods was more important than their quality. The silent assumption was that “it suffices to check quality.”

The price of this model was the high costs of extensive inspection systems. Less attention was paid to quality (process capability), as reducing the defectiveness of final products increased of the evaluation costs, and total elimination of defective products increased of prevention and assurance costs to infinity [11]. As a result, at least in theory, a certain optimal defectiveness higher than 0% of production remained, determined by an optimal value of total quality costs. On both sides of this optimum, there were zones for potential cost reduction by prevention of defects or by reduction of quality control costs [10]. Based on this model, a curve of total quality costs can be divided into three zones [11]: status quo, improvement of projects, and perfection.

By the 1970s, the definition of quality included meeting client requirements, determined not by final inspection, but rather by improvement of manufacturing processes. Developed in the era of mass production, this was a beginning of a process of integration of both internal quality, focused on methods of evaluation of products and processes, and external quality, focused on perception and evaluation of a product by a client. Previously, determination of quality had been limited solely to conformance with the design; communication with the client, known as marketing, had been mostly limited at the stage of distribution and sales, aimed at encouraging clients to buy manufactured products. Over time, marketing tasks were now expanded so that communication with the client occurred before the product was manufactured. Moreover, activities perceived as separate up to this point—marketing and quality assurance—became integrated.

This generated an increase in activities to prevent non-conformance and foster continuous improvement. Schneiderman (1986) [12] presented continuous improvement as a never-ending effort to eliminate all wastage, such as modifications, decrease of productivity, downtimes, work-related accidents, or less visible factors related to unexploited individual or team potential. Later, researchers found that a program of continuous improvement is not necessarily cause an infinite increase of costs. Instead, the minimal level of total quality costs was present at the point where conformance with requirements was 100%, as the zero defect rule can be realized with finite costs. This is the model of continuous improvement costs.

Changes and advancements, both in technology and management, were also noted by Juran and Gryna, who proposed a similar interpretation of relationship between different groups of quality costs. In the models presented by Juran and Gryna or by Schneiderman, quality costs are analyzed in the coordinate system, where the Y-axis represents costs per unit of a product, while the X-axis represents conformance with requirements (expressed as a percentage of defective products). However, quality costs can also be considered in function of time, corresponding to the time of existence and development of a company, or a time of product life.



Researchers such as Bank [3] found that activities related to prevention could have a long-term result of cutting of total quality costs by as much as half. A model of costs describing such activities can be considered a model of prevention costs.

In this model, it is assumed that increase of prevention costs is related to continuous improvement of quality by investing in training, prevention, correction of systems, and economic processes. As the awareness and qualification level of employees increases, a portion of these costs stabilizes. Taking preventive actions lowers the costs of internal and external errors, the costs of exceeding requirements, as well as the costs of lost possibilities [3]. One method of decreasing such costs is focusing attention on client's requirements and considering his/her input while designing products and manufacturing processes. The value of this method is confirmed by the fact that most errors—as many as 75%—occur at the initial stage of design and planning of products [13].

Thus analyzing the costs of quality in an entire product lifecycle is a key problem. Such an analysis enables a producer to plan the costs of manufacturing a product and assess whether it is necessary to incur them and whether they can be reduced. However, such analysis requires application of an integrated system of tools, methods, and trainings, incorporating improving as a goal in all processes within an organization [14]. In such a system, quality becomes one of the basic characteristics of a company, along with management of finances, personnel, logistics, etc. [4]. This approach, management through quality, is well-known as total quality management (TQM).

In the late 90s, some researchers predicted that future social and economics conditions—such as focusing on the client, developing new technologies, or creating different organizational methods—would make prevention a part of everybody's work, and self-management would be the only method of quality control [15]. General and simply intuitive prevention of errors would result in non-conformance costs decreasing to zero, as conformance costs would become synonymous with operational costs in the company.

Today, activities related to assurance of quality have become standard practice. Based on this model, the problem of quality costs will cease to exist at some point in time [16].

Considering this reality, quality assurance should be treated as an ultimate model.

## 4 Technique to Evaluate QMS Maturity

Conclusions drawn from analysis of development of the quality cost concept and described characteristics of companies corresponding to particular models of the quality costs have become a basis for preparation of technique of evaluation of quality management system maturity in a manufacturing company. For its purposes, four models of quality costs were integrated (Fig. 1).

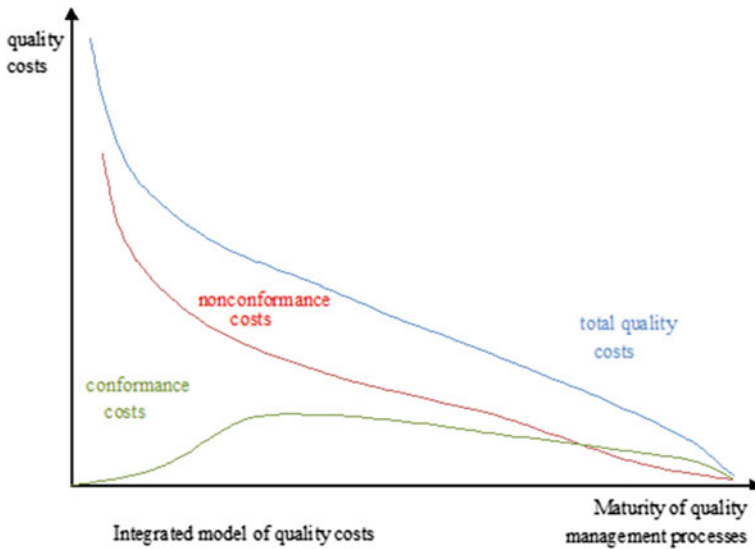


Fig. 1 Integrated model of quality costs

To connect the models, it was a key factor to indicate differences between them and their characteristic features (Table 2). The integrated model of quality costs was joined with a prepared description of conditions of functioning of companies during the years when models of costs of evaluation, improvement, prevention, super-prevention were developed [17], [18].


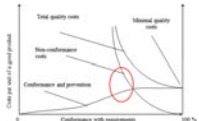
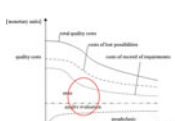
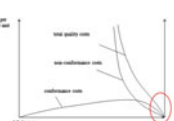
The integrated quality cost model (Fig. 1) in connection with the indicated ACO (Table 1) are basic elements of a technique developed by the authors for the assessment of maturity of quality management processes. The procedure consists of four stages.

The first stage is identification of values of conformance and non-conformance costs in a studied company. To conduct the studies on technique of evaluation of quality management processes maturity, a classification of quality costs according to the PAF (prevention, appraisal, failure) model was assumed.

Depending on the level of company’s advancement in maintaining an account of quality costs, three situations can be distinguished:

- in the companies in which there is a quality cost account, review of its adequacy to the current operation conditions must be made,
- in the companies in which a classic cost account is run (without separation of the quality costs), the quality costs must be separated, with division into conformance and non-conformance,
- in the companies in which there is neither cost account nor a quality cost account, a procedure of gathering data about conformance and non-conformance costs must be introduced.

**Table 2** Comparison, characteristics, and integration of models of the quality costs

Evaluation costs	Continuous improvement	Costs of prevention	Super-prevention
Model of quality costs			
			
Relations between costs of compatibility and incompatibility characteristic for models			
Decrease of values of the incompatibility costs with insignificant increase of the compatibility costs. Tendencies of changes between groups of costs are opposite: if compatibility costs increase, then incompatibility costs decrease and vice versa. Gradual stabilization of compatibility costs occurs	Decrease of values of the incompatibility costs is accompanied by small increase of the compatibility costs. Stabilization of compatibility costs occurs along with step of step decrease of incompatibility costs	Both compatibility and incompatibility costs go to zero	

**Table 3** Guidelines for analysis of relations between types of quality costs

Type of costs Class	Costs of conformance	Costs of non-conformance	Total quality costs
Class I	Value increases insignificantly, then stabilizes	Value decreases	Value decreases
Class II	Value is constant, then it decreases	Value does not change or insignificantly decreases	Value does not change or insignificantly decreases
Class III	No separation, identical with operational costs	Value decreases then stabilizes	Value does not change or insignificantly decreases

The second stage of the method is monitoring values of quality costs in time and monitoring relations between conformance and non-conformance costs (Table 3).

In the third stage of the method, results of observations of relations between the conformance and non-conformance costs (Table 3) must be compared with the

integrated model of quality costs (Fig. 1) and on that basis, the quality management processes should be assigned to maturity classes I, II, III.

The fourth stage of the methodology consists of the analysis of weak points of a quality management system and indication of areas for improvement. Guidelines for accomplishment of these tasks are descriptions of management areas (Table 1).

On this basis, the integrated model of quality costs was proposed and its parts were assigned to various classes of quality management processes maturity. Based on the findings of research carried out in production companies, it was found that a critical factor in the cost of quality is the human error [19, 20]. This observation led to combine quality costs with the learning curve. As product lifecycles shorten because manufacturers are trying to adapt to customer's changing requirements the pace of learning is a critical factor in the success of the company. This is a problem from the standpoint of standardizing manufacturing processes and reduces the cost of their implementation because the system always includes products that are in the phase of design and development. In the first phase of the product lifecycle is generated relatively high cost, including the cost of quality. That is why quality costs analysis should be conducted according to products, not to entire enterprise. Quality costs depend on skills and knowledge about product and processes [21]. Continuous improvement can be realized without high investment because prevention in mature quality management processes. Improvement of processes can be implemented with the involvement of relatively small investments or no cost, due to the fact that prevention in enterprises with mature management systems becomes part of each employee's work.

## 5 Conclusion

The proposed technique to assess QMS maturity can be a useful tool for management of a company in terms of indication of areas for improvement. This technique may be also used to facilitate communication between auditors, employees, or external consultants as well as the management of a company or owners of processes. Transferring information about immature or averagely mature processes using numerical data and data visualization tools is more credible and does not leave an impression of being solely a subjective opinion and feelings of an evaluator.

**Acknowledgements** The research work reported here was financed by the science grant admitted by the Ministry of Science and Higher Education under theme 02/23/DSPB/7695.

## References

1. Lasrado, F., Gomiscek B.: A tool to measure maturity of employee suggestion scheme. *Manage. Prod. Eng. Rev.* **6**(2) (2015)
2. Lari, A., Asllani, A.: Quality cost management support system: an effective tool for organisational performance improvement?. *Total Qual. Manage. Bus. Excellence* **24**(3–4), 432–451 (2013)
3. Bank J.: *The Essence of Total Quality Management*. Prentice Hall, United States (1993)
4. Campanella, J.: *Principles of Quality Cost. Implementation and Use*, ASQ Quality Press, Milwaukee, Wisconsin, Principle (1999)
5. Crosby, P.B.: *Let's Talk Quality, 96 Questions You Always Wanted To Ask Phil Crosby*. McGraw-Hill Publishing Company, USA (1989)
6. Dahlgaard, J.J., Khanji, G.K., Kristensen K.: *Fundamentals of Total Quality Management*. Taylor & Francis, United Kingdom (2002)
7. Drucker, P.F.: *Drucker's Guiding Thoughts*. MT Biznes sp. z o.o, Warsaw (2002)
8. Feigenbaum, A.V.: *Total Quality Control*. McGraw-Hill Inc., New York (1991)
9. Juran, J.M.: *Quality Control Handbook*, 1st edn. McGraw Hill, New York (1951)
10. Jasarevic, S., Brdarevic, S., Imamovic, M., Diering, M.: Standpoint of the top management about the effects of introduced quality system and continuation of activities of its improvement. *Int. J. Qual. Res.* **9**(2), 209–230 (2015)
11. Juran, J.M., Gryna, F.M.: *Juran's Quality Control Handbook*, 4th edn. McGraw-Hill, US (1988)
12. Schneiderman, A.M.: Optimum quality costs and zero defects: are they contradictory concepts? *Qual. Prog.* (1986)
13. Hamrol, A.: *Quality Management With Examples* (in Polish). PWN, Warsaw (2008)
14. Jasarevic, S., Diering, M., Brdarevic, S.: Opinions of the consultants and certification houses regarding the quality factors and achieved effects of the introduced quality system. *Tehnicki Vjesnik-Technical Gazette* **19**(2), 211–220 (2012)
15. Hand, M., Plowman, B.: *Quality Management Handbook*. Professional Handbook Series, Butterworth Heinemann, Oxford (1992)
16. Zymonik, Z.: *Quality Costs in Company Management*. Wroclaw University of Tehnology, Wroclaw (2002)
17. Stoner, J., Wankel, Ch.: *Managing*. PWE, Warsaw (1996)
18. Wood, D.C.: *Principels of Quality Costs, Financial Measures for Strategic Implementation of Quality Management*, 4th edn. ASQ Quality Management Division, ASQ Quality Press. Milwaukee, Wisconsin, US (2013)
19. Al-Zoubi M.T.: Generating benchmarking indicators for employee job satisfaction. In: *Total Quality Management & Business Excellence*, Taylor & Francis Group, London **23**(1) (2012)
20. Hamrol, A., Kowalik, D., Kujawinska, A.: Impact of selected work condition factors on quality of manual assembly process. *Hum. Factors Ergon. Manuf. Serv. Ind.* **21**(2), 156–163 (2011)
21. Starcevic, D.P., Mijoc, I., Mijoc, J.: Quantification of quality costs: impact on the quality of products. *Ekonomski Pregled* **3**, 231–251 (2015)

# Organization of Visual Inspection and Its Impact on the Effectiveness of Inspection

Agnieszka Kujawinska, Katarzyna Vogt, Magdalena Diering,  
Michal Rogalewicz and Sachin D. Waigaonkar

**Abstract** The research presented in this paper was aimed to analyse and evaluate the impact of organizational factors on the effectiveness of visual inspection in the manufacturing of electronic systems for the automotive industry. The study was carried out according to the authors' own methodology consisting of three stages: detailed description of the process, developing a study plan and analysis of the results. The experiment was conducted and influence of three factors: type of inspection, shift and type of defect, was taken into consideration and evaluated. Recommendations were made to improve the quality of such inspections that will lead to the improvement in the final quality of the product.

**Keywords** Visual inspection · Effectiveness of inspection · Organizational factors

## 1 Introduction

Quality inspection is defined in the literature as assessment of compliance of selected product features or process parameters with the predefined requirement on the basis of observation or measurement [1, 2]. It is expected from quality inspection that it actively improves the production and quality as well as reduces the costs [3]. The key characteristics of the inspection should be in accordance with the KPI of the process and/or product [4].

---

A. Kujawinska (✉) · K. Vogt (✉) · M. Diering · M. Rogalewicz  
Chair of Management and Production Engineering,  
Poznan University of Technology, Poznań, Poland  
e-mail: agnieszka.kujawinska@put.poznan.pl

K. Vogt  
e-mail: katarzyna\_vogt@o2.pl

S.D. Waigaonkar  
Department of Mechanical Engineering,  
BITS Pilani K K Birla Goa Campus, Sancoale, Goa, India

The method of quality inspection depends on the nature of the manufacturing process. Unit inspection involves a series of measurements for the assessment of each product on an individual basis. In large-series production, evaluation of each product is often economically unjustified or even unfeasible. For the purpose of quality inspection, techniques of statistical analysis of random sample data are used instead, which provide information for quality assessment of the entire lot (or process, respectively). In some cases, however, 100% quality inspection is applied in mass production, where delivery of products noncompliant with the requirements may result in serious consequences, for example, in the food, pharmaceutical, medical, aviation or automotive industry.

Considering the method of conducting quality inspection, it can involve assessment of measurable (quantitative) or qualitative (assessed alternatively) features [5]. The latter type of quality inspection is applied where direct or indirect measurement is unfeasible, impeded or uneconomic. Alternative assessment does not provide data on the degree in which the examined feature meets predefined requirements, but rather serves as a basis for a decision whether the product under analysis should be accepted or rejected as defective. Typically, as a result of the inspection, the product is assigned to one of two (or—less frequently—a larger number) possible states [5, 6].

Alternative assessment can be carried out with the use of specialized equipment which classifies products automatically (e.g. equipment for the assessment of location and orientation of components, optical systems for identification of impurities on the surface). However, it can also have the form of sensory testing. One type of sensory evaluation is visual inspection [7, 8].

Visual inspection is commonly believed to be economic as it does not require any costly equipment and is not destructive. However, it has its downsides—no matter how diligently performed, it is never 100% reliable and does not guarantee proper assessment [9].

As any type of inspection, visual inspection must be appropriately prepared and planned. The inspection plan should specify the timeframes (before, during or upon completion of a process), the feature under examination and its characteristics (whether it is measurable or evaluated alternatively) and the purpose of evaluation (quality estimation, acceptance or rejection of products on an individual basis) [10]. Information quality is very important to use and improve quality inspection [11]. The inspection plan has a large impact on the effectiveness of the inspection and maintenance management [12], also on cost of the quality control [13].

Effectiveness of visual inspection is determined by various technical, organizational, work environment and human-related factors [14, 15]. Technical aspects concern the physical process of inspection and include the product features under evaluation (their availability for visual assessment), the standards (templates) against which the product is assessed, availability of assessment tools, etc. Organizational factors may include the type and number of inspections, availability of decision-making support, information on efficiency and effectiveness of past inspections, the work shift on which the inspection is carried out, etc. Work environment-related factors may be physical, such as lighting, noise level, ambient

temperature, as well as organization of the workstation at which the inspection is carried out. Human-related factors are the sex, IQ level, character, health and type of motivation of the inspector.

Effectiveness of a visual inspection is determined by effectiveness of each of its components. While work environment, organization of the workstation and work itself, and technical condition of equipment are all controllable and can be corrected or improved, human mental and physical condition, for example the biorhythm (daily cycle), remains constant or changes only slightly [16].

The impact of a selected group of organizational factors on the effectiveness of visual inspection in the manufacturing of electronic systems for the automotive industry was examined in the paper. It presents a three-stage procedure adapted by authors to assess the visual inspection procedure in the organization. It was evaluated scientifically and the factors affecting the quality of evaluation are discussed.

## 2 Methodology of the Study

The organizational factor on the effectiveness of visual inspection was identified by means of an experiment. The study was carried out according to the research methodology consisting of three stages.

**STAGE 1:** Description of the process: development of a process map specifying the operations of visual inspection; identification of the number of inspectors; identification of work shifts; identification of possible defects and their location.

**STAGE 2:** Study plan: development of the study sample—number and types of defects (known to the expert); selection of inspection operations for evaluation; determination of the study schedule taking into consideration work shifts at the manufacturing facility; appointment of quality inspectors; development of data acquisition forms.

**STAGE 3:** Analysis of study results: analysis of the results of evaluation, by: *type of inspection, shift, type of defect.*

At stage 1, the process under examination is presented as a map specifying the operations performed as part of the visual inspection, number of inspectors, number of shifts and possible defects (based on value stream mapping analysis [17]). At stage 2, a detailed plan of the experiment is developed, specifying timeframes, product samples with the number and types of defects, work shifts at the manufacturing facility and location of the defects. At stage 3, the study results are analysed and conclusions are formulated.



### 3 Results (Case Study)

A case study of the process of mass production of electronic panels was conducted in order to assess the impact of the above-mentioned factors on the effectiveness of visual inspection.

#### 3.1 Stage 1: Description of the Process

At stage 1, visual inspection operations were identified. In the process under analysis, the operations are conducted upon completion of soldering of components, during the functional test and during the final inspection upon completion of the operation of cutting the panel (Fig. 1).

The process under analysis is carried out from Monday to Friday on three work shifts: the morning shift from 6:00 am to 2:00 pm, the afternoon shift from 2:00 pm to 10:00 pm, and the night shift from 10:00 pm to 6:00 am. Visual inspection is carried out by 14 operators. Electronic circuit boards are inspected in panels or on trays. One panel or tray contains 56 boards (Fig. 2).

The possible defects include a cracked seam, the diode pulled out of the seam, a scratched board, exposed copper, a scratched resistor, cracked component, damaged component, damaged pad (Fig. 3). Locations of some defects are identified, for example the capacitor or the diode. However, a large number of defects do not have an assigned location.

Most of the defects can be detected “with the naked eye”—e.g. a missing component (pulled out of the seam) or scratches/exposed copper on the circuit board (pellets or stains of solder). Some defects, however, can be identified only with the use of a magnifying glass.

There are three visual inspection operations in the process: inter-operative (no. 1), intra-operative (no. 2) and final (no. 3) [18]. The first inspection is aimed to evaluate the circuit board upon completion of the soldering process.<sup>1</sup> According to the workstation instruction, the worker’s task is to evaluate the quality of the soldered seam and the position of components on the surface of the printed circuit board, as well as to verify whether the soldered components are free from mechanical defects. The second visual inspection is carried out during the functional (electric) test. The operator performs visual assessment of the panel once it is taken out of the tester bed. If any errors are detected, the operator’s task is to look for potential defects of the components on the board, resulting from improper mounting or soldering of components.

Before the final inspection, the panels cut at a milling centre and automatically placed on trays. In the final inspection, the operator verifies the quality of mounting and soldering of components. Additionally, they check for any mechanical defects,

---

<sup>1</sup>Soldering is done using the “pick and place” technology.

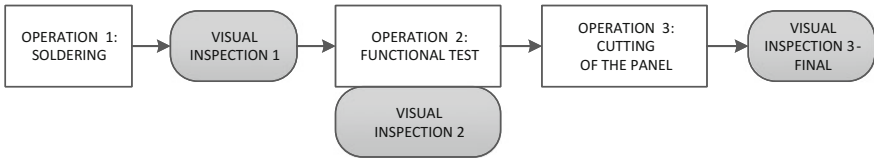


Fig. 1 Process diagram specifying the visual inspection operations

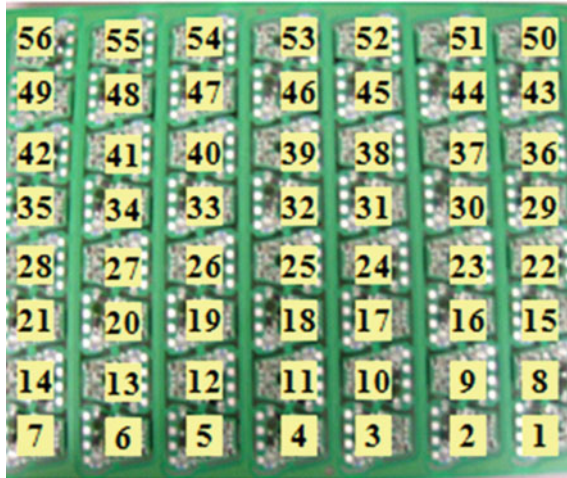


Fig. 2 The panel (multi-block) with 56 boards [source own work]

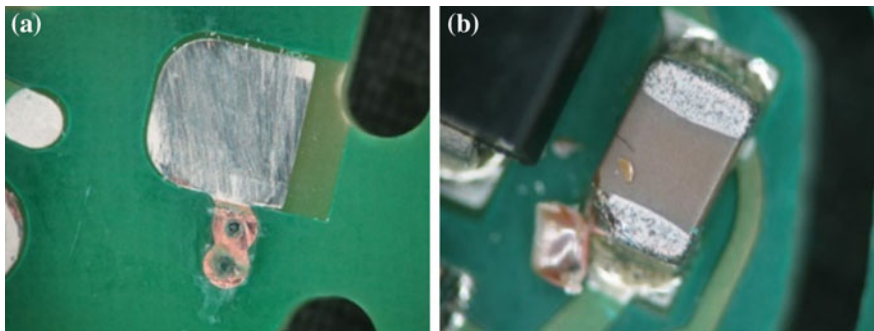


Fig. 3 Example defects a exposed copper b a component pulled out [source own work]

which may occur mainly as a result of inter-operational transport and handling of panels or single boards in the inspection process. The most common mounting errors include improper polarization of components and displacement of components relative to the soldering pads. The most common soldering errors are pellets

of solder, short circuit and stains of solder. While in the first and second inspection entire panels are evaluated, the final inspection consists in one-sided evaluation of single boards. In the case of any doubts, the operator takes the board in their hand and evaluates it on both sides. Evaluated boards are put away onto a transporting tray (56 boards per tray). If a board is considered defective, it is put away for repair or scrapping.

Figure 4 shows a diagram of the conditions in which boards are inspected in visual inspections 1, 2 and 3 (final).

### **3.2 Stage 2: Study Plan**

The experiment was scheduled for 11 weeks on three work shifts in the real manufacturing process. In total, 20 work shifts were included in the study, of which 6 were morning shifts, 11—afternoon and 3—night shifts. The study was conducted on Mondays (the beginning of the week), Wednesdays (the middle of the week) and Fridays (the end of the week).

Fourteen operators, men and women of 25–51 years of age and various work experience, participated in the study.

It was agreed that at each shift, a fixed (repeated) number of defected boards with a known structure of defectiveness would be admitted to the lot on which the experiment was conducted. Each sample contained 16 defective boards on 6 panels. To avoid the delivery of a defective product to the end customer, serial numbers of defective boards were blocked in the IT system.

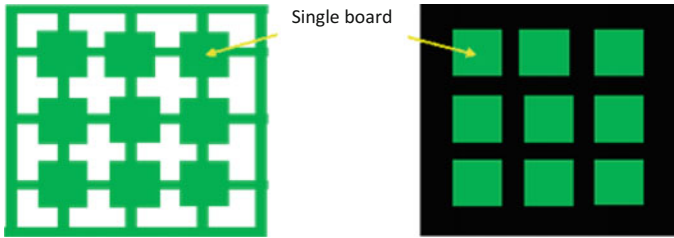
Table 1 shows the structure of defectiveness in a 16-component sample, with the location of defects.

Locations of defects of the boards were the same in each lot under analysis. The operators received a transportation basket with 21 panels of which 6 had the defects listed in Table 1. The defective panels constituted 28.6% of the transportation unit. The operator took the components out of the transportation basket for the operation of soldering, functional test and cutting. The operators noted down the detected defects on dedicated forms.

### **3.3 Stage 3: Analysis of Results**

The analysis of the results collected within 11 weeks and across 20 experiments took into consideration the type of inspection, work shift and type of defect.

The type of inspection depends on where it is conducted in the process. Two types of inspection were identified: in-process (online) and upon completion of the process (offline). Inspections no. 1 and 2 are online—conducted on an ongoing basis during a technological operation (soldering of components and the functional test). The offline inspection is a separate stage of the process which does not



**Fig. 4** Conditions of board inspection: inspection 1 and 2—boards in a panel (left); inspection 3—boards on a tray (right)

**Table 1** List of defects and their locations in the study sample

Defect	Board number	Panel designation	Location of defect
Cracked seam	52	A	Capacitor
Exposed copper	13	A	N/A
Seam pulled out	42	A	Diode
Exposed copper	56	B	N/A
Exposed copper	7	B	N/A
Exposed copper	1	B	N/A
Damaged component	2	C	Capacitor
Exposed copper	3	C	N/A
Exposed copper	4	C	N/A
Scratched resistor	5	C	Resistor
Exposed copper	50	D	N/A
Cracked component	49	D	Capacitor
Damaged component	56	E	Capacitor
Damaged pad	55	E	Diode
Exposed copper	50	F	N/A
Exposed copper	7	F	N/A

accompany any technological operation. In the case under analysis, inspection no. 3 is offline.

An analysis of effectiveness of the three inspections, expressed as percentage values of detected defects in proportion to all the defects at a given stage of the process (Fig. 5), leads to a conclusion that inspection no. 2 is ineffective. No defects were found as a result of inspection no. 2; probably due to the fact that the inspection is treated by the operator as additional to the functional test.

Effectiveness of the final inspection no. 3 is also low—defects were spotted only in 3 out of 20 cases. What is more, the percentage of identified defects is very low (10–36%). The circuit boards are evaluated after the panel is cut and the boards were placed on a tray. The fact that manipulation with the boards on a tray is restricted has a negative impact on effectiveness of the evaluation. The highest rate

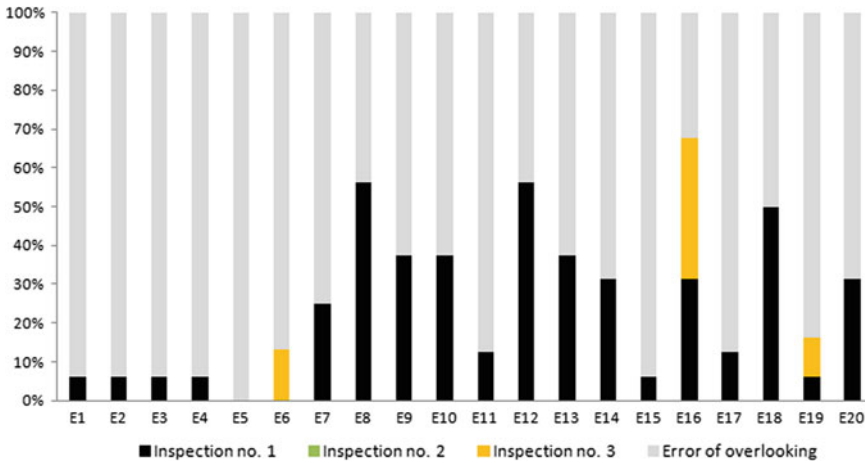


Fig. 5 Effectiveness [%] of inspections no. 1, 2 and 3 in particular experiments

of error detection was noted for inspection no. 1, upon completion of the soldering operation (mean effectiveness at 23%).

The company works on a three-shift system. An analysis of the impact of the shift system on the effectiveness of visual inspection was not statistically significant between the morning and afternoon shift (Fig. 6). Limited effectiveness on the night shift (18%) in comparison to the morning and afternoon shifts most likely results from variability of the mental and physical aptitude of operators during the daily cycle.

A comparison of the defect detection rate with the type of defect (Fig. 7) shows that location of the defect on the circuit board has no material impact on the detection rate.

Defects located randomly on the board did not pose any problem to the operators, although, in principle, they should be more difficult to detect. Defects of known location, on the other hand, for example pulled out seams or cracked components, went unnoticed.

On the basis of the of the conclusions presented above, further study was conducted and improvement actions were undertaken, including training sessions for inspectors and changes in the organization of visual inspection operations.

## 4 Discussion and Summary

The complexity of the issue of effectiveness of visual inspection carried out by human beings results from the fact that it is influenced by many human-related factors, such as the physical and mental aptitude of the operator, their personality, character, motor abilities, level of motivation and knowledge, experience,

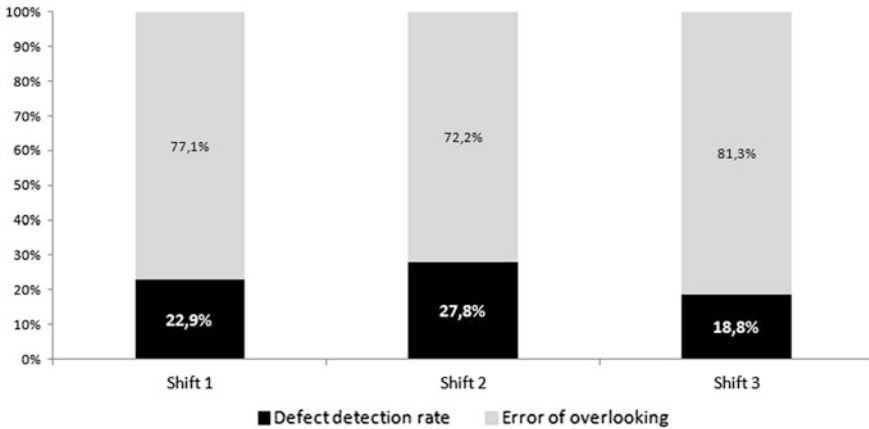


Fig. 6 Effectiveness [%] of visual inspection on shift 1, 2 and 3

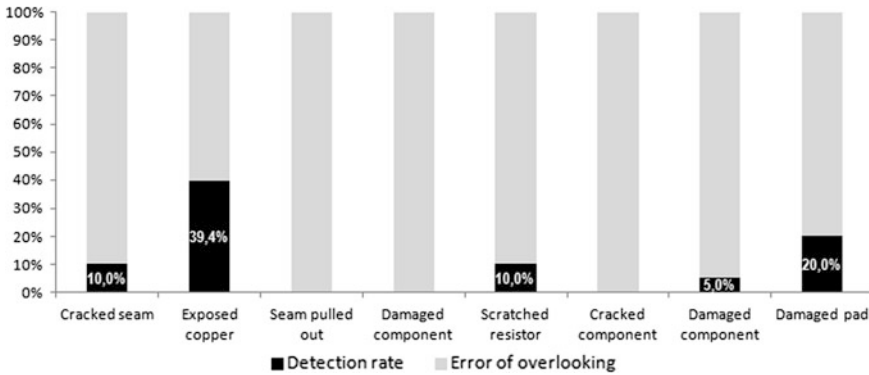


Fig. 7 Detection rate [%] of defect types in visual inspection (results of the functional test are not taken into account)

mindfulness, ability to focus, ability to solve complex issues, ability to process information, perception, intelligence, memory, as well as cultural aspects and behaviour standards.

Factors related to work environment and work organization are equally influential. In order to identify their impact on the effectiveness of visual inspection, a study was conducted of three visual inspection operations in the process of manufacturing printed circuit boards for the automotive industry.

The following factors were taken into consideration in the study, scheduled for 11 weeks: timeframes of inspections within the manufacturing process, types of defects and work shifts at the manufacturing facility.

An analysis of visual inspection expressed as percentage values of detected defects in proportion to all the defects at a given stage of the process leads to a conclusion that inspection no. 2 is ineffective. Incorporation of control activities

(so-called self-control) in the operator's basic duties failed. They treated them as additional activities and probably did not perform them. The lack of proper training of employees is often a factor that diminishes the effectiveness of ongoing controls. The effectiveness of the operator training process is reflected in the repeatability and reproducibility of the decision taken considering quality of controlled products.

Visual inspection can be performed on individual pieces, but also on a package of products. In the described experiment, the effectiveness of ongoing visual inspection on a package of products was analysed. Described studies have confirmed that the chances of its success are low (between 10 and 36% of defects detected).

Moreover, the low effectiveness of the detection of nonconformities was also characterized by a final control. The high value of this indicator was expected because the rate of final evaluation is not enforced by the production cycle as in the case of ongoing inspection. At the end of the inspection, the operator usually can spend more time on inspection than on the ongoing inspection.

For the final inspection, even the aspect of the background contrast on the tile was taken into account in the experiment being performed—after cutting, the panel was placed on a black tray. It turned out, however, that cutting the panel deprived the operator of the ability to rotate the tiles in space. Placing parts (already separated) in the tray reduced the rating to a 2D rating. This was the main reason for the low effectiveness of final control.

Correct organization of the control post is just as important as the selection and training of visual inspection staff, control methods or assessment aids. The reliability of any of these elements directly affects the effectiveness of the visual inspection.

**Acknowledgements** The paper is prepared and financed by scientific statutory research conducted by Chair of Management and Production Engineering, Faculty of Mechanical Engineering and Management, Poznan University of Technology, Poznan, Poland, supported by the Polish Ministry of Science and Higher Education from the financial means in 2017 (02/23/DSPB/7695).

## References

1. Starzyńska, B., Hamrol, A.: Excellence toolbox: decision support system for quality tools and techniques selection and application. *TQM&BE* **24**(5–6), 577–595 (2013)
2. Sika, R., Rogalewicz, M.: Demerit control chart as a decision support tool in quality control of ductile cast-iron casting process. In: *MATEC Web of Conferences* 121, 05007, 8th International Conference on Man, Science and Education—Trends in new industrial revolution. 2017
3. Borkowski, S., Knop, K.: Challenges faced in modern quality inspection. *Manag. Prod. Eng. Rev.* **7**(3), 11–22 (2016)
4. Lewandowska, E., Wiecek-Janka, E.: European version of a balanced scorecard in family enterprises. In: Xu, Y., Zhao, S., Xie, H. (eds.) *3rd International Conference on Management Science and Management innovation, AEBMR*, vol. 10, pp. 219–223 (2016)

5. Diering, M., Dyczkowski, K.: Assessing the raters agreement in the diagnostic catheter tube connector production process using novel fuzzy similarity coefficient. In: IEEE International Conference on Industrial Engineering and Engineering Management, 228–232 (2016)
6. Jasiulewicz-Kaczmarek, M., Saniuk, A.: Human factor in sustainable manufacturing. In: Antona, M., Stephanidis, C. (eds.) *Access to the Human Environment and Culture*, vol. 9178, pp. 444–455 (2015)
7. Drury, C.G., Sinclair, M.A.: Human and machine performance in an inspection task. *Human Factors Ergonomics Manuf.* **25**(4), 391–399 (1983)
8. Hamrol, A., Kowalik, D., Kujawińska, A.: Impact of selected work condition factors on quality of manual assembly process. *Human Factors Ergonomics Manuf. Serv. Ind.* **21**(2), 156–163 (2011)
9. Drury, C.G., et al.: The two-inspector problem. *IIE Trans.* **18**, 174–181 (1986)
10. Harold, S.: Effect of type of task and number of inspectors on performance of an industrial inspection-type task. *J. Hum. Factors Erg. Soc.* **37**(1), 182–192 (1995)
11. Grudzień, Ł., Hamrol, A.: Information quality in design process documentation of quality management systems. *Int. J. Inf. Manag.* **36**, 599–606 (2016)
12. Jasiulewicz-Kaczmarek, M.: Integrating lean and green paradigms in maintenance management. In: Boje, E., Xiaohua, X. (eds.) *19th IFAC World Congress Cape Town, IFAC-Papers OnLine*, vol. 47, no. 3, pp. 4471–4476 (2014)
13. Mahato, S., Dixit, A.R., Agrawal, R.: Application of lean six sigma for cost-optimised solution of a field quality problem: a case study. *J. Eng. Manuf.* **231**(4), 713–729 (2017)
14. Kujawińska, A., Vogt, K., Wachowiak, F.: Ergonomics as significant factor of sustainable production. In: Golińska, P., Kawa, A. (eds.) *Technology Management for Sustainable Production and Logistics, EcoProduction*, pp. 193–203 (2015)
15. Górski, F., Bun, P., Wichniarek, R., Zawadzki, P., Hamrol, A.: Effective design of educational virtual reality applications for medicine using knowledge-engineering techniques. *EURASIA J. Math. Sci. Tech. Edu.* **13**(2), 395–416 (2017)
16. Kaliom, R., El-Batawi, M.A., Cooper, C.L.: *Psychosocial factors at work and their relation to health*. World Health Organization (WHO), Geneva (1987)
17. Gangala, C., Modi, M., Manupati, V.K., Varela, M.L.R., Machado, J., Trojanowska, J.: Cycle time reduction in deck roller assembly production unit with value stream mapping analysis. In: Rocha, Á., et al. (eds.) *WorldCIST, Advances in Intelligent Systems and Computing*, vol. 571, pp. 509–518. Springer, Berlin (2017)
18. Viera, A.J., Garrett, J.M.: Understanding interobserver agreement: the kappa statistic. *Fam. Med.* **37**(5), 360–363 (2005)



**Part V**  
**Materials Engineering**

# On the Formation Features and Some Material Properties of the Coating Formed by Laser Cladding of a NiCrBSi Self-fluxing Alloy

Oleg Devojno, Eugene Feldshtein, Marharyta Kardapolava  
and Nikolaj Lutsko

**Abstract** In the present paper, the influence of laser cladding conditions on the powder flow conditions as well as the microstructure, phases, and microhardness of a Ni-based self-fluxing alloy coating is studied. The formation regularities of a coating microstructure with different cladding conditions as well as patterns of element distribution over the coating depth and in the transient zone are defined. The microhardness distribution patterns by depth and length of a coating for various laser cladding conditions have been studied. It was found that the laser beam speed, track pitch, and the distance from the nozzle to the coated surface influence the changes of the coating microstructure and microhardness.

**Keywords** Laser cladding · Ni-based self-fluxing alloy · Powder flow · Coating microstructure · Microhardness

## 1 Introduction

Laser cladding is one of efficient methods to deposit different coatings on machine parts. In this method, the powder melting and solidification processes lead to the fabrication of single- or multi-layer coatings. Generally, laser cladding can be affected by very large number of factors, and several groups can be identified among them [1–9]. These groups include the following:

- a dependence on laser radiation conditions (laser power, pulse energy, pulse duration, pulse frequency, laser wavelength, laser beam spot diameter, focal distance),

---

O. Devojno · M. Kardapolava · N. Lutsko  
Belarusian National Technical University, Minsk, Belarus

E. Feldshtein (✉)  
University of Zielona Góra, Zielona Góra, Poland  
e-mail: E.Feldshtein@ibem.uz.zgora.pl

- a dependence on conditions of layer forming (laser scan speed, scan strategy rotation, number of spots, scanning space, stripe width, stripe overlap, hatch or track distance, layer thickness, gas content control),
- a dependence on characteristics of powders that was used (size of the powder particles, powder mass flow, temperature of the powder).

A number of studies have been carried out to investigate the properties of single tracks, as well as the coating layer as a whole. In [10], the surface morphology and microstructure of the layer of 316L steel after introduction of a NiB additive were described. The microstructure and nano-mechanical properties of the layer of AlSi10 Mg alloy after selective laser melting were researched in [11], and the density, roughness, and microstructure of AlSi10 Mg layer were described in [12]. The microstructural and mechanical properties and surface quality of CoCrMo alloy and their relationship with some of the selective laser melting parameters were studied in [6, 13] for the surface.

The cladding of self-fluxing alloys on different substrate materials is widely applied. Three groups of these alloys are known now: Fe-based, Ni-based, and Co-based self-fluxing alloys [7, 14–22]. The Ni- and Co-based self-fluxing alloys are characterized by wettability, deoxidization, and by a fluxing effect as well as high physical and mechanical properties, and a good resistance to wear, oxidation, and high-temperature corrosion.

The aim of the present investigation is to study the formation features, microstructure, chemical composition, and microhardness of a NiCrBSi self-fluxing alloy coating formed on AISI 1045 steel's substrate by laser cladding.

## 2 Experimental Procedure

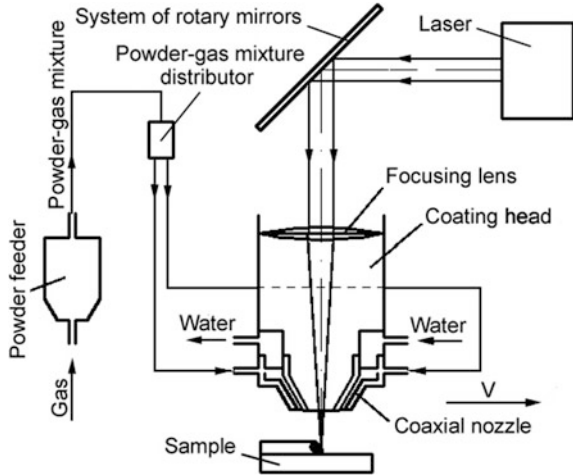
The research was carried out with Ni-based self-fluxing hard alloy. The chemical composition of the powder and the hardness of the material are shown in Table 1.

The coatings were applied to a substrate of AISI 1045 steel (EN 10277-2-2008 C45 steel). The starting powder was sieved to appropriate granulations using a set of sieves and then was dried in an electric furnace at 200 °C for two hours. Cladding was performed using a continuous-wave CO<sub>2</sub> laser “Comet 2” with the power of 1 kW (Fig. 1). Powder was fed to the work area through a lens with a nozzle for spot coaxial laser cladding which can operate with the CO<sub>2</sub> laser in the range of focal lengths 100–200 mm. The lens can work in conjunction with different gas-powder feeders and provides a simultaneous or programmable flow of up to four different components. The powder components are mixed in a special

**Table 1** Powder composition and the material hardness

C (%)	B (%)	Si (%)	Cr (%)	Fe (%)	Ni (%)	Hardness
0.3–0.6	1.7–2.5	1.2–3.2	8–14	1.2–1.3	The rest	HRC 35–40

**Fig. 1** Scheme of coating deposition



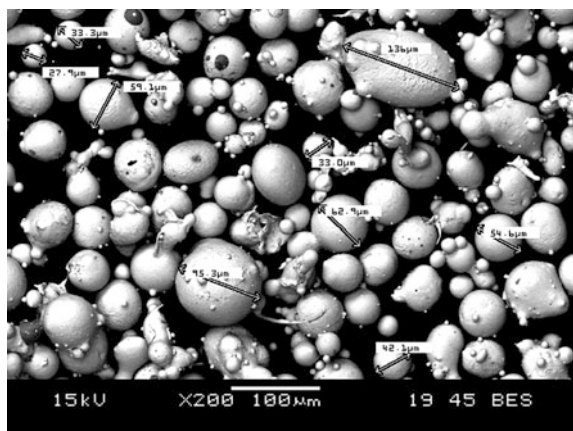
chamber and supplied to the laser target area with the nozzle channels. The lens has an air-cooled lower part of the nozzle and a body that ensures its long service life. The compressed air is used as a transporting gas. The focal length was of 200 mm, and a focused spot was of 1.0 mm.

To determine the optimal particle sizes, the segregation of an in situ powder (Fig. 2) was performed and three fractions were used: less than 20  $\mu$ , 20–80  $\mu$  and 80–100  $\mu$ .

Cladding layers of the Ni-based alloy were tested in the speed range of 40–120 mm/min when the distance between the nozzle and the surface of sample was of 10–14 mm. The diameter of the laser spot was of 1 mm, which corresponds to a power density of  $1.27 \times 10^5$  W/cm<sup>2</sup>.

The powder flow was measured by powder blowing through the feeder nozzle per unit of time when operating the laser, and then samples with deposited powder

**Fig. 2** In situ NiCrBSi powder



were weighed on a CITIZEN CY-124 analytical balance. Compressed air flow was measured with a P5 rotameter with precision  $\pm 4\%$ . The air pressure was regulated by a feeder control system. All measurements were repeated three times.

The coating height was measured using an optical microscope with accuracy of 0.001 mm.

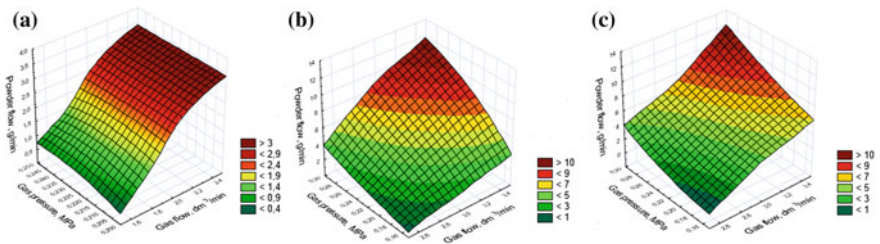
The microstructure, morphology, and chemical composition of coatings were analyzed by a scanning electron microscope “Mira.” The microhardness was measured using a MICROMET II Hardness Tester. The indenter for Vickers tests with the load of 100 gf was used (further the designation HV 100 was applied).

Statistica 12 software was used for a graphical interpretation of some results.

### 3 Results and Discussion

#### 3.1 Powder Flow When Passing Through the Nozzle

The research results of the powder passage through the nozzle of the lens are shown in Fig. 3. With increasing gas pressure and gas flow, the flow rate of self-fluxing powder increases, but the behavior of this influence depends on the particle size. In the case of the fraction with particle sizes of 80–100  $\mu\text{m}$ , the effect of the pressure increases, but the intensity of the gas flow effect decreases. For the fraction having particle sizes less than 20  $\mu\text{m}$ , the significant gas flow inhibits the flow rate of particles and the pressure is not affected. This is probably due to packetizing particles in the feeder, which prevents the particles exit from the nozzle. Thus, the powder with the size of 20–80  $\mu\text{m}$  was the best and was accepted for further studies.



**Fig. 3** Efficiency of the powder particles passage with dimensions less than 20  $\mu\text{m}$  (a), 20–80  $\mu\text{m}$  (b), and 80–100  $\mu\text{m}$  (c) through the lens nozzle depending on the pressure and flow of the transporting gas

### 3.2 Microstructure and Phase Composition of Single-Layer Coating

The analysis of the deposited coating layer (Fig. 4) showed that a clear tendency for reducing dimensions of the structural components and the depth of the heat-affected zone is observed with increasing the deposition rate. Favorable conditions for the carbide eutectic  $\gamma\text{-Ni}-(\text{Cr}_3\text{C}_2 + \text{Cr}_7\text{C}_3)$  formation, as well as the formation of a low-melting eutectic  $\gamma\text{-Ni-Ni}_3\text{B}$ , whose crystallization occurs in the interdendritic space during cooling, are created in this case.

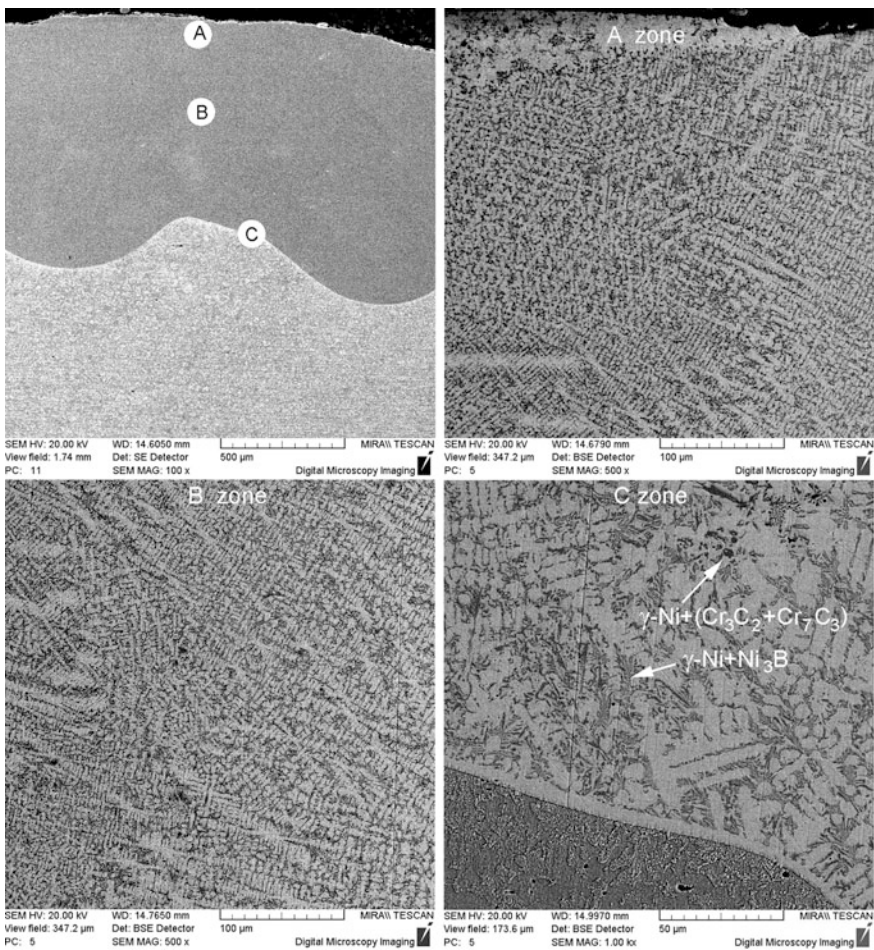


Fig. 4 Microstructure of a coating layer

The cladding distance affects the coating microstructure similarly. Dimensions of the dendrites decrease with its increasing, and their direction is clearly defined only in the upper part of the coating layer.

The differences in the microstructures are caused by the conditions of the heat exchange between the molten coating layer and the substrate. An additional time is required for the reduction of the oxide films when cladding tracks. It includes the recovery time of an oxide film between the substrate and the deposited layer, the recovery time between the powder particles as well as the recovery time of oxides between the tracks. Areas adjacent to a neighboring layer are subjected to the double thermal effect, whereby the sizes of the solid solution dendrites adjacent to the track edge are somewhat increased. The heat-affected zone with the depth of 40–100  $\mu\text{m}$ , depending on deposition conditions, indicates the presence of a chemical bond between the clad layer and the substrate.

With the increase of a laser beam speed and a distance from the nozzle to the coated surface, structural components are crushed, transforming into quasi-eutectic structures. Most of the close-packed planes of a crystal lattice are located on the surface, because dendrites are crystallized at an angle of  $45^\circ$  to it.

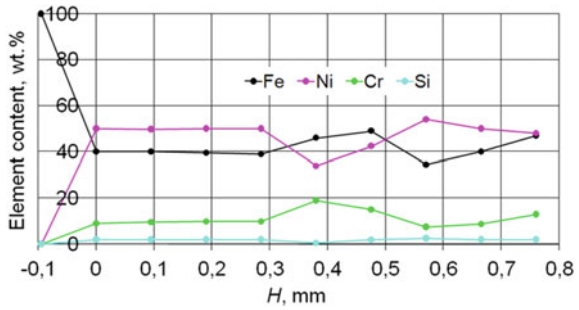
As it was noted above, the alloy microstructure consists of two kinds of eutectics:  $\gamma\text{-Ni-Ni}_3\text{B}$ , whose melting point is 1000  $^\circ\text{C}$ , and  $\gamma\text{-Ni-(Cr}_3\text{C}_2 + \text{Cr}_7\text{C}_3)$ , which crystallizes at higher temperatures and is a strong coating corset. Secondary borides crystallize in the form of small nucleuses and have no time to grow. According to our researches and other investigations [23, 24], the strong coating corset contributes to a high corrosion resistance in alkalis and acids, and low-melting eutectic heals the pores, cracks, and other single defects.

### ***3.3 The Distribution of Elements Over the Depth of a Single-Layer Coating***

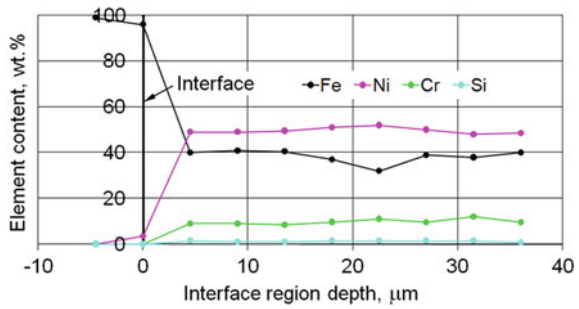
The results of the study on the elements distribution over the depth of a single-layer coating are shown in Fig. 5. The stable content of the elements was observed practically all over the depth of the coating. The nickel content is about 50% all over the depth of the coating and is much lower than in the in situ powder. At the same time, 40% of the iron is contained in the coating and is also uniformly distributed over the entire depth.

This indicates a significant diffusion of the iron from the substrate since the iron content of the in situ powder does not exceed 1.3% (see Table 1). Chromium and silicon are also uniformly distributed across the depth of the coating and their content corresponds to the in situ powder. The uniform content of elements by coating depth indicates uniform mixing of materials in the melt pond and the same conditions of coating material heating throughout the depth. Nickel, chromium, and silicon do not penetrate from the coating into the substrate.

**Fig. 5** Distribution of elements at a depth of a coating



**Fig. 6** Distribution of elements in the transient zone of a coating



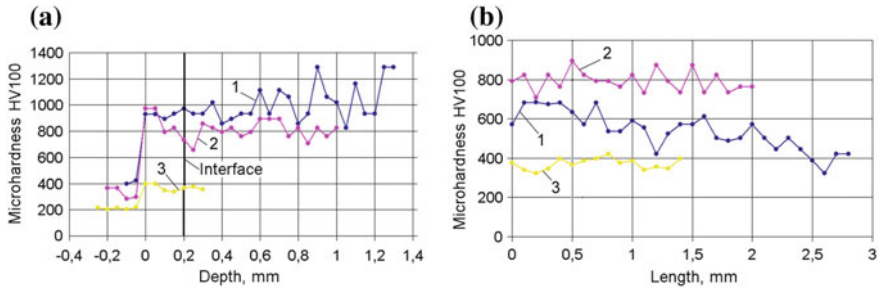
The finding that the coating elements do not penetrate the substrate is also supported by Fig. 6, which shows the distribution of the elements in the transient zone from the substrate to the coating. Nickel, chromium, and silicon contents are equal to zero already at a depth of 4.5 μm under the interface, and the Ni content was 4% and the Fe content was 95% on the interface. At a height of 4.5 μm above the substrate, the content of elements in the transient zone corresponds to their content all over the depth of the coating.

### 3.4 Microhardness of the Coating

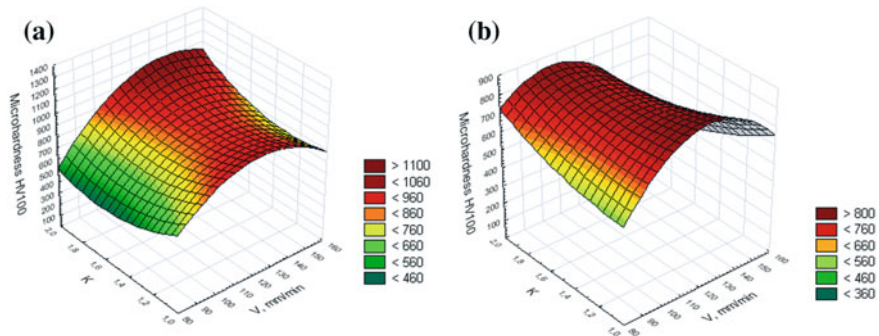
Microhardness changes by depth and along the coating are shown in Fig. 7. It is easy to notice that the microhardness increases in the “substrate—coating” interface, and then for each cladding condition, it is about at the same level throughout the coating depth (Fig. 8a). Microhardness fluctuations are of HV 100 = 200. Points with an extremely high or extremely low value of microhardness also occur, i.e., HV 100 = 1280 and HV 100 = 200. These changes are caused by the microstructure changes in different areas of the coating.

It is seen from the results of microhardness measurements in the longitudinal direction (Fig. 7b) that for each condition of laser cladding, the microhardness is





**Fig. 7** Changes of microhardness by depth (a) and length (b) of a coating: 1 –  $v = 80$  mm/min,  $L = 10$  mm,  $K = 1.0$  mm; 2 –  $v = 120$  mm/min,  $L = 12$  mm,  $K = 1.5$  mm; 3 –  $v = 160$  mm/min,  $L = 12$  mm,  $K = 2.0$  mm



**Fig. 8** Effect of laser cladding parameters on the microhardness of coating layer for the distance from the nozzle to the sample surface of  $L = 10$  mm (a) and  $L = 12$  mm (b)

approximately at the same level all over the length. Fluctuations of microhardness as well as its maximum and minimum values are similar to those in the depth of the single-layer coating.

The effect of laser cladding conditions (speed of the laser beam  $v$ , pitch  $K$ , and the distance from the nozzle to the sample surface  $L$ ) on the average microhardness has a complicated character (Fig. 8).

It is known that the crystal growth rate is always less than the nucleation rate and does not depend on the cooling rate and rate of cladding. At the same time, the rate of nucleation of crystals increases with increasing the cooling rate and cladding rate. For this reason, with an increase of the cladding rate from 80 to 120 mm/min, a decrease in the grain sizes and microhardness growth is observed. It is due to the growth of a crystal nucleation rate and to the essentially constant crystal growth rate. With a further increase of the cladding speed to 160 mm/min, despite the continuing reduction in the grains size, the lack of laser power input and a reduction of the fusion strength of grains cause a decrease of the microhardness.

## 4 Conclusions

Coatings of a Ni-based self-fluxing alloy have been formed by laser cladding using the CW CO<sub>2</sub> laser. The optimal granulation of a self-fluxing alloy powder and the relationship between the flow of powder of various fractions and the flow rate and pressure of the transporting gas have been determined for conditions of coaxial laser cladding. The formation regularities of a single-layer coating microstructure with different cladding conditions as well as patterns of element distribution over the coating depth and in the transient zone are defined. The microhardness distribution patterns by depth and length of the coating for various laser cladding conditions have been studied. It was found that optimal powder grain sizes are of 20–80 μ and reducing dimensions of the structural components and the depth of the heat-affected zone is observed with increasing the speed of the laser beam. The effect of speed of the laser beam, track pitch, and the distance from the nozzle to the coated surface on the average microhardness has a complicated character depended on the cooling conditions.

## References

1. Vandenbroucke, B., Kruth, J.-P.: Selective laser melting of biocompatible metals for rapid manufacturing of medical parts. *Rapid Prototyping J.* **13**, 196–203 (2007)
2. Dimitrov, D., Schreve, K., Beer, N.D.: Advances in three dimensional printing—state of the art and future perspectives. *Rapid Prototyping J.* **12**, 136–147 (2006)
3. Yadroitsev, I., Bertrand, P., Smurov, I.: Parametric analysis of the selective laser melting process. *Appl. Surf. Sci.* **253**, 8064–8069 (2007)
4. Ciurana, J., Hernandez, L., Delgado, J.: Energy density analysis on single tracks formed by selective laser melting with CoCrMo powder material. *Int. J. Adv. Manuf. Technol.* **68**, 1103–1110 (2013)
5. Averyanova, M., Cicala, E., Bertrand, P., Grevey, D.: Experimental design approach to optimize selective laser melting of martensitic 17–4 PH powder: part I—single laser tracks and first layer. *Rapid Prototyping J.* **18**, 28–37 (2012)
6. Pupo, Y., Monroy, K.P., Ciurana, J.: Influence of process parameters on surface quality of CoCrMo produced by selective laser melting. *Int. J. Adv. Manuf. Technol.* **80**, 985–995 (2015)
7. Arisoy, Y.M., Ciales, L.E., Özel, T., Lane, B., Moylan, S., Donmez, A.: Influence of scan strategy and process parameters on microstructure and its optimization in additively manufactured nickel alloy 625 via laser powder bed fusion. *Int. J. Adv. Manuf. Technol.* **90**, 1393–1417 (2017)
8. Ciales, L.E., Arisoy, Y.M., Lane, B., Moylan, S., Donmez, A., Özel, T.: Predictive modeling and optimization of multi-track processing for laser powder bed fusion of nickel alloy 625. *Add. Manuf.* **13**, 14–36 (2017)
9. Dunbar, A.J., Denlinger, E.R., Heigel, J., Michaleris, P., Guerrier, P., Martukanitz, R., Simpson, T.W.: Development of experimental method for in situ distortion and temperature measurements during the laser powder bed fusion additive manufacturing process. *Add. Manuf.* **12**, 25–30 (2016)

10. Stašić, J., Božić, D.: The effect of NiB additive on surface morphology and microstructure of 316L stainless steel single tracks and layers obtained by SLM. *Surf. Coat. Technol.* **307**, 407–417 (2016)
11. Aboulkhair, N.T., Maskery, I., Tuck, C., Ashcroft, I., Everitt, N.M.: On the formation of AlSi10 Mg single tracks and layers in selective laser melting: Microstructure and nano-mechanical properties. *J. Mater. Process. Technol.* **230**, 88–98 (2016)
12. Kempen, K., Thijs, L., Van Humbeeck, J., Kruth, J.: Processing AlSi10 Mg by selective laser melting: parameter optimization and material characterization. *Mater. Sci. Technol.* **31**, 917–923 (2014)
13. Monroy, K.P., Delgado, J., Sereno, L., Ciurana, J., Hendrichs, N.J.: Effects of the selective laser melting manufacturing process on the properties of CoCrMo single tracks. *Met. Mater. Int.* **20**, 873–884 (2014)
14. Fernández, E., Cadenas, M., González, R., Navas, C., Fernández, R., De Damborenea, J.: Wear behaviour of laser clad NiCrBSi coating. *Wear* **259**, 870–875 (2005)
15. Chen, H., Xu, C., Qu, J., Hutchings, I.M., Shipway, P.H., Liu, J.: Sliding wear behaviour of laser clad coatings based upon a nickel-based self-fluxing alloy co-deposited with conventional and nanostructured tungsten carbide–cobalt hardmetals. *Wear* **259**, 801–806 (2005)
16. Wang, X.H., Zhang, M., Liu, X.M., Qu, S.Y., Zou, Z.D.: Microstructure and wear properties of TiC/FeCrBSi surface composite coating prepared by laser cladding. *Surf. Coat. Technol.* **202**, 3600–3606 (2008)
17. Tong, X., Li, F.-H., Liu, M., Dai, M.-J., Zhou, H.: Thermal fatigue resistance of non-smooth cast iron treated by laser cladding with different self-fluxing alloys. *Opt. Laser Technol.* **42**, 1154–1161 (2010)
18. Aghasibeig, M., Fredriksson, H.: Laser cladding of a featureless iron-based alloy. *Surf. Coat. Technol.* **209**, 32–37 (2012)
19. Hemmati, I., Huizenga, R.M., Ocelík, V., De Hosson, J., Th, M.: Microstructural design of hardfacing Ni–Cr–B–Si–C alloys. *Acta Mater.* **61**, 6061–6070 (2013)
20. Feldshtein, E., Kardapolava, M., Dyachenko, O.: On the effectiveness of multi-component laser modifying of Fe-based self-fluxing coating with hard particulates. *Surf. Coat. Technol.* **307**, 254–261 (2016)
21. Janka, L., Norpoth, J., Eicher, S., Ripoll, M.R., Vuoristo, P.: Improving the toughness of thermally sprayed Cr 3C 2-NiCr hardmetal coatings by laser post-treatment. *Mater. Des.* **98**, 135–142 (2016)
22. Krolczyk, G.M., Nieslony, P., Krolczyk, J.B., Samardzic, I., Legutko, S., Hloch, S., Barrans, S., Maruda, R.W.: Influence of argon pollution on the weld surface morphology. *Measurement* **70**, 203–213 (2015)
23. Paulin, C., Chicet, D.L., Istrate, B., Panțuru, M., Munteanu, C.: Corrosion behavior aspects of Ni-base self-fluxing coatings. *IOP Conf. Ser. Mater. Sci. Eng.* **147**, 012034 (2016)
24. Sadeghimeresht, E., Markocsan, N., Nylén, P.: Microstructural characteristics and corrosion behavior of HVAF- and HVOF-sprayed Fe-based coatings. *Surf. Coat. Technol.* **318**, 365–373 (2017)

# Fracture Toughness of Plasma Paste-Borided Layers Produced on Nickel-Based Alloys

Magdalena Frackowiak, Natalia Makuch, Piotr Dziarski,  
Michal Kulka and Sukru Taktak

**Abstract** The boriding treatment is the suitable process which caused an increase in surface hardness and wear resistance of nickel and its alloys. However, the phase composition of boride layers strongly influences on layer properties—especially hardness and brittleness. The method of plasma paste boriding was used in this study to produce the hard boride layers on nickel-based alloys: Ni201, Inconel 600, and Nimonic 80A. This process was carried out at 800 °C (1073 K) for 3 h. The chemical composition of substrate material was the reason for producing of layers which were characterized by different thickness: 55 μm for Ni201, 42 μm for Inconel 600, 35 μm for Nimonic 80A. The lowest hardness (1000–1400 HV) and the highest fracture toughness (up to 2.6915 MPa m<sup>1/2</sup>) were measured for layer produced on Ni201. In this specimen, only nickel borides were detected. However, due to high content of chromium, in case of Inconel 600-alloy and Nimonic 80A-alloy, the higher hardness (in the range of 1000–2450 HV) and higher brittleness (average value of  $K_c = 0.77$  MPa m<sup>1/2</sup> for Inconel 600-alloy and  $K_c = 0.67$  MPa m<sup>1/2</sup> for Nimonic 80A-alloy) were calculated. This situation was caused by the appearance of hard ceramic phases (chromium borides CrB and Cr<sub>2</sub>B) in borided layer. Simultaneously, at the cross section of each sample, the strong fluctuation of hardness occurred, due to the variable participation of chromium and nickel borides.

**Keywords** Borided layer · Fracture toughness · Boriding · Hardness, nickel-based alloys

---

M. Frackowiak (✉) · N. Makuch · P. Dziarski · M. Kulka  
Institute of Materials Science and Engineering,  
Poznan University of Technology, Poznan, Poland  
e-mail: frackowiak.magdalena@doctorate.put.poznan.pl

S. Taktak  
Department of Metal Education, Technical Education Faculty,  
Afyon Kocatepe University, Afyonkarahisar, Turkey

## 1 Introduction

In the widely known industry, it is obvious for technology or production methods to change trying to follow the progress in knowledge. This process applies furthermore to materials' properties as a natural consequence of transformation. The most common procedure of material modification is a surface treatment as a faster and cheaper way. It also could be provided to elements that are already formed and shaped or those in need of slight renovation of surface.

In a wide range of different surface procedures, the most common is the thermo-chemical treatment wherein beside the heat energy also chemical reactions are involved because addition of other material like media containing carbon- [1], nitrogen- [2, 3], or boron-source [4] depending on the demanded result. Nickel alloys are unique due to the combination of their very good mechanical properties [5–8] and an excellent corrosion resistance [9, 10] in so many media. From common use of nickel alloys are restrained by serious disadvantage which is their low hardness and as a consequence of this also very poor wear resistance and therefore a surface treatment must be involved. For nickel alloys, only nitriding and boriding can be brought, not the carburizing because of very low solubility of carbon in nickel and therefore non-effective treatment [11].

The layers characterized by high hardness can reveal the tendency to cracking, chipping, and delamination in the working environment of high stress or dynamic loads. In order to investigate the fracture toughness of boride layers cracking examination, including Berkovich and Vickers marks was proposed by Anstis and others [12, 13]. All of these techniques can be summarized as a procedure consisting of few steps—producing indentation marks, measurement of necessary parameters like cracks length, hardness, or Young's modulus, and finally applying these values to appropriate equation. As a result of this calculation, the stress intensity factor ( $K_c$ ) is provided to describe material behavior under stress condition—the lower is this value the more brittle is investigated material.

In this paper, three different Ni-based alloys were subjected to the process of plasma boronizing using borax paste as a boron source. The influence of chemical composition of substrate on layer properties like thickness, microhardness, and fracture toughness was investigated.

## 2 Experimental Procedure

Samples used in the plasma boriding process were featured in flat slices with the thickness of 7 mm and diameter of 25 mm. They were made of Ni201, Inconel 600, and Nimonic 80A alloys. The chemical composition of materials used for this study is shown in Table 1.

Prior to the treatment, all of the samples were prepared by polishing (using paper gradation in presented order: 60, 120, 240, 360, 600). After polishing, it was

**Table 1** Chemical composition of substrate materials used in this study (wt%)

Material	Cr	Mn	Cu	Fe	Ti	Si	C	Al	Ni
Ni201	–	≤ 0.35	≤ 0.25	≤ 0.40	–	≤ 0.40	≤ 0.02	–	Balance
Inconel 600	15.72	0.16	0.04	8.63	–	0.18	0.078	0.06	Balance
Nimonic 80A	19.52	≤ 0.01	0.01	0.25	2.55	0.09	0.085	1.44	Balance

necessary to purify the sample surface with alcohol and dry thoroughly. The next step included covering samples with the paste (consisting of borax and ethyl alcohol) that was thick enough to keep the demanded feature of layer during the whole time of paste drying. The thickness of this layer was kept in the range of 1–1.5 mm. The last stage of preparation was to let the paste dry for about 24 h. The devices, applied to the plasma boriding process, consisted of the vacuum chamber, turbomolecular pump, vacuum meter, rotational pump, gas mixing chamber, and cylinders with the gases used during the process. The prepared samples were placed into the vacuum chamber, and the pressure was set to 0.01 Pa. The samples were plasma paste boronized at 800 °C (1073 K) for 3 h in a gas mixture of 70% H<sub>2</sub>–30% Ar under a constant pressure of 400 Pa. After the process finished, the specimens were cooling in the chamber in the atmosphere of argon.

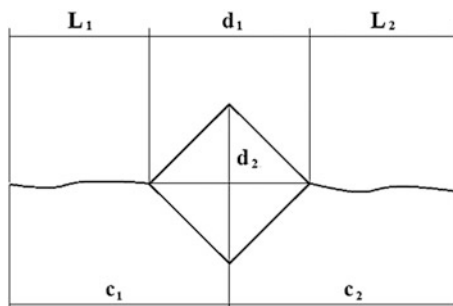
Directly after plasma paste boriding process, the investigation of phase composition was carried out by PANalytical EMPYREAN X-ray diffractometer using Cu K<sub>α</sub> radiation. Then the samples were cut perpendicular to the top surface in order to reveal the cross section of the produced layer and a matrix. The next step was preparing the samples to optical microscopy (OM) observation by grinding and polishing with aluminum oxide suspension. The last step was etching using the Marble's reagent, which consisted of HF, HNO<sub>3</sub>, and H<sub>2</sub>O mixed by volume ratio of 2:1:47. Microhardness test was carried out using the Vickers indenter with load (*F*) of 0.49 N (HV 0.05) by 15 s, according to PN-EN ISO 6507-1. In this study, the diamond pyramid with the α-angle of 136° was used as an indenter to produce the indentation marks. In order to determine the microhardness value, the following relation was used:

$$HV = 1.891 \left( \frac{F}{d^2} \right) \quad (1)$$

where *F*—load, N; *d*—the arithmetic average of the length of two mark's diagonals *d*<sub>1</sub> and *d*<sub>2</sub>, mm.

In order to evaluate fracture toughness of plasma-borided layers, the Vickers indenter was applied to obtain indentation marks with cracks that were measured as shown in Fig. 1. The indentation marks were placed on polished and etched cross section. The load value was set on 0.98 N, and the time of load was 15 s. This method uses a model of elastic–plastic behavior of the material under the impression—a system of the central and radial cracks is a result of the tensile stresses

**Fig. 1** Schematic views of the obtained indentation mark with cracks



caused without load. In this study, the fracture toughness of borided layer produced on Ni-based alloys has been determined based on the measurements of  $K_C$  factor according to equation [14]:

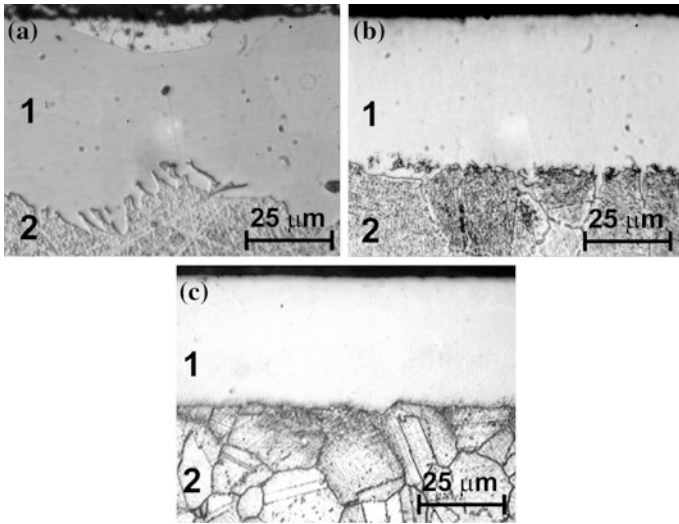
$$K_C = A \frac{P}{c^{\frac{3}{2}}} [\text{MPa m}^{1/2}] \quad (2)$$

$$A = 0.028 \left( \frac{E}{H} \right)^{\frac{1}{2}} \quad (3)$$

where  $P$ —load, N;  $c$ —the radial crack length, m;  $A$ —residual indentation coefficient;  $E$ —Young's modulus, MPa;  $H$ —hardness, MPa.

### 3 Results and Discussion

The microstructures of borided layers, produced on Ni-based alloys, obtained by optic microscopy are shown in Fig. 2a–c. Microstructure analysis showed that all of the layers were dense, very fine-grained, and porous-free. Layer thickness depended on the chemical composition of the substrate, because of its influence on the phases that could be formed in layer and hence a different growth kinetics of these phases. In case of Ni201 material, the characteristic shape of the transition zone between the layer and the matrix was noticeable—the needle-like structure coming from the nickel borides. For Nimonic 80A and Inconel 600 alloys, the transition zone featured as a way more smooth, flatline. This situation was caused by the high concentration of chromium in Inconel 600-alloy and Nimonic 80A-alloy. Moreover, the high concentration of chromium was the reason for difficult diffusion of boron atoms during boriding process as assumed. Therefore, the thickness measured for borided layers produced on Nimonic 80A-alloy and Inconel 600-alloy was lower (average value of 35 and 42  $\mu\text{m}$ , respectively) when compared with borided Ni201 (55  $\mu\text{m}$ ).

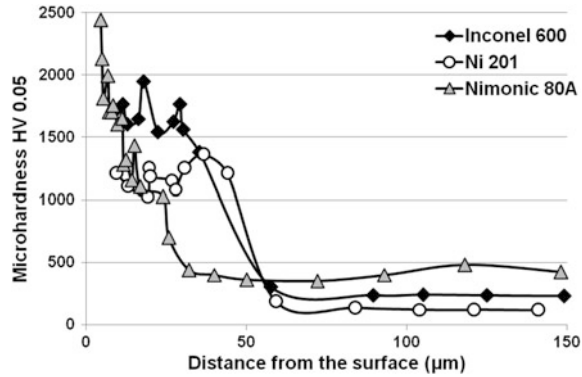


**Fig. 2** Microstructure of plasma paste-borided layers formed on **a** Ni201, **b** Inconel 600-alloy, and **c** Nimonic 80A-alloy; 1—compact boride zone; 2—substrate (base material), obtained from optic microscopy

In case of borided Ni201, the presence of nickel borides ( $\text{NiB}$ ,  $\text{Ni}_2\text{B}$ ,  $\text{Ni}_3\text{B}$ , and  $\text{Ni}_4\text{B}_3$ ) was detected. The high concentration of chromium in Inconel 600-alloy and Nimonic 80A-alloy caused the appearance of chromium borides ( $\text{CrB}$  and  $\text{Cr}_2\text{B}$ ). Moreover, the nickel borides ( $\text{NiB}$ ,  $\text{Ni}_2\text{B}$ ,  $\text{Ni}_3\text{B}$ , and  $\text{Ni}_4\text{B}_3$ ) were also identified. The microhardness profiles of plasma paste-borided nickel-based alloys are presented in Fig. 3. The boriding process caused the significant increase in hardness of the surface layer for all of the samples. The lower values of hardness were characteristic of borided layer produced on Ni201. The obtained microhardness was in the range of 1000–1400 HV. Ni201 contained only nickel without chromium or iron addition. Therefore, in this case, only the nickel borides occurred in the produced layers. These results confirmed also the papers [15, 16]. The higher microhardness was obtained for borided Nimonic 80A-alloy. The maximal hardness of 2450 HV was measured near the top surface. However, in the compact borides layer, the high differences between the lowest and the highest hardness occurred. The fluctuation of hardness through the cross section of plasma paste-borided layer produced on Nimonic 80A-alloy probably was caused by a change in volume fraction of chromium borides. According to earlier paper [4], the lower values (1000–1500 HV) corresponded to the measured area in which the amount of nickel borides was higher, whereas the higher hardness (1600–2450 HV) was characteristic of areas in which higher content of hard chromium borides occurred. The same effect can be observed for plasma paste borided Inconel 600-alloy. However, the lower concentration of chromium in this alloy could be the reason for the

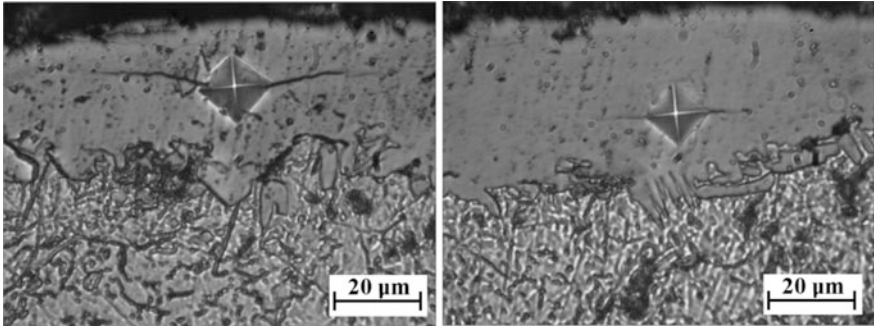


**Fig. 3** Microhardness profiles of plasma paste-borided layers formed on Ni201, Inconel 600-alloy, and Nimonic 80A-alloy

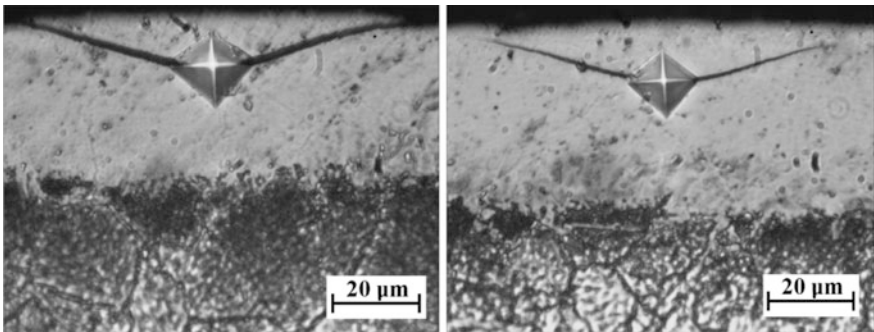


diminished amount of chromium borides in borided layer. Therefore, the slightly lower hardness was measured in this layer.

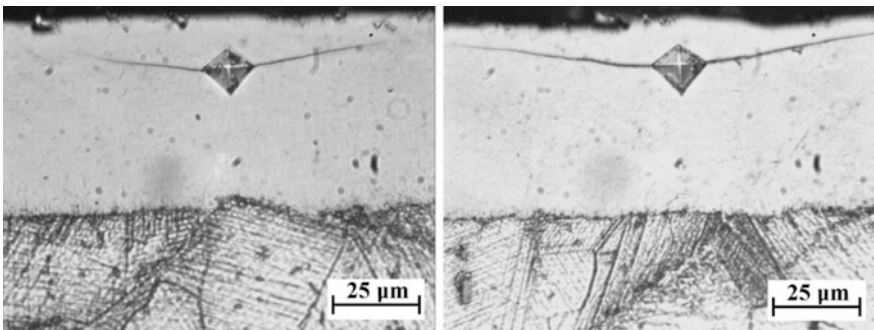
The fracture toughness measurements were carried out through a cross section of the specimens at the distance from the surface of about 15 µm. As a result of the Vickers hardness test, the indentation marks with cracks were generated. For the fracture toughness calculation, the Young's modulus was necessary. In case of borided layer produced on Ni201 substrate, it was obvious that the value typical for nickel borides could be used. Therefore, according to earlier study [17], for  $K_c$  calculation, the  $E$  value of 287.91 GPa was taken. In case of borided layers produced on high-chromium alloys (Inconel 600 and Nimonic 80A), the average value of Young's modulus was evaluated. These layers consisted of nickel and chromium borides mixture, which suggested that the higher  $E$  value should be taken for fracture toughness measurements. The Young's modulus of chromium borides evaluated in paper [17] was equal to 355.11 GPa. Therefore, in this study, the average value of  $E$  was used for calculation (321.51 GPa). The OM micrographs of the indentation marks with visible microcracks are presented in Figs. 4, 5 and 6. First, it should be noticed that the cracks were generated only in a direction parallel to the surface. Some authors reported [18] that the strong influence on brittleness has stress distribution across the borided layers. The presence of compressive stresses in the normal (perpendicular to the surface) direction caused that the growth and propagation of microcracks produced by an indentation in this direction were blocked. As a result, the cracks appeared only in the direction parallel to the surface. The chemical composition of substrate material doesn't influence on this behavior. However, the differences in cracks length were observed. In case of borided layer produced on Ni201 (Fig. 4), the cracks' length was lower when compared to those obtained in case of layer produced on Inconel 600-alloy (Fig. 5) or Nimonic 80A-alloy (Fig. 6). The longest crack length was measured for Nimonic 80A-alloy. Obviously, the higher crack length caused diminished fracture toughness. In Table 2, the  $K_c$  values for all the samples were compiled. The six indentation marks were performed for each specimen. Due to the anisotropy of the borided layer, it was possible to calculate the fracture toughness only for the microcracks, obtained



**Fig. 4** OM images of Vickers indentation marks with cracks generated in borided layer produced on Ni201



**Fig. 5** OM images of Vickers indentation marks with cracks generated in borided layer produced on Inconel 600-alloy



**Fig. 6** OM images of Vickers indentation marks with cracks generated in borided layer produced on Nimonic 80A-alloy

**Table 2** Results of  $K_c$  measurements for borided layers produced on Ni-based alloys

Indentation mark	$K_c$ (MPa m <sup>1/2</sup> )		
	Ni201	Inconel 600	Nimonic 80A
1	1.0220	0.4929	0.3046
2	1.1116	0.6146	0.4899
3	1.2057	0.6616	0.5211
4	2.1261	0.7117	0.7607
5	2.2298	1.0334	0.8277
6	2.6915	1.1105	0.9821

in the direction parallel to the surface. The chemical composition of substrate material strongly influenced the brittleness of borides layers. In case of Ni201 layer consisted only of nickel borides. Such a phase composition was the reason for lower hardness and higher fracture toughness (average value  $K_c = 1.73$  MPa m<sup>1/2</sup>). The more brittle were layers contains nickel and chromium borides. The presence of hard chromium borides caused a decrease in fracture toughness for borided layers produced on Inconel 600-alloy (average value  $K_c = 0.77$  MPa m<sup>1/2</sup>) and Nimonic 80A-alloy (average value  $K_c = 0.67$  MPa m<sup>1/2</sup>). After analysis of data compiled in Table 2, it can be found that for each material the differences in  $K_c$  values occurred. The lowest fracture toughness for borided layer produced on Ni201 was equal to 1.022 MPa m<sup>1/2</sup>, whereas the higher  $K_c$  for the same sample was equal to 2.6915 MPa m<sup>1/2</sup>. Similar behavior was noticed in the case of nickel–chromium alloys examined in this study. These differences between the lowest and the highest value of fracture toughness could be related to the variable phase composition across the borided layers and stress distribution in the cross section of layers.

## 4 Summary and Conclusions

Plasma paste boriding at temperature of 800 °C (1073 K) for 3 h was used to produce the hard borided layers on Ni-based alloys, which differed in chromium content. The following conclusions can be formulated from the obtained results:

- All of the produced layers were compact and porous-free. The fine-grained microstructure was the characteristic of these layers.
- The chemical composition of substrate material strongly influenced on layer thickness. The higher thickness of 55 μm was measured for layer produced on Ni201 (alloy without the addition of chromium). The high content of chromium in Inconel 600-alloy and Nimonic 80A-alloy was the reason for diminished layer thickness, 42 and 35 μm, respectively.
- The phase composition of the produced layers was the reason for differences in hardness and fracture toughness.
- The presence of chromium borides caused an increase in hardness (up to 2450 HV in case of Nimonic 80A-alloy).

- Simultaneously, the higher participation of chromium borides caused a decrease in fracture toughness (for Nimonic 80A-alloy, the lowest value  $K_c$  of 0.3046 MPa m<sup>1/2</sup>).

**Acknowledgements** During the realization of this work Ph.D. Natalia Makuch was supported by the Foundation for Polish Science (FNP).

## References

1. Flis-Kabulska, I., Sun, Y., Zakroczymski, T., Flis, J.: Plasma carburizing for improvement of Ni-Fe cathodes for alkaline water electrolysis. *Electrochimica* **220**, 11–19 (2016)
2. Paosawatyanong, B., Pongsopa, J., Visuttiptitaku, P., Bhanthumnavin, W.: Nitriding of tool steel using dual DC/RFICP plasma process. *Surf. Coat. Technol.* **306**, 351–357 (2016)
3. Aw, P.K., Batchelor, A.W., Loh, N.L.: Structure and tribological properties of plasma nitride surface films on Inconel 718. *Surf. Coat. Technol.* **89**, 70–76 (1997)
4. Makuch, N., Kulka, M.: Fracture toughness of hard ceramic phases produced on Nimonic 80A-alloy by gas boriding. *Ceram. Int.* **42**, 3275–3289 (2016)
5. Pirowski, Z., Uhl, W., Wodnicki, J., Gwiżdż, A., Jaśkowiec, K.: Effect of heat treatment of structure of the Inconel 740 type alloy. *Inst. Cast.* **2**, 5–22 (2011)
6. Jiang, T., Chen, L., Jiang, F., Cai, H., Sun, J.: Microstructural evolution and mechanical properties of a nickel-based superalloy through long-term service. *Mater. Sci. Eng.* **656**, 184–189 (2016)
7. Zla, S., Smetana, B., Žaludova, M., Dobrovska, J., Kalup, A., Vodarek, V., Konecna, K.: Determination of thermophysical and structural properties of nickel super-alloy. *Metalurgija* **54**, 639–642 (2015)
8. Srinivasan, N., Prasad, Y.V.R.K.: Hot working characteristics of Nimonic 75, 80A and 90 superalloys: a comparison using processing maps. *J. Mater. Process. Technol.* **51**, 171–192 (1995)
9. Petrova, R.S., Suwattananont, N., Pallegar, K.K., Vangaveti, R.: Boron coating to combat corrosion and oxidation. *Corros. Rev.* **25**, 555–569 (2007)
10. Soo-Haeng, C., Jin-Mok, H., Chung-Seok, S., Seong-Won, P.: High temperature corrosion of superalloys in a molten salt under an oxidizing atmosphere. *J. Alloy. Compd.* **452**, 11–15 (2006)
11. Rosier, J., Mtiller, S.: Life extension of IN706 type disc materials by surface modification with Boron, RTO MP, vol. 17, pp. 1998.
12. Anstis, G.R., Chantikul, P., Lawn, B.R., Marshall, D.B.: A critical evaluation of indentation techniques for measuring fracture toughness: I, direct crack measurements. *J. Am. Ceram. Soc.* **64**, 533–538 (1981)
13. Anstis, G.R., Chantikul, P., Lawn, B.R., Marshall, D.B.: A critical evaluation of indentation techniques for measuring fracture toughness: II, strength method. *J. Am. Ceram. Soc.* **64**, 539–543 (1981)
14. Ucisik, A.H., Bindal, C.: Fracture toughness of boride formed on low-alloy steel. *Surf. Coat. Technol.* **94–95**, 561–565 (1997)
15. Ozbek, I., Akbulut, H., Zeytin, S., Bindal, C., HikmetUcisik, A.: The characterization of borided 99.5% purity nickel. *Surf. Coat. Technol.* **126**, 166–170 (2000)
16. Gunes, I., Kayali, Y.: Investigation of mechanical properties of borided Nickel 201 alloy. *Mater. Des.* **53**, 577–580 (2014)

17. Kulka, M., Makuch, N., Dziarski, P., Piasecki, A.: A study of nanoindentation for mechanical characterization of chromium and nickel borides' mixtures formed by laser boriding. *Ceram. Int.* **40**, 6083–6094 (2014)
18. Campos, I., Rosas, R., Figueroa, U., VillaVelazquez, C., Meneses, A., Guevara, A.: Fracture toughness evaluation using Palmqvist crack models on AISI1045 borided steels. *Mater. Sci. Eng. A* **488**, 562–568 (2008)

# Effect of Residual Stresses in Surface Layer of Nickel-Based Alloy—Inconel 718 on the Safety Factor of Construction

Joanna Krajewska-Spiewak and Jozef Gawlik

**Abstract** Characteristics of the surface layer of difficult-to-cut materials have been presented in the article. Residual stresses generated in the material during machining process can be distinguished among many other properties of the surface layer. The main goal of the research was to determine the influence of peripheral milling on residual stresses state in the surface layer of the workpiece made out of Inconel 718. In order to determine safety factor of construction (based on stochastic dependence), residual stresses and exploitation stresses were taken into account.

**Keywords** Inconel 718 · Residual stresses · Safety factor of construction

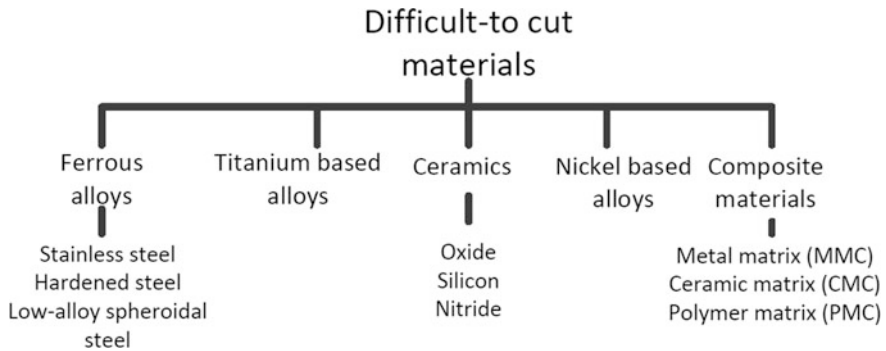
## 1 Introduction

Development of new constructions is associated among others with increasing demand for new engineering materials. These materials, in general, belong to the group of difficult-to-cut materials and are most commonly used in following types of industries: aerospace, maritime, petrochemical, and biomedical engineering. The increasing demand of these materials is justified through their unique properties, which include high strength at relatively low density, creep resistance, and resistance to fatigue failures.

Ezugwu in his work [1] suggested the division of difficult-to-cut materials into four main groups: titanium-based alloys, nickel-based alloys, ceramics, and ferrous alloys. Additional type of material (composite materials) has been added to this division which is presented on Fig. 1.

---

J. Krajewska-Spiewak (✉) · J. Gawlik  
Cracow University of Technology, Cracow, Poland  
e-mail: jkspiewak@mech.pk.edu.pl; jgawlik@mech.pk.edu.pl



**Fig. 1** Division of difficult-to-cut materials

## 2 The Characteristics of the Surface Layer Formed in the Cutting Process

Machining is an oriented and controlled process of cracking which is accompanied by progressive separation of the material in form of the chip with the use of wedge blade [2]. The cutting tool is a carrier of focused, external mechanical energy. The energy inside the material increases with the increase of plastic deformation. Crystal lattice is subjected to the increasing value of plastic deformation which alters properties of the workpiece.

During machining process, new stress state is generated which results in energy changes in the cutting zone. Stresses which are present in the material during external load and stresses present in the material in the absence of the influence of external forces can be distinguished [3]. Another division of stresses is based on the area of size in which they balance. According to Davidenkov's classification, stresses can be divided into:

- Macro-residual stresses (1st type of RS) appear in the area where their size is compared with the size of the workpiece. The existence of these stresses can be determined based on the displacement of diffraction lines in proper direction.
- Micro-residual stresses (2nd type of RS) appear in the area where their size is compared with the size of the grain. These residual stresses can be further divided into oriented residual stresses which arise as a result of oriented plastic deformation, and they cause an angular shift of diffraction lines. Unoriented residual stresses cause diffraction line broadening.
- Sub-residual stresses (3rd type of RS) appear in the area of the few atomic distances. The force and moment equilibrium exist in sufficiently large parts of a crystallite. These stresses are caused by numbers of deformations in crystal lattice (e.g., delamination and dislocations).

Stresses can be also distinguished based on the cause of their formation. Thereby, following types of stresses can be given: mechanical, thermal, and

structural. Structural stresses arise from volumetric changes [4, 5]. They are generally caused by phase transitions and are determined by temperature and time. In case of increased specific volume, compressive stresses are present, otherwise tensile stresses occur. The uneven heating or cooling process of particular layers of the material leads to thermal stresses. After reaching a temperature below core temperature, compressive residual stresses are formed, while tensile stresses occur inside of the core. During machining process, mechanical stresses arise as a result of uneven deformation of the surface layer of the workpiece.

### 3 Impact of Cutting Conditions on Stress State in the Surface Layer of Inconel 718

Research was carried out on samples made out of nickel-based alloy—Inconel 718 through the wide range of its industrial applications. The main goal of the research was to determine the influence of peripheral milling on residual stresses state in the surface layer of the workpiece. During machining process, cutting forces were recorded by a Kistler three—component piezo dynamometer. The scheme of the workstation is presented on Fig. 2. The course of cutting forces was registered to correlate the obtained data with calculated values of residual stresses. After milling process, residual stresses were determined by X-ray diffractometer. Measurements were performed at the Institute for Sustainable Technologies—National Research Institute in Radom.

Table 1 presents scheme of the research program, while Table 2 contains ranges of variable parameters during milling process of Inconel 718.

The values of calculated residual stresses are presented in Table 3. Residual stresses were identified in samples made out of nickel-based alloy—Inconel 718 after peripheral, down-cut milling. Research was carried out on a diffractometer (Bruker's company), where  $\sigma_r$ —stresses calculated in the parallel direction toward milling process,  $\sigma_p$ —stresses calculated in the perpendicular direction toward milling process.

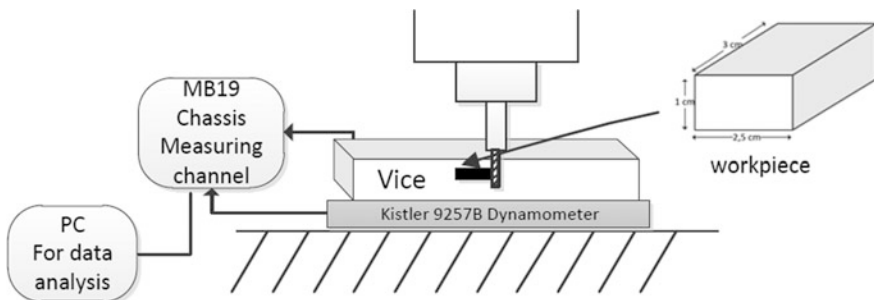


Fig. 2 Scheme of the work station and dimensions of the test sample [6]



**Table 1** Scheme of the research program

No.	Code		
	x1	x2	x3
1.	-1	-1	-1
2.	+1	-1	-1
3.	-1	+1	-1
4.	+1	+1	-1
5.	-1	-1	+1
6.	+1	-1	+1
7.	-1	+1	+1
8.	+1	+1	+1
9.	$-\alpha$	0	0
10.	$+\alpha$	0	0
11.	0	$-\alpha$	0
12.	0	$+\alpha$	0
13.	0	0	$-\alpha$
14.	0	0	$+\alpha$
15.	0	0	0

**Table 2** Variable cutting parameters used during milling process

$\alpha = 1.215$	Rotation speed $n$ (rot/min) $x_1$	Feed $f$ (mm/min) $x_2$	Depth of cut $a_p$ (mm) $x_3$
$-\alpha$	955	100	0.2
-1	1485	280	0.35
0	1978	550	0.5
+1	2470	820	0.65

Carried out research confirms that a texturization of crystal lattice occurs in the surface layer during machining process in the direction of feed motion. Tensile stresses occurred in the surface layer of nickel-based alloys after milling.

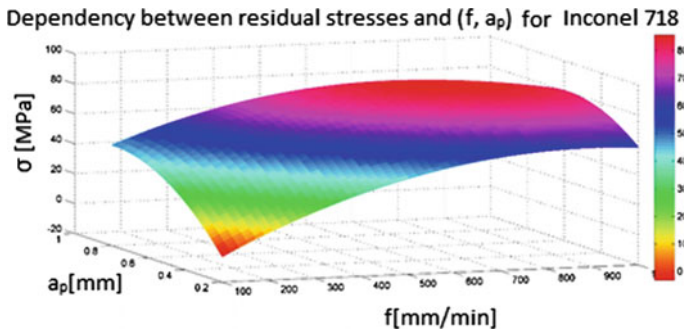
The function of the research object was developed in order to determine the dependence between cutting parameters and residual stresses. Second degree of a polynomial function was created with interaction for three input parameters ( $v_c$ ,  $f$ , and  $a_p$ ). Obtained results are shown in a graphical form in Figs. 3, 4, and 5.

## 4 Safety Factor in Terms of Construction Reliability

Heterogeneity of the structure of materials, dispersion of values of strength characteristics, and instability of exploitation conditions are factors which justify consideration of safety factor of construction. Based on the research developed by Loladze [7] and Betanelego [8], safety factor ( $\vartheta$ ) can be presented as followed:

**Table 3** Calculated stresses values generated in the surface layer of Inconel 718 [6]

No.	$\sigma_r$ (MPa)	$\sigma_p$ (MPa)	No.	$\sigma_r$ (MPa)	$\sigma_p$ (MPa)	No.	$\sigma_r$ (MPa)	$\sigma_p$ (MPa)
N1-1	545	439	N33-1	639	618	N6-1	352	199
N1-2	582	452	N33-2	706	654	N6-2	549	370
N1-3	588	547	N33-3	737	693	N6-3	611	448
N1-4	604	558	N33-4	680	640			
N11-1	489	376	N4-1	833	792	N66-1	703	658
N11-2	369	369	N4-2	890	813	N66-2	893	755
N11-3	365	365	N4-3	850	804	N66-3	870	724
N11-4	425	346	N4-4	795	815			
N2-1	677	720	N44-1	986	928	N7-1	544	418
N2-2	856	820	N44-2	1002	933	N7-2	536	375
N2-3	841	827	N44-3	919	860	N7-3	549	393
N2-4	733	774	N44-4	956	904	N7-4	625	462
N22-1	767	762	N5-1	719	693	N77-1	585	747
N22-2	822	766	N5-2	721	712	N77-2	823	803
N22-3	770	773	N5-3	486	475	N77-3	845	837
N22-4	750	730	N5-4			N77-4	820	816
N3-1	513	546	N55-1	538	564	N8-1	766	733
N3-2	703	615	N55-2	820	748	N8-2	814	716
N3-3	638	597	N55-3	689	594	N8-3	786	734
N3-4	550	568	N55-4	674	626			

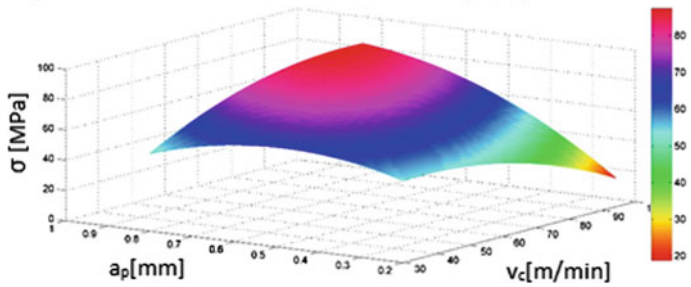


**Fig. 3** Relationship between residual stresses and variable values of cutting parameters—feed and depth of cut ( $f, a_p$ ) at constant cutting speed  $v_c = 62.1$  [m/min] [6]

$$\vartheta = \frac{X_\sigma}{X_g} \tag{1}$$

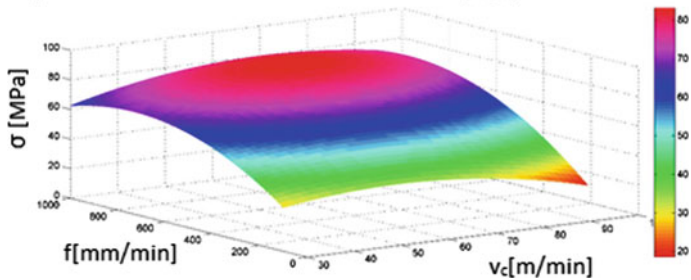
where  $X_\sigma$ —determines the stress state in the material;  $X_g$ —determines the limit of ultimate strength of the material.

Dependence between residual stresses and ( $v_c, a_p$ ) for Inconel 718



**Fig. 4** Relationship between values of residual stresses and variable values of cutting parameters—cutting speed and depth of cut ( $v_c, a_p$ ) at constant feed  $f = 550$  [mm/min] [6]

Dependence between residual stresses and ( $v_c, f$ ) for Inconel 718



**Fig. 5** Relationship between residual stresses and variable values of cutting parameters—cutting speed and feed ( $v_c, f$ ) at constant depth of cut  $a_p = 0.5$  [mm] [6]

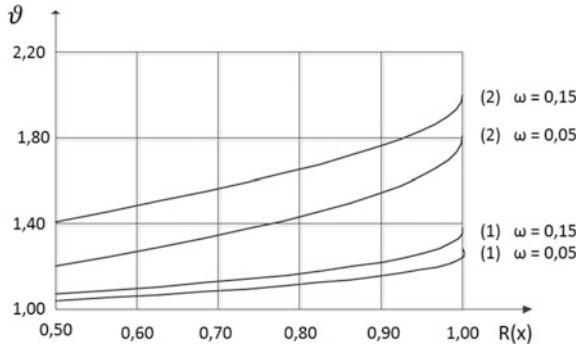
Strength characteristics of construction materials can be usually described by normal distribution. For a given quantile percentage ( $\gamma$ ), the safety factor of the construction can be presented as followed:

$$\vartheta = \frac{1 - \omega_\sigma \cdot \gamma_R}{1 - \omega_d \cdot \gamma_{1-R}} \tag{2}$$

where  $\omega_\sigma = \frac{D_{X_\sigma}}{X_{\sigma_s}}$ —variation coefficient of stresses  $\omega_d = \frac{D_{X_g}}{X_{g_s}}$ —variation coefficient of the limit of ultimate strength of the material;  $\gamma_R$ — $R$ —quantile percentage of normalized normal distribution and  $\gamma_{1-R}$  ( $1-p$ ) quantile percentage of normalized normal distribution for determined level ( $p$ ) of construction reliability ( $s$ );  $D_{X_\sigma}$ —standard deviation of stresses dispersion and  $D_{X_g}$ —standard deviation of the limit of ultimate strength of the material;  $X_{\sigma_s}$  average value of stresses and  $X_{g_s}$ —average value of the ultimate strength of the material.

The analysis of Eq. 2 indicates the safety factor of the construction that strongly depends on the dispersion of mechanical properties of the material and

**Fig. 6** Dependence between safety factor ( $\vartheta$ ); reliability level ( $R$ ); and coefficient of variation  $\omega$  for two values of probability ( $p$ ) of achieving assumed reliability ( $R$ ); 1  $p = 0.90$ ; 2:  $p = 0.975$



assumed/established level of construction reliability [9, 10]. To simplify (the model, the calculations), the authors assumed  $\omega = \omega_{\sigma} = \omega_d$ . Figure 6 shows the change of safety factor  $\vartheta$ .

The results obtained from carried out research show that residual stresses arise after machining process and are present on the surface layer of the workpiece. These stresses affect the behavior of the element and they have an impact on the construction reliability. Stresses arise in the material as a result of external load. Generated residual stresses can add up and cause number of undesired effects (e.g., delaminations, cracing, tribological wear). Therefore, residual stresses should be taken into account during determination of safety factor.

With the use of chi-square test  $\chi^2$  authors demonstrated that in significance level equal to  $\alpha = 0.05$ , there is no reason to reject the hypothesis of the normal distribution of residual stress in the surface layer of Inconel 718 alloy. The dependence of safety factor takes the following form:

$$\vartheta = \frac{1 - \omega_{\sigma_w} \cdot \gamma_R}{1 - \omega_d \cdot \gamma_{1-R}} \tag{3}$$

where  $\omega_{\sigma_w} = \frac{D_{X_{\sigma}} + D_{X_r}}{X_{\sigma_s} + X_{\sigma_r}}$ —variation coefficient of combined stresses in a material, ( $X_{\sigma}$ ) exploitation stresses, ( $X_r$ ) residual stresses,  $D_{X_r}$ —standard deviation of residual stresses and  $X_{\sigma_r}$ —average value of residual stresses.

## 5 Conclusions

Multi-blade milling process of Inconel 718 alloy generates residual stresses in formed surface layer of the workpiece. The possibility of residual stresses summation must take into account during strength calculations when structures are subjected to external loads at the allowable level. Therefore, in order to ensure reliable operation of construction determination of the proper safety factor is necessary.

## References

1. Ezugwu, E.O.: High speed machining of aero-engine alloys. *J. Braz. Soc. of Mech. Eci. Eng.* **XXVI**(1), (2000)
2. Dornfeld, D.: Process monitoring and control for precision manufacturing. *Prod. Eng.* **6**, 29–34 (1999)
3. Burakowski, T.: *Areology, Theoretical basics* (in Polish) Scientific Publishing of the Institute for Sustainable Technologies—PIB 2013
4. Radziejewska, J., Skrzypek, S.J.: Microstructure and residual stresses in surface layer of simultaneously laser alloyed and burnished steel. *J. Mater. Process. Technol.* **209**, (2009)
5. Toshiaki, S., Hiroyuki, S., Masaomi, T.: Development of a new tool to generate compressive residual stress within a machined surface. *Int. J. Mach. Tools Manufac.* **44**, (2004)
6. Krajewska-Śpiewak, J.: Identification of the properties of surface layer of difficult-to-cut materials (in Polish). Dissertation, Cracow University of Technology, (2016)
7. Stakhniv, N.E., Devin, L.N.: The study of wear of cutting tools of cBN-based composite material and the influence of tool wear on cutting forces in turning hardened steel. *J. Superhard Mater.* **33**, 129 (2011)
8. Wang, P., Gao, R.X.: Stochastic tool wear prediction for sustainable manufacturing. *Procedia CIPR* 48, (2016)
9. Gawlik, J., Karbowski, K.: Forecasting of the wear state of the cutting tools in the cutting process (in Polish). Published by Cracow University of Technology. Monograph No. 66, (1998)
10. Odelros, S.: *Tool wear in titanium machining*. Uppsala University, (2012)

# Influence of Preparation Conditions on Final Dielectric Properties of Pure and Ca-Doped BaTiO<sub>3</sub> Ceramics

Izabela Szafraniak-Wiza, Anna Włodarkiewicz, Ewa Markiewicz, Bożena Hilczer, Kamil Feliksik and Lucjan Kozielski

**Abstract** Improvement of dielectric properties of commonly used electroceramic materials plays an important role in the development of modern electronics. This paper has described the preparations and properties of lead-free BaTiO<sub>3</sub>-based ceramics obtained from mechanochemically synthesized powder. Ba<sub>1-x</sub>Ca<sub>x</sub>TiO<sub>3</sub> powders with different calcium contents ( $0 \leq x \leq 0.20$ ) have been successfully obtained by mechanochemical synthesis directly at room temperature (without any additional thermal treatment). Mechanochemically triggered reaction, leading to the formation of perovskite phase, has been monitored by XRD at different stages. Pure and Ca-doped barium titanate powders have been consolidated (1) by pressing and subsequently conventional sintering or (2) by hot pressing. The influence of the sintering method on the dielectric properties of the ceramics has been investigated by dielectric spectroscopy in the temperature range from 25 to 180 °C. Both the sintering method and the doping with Ca have a strong effect on the dielectric permittivity and dielectric losses of barium titanate ceramics.

**Keywords** Lead-free piezoceramics · Mechanochemical synthesis  
Hot pressing · Perovskite · Dielectric properties

---

I. Szafraniak-Wiza (✉) · A. Włodarkiewicz  
Faculty of Mechanical Engineering and Management,  
Institute of Materials Science and Engineering, Poznań University of Technology,  
Poznań, Poland  
e-mail: izabela.szafraniak-wiza@put.poznan.pl

E. Markiewicz · B. Hilczer  
Institute of Molecular Physics, Polish Academy of Sciences, Poznań, Poland

K. Feliksik · L. Kozielski  
Faculty of Computer Science and Material Science, Institute of Technology  
and Mechatronics, University of Silesia, Sosnowiec, Poland

## 1 Introduction

Ferroelectric ceramic materials play a very important role in modern technology. Broad range of applications comprises devices based on dielectric, piezoelectric, pyroelectric, or electro-optic properties of ferroelectric materials, to list just a few [1–3]. For a long time, lead zirconate titanate (PZT) has been the most widely used piezoceramic material because of its excellent properties and low cost. Recently, the awareness of the environmental and health hazards caused by the toxicity of lead is increasing, and as a result, several regulations limiting the usage of this element are introduced and lots of scientific research are focused on the development of lead-free materials [4–6]. Despite the fact that the candidates, considered as the future replacements for lead-based piezoelectric, are not as versatile in properties as PZT, it should be possible to find a set of different materials tailored to the specific applications. One of the most attractive lead-free materials for devices operating mainly at room temperature, like X7R multilayer ceramic capacitors, is barium titanate ( $\text{BaTiO}_3$ ) [2]. Doping with calcium has been found to be an effective way to improve the thermal stability of its properties [1, 7, 8].

Growing demands for higher performance and more efficient devices, as well as for less time- and energy-consuming manufacturing processes, are directly connected to the properties and quality of the materials. In the case of perovskite-type piezoelectric ceramic powders, conventional solid-state synthesis is the most commonly used preparation method. Nevertheless, there are several problems arising from the high-temperature treatment. Volatilization of some elements can lead to the changes in the stoichiometry, chemical inhomogeneity of the material, and formation of secondary phases. The grain growth and the agglomeration of the powder particles, obtained by conventional solid-state synthesis, lead to poor material sinterability. Mechanochemical synthesis is the novel processing technique that allows the preparation of crystalline piezoceramic powders at room temperature or at least significantly decreases the thermal treatment, at which the reaction occurs [9–11].

Pure and Ca-doped barium titanate has been successfully obtained directly after milling, without any additional calcination step [11–13]. In the mechanochemical synthesis process, thermal activation of the diffusion, necessary for the reaction to proceed, is replaced by the mechanical activation originated from the high energy of the collisions between milling balls, powder particles, and the walls of the vial. The generation of many structural defects and the increase in the specific surface area of the powders are the main factors that accelerate the diffusion rate. The product layer, formed at the interface of the reactants, is repeatedly crushed, and the new, fresh surfaces are created. As a result, the powders become much more reactive and the desired phase can be obtained directly at room temperature [9–12].

In this work,  $\text{Ba}_{1-x}\text{Ca}_x\text{TiO}_3$  nanopowders with different calcium contents ( $0 \leq x \leq 0.20$ ) have been obtained directly by mechanochemical synthesis at room temperature. The calcium content has been selected to be below the solubility limit of Ca at A-site of  $\text{BaTiO}_3$  which is  $x \sim 0.23$  [14]. The influence of milling

time and calcium content on the formation of perovskite phase and on the morphology of the nanopowders has been investigated. The effect of the sintering method has been determined with respect to final physical properties of the material, including dielectric permittivity, dielectric loss tangent, and Curie temperature.

## 2 Experimental Procedure

The high-purity oxides (BaO, CaO, and TiO<sub>2</sub>-anatase, Aldrich, 99% purity or higher) in the stoichiometric ratio were used for the synthesis of pure and Ca-doped barium titanate Ba<sub>1-x</sub>Ca<sub>x</sub>TiO<sub>3</sub> ( $0 \leq x \leq 0.20$ ) nanopowders. The starting materials were loaded into the stainless steel vial with stainless steel balls (ball-to-powder weight ratio BPR = 6:1) and milled in the high-energy shaker-type mill SPEX 8000 for different periods up to 100 h at room temperature.

The formation of the perovskite crystal structure as a function of milling time and Ca content was monitored by XRD studies using PANalytical Empyrean X-ray powder diffractometer (CuK<sub>α</sub> radiation, 45 kV, 40 mA). The pure BaTiO<sub>3</sub> nanopowders were uniaxially pressed to form the pellets. The Ca-doped barium titanate powders were cold isostatically pressed at 2.5 GPa into cylindrical pellets and conventionally sintered at 1300 °C for 2 h in the air. For the comparison, pure barium titanate nanopowders milled for 70 h were hot pressed at 1250 °C for 2 h under the uniaxial pressure of 20 MPa. The hot-pressing conditions were determined on the basis of the observation of dimensional changes of the sample during heating using heating stage microscope, Leitz, Version 1A, at a heating rate of 10 °C/min.

The microstructure of the powders and ceramic samples was investigated by scanning electron microscope (SEM). The chemical homogeneity of the hot-pressed ceramics was evaluated by energy-dispersive X-ray spectroscopy (EDS). For dielectric measurements, silver paste was applied on the both sides of the pellets and fired at 150 °C for 30 min to form the electrodes. Temperature dependence of dielectric permittivity and dielectric loss tangent at different frequencies, between 1 kHz and 1 MHz, was determined in the temperature range from 20 to 180 °C.

## 3 Results and Discussion

### 3.1 X-Ray Diffraction

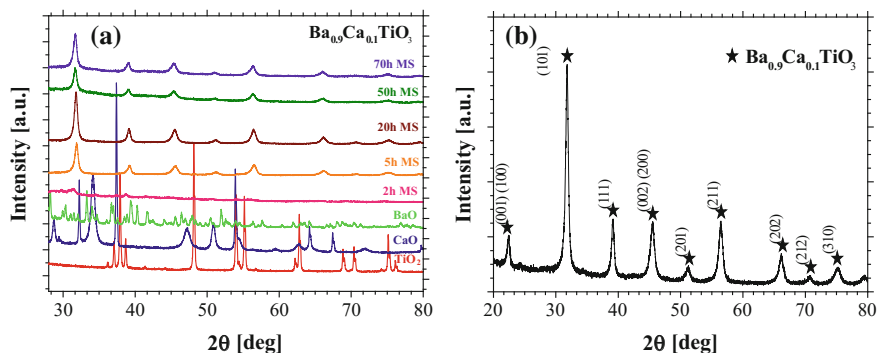
XRD studies performed at different stages of the milling process revealed that the perovskite phase with the tetragonal crystal structure is formed directly in the milling process, after 10 h or 5 h of mechanochemical synthesis in the case of pure and Ca-doped barium titanate, respectively. For all of the compositions,



investigated in this work, the perovskite phase formation during milling proceeded similarly. Figure 1a shows the XRD patterns of starting oxides and of the  $\text{Ba}_{0.9}\text{Ca}_{0.1}\text{TiO}_3$  composition obtained after milling time between 2 h and 70 h. At the initial stage of the process, after 2 h of milling, complete amorphization of the reactants occurred. Upon further milling for 5 h, new, well-visible peaks emerged on the XRD pattern, indicating that the perovskite tetragonal phase was formed. Longer milling, up to 70 h, resulted in the gradual changes in the width and intensity of the diffraction peaks.

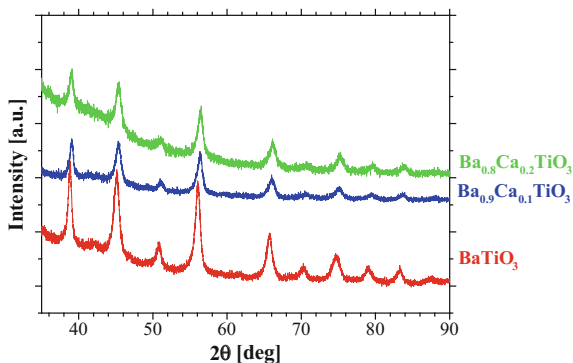
The course of these changes was slightly dependent on the Ca content in the  $\text{Ba}_{1-x}\text{Ca}_x\text{TiO}_3$  powder, and for  $x = 0.1$ , the highest crystallinity of the material was obtained after 20 h of milling (Fig. 1b). After longer milling time, the diffraction peaks became broader and their intensity decreased. For  $x = 0.2$ , the most intensive XRD peaks were observed in the milling time range between 20 and 50 h. XRD patterns of the  $\text{Ba}_{0.8}\text{Ca}_{0.2}\text{TiO}_3$  powders milled for longer than 50 h revealed significant broadening and decreased intensity of the diffraction peaks. The changes in the diffraction patterns observed at different stages of the milling process can be explained as follows. Initially, as the perovskite phase content increases, diffraction peaks become more intense. For longer milling times, the refinement of the crystallite size and the generation of many structural defects are the dominant phenomena affecting the XRD pattern of the powder.

XRD patterns for pure and Ca-doped  $\text{Ba}_{1-x}\text{Ca}_x\text{TiO}_3$  powders ( $0 \leq x \leq 0.20$ ) are shown in Fig. 2. An increase in the Ca content results in the slight shift of the diffraction peaks to the higher values of  $2\theta$  angle, which can be explained by the decrease in the interplanar spacings because of the substitution of some  $\text{Ba}^{2+}$  ions with the smaller  $\text{Ca}^{2+}$  ions.

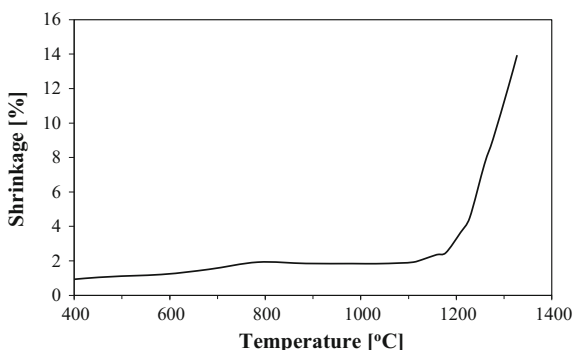


**Fig. 1** XRD patterns of the starting materials and  $\text{Ba}_{0.9}\text{Ca}_{0.1}\text{TiO}_3$  powder at different stages of mechanochemical synthesis (a) and XRD pattern of 20 h mechanochemically synthesized  $\text{Ba}_{0.9}\text{Ca}_{0.1}\text{TiO}_3$  (b)

**Fig. 2** XRD patterns of pure and Ca-doped barium titanate powders after 70 h of mechanochemical synthesis



**Fig. 3** Temperature dependence of shrinkage of pure  $\text{BaTiO}_3$  ceramic pellet



### 3.2 Hot-Pressing Conditions

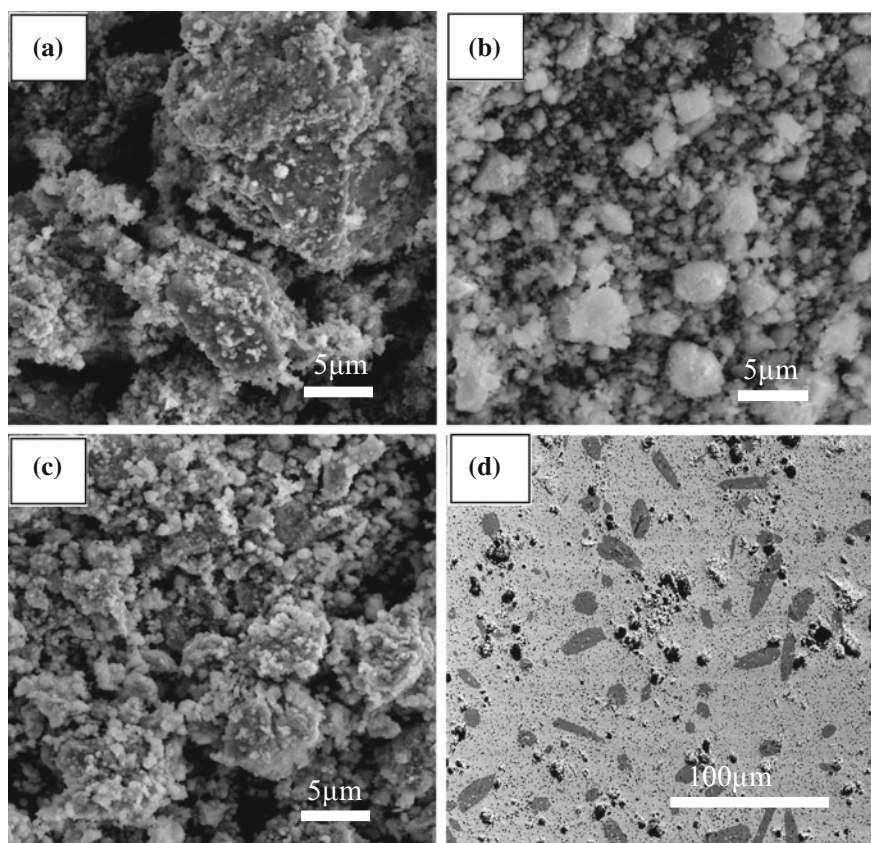
In order to determine the appropriate hot-pressing conditions of pure  $\text{BaTiO}_3$  ceramics obtained from the 70-h milled powder, dimensional changes of the pellet during heating were measured using the heating stage microscope (Fig. 3). It was found that the shrinkage of the sample takes place in two steps. The first one is very slight and occurs in the temperature range from 400 to 780 °C. Then, a plateau is observed on the shrinkage curve up to 1150 °C. At this temperature, the main shrinkage step begins, occurring from 1150 to 1350 °C. The total shrinkage of the sample in the temperature range from 400 to 1350 °C is 13.9%. Based on these results, temperature of 1250 °C was chosen as the most suitable for the hot pressing of pure barium titanate.

### 3.3 Microstructure of the Powders and Ceramic Samples

The morphology of the mechanochemically synthesized powders and ceramic samples obtained from these powders by conventional sintering and by hot pressing

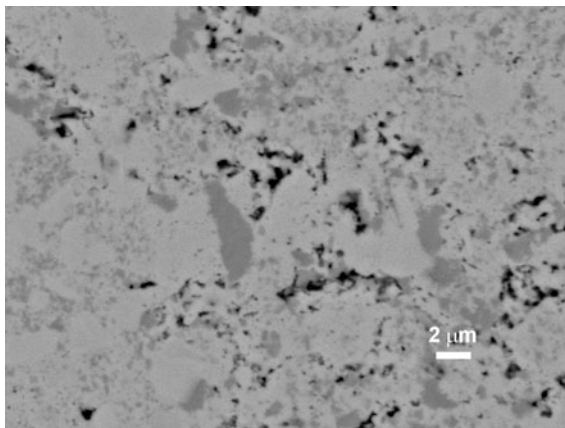
was investigated using scanning electron microscopy. The SEM images of  $\text{Ba}_{0.8}\text{Ca}_{0.2}\text{TiO}_3$  powders milled for 1, 50 and 100 h are shown in Fig. 4a–c. The powder particles have irregular shapes and form agglomerates of different sizes. After longer milling time (100 h), agglomerates are composed of smaller particles with a narrower size distribution. Figure 4d shows the microstructure of  $\text{Ba}_{0.8}\text{Ca}_{0.2}\text{TiO}_3$  ceramic sample obtained from the powder milled for 50 h by conventional sintering at 1300 °C for 2 h.

Pure  $\text{BaTiO}_3$  powders prepared by 70 h of mechanochemical synthesis were consolidated by hot pressing at 1250 °C. Conditions of the process were chosen on the basis of shrinkage behavior of the sample during heating (see Sect. 3.2). As shown in Fig. 5, well-densified ceramics with a low porosity content was obtained (note the difference in the magnification between Figs. 4 and 5).



**Fig. 4** SEM images of  $\text{Ba}_{0.8}\text{Ca}_{0.2}\text{TiO}_3$  nanopowders after **a** 1 h **b** 50 h **c** 100 h of mechanochemical synthesis and SEM image of conventionally sintered  $\text{Ba}_{0.8}\text{Ca}_{0.2}\text{TiO}_3$  ceramics derived from powder milled for 50 h (**d**)

**Fig. 5** SEM image of hot-pressed BaTiO<sub>3</sub> ceramics

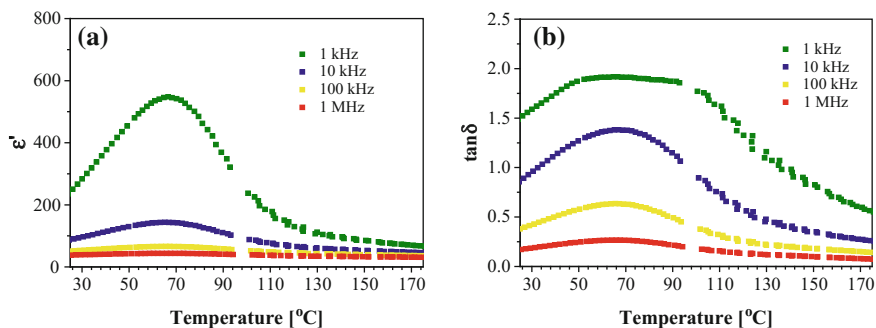


In order to determine the chemical homogeneity of the hot-pressed ceramics, EDS analysis was performed on these areas. It was found that there is a difference in Ba/Ti ratio between dark and bright regions of the sample (Fig. 5). The chemical composition of the bright regions is almost equal to the nominal one, calculated due to the stoichiometry of the compound. In the dark regions, decreased concentration of Ba and increased concentration of Ti were detected, resulting in the lowering of Ba/Ti ratio. This compositional inhomogeneity of the sample may be attributed to some chemical segregation processes that occur at the sintering step.

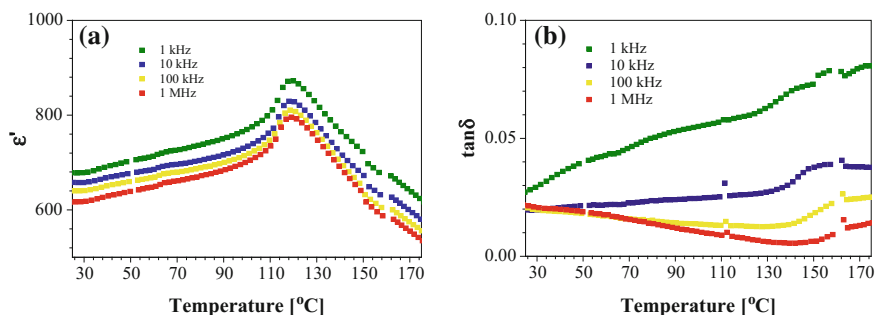
### 3.4 Dielectric Properties

The temperature dependence of dielectric properties of pure and Ca-doped barium titanate ceramics derived from the powders milled for 70 h was investigated at different frequencies of the electric field, in the range between 1 kHz and 1 MHz. It has been stated that both the sintering method and the compositional modification with calcium significantly affect the dielectric characteristics of barium titanate ceramics. The pressed, unsintered powder of pure BaTiO<sub>3</sub> exhibits poor dielectric properties (Fig. 6), as evidenced by very high dielectric losses.

The temperature dependence of dielectric permittivity has shown one very broad maximum, only at the lowest frequency (1 kHz). Dielectric anomaly disappears almost completely when the measurement is performed at higher frequencies. The lack of a distinct maximum of the dielectric permittivity at the temperature of transition from ferroelectric to paraelectric phase indicates that the pressed, unsintered BaTiO<sub>3</sub> does not possess the typical ferroelectric properties. Such behavior is closely related to nature of materials. The mechanochemically synthesized powders usually exhibit the core-shell structure with well-crystallized cores that are surrounded by amorphous layers [15]. The presence of the amorphous phase suppresses the ferroelectric response of the material.



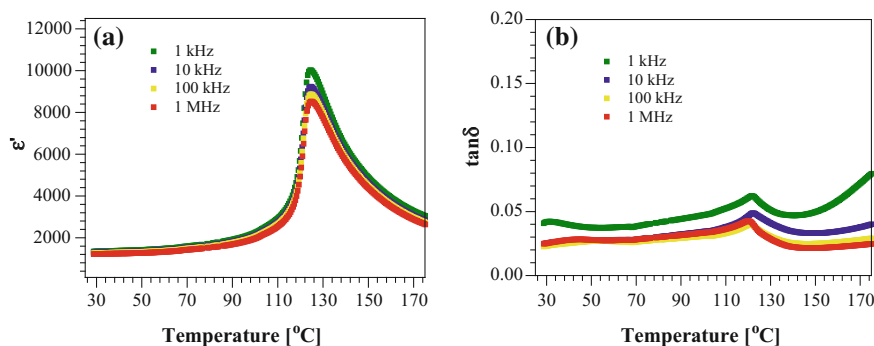
**Fig. 6** Temperature dependence of **a** dielectric permittivity ( $\epsilon'$ ) and **b** dielectric losses ( $\tan\delta$ ) measured on pressed, unsintered BaTiO<sub>3</sub> pellets



**Fig. 7** Temperature dependence of **a** dielectric permittivity ( $\epsilon'$ ) and **b** dielectric losses ( $\tan\delta$ ) measured on hot-pressed BaTiO<sub>3</sub> ceramic samples

The hot pressing of pure barium titanate results in the significant change of dielectric properties of the ceramics (Fig. 7). The single anomaly of the dielectric permittivity appears at 120 °C, which is known as the Curie point of pure barium titanate. The dielectric permittivity of hot-pressed barium titanate ceramics decreases as the frequency increases, but the temperature of the peak permittivity is independent of the frequency of the electric field. The hot pressing allows the preparation of barium titanate ceramics with substantially lower dielectric losses as compared to the pressed, unsintered samples. Dielectric losses of hot-pressed barium titanate are below 0.1 in the whole temperature range. The improvement of dielectric properties of hot-pressed samples can be attributed to the higher densification of the ceramics. Moreover, the temperature treatment, taking place during hot-pressing stage, allows the crystallization of amorphous part of sample [16]. Since the ferroelectric properties are very closely connected to perovskite phase, the improvement of dielectric properties of hot-pressed sample has been observed.

In order to investigate the influence of calcium on dielectric properties of barium titanate, composition with Ca content of  $x = 0.2$  was selected for the measurements.



**Fig. 8** Temperature dependence of **a** dielectric permittivity  $\epsilon'$  and **b** dielectric losses ( $tg\delta$ ) measured on for conventionally sintered  $Ba_{0.8}Ca_{0.2}TiO_3$  ceramic samples

The  $Ba_{0.8}Ca_{0.2}TiO_3$  ceramic pellets were obtained by conventional sintering at 1300 °C of mechanically synthesized powders. The Ca-doping greatly improves dielectric properties of barium titanate (Fig. 8). The dielectric permittivity of  $Ba_{0.8}Ca_{0.2}TiO_3$  ceramics is much higher in comparison with the results obtained for pure  $BaTiO_3$ . The temperature dependence of dielectric permittivity exhibits one sharp maximum at 125 °C. This anomaly related to the Curie temperature is observed slightly higher than in the case of undoped barium titanate. The value of the dielectric permittivity above  $T_c$  decreases slightly with increasing frequency and is almost independent of the frequency when the material is in the ferroelectric phase. Dielectric losses of  $Ba_{0.8}Ca_{0.2}TiO_3$  are very low, especially at the higher frequencies of the electric field, which confirms excellent dielectric properties of Ca-doped ceramics.

## 4 Conclusions

The tetragonal perovskite phase formation at room temperature, directly during mechanochemical synthesis of pure and Ca-doped barium titanate, has been confirmed by XRD studies. The doping with calcium significantly improves the dielectric properties and thermal stability of barium titanate ceramics. In the case of pure barium titanate, better properties, especially in terms of lower dielectric losses, can be obtained by hot-pressing method. The compositional modification and optimization of the processing conditions of barium titanate allow the improvement of the functional properties of the material.

**Acknowledgements** The authors acknowledge the help of Prof. B. Malic (Jozef Stefan Institute, Ljubljana, Slovenia) for hot-pressed experiment. The research work reported here was partially financed by Polish Ministry of Science and Higher Education within statutory activity.

## References

1. Zhang, L., Thakur, O.P., Feteira, A., Keith, G.M., Mould, A.G., Sinclair, D.C., West, A.R.: Comment on the use of calcium as a dopant in X8R BaTiO<sub>3</sub>-based ceramics. *Appl. Phys. Lett.* **90**, 142914 (2007)
2. Puli, V.S., Pradhan, D.K., Riggs, B.C., Chrisey, D.B., Katiyar, R.S.: Investigations on Structure, Ferroelectric, Piezoelectric and Energy Storage Properties of Barium Calcium Titanate (BCT) Ceramics, vol. 584, pp. 369–373 (2014)
3. Auciello, O., Scott, J.F., Ramesh, R.: The physics of ferroelectric memories. *Phys. Today* **51**, 22–27 (1998)
4. Priya, S., Nahm, S.: *Lead-Free Piezoelectrics*. Springer, New York (2012)
5. Coondoo, I., Panwar, N., Kholkin, A.: Lead-free piezoelectrics: current status and perspectives. *J. Adv. Dielectr.* **3**(2), 1330002 (2013)
6. Damjanovic, D., Klein, N., Li, J., Porokhonskyy, V.: What can be expected from lead-free piezoelectric materials? *Funct. Mater. Lett.* **3**(1), 5–13 (2010)
7. Savinov, M.E., Trepakov, V.A., Kamba, S., Kapphan, S.E., Petzelt, J., Pankrath, R., Kislova, I.L., Kutsenko, A.B., Jastrabik, L.: Dielectric and infrared response of Ba<sub>0.77</sub>Ca<sub>0.23</sub>TiO<sub>3</sub>. *Ferroelectrics* **295**, 31–38 (2003)
8. Kuper, C., Pankrath, R., Hesse, H.: Growth and dielectric properties of congruently melting Ba<sub>1-x</sub>Ca<sub>x</sub>TiO<sub>3</sub> crystals. *Appl. Phys. A* **65**, 301–305 (1997)
9. Kong, L.B., Zhang, T.S., Ma, J., Boey, F.: Progress in synthesis of ferroelectric ceramic materials via high-energy mechanochemical technique. *Prog. Mater. Sci.* **53**(2), 207–322 (2008)
10. Suryanarayana, C.: Mechanical alloying and milling. *Prog. Mater. Sci.* **46**, 1–184 (2001)
11. Stojanovic, B.D., Jovalekic, C., Vukotic, V., Simoes, A.Z., Varela, J.A.: Ferroelectric properties of mechanically synthesized nanosized barium titanate. *Ferroelectrics* **319**, 65–73 (2005)
12. Stojanovic, B.D., Simoes, A.Z., Paiva-Santos, C.O., Jovalekic, C., Mitic, V.V., Varela, J.A.: Mechanochemical synthesis of barium titanate. *J. Eur. Ceram. Soc.* **25**, 1985–1989 (2005)
13. Szafraniak-Wiza, I., Hilczer, B., Talik, E., Pietraszko, A., Malic, B.: Ferroelectric perovskite nanopowders obtained by mechanochemical synthesis. *Proc. Appl. Ceram.* **4**(3), 99–106 (2010)
14. Wang, X., Yamada, H., Xu, C.-N.: Large electrostriction near the solubility limit in BaTiO<sub>3</sub>-CaTiO<sub>3</sub> ceramics. *Appl. Phys. Lett.* **86**, 022905 (2005)
15. Szafraniak, I., Połomska, M., Hilczer, B., Pietraszko, A., Kępiński, L.: Characterization of BiFeO<sub>3</sub> nanopowder obtained by mechanochemical synthesis. *J. Eur. Ceram. Soc.* **27**, 4399–4402 (2007)
16. Szafraniak-Wiza, I., Bednarski, W., Waplak, S., Hilczer, B., Pietraszko, A., Kępiński, L.: Multiferric BiFeO<sub>3</sub> nanoparticles studied by electron spin resonance. X-ray Diffract. Trans. *Electr. Microsc. Meth. J. Nanosci. Nanotechnol.* **9**, 3246–3251 (2009)

# Wear of Solid Carbide Ball Nose End Mill

Iwona Lapunka, Piotr Wittbrodt and Katarzyna Marek-Kolodziej

**Abstract** The cutting tools are an important part of the production process and represent a significant share in the costs of manufactured products. Evaluation of their condition is an important task, and efficient use of cutting abilities is one of the ways to reduce production costs. This paper outlines the methods for determining the tool life and wear level of solid carbide ball nose end mills. There have been considerations of the wear of the ball nose end mill's cutting edge involved in the machining process. We demonstrate the need for developing a computer system for the prediction of wear of ball nose end mills operating under variable (random) technological and geometric machining parameters.

**Keywords** Durability and wear · Monitoring · Prediction

## 1 Introduction

Turning, milling, and drilling are typical and most commonly applied machine cutting operations in the metallurgical and mechanical engineering industry. Owing to the modern computer solutions for computer-aided design and computer-aided manufacturing (CAD/CAM) and to the use of open architecture controller (OAC), such operations can develop dynamically in large companies. Recent improvements in the field of production organization, such as adaptive machining and agile manufacturing, allowed, to a degree, to transfer innovative machine cutting

---

I. Lapunka · K. Marek-Kolodziej  
Faculty of Production Engineering and Logistics,  
Department of Project Management, Opole University of Technology,  
Opole, Poland

P. Wittbrodt (✉)  
Faculty of Production Engineering and Logistics,  
Department of Management and Production Engineering,  
Opole University of Technology, Opole, Poland  
e-mail: p.wittbrodt@po.opole.pl



solutions into the sector of small- and medium-sized enterprises (SMEs). Modern economy is largely based on these enterprises, which naturally creates an incentive to implement novel industrial solutions with the aim of improving their technical standing.

Despite the continued adoption of modern organization and technological methods by enterprises, many technical issues remain to be solved. One of the outstanding issues is to ensure a high level of the use of machines and manufacturing equipment of an enterprise. Continuity of operation can be disrupted by mechanical failure, resulting in machine stoppage. Machine stoppage is understood as a period of time, during which no machining takes place. Reasons for machine stoppage include the following:

- organizational and logistics issues of the manufacturing system, e.g., the diversity of manufactured assortment, which increases machine retooling rate;
- technical issues, e.g., periodic equipment maintenance needed to ensure its continuous operation, or excessive wear or breaking of a tool.

Machine stoppage can often be mitigated or eliminated. Some organizational issues are known in advance, making it possible to employ, e.g., clustering methods, whereby assortment is grouped according to its technological features; this allows manufacturing similar elements without the need for machine retooling. More difficult to manage are the technical issues leading to machine stoppage, in particular the excessive wear or breaking of a tool under stochastic conditions of machine cutting.

## 2 Cutting Tool Wear

The main reason for the unplanned stoppage in a technical environment is the wear and breaking of a cutting tool during machining, often leading to severe machine breakdowns. Such stoppage is expensive, not only because of the lost time, but also due to the cost associated with having to replace the tool. Excessive wear has a detrimental impact on the cutting conditions (e.g., increased cutting force, increase in temperature and vibration level), resulting in quality deterioration of the work-piece. Mean machine stoppage rate due to a broken tool has been estimated as 6.8% [1] (or as much as 20% [2]). Studies carried out as early as twenty years ago [3, 4] demonstrated that the use of reliable systems for monitoring the condition of the tool nose can increase cutting speed by 10–50%, reduce total costs by 10–40%, as well as predict the condition of the tool, which can reduce machine stoppage. The quoted improvement rates remain valid today, and an accurate assessment of cutting tool wear is considered crucial to increase productivity and effectiveness of the entire manufacturing process.

Tool wear is a continuous process, with its intensity, along with machining conditions significantly influencing the dynamics of every machining process. The

increase in tool wear during machining, particularly on the tool flank, leads to increased friction, in turn causing an increase in the cutting force [5]. Tool wear, apart from its direct impact on tool durability, also affects the microhardness of work surface [6].

Currently, milling is considered the dominant machine cutting process. The literature review demonstrates that the particularities of end mill wear are not fully understood. This is due to the fact that milling is widely used in the manufacturing of molds and dies with a large number of 3D surfaces. To machine these, ball nose end mills are used, for which the tool wear has not been thoroughly researched. Whether a ball nose end mill is used also depends on the choice of machining strategy as well as on the inclination angle [7]. These parameters have a significant impact on the machining time, quality of the machined surface, and tool life [8].

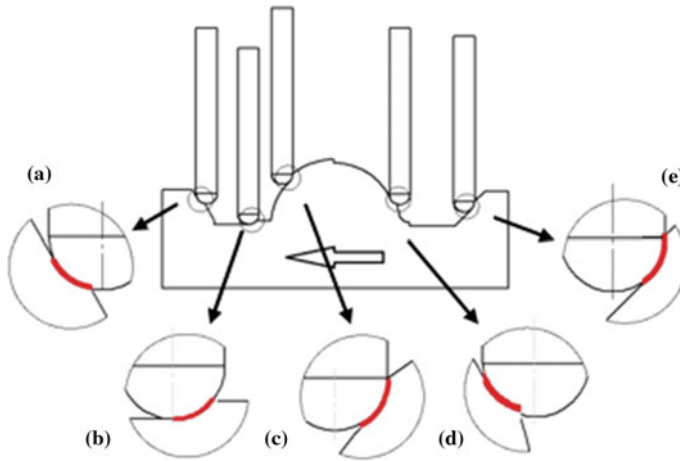
The challenging conditions of machining 3D surfaces decrease tool life through intensive wear, which is stochastic in nature. Studies have demonstrated the dependence of tool life and cutting parameters [e.g., 7, 8]; however, the tool wear of the entire ball nose edge under random machining conditions has not been comprehensively investigated to date. The abundance of input data is an obstacle to diligent analysis, making computer systems for the prediction of tool wear a noteworthy option [9].

### 3 Nose Tool Life Under Variable Machine Cutting Conditions

At present, milling is the most common technique of manufacturing 3D elements. In contrast to machining 2D elements with typical end milling cutters, where machining conditions are constant, determining the conditions of machining 3D elements is often challenging. This is due to the specifics of the operation of a ball nose end mill, which is typically used for this kind of machining. It is possible to minimize their impact when assessing tool's operating conditions by using a 5-axis computer-numeric-controlled (CNC) machines (this allows machining with the same tool part); however, due to the costs of purchase and maintenance of such equipment, this approach is not viable in the SME sector.

Instead, SMEs typically use 3-axis machines, where the tool is perpendicular to machine tool table, leading to the high variability in machining parameters. Figure 1 shows a typical setup (machining diagram) for a ball nose end mill in a 3-axis machine, highlighting typical local features in machining. It is assumed that milling local features (a, c, d, e in Fig. 1) accounts for ca. 40% of the manufacturing time of the entire form [10].

The contact point between the ball nose end mill and the workpiece is denoted with a thick line. The manner in which the tool comes in contact with the worked material during machining is non-deterministic. Certain parts of the cutting-edge arc (those closer to the rotation axis of the tool) work with greater intensity compared



**Fig. 1** Types of features machined using a ball nose end mill: **a** downward slope, **b** plane, **c, d** convex protrusion, and **e** upward slope

with the parts closer to the cylindrical section (is it related to the variable cutting forces?). Practical observations of operating conditions reveal that the ball-shaped section of the tool is subjected to maximum use when machining protrusions (c, d in Fig. 1). With other features, in most cases in practice, the fragments of the cutting edge of the tool operate under variable machining conditions.

During the operation of the tool, the local contact point of the ball nose end mill with the machined object moves along the arc of the cutting edge. This results in a change of local operating conditions of the tool, which leads to varying intensities of its wear, making the determination of tool life under non-stationary machining conditions very difficult. Figure 2 shows a graphical interpretation of tool nose wear for alternating variable cutting parameters. Assuming that the curves 1–4 represent the tool's wear at constant but different variables of the machining parameters (speed, depth, and the machining width), and the horizontal lines represent different variables of the wear, the wear curve may be determined according to the alternately changing machining parameters. In order to determine this relationship, curves 1–4 must be translated horizontally, giving rise to a combined curve 5. In doing so, we obtain a plot representing wear with alternating variable cutting parameters.

Determining the contact point between the ball nose end mill and the workpiece, and obtaining a wear curve, is possible under laboratory conditions. Under industrial conditions, however, this process is overly time-consuming. Moreover, the motion of the contact point along the arc of the cutting edge depends on the chosen milling strategy, which significantly hinders the assessment of the condition of the tool nose.

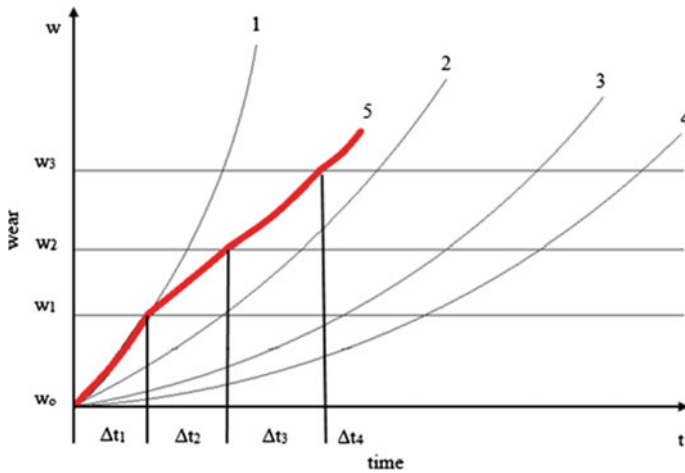


Fig. 2 Tool nose wear with alternating variable cutting parameters

#### 4 Mill Tool Life and Wear with Alternating Variable Cutting Parameters

The aim of the study was to determine the wear distribution of the spherical part of a ball nose end mill for alternating variable cutting parameters. The change in parameters was obtained through a suitably prepared study sample. The machined material was quenched and tempered with 55NiCrMoV7 steel (according to EN 96-79), HRC  $42 \pm 2$ .






The experiment was conducted using a 3-axis CNC milling machine, with the program controlling the machine generated by CAM.

The operation of a 4-flute solid carbide ball nose end mill [6 mm diameter, h10 tolerance ( $\varnothing 6_{-0.048}^0$ )] was studied. Table 1 presents the basic specification of the tool. Table 2 presents the technological and geometric machining parameters employed during the tests. The values recommended by the tool manufacturer are shown for reference.

Based on the definitions of selected tool wear indicators [12], procedures for their determination were elaborated for ball nose end mills (Fig. 3). The following wear indicators were evaluated for the flank face: VB—flank wear, and for the rake face: KB—crater width, KF—distance from the crater to the primary cutting edge, KT—crater depth.

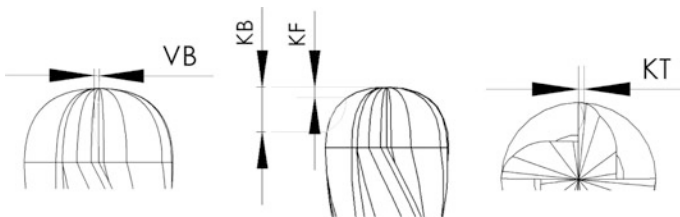
Ball nose end mill wear was measured using a microscope equipped with a measuring head with an accuracy of 0.001 mm.

**Table 1** Specification of the ball nose end mill for machining forming [11]

Solid carbide ball nose end mill for machining		
d = 6 mm		
Z 4		
		
< 48 HRC		

**Table 2** Technological and geometric parameters—recommended and actually employed values

Steel grade	Values	Parameters			
		Technological		Geometric	
		Cutting speed [m/min]	Rate of feed [mm/min]	Cutting depth [mm]	Cutting width [mm]
55NiCrMo V7	Recommended	<95	1400	0.3	0.3
	Actually employed	25–60	200–500	0.15–6	0.15–6



**Fig. 3** Wear indicators for ball nose end mills

## 5 Measurement Results

Several measurements were obtained in the course of studies on the selected wear indicators. We observed that the wear of ball nose end mill teeth is variable and random; i.e., the changes in wear indicators for individual edges are different. Figures 4, 5, 6, and 7 show changes in wear indicators as a function of cutting time (separately for each tooth). Points represent the accomplished measurement, and color—the examined blade. The solid line indicates mean values from the obtained measurements. The curves are qualitatively similar, with only minor differences between them. The values of indicators increase for mean values (for four tool teeth a, b, c, d, Figs. 4, 5, 6, and 7). However, it is impossible to determine the tool (or

individual tooth) condition from the mean value alone (e, Figs. 4, 5, 6, and 7). A detailed analysis confirms that tool teeth wear occurs at random. Moreover, at any given time, one of the teeth (e.g., tooth 1) experiences higher wear relative to the other teeth. At the same time, the remaining teeth (e.g., 2, 3, 4) do not participate in the cutting process. When the first tooth becomes worn out, e.g., due to excessive abrasion or crumbling, the next one (e.g., 2) takes over and so on. Importantly, the subsequent teeth work with different, more demanding geometric and technological parameters. In addition, an increase in cutting speed (during the machining of 3D elements, the changes in speed are frequent) increases the intensity of tool teeth wear.

The results of direct observations of ball nose end mill teeth are in line with the above discussion. The observed KF index decreases, as with the progress of machining time, the blade's wear occurs increasingly closer to the rotation axis of the mill (the measurement rule of the KF index, see Fig. 3).

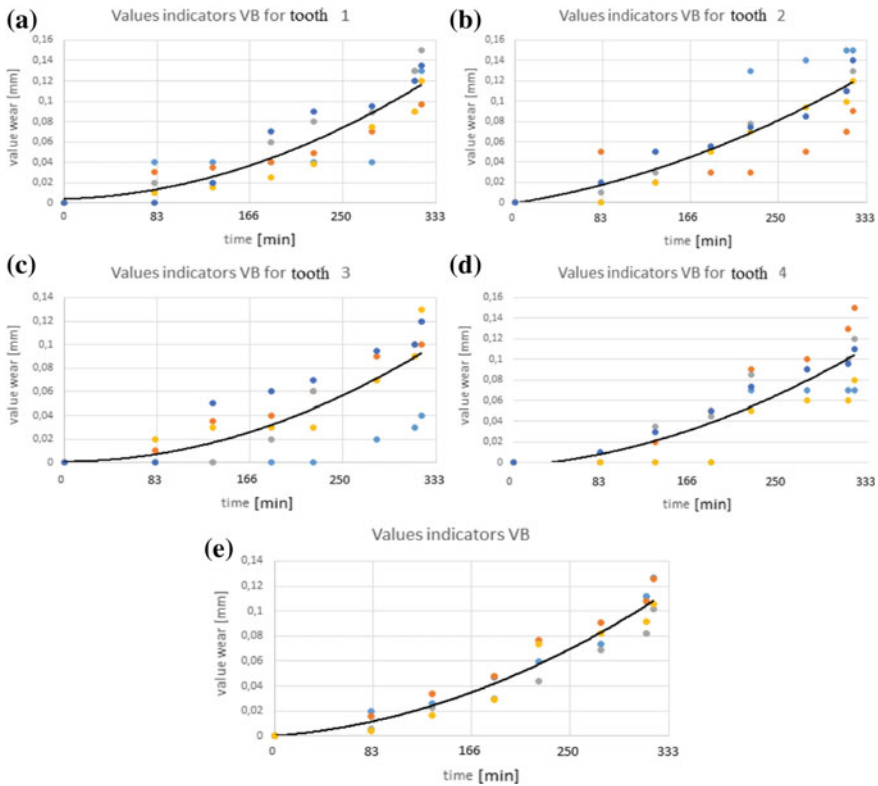
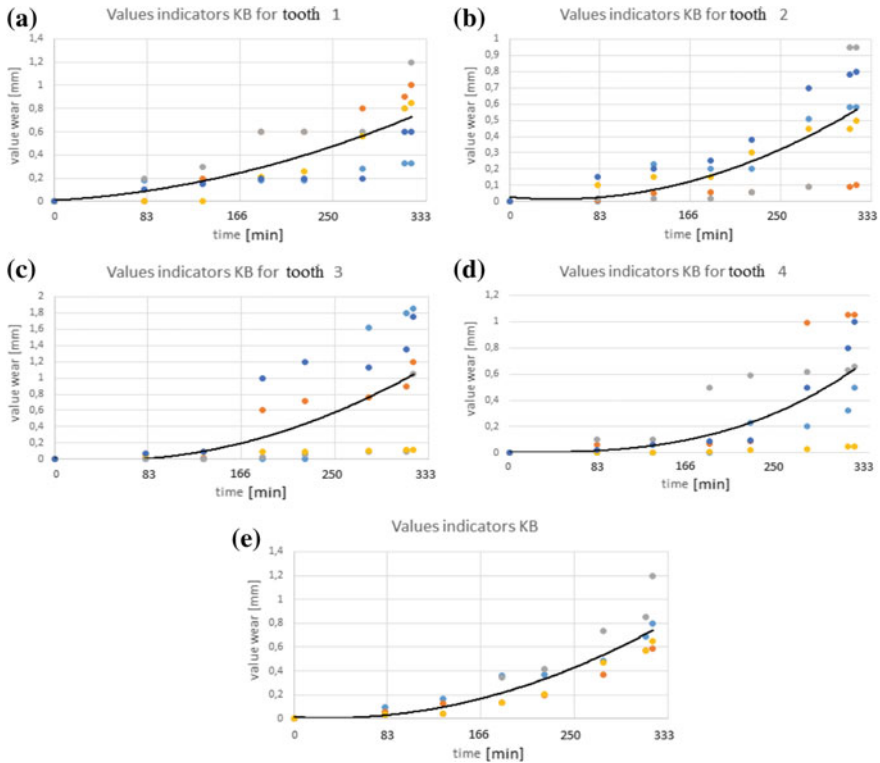


Fig. 4 Changes in the VB indicator as a function of cutting time (solid line corresponds to mean)



**Fig. 5** Changes in the KB indicator as a function of cutting time (solid line corresponds to mean)

A detailed analysis demonstrates that the values of wear of individual teeth and corresponding indicators show significant variance. It is impossible to unify them and identify common features or even similarities. This explicitly demonstrates the necessity to approach the analysis of selected teeth indicators and established geometric and technological parameters on a case-by-case basis.

## 6 Summary and Conclusions

Our results confirm the lack of repeatability in the wear of ball nose end mills under alternating variable machining conditions. The analysis reveals no explicit interdependence between wear and cutting parameters, nor any correlation between the wear and the feature shape at the mill-workpiece contact point. Therefore, the wear of individual teeth is random and cannot be predicted in a traditional, direct manner. The evaluation of tool condition under the transient industrial conditions is time-consuming and often infeasible.

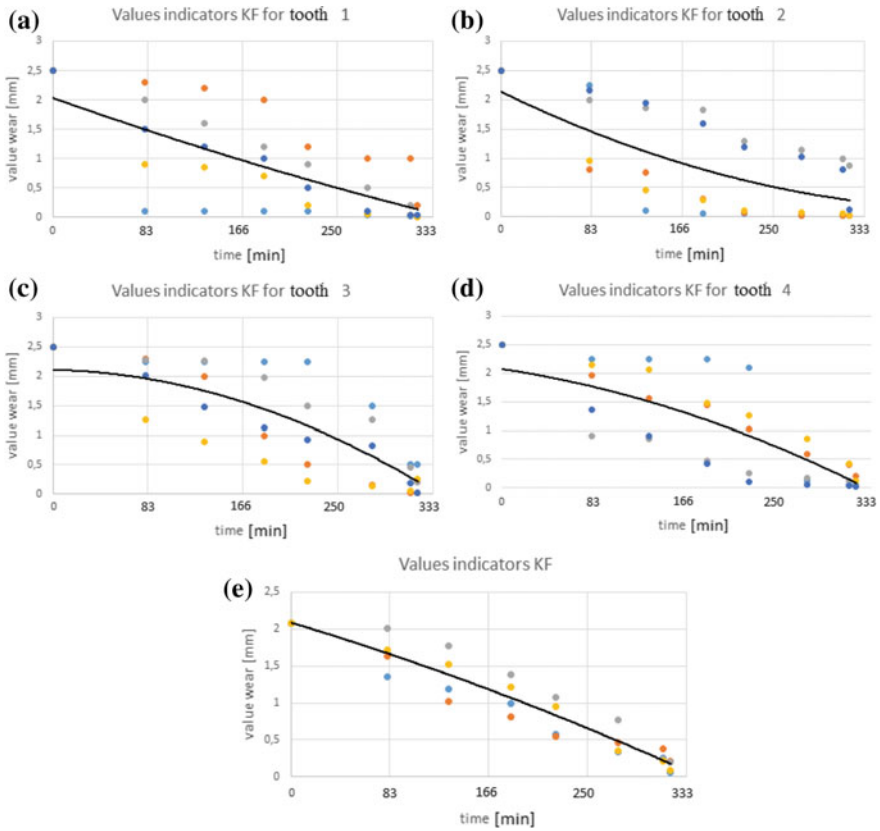


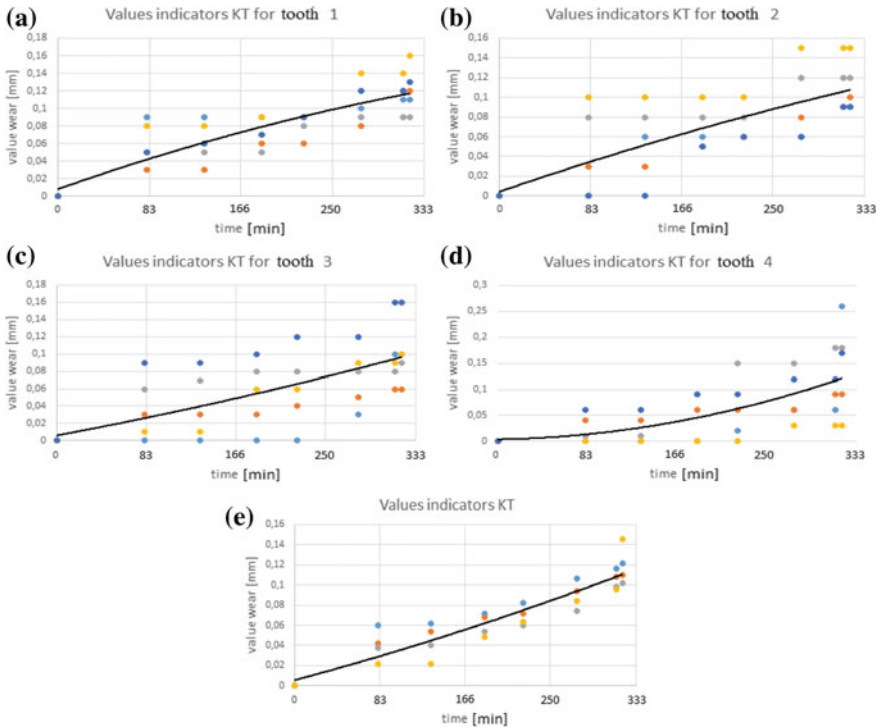
Fig. 6 Changes in the KF indicator as a function of cutting time (solid line corresponds to mean)

We indicated the need to employ ball nose end mills when machining curvilinear surfaces, therefore, from the perspective of machining economics, and it is important to minimize stoppages in the cutting process. Increasing useful tool life is extremely challenging, especially under the industrial conditions of SMEs, which are not equipped with computer-aided systems, such as expert systems.

A further difficulty lies in the lack of suitable norms that would standardize the measurement of ball nose end mill wear. Developing an appropriate study methodology is necessary.

As it was mentioned before, the wear of multi-flute tools is random and its intensity is different for each tooth. Mean values are not representative of actual wear, leading to excessive machine stoppages. To mitigate the unplanned stoppages caused by replacing a tool whose remaining useful tool life is nonzero, an effective computer system for the prediction of the wear of ball nose end tools must be analyzed anew and elaborated.





**Fig. 7** Changes in the KT indicator as a function of cutting time (solid line corresponds to mean)

The above considerations are a part of wider studies, which focused on elaborating an integrated computer system for aiding the production process based on tool use diagnostics. The main principles of the system under construction were presented, e.g., in [13, 14].

## References

1. Yeo, S.H., Khoo, L.P., Neo, S.S.: Tool condition monitoring using reflectance of chip surface and neural network. *J. Intell. Manuf.* **11**, 507–514 (2000)
2. Kurada, S., Bradley, C.: A review of machine vision sensors for tool condition monitoring. *Comput. Ind.* **34**, 55–72 (1997)
3. Najafi, B., Hakim, H.: A comparative study of non-parametric spectral estimators for application in machine vibration analysis. *Mech. Syst. Signal Process.* **6**, 551–574 (1992)
4. Fu, P., Hope, A.D., King, G.A.: *Intelligent Tool Condition Monitoring in Milling Operation*. Systems Engineering Faculty Southampton Institute, UK (1998)
5. Tönshoff, H.K., Arendt, C., Amor, R.B.: Cutting of hardened steel. *CIRP Ann. Manufact. Technol.* **49**, 547–566 (2000)
6. Krolczyk, G.M., Nieslony, P., Legutko, S.: Determination of tool life and research wear during duplex stainless steel turning. *Arch. Civ. Mech. Eng.* **15**, 347–354 (2015)

7. Ventura, C.E.H., Hassui, A.: Evaluation of static cutting forces and tool wear in HSM process applied to pocket milling. *Int. J. Adv. Manuf. Technol.* **65**, 1681–1689 (2012)
8. Duspara, M., Sabo, K., Stoic, A.: Acoustic emission as tool wear monitoring. *Tehnički vjesnik [Tech. Gaz.]* **21**, 1097–1101 (2014)
9. List, G., Sutter, G., Bi, X.F.: Investigation of tool wear in high speed machining by using a ballistic set-up. *Wear* **267**, 1673–1679 (2009)
10. Kecelj, B., Kopac, J., Kampus, Z., Kuzman, K.: Speciality of HSC in manufacturing of forging dies. *J. Mater. Process. Technol.* **157–158**, 536–542 (2004)
11. [http://www.kometgroup.pl/upload/Katalog\\_URPOL\\_2012.pdf](http://www.kometgroup.pl/upload/Katalog_URPOL_2012.pdf), 27
12. PN-ISO 8688-1:1996, PN-ISO 8688-2:1996
13. Wittbrodt, P., Paszek, A.: Decision support system of machining process based on the elements of fuzzy logic. *Int. J. Mod. Manuf. Technol.* VII **1**, 81–85 (2015)
14. Wittbrodt, P., Paszek, A.: The operating diagnostics in the computer aided systems of production processes. *Appl. Mech. Mater.* **791**, 3–9 (2015)

# Author Index

## A

Abramov, Andrey, 573  
Adamczak, Michal, 89  
Aleksenko, Borys A., 509  
Antas, Dawid, 67  
Antczak, Lukasz, 393  
Antosz, Katarzyna, 45  
Araújo, Adriana F., 129

## B

Bachtiak-Radka, Emilia, 649  
Banaszak, Zbigniew, 213  
Barreto, Raissa C.C., 129  
Bartkowiak, Tomasz, 13  
Bartoszek, Jakub, 393  
Bocewicz, Grzegorz, 213  
Bogdan-Chudy, Marta, 659  
Borsekova, Kamila, 193  
Bozek, Mariusz, 3, 835  
Budniak, Zbigniew, 473  
Bun, Pawel, 563, 597

## C

Carach, Jan, 803  
Cepova, Lenka, 813  
Chabera, Petr, 573  
Chattopadhyaya, Somnath, 803  
Chudy, Roman, 695  
Cizak, Olaf, 13, 519  
Cyplik, Piotr, 89  
Czajka, Piotr, 553, 775

## D

Davidrajuh, Reggie, 119, 287  
Devojno, Oleg, 911  
Diakun, Jacek, 109, 119, 309  
Diering, Magdalena, 835, 879, 897  
Dixit, Amit R., 803  
Dobrovorskiy, Sergey S., 509

Dobrovolska, Ludmila G., 509  
Domínguez, Alejandro Pereira, 813  
Dostatni, Ewa, 309, 319  
Duda, Jan, 79  
Dudzinska, Sara, 649  
Dziarski, Piotr, 921  
Dzionk, Stefan, 585

## E

Erkoyuncu, John A., 563

## F

Feldshtein, Eugene, 911  
Feliksik, Kamil, 939  
Fertsch, Marek, 89  
Figueiredo, Luis, 725  
Frackowiak, Magdalena, 921  
Frackowiak, Piotr, 383, 403

## G

Gabka, Joanna, 169  
Galusik, Dariusz, 23  
Gapinski, Bartosz, 775, 813  
Gawlik, Jozef, 931  
Gestwa, Wojciech, 639  
Giesko, Tomasz, 541  
Gladysz, Bartlomiej, 267  
Golinski, Marek, 193  
Gomes, Marivan S., 129  
Gorski, Filip, 563, 597  
Goslinski, Jaroslaw, 373  
Grabowska, Marta, 3, 887  
Graczyk-Kucharska, Magdalena, 193  
Grajewski, Damian, 309  
Grochala, Daniel, 649  
Grudzien, Lukasz, 299  
Grzesiak, Dariusz, 531  
Grzesik, Wit, 695  
Guerreiro, Bruno V., 159

**H**

Habrat, Witold, 763  
 Hajkowski, Jakub, 619  
 Hamrol, Adam, 3, 319, 867  
 Harugade, Mukund, 425  
 Hawryluk, Marek, 751  
 Helman, Joanna, 169  
 Herbin, Pawel, 437, 531  
 Hilczer, Bozena, 939  
 Hloch, Sergej, 495, 803

**I**

Ingaldi, Manuela, 855

**J**

Jablonski, Piotr, 13, 553, 775  
 Jacso, Adam, 353  
 Jakobczyk, Adrian, 119  
 Jakubowicz, Michal, 731  
 Jakubowski, Arkadiusz, 373, 455  
 Jarczoch, Andrzej, 99  
 Jasarevic, Sabahudin, 299

**K**

Kacalak, Wojciech, 473  
 Kardapolava, Marharyta, 911  
 Karwasz, Anna, 139, 309  
 Klos, Slawomir, 33  
 Knop, Krzysztof, 855  
 Knosala, Ryszard, 57  
 Kolinski, Adam, 23  
 Koper, Jeremiasz K., 483  
 Kosturek, Robert, 679  
 Koterak, Robert, 785  
 Kowalczyk, Malgorzata, 795  
 Kowalski, Arkadiusz, 169  
 Kozielski, Lucjan, 939  
 Krajewska-Spiewak, Joanna, 931  
 Krawczyk-Dembicka, Elzbieta, 257  
 Kreibich, Viktor, 685  
 Krenczyk, Damian, 287  
 Krolczyk, Grzegorz, 495, 659  
 Krolczyk, Jolanta, 763  
 Krolikowski, Marcin A., 531  
 Kruszynski, Bogdan, 705  
 Kubacki, Arkadiusz, 277, 373, 455  
 Kuczko, Wieslaw, 563  
 Kuczmaszewski, Jozef, 669  
 Kudlacek, Jan, 573, 631, 685  
 Kujawinska, Agnieszka, 835, 867, 897  
 Kulka, Michal, 921  
 Kupiec, Robert, 795

**L**

Lajmert, Pawel, 705  
 Lapunka, Iwona, 949  
 Legutko, Stanislaw, 685, 715, 803  
 Lehocka, Dominika, 715, 803  
 Lemes, Samir, 823  
 Lins, Romulo G., 159  
 Login, Waldemar, 669  
 Luczak, Marcin, 835  
 Lutsko, Nikolaj, 911

**M**

Machado, Jose, 23, 149, 725  
 Majchrowski, Radomir, 731  
 Majewski, Maciej, 473  
 Makuch, Natalia, 921  
 Malec, Elzbieta, 203  
 Malopolski, Waldemar, 607  
 Marciniak-Podsadna, Lidia, 785  
 Marek-Kolodziej, Katarzyna, 949  
 Markiewicz, Ewa, 939  
 Matyszczak, Jakub, 393  
 Mazurkiewicz, Adam, 541  
 Mendonca, Joao P., 725  
 Miadlicki, Karol, 413, 463  
 Milecki, Andrzej, 331  
 Minorowicz, Bartosz, 363, 393, 741  
 Myszkowski, Adam, 13, 343

**N**

Najwer, Michal, 679  
 Nieslony, Piotr, 659, 679  
 Nogaj, Kamil, 119

**O**

Osinski, Filip, 299  
 Ostrowska, Ksenia, 795  
 Ostrowski, Dariusz, 705  
 Owczarek, Piotr, 343, 373, 455

**P**

Pajor, Miroslaw, 413, 437, 463  
 Palubicki, Mariusz, 393  
 Parus, Arkadiusz, 413  
 Paszek, Alfred, 225  
 Patalas, Adam, 553  
 Patalas-Maliszewska, Justyna, 33  
 Pawlewski, Pawel, 213  
 Peplowsky, Stefan, 845  
 Perz, Karolina, 449  
 Piesko, Pawel, 669  
 Pittner, Grzegorz, 363, 741

Pobozniak, Janusz, 247  
Podsadna, Lidia Marciniak, 813  
Popielarski, Pawel, 619  
Przybylski, Włodzimierz, 585  
Putnik, Goran D., 149

**R**

Regulski, Roman, 363  
Regus, Michal, 553, 775  
Reis, Luis P., 109, 867, 879  
Rejek, Michal, 495  
Rewers, Paulina, 67, 109  
Rewolinska, Aleksandra, 449  
Rey, Anton Martinez, 813  
Rich, Beatrice M., 845  
Rocha, Alvaro, 109, 879  
Rogalewicz, Michal, 835, 867, 897  
Rojek, Izabela, 319  
Rosienkiewicz, Maria, 169  
Rostek, Michaela, 57  
Rucki, Mirosław, 631, 731  
Rybarczyk, Dominik, 277, 343, 373  
Rychlik, Marcin, 751

**S**

Sakow, Mateusz, 413, 463  
Salwin, Mariusz, 267  
Santarek, Krzysztof, 267  
Sawicki, Lukasz, 373  
Schmitt, Robert, 159  
Siemiatkowski, Zbigniew, 631  
Sika, Robert, 619  
Sikora, Malgorzata, 705  
Simkulet, Vladimir, 715  
Skobiej, Bartosz, 99  
Skolud, Bozena, 287  
Skorska, Halszka, 795  
Sladek, Jerzy, 795  
Smilek-Starczynowska, Marta, 855  
Smuskiewicz, Pawel, 867  
Sobkow, Lukasz, 67  
Sousa, Joao, 725  
Spychala, Malgorzata, 193  
Stadnicka, Dorota, 45  
Starzynska, Beata, 879  
Stec, Natan, 393  
Stefanski, Frederik, 741  
Sun, Jianing, 159  
Susz, Slawomir, 169  
Svoboda, Jakub, 685  
Szafraniak-Wiza, Izabela, 939

Szafranski, Maciej, 193  
Szajkowska, Karolina, 139, 879  
Szalanska, Karina, 597  
Szalay, Tibor, 353  
Szydłowski, Michal, 649

**T**

Takala, Josu, 887  
Taktak, Sukru, 921  
Talar, Rafal, 553  
Trojanowska, Justyna, 23, 109, 129  
Turek, Pawel, 763

**U**

Urban, Wieslaw, 257

**V**

Varela, Maria L.R., 23, 129, 149  
Varga, Gyula, 731  
Vieira, Gaspar G., 149  
Vogt, Katarzyna, 897

**W**

Wachowski, Marcin, 679  
Waigaonkar, Sachin D., 425, 835, 897  
Weber, Markus, 3  
Wichniarek, Radoslaw, 309, 563, 597  
Wieczorowski, Michal, 785, 813  
Wiercioch, Adam, 607  
Wisniewski, Marcin, 13  
Wittbrodt, Piotr, 949  
Włodarkiewicz, Anna, 939  
Wojakowski, Pawel, 795  
Wojciechowski, Jakub, 519  
Wojtko, Kamil, 383, 403  
Woll, Ralf, 845  
Worlitz, Jane, 845  
Wrobel, Nikodem, 495

**Z**

Zaimovic-Uzunovic, Nermina, 823  
Zak, Krzysztof, 695  
Zak, Maciej, 763  
Zawada-Michalowska, Magdalena, 669  
Zawadzki, Przemyslaw, 183, 237, 597  
Zerbst, Slawomir, 3  
Ziamba, Jacek, 751  
Znaniiecki, Piotr, 785  
Zoubek, Michal, 573  
Zywicki, Krzysztof, 67, 183